CISBAT

PROCEEDINGS VOL. II

INTERNATIONAL CONFERENCE

CLEANTECH FOR SMART CITIES & BUILDINGS
FROM NANO TO URBAN SCALE

4-6 SEPTEMBER 2013 EPFL

LAUSANNE - SWITZERLAND

LESO-PB
EPFL
ÉCOLE POLYTECHNIQUE FÉDÉRALE DE LAUSANNE

Schweizerische Eidgenossenschaft
Confédération suisse
Confederazione Svizzera
Confederaziun svizra

Swiss Federal Office of Energy SFOE

Fondation ZENO KARL SCHINDLER
ZENO KARL SCHINDLER Foundation
ZENO KARL SCHINDLER - Stiftung

Cambridge University

Massachusetts Institute of Technology

IBPSA CH

LABORATOIRE D'ENERGIE SOLAIRE
PHYSIQUE DU BÂTIMENT

ÉCOLE POLYTECHNIQUE
FÉDÉRALE DE LAUSANNE

CISBAT 2013

PROCEEDINGS VOL. II

CLEANTECH FOR SMART CITIES & BUILDINGS
From Nano to Urban Scale

4-6 September 2013
EPFL, Lausanne, Switzerland

CISBAT

Schweizerische Eidgenossenschaft
Confédération suisse
Confederazione Svizzera
Confederaziun svizra

Swiss Federal Office of Energy SFOE

IBPSA-CH

Cambridge University

Massachusetts Institute of Technology

CISBAT 2013

International Conference
4-6 September 2013, EPFL, Lausanne, Switzerland

CLEANTECH FOR SMART CITIES & BUILDINGS –
FROM NANO TO URBAN SCALE

ISBN Electronic version: 978-2-8399-1280-8
ISBN Print-version: Vol.I 978-2-8399-1281-5 Vol.II 978-2-8399-1282-2

Conference Host / Editor
Solar Energy and Building Physics Laboratory (LESO-PB)
Ecole Polytechnique Fédérale de Lausanne (EPFL)
Station 18, CH - 1015 Lausanne / Switzerland
leso@epfl.ch
http://leso.epfl.ch
Conference Chair: Prof. J.-L. Scartezzini
Conference Manager: Barbara Smith

Scientific partners
Cambridge University, United Kingdom
Massachusetts Institute of Technology, USA
Swiss Chapter of International Building Performance Simulation Association, Switzerland

Scientific committee
Chairman:
Prof. J.-L. Scartezzini, EPFL, Switzerland

Members:
Prof. Leon Glicksmann, MIT, USA
Prof. Anne Grete Hestnes, NTNU, Norway
Prof. Hans Martin Henning, FhG-ISE, Germany
Dr. Nicolas Morel, EPFL, Switzerland
Rolf Moser, Enerconom SA / SFOE, Switzerland
Dr Jérôme Kaempf, EPFL, Switzerland
Dr Maria Cristina Munari Probst, EPFL, Switzerland
Prof. Brian Norton, DIT, Ireland
Prof. Christoph Reinhart, MIT, USA
Christian Roecker, EPFL, Switzerland
Prof. Claude-Alain Roulet, EPFL, Switzerland
Dr Andreas Schueler, EPFL, Switzerland
Prof. Koen Steemers, Cambridge University, United Kingdom
Prof. Jacques Teller, Univ. of Liège, Belgium
Prof. Thanos Tzempelikos, Purdue Univ., USA

Members IBPSA Switzerland:
Prof. Achim Geissler, FHNW, Switzerland
Prof. Thomas Afjei, FHNW, Switzerland
Dr Stefan Barp, AFC Zurich, Switzerland
Dr Christian Struck, HSLU, Switzerland

Under the patronage of
Swiss Federal Office of Energy (SFOE)
Ecole Polytechnique Fédérale de Lausanne (EPFL)

Generously supported by
Zeno Karl Schindler Foundation

Private sponsor
SwissINSO Holding Inc.

PREFACE

"Clean Technology for Smart Cities and Buildings" was the topic of the international scientific conference CISBAT 2013, which took place in the Swiss lakeside city of Lausanne from 4 to 6 September 2013.

Designed as a platform for interdisciplinary dialog and presentations of innovative research and development in the field of sustainability in the built environment, the conference covered a wide range of subjects from solar nanotechnologies to the simulation of buildings and urban districts.

CISBAT 2013 was the 12th edition of CISBAT, whose vocation is to present new perspectives offered by renewable energies in the built environment as well as the latest results of research and development in sustainable building technology, in a setting that encourages interdisciplinary dialogue and networking at the international level. The conference assembled 270 building scientists and architects from all over the world in an effort to promote clean technologies for sustainable buildings and cities. Close to 200 scientific papers were presented during three intense days of conference.

CISBAT 2013 was organized in scientific partnership with the Massachusetts Institute of Technology (MIT) and Cambridge University. Furthermore, the organizing committee was proud to be able to count on an international team of confirmed scientists to ensure the scientific quality presented papers. This year the conference also teamed up for the second time with the Swiss Chapter of the International Building Performance Simulation Association (IBPSA-CH), to strengthen the subject of “Building and Urban Simulation”, one of the conference's leading topics.

Organised under the auspices of the Swiss federal Office of Energy (SFOE) and generously supported by the Zeno Karl Schindler Foundation, CISBAT 2013 connected researchers and projects and gave an exciting insight into research and development in the field of sustainable buildings and cities. We look forward to seeing you at the next edition.

Prof. Dr Jean-Louis Scartezzini
Conference Chairman
Solar Energy and Building Physics Laboratory
Swiss Federal Institute of Technology Lausanne

CONTENTS VOL. I

Author index see back of book

Keynotes

Nanostructured Materials for Renewable Energies

Sustainable Building Envelopes

Solar Active and Passive Cooling

Daylighting and Electric Lighting

Indoor Environment Quality and Health

Advanced Building Control Systems

Urban Ecology and Metabolism

CONTENTS VOL. II

Integration of Renewables in the Built Environment

Building and Urban Simulation

Information Technologies and Software

Integration of Renewables in the Built Environment

ARCHITECTURAL INTEGRATION OF TRANSPIRED SOLAR THERMAL FOR SPACE HEATING IN DOMESTIC AND NON-DOMESTIC BUILDING ENVELOPES

Hasan Alfarra; Vicki Stevenson; Phil Jones

Welsh School of Architecture, Cardiff University, Bute Building, King Edward VII Avenue, Cardiff, CF10 3NB, UK, email: alfarrah@cf.ac.uk

ABSTRACT

In response to climate change, energy poverty, and increasing prices of fossil fuel energy; building integrated renewable energy should find a quick and strong stream in design and construction fields. Solar thermal appears as a promising technology for domestic and non-domestic building envelopes, particularly for space heating which counts for 61% the total domestic energy consumption in countries with long cold seasons like UK. The integration of transpired solar collectors (TSC) technology however suffers lack of adoption in building envelopes despite its apparent technical competitiveness for using solar pre-heated external air for space heating since patented in the late-1980s. Architectural integration seems to play a major role in developing and encouraging the use of TSC in buildings. This paper therefore investigates the innovative possibilities of improving the architectural integration of TSC into building envelopes at both multi-functional and aesthetic levels.

An international web-based survey was distributed to architects, engineers, and other academic and professionals in design and construction fields with intensive focus on countries with long heating seasons and potential integrations of TSC such as Canada, USA, and UK and mainland Europe. The responses of 1,295 participants, the largest pool ever for previous comparative studies in this field, were analysed quantitatively and qualitatively. Unlike previous studies the outcomes were statistically examined using Pearson's Chi-square and Spearman's correlation Coefficient tests. Although respondents only had a moderate awareness of the TSC technology they were very interested in integrating solar energy into the built environment. Seven selective integration images of TSC and photovoltaic (PV), from existing projects in Canada, USA and Europe were rated by respondents in terms of multi-functional and aesthetic roles of integration. The barriers and limitations along with preferable integration schemes were investigated and discussed. Integration parameters such as function, type, and position of TSC which were found to be the most favoured by the participants were identified. The survey results provide valuable contributing information of architecturally integrating transpired solar thermal in the built environment. This contribution is necessary for researchers and professionals in design and construction fields.

Keywords: architectural integration, transpired solar, architect(s),

INTRODUCTION

The built environment is generally powered by conventional energy sources which contribute CO2 emissions and have an impact on climate change as well as consuming more than 40% of the total annual energy consumption worldwide [1]. Increasing energy demand and continuing fossil fuel dependency threatens global power sectors; as an example, the United Kingdom (UK) became a net energy importer in 2004 [2]. This leads to increasing energy prices and levels of energy poverty. It is necessary for further prosperity to ensure secure, equitable, affordable and sustainable supply of energy. Methods of meeting this demand through energy efficiency and renewable energy should be explored. Some renewable energy

options have drawbacks such as occupying fertile land and being positioned where there are significant energy losses through distribution. Therefore, building-integrated renewable energy should find a quick and strong stream in design and construction fields.

Space heating in UK counts for 61% of the total domestic energy consumption [3]. Therefore, almost two-third of the energy savings in dwellings seems achievable through space heating. Furthermore, the operation control of many heating systems (boilers and heat emitters) in use in the UK is found to be inefficient [4, 5]. Novel efficient systems therefore are in a real demand for UK market as well as other countries with long heating seasons. These efficient systems are more likely to prosper if they appeal to architectural aesthetics, sustainability measures, and social parameters such as thermal comfort and energy saving.

Integrating solar thermal systems in building envelopes differs according to the solar collector type, design, function and the economic feasibility. According to Zhai, Wang [6], the integration of solar thermal technologies with green buildings, for supplying space heating, is recently under rapid development. Transpired Solar Collectors (TSC) technology pre-heats the ambient outdoor air which is drawn into the building for space-heating. The TSC technology was patented in Canada in the late-1980s with the first application in 1990 [7-10]. The TSC consist of perforated solar absorbing sheet, ducting and fan. The perforated pane is placed approximately fifteen centimetres to building's external wall creating a plenum of air, and it is usually a dark colour to maximize the solar absorption. The fan is fixed in a cut-out through the building's exterior wall and connected to the duct work connection or HVAC (Heat, Ventilation, and Air-Conditioning) system. The fan draws fresh air into the plenum through the perforations in the outer pane by creating negative pressure [7, 8, 11]. The TSC proved in their early development to be a competitive technology with instantaneous thermal efficiencies that exceeded 70% and low capital costs. Those two factors constitute the basic potential of simple economic payback of almost two years for large installations [8, 12, 13]. The orientation of TSC is ideally south-facing although, orientation between east and west remain possible at lower solar gain [14]. The TSC can be integrated into the building envelope through wall or roof mounting; it can also be stand-alone. The TSC can be combined with photovoltaic panels as a hybrid system to produce space heating and electricity.

Although, TSC has proved competent for air preheating and performance, it is rarely integrated with building envelopes. Almost all the current applications are for non-domestic buildings [8] with little information about installations in the domestic sector. Furthermore, most of the existing solar thermal integrations in buildings have fairly poor architectural quality which discourages further take-up [15]. The quality of architectural integrated solar thermal is defined as the controlled and coherent interaction of solar thermal collectors in the building envelope. This interaction should simultaneously satisfy the multi-functional and aesthetic aspects of architectural form and space [15, 16]. The paper aims to investigate the socio-technical and socio-cultural parameters important to the legitimisation lobby (architects, researchers, authorities, building owner…etc.). It focuses on the optimum features of integrating TSC in domestic and non-domestic building envelopes to improve the architectural integration quality at both multi-functional and aesthetic levels.

METHOD

In order to analyse the perception of the legitimatisation lobby about integrating TSC, an international web-based survey was designed to investigate parameters like awareness, limitations, and recommendations of the technology and integration. Following a pilot study with selected experts in the field, the questionnaire was distributed to architects, engineers, and other academics and professionals in design and construction fields. The geographical

focus was on countries with long heating seasons and potential integrations of TSC such as Canada, USA, and UK and mainland Europe. The responses of 1,295 participants were analysed quantitatively and qualitatively.

The quantitative data were investigated statistically to examine the significance of the results unlike similar previous studies in this field; a drawback which was acknowledged by Horvat, Dubois [17]. The survey data are non-parametric; therefore; there were two suitable statistical tests to address the data: 1. "Pearson's Chi-square test" which explores the significance of relationship and association between two categorical variables, and 2."Spearman's correlation coefficient" which determines the correlational strength and direction between variables [18, and 19]. The software used to carry these investigations is IBM SPSS 20 "Statistical Product and Service Solutions".

RESULTS

The respondents were 62.1% architects, 22.9% engineers, and 15% other professions distributed at different working fields and with various years of experience. The respondents were distributed on 73 countries; with 73% of them concentrated in USA, UK, and Canada.

Awareness: A key area to explore was the respondent's awareness of TSC (categorised as: expert, aware and unaware). Commercial brands of TSC were listed to ease recognition. It became apparent that 48.6% of the surveyed professionals were unaware of the technology. A further 49.7% were aware of the technology with 1.7% considering themselves to be expert. There was a significant association, according to Chi-Square statistical test, between awareness and respondents geographic region. The Canadian participants had the highest rate of awareness (71.0%) followed by 53.3% for Europe mainland excluding UK. The American respondents recorded 41.4% awareness.

Decision: The participants were asked to identify the stakeholder with most power to decide to use TSC in domestic buildings. Almost 74.2% of the participants identified the client, while 50% identified the architect. There is a statistically significant association of those architect respondents who selected client and architect as well as geographic regions association. For non-domestic buildings, 58.7% identified the client as having the most decision power, followed by the integrated design process "IDP" team (49.9%), then the architect (42.5%). Furthermore, 63.8% if the participants agreed that the architect had the lead in deciding the type of integration in building envelopes (i.e. wall-mounted…etc.) for both domestic and non-domestic buildings.

Integration Examples: Seven selective integration images of TSC and PV, from existing projects in Canada, USA and Europe were rated by respondents in terms of multi-functional and aesthetic roles of integration. All of those examples were from non-domestic buildings due to the lack of availability of domestic images. Integration was considered in terms of multi-functionality and in terms of aesthetics. The façade integration generally rated above roof integration in terms of multi-functions. In terms of aesthetics, rating of façade integration was further extremely in higher acceptance than roof integration. Figure 1 for instance represents the integration image which was ranked the highest for both multi-function and aesthetics. This project is for a governmental building in USA which included a façade integration of TSC along with dummy cladding in order to conceal the areas which did not have TSC panels. The building was rated on a Likert scale from -2 to +2, by 1,051 participants for multi-function and 1,058 for aesthetics. Where -2 represented a very poor integration and +2 represented a perfect integration. By investigating the relationship between multi-function and aesthetics using Spearman's Correlation, there was a strong direct relation

between multi-function and aesthetics for architects versus medium correlation for the other professions.

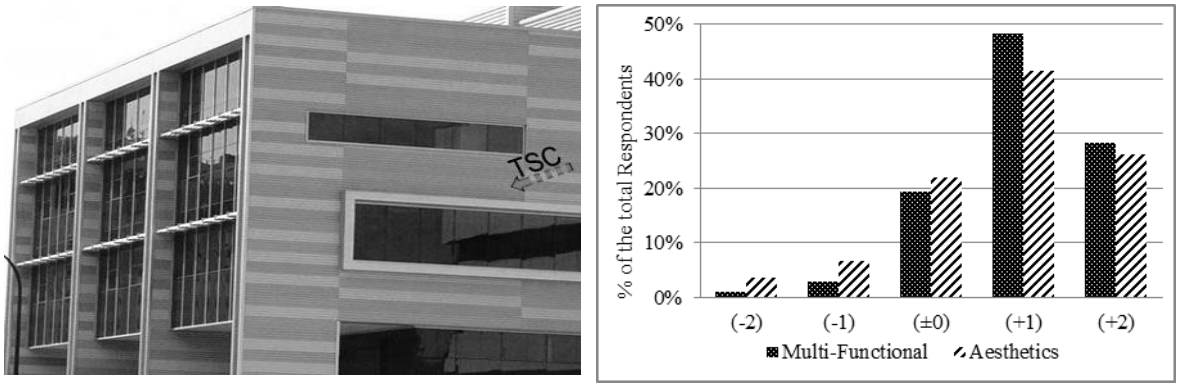

Figure 1: (a) Ann Arbor Municipal Building, USA. InSpire wall [20]. (b) Likert scale rating by total respondents for Multi-function and Aesthetics

Multi-function Integration: When questioned the priority of integrating TSC in building envelopes, the majority of votes (71.6%) were given to the multi-functional role of the technology to act as an architectural element in the building envelope as well as functions as an energy source, rather than as an isolated energy generating device or aesthetic feature. There was a significant association between professions and the selection of multi-function as the architects were found committed to prioritize the multi-functional role more than others. There was no association in selection with location, work field or experience.

Integration Scheme: For domestic buildings, all professions preferred roof installations for TSC and then hybrid PV/TSC installations. For non-domestic buildings, there was more acceptance of TSC façade installations, but roof installations were still the most preferred for PV/TSC hybrids (Fig. 2). There was no significant association within professions, location groups, or experience which means that all respondents were in agreement with the selections.

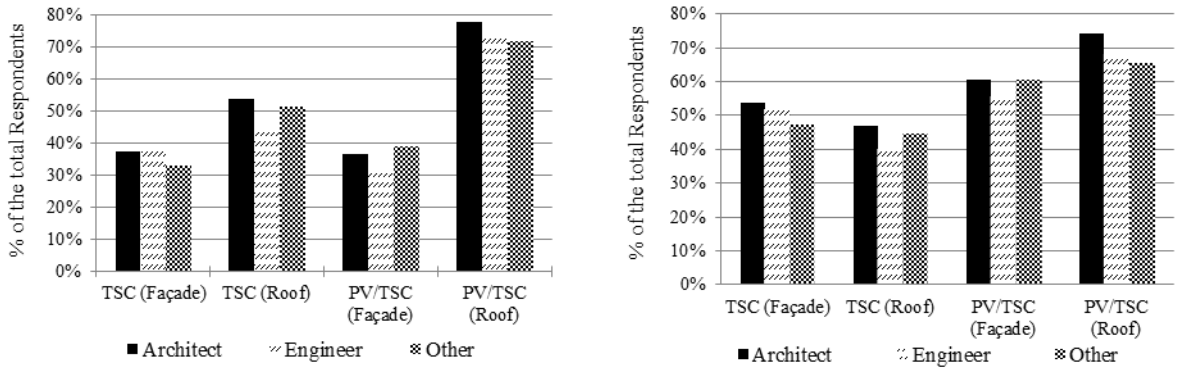

a) Domestic building envelope *b) Non-domestic building envelope*

Figure 2: Recommended constructive integration schemes of TSC for Domestic and Non-domestic building envelopes

DISCUSSION

Although the majority of responses are from architects approximately one third of the response is from engineers and others which reduces the architectural bias in comparison to some previous surveys like Farkas and Horvat [21] and Horvat, Dubois [17], while being a similar mix to Probst and Roecker [15].

The high awareness of Canadian participants was to some extent expected as the TSC technology was patented in Canada. Canada furthermore is the home country of the chief four TSC providers. The low rate of awareness in USA was quite surprising nevertheless, it could be attributable to the fact that space heating is in lower need in the southern part of USA. This notice was in some way reflected in respondents' comments from States in the southern part of USA such as Arizona, New Mexico, and South Carolina. The participants from those hot-dry and hot-humid States [22] were almost quarter of the total USA respondents with overall awareness of about 30%.

Of the respondents who see the client as the most important stakeholder in decision making, the majority were architects who are likely to have a good picture of the client's role as the architect is usually the principle dealer with clients. On the other hand, there might be some bias in selecting architect as a decision maker by architect respondents. However, the effect size is statistically small and furthermore, the other respondents achieve balance level which leads to gain reliability confidence in the results.

The most highly rated aesthetic integration example (illustrated in Fig 1) is likely to be highly rated due to the unity and coherence of integration within the building envelope, and the use of dummy panels. On the contrary, very few participants (8.2%) supported the use of dummy panels when they were directly asked their opinion on using dummy panels to achieve unity of building façades. This truly reflects that good integration is acceptable despite possible conflict with existing opinions or beliefs at some extents.

Similarly, the roof integration scheme of TSC/PV was most favoured for both domestic and non-domestic building envelopes (illustrated in Fig 2) in spite the fact that the example of TSC/PV roof integration was rated the lowest out of the examples. Furthermore, this could be explained by the concept of integration being favoured but the example question was not a good presentation of the concept. The visualisation of the concept might moreover supress the theoretical belief. This leads to adopting a concept in theory but neglecting it on the visualisation stage. Another possible interpretation is that the roof integration could be preferred because it can be easily hidden especially when roofs are mostly not used spaces therefore, there will be no complication for the façade design. Façade integration however is found more acceptable for non-domestic buildings than domestic where roof integration is more preferred.

CONCLUSION

An international survey with a significant response of 1,295 built environment professionals was statistically analysed.

The legitimatisation lobby relating to the built environment (architects, engineers, academics, authority…etc.) in countries including Canada, USA, and Europe mainland were surveyed to investigate their perceptions and recommendations about transpired solar thermal for space heating. The participants were equally divided in term of previous awareness of TSC despite its availability since the late-1980s and laboratory proven competence. Even fewer respondents had knowledge of the working principles of the TSC technology.

The clients of the buildings were found to be the most important stakeholder for decision making in choosing to use TSC. The architects almost agreed certain guidelines of integrating solar thermal in building envelopes for both domestic and non-domestic building envelopes; these guidelines included: types; positions; and function. For domestic buildings, the position of integration outweighed the function. There was a strong preference for TSC to be integrated on the roof rather than the façade. A stronger preference was for the type of hybrid PV/TSCs to be installed on the roof (Fig. 2a). For non-domestic buildings, the preference was

different as the type and function of integration was given the priority. There was a stronger preference for hybrid PV/TSCs rather than only TSC to be installed either on the roof or façade; however, there was more support for TSC façade integration (Fig. 2b) than domestic buildings.

ACKNOWLEDGEMENTS

The authors would like to thank the respondents to the survey and the pilot study for their participation, time, efforts, and information. The authors also would not forget to express acknowledgement to anyone who helped in guiding this research to success.

REFERENCES

1. Shi, L. and M.Y.L. Chew, A review on sustainable design of renewable energy systems. Renewable and Sustainable Energy Reviews, 2012. 16(1): p. 192-207.
2. DECC, UK Energy Sector Indicators 2011, 2011, Department of Energy and Climate Change Business Plan Quarterly Data Summary.
3. DECC. Energy consumption in the United Kingdom 2011 [cited 2012 28 February]; Available from: http://www.decc.gov.uk/en/content/cms/statistics/publications/ecuk/ecuk.aspx.
4. Liao, Z., M. Swainson, and A.L. Dexter, On the control of heating systems in the UK. Building and Environment, 2005. 40(3): p. 343-351.
5. BRECSU, Energy consumption guide 81: Benchmarking tool for industrial building—heating and internal lighting, 2002, Building Research Energy Conservation Support Unit.
6. Zhai, X.Q., et al., Experience on integration of solar thermal technologies with green buildings Renewable Energy, 2008. 33(0): p. 1904-1910.
7. McLaren, B., S.A. Parker, and C. Christensen, Transpired Collectors (Solar Preheaters for Outdoor Ventilation Air), in Federal Energy Management Program, Federal Technology Alert, B. McLaren, S.A. Parker, and C. Christensen, Editors. 1998, US. Department of Energy.
8. Hall, R., et al., Transpired solar collectors for ventilation air heating. Proceedings of the ICE - Energy, 2011. 164(3): p. 101-110.
9. Hollick, J.C., Solar cogeneration panels. Renewable Energy, 1998. 15(1–4): p. 195-200.
10. Kutscher, C.F. Transpired solar collector systems: a major advance in solar heating. in Proceedings of the 19th World Energy Engineering Congress. 1996. Atlanta, GA.
11. Brown, D.S., An Evaluation of solar air heating at United states air force instalations, in Department of Systems and Engineering Management2009, Air Force Institute of Technology, Air University.
12. Brunger, A.P., C.F. Kutscher, and J. Kokko, Low Cost, High Performance Solar Air-heating Systems Using Perforated Absorbers, 1999, International Energy Agency: Paris.
13. Brewster, A., Using the sun's energy. Building Engineer, 2010. 85(6).
14. CA-Group. SolarWall®: Transpired Solar Collector (TSC). n.d [cited 2012 15 January]; Available from: http://www.cagroupltd.co.uk/pages/cabp/products/cabp_solarwall.php.
15. Probst, M.C.M. and C. Roecker, Architectural Integration and Design of Solar Thermal Systems. 2011, Italy: Taylor & Francis Group Ltd.
16. Krippner, R. and T. Herzog. Architectural Aspects of Solar Tecniques: Studies on the Integration of Solar Energy Systems into the Building Skin. in Eurosun 2000, 3rd ISES-Europe Solar Congress. 2000. Copenhagen, Denmark.
17. Horvat, M., et al., International survey about digital tools used by architects for solar design, in Task 41 - Solar Energy and Architecture. Subtask B - Methods and Tools for Solar Design2011, International Energy Agency Solar Heating and Cooling Programme.
18. Pallant, J., SPSS survival manual. 4th ed. 2010, New York: Allen & Unwin Book Publishers, australia.
19. Field, A., Discovering statistics using SPSS. 3rd ed. 2009, California: Sage Publication Lts.
20. Atas, Ann Arbor Municipal Building, 2010, ATAS International, Inc.
21. Farkas, K. and M. Horvat, Building Integration of Solar Thermal and Photovoltaics – Barriers, Needs and Strategies, in IEA SHC Task 41: Solar Energy and Architecture. Subtask A: Criteria for Architectural Integration2012, International Energy Agency Solar Heating and Cooling Programme.
22. Ramirez, D. Natural Remodeling with Kelly Lerner: Considering Your Home's Climate. 2008 [cited 2013 12-Apr]; Available from: http://ecohomeresource.com/2008/08/natural-remodeling-10-weeks-wi.html.

LUMINESCENT, TRANSPARENT AND COLORED, PV SYSTEMS IN ARCHITECTURE: POTENTIAL DIFFUSION AND INTEGRATION IN THE BUILT ENVIRONMENT

G. Scudo[1], A. Rogora[1], B. Ferrari[1], Daniele Testa[2]

[1]*Politecnico of Milano, Dept. ASTU, via Bonardi 3, 20133 Milano, +39 0223995175, alessandro.rogora@polimi.it*

[2]*Process Technologies Unit (TECNOP), Research Center for Non-Conventional Energies - Istituto ENI Donegani, Via Giacomo Fauser, 4 - 28100 Novara, +39 0321447801, daniele.testa@eni.com*

ABSTRACT

The Luminescent Solar Concentrators (LSC) are transparent plates (plastic or glass) which contain dispersed fluorescent dyes that absorb a part of the solar light and emit it into the inside of the plate. By means of the total internal reflection, the emitted radiation is led towards the thin edges of the plate where it is concentrated on small surfaced conventional solar cells, which converts it into electrical energy.

The LSC seems a promising technology with large diffusion potentialities in architecture thanks to the transparency combined with energy production. In fact LSC technology could be positively integrated in transparent envelope components and systems (i.e. shading devices, bow windows, fanlights, arcades, agricultural greenhouses, glazed courtyards). The colour of the LSC can be considered a problem but also a potential element to introduce colours pattern in the built environment and to modify the colour temperature in the interiors especially in office buildings where the dominant white finishing and artificial light with cold temperature require a warmer contribution.

The research carried out by the Milan's Polytechnic for ENI S.p.A. has the objective to study the development of building components based on LSC technology. The research focuses on the possible diffusion and integration of LSC technology in the built environment, analyzing mainly two aspects: the production of electrical energy and the interior lighting. The parameters to be considered are energy transmitted (transparency) and PV production. The use of LSC allows the exterior view of the used spaces and the modification of the lighting tone inside the building. The possibility of combining different colors and of coupling translucent materials to the LSC allows also to obtain effects of polychromy and/or diffused light. The possibility to interact with sensorial and design variables both of the interior spaces and of the exterior volumes are consequently significantly high.

The first experimental application of LSC technology at real scale is a bicycles shelter in Rome. The architectural and structural project has been designed in order to assess the LSC components performance in three different orientations (tilted east and west facing and a vertical west facing) and in combination with a shading system which improves the PV production.

Keywords: Luminescent Solar Concentrator, coloured light, PV system, Building envelopes

INTRODUCTION

The Luminescent Solar Concentrators (LSC) are transparent plates (plastic or glass) which contain dispersed fluorescent dyes that absorb a part of the solar light and emit it into the inside of the plate. By means of the total internal reflection, the emitted radiation is led towards the thin edges of the plate where it is concentrated on small surfaced conventional solar cells, which convert it into electrical energy.

This technology enables designers with a new tool to generate electricity while providing natural light inside the building thanks to its transparency. The LSC technology offers significant potential advantages over conventional silicon panels and solar concentrators based on mirrors or lenses. The plates can in fact collect both the direct and diffuse solar radiation, being efficient even under cloudy skies, and their installation is not subject to orientation problems. LSC plates are also made of cheap materials and significantly reduce the silicon surface needed to generate the same energy power. Even if the performance of LSC technology is not comparable to that of traditional photovoltaic (PV), its complete transparency allows to make all glass surfaces energy producers. In particular this aspect is related to the desire of lightness and visual permeability of contemporary architecture. In addition, the presence of colour allows to characterize the building envelope with a wide number of formal, sensorial and communicative variables.

The research carried out by Milan's Polytechnic for ENI S.p.A., has the objective to study the development of building components based on LSC technology. The research focuses on the possible diffusion and integration of LSC technology in the built environment, analyzing mainly two aspects: the production of electrical energy and the interior lighting conditions.

METHOD

LSC panels can be used in a lot of different ways both in new buildings and in retrofit. On a morphological level the application of these components depends on their shape and their position relative to the building. The terms, purely evocative, that have been identified to indicate the different "scenarios of use" are: "between" (connection spaces between buildings, vertical connections, stairs and elevators, atria, light chimneys); "front" (curtain wall, fixed or opening windows, bow-window, double skin envelope, vertical or horizontal shading devices); "top" (volumes added as coverage as skylights, sheds, top of light chimneys, and technological spaces); "outdoor" (where instead LSC are used to build a very numerous series of installations in open spaces such as urban equipment in parks and streets, temporary buildings, bridges, road barriers, parking areas, urban shelters, greenhouses and volumes for heat collection).

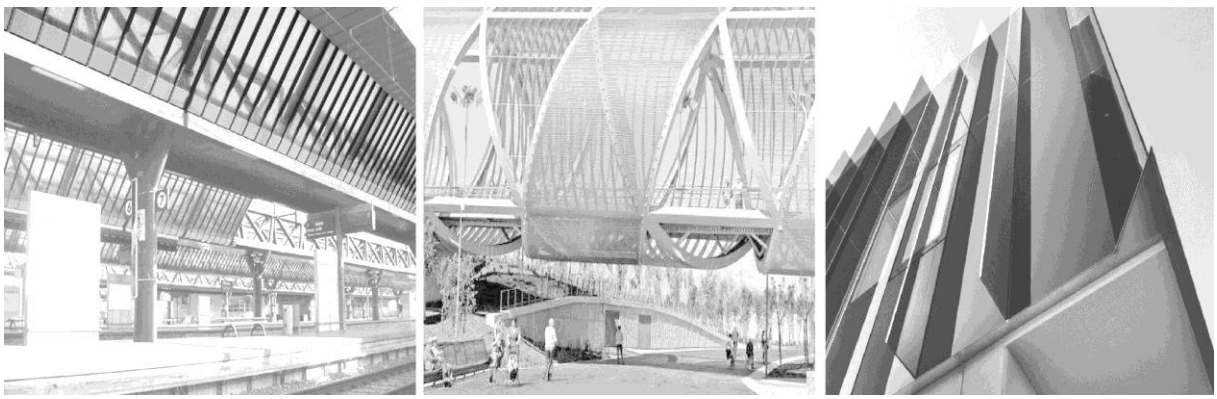

Figure 1: Examples of application of LSC in infrastructures, in open spaces and as shields on building facades (i.e. from left to right: A. Mangiarotti, D. Perrault, Buratti+Battiston).

The application possibilities of LSC become even more interesting if measured at the sensorial level considering also the possible combinations with other materials: it is possible to emphasize the plate transparency or couple it with translucent materials (such as the satin glass) to obtain a component that reduces visual permeability but lets the light pass through and therefore it is able to emphasize the value and charm of diffuse light.

Different chromatic effects can be obtained: monochromatic ones using only panel of the same colour alternating with clear glass, or polychromatic ones combining the available colours of LSC (i.e. yellow, orange, red). Moreover modulating the size and the number of LSC panels and combining them with other materials (i.e. metal, glass, wood), different aesthetic effects can be achieved.

The experimental application

The first application at real scale of Eni technology was a shelter for electric bicycles in Rome. This project allowed to verify the strengths and the limitations of LSC panels from the energy production viewpoint (the shelter is currently still under monitoring) and from the construction process integration viewpoint (planning, design and implementation). The shelter is the ideal tool to simultaneously test the panel in different positions and environmental conditions since the PV modules can be positioned with different orientations. Three orientations have been selected: facing east, facing west and vertical. The bike shelter was also equipped with a shading system made of reflective slabs and milled plates placed at proper distance from the LSC plates to verify the PV production due to the materials able to increase the amount of indirect radiation on the LSC plates. The concept chosen for the project, called "energy module", defines the shelter as a set of modular free-standing elements that can be placed in different configurations in urban contexts. The module is made of a frame that can be composed with solid elements, vertical/horizontal slats, etc.. The same applies to the horizontal plane of coloured polymethylmethacrylate (PMMA) that can be left transparent or can be shielded with metal sheets, strips, plates of satin or reflective materials to increase the light component (diffuse of reflected).

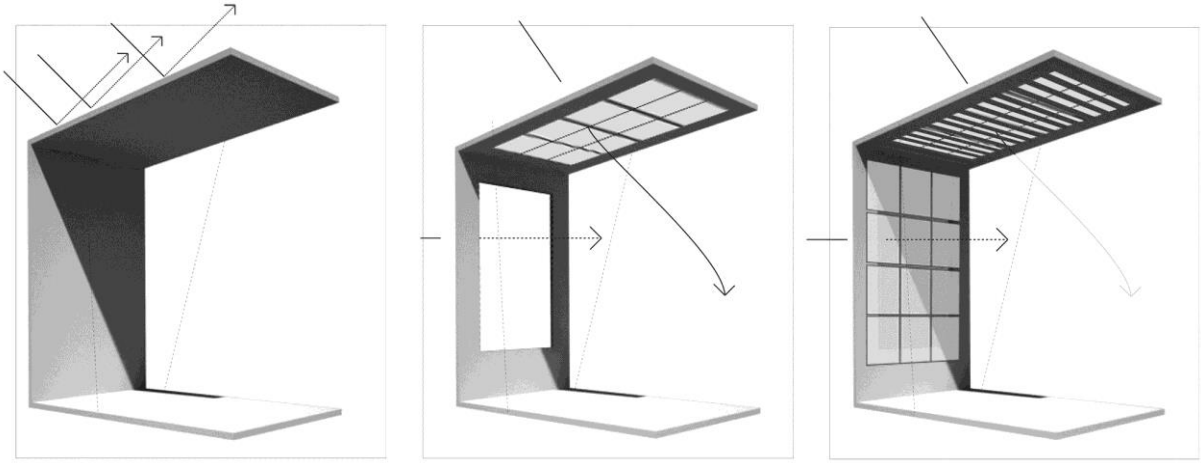

Figure 2: The three possible types of energy modules (from left to right): "full module" (with a reflective panel), "empty module" (the coloured light pass through) and "shielded module" (with slats that filter light).

The modules can be combined, with more or less spacing between them, with different logics depending on the context in which they are placed. To build the experimental shelter the modules were designed to include six LSC panels into a single component of 100x150 cm.

The selected steel frame ensures mechanical strength, water resistance, modularity and the possibility to easily interface with the elevation structure of the shelter.

Figure 3: Pictures of the Rome LSC bike shelter on its opening day (November 27th, 2012).

The frame module was developed by Milan's Polytechnic in collaboration with Secco Sistemi S.p.A using only their standard products to minimize the process due to time constraints. The steel frame makes the module self-supporting and able to withstand the final assembly loads. The photovoltaic modules are made of 6 LSC panels each obtained with PMMA plates with dimensions of 50x50 cm assembled with properly dimensioned silicon solar cells connected in series/parallel. The panels are then connected in series to the stiffening structure made of painted steel, with dimensions of 108,4x161,8 cm. The panels are inserted into the frame and glued to ensure the resistance to atmospheric agents.

Figure 4: Panel drawing (left) and picture of a steel frame (right).

The selected steel profiles are glass retention systems bolted to steel box-shaped profiles for securing the LSC plates. A C-shaped aluminum frame is applied to the panel to protect the cells and bus. The profiles are equipped with butylic gaskets. Electric wires are placed outside the aluminum frame and inside the main metal profile. The LSC panels fixation inside this structure is achieved through box-shaped steel profiles screwed to the main profile that was welded to make the frame. Two cables, positive and negative, collecting the energy from the series of the 6 LSC panels inside, extend out of the steel frame.

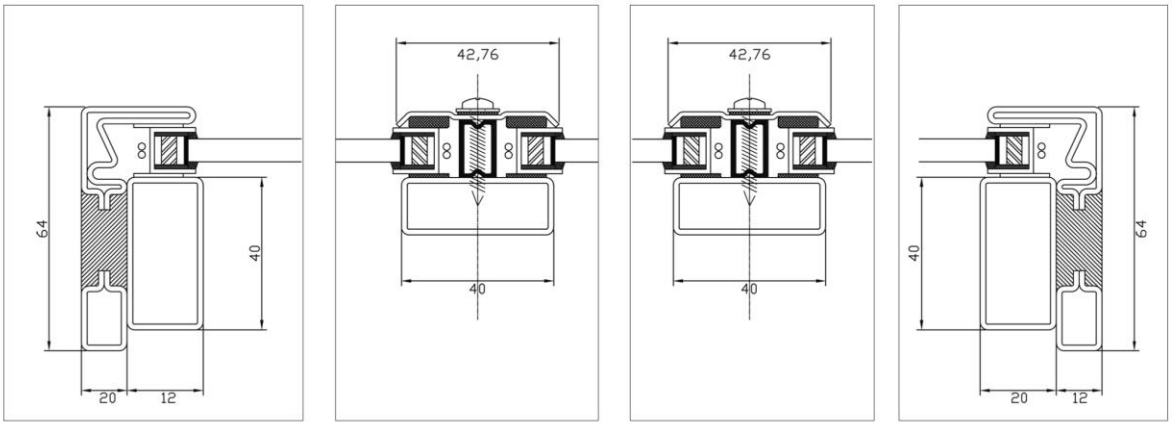

Figure 5: Design of the steel profile of the window. longitudinal section.

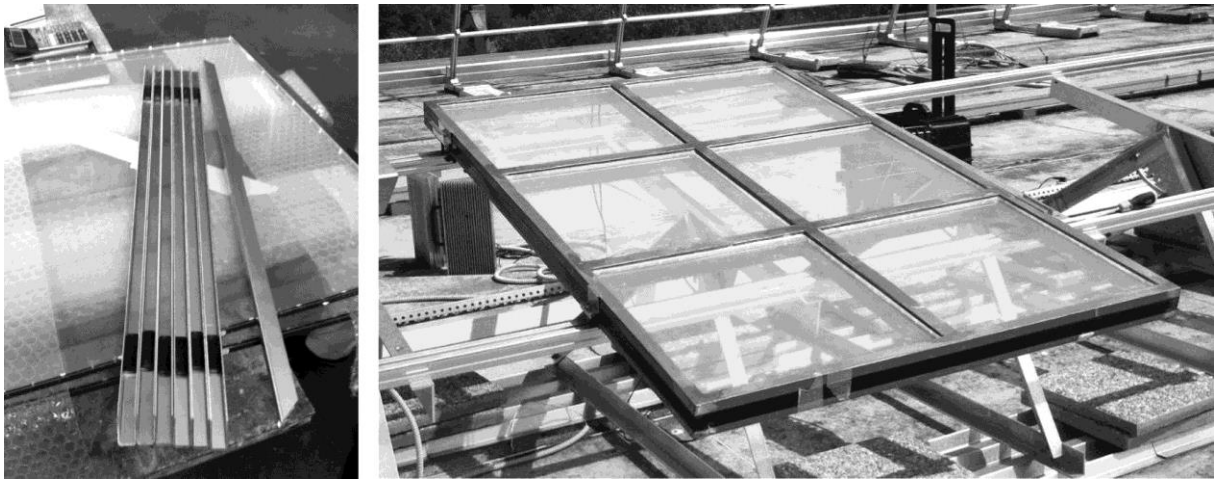

Figure 6: Metal edges for the LSC plates (left) and complete PV panel (right).

Electrical scheme

The plant in question is stand-alone, with island operation. All the electrical loads need to be fed with alternating current at 230V, therefore the facility is equipped with an inverter able to supply the 230V to the loads drawing the necessary energy from the batteries. In detail, the generator of this photovoltaic system, made of photovoltaic modules and their connections and mechanical supports, is composed of a total of 32 prototype modules with monocrystalline silicon cells, installed at 3 different orientations and inclinations, as shown in the following summary table.

Type	Inclination °	Azimut surface γ	N° modules	N° Strings
1	20°	-90°	12	6
2	20°	+90°	12	6
3	90°	0°	8	4

Table 1: Types and quantities of PV panels used for the shelter.

The different PV modules are connected in series of two modules each, thus forming a total of 16 strings. These strings are then grouped into three different sections, each of which is characterized by a uniform application type and is constituted by the electrical connection in

parallel of the strings that compose it. The entire system is then equipped with a monitoring system able of measuring the voltage and current produced by each string, in addition to the main environmental data.

System monitoring and remote control

The photovoltaic plant in question is equipped with an acquisition and monitoring system able to measure the following parameters: current strength of each string, the tension of each string, operating temperature of 3 photovoltaic modules, ambient temperature, radiation on the 3 different orientation planes under which the modules were mounted.

The criteria selected for the analysis are: comparison between the integrated production of the LSC modules and the one estimated for traditional PV panels, definition and selection of significant days and tracking of the power supplied under different irradiation conditions, keeping the data coming from different panels orientations separate (bicycles side, motorcycle side, vertical wall), distinction of the strings according to the presence or absence of a back reflective panel, analysis of the historical production of the best performing strings.

RESULTS

The shelter, which is still in the monitoring phase, showed that the LSC are far less sensitive to the orientation than traditional photovoltaic panels; LSC are therefore able to exploit the diffused light and to work even in low lighting conditions (cloudy sky, sun low on the horizon). The demo bike shelter plant will be used as an outdoor laboratory for testing the behavior of new devices. The Eni photovoltaic shelter can nominally produce about 500 watts of electricity generated by 192 yellow transparent photovoltaic slabs, each of which is made of a plastic material with a minimum amount of dyes patented by Eni.

From the point of view of the type of component for the realization of the PV module, the initial choice fell on a frame with steel profiles with standard press-bents. The selected frame therefore guaranteed the same durability and mechanical strength of a traditional window frame with also the possibility to be easily opened for slabs repositioning. The next step is focused on a new fiberglass component structure which guarantees lightness, higher thermal and electrical insulation and minimum interference with the LSC energy performance in terms of minimum shading effect on solar cells. Furthermore we are investigating the possibility of producing new components based on LSC technology.

REFERENCES

1. Millet, M. S.: Light Revealing Architecture. Van Nostrand Reinhold, New York, 1996.
2. IEA: Photovoltaics in Buildings. James & James: London, 1996.
3. Oleari, C.: Misurare il colore, Hoepli, Milano, 2008.
4. Wilson L. R.: Luminescent Solar Concentrators. A Study of Optical Properties, Re-absorption and Device Optimisation, B.Sc. Submitted for the degree of Doctor of Philosophy (Ph.D.), Heriot-Watt University, Edinburgh, 2010.
5. Abbondanza L., Caccianotti L., Fusco R., Scudo P. F.: Spectral converters and luminescent solar concentrators, SOLMAT5099, Solar Energy Materials and Solar Cells Online publication complete, 2010.
6. Debije M.G., Verbunt P.P.C.: Thirty Years of Luminescent Solar Concentrator Research. Solar Energy for the Built Environment, Advanced Energy Materials, Volume 2, 2012.

SURROUNDING PHOTOVOLTAIC FAÇADE SIHLWEID FIRST YIELD RESULTS AND ANALYSIS

Joss David; Münger Monika; Muntwyler Urs

Bern University of Applied Sciences (BUAS), Division of Engineering and Information Technology, Institute for Energy and Mobility Research, Laboratory for Photovoltaics, Jlcoweg 1, CH-3400 Burgdorf BE, Switzerland Phone: +41 (0)34 426 68 86, Fax: +41 (0)34 426 68 13, Email: info@pvtest.ch, Internet: www.pvtest.ch

ABSTRACT

As part of a core refurbishment of two 60 meter high tower blocks in Zurich Leimbach, all four façades of each building were covered with standard micromorphous thin film modules. As in January 2012 the renovating process of the first tower block was completed, its photovoltaic plant started energy generation and feed into the local electricity grid. The production data have been analyzed and evaluated for all four façade sides as well as for the overall system. Unconventional module circuitry considering partial shading, inverter configurations as well as energy yields and plant efficiencies had been calculated by students as part of their bachelor thesis at the Laboratory for Photovoltaics of Bern University of Applied Sciences BUAS. These calculations were used as a basis for planning and implementation of the refurbishment. Thanks to the yield data of the first year of operation, it is now possible to verify the calculations and evaluate the utility of the selected configurations. Of special interest is the photovoltaic plant unit on the building's north side and its working behavior. In total 288 panels have been mounted on the north façade and connected to 6 inverters. Finally, the evaluation of the first year's yield and operation data will deliver findings on technical aspects and the economy of this non common PV plant.

Keywords: BIPV, PV System, PV Façade, Yield, First Results

INTRODUCTION

Total renovation process - With the renovation of the Sihlweid-buildings from the 1970s, the first skyscrapers of Switzerland that meet the criteria of the 2000-watt society emerged. Special emphasis was put on optimal energy renewal by providing new windows and an overall improved insulation. The most striking intervention in the course of the 30-million refurbishment was the use of photovoltaic elements: The entire façade of the 2 towers was clothed with modular sheet metal elements, which each frame a thin-film solar module. The initial steps of the first builing's renovation took place in May 2011. The photovoltaic plant is fully operational since February 2012 and the total project is expected to be completed in late 2013. For all subsequent considerations only the building at Sihlweidstrasse 1 is taken into account.

System planning as part of a bachelor thesis - The building orbiting photovoltaic system was planned during a preliminary project study and a bachelor thesis. Besides the selection and analysis of the system components some tests and measurements were carried out to obtain first characteristics. In particular, special aptitude tests were carried out on the photovoltaic module. In the laboratories of BUAS-AHB wind load simulations were performed. Since the used module is in only certified in accordance with IEC 61646/10.16 (pull/pull stress $\leq$ 2400kN/m^2), these tests were necessary on the basis of compliance with wind load resistance for high-rise buildings according to SIA 261. After defined cycles with

2400kN/m^2 (wind), 5400kN/m^2 (snow) the burst behavior of the modules was finally analysed. The by 2 additional cross struts strengthened module showed permanent fault structures in the glass after an applied force of 13000kN/m^2. The shards did not peel up from the module and hence the suitability for the intended application was confirmed. The burning resistance of the EVA back sheet also was an issue. A fire-retarding sealing of the modules by mineral wool towards the stone façade was to be examined after a request of the fire security department of Zurich. Thus, temperature characteristics tests were carried out with a PTFE-coated glass cloth insulation (D = 20mm) within the modules frame and without insulation (3). Due to the massive module temperature growth (15-20 ° C vs. non-insulated) and the estimation of associated consequences, the idea with back insulation was dropped. The inverter type (Pdc=3.71kWp galv. isol.) was already specified by the executive electric installation company.

Type of Module	NA-128G5	**Voltage Voc/Vmpp**	59.8V/45.4V
Series	NA-121G5/NA-121A5/ NA-128G5	**Current Isc/Impp**	3.45A/2.82A
Technology	Tandem a-si/µc-si	**Efficency**	9%
Manufacturer	Sharp	**Bypass Diode**	1
Nominal Power	128 Wp	**Cross Struts**	2
Type	IG Plus 35(V)	**Grid Connection**	1~NPE 230V/50Hz
Series	IG Plus	**Power Factor**	0.85-1 ind./cap.
Technology	galvanically isolated with HF-Transformator	**DC-Voltage Min/Max/Mpp**	230V-600V/ 230V-500V
Manufacturer	Fronius	**Current Imax**	16.1Adc/15.2Aac
Nominal Power	3710Wpdc/3500Wpac	**Efficiency**	95.7%Max/95%EU

Table 1: Characteristics of photovoltaic module and inverter

Building Side	**Modules con./tot.**	**Strings/Modules per String**	**Amount of Inverters/Type**	**P_{DC}**	**E_{AC}**	**Specific Yield**
	pcs./pcs.	pcs./pcs.		kWp	kWh	kWh/kWp/a
North	281/385	17/7 & 18/9	2/IG Plus 100V & IG Plus 150V	35.968	7220	200.73
East	144/196	4/9	4/IG Plus 35V	18.432	9680	525.17
South	216/266	3/9	8/IG Plus 35V	27.648	15420	557.73
West	216/266	3/9	8/IG Plus 35V	27.648	9460	342.16
Total	**857/1113**			**109.696**	**41780**	

Table 2: PV plant configuration: Recommendation from the bachelor thesis

During the bachelor thesis 4 circuitry concepts were worked out for every façade. Different circuit concepts were considered in which identically oriented (horizontal / vertical) solar modules on the same side of the façade, modules in a local area with close vicinity, all or only some modules are connected in strings. At this point the link to the bachelor thesis' documentation (2) shall be made for more circuitry information. Below, only extracts of the Thesis and the final plant configuration are presented. Of all 4 possible sub-configurations per side, yield simulations were carried out using the program PVsyst 5.06 (Meteo data source: Meteonorm 2000/ref. stat. Zurich/synth. gen. stat. Sihlweid) including horizon and near shading effects to finally make precise and practical efficiency calculations.

Recommendation from the bachelor thesis - The findings from the module shading tests, yield simulations with different circuitry and detailed fine-resolution shading analysis plus economic considerations led to a recommendation by the students and the Laboratory for Photovoltaics to the builders. To minimize mismatch and MPP tracking losses, connection groups by 3 strings times 9 modules per inverter were suggested. The recommended configuration is listed in Table 2, as well as the field power and the simulated rounded final yield. A special connection configuration was proposed for the north façade. As known from the theory (1) and from measurements, the radiation on the north side will not exceed 300W/m^2 and thus with an expected theoretical inverter load of 30% of its nominal power, a field division of the 281 modules distributed to 2 inverters was suggested.

Effectively implemented interconnection concept - The system effectively implemented differs from the recommended system concept. On one hand 27 modules less than planned were integrated into the building envelope while on the other hand 25 additional panels were electrically connected. Finally, of 1086 mounted modules a total of 882 were wired functionally. The remaining 204 modules are located in nearby balconies or otherwise referred to high shading losses, so they were not connected. Table 3 shows a summary of the effectively implemented system concept.

Building Side	**Modules con./tot.**	**Strings/Modules per String**	**Amount of Inverters/Type**	**P_{DC}**	**E_{AC}**	**Specific Yield**
	pcs./pcs.	pcs./pcs.		kWp	kWh	kWh/kWp/a
North	288	3x(6/9) & 3x(6/7)	6/IG Plus 35	36.864	7190.8	195.1
East	162	2x(3/9) & 3x(4/9)	5/IG Plus 35	20.736	10195.5	491.7
South	216	6x(4/9)	6/IG Plus 35	27.648	17904.0	647.6
West	216	6x(4/9)	6/IG Plus 35	27.648	10800.0	390.6
Total	**882/1086**		**23/IG Plus 35**	**112.896**	46090.3	

Table 3: PV plant configuration: effectively realized system concept with energy yield

METHOD

Measurement setup and data acquisition - The center of the system is the Datalogger Web, which can record and store the operating data from so called ComCards connected via a bus system, the temperature sensors (module / environment) and the reference cell (m-Si). The data logger is web-enabled and can be controlled remotely with an appropriate network configuration. The data acquisition system has an overall accuracy of ± 5%, a temperature measurement accuracy of ± 0.8K, a irradiation measuring accuracy of ± 5% and the current/voltage measurement uncertainty is ± 5% (7) The ambient temperature sensor, as well as the reference cell and the module temperature sensor are mounted on the 6th floor at the center of the building with an azimuth of -5 °. The data sampling interval is 15 minutes. On 01.02.2012 for the first time, the whole photovoltaic system produced electricity and on 05.06.2012, the complete system including all sensors was ultimately installed. The detected and evaluated operational data interval extends from 01.02.2012 to 31.01.2013.

Geodata Reference - Since in the system, the irradiation and temperature data only in the generator plane "south" (azimuth: -5 °) are detected, another source has been consulted. As reference for the assessment, the weather station on Uetliberg with a distance of 3100m was used. The reference value taken from this source is the global radiation in the horizontal plane

(gre000z0) with 10 minute averages. The quality information of the data can be found in source (8). All other data used for the analysis are from the data logging system on site.

RESULTS

Energy yield - Figure 1 shows the simulated values plotted towards the real yield data as a bar chart. Superimposed there is a line graph to visualize the relationship between real operating data and the simulated yield expectations.

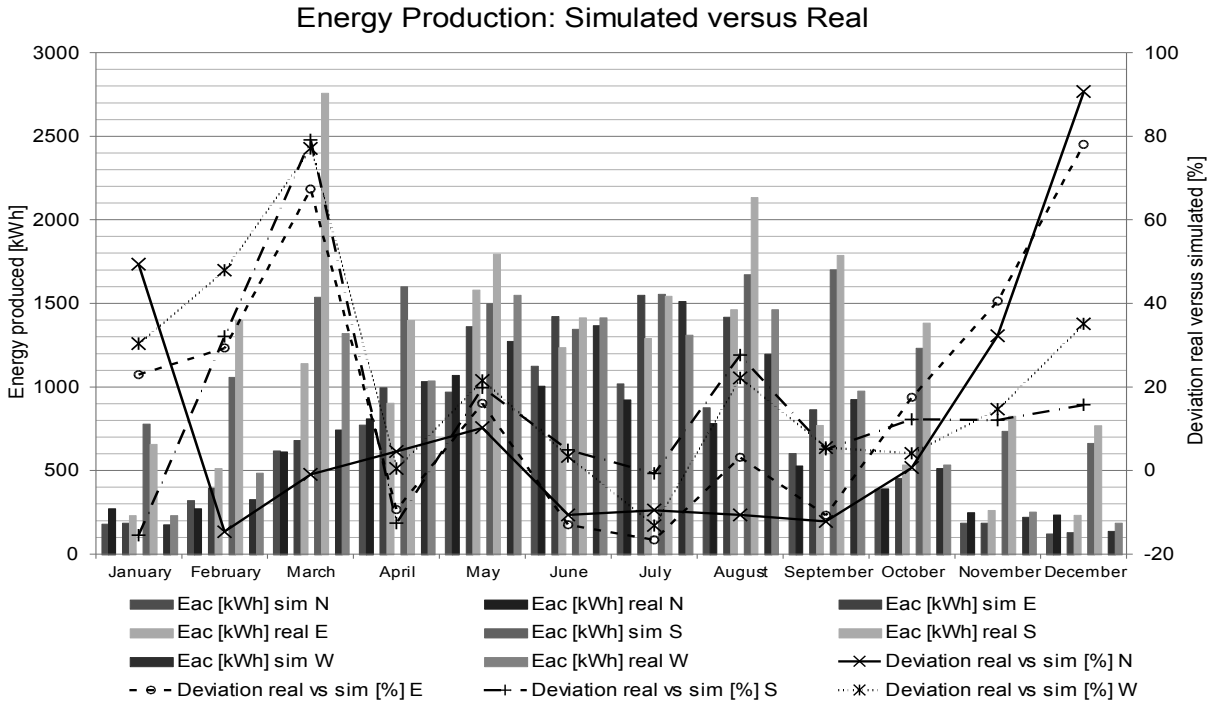

Figure 1: Simulated yield data versus real energy production with deviation (Real/Sim)

Economic yield – The analysis of economic operation data was not completed at the time of submission of this manuscript. Hence an illustration of the economics will not take place here. The results and their discussion will be reported in the oral presentation.

Summer Energy Share/Winter Energy Share - Table 4 lists the energy shares for the summer and winter months. Given are the simulated values and the real operating data.

	North		**East**		**South**		**West**	
	Sim	Real	Sim	Real	Sim	Real	Sim	Real
E_{AC} Summer [%]	74.6	71.5	78.8	71.3	60.9	56.4	77.4	71.9
E_{AC} Winter [%]	25.4	28.5	21.2	28.7	39.1	43.6	22.6	28.1

Table 4: Summer energy share/Winter energy share

Daily course of production curves for each building side – Figure 2 shows the course of production of the whole photovoltaic system with the superimposed courses of the northern, eastern, southern and western plant. The figure shows the ambient and module temperature profile as well as the global radiation in the horizontal plane, too. The abrupt decrease of radiation by about 18:00 is derived from the horizon shading from the "Uetliberg". The figure was edited for Monday, 20.08.2012, a warm and cloudless day.

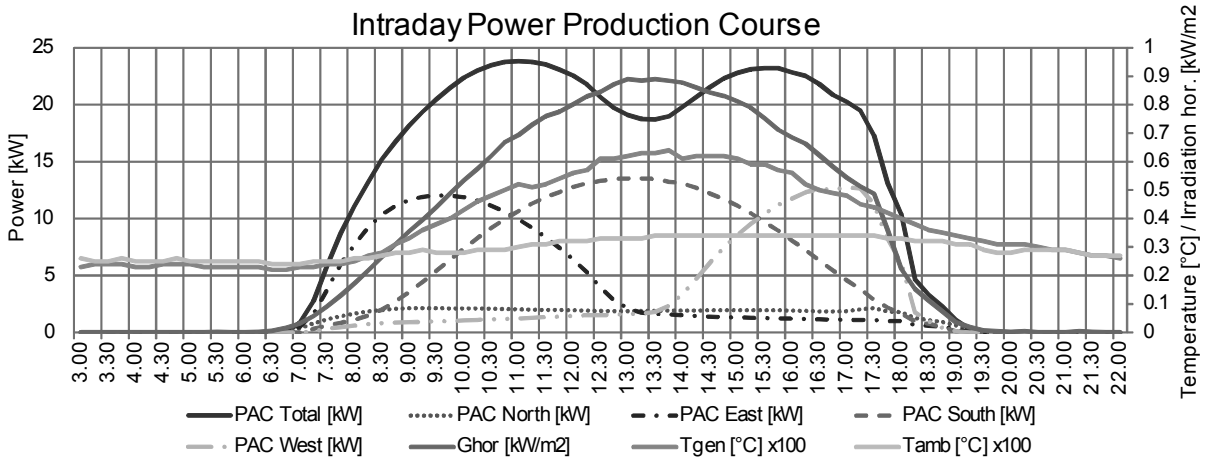

Figure 2: Daily course of AC power (total, east, south, west) supperimposed by the generator and ambient temperature

Module temperature history plant "south" - The measurement of the generator temperature pointed out a maximum value of 64°C. This value was recorded on 20.08.2012 at 13:45. The lowest operating start temperature of the generator (-2°C) was recorded on the same day in the morning at 09:00.

DISCUSSION

Energy yield - With a production surplus of the total system of 4310.3kWh there results a higher yield of 10.3% compared to the simulations. In particular, the photovoltaic system on the south façade brings with 17904.0kWh 16.1% more energy than calculated. The west façade generates, although horizontal shading is present through the nearby Uetliberg and near shading by the two neighbouring high-rise buildings, 14.1% more annual energy as predicted. 5.3% more final yield than simulated was produced by the east façade with 10195.5kWh. Only the north facing system has a reduced yield of 0.5% versus the simulations. The latter is clearly located within the measurement and simulation uncertainty. With an average of 21% higher winter energy fraction (15820.1kWh) the winter energy demand of the high-rise building can be supported. The question of whether the winter-summer energy ratio remains so in the future will have to be determined. Because of the very sunny month of March (record values of sunshine duration according to (9)) there was with 61.0% massively more energy output produced than calculated in the simulations, which were based on multi-year values. In general it can be said that the calculated yield for the total plant was too pessimistic for the winter months. The summer earnings, however, were lower than expected.

Intraday course – A very interesting subject is the lack of the production noon peak well visible in Figure 2. By the angle of the east and west side façades systems there is a steep rise in production in the morning and abrupt production reduction in the evening, respectively. The two façades contribute in combination with the plant "south", for the midday sun suboptimal aligned and partially shaded in the afternoon, to a “homogeneous” intraday course. In winter, the saddle-shaped course of the production curve, as it occurs in the summer, flattens further.

Configuration and production of the northern façade – Although the north façade system is at 0.5% and with a normalized annual energy of 195.1kWh/kWp below the calculated energy yield value, its electricity production should be analysed further. It is interesting that in November, December and January, the production by an average of 57.4% is substantially

higher than expected. A corresponding influence could have been the snowy winter with good beam reflection behavior of the ambient as well as the good diffuse radiation properties of thin-film modules used. Future income yield data, also from the system in the building envelope of the 2nd high-rise building with another inverter configuration can bring clarity to this issue and to the assumption that simulations took place with too low Albedo values.

White Spots - The phenomenon of white spots that can occur in thin-film photovoltaic modules of the NA F1xxG5 series (10) was also investigated. According to the manufacturer, such visual types of damage as a result of shading and local current concentration at low ohmic cell surfaces will not affect the energy yield. A possible occurrence of white spots was subjectively judged by experts from the ground with sight on low mounted modules. By the time of manuscript writing no white spots were seen.

Temperature – The lowest initial operation temperature was -2°C (12.12.2012 09:00). The light radiated into the generator plane then heated up the photovoltaic modules within 1.5h to 35°C. The minimum as well as maximum recorded temperatures in the generator "south" are within the expected range. The maximum operating temperature reached is 26°C below the by the manufacturer specified maximum module cell temperature (90°C). The acquisition of additional position-dependent temperature behaviour data will in future provide more detailed information of photovoltaic façade of this dimension.

Forecast - The second tower with other configurations and design principles is 2 floors higher than the first building and has additional partial shadowing. It was finally renovated in spring 2013. For economic and technical reasons the inverters of the north façade system were undersized by an average factor of 4,5 out of the knowledge that there will not be a specific plant power over ~20-25% below STC-conditions.

ACKNOWLEDGEMENTS

The team of the Laboratory for Photovoltaics at BUAS thanks the electrical installation company Kälin & Müller AG and especially Stefan Kälin for the open, straightforward and competent professional cooperation. Other thanks go to the students Nicole Reber and Daniel Bützer for their good base of simulations which they developed during the bachelor thesis.

REFERENCES

1. Häberlin, H.: Photovoltaics – System Design and Practice, RB, Electrosuisse, Fehraltdorf, 2012
2. Bützer, D. and Reber, N.: PV-Fassade Sihlweid Zürich, BT, Burgdorf, 2011
3. Bützer, D. and Reber, N.: PV-Fassade Sihlweid Zürich, PW, Burgdorf, 2011
4. Jäggi, J. and Schaad, S.: PV-Fassade Hochhaus Leimbachstrasse 215, BT, Burgdorf, 2012
5. Zurlinden, Baugenossenschaft: Vorzeigeprojekt Sihlweid, IN, Zürich, 2013
6. Zurlinden, Baugenossenschaft: Terminplan, IN, Zürich, 2013
7. Fronius, Internat. GmbH: Fronius DATCOM Detail, UM, Wels, 2012
8. MeteoSchweiz: Werkzeuge für die Qualitätskontrolle und die Bearbeitung von Meteorologischen Daten, TS, Zürich, 2009
9. MeteoSchweiz: Klimabulletin Jahr 2012, TR, Zürich, 2013
10. Sharp, Electr. GmbH: CS1105008 White Spot on Thin Film PV, TS, 2011

METHOD AND DATA ANALYSIS FOR ASSESSMENT OF LOCAL ENERGY POTENTIALS FOR URBAN TRANSFORMATION: CASE STUDY OF A MIXED USE CITY QUARTER.

Jimeno A. Fonseca[1], Arno Schlueter.

Architecture & Sustainable Building Technologies (SuAT), Institute of Technology in Architecture (ITA), ETH Zürich

ABSTRACT

This paper introduces the intermediate results of an on-going research project addressing the assessment of local energy potentials for the transformation of a mixed-use city quarter. We describe the allocation and analysis of energy data of commercial and industrial buildings and uses on site. A general method is proposed to identify and assess plausible infrastructural and building retrofit measures under the framework of the Swiss 2000-watt society, combining different techniques used in urban and energy planning fields. In conclusion, the method facilitates the comparison of global and local alternatives to obtain well-performing and feasible solutions for sustainable urban transformations.

Keywords: Urban transformation, energy potentials, Swiss 2000-watt society.

1.1 INTRODUCTION

In the future, urban areas will increasingly constitute not only the places for affordable and comfortable living, but also the centres of highest energy demand and related greenhouse gas emissions. Setting strategies to decrease their impact on the environment while supplying the future energy demand remains one of the biggest challenges for the 21st century [1]. Under this premise, the exploitation of renewable energy sources and energy-saving measures constitute the most urgent actions to support energy supply with low environmental impact [1], [2]. The assessment of local opportunities facilitates the implementation of these actions in the urban context, promoting future sustainable forms of urban development. This research addresses the assessment of local energy potentials at the city quarter scale. This granularity is minimum to identify main opportunities and constraints of the urban context at social, environmental and economic levels [3], [4]. It is on this scale where characteristic vectors of supply and demand clearly interact.

We propose the assessment of local energy potentials by combining existing techniques in both urban and energy planning domains. Geographic information systems, district energy system analysis and strategic planning methods constitute the way to make this task possible. In detail, our methodology is based on the analysis of energy quantities, qualities and interactions taking place in an urban energy system composed by buildings, infrastructure and sources of energy. Within these system boundaries, local energy potentials vary from infrastructural upgrades with potential integration of renewable energy sources to local improvements of building performance (building retrofits).

The proposed method is applied on a case study targeting the urban transformation of an industrial area in regards to the framework of the 2000-watt society [5]. The area of study is composed of industrial and commercial uses hosted in 24 buildings that are connected to a shared district heating, cooling and electrical network. The research on the case study is divided into three modules: A. Buildings and Infrastructure, B. Industrial Processes, and C.

[1] Corresponding Author: fonseca@arch.ethz.ch. Tel: +41 44 633 81 21
ETH Zürich, Building HPZ, floor G, Schafmattstrasse 32,CH-8093 Zürich, Switzerland

People and Mobility. To synthesize the research of the different modules, three possible development scenarios will be established for 2035. By the time of writing, the general methodology, developed in the module A, is applied to a "*business as usual"* scenario representing the prolonging of the on-going development at the site.

1.2 METHOD

1.2.1 Goal setting

The concept of 2000-Watt society is simple in its definition but complex in its quantification. One of the key problems to assess the benchmarks of the 2000-Watt Society for a dedicated area is that they are mainly oriented at the consumption per capita. This can be solved by converting the goals to square meters of built area as shown in Lenzlinger, 2010 [6].

This approach has been carried out for the *building categories* of residential, offices, and industry. Extending this approach to fit the requirements of the case study, industrial uses are furthermore divided into goals for buildings and processes. This separation aims to compare scenarios where the performance of industrial buildings is improved but the performance of industrial processes is not and vice versa, allowing for modelling these two different entities in terms of energy intensity. The estimation of goals is based on the Swiss prospects of energy reference area by Haag, 2004 [7], the grey emissions of the Swiss building stock by Lenzlinger, 2009 [8] and the Swiss energy consumption statistics of Switzerland 2000-2011 by Kemmler et al., 2012 [9]. The result is a set of goals for reduction of CO_2 emissions and primary energy consumption of the average Swiss building stock. These values are compared to those of the buildings in the area of study, obtaining goals for each *category of use* in the area on the time line of the suggested transformation (*Table 1*).

Factor	Unit	Year	Category of use							
			Residential		Offices		Industry (buildings)		Industry (Processes	
			CH	Area	CH	Area	CH	Area	CH	Area
Ep (non-renewable)	$MJ/m_2.a$	2005	890	-	1168	1192	802	1431	2552	1828
CO_2-eq emissions	$Kg/m_2.a$		39.9	-	60.7	32.7	28.1	42	89.4	40
Ep (non-renewable)	%	2035	47%	-	54%	55%	48%	71%	48%	28%
CO_2-eq emissions	%		58%	-	64%	32%	59%	72%	59%	8%

Table 1 Abstracts of estimated goals 2000 W-society. CH: Switzerland. Area: area of study/city quarter.

1.2.2 Data allocation

For buildings and infrastructure, different data sources were exploited and combined to achieve the best possible repository: *official data* obtained from local and regional public entities, *measured data* obtained through metering and monitoring in-situ, and *estimated data based on* plausible estimates combining statistical methods and official data.

In terms of resources, the system boundaries are extended to the local and regional context. At the local context previous analysis of renewable energy potentials such as solar and ambient heat is referenced. At this scale, restrictions of use of renewables and their related infrastructure are examined, such as protected zones for geothermal/ groundwater exploration, and restrictions in use of solar panels on heritage buildings. At the regional level, official data referencing energy and environmental policies is studied in order to obtain economical incentives for energy infrastructure, and availability of resources disposed at this scale such as biomass.

At the infrastructural level, measured energy data, existing technical reports, and record plans of energy infrastructure are obtained from the district system's operator. This data is allocated

in order to identify the annual dynamics of the infrastructural system, main energy carriers, end-uses of energy, fuel consumption, yearly energy demand and delivery, main infrastructural components, district system's configuration and foreseen improvements if any.

In order to identify possible ambiguities in measured energy data, the energy data reported by the district systems' operator is compared to the data recorded by the local utility. From this process, additional "third parties" not connected to the district' network consuming fuel and electricity in the area are identified. This process constitutes one of the most time-consuming efforts during data allocation.

At the building scale, existent categories of use and their related built area are assessed. Energy reference areas are measured according to existing plans, and if not available, they are estimated as the total area above ground of buildings from nationally geo-referenced official data. On site, it is determined the amount of area/space unoccupied during the periods where the energy consumption data is measured. During the next stage (see section 1.2.3) the amount of area occupied is used as basis for the estimation of future energy consumption and current performance on site.

Finally, all data is stored in a geo-referenced database, reported and visualized as "*energy profiles of the site*"[2].

1.2.3 Data processing

During this stage, the energy consumption and production on site is analysed on qualitative and quantitative levels. A special emphasis is put on the quality (i.e. temperature or voltage) and yearly dynamics of the energy demand, and related patterns of fuel consumption. This analysis leads to estimate the current seasonal efficiencies and performance factors of the system according to the standard EN 15316-4-5:2007 [10]. These parameters are of outmost importance to define the performance of the system in terms of current CO_2-eq emissions and primary energy consumption (non-renewable).

Additionally, the diverse end-uses of energy identified in the area are estimated in terms of *energy performance values* (EPV, $MJ/m_2.a$) of each building. EPV estimates allow benchmarking the performance of the current building stock with existing standards and local averages, targeting the identification of buildings for retrofit. An example of this analysis and visualization using the GIS database is shown in Fig. 1.

To evaluate the end-uses of energy approximately 20% of the measured energy data has to be augmented using standard EPVs values[3]. The validation of this data is carried out by comparing end-uses of energy for the same building use built at the same period of time. When the estimated values are out of the normal deviation of the sample, the end-use of energy is assumed as the mean value within the same category of use. The validation of this data constitutes one of the biggest challenges in data processing due to the high dispersion of measured values in comparison with standards (30%). Taking into consideration that this method was used on 20% of the measured data, the deviation of the total end-uses of energy is estimated to be around 6%.

[2] Format to report data data and analysis of economical, environmental, technical and other aspects related to energy issues in the area. Method quite used for survey and auditioning of energy performance in communities for strategic land planning since early 80's [3]
[3] Based on the local building standards SIA 380/1 and SIA 380/4

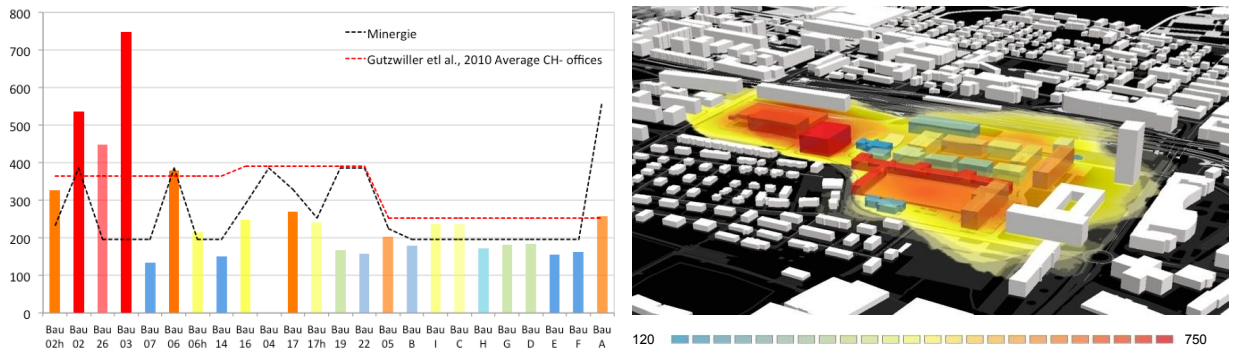

Fig. 1 2D and 3D Visualization of energy performance values end-uses for room heating, domestic hot water and humidification (MJ/m^2.yr) in comparison to Minergie standard Q_h<=90% Q_{hlim} and the regional average after Guzwiller et al., 2010 [11]

1.2.4 Definition and assessment of potentials

Following a SWOT Analysis method, widely applied in both urban and energy planning domains [12–14], we evaluate the weaknesses of the current system, the existing threats concerning its improvement and finally the strengths and opportunities available to overcome those drawbacks. An abstract of the SWOT analysis performed during the research is presented in *Table 2*.

Strengths	Weaknesses	Opportunities	Threats
District cooling is operated by extracting free cooling from the lake of Zug at a temperature 6°C/13°C. The network provides refrigeration to the district with an average performance ratio of 17.2. It is active during winter time due to the existence of a data centre with an annual cooling need of 1.5 GWth. Good amount of planar rooftop areas with good solar insolation. Low amount of heritage buildings (1 out of 24)	High temperature Network operating at 160°C /120°C when most consumers require only 75°C /45°C. The central boiler operates at low capacity and thus low efficiency during summer time to supply DHW, H and PH. Low thermal performance of Bau 02, 03 and Bau 26. Values out of Minergie standard range, site average and regional average.	Possibility to decentralize high temperature loads H and PH loads during summer with a NG-boiler. A temperature of 6°C/13°C of lake water could be used for heating purposes as well. Previous studies in the area suggested that by lowering the temperature of the network (return) a cold condensator heat exchanger could be uses to raise efficiency to 10%. Supply of biomass nearby for possible joint supply to the area. Possible transformation of Bau 02 into new offices and Bau 03 to open space	Limits on concession for cooling capacity and possible heating capacity to be extracted from the lake. Existing restrictions in use of CHP units (in terms of control system) No geothermal exploration allowed.

Table 2 Abstract from SWOT Analysis

A set of 12 potential measures is derived from the analysis and presented in *Fig. 2*. These measures consist on global infrastructural upgrades involving a partial integration of renewable energy sources and building retrofits.

Potential infrastructural upgrades No.1 (CHP unit providing 100% of heat load, 60% of electrical load) and No.2 (flue gas boiler providing 100% of heat load) are a result of a possible joint supply of biomass to the area considering a low trade-off in emissions. The infrastructural upgrades No. 3 (shut-down of existing boiler) and No.4 (utilization of lake water for heating) leverage the opportunity to decentralize high quality/low demanding end-uses of energy with NG-fired boilers and to integrate ambient heat for heating purposes with heat pumps. These measures are tailored to overcome the weakness of the heating network in terms of high temperature and inherent low performance during summer. Potential measures No. 5 (solar collectors providing 60% of heat load) and No. 6 (PV panels providing 30% electrical load) employ 80% of available rooftop areas for solar harvesting. The amount of energy that can be covered is estimated according to the analysis of solar potential on rooftops in the city of Zug [15].

Local measures No.7 (retrofit of building 6h), No.8 (retrofit of building 26), No.9 (retrofit of building 02), and No.10 (demolition of building 03) address measures related to buildings with high thermal losses. As inputs from the other modules of the project production processes on site are targeted to be 10% more efficient by 2035 (measure No.11). No.12 (business as usual) proposes a transformation and retrofit of four buildings to residential industrial and commercial use accompanied by an increase in production of 50%.

For each measure the potential reduction of primary energy consumption and CO_2-eq emissions is estimated. For this, the characteristic efficiencies of infrastructural components, primary energy and emission factors described in SIA 2040 [16] and KBOB, 2012 [17] are used.

Finally, in measure No 13, the most high-performing measures (1 and 12) addressing both improvements of the infrastructure and building retrofit are aggregated to achieve the reduction goals for each category of use as shown in *Fig. 2*.

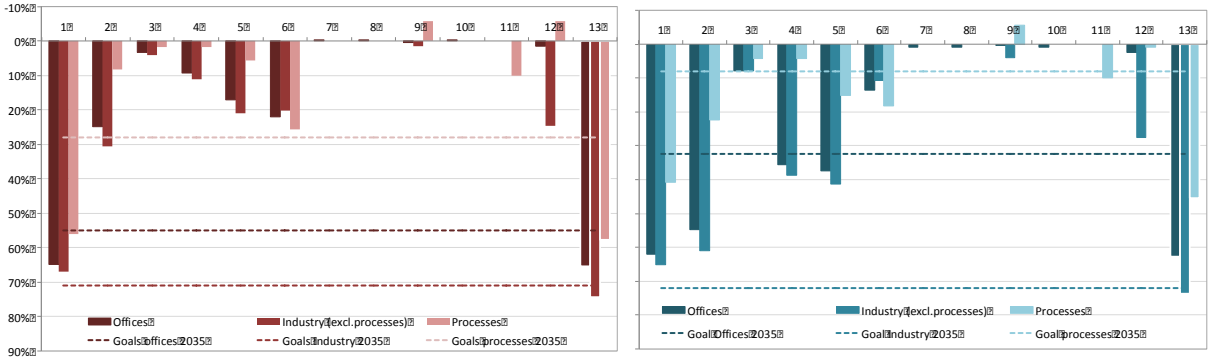

(a) (b)

Fig. 2 Estimated reduction of primary energy consumption (non-renewable) (a) and CO_2-eq emissions (b) of energy potentials in the area in comparison to estimated goals.

1.3 DISCUSSION AND CONCLUSIONS

This work proposes a method to identify and assess plausible infrastructural and building retrofit measures in regards to the framework of the Swiss 2000-watt society. The results are presented in terms of potential reduction of primary energy and CO_2-eq emissions of different alternatives in diverse categories of use.

The approach provides simplified estimations of the effects of individual and aggregated measures addressing the future operational performance of an urban energy system. Other criteria such as grey emissions, economic, financial and social issues are at this time neglected but would generally provide a more inclusive analysis of the phenomena, however also increasing the overall complexity of its assessment.

The data allocation and analysis of building related, end-uses of energy facilitate the identification of infrastructural upgrades addressing end-uses requiring high qualities of energy (e.g. process heat, humidification, compressed air etc.) as well as the integration of sources of excess heat (e.g. servers cooling, process heat etc.). It also provides the comparison of the performance of the current building stock with standard values. As shown for the case study, the allocation, structuring and analysis of the relevant energy data from different sources is time consuming and a challenge itself.

For the case study area, it can be observed that infrastructural upgrades provide a higher impact towards the targeted goals than the retrofit of the existing buildings. This is mainly due to the good average energy performance and quality of the existing building stock on site.

Infrastructural interventions improve the efficiency of the district energy system by performing modifications achievable in short periods of time (e.g. potential No. 3). In

contrast, for the quality of the existing buildings, retrofit measures by its nature require a more invasive and in general more expensive intervention with potentially lower impacts in reduction of emissions (i.e. potentials No. 7 – 9), not even considering grey energy and related emissions. From an energy point of view, building retrofits in the area of the case study are advisable when either infrastructure solutions prove to be not economical, or when a major functional transformation of the area are tailored to improve the performance of a low performing category of use (i.e. industry- buildings category in potential No 12.)

The assessment of local energy potentials is dependent on the efficiency of technology considered, and related factors for primary energy and CO_2-eq emissions. Further research in the project will consider the impact of these variables in the general assessment of local energy potentials as well as the integration of further economic and social aspects.

1.4 ACKNOWLEDGEMENTS

We would like to thank Anja Willmann of SuAT for research and management, Martin Schaer and Benno Moser from Siemens Building Technologies, Zug, furthermore our project partners Michael Stauffacher, Corinne Moser, Christian Wirz and Sandra Moebus. This research is financed by the Swiss Commission for Technology and Innovation (CTI).

1.5 REFERENCES

[1] Intergovernmental Panel on Climate Change (IPCC), *Renewable Energy Sources and Climate Change Mitigation: Special Report of the Intergovernmental Panel on Climate Change*. New York: Cambridge university press, 2012, p. 1088.
[2] International Energy Agency (IEA), "Energy technology perspectives: Scenarios and strategies 2050," 2010.
[3] R. Lang, A. Armour, and Land Armour Associates, *Planning land to conserve energy: 40 case studies from Canada and the United State*, vol. 25. Ottawa: Lands Directorate of Environment Canada, 1982, p. 212.
[4] A. van den Dobbelsteen, S. Broersma, and S. Stremke, "Energy Potential Mapping for Energy-Producing Neighborhoods," *International Journal of Sustainable Building Technology and Urban Development*, vol. 2, no. 2, pp. 170–176, Jun. 2011.
[5] R. Iten, S. Schneider, and K. Schulte, "Grundlagen für ein Umsetzungskonzept der Fehler! Keine Index-einträge am Beispiel der Stadt Zürich LSP 4 - ' Nachhaltige Stadt Zürich - auf dem Weg zur 2000-Watt-Gesellschaft ' Ein Gemeinschaftsprojekt von Stadt Zürich , Bundesamt für Ener- Unterstützung," 2009.
[6] M. Lenzlinger, "SIA Effizienzpfad: Bestimmung der Ziel- und Richtwerte mit dem Top-Down Approach," Bern, 2010.
[7] M. Haag, "Zukünftige Entwicklung der Energiebezugsflächen," 2004.
[8] M. Lenzlinger, "Graue Energie im Gebäudebestand der Schweiz," Schlieren, 2009.
[9] A. Kemmler, A. Piegsa, A. Ley, M. Keller, M. Jakob, and G. Catenazzi, "Analyse des schweizerischen Energieverbrauchs 2000 - 2011 nach Verwendungszwecken," Bern, 2012.
[10] Technical Comitee CEN/TC 228, *Heating systems in buildings — Method for calculation of system energy requirements and system efficiencies — Part 4-5 Space heating generation systems , the performance and quality of district heating and large volume systems*. 2006, p. 20.
[11] L. Gutzwiller, B. Aebischer, O. Brüggimann, A. Eckmanns, and C. Gmür, "Energieverbrauch von büro-gebäuden und grossverteilern," Bern, 2010.
[12] J. Terrados, G. Almonacid and L. Hontoria, "Regional energy planning through SWOT analysis and strategic planning tools.," *Renewable and Sustainable Energy Reviews*, vol. 11, no. 6, pp. 1275–1287, Aug. 2007.
[13] H. Strasser, O. Pol, K. Church, S. Svendsen, A. Dalla Rosa, A. Koch, and R. Jank, *Annex 51: Energy Efficient Communities - Case Studies and Strategic Guidance for Urban Decision Makers: Subtask A Description of the state-of-the-art of energy efficient projects on the scale of neighbourhoods*, no. April. Karlsruhe: International Energy Agency, 2011, p. 89.
[14] J. Cherni and N. Kalas, "A Multi-criteria Decision-Support Approach to Sustainable Rural Energy in Developing Countries," in *Handbook on Decision Making*, 2010, pp. 143–162.
[15] Stadt Zug -Umwelt und Energie, "Zug Map: Planung und Bau - Solarkataster Stadt Zug," 2013. [Online]. Available: http://zugmap.ch/zugmap/BM3.asp. [Accessed: 10-Apr-2013].
[16] Schweizerischer Ingenieur-und Architektenverein (SIA), "SIA-Effizienzpfad Energie: Merkblatt 2040," Zuerich, 2011.
[17] Die Koordinationskonferenz der Bau und Liegenschaftsorgane der Oeffentlichen Bauherren (KBOB), "Ökobilanzdaten im Baubereich: 2009/1," 2012.

A CONSENSUS-BASED APPROACH TO TEST THE APPLICABILITY OF INTERNATIONAL SUSTAINABLE ASSESSMENT SCHEMES FOR SAUDI ARABIA CONTEXT

Saleh. H. Alyami[1]; Prof. Yacine Rezgui[2]; Dr. Alan Kwan[3].

(1) Saudi Environmental Society (SENS) & School of Engineering- Cardiff University- the UK. (2) Professor and Institute leader (BRE Institute in Sustainable Engineering) School of Engineering- Cardiff University- the UK. (3) Reader and Head of the Architectural, Civil and Civil & Environmental; School of Engineering- Cardiff University- the UK.

ABSTRACT

Stimulating market demand on sustainable and green building has increased the utilization of sustainable assessment tools (e.g. BREEAM and LEED). The evolution of those schemes created a competition, amongst well-known sustainable assessment tools, toward worldwide use. However, practical evidences show that regional and socio-cultural variations have hindered the direct global use of those sustainable assessment tools. Therefore, this paper proposes to test the applicability of international leading sustainable assessment tools such as BREEAM and LEED for the assessment of Saudi's built environment. Scientific evidence suggests that building assessment tools involve multi-dimensional criteria; therefore a consensus-based approach is used to conduct this study. Hence, the Delphi technique is a reliable approach to reach consensus amongst panel of experts; it has been selected and conducted in three successive consultation rounds involving world leading experts in the domain of environmental and sustainable assessment schemes, as well as professionals and highly-informed local experts from academia, government and industry. The results reveal that international assessment schemes are not fully applicable to the Saudi built environment, as reflected in the development of a new building environmental and sustainability assessment scheme.

Keywords: Built environment, Sustainability assessment schemes, Delphi technique

1. INTRODUCTION

Since 1990s, there has been a widespread development of sustainable and environmental building assessment tools, many of which have subsequently gained considerable success [1]. The Building Research Establishment Assessment Method (BREEAM) was the first real attempt but various schemes such as Sustainable Building Tool (SBTool), Leadership in Energy and Environmental Design (LEED) and Comprehensive Assessment System for Building Environment Efficiency (CASBEE) have subsequently emerged. However, almost all sustainable assessment tools have been designed to suit a specific territory. Evidence suggests [2, 3] that existing environmental assessment methods were developed for different, local purposes. More specifically, certain environmental factors may hinder the direct use of any existing assessment tool. Examples of such factors are: climatic conditions; geographical characteristics; potential for renewable energy gain; resource consumption (such as water and energy); construction materials and techniques used; population growth and public awareness.

This paper aims to examine the applicability of sustainable building assessment categories and criteria, which applied by well-known tools; and thereby establishes applicable categories and criteria for Saudi Arabia built environment. The outline of this paper include (a) explanation of the used research instrument (b) the approved sustainable building assessment categories for Saudi Arabia built environment (c) brief discussion about the distinctions of the Saudi context, which have not been covered by leading sustainable assessment tools.

2. METHOD

The field of sustainable assessment method is vast and diverse. Therefore, to establish a new customization for specific region, a comparison process between well known assessment tools is firstly considered as a robust starting point [4]. Given that, the authors conducted comparative analysis between *BREEAM, LEED, SBTOOL and CASBEE* at the aim of building a consolidated categories and criteria, by which the development of new sustainable assessment tool will be enhanced. The main research instrument in this paper is the Delphi technique, which was developed by the American defence industry in the early 1950s. The "*Project Delphi"* was the name of a study undertaken by the RAND Corporation for the US Air Force. Then, the technique was first published by Dalkey and Helmer. The main purpose of Delphi study is to "*obtain the most reliable consensus of opinion of a group of experts by a series of intensive questionnaires interspersed with controlled opinion feedback*" [5].

Ranking Delphi is the followed technique in this consultation; which is nowadays the most commonly used Delphi technique. This is because the ranking technique draws its robustness from the four fundamental characteristics of Delphi, which are: **"***Anonymity, Iteration, Controlled feedback and Statistical group response***"** [6]. The major steps of conducting Delphi technique in this study include: (I) composition of the Delphi panel; (II) Delphi survey rounds and (III) analysing the result. *Composition of Delphi panel* is the key factor for a well-established study. For this reason there has been a compliance with recommended guidelines of expert selection. While the expert's nomination is a recommended approach to compose a well-built panel; a number of different institutions were visited to meet this objective. These institutions included: King Abdul-Aziz City for Science and Technology (KACST), Sustainable Energy Technology Centre (SETC), King Saud University, Saudi Environmental Society (SENS), Saudi Green Building Council (SGBC), Riyadh Municipality and Saudi Oger Ltd. Furthermore, a number of recommended criteria have been taking into

consideration when forming the Delphi panel; the participants should be (a) Academic specialist in the area of Sustainable Development (b) Decision-maker, manager, or practitioner in the field of sustainable and green building (c) Accredited professional in one of the leading sustainable assessment systems (d) Practical experience and sufficient knowledge of the sustainable development potential within the kingdom of Saudi Arabia (e) Expert with a level of influence regarding the adoption of the resulting methodology and (f) Willingness to participate. The Delphi panel in this study comprises thirty-three members, including some of the world's leading experts in the domain of sustainable and environmental assessment schemes, as well as professionals and highly-informed local experts from academia, government and industry (9% Professors, 21% Doctors, 37% AEC professionals and 33%Multi- disciplines).

Delphi survey rounds were designed and administered using a web based survey "Survey Monkey" (http://www.surveymonkey.com/). This software tool was extremely effective, to enable collection of the entire data within 4 months in three separate rounds. The first round sought to create a list of sustainable building assessment criteria, that are applicable to the Saudi Arabia built environment. This was based upon brainstorming process, with open-ended solicitation of criteria, in an attempt to obtain and clarify the key sustainable criteria for the Saudi context. The second round allowed the Delphi panellists to anonymously view the responses and feedback from the first round. This gave them the opportunity to revise their previous thoughts and reassess their initial judgements. Within a Delphi study, the results of any previous iteration, whether specific statements or criteria can be changed or modified by individual panel members in later versions. The third round summarised the outcomes of the previous rounds, reflecting the opinion of the experts in the form of "*Statistical group response"* (Mean/Median). The survey was then sent again to the Delphi panel, to invite their final judgement, as this approach generally leads to improved judgements and increased overall accuracy [7].

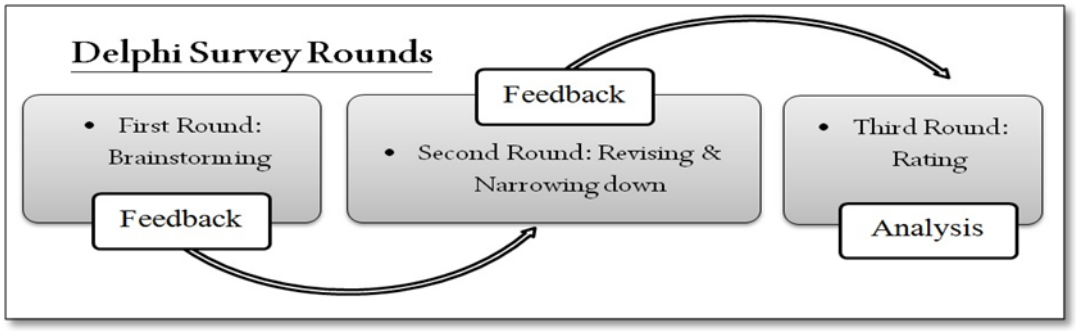

Fig. 1 Ranking Delphi rounds

Analysing the result; each round was followed by analytical stage to evaluate the level of consensus as well as to test the applicability of building assessment categories and criteria that will form the new framework.

3. RESULTS

The result of this consultation process strongly suggests that international schemes such as *BREEAM* and *LEED* are inapplicable for the Saudi context. Expert consensus converge in that building environmental and sustainable assessment categories should include: ***Indoor environmental quality, Energy efficiency, Water efficiency, Waste management, Site***

quality, Material, Pollution, Quality of services, Economic aspects Cultural aspects and Management and Innovation. Each of the above categories includes a list of related criteria (shows in Fig.2 in the proposed Framework), creating a 92 item list of criteria for sustainable residential building assessment in Saudi Arabia. The consensus of Delphi panel was determined by calculating the interquartile range (IQR). In this study, the values of IQR were between 0.12 - 0.48 which is a reliable indications of reaching the consensus [7].

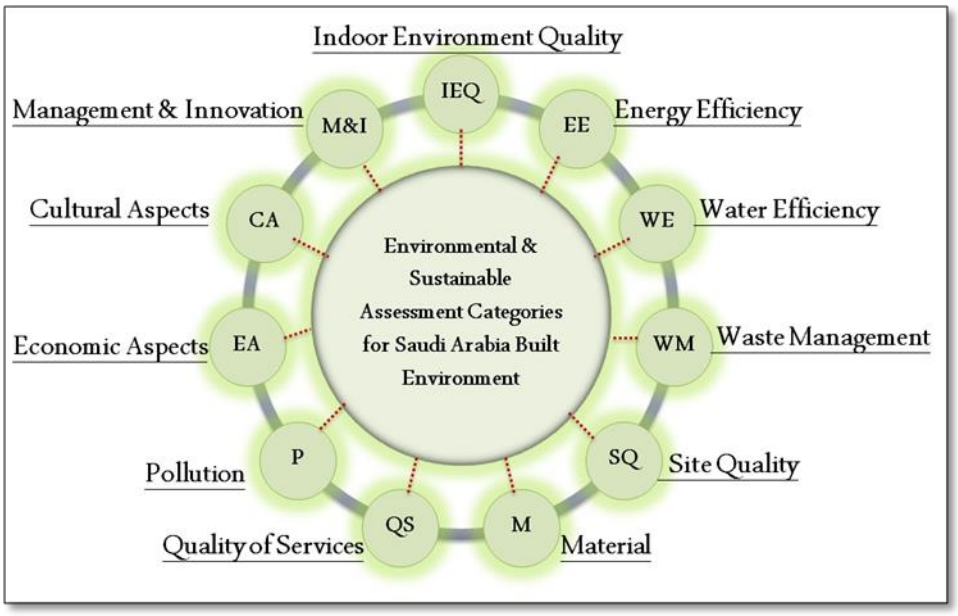

Fig. 2 Sustainable building assessment categories

The judgement of the panel is that water efficiency is the top priority. Subsequently, energy efficiency design and indoor environmental quality are almost at the same level. This agreement by the Delphi panel about the prioritisation of the above three categories are compatible with current concerns in relation to the Saudi Arabian built environment [8].

4. DISCUSSION

The well-known assessment tools attempt to be comprehensive in order to be applied in global scale. For instance *BREEAM Bespoke* is a strategic way to cover any building type in any region in the world, but this is greatly influenced by the original *BREEAM* categories and criteria. Moreover, there is a lack of transparency regarding the utilized instruments to identify international *BREEAM Bespoke* criteria. Another example is that *LEED* uses a simple additive system to determine the level of green practice. However the absence of an adjusted weighting system is still major drawback of *LEED* system. In spite of *BREEAM* lunching *BREEAM Gulf*, there is no building assessed by this scheme in Saudi Arabia so far. This reflects the influence of market basis, which are affected by political aspects, for assessing the built environment regardless the actual outcomes that reflect reliable results.

However, to obtain best possible outcomes of building rating system; leading assessment schemes, such as *BREEAM*, *LEED* and *SBTool*, have been critically revised in the development of potential assessment scheme for Saudi Arabia. Hence, regional and cultural variations in hot arid climate (Saudi Arabia) advocate the further development of appropriate categories and criteria. A clear consensus has been reached using Delphi technique that a number of categories and criteria have not been recognised by the leading schemes, which are essential for the assessment of Saudi's built environment. This study develops a coherent

framework to assess Saudi Arabia's built environment, based upon the three pillars of sustainability development (*Environmental, Economic and Social aspects*).

Environmental aspects: The hot arid climate coupled with varies topography of Saudi Arabia requires AEC professionals to observe certain considerations. For instance, heavy sandstorms are a common phenomenon in the Arabian Peninsula [9], with a severe impact on inhabited cities, causing health problems and communication disruption. Therefore, specific criteria are essential in this case in order to promote heather built environment design. In this study the Delphi panel recognise the need for such criteria. These criteria include: *Air tightness of buildings (as an effective barrier to dust), and Internal landscaping (Vegetation).* Another important consideration is that the clear skies and extremely hot arid weather significantly increase building exposure to bright sunlight, meaning that *shading strategies* should be used to protect building envelopes and occupants from solar radiation. The shading strategy can also play an important role in energy saving and enhancing the comfort of the indoor environment [10]. In addition, due to climate change and global warming indicators in the middle east, the panellists agreed that the degree of *building adaptability for future change is* significant, especially given evidence that predicts the temperature of Saudi Arabia will rise by approximately 2.0–2.75 °C in the next 30 years [11].

Saudi Arabia is not densely populated, and electrification and desalination plants, along with other basic networks have been expanded over thousands of kilometres to cover the most populated cities [12], but, certain rural and remote areas are not yet connected to the network, and connecting them will require an additional increase in power generation. Therefore, various criteria were recommended to manage this expansion, including: *Renewable energy technology and, Sub-metering of electricity use*. Moreover, Saudi Arabia has poor water resources and is heavily dependent on energy-intensive means such as groundwater and sea water treatment (desalination) [13]. This study ranked water as the top priority category, with the aim of raising awareness amongst utility customers regarding water scarcity. Therefore, the panellists recommended encouraging innovative strategy of water conservatives and *ensuring that the restriction level of water supply should not lead to unsustainable practices.* Another important consideration is that building material requires large amount of embodied energy that also put intensive pressure on the natural environment [14]. However, the Delphi panel add that buildings should be *designed to deal with future climate change***,** using *environmentally friendly material with high thermal mass* that can cope with the environmental and climatic conditions of Saudi Arabia.

Economic aspects: Financial considerations are essential in sustainability development in both developed and developing countries. Developed countries are concerned with the reduction of environmental impact while maintaining standards of living. However, in developing countries economic and social issues are often as important as environmental considerations [15]. However, neither BREEAM nor LEED consider financial aspects in their evaluative framework. This arguably contradicts the ultimate principle of sustainable development, as financial returns are essential for all projects, with environmentally friendly projects potentially being very expensive to build. Therefore, this scheme has incorporated economic criteria that play an important role in Saudi Arabia's built environment, including: *Use of whole life costing mechanism in building choice (WLC); Affordability of residential rental; and constructions cost & pay back.*

Cultural aspects: Residential buildings in Saudi Arabia are greatly influenced by cultural considerations. Typical Saudi families are large and dynamic, keeping strong ties with even

distant relatives and neighbours. Therefore, buildings need to be designed and built to accommodate social events and needs. This issue was raised by various local experts in the consultation rounds. A consensus was reached by the Delphi panel in the subsequent rounds. The required criteria for the assessment of residential buildings include: *Male and Female space privacy; Heritage and Cultural Identity; Habits and custom effects on the built environment and; Constancy of Islamic faith.* These issues are completely overlooked by the leading international schemes, which also contradict sustainable development principles.

ACKNOWLEDGEMENTS

The authors are grateful to Dr. Majida Abu-Ras, *Deputy Executive Director of Saudi Environmental Society (SENS)* for the help and support during the consultation process; also they express their great gratitude to the anonymous thirty three Delphi panel for their valuable contributions in this study.

REFERENCES

[1] Cole, R., *Shared markets: coexisting building environmental assessment methods.* Building Research and Information, 2006. 34(4): p. 357-371.

[2] Cole, R.J., *Emerging trends in building environmental assessment methods.* Building Research and Information, 1998. 26(1): p. 3-16.

[3] Cooper, I., *Which focus for building assessment methods – environmental performance or sustainability?* Building Research & Information, 1999. 27(4-5): p. 321-331.

[4] Cole, R., *Building environmental assessment methods: redefining intentions and roles.* Building Research and Information, 2005. 33(5): p. 455-467.

[5] Linstone, H.A., Turoff, M., and Helmer, O., *The Delphi method: Techniques and applications*. 1975: Addison-Wesley Publishing Company, Advanced Book Program.

[6] Rowe, G., Wright, G., & Bolger, F., *Delphi: A reevaluation of research and theory,*Technological Forecasting and Social Change, 1991. 39(3): p. 235–251.

[7] Von der Gracht, H.A., *Consensus measurement in Delphi studies: Review and implications for future quality assurance.* Technological Forecasting and Social Change, 2012. 79(8): p. 1525-1536.

[8] Hepbasli, A. and Alsuhaibani Z., *A key review on present status and future directions of solar energy studies and applications in Saudi Arabia.* Renewable and Sustainable Energy Reviews, 2011. 15(9): p. 5021-5050.

[9] Al Saud, M., *Assessment of flood hazard of Jeddah area 2009, Saudi Arabia.* Journal of Water Resource and Protection, 2010. 2(9): p. 839-847.

[10] Chan, A.L.S., *Effect of adjacent shading on the thermal performance of residential buildings in a subtropical region.* Applied Energy, 2012. 92(0): p. 516-522.

[11] Almazroui, M., *Recent climate change in the Arabian Peninsula: Seasonal rainfall and temperature climatology of Saudi Arabia for 1979–2009.* Atmospheric Research, 2012. 111(0): p. 29-45.

[12] Alnaser, W.E. and Alnaser N.W., *The status of renewable energy in the GCC countries.* Renewable and Sustainable Energy Reviews, 2011. 15(6): p. 3074-3098.

[13] Taleb, H.M. and S. Sharples, *Developing sustainable residential buildings in Saudi Arabia: A case study.* Applied Energy, 2011. 88(1): p. 383-391.

[14] Ortiz, O., Castells F., and Sonnemann G., *Sustainability in the construction industry: A review of recent developments based on LCA.* Construction and Building Materials, 2009. 23(1): p. 28-39.

[15] Libovich. *Assessing green buildings for sustainable cities.* in *SB05 Tokyo: Action for Sustainability - The 2005 World Sustainable Building.* 2005. Tokyo, Japan.

ENERGY MODELING AND PERFORMANCE ASSESSMENT OF BUILDING INTEGRATED PHOTOVOLTAIC THERMAL SYSTEMS WITH TRANSPIRED SOLAR COLLECTORS

Siwei Li[1], Panagiota Karava[2*]

1: School of Civil Engineering, Purdue University, 550 Stadium Mall Dr.,West Lafayette 47907, USA

2: School of Civil Engineering, Division of Construction Engineering and Management, Purdue University, 550 Stadium Mall Dr.,West Lafayette 47907, USA

ABSTRACT

Building-integrated photovoltaic-thermal (BIPV/T) systems with unglazed transpired solar collectors (UTCs), can be a key solution to address the energy and environmental challenges associated with buildings. So far, although the energy savings potential of such systems has been proved to be significant, no systematic thermal analysis model has been developed to accurately predict its performance and consequently to enable optimal design, further optimization and smart operation control. This paper presents detailed transient energy models for this system, using a fully-explicit finite difference scheme on the thermal network representation. The unknown convective heat transfer coefficients ($h_{conv.ext}$ and $h_{conv.int}$), as well as the suction air temperature T_s, are calculated based on the correlations obtained from validated Computational Fluid Dynamics (CFD) simulations, using high resolution grids and the Renormalization Group Methods k-ε (RNG k-ε) turbulence closure model. Eight plates with different geometry shapes have been studied under various wind speeds (1 – 10 m/s) and suction velocities (0.01 – 0.06 m/s), to investigate the most efficient PV module dimensions and optimal geometry shape, and to develop the correlations. The agreement between the correlation prediction and CFD simulation results is satisfactory, with the error within 20 %. The overall system performance has been evaluated, based on the cavity exit air temperature and the PV surface temperature, since all the other conditions are the same in the simulations. The results show that maximum combined electrical-thermal efficiency can be achieved with small PV modules and large coverage area. The study also suggests increasing the corrugation wavelength to improve the thermal performance. On the contrary, decreasing the crest length and increasing the corrugation amplitude will reduce the thermal efficiency significantly. Small surface temperature differences of the PV modules have been observed for different geometry shapes, which, however, are not expected to cause major efficiency drops.

Key words: unglazed transpired solar collector, BIPV/T, energy modeling, Nusselt correlations

INTRODUCTION

The concept of replacing conventional building cladding with a system that generates electricity and heat (namely building-integrated photovoltaic-thermal, BIPV/T) is an area that, until recently, has received only limited attention although the potential energy and cost savings from integrated and optimized solar technologies are high [1]. For example, unglazed transpired solar collectors, known as UTCs can be integrated with open-loop photovoltaic thermal (PV/T) systems to preheat ventilation air and/or to feed hot air into an air source heat pump, thus satisfying a significant part of the building's heating and/or hot water

requirements while also generating electricity. Although the concept of this system integration is relatively simple and the energy savings potential is significant, no systematic thermal model has been developed to analyze and optimize its performance. The objective of this study is to develop models for design, analysis, and optimal control of open-loop UTCs integrated with Photovoltaic systems. These models have been used to create a new component in TRNSYS in order to evaluate the system's annual performance and to explore system integration approaches with building HVAC systems and thermal storage mechanisms.

METHOD

Although Computational Fluid Dynamics (CFD) simulations can be a powerful tool to analyze the airflow and thermal field for UTCs and UTCs integrated with PV modules, using CFD simulations to predict annual performance and parameter optimization for buildings would be computational expensive and time consuming. There are numerous mathematical models, with correlations for convective heat transfer coefficients, developed for both UTCs and BIPV/T systems, based on energy balance in control volumes, i.e. both steady and transient models for an open-loop air-based BIPV/T system [2], flat UTC [3], etc. Most of these models are based on a steady state approach, neglecting the thermal capacitance effects of the PV module. In contrast, recently it has been reported [2] that a transient model is more responsive to the effects of rapid changes (e.g. variable solar irradiance, wind speed fluctuations, etc.) and better represents the system thermal dynamics.

In this study, a fully-explicit finite difference scheme, in which the temperature for the current time step depends only on the temperatures of the previous time step, is used to develop a transient model for UTCs with PV systems. The cavity beneath the UTC plate is divided into control volumes and each control volume corresponds to one corrugation, as shown in thermal network in Figure 1 left.

In this figure, $T_{p\text{-}i}$, $T_{c\text{-}i}$, $T_{b\text{-}i}$, T_a and T_{sky} are the UTC surface temperature, cavity air temperature, back wall surface temperature, ambient air temperature and sky temperature, respectively (K). G is the incident solar radiation on the UTC plate (W/m^2) and h_{rad} and h_{conv} represent the radiative and convective heat transfer coefficients (W/m^{2}K). Q_s is the heat flux from the suction air (J) and $Q_{i\text{-}1}$ is the heat flux from the previous control volume (J). The two terms can be calculated using the equations shown in Figure 1 left.

In order to simplify the problem, some basic assumptions for the model are listed below, based on the CFD simulation results and analysis presented in [4]:

1. The temperature differences between different regions (crest, valley, leeward and windward slopes) within one control volume are neglected.
2. The temperature of the surfaces (PV, UTC plate, back wall) and the cavity air temperature are assumed to be uniform inside each control volume.
3. Air flow rate of each control volume is assumed to be the same.
4. There is no reverse flow or air leakage after entering the cavity and no edge effects.
5. Properties of solid materials remain constant and uniform.
6. There is no humidification or dehumidification of the air stream.

According to experimental results reported in [1] and our initial CFD analysis, the difference between the surface temperature of the UTC plate T_p and cavity air temperature T_c is no more than 0.5 ˚C. Thus, in the energy model, T_p is considered equal to T_c and these two nodes can be merged into one. The unknowns needed to complete the energy balance equations are the

convective heat transfer coefficients ($h_{conv.ext}$ and $h_{conv.int}$), as well as the suction air temperature T_s. Validated CFD simulations, with high resolution grids and the Renormalization Group Methods k-ε (RNG k-ε) turbulence closure model [4], are used to obtain the correlations for the unknown heat fluxes.

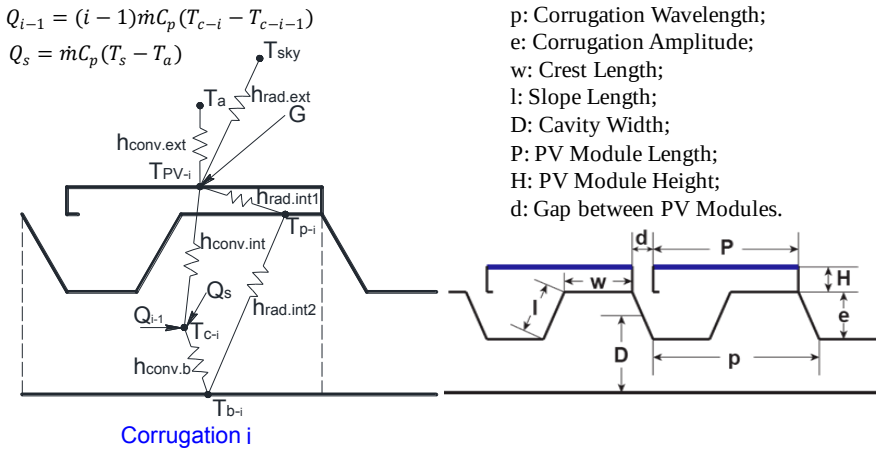

Figure 1: Thermal network for UTC integrated with PV (left) and the detailed geometry (right)

RESULTS & DISCUSSION

The parameters considered to have significant impact on the convective heat transfer process include suction velocity, wind speed and corrugation geometry (as shown in Figure 1, right). Perforation dimension has been excluded based on previous analysis [4] and the fact that in real applications the porosity of corrugated UTC varies within a very small range (usually between 1–2 %). Eight plates with different geometry shapes have been considered under various wind speeds (1 – 10 m/s) and suction velocities (0.01 – 0.06 m/s), to investigate the most efficient PV module dimensions and develop the heat transfer correlations. All the cases are simulated with 1000 W/m^2 solar radiation and 300 K ambient air temperature, with 0.1 % incident turbulence intensity.

PV Module Dimensions

Results reported in [1], for two UTCs with different PV module dimensions indicate that the configuration with smaller PV modules provides significant improvement on the electrical performance. Similar conclusions can also be found in [5], which shows that using smaller PV modules can generally reduce the PV surface temperature by 4-5 K, which corresponds to 0.3 % higher PV efficiency. The present study investigates four different PV dimensions on the same UTC plate, as shown in Figure 2, using CFD simulations. The PV module dimension is the same for plate 3 and 4, but the coverage ratio in plate 3 is only half of plate 4. The plates are simulated under 3 m/s wind speed with the suction velocity ranging from 0.015 m/s to 0.065 m/s. The comparison is not limited to the electrical efficiency as in previous studies, but also considers the thermal efficiency of the system.

Figure 3 shows results for the PV surface temperature and cavity exit air temperature, which is related to the electrical and thermal energy output, respectively. It can be seen that the medium PV module used in plate 2 can reduce the PV surface temperature to the maximum level; however, considering the impact of PV surface temperature on its efficiency, this small temperature difference cannot affect the electrical energy efficiency significantly (less than 0.5 %). On the other hand, using small PV modules can provide the highest cavity exit air

temperature, which will result in more than 10 % thermal energy output. Therefore, the small PV module is recommended to be the optimal choice for the PV module design, for its maximum combined electrical-thermal energy output.

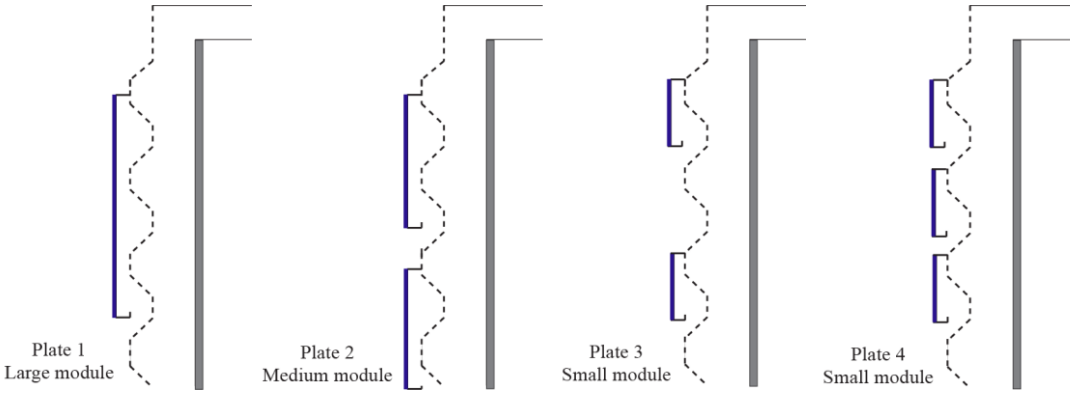

Figure 2: Sketch of different PV module dimensions mounted on UTCs

Furthermore, there is almost no temperature difference between plate 3 and plate 4, which indicates that adding more PV modules will not influence the energy efficiency, but it will increase the effective PV module area and therefore provide higher energy output.

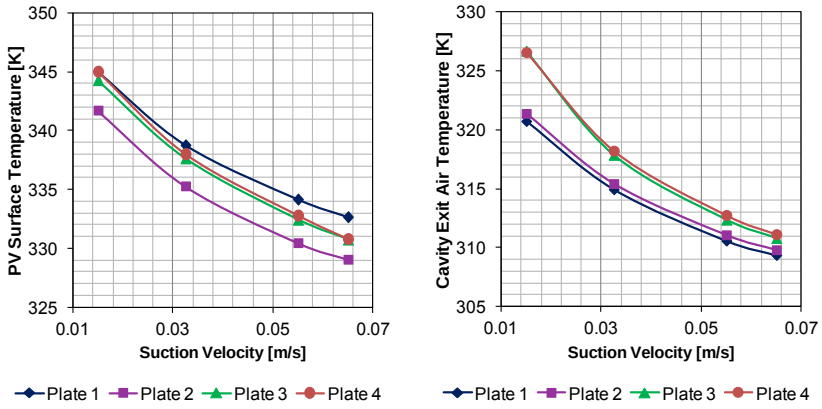

Figure 3: Comparison of PV surface temperature (left) and cavity exit air temperature (right) for plates 1 – 4 under different suction velocity

Heat Transfer Correlations

Based on the results presented in the previous section, the smallest PV module dimension has been selected for further analysis. Plate 4 and another four plates, with only one parameter changed compared to plate 4, have been used to develop the heat transfer correlations. As shown in figure 1 (right), once the eight parameters are fixed, the geometry shape of the corrugation and PV panels is determined. The correlations for convective heat transfer coefficients are expressed using Nusselt number, which is based on the plate length and $h_{conv.ext}$ (or $h_{conv.int}$). The air temperature through the perforations is calculated using the effectiveness ε, defined in the following equation:

$$\varepsilon = \frac{T_s - T_a}{T_p - T_a} \quad (1)$$

From the simulation results, the following correlations can be obtained for the average exterior Nusselt number Nu_{ext}, average interior Nusselt number Nu_{int} and ε:

$$Nu_{ext} = \left(\frac{p}{e+H}\right)^{-0.0392}\left(\frac{e}{l}\right)^{0.762}\left(\frac{w}{p}\right)^{-0.125}\left(\frac{P}{d}\right)^{0.552}(0.00608 \cdot {Re_U}^{0.863} + 0.0869 \cdot {Re_V}^{0.88}) \quad (2)$$

$$Nu_{int} = \left(\frac{p}{e+H}\right)^{-0.869}\left(\frac{e}{l}\right)^{-2.996}\left(\frac{w}{p}\right)^{-0.175}\left(\frac{e}{D}\right)^{0.413}(0.005 \cdot {Re_U}^{0.922} + 0.482 \cdot {Re_V}^{1.004}) \quad (3)$$

$$\varepsilon = \left[2.1154 + \left(\frac{p}{e+H}\right)^{-1.154}\left(\frac{e}{l}\right)^{-0.776}\left(\frac{w}{p}\right)^{-0.265}\left(\frac{P}{d}\right)^{-1.952}(Re_V^2/Re_U)^{0.907}\right]^{-1} \quad (4)$$

where, the Reynolds number Re_U is based on the wind speed and plate length, while the Reynolds number Re_V is based on the suction velocity and plate length.

The corresponding R^2-value for Nu_{ext} and Nu_{int} is 0.992 and 0.972, respectively, which shows a good agreement with the CFD simulation results. The largest bias for Nu_{ext} appears when the wind speed is low (1 m/s) while the suction velocity is high (0.06 m/s), whilst for Nu_{int} the correlation gives less accurate prediction when the wind speed is high (10 m/s) and the suction velocity is low (0.01 m/s). For both scenarios, the prediction error is around 20 %. The R^2-value for ε is less satisfactory and equal to 0.733, which requires further investigation. However, the prediction error is still within 20 %.

Optimal Geometry

Similarly with the analysis presented above, although the PV surface temperature will vary for different geometry shapes, the differences are within 5 ˚C, which will result in an electrical efficiency change less than 0.5 %. Thus, the performance of each geometry shape is evaluated mainly based on the thermal energy efficiency, which can be assessed by the cavity exit air temperature when all the other conditions are the same.

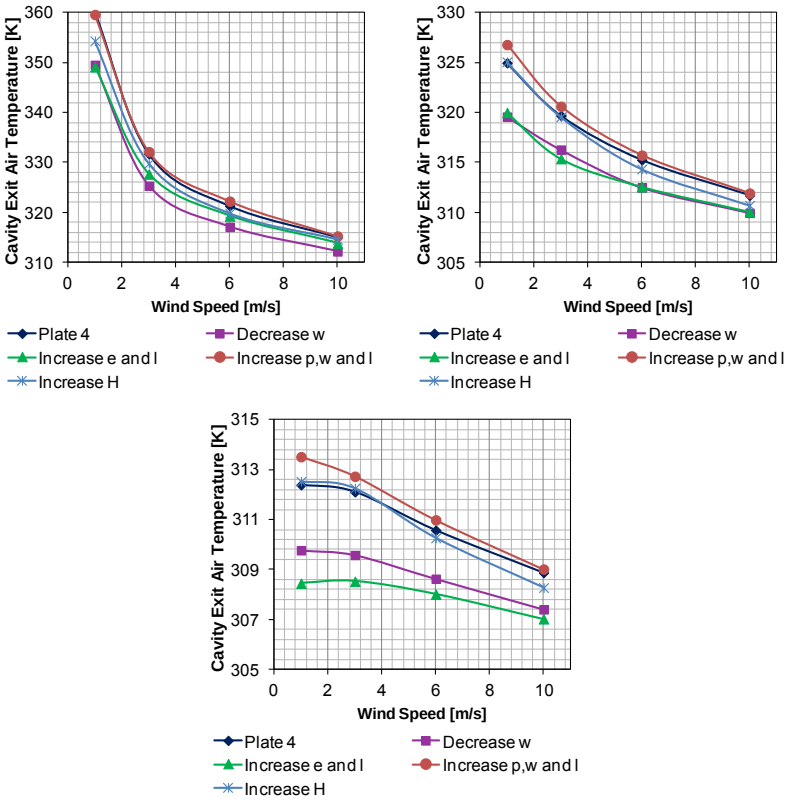

Figure 4: Comparison of cavity exit air temperature for different geometry shapes under different suction velocity: 0.01 m/s (left), 0.03 m/s (middle) and 0.06 m/s (right)

Plate 4 is considered as a base case since its UTC geometry is already an existing product in the market. Figure 4 shows the comparison of cavity exit air temperature for different corrugation geometry shapes, each with only one important parameter changed. The results shown in Figure 4 indicate that the plate with increased wavelength *p* (the crest *w* and slope length *l* will increase accordingly, as well as the PV module dimension *P* and gap distance *d*) can provide higher cavity exit air temperature compared to plate 4, especially when the suction velocity is high while the wind speed is low, the temperature difference is about 3 ˚C, which can result in 27 % more thermal energy. Other geometry shapes will reduce the system efficiency. The most unfavorable geometry change would be decreasing the crest length *w* and increasing the amplitude *e* (the slope length *l* will also increase accordingly), which will cause 50 % thermal energy decrease at most. The possible explanation would be that this geometry will enlarge the space between the PV modules and the UTC plate, which will cause recirculation inside and therefore trap more heated up air and reduce the captured heat at the cavity exit.

CONCLUSIONS

A detailed transient energy model for BIPV/T systems with UTCs has been developed, based on the thermal network representation, using a fully-explicit finite difference scheme, and it is used to evaluate the overall performance based on the cavity exit air temperature and the PV surface temperature. The results show that maximum combined electrical-thermal efficiency, more than 10 % higher than the case with largest PV modules, can be achieved with small PV modules and large coverage area. It is also recommended to increase the corrugation wavelength to improve the thermal performance, which can result in an increase of the thermal energy extraction up to 27 %. On the contrary, decreasing the crest length and increasing the corrugation amplitude will reduce the thermal efficiency significantly (up to 50%). Small temperature differences have been observed for different geometry shapes, which, however, are not expected to cause major efficiency drops.

REFERENCES

1. Athienitis, A.K., Bambara, J., O'Neill, B., & Faille, J.: A prototype photovoltaic/thermal system integrated with transpired collector. *Solar Energy*, 85: 139-153, 2011.
2. Candanedo, L.M., Athienitis, A.K., Candanedo, J., O'Brien, W. & Chen, Y.X.: Transient and steady state models for open-loop air-based BIPV/T systems. ASHRAE Transactions, 116: 600-612, 2010.
3. Leon, M.A. & Kumar, S.: Mathematical modeling and thermal performance analysis of unglazed transpired solar collectors. Solar Energy, 81: 62-75, 2007.
4. Li, S., Karava, P., Savory, E. & Lin, W.E.: Airflow and thermal analysis of flat and corrugated unglazed transpired solar collectors. Solar Energy, 91: 297-315, 2013.
5. Li, S., & Karava, P.: Evaluation of turbulence models for airflow and heat transfer prediction in BIPV/T systems optimization. Proceedings of 1st International Conference on Solar Heating and Cooling for Buildings and Industry, Energy Procedia, 30: 1025-1034, 2012.

DESIGN AND FIRST EXPERIENCES OF A SOLAR THERMAL HEATING SYSTEM WITH HEAT PUMP AND ICE STORAGE

Daniel Philippen, Michel Y. Haller, Stefan Brunold, Elimar Frank

Institut für Solartechnik SPF, Hochschule für Technik Rapperswil, Oberseestrasse 10, 8640 Rapperswil, Switzerland, Phone: +41 55 222 48 30, daniel.philippen@solarenergy.ch

ABSTRACT

The development and realization of a heating system that uses solar collectors, a heat pump and an ice storage is described and first results of the operation phase of a pilot plant are presented. The heating system is designed to reach a seasonal performance factor (SPF_{sys}) of 6 in a climate like the one of Zurich and in buildings with low temperature heat distribution system and with a heating demand for space heating of 100 kWh per year and square meter of energy supply area.

A comparison of different concepts for heating systems consisting of a solar collector field and a heat pump is drawn. With computer simulations the sizes of the main components that are needed in order to reach an SPF_{sys} of 6 are determined. The dynamic performance of a chosen system concept in a building is simulated with computer simulations in TRNSYS. The simulations show that an SPF_{sys} of 6 can be reached with a solar collector field of 30 m^2, a brine-water heat pump, and an ice storage of 30 m^3 where solar heat can be stored from summer to winter time. The simulations are also used to develop the system´s control strategy.

A new feature of the ice storage that was developed for this project is the ability to de-ice the heat exchanger surfaces periodically in order to maintain the high heat transfer coefficient that is decreasing when the thickness of the ice on the surface of the heat exchanger is increasing. Thus, the heat source temperatures for the heat pump remain relatively high at all times. To enable de-icing special immersed heat exchangers were developed that are mounted at the bottom of the ice storage.

A pilot plant which is based on the developed system concept was installed in a kindergarten in Rapperswil (SG) end of 2012. Performance factors are presented and compared with the system simulations.

Keywords: solar thermal heat pump system, high efficiency, ice storage, de-icing, pilot plant

INTRODUCTION

In most of the new buildings in Switzerland and also for refurbishment of heating systems heat pumps are used to provide heat for space heating and domestic hot water [1]. To reduce the electric energy demand of the heat pump solar thermal collectors can be used in order to reduce the operating hours of the heat pump or to increase the source temperature at the evaporator of the heat pump [2]. Both measures reduce the electricity consumption of the heat pump and thus lead to lower costs of operation and environmental impact caused by the use of electricity.

The development of a heating system which combines a heat pump, solar collectors and an ice storage is presented in the following. The heating system consumes a smaller amount of electricity due to the use of solar heat and reaches high seasonal performance factors (SPF_{sys} 6 for buildings with low temperature heat distribution). Solar heat that is used directly or stored

temporary in an ice storage is the solely heat source of the heat pump. With this approach no boreholes or air heat exchanger for the heat pump is necessary.

Definition of the system's seasonal performance factor, SPF_{sys}

To assess the efficiency of a heating system concerning its consumption of electricity while a fixed amount of useful heat is provided the system's seasonal performance factor (SPF_{sys}) is used. The SPF_{sys} takes into account the losses of storages in the heating system which is especially relevant in systems with large storages. Only heat that is delivered to the space heat distribution pipes and to the domestic hot water distribution pipes is counted as useful heat. The SPF_{sys} is calculated as ratio of the useful heat and the total electricity demand of the heating system (including e.g. compressor, circulating pumps and controls) for one year:

$$SPF_{sys} = \frac{Q_{Spaceheating} + Q_{DomesticHotWater}}{W_{Electricity}} \quad (1)$$

Ice storage as components of a solar heat pump system

Ice storages are heat storages that besides sensible heat also deliver latent heat of the water that is used as storage medium. A heat pump can be used to increase the temperature of the extracted heat to a level that is needed in the building for space heating and domestic hot water. Due to the utilization of the latent heat ice storages have a high volumetric storage capacity and their size can be reduced compared to normal heat storages. Lower or even reversed temperature differences to the surroundings allow a reduction of insulation leading to lower costs of material.

There are only a few solar thermal heat pump systems available on the market that use ice storages to store solar heat diurnally or seasonally. The heat exchangers in these ice storages mostly are ice-on-coil types where heat is extracted from the storages with long tubes serving as heat exchangers [3]. Ice is formed on the tubes if the temperature on its surface drops below the freezing point of water. Depending on the distances between the tubes and the amount of heat extracted, the ice layer can reach a thickness that leads to a significant increase of the heat transfer resistance from the water/ice boundary layer (where latent heat is released) to the brine inside the heat exchanger. This leads to decreasing temperatures in the brine and hence to a decreasing coefficient of performance of the heat pump.

In this project a flat plate heat exchanger was developed that can be de-iced by removing the ice layers on the heat exchanger's surfaces if the overall heat transfer coefficient drops below a certain threshold.

METHODS

System simulations

Different concepts for the principle design of a heating system that combines solar collectors and a heat pump and reaches an SPF_{sys} of 6 were simulated and compared. A mathematical model for these systems was build up that takes into account climatic conditions, the heating demand of the building and the energy flows of the systems components in 1-hour time steps. The comparison was used to choose a promising system concept for the further analyses. The selected system concept was simulated with the software TRNSYS to find suitable sizes of the system components and a suitable control strategy. The simulation model consists of a building and its heating system and takes transient heat sources and sinks into account like climate and heating demand in the building. The simulations in TRNSYS were done in time steps of 2 minutes.

Development of a heat exchanger that can be de-iced
As the ice storage in the heating system that was designed has a large volume a flat plate heat exchanger was developed that ensures a high heat transfer rate with low costs of materials.

Validation of the mathematical model of the ice storage with experimental data
For the TRNSYS simulations a mathematical ice storage model including the newly developed heat exchangers was programmed and validated with data derived from experiments in a lab-sized ice storage with 1 m^3 volume.

Construction and monitoring of a pilot plant
A heating system with solar collectors, a heat pump and an ice storage as main components was constructed and put into operation in January 2013. All relevant quantities like temperature, mass flow and irradiation that have an effect on the system's performance are measured with a monitoring system.

RESULTS

Simulation of system concepts

A main distinction between the system concepts that were examined is the way the solar heat is used: with a parallel combination the collectors and the heat pump are loading the warm storage independently from each other. With a serial combination the solar heat of the collectors is used solely as a heat source of the heat pump's evaporator. Systems where the solar heat is used in both ways are combined parallel-serial [4].

The simulations are done for a single family house that has a heating demand of 14 MWh/a with an energy reference area of 140 m^2, a low temperature heat distribution system and a warm water demand of 3 MWh/a [5]. In Table 1 simulation results for the sizes of the main components of different heating systems and the seasonal performance factors are listed. System concept No.1 is a reference system without solar support for the heating. In concept No.2 solar collectors and the heat pump are combined in parallel. The other concepts include an ice storage and have a combined parallel-serial implementation of solar collectors and the heat pump. In concept No.3 a heat pump is simulated that can either use heat from air or from the ice storage as heat source. In concept No.4 the only heat source of the heat pump is the ice storage that is loaded by the solar collector.

No.	System concept	Type of heat pump	SPF_{sys}	Collector area [m^2]	Volume of warm storage [m^3]	Volume of ice storage [m^3]
1	Air source HP without solar collectors	Air-water	2.8	-	0.5	-
2	Air source HP with solar collectors	Air-water	6.0	100	3	-
3	Air/brine source HP & Solar & Ice storage	Air/Brine-water	6.0	45	2	5
4	Brine source HP & Solar & Ice storage	Brine-water	6.0	32	2	35

Table 1: Simulated sizes of the main components of solar thermal heating systems reaching an SPF_{sys} of 6 in a single family house (System No.1: reference system with SPF_{sys} 2.8; HP: heat pump, Solar: solar collectors).

The analysed solar-heat pump systems with air-brine heat pumps which store the solar heat only in a warm storage (system concept No.2) need both a large collector field (100 m^2) and a large warm storage (3 m^3) to reach an SPF_{sys} of 6. In systems where solar heat is stored also in

an ice storage and used afterwards as a heat source of the heat pump (concept No.3) the sizes of the system components can be reduced significantly. However, in these systems the heat pump has to be equipped with a special evaporator that can handle both air and brine as heat source. System concept No.4 with brine-water heat pump reaches an SPF_{sys} of 6 with a comparatively small collector field but it needs a large ice storage.

It was decided to design a heating system in accordance with system concept No.4 as it can be realized mainly with standard components (normal brine-water heat pump) and has no visible components outside the building apart from the collectors.

To get more reliable results the dynamic performance of the chosen system concept was simulated with computer simulations in TRNSYS. The simulations were used to resize the components of the heating system to reach an SPF_{sys} of 6 and to develop the system´s control strategy (fig. 1).

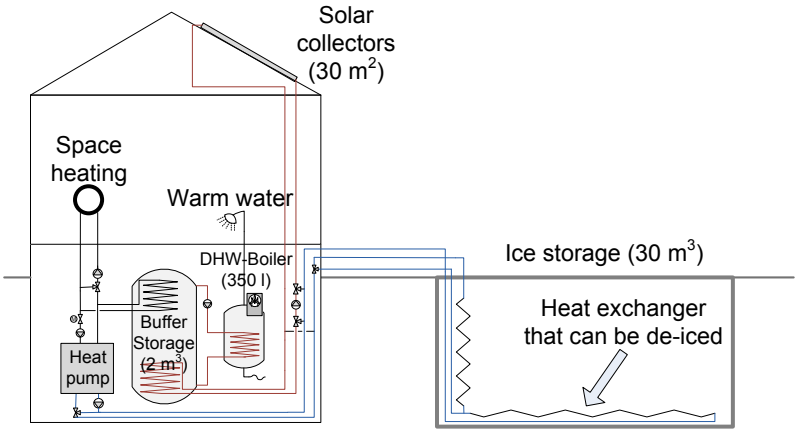

Figure 1: Simplified hydraulic scheme of the simulated heating system with ice storage and SPF_{sys} of 6 and sizes of the main components for a single family house.

The monthly balances of the energy flows through the heating system for a simulated year are shown in fig. 2. Highest solar gains occur from March to May when the water in the ice storage is melted. Solar heat is stored in and extracted from the ice storage throughout the whole year. The relative amount of energy that is provided by the solar collectors during one year (solar fraction) is 84%.

Development of a heat exchanger that can be de-iced

A flat plate heat exchanger was developed that can be de-iced periodically with heat (fig. 3, right) [6]. When the heat pump has produced ice on the heat exchanger and is switching off the heat exchangers are heated up shortly for de-icing. The de-icing is mainly made with heat from the solar collectors. In times with low irradiation on the collector field, heat from the lower part of the buffer storage can be used (fig. 1). The ice layers separate from the heat exchanger surfaces due to their buoyancy and float upwards to accumulate at the surface of the water.

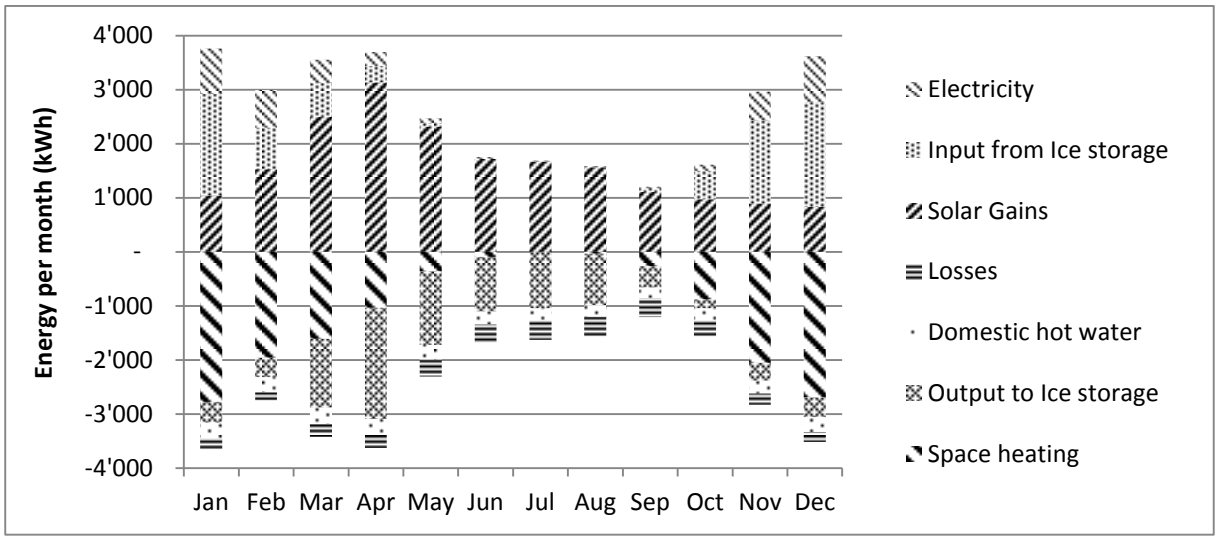

Figure 2: Simulated energy flows per month of the heating system with ice storage reaching an SPF_{sys} of 6 in a single family house with space heating demand of 14 MWh per year.

Pilot plant

A pilot plant with the developed heating system was put into operation in January 2013 (fig. 3). The pilot plant was installed in a kindergarten with a heating demand of 35 MWh/a and with a high temperature heat distribution system. The sizes of the main components of the installed heating system are 50 m^2 glazed collectors, 17 m^2 unglazed façade collectors, 3.5 m^3 warm buffer storage, 75 m^3 ice storage and an 18 kW (@ B2W45) heat pump.

Figure 3: The collector field of the pilot plant on the roof of the kindergarten in Rapperswil SG (left) and view into the buried ice storage of the pilot plant before filling with heat exchangers at the bottom that can be iced and de-iced (right).

The measurement data derived from the monitoring of the pilot plant is used to validate the TRNSYS simulations of the system. A first comparison for 17 days in April 2013 (9.4. - 25.4 2013) was drawn (fig. 4). The demand for domestic hot water is not shown as the demand in the kindergarten is generally low and can be neglected for the analysed period of time. The performance factors for this period are 6.9 for the measurement and 6.7 for the simulation.

Generally the results of the simulation show a good agreement with the measurement for the period that was evaluated. However the differences between the measured and the simulated performance factors and a difference in the measured and the simulated exchange of heat with the ice storage has to be analysed in further work.

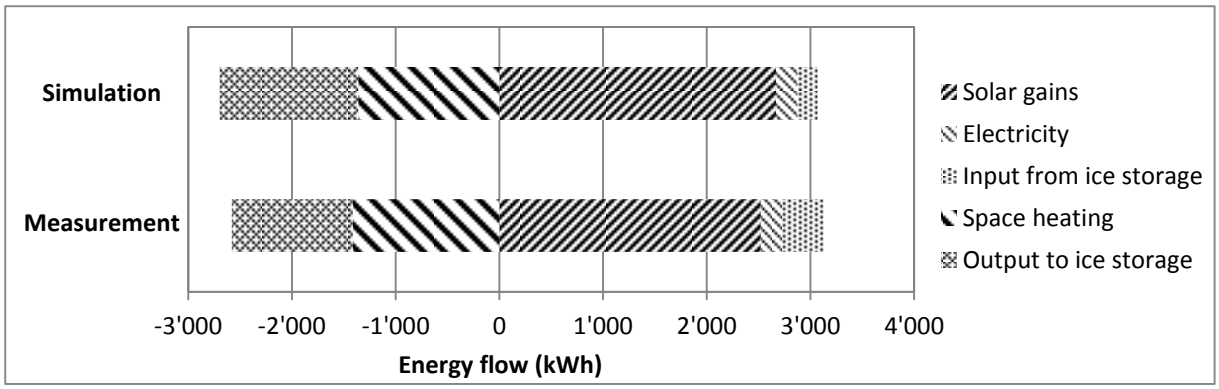

Figure 4: Comparison of simulated and measured energy flows in the heating system of the pilot plant for 17 days in April 2013.

CONCLUSION

Different ways of how solar thermal heat pump systems can reach a high efficiency regarding the use of electricity were compared. A promising concept with a large outside buried ice storage was chosen that uses solar heat as solely heat source for the heat pump. As a consequence the heating system does not need boreholes or air heat exchangers outside the building. Simulations show that an SPF_{sys} of 6 in a single family house can be achieved with 30 m^2 solar collectors, 30 m^3 ice storage, 2 m^3 buffer storage and a newly developed concept for unloading of the ice storage. The pilot plant that was put into operation 2013 is running properly. The simulations of the energy flows and the system performance show a good agreement with the measured data of the pilot plant. We expect to be able to present the first annual balance and SPF_{sys} of the pilot plant in spring 2014.

The work presented was carried out in an R&D project financed by the Elektrizitätswerk Jona-Rapperswil AG, Switzerland.

REFERENCES

1. CS 2009: Swiss Issues Immobilien, Immobilienmarkt 2009, Fakten und Trends. Credit Swiss Economic Research, Zürich
2. Frank E., Haller M. Y., Herkel S. & Ruschenburg J., 2010. Systematic Classification of Combined Solar Thermal and Heat Pump Systems. In: Proc. of the EuroSun 2010 Conference, Graz, Austria.
3. Hadorn J-C (Ed.): Thermal energy storage for solar and low energy buildings, IEA Solar Heating and Cooling Task 32 (2005).
4. Haller M. Y., Frank E. (2010): Kombination von Wärmepumpen mit solarthermischen Kollektoren – Konzepte und Fragestellungen, BRENET – 16. Status-Seminar „Forschen und Bauen im Kontext von Energie und Umwelt“, ETH Zürich, 2./3. September 2010
5. Heimrath R. und Haller M. Y., 2007. Project Report A2 of Subtask A: The Reference Heating System, the Template Solar System [Bericht]. - Graz : Institut für Wärmetechnik, Graz University of Technology, 2007.
6. Philippen D., Haller M. Y., Logie W., Thalmann M., Brunold S., Frank E., 2012. Development of a heat exchanger that can be de-iced for the use in ice stores in solar thermal heat pump systems. SPF, Rapperswil, EuroSun2012

AIPV VISUAL ASSESSMENT FOR ARCHITECTURE RETROFITTING

R. Xu; S.K. Wittkopf

Competence Centre Envelopes and Solar Energy, Lucerne University of Applied Sciences and Arts

ABSTRACT

Typical architecture designers convey through vague and qualified notions. With the increasing number of PV installations on buildings, architects are forced to corporate with technicians and engineers in the design processes. However, the communications between them are often hindered because unlike architects who communicate through semantic descriptors and visual images, engineers are used to interact with quantified terms. One way to solve this problem is adapting visual impact assessment for PV installed on façade so that one can foresee and evaluate its final overall effect in a way that is comprehensible for both sides. The visual impact assessment is a method mainly used in landscape design for evaluating the influence manmade changes caused on natural landscape. Now it is vastly used on aesthetic assessment for wind farms being built on open landscapes all over the world. Comparing with wind farms, the relevant researches for Photovoltaics are rather underdeveloped. The estimation of visual effect created by integrating solar energy components on open landscape is rarely investigated, let alone on architecture where it is more complicated because more aesthetic factors are involved. With the increasing number of Photovoltaics installed or to be installed on architecture facades, it is necessary to develop a rational visual assessment tool to better evaluate the appearance outcome of the final installation. Based on summarizing research experiences and literatures from former visual impact assessments, this paper tries summarize the possible factors that are relevant for AIPV installation, and changes and extensions on existing theories are being made when necessary. The final results will benefit architects, engineers during the planning process, and eventually for law regulator in laying down clear and reasonable urban planning regulations regarding installing PV in urban areas. In the end, the author will apply the visual impact theory on a retrofitting project where AIPVs are assigned to be installed on a church in Lucerne, Switzerland.

Keywords: AIPV, Architecture Integrated Photovoltaics, Visual Assessment, retrofitting, Visual Impact

1. INTRODUCTION

Solar energy production is a booming technology and is welcomed especially among private investors in cities and suburbs. The government tries to encourage this trend by authorizing legal and bureaucratic simplification [1]-[4], but often the process is hindered due to administrational obstacles such as from historical preservation department, claiming many of them to be visually destructive to the existing architecture/environment [5]-[7]. Traditional architectural design process uses very vague notions, participants mostly communicate semantically to explain their pictorial demonstrations, as is the case when the historical restoration department explains their rejection reasons to the applicants, who are often even more confused after the explanation where mostly qualitative descriptors are used. Also architects and engineers often have very different understandings of certain words and what a good combination of PV on architecture is, which sometimes leads to bi-poled opinions on same subjects [8]. Survey shows that the main problems of solar architecture today can be summarized as following: the lack of diversity in solar panels; the professional tools that are available for solar energy assessment are mainly oriented to the engineers instead of to architects or to both [9]. The blockage between architects and engineers needs to be counteracted and one of the solutions would be to transform these vague notions into parameters and to lay clear defined physical features to those semantic descriptors in the design process. Visual impact assessment is one way to quantitative the evaluation on the effect of renewable energy, with practices done on wind energy in open landscapes substantially outnumbering the practices done on solar plants on open landscape, let alone on solar panels on architecture. This is why this paper would like to dedicate the research to develop a tool to appropriately evaluate the visual fitness of PV on architecture, to both lay a sound and sophisticated foundation for urban planning guidelines and regulations regarding solar energy, and to clear the communication barrier between architects, engineers and other stakeholders.

2. LITERATURE REVIEWS

The importance of visual impact caused by using renewable energy technology is getting more recognized by the public over the years. Especially the subjective evaluation of wind farms on open landscape, both theories and methods are already well established [10]-[14]. In the paper of Tsoutsos [15], even though no evaluation methods were discussed, the author states that the trend of "hiding" solar elements is fading and that the architects are beginning to realize the aesthetic appeal of solar elements and use them in attractive and visible ways. Work by Torres Sibille et al [16] is one of the very few works done on scientifically evaluating the visual impact of solar plants in open landscape. This work was carried out on the basis of their former work [17] on evaluating visual impacts on wind farms in open landscape. They have developed a parameter called Objective Aesthetic Impact of a Solar Power Plant installed on a landscape (OAIWF), which is dependent on the following sub-parameters: visibility, color, climatology coefficient, fractality and concurrence parameters of the technology and site. With the reference to and some modifications on the work of Torres Sibille et al [16] mentioned before, Chiabrando [18] applied the similar theory on the visual impact assessment of solar power plants (can be both solar thermal collectors or photovoltaic) with the term OAISPP, which varies between the value 0 – 1 (0 being the least, 1 the most effective impact), decisive by the following sub-parameters: the visibility of the plant (Iv); the colour of the plant compared to the colour of the immediate surrounding (Icl); the shape of the plant (If); the concurrence of various forms and types of panels in the same plant (ICC). However, it is undeniable that the solar energy implementation on buildings requires more care and caution as compared to installing renewable energy farms on open landscape, as architecture is a small scaled and delicate work of art itself. Probst and Roecker [19] evaluated the architectural integration of solar thermal systems by dividing them into functional (integrating solar heat collection function and other envelope functions), constructional (mainly constructive issues) and formal aspects. Formal aspect refers to how well the equipment is integrated architecturally with the building and can be graded with three progressive levels: basic, medium to advanced level. The advanced level means that beside offering flexibility in terms of the solar collectors' shape, size, module jointing, color, visible surfaces textures and finishes, dummy modules and complementary interface elements (jointing/finishing/angular components) should also be provided by the producers. The theory developed is mainly based on acceptance surveys on different stakeholders. The methods of the above mentioned visual assessment theories vary from strictly parametric analysis to doing acceptance surveys and to merely semantic descriptions. These theories and methods can be used as foundation as references for assessing visual impacts of AIPV.

3. DISCUSSION

In this part, the author will discuss about the aspects that are important to the formal aspects of implementing AIPV (Architecture Integrated Photovoltaic) on building facades. Hereby the technical aspects, such as efficiency of the PVs, are omitted and the focus will be solely on the architectural formal integration, and theories from related architecture design aspects will be introduced and referred.

3.1 Location

Often during the design phase, it is difficult to decide where exactly to locate the PV panel that is the most efficient and at the same time will lead to the most appropriate visual impact. The method of setting up a 3D digital model in helping to visualize the design is a routine in architecture branch. Several practices show that Ecotect to be an efficient tool in solar optimizing of the digital 3D model [20]-[22]. Compared to wind farms on open spaces, AIPV will stay still for the most of the time, therefore Ecotect combined with 3D renderings will be used to balance the most probable locations for gaining sufficient solar radiation and architecture aesthetic.

3.2 Silhouette and Detail

To install AIPV on the façade of a building, it is important to know ahead how its size, detail and texture are going to affect the overall appearance of the building. There had been precedents in investigating the silhouette and complexity effects.

According to Van der Laan's [23] theory, if one form is intended to appear to be part of the other form, its respective dimensions have to be in the range of 1–1/7 of the latter form. If the ratio falls

between 1/7 and 1/49, then it will be the ornament of the latter, and below 1/49, the form will come out as trim, detail and texture. Stamps III [24] tested this theory and his results suggests that trim and ornament affect the architecture detail more than texture does. He [25] also states that surface complexity would make the most in the architectural façade, followed by silhouette complexity and façade articulation. Therefore it is meaningful to seriously consider the different size of the AIPV as it will cause different impacts on the overall appearance on the building façade. When necessary, the details of AIPV should be handled thoughtfully, which means that e.g. the gaps between the panels should not be defined arbitrarily but with regard to the architecture details. Also module jointings should be chosen carefully such as the material (EPDM or metal), color (same or contrast color as the absorber) and size (large jointing width or rather as a slim embroider) (Fig. 1).

Fig.1 Megaslate from 3S Photovoltaics, Suntech PV Module, First Solar PV Modules

The work of Attneave [26] suggests that for random polygons, the most important effect will be caused by the number of turns. Also Stamps [27] reports that the number of turns in the architecture silhouette has the most effect on shape complexity. Neither of the other parameters such as symmetry, the number of lengths of line silhouette segments nor the number of angles between those silhouette segments share comparable importance. Both cases indicate that for architectural silhouettes, the impression of complexity can be indicated very well from the turns in the form-outlines. Akalin [28] made experiments on the impressiveness and preference in residential architecture. The students will see a set of houses where they will decide their favor for the house with a changing variety on complexity details. It turns out that preference (fondness) was much stronger than impressiveness in both the minimum and intermediate complexity levels, but this relationship seems reversed at maximum complexity level, i.e. impressiveness was much stronger than preference (fondness). At present the PV panels can exist in many shapes thanks to dummy parts. These literatures suggest that special attention should be paid to the silhouette forms of the architecture and the PV panels (complexity, number of turns etc.), so that they share a certain connection with each other, and can exits harmoniously together, and that the PV panels will not be standing out boldly and conspicuously.

3.3 Style of architecture

Dalit Shach-Pinsly et al [29] argues that façade openings will link with human`s feel of privacy and comfort. [30] proposed a term called void-to-solid ratio, which is defined by the proportion of openings (such as windows or glasses) to the solid part (such as walls) on a façade. He believes that it can be an implication to the style and function of the certain architecture. Since PV panels are usually highly reflective and share the same reflectivity feature with window glasses, meaning that it can be treated as window components for observers. The ratio between window and wall ratio, or between the reflective and antireflective surfaces should be cautiously arranged, e.g. for historical architectures, it is the best to keep the ratio as original as possible, and for newer buildings, the ratio can be changed but should overall be kept in balance.

Architecture is also a design process that deals with ratio and proportion. Further literature studies should be made on theories about these areas. However, it is certain that e.g. if a building that was designed to have a horizontal trend and meant to give out a massive and stable atmosphere, then a single vertical PV panel component sticking out from the façade would certainly be inappropriate.

3.4 Material, Colour parameters and Light

[31] carried out the evaluation of the architecture façade only by changing the one parameter, namely the hue based on the similarity between the façade color and its natural surroundings. Torres Sibille et al [16], [17] and Chiabrando et al [18] deepened the definition of color contrast by using CIE color formulae to define the difference between the equipment and its surroundings. Here the color is identified by the colorimetric coordinates hue, saturation and brightness. L. Oberascher [32] claims

that perception of color in architecture is dependent on space and time, material and form, light and surface and the user itself. The last method might be the most appropriate for analyzing architecture integrated solar panels impacts, because unlike being on an open landscape, the color combination of architecture is more meticulous and is mostly comprised of multiple complex colors and materials where bumping and texture (based on their scale) can also be an issue. Thus same prudence shall be given to PV modules when choosing their color. Moreover, special attention should be dedicated to the unique feature of AIPV color that changes all the time with the shifting angle of the incoming light.

4. AN EXAMPLE OF APPLICATION

The following part is a progress report where it is the author's first attempt to design AIPV on a church façade by taking visual impact assessment into account. Due to time constraint, only location analysis and void-solid ratio theories are adopted. Further analyses are to come. Since the installing PVs on the roof of the buildings and hiding behind the parapet wall is clearly a natural choice without any effect on the façade, this option will be omitted from the discussion. Only options where the AIPV will take an effect the façade will be paid attention to.

The Catholic Church St. Michael lies in Lucerne, Switzerland and is required to be retrofitted with Photovoltaic. The church as a representative of 1960`s Brutalism and has an emphasis on the massiveness and horizontality, the installation requires extra care to be well integrated with the architecture, since for retrofitting projects that are under the protection of historical preservation, it is important to retain the original atmosphere. The suitable locations of the PV were carefully defined using simulations per Ecotect based on digital 3Dmodel made from sketch up. The findings in annual solar radiation analysis and shadow range in winter and summer are shown in Fig. 2 – Fig. 4.

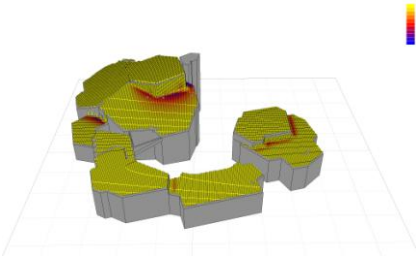

Fig.2 Annual Solar Radiation Analysis via Ecotect

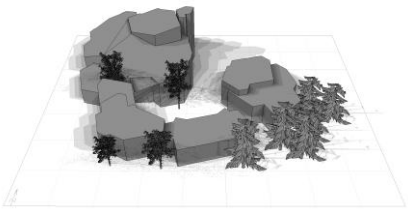

Fig.3 Shadow range summer via Ecotect

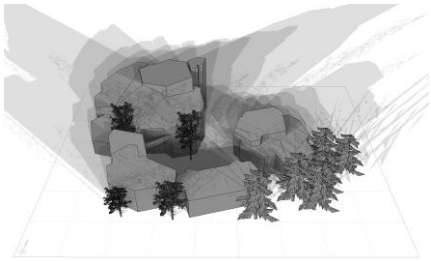

Fig.4 Shadow range winter via Ecotect

Since this church is under restoration protection, it will be very necessary to maintain its original style, and eventually its original solid-void ratio. As in this case, the solid void ratio refers to the proportion between the windows and opaque walls. Fig. 5 demonstrates the analysis of solid void ratio on different facades via AutoCad. The findings are that the main facades of the church possess an average ratio that is normally under 0.1, with less windows and a more sacral, monumental appearance; while on the side with residential function the ratio being much higher (0.15 or more) as there are more transparent areas.

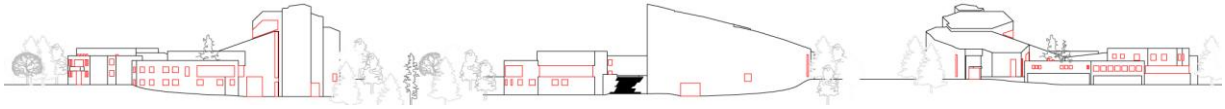

Fig.5 Solid-void-ratio

5. RESULTS

Based on the findings from above, it can be concluded that for large area AIPV installation, it can only be processed in the following 4 ways: (a) outside the church building complex (e.g. parking area)

where the appliances are practically "invisible" and the ratio will not be affected, (b) on the sloping roof of the church where the ratio will only be very slightly affected, (c) on the original window area where the ratio will stay the same, and (d) on the residential part of the building, where the higher ratio will not do much harm to the original atmosphere. Do to the reflecting characteristic of the PV panel surface, a lowering of the ratio will not be feasible. The results are presented in the Fig. 6.

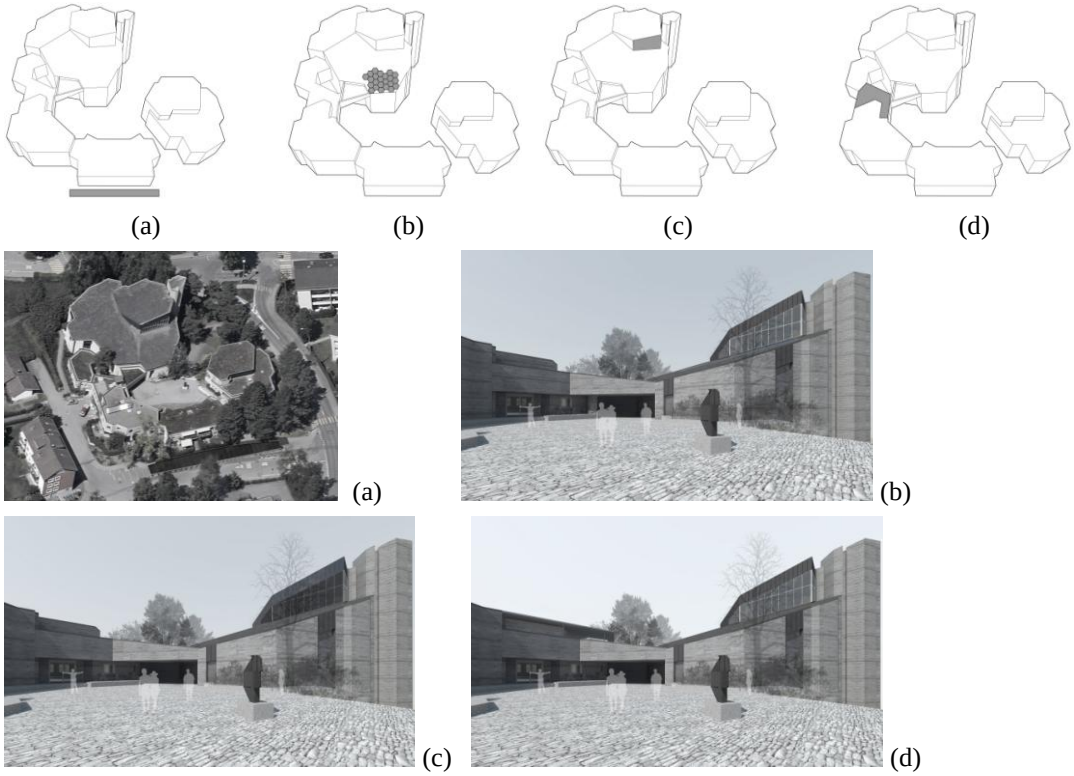

Fig.6 (a) on the roof of the church, (b) on the parking space (c) on the original window area and (d) on the residential part of the building

6. DISCUSSION ON THE RESULTS AND OTHER PROBLEMS

This work is the author's first attempt to develop a design methodology based on analyzing the visual impact of the AIPV on facades beforehand. Even though the results are developed on the basis of quantifying the parameters and rational reasons, there is still a lot of architectural design thinking involved. This kind of thinking needs to be clarified in the future so as to better serve the purpose of processing a rational design. Other problems also involve:

1. In this paper, only the existing theories are being looked into so far. In the upcoming future, crystallizing parameters that are fit for visual impacts of AIPV should be developed.
2. The energy production (which is proportional to the area of PV) of AIPV hasn't been taken into consideration yet. This is of course a crucial point that separates PV from any other architectural components.
3. For architecture observer, the height and viewpoint is decisive in the design process. Visual impacts strongly depends on the AIPV's visibility to the observer, whereas different from the wind farms, the distance is by far not as pivotal as the observation angle. Thus theories about how to define the most suitable viewpoints should be investigated.

REFERENCES

[1] Schweizerischer Bundesrat, "Bundesgesetz über die Raumplanung (Raumplanungsgesetz, RPG)(Vom 22.6. 1979)," Bern, SR, vol. 700, 1979.

[2] Department Bau, Verkehr und Umwelt, Department Bildung, Kultur und Sport Kanton Aargau, "Merkblatt Solaranlagen," pp. 1–5, Feb. 2012.

[3] Bau und Verkehrsdepartment des Kantons Basel-Stadt and Department für Wirtschaft, Soziales und Umwelt des Kantons Basel Stadt, "Richtlinie_Solaranlagen_BS_PDF.indd," pp. 1–6, Dec. 2012.

[4] Regierungsrat des Kantons Bern, "Richtlinien - Baubewilligungsfreie Anlagen zur Gewinnung erneuerbarer Energien," pp. 1–32, Jul. 2012.

[5] “Ortsbild kommt Solaranlagen in Zunzgen nicht mehr lange indie Quere,” http://www.bzbasel.ch/basel/baselbiet/ortsbild-kommt-solaranlagen-in-zunzgen-nicht-mehr-lange-in-die-quere-124869377,7/ 2012
[6] “Familie Wildhaber ändert Rechtspraxis, 8890 Flums, SG,” http://www.solaragentur.ch/images/content/PDF/Seiten%20aus%20G-11-10-31%20Wildhaber%20def_KA.pdf?PHPSESSID=815a2ae977ea39ba06b642aa69ea6f03, Oct. 2011.
[7] “Keine Sonne über den Weilern,” http://www.aargauerzeitung.ch/schweiz/keine-sonne-ueber-den-weilern-5276784, Dec. 2009.
[8] M. Munari Probst and C. Roecker, “Towards an improved architectural quality of building integrated solar thermal systems (BIST),” Solar Energy, vol. 81, no. 9, pp. 1104–1116, Sep. 2007.
[9] M. Wall, M.C. M. Probst, C. Roecker, M.-C. Dubois, M. Horvat, O. B. Jørgensen, and K. Kappel, “Achieving Solar Energy in Architecture-IEA SHC Task 41,” Energy Procedia, vol. 30, pp. 1250–1260, Jan. 2012.
[10] J. HURTADO, “Spanish method of visual impact evaluation in wind farms,” Renewable and Sustainable Energy Reviews, vol. 8, no. 5, pp. 483–491, Oct. 2004.
[11] J. Molina-Ruiz, M. J. Martínez-Sánchez, C. Pérez-Sirvent, M. L. Tudela-Serrano, and M. L. G. Lorenzo, “Developing and applying a GIS-assisted approach to evaluate visual impact in wind farms,” Renewable Energy, vol. 36, no. 3, pp. 1125–1132, Mar. 2011.
[12] Jacob Ladenburg, “Visual impact assessment of offshore wind farms and prior experience,” Applied Energy, vol. 86, no. 3, pp. 380–387, Mar. 2009.
[13] T. Tsoutsos, A. Tsouchlaraki, M. Tsiropoulos, and M. Serpetsidakis, “Visual impact evaluation of a wind park in a Greek island,” Applied Energy, vol. 86, no. 4, pp. 546–553, Apr. 2009.
[14] G. B. Jerpåsen and K. C. Larsen, “Visual impact of wind farms on cultural heritage: A Norwegian case study,” Environmental Impact Assessment Review, vol. 31, no. 3, pp. 206–215, Apr. 2011.
[15] T. Tsoutsos, N. Frantzeskaki, and V. Gekas, “Environmental impacts from the solar energy technologies,” Energy Policy, vol. 33, no. 3, pp. 289–296, Feb. 2005.
[16] A. D. C. Torres Sibille, V.-A. Cloquell-Ballester, V.-A. Cloquell-Ballester, and M. Á. Artacho Ramírez, “Aesthetic impact assessment of solar power plants: An objective and a subjective approach,” Renewable and Sustainable Energy Reviews, vol. 13, no. 5, pp. 986–999, Jun. 2009.
[17] A. D. C. Torres Sibille, V.-A. Cloquell-Ballester, V.-A. Cloquell-Ballester, and R. Darton, “Development and validation of a multicriteria indicator for the assessment of objective aesthetic impact of wind farms,” Renewable and Sustainable Energy Reviews, vol. 13, no. 1, pp. 40–66, Jan. 2009.
[18] R. Chiabrando, E. Fabrizio, G. Garnero, “On the applicability of the visual impact assessment OAISPP tool to photovoltaic plants,” Renewable and Sustainable Energy Reviews, vol. 15, no. 1, pp. 845–850, Jan. 2011.
[19] M.C. M. Probst and C. Roecker, Architectural Integration and Design of Solar Thermal Systems, EPFL Press, 2011.
[20] E. Mark, “Optimizing solar insolation in transformable fabric architecture: A parametric search design process,” Automation in Construction, vol. 22, no. C, pp. 2–11, Mar. 2012.
[21] J. Kanters and M. Horvat, “Solar Energy as a Design Parameter in Urban Planning,” Energy Procedia, vol. 30, pp. 1143–1152, Jan. 2012.
[22] X. Shi and W. Yang, “Performance-driven architectural design and optimization technique from a perspective of architects,” Automation in Construction, vol. 32, no. C, pp. 125–135, Jul. 2013.
[23] H. Van der Laan, Architectonic Space: Fifteen Lessons on the Disposition of the Human Habitat. Leiden, The Netherlands: Brill Academic Publishers, 1983.
[24] A. E. Stamps III, “Architectural detail, Van der Laan septaves and pixel counts,” Design Studies, vol. 20, no. 1, pp. 83–97, 1999.
[25] A. E. Stamps III, “Physical Determinants of Preferences for Residential Facades,” Environment and Behavior, vol. 31, no. 6, pp. 723–751, Nov. 1999.
[26] F. Attneave, “Physical determinants of the judged complexity of shapes”, Journal of Experimental Psychology, vol. 53, no. 4, pp. 221–227, Apr. 1957.
[27] A. E. Stamps III, “Complexity of architectural silhouettes: From vague impressions to definite design features”, Perceptual and Motor Skills, vol. 87, no. 3, pp. 1407–1417, Dec. 1998.
[28] A. Akalin, K. Yildirim, C. Wilson, and O. Kilicoglu, “Architecture and engineering students • evaluations of house facades: Preference, complexity and impressiveness,” Journal of Environmental Psychology, vol. 29, no. 1, pp. 124–132, Mar. 2009.
[29] D. Shach-Pinsly, D. Fisher-Gewirtzman, M. Burt, “Visual Exposure and Visual Openness: An Integrated Approach and Comparative Evaluation,” Journal of Urban Design, vol. 16, no. 2, pp. 233–256, May 2011.
[30] M. M. Alkhresheh, “Preference for void-to-solid ratio in residential facades,” Journal of Environmental Psychology, vol. 32, no. 3, pp. 234–245, Sep. 2012.
[31] Z. O'connor, “Bridging the Gap: Façade Colour, Aesthetic Response and Planning Policy,” Journal of Urban Design, vol. 11, no. 3, pp. 335–345, Oct. 2006.
[32] L. Oberascher, “‘Luminos 3’: a new tool to explore color and light in 3D,” Proc. SPIE 4421, 9th Congress of the International Colour Association, vol. 4421, Jun. 2002.

METHODS AND TOOLS TO EVALUATE VISUAL IMPACT OF SOLAR TECHNOLOGIES IN URBAN ENVIRONMENT

Dessi Valentina

Politecnico di Milano, Dept. DASTU. Via Bonardi 3, 20133 Milan

ABSTRACT

The last Italian rules regarding the authorization of the renewable energy technologies were proposed in 2010 in order to make easier and easier the diffusion of this kind of technologies. Nevertheless the good goals of the guidelines risk to get in conflict with the need to have an harmonious integration of them in the landscape.

The evaluation of the visual impact was in the past considered at local level by building codes or by the superintendence in particular cases. The new guidelines neglect completely the perceptive and visual impact of new installations in urban context as well as in open field.

A research activity based on the development of strategies and tools to minimise negative impacts in the urban "sensitive" environment was carried out by the Politecnico of Milano and by other Italian Schools of Architecture through a Scientific research national program of relevant interest (PRIN) [1]. The part of the research presented in this paper starts with the consideration that now it is quite hard to separate the city development from the energy supply. For this reason the design of technologies from renewable energy can't be done only on the basis of energy production but it should also be consistent with the territorial analysis in terms of visual impact. Designers who want to integrate the solar technologies in a building or in a space need some tools to evaluate visual impact before presenting the project. On the other hand the public administration needs suitable tools to evaluate the proposal and the project as well.

First the paper presents some examples on how different Italian Regions implemented the national rule. In the second part a rapid glances is given at different tools that can be implemented especially by the local administration. As third, according to the need to have very simplified tools accessible to everyone, a simple graphic evaluation tool is proposed that can be used by private people or by persons in charge. Trough this graphic tool it is possible to quickly understand whether a solar panel is visible from the street, according to the distance, the height of the building and the roof tilt.

Keywords: *Visual impact, building integration, graphic evaluation tool*

INTRODUCTION

In September 2010 national guidelines were approved relating to the authorization of plants powered by renewable sources (Decree of September 10, 2010: *Guidelines for the authorization of plants powered by renewable sources),* provided from the Legislative Decree no. N. 387/2003. The application of guidelines from the Regions, seems to represent an incomplete and somewhat critical framework that only allows us to hypothesize a number of possible scenarios. The exclusion of local authorities, such as the City and the Province, is only the first result of this regulatory approach. The simplification of procedures for authorization of technologies by Renewable Energy Source (RES) is its sole objective, expanding their spread, especially in terms of micro-interventions, on the whole national territory. Unfortunately, the "virtuous" goal that the guidelines are placed is likely to get into

conflict with the need to ensure the harmonious integration of plants in the landscape, by the bodies responsible for protecting the environment, both natural and urbanized. The issue is being addressed through the identification by the Regions of “not suitable areas”. According to the guidelines, "*the identification of not suitable areas has to be based solely on objective technical criteria related to environment protection aspects, landscape, cultural and artistic heritage aspects, linked to the intrinsic characteristics of the territory and the site”.* According to what is defined by law, it is interesting to note that there are regions that have adopted the recommendations of the guidelines in full, identifying not suited areas to the areas listed in the guidelines as an example, while others decided not to follow the national law and continue to operate in its autonomy, considering the local rules (mandatory or voluntary building regulations) more careful and protective to the landscape.

Another important question remains open and unsolved, and it relates to the instrumental help necessary for the evaluation of this type of impact. The problem can be approached from two points of view: from one hand, the designer who intend to carry out the project needs to have tools, to verify and possibly modify it, in order to make it more acceptable. From the other hand is the public administration that needs to be equipped with tools to monitor and control the proposed projects. The solutions can be different and vary depending on the degree of difficulty and complexity of the environment in which the plant should be inserted. The protection of visual cones or settlement of historical interest visible also from high territory parts should not prevent the installation of technologies from RES or rather, new installations of solar technologies should not "disturb" the perception of a sensitive landscape, which can be, for example, all the buildings included in the historical center of a medieval village.

Amendments to the regulatory scenario at local scale: some examples and doubts

The example of the Autonomous Province of Bolzano

It is important to note the appeal on jurisdictional dispute between agencies, promoted by the Autonomous Province of Trento against the Ministerial Decree of September 10, 2010 for the approval of the national guidelines. The decree, according to the Province, would be contrary to the legal rules of implementation of the provincial Statute that governs the relationship between legislative state and regional and provincial laws. The decree n. 37, of 25 October 2010, provides for the installation of photovoltaic panels in particular, in art. 2, p. 3, that (a) "*installation is forbidden on all the buildings subject to the protection of cultural goods”*, that (b) “o*n residential buildings in the area A the claim shall be subject to the approval of provincial Cultural Heritage Division*," and that (c) “*in residential areas it is allowed only if the installation is parallel to the roof or the facades, with a maximum height of 1.20 m (*1,20 m is the maximum height that can be reached by the tilted panel in a flat roof). *The derogation is only possible if it is proved the non-road visibility*". It shall also specify requirements to be met by plants in areas not particularly sensitive. In any case, the project should always be verified by the office of the Cultural Heritage of the Province. This is a fundamental difference compared to the other Regions which implement the guidelines that are not in fact required to specify the mode of application in contexts considered appropriate. If we read the art. 19/ter of the building code of Bolzano, on energy saving and renewable energy sources in step 3 is even more specific: "*In the case of pitched roofs, solar panels must be positioned adjacent to the flap mode (retrofit), or rather incorporated it (structural modes). In the case of flat roofing panels will be installed with optimum tilt, however, so not visible from the street*”. In this case the building code of the city still remains a valuable tool control while in the case of implementation of the national guidelines the building code, apparently only in this respect, it loses any value.

The example of the Campania Region

The Campania Region has adopted the national guidelines so far in incomplete way since they were not mentioned areas not suited by the Region. In the absence of indications, they continue to seek the opinion (non-binding) of the Superintendent, and assumes instead as binding the decision of the Conference of the Services, which evaluates each case. The historic center of Naples is patrimony of UNESCO and object of number of programs of urban redevelopment. The Grand Plan for the Historic Centre of Naples UNESCO World Heritage aims to achieve development and significantly improve the environment and quality of life of the inhabitants. The *Real Albergo dei Poveri* building is included in this program. It has recently undergone a major redevelopment promoted by the municipality that approved the master plan in 2005, which also includes a renovation in energy terms. In particular, the design team, B5 engeneering, winner of the competition, proposed to replace the cover in reinforced concrete with semitransparent photovoltaic modules (Fig.1).

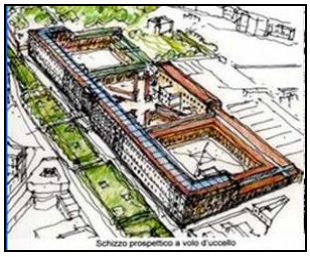

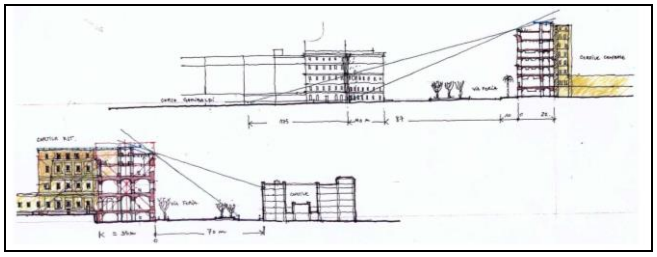

Figure 1: Bird's eye perspective of the restoration
Figure 2: Drawings of the visual impact from the ground of the photovoltaic roof.

The environmental impact of this integration was carefully considered (Fig. 2). As consequence of the evaluation a reduction in the production of energy was proposed- due to an adaptation of the envelope (tilt and orientation). Compared to the optimum production it has decreased the productivity by 16.9% to a specific producibility of energy equal to 1269 kWh / kWp year. Despite the Campania Region has already partly implemented the national guidelines, the planning process that today would lead to a realization of this type would not be very different, if not for the fact that the opinion of the superintendent would not be binding. It is believed, in fact, that the Conference of Services takes proper account of an opinion of that authority.

METHODS: SOME EUROPEAN EXAMPLE OF INSTRUMENTS AND METHODS TO EVALUATE THE VISUAL IMPACT IN THE LIVED LANDSCAPE

Guidelines for installation in historic buildings: the search for SUPSI in Switzerland

The competence centre BiPV - SUPSI, placed in Cannobio, has developed a method for assessing the impact of solar technologies for buildings historical and cultural interest. The work, titled "*Development of technical guidelines and architecture for the integration of solar systems in historic buildings*" [2], was commissioned by the City of Bellinzona and develops from a series of criteria already taken into account in some cantons Switzerland. Existing policies are mainly based on the geometry and placement of solar panels on the roofs. Research has identified other criteria, focusing in particular on the visual impact.

One of the first requirements to enhance the architectural quality of new and existing buildings that include the installation of solar systems is to define, and then try to reduce, the formal limitations that negatively characterize the installation, so you can identify the most appropriate solutions. It is the objective requirements which do not exclude the analysis of

each specific case and which is especially crucial in buildings or areas of historical interest as the proposal of intervention must be evaluated from different points of view. The table below summarizes the possible relationship between different building types and six requirements (compulsory) and five criteria (not required).

Finally, a check list can be used to make a quick assessment of the compatibility of the building with the solar system with a check list that takes into consideration various aspects. The aspects are divided into three categories: general aspects related to the location and the building and other referring to the specific technology, ownership or right to use (in particular, cover and walls).

Green: criteria / recommendations you can easily meet.
Yellow: criteria / recommendations can be met if plant installations are taken into account from the earliest stages of the project.
Red: criteria / recommendations can be followed, but you should consider very carefully the various aspects.

Figure 3: Table of verification of criteria and recommendations with different morphologies.

Visual impact from large parts of the territory: the research of the University of Pisa

Although the majority of prescriptions focus more attention on the visibility from the street, there is also a question of protecting visual cones and protection from the highest points of land, or top view of the monuments. In these cases, it's necessary to have more sophisticated tools and methodologies that match needs and availability of areas with the protection of the landscape. In this regard it is useful to quote an interesting study based on an approach of integration between energy and territorial issues proposed by the University of Pisa [3].

Through the three-dimensional reconstruction of the urban context, identifies the portions of land most suitable for installation of solar panels, i.e. those that maximize the efficiency of the panel ensuring optimal exposure and inclination, but at the same time minimize the visual impact for the privileged observers (in the case of Pisa, tourists). The supply of solar energy is then crossed with the demand for tourism and residential, identifying those roofs where supply can match demand (Fig.6).

The specific results from the conducted analyzes revealed that the majority of facilities are able to meet their needs with solar thermal technology without cause significant visual impacts to the urban context in which they are found, whether in the historical center or in the peripheral areas. In addition, the use of GIS software allowed to combine statistical data

(registry office), energy (hot water demand in the residential and tourism) and territorial (physical form of the city) in an innovative way.

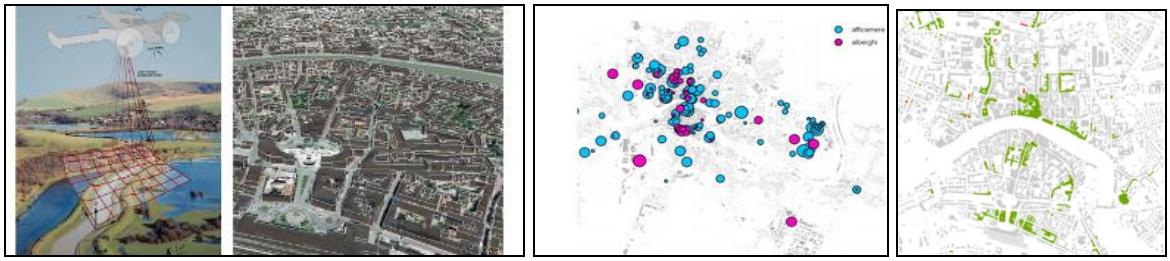

Figure 4: View from GoogleEarth of the buildings with the tool LiDAR Analyst, ArcGIS.
Figure 5: Requirement for hot water receptive.
Figure 6: Buildings in receptive use (in green) results suitable for the installation of solar panels, that is not visible and sunny.

RESULTS: THE ASSESSMENT OF THE VISUAL IMPACT FROM THE STREET

It's possible to have a designer responsible for checking the visibility from the street, or to have a body that needs to verify that the proposed project meets certain requirements related to the visual impact. It would be necessary to have available evaluation tools, very simplified tools in order to make some preliminary verification about the visibility impact, at least from the street. The proposed one is a graphical tools that allow the verification from different points of the road. As can be seen from the figure, the point that represents the panel on a roof slope of 15 ° is not visible at a distance less than 25 meters if the building is 7 meters high and at a distance of 30 meters if the building is high 10 meters.

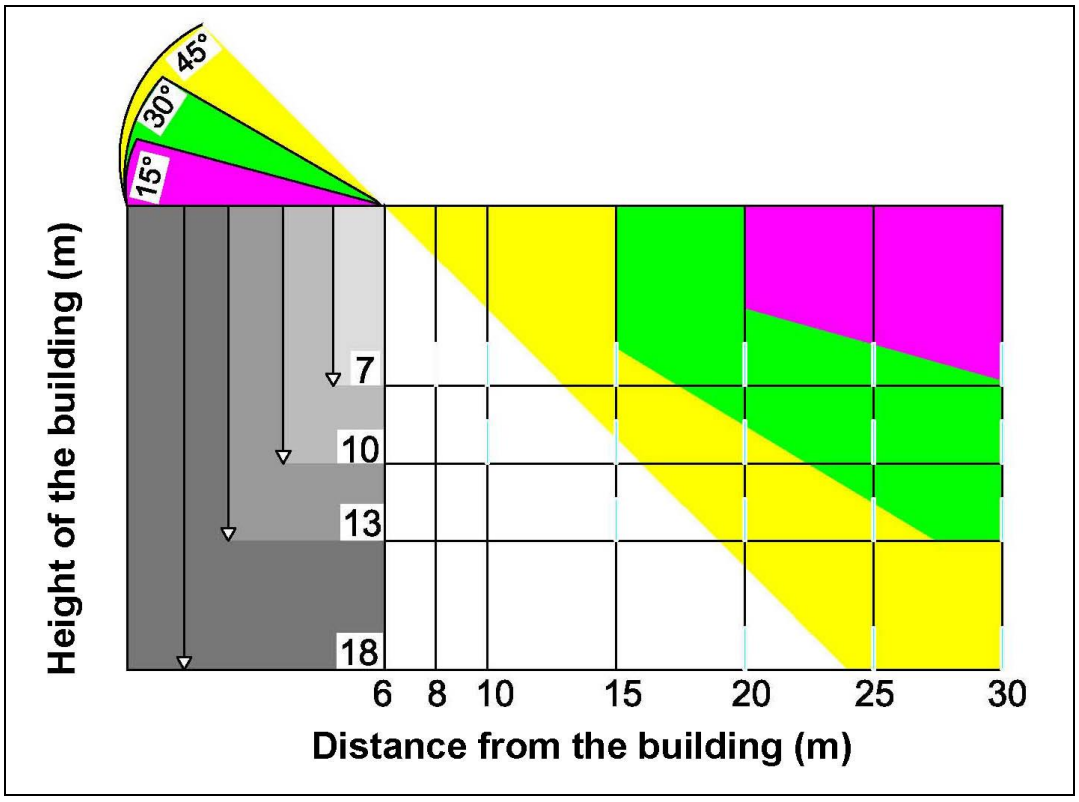

Figure 7: Graph for the visibility assessment of a solar panel from the road

Because the panel is visible on a roof slope of 30 ° we must find a minimum distance of 10 meters if the building is 7 meters high, 15 meters if the building is 10 meters high, at a distance of 20 meters if the building is 13 meters high and at a distance of 30 meters if the building is 18 meters high, ie 6 floors. If the coverage is 45 ° inclined panel is much more visible. As you can see from the chart, the stitch is evident from a distance of 8 meters, even on a high-rise 7 meters.

CONCLUSIONS

The paper focused on two important aspects:

1- The issue about the question of solar systems installation in buildings is by now more and more pressing. Unfortunately it can be in conflict with an harmonic integration in the natural and built environment, in particular where more difficult could be the integration between the two aspects related to the energy sustainable management and the heritage protection. It's the case of existing buildings, maybe under the Superintendence protection (for instance the Real Albergo dei Poveri in Naples).

2- The reported examples about the evaluation tools represent two different approaches. From one hand, simplified guidelines (competence centre BiPV-SUPSI) connect among them some criteria-requirements with the building morphology. But not always they help to verify the visibility, especially for those building or part of the city where the visibility should be reduced as much as possible. On the other hand, sophisticated tools suitable to verify the visibility from wherever exist (method proposed by the University of Pisa) but the necessary data to implement it are not always available or they are quite hard to use and require specialised people.

For this reason a graphical tool very rapid in use is proposed, dedicated to the public administration as well as the private citizen who asks the authorization for the installation of the plant. This tool represent a quick check combining some elements related the building and the position of the observer. Very often to obtain the authorization it is in effect enough to know if the plant is visible or not. In case of other requirements, like the integration of the plant in the building it is possible to go beyond using other complementary methods and tools (like the one proposed by the competence centre BiPV-SUPSI) that the local or national control body should have.

REFERENCES

1. Scudo G.: Integrazione di tecnologie di fonti energetiche rinnovabili nell'ambiente costruito. Processi, progetto,/strumenti, sistemi e componenti. Wolters Kluwer Italia, Assago (Mi), 2013
2. Zanetti I., Frontini F., Ferrazzo M. (Swiss BiPV): Development of technical and architectural guidelines for solar system integration in historical buildings. Determination of solar energy opportunities, Canobbio (CH), 2011
3. Casini C.: Il rapporto tra energia e territorio: analisi degli strumenti normativi, pianificatori e operativi e applicazione alla valutazione delle potenzialità solari del comune di Pisa, in XXXII Conferenza Italiana di Scienze Regionali, Il ruolo delle città nell'economia della conoscenza, Torino, 2011

INNOVATIVE SOLUTION FOR BUILDING INTEGRATED PHOTOVOLTAICS

Laure-Emmanuelle Perret-Aebi[1]*, Patrick Heinstein[2], Valentin Chapuis[2], Christian Schlumpf[2], Heng-Yu Li[2], Christian Roecker[3], Andreas Schueler[3], Virginie Le Caër[3], Martin Joly[3], Robert Tween[4], Yves Leterrier[4], Jan-Anders Månson[4], Jean-Louis Scartezzini[3], Christophe Ballif[1,2]

[1] *CSEM Centre Suisse d'Electronique et de Microtechnique SA, PV-center, Jaquet-Droz 1, 2002 Neuchâtel, Switzerland*

[2] *Photovoltaics and Thin Film Electronics Laboratory, Institute of Microengineering (IMT), Ecole Polytechnique Fédérale de Lausanne (EPFL), Rue A.-L. Breguet 2, 2000 Neuchâtel, Switzerland,*

[3] *Solar Energy and Building Physics Laboratory, EPFL-ENAC-IIC-LESO-PB, Station 18, 1015 Lausanne, Switzerland*

[4] *Laboratory of Polymer and Composite Technology, EPFL-STI-IMX-LTC, MXG 133, Station 12, 1015 Lausanne, Switzerland.*

*Corresponding author.: laure-emmanuelle.perret@csem.ch

ABSTRACT

Among the main challenges of our century, the climate change and the need of diversification of the energy sources are of most importance. Renewable energies undoubtedly have an important role to play, photovoltaic (PV) electricity being especially well suited to face these energy challenges. However, the current integration of PV panels often comes without architectural consideration. In this context, the Archinsolar project [1] aims to develop a new generation of photovoltaic elements based on silicon thin films technologies (amorphous and micromorph), ultra-reliable and manufacturable at a very low cost, allowing a unique architectural integration, respectful of the built environment and overall landscape. Here we will present our new developments on innovative PV elements including colored PV panels and a solar tile using a composite back-structure.

GENERAL CONTEXT

The renewed debate on nuclear energy following the recent events in Japan, the numerous political decisions made in favor of the development of renewable energies as well as the attitude of the public, which is always more concerned about environmental issues, lead to the development of new and more adequate technologies adapted to our current energy needs.

Photovoltaic energy is particularly well positioned as it is proven that a large part of the electricity needs of our modern society could be covered by photovoltaics, providing intelligent energy management if applied. In the long-term, solar energy should even be used to provide a significant part of the world's energy consumption. As an example, the well oriented roofs of Switzerland (130 km^2) could cover around $1/3^{rd}$ of the 58 annual TWh with standard crystalline modules.

It is then reasonable to argue that, today, there is no "versatile" solution available on the market which is inexpensive, aesthetically acceptable and easy to install. Nowadays photovoltaic energy is still limited by to heavy investments. These investments are notably associated to the unit prices, to the BOS costs (mounting, support, inverter) and to the

planning costs (linked to the experience). Indeed, the price of the modules proposed on the market is still one of the most important factors which retain potential purchasers. In the built-environment and in specific landscape, aesthetic aspects will play an increasingly important role, as the pressure not to install PV in areas reserved to agriculture is increasing.

These crucial aspects are of utmost importance to succeed in competitively positioning photovoltaic energy either on the electricity market or for internal use. Only then photovoltaic electricity will be able to contribute significantly to the general electricity production.

SIMPLICITY OF INSTALLATION AND MULTI-FUNCTIONALITY FOR LOWER COSTS

Technologies based on thin-films such as amorphous or microcrystalline silicon [2-3], have the potential to lead to a stronger cost reduction of the solar kWh (<30€/m^2 for the thin layers) and offers the unique potential to cover large surfaces at a particularly low cost. Furthermore, thin film Silicon technology is based on abundant and non hazardous materials.

To reduce the high expenses related to the installation of photovoltaic modules, solutions to simplify the installation of system is required. Currently, an installation of photovoltaic modules on a roof remains complex and needs the intervention of several working corporations, from engineers to roofers. A general simplification of the systems, in particular an improvement of the mechanical stability and a simplification of the electrical connections are taken into consideration. Furthermore, the size and the weight of the module, using composite materials [4] is taken into account and should be adapted to allow only one roofer to be able to install the system.

Integration solutions allowing the replacement of other building components by photovoltaic panels will reduce the overall cost of the installed system. Simple and modular building elements such as roof tiles and slates, or solar roof windows (semi-transparent), and other components are certainly the most innovative aspects. These elements should then ensure multifunctionality such as mechanical stiffness, water vapour barrier [5-6], building element, insulation, sun protection or capturing the heat energy in addition of solar power generation.

SOLAR TILES WITH COMPOSITE BACK-STRUCTURE

Solar tiles based on thin film silicon technology and a new thermoplastic composite backing structure were introduced as cost-effective solutions fully compatible with building integrated PV. The molded back-structure provides mechanical stability to the module and protects the fragile glass solar cell. It moreover ensures water tightness to the roof by its specific profile. A novel integrated process approach was introduced, in which the lamination step of the glass module to the composite backing (Fig.1. right) is suppressed by direct overmolding of the composite backing on the glass with or without adhesive layer (Fig. 1. left). The main challenges of this new molding process are i) the risk of breaking the glass due to thermal shock during the molding process and ii) durability issues in case no adhesive is used. A small series of solar tile demonstrators were produced and mounted together with TEGALIT tiles on a real size mock-up roof (Fig. 2). The cost and environmental impacts for the production of these novel BIPV compatible solar tiles were evaluated and found to be comparable with standard rack-mounted glass-glass modules.

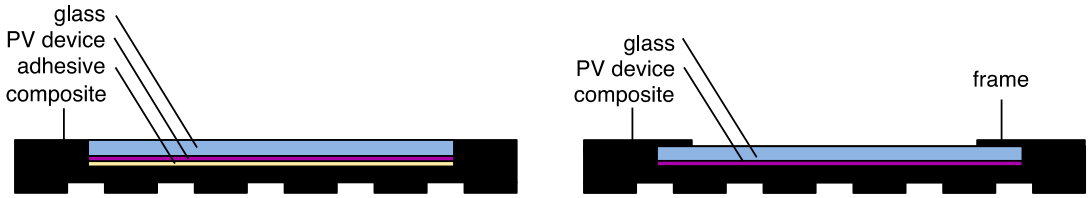

Fig.1. Standard lamination (left) and integrated process (right).

Fig. 2. New solar tiles developed in the Archinsolar project framework

ARCHITECTURAL ASPECTS AND AESTHETICS OF THE PV MODULES IN THEIR ENVIRONMENT

From an esthetic point of view, the color variation, going from the typical brown of amorphous silicon to the typically black for micromorph, constitutes one of the great starting advantages of these kinds of modules.

The desire for optimum equipment performance is sometimes in conflict with site and building conditions. While effective in establishing proper orientation of solar panels, these installations give a discontinuity in the building and its architecture.

Providing architects with a pallet of various products, with amongst other aspects, different color levels, is essential. In the long term, we can imagine that every roof could be completely covered with suitable tainted photovoltaic modules and cost effective. Due to the inherent homogeneous aspect of the thin films based modules, as well as the possible modification of these colors by the introduction of colored filters [7-8] or polymers, it is possible to consider a whole pallet of modules aesthetically interesting which will be better integrated in their environment.

COLORED PV ELEMENTS

A new generation of orange coated glasses with improved angular color stability have been industrially produced on large glass panes by Swissinso S.A. and laminated to real-size (1.10 x 1.30 m2) PV a-Si modules (Fig.3).

Fig. 4: Orange glass panes laminated on real-size PV modules (1.10 x 1.30 m^2) on which strong angular dependency of the color is observed.

In parallel, new terra-cotta like modules have been developed, using a specific encapsulation scheme without additional coating. These new framed terra-cotta like PV modules have been installed on a demonstration roof at IMT (Fig.4) and show a perfect integration by their color and the water tightness ensured by the special design of their frame. This allow, in addition, a very easy mounting without any special preparation of the roof underneath. The max-Power voltage of these modules if of 107 V with an efficiency of 6%.

Fig. 4: Demonstration roofs with the new orange colored PV modules

CONCLUSION

Only a very small fraction of the installed PV capacity has been actually integrated in the built environment. Landscape protection, competition with agricultural lands or public opinion are putting pressure on PV developers to increase the use of the build environment as a space to produce PV electricity. At the same time, higher module and/or BOS (Balance Of System) costs when installing on buildings and poor aesthetics of several existing PV integration are additional elements working against PV on buildings. There is therefore a necessity to come up with new PV modules addressing the two major barriers against a wider spread of PV in the build environment: cost and aesthetics.

Innovative coloured solar tiles were developed and shown on full size demonstrator in this project. The results presented here clearly show the potential for developing innovative PV systems allowing improved architectural integration by developing coloured PV modules, either using interferential coloured filters on thin film amorphous silicon modules or by working on different cell and encapsulation designs. These multifunctional BIPV solutions, especially when based on thin film technologies are extremely promising and cost effective if compared to conventional building elements.

ACKNOWLEDGMENTS

The authors are thanking the company SwissInso for their effort and support in providing large scale coloured glass.

Swiss Electric Research (SER), the Center of Competence for Energy and Mobility (CCEM), the Services Industriels Genevois (SIG) and the Swiss Federal Office for Energy (SFOE) are thanked for their financial support in the framework of the Archinsolar project.

REFERENCES

1. Archinsolar: “Unique and innovative building integration solution”, demonstration project financed by Swiss Electric Research (SER), Competence Center Energy and Mobility (CCEM.CH), Services Industriels Genevois (SIG), Office Fédérale de l’ Energie (OFEN), 04.2010-04.2013.
2. Schropp, R.E.I., Zeman, M., Amorphous ans microcrystalline silicon solar cells: modeling, materials and device technology (electronic Materials: Sciences & Technology), Springer US 1998.
3. Vallat-Sauvain, E., Advances in microcrystalline silicon solar cell technologies, Wilex Series in Materials for Electronic & optoelectronic Applications, John Wiley & sons Ltd, pp.133-165 (2006)
4. Rion J., Leterrier Y., Månson J.-A.E. Ultra-Light Asymmetric Photovoltaic Sandwich Structures, Compos. Part A., 40 (2009), p.1167-1173.
5. Pélisset, S., Perret-Aebi, L.-E., Théron, R., Dunand, S., Prongué, L., Ballif, C., Damp heat stability of transparent conductive zinc oxides: role of encapsulants and protective layers, PVSEC 2010, Valencia.
6. Pélisset, S., Théron, R., Barnéoud-Raeis, M., Perret-Aebi, L.-E., Benkhaira, M., Ballif, C., Monitoring water vapour penetration using a contactless techniques, PVSEC 2009, Hamburg.

7. Schüler, A., Roecker,C., Scartezzini, J.-L., Boudaden, J., Videnovic, I.R., Ho, R.S.-C., Oelhafen, P. On the feasability of coloured glazed thermal solar collectors based on thin film interference filters, Solar Energy Materials & Solar Cells, 84 (2004), p. 241-254.
8. Munari-Probst, M.-C., Roecker, C., Integration and formal development of solar thermal collectors, PLEA 2005, Beirut, Lebanon, November 13-16, 2005.

PRE-ASSESSMENT TOOL FOR THE EVALUATION OF OPTIMAL RENEWABLE ENERGY INTEGRATION STRATEGIES.

CASE STUDY IN THE EXTENSION EAST OF BRUSSELS.

Galan Gonzalez A.[1], Stevanovic M.[1], Acha Román C.[2], Bouillard P.[1]

1: Building, Architecture and Town Planning, Université Libre de Bruxelles (ULB)
2: Construccion y Tecnologia Arquitectonica, Escuela Técnica Superior de Arquitectura de Madrid (ETSAM)

ABSTRACT

Renovating the existing building stock is well recognized in the construction industry as a very important issue. While the number of new buildings annually provides maximum 1% to the building stock [1], the other 99% represent buildings which are already built [2]. Studies show that the environmental impact to extend the life of a building is definitely smaller than that of demolition and new construction [3]. Recent figures suggest that the residential sector can provide significant reductions in energy consumption [4].

As many vital decisions are taken in the early stages of the refurbishment process, planners need **tools** that will help them create better and more sustainable rehabilitation projects based on the integration of renewable energy [5].

This study describes a **methodology** to support decision making and enable the development of an integration strategy for different cases and specifications. It is intended that the planners know the energy impact of the project according to the adopted solutions. To do this, the possible solutions are organized in the form of a matrix (**TCS: building Typology, building Component, Solution**). This **matrix** is basically a compendium of the integration of renewable energy techniques to apply in rehabilitation projects, sorted by building typology and its major components, so that it gives an overview of the integrated strategy of the rehabilitation process.

It is essential to know how they affect the modifications to the improvement of the energy efficiency, which is why it is possible to obtain an estimation of the savings value in economic terms. From all the data collected a theoretical **TCS matrix** is built that will serve as a baseline to compare with the actual data.

Keywords: Building stock; Building energy retrofit; energy integration strategies; renovation; renewable energy, methodology, tools, matrix.

INTRODUCTION

According to the Directive 2010/31/EU, new buildings will have to be nearly zero energy buildings by 31st December 2020. However, the directive gives no specific targets regarding refurbished buildings, which present a large proportion of the building stock and the first cause of CO2 emissions in the building sector.

Gaterell and McEvoy [4] suggest that the domestic sector could potentially make a significant contribution to reducing energy consumption. Residential buildings account for the 2/3 of final energy consumption in the building sector and 70% of buildings' floor area, so it seems important to focus on the improvement of energy efficiency in the existing residential building stock.

It is necessary to develop a methodology to tackle the energy renovation analysis in residential building that assures success since the design phase. There is an individual and

often fragmental approach to energy renovation projects even when the solutions are applied in an individual residential building.

This paper discusses an approach to the designing of refurbishment projects, as a way to improve the energy efficiency of the residential stock. It presents answers to specific technical problems and determines how improvements in the environmental performance can be reached.

The discussion starts introducing the TCS matrix, which is the centrepiece of the approach, to later present how the TCS is used through our proposal of methodology. Both the methodology and the TCS will be developed in a technical tool, which is currently an on-going prototype.

1. A METHODOLOGY FOR SUSTAINABLE HOUSING REFURBISHMENT

Housing refurbishment is taking a central place in the efforts for integral refurbishment and revitalization of larger areas, especially in larger housing states (Ruano, 2002). The concept of sustainable refurbishment should cover and integrate economic, social and environmental needs as much as possible. Reddy, Socur and Ariaratnam (1993) offer a frame-based decision support model for building refurbishment, while Rosenfiels and Shohet (1999) and Lavy and Shohet (2007) talk about a decision support model for semi-automated selection of renovation alternatives. Alanne (2004) proposes a multi-criteria model to help designers choose the most feasible refurbishment actions in the conceptual phase of the project.

The methodology proposed in the study can be considered as a toolbox in the form of a matrix that intends to accelerate the construction process. *T. Konstantinou and U. Knaack (2011)* defined a toolbox with the same goal for a specific project where they identified components and solutions. It can be considered as a huge step in the process of standardising the construction process.

Nevertheless there are three elements that we miss from their toolbox, and that we consider critical to ensure the success and reusability of the model. Firstly, their model is focused on a type of building, and is to be redefined in each work. This constraint triggers the need to extend the toolbox with the inclusion of building typologies, as components and solutions are roughly the same in a building typology. Secondly, and based on the Deming cycle[1], the toolbox lacks of a continuous improvement process that will allow the system to learn from its deviations. Finally, it will offer the possibility of being parameterised to calculate the efficiency based on different constraints such as the budget of the work.

1.1. Decision making process

When refurbishment reasons are clarified, further activities to achieve the main tasks are discussed. It must be decided if complete refurbishment of a building is needed or just a partial one.

Once the refurbishment scope is defined, the next and very important phase is decision making. Decision making means selection of the best alternative from numerous ones. In this phase the information about already implemented refurbishment projects, best practice examples, projects strengths and weaknesses is needed.

[1] Deming defined the PDCA (plan-do-check-act) model as an iterative four-step management method used in business for the control and continuous improvement of processes and products. Further information can be found in http://en.wikipedia.org/wiki/PDCA

In practice, the measures have to fit the individual project in terms of the building´s existing condition, location, project specifications, budget and ambition of client and architect´s decisions.

1.2. Matrix TCS

The matrix Typology-Component-Solution (TCS), shown below, is the artefact that we will put in place to ensure the reusability of the solution across different tasks. The different solutions applicable are structured in a matrix with:

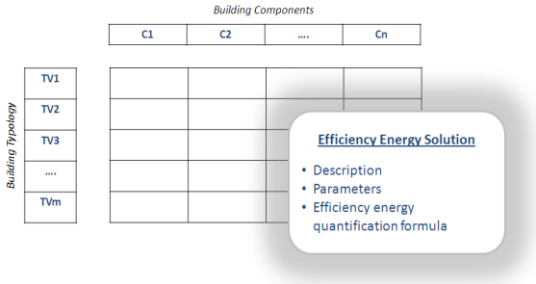

- the different Typologies of buildings to which the methodology is applicable in the rows;
- the different building Components in a house in the columns;
- each cell contains the possible solutions suitable for the component in each building type. Solutions in the cell are described with three main elements: (i) description of the solution; (ii) the list of parameters needed to calculate the energy consumptions; and (iii) the formula to use to calculate the energy consumption.

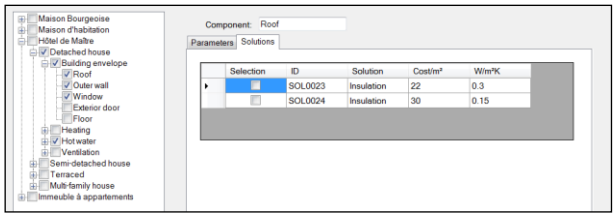

The picture in the left shows an example of a cell in the TCS matrix in the current version of the tool, which contains different solutions applicable to roofs in buildings in the scope of the study. The final number of solutions will be increased along with the study,

The TCS matrix is the main element around which the model revolves. The accuracy of the model depends on the level of identification of the different solutions and how precise the formulas included are.

During the project a TCS Matrix will be designed including the different building typologies subject of the study. Nevertheless, it is important to note that the TCS matrix needs to be enriched along with new building typologies to make it more extensible. This process will be supported by the tool which will automate registering all the information required for further used.

1.3. Methodology phases

Our methodological approach aims to implement a continuous improvement process to validate the results offered during the pre-assessment phase of the work with the final measures obtained once the solutions are applied. The continuous improvement process ensures long-term use of the system as the results will remain accurate as long as the methodology is used.

Four phases are defined in the methodology, in line with the Deming PDCA model:

1. **TCS Matrix Elaboration:** This phase intends to complete the TCS Matrix with the information required for the work. Depending on the type of building, it might require more or less effort. When the type of building has already been entered, only a

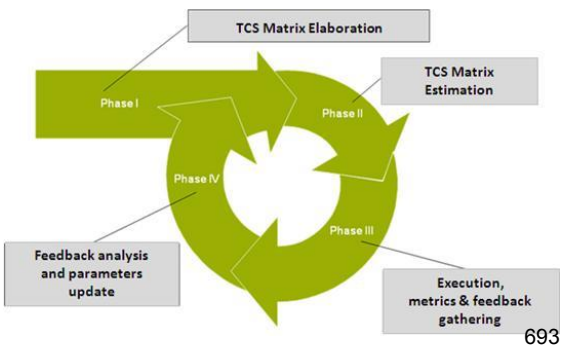

validation that the TCS matrix contains all the components and the possible solutions is required. Whenthe building is of a new type, this type needs to be created and matched with the different components in the database. Once this is done, the team will confirm that all the components and solutions are in the matrix, providing the missing information.

2. **TCS Matrix Estimation:** Once the TCS matrix is set, it is used to make an estimation of the best work. This phase corresponds to the real pre-assessment that the team will use to define the target efficiency that can be achieved. It is also important to note that constraints could be applied during this process, such as the maximum budget for the work; the components where solutions can be applied among all the components of this building type; etc.
3. **Execution, metrics & feedback gathering:** Once the work is done, it is important to perform measurements and to gather feedback from the work. Measures will collect information about the consumptions of energy of each component and of the whole building as well. The procedure and the feasibility to gather metrics depends on each component involved in the work.
4. **Feedback Analysis and parameters update:** The system will log estimations to later be able to check the quality of the pre-assessment provided. The feedback collected in Phase III will be analysed and compared with the pre-assessment. As a result, the TCS matrix may be updated with, for example solutions that have been discovered later during the work but that are not listed in the TCS, formulas that are incorrect or which require some adjustment depending on certain conditions, etc.

After each cycle, the effectiveness of the TCS Matrix is tested. Thus, next usages of the Methodology will reap the benefits from the historical information.

1.4. Estimation methods

During the first phase of the study, we will define two possible refurbishment estimation methods.

The first one, depicted on the right, it is the ***Optimal Refurbishment***. It aims to identify the best refurbishment possible considering the components that will be updated during the work. The result will be a list of the solutions that will be applied to obtain optimal energy refurbishment.

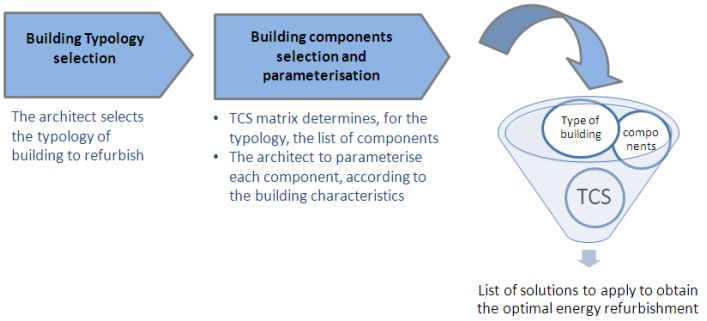

The second, named ***Best Refurbisment in Price*** intends to define a list of solutions to apply to obtain optimal refurbishment within the budget of the work, so that the solutions will be adapted to the context of the work.

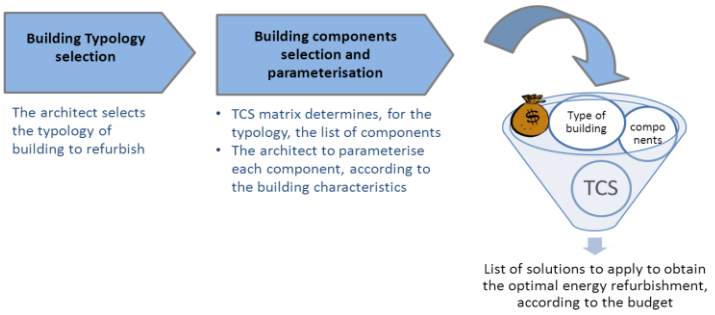

2. CASE STUDY

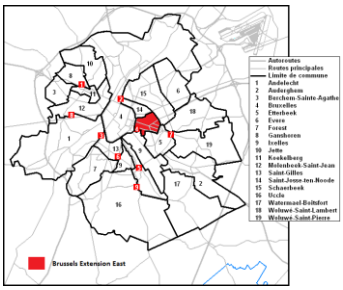

The TCS matrix tool is developed and applied in the context of the upcoming refurbishment of residential buildings in the **Extension East of Brussels**. The revitalization of old cities would imply the increment of dwelling availability in areas where greater social diversity is needed and higher population density can be beneficial. The older the construction, the more delicate and necessary the upgrading process is and the more specialised the knowledge is required.

It is a predominantly residential area, where *Maison d´habitation, Maison d´architecte and Hôtel Particulier* represent the main types of dwellings (Figure 2).

Building Typology	Number of Buildings	Example
Hôtel Particulier	21	(1) Rue Philippe Le Bon 70 (1901)
Maison d'habitation	More than 900	(2) Maison Saint Cyr (1903)
Maison ouvrière	1	(3) Rue de l'Inquisition 37 (1895)
Maison d'architecte	22	(4) Avenue de la Brabançonne 7 (1894)
Maison et Atelier d'artiste	4	(5) Rue des eburons 63 (1904)

The majority of the houses are in good standing with almost invariably the same plane-type three rooms in a row, along with attic reserved for domesticity. The facade has usually two or three unequal spans, decorated with a balcony or loggia. In contrast, this program can be found amplified in mansions for the upper class. Moreover, their plots allow the development of additional parts such as lobbies or an office. The facades are richly ornamented and with cubicles, with bow-windows or even turrets.

Although the research focuses on passive measures exclusively, being its main challenge to improve historic buildings through redesign, it has been found necessary to approach active systems as well, due to the big energy problem identified.

The project team is currently focused on completing the TCS matrix for the Case Study. This process is planned to be finish by the end of this year. Further advances will be presented during the congress.

CONCLUSION

Sustainable refurbishment is a significant problem in current building stock, taking much scientific attention as well as European Commission initiatives. Sustainable refurbishment is widely discussed in the literature and various models and decision making tools that are proposed. This paper **integrates sustainable development principles in the decision making process** and influencing factors into one unique conceptual sustainable refurbishment model.

The model involves environment factors analysis and integrates participating in refurbishment stakeholder's decisions and needs. Accordingly to sustainable refurbishment principles, refurbishment not only decreases energy consumption but also improves whole condition of the building. Much attention is paid to the decision making process. In order to design and implement buildings refurbishment based on sustainable development principles it is necessary to follow these principles from idea to implementation. There is still a **need of specialised knowledge to assist the design of holistic refurbishment strategies** in the early stages when decisions have a bigger impact.

This paper presents a holistic approach to the energy refurbishment focusing on **pre-assessment and feedback as the key elements** at the disposal of the technical teams to develop sustainable refurbishment projects and to continuously improve future works. This approach relies on the maturity of the process as the enabler to increase future efficiency. The methodology is accompanied by a tool that will support the implementation of the method.

This approach recognises the diversity of each project as well as the designer decision freedom. In a future stage, **the tool will provide solutions for technical issues to be solved in the implementation phase**. Its aim is to be a support instrument throughout the design process which **will provide knowledge on the effectiveness of the measures**, without compromise the project intentions.

At this stage the tool is an on-going prototype whereas the project team is focused on completing the TCS matrix for the Case Study. This process is planned to be finished by the end of this year. Further advances over this paper will be presented during the congress.

REFERENCES

1. [1]. Power: Does demolition or refurbishment of old and inefficient homes help to increase our environmental, social and economic viability? Energy Policy 2008. 36(12): 4487-4501.
2. [2]. Eurostat, Europe in figures, Eurostat yearbook 2009. Luxembourg: Office for Official Publications of the European Communities; 2009.
3. [3]. A.F. Thomsen y C.L. van der Flier: *Replacement or reuse? The choice between demolition and life cycle extension from a sustainable viewpoint, in Shrinking Cities, Sprawling Suburbs, Changing Countrysides* 2008; Centre for Housing Research, UCD.
4. [4]. M.R. Gaterrel y M.E. McEvoy: *The impact of climate change uncertainties on the performance of energy efficiency measures applied to dwellings*. Energy and Buildings 2005. 37(9): 982-995
5. [5]. T. Konstantinou, U. Knaack: *Refurbishment of residential buildings: a design approach to energy-efficiency upgrades*. 2011 International Conference on Green Buildings and Sustainable Cities. Procedia Engineering 21 (2011) 666-675.
6. [6]. J. Rodríguez Álvarez: *Rehabilitación energética del tejido urbano residencial. Evaluación previa para una mayor eficiencia*. SB10mad Sustainable building conference. Madrid 2010.
7. Alanne, K: *Selection of renovation actions using multi-criteria « knapsack » model*, Automatisation and Construction 2004, 13(3), pp. 377-391
8. Lavy, S. and Shohet I.M. *A strategic integrated healthcare facility management model*, 2007, International Journal of Strategic Property Management, 11(3), pp. 125–142.
9. Reddy, P.V., Socur, M. and Ariaratnam, S.T: *Building renovation decision support model*. 1993. In: Proc. of the ASCE 5th International Conference on Computing in Civil and Building Engineering, Anaheim, CA, USA, June 7–9, pp. 1547–1554.
10. Rosenfiels, Y. and Shohet, I.M: *Decision support model for semi – automated selection of renovation alternatives*, 1999, Automation in Construction, 8(4), pp. 503–510.
11. Ruano, M: *Eco-Urbanism Sustainable Human Settlements: 60 Case Studies*, 2002, Barcelona: G.Gilli.
12. Sitar, M., Dean, K. and Kristja, K: *The Existing Housing Stock – New Renovation Possibilities; A Case of Apartment building Renewal in Maribor*. 2006. Research Report presented at the Conference Housing in an expanding Europe: theory, policy, participation and implementation (ENHR). Urban Planning Institute of the Republic of Slovenia, Jul. 2006, Slovenia.
13. Sunikka, M: *Sustainable housing policies for the existing housing stock in Europe*, 2003, Open House International, 28(1), pp. 4–11.
14. T. Konstantinou, U. Knaack: *Refurbishment of residential buildings: a design approach to energy-efficiency upgrades*. 2011 International Conference on Green Buildings and Sustainable Cities. Procedia Engineering 21 (2011) 666-675.

HYBRID ROOFSCAPES – ARCHITECTURAL IMPACTS OF ROOF-INTEGRATED PV/T-COLLECTORS

N. Haller[1*]; P. Furrer[2]; C. Wieser[2]; H. Leibundgut[1]

1: Swiss Federal Institute of Technology (ETHZ); Institute of Technology in Architecture (ITA); Chair of Building Systems; Schafmattstrasse 32, CH-8093 Zürich

2: Zurich University of Applied Science (ZHAW); School of Architecture, Design and Civil Engineering; Institute for Constructive Design; Tössfeldstrasse 11, CH-8401 Winterthur

**main author email: haller@arch.ethz.ch*

ABSTRACT

In the future, buildings must be operated free of CO_2-emissions. To achieve this goal the chair of building systems at ETHZ has developed a system named Sol^{2}ergie. In a Sol^{2}ergie building large surfaces of PV/T-collectors (PV/T) are needed to regenerate the deep ground heat exchanger. The system covers up to 90% of all the thermal demand for heating and domestic hot water by locally stored heat and considerably decreases the maximum power requirement.

Architecturally, the PV/T is the most sensible element of the system. For energetic and economic reasons it makes sense to integrate the PV/T into the building skin, but replacing the modular application with functional integration implies a complete new interpretation of historical and contemporary roof constructions. For that reason, this study is part of a research project based on an interdisciplinary cooperation between ETHZ and the institute for constructive design at the ZHAW.

The aim of the presented study is to investigate how this new technology may change the roof on a typological and urban level. Seven scenarios in four different existing urban situations show future transformation strategies. In the conservative scenarios the roofs do not offer enough PV/T-surfaces, whereas in the more progressive and innovative ones the new roof typologies may cover the whole annual energy demand. Therefore we argue that the design of roofs is going to be one of the key aspects on the way towards a more sustainable built environment. In addition this study is also a contribution to the discussion about the vertical densification of central urban districts.

Keywords: PV/T, Sol^{2}ergie, LowEx, Sustainable Architecture, Building integration

INTRODUCTION

Buildings are artefacts, artificial sub-systems embedded in a larger system, the natural environment. They result from intelligent processes of analysing and adapting natural laws and cultural patterns. While natural laws can't be manipulated, cultural patterns are in constant change. Today, the building systems we have created cause too much stress to our own natural environment. Buildings' impact on climate change, mainly due to an extensive and inefficient use of fossil fuels (and other natural resources), presents a major challenge for the construction industry and on a larger scale, society as a whole.

There are many ideas about how this process can be transformed to lead to a more sustainable built environment. New technologies have been developed that significantly decrease a building's ecological footprint, but many of these solutions lack acceptance, for manifold reasons. So instead of trying to "reinvent the wheel", we need to develop these existing ideas in such a way that they better fit their respective contexts. In the last decades solar

installations have made a huge progress, both in technology and market penetration. However this clearly illustrates the intricacy between the development of new technologies and their application, especially in domains like the construction sector. Despite some recent advances, a large fraction of products in the field of domestic solar systems has little or nothing to do with their designated ambit, mostly being the roof.

The roof is the uppermost ceiling and thus the vertical completion of a building. It's part of the building envelope but its exposed situation embodies the constitutional element of a house; to keep the space underneath protected from the natural environment. Due to this dominant primary function almost all historical roof typologies are variations of a pitched roof. Their structure, form and materiality may be diverse, but they all evoke the feeling of security. Since the period of the Renaissance the idea of a horizontal building completion has fascinated architects and their mentors[1], yet the big breakthrough came with the advances in the field of sealing technology and structural engineering in the 19th and 20th century. Despite the fact that until today a flat roof is widely presumed as a modernist statement, its symbolism has never achieved the power of historical roof constructions. Maybe this is because a flat roof has somehow lost the correlation between its primary function and its form[2].

The objective of this study is a similar conflict between a technological development and the architectural inheritance in its wide spectre. Sol^{2}ergie is a building system that is based on the ZeroEmission-LowEx approach and can be applied in new or existing buildings, providing them with emission-free heating and cooling.[1] It only requires electrical energy from the outside. The use of deep ground as a seasonal heat storage for the thermal share of the primary source, the solar irradiation, allows large reductions in electricity required to operate a heat pump in winter. The boundary conditions for the passive components of a building with a Sol^{2}ergie system are set by the low temperature lift between the heat source and sink to reach a high COP of the heat pump a reduced maximum load. With regard to the overall reduction of CO_2-emissions, this approach constitutes an interesting strategy, especially in the case of refurbishments.

PV/T are an essential part of the system. In principle they consist of water-cooled PV-modules, which can be thermally insulated on the backside. Their characteristics correspond to those of unglazed thermal collectors. The cooling effect of the heat absorber increases the electrical output whilst the insulation enhances the thermal gains[3]. In total, PV/T embedded in a low-temperature heat pump system with seasonal heat storage have exergetically wise the highest surface efficiency in transforming the solar irradiation[4]. The surface efficiency of PV/T is a significant advantage compared to other systems, however the current high cost of installation and system integration as well as the bulky modularity of contemporary products represents a major hurdle. The integration analogous to the developments in the BIPV would lead to economic synergies and alleviate the need for maximum surface efficiency in favour of higher design liberty[5, 6]. For this reason the chair of building systems at ETHZ is developing a new hybrid roof construction with integrated PV/T. A first prototype is completed and currently being tested. A large-scale application is scheduled for autumn 2013.

Eventually Sol^{2}ergie isn't just a technical system that replaces the old ones. Moreover it is an approach that tries to find a balance between the culturally inherited patterns and the exigencies of our contemporary society as well as of the natural environment.

[1] For further information: www.solergie.org.

For this study three main research questions were formulated:

- How could the roofs of the considered buildings be transformed so that they contribute a significant part of the thermal need following the Sol^{2}ergie concept?

- How can the numerous synergetic effects of constructively integrated PV/T affect and maybe revive the almost abandoned typology of the pitched roof?

- How could this approach influence the contemporary discussion about the vertical densification of central urban districts?

METHOD

In most studies technical aspects and numerical analysis dominate the evaluation of solar installations as a contribution to a more sustainable future energy system. Furthermore they consider existing structures as to be conserved. The result is a countrywide rag rug of little solar fields that is driven by the idea of efficiency of the single surface and has little to do with the phenomenology of existing roofscapes.

For this reason we have developed a method, which combines numerical modelling with spatial analysis using detailed 3d visualisations. This combination allows an assessment on different scales, as well as the appraisal of objective and more subjective parameters.

In this study, a total of 122 buildings in four existing areas are investigated and 7 different scenarios are developed. All of them are situated in urban centres (Zurich and St. Gallen) where the pressure for transformation is high but which are also admitted to be maintained or strengthen in their physical substance and overall architectural character. Most of the buildings date from the late 19th and early 20th century implicating all the well-known difficulties when it comes to questions of energy saving refurbishments. The typological inventory ranges from perimeter block development to single, multi-storey houses and covers a wide range of roof typologies.

In a first phase the 3d model is set up and every building is characterised by quantitative indicators with an emphasis on the roofs. Illustrations of these indicators allow an additional and more objective comparison between the areas and serve as a basis to develop the different transformation scenarios.

Energy model

The geometric data is used to establish the buildings energy balance and the dimensioning of the Sol^{2}ergie building system. Passive measures are defined so that the temperature in the heat distribution system can be set to a maximum of 35-40°C. The second target for the passive transformation is the symmetry of radiation to guarantee the users' thermal comfort. Subsequently the resulting u-value of the vertical façade must be lower than 0.65 W/m^{2}K in the weighted average. This is achievable with economical and aesthetically acceptable. Invisible parts like basement ceilings are highly insulated ($u < 0.20$ W/m^{2}K). Together with an adapted domestic hot water system, these transformations lead to an average energy demand of 60 kWh/m^{2}a and a max. load of 36 W/m^{2}a according to SIA 380/1 (2009). The other important system temperature depends on the source for heat pump. To achieve a constantly high source temperature, Sol^{2}ergie uses the deep ground under or nearby the building as a seasonal heat storage, which must be regenerated in summer. In this study the only sources for this process are local PV/T. Consequently their summer yield must match the whole annual thermal energy demand minus the electrical input to the heat pump. Assuming a performance factor of the heat pump g=0.5, the thermal yield that must be generated by the PV/T can be defined. The thermal output of the PV/T for the specific locations and

orientations is simulated with TRNSYS (Table 1). The absolute value for the best orientation (Azimuth 20°;180°S) are 451 kWh/m^2 in summer for Zurich and 436 kWh/m^2 for St. Gallen. This reduction ratio is applied to determine the thermal yield of every specific roof surface.

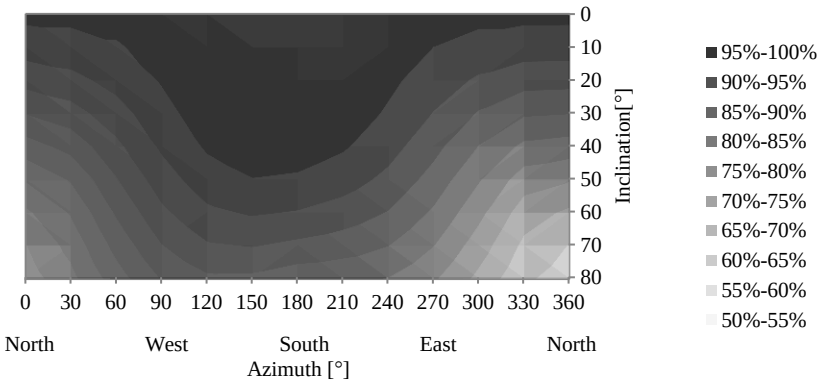

Table 1: Relative PV/T surface efficiency (thermal yield in summer). The system configuration allows more flexible placement compared to installations, which focus on the yearly gains.

Transformation scenarios

The seven scenarios are described in table 2. They vary in terms of their conceptual approach and their depth of penetration into the existing structures. For each scenario the contribution of the PV/T is calculated as a ratio between the thermal yield and the demand of the specific building. To discuss the spatial and typological transformation, every scenario is illustrated in two street views, one view from the roof level and one bird's eye view (Figure 1-3).

Scenario 1	S1_SG_P S1_SG_S S1_ZH_K S1_ZH_S		All existing surfaces larger than 5m^2 and a surface efficiency above 60% are replaced by integrated PV/T-collectors. It shows the theoretical potential of the present roof surfaces.
Scenario 2	S2_SG_P S2_SG_S S2_ZH_K S2_ZH_S		PV/T-collectors are applied as standard modules (PV/T-collector 3S-PV, size: 1.65*1m) according to the current building legislation and recommendations for the integration of PV and solar thermal installations in Zurich.
Scenario 3	S3_SG_P S3_ZH_K		A secondary building element is applied in the form of a shed dormer that offers a good surface orientation for PV/T and additional useable volume underneath. The shape of the primary roof construction is not manipulated whereas the secondary structure is a modification of an existing typology.
Scenario 4	S4_SG_S S4_ZH_S		The kerb roof serves as a typological reference to establish a horizontal zoning. The 1st level mediates between the corpus and the roof. The 2nd level accommodates well-oriented, integrated PV/T-surfaces and the 3rd level is used as a terrace as soon as the energy benchmark is accomplished. Additional living space.
Scenario 5	S5_SG_S	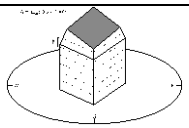	An integrated PV/T surface is applied on every building. The size, orientation and inclination are chosen to achieve the benchmark with a minimal PV/T area. The emphasis is placed on efficiency and autonomy with no regard on existing typologies. Additional living space.
Scenario 6	S6_SG_S	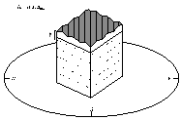	A layer of integrated PV/T replaces the existing roof scape. This scenario is deduced from the idea of a superior, communal infrastructure. The maximal total yield is attained with an E-W orientation and a 15° inclination (minimal shadows). The building corpus is heightened to maintain the initial volume.
Scenario 7	S7_SG_S	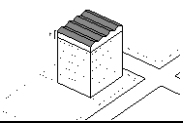	Similar to S6 a "solar layer" replaces the existing structures. But the homogeneous pattern is altered by the size and orientation of the buildings to merge the existing urban layout.

Table 2: Schematic illustration and description of transformation scenarios.

RESULTS AND DISCUSSION

To compare the scenarios the thermal contribution potential of the PV/T-collectors are shown in table 3. Since the energy and the power demand per m^2 heated are normalised, the remaining variables are the ratio between the heated floor area and the PV/T area as well as the quality of the latter (surface efficiency). This becomes obvious in scenario S3. The buildings in Paradiesstrasse, St.Gallen (S3_SG_P) are mainly 3-4 stories high and have well oriented and simple primary roof structures while they are 5-6 stories high and have a lot of very steep roof surfaces in the case of Kanzleistrasse, Zurich (S3_ZH_K). The district ratio raises the possibility of trade-off systems between several buildings (e.g. perhaps some buildings should be preserved whereas others offer good installation opportunities).

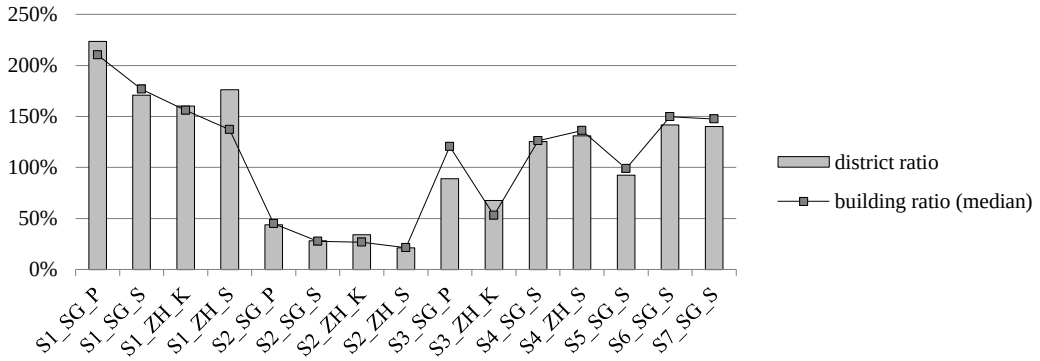

Table 3: Thermal contribution potential of PV/T-collectors for the different scenarios.

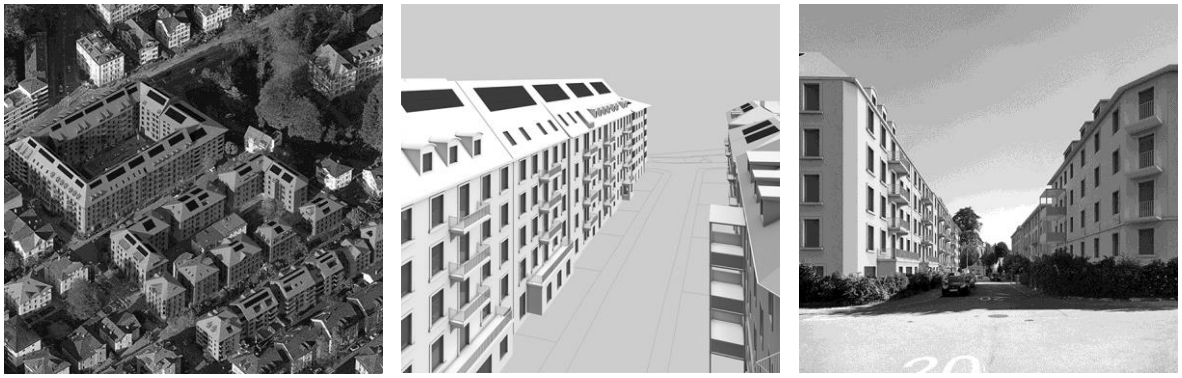

Figure 1-3: 3d-visualisations from different viewpoints (ex. S2_SG_S)

Figure 4-6: 3d-visualisations of three different scenarios (ex. S3_SG_S; S4_SG_S; S7_SG_S)

In general one can see that a consequent accomplishment of contemporary installation paradigms does not lead to satisfying results in terms of energy as well as roof design (S1.3).

On the other hand, all the scenarios that are emphasising the maximum energy yield while neglecting the physical heritage lead to abrupt ruptures. S3 and S4 may be successful strategies, because they are developed from existing typologies in an "amalgamating" process.

CONCLUSION

As a conclusion of this study we argue that:

1. Even though technology will become more surface-efficient, the problem lies in the lack of well-suited surfaces. If the entire thermal energy demand is locally generated by PV/T, the roof needs to be reinterpreted. The additional function must be carefully brought in line with traditions, but by doing so the functional densification increases the (positive) ambiguity and (lost) integrity of the building element. Instead of creating a rig rug, the roof as whole must be seen as an energy-generator. Pursuing the synergetic effects of the building integration will lower costs and facilitate architecturally coherent and energetically sufficient constructions.

2. The indirect correlation between energy consuming area and energy generating area may launch a new planning instrument. Given a certain energy standard, a building should be able to generate the heat on-site and therefore offer enough well suited surfaces as long as there is no other heat source available.

3. Despite the fact that the a large portion of new roof constructions are flat roofs, the aesthetic legacy of the modernist movement and the subsequent developments in the construction industry, the archetype is still a pitched roof. The technical benefits of slanted solar installations may introduce a renaissance of pitched roof constructions.

4. These new hybrid roofscapes have manifold economical leverage effects to be studied. They increase the buildings' value by creating additional and attractive living space and supply their host buildings with CO_2-emission free energy without burdening the existing communal infrastructure.

ACKNOWLEDGEMENTS

The authors would like to thank the city of Zurich and St. Gallen as well as FA. Velux AG, ZZ Wancor AG and Eternit AG (Switzerland) for their financial support.

REFERENCES

1. Schittich, C., *Das flache Dach: eine Entwicklungsgeschichte*, in: *Flachdach Atlas Werkstoffe, Konstruktionen, Nutzungen*, K. Sedlbauer, Editor 2010, Basel, Birkhäuser, S. 10 - 21
2. Burren, B., C. Vogt, und M. Tschanz, eds., *Das schräge Dach: ein Architekturhandbuch*, 2008, Sulgen, Niggli
3. Bätschmann, M. und H. Leibundgut, *LowEx Solar Building Systems: Integration of PV/T collectors into low exergy building systems*, in: Solar Heating and Cooling SHC, 2012, San Francisco
4. Meggers, F., et al., *Low exergy building systems implementation*, Energy, 2012, 41(1), S. 48-55
5. Anderson, T.N., et al., *Performance of a building integrated photovoltaic/thermal (BIPVT) solar collector*, Solar Energy, 2009, 83(4), S. 445-455
6. Reijenga, T. und H. Kaan, *BIPV in Architecture and Urban Planning*, in: *Comprehensive Renewable Energy*, A. Sayigh, Editor 2012, Amsterdam, Elsevier, S. 697 - 707

OPTIMIZATION OF THE BUILDING ENVELOPE'S GEOMETRY TO MAXIMIZE SOLAR ENERGY COLLECTION

N. Kotelnikova-Weiler [1]; O. Baverel [1,2]; J.-F. Caron [1]

1: UR Navier, Université Paris-Est, Ecole des Ponts ParisTech, 6-8 avenue Blaise Pascal, 77455 Marne-la-Vallée cedex 2, France

2: Ecole Nationale Supérieure d'Architecture de Grenoble

ABSTRACT

The concept of a Solar Shell emerged from a paradox. Indeed it is common sense that to reduce energy losses through external surfaces, the building must be as compact as possible and at the same time these same surfaces need to expand in the interest of collecting solar energy. The idea is to separate the two functions of the building facade into two different envelopes: isolating and collecting. In refurbishment projects the first step consists in insulating the existing envelope in order to reduce energy losses. The next step proposed in this approach would allow a building to cross the gap between zero energy and plus energy. It consists in installing around the insulated envelope a second skin, the Solar Shell. The geometry of this skin is free from internal functional constraints. The present study is aiming at the optimization of its geometry and the distribution of energy collectors (such as solar cells) on its surface. Thus the present work fits into a climate-driven design strategy.

The following environmental conditions were taken into account: sun's path in the sky according to the geographic location of the considered building, daily and seasonal variation of the solar energy perceived on the ground level, surrounding and distant obstacles masking the sun. The surface of the envelope to be optimized is divided into triangular facets. Each facet is described by the position of its edge points and the type of filler it contains (either energy collector of a certain nature or glass/opaque pane). Then genetic algorithms are used to optimize the envelope. Each given envelope represents an individual. The initial population is random. That is for each individual the position of the edge points of the facets forming the envelope and the type of filling panels are chosen randomly. Then the individuals' fitness is evaluated with the aim of maximizing the energy produced by the panels. Next, a new generation is formed using the best fitted individuals.

The tool was then applied to optimize the geometry of a building's envelope and the spatial distribution of solar panels on it. The building was partially shaded with neighbouring constructions of various heights and widths. This results in different optimal solutions. Robustness of such a design approach was then assessed by comparing the performances of a given optimized solution placed in a modified shading context. This highlights the issue of solar rights in the evolving urban context.

Keywords: solar energy, genetic algorithms, geometry optimization, solar cell, shading mask

INTRODUCTION

Today's energy and environmental context demands urgent solutions to reduce buildings energy demand. This will be reached by reducing energy losses through the building's envelope and at the same time by using its surface to collect solar energy. The concept presented in this work is illustrated in the figure 1. The building' envelope is separated into two envelopes. The internal envelope's role is to thermally isolate the building. Its geometry can therefore be as compact as possible. The external envelope's role, on the other hand, is to

collect solar energy. This solar energy can then be converted to either electrical power or heat depending on the solar collectors installed (thermal collectors or solar cells). The geometry of this Solar Shell is relatively free from internal constraints. Solar collectors spatial distribution and the geometry of the Solar Shell can therefore be optimized in order to maximize solar energy production. The problem of optimizing buildings envelope geometry was already addressed in several theoretical works (such as [1,2,3]) but in the present work, close obstacles partially shading the optimized building were also treated and different geometric description of the envelope was also adapted (see PhD thesis [4] for more details).

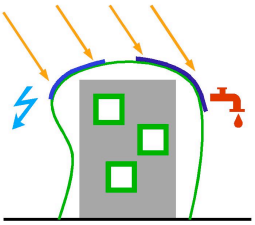

Figure 1: Solar Shell concept. External envelope's role is to produce heat and power.

SOLAR OPTIMIZATION METHODOLOGY

Objective function

Solar radiation reaching the atmosphere is partially transmitted forming the beam component. Another fraction of the solar radiation is diffused by the atmosphere. When reaching the ground it is reflected towards buildings. Thus the solar radiation reaches solar collectors installed on a building envelope in three different forms: beam, diffuse and reflected radiation. In the present work solar collectors were chosen to be characterized by the various components yield. Equation (1) gives the energy produced by the solar collector i. $\mu_{i,j}$ is the yield of the collector i from the component j (b – beam, d – diffuse, r – reflected). Opaque panels that do not produce energy have zero yields.

$$E_{p,i} = \mu_{i,b}E_{b,i} + \mu_{i,d}E_{d,i} + \mu_{i,r}E_{r,i} \quad (1)$$

The energy produced by the envelope of the building is therefore equal to the sum of the energy produced by its solar collectors. This is expressed in the equation (2.b). In the present work, the aim of the optimization process is to maximize the total energy production divided by a weighted surface of the envelope. The weighting coefficients α enable to represent the cost associated with solar collectors and opaque panels. Equations (2.a) and (2.c) give respectively the expressions of the objective function and the weighted surface of the envelope.

$$\max\left(\frac{E_{p,tot}}{S}\right) \text{ (a)} \qquad E_{p,tot} = \sum_i E_{p,i} \text{ (b)} \qquad S = \sum_i \alpha_i S_i \text{ (c)} \quad (2)$$

Envelope description

The figure 2 illustrates the envelope description used in this work. The envelope is described as a faceted surface (fig 2.a). Each facet is either a solar collector of a given type (characterized by its yield) or an opaque panel. Facets are triangular in shape and each vertex of the triangles becomes a control point of the geometry (fig. 2.b). During the optimization process, the control points can take several positions defined between an internal constraint (corresponding to the internal volume of the building) and an external constraint (such as the constructible volume of the site) (fig. 2.c).

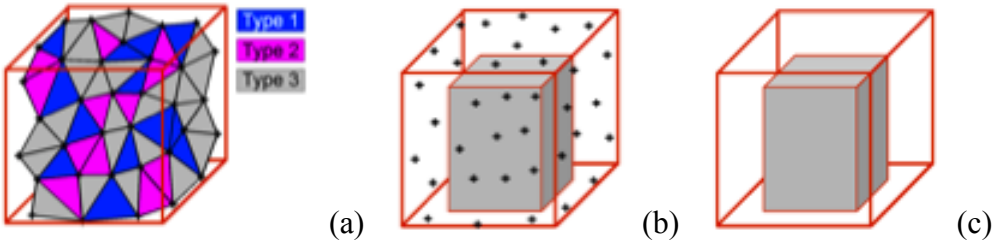

Figure 2: Envelope description. a – triangular facets and their types; b – control points of the geometry; c – internal and external constraints restraining control points positions

Genetic algorithms

Optimizing the envelope means optimizing the position of each control point (parameter X_i) and the type of filling panel of each facet (parameter T_j). The objective function in this problem is non linear, the combinations of X_i and T_j parameters are numerous. In these conditions genetic algorithms can be used to solve the optimization problem. A given envelope (its geometry and collectors spatial distribution) is considered as an individual. X_i and T_j represent the "genetic code" of this individual. A group of different individuals form a population. Figure 3 represents the three scales of genetic representation of the optimization problem.

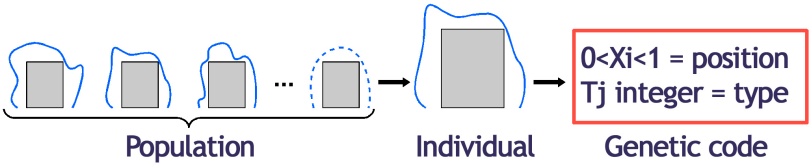

Figure 3: genetic representation of the optimization problem

Main steps of the optimization using genetic algorithms are: the first population is generated defining random individuals; these individuals are assessed: their objective function is evaluated; best individuals are chosen to form "parents" for the next generation; cross-over and mutations are performed to form the next generation population. In the present work, genetic algorithm BIANCA was used [5,6,7]. A specific research tool called "SolarOptiForm" was developed able to correctly evaluate the objective function, that is evaluate beam, diffuse and reflected components of solar radiation received on collectors, depending on time and location of the building studied, and taking into account the potentially complex shape of the envelope leading to self-shading. This tool then uses BIANCA to optimize the envelope.

OPTIMIZATIONS WITH DIFFERENT SHADING PATTERNS

Optimization conditions

The optimization was performed for solar radiation conditions of Paris, France. The optimization is performed over a year represented by 4 characteristic days. For each date 4 calculations of the radiations are performed. Internal and external geometric constraints are two parallelepipeds of respective dimensions 50*50*30 and 110*110*60 (Length*Width*Height). The envelope is optimized in the case of two different shading configurations. In the first configuration a small obstacle is placed close to the South-West corner of the building. In the second configuration, a large and tall obstacle is placed facing the South façade of the building. The envelope is described with 45 control points (approximately 85 triangular facets – potential collectors). In each generation, a population of 6000 individuals is treated. The optimization stopped after 1200 generations, which enabled,

in both cases to reach a stabilization of the objective function over generations. Three possible types of fillers are defined as follows: opaque panel with zero yields; diffuse-sensitive collectors with a 100% yield for diffuse and reflected radiations and zero yield for beam radiation; direct-sensitive collectors with a 100% yield for beam radiation and zero yield for diffuse and reflected radiation. Opaque panels have a weight coefficient of 0,3 and solar collectors have a weight coefficient of 1.

Results and comparison for different shading patterns

Figures 4 and 5 represent the best individual, envelope, of the last generation respectively for a small and the large and tall obstacles. The geometry of the envelope optimized in the presence of a small obstacle is rather flat. On the North façade, most of the collectors are diffuse-sensitive, whereas on the South façade, the collectors are direct sensitive. The geometry obtained with no obstacles at all is slightly modified by the presence of this small obstacle.

The strategy of energy collection used in the presence of a large and tall obstacle is to avoid the shade of the obstacle by elevating the whole geometry. On the South façade, where direct-sensitive collectors were located in the case of the small obstacle, they are replaced with diffuse-sensitive collectors as this part of the envelope is most of the year in the shade of the obstacle placed in front of the building.

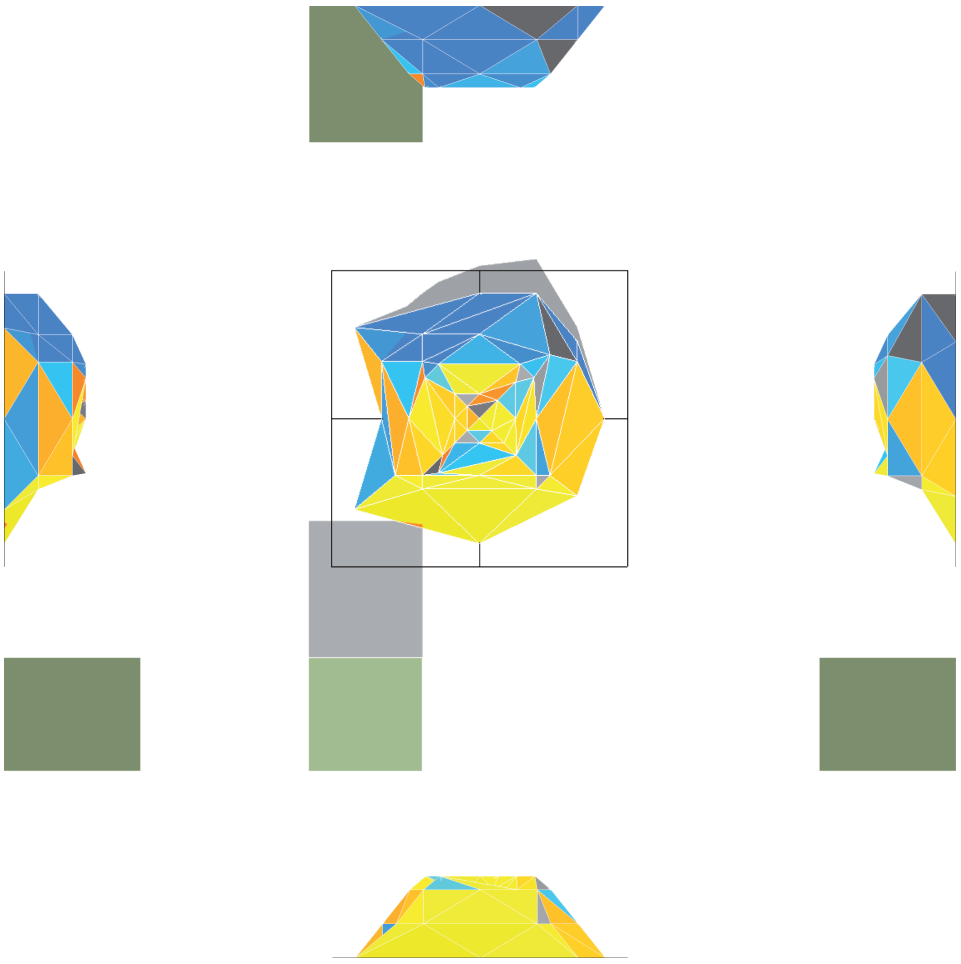

Figure 4: Best individual of the last generation in the optimization with a small obstacle. Top view in the centre, East, South, West and North façades respectively on the right, bottom, left and top.

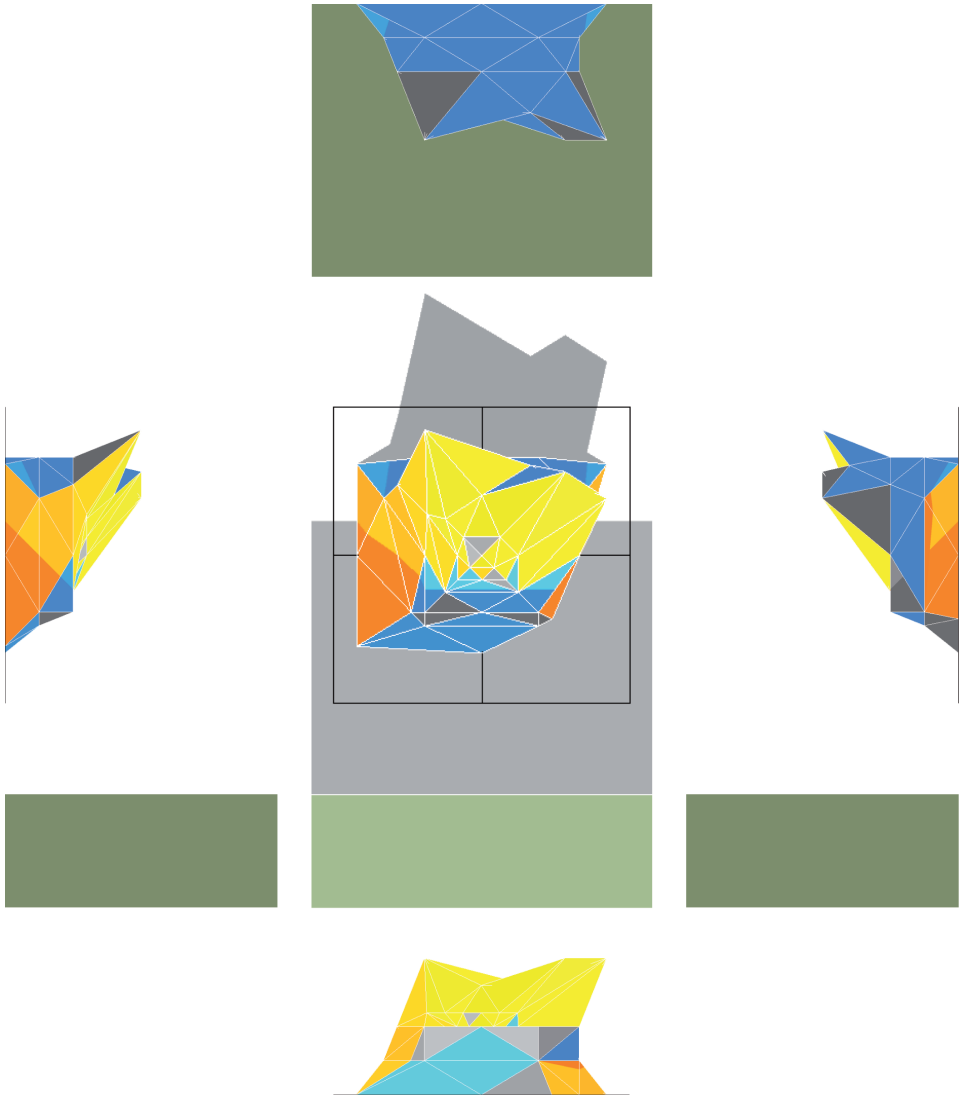

Figure 5: Best individual of the last generation in the optimization with a large and tall obstacle. Top view in the centre, East, South, West and North façades respectively on the right, bottom, left and top.

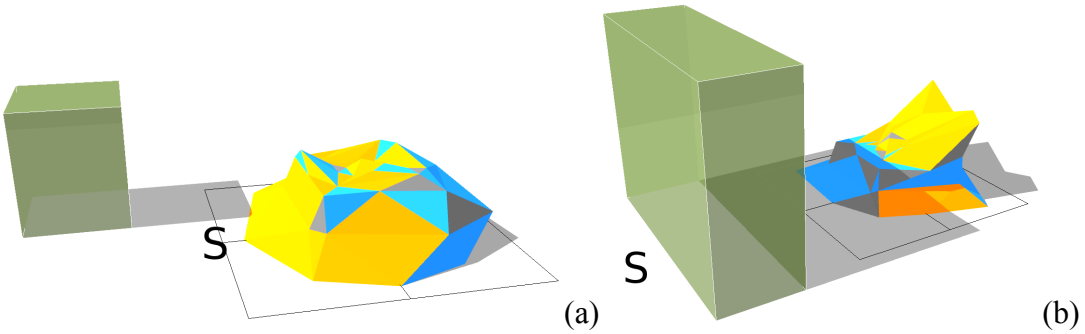

Figure 6: Perspective view of the optimized envelopes in the presence of a small (a) and a large and tall (b) obstacles.

The figure 6 gives a perspective view of the two optimized envelopes and represents the obstacle partially shading them. The South orientation is indicated with “S”. Comparison of the two optimized envelopes shows that although the geometries and collector types distributions are rather different, the proportions of energy production from beam, diffuse and

reflected radiations are similar. In the case with a larger obstacle, the proportion of reflected radiation is greater (6.5% vs 2.9% of total energy produced). An efficiency of the envelope could be defined by the ratio between the total energy produced and the total energy received on its surface. In the two optimization cases presented here, both optimized envelopes have the same efficiency of 55%. However, the envelope optimized in the presence of the large and tall obstacle sees its objective function (total energy produced divided by the weighted surface) reduced by 16%.

SOLAR RIGHT

The optimization cases presented above show that in constrained urban contexts leading to more shading on the envelope, it is still possible to achieve the same efficiency but at higher production costs. In this part the robustness of the optimized solution will be explored.

The envelope optimized with the small obstacle is placed in the presence of the large and tall obstacle and its impact on the envelope's efficiency and objective function is investigated. This case is representative of a situation when new buildings are constructed in the vicinity of a building equipped with finely-tuned solar installation.

In this case it was observed that the total energy production is reduced by 9%. Beam radiation source is the most affected, with a reduction of 14%. The proportion of energy production from the reflected source is increased by 3%, whereas diffuse radiation source is almost unchanged (-1%).

These observations clearly highlight the problem of solar right in urban environment [8]. Today optimization techniques are beginning to be applied in the buildings design. Structural, thermal, lighting and energy generation aspects are increasingly treated with these techniques. This works underlines the importance of robustness studies in these applications.

REFERENCES

1. Kämpf, J.H., Robinson, D., Optimisation of building form for solar energy utilisation using constrainted evolutionalry algorithms. *Energy and buildings*, Vol. 42, 2010.
2. Merello, R., Design of a building structural skin using multi-objective optimization techniques, MIT, Master Degree Thesis, 2006
3. Yi, Y.K., Malkawi, A.M., Optimizing building form for energy performance based on hierarchical geometry relation. Automation in Constrction, Vol. 18, pp. 825-833, 2009.
4. Kotelnikova-Weiler, N., Optimisation mécanique et énergétique d'énveloppes en matériaux composites pour les bâtiments, PhD thesis, Université Paris Est, 2012
5. Montemurro, M., Vannucci, P.n Vincenti, A., Bianca, a genetic algorithm for engineering optimisation – user guide, 2012.
6. Montemurro, M., Vincenti, A., Vannucci, P., A two-level procédure for the global optimum design of composite modular structures – application to the design of an aircraft wing. *Journal of Optimization Theory and Applications*, vol. 155, 2011.
7. Vincenti, A., Ahmadian, M.R., Vannucci, P., Bianca : a genteic algorithm to solve hard combinatorial optimisation roblems in engineering. *Journal of Global Optimisation*, Vol. 48, pp. 399-421, 2010.
8. Etzion, Y., A general expression for solar rights determination. Energy and Buildings, Vol. 12, pp. 149-154, 1988

HEATING AND ELECTRICAL LOAD SHIFTING IN A BUILDING WITH PHOTOVOLTAIC PANELS AND AN ELECTRICAL RESISTANCE HEATER

Amar Abdul-Zahra, Tillman Faßnacht, Andreas Wagner

Building Science Group, Karlsruhe Institute of Technology (KIT), Englerstr. 7, 76131 Karlsruhe, Germany

ABSTRACT

The rapid growth of installed renewable energy systems in Germany causes higher amplitudes and frequencies of the fluctuations in the electric grid. This goes along with increasing electricity tariffs and a decrease of feed-in tariffs. One strategy to compensate for that is to increase own energy consumption of electricity from photovoltaic (PV) modules, which are installed in single family houses. This could be extended by using electricity from PV for heating which represents a large portion of the energy demand for residential buildings.

One goal of this paper was to investigate how the own energy consumption from PV panels could be increased by using a simple and low cost heating system that can be directly coupled with PV panels. A simulation scenario has been set up using TRNSYS 17 for a single family house. The low energy consumption of the building (15 kWh/m^2 year) is covered by an electrical resistance heater installed inside a storage tank and connected to PV panels and the grid. Different control strategies and storage volumes have been investigated to maximize own energy consumption. For a given PV-systems maximum power of 3.33 kWp, load shifting leads to an increase of own energy consumption from 44% to 80% (electrical household and heating system considered). A full cost calculation shows that the use of an electrical resistance heater connected to PV panels along with a load shifting strategy can be cheaper than a gas heating system and can have approximately comparable total costs to a gas heating system complemented with a PV system. However the primary energy consumption and CO_2 emissions of the electrical resistance heater heating system is significantly higher compared to the gas heating system complemented with a PV system, but lower compared to a standalone gas heating system.

Keywords: Heating, Electrical Load Shifting, Photovoltaic Panels, Electrical Resistance Heater

INTRODUCTION

The government support of electricity generated from renewable sources in Germany (Renewable Energy Electricity, REE) led to an increase in REE from 17 TWh in 1990 to 123 TWh [1].

The amount of REE supplied to the grid is amongst other things depending on the short-term climatic conditions, e.g. on the solar irradiation, wind and more. The feed-in of the power produced can lead to higher frequency and amplitude of the fluctuations in the electric grid in time periods with high availability of energy from renewable sources. In order to reduce such phenomena, the energy generated from PV modules can be conserved locally, e.g. by thermal energy storage. The goal of this approach is to use a high fracture of the generated energy by PV for own usage.

The increase of own energy consumption (or: "electricity consumption") from PV panels can further have an economic advantage due to the ongoing rise of electricity tariffs, which have increased from 19.0 €cent/kWh in 2007 to 25.7 €cent/kWh in 2012 [2]. This tariff is expected to increase more in the future, while the feed-in tariffs have decreased from 49.3 €cent/kWh in 2007 to 17.0 €cent/kWh in Jan 2013 [3].

One possible method for load shifting is to store the electricity generated from PV panels in the form of heat in thermal storage tanks and discharge the storage at times when less or no solar radiation is available. For the transformation from electricity to heat either heat pumps or electrical resistance heaters (ERHs) can be used. The main disadvantage of ERHs are the lower efficiency compared to heat pumps. However, ERHs are very cheap at almost no maintenance cost, require less space and can provide higher temperatures (>65 °C), which can lead to lower storage tanks volumes for load shifting. This are the causes, why in this paper is evaluated, if an ERH system coupled with a PV system can be a viable option for new buildings of passive house standard. In order to do that, a simulation study in TRNSYS 17, a full cost calculation and a primary energy consumption and CO_2 emission calculation have been performed.

BOUNDARY CONDITIONS OF THE SIMULATIONS SCENARIO

A single family house with an area of 186 m², built according the German passive house standard, has been modelled at the location of Würzburg, Germany. The modelled building leads to a space heating demand of 2790 kWh (15 kWh/(m^2 year)). The electrical demand has been modelled as a typical single family demand profile [4] of 4000 kWh. As domestic hot water (DHW) profile a simplified profile developed in IEA Task 44 has been used. The consumption is 140 l/day at 45 °C [5] and yields to a demand of 2033 kWh/year. The building is equipped with a PV panels area of 23.5 m^2 with a maximum peak power of 3.33 kWp. The maximum efficiency of the modules and inverter are chosen to 14 % and 92 % respectively, while the PV panels direction is assumed to south and the inclination to 40°. This comes to 3886 kWh/year generated by the PV-system. A stratification storage tank is installed inside the building. An ERH with a maximum power of 10 kW is installed inside the thermal storage. The ERH can be supplied by the PV panels directly, or from the grid.

SIMULATION SCENARIO AND CONTROL STRATEGY

The heating system of the building consists of the floor heating, the ERH installed in a multi-mode cylinder and the PV installation. The flow temperature to the floor heating is calculated by a heating curve (i.e. $T_{h\_d} = f(T_{amb})$ and between 25-35 °C). Based on this system the ERH will start to operate to ensure the supply for the heating and DHW demand, if:

$$T_{s\_m} < T_{h\_d} \quad \text{or} \quad T_{s\_up} < T_{set\_dhw} - 3K \tag{1}$$

Where:

T_{s_m}, T_{s_up}: water temperatures at levels of 0.58 and 0.66 relative height of the storage tank.

T_{h_d}: set temperature of the supply water to the building $T_{h\_d}=f(T_{amb})$

T_{set_dhw}: set temperature in the top part of the tank, which is used for DHW heating.

Without load shifting the ERH will work until the following conditions are met:

$$T_{s\_m} \geq T_{h\_d} + 3 \quad \text{and} \quad T_{s\_up} \geq T_{set\_dhw} \tag{2}$$

The load shifting is achieved by operating or using the ERH as often as possible when more PV-Power is available then required by the household. Therefore the ERH will run when:

$$PV_{Power} > 0 \quad \text{and} \quad T_{s\_m} < T_{\max} \quad \text{and} \quad T_{s\_up} < T_{\max} \tag{3}$$

T_{max} is the maximum temperature in the storage for the load shifting and has been varied in the simulation study. The current generated by the PV panels is first supplied to the household demand, then to the ERH and at last to the grid.

FULL COST CALCULATION

A full cost calculation was performed and the results compared to the cost of a gas heating system and a gas heating system complemented with a PV system. The cost calculation includes:

1- Investment cost (cost of boiler/ERH, heat distribution, thermal storage, gas connection, chimney, heating system installation, PV system, VAT, etc).

2- Operation cost

a- Maintenance (e.g. chimney sweep and tank cleaning per year).

b- Energy cost of the heat source (gas / electricity).

The cumulative costs after 20 years are then

$$C_T = C_I + \sum_{n=1}^{L} C_o \cdot (1+r)^{(n-1)} + \sum_{n=1}^{L} C_M \cdot (1+p)^{(n-1)} \tag{4}$$

Where: C_T= total cost after 20 years, C_I= investment cost, C_o= operation cost, r_o: energy price increase rate per year (assumed to be constant), C_M= maintenance cost per year, p= maintenance price increase rate per year, L= lifetime.

PRIMARY ENERGY DEMAND AND CO_2 EMISSIONS

In order to assess the energy performance of buildings with different heating systems, the primary energy and CO_2 emissions have been calculated for the ERH + PV system, gas + PV and gas heating system. The calculation is based on the standards EnEV 2009 and prEN 15203 [7, 8]. Table (1) shows the used primary energy and CO_2 factors.

Energy carrier	**primary energy factor**	**CO2 production [kg/kWh]**
Natural gas	1.1	0.277
Electrical energy	2.6	0.617

Table (1): Primary energy and CO_2 emission factors.

RESULTS

Own electricity energy consumption from the PV array

The energy from the PV panels is at first supplied to the electricity demand of the household and then to the heating system and at last to the grid. The own energy consumption for the household demand and the heating system without special control for load shifting is 44%. Figure (1) includes the own energy consumption from the PV system (black columns) with applied control for load shifting. One can see that it is greatly influenced by the value of T_{max}. The x-axis in Figure (1) represents the maximum temperature while the load shifting at the sensor T_{s_m} inside the storage. The two numbers ((80, 60), (80, 55),…) in the x-axis indicate the use of a different control strategy for T_{max} adopting two values during the year depending on the season. The first number is the maximum temperature allowed in heating season and

the second number is the maximum temperature allowed during summer season. When electricity is available from the PV panels, the temperature set point of the thermal storage is increased during the heating season. During the summer season, the set point is lowered to decrease the amount of heat losses from the storage. To further compare the different control parameterizations figure (1) also includes as gray columns a static cost balance. The energy cost balance represents the difference between the price of purchased electricity from grid and the price of electricity from PV array sold to the grid. According to this cost esteem, the best control strategy of the investigated cases was found to be T_{max} = (70, 60). Based on the approach that the system should have a high own consumption rate, but should be economic competitive, the parameterization with T_{max} = (70, 60) is used further on in the following investigations.

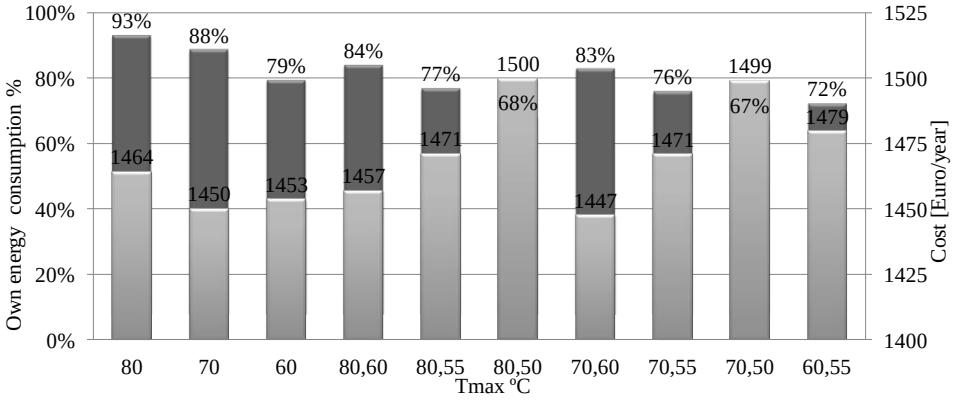

Figure 1: The black columns are total energy consumption from PV panels and the gray columns are energy costs balance with different values of Tmax.

Thermal Storage volume

The achievable own energy consumption from PV depends on the storage size. To find out the best storage tank volume in regard of own consumption and energy cost balance, four different storage tank volumes have been tested. The maximum own consumption from PV panels was observed to be 94% at a storage tank volume of 3 m^3 (see figure 2). The best case from the economic standpoint was obtained with a storage tank of 0.56 m^3 and 80% own energy consumption from the PV panels. This is mainly caused because of lower heat losses compared to the simulations with bigger storage sizes. Based on this results a storage tank with 0.56 m³ volume has been taken into consideration for the full cost and primary energy calculations.

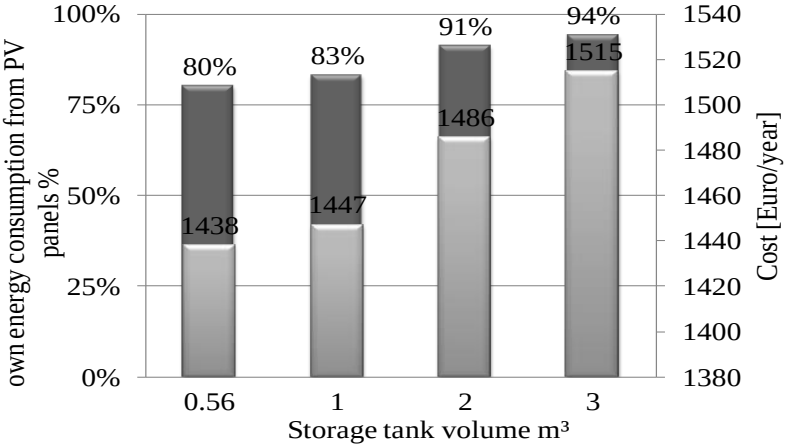

Figure (2): Own energy consumption from PV panels and energy cost balance with different storage volumes

Full cost calculation

Table (2) and figure (3) present the cumulative cost within 20 years lifetime for a gas and a gas heating system complemented with a PV system as well as the ERH+PV heating system. In the calculation the electricity demand of the household is implemented. The Gas+PV heating system present here the lowest cumulative cost in 20 years lifetime due to its low operation cost and the feed-in tariff, where idle energy can be sold to the grid. While the ERH+PV is cheaper than standalone gas heating system due to its low investment cost, the low electricity demand from grid (= high PV own consumption) and the feed-in tariff.

Details	Gas+PV	Gas	ERH+PV
Investment cost: heating source, distribution, installation, storage tank, floor heating, etc [€]	23744	17969*	15057
Maintenance cost per year [€]	250	180*	100
Yearly efficiency of heating system	0.85*	0.90*	0.94
Energy from PV panels supplied to the building [%]	41%	0	80%
Money from sold PV current to grid (feed-in tariff) [€/year]	389	0	131
End energy demand of the heating system [kWh/year]	6531	5844	3070
Energy costs heat source [€cent/kWh]	9.0	7.0	25.7
Energy price increase rate per year	5.4%	5.4%	5.4%
Maintenance cost price increase rate per year	2%	2%	2%
Lifetime [year]	20	20	20
Total costs for 20 year [€]	64000	76609	66314

*Table 2: Results of full cost calculation. (*taken from [6]).*

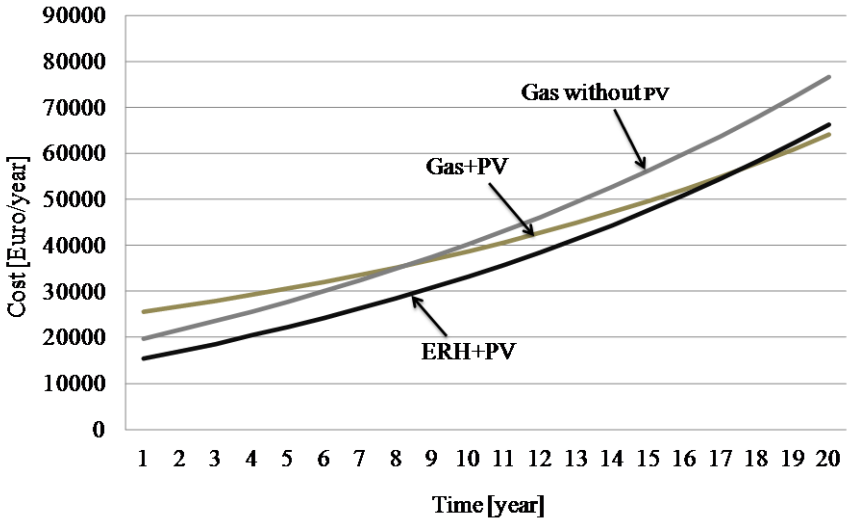

Figure (3) cumulative cost within 20 years lifetime

Primary energy and CO_2 emissions

Figures (4) represent the primary energy and CO_2 emissions for the same systems as in the full cost calculation. It can be seen that the primary energy consumption and CO_2 emissions for the building with ERH+PV are advantageous over the gas heating system alone, but if additive a PV system is installed the gas+PV system has significant lower primary energy consumption and CO_2 emissions. In this calculation the PV energy, which is fed into the grid, has not been considered for the primary energy and CO_2 calculation.

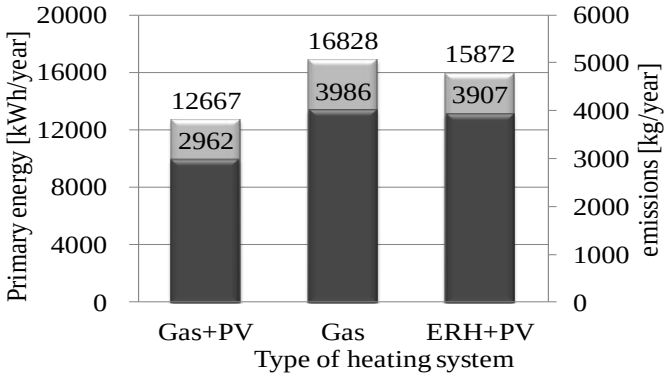

Figure 4: Primary energy consumption and CO_2 emissions for different heating systems.

CONCLUSIONS

This study shows the effect of applying electrical load shifting with an ERH to increase own energy consumption from PV panels. An increase was achieved from 44% to 80%. The load shifting strategy leads to a decreased energy cost by 8 % compared to the energy cost without electrical load shifting and 40 % to that without using PV panels at all. The full cost calculation for different heating systems shows that the ERH with PV panels and electrical load shifting has approximately the same costs, as a gas heating system complemented with PV and is cheaper than a gas heating system. The ERH+PV system has in the case at hand with a passive house a better cost structure than the gas heating system, due to its low investment and maintenance costs in addition to financial returns from supplying the additional produced electricity to the grid. In the future the feed in tariff will further decrease, this has a bigger impact on the gas+PV system than on the ERH+PV, because of the lower own consumption rate of the gas+PV system. For that reason the ERH+PV system will be cheaper when the feed-in tariff falls below approximately 10 €cent/kWh. However, the disadvantage of the ERH heating system is a higher primary energy consumption and higher CO_2 emissions compared to gas+PV due to additional back up electricity consumption which has to be taken from the grid at low PV energy production rates. But compared with a standalone gas heating system the ERH+PV heating system is cheaper and yields to a lower primary energy consumption.

REFERENCES

[1] BMU-KI III 1 according to Working Group on Renewable Energy-Statistics (AGEE-Stat); as at: July 2012

[2] Bundesverband der Energie- und Wasserwirtschaft e.V.: "BDEW-Strompreisanalyse Mai 2012", www.bdew.de .

[3] Erneuerbare-Energien-Gesetz – EEG, veröffentlicht durch die Bundesnetzagentur (Stand: 31.01.2013).

[4] E.ON Mitte: http://www.eonmitte.com/de/netz/veroeffentlichungen, April 2013 .

[5] Haller, M.: "IEA SHC Task 44 / A38 Simulation boundary conditions. IEA Task 44 Meeting", Barcelona, April 8th, 2011.

[6] Wirtschaftsministerium Baden-Württemberg: "Energie sparen durch Wärmepumpenanlagen", aktualisierte Auflage Oktober 2005.

[7] EnEV 2009: „Energieeinsparverordnung", 2009.

[8] prEN 15203 / 15315: „Energy performance of buildings — Overall energy use, CO2 emissions and definition of energy ratings", 2006.

URBAN WIND TURBINES: POTENTIALS AND CONSTRAINTS

Islam Abohela; Neveen Hamza; Steven Dudek

School of Architecture, Planning and Landscape, Newcastle University, Newcastle upon Tyne, UK, NE1 7RU.

ABSTRACT

This paper, is part of a research investigating variables affecting the performance of urban wind turbines, specifically roof mounted wind turbines. These variables include wind direction, roof shape, building height and surrounding urban configuration. Computational Fluid Dynamics (CFD) is the tool used for assessing wind flow around the investigated cases. The CFD simulations are validated by comparing the results with in-situ measurements and wind tunnel tests results for wind flow around a surface mounted cube in a turbulent channel flow. The validation study shows that the CFD simulations compare favourably with both the wind tunnel tests results and the in-situ measurements. Results show that for each roof shape there is an optimum mounting location for roof mounted wind turbines and among the investigated roof shapes, the barrel vaulted roof had the highest accelerating effect on wind flow above the roof. Also, it is evident that changing wind direction, building height and surrounding urban configuration had an effect on choosing the optimum mounting location and the energy yield. In addition to presenting the results of the simulation work, this paper focuses on presenting the effect of the investigated independent variables on the wind velocity and turbulence intensity at the wind turbine's proposed mounting location, accordingly, on the energy yield of the proposed wind turbine. Recommendations of the research are also outlined focusing on the potentials of integrating wind turbines within buildings and what is needed for this kind of integration to be successful. In light of the obtained results of the research, the paper concludes by discussing how architects can implement the available wind assessment tools and their knowledge of the design process in providing an informed decision regarding integrating wind turbines within the built environment and in the vicinity of buildings and to what extent should the design of a building be affected by the decision of integrating wind turbines.

Keywords: Urban Wind Turbines, CFD, Roofs, Architects, Design

INTRODUCTION

The state of uncertainty regarding the viability and feasibility of urban wind turbines is evident. The unfavorable wind conditions in urban areas due to the variation in the surface features are well established in research [1, 2, 3]. On the other hand, the wind accelerating effect of buildings and the potentials of wind turbines taking advantage of the augmented wind presents itself as a potential for harnessing wind energy [4, 5]. Urban wind turbines send visual messages for tackling climate change which might encourage people on cutting down on their energy consumption while generating their own electrical power. On the other hand, the main idea behind urban wind turbines is to generate electricity where it is consumed, thus cutting down on the extra costs of infrastructure, cabling and power losses [6]. Accordingly, positioning roof mounted wind turbines at the optimum mounting location and the optimum roof shape for mounting wind turbines needed to be investigated. In addition, other factors such as wind direction, building height and surrounding urban configuration have an effect on the energy yield and positioning of roof mounted wind turbines, thus needed investigation. This work provides a scientific framework to assess wind flow around buildings for

accurately positioning wind turbines to help in improving the energy yield of roof mounted wind turbines. Investigated cases include wind flow around flat, domed, gabled, pyramidal, barrel vaulted and wedged roofs (Figure 1). Investigated urban configurations include an urban street canyon configuration and a staggered urban configuration.

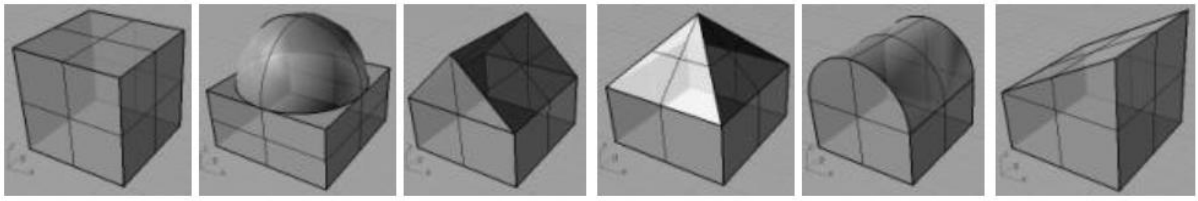

Figure 1: Different investigated roof shapes.

METHOD

Specifying the mounting location of a wind turbine within the built environment or close to buildings requires an understating of the nature of urban wind flow regimes. Accordingly, the available tools for assessing wind flow within the built environment were reviewed to specify the most relevant tool for assessing urban wind which, in this case, was the Computational Fluid Dynamics (CFD) simulations. Literature on CFD and its usage for assessing urban wind flow was reviewed in order to specify the best practice guidelines for using CFD in assessing urban wind flow. Based on the reviewed literature, the Realizable k-ε turbulence model was used. Reviewed research recommended running validation studies to assure the consistency of the yielded results. Thus, a validation study was required to give confidence in the data entry of simulations variables in order to yield consistent results of the investigated flow problems. For a detailed discussion on the best practice guidelines for CFD simulations, the set of used simulation variables and the validation study, the reader is referred to the publication by the authors titled: *Validating CFD simulations of wind flow around a surface mounted cube in a turbulent channel flow* [7].

Despite the limitations of the used wind assessment tool, the results were consistent and compared favourably with the results from other published wind assessment tools such as wind tunnel tests and in-situ measurements. Accordingly, the simulation conditions were used for investigating the main flow problems in this research to identify the optimum roof shape for mounting wind turbines, in addition to identifying the effect of wind direction, buildings height and surrounding urban configuration on the energy yield and positioning for roof mounted wind turbines.

RESULTS

Validating CFD simulation results

The extracted best practice guidelines for CFD simulations were used as the start point for the validation study. The validation study investigated wind flow around a cube in a turbulent channel flow and compared the obtained CFD results with in-situ measurements, wind tunnel tests results and validated CFD simulations results. Figures 2a and b show the vertical and horizontal stream wise velocity path lines for the obtained CFD simulation results showing the main flow features and their positions which was compared with wind tunnel tests, in-situ measurement's and validated CFD simulation results. In addition, Figure 2c shows the obtained pressure coefficients along the centreline of the cube compared to other results using the previously mentioned tools. It can be argued that the obtained CFD simulation results in this work compared favourably with the reviewed results. In addition, the obtained results in

this work can be considered the closets results among the reviewed CFD simulation results to published wind tunnel tests and in-situ measurements.

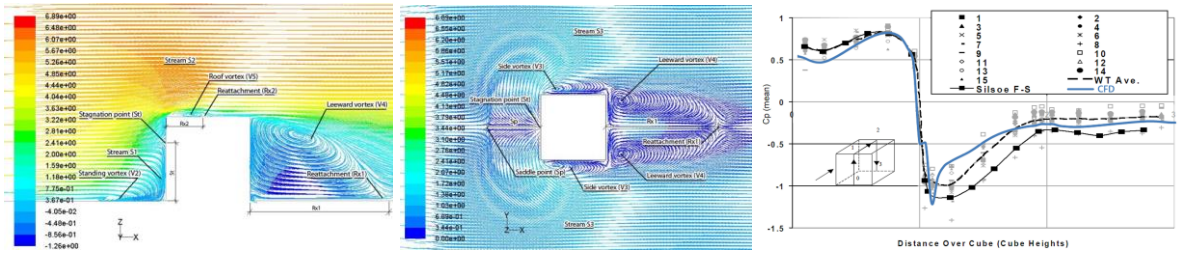

Figure 2 Left (a), middle (b) vertical and horizontal stream wise velocity path lines. Right (c) Pressure coefficients along the centreline of the cube.

Investigated independent variables

In order to assess the effect of wind direction, roof shape, building height and surrounding urban configuration on the energy yield and positioning of roof mounted wind turbines, two dependent variables should be investigated; these are the wind velocity and the turbulence intensity as they are the main variables affecting the performance of wind turbines since the nergy yield of the wind turbine is directly proportional to cube the wind speed.

Wind direction variable

It was hypothesized that studying the variation in wind directions may or may not change the optimum mounting location of a roof mounted wind turbine. It was noticed that for all roof shapes except the domed roof, specifying the optimum roof mounting location for a wind turbine depends on the wind direction since the optimum location on top of each roof shape changed with the change in wind direction. Accordingly, identifying the effect of different wind directions on the optimum roof mounting location of a wind turbine is achieved.

	Flat	Domed	Gabled	Pyramidal	Barrel vaulted	Wedged
Max. stream wise velocity	1.12	1.14	1.09	1.08	1.16	1.14
Wind direction	45^0	45^0	45^0	45^0	0^0	135^0
Increase in energy yield	40.5%	48.2%	29.5%	26%	56.1%	48.2%

Table 1 Maximum recorded acceleration above the investigated roofs under different wind directions

For the domed roof, the location of maximum acceleration under different wind direction was always the same (midpoint of the roof) and since the energy yield of a wind turbine directly proportional to cube the velocity [8], the increase in energy yield for an integrated wind turbine at that location would yield 40.5% to 48.2% more power based on the wind direction. The consistency in the location can be attributed to the symmetrical properties of the domed roof.

As seen in Table 1 all roof shapes under different wind directions had an accelerating effect on wind above the roof. Maximum acceleration above flat, domed, gabled, pyramidal, barrel vaulted and wedged roofs reached 1.12U, 1.14U, 1.09U, 1.08U1.16U and 1.14U respectively (where U is the wind velocity under the same flow conditions, at the same location in an empty domain), at wind directions 45^0, 45^0, 45^0, 45^0, 0^0 and 135^0 respectively. All roof shapes under different wind directions increased the turbulence intensity on top of the investigated roof shapes.

Roof shape variable

For each roof shape there is an optimum mounting location for wind turbines. Thus, if wind flow above each roof shape is assessed, the optimum mounting location can be identified and the performance of the integrated wind turbine can be improved. Through comparing the results of the CFD simulations of wind flow around the investigated roof shapes, it was noticed that the location of maximum wind speed on top of each roof shape differed from one roof to another. For the flat roof the increase in energy yield at different locations above the roof ranged between 31.3% (between the roof windward edged and the middle of the roof) - 40.5% (midpoint between the windward roof edge and he center of the roof), for the domed roof: 40.5% (roof midpoint) - 48.2% (roof midpoint), for the gabled roof: 15.8% (the leeward corner of the roof) - 29.5% (midpoint along the leeward inclined edge), for the pyramidal roof: 15.8% (leeward hip, midway between the middle of the roof and the leeward roof edge) - 26% (on the roof stream wise axis between the midpoint of the roof and the leeward corner), for the barrel vaulted roof: 27% (midpoint between the windward roof edge and the center of the roof) – 56.1% (midpoint of the roof) and for the wedged roof: 9.3% (the leeward corner of the roof) to 48.2% (midpoint between the centerline and the windward horizontal edge). Thus, identifying the optimum roof mounting location for a wind turbine on top of the investigated roof shapes is achieved.

It is also noticed that different roof shapes have different effects on wind flow above them. Among all roof shapes, the barrel vaulted roof is the optimum roof shape for roof mounting wind turbines since it caused the highest acceleration which reached 1.16 times the wind velocity at the same location under the same flow conditions in an empty domain when the wind was flowing parallel to the roof profile, which means that a wind turbine mounted on top of a vaulted roof would yield 56.1 % more power than a free standing wind turbine at the same location under the same flow conditions. Thus, this case was chosen for further investigations of other independent variables. On the other hand the lowest maximum acceleration occurred on top of the pyramidal roof since it reached only 1.08U which corresponds to an increase in the energy yield of the installed wind turbine by 26%.

Building height variable

Another variable affecting wind flow above buildings' roofs is the building height. Thus, for a single roof shape, if the height of the building is changed, that would have an effect on the wind flow above it, it was noticed that changing the building height had no effect on the optimum mounting location of the wind turbine. However, it was noticed the increase in the accelerating effect above the roof with the increase in the building height. Figure 4 shows a comparison between the accelerating effects above the investigated three cases. For the 6m case the increase in power reached 56.1%, the 12m case caused acceleration in wind equivalent to an increase in power equal to 60.1%, as for the 24m case, the increase in power reached 64.3%. Accordingly, it can be argued that high rise buildings are more preferable for mounting wind turbines rather than low rise buildings.

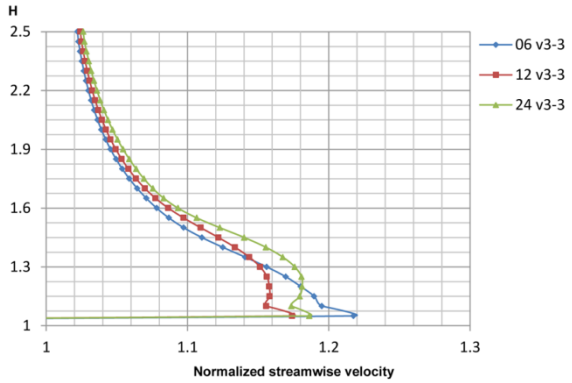

Figure 3 Comparison between the maximum recorded velocities at location v3-3 for the 3 heights

Urban context variable

Another variable affecting urban wind flow is the urban setting. Thus, it is assumed that different urban configurations would have different effects on wind flow above buildings' roofs', the height of the barrel vaulted roofed building was changed between 4.5m, 6m, 12m and 24m to identify the effect of varying the height within different urban configurations. It can be argued that the closer the building to its surroundings the more the effect of the surroundings on the wind flow above the roof.

In terms of the flow patterns, the staggered urban configuration had less effect on the flow above the investigated cases than the urban canyon configuration, this can be attributed to the bigger stream wise space in front of the investigated building when compared to the urban canyon configuration.

In terms of the effect of the urban configuration on the accelerating effect above the investigated cases, two patterns were observed; the first applies to the cases where the building height is the same as or less than the surrounding urban configuration. And the second applies to the cases where the building height is larger than the surrounding urban configuration. In the first group, the urban canyon configuration had less accelerating effect than the staggered urban configuration since the acceleration above the barrel vaulted roof reached 1.07U which corresponds to an increase in power of 22.5% while for the staggered configuration it reached 1.09U which correspond to an increase in power of 29.5%.

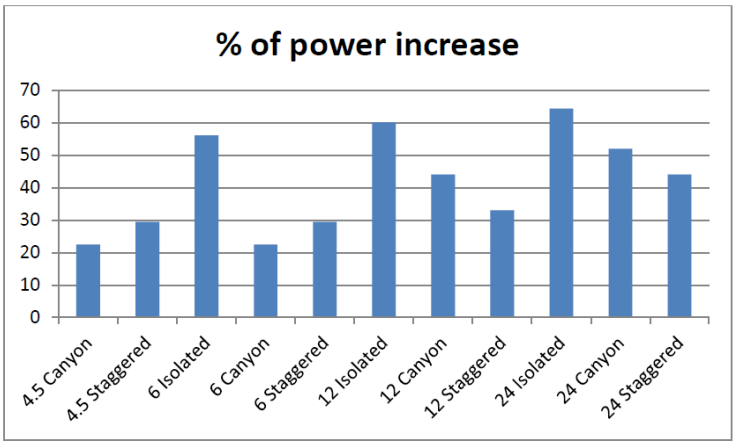

Figure 4 Comparison between the increase in the energy yield of the proposed wind turbine

However, for the second group, the urban canyon configuration had more accelerating effect than the staggered urban configuration since the acceleration above the vaulted roof reached 1.13U and 1.15U which corresponds to an increase in power of 44% and 52% for the 12m case and the 24m case respectively. As for the staggered urban configuration cases, the acceleration reached 1.10U and 1.13U which corresponds to 33% and 44% increase in power for the 12m and 24m cases respectively. Figure 5 shows a comparison between all the investigated cases in terms of the estimated increase in power output.

DISCUSSION

It should be noted that the idea of integrating wind turbines in urban areas is still questionable due to the low mean wind speed and high levels of turbulence in addition to the difficulty of assessing, to a high degree of accuracy, the wind resources at the proposed mounting location. However, when it comes to mounting wind turbines near buildings in rural areas or on top of isolated buildings' roofs in open fields, the integrated wind turbines would have more potential in terms of being mounted at the optimum mounting location to take advantage of the accelerating effect of the building which has been demonstrated in this paper.

These areas are usually located away from the grid and energy consumption is minimal which makes the idea of integrating renewables more viable. For roof mounting wind turbines, the case will either be retrofitting an existing building with a roof mounted wind turbine or a new building is being built and the decision has been made to rely on wind energy as part of energy supply of the building. In the first case, the wind resources can be assessed to a high degree of accuracy due to the simplicity of the surrounding context. Thus, the optimum mounting location can be determined. However, the structural integrity of the building and any other potential problems from retrofitting the existing building with the wind turbine should always be assessed before installing the wind turbine.

REFERENCES

1. Dutton, A.G., Halliday, J.A. and Blanch, M.J. (2005) *The Feasibility of Building Mounted/Integrated Wind Turbines (BUWTs): Achieving their Potential for Carbon Emission Reductions.*
2. Mertens, S. (2006) *Wind energy in the built environment : concentrator effects of buildings*. Essex: Multi-Science.
3. Stankovic, S., Campbell, N. and Harries, A. (2009) *Urban wind energy*. London: Earthscan
4. Abohela, I., Hamza, N. and Dudek, S. (2010) 'Integration of wind turbines in the built form and environment', *The Second International Conference on Sustainable Architecture and Urban Development*. Amman, Jordan. The centre for the study of Architecture in the Arab Region, pp. 63-78.
5. Abohela, I., Hamza, N. and Dudek, S. (2013) 'Effect of roof shape, wind direction, building height and urban configuration on the energy yield and positioning of roof mounted wind turbines', *Renewable Energy*, 50(0), pp. 1106-1118.
6. Ritchie, A. and Thomas, R. (2009) *Sustainable urban design : an environmental approach*. 2nd edn. London ; New York: Taylor & Francis.
7. Abohela, I., Hamza, N. and Dudek, S. (2012) 'Validating CFD simulations of wind flow around a surface mounted cube in a turbulent channel flow', *PLEA2012 - 28th Conference, Opportunities, Limits & Needs Towards an environmentally responsible architecture* Lima, Perú, 7-9 November 2012. p. Under publication.
8. Tong, W. (2010) *Wind Power Generation and Wind Turbine Design*. Wit Pr/Computational Mechanics.

INDEX OF ENERGY PRESENT VALUE: ASSESSMENT TOOL FOR ENERGY SAVINGS AND DISTRIBUTED ENERGY PRODUCTION

Philippe Bélanger

Ecole Polytechnique Fédérale de Lausanne (EPFL), REME INTER ENAC, BP 2138, CH-1005 Lausanne, Switzerland

ABSTRACT

Today's simulation technology in engineering and architecture are very impressive. As a result technology developers have a good idea of the resulting energy consumption of a building. They even have an idea of the distribution of the possible output. At CISBAT 2011, some authors presented innovative technologies with detailed impact on energy consumption (energy quantity, type, time of consumption) but very limited value conclusion. When asked why with such data quality they did not have more information about value. They answered with a question. Do you know of a paper that describes the methodology to achieve such valuation?

This paper intends to present a simple method that allows energy efficient technology to better assess the value of the energy savings. This value can be compared to the cost underlying this improved efficiency.

Index are easy to build and duplicate. For example, anybody could compute most of the stock market indices. While it is quite easy, it is time-consuming and it is convenient to use one publicly available in spite of the fact that it may not be the perfect one for the purpose it is used to. This paper applies typical methodology in investment valuation derived from the discounted cash flow (DCF).The proposed index is built using national and international agency forecast for future energy price. It also uses national real estate industry income return to obtain present value of energy efficiency.

Proposed index computation are given for different maturity, different years, different forecast sources (US Energy Information Administration and UK department of Energy and Climate Change) and different geographic space (UK and US). The same methodology can be used for other and more specific countries given available data.

While the method presented here is not perfect, it is better than a method that does not account for discount rate, energy mix and price forecast. Application to a specific project makes the assumption that local price growth and expected return are similar to the one on the country level.

New technology both distributed production and saving can use presented index to assess the economic value of the technology.

While a simple approach, it appears that such index for future energy value does not exist yet. This paper intends to answer this need.

Keywords – Energy efficiency, Real estate, Technology

INTRODUCTION

Energy prices are not the same for each energy source. Moreover expected future energy price growths are not the same for each energy source. As example, in 2013 future natural gas prices are expected to remain stable with expected growth around 0% in a foreseeable future due to new resources in US. In the same time, electricity and oil price are expected to grow faster than inflation. Nuclear power plants shutdowns explain electricity behaviour. Oil price behaviour is explained by many variables, international instability, resources rarity and transportation issues to

name just a few. One franc of natural gas in 10 years does not worth the same value than one franc of oil. Figure 1 shows the historical price of different energy sources in Switzerland.

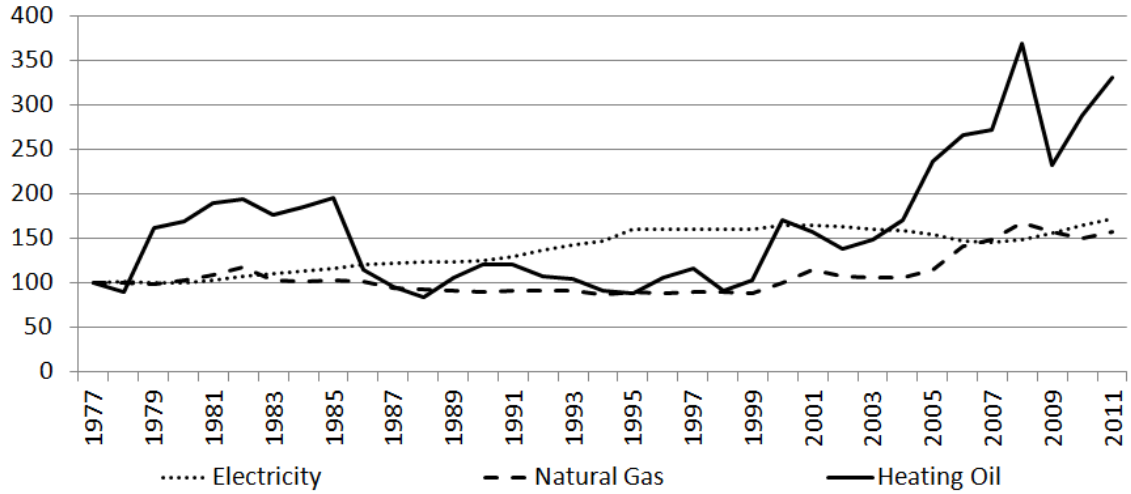

Figure 1: Index of Swiss Energy Prices, 1977=100, source BFS historical data.

We can observe in figure 1 that not only the energy price trends are not the same but also the volatility of those prices are different. We can show that if energy price growths are different for different sources, energy mix will change the value of the energy expenses in the future. Therefore it is important to take energy mix into account in the valuation process of energy efficiency investment. Figure 2 shows the present value of 100CHF of energy saving each year for 20 years for different energy mix if price growths are not the same.

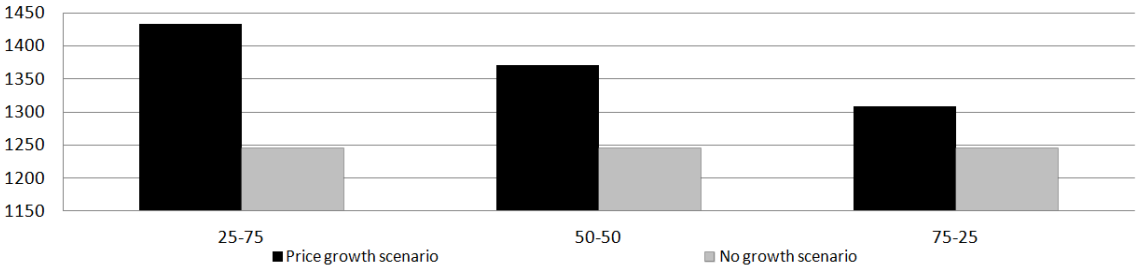

Figure 2: Present value of 20 years of energy saving for given energy mix (natural gas - electricity) with 5% expected return. Growth rate 2% - 0%.

The valuation process of energy efficiency process will take into account the quantity of energy saved for each possible source. For example, isolation will decrease heating oil expenses in winter and decrease electric cooling expenses during the summer. Valuation will need to take into account the value of saving from each source. To make the process easier it would be nice to have an *index of the present value* of each source of energy saving for different project maturity and countries.

Indices are broadly used around the world. Financial companies used them to measure performance, civil engineer use them to approximate the resistance of materials, etc. Index are easy to build and quite easy to duplicate. For example, anybody with basic access to data and basic knowledge can compute most of the stock market indices. While it is quite easy, it is time-consuming and it is convenient to use one publicly available in spite of the fact that it may not be the perfect one for the purpose it is used for. Every user knows that these indices are not perfect but they are a fair representation of what is needed. The index developed here is not perfect but it is intended to be a fair approximation of the present value of energy savings.

METHOD

Any finance 101 course [1] teaches that the value of an investment is equal to the discounted value of the future cash flows generated by the investment. It is reasonable to assume that it should be the same for an investment in energy efficiency, at least if the project is sold as a way to obtain higher return. The discounted value of the future cash flows is generally called "present value" and mathematically given by equation 1.

$$PV = \sum_{t=0}^{M} \frac{CF_t}{(1+r)^t} \tag{1}$$

Where:

PV is the present value of the investment (discounted value of the cash flows)
M is the maturity of the investment
CF_t is the value of the cash flow generated by the project at period t
r is the return expected from the investor for this investment

If PV is greater than the cost, the investor will invest in the project, otherwise the project is rejected. Therefore in order to decide whether or not he will invest in energy efficiency the investor will need to compute equation 1.

Future energy price

Cash flows generated from energy efficiency is function of the value of the energy saved. This value is obtained when we put together the energy price and the quantity of energy saved for each period. Then we need to know the future price expectation of the investor. For the need of index building we assume that the aggregate investor's expectations are the same than some major institution that deliver periodic updates of their prediction. It is fair to assume that energy efficiency investor's expectations are relatively similar to those of these organisations.

Public and private organisations that provide future energy price forecast usually do so in real term. The investor usually works with nominal prices because his discount rate already takes into account inflation. Then, we need to use deflated expected return or nominal energy price. In order to compute nominal prices we will need to use inflation forecast in order to transform real price into nominal, unless organisation provides nominal prediction. Since energy price can behave differently among countries, it is important to use indices that are built from predictions that represent best the behaviour of prices local to the considered investment.

Expected return

Real estate investments are expected to give some return. Since energy efficiency investment will be made into the building we expect the energy efficiency investment to return at least as much as the rest of the building. If it is not the case the investor will use his capital to invest into other buildings instead of investing into energy efficiency. It is possible that the investor ask for some premium for energy efficiency. He will do so if the perceived risk of the investment is higher than the one on his regular operation. Since energy expense represent about 30% of the operation cost of a building [2] it is reasonable to assume that energy price exposition is already somehow included in the actual expected return. Public real estate investor needs to publish their financial results. From these results some companies compute indices of real estate return. The best approximation of the return expected on investment is the actual or historical return that the investor does.

Computation

In the case of energy efficiency investment cash flows are equivalent to the energy expenses that have not been done. Then, we can express the cash flow as equation 2. In the case of distributed energy production, the cash flow generated is equivalent to the energy that the investor doesn't need to buy elsewhere at the price he would have paid.

$$CF_{St} = Q_{St} * P_{St} \tag{2}$$

Where:

Q_{St} is the amount of energy from source S that the project will save for each period.
P_{St} is the price per unit of $Q_{St}$of energy from source S for period t.

We can assume, as many energy efficiency research does, that the quantity of energy saved each year is equal over all the investment period. If we replace the cash flow in discount cash flow model formula, we can rewrite as equation 3.

$$PV = \sum_{S=1}^{N} Q_S \sum_{t=0}^{M} \frac{P_{St}}{(1+r)^t} \tag{3}$$

Where:

Q_S is the quantity of energy saved each period $Q_S = Q_{St}$ for each t.
S is the different source of energy. For instance 1 = oil, 2 = natural gas.
N is the total number of different energy source involved in the project.

The investor will need to solve equation 3 in order to know if the cost of the energy efficiency project is lower than its present value. We define the first index as I_S.

$$I_{SM} = \sum_{t=0}^{M} \frac{P_{St}}{(1+r)^t} \tag{4}$$

Where:

I_{SM} is the value of one unit of energy saved for the duration of the project.
M is the maturity of the project.

An index of the value of energy efficiency is needed for each energy source. With I_{SM} available the investor can rapidly multiply the quantity of energy saved by the index to find a good approximation of the value of the project's energy savings.

Price of energy grows each year (growth can be negative for some year), so we can express the energy price as equation 5.

$$P_{St} = P_{St-1} * (1+g_{St}) \tag{5}$$

Where:

g_{St} is the price growth rate for period t.

From equation 5 we can write equation 6.

$$P_{S2} = P_{S0} * (1+g_{S1}) * (1+g_{S2}) \tag{6}$$

Let define G_t as equation 7. G_t is the expression of the total price growth since t=0.

$$G_{St} = \prod_{i=1}^{t} (1+g_{Si}) \tag{7}$$

We can rewrite equation 5 as equation 8.

$$P_{St} = P_{S0} * G_{St} \tag{8}$$

If we replace P_{St} in equation 3 we obtain equation 9.

$$PV = \sum_{S=1}^{N} Q_S P_{S0} \sum_{t=0}^{M} \frac{G_{St}}{(1+r)^t} \tag{9}$$

Each G_t is obtained from prediction of the future energy prices from renowned sources. From equation 9 we can define a normalized index as equation 10.

$$I_{SM}^{Normalized} = \sum_{t=0}^{M} \frac{G_{St}}{(1+r)^t} \tag{10}$$

Normalized index can be use when the national price used for the forecast by the organisation is different from those actually observed in the area of the project. If the investor believes, despite the fact that the energy price is different, that the long term energy price growth will be similar to the one expected from the forecast organisation; the normalized index will gives a good approximation. This situation can often be observed in area where there is energy transportation constraint or local taxes. In that case, it is reasonable to assume the long term growth to be similar to the one observed on the national level. The user of the normalized index will multiply index by the quantity of periodic energy saving and by the energy price observed on the specific market.

RESULTS

Data

In order to compute the indices we use energy price forecast from UK Department of Energy and Climate Change [3-6] and US Department of Energy, Energy Information Administration [7-11]. Recent forecast include real and nominal value for energy price. For the years where nominal forecast are not available we assume an expected inflation of 2% each year which correspond to the usual targeted inflation by central bank. UK prices are given in pence per kilowatt-hour while US prices are in dollar per million British thermal unit. Since those units are the one commonly used in those countries the indices keep them. Indices cannot be compared as such between countries but to express the indices in the common denomination make it easier to use them.

IPD is a company that compute some real estate index from a database of more than sixty thousands properties. Among those indices there is one index called Income return and is the percentage of net income over the total capital employed. Since real estate is a long term investment we assume the 10 year income return to be a good assumption of the future expected return.

UK and US indices

Here is a sample of the index that can be computed from the IPD income return and official price forecast[1].

	2008	**2009**	**2010**	**2011**	**2012**
United States, Residential ($/mBtu)					
Electricity	382	385	388	389	431
Gas	147	146	146	134	141
Distillate Fuel Oil	197	259	272	289	361
United Kingdom, Residential (p/KWh)					
Electricity	189	-	201	205	243
Gas	47	-	63	57	83
Petroleum Average	146	-	190	110	219

Table 1: Sample of UK and US energy savings value index for 20 years maturity

[1] More indices based on UK, US and International Energy Agency forecast will be available on the author website. Forecast sources and country specific suggestions are welcome and will be made available if possible.

	2008	2009	2010	2011	2012
United States, Residential					
Electricity	12.33	11.85	11.83	11.51	12.39
Gas	11.52	10.98	12.60	12.09	13.28
Distillate Fuel Oil	10.01	10.61	14.89	13.85	13.41
United Kingdom, Residential					
Electricity	13.60		14.24	15.87	17.29
Gas	12.93		13.62	14.35	13.80
Petroleum Average	11.81	13.94	16.46	13.49	15.55

Table 2: UK and US energy savings value normalised index for 20 years maturity

CONCLUSION

Let assume an isolation investment in UK that will save 500KWh of cooling (electricity) and 500KWh of heating (gas). The investor could apply the indices to find that if the investment cost less than 1'630 pounds it is a good investment. One could propose to use other assumptions for expected return but the usefulness of the kind of indices presented here appear obvious. It will add a lot to energy savings technology valuation. Even if not perfect, uses of these indices are better than usual approaches that omit future energy prices and energy mix. It can be used to figure out the cost target that one should reach in order to make such technology commercially viable.

REFERENCES

1. Berk, J.B. and P.M. DeMarzo, *Corporate finance*. 2nd ed. 2011, Boston: Prentice Hall.
2. Eichholtz, P., N. Kok, and J.M. Quigley, *The Economics of Green Building*. 2010, European Property Research Institue.
3. UK Department of Energy and Climate change, *Updated Energy and Carbon Emissions Projections*. 2008. p. 51.
4. UK Department of Energy and Climate change, *Updated Energy and Emissions Projections*. 2010. p. 38.
5. UK Department of Energy and Climate change, *Updated Energy and Emissions Projections*. 2011. p. 51.
6. UK Department of Energy and Climate change, *Updated Energy and Emissions Projections*. 2012. p. 48.
7. US Energy Information Administration, *Annual Energy Outlook*. 2012. p. 252.
8. US Energy Information Administration, *Annual Energy Outlook*. 2011. p. 246.
9. US Energy Information Administration, *Annual Energy Outlook*. 2010. p. 231.
10. US Energy Information Administration, *Annual Energy Outlook*. 2009. p. 230.
11. US Energy Information Administration, *Annual Energy Outlook*. 2008. p. 224.

FINANCIAL IMPLICATIONS FOR COMPANIES RUNNING STANDBY GENERATORS IN SUPPORT OF A SMART GRID

L. A. Daniels[1*], B. A. Potter[2], P. J. Coker[3]

[1]*Technologies for Sustainable Built Environments Centre, University of Reading, UK*
[2] *School of Systems Engineering, University of Reading, UK*
[3]*School of Construction Management and Engineering, University of Reading, UK*
[*]*Corresponding Author: l.daniels@pgr.reading.ac.uk*

1. ABSTRACT

Integrating renewable energy technologies into built environments requires additional attention to the balancing of supply and demand due to their intermittent nature. Demand Side Management (DSM) has become a popular measure in order to reduce load at peak times and has the potential to become an additional revenue stream for organisations as well as support the System Operator as the generation mix changes. There is an opportunity to improve the current use or increase the running hours of existing technologies in order to manage demand. Company-owned standby generators are a rarely used resource; their maintenance schedule often accounts for a majority of their running hours and carry costs of man hours and fuel. There are existing regulated services in place to incentivise the running of generators in support of the network. However, this paper shows that the incentives that are inherent in the end use charging structure in Great Britain (GB) can be enough to encourage the use of standby generators for DSM measures. As well as a range of technologies, DSM encompasses a range of organisations; energy supply companies, Distribution Network Operators (DNOs), Aggregators and Customers all stand to benefit from DSM. It is therefore important to consider impact of DSM measures to each of these stakeholders. This paper assesses the financial implications of organisations using existing standby generation equipment for DSM in order to avoid peak electricity charges. It concludes that under the current GB electricity pricing structure, there are several regions where running diesel generators at peak times is financially beneficial to organisations. Fuel costs, Carbon Reduction Commitment (CRC) charges, maintenance costs and electricity prices are discussed and future work areas are identified including the impact on the network.

Keywords: Smart Grid, Demand Side Management, Standby Generators, Load Shedding.

2. INTRODUCTION

Standby generators have historically been installed on sites where loss of electricity supply would be detrimental to organisational operation. This could be in a hospital where a power cut could result in loss of life, however in this paper a retail setting is discussed, where loss of profits have been the concern. Their maintenance schedules carry costs through the man hours and purchasing of fuel and it should be considered whether the use of these generators could provide mutual benefit to both the System Operator (SO) and the company owning the generator. In order to understand how these generators could be used for Demand Side Management (DSM) measures, it is important to evaluate the implications of their use under current frameworks. There are two main frameworks:

- Regulated Services by one generator or across a number of sites via an Aggregator
- Non-regulated, to benefit from inherent incentives in the end use charging structure

In a recent study it was shown that standby generators have the potential to increase the overall reliability of the South African network [1]. However, the electricity network in the UK is reliable at present and standby generators are rarely used in emergencies, making their potential for use in DSM measures a benefit that companies may otherwise not see.

Much of the literature available focuses on contracted services in international settings where the financial incentives are well established and many aggregators are available [2] This paper considers the financial implications of running generators outside of the regulated services that are offered by the SO; a) for generator maintenance tests running during the most expensive charging periods and b) for running the generators for additional hours. This is partly due to external costs and long lead times associated with obtaining grid contracts but also allows for a clearer understanding of the effectiveness of regulated services in future work

3. BACKGROUND

3.1. Electricity Pricing Structure

In Great Britain (GB) there are a number of components that contribute to the final electricity charge. These components, including charges to account for the use of the Transmission Network and Distribution Network vary by time, season and region. There are 14 DNO regions across the GB network representing a geographic region of the distribution network. It has been suggested that the pricing structure in 1999 offered 'tangible payback' [3]. Since the time of writing there has been a change to the electricity pricing structure – carbon emissions can now be attributed to a direct cost for example.

3.1.1. Transmission Use of System (TUoS) Charges

These charges, shown in Table 1 are calculated by the SO and vary regionally. Part of this charge is the 'Energy Consumption Tariff' which 'is based on the annual energy consumption during the period 16:00 hrs to 19:00 hrs (i.e. settlement periods 33 to 38 inclusive) over the relevant financial year' [4]. The other aspect of this charge is calculated based on the demand of a customer at the TRIAD periods, which:

> *'describe the three settlement periods of highest transmission system demand within a Financial Year, namely the half hour settlement period of system peak demand and the two half hour settlement periods of next highest demand, which are separated from the system peak demand and from each other by at least 10 Clear Days, between November and February of the Financial Year inclusive' [5].*

3.1.2. Distribution Use of System (DUoS) Charges

The DUoS charge, shown in Table 1, covers the cost of receiving electricity from the national transmission system and feeding it directly into homes and businesses through the regional distribution networks [6]. The charges are broken down into three bands: *red, amber* and *green*. Each DNO has different periods of the day and week covered by the higher (red and amber) charging periods and these charges depend on whether a customer is connected to the High Voltage or Low Voltage Distribution Network.

3.1.3. Fixed Unit Charges and Fixed Standing Charges

There are a number of additional 'pass through charges including reactive capacity charges [6]. These fixed standing charges are not included in the analysis in this paper. as they are unaffected by the time of generator operation. Fixed unit charges are summed to 6p/kWh, including the base unit charge and additional 'uplift charges' [7] including the UK feed in

tariff. Base unit prices are split into 'day' and 'night' charges, but generator maintenance tests are only run in the day so these differences are ignored.

DNO Number	DUoS Charge			TUoS Charge	
	Low Voltage (p/kWh)			Unit Tariff (p/kWh)	TRIAD Charge (£/kW)
	Low (GREEN) Rate	Mid (AMBER) Rate	High (RED) Rate		
10	0.109	0.216	7.744	3.63	25.95
11	0.033	0.569	8.255	3.6	25.45
12	0.013	0.137	1.771	4.17	31.17
13	0.068	0.386	3.535	3.39	23.64
14	0.155	0.908	12.403	3.94	27.36
15	0.048	0.604	7.706	2.72	19.66
16	0.095	0.622	8.918	3.31	22.84
17	0.535	1.865	6.387	1.48	10.74
18	0.156	0.787	8.582	2.26	16
19	0.055	0.295	8.858	3.99	28.25
20	0.061	1.078	9.729	4.35	30.61
21	0.144	0.972	13.796	3.37	25.26
22	0.161	0.251	20.727	4.23	31.06
23	0.044	0.734	7.216	3.22	23.18

Table 1: Variable Electricity Charges by Region [4,10]

3.1.4. Carbon Reduction Commitment (CRC)

The CRC Energy Efficiency Scheme is a mandatory UK scheme initiated by Government aimed at cutting emissions in large public and private sector organisations [8]. The method of calculating emissions is published by the Environment Agency and organisations are charged at £12/tonne carbon [9]. Although the CRC is not a direct component of the electricity unit charge, it is considered here due to the correlation between a charge per unit consumed and to its mandatory nature.

4. FINANCIAL IMPLICATIONS

In order to calculate the financial implications of running standby generators, two potential uses of these standby generators for DSR are considered: a) shifting the current maintenance schedule to coincide with higher charging periods and b) running the generators for additional hours outside the current maintenance schedule. The impacts of DUoS charges and TUoS unit consumption tariff are considered as these are the components of electricity charges that change with time throughout the day.

4.1. Shifting Maintenance Schedule

The current maintenance schedule can be shifted in order to coincide with the higher charging periods. This involves no further running hours and therefore no additional fuel. For this scenario it is also assumed that no extra man hour charges are incurred and no additional maintenance will be required due to breakdowns than is already expected. Only the current 'on load' tests are considered as this will involve the minimum in changes to the current process. This means that the base cost of electricity is not offset any further than already experienced. For this scenario, no additional charges will be incurred under the CRC. As the maintenance tests considered are 'on load' there will be no savings on CRC from grid electricity imports. Fuel is already purchased for the maintenance schedule so it can therefore be considered that any savings on electricity costs offset this existing expenditure. The TUoS consumption charge is also saved as grid connected load is reduced in the TUoS unit charging period (16:00-19:00). The proportion of fuel costs offset by the generators partially depends on this regional charge as well as the difference in cost per kWh between green and red DUoS

charges. As it can be seen from Table 2, running maintenance tests in red DUoS periods can offset at least 45% of the fuel costs depending on the region. The offset exceeds 100% in three DNO regions – where it is cheaper to run the maintenance tests in red DUoS periods than to import grid electricity – i.e the maintenance tests make a profit for the organisation.

DNO Number	Offset of Maintenance Fuel Costs (%)
	Low Voltage
10	71.41
11	77.15
12	48.28
13	**106.92**
14	72.19
15	48.36
16	76.53
17	45.51
18	68.01
19	81.43
20	90.29
21	**105.81**
22	**151.06**
23	65.52

Table 2: Shifting Maintenance Schedule Fuel Offset

4.2. Additional Running

The generator sets could be run for additional hours in order to reduce the grid connected loads for a higher proportion of the red DUoS charging periods. Additional fuel, CRC and maintenance charges need consideration in this scenario. An assessment of the financial implications of running generators at other red, amber and green DUoS periods show the differences in financial implications throughout the day.

In this scenario, base unit cost of electricity will be offset in addition to the DUoS charges. The calculations are based on the DUoS periods coinciding with the TUoS unit consumption charging period (16:00-19:00); this means that DNO charging regions with two red DUoS periods, the savings in the early afternoon peak will not be the same as shown in Figure 1.

Under the CRC, a number of factors are applied to a range of activities that produce carbon emissions. Emissions from grid imports are calculated using a factor of 0.51kg/kWh which equates to 0.65p/kWh [9]. Using a standard fuel consumption chart and the EA diesel emissions factor of 2.639kg/litre, the emissions from the standby generators are charged at 0.85p/kWh. The additional charge incurred by offsetting grid electricity with standby generators is 0.2p/kWh. The cost of fuel has been calculated using the same consumption chart and internal charging documents for fuel contracts and is approximated to 16.3p/kWh.

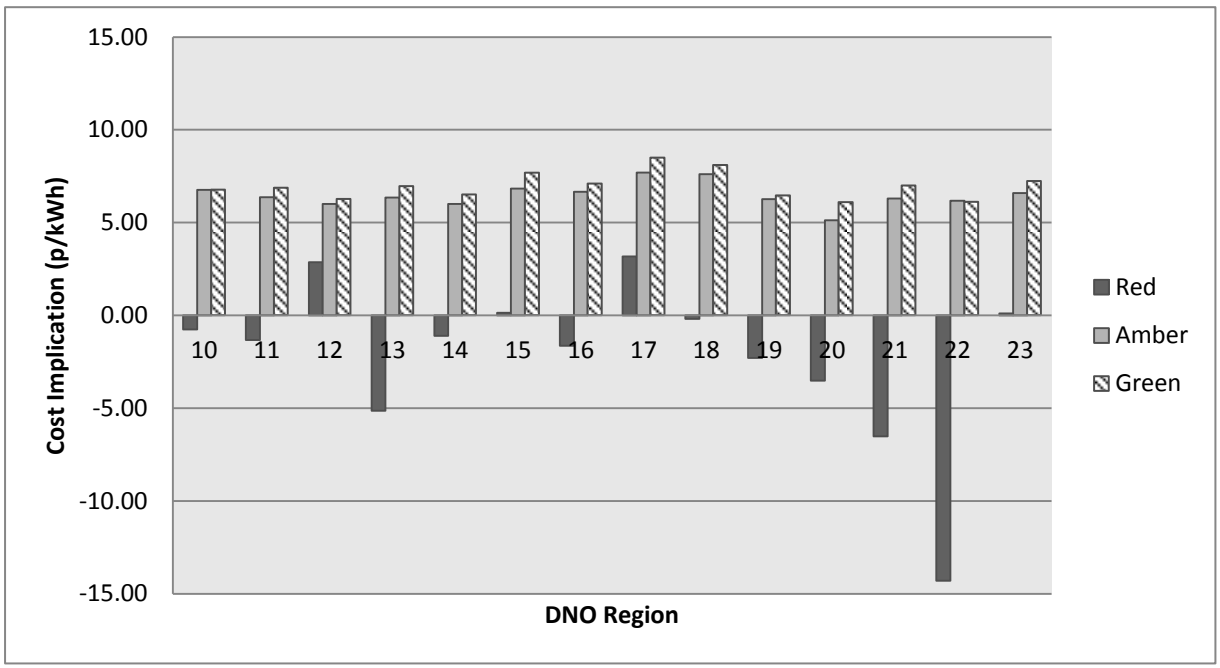

Figure 1: Cost Implications of Diesel Generators at Different Charging Periods (Low Voltage)

A ‘total’ cost implication calculation has been carried out for each DNO region. The results are shown in Figure 1. Where the number is below zero, it is financially beneficial for the organisation to run the diesel generators during RED DUoS periods that coincide with TUoS unit consumption charging periods.

5. DISCUSSION

The value of running standby generators for DSR for companies depends on the pricing structure in place. It has suggested that standby generators could be up to 10p/kWh less in fuel costs than grid charging at peak periods [3]. Under today’s pricing structure, it can be seen that the price varies according to the DNO region and time of day. This pricing structure provides an inherent incentive for customers to reduce their demand at these peak times but as the generation mix changes, the SO and DNOs will have to manage more intermittent supply. It is possible that the electricity pricing structure may change to accommodate this and to encourage DSR at times of low renewable supply as well as times of high demand. DNO’s have suggested that a network wide DUoS charging structure may not deal well with localised peaks within their DNO region [11] and with more renewable supply, the charging structure may even see changes within DNO regions.

It is difficult to equate TRIAD savings in terms of a unit cost because it is based on a kW demand rather than kWh consumption. There is one, two hour maintenance test in an average TRIAD season between November and February. There are three, half hour periods that are used to calculate TRIAD periods and these are allocated after the event has occurred. The likelihood of these events coinciding is slim and it is therefore not unreasonable to discount them from the calculations. However, if tests could be run during TRIAD periods there would be potential for greater savings.

Maintenance costs have not been considered in the calculations presented. Previous literature has claimed that additional maintenance will be ‘*unlikely to outweigh the savings’* [3]. However, a more quantified approach should be taken when assessing the potential use of standby generators across a large estate where maintenance costs are significant. Approximating maintenance costs is difficult as it is somewhat unknown whether required repairs can be directly attributed to the additional running hours. Preliminary calculations have suggested that additional maintenance costs can add up to 50% of fuel costs to running hours. Further work needs to be carried out to assess the accuracy of these results.

6. CONCLUSIONS AND FURTHER WORK

Current maintenance schedules should be optimised for maximum savings that can be seen when generators are run during higher electricity charging periods. In some regions, simply moving the maintenance schedule can not only save the entire cost of fuel but also make profits. Standby generators in some regions have the potential to save companies money if they are run for additional hours at periods of the day where electricity pricing is higher. In regions where the DUoS and TUoS charges are high enough, savings could be up to 14.3p/kWh in RED charging periods. An initial assessment of the financial implications has allowed for an understanding of the potential savings available although further consideration of other issues is required.

Initially, further work needs to be carried out on the effect on maintenance of running generators for additional hours as well as the interaction between voluntary generation and contracted services with the SO. The impact that these generators could have on the network is an important next stage of research. At a national and DNO level, investigation into the

potential benefits of these standby generators should be carried out. Further work on TRIADS should be carried out to analyse the potential impact on load reduction in these periods. Carbon emissions are a large consideration in the use of these generators. An evaluation of the carbon impacts of generators based on marginal grid emissions factors should be carried out for particular usage patterns. Other non-financial issues such as noise and air pollution should be considered, although these issues are location dependent and this is likely to be needed on a site by site basis. This paper has demonstrated that there are savings inherently available in the end user pricing system for standby generators in DSM measures. With further work on the consideration of regulated services that are available, the potential benefits to organisations could increase.

7. REFERENCES

1. Van Es, D. 2008. A Case for Incorporating Standby Generators into the South African Electricity System. [pdf] Cape Town, University of Cape Town. Available: http://www.erc.uct.ac.za/Research/publications/07VanEs-Bennett_Standby_generators.pdf
2. Whitham, J. 1996. Utility Deregulation and The Role of Standby Generators. In: *Power-Gen '96*, Orlando, Florida, December 5, 1996. Unknown: Power-gen.
3. Dixon, M.J., 1999. Profitable Use of Standby Generators in a Competitive Electricity Market. In: INTELEC Telecommunication Energy Conference, 1999. The 21st International. Copehhagen, Denmark June 6-9 1999. Unknown: INTELEC
4. National Grid, 2012a. *The Statement of Use of System Charges.* [pdf] Warwick, National Grid. Available: http://www.nationalgrid.com/NR/rdonlyres/00233587-FCF6-4F54-9537-7EC361B1F7AC/52839/UoSCI8R0Final_Issued.pdf
5. National Grid, 2012b. *The Connection and Use of System Charge (CUSC) Section 14 Charginng Methodologies.* [pdf] Unknown, National Grid. Available: http://www.nationalgrid.com/NR/rdonlyres/8FFA9408-9DC7-44C2-AF68-93E684A176D8/57848/CUSC_Section_14combined_CMP206_3December12.pdf
6. Eon Central Networks, unknown. *Distribution Use of System Charges (DUoS) for Half Hourly Customers.* [pdf] Eon Central Networks, Coventry. Available: http://www.eon-uk.com/downloads/DUoS_leaflet_final.pdf
7. EDF, 2011. *Electricity Prices Explained.* [pdf] London, EDF. Available: http://www.edfenergy.com/products-services/large-business/PDF/B2B_ePublications/B2B-FS-EPC.pdf
8. DECC, 2013. *CRC Energy Efficiency Scheme.* Available: https://www.gov.uk/crc-energy-efficiency-scheme
9. Environment Agency, 2012. *CRC Energy Efficiency Scheme Guidance for participants in Phase 1.* Bristol, Environment Agency. Available: http://www.environment-agency.gov.uk/business/topics/pollution/127831.aspx
10. Energy Networks Association, 2013. *Distribution Use of System Charges.* Available: http://www.energynetworks.org/electricity/
11. Sustainability First, 2012. *What Demand-Side Services Can Provide Value to the Electricity Sector?* [pdf] London, Sustainability First. Available: http://www.sustainabilityfirst.org.uk/docs/

DAYLIGHTING THROUGH SEMI-TRANSPARENT PV WINDOW: A WAY TO REACH ENERGY EFFICIENT BUILDINGS

E. L. Didoné[1]; A. Wagner[1]; F. O. R. Pereira[2]

1: Building Science Group, Karlsruhe Institute of Technology (KIT) / Englerstr. 7, 76131 Karlsruhe, Germany.

2: PósARQ - Federal University of Santa Catarina (UFSC) / Campus Universitário Reitor Joao David Ferreira Lima, Trindade, 88040-900, Florianopolis-SC, Brazil.

ABSTRACT

Artificial lighting and air conditioning systems are responsible for a large amount of energy consumption in contemporary office buildings. This situation can be changed when buildings are constructed using design strategies that prioritize the use harnessing of daylight to save energy and are equipped with devices that generate electricity. The large available amount of solar radiation is a significant usability factor for solar energy in Brazil. Therefore, Building Integrated semi-transparent Photovoltaic (BIPV) solar systems interlinked to the electric network are becoming a promising alternative for the future. This research aims to evaluate the potential of semi-transparent PV windows for energy efficient buildings considering the use of daylight. The methodology entails modeling a semi-transparent PV window for evaluating energy and light performance through computer simulation. The modeling is performed using Optics 6 and WINDOW 7 programs. The daylight simulation for the investigation of the available annual daylight with different window systems is performed using Daysim/RADIANCE program and the simulation of the energetic performance using the program EnergyPlus. The simulations are accomplished for two cities in two different climatic zones of Brazil: Fortaleza/CE in the Northeast and Florianopolis/SC in the South. The results show that semi-transparent PV windows in combination with a control system for artificial lighting provided a reduction of the total energy consumption that can reach 24% with ASI thru and 22% with organic PV, due to the electricity reduction for cooling and generated energy. However, in environments where cooling is not necessary, more electricity is used with the BIPV than with a single glass window due to artificial lighting. In conclusion, the semi-transparent PV window is an appropriate choice for environments with air conditioning or environments with low light demands.

Keywords: daylighting, energy efficiency, semi-transparent PV window, building simulation

INTRODUCTION

Daylight is an important factor for reducing energy consumption in buildings due to its wide availability during the day when non-residential buildings are occupied. In Brazil most office buildings present few strategies to improve the use of natural resources. A lot of these buildings were projected to prioritizing its aesthetic value with characteristics of international architecture that are inappropriate for the local climate.

Nowadays a promising technology using natural resources and capable of in-situ energy generation has been incorporated into building envelopes substituting conventional construction materials. Building integrated photovoltaic (BIPV) have been used as part of the facade for energy efficiency and aesthetic considerations. Some studies have been conducted on semi-transparent PV modules as window [1-3]. One of them [2] shows that for a building in Tokyo energy savings of 54% are possible using semi-transparent PV modules in windows.

Semi-transparent PV windows have a significant potential to reduce the annual electrical consumption for cooling and in addition generate energy, compared to standard glazing systems using tinted glass or dark plastic films, which, together with clear glass, are most commonly used in Brazilian buildings according to some studies [4-5]. This paper aims to evaluate the potential of semi-transparent PV windows for energy efficient buildings, considering the use of daylight.

METHOD

Building model

A representative model for Brazilian office buildings was chosen. The building characteristics, materials and internal heat loads were obtained from previous studies [5]. For the simulations a room with a base area of 8 m x 11 m and a height of 2.7 m was used. Simulations were made for models with different window to wall ratios (WWR) of the main facade which represent the most common window sizes in Brazilian office buildings and office buildings with large windows (Table 1).

M1: WWR < 50% (8 m²)			**M2: WWR > 50% (16 m²)**		
Single glass window	Organic PV window	ASI Thru PV window	Single glass window	Organic PV window	ASI Thru PV window
Case 1	Case 2	Case 3	Case 4	Case 5	Case 6
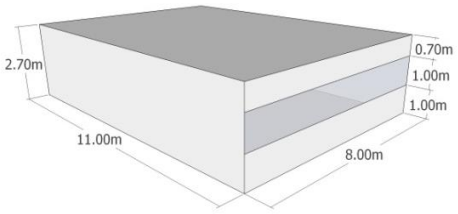			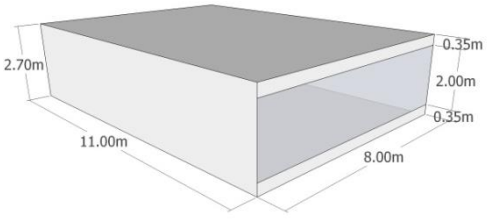		

Table 1: Simulation models.

Three different window systems were analyzed[1]: I. Single glass window: U = 5.82 W/m² K, VT = 0.88 and SHGC = 0.82; II. Organic PV window: U = 1.67 W/m² K, VT = 0.23 and SHCG = 0.22; III. ASI Thru PV window: U = 1.67 W/m² K, VT = 0.09 and SHCG = 0.13.

The building is occupied from 8 am to 6 pm with an average occupancy of 14.7 m²/person. The internal gains are 8 W/m² for lighting and 9.7 W/m² for equipment. The HVAC system is a window unit with a coefficient of performance (COP) of 2.8 and a set point for heating of 18°C and of 24°C for cooling [5]. An automatic dimming system to control artificial lighting was used in order to ensure that artificial lighting was turned off when the available daylight reached 500lux [6].

The internal surfaces (ceiling, wall and floor) were considered with 80%, 50% and 20% of reflectance, respectively. The models were evaluated for four different orientations: North (0º), East (90º), South (180º) and West (270º). The building was regarded as detached in the simulation and the surrounding was not considered.

Semi-transparent PV window model

The used semi-transparent PV window is composed of two glass layers with a thickness of 3 mm separated by an air filled of 12 mm wide gap. The encapsulated PV cell is placed at the inner side of the exterior glass.

[1] U = Thermal Transmittance; VT = Visible Transmittance; SHCG = Solar Heat Gain Coefficient.

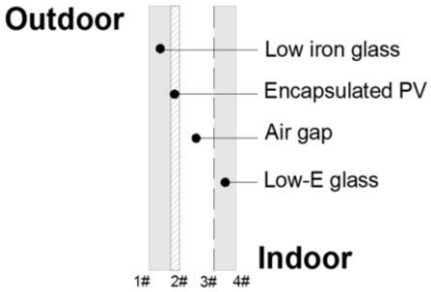

Fig. 1: Schematic of the PV window.

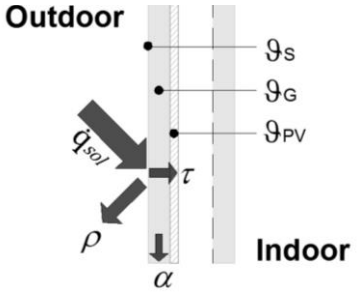

Fig. 2: Detailed scheme for solar radiation balance.

Two windows with different PV solar cell types were evaluated. One organic solar cell with a cell efficiency of 3% and transmittance of 30% [7] and a Schott ASI® thru solar cell with an efficiency of 5% and a transmittance of 8% [8]. The encapsulated organic PV cell was modeled and integrated on the outer glass sheet as a thin film by the program Optics 6 [9]. Optical and thermal characteristics of this module were modeled with the WINDOW 7 program [9].

As it is not possible to directly integrate a model for semi-transparent PV windows into EnergyPlus it was necessary to separate the thermodynamic energy balance of the glazing system as well as the energy yield calculation of the PV from the simulation of the whole environment to obtain the total energy consumption. Figure 2 shows the scheme used for the thermodynamical calculations to extract the temperatures inside the window [3]. The generated electricity can then be calculated by multiplying the result of (1) by the window area

$$\dot{q}_{el} = \dot{q}_{sol}\,(1-\alpha)(1-\rho)n_{PV}[1+K\,(\vartheta_{PV}-25)] \qquad (1)$$

Here α is the absorption, ρ the reflection, η_{PV} the solar cell efficiency, K the temperature power output coefficient (obtained from the PV manufacturer), ϑ_{PV} the solar cell temperature in °C, $\dot{q}_{sol}$ the solar radiation and $\dot{q}_{el}$ the generated electricity.

Building analysis

The energy consumption of the two building models was obtained through an integrated computer simulation using two programs: Daysim/RADIANCE and EnergyPlus. Daysim was used to evaluate the daylight behavior and to obtain the use of artificial lighting for the integrated simulation with EnergyPlus, which was used to obtain the overall energy consumption.

The dynamic daylight results were analyzed using the Daylight Autonomy (DA)[2] and Useful Daylight Illuminance (UDI)[3] parameters. For the analysis a grid of 88 equally spaced sensors was used, which was located in a plane 0.75 m above the floor.

The simulations were carried out for two Brazilian capital cities: Fortaleza/CE which is close to the equator (latitude of 3°78' S - tropical climate - solar irradiation of 5.67 kWh/m².dia) and Florianopolis/SC in the southernmost part of Brazil (latitude of 27°67' S - subtropical climate

[2] *Daylight Autonomy* (DA) is defined as the percentage of occupancy hours per year, for which a minimum illuminance level (e.g. 500 lux) is reached by daylight [10].

[3] *Useful Daylight Illuminance* (UDI) is defined as the annual occurrence of illuminances (E) that are within a predetermined range considered useful by occupants [11]. The ranges are: E < 100 lux: UDI fell-short (UDI-f); 100 < E < 300 lux: UDI supplementary (UDI-s); 300 < E < 3000 lux: UDI autonomous (UDI-a) and 3000 < E lux: UDI exceeded (UDI-e).

- solar irradiation of 4.77 kWh/m².dia). The weather data of the cities was obtained from the website of the U.S. Department of Energy [http://apps1.eere.energy.gov].

RESULTS

Daylighting performance

For the UDI analysis, the office room was divided into nine areas and the number of hours (total of 2500 hours) which attend the illuminance intervals were determined. In the Table 2 below the resulting hours are written into each area. The different shades of gray give a visual impression of the attained number of hours for the studied room.

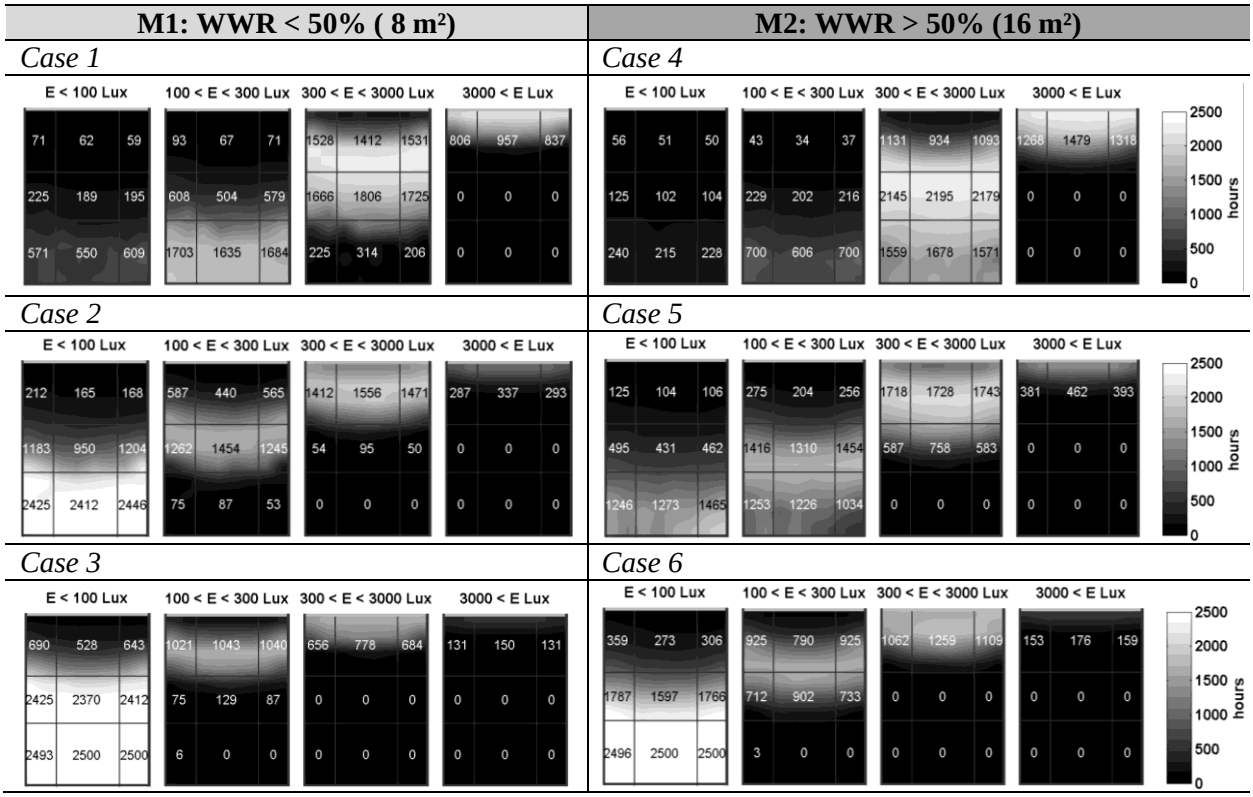

Table 2: UDI for the North facade in Florianopolis.

The results show that in Florianopolis, the illuminance inside the rooms for the cases with a single glass window (Case 1 and Case 4) reach the range of UDI-a (300 < E < 3000 lux) many hours per day almost in the whole room. While for both PV windows similar values occur only in the region near the window (1/3 of the room). The UDI-e (3000 < E lux) represents the highest illuminance values, and is achieved in the region near the window for the cases with single glass window. For the PV window cases the UDI-e values are considerably lower and the region where they appear is smaller. Instead the values for the UDI-f (E < 100 lux) range are higher and their distribution reaches from the middle to the bottom of the room, as expected considering the lower VT (Table 2).

Figure 3 and Figure 4 present the results using the DA metrics for an illuminance of 500 lux for the North facade. In Florianopolis, the illuminance near the window varies between 70% and 100% depending on the case. In contrast, for Fortaleza these values are significantly lower, between 20% and 90%. This is caused by the latitude of Florianopolis at which more daylight is available on the North facade. Using a PV window, it is possible to reach the

required illuminance only near the window with WWR < 50%: within a maximum depth of 3.5 m in Florianopolis and 2.5 m in Fortaleza. For WWR > 50% the distance increases.

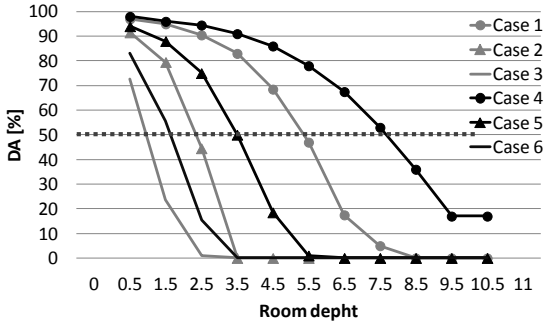

Fig. 3: DA(500lux) for the North facade in Florianopolis.

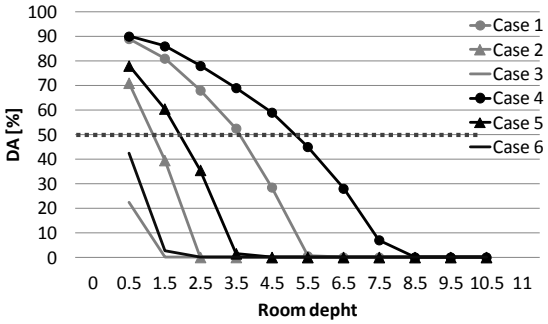

Fig. 4: DA(500lux) for the North facade in Fortaleza.

Energy consumption vs. generated energy

The figures ahead contain the final energy consumption for lighting and cooling obtained by the simulations. The black dots represent the percentage of the total required energy (actually consumed - generated) compared to the Case 1. Generally, in Florianopolis the total consumption values are lower than in Fortaleza, mainly due to cooling loads.

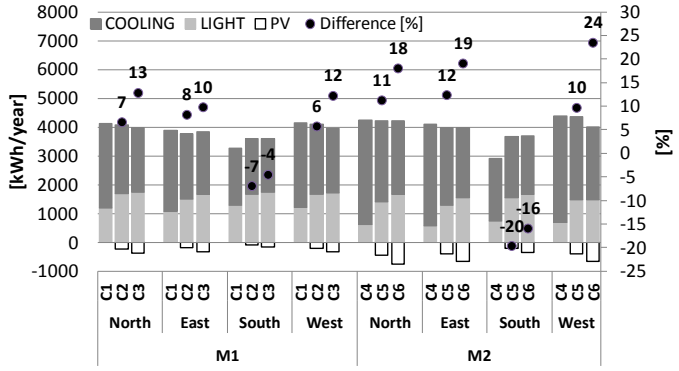

Fig. 5: Energy balance for Florianopolis.

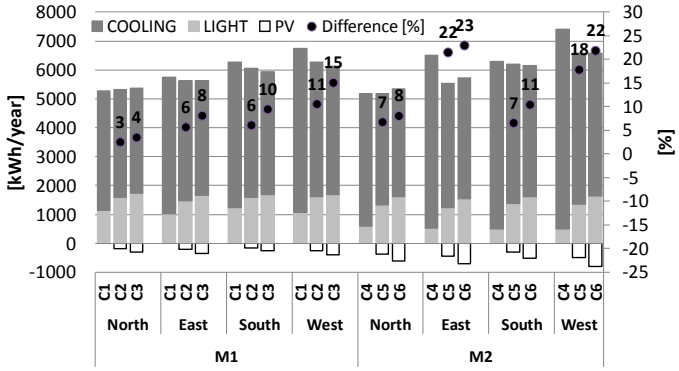

Fig. 6: Energy balance for Fortaleza.

Comparing the PV window with the single glass window, it is necessary to increase artificial lighting to reach 500 lux in the work plane for all PV window cases, since the transmittances of the PV windows (9% to 23%) are lower than the single glass window (88%). In addition, the larger the window size is, the higher is the energy consumption for lighting in the PV window in comparison to a single glass window. This increase reaches 81% for the organic PV window and 79% for the ASI Thru window in Florianopolis. In Fortaleza, these values can reach 112% and 122%, respectively.

In contrast, the energy consumption for cooling decreases in all cases, maximum of 32% with ASI Thru window in East facade for Florianopolis and 30% for Fortaleza. The energy generated by PV windows also reduces the final energy consumption in the office. However, in Florianopolis the South facade presents better final energy consumption with single glass window. This happens due to the lower levels of solar radiation which reduce cooling loads, energy generation and daylighting in this orientation.

DISCUSSION

The semi-transparent PV window is an appropriate choice for environments with air conditioning or environments with low light demands, for example corridors and hotel rooms; since the use of the PV window in conjunction with dimmer sensors that control artificial lighting reduces the total electricity consumption. A trade-off analysis between increased daylighting causing more heat gain on the one side and more electricity production requiring less cooling but more artificial lighting on the other side has to be made for each case.

In conclusion, the PV window technology is not applicable for all orientations and cities (e.g. South facade in Florianopolis). The local climatic conditions, especially the available daylight and temperature have to be considered carefully. For the use of PV windows in environments that do not require artificial cooling, a study using different transmittances and efficiencies is recommended.

ACKNOWLEDGEMENTS

The authors would like to thank CAPES for the financial support.

REFERENCES

1. Chow T.T., Pei G., Chan L.S., Lin Z., Fong K.F. A comparative study of PV glazing performance in warm climate. *Indoor and Built Environment* 18. Pp. 32-40. 2009.
2. Miyazaki T., Akisawa A., Kashiwagi T. Energy savings of Office buildings by the use of semi-transparent solar cells for Windows. *Renewable Energy* 30, pp. 281-304.
3. Wah W.P., Shimoda Y., Nonaka M., Inoue M., Mizuno M. (2005) Field study and modeling of semi-transparent PV in power, thermal and optical aspects. *Journal of Asian Architecture and Building Engineering*. P. 556. Nov 2005.
4. LABEEE. Carlo, J., Toccolini, G. *Survey data aiming the definition of Brazilian prototype buildings*. Eletrobras/PROCEL. Florianopolis, 2005 (In Portuguese).
5. Santana, M. V. *Influence of constructive parameters on energy consumption of office buildings located in Florianopolis-SC*. 2006, 181p. Dissertation. Federal University of Santa Catarina, Florianopolis, 2006 (In Portuguese).
6. ISO/CIE 8995. *Lighting of Indoor Work Places*. Viena, Austria. ISO 2002.
7. Lichttechnisches Institut - LTI. Karlsruhe University. Personal Information. Germany, 2012.
8. Glassdbase. *Schott Solar: ASI Thru Laminated*. Acessed at <http://glassdbase.unibas.ch> in April 2012.
9. WINDOW 7 / OPTICS 6. LBNL. *Windows & Daylighting Software*. National Fenestration Rating Council (NFRC). 2011.
10. Reinhart, C. F.; Morrison, M.: The lightswitch wizard – reliable daylight simulations forinitial design investigation. In: Buildings Simulation, 2003, Eindhoven, The Netherlands. *Proceedings…* Eindhoven: BS, 2003. Vol. III. p.1093-1100.
11. Nabil, Azza; Mardaljevic, John. Useful daylight illuminances: A replacement for daylight factors. Science Direct. *Energy and Buildings* 38. P. 905-913. 2006.

ENERGY CONCEPTS FOR FLOATING HOMES

Dr.-Ing. Peter Engelmann, Dipl.-Ing. (FH) Thomas Kramer, Sascha Strutz, M.Sc.

Fraunhofer Institute for Solar Energy Systems ISE, Heidenhofstr. 2, 79110 Freiburg, Germany, peter.engelmann@ise.fraunhofer.de

ABSTRACT

For floating buildings the connection to a supply grid is more difficult than for onshore constructions. In combination with the surrounding water as heat source, heat pumps allow all-electric solutions for an efficient energy supply for space heating and domestic hot water (DHW). With on-site photovoltaics (PV) the power supply can be partly covered locally. This paper analyses the match or mismatch of local generation and consumption based on a monitored demo building. In addition to measured loads, a simulation study is used to investigate the load-shifting potential of the heat pump system with the goal of increasing the own consumption of renewable (PV) power and minimizing the connection power.

The results of the simulation show that in very low energy homes (in this case according to passive house standard) the fraction of heat for space heating is too small to be used for load shifting – additionally the highest heating loads are typically complementary to solar radiation. More promising is to implement the PV output in the control strategy for heating up the DHW storage tank: the own usage can be increased, with the downside of a lower efficiency of the heat pump. Looking at the overall electric consumption, including the extremely user dependant load patterns in small apartments, the influence a heat pump system has on the overall solar fraction is rather small.

Keywords: net-zero energy buildings, load and store management, smart buildings

INTRODUCTION

Floating constructions are an exotic or uncommon environment for buildings. Examples and Activities in this area are based not only on the desire to ever more exclusive buildings - there are also increasingly objectively related requirements for the use and exploitation of water areas for construction, such as after use of mining landscapes and abandoned city harbors, unused waterways and channels, to the use in flood-prone areas or districts with rising sea levels. In a joint research project the Fraunhofer ISE investigates energy supply systems for these floating buildings. A typical restriction for floating buildings is the access to grid-bound supply systems: water, sewerage and electricity or other energy sources. For this study, we assume a connection to the electric grid and a fresh water supply. The focus is to minimize not only the overall energy consumption of the building, but also the connection power.

A prototype was built in 2011, located on a flooded gravel-pit (see Figure 1). The research building floats on steel pontoons, the construction is realized as a timber-framed building clad with white Eternit panels. The inside is devided up into a large conference or classroom and smaller individual rooms, which are used as a bathroom, kitchen and for technical equipment. The building is used as conference/training classroom.

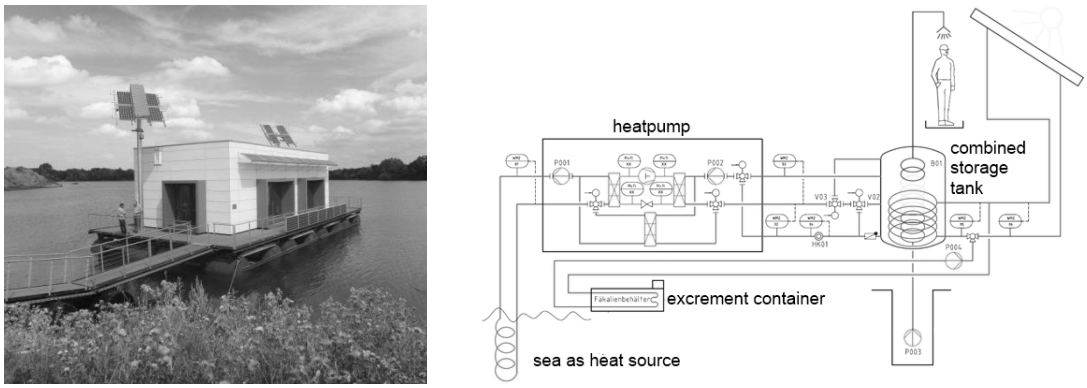

Figure 1: Picture of the prototype demonstration-building in Kalkar, Germany (left) and schematics of the energy supply system (right).

A summary of the design and technical systems:

- thermal heat supply: heat pump (prototype, downscale-modification of existing unit; <5 kW thermal) with lake as heat source
- different supply systems for space heating: floor heating or low-temperature convectors
- small solar panel for freeze protection of the pontoon housed feces container
- passive-house design with additional PV systems to compensate the overall energy consumption, designed as "plus-energy" building: positive energy balance on a yearly basis
- different PV systems: tilted, fixed, south-oriented; vertical, fixed, south-oriented; tracker, with and without additional lens- system

Except for a small solar thermal collector, which is only used to prevent the fecal-container from freezing, the buildings is “all-electric” in terms of energy-supply. Numerous integrated sensors allow a detailed analysis of the performance and dynamic interaction of the technical components.

BACKGROUND

In todays "net-zero" or “plus-energy” concepts, typically grid connected energy efficient buildings are combined with an on-site renewable energy source (typically photovoltaics, PV) to compensate the remaining energy consumption by renewable generation on a yearly energy balance. According to [1] the schematic is shown in Figure 2.

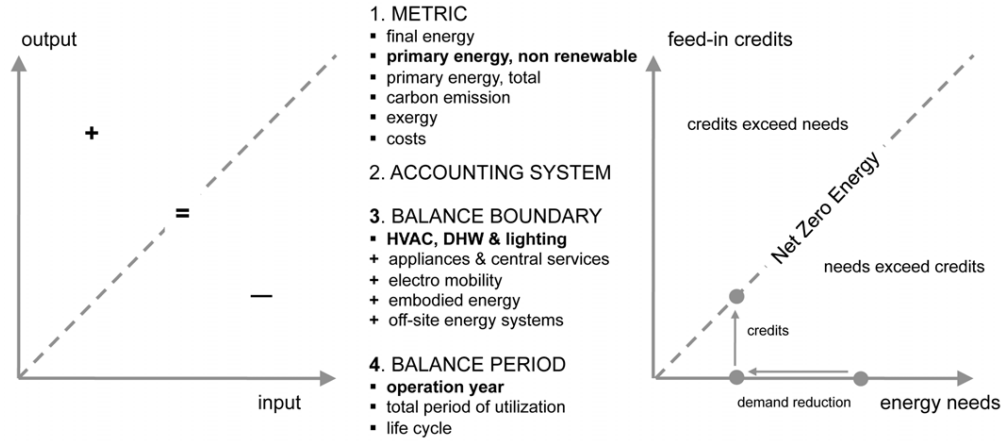

Figure 2: Schematic input/output balance of a building (from [1]). By defining a metric, an accounting system, the boundaries for the energy balance and a balance period a building (or district) can be evaluated. By applying efficiency measures a demand reduction is realized, covering the remaining energy needs with renewable sources leads to a net zero balance.

Without the availability of seasonal on-site energy storage, the public grid is used as reservoir whenever the renewable generation exceeds to local demand, at the same time the grid is used as source, when no renewable power is available. While these concepts show a match of demand and generation on a yearly basis, the energy balance on smaller time steps looks different. Seasonal variation of ambient conditions (temperature and solar radiation) as well as the course of day and night cause temporal mismatch. Figure 3 (left) shows the solar fraction for different periods: whereas on a yearly basis PV generated more energy than the building used, the solar fraction declines significantly when looking at smaller periods. At the same time the discrepancy between maximum consumption and generation increases. For demo building, it appears that the highest loads for the grid connection are caused by feed-in from PV, not from internal loads – see Figure 3, left. Additionally the correlation plot indicates that load and generation are mostly decoupled.

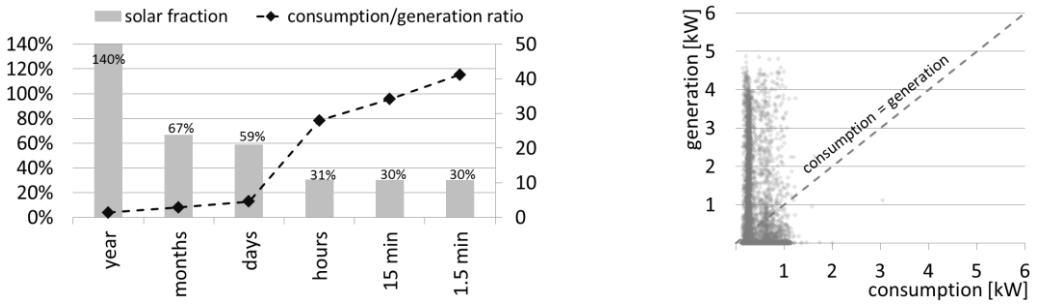

Figure 3: Solar fraction for the demo- building, relating to different time periods and equivalent ratio of consumption and generation (left) correlation plot of generation and consumption (right).

Another way to visualize the time-dependency of a value are "carpet-plots": the x-axis represents the time of the year, the y-axis time of a day; the power is color-coded, plotted against date and time. Again these plots illustrate the mostly contracyclical pattern of load and PV generation.

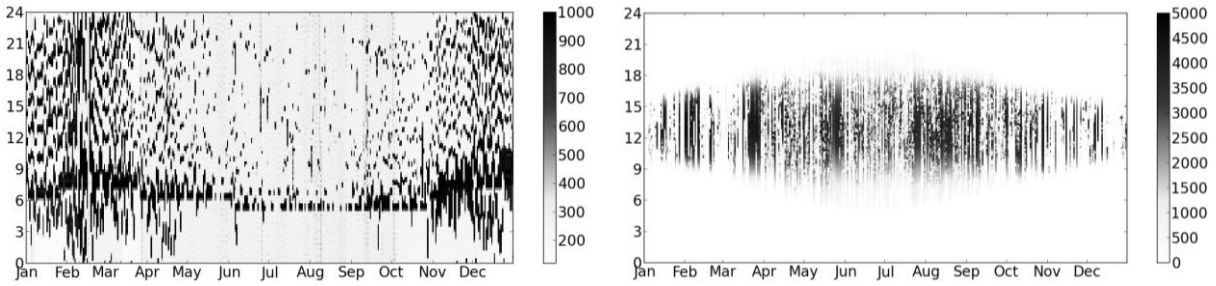

Figure 4: Carpet Plot for electric consumption (left) and PV generation (right) for the floating demo-building (time: CET, latitude: 51.7°)

In Figure 5 electric consumption and PV generation are classified depending on their occurrence in 6h-periods over a day, summarized for a whole year and for the seasons (Winter: Jan, Feb, Nov, Dec; transition: Mar, Apr, Sep, Oct; Summer: May, Jun, Jul, Aug). Additionally the sum of (electric) energy is shown on the left axis. This reflects Figure 4: whereas the majority of PV power is available from noon to 6 PM and the summer season has the highest yield, the electric consumption is more equally distributed throughout a day with higher loads in winter (note: the building is heated, but only temporarily used).

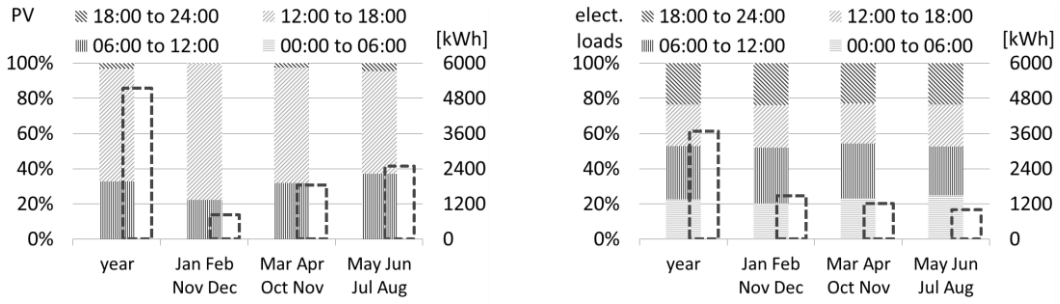

Figure 5: Percental distribution and sum of electric load (left: generation, right: consumption) divided up into four 6h- periods; for the whole year and in 4-month periods.

Because the demo- building is only temporarily used as conference room, the (electric) loads are not comparable to a residential building. To transfer the results from the monitored building to other uses and to investigate the influence of different usage- profiles and control strategies for the building equipment (mainly the heat pump), the building is modeled in the dynamic simulation environment Dymola/Modelica. The simulation models were validated with detailed measurement data as far as possible. The main differences of the real building and the simulation model are:

- implementation of a DHW tap- profile
- implementation of electric load- profiles: the household-electricity load profiles from different units of a multi-family home are analysed; different load profiles are selected and used with the simulation model
- the buffer tank was changed from serial to parallel connection, to decouple the operation of the heat pump from space heating

Goal of a parameter variation-study is to test the influence of different control strategies and variation of thermal storage capacities on the residual loads. The question is: to which extend own consumption of PV power can be increased by running the heat pump with availability of PV power as command variable in addition to standard demand-based control strategies.

The different parameters used in the simulation are:

- reference: reference scenario – space heating (SH) is controlled by an ambient-temperature dependant heating curve, DHW tank is set to 50°C.
- off-time: operation of the HP is blocked for SH from 21:00 to 8:00, for DHW from 23:00 to 7:00, buffer tank is increased to 2000 l.
- SH 750l: whenever PV power is available, the heating curve is increased by 10 K, the buffer tank is increased to 750 l
- DHW 750l: whenever PV power is available, the setpoint for DHW is increased by 10 K, buffer tank is increased to 750 l.
- SH+DHW 750l: combination of the above – heating curve and DHW setpoint are increased
- SH+DHW 200l/4000l: same as above, capacity of buffer tank is increased to 2000 l and 4000 l respectively.

RESULTS

Figure 6 shows the results for the operation of the heat pump: by changing the control strategy, loads from the heat pump can be shifted towards periods with available PV power: the net grid-supply of decreases. At the same time, the heat pump is more often operated with lower efficiency – mainly because of higher supply temperatures for the heat sink: the electric consumption of the heat pump increases. By increasing the size of the buffer storage, the capacity for load shifting increases, as well as thermal losses.

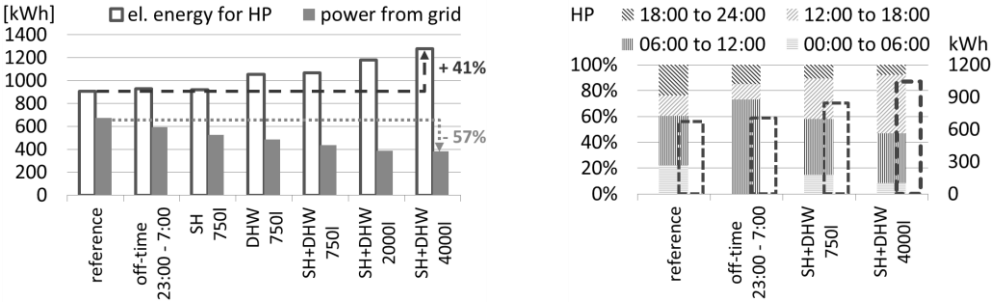

Figure 6: Due to changes in the control strategy the electric energy demand of the heat pump increases by 40%, because the heat pump is operated in unfavourable conditions (high supply temperatures) more often. Because the additional consumption is covered by PV the net electricity demand from the grid is reduced by nearly 60%.

To investigate the influence of an own-consumption optimized control-strategy in a small residential building, different measured load profiles from apartments (occupied by 2 – 4 people) are analysed and compared. In single-family homes the load pattern is extremely user-dependent [2]. For a comparison we used five different apartments, three of them are shown in Figure 7 and Figure 8 (named AP01 – AP03).

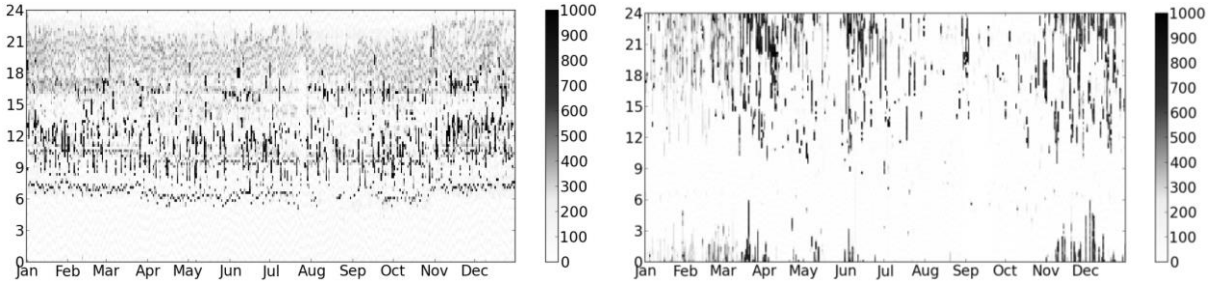

Figure 7: Carpet plot of electric load profiles for different households. Some have very regular daily patterns (left: AP02), especially the loads during night and day can differ significantly (right: AP03).

The figures illustrate that in addition to the summarized electric consumption, the dynamics of the load patterns is important. Even though AP01 and AP03 have a similar electric consumption for household electricity (incl. ventilation), in AP01 59% of the electric energy is used at daytime (6:00 to 18:00), whereas it is only 35% in AP03 (see Figure 8). In addition to the household electricity, the electric demand of the heat pump is shown (Figure 8, left graph, reference scenario). As the demand for the heat pump (=space heating and DHW) is nearly the same for every apartment, the ratio of heat pump and household electricity varies.

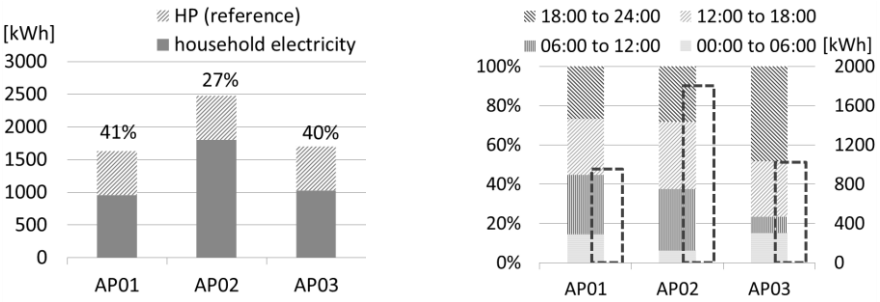

Figure 8: Comparison of different electric consumption-profiles from different households (size: 2 – 4 inhabitants).

Combining the heat pump with the different control strategies with electric load patterns from small apartments levels the small achievements that are shown in Figure 6. For a cross-comparison the summarized load patterns (HP plus household consumption) are combined with a downscaled PV system (2.1 kW_p, 2000 kWh yield) and the net grid supply, the feed-in surplus and the solar fraction are calculated for the different apartments and the different control strategies – see Table 1.

Table 1: Comparison of overall household electricity with different control strategies for the HP system. Net grid supply: sum of electric energy during time when demand is bigger than PV supply.

		reference	off-time 23:00 - 7:00	SH+DHW 750l	SH+DHW 4000l
AP01					
gross consumption	[kWh]	1426	1456	1598	1798
net grid supply	[kWh]	1025	1018	976	977
PV feed-in	[kWh]	574	544	402	202
hourly solar fraction	[%]	33%	31%	29%	27%
AP02					
gross consumption	[kWh]	2275	2305	2447	2647
net grid supply	[kWh]	1388	1359	1226	1174
PV feed-in	[kWh]	2875	2844	2703	2503
hourly solar fraction	[%]	34%	33%	32%	32%
AP03					
gross consumption	[kWh]	1496	1527	1669	1869
net grid supply	[kWh]	1123	1080	934	879
PV feed-in	[kWh]	3649	3619	3477	3277
hourly solar fraction	[%]	40%	39%	40%	40%

The results in Table 1 again show that the overall consumption increases due to lower efficiency of the heat pump. Even though the net grid supply decreases, the PV feed-in decreases even more. The hourly solar fraction is not getting better – on the contrary, even though the availability of PV power is used as parameter in the controls, the solar fraction decreases.

CONCLUSION

For buildings located on the water, HVAC systems based on heat pumps, using the water as heat source, can be seen as efficient solution. To minimize connection power and increase own-consumption for on-site PV, the load-shifting potential of using the heat pump is rather low. The influence of user dependant load patterns is bigger than adapted control strategies.

REFERENCES

1. A.J. Marszal, J.S. Bourrelle, E. Musall, P. Heiselberg, A. Napolitano, I. Sartori, K. Voss: Zero Energy Buildings - A review of definitions and calculation methodologies, Energy and Buildings 43, 2011
2. Engelmann, P., Roth, K. : Comfort, Indoor Air Quality, and Energy Consumption in Low Energy Homes, NREL Report No. SR-5500-56023, Golden, CO, December 2012

SMART BUILDING AS A POWER PLANT – ENERGYPLUS HOUSE WITH ENERGY CHARGE MANAGEMENT AND E-MOBILITY

Prof. Dr.-Ing. M. Norbert Fisch, Dipl.-Ing. Christina Stähr, Dipl.-Ing. Franziska Bockelmann

Technical University of Braunschweig IGS – Institute of Building Services and Energy Design, Mühlenpfordtstraße 23, 38106 Braunschweig, Germany, Phone: +49-531-39163403, Fax: +49-531-3918125, staehr@igs.tu-bs.de

ABSTRACT

The energyPLUS building demonstrates an integral solution of appealing architecture, energy efficiency and optimal usage of solar power through photovoltaic. The "only-electricity-building" has an annual demand of approx. 9,500 kWh for space heating, domestic hot water, white goods and user equipment. The PV-system delivers approx. 14,500 kWh/a.
The goal is to achieve an intelligent power load management with an intrinsic power-usage share of 50% for the building's internal power consumers.

To achieve this goal the following measures were realized: In the heating period the heat pump is only powered by the public grid in exceptional cases during night time. White goods such as dishwasher, washing machine, laundry dryer etc. are preferably run during daytime. Fridge and freezer get switched off at night for a few hours (observation of internal temperature) in exchange an "under cooling" is realized during daytime using PV-power.
By a backup-system of two batteries (storage-capacity 7 kWh and 20 kWh) and an inverter the small-scale users such as lighting, IT and the phone would get supplied in times at which the PV-System provides no power.

Besides the prior direct usage in the building, the solar power is used to charge the electric car. The charging station is located in the garage of the residential building. Further surplus is fed into the public grid and drawn back out for the times the energy demand is higher than the PV energy yield. Unlike the common case where the public grid is used for energy storage to 100% here it is relieved.

The existing building is one of the answers to the challenges of our future energy supply with a high fraction of renewable energy. The project is a role model example of integral planning and allows researching future orientated technology- and energy strategies today. The high rate of PV-self-supply (direct and using batteries) makes this building a trendsetting pilot project rather than the plus balance on feeding PV-power into the public grid.

Keywords: EnergyPLUS, PV-self-supply, energy storage, smart grid, sustainable architecture and design

INTRODUCTION

The goal of this project was to create a building that would meet the future energy-efficiency and living comfort demands as well as eco-friendly mobility. It combines these energetic goals with an ambitious architecture. In the future it will be not only important to reduce the heating energy demand but to have an integral overview on the entire electricity demand and the utilization of energy for private mobility. Important parts in this concept are the interfaces between building, e-mobility and building power grid. The monitoring of the research project (SF-10.08.18.7-11.32) is founded by the BMVBS by the research initiative 'ZukunftBAU'.

METHOD

Due to the active solar energy use the annual regenerative energy yield balance is higher than the whole power demand. It was only achievable with the high energy efficiency of the building: the orientation, the shape of the building, high quality air-tight building envelope with low heat transfer coefficients and the innovative building technology. The electricity from the PV system is fed into the two batteries with a capacity of 7 and 20 kWh. The implementation of the batteries increased the fraction of electricity used at home in comparison to electricity sent to the grid.

Implementation of a monitoring enables an assessment of particular systems and the overall performance of the building and an identification and optimization in the direction of the target values. Furthermore the significant loads of heat and electricity, temperatures, humidity levels and local weather data are collected. The measurement data and the calculated energy values are optionally displayed to the users via an online energy monitor to make the current energy efficiency transparent and to influence the user behaviour if necessary.

Architecture

The single family home completed in the end of 2010 is built on the south-orientation estate with an area of around 900 m². The building has a floor area of approximately 260 m². The northern part of the basement points towards the hillside and is below the ground, while the southern part opens up to the valley with a large window front. The north, east and west façades are kept much more opaque. Because of the location on a slope, all living spaces are oriented towards the south. The different floors are staggered and the structural bearing-out forms a sun protection for the ground floor. As an integral part of the architecture the shed roof, facing 18 degrees south, becomes an active solar collector area. Around 15 kW_p of polycrystalline photovoltaic modules and 7 m² of solar thermal collectors (switch off 2012) are fitted on the roof. The building is accessible from the lower located street over a stone staircase, built into the hillside, or through the underground garage.

Figure 1: South and north-west side

Energy concept

The energy concept for the energyPLUS building is being developed in an integral design process.

Due to the active solar energy use the annual regenerative energy yield balance is higher, than the whole power demand for space heating, hot domestic water, lighting, ventilation, household electricity etc..The basis to achieve this goal is a high energy efficiency of the building. The key for the consistent energy design of the dwelling place is the smooth teamwork between architecture and technology: The orientation and shape of the building on the one hand, high quality air-tight building envelope with low heat transfer coefficients on

the other hand, in combination with the innovative building technology add together to a sophisticated concept for an energyPLUS building.

Optimized use of daylight and innovative and energy-efficient building equipment exclusively based on electricity reduce the power consumption of the building. Coverage is primarily realized through a high solar electricity direct use. The technical components of the building are equipped with battery storages and are linked to a smart electricity load management system. Primarily the solar-generated electricity is used to cover the building demand in addition the produced electricity beyond this load is stored in batteries inside the building and in the electric vehicle batteries allowing a fossil fuel independent mobility. Not until then further solar electric yield is supplied to the public grid. Thus the public grid is unloaded and not used 100% as power storage, as is usually the case otherwise.

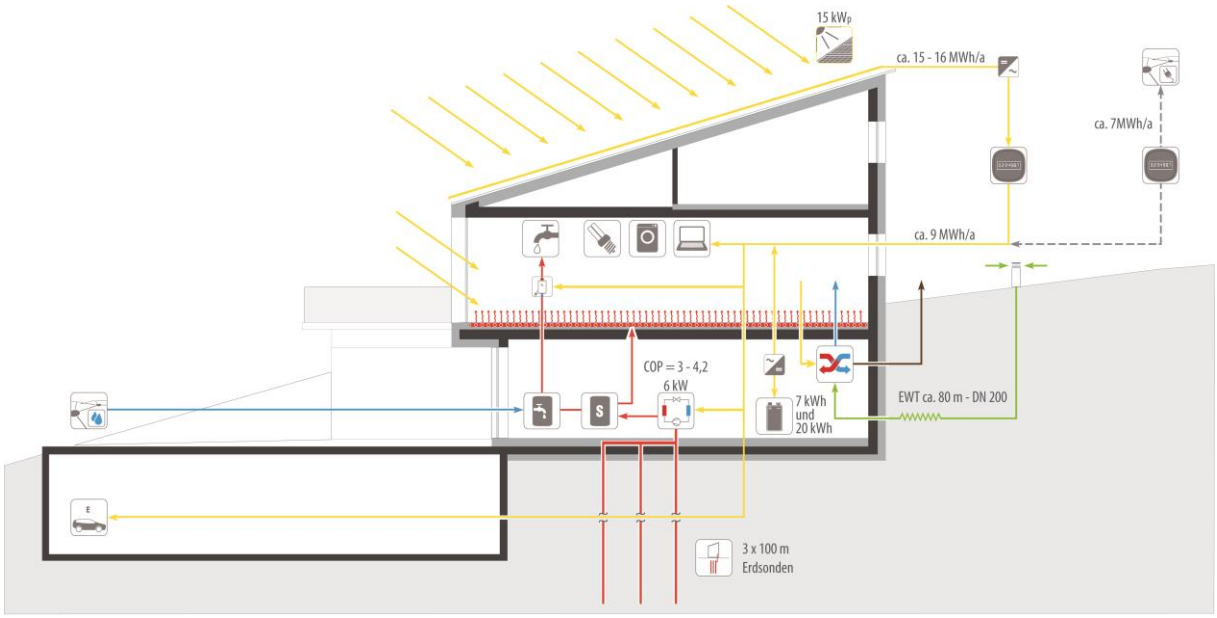

Figure 2: Energy concept

The electricity from the PV system is fed into the two lead-acid batteries with a capacity of 7 kWh respectively 20 kWh and supply the building via an inverter to power lighting.

Besides the prior direct usage in the building, the solar power is used to charge the electric car. Charging station is located in the garage of the residential building. Further surplus is fed into the public grid and drawn back out for the times the energy demand is higher than the PV energy yield. Unlike the common case where the public grid is used for energy storage to 100% here it is relieved.

Building services engineering

The heating system is based on a ground coupled monovalent heat pump powered electrically (max. 3.5 kW_{el}) with 3 vertical ground probes of 100 m each, low temperature floor heating and a central hot domestic water system. The mechanical ventilation with heat recovery is coupled with a ground heat exchanger. Systems for energy storage are the thermally active building mass itself, a buffer storage (800 l) and two electric batteries (7 and 20 kWh). Further energy-efficient features are especially energy-saving white goods (washing machine and dishwasher with hot water supply) and energy-efficient lighting.

Energy Charge management

The intelligent power-load-management is connected to all major intra-building electricity consumers. The idea behind this is to directly use the generated PV-power. To achieve this goal the following measures were realized: In the heating period the heat pump is only powered by the public grid in exceptional cases during night time. White goods such as dishwasher, washing machine, laundry dryer etc. are preferably run during daytime. Fridge and freezer get switched off at night for a few hours (observation of internal temperature) in exchange an "under cooling" is realized during daytime using PV-power. All relevant technical system components are controllable over the central building management system (BMS). The BMS is connected to the internal Ethernet-network through a LAN-interface. This allows changing parameters and selecting functions of the BMS using a PC, a touch panel or a Wi-Fi handheld device.

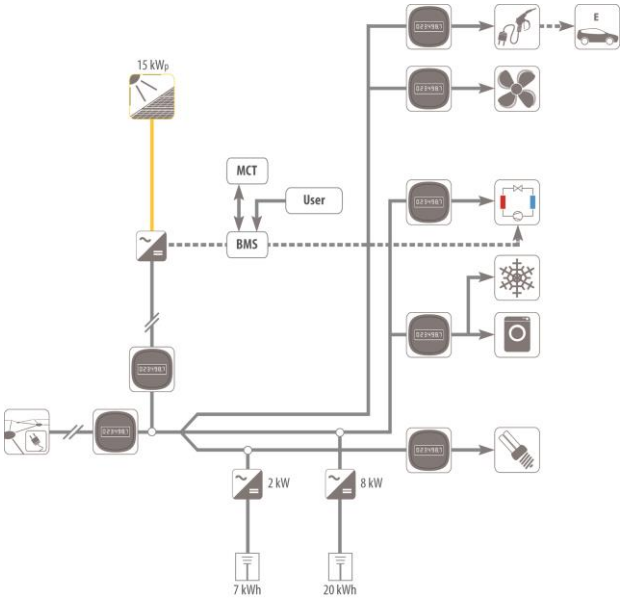

Figure 3: Electricity supply, -storage and -distribution and electricity meter concept

Monitoring

The implementation of a monitoring the partial energy characteristics and the overall performance of the building are identified and optimized in the direction of the target values (annual primary energy demand, KfW Efficiency House 55 and high fraction of self-generated power usage). Furthermore the significant loads of heat and electricity, temperatures, humidity levels and local weather data are collected. The measurement data and the calculated energy values are optionally displayed to the users via an online energy monitor to make the current energy efficiency transparent, and to adapt the user behavior if necessary. In addition to the energetic goals the acceptance of such long-range systems is examined and evaluated in a long-term test. It is interesting to see how the monitoring influences the user behaviour.

RESULTS

The data from the first two years of operation (2011/2012) for the energy balance surpassed expectations. In comparison to the calculated annual PV energy yield of 14,500 kWh/a, a total of approx. 16,000 kWh/a was collected in each year, which is about 12% more than predicted (Figure 4). This corresponds to a specific annual yield of 1,085 kWh/kW$_p$. The photoelectric

energy yield over the first year of operation was approximately 1.8 times the annual electricity consumption. A total of 2,857 kWh/a (2012: 5,262 kWh/a) was used directly in the house and consequently 13,417 kWh/a (2012: 10,661 kWh/a) was fed into the grid. Of the total electricity consumption of 9,027 kWh/a (2012: 11,060 kWh/a), about 32% (2012: 48%) was covered directly by the PV system. The direct usage of the self-generated electricity reached approximately 18% in the first year of operation. The balance sheet shows a surplus of about 7,250 kWh/a, which would be sufficient to power the electric vehicles (about 20 kWh per 100 km) over a distance of 36,000 km/a or to cover the electrical demand of a house with five or six persons.

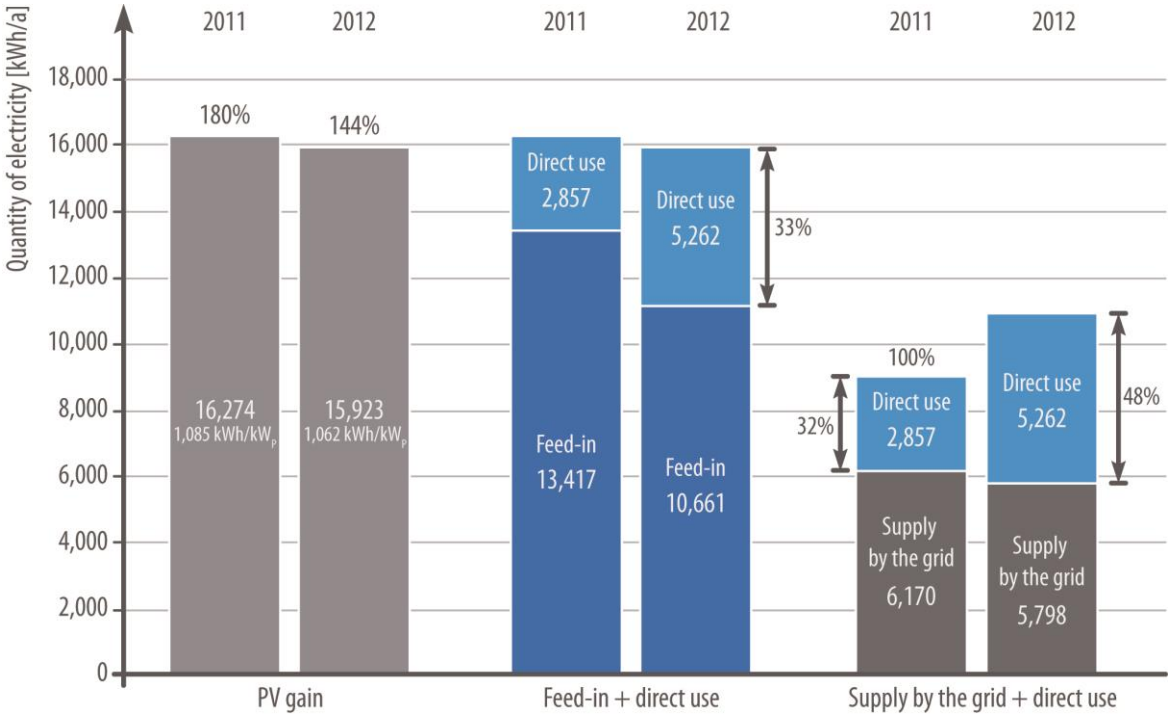

Figure 4: Annual balance of total electricity of house (2011 and 2012)

Due to modifications in load management and optimization of the control strategies for operation of the heat pump, the share of solar energy in the overall electrical consumption increased to 48% in 2012. A battery was additionally installed for optimal storage and utilization of the photovoltaic energy. Since the shutdown of the solar thermal system in March 2012, supply has been effected monovalently via the heat pump, resulting in a decrease to 144% in the balance for 2012 in connection with increased self-consumption of electricity.
The overall specific electrical consumption in 2011 was about 35 kWh/(m^2_{LS}a) in respect of the living space; as a result of the changes described above, the figure increased to 42.5 kWh/(m^2_{LS}a) in 2012. With the relevant primary energy factor of 2.6 for the German electrical energy mix in 2012, the effective primary energy consumption is about 58 kWh_{PE}/(m^2a), with a primary energy surplus of around 56,8 kWh_{PE}/(m^2a).

Figure 5 shows the shares of heat supply and heat consumption in the building, broken down according to heat source (heat pump and solar thermal), heat distribution (buffer storage/distribution), and heat transfer (heating and domestic hot water). The total heating consumption amounted to 11,202 kWh/a in 2011 and 13,918 kWh/a in 2012. The corresponding specific heating energy consumption figures were 43.1 kWh/(m^2_{LS}a) and 53.5 kWh/(m^2_{LS}a). The heat demand in 2011 was covered to 73% by the heat pump and to 27% by the solar thermal collectors.

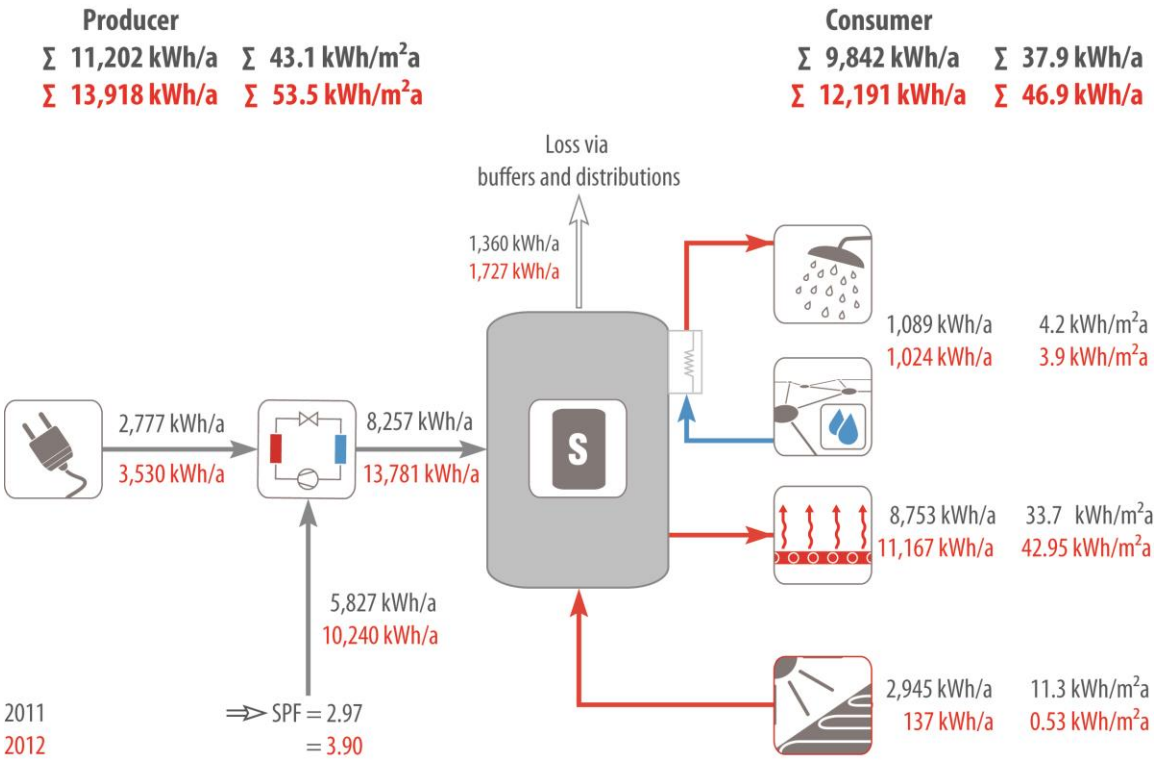

Figure 5: Annual energy balance of the buffer storage (2011 and 2012)

Since the solar collectors were shut down in March 2012, the solar thermal benefit for that year was reduced to 1%; 99% was covered by the heat pump. The fraction of heat used for domestic hot water was 10% (1,089 kWh/a) in 2011 and 7% (1,024 kWh/a) in 2012; whereas 78% (8,753 kWh/a) were used for heating in 2011 and 81% (11,167 kWh/a) in 2012. This corresponds to specific values of 4.2 and 3.9 kWh/(m2LSa) respectively for domestic hot water, and 33.7 and 43.0 kWh/(m2LSa) for heating. The energy heat losses due to storage and distribution amounted to around 12% for each of the two years of operation.

CONCLUSION

The energyPLUS building with e-mobility and a high PV-power self-supply is one of the answers to the challenges of our future energy supply with a high fraction of renewable energy. The project is a role model example of integral planning and allows researching future orientated technology and energy strategies today. The high rate of PV-self-supply makes this building a trendsetting pilot project rather than the plus balance on feeding PV-power into the public grid.

REFERENCES

Fisch, M. N., Wilken, T., Stähr, C: EnergiePLUS – Gebäude und Quartiere als erneuerbare Energiequellen, Leonberg, 2012

MONITORING TECHNIQUE, EVALUATION METHODOLOGY AND RESULTS FOR A MULTIFUNCTIONAL BUILDING WITH GEOTHERMAL ENERGY

Johannes P. Fuetterer; Ana Constantin, Martin Schmidt, Rita Streblow and Dirk Müller

RWTH Aachen University, Institute for Energy Efficient Buildings and Indoor Climate, Mathieustraße 10, 52074 Aachen, Germany, jfuetterer@eonerc.rwth-aachen.de

ABSTRACT

Higher complexity of energy concepts in modern buildings leads to an increase of the amount of data points within a building automation system. More and more degrees of freedoms for different control strategies and approaches are available and energy efficiency of complex energy systems hardly depends on their operation mode.

The authors implemented an extensive monitoring system into a multifunctional 7222 m² building for offices, laboratories and conferences. A complex energy concept with virtually all state-of-the-art building technologies satisfies the building's energy needs while aiming for high energy efficiency.

The paper presents guidelines for sensor placement via introducing four theoretical monitoring layers. Accomplishing sensor equipment at all four monitoring layers leads to a complete system that enables analysis toward technical operation and energy efficiency. They further present a data processing methodology. The paper explains how data is gathered from an OPC data access server and stored into an event-based SQL data base. The data is either processed on demand via different software tools or analysed within automatically generated reports. The authors present their evaluation methodology by introducing the content of their monitoring reports. The four existing report types are: a daily energy report for the building, a daily energy report for the systems of energy conversion, a daily energy report for the systems of distribution and demand, and a monthly energy report.

With the presented reports it is possible to assess a complex energy concept and a huge amount of data and derive clear and meaningful statements. Optimization can be relevantly supported by such system. Without ongoing information and system insight optimization can only be hardly conducted. For the monitoring object it is obvious that the energy concept is currently not working according to its expected energy consumption and efficiency. The monitoring system will as such support further work towards control strategy and operation optimization.

Keywords: monitoring, data storage, data processing, evaluation, visualization,

INTRODUCTION

Higher complexity of energy concepts in modern buildings leads to an increase of the amount of data points within a building automation system. More and more degrees of freedoms for different control strategies and approaches are available and energy efficiency of complex energy systems hardly depends on their operation mode.

We implemented a complex energy system with virtually all state-of-the-art building technologies into a multifunctional office building with additional conference and laboratory use. Further we implemented an extensive monitoring system for energetic and operational analysis of the energy system. Via detailed monitoring reports it is possible to get a clear

picture of the system's operation mode and behaviour. It is possible to identify malfunctions and failures. Our monitoring results show that the prior to the building's construction designed control strategy is not working with satisfying energy efficiency. The actual control strategy has to be improved and research towards new advanced control strategies and approaches has to be done.

In this paper, we present how we placed sensors following theoretical monitoring layers which allow for detailed analysis of building energy systems. We introduce our technical data gathering and storage system. From a technical point of view, we present our methodology for data processing, either on demand or by automatic reporting. We present a solution for dealing with huge amounts of data and build monitoring reports in order to support system evaluation and optimization. As results we present an extract of a monitoring report.

BUILDING, ENERGY CONCEPT AND MONITORING PRINCIPLE

The object of interest for our monitoring system is the new main building of the E.ON Energy Research Center at the RWTH Aachen University. The building offers facilities for 250 employees. Its energy concept meets the trade-off between fulfilling all demands while maintaining a high energy efficiency. As shown in Figure 1 the concept consists of different energy conversion and distribution units. The system's heart is a turbo compressor driven heat pump. A glycol cooler and a field of 40 borehole heat exchangers keep the energy balance of the heat pump's hot and cold side throughout the whole year. A co-generation plant provides electricity, mainly used for the heat pump process, and high temperature heat for integration into a heat-to-cold shifting sorption process, or for direct use in laboratories or for additional heating energy.

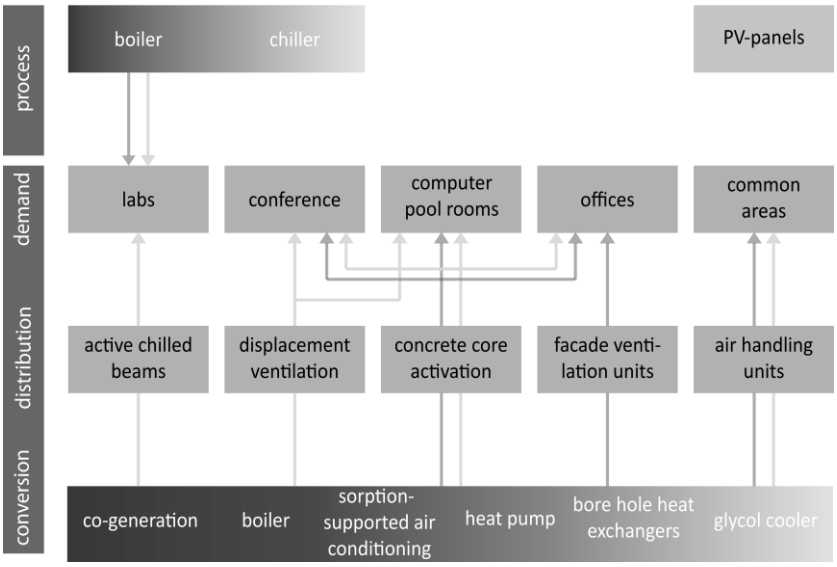

Figure 1: Energy concept of the monitored multifunctional office building.

We organized the system in conversion, distribution, demand, and process layer. In order to gather data in required detail the sensors of the building automation system it was necessary to install additional sensors. We added sensors to provide a complete energetic and system operation monitoring data within four layers, which are detailed below. The sensor placement guarantees holistic and complete sensor equipment for monitoring purposes towards system optimization and energy efficiency.

Global consumption layer: This layer consists of all energy and mass flows that enter or leave the building. The electricity, water and gas consumption and the transfer of ambient energy are part of this layer.

Energy conversion layer: All energy conversion related energy and mass flows are part of this layer. Inlet and outlet energy flows occur for every energy conversion unit, e.g. for the heat pump these flows are the electrical energy, the absorbed ambient energy and the emitted heat flow. Furthermore, sensors that map and image the conversion and generation process internally, such as temperature, pressure, control parameters, etc. within conversion units belong to this layer

Energy distribution layer: Energy flows supplied by the energy conversion system are allocated and distributed within the building. Buildings can be separated in zones, following their use, their energy distribution principle and their geographical orientation. For each distribution system and for each use of the building the energy consumption has to be calculated. The distribution layer monitoring sensors are gathering the energy flows supplied to or extracted out of these different zones.

Utilization layer: Each energy or mass flow satisfies a certain goal, within multi-functional buildings e.g. thermal comfort in office rooms or staff facilities, heating for test benches or cooling for server rooms. The evaluation of the goal-satisfaction is the last elementary monitoring layer.

Given physical sensor equipment at all four layers, it is possible to conduct variable and complete assessments. Such assessments are orientated towards different key performance indicators (KPI), distinct parts of the equipment, system interaction, user behavior and so on.

We used the four theoretical layers to place our sensors as follows: at the global consumption layer electricity flows entering the building from the grid or leaving the building due to cogeneration plant and PV production are measured. The gas consumption and the fresh water amount are observed. Furthermore, the energy exchange with the environment via the geothermal field and via the glycol cooler is included. At the energy conversion layer all energy flows entering and leaving all different conversion units are measured. KPIs of the heat pump, the boilers, the cogeneration plant, the chiller, and the sorption-supported air handling unit can be calculated. Data for other parts of the hydraulic systems, e.g. buffer storages and distribution systems is available. Concerning the energy distribution layer each energy distribution principle, such as concrete core activation, façade ventilation displacement ventilation, active chilled beams, air handling units and circulation air coolers, is separately monitored. Distinctions between different zones, like the east and the west energy supply hydraulic network for façade ventilation units and the four different zones of the concrete core activation are made. The monitoring system gathers data of the ventilation mass flows for each room. All operation data of the façade ventilation units, altogether 40 data points, is logged. At the utilization layer due to the immense sensor amount ten reference rooms have been chosen. These reference rooms are equipped with sensors measuring all supplied and extracted energy flows. In every room of the building, the room temperature, humidity, CO_2 and volatile organic compounds (VOC) are monitored. Installed sensors measure the energy transfer for all special demands, such as server cooling.

ARCHITECTURE OF THE MONITORING SYSTEM

A common building automation system – field, automation and management layer – was installed in the building during its construction. Programmable logic controllers automate field devices, such as control panels, sensors and actuators. A management server provides a supervisory control and data access system that is able to access all network data points.

BACnet integrates BACnet-compatible parts of the technical building equipment directly into the system's management layer.

We connected the institute's intranet with the building management network and added a cloud server infrastructure. The cloud is connected to the building management network and to the institute's intranet; see Figure 2 left. We virtualized the building management server, moved it into the cloud and added a monitoring server hosting all necessary services.

A service logs every data point occurring in the building automation system and redundantly stores it into two event-based databases. The service uses an OPC (object linking and embedding for process control) data access server to gather data. OPC is a standard and commonly used data access protocol. The OPC server scans PLCs and BACnet devices within the building management network and provides data objects. Two other services include weather forecast, a weather station and a wireless sensor network into the database. Temporary measurements are integrated via a data import tool; see Figure 2 right.

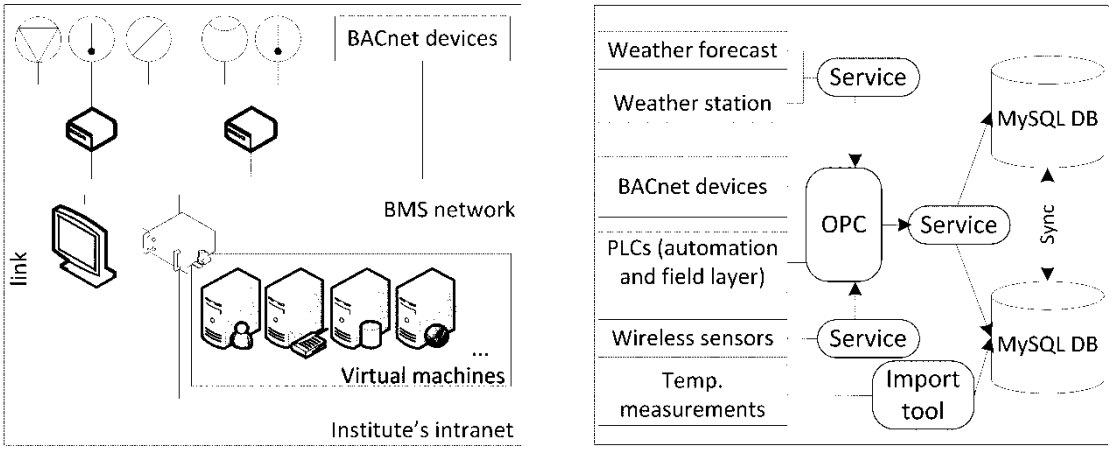

Figure 2: left: Building automation infrastructure with cloud server and link to the institute's intranet; right: Schematic of the data logging and storage system

DATA PROCESSING METHODOLOGY

Basically, different software tools and programming language are able to access SQL data bases and process data. We implemented routines for data processing in Python, Excel, MATLAB and Java in order to be as interoperable as possible and in order to provide flexible data access for data user'spreferences. The data bases are accessible via VPN through the internet. An extensive building data catalogue is available for data users. The data catalogue consist of a description every data point that is available through the system. Every data point is included in a schematic which is linked out of the building catalogue.

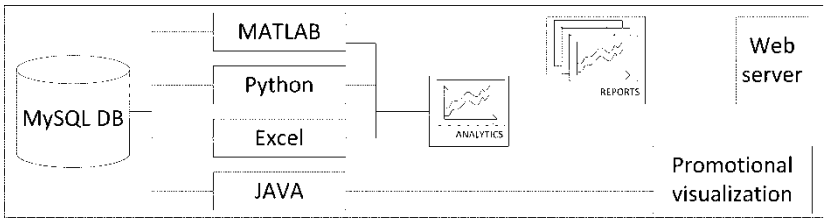

Figure 3: Schematic of the data access and processing system with online publication

A data analytic and report generation system operates on a virtual machine in our cloud infrastructure. It generates detailed daily, weekly and monthly reports on energy consumption and KPIs; from whole building scale down to every single energy conversion unit and

distribution system. Reports are generated in HTML format. A cloud-based web server hosts generated reports to the internet.

Daily energy report for the building

The daily energy report for the building consists of an energy flow diagram, a table with additional information about the system performance and a plot with weather data.

The energy flow diagram as shown in Figure 4 gives an overview of the total amounts of heating and cooling energy produced and distributed in the building. Different grey types indicate the temperature levels of the energy flows, starting from cooling energy at 6°C and 17°C on to heating energy at 35°C and 80°C. The systems of energy conversion and distribution are shown together with the related amounts of energy for the day. More information about the systems can be found in the table, which additionally contains information about maximum heat flow, as well as maximum and minimum temperatures of the day. Another diagram shows the outside air temperature and global radiation that we obtain from our own weather data monitoring system.

Daily energy report for the systems of energy conversion

In order to get a deeper insight in the performance of the most important systems of energy conversion, detailed reports are created daily for the heat pump, the condensing boiler, the central heat and power unit as well as for the geothermal field.

A table gives information about total amounts of energy, maximum and minimum values of heat flows and temperatures, the operating mode and operating coefficients. Two plots show the temperatures and heat flows during the day. The report is completed by information about outside air temperature and global solar radiation.

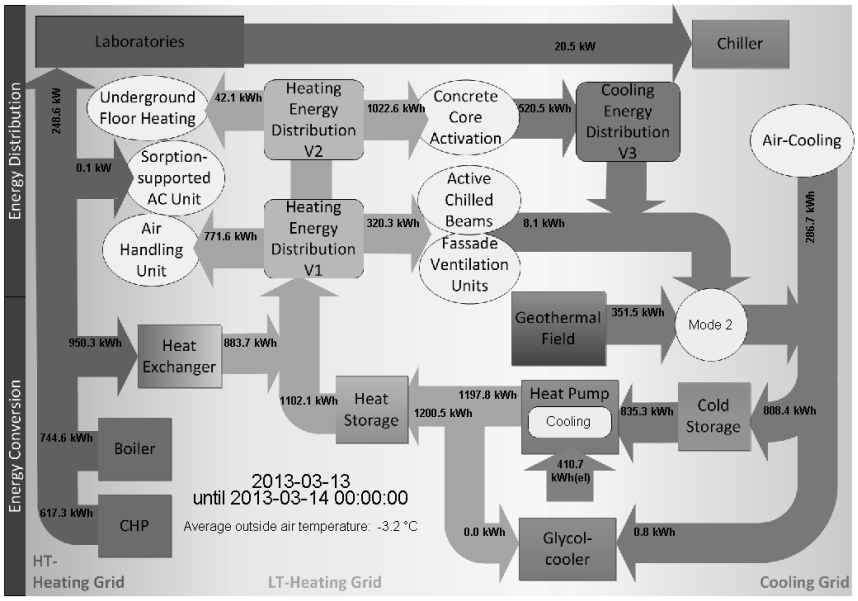

Figure 4: Daily building report's energy flow diagram

Daily energy report for the systems of distribution and demand

Reports about the high temperature heating, low temperature heating, and cooling energy distribution show the daily characteristics of how the energy is used in the building.

Again a table summarizes information about amounts of energy, maximum and minimum heat flows and temperatures for the day. A plot shows the heat flows going to or coming from

the different systems, e.g. for the systems of low temperature heating. Additional plots display the temperatures of the flows over time and the weather conditions at the building for the day.

Monthly energy report

Once in a month a report is created that summarizes the total energy production and consumption of the building's systems. Furthermore it shows how these amounts of energy are allocated to the different days of the month. Information about the outside air temperature and the total amount of global radiation in the month completes the report.

The monthly energy reports are a basis for long time observation of the overall building performance.

RESULTS

As a representative result we present the energy flow diagram from an example building report for a cold day in March 2013. It is shown in Figure 4. On this day with an outside mean temperature of -3.2 °C high amounts of energy are needed for thermal heating. As can be seen in the figure the heating energy is provided by the heat pump, the CHP and the boiler. The CHP produces 617.3 kWh, the Boiler 744.6 kWh of high temperature energy this day. The major part of these amounts (950.3 kWh) is transferred to the low temperature grid where it is used for thermal heating purposes additionally to the energy from the heat pump. A smaller part (248.6 kWh) is used as process heat for the laboratories. The figure gives an overview about how the system operates to satisfy the building's demand. It shows how the energy conversion units interact.

CONCLUSION

We presented four theoretical layers for sensor placement that lead to a complete sensor equipment for analysis towards evaluation and optimization of complex energy concepts. We outlined a solution for gathering data out of a common building automation system, for storing it and for making it accessible for analysis. We presented automated reports that evaluate the energy system from an energetic and operational point of view. They provide a clear insight about what is happening within the system. They enable the identification of malfunctions and disadvantageous operations.

Our energy concept is currently not working according to its expected energy consumption and efficiency. The monitoring system will as such support further work towards control strategy and operation optimization.

With the presented reports it is possible to assess a complex energy concept and a huge amount of data and derive clear and meaningful statements. Optimization can be relevantly supported by such system. Without ongoing information and system insight optimization can only be hardly conducted.

REFERENCES

1. J. Fuetterer, A. Constantin and D. Mueller, "An energy concept for multifunctional buildings with geothermal energy and photovoltaic," in CISBAT international scientific conference 2011 - proceedings Vol. 2., Lausanne, Switzerland, 2011.
2. American Society of Heating, Refrigerating and Air-Conditioning Engineers, „ANSI/ASHRAE 135-2010 Standard 135-2010 - BACnet A Data Communication Protocol for Building Automation and Control Networks (ANSI Approved) SSPC 135 and TC 1.4, Control Theory and Application," ASHRAE, 2011.

EXPERIENCE AND OUTLOOK ON A THERMO-CHEMICAL STORAGE SYSTEM BASED ON AQUEOUS SODIUM HYDROXIDE

B. Fumey; R. Weber; V. Dorer; J. Carmeliet

EMPA, Building Technology Laboratory, Überlandstasse 129, 8600 Dübendorf

ABSTRACT

Application limitations for solar heating are overcome by greatly improving heat storage. Adequate heat storage is achieved by reducing the time dependent thermal losses, reducing storage volume and allowing storage geometries to easily adjust.

To this purpose much work has been done at Empa on a laboratory scale proof of concept of a closed sorption heat storage. This work has provided valuable insight into the potential as well as the challenges and limitations of this technology for the application as heat storage.

The closed sorption heat storage concept is based on a continuous, but not full cycle, liquid state absorption heat pump. Heat is not directly stored, instead the potential to regain heat at a desired temperature from a low temperature thermal input is stored. The markable benefit in this is undoubtedly the time independent energy losses. Losses are encountered in the conversion processes during charging as well as discharging but not during storage time. For this reason there is great potential in the application of the closed sorption heat storage as a long term solar heat storage. Due to the losses during the conversion process the closed sorption heat storage is less suitable for short term heat storage. Therefore for a 100 % solar heated home a hybrid system is proposed. This hybrid system contains a hot water storage for short to intermediate term storage and a closed sorption heat storage for seasonal storage.

In the scope of the EU funded project COMTES a prototype system based on the working pair aqueous sodium hydroxide is under construction. The system is dimensioned to cover space heating as well as domestic hot water in a single family house in Zurich, built to passive energy standards. The two major challenges in the system design are: keeping the system volume favourable and keeping the parasitic electric energy consumption at a minimum.

Keywords: Longterm Thermal Storage, Thermo-chemical Material, Sodium Hydroxide, Absorption Heat Pump, Closed Sorption Heat Storage

NOMENCLATURE

T_{Ain}	Temperature of the fluid to be heated entering the absorber
T_{Aout}	Temperature of the heated fluid departing the absorber
T_{Eout}	Temperature of the fluid departing the evaporator to the bore hole heat exchanger
T_{Din}	Temperature of the fluid entering the desorber coming from the solar collectors
T_{Cin}	Temperature of the fluid entering the condenser coming from the bore hole heat exchanger
w_{sh}	concentration of the regenerated sorbent containing a high sodium hydroxide content
w_{sl}	concentration of the diluted sorbent containing a low sodium hydroxide content
Δw_s	concentration difference between w_{sh} and w_{sl}

INTRODUCTION

In sorption heat storage, heat is stored by separation of substances [1, 2]. To retrieve heat, the substances are recombined. No thermal insulation is required. The process functions under exclusion of non condensing gasses and is represented by the following reaction scheme:

$$\begin{aligned} &\text{Step 1:} && \text{AB (liquid or solid) + heat} \rightleftarrows \text{A (liquid or solid) + B (gaseous)} \\ &\text{Step 2:} && \text{B (gaseous) - heat} \rightleftarrows \text{B (liquid)} \end{aligned} \qquad (1)$$

Closed sorption heat storage is based on a continuous, but not full cycle, liquid state absorption heat pump [3]. The operating principle is as follows: two chambers are connected, as shown in figure 1. Chamber 1 functions as desorber as well as absorber containing the liquid working pair. In the scope of this task the working pair is water and sodium hydroxide. Chamber 2 is the condenser and evaporator, containing the working fluid water. The reversible chemical reaction, in the case of sodium hydroxide and water, is:

$$NaOH \cdot nH_20 + \text{heat} \ ^{TM} \ NaOH + nH_2O \qquad (2)$$

The system is facilitated with storage vessels to contain the working pair in its separated as well as combined state. Heat is not directly stored, instead the potential to regain heat at a desired temperature from a low temperature heat input is stored. In addition to achieving a potential increase in volumetric energy density compared to hot water storage, the closed sorption heat storage system has the markable benefit of time independent thermal loss. Thermal energy losses occur in the conversion processes, but not during storage. This technology is thus highly attractive for seasonal solar heat storage.

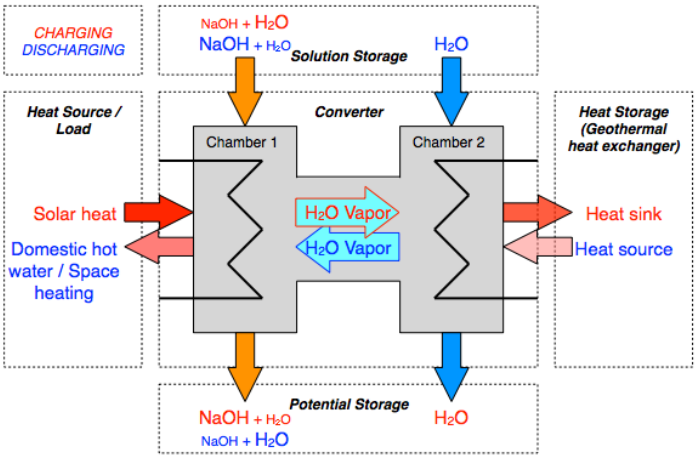

Figure. 1. The concept of the closed sorption heat pump based heat storage.

Regeneration or charging occurs by supplying heat from a heat source such as solar collectors to chamber 1. Water vapour is driven from the diluted sorbent to chamber 2, where it is condensed. The latent heat of evaporation is then released to the environment. In this process chamber 1 and 2 function as desorber and condenser respectively.

This process is temperature regulated so that the desired sodium hydroxide concentration in chamber 1 can be reached. The achievable concentration is directly dependent on the temperature difference of the temperature in chamber 1 to the temperature in chamber 2.

Both the resulting sorbent with high sodium hydroxide content and the water are stored separately. The liquids may then reach room temperature without potential loss, as long as reversed vapour transport is inhibited. The losses in storage are restricted to sensible heat loss of the liquids, which is a small fraction of the totally stored energy.

In heating or discharging mode, chamber 1 and 2 function as absorber and evaporator respectively. Water is introduced to chamber 2 and evaporated by employing a low temperature heat source. Water vapour is thus driven from chamber 2 to chamber 1, where it is absorbed by the sorbent, releasing the latent heat of evaporation. Due to the high affinity of water to sodium hydroxide, vapour is readily absorbed by the sorbent whereby a temperature increases results.

The output temperature T_{Aout} is dependent on the sodium hydroxide content in the sorbent w_{sh} entering chamber 1 as well as the output temperature T_{Eout} of chamber 1. Figure 2 illustrates this.

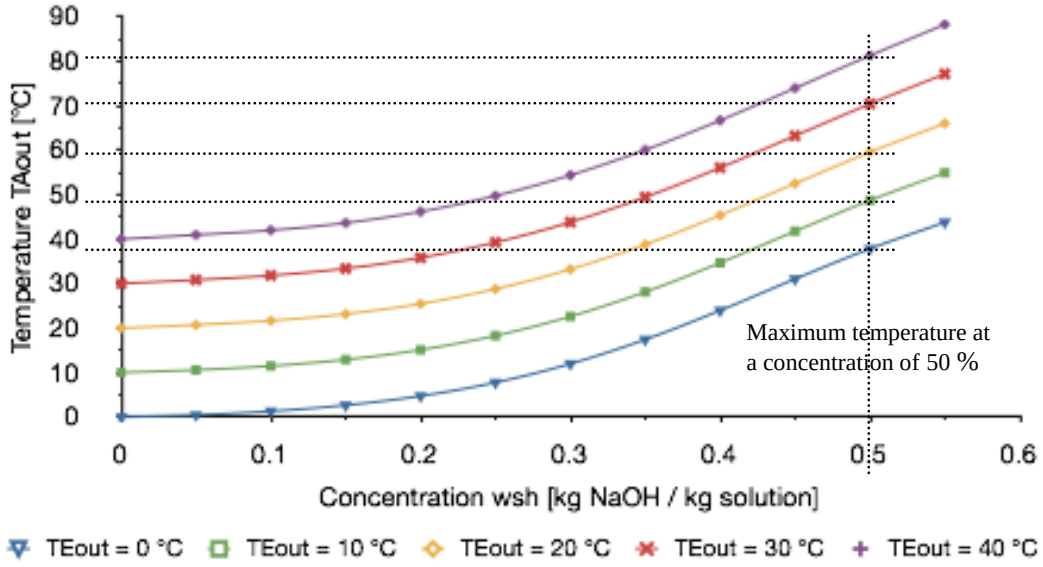

Figure. 2. Maximum output temperature in respect to sodium hydroxide concentration and solvent evaporation temperature.

In respect to the heating capacity the parameter of interest is the change in sodium hydroxide concentration Δw_s in the sorbent. At this point it is important to note that the increase in capacity is not linear to the concentration increase. As illustrated in figure 3. The higher the concentration, the lower the capacity increase in respect to concentration increase. It is thus important that a low concentration is achieved in the heating mode.

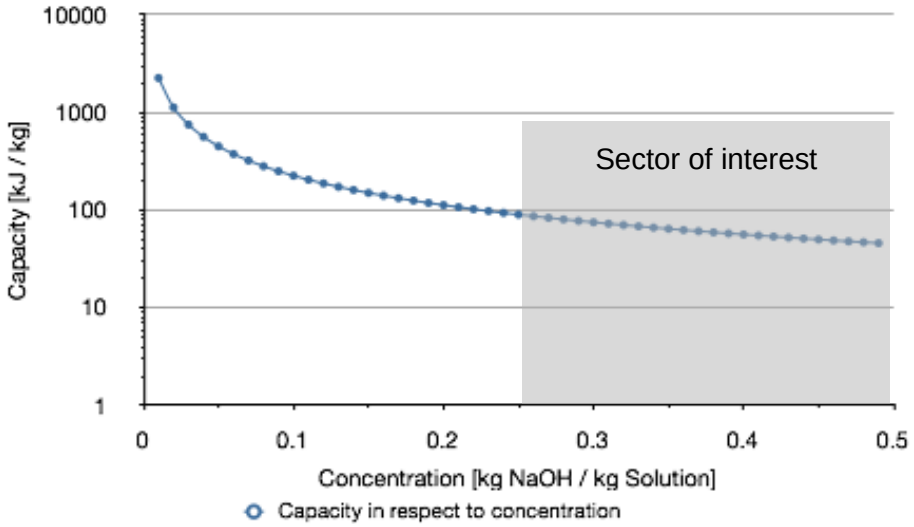

Figure. 3. Shows the reduction of the capacity gain in respect to the sodium hydroxide concentration in the solution.

It can be concluded that the energy stored is a function of the resulting concentration and the concentration increase. In other words, the heat capacity stored is dependent on the quantity of water vapour m_v transported.

It follows that in order to determine the energy capacity of the closed sorption heat storage system the maximum sorbent dilution has to be found. This in turn is dependent on the temperature of the water entering the absorber T_{Ain} and the temperature of the thermal supply leaving the evaporator T_{Eout}. The difference between T_{Ain} and T_{Eout} must be as low as possible to achieve a high exploitation, and so reach a high capacity.

The concentration difference of the working pair Δw_s is the difference between w_{sl} and w_{sh}. The high concentration or final regenerating concentration is dependent on the temperature difference between chamber 1 and chamber 2 during the regenerating mode. The greater the temperature difference the greater the resulting NaOH concentration in the solution. A limiting factor to w_{sh} is the solidification of the solution. This is dependent on concentration and temperature. For the working pair aqueous sodium hydroxide 50 w% sodium hydroxide in water is an upper limit whereby the solution does not solidify at temperatures above 15 °C.

From the discussion it can be concluded that the output temperature and the storage capacity are based on the same parameters, namely T_{Eout}, T_{Din} and T_{Cin} whereby the capacity additionally depends on T_{Ain}.

LABORATORY SCALE PROOF OF CONCEPT

Initial experience has been gained from a lab scale setup built with financial support from the Swiss Federal Office of Energy. Figure 4 left shows the schematic diagram of the system. Figure 4 right shows the laboratory setup.

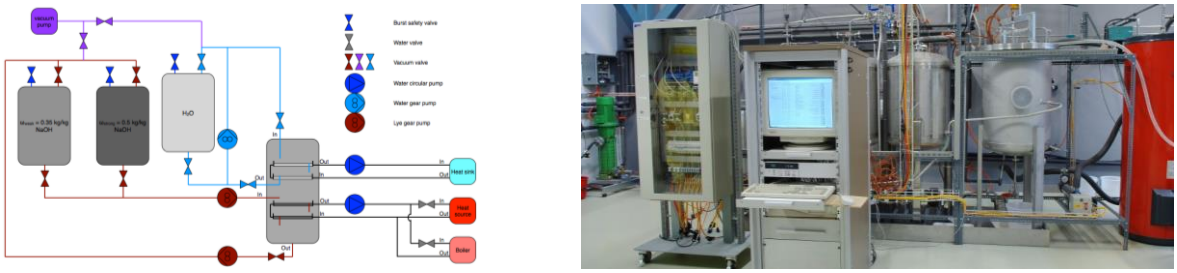

Fig. 4. Laboratory scale proof of function

The laboratory setup consists of three storage vessels containing concentrated lye, diluted lye and water. Gear pumps are used to transport the liquids to and from the converter. An electric resistor heater is used to simulate the solar collector input and the facilities chilled water supply serves as heat sink and low temperature heat source. The system is controlled using Labview. This setup enabled an initial proof of function. The exclusion of non condensing gasses and the transport of highly concentrated NaOH solutions demanded a very solid build. This in turn made the transport of solution concentrations of 50 w% and higher very difficult and crystallisation was often encountered. Never the less, it was possible to increase and decrease the NaOH concentration in the solution and heat transport in the form of water vapour could be measured.

The following diagram in Figure 5 shows the varying temperatures in the regenerating process. In the diagram one can see that up to the regenerating starting point the desorber plates are pre heated. The condenser plates are not pre cooled, resulting in a temperature rise

in plate C4 due to direct infrared radiation from plate D3. At the point "Start" the condenser plates are cooled and solution with low sodium hydroxide concentration is introduced to the desorber. The desorber is heated at a constant power. Due to the evaporation of water from the solution the temperatures T_{D1} to T_{D3} drop. In this process water is separated from the diluted sorbent to gain concentrated sorbent and water.

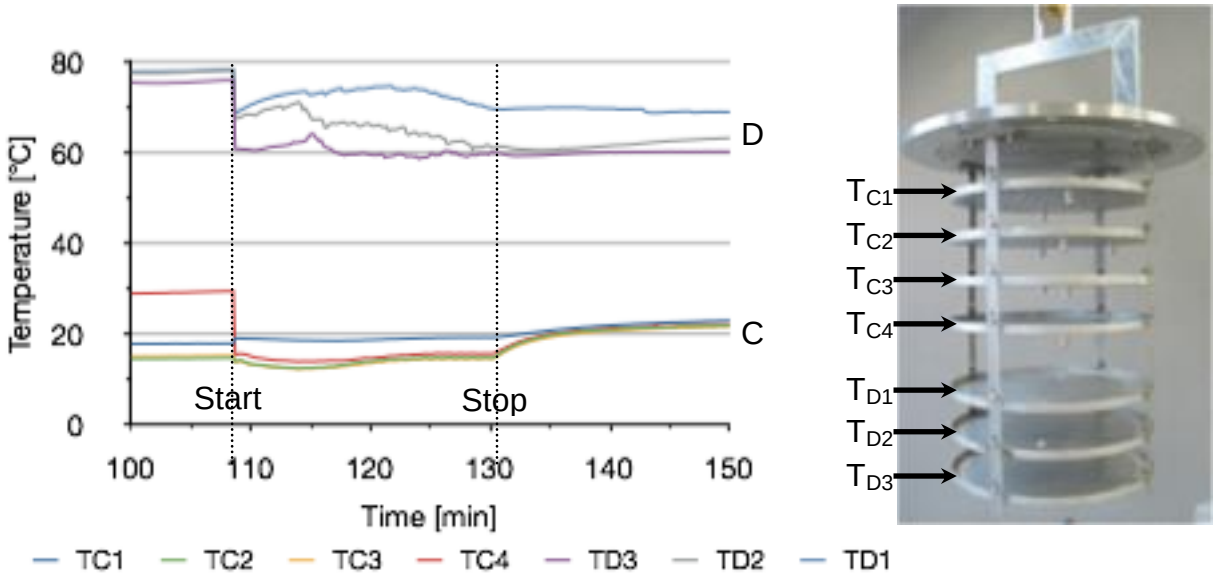

Fig. 5. Diagram of the regenerating process. The temperatures of the desorber as well as the condenser plates are shown.

The laboratory system was successful in proofing the concept of the closed sorption heat storage. Nevertheless operating the setup was complex and conversion efficiencies were low due to thermal radiation between the hot and cold plates, thermal convection due to reverse water vapour flow and thermal conduction through the massive steel body. This problem was most critical during heating mode, due to the considerably lower power input from the low temperature heat input. Much experience has been gained from this proof of concept that can be directly implemented into the prototype system now under development.

PROTOTYPE SYSTEM

With financial support from the European Union a prototype system is now under construction. The aim of the development is to build a heat storage system able to provide 100 % solar coverage for a single family house built to passive energy standards and located in Zürich. It is based on a hybrid concept and consists of sensible heat storage in water tanks as well as the new developed sodium hydroxide storage system. The setup contains solar collectors as heat source and a vertical bore hole heat exchanger as heat sink and source. In the general mode of operation the sensible heat storage tanks are always initially charged from the solar input. If there is excess solar thermal input, it is used to regenerate the absorption heat pump. If the solar heat input is insufficient, the absorption heat pump is employed to gain heat at the desired temperature either from the sensible heat storage or from the vertical bore hole heat exchanger. In this manner the hybrid heat storage system is able to continuously supply heat at the required temperatures.

CONCLUSION AND OUTLOOK

The basic concept of the closed sorption heat storage based on sodium hydroxide and water is presented. Theoretical and experimental results are discussed. A proof of concept has been successfully built and operated and much experience has been gained. In a next step these results are used to design a full sized prototype to supply all heat requirements of a single family house. The running storage development is part of the COMTES (combined development of compact thermal energy storage technologies) collaborative project.

ACKNOWLEDGEMENTS

Financial support by the Swiss Federal Office of Energy is gratefully acknowledged. Further we gratefully acknowledge financial support by our research institution EMPA Swiss Federal Laboratories for Materials Science and Technology as well as by the European Union in the seventh framework program (FP7 / 2007-2013) under the grant agreement No295568.

REFERENCES

K. Edem N'Tsoukpoe et al., A review on long-term sorption solar energy storage, Renewable and Sustainable Energy Reviews, 13 (2009) 2385–2396.

Hadorn J. C. et al., Thermal energy storage for solar and low energy buildings - State of the art, IEA SHC Task 32 ISBN: 84-8409-877-X, 200

Weber R., Dorer V., Long-term heat storage with NaOH. Vacuum 82, 708-716.

DEVELOPMENT AND VALIDATION OF SOLAR COOLING AND SOLAR COOLING COMBINED WITH FREE COOLING SIMULATION MODELS

P. Gantenbein; L. Leppin; H. Marty; E. Frank

Institute for Solar Technologies SPF, University of Applied Sciences of Rapperswil, Oberseestrasse 10 CH-8640 Rapperswil - Switzerland.

ABSTRACT

In the design and planning process for solar cooling and free cooling systems simulation tools are required to optimize the final version and control strategies. There exists different simulation tools equipped with differential equation solvers which can be applied for this task. The POLYSUN software offers modules of small scale solar thermal driven sorption cooling machines as well as modules for electric driven compressor cooling machines. For the validation of thermal driven cooling systems POLYSUN simulation templates of two real installations of solar thermal driven sorption chiller implemented in systems have been developed. The challenge in this set up process was not only the thermodynamic equivalent transfer of installed components into the simulations environment but also to map the controller settings into the template. For this task an individually programmable controller is available in the software giving a wide range of possibilities in system controlling. The results of the simulation were compared with the measured data. For the comparison it was necessary to read in measured local weather data for the simulation. The comparison shows a good coincidence of the energy yield of the solar collector field, cooling energy output of the absorption machine and the electric energy used. A larger deviation of the simulation results in the thermal power of the heat rejection sub-system can be observed. But in both systems the simulated temperatures are qualitatively correct but deviate from the measured data. Therefore further adjustments of the component parameters and the controller setting will be done to reach an even better consistency. In an engineering design process different system versions can be checked or - for a real installation - a controller settings optimisation can be done with a POLYSUN template.

INTRODUCTION

The increasing need of comfort in living and working rooms as well as in shops, sports stadiums and activity areas in general will be a driving force for the planning and installation of air conditioning systems. Predominantly in summer time the energy consumption of air conditioned buildings will increase. Because of the coincidence of solar radiation and cooling need solar energy supported or even solar driven cooling systems are preferred to reduce electric and thermal energy from non-renewable sources [1, 2, 3, 4]. The design and the assessment of system versions should be done by the use of simulation software tools.

There are different tools equipped with component catalogues and differential equation solvers which can be applied for this task [5, 6]. The special developed POLYSUN software [6] offers in the component catalogues beside of collectors, storage tanks, heat exchangers pumps etc. modules of small scale (max. 20kW) solar thermal driven cooling machines (absorption & adsorption) and electric driven compressor cooling machines. With this software a high flexibility tool for the combination of different components like collectors,

water storage tanks (hot and cold), cooling machines etc. is available. Based on two real installations of solar thermal driven sorption systems – AbKM Klimatechnik GmbH LiBr-H_2O absorption and SorTech Silica Gel-H_2O adsorption – for each a POLYSUN simulation template was set up and tested. The results from the simulation and the measured data were compared.

SYSTEM DESIGN AND GRAPHICAL USER INTERFACE - TEMPLATES

Both systems – AbKM Klimatechnik GmbH LiBr-H_2O absorption and SorTech Silica Gel-H_2O adsorption – are driven by solar heat gained through solar flat plate collectors. In addition there are hot water storages due to buffer energy for times with no solar gains but cooling demand in the building. As cold distribution cooling ceilings or fan coils are installed. The heat rejection is either realized by a wet cooling tower or a dry/hybrid cooling tower. In the adsorption system the heat rejection sub-system can also be used for free cooling application if the temperatures of the ambient air, the server room and the cold storage tank have the necessary values. In Figure 1 the scheme of the installed adsorption cooling system is presented and the parameters like collector area and storage volume are indicated therein. The schematic, the template and the data of the absorption cooling system are shown in an earlier presentation [7].

The system schemes were transferred into the POLYSUN simulations user interface by using the relevant catalogues libraries. Working with the component catalogues in POLYSUN the required modules easily can be called up or defined i.e. parameterised and interconnected through tubes. For the simulation unnecessary components like expansion tank, pressure relief and check valves or water filters are neglected. Also volume flow meters and temperature sensors don't need to be invoked manually but the knowledge of the position of the temperature sensor is important for comparison with the measurement results and separate additional tubes at the (real) sensor position can be defined. POLYSUN automatically logs temperatures, flows etc. of every component. The POLYSUN Version 6 controller catalogue is now extended with a programmable controller of each 16 input, output, operating state and auxiliary variables.

This high flexibility allows, beside of others, different flow set-points of one pump through different settings in the programmable controller. In Figure 1 the pump P5 (main pump in the low temperature circuit - LT) has three different set-points. In a transfer of the installation schematic correctly into a POLYSUN simulation template this has to be kept in mind. In case of the adsorption system where the heat rejection sub-system can be used for free cooling in the POLYSUN GUI two pumps were used to realise the hydraulic loops "adsorption low temperature" (LT) and "transfer low temperature free cooling" (via the heat exchanger to the Drycooler), Figure 1. These two pumps can be used to set the three different flows VT3 LT, VT5 HRF (1) and VT5 HRF (2), Figure 2.

These flows are necessary because of the several system operation modes – for example solar cooling of the server room and/or the cold storage tank, free cooling of the storage and the server room, cooling of the server room through the cold storage etc. – which are active depending of temperature levels in the server room T6, the ambient air temperature T9 and the hot water storage tank temperature T4 and certain conditional relations between them. The resulting template for the adsorption cooling system is shown in Figure 3.

RESULTS AND DISCUSSION

In the simulation local weather data were read in and the results are compared with the measurement data of the real absorption located in Switzerland at Rapperswil. For the adsorption system located in Hedingen Switzerland the Meteonorm weather data [8] implemented in POLYSUN were used. The comparison shows a good coincidence of the energy yield of the collector field in period of one month [7]. For the same period the measured temperatures of the hot water storage tank and the simulation results show a good qualitative agreement but a deviation – the faster measured temperature decrease in the storage tank - of the lowest layer has to be analysed.

If the fluid inlet and outlet temperatures to the cooling machine have the same absolute deviation there will be no influence on the energy and power analysis. But with the COP characteristic of the machine depending of the inlet temperature a higher cooling power could be realised in the simulation because of the higher temperatures compared to the measurement. For the absorption machine measurement data of the generator power (Q'_G), the cooling power (Q'_E) and the heat rejection power (Q'_AC) and the simulation results of the analogous apparatus are in good agreement for the operation period of one day.

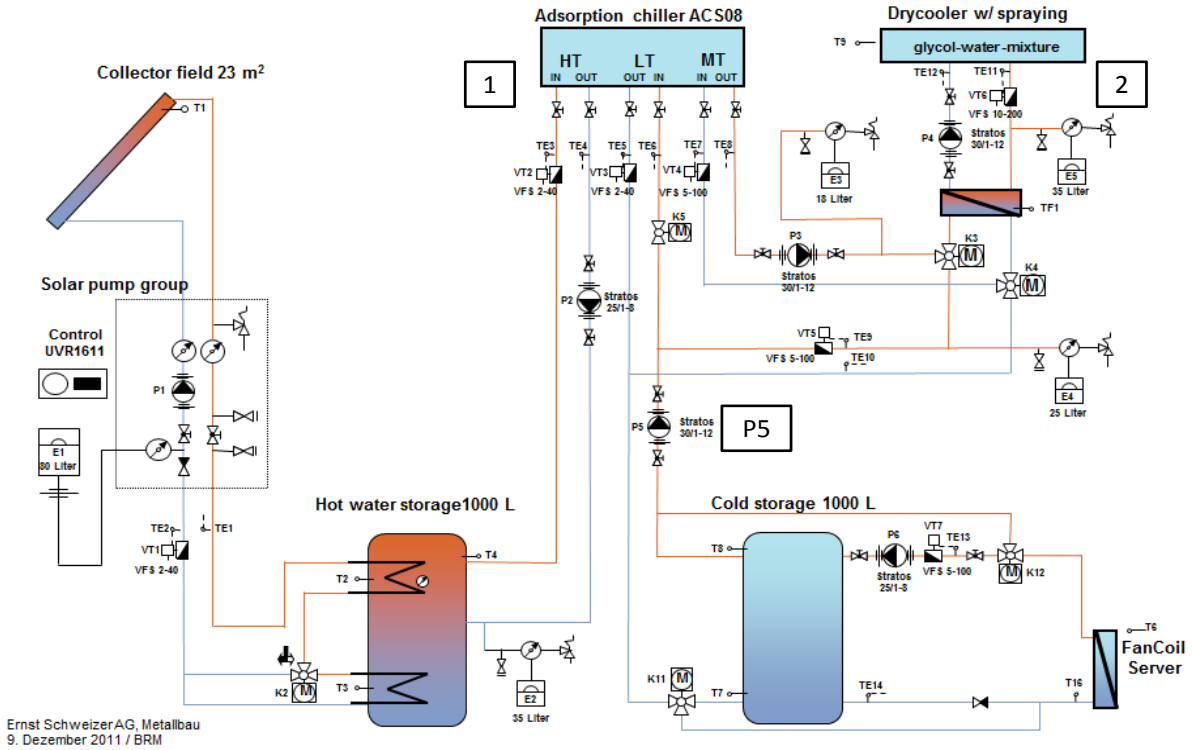

Figure 1: Schematic of the solar thermal driven 8kW ACS08 Silica Gel-H_2O adsorption cooling machine of SORTECH AG (1). The heat rejection sub-system of the solar cooling system (2) can be used in the server room free-cooling mode (schematic: E. SCHWEIZER AG).

In the evaluation of the cooling technologies the electric energy consumption plays an important role and thermal driven machines, in principle, have the advantage of a lower need compared to compressor machines. The electric energy need for pumps and ventilators of the thermal absorption cooling systems is in good agreement for the period of one month.

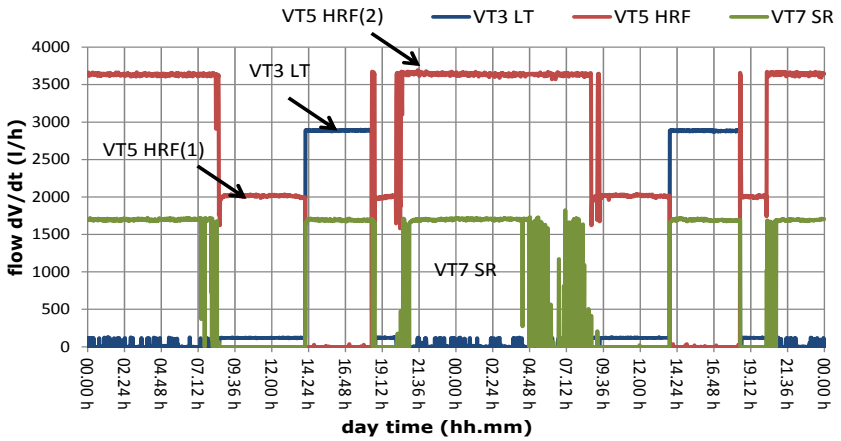

Figure 2: Volume flow data from the solar thermal driven 8kW ACS08 cooling machine. In the simulation environment of POLYSUN the three different flows in VT3 LT, VT5 HRF(1) and VT5 HRF(2) will be realised with two different pumps and a programmable controller. For the nomenclature of VT3 LT, VT5 HRF and VT7 SR see Figure 1.

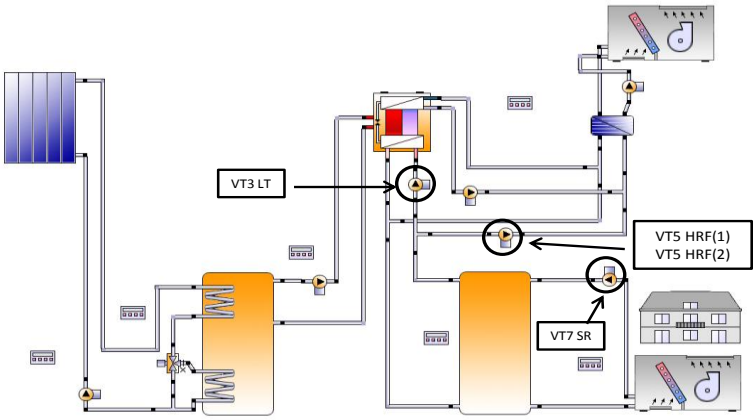

Figure 3: Schematic of the graphical user interface in the POLYSUN-Software of the solar thermal driven 8kW adsorption cooling machine ACS08 of SORTECH AG. In the simulation the volume flows of VT3 LT, VT5 HRF(1) and VT5 HRF(2) will be realised by two pumps running with a programmable controller.

Figure 4 shows first simulation results of the adsorption cooling system. The temperature curve in the lowest layer of the cold storage tank reveals the cooling mode of the system. At outdoor temperatures T_{amb}>20°C and high enough solar radiation the systems cools down the cold storage tank and the server room. After a decrease of the outdoor temperature T_{amb} below 20°C the server room is cooled by free cooling and at a further decrease of T_{amb} below the temperature of the cold storage tank both the server room and the cold storage are cooled by free cooling. In the morning time of too low solar radiation and too high T_{amb} the server room is cooled by the cold storage tank – the temperature in the tank is increasing.

In case of an installed cooling system related to the target function – for example a low electric energy consumption - an optimisation still can be done through the set-points of the system controller. With the developed template in POLYSUN this work can be done in advance of the start-up of the system.

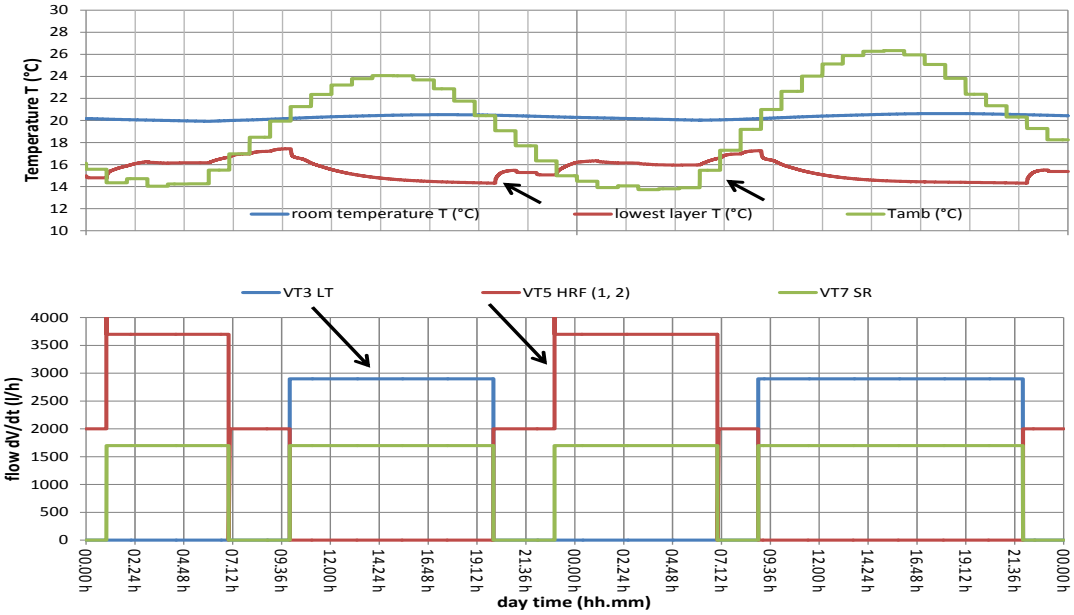

Figure 4: Temperature of the server room, the lowest layer in the cold storage tank and the ambient air in function of time over two days (above). The building in the template of Figure 3 represents the server room (SR). The ambient temperature has a hourly resolution and is staircase-shaped. The lower graph of the Figure shows the fluid flow in the pumps VT3 LT, VT7 SR and VT5 HRF (1, 2) of the template in Figure 3.

In Figure 5 the measurement data and the simulation results are shown over a period of one day for the adsorption system. The Figure 5 shows the ambient temperature, the temperature of the cold storage tank and the status of the cooling machine ACS08 and the free cooling status are also shown. A qualitative agreement can be seen but for the temperatures the absolute values are different. One part to explane this deviation is the difference of the real and „synthetic weather" data in the measurement and the simulation, because for this system too low weather parameters were measured at to location of installation. But the time dependent oscillation behaviour of the storage tank temperature is in good agreement related either to the status of the ACS08 or the free cooling system.

CONCLUSION AND FURTHER WORK

The analysis of the measurement data and the comparison with simulation results are showing good results. The observed deviations require a refinement of the components in the templates and a check and calibration of the temperature sensors as well as the flow meters in the field installations. The refinement of the component "cooling machine" in the POLYSUN catalogue for example means an extension of temperature and COP data table in the read-in csv-file. Nevertheless at this level of validation of the models they enable a planner to define the system parameters of the real installation and to vary the control strategy to optimise the electric energy consumption. This can be done by systematic variation of the conventional controller and the programmable controller settings in the simulation template.

With the known location of the building, the building size and its use and the determined cooling need of the engineering designed system the POLYSUN software allows a comparison of different versions in relation to energetic and economic points of view. In a next project the absorption system could be operated with hybrid cooler in the heat rejection sub-system. This

type of cooler component opens the potential to reduce the water consumption. A further analysis and assessment of the results can be done.

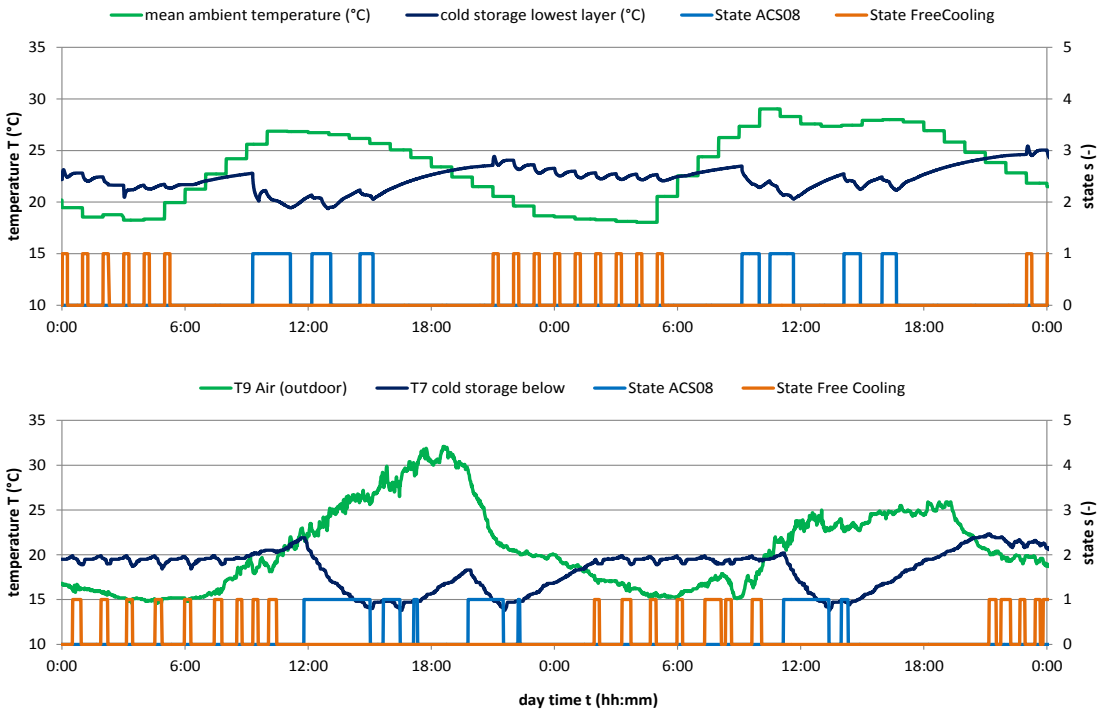

Figure 5: Ambient temperature at the location and temperatures in function of time in the cold storage (lowest layer) as well as the states of the cooling machine ACS08 and the free cooling (ON=1 & OFF=0) in the simulation (above) and in the measurement (below).

ACKNOWLEDGEMENTS

The financial support of the Swiss Commission of Technology and Innovation (CTI) and of the HSR University of Applied Sciences Rapperswil is gratefully acknowledged.

REFERENCES

1. Solar Engineering of Thermal Processes, J A. Duffie & W. A. Beckman; ISBN 13 978-0-471-69867-8, John Wiley & Sons, Inc.
2. ASHRAE Handbook 2005, Fundamentals – chapter 8 thermal comfort.
3. www.esttp.org & www.iea-shc.org/task38.
4. Solar-Assisted Air-Conditioning in Buildings - A Handbook for Planners. Hans-Martin Henning (Ed.). ISBN 3-211-00647-8 Springer Wien New York (2004).
5. http://www.transsolar.com Transsolar Energietechnik GmbH.
6. http://www.velasolaris.com. Vela Solaris AG.
7. Development and validation of solar cooling and free cooling simulation models. P. Gantenbein et al. EUROSUN 2012, Opatija, Croatia.
8. http://www.meteotest.ch METEOTEST.

PROGRESSING TOWARDS NET ZERO ENERGY BUILDING IN HOT CLIMATE USING INTEGRATED PV MODULES AND PARABOLIC TROUGH COLLECTORS

Adel A. Ghoneim*, Adel M. Mohammedein
*Applied Sciences Department, College of Technological Studies, P.O. Box 42325, Shuwaikh 70654, Kuwait , *email: aa.ghoniem@paaet.edu.kw*

ABSTRACT

Kuwait is located in the desert geographical region and has a continental climate characterized by its dry hot long summer and short warm winter with occasional rainfalls. The mean annual temperature in Kuwait is 25.6 °C, and it receives annual total radiation more than 5280 MJ/m^2 with approximately 3347 h of sunshine. The potential for reduction of greenhouse gases emissions is an important issue for the wide spread of renewable energy systems. In most existing buildings cooling and heating loads lead to high primary energy consumption and consequently high CO_2 emissions. These can be substantially decreased with suitable energy concepts using appropriately integrated renewable systems. Solar energy systems consist of PV modules and parabolic trough collectors are considered to satisfy electricity consumption, domestic water heating, and cooling loads of an existing building. This paper presents the results of an extensive program of energy conservation and energy generation using integrated photovoltaic (PV) modules and parabolic trough collectors (PTC). The program conducted on an existing institutional building intending to convert it into a Net-Zero Energy Building (NZEB) or near net Zero Energy Building (nNZEB). The program consists of two phases; the first phase is concerned with energy auditing and energy conservation measures at minimum cost and the second phase considers the installation of photovoltaic modules and parabolic trough collectors to provide considerable portion of the energy consumption in the building. The 2-storey building under consideration is the Applied Sciences Department building at the College of Technological Studies, Kuwait. The performance of different solar components is simulated using transient simulation program (TRNSYS). A single effect lithium bromide water absorption chiller is implemented to provide air conditioning load to the building. The economic calculations for this study are based on life cycle savings (LCS) method. In addition, a numerical model is developed to assess the environmental impacts of building integrated renewable systems. The first phase results in an energy conservation of about 25% of the building consumption. In the second phase, the integrated PV completely covers the lighting and equipment loads of the building. On the other hand, 78% of the building cooling load can be accomplished by integrating parabolic trough collectors. The annual avoided CO_2 emission is evaluated at the optimum conditions to assess the environmental impacts of the solar heating and cooling systems. The total annual avoided CO_2 emission is about 1100 tonne/year which confirms the environmental impacts of these systems in Kuwait.
Keywords: building integrated renewable systems, Net-Zero Energy Building, payback period, emission factor, avoided CO_2 emission.

INTRODUCTION

Energy use in buildings represents a significant part of final energy end-use, making building energy efficiency a top priority. Buildings are typically responsible for significant part of the total primary energy consumption. Net-Zero Energy Building (NZEB) is the building which, on an annual basis, produces energy from renewable sources that equals the amount of consumed energy by the building. If the produced energy from the building is slightly less than consumed; such building is called nearly net zero energy building (nNZEB). In the future nNZEB concept may be extended to a life cycle zero energy approach, as proposed by Hernandez and Kenny [1]. An early example of a solar based zero energy home is presented by Voss et al. [2]. A number of zero energy homes and buildings have been built and tested throughout the world [3,4]. NZEB performance is usually measured and evaluated using various indicators, i.e. net primary energy

consumption, net energy costs, and carbon emissions [5]. Many research works have implemented audit standards for the buildings and their results showed substantial energy reductions [6-8].
The potential impact in energy demand reduction at the Florianopolis International Airport in Brazil with the use of building-integrated photovoltaic (BIPV) systems is analyzed by Rüther et al.[9]. Their results showed that the integration of PV systems on airport buildings in warm climates can supply the entire electrical power consumption of the airport. A life cycle inventory model is presented by Keoleian et al. [10] to characterize the energy and environmental performance of BIPV systems.
Zhai et al. [11] concluded that under the weather condition of Shanghai, 150 m^2 vacuum tube solar collector arrays can be used to satisfy heating and air-conditioning for covered area of 460 m^2. A building integrated multifunctional roofing system is designed by Yin et al. [12] to harvest solar energy through photovoltaics and heat utilization. Their performance analysis indicates that the proposed solar roofing system provides significant advantages over the traditional asphalt shingle roof and PV systems without cooling.
In the present work, a mid-size existing institutional building is considered as a model for existing public buildings that can be moved toward NZEB in Kuwait. This study has two purposes; the first is to carry out an energy audit to reduce the energy consumption in the building to its lowest possible value by implementing the appropriate energy conservation measures. The second objective is to design building integrated PV modules and parabolic trough collectors in Kuwait to achieve Net Zero/near Net Zero Energy Building (NZEB or nNZEB). In addition, the performance and environmental impacts of the designed building integrated photovoltaic parabolic trough collectors are evaluated.

BUILDING LOAD

The 2-storey building under consideration is the Applied Sciences Department in the College of Technological Studies, Kuwait. On average, 500 people use the building with irregular occupancy from 8 am to 5 pm, 5 days per week during the academic semesters. The building wall construction can be considered heavy mass, with an overall heat transfer coefficient of 0.498 W/m²K. The roof of the building is constructed from light mass construction that is well insulated with an overall heat transfer coefficient of 0.185 W/m²K. The windows and entrance doors are aluminum-framed constructed from 6 mm double-tinted glazing with an overall heat transfer coefficient of 3.64 W/m²K. In dry and harsh hot weather such as the case in the State of Kuwait, the heating, ventilation and air-conditioning (HVAC) system of the building is the most energy consuming equipment in buildings.

Type 56 included in TRNSYS [13] is employed to carryout building simulation. This component models the thermal behavior of building having multiple thermal zones. The building description is ready by this component from a set of external files. The files can be generated based on user supplied information by running the pre-processor program called TRNBuild. From the simulation done with TRNSYS to determine the demand for air conditioning in the house under study, we obtained results that indicate that this demand starts from April to October, with critical periods for the months of June, July and August in which occurs the maximum load of about 228 kW. In this study, the HVAC system is found to consume about 85% of the total building energy consumption. The remaining energy consumption in building is distributed between lighting system, 10%, and equipments, 5%.

RESULTS AND DISCUSSIONS

Phase-I: Energy Auditing and Energy Conservation

A preliminary energy audit assessment is carried out, which revealed an inefficient practice upon the building and by the occupants. The main entrance and emergency doors were deliberately left open for a long time while the HVAC system was running. This increases the amount of air infiltrated into the building and consequently the HVAC energy consumption dramatically.

Moreover, visits at night and weekend to the building revealed that the lights and plug-in equipment of some offices and laboratories were left on after working hours and during the weekends. In addition, the light intensity in offices, laboratories, workshops, classrooms, and corridors are not to comply with the recommended intensity levels. In general, to reduce energy consumption, it is important to increase the awareness of the users to switch off the room lights and equipment before leaving. This asked to be checked by the security officers. This audit assessment revealed that there is a potential opportunity of energy conservation that could be achieved by applying the above mentioned energy conservation measures. It is estimated that as a result of applying the preliminary auditing of the building an annual saving of about 6% of the building consumption can be achieved. An additional energy saving of about 4% can be achieved if the temperature is set to 28 ºC instead of 24 ºC after working hours. Additional, 15% of the building's energy consumption can be saved if the HVAC system is switched off during weekends and proper operation and maintenance are exercised. Implementation of above mentioned procedures can yield considerable energy savings as it reduces the annual energy consumption of the building from 2 GWh to 1.5 GWh.

Phase-II: Building Integrated Solar Energy

The second phase is concerned with integrating the building with photovoltaic modules and parabolic trough collectors to provide the energy consumption of the building in an attempt to convert it into NZEB. Building integrated photovoltaic (BIPV) system is adapted to provide the lighting and equipment load of the building. For the power to drive absorption chillers, the parabolic trough solar collectors are considered for the building under study. The weather data used in this study have been measured and collected for over two years in the College of Technological Studies, Kuwait.

Building Integrated Photovoltaic (BIPV)

Grid connected PV system is proposed for the present work because the PV array does not have to be sized large enough for worst weather conditions. The PV array charges the battery during daylight hours and the battery supplies power to the loads as needed. The electricity is started during extended overcast situations or at periods of increased load. When the batteries are low, the electricity will power the AC loads in the building as well as the battery charger. The system includes a DC to AC inverter to convert the direct current (DC) produced by the PV array to alternating current (AC). In the present work, the five parameter model [14] is used to simulate the characteristic of mono-crystalline solar cells at different weather conditions. This model adds the shunt resistance to the four-parameter model. At a fixed temperature and solar radiation, the I-V characteristic for the five parameter model is:

$$I = I_L - I_D - \quad I_{sh} = I_L - \quad I_o\,[exp(\frac{V + IR_s}{a}) - 1] - \frac{V + IR_s}{R_{sh}} \qquad (1)$$

Where, I current at the load, I_D diode current, I_{sh} shunt resistance current, I_L photocurrent, I_o diode reverse saturation current, V voltage at the load, R_s series resistance, and R_{sh}, shunt resistance.
Assumptions of angle of orientation, local temperature and radiation levels, inverter efficiency and module efficiency are the most important factors that determine the output of the PV system. Each simulation has a length of one year period and employing mono-crystalline solar cell (BP Solar PB 2140 S) rated at 140 W. The five parameter model is implemented into TRNSYS to determine the PV output. The data used are weather data, building load, utility rate schedules and total utility demand. The weather data used are hourly global solar radiation on horizontal surface, and hourly ambient temperature.
The variation of the annual energy production for various PV orientations is studied. The slope of the PV array is changed from 0° to 60° (i.e. latitude ± 30°). In addition, different azimuth angles are examined ranging from 0° (due south) to 40° west of south. It is found that the maximum energy generation from the PV arrays corresponds to array slope equal to 40° (i.e. latitude+10°) and for arrays facing south (azimuth angle=0°). So, annual energy production can be maximized

by using an array sloped at an angle 10° greater than the latitude. The annual PV generation from 952 mono-crystalline cells in this case is about 225 MWh, i.e. 15% of the total building energy consumption. This means that the lighting and equipment loads of the building can be completely satisfied with the integrated PV modules. Since each module area is 1.26 m^2, so the total area required for integrated PV about 1200 m^2.

The overall benefit of BIPV systems over conventional electricity sources can be demonstrated also by calculating energy payback times. The Energy Payback Time (EPT) of a PV system is the time in which the energy input during the module life cycle is compensated by the electricity generated with the PV module and it depends on several factors including cell technology, PV system applications. The variation of EPT for the proposed BIPV system with tilt angle at fixed azimuth angle (azimuth=0°) is presented in Figure 1. This figure suggests that employing tilt angle of 40° (i.e. array with a slope of 10° greater than latitude) gives the best EPT which is approximately 9.4 years i.e. less than 10 years. These results indicate that the BIPV system can produce net or free power after 10 years of its operation. The variation of annual avoided CO_2 emission with tilt angle is determined. Again, the optimum tilt angle which maximizes the avoided CO_2 emission is 40°. At this angle, the avoided CO_2 emission is found to be about 200 tone/year.

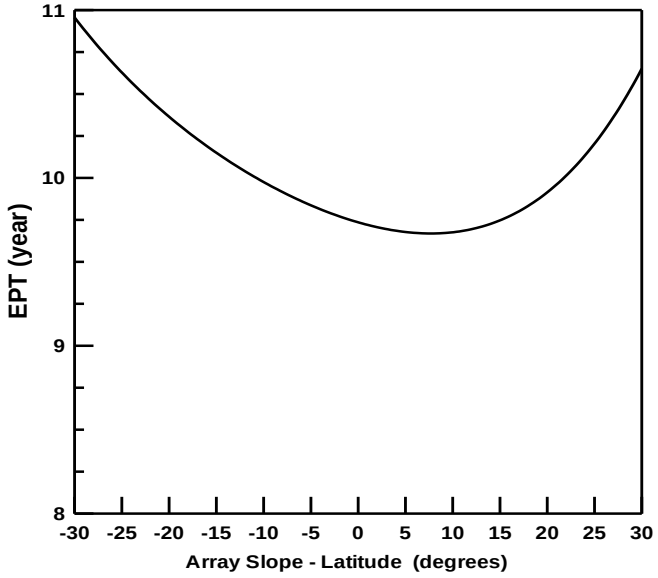

Figure 1: Variation of EPT with tilt angle at fixed azimuth angle (azimuth=0 °)

BUILDING INTEGRATED PARABOLIC TROUGH COLLECTORS

Parabolic trough collector is assumed to be integrated with the building to satisfy the cooling load which represents about 85% of the building load (1.275 GWh). A performance model has been developed for parabolic trough solar collector (PTSC) based on a linear, tracking parabolic trough reflector. The developed PTSC model is a steady-state model and based on the energy balance and radiative and convective heat transfer mechanisms within PTSC's receiver tube. It can calculate the collector efficiency, detailed thermal losses from collector, and the temperatures of various collector components and of the fluid throughout the receiver under different conditions. In addition, the model could be used for optimizing PTSC design by varying the size of receiver tube, the size of glass envelope, receiver tube material, coating material and so forth. The efficiency of PTSC which is given by:

$$\eta_c = F_R(\tau\alpha) - \frac{A_r}{A_a} F_R U_L \frac{(T_i - T_a)}{G} \qquad (2)$$

where A_r is the receiver area, A_a is collector aperture area, G is the incident radiation on horizontal surface, F_R is the heat removal factor, $(\tau\alpha)$ is the transmittance-absorptance product, U_L is the

collector overall heat transfer loss coefficient, T_i is the inlet collector temperature, and T_a is the ambient temperature. The storage tank is modelled as a stratified tank. A computer program is developed to simulate and design a solar single effect lithium bromide-water cooling absorption system to supply demand of cooling for sunshine hours from April to October. To obtain optimum collector area, several data files of absorption chiller of single-effect employing LiBr–H_2O solution as working fluid according toYazaki chillers WFC SH10 are adapted. This system operates with a relatively good coefficient of performance at generator temperature between 70°C and 95 °C [15]. Other TRNSYS types are adapted to simulate different system components. The variation of solar fraction (F), life cycle savings (LCS) and overall system efficiency (η) with collector area is presented in Figure 2. The results of simulation showed that for each ton of refrigeration, it is required to have a minimum collector area of about 25 m^2 for a system to operate solely on solar energy and the maximum cooling load of 140 KW (40 refrigeration tons) in August.

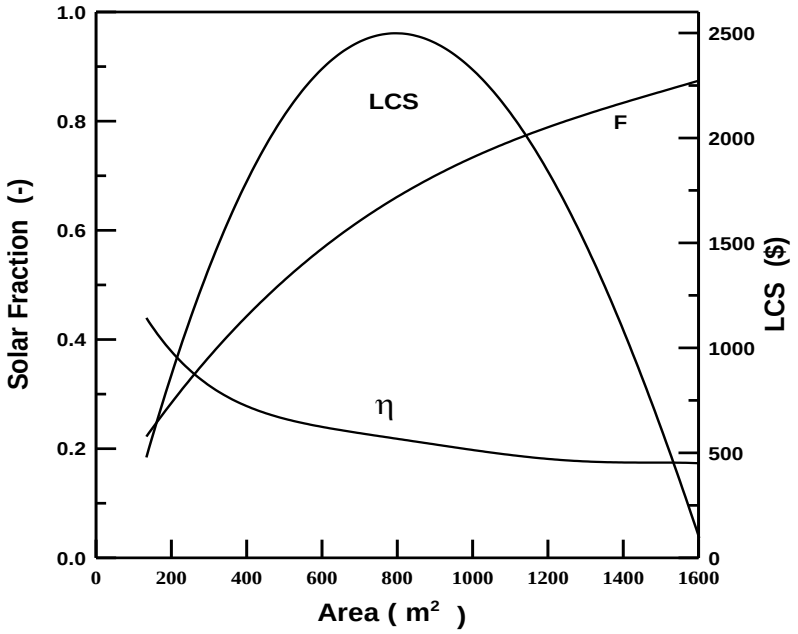

Figure 2: Variation of system parameters with collector area

As seen from the figure, the optimum area which corresponding to maximum solar savings is approximately equals to 800 m^2. It should be noted that the optimum area neither corresponds to maximum system efficiency nor to the maximum solar fraction. Also, the total solar fraction (F) for parabolic trough solar collector satisfies great portions of the cooling load about 0.78. The value of life cycle savings (LCS) is found to be $2400 per year for the optimum conditions. In the present study, the cost of 1 kWh provided by the proposed solar system is about 0.017 $/kWh which represents 68% of the value provided by the conventional fuel system (0.025 $/kWh) emphasising the feasibility of solar cooling systems in Kuwait.

The variation of annual avoided CO_2 emission with collector area is studied. It is found that the optimum area which maximizes the avoided CO2 emission is again 800 m2. At this optimum area, the avoided CO2 emission approximately equals to 900 tonne/year. In addition, the costs due to the application of the Kyoto Protocol, which penalizes the emissions of green house effect gases should be added to the costs of conventional energy resources. Considering application of this protocol will enhance the economical and environmental aspects of solar systems in Kuwait much more. In addition, the ongoing research on solar cells claims fast developing with respect to higher efficiency and lower cost. The present results should encourage governments for wide installation of solar heating and cooling systems in different applications which will significantly reduce energy consumption of conventional fuel as well as reducing environmental pollution to keep our community healthy and clean.

CONCLUSIONS

This work evaluates the outcomes of energy auditing, energy conservation and energy generation, using photovoltaic modules and parabolic trough collectors on an existing institutional building in a trial to convert it into NZEB or nNZEB. Based on the present results, the following conclusions can be drawn:

Preliminary energy audit, energy conservation and efficient operation strategies of the building result in an annual energy saving of about 500 MWh which is equivalent to 25% of the building consumption without the need to any retrofitting or investments.

Efficient energy conservation can play an important role in converting the existing buildings into NZEBs as it saves a significant portion of annual energy consumption of the building.

The integration of PV modules into the building produces about 15% of the building energy consumption (225 MWh) and can completely cover the lighting and equipment load.

Parabolic trough collectors of optimum area of 800 m^2 can satisfy 78% of the total building cooling load (1.275 GWh).

The total area of BIPV and parabolic trough collectors required is about 2000 m^2, i.e. about half the area of the building roof (4000 m^2) enabling PV modules and collectors to be spaced widely in rows to minimize shading losses.

Total avoid CO_2 emission of about 1100 tone/year can be achieved.

Nearly NZEB can be achieved in existing buildings by re-commissioning the building, installing better performance HVAC systems and other equipment and integrating efficient PV modules and parabolic trough collectors.

The results of the present work should encourage governments for wide installation of solar energy systems to keep our environment healthy and clean.

ACKNOWLEDGEMENTS

The authors would like to express their sincere gratitude to The Public Authority for Applied Educa-tion and Training (PAAET), Kuwait for financial support of this research under project No. (TS–11-09).

REFERENCES

1. Hernandez, P., Kenny, P.: From net energy to zero energy buildings: Defining life cycle zero energy buildings (LC-ZEB). Energy and Buildings Vol 42 (6), pp 815–821, 2010.
2. Voss, K., Goetzberger, A., Bopp, G., Ha¨berle, A., Heinzel, A., Lehmberg, H. : The self-sufficient solar house in Freiburg—Results of 3 years of operation, Solar Energy Vol 58, pp 17-23, 1996.
3. Reijenga T.H. Energy efficient and zero-energy building in the Netherlands. In: International Workshop on Energy Efficiency in Buildings in China for the 21st Century, CBEEA, Beijing; December, 2000.
4. Gilijamse W. : Zero-energy houses in the Netherlands. In: Proceedings of Building Simulation '95. Madison, Wisconsin, USA, pp 276-283, August 14–16, 1995.
5. Tsoutsos, T., Aloumpi, E., Gkouskos, Z., Karagiorgas, M. : Design of a solar absorption cooling system in a Greek hospital. Energy and Buildings Vol 42 (2), pp 265-272, 2010.
6. Marszal A.J., Heiselberg P., Bourrelle P., Musall E., Voss K., Sartori, I., Napolitano, A.: Zero energy building – a review of definitions and calculation methodologies. Energy and Buildings Vol 43 (4), pp 971–979, 2011.
7. Rahman M.M., Rasul M.G., Khan M.M.K : Energy conservation measures in an institutional building in sub-tropical climate in Australia. Applied Energy Vol 87, pp 2994-3004, 2010.
8. Oliver M., Jackson T.: Energy and economic evaluation of building integrated photovoltaics. Energy Vol 26, pp 431-439, 2001.
9. Rüther R., Braun, P.: Energetic contribution potential of building-integrated photovoltaics on airports in warm climates. Solar Energy Vol 83, pp 1923-1931, 2009.
10. Keoleian A., Lewis G.: Modeling the life cycle energy and environmental performance of amorphous silicon BIPV roofing in the US. Renewable Energy Vol 28, pp 271-293, 2003.
11. Zhai X.Q., Wang R.Z., Dai Y.J., Wu J.Y.: Experience on integration of solar thermal technologies with green buildings. Renewable Energy Vol.33, pp 1904–1910, 2008.
12. Yin H.M., Yang D.J. Kelly G., Garant J.: Design and performance of a novel building integrated PV / thermal system for energy efficiency of buildings. Solar Energy Vol 87, pp 184-195, 2013.
13. Klein S.A. et al.: TRNSYS, A Transient Simulation Program", Version 16, Univ. of Wisconsin-Madison, 2006.
14. Ghoneim A. A., Al-Hasan A.Y., Abdullah A.H. : Economic analysis of photovoltaic powered solar domestic hot water systems at Kuwait. Renewable Energy Vol 25, pp 81-100, 2002.
15. Duffie J.A., Beckman W.A.: Solar Engineering of Thermal Processes. John Wiley & Sons Inc, New York, 2004.

MONTHLY BALANCED PRODUCTION AND CONSUMPTION OF HEAT AND ELECTRICITY WITH LOW NON-RENEWABLE PRIMARY ENERGY INPUT AT DISTRICT LEVEL

M.Y. Haller[1]; T. Selm[2]; E. Frank[1]

1: Institut für Solartechnik SPF Hochschule für Technik HSR, Oberseestr. 10, CH-8640 Rapperswil

2: Selm Heizsysteme AG, Fischhausenstr.5, CH-8722 Kaltbrunn

ABSTRACT

A concept is presented for the supply of heat and electricity within an urban development area including multifamily, two family, single family and row homes, aiming at a significant improvement in terms of non-renewable energy use compared to the current standard, with a balanced local production and consumption of electricity for each single month of the year. This can be achieved on a district level using a combination of combined heat and power and solar thermal energy to provide heat for a small local network that covers the most densely populated parts of the development area. The heat demand of the less densely populated areas is covered by geothermal heat pumps. The electricity for households and heat pumps in both areas is served from solar photovoltaics in summer and predominantly from electricity generated by the combined heat and power in winter. The proposed concept reduces the yearly non-renewable primary energy consumption for heating and power supply by 53% if natural gas is used for the combined heat and power plant, and by 81% if biogas is used. However, not only the yearly values but also the monthly balance of renewable energy supply and energy use has to be considered as Switzerland is a country that imports electricity in winter and exports in summer. With increasing installations of photovoltaic power production and heat pumps, this discrepancy may even increase in the future. The presented concept includes heat pumps and photovoltaic electricity production, but at the same time levels out the imbalanced electricity production with the combined heat and power plant. This overall concept has thus a higher chance for unlimited reproduction than a net-zero-energy concept alone, reducing the non-renewable primary energy demand substantially compared to standard solutions for supplying heat and electricity.

Keywords: small-scale district heating, solar thermal, photovoltaics, heat pump, combined heat and power, smart grid

INTRODUCTION

The Institut für Solartechnik SPF, on behalf of Bildstöckli AG (Eschenbach), has simulated a concept for a predominantly local production of both electricity and heat for a planned development area in in the Swiss midlands, consisting of multifamily, two family, single family and row homes. The focus was on providing a solution that may serve as a role-model in terms of sustainability and cost-efficiency. In view of an unlimited duplicability of the concept, a balanced heat and power production for each month of the year was aimed for. This distinguishes the concept from most of the presented "net-zero-energy" approaches in which lacking electricity in winter leads to imports that are counterbalanced by exporting excessively produced electricity in summer. The Swiss government decided after the Fukushima nuclear disaster that the currently existing atomic power production facilities in Switzerland will not be replaced and thus will be phased out. Currently, Switzerland is

exporting electricity in summer, but importing it in winter. Additionally, the amounts of electricity from nuclear production and from unknown production are considerably larger in winter than in summer [1].

It is not difficult to reach a balanced production and consumption of electricity on a yearly basis with a combination of photovoltaics (PV, predominantly producing in summer) and heat pumps for domestic hot water preparation (DHW) and space heating (predominantly consuming in winter)However, a monthly balance between production and consumption of electricity cannot be reached with these two technologies alone. In this paper simulation results and cost calculations are presented for a concept that reaches a monthly balanced production and consumption of electricity and heat for a small development area designed for 85 homes.

METHOD

In a first step, the development area was split into a more densely populated part A where heat will be provided by a small district heating network fed by a combined heat and power (CHP) plant in combination with solar thermal installations, and a less densely populated area where heat is provided by geothermal heat pumps in combination with solar thermal DHW production (Table 1).

	Zone A		**Zone B**	
	heat	electricity	heat	electricity
summer	solar thermal	photovoltaic	solar thermal	photovoltaic
winter	CHP	CHP	heat pump	CHP

Table 1: Overview of technologies that cover heat and electricity demand in zones A and B.

In a second step the demand for heat and electricity within the two zones was estimated. The space heating demand was based on the limits for new homes of SIA 380/1 (2009). The demand for domestic hot water was estimated based on Nipkow et al. [2]. The solar thermal installations were sized in order to cover the heating demand for the district heating network (including losses) during the summer months, such that the network will remain in operation over the whole year. The sizing of the CHP for the district heating was based on the given heat demand profiles. The climate dependent heat loads and yields for solar thermal and solar PV were simulated with TRNSYS.

RESULTS

The demand for space heating, DHW, and household electricity for the two zones is given in Table 2. The small district heating network is equipped with a CHP plant (133 kW_{th}, 90 kW_{el}), a peak demand gas boiler (200 kW_{th}), a central heat storage (50 m^3) and two solar thermal collector fields (in total 413 m^2 absorber surface). The heat storage enables a better management of the CHP as well as the storage of solar heat. The solar installations (both solar thermal and PV) are sized in order to reach 100% heat and electricity coverage for the summer months (on a monthly averaged base in the case of PV). One of the solar thermal installations feeds directly into the heat storage, the other one into the distribution network.

Figure 1 shows the simulated monthly energy balances of the small district heating network. In the less densely populated zone it was assumed that heat is provided by ground source heat pumps in combination with solar thermal DHW systems that improve the seasonal performance factor of the overall system because the ratio of heat output per electricity input is about 20 times higher for solar thermal than for heat pumps. The seasonal performance

factor of the overall system that provides space heating and DHW resulted to be 4.3 for a ground source heat pump alone, and 4.9 combined with the solar thermal DHW production. The monthly heat balance of zone B is shown in Figure 2.

Zone A:		**1FH**	**2FH**	**RH**	**MFH**	**sum**
number	-	8	4	0	5	17
space heat	MWh/a	111	98	0	318	527
DHW	MWh/a	22	22	0	112	157
Zone B:		**1FH**	**2FH**	**RH**	**MFH**	**sum**
number	-	13	5	2	0	20
space heat	MWh/a	180	122	70	0	373
DHW	MWh/a	36	28	17	0	81
Zones A+B:		**1FH**	**2FH**	**RH**	**MFH**	**sum**
household electricity	MWh/a	105	90	30	180	405
1FH: single family home; 2FH: two family home; RH: row home (3 units); MFH: multifamily house.						

Table 2: Energy demand for zone A (district heating) and zone B (heat pumps).

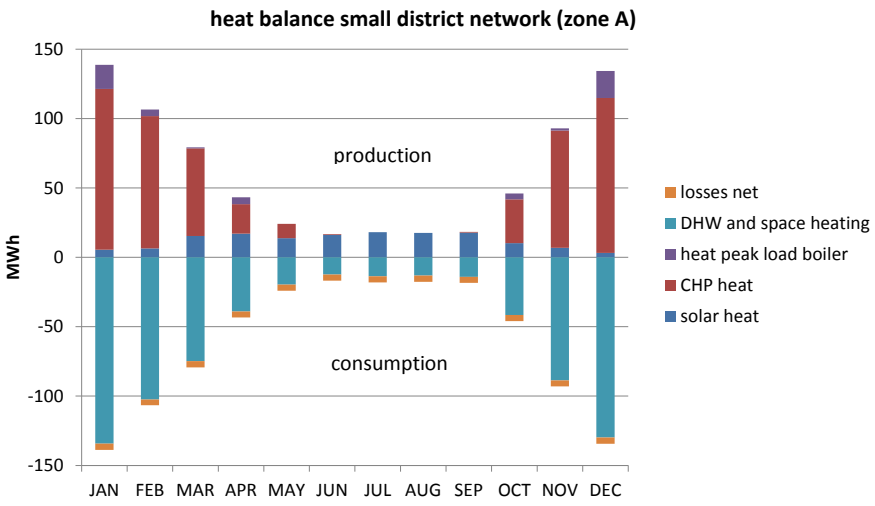

for correct legibility of this figure, please refer to the colour version available in the electronic form of the proceedings

Figure 1: Monthly heat balance of zone A (small district heating network).

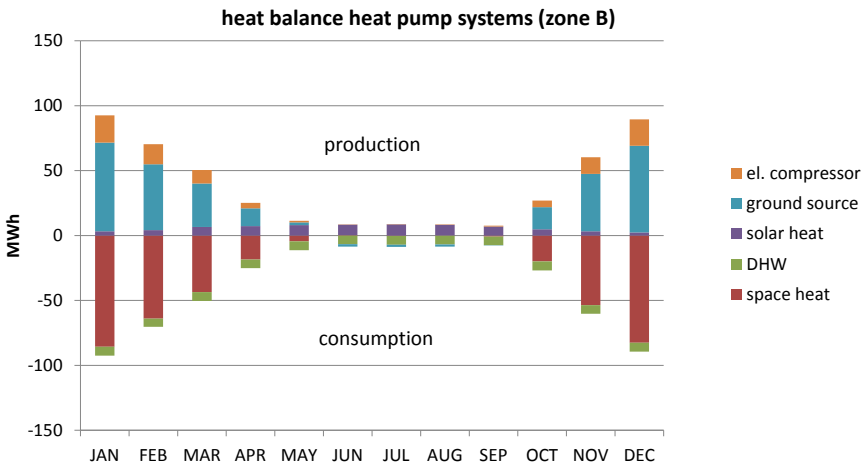

for correct legibility of this figure, please refer to the colour version available in the electronic form of the proceedings

Figure 2: Monthly heat balance of zone B (heat pumps with solar thermal).

The expected electricity production by the CHP is 310 MWh/a and exceeds by far the 92 MWh/a needed to operate the heat pumps. However, in order to additionally cover the household electricity demand of both zones 497 MWh/a are needed. The missing electric energy (187 MWh/a) can be supplied by 1300 m^2 photovoltaic panels, resulting in a net electricity production of 1.2% over the year. Thus, a balanced production and consumption of electricity can be achieved even on a monthly basis (Figure 3). In summer, the production is a bit lower than the consumption (∅ -9 MWh/mt) and in winter some electricity can even be exported (∅ +10 MWh/mt). By adding an additional 19 single family homes with heat pumps and increasing the PV area by 1000 m^2 (53 m^2 per additional single family home), a better balance between electricity production and consumption could be reached, with a maximum monthly deviation of -15 MWh for the month of September. Figures 4 and 5 show the monthly and annual balance of energy input and output into the whole development area. It can be seen that a mix of solar thermal, photovoltaic, ground source, heat pump and combined heat and power leads to a relatively balanced production and consumption both for heat as well as for electricity, not only on an annual average basis, but also for each single month.

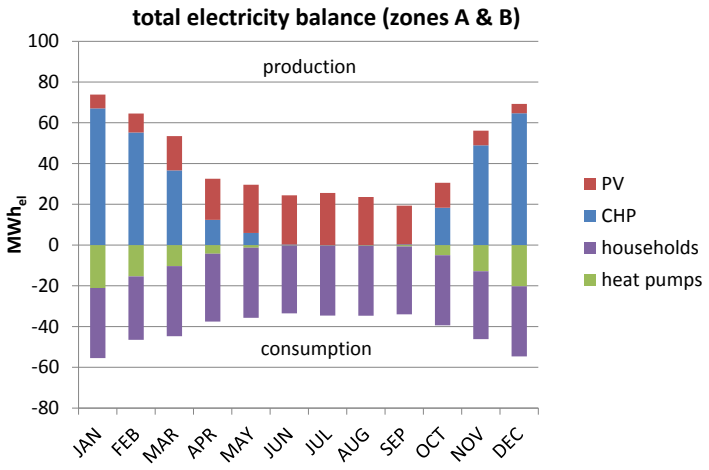

for correct legibility of this figure, please refer to the colour version available in the electronic form of the proceedings

Figure 3: Monthly electricity balance of both zones including household electricity.

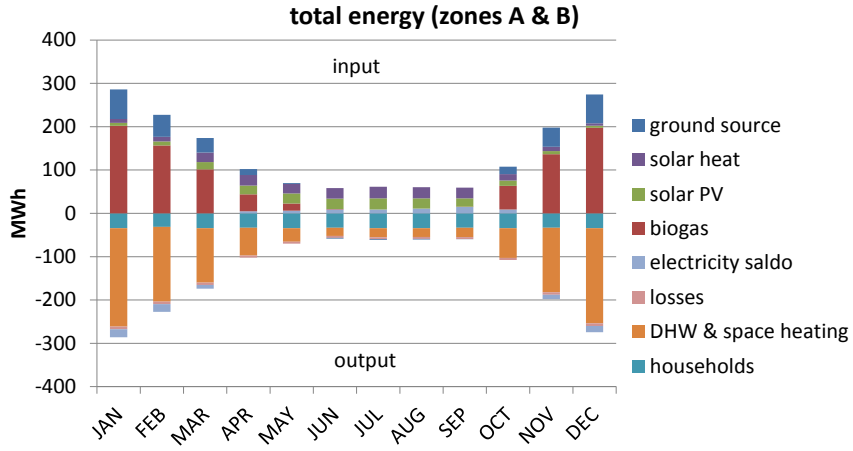

for correct legibility of this figure, please refer to the colour version available in the electronic form of the proceedings

Figure 4: Monthly balance of all energy inputs and outputs of the whole development area.

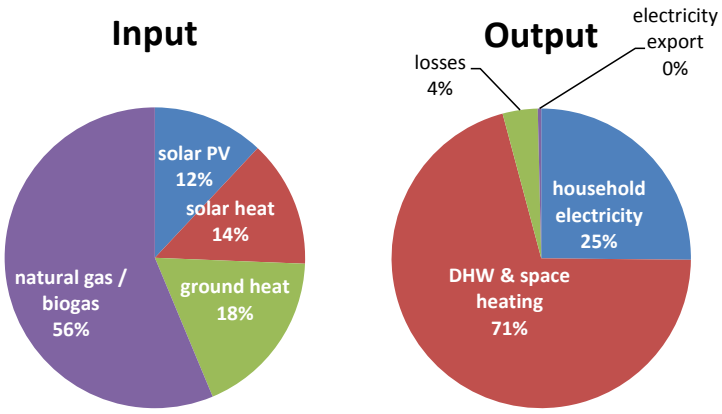

for correct legibility of this figure, please refer to the colour version available in the electronic form of the proceedings

Figure 5: Annual balance of energy inputs and outputs of the whole development area.

Figure 6 shows the comparison of non-renewable primary energy demand (fossil and nuclear) of the proposed concept with conventional heating with natural gas and consumption of household electricity from the grid (Swiss consumption mix), based on data from [3]. The most sustainable variant with biogas for the CHP reduces the non-renewable primary energy demand by 82%. If natural gas is used for the DHP the reduction is 55%. Not included are the grey energy included in the construction of the heat pumps, the CHP and the heat distribution network. Also for the reference system the grey energy for the decentralized natural gas units are not included.

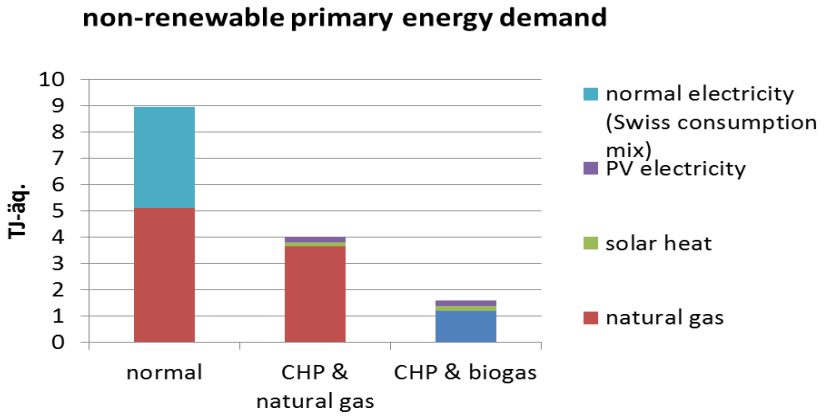

for correct legibility of this figure, please refer to the colour version available in the electronic form of the proceedings

Figure 6: Non-renewable primary energy demand in comparison to conventional natural gas heating and consumption of household electricity from the grid.

If the system could be extended with additional 19 singe family homes and additional 1000 m^2 PV as mentioned before, the non-renewable primary energy savings would be 84% for the variant with biogas CHP and 63% for the variant with natural gas CHP.

The investment costs of the different components for the CHP, the small district heating network as well as the solar thermal systems were estimated based on experiences from past projects and/or preliminary offers that were obtained for this particular project. Annual costs were calculated with the annuity method assuming an interest rate of 3% and a lifetime of 15 to 30 years, depending on the component. The PV installations were not included in the cost calculation since a financing by the cost-covering feed-in tariffs (government subsidies) is assumed. Furthermore, also the heat production in zone B based on heat pumps in combination with solar thermal is excluded from the cost analysis. The average price for end-

energy produced by the CHP in combination with the solar thermal installations (heat and electricity combined, including capital bound as well as maintenance costs) for different variants is shown in Table 3. Table 4 shows the end energy price for conventional heating systems as well as the average electricity price for single family homes in 2012 according to Elcom [4].

Variant	end energy price [Rp/kWh]
biogas CHP (certificates), with solar thermal	30.3
natural gas CHP, with solar thermal	23.5
natural gas CHP, with solar thermal, including incentives	22.9
natural gas CHP, without solar thermal	20.9

Table 3: Average end-energy price of the presented concept for zone A (incl. electricity from the CHP as well as heat).

Variant	end energy price [Rp/kWh]
ground source heat pump SFH, without solar thermal	21.6
natural gas heating SFH	24.1
natural gas heating MFH	16.4
electricity SFH [4]	19.7

Table 4: Average end-energy price of conventional heating systems, including investment cost and maintenance (exception: electricity, where no additional investment is assumed).

DISCUSSION & CONCLUSION

The proposed concept reaches a quite balanced local production and consumption of both, heat and electricity, at a small district or community level. However, the photovoltaic environmental benefit is lost if PV electricity is fed into the grid, compensated by a feed-in tariff, and thus sold to others. In order to get the full credits of this "green" electricity that is produced on site, the same amount of PV generated electricity that is fed into the grid and sold has to be bought back by the inhabitants. If this is the case, quite important primary energy savings can be achieved compared with standard solutions even if the CHP plant is operated with natural gas. Assuming a feed-in tariff of 18 Rp/kWh and a one-time connection fee for the district heating of 15'000 SFR per home, the average cost for heat from the heat distribution network (with natural gas CHP and solar thermal) is at an acceptable 2066 SFR/a. However, the local electricity provider is only willing to pay 6.3 – 8.2 Rp/kWh for the fed-in electricity from CHP. With a price for natural gas of 7.4 Rp/kWh, the fed-in electricity would have to be cross-financed by the heat price which was not accepted by the investors.

REFERENCES

[1] Jakob, M., Vokart, K. & Widmer, D., 2009. *CO2-Intensität des Stromabsatzes an Schweizer Endkunden - Schlussbericht*. TEP Energy GmbH im Auftrag von FOGA und FEV, Zürich.

[2] Nipkow, J., Gasser, S. & Bush, E., 2007. *Der typische Haushalt-Stromverbrauch*. Bulletin SEV/VSE, 19, p.24–26.

[3] Frischknecht, R., Tuchschmid, M. & Itten, R., 2011. *Primärenergiefaktoren von Energiesystemen - Version 2.2*. ESU-services Ltd.

[4] ElCom, 2012. *Strompreise 2012*. Available at: http://www.news.admin.ch/message/index.html?lang=de&msg-id=40988 [Accessed July 2, 2012].

FULL SCALE EXPERIMENTS AND MODELLING OF A PHOTOVOLTAIC - THERMAL (PV-T) HYBRID SYSTEM

P. Haurant[1,2], C. Ménézo[1,2] , P. Dupeyrat[3]

1 *Centre Thermique de Lyon (CETHIL UMR CNRS 5008 / INSA Lyon / UCB Lyon 1), Lyon, France*

2 *Chaire INSA/EDF « Habitats and Energy Innovations », Lyon, France*

3 *EDF R&D, Département Enerbat, Moret sur Loing, France*

ABSTRACT

Although a classic photovoltaic module absorbs 80 to 90 % of incident solar radiation, typically only 10 to 20 % of the solar energy is converted into electricity. The remainder is dissipated into heat.

Photovoltaic-Thermal (PV-T) hybrid collectors are multi-energy components that convert solar energy into both electricity and heat. They make possible the use of this large amount of solar radiation wasted in PV modules as usable heat in a conventional thermal system.

In 2012, a research project led by CETHIL Lyon in collaboration with EDF / R&D and ADEME started with the goal to develop, monitor and model an improved PV-T system of solar electricity/heat cogeneration to meet the energy needs of the building to which they are fitted (Project PHOTOTHERM). At this stage of developments, the project is focussed upon the monitoring and modelling of a full scale PV-T system under real climatic conditions. Leading up to this phase, a full and in-depth study of the constituent materials and fabrication processes was undertaken regarding hybrid PV-T modules, resulting in a prototype offering an unprecedented level of solar energy conversion [1].

All the phases of the design and the development of the hybrid PV-T solar collector prototype have been optimized. Moreover we have experimental data obtained in both controlled and real climatic conditions. This allows us to achieve the development of a reliable dynamical component model that could be validated at each stage. From this validated model, some complete systems will be implemented in order to elaborate optimal strategies for component interconnection, management of the cogeneration system, and adapting of the system to the heating and electricity requirements of the building.

As an essential part of the performance evaluation, the basis of the new simulation tool will be presented in this article. Results comprising system-data comparisons involving in-situ measurements will be presented for domestic hot water configuration. The performance of the model under development is compared to those of existing models available in the TRNSYS software library.

Keywords: Photovoltaic-thermal collector dynamic model

INTRODUCTION

PV-T solar collectors are hybrid collectors where PV modules have the function of absorber of a thermal collector while it produces electricity. Although numerous research and development works about such solar components have been conducted these three last decades, applications are still limited to R&D [2]. In this context, the PHOTOTHERM project was launched in 2012 with the goal to develop, monitor and model a new generation of PV-T modules. The aim of this paper is to introduce the dynamic thermal/electric model

implemented in this framework. Thus the PV-T component will be briefly presented in a first section followed by the modelling approach and then first results will be introduced. Finally, a sample of monitoring results will be showed.

PV-T HYBRID COMPONENT

In this research led at the Fraunhofer Institute for Solar Energy Systems (ISE) in Germany with the support of EDF R&D, a broad, multi-scale and multi-competence approach was used to improve not only the PV and the thermal components separately, but also to find synergetic and specific solutions for the PV-T collector as a whole [3, 4].

PV-T absorber was built consisting of a flat heat exchanger coated with an electrically insulating film and was laminated with 32 interconnected mc-Si PV cells, EVA films and a polymer film as front cover. The aperture area of each collector is 1.01 m² and the PV packing factor is 0.79. The front cover is a 4 mm AR glass with a transmission around 0.93 and the distance between cover and absorber was 20 mm. A 20 mm thick thermal insulation with a conductivity below 0.03 W/(mK) was used at the back.

Thermal and electrical performances of this PV-T collector were measured at the TestLab Solar Thermal Systems of Fraunhofer ISE. These results, presented in a previous paper at CISBAT showed an overall efficiency above 82% which represents a major improvement of both thermal and electrical efficiency in comparison to previous works on PV-T concepts found in literature [5].

DYNAMIC 3D THERMAL MODEL

It is essential to accurately determine the thermal state of these hybrid components because it is conditioning thermal efficiency but also electrical power generation and its reliability. This is why we put research efforts in this direction through the development of a 3D time dependent model. The panel is described according to 3D meshing, each volume of control following the heat balance equation:

$$\rho c_p V \frac{\partial T}{\partial t} = \Phi_{CONV} + \Phi_{COND} + \Phi_{SW} + \Phi_{LW} \quad (1)$$

with ρ and C_p are respectively the mass density [kg/m^3] and the specific heat capacity [J/(m^{3}K)] of the volume of control, V [m^3] are their volumes and

- Φ_{CONV} [W/m²] refer to the convective flux that are zeros for the layers except the surfaces that are into contact with the air, over the top-glass on one hand, between the top-glass and the PV-absorber plate on the other. In those cases, we consider

$$\Phi_{CONV} = h_{air}\left(T_{layer} - T_{air}\right) \quad (2)$$

  where the convective coefficients h_{air} [WK^{-1}] are calculated from Nusselt numbers that result from correlations defined in [6] at the inner air layer and $h_{air} = 2.8+3.0u_{wind}$ outside.

- Φ_{COND} [W/m²] are the conductive flux in calculated in all the directions according to the formula :

$$\Phi_{COND} = k\Delta T \quad (3)$$

  where k is the thermal conductivity [Wm^{-1}K^{-1}].

- Φ_{SW} [W/m²] are short wavelength radiative flux :

$$\Phi_{SW} = S.\tau_{\alpha} E_{SW} \quad (4)$$

S are the surfaces of control volumes that are illuminates and E_{SW} the radiations they received. τ_{α} is a transmission-absorption coefficient for short wave radiations that take into account multi-reflexion in the air layer.

- Φ_{LW} [W/m²] are long wavelengths radiation. For control volumes that are in contact with outside, over the top-glass

$$\Phi_{LW} = S\varepsilon\sigma\left(Frc\left(T_{sky}^{4} - T_{glass}{}^{4}\right) + Frs\left(T_{grd}^{4} - T_{glass}{}^{4}\right)\right) \quad (5)$$

calculating $F_{rc}=(1-cos(p))/2$ and $F_{rs}=(1-cos(p))/2$, with *p* the inclination, and defining α_{LW} their long wavelength radiations absorption coefficients of control volumes.

For surfaces of the top glass and the PV-plate that are in contact with the inner air layer:

$$\Phi_{LW} = S\frac{\varepsilon_{glass}\varepsilon_{plate}}{\varepsilon_{glass} + \varepsilon_{plate} - \varepsilon_{glass}\varepsilon_{plate}}\sigma\left(T_{glass}^{4} - T_{plate}^{4}\right) \quad (6)$$

Once the thermal model of the combi-panel implemented, the evolution of the fluid temperature is computed as follows [6,7]:

$$\rho_w C_{p,w} V_w \frac{\partial T_w}{\partial t} = Nu_w \pi k_w L\left(T_{abs} - T_w\right) + \dot{m} C_{p,w} L \nabla T_w \quad (7)$$

Nu_w designates the Nusselt characterizing the thermal exchange with water, calculate from the relations in [6, 7] depending on the turbulent or laminar behaviour of the fluid. $\dot{m}$ is the mass flow ([kg/s]), L ([m]) the length of the path segment.

ADAPTED TESSELATION

The heat exchanger of the hybrid PV-T component has a bionic channels structure designed by Hermann's FRACTHERM algorithm [8]. This absorber performs better usual drawbacks observed on conventional exchangers: it reduces the pressure drops and allows an uniform flow distribution.

An adapted meshing has been implemented for the model in order to respect the specific geometry of the exchanger. In that view, the channel structure has been designed following the description introduced by Hermann [8] and Pieper and Klein [9], reproducing the geometry. Then branching points and other central points of the paths defined a vertices network that are used as cells' centres of an adapted Voronoi meshing, as recommended in [9]. Thus, Voronoi polygons were used as a basis of a 3D tessellation applied to all the layers that constitute the PV-T module. The prisms' thickness are the characteristic height of each layer.

PHOTOVOLTAIC CONVERSION

At this stage of development we consider the photo-conversion through an entirely conventional. This approach is clearly insufficient for such component. In further developments we intend to increase the level of accuracy of its modelling and also take into consideration the location of PV cells at the absorber. Although the current approach we present is limited, we even include it to be consistent in the energy balance. The electrical

production computation is based on the Shokley diode equation. It outputs the I-V characteristics as functions of the temperatures and the irradiance according to the relations:

$$I = I_{PV} - I_0\left(\exp\left(\frac{q(V + IR_s)}{nkT} - 1\right)\right) \quad (7)$$

I_{PV} is the photocurrent and I_0 the saturation current of the diode, which expressions are developed in [10]. R_s are internal resistances, q the electron charge, k the Boltzmann constant and n a calibration factor.

This model takes into account the temperature dependence of the photovoltaic conversion. The PV cell temperatures are obtained by the thermal model exposed previously. As the meshing used in the thermal model is not adapted to the cells geometry, their temperatures are computed as weighted means of temperatures of Voronoi polygons.

Then, the electrical efficiency is

$$\eta(T) = \frac{I_{mpp}(T).V_{mpp}(T)}{G.A_{PV}} \quad (8)$$

It will be used to calculate the short wave irradiance E_{SW} that is converted into heat :

$$E_{SW} = \tau_\alpha(1-\eta)G \quad (9)$$

FIRST RESULTS

The PV-T hybrid panel introduced in a previous has been modelled according to the theory developed above, using to the specific meshing recommended by [9]. The main equations (partial differential equations (1) and (7)) are solved thanks to an explicit Runge-Kutta (2-3) method implemented in Matlab for all the control volumes and the fluid.

Figure 1 show the temperature field along the exchanger path for a mass flow $\dot{m} = 0.005\,\text{kg/s}$ (18kg/h) and different inlet temperatures of the fluid. The exchanger path is drawn in black.

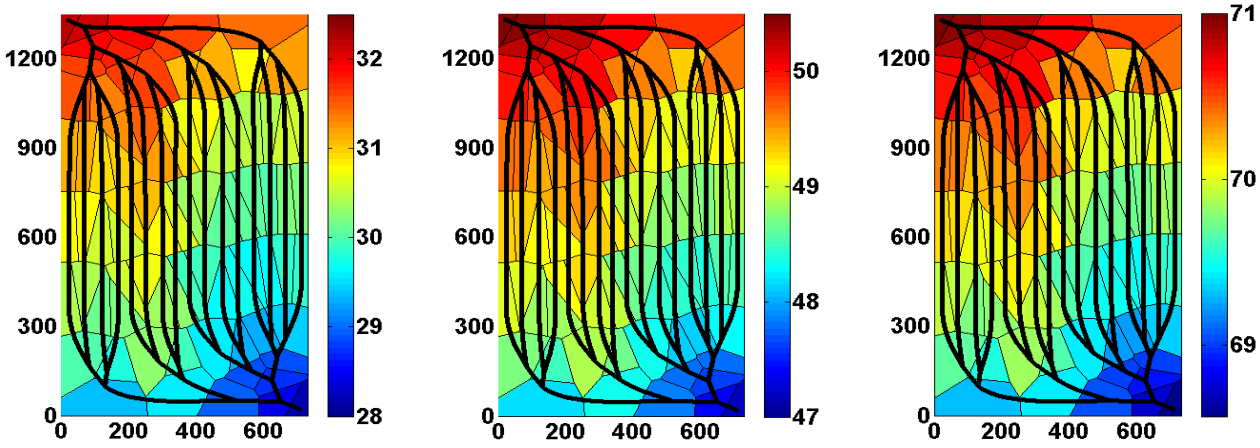

Figure 1: Temperature fields in the exchanger for T_{inlet} = 28.1°C ; T_{intlet}=48.5 °C and T_{inlet}=68.2 °C

Since the environmental conditions are fixed (T_{air} = 29 °C ; G = 956 W/m²), we can consider that we are in steady state regimes. As expected, we can observe that the temperature of the fluid increases while it crosses the path, following a logic evolution. Besides, whatever the

inlet temperature of the fluid, we can observe that the outlet temperatures are still between 4°C and 5°C greater.

The robustness and coherence of the model is been evaluated. In that view, different values of mass flow have been tested with different values of T_{inlet} in steady state conditions (Fig. 2).

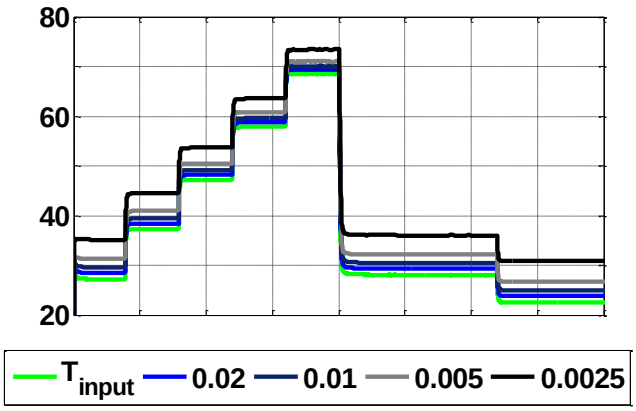

Figure 2 : Outlet temperatures for $\dot{m} = 0.02$ *kg/s ;* $\dot{m} = 0.01$ *kg/s ;* $\dot{m} = 0.005$ *kg/s and* $\dot{m} = 0.0025$ *kg/s ; with* T_{inlet} *=27.2°C ;* T_{inlet} *=37.2°C ;* T_{inlet} *=47.2°C ;* T_{inlet} *=57.9°C;* T_{inlet} *=68.5°C ;* T_{inlet} *=28.1°C and* T_{inlet} *=22.5°C*

As expected, the smaller the mass flow is, the greater are the temperature gradients between inlet and outlet.

We can also observe that for a mass flow value, the fluid temperatures increase the same way whatever the inlet temperature. Thus, for $\dot{m} = 0.02$ kg/s for example, the outlet temperature is 1.2 to 1.5 °C higher that the inlet temperature. For $\dot{m} = 0.0025$ kg/s, the difference hit 7.5 to 8 °C.

We can thus confirm the coherence of the model but confrontations to experimental data have to be realized.

CONCLUSION AND PERSPECTIVES

The PV-T hybrid collectors are components that convert solar energy into both electricity and heat. Many attempts have been made in the past developing without leading to real products. In 2008, a collaborative project with EDF and the Fraunhofer ISE has allowed to develop a component with unequalled electrical and thermal performances. This project goes on since 2012, with the goal to develop, monitor, model and demonstrate the reliability of a PV-T system dedicated to domestic hot water.

Facing the complexity of such component and the interrelated implied phenomena that are governing their behaviour and reliability, classical simple modelling approaches can not be adopted. We focused this paper on the development of a 3D thermal/electric model of the component which area key points of the accuracy of the power production prediction. Its specificity lies in the application of a Voronoi meshing particularly adapted to the bionic geometry of the exchanger.

First results of the model have been shown, confirming its coherence, robustness and fast computation. Electrical modelling improvement are now required and under implementation. At this study stage, experimental confrontations in controlled conditions and steady state regime are in progress.

Besides, additional experimental data are collected in real conditions and dynamic regime at the test facilities BESTLAB (Building Envelope & Solar Technologies Laboratory of EDF R&D): six PV-T modules oriented south with an inclination of 45° are coupled to a real domestic hot water system. A pump drives the circulation of glycolic water from the heat exchanger in the tank to the PV-T collectors, and inverters inject electricity produced by the PV-T modules to the local grid. All the experimental data are collected minute wise monitored since summer 2012. In the future, our PV-T model will integrate a global Domestic Hot Water system model and the results will be confronted to the monitored data.

ACKNOWLEDGEMENT

This project, PHOTOTHERM, is supported by the French Environment and Energy Management Agency (ADEME).

REFERENCES

1. P. Dupeyrat, C. Ménézo, S. Fortuin. Study of the thermal and electrical performances of PVT solar hot water system. Energy and Buildings, In Press, Corrected Proof, Available online 29 September 2012.
2. T.T. Chow. A review on photovoltaic/thermal hybrid solar technology. Applied Energy 87 (2010) 365–379,.
3. P. Dupeyrat, C. Ménézo, H. Wirth and M. Rommel. Improvement of PV module optical properties for PV-thermal hybrid collector application. Solar Energy Materials and Solar Cells 95 (2011) 2028-2036.
4. P. Dupeyrat, C. Ménézo, M. Rommel and H-M. Henning. Efficient single glazed flat plate photovoltaic–thermal hybrid collector for domestic hot water system. Solar Energy 85 (2011) 1457-1468.
5. P. Dupeyrat, C. Ménézo, Y. Bai, S. Fortuin, G. Kwiatkowski, M. Rommel and G.Stryi-Hipp. Hybrid photovoltaic-thermal (PV-T) solar cogeneration at the building's scale. in: Proceedings, CISBAT 2011, "CleanTech for Sustainable Buildings - From Nano to Urban Scale", Lausanne, Switzerland, 14-16.9.2011
6. H.A. Zondag, D.W. De Vries, W.G.J. Van Helden, R.J.C. Van Zoligen, A.A. Van Steenhoven. The thermal and electrical yield of a PV-Thermal collector. Solar energy Vol. 72, N°2 (2002), 113 - 128.
7. C. Cristofari, G. Notton, J.L. Canaletti. Thermal Behaviour of a copolymer PV/T solar system in low flow rate conditions. Solar energy Vol. 83 (2002), 1123 - 1138,
8. M. Hermann Bionische Ansätze zur Entwicklung energieeffizienter Fluidsysteme für den Wärmetransport. PhD thesis, University of Karlsruhe, 2005.
9. M. Pieper, P. Klein. A simple and accurate numerical network flow model for bionic heat exchangers. Heat Mass Transfer 47 (2011), 491-503.
10. F.M. Gonzales-Longatt. Model of Photovoltaic Module in Matlab™. 2do congreso IberoAmericano de estudiantes de ingenieria electrica, electronica, electronica y computation (II CIBELEC) 2005.

A NET ZERO EMISSION CONCEPT ANALYSIS OF A NORWEGIAN SINGLE FAMILY HOUSE - A CO_2 ACCOUNTING METHOD

A.HoulihanWiberg[1]; T. Dokka[1,2]; S.Mellegård[2]; L.Georges[1,3]; B.Time[1,2];M.Haase[1,2]; A.Lien[1,2]

1: Zero Emissions Research Centre (ZEB), NTNU, N-7491 Trondheim, Norway
2: SINTEF Byggforsk Oslo & Trondheim, NO-7465 Trondheim & 0314 Oslo, Norway
3: Energy and Process Engineering Department, NTNU, NO- 7491 Trondheim, Norway

ABSTRACT

In order to reach the goal of a zero emission building (ZEB), CO2 emission data has to be made available and verified for traditional building materials, new 'state-of-the-art' building materials and the active elements used to produce renewable energy. However, an initial literature review found that although there are databases of embodied carbon values for most building materials, the range in results for some materials are varied and inconsistent [1].

This paper follows on from previous work [1] on the development of a transparent and robust method to calculate CO_{2eq} emissions of the materials used in the concept analysis of the ZEB residential model, single family house [2]. The aim of the concept analysis was to investigate if it was possible to achieve an "all-electric" ZEB-building by balancing operational and embodied emissions by PV-production on the building. The analysis has not considered minimising the embodied emissions but is rather a documentation of the embodied carbon dioxide emissions using traditional materials in the envelope and in the ventilation and heating systems, as well as, those associated with the renewable energy system, such as the photovoltaic panels and solar thermal collectors. Material inventories have been imported from the Revit BIM model [3], via MS Excel. The material inputs are structured according to the Norwegian table of building elements, NS 3451-2009 [4] and emission factors ($kgCO_{2eq}$ per functional unit) for the calculations are sourced from SIMAPRO/ Ecoinvent version 2.2 [5][6].

The goal of these calculations is to estimate, and thus provide an overview of the materials and components in the ZEB residential model, which contribute the most to the embodied carbon dioxide emissions. The calculations are based on the principles of environmental assessment through life cycle analysis. It should be noted that in this first round of calculations, not all life cycle phases are included. In the next stage of the calculations, the model will be optimised and the impact on emissions recalculated accordingly.

Keywords: Net ZEB, Residential Concept Model, BIM, LCA, CO_{2eq} Emissions Calculation

INTRODUCTION

The main aim of this work is to do realistic simulations of the energy use, embodied emission and the total CO_{2eq} emission for a typical residential building in Norway. By doing this the main drivers for the CO_{2eq} emission will be revealed, and also what performance is necessary for components and solutions in a Zero Emission Building according to the current net ZEB-definition levels [7]. The minimum requirements on energy efficiency are proposed to be in accordance with those stated in NS3700 [8]. The net ZEB definition levels of ZEB-O[1] and ZEB-OM[2] are aimed to be achieved in this study. The study evaluates the embodied carbon (EC) and the impact related to different building components and materials. The goal of these calculations is to estimate, and thus provide an overview of the materials and components in the ZEB residential concept model, which contribute the most to the embodied carbon dioxide emissions. The study also questions whether net ZEB-O and net ZEB-OM can be achieved with current technologies.

[1] ZEB-O: Emission related to all energy used for operation shall be zero, also energy use for equipment.
[2] ZEB-OM: Emission related to all energy used for operation plus all embodied emission from materials and installations shall be zero.

Building Model

The concept building is a timber frame, 2 storey, single family home with concrete slab on ground. The building has a high performance building envelope achieved by using materials and solutions already on the market.

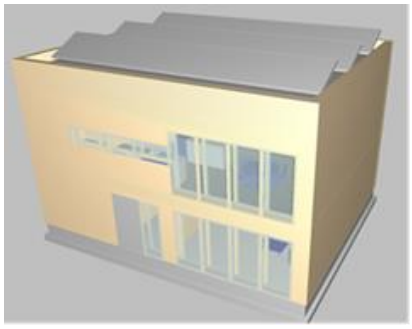

Figure 1 Revit model

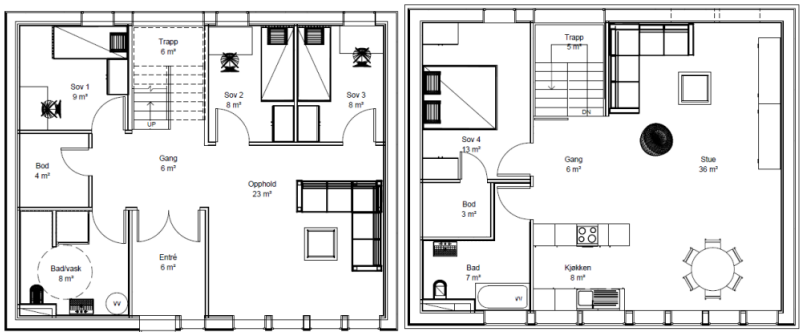

Figure 2 First and second floor plans

The envelope consists of a well-insulated timber frame wall construction with 350 mm mineral wool insulation. Table 1 gives the thermal specification of the building envelope. Even though this is a high performance building envelope, these figures can be achieved by materials and solutions already on the market.

	Values	Solution
External walls	U = 0.12 W/m²K	Timbered wall with 350 mm insulation.
External roof	U = 0.10 W/m²K	Compact roof with approximately 450 mm EPS insulation.
Slab on ground	U = 0.07 W/m²K (U = 0.06 W/m²K)	Floor construction with 500 mm EPS insulation. U-value in brackets takes into account the thermal resistance of the ground.
Windows	U = 0.65 W/m²K	Three layer low energy windows, with insulated frame.
Doors	U = 0.65 W/m²K	Well insulated doors.
Normalized thermal bridge value	ψ" = 0.03 W/m²K	Detailed thermal bridge design
Air tightness	N50 < 0.3 ach@50 Pa	Detailed design of a continuous vapour and wind barrier, good quality assurance in craftsmanship and pressure testing of the building in two stages (when the wind barrier is mounted and when the building is finished).

Table 1 Specifications for the building envelope

Energy Supply System

The energy supply solution for heating, cooling and electricity is an "all electric" solution based on a combined system of an 'air to water' heat pump and solar thermal collectors covering the total heat demand, giving a high COP. The electricity demand is covered by high efficiency PV panels on the roof. This solution is chosen due to its relatively mature technology and it is commonly used on buildings with high energy ambitions (nearly zero, zero or plus energy houses).

The vacuum tube solar collectors placed on the vertical south façade are designed to cover most of the heat demand (DHW and space heating) in the summer. Test data for vacuum collectors from APRICUS is used, with an optical efficiency of 69 % and a U-value of 1.51 W/m²K. The collectors are mounted on the south vertical façade. The storage capacity is set to 600 litres. It should be noted that other solar producers can deliver collectors with a similar performance. The heat pump system is an air to water heat pump, using the outdoor air as heat source. Consequently, due to fluctuations in the outdoor air temperature, the COP fluctuates accordingly. The data used in the simulation is for the AEROTOP T07 heat pump system from the Swiss manufacturer, Elco. The PV panels are normally arranged on a flat roof with arrays of south facing panels with an optimal tilt of around 30-45 degrees for Nordic conditions. However, with the low solar height in Norway, there needs to be a large space between the arrays or significant self-shading will occur. An alternative way to solve this is to angle the panels with a low tilt of

10-15 degrees and position them so that they face north and south alternatively. To analyse this, a module from the manufacturer Sunpower (spr-333ne-wht-d) has been chosen. This is a monocrystalline cell type with a very high nominal efficiency (20.3 %). Each module is 1.56 m high and 1.05 wide. A grey-water heat recovery has been used. Its efficiency has been set to 20% as it considered as a preheating of the cold water by the hot-water draw-off.

SIMULATION TOOLS AND METHODS USED

The 3D architectural drawings and 3D BIM modelling have been done in Revit, version 2012 [3]. Embodied emission and embodied energy calculation have been done in the LCA Software tool SimaPro version 7.3 [6] which uses data from the LCA database EcoInvent [5]. Material inventories have been imported from the Revit BIM-model, via Excel. Simulation of the annual heating and cooling demand, peak heating and cooling load, net energy budget, delivered energy and heat loss calculation has been done in SIMIEN version 5.011 [9]. The performance of the solar collector system and the heat pump system have been simulated using PolySun [10]. The performance of the PV-systems have been simulated with PV-syst [11].

Calculation Method

The calculations are based on the principles of environmental assessment through life cycle analysis. It should be noted that in this first round of calculations, not all life cycle phases are included. The analysis focuses on module A1-A3 from the standard EN15978 [12], which include material inputs to gate. The use phase B4, replacements and replacement of new materials over the lifetime of the building has also been included. The functional unit is 1 m^2 of heated floor area (BRA) in the residential building over an estimated life time for the building of 60 years. The heated floor area is 160 m^2. The results are mainly presented for emissions on an annual basis, where the functional unit of 1 m^2 is divided by 60 years. The estimated service lifetime of the different inputs is mainly based on product category rules for different materials and components. The estimated service lifetime for the solar PV panels is 30 years and is based on guidelines from the IEA for the LCA of PV panels. [13] The service lifetime for PV panels is uncertain and is dependent on the quality of the actual PV panels used. Chemicals such as glue –paint and primers are not included in the analysis.

The ZEB emission factor (130gCO_2/kWh) [14] is used to calculate the emissions for operational electricity. With an assumed life time of the building of 60 years (standard value used in the ZEB centre), and a constant energy use assumed for the duration of the lifetime, the average CO_{2eq} factor for electricity can be calculated to 130 g/kWh (for a building constructed in 2013). The average factor of 130 g/kWh is based on a several choices, assumptions, simplifications and scenarios. In addition, no official value or consensus on a CO_{2eq} factor for electricity currently exists in Norway. However, the approach taken in the ZEB Centre is in line with the long term political goals for the electricity system in Europe [7]. The calculations for materials are based on emission factors based on the electricity mix used in the different processes for each respective material and are sourced from the Ecoinvent database. For example, the concrete used in the analysis is based on a concrete process from Switzerland with the Switzerland electricity mix as an input. The solar cell production is based on the UCTE electricity mix (average European mix). Further work on the ZEB-residential concept model will include scenarios using different electricity mixes in addition to the ZEB emission factor. The impact of the different emission factors on overall emissions for the building will then be assessed.

RESULTS

In Figure 3 below, the emissions from the main material inputs and technical installations are shown. The total emission amounts to 7.2kgCO_{2eq}/m²a, the initial material inputs 5.25 kgCO_{2eq}/m²a and the use phase replacements 1.95 kgCO_{2eq}/m²a. The PV panels, external walls and foundation are the largest contributors to the emissions. The concrete used in the foundation

and ground works is responsible for the emissions from this part of the building. Another contributor is the insulation, in particular, the use of EPS insulation in the ground floor slab and the roof and also, the glass wool insulation used in the outer and inner walls.

If the solar cells are not estimated to be produced in a 50% more efficient way in 30 years [15] and the same EcoInvent process is unchanged for the use phase, the total emissions will be 7.6 $kgCO_{2eq}/m^2$ per year i.e. 0.7 kg higher. This indicates that the PV panels alone account for between 2.1-2.9 $kgCO_{2eq}/m^2$ per year or approximately 30-38 % of the current total emissions dependent on the replacement scenario. It should be noted that an emission factor of 261 $kgCO_{2eq}/m^3$ per year is used for "normal" concrete. By replacing the "normal" concrete with low carbon or "green" concrete, the emissions from concrete could be reduced significantly.

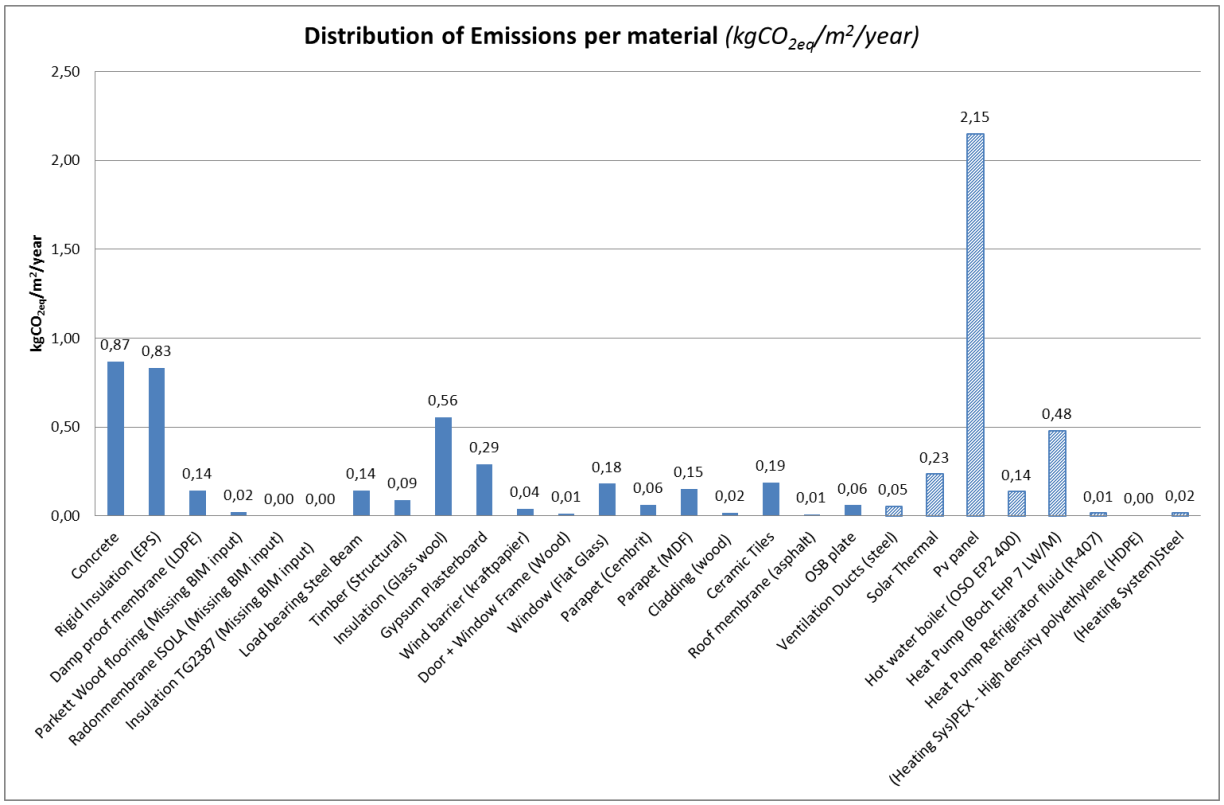

Figure 3 Distribution of carbon dioxide emissions ($kgCO_2eq$ per m^2 per year) from material and technical inputs.

Design of on-site electricity production and total CO_2 balance

The total CO_2 emission (from the materials and from the energy used for operation of the building) amounts to 12,3 $kgCO_{2eq}/m^2$ per year, or 1964 $kgCO_{2eq}$ per year. With a CO_2 factor of 0.13 $kgCO_{2eq}$/kWh, the necessary PV production[1] has to be 1964/0.13 = 15109 kWh per year. That amounts to 94 kWh per m^2 heated floor area per year, which is a very high number to achieve under Norwegian climate conditions. The flat roof mounted PV will have a yearly production of 11344 kWh. This is equal to 71 kWh per m^2 heated floor area per year, which is well above the yearly energy used for operation (delivered electricity, 39 kWh/m² per year). Thus, this alternative can be called a plus energy house, producing more energy than it consumes. The PV production covers 75 % of the total CO_2 emissions, as illustrated in figure 4 below and therefore fails to achieve the ZEB-OM target, however, it does satisfy the ZEB-O level.

[1] This is based on the assumptions that exported electricity to the grid will offset equivalent amount of electricity in the central el-grid system, produced with the same mean CO_2 emissions as the imported (bought) electricity i.e. the same CO_2 factor is used for both exported and imported electricity (symmetric CO_2 factor).

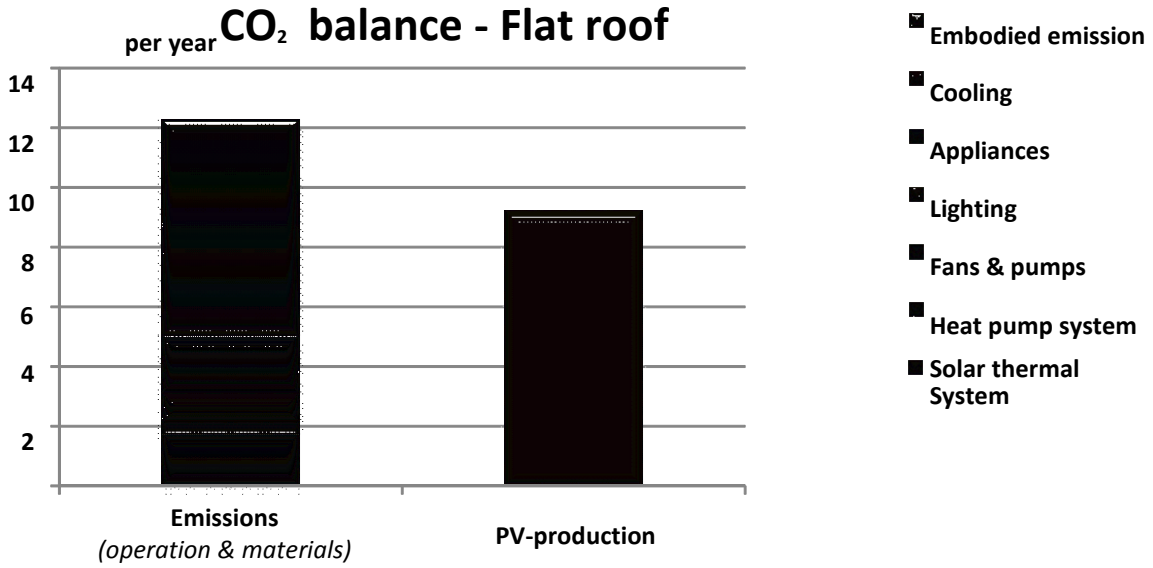

Figure 4 CO_2 balance between emissions from energy used for operation & embodied emissions from materials, and PV production with roof mounted PV.

DISCUSSION

One of the main outputs of this research has been the inter-operability of Revit/BIM with Ecoinvent using Excel. This inter-operability is part of the development of a robust, flexible and transparent emissions calculation method for use at early design stage. Such application of the method to the concept model has demonstrated that it can be used to assess the impact on emissions of different material choices and energy systems, as well as testing and ensuring consistency in environmental input data. The main findings have shown that the emissions from PV panels account for 30-38% of the total emissions depending on the predicted production efficiency chosen. The preliminary conclusions from this study are:

1. For a typical single family home (2 storeys) it is rather easy to achieve a ZEB-O level, which in this case can be labelled a net zero energy building (energy produced on-site with PV equals total electricity demand).
2. Taking into account also the embodied emissions from materials and installations it is difficult to achieve the ZEB-OM (operation and material) level by using only the flat roof for PV production. However, it should be noted that the calculation of embodied emissions for operation are highly dependent on the emission factor chosen for the electricity mix.
3. Even if the calculation of embodied emission (EE) has considerable uncertainties, preliminary results indicate that EE is significantly higher than the emission related to energy used in operation. However, in the current calculations no effort has been made to reduce EE, in contrast to energy used in operation where high performance solutions are used.
4. To achieve a ZEB-OM level a combination of further reduced energy demand, high COP/SPF thermal systems, reduced embodied emissions and increased PV-production seems to be the solution.

This study does not consider other on-site electricity production alternatives like bio-CHP, or building integrated wind generators. This study is also restricted to analyse operational and embodied emission, not taking into account emissions related to the construction and demolition phase. Despite the fact that this first round of calculations has presented many challenges and provided a large learning curve and interpretation of the data involved, it is expected that future optimisation of the design will be much less challenging. In the next stage of this research, the impact on total emissions of different lifetime and durability assumptions should be investigated and a series of scenario tests should be conducted to analyse the impact on emissions of the following;

1. Using Hybrid PV/T modules instead of separate PV panels and solar thermal collectors.
2. Comparing the emissions for the monocrystalline, silicon PV panels (199 $kgCO_{2eq}/m^2$) used in this first round of calculations with less efficient thin film PV panels such a-Si (73,8 $kgCO_{2eq}/m^2$) and CIS (123 $kgCO_{2eq}/m^2$) which less energy intensive to produce and are less sensitive to over-heating.
3. Replacing normal concrete with "green" concrete and replacing glass wool insulation with emerging materials such as VIP, PCM and aerogel. The corresponding structural implications would also need to be considered.
4. Generic data should be replaced with specific data from Norwegian manufacturers where applicable. The boundary condition, year of the data and place of production of the material should be noted carefully when extracting data from the EPD. The emissions should be calculated by using the kWh for production and the ZEB emission factor. [14]
5. Using different emission factors for the electricity grid. The current ZEB emission factors for electricity have been established assuming a massive and progressive de-carbonization of the grid until 2050, a so-called ultra-green scenario.[7]

ACKNOWLEDGEMENTS

This paper has been written within the Research Centre on Zero Emission Buildings (ZEB). The authors gratefully acknowledge the support from the ZEB partners and the Research Council of Norway.

REFERENCES

1. Houlihan Wiberg, A.A-M., Hestnes, A.G., 2011. Development of a CO_2 accounting method for Norwegian zero emissions buildings (ZEB). In: Proceedings from CISBAT 14-16 September 2011; Lausanne, Switzerland.
2. Dokka TH, Houlihan Wiberg A.A-M, Mellegård S., Georges L, Time B., Haase M., Lien A.G. (In press) A zero emission concept analysis of a single family house, The Research Centre on Zero Emission Buildings (ZEB Technical Report, 2013.
3. Revit Architecture Suite, version 2011.
4. Standards Norway, 2009. NS 3451-2009 Table of Building Elements. Oslo, Norway: SN.
5. Ecoinvent 2010. Ecoinvent version 2.2. Online Life Cycle Inventory Data (LCI). Swiss Centre for Life Cycle Inventories, Dübendorf, Switzerland.
6. Simapro, 2012, Simapro 7.3.3, PRé Consultants, Amersfoort, The Netherlands.
7. Dokka, T.H., Sartori, I., Thyholt, M., Lien, K., Byskov Lindberg, K., 2013. A Norwegian Zero Emission Building Definition. In: Proceedings from Passivhus Norden 2013, 15-17 October2013; Göteborg, Sweden.
8. NS3700:2010 Criteria for passive houses and low energy buildings – Residential buildings. Standard Norway 2010.
9. SIMIEN 5.11, SIMulation of Indoor climate and ENergy use. [online] Available at: <http://www.programbyggerne.no> [Accessed 10 April 2013].
10. Polysun 5.1 Simulation Software. Vela Solaris AG. Winterhur, Switzerland. [online] Available at: <http://www.velasolaris.com > [Accessed 10 April 2013].
11. PV-syst 5.62 Photovoltaic System Software. [online] Available at:< http://www.pvsyst.com/en/ > [Accessed 10 April 2013].
12. British Standards Institution, 2011. EN15978:2011 Sustainability of construction works. Assessment of environmental performance of buildings. Calculation method. British Standards Online [online] Available at: <http://shop.bsigroup.com>[AccessedApril 2013].
13. Methodology Guidelines on Life CycleAssessment of Photovoltaic Electricity http://www.iea-pvps.org/fileadmin/dam/public/report/technical/rep12_11.pdf
14. Dokka, TH, 2011. Proposal for CO_2 factor for electricity and outline of a full ZEB-definition. The Research Centre on Zero Emission Buildings (ZEB) Internal Report, 2011.
15. Alsema E. 2006. Life Cycle Assessment of PV technology: current status and further needs [pdf] Available at: <http://www.sense-eu.net/fileadmin/user_upload/intern/documents/Results_and_Downloads/SenseWorkshopLCAinGeneral.pdf> [Accessed 10 April 2013].

INTEGRATION OF SOLAR TECHNOLOGIES INTO URBAN COOLING SYSTEMS: A COST OPTIMAL APPROACH

A.M. Kamali; C. Felsmann

Professorship of Building Energy Systems and Heat Supply, Institute of Power Engineering, Faculty of Mechanical Science and Engineering, Dresden University of Technology, Helmholtzstr. 14, 01069 Dresden, Germany

ABSTRACT

In recent years, the demand for urban or district cooling technologies and networks has been increasing significantly due to their higher efficiency and better ecological impact. Such impact is strongly expected to improve further integrating renewable energy technologies. Recent studies have been in favour of de-centralized District Cooling where the cooling network is divided into sub-networks instead of one central network. This raise the issue of which system is considered a better option or solution: Separated, De-Centralized or Urban Cooling System (UCS)? Which cooling technology is to be adopted and consequently which solar-assisted cooling system represents a better choice?

A cost optimization model has been developed to optimize several elements of UCS such as: cooling network, cooling technologies (compression or absorption), capacity of cooling devices, cold and hot storage locations and sizes. Both conventional and renewable energy resources have been taken into consideration. Different solar technologies have been included in the optimization process such as: trough solar concentrators, vacuum solar collectors and PV panels. The model was developed based on the mixed integer linear programming method (MILP) and implemented using GAMS language. In this paper, the model developed as well as the results of two case studies are briefly presented. The aim of the investigation is to provide the decision makers with a preliminary idea of where to invest among all these design options, varying from Separated (one building) Systems to UCS, and the different solar technologies investigated. The work is also an attempt to answer the questions concerning the financial affectivity of integrating solar technologies into Urban Cooling Systems.

It was observed that UCS represents a more efficient choice when dealing with residential districts. The decision of integrating solar technologies into UCS, especially in sub-tropical regions, is a technically feasible way to reduce the effect of climate change and global warming. Among the three solar technologies investigated in this research, PV-Panels emerged to be more economic option to adopt. This work is a starting effort to develop a multi-objective decision making model optimizing cost, primary energy consumptions and CO2 emissions.

Keywords: Urban / District Cooling, Cost Optimization, MILP, Solar Energy Integration, Decision Making.

INTRODUCTION

A typical urban cooling system (UCS) consists of several cooling consumption locations (Buildings) which are usually different in application type and occupation pattern and therefore, different cooling load profiles. Each building is assumed to have an available area which can be utilized to install cooling energy production unit, cold water storage and/or user-end unit.

Considering the wide range of possible network structures and capacity planning options, it becomes extremely essential to compare and analyse the trade-off between the scale economies in centralized solutions and those in the decentralized solutions in order to reach optimal solutions. This can be achieved by using binary variables accounting for fixed cost components [1]. MILP techniques already have been applied in the optimization of cogeneration and tri-generation systems by several researchers [2, 3, 4 & 5]. Thus the choice of using MILP in urban cooling systems (UCS) was driven by the necessity of producing a realistic comparison of centralized and decentralized solutions.

The decision of integrating solar technologies into urban cooling, especially in sub-tropical regions, is a technically feasible way to replace the electric refrigeration machines, minimise the consumption of fossil fuels, subsequently reduce the green house emission and eventually reduce the effect of climate change and global warming [6, 7]

In this work, two cooling technologies to produce cooling energy have been considered: a) Compression chillers powered by electricity grid, PV-panels or both. b) Absorption chillers connected to a boiler powered by natural gas supply line or to solar energy technologies (e.g vacuum tube collectors and/or trough solar concentrators). Figures (1a & b) represent the possible constructions of the cooling energy generation unit to be installed at each site including all the technologies integrated to the model.

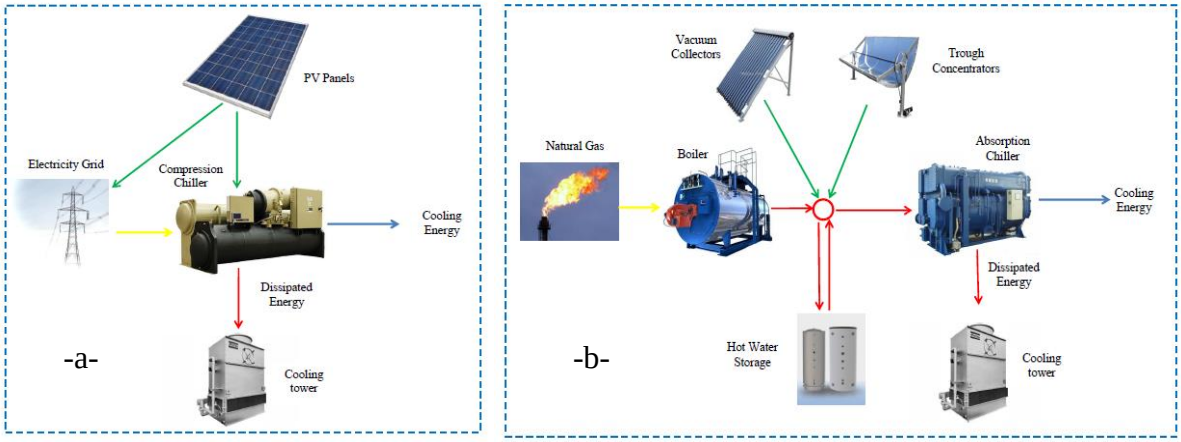

Fig. (1a & b): Configuration options for the cooling energy generation plant on site (i).

METHODOLOGY

A MILP model was developed, considering local energy balances and overall network configuration, to optimize the structural design and operational parameters of the urban cooling system. That includes: Size and location of each equipment in the system, type of cooling technologies (type of chiller: compression or absorption) to be used, type of energy resources, size and location of the each distribution pipeline in the DC network, energy flow rates in those pipelines and how the production and storage units should be hourly operated to cover the hourly cooling load of each building in the UC system. On a later stage, the model was upgraded to include the structural design and operational parameters of three solar technologies (PV-panels, Trough concentrators and Vacuum tube collectors).

Figure (2) shows, schematically, the basic energy flow structure of the UC network. The nodes (i, j and k) represent the physical locations where the cooling energy can be offered or requested (e.g. buildings, storages, or plants). Figure (3) shows a superstructure at any location i, comprising all equipment and technologies which are possible to be installed at this site. In this model, each location is a possible plant, storage, consumer or all three together.

It is up to the optimization model to decide which type of cooling technology is to be installed in each energy generation site among the technologies presented in Figure (1).

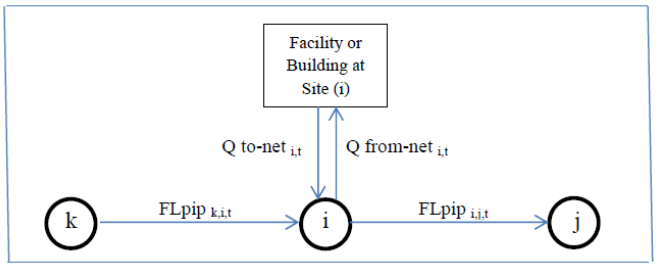

Fig. (2): energy-flow structure of the UC network at site (i).

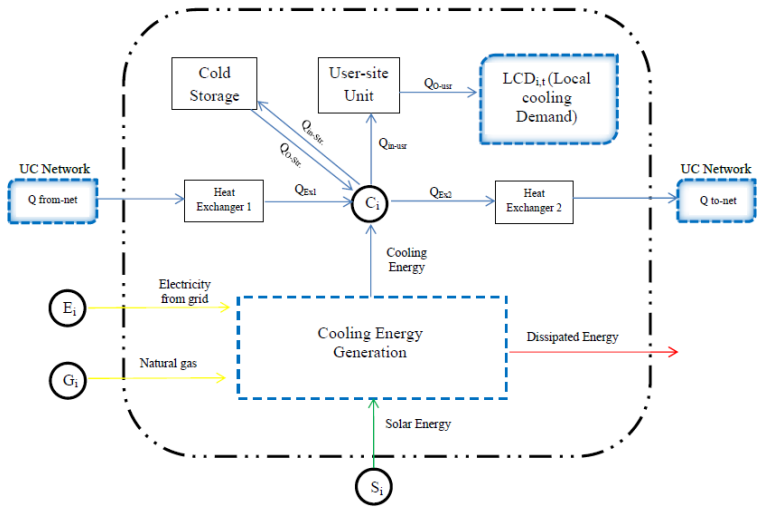

Fig. (3): Local Cooling Energy System (Superstructure) at site (i). Where : Gi represents the local fuel (Gas) supply system, Ei represents the local electricity supply grid, Si represent the solar energy resources and Ci represents the local cooling supply piping system.

The optimization is defined as to minimize the overall annual cost of UC system. As presented in (eq. 1) the objective function considers both the investment and operational costs of all equipment and network of the UC system.

$$min. \quad Z = \{C_{inv} + C_{opr}\} \tag{1}$$

The MILP model for the multi-period design and operational planning problem is characterized by bainary variables ($Y_{equ,i}$) which determines the location and number of units installed, and also by continuous variables ($CAP_{equ,i}$) for the representation of nominal capacities and energy flows [3, 4]. The investment cost of each equipment or network pipeline is defined using the annuity method as presented in (eq.2) where (f_{equ}) represents the annuity factor [1, 2]. CCv_{equ} and CCf_{equ} are the linearized price function parameters of equipment. For solar technologies, the equipment capacity variables were replaced with gross area variables ($A_{equ,i}$). On the other hand, the annual operational costs were calculated as the sum of operational costs in all time periods [1].

$$PC_{inv} = \sum_i \sum_{equ} f_{equ} \cdot \left[CCv_{equ}.CAP_{equ,i} + CCf_{equ}.Y_{equ,i}\right] \tag{2}$$

$$C_{opr} = PC_{opr} + EC_{net-opr} + EC_{comp-opr} + FC_{opr} - EC_{pv} \tag{3}$$

Where; PC_{opr} is the sum of operational costs of the plant equipment for all time periods, $EC_{net-opr}$ is the sum of electricity costs of pumping the cooling water through the network for all time periods, $EC_{comp-opr}$ is the sum of electricity costs to operate the compression chillers for all time periods, FC_{opr} is the sum of fuel (natural gas) costs used to operate the boilers for all

time periods, EC_{pv} is the sum of incomes of produced electricity at PV-Panels and sold to the national grid for all time steps (h) and Cpv_t is the selling price (ct./kWh).

$$EC_{pv} = \sum_i \sum_h Cpv_h \left(Epv_{i,h}\right).\Delta t_h \quad (4)$$

Both electricity and fuel (natural gas) prices are time dependent in this model. Thus a time related purchase tariff including various prices of electricity (depending on the hour of the day) and fuel (depending on the time of the year) can be easily adopted.

The annual demand is expressed considering a number of representative days throughout the year (e.g. one representative day for each month of the year) divided into 24 periods of (1 hour). However, although only representative days have been included in the time set of the model, the operational costs were calculated for the full year by assuming similar operation costs at similar time periods. The objective function was subjected to several constraints regarding energy balances, capacity limits, consistency bounds and available area constraints. All of which were applied on the local equipment and the pipeline network.

RESULTS

The MILP optimization model was implemented using GAMS language and solved using the commercial solver CPLEX 12. Two realistic case studies were investigated. The first case study is a small sector of a university campus consisting of four buildings, three office buildings (N1, N2 & N4) and one dormitory (N4), as presented in Figure 4. The second case study is a residential neighbourhood consisting of five multi-apartment residential buildings and two office buildings, a school (N4) and a health centre (N8), as presented in Figure 5.

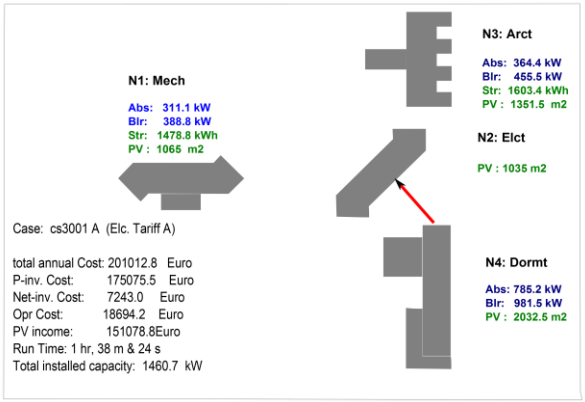

Figure (4): optimized cooling system obtained for Case study 1 for: Tariff A.

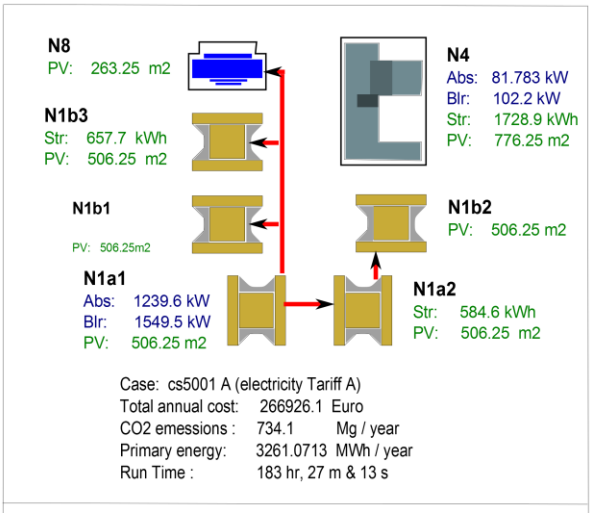

Figure (5): optimized cooling system obtained for Case study 2 for: Tariff A.

Two different electricity tariffs were adopted. Tariff A is a constant tariff: 26 ct/kWh (01:00 – 24:00) and Tariff B is a variable tariff: 26 ct/kWh (01:00 – 05:00) & (22:00-24:00) and 19.4 ct/kWh (06:00 – 21:00) [8]. Other scenarios with different conditions, such as limited available area and prices changes, were also performed in order to reach a general conclusion about the impact of some decision making parameters, related to the solar technologies, on the cost optimized system.

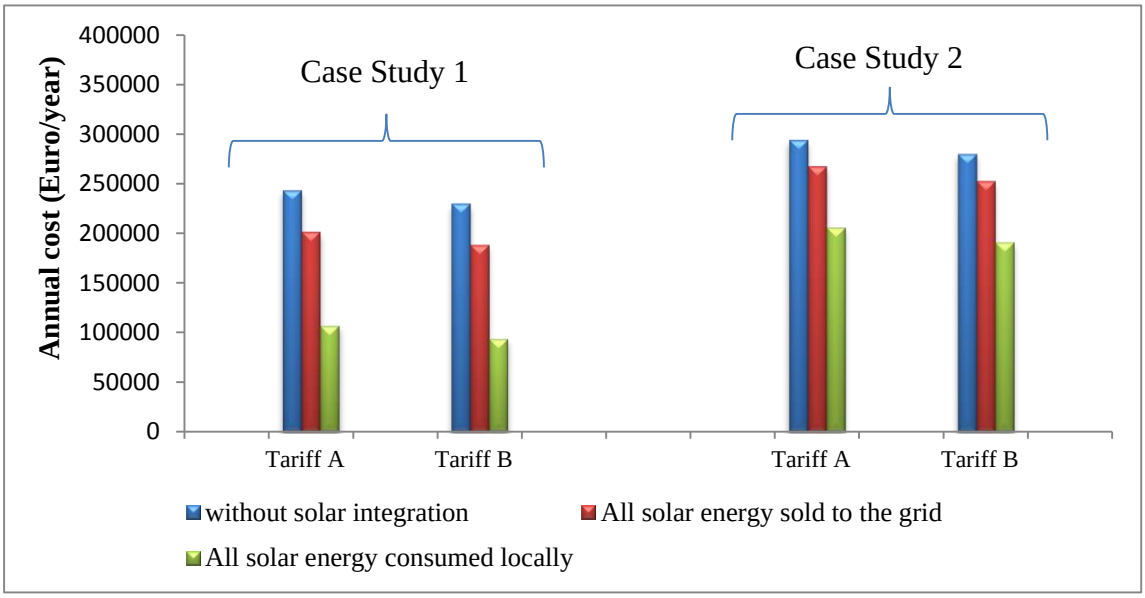

Figure (6): Annual costs of case studies 1 & 2 and for three different scenarios.

DISCUSSION

It is noticed that the results were strongly affected by the nature of the buildings under investigation and also the distances among those buildings. The buildings in the first case study were relatively big with high peak loads but their occupation pattern were limited for a certain period of time, the working hours, except of the student dormitory (N4). On the other hand the buildings in the second case study were mostly residential buildings with shorter distances among them. It is observed that UCS is a more efficient choice to make when dealing with residential districts. Although conventional compression chillers have less investment costs within the range of design capacities chosen by the model, absorption chillers driven by natural gas fired boilers seem to have less annual cost (both investment and operational costs).

Among the three solar technologies investigated in this research, PV-Panels emerged to be more economic due to their annual income of locally produced energy. The energy produced in the local PV-Panels were assumed, at first, to be sold completely to the national electricity grid due to the difference in timing between the solar energy production hours, daylight hours, and the operation hours of the cooling chillers which are more related to the cooling load profiles. This difference was more obvious in the variable electricity Tariff (B) when compression chillers were to be installed at the production site, as a substitute for the absorption chillers, where most of the cooling energy was produced during low tariff period (night hours). However the selling prices of the locally produced energy where 16 ct./kWh [9] which is less than the purchased electricity tariffs A and B. This indicates that a better solution, less total cost, might be suggested by the model if electricity produced by the PV-Panels were used directly to operate the compression chillers. Such a scenario was performed by assigning PV energy sell prices equal to the purchase tariffs. This scenario showed a

sufficient reduction in the annual cost, up to 59 % in case 1 and 32 % for case 2 (Fig. 6). However the configurations presented in figures (4 & 5) were still chosen by the model as optimal solutions.

The condition of no fuel to drive the boiler was also investigated for case study 1 as a special scenario combined with the condition of no PV panels to be installed. The goal of this special case was to investigate which of the other two solar technologies represent the more economic option. Although trough concentrators have less investment cost, vacuum tube collectors have lass operational costs due to the absence of sun tracking systems. However, the model has chosen compression chillers operated by national grid electricity over the option of absorption chillers operated by solar energy. This can be explain by the relatively low amount of energy produced by each square meter of solar collectors which requires a wide area to be invested to operate the absorption chillers and big sized hot water storages to be installed as well which will eventually result in higher total cost of the system.

In general, it is observed that integrating solar technologies into urban cooling system has a positive impact not only on the economic aspect but also on the ecological aspects as well where CO2 footprint and primary energy consumption rates where reduced significantly. Separated single-objective optimization models for minimizing the CO2 emissions and primary energy consumption have been developed and implemented for both case studies (1 & 2). On the long-term future plan, the design and optimization model is to be further developed into a multi-objective optimization model where the ecological objective (minimizing the CO2 emissions and primary energy consumption) is to be included along with cost optimization.

REFERENCES

1. D. Chinese. “Optimal size and layout planning for district heating and cooling networks with distributed generation options”. International Journal of Energy Sector Management. Vol. 2, No. 3, 2008, pp. 385-419.
2. M. A. Lozano, J. C. Ramos, L. M. Serra (2010). “Cost optimisation of the design of CHCP (combined heat, cooling and power) Systems under legal constraints”. Energy, 35, 794-805.
3. J. Söderman, F. Pettersson (2006). “Structural and operational optimisation of distributed energy systems”. Applied Thermal Engineering, 26, 1400-1408.
4. J. Söderman (2007). “Optimisation of structure and operation of district cooling networks in urban regions”. Applied thermal engineering, 27, 2665-2676.
5. D. Buoro, M. Casisi, P. Pinamonti. “Optimization of distributed Trigeneration systems integrated with heating and cooling micro-grids”. Distributed Generation and alternative energy Journal. Vol. 26, No.2, 2011.
6. K.F. Fong , C.K. Lee, , T.T. Chow. “Comparative study of solar cooling systems with building-integrated solar collectors for use in sub-tropical regions like Hong Kong“. Applied Energy. Volume 90, Issue 1, February 2012, Pages 189–195.
7. S. A. Kalogirou. “Solar thermal collectors and applications“. Progress in Energy and Combustion Science. Volume 30, Issue 3, 2004, Pages 231–295
8. DREWAG. “Allgemeine Preise Strom - Grundversorgung für den Haushalt“. www.drewag.de
9. Erneuerbare-Energien-Gesetz – EEG, veröffentlicht durch die Bundesnetzagentur (Stand: 31.01.2013).

SOLAR CADASTRE 2.0: UPDATED MONTHLY PRODUCTION VALUES FOR EACH ROOF OF A CITY

D. Klauser; J. Remund

Meteotest, Fabrikstrasse 14, CH-3012 Bern

ABSTRACT

With the availability of accurate digital surface models over large areas, there is growing interest in solar cadastre, i.e. calculations of the irradiation for every roof of a city. Currently a solar cadastre gives a prediction for the yearly production of a PV plant on a specific roof as well as the orientation, inclination and area of the roof plane. This information together with the horizon calculated when developing the solar cadastre may be used to do update a solar cadastre with monthly production values for each roof.

The irradiation calculation for a solar cadastre is rather time consuming. Thus it is not feasible to repeat the full calculation for a large area every month. Instead we have developed a simple model to approximate the monthly production values based on the irradiation calculation for an average year and measured current irradiation data from ground stations.

The irradiation calculation for an average year that is performed for a standard solar cadastre takes into account orientation, inclination and shadowing for a specific roof. This result for an average year is scaled by comparing the direct and diffuse irradiation on a horizontal surface for the current month with the corresponding month of the typical year. The precision of this method was validated over a 10-year period showing that the standard deviation of the relative error is only 4% for roofs with an inclination between 20 and 60 degrees.

The resulting monthly production values are presented in a web application accessible to the general public. The most important value presented is the estimated production in kWh/kWp. This allows owners of small private PV plants to compare the estimated production with the production of their plant to have a simple kind of plant surveillance.

Keywords: Solar Cadastre, Solar Energy, Web Application, Monthly Production Values.

INTRODUCTION

For the first solar cadastre in the 1990's the information on the geometry of the roof planes was derived from photogrammetric data [1]. In recent years the availability of airborne laser scanning provided a new option to obtain the digital surface model data needed for the derivation of a solar cadastre [2]. A further possible data source is an already existing 3D city model.

The derivation of a solar cadastre may be divided into three steps. First of all, the input data need to be rasterized to obtain a digital surface model. From this aspect and slope of each raster cell may be derived based on the heights of neighbouring pixels. In the second and central step, the irradiation for each raster cell is calculated taking into account aspect and slope as well as shadowing effects. Finally, the results from the irradiation calculation are aggregated per roof plane.

In particular the second step of the derivation, the irradiation calculation, is rather time consuming. In order to obtain accurate results, usually the irradiation and the shadowing

effect are calculated for each hour of an average year with a special resolution of less than 1 meter. To repeat this calculation every month with current irradiation data takes several days up to weeks for larger areas and is thus not feasible.

METHOD

We use hourly irradiation data for an average year (period 1986-2005) from meteonorm [3] on an un-shadowed horizontal plain as the basis for the calculation. For the direct irradiation the analysis of the shadowing effect is straight forward: for each hour of the year one needs to determine whether the sun position is above the horizon or not. For the diffuse irradiation the method is a bit more complicated. In order to calculate the effect of the horizon on the diffuse irradiation it is necessary to calculate the radiation distribution of the diffuse radiation over the sky hemisphere. For this we use the Perez model [4]. As the radiation distribution depends on the sun position and the sky's clearness and the sky's brightness the radiation distribution needs to be calculated for each hour separately. Weighting the hourly radiation distribution with the diffuse radiation in the corresponding hour, one obtains the yearly diffuse radiation distribution. This yearly diffuse radiation distribution is then masked with the horizon for each raster cell (see Figure 1).

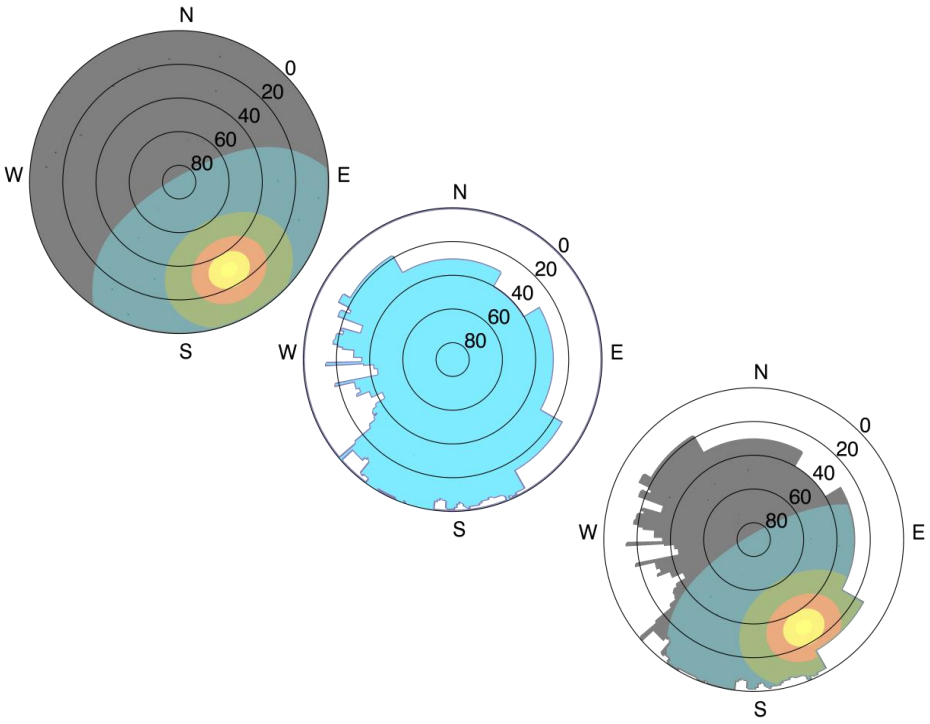

Figure 1: Illustration of the shadowing analysis for the diffuse irradiation for a specific point in time: radiation distribution (left), horizon (center) and un-shadowed part of the radiation distribution.

For each raster cell the results of the hourly irradiation calculation are summed for each month for direct and diffuse irradiation separately. These are then aggregated per roof plane in order to obtain for each roof plane the direct and diffuse irradiation for each month of a typical year.

In order to obtain the estimated production for the current year, the measured direct an diffuse irradiation on a horizontal plane are compared with the values for the average year and the values for each roof are scaled accordingly (see Figure 2).

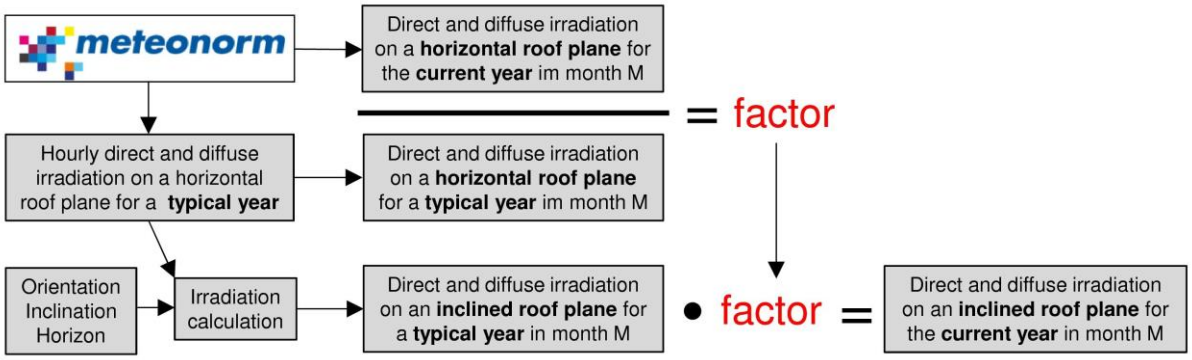

Figure 2: Illustration of the method to estimate the monthly irradiation values for the current year based on measured irradiation date on a horizontal plane.

Validation

The results of the method were validated for a place near Berne, Switzerland for the 120 months during the period 2002-2011. The validation was performed for roof planes with all orientations and an inclination between 0° and 60°. First the irradiation was calculated directly with the Perez-Modell for each month based on the hourly data from meteonorm as is was done for the average year. These results were then compared with values obtained by scaling the values from the average year using method described above.

The mean relative error was found to be less than 1%. The distribution of the mean relative error depending on the orientation and inclination of the roof plan is shown in Figure 3. The standard deviation of the distribution of the relative error was found to be 4%.

In a first attempt a more simple method was tried by using only the global horizontal irradiation for the current month in comparison with the average year for scaling. While the mean relative error also is less than 1%, the standard deviation of the distribution of the relative error is 8%. This shows that it is necessary to look at the direct and diffuse irradiation separately.

With the error of the method used typically being less than 4%, the accuracy of the measured irradiation is likely to have a similar or even larger error. Thus the accuracy of this method is comparable to performing an irradiation measurement at the site of the plant or using satellite data for plant surveillance. The last two have of course the advantage of higher time resolution. In contrast it is not advisable to use the method presented in this article to calculate daily values. On one hand because the data to be stored becomes much larger and the day of the current year may have a completely different ratio of direct to diffuse irradiation compared to the average year.

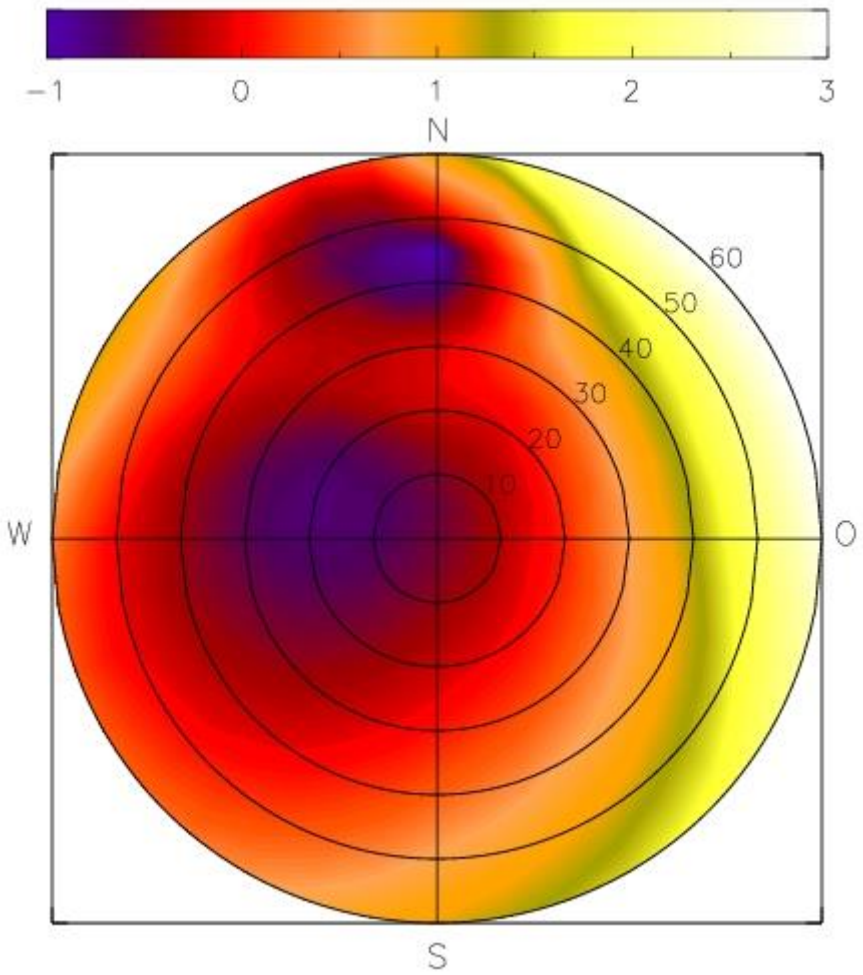

Figure 3: Distribution of the mean relative error (MRE) in % depending on the orientation and inclination of the roof plane for 120 months the validation period 2002-2011.

RESULTS

The results of the calculation were integrated into an interactive website [5] (see Figure 4). For each roof the standard parameters of a solar cadastre (orientation, inclination, area, mean annual irradiation) are given. On top of that the monthly irradiation values of the last and the current year are given and compared with the average year. This comparison is also displayed in a graphic. Further, the estimated production in kWh/kWp is given.

To estimate the monthly production the mean monthly irradiation in kWh/m^2 for a specific roof is multiplied with a performance ratio of 85% to obtain the estimated production in kWh/kWp.

The data presented allows owners of small PV plants to check whether their plants production reaches the estimated production, thus performing a simple kind of plant surveillance.

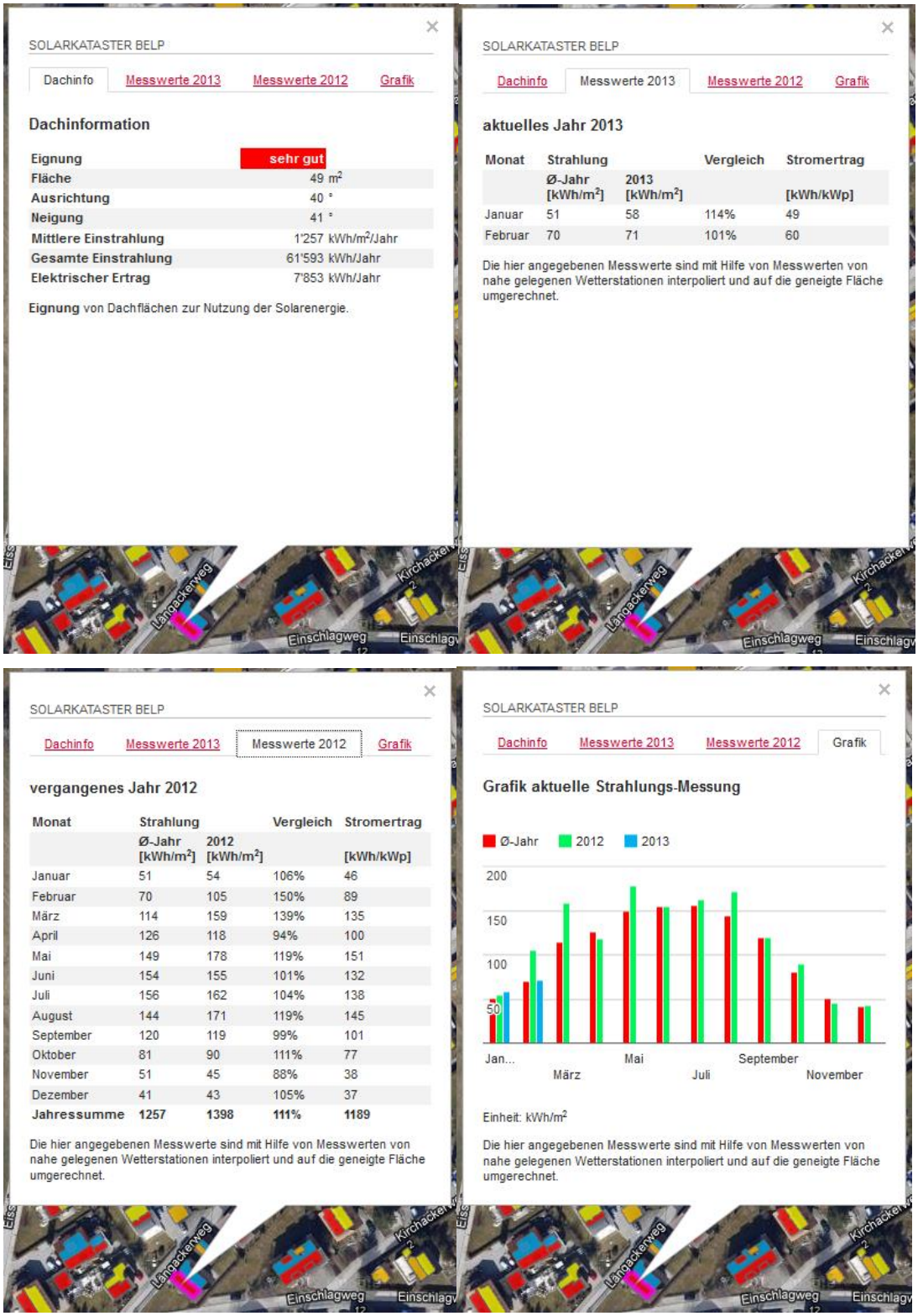

Figure 4: Screenshots from the website http://solarkataster.meteotest.ch/belp which shows the monthly irradiation data and the estimated production.

REFERENCES

1. Wittmann, H. et al. : Identification of roof areas suited for solar energy conversion systems, Renewable Energy, Vol. 11, no. 1, pp. 25-36, 1997.
2. Voegtle, T. et al. :Airborne laserscanning data for determination of suitable areas for photovoltaics, ISPRS WG III/3, III/4, V/3 Workshop "Laser scanning 2005", Enschede, the Netherlands, September 12-14, 2005.
3. http://www.meteonorm.com
4. Perez, R. et al., All-weather model for sky luminance distribution – preliminary configuration and validation, Solar Energy, Vol. 50, No. 3, pp. 235-245, 1993.
5. http://solarkataster.meteotest.ch/belp

USING A BAYESIAN NETWORK TO EVALUATE THE SOCIAL, ECONOMIC AND ENVIRONMENTAL IMPACTS OF COMMUNITY RENEWABLE ENERGY

Philip A. Leicester[1,2], Chris I. Goodier[1], Paul Rowley[2]

1. School of Civil and Building Engineering, Loughborough University, Epinal Way, Loughborough, LE11 3TU, UK.

2. Centre for Renewable Energy Systems Technology, School of Electronic, Electrical and Systems Engineering, Loughborough University, Epinal Way, Loughborough, LE11 3TU, UK.

ABSTRACT

Social, economic and environmental (**SEE**) impacts resulting from the adoption of solar PV have been modelled at a community scale for the first time using a probabilistic graphical model in the form of a Bayesian Network (**BN**). Model parameters required to conceptualise this multi-disciplinary problem domain are characterised by uncertainty due to stochastic variability, measurement and modelled data errors, or missing or incomplete information. A **BN** conveniently represents the model parameters and the associations between them and endogenises the uncertainty in probability distribution functions or mass functions.

The theory and method of construction of an object-oriented **BN** which encapsulates a number of **SEE** parameters is described. This is used to model small urban areas as potential adopters of solar PV technology. The **BN** has been populated with modelled and empirical quantitative data from a variety of disciplines to create an inter-disciplinary knowledge representation of the problem domain.

The model has been used to explore a number of scenarios whereby 'observations' are made on one or more variables of interest thus altering their prior probability distribution. The updated or posterior distributions of all the other variables are then recalculated using inference algorithms. Results are presented which show the utility of this approach in diagnostic and prognostic inference making. For example it is shown that Solar PV can have a small but significant impact on energy poverty.

It is concluded that the adoption of a BN modelling approach that endogenises uncertainty, and reduces investment and policy risks associated with energy technology interventions within communities, can act as a useful due diligence and decision support tool for a number of private, public and community sector stakeholders active in this sector, in particular key decision and policy makers.

Keywords: Solar PV, Bayesian Networks, Community Energy, Uncertainty

INTRODUCTION

Community scale energy efficiency and renewable energy technologies are seen as a valuable means for contributing to a number of energy policy objectives, and are benefitting from a range of financial support mechanisms internationally. These incentives in turn are resulting in rapidly increasing investment in the community scale renewables sector. However, significant uncertainty exists with respect to the potential impacts of community scale renewables in terms of specific policy goals, including actual (as opposed to projected) greenhouse gas reductions, renewable energy generation capacity and socio-economic benefits such as fuel poverty alleviation. This uncertainty represents significant risk for investors and policy makers alike. A multivariate problem domain characterised by uncertainty is ideal for representation by a probabilistic graphical model and more specifically

by a Bayesian Network (**BN**) (Pearl, 1990).

The aim of the broader research project to which the work here contributes is to use a **BN** methodology to evaluate the potential **SEE** impacts of low carbon interventions for urban areas in order to endogenise uncertainty in the modelled outputs and thus explore risk. A **BN** as a decision and policy making tool in this arena will be evaluated.

This paper demonstrates how a candidate **BN** was constructed. The two key elements of the method are discussed; firstly the construction of the **BN** to represent the problem domain as a qualitative conceptual model; and secondly the elicitation of quantitative data to define the marginal and conditional probabilities for all the variables in order to construct an accurate knowledge representation. Some preliminary outputs of the model are presented. Finally the efficacy of **BN**s as a tool for decision and policy making pertaining to the deployment of community renewable energy is discussed.

BAYESIAN NETWORK THEORY

A **BN** is encoded over a directed acyclic graph (**DAG)** in which the vertices (nodes) correspond to random variables and directed edges represent direct dependencies between them (see Figure 1). A directed edge from a parent node $\boldsymbol{A}$ to child node $\boldsymbol{B}$ implies that variable $\boldsymbol{B}$ has a causal or influential dependence on variable $\boldsymbol{A}$.

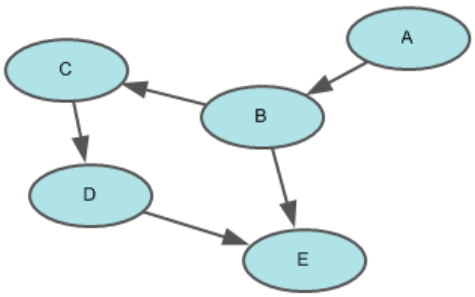

Figure 1. Bayesian Network modelled as a directed acyclic graph

The variable is represented as a *probability mass function* (**pmf**) which gives the probability of each disjoint state. A variable **A**, with n discrete states, a_1, a_2, a_3... a_n, has a **pmf,** $P(\boldsymbol{A})$, represented by a set as in equation 1.

$$P(\boldsymbol{A}) \equiv \{p(\boldsymbol{A} = a_i)\ \forall i = 1,2,3 \dots n\} \qquad \textit{Equation 1}$$

The dependency of a child variable on a parent variable is modelled using a conditional probability table (**cpt**) $P(\boldsymbol{B}|\boldsymbol{A})$, whereby each state of a child variable **B** has a probability conditional on the state of the parent variable **A**. The joint probability distribution (**jpd**), $P(\boldsymbol{A},\boldsymbol{B})$, is calculated using the fundamental rule from the prior **pmf** of the parent and the **cpt** (equation 2).

$$P(\boldsymbol{A},\boldsymbol{B}) = P(\boldsymbol{B}|\boldsymbol{A}) \cdot P(\boldsymbol{A}) \qquad \text{Equation 2}$$

Using the **jpd,** the prior **pmf** of the child variable **B** can be deduced by the process of marginalisation which involves summing the probability of the child variable for each value of the parent:

$$P(\boldsymbol{B}) = \sum_{i=1}^{m} P(\boldsymbol{B}, a_i) \qquad \text{Equation 3}$$

These techniques, which follow from the axioms of probability, can be applied to all the variables in a BN. The fundamental rule yields the chain rule which can be factorised to a more tractable form. Thus the **jpd** for all the variables in the **BN** shown in Figure 1 can be represented using the factorised chain rule as in equation 4.

$$P(\boldsymbol{A},\boldsymbol{B},\boldsymbol{C},\boldsymbol{D},\boldsymbol{E}) = P(\boldsymbol{A})P(\boldsymbol{B}|\boldsymbol{A})P(\boldsymbol{C}|\boldsymbol{B})P(\boldsymbol{D}|\boldsymbol{C})P(\boldsymbol{E}|\boldsymbol{B},\boldsymbol{D}) \qquad \text{Equation 4}$$

The **pmf** for each variable can be calculated by a repeated process of marginalisation. Such a

calculation produces the prior probability distribution - a measure of the prior uncertainty - of each variable. The utility of a **BN** is realised when one or more variables are fixed to a particular state (hard evidence), or state probabilities are adjusted in the light of new observations (soft evidence). The **jpd** can be updated and the **pmf**s for all other variables recalculated using Bayes Rule and the chain rule. The new posterior distributions allow the **BN** to be used as a decision support tool.

For a large **BN**, with say 20 variables each with 10 discrete states, the number of elements in the **jpd** would number 10^{20}. Its calculation is intractable and computationally NP-hard (Cooper, 1990). Software algorithms enable **pmf**s to be calculated without determining the entire **jpd**, rendering the problem feasible for all **BN** structures (Jensen et al., 1990).

Software packages are available which allow the encoding of a **BN** and the execution of rapid inference calculations. In this work AgenaRisk® was used. This software allows the encoding of hybrid **BN**s which have both discrete and continuous random variables (Neil et al., 2005). Continuous variables, parameterised by a probability distribution function (**pdf**), are automatically discretised (converted to intervals) to yield a **pmf**. AgenaRisk® makes use of dynamic discretisation algorithms to create non-uniform intervals. This ensures that narrower intervals are used in regions of the **pdf** where broad intervals would lead to approximate inference. AgenaRisk® thereby maximises the fidelity of the resultant discretised **pmf** to the **pdf** without a "*heavy cost of computational complexity"* (Neil et al., 2007).

CONSTRUCTING THE BN

The first task is to construct the qualitative component of the **BN**, namely the **DAG**, by deciding upon the key variables of interest and determining the causal influence between them using expert knowledge in a fashion similar to causal mapping (Goodier et al., 2010). For a large interdisciplinary problem domain it is convenient to break the graph into smaller connected sub-domains to create an object-oriented BN (Koller and Pfeffer, 1997; Molina et al., 2010). Each object encapsulates a more granular **BN** in which a number of variables define the object's domain. The prior, or posterior, **pmf** of an object's variables can act as inputs for other objects thus creating a declarative object-oriented application. This approach was adopted here and eight objects which encapsulate a total of 40 variables have been defined, with their relationships shown in Figure 2. These are discussed further below.

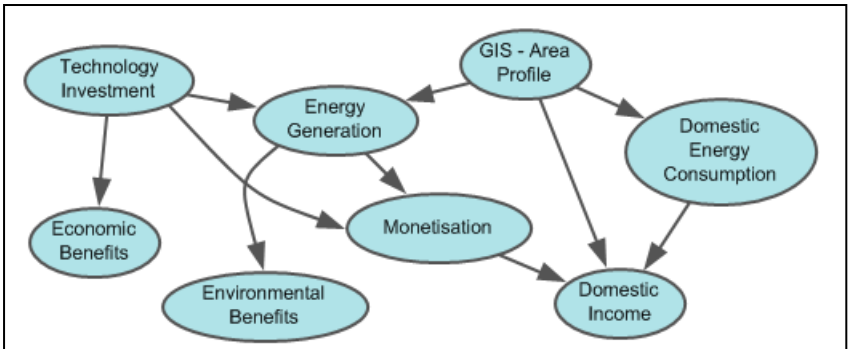

Figure 2. Object-oriented BN for community renewables

The second task is to populate each node with quantitative probabilistic data. For each variable a node probability table (**npt**) needs to be entered. For variables with parents, the data must convey conditional probabilities for each parent state. Preparing data for entry into the **npt** requires processing and conditioning. Occasionally it is convenient to parameterise a dataset into a continuous probability distribution using multivariate fitting algorithms.

In the following section the resulting **BN**'s objects are described. Some key data sources used to populate the **npt**s of variables are described and posterior **pmf**s resulting from observations are demonstrated.

RESULTS AND DISCUSSION

1. **GIS Area Profile** - In this work the geographic unit of analysis was the Lower Super-Output Area (**LSOA**), which is derived from socially homogeneous UK census output areas (Martin et al., 2001) and comprises, on average, 600 dwellings. Variables from several sources have been combined to create a Graphical Information system (**GIS**). Thus far, 4 **LSOA**s have been included (Figure 3). Geo-location, size, aspect and pitch of roofs have been derived using Light Detection and Ranging (LiDAR). Building type, height, footprint and age have been obtained from a commercial database. A **pmf** of the domestic household income has been estimated using spatial micro-simulation modelling. This has been estimated using census and family resource survey data (Anderson, 2013) and fitted with a β-distribution for ease of entry into AgenaRisk®. Figure 4 shows the **pmf** and fitted **pdf** for household income in LSOA E01025703 (Loughborough).

Figure 3. LSOA locations in England

2. **Technology Investment** - This object models the probabilistic relationships between technology costs, loan finance and discount rates to give net present value distributions.

3. **Energy Generation** - This object takes as a key input the solar potential of the **LSOA** from the **GIS** object and uses PVGIS CM-SAF model (Huld et al., 2012) to calculate the solar potential **pmf** of the **LSOA.** The results for LSOA E01018870 (Camborne) are shown in Figure 5.

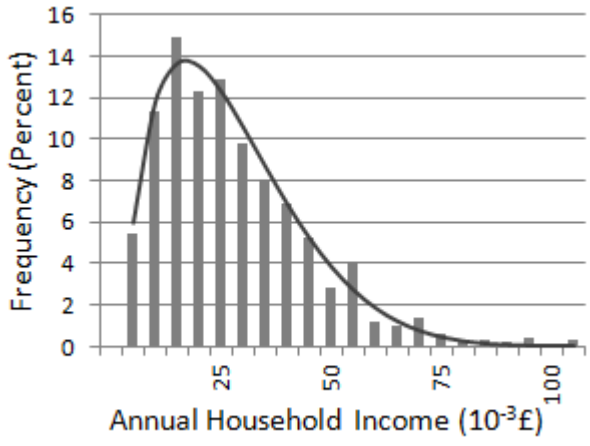

Figure 4. Distribution of annual household income

The deterministic PVGIS Yields are combined with empirical data to estimate system losses in a statistically robust way to introduce a realistic probabilistic measure of solar PV yield for any one property. This is coupled with empirical data for typically deployed UK Solar PV system ratings to calculate probabilistic annual yields.

4. **Monetisation** - The UK FiT scheme pays PV owners a generation and export tariff. This object takes as an input the energy generated and monetises this using current tariffs. A **pmf** of the self-consumption of the PV generated electricity has been estimated using data from Solar PV field trials which enables a **pmf** for export income to be estimated.

5. **Domestic Energy Consumption** - key variables in this object are domestic electricity and gas consumption. Inputs from other objects are the household income and property attributes from the GIS object and building energy performance. Fuel consumptions conditional on the

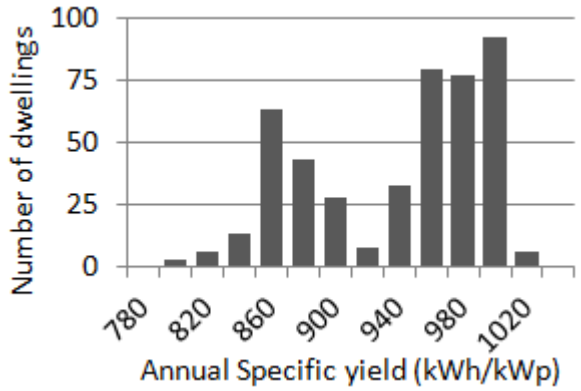

Figure 5. Solar potential for LSOA E01018870,

building performance and household income were derived from literature data (DEFRA, 2005) and deconvolution methods.

6. **Domestic Income** - The income distribution from the GIS object is combined with cash flows from the monetisation and energy consumption objects. This object provides a **pmf** of the change in household income as a probabilistic economic indicator.

7. **Environmental Benefits** - Using carbon intensity of displaced grid electricity, this object delivers a **pmf** of the carbon emission reduction for the technology.

8. **Economic Benefits** - Cash flows into business from the Technology Investment object can be used to estimate business income, growth and employment creation.

The model allows variables from a range of knowledge domains to be rendered as distributions in the form of **pmf**s. Such a representation of uncertainty is commensurate with Bayesian statistical inference. This is potentially more intuitive for stakeholders since a **pmf** gives an immediate and tangible variability of model parameters as opposed to alternative statistical inference methods using p-values and confidence intervals (Iversen, 1984). There are numerous aspects of this that can be demonstrated using this model across a range of **SEE** indicators e.g. carbon emission savings, domestic household income impacts and contributions to business growth. Figure 6 shows the **pmf**s for income from displaced electricity saving under 3 observations of solar PV system rating.

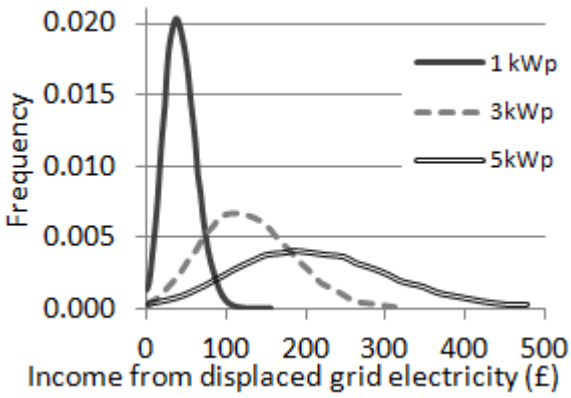

*Figure 6. **pmf**s of saving due to displaced grid electricity in LSOA E0102570, Loughborough.*

kWp	%
0	22.9
1	20.5
3	17.8
5	15.0

Table 1. Percentage households spending over 10% on fuel.

In the UK context one pressing policy concern is fuel (energy) poverty (Boardman, 2012) and questions arise as to whether microgeneration can have an impact (Walker, 2008). Posterior **pmf**s for the percentage of household income spent on fuel have been generated by the **BN** for several PV system rating observations. From these the percentage of households spending over 10% of their income on fuel has been calculated. The results are shown in Table 1. This demonstrates how the **BN** allows scenarios to be tested and recalculates the posterior distributions accordingly.

CONCLUSIONS AND FURTHER WORK

An extensive interdisciplinary knowledge representation for the deployment of solar PV in four communities has been created. The probabilistic assessment of a number of **SEE**

parameters has been made, providing a powerful inference making tool to aid multi-criteria decision making (**MCDM)**. This robust whole-system approach facilitates multi-scale (e.g. building, community, or city) analysis whilst managing constraints such as cost or carbon emissions (Rowley et al., 2013). Further development will incorporate probabilistic impact distributions for a range of domestic low carbon technical and behavioural interventions. This can be further enhanced by adding utility and value nodes (Delcroix et al., 2013) for various **SEE** indicators to create a triple bottom line **MCDM** tool to aid deliberative policy making.

ACKNOWLEDGEMENTS

The authors are immensely grateful to James Eddy, Blue Sky Solutions, Coalville; Alastair Buckley and the Sheffield Solar Hub, Sheffield University; Ben Anderson, Essex University. This work is funded by the Loughborough University Centenary Fund.

REFERENCES

Anderson, B., 2013. Estimating small area income deprivation: an iterative proportional fitting approach, in: Tanton, R., Edwards, K. (Eds.), Spatial Microsimulation: A Reference Guide for Users. Springer, pp. 49–67.

Boardman, B., 2012. Synthesis fuel poverty: Lessons learnt, actions needed. Energy Policy 49, 143–148.

Cooper, G.F., 1990. The computational complexity of probabilistic inference using bayesian belief networks. Artificial Intelligence 42, 393–405.

Delcroix, V., Sedki, K., Lepoutre, F.-X., 2013. A Bayesian network for recurrent multi-criteria and multi-attribute decision problems: Choosing a manual wheelchair. Expert Systems with Applications 40, 2541–2551.

Department for Environment and Rural Affairs, Building Research Establishment, The Energy Saving Trust, 2005. Energy Use in Homes - Fuel Consuption.

Goodier, C., Austin, S.A., Soetanto, R., Dainty, A.R.J., 2010. Causal mapping and scenario building with multiple organisations. Futures 42, 219–229.

Huld, T., Müller, R., Gambardella, A., 2012. A new solar radiation database for estimating PV performance in Europe and Africa. Solar Energy 86, 1803–1815.

Iversen, G.R., 1984. Bayesian Statistical Inference. SAGE Publications.

Jensen, F.V., Olesen, K.G., Andersen, S.K., 1990. An Algebra of Bayesian Belief Universes for Knowledge-Based Systems. Networks 20, 637–659.

Koller, D., Pfeffer, A., 1997. Object-Oriented Bayesian Networks, in: Proceedings of the Thirteenth Annual Conference on Uncertainty in AI (UAI-97). pp. 302–313.

Martin, D., Nolan, A., Tranmer, M., 2001. The application of zone-design methodology in the 2001 UK Census. Environment and Planning A 33, 1949–1962.

Molina, J.L., Bromley, J., García-Aróstegui, J.L., Sullivan, C., Benavente, J., 2010. Integrated water resources management of overexploited hydrogeological systems using Object-Oriented Bayesian Networks. Environmental Modelling & Software 25, 383–397.

Neil, M., Fenton, N., Tailor, M., 2005. Using Bayesian networks to model expected and unexpected operational losses. Risk analysis 25, 963–72.

Neil, M., Tailor, M., Marquez, D., 2007. Inference in Hybrid Bayesian Networks using Dynamic Discretisation. Statistics and Computing 17, 219–233.

Pearl, J., 1990. Reasoning Under Uncertainty. Annual Review of Computer Science 4, 37–72.

Rowley, P., Gough, R., Doylend, N., Thirkill, A., Leicester, P.A., 2013. From Smart Homes to Smart Communities: Advanced Data Acquisition and Analysis for Improved Sustainability and Decision Making, Proceedings of the I-Society Conference, Toronto, June 2013.

Walker, G., 2008. Decentralised systems and fuel poverty: Are there any links or risks? Energy Policy 36, 4514–4517.

OPTIMIZED BUILDING GEOMETRY FOR PHOTOVOLTAIC AND SOLAR THERMAL FIELDS TO OBTAIN MAXIMUM SEASONAL YIELDS

Stephan A. Mathez

Solar Campus GmbH, Technologiepark Wetzikon, Buchgrindelstr. 13, CH-8620 Wetzikon, Fon: +41 (0)43 495 21 01, Fax: +41 (0)43 495 21 26, stephan.a.mathez@solarcampus.ch

ABSTRACT

Developing towards sustainable buildings with a high degree of energy independence, an increase of the solar thermal yield can only to some extent be achieved by improving solar components such as collector, storage tank, or controller. Beyond that, the geometric setup, combination and integration of solar PV and thermal modules into the architectural concept yield many opportunities in terms of orientation and inclination angles, seasonal shadings, reflection and convection effects.

Another optimization aspect for thermal systems is to align the concept according to the exergetic operating conditions of the supplied energy consumers. I.e. heat storage capacities and temperature levels have to reflect the energy demands and the fluctuation band of solar energy.

All these concepts are taken into account in a building that is presently under construction and that aims at a thermal solar fraction of 75% without seasonal storage but using a concrete core activation to store heat on a weekly basis. Investigating the mentioned phenomena and optimizing the geometric aspects are important steps towards a self-sustaining building managing to make use of the sufficient amounts of solar energy that are available even in winter time. Beyond the demonstration of these special features we hope to inspire energy specialists and architects to develop further concepts along these lines.

Keywords: self-sustaining building, concrete core activation, high solar fraction, mirror effect

BASE CONCEPT OF A PILOT AND DEMONSTRATION BUILDING IN WETZIKON ZH

The design process for the pilot and demonstration project "75% active solar building (without seasonal storage)", supported by the Swiss Federal Office of Energy SFOE was driven by the above mentioned strategies. The one-family-building with a separate office apartment and studio is built according to the Swiss standard Minergie-P-ECO (passive house) with a specific heating demand of 15 kWh/m^2/a. This is achieved by U-values of 0.1 W/m^2/K for the walls, 0.09 W/m^2/K for the roof, and 0.95 W/m^2/K for the windows (incl. the frame) respectively. The mechanical ventilation uses a soil heat exchanger to preheat the fresh air and a membrane-based enthalpy exchanger. Due to overtopping and CO_2 sensors, the ventilation flowrate can be reduced to a minimum. Loam elements and loam rendering in all inhabited rooms are further measures to keep the relative humidity in the comfortable range of 40 – 50% and to lessen the overheating in case of high passive gains. In this way, a healthy indoor climate and an ecological optimization are obtained simultaneously.

A crucial point of a predominantly solar driven building is the heat storage. It is known since 1991 that the irradiated energy in summer can be stored in a huge water tank and withdrawn in winter for heating. A certain disadvantage of this seasonal storage concept is that the collector runs on high temperatures to obtain high energy densities in the tank.

In the here presented project, the heat storage is the concrete mass of the building, including the cellar floor and ceiling and the timber-concrete composite of the upper floor. 90% of the floor area can be activated and is directly linked (without heat exchanger) to the solar circuit. In this way the concrete mass can be used as storage on a weekly basis. In order to release the heat retarded, the concrete is covered above and below by insulating materials. The U-values are chosen such that heat transfer just covers the buildings transmission and ventilation losses. As soon as internal or passive gains raise the room temperature, the heat transfer diminishes due to the reduced temperature difference. This self-controlling of the power release according to the room temperature is also known from common floor heating. But in the present building, 60 m^3 of concrete with a heat equivalent of 50 kWh/K help to keep the temperature up over a long period: Taking very moderate passive gains into account, 1 K of concrete temperature covers the energy demand of a severe winter day. Since the temperature spread of about 5 K in the concrete (from 25 to 30°C) can be fully charged about 20 times per year, yielding an estimated integrated storage capacity of app. 5000 kWh. This is comparable to the annual heating demand of 6000 kWh.

In contrary to the case of seasonal storage, the collector temperature in the present concept is always around 30 – 35 °C. The small temperature difference to the inlet temperature is possible because the solar circuit runs on water and is directly connected to the heating circuit, without heat exchanger. Furthermore, the water that drains properly down when the solar circuit stops has better heat transfer and turbulence properties than glycol mixtures, especially at these moderate temperatures.

These collector operating conditions allow for significantly higher solar gains from diffuse irradiance in winter and for a high efficiency for direct solar irradiance. In order to use this to the highest extend, the collector inclination of 70° and exact south exposure has been chosen. In addition to the direct sun light, reflected sun light from the PV panels increases the total collector irradiance. This is further described in the over next chapter.

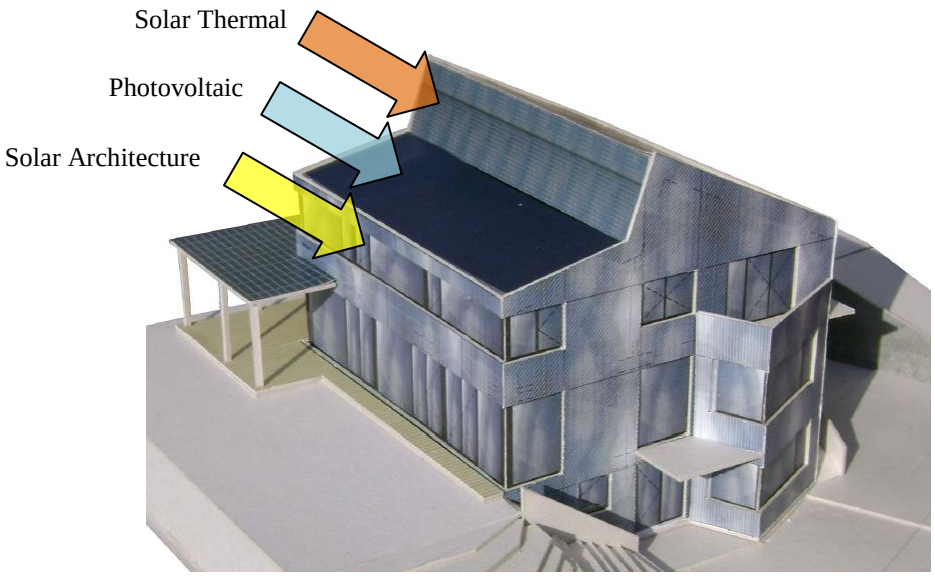

Figure 1: Pilot and demonstration building (here a picture of its model) aiming at a 75% thermal solar fraction (heating and hot water), 25% are covered by wood pellets. The photovoltaic field covers the buildings electricity demand about four times. The construction will be/was terminated in summer 2013.

GENERAL CONSIDERATIONS TO OPTIMIZE SOLAR THERMAL AND PHOTOVOLTAIC INSTALLATIONS

For solar buildings that are planned from scratch, instead of a side-by-side of PV and solar thermal, a mutual assistance can be achieved under certain conditions. For the two technologies, the following characteristics have to be considered when planning an installation [1]:

Photovoltaic:

- For Switzerland, flat inclination of 25 – 35° are optimal (steeper in the mountains)
- A good cooling (ventilation) of the modules increases the solar yield
- South or slightly south-east orientation are optimal (mornings are cooler)
- Should not be shaded by obstacles, especially in summer

Solar thermal:

- For Switzerland, steep inclination of 50 – 75° are optimal (in particular for heating)
- Warm air around the collector increases the solar yield
- South or slightly south-east orientation are optimal (afternoons are hotter)
- Should not (heavily) be shaded in winter time

Beside these two technologies, the shape of the building is another energy relevant element. The daily and seasonal variation of the irradiance orientation and intensity of direct and diffuse sunlight can be systematically used for passive heating purposes in winter and preventing overheating in summer. Therefore, the following aspects are important:

- Building orientation, big windows towards south
- East and west side: smaller windows to prevent overheating in summer
- Using a porch roof to shade windows in summer
- Special glazing with seasonally variable transmission of sunlight ("SunPattern" [2])
- Compact building shape to minimize the surface
- Thermally optimized placing of the rooms in the building interior

All these aspects should be taken account of, or should be combined together as optimally as possible. Especially on the south façade, the considered applications rival one another, but when cleverly combined (for instance a flat PV porch roof shading a window below) the technologies support each other.

IRRADIANCE AND THERMAL YIELD INCREASE DUE TO REFLECTION FROM THE PV FIELD

The reflection concept is shown in Figure 2: A relatively flat PV field with an inclination of 11° serves as a mirror for steeply inclined (70°) thermal collectors, installed above the PV field. For low sun elevations, parts of the sunlight are reflected from the PV to the thermal field. For high sun elevations, the mirror effect works the other way round, even though to a lower extend.

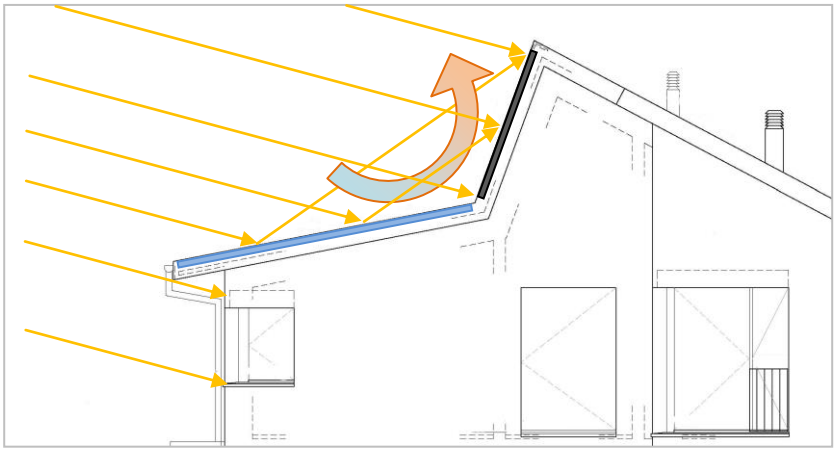

Figure 2: Mirror effect on the photovoltaic field (blue, 11° inclined) onto the thermal collectors (black, 70° inclined) for low solar elevation (15 – 25°). This yields a 20% increase in the solar thermal gain during wintertime. In addition, the rising warm air from the PV field (round arrow) reduced the losses of the thermal field (in winter and summer) and hence increasing the yield furthermore.

In order to calculate the irradiance increase due to this mirror effect, not only the geometric effects but also the polarization of the irradiance has to be taken into account. These two formulas represent the transversal and longitudinal reflectivity for an incidence angle θ and a PV glazing refraction index n:

$$R_s = \left(\frac{\cos(\theta) - \sqrt{n^2 - \sin(\theta)^2}}{\cos(\theta) + \sqrt{n^2 - \sin(\theta)^2}} \right)^2 \qquad R_p = \left(\frac{n^2 \cdot \cos(\theta) - \sqrt{n^2 - \sin(\theta)^2}}{n^2 \cdot \cos(\theta) + \sqrt{n^2 - \sin(\theta)^2}} \right)^2$$

Incident angle modifier (IAM) for transversal, longitudinal and mixed polarization modes:

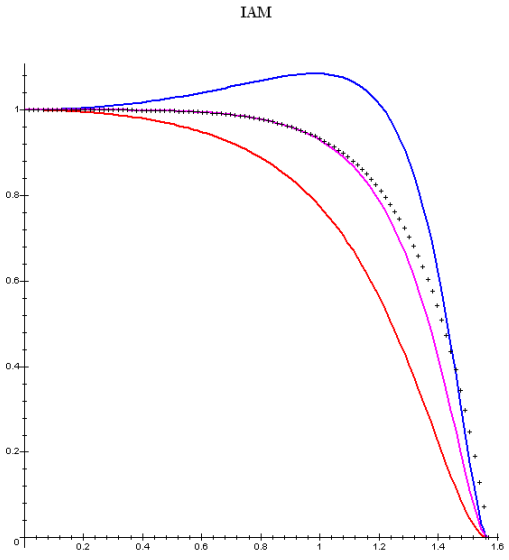

Figure 3: Angle dependence of the transmission of the transversal (upper solid line) and the longitudinal (lower solid line) polarization axis, as well as for unpolarized light (intermediate solid line). The dotted line is the IAM (incidence angle modifier) according to Ambrosetti, adjusted at 50° to the Fresnel equation.

Since the reflection angles in winter are close to the Brewster angle where the polarization effect is maximal, the irradiance amplification is slightly diminished. The mirror effect results in wintertime in total up to a 20% increase of the collector irradiance, in case of snow on the PV field even to a 40% increase. As a consequence, the solar thermal yield during wintertime increases by 20%. This demonstrates the effectiveness of the implemented mirror effect.

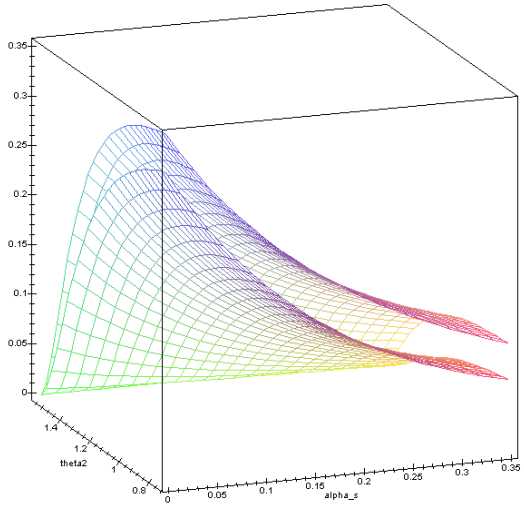

Figure 4: Irradiance increase onto the collector plane, with respect to the sun elevation (α_s) and collector plane irradiance angle (θ_2) when taking the polarization effect into account (lower plane) resp. when neglecting it (upper plane). Over all, the effect lowers the irradiance enhancement by 1/5.

On top of the irradiance effect, the mutual position of photovoltaic and the thermal field makes the waste heat from the PV field (about 80% of the irradiance turns into hot air) available for the above installed thermal field, i.e. it reduces its thermal losses. How much this effect is able to additionally increase the thermal yield will be observed by the measurements starting in summer 2013.

BUILDING AND SOLAR OPTIMIZATION USING THE SIMULATION FRAMEWORK *TACHION*

The building model of the simulation framework Tachion that was used to simulate and optimize the present building is based on the "hourly method" of the EN ISO 13790 [3]. Compared to the standard method, the computation of the passive gains in Tachion is considerably refined (window size and orientation, niche depth, porch roofs, g-value, glazing IAM, simulation of sun-blinds). For the above described object, the following solar fraction (SFu: „solar fraction to user",) has been obtained:

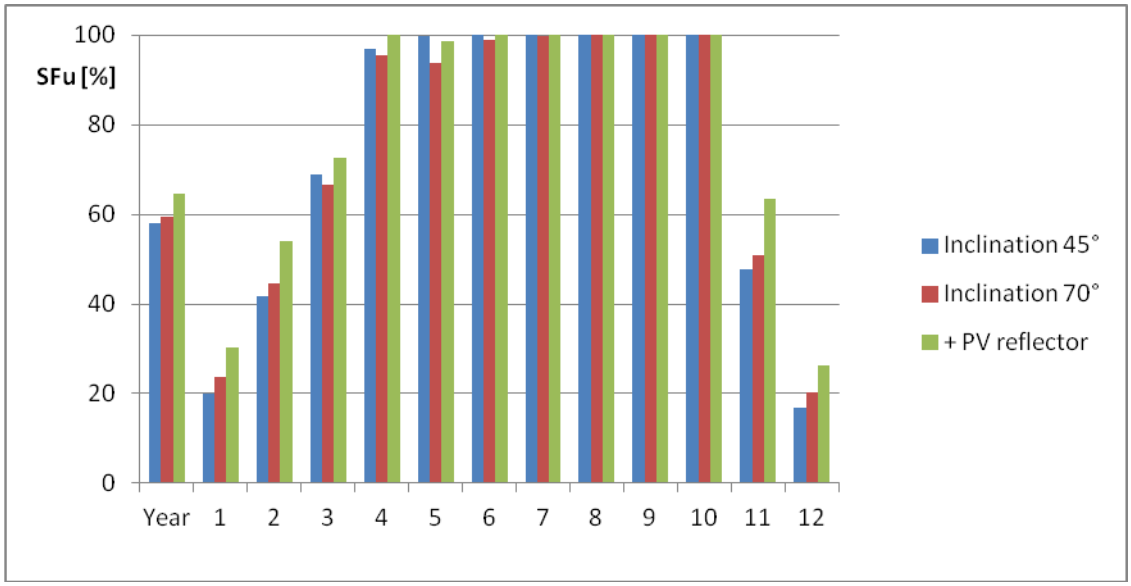

Figure 5: Solar fraction for the Minergie-P-ECO building with a specific consumption of 15 kWh/m^2 of energy reference area. The building is exactly southwards oriented. The thermal field has once been simulated with 45° inclination, than with an inclination of 70°, and finally with 70° inclination and a PV field below the thermal field with 11° of inclination.

It can well be recognized in Figure 5 how the PV field acting as a reflector for the thermal field clearly increases the solar fraction in the winter season. The total solar fraction SFu rises from 59.3% to 64.6%. If the same increase should be obtained by a larger collector field, its size would have to be enlarged by a third. Thanks to the reflectors angle, no direct sunlight it directed to the thermal collector in summertime and hence does not intensify the overheating problem.

The photovoltaic yield is reduced due to the flat inclination by 4% compared with the optimal inclination angle of 32°. But in the summer, the reflection from the thermal to the PV field again makes up about half of this reduction.

CONCLUSION

Solar irradiance is a high-valued and multi-purpose form of energy. Thanks to modern building technologies and sophisticated irradiance collection and heat storage, a net consumer building can be turned into a net energy producer. The presented pilot building demonstrates that the "best" form of using the solar energy involves a bunch of aspects and that dedicated software tools are required in order to release the maximum potential of these technologies.

REFERENCES

1. Mathez, S.A. (2012): Synergie-Effekte zwischen Solarthermie, Photovoltaik und Solararchitektur mit Hilfe des Simulationsframework *Tachion* modellieren und sichtbar machen. Proceedings of the Symposium on Solar Thermal Energy, OTTI 2012, Staffelstein, Germany.
2. Mathez, S.A. and Sachs, W. (2011): Glazing structures with a maximum seasonal contrast ratio and the simulation of such building envelopes. Proceedings of the CISBAT 2011, EPFL, Lausanne, Switzerland.
3. EN ISO 13790:2008, Energy performance of buildings - Calculation of energy use for space heating and cooling (ISO 13790:2008)

HEAT PUMP SYSTEMS WITH UNCOVERED AND FREE VENTILATED COVERED COLLECTORS AS ONLY HEAT SOURCE

I.Mojic[1]; M.Y. Haller[1]; B.Thissen[2]; E. Frank[1]

1: Institut für Solartechnik, HSR Hochschule für Technik Rapperswil, Oberseestrasse 10, CH-8640 Rapperswil

2: Energie Solaire S.A., Rue des Sablons 8, Case postale 353, CH-3960 Sierre

ABSTRACT

In the past years the research and development activities for heat pumps in combination with solar thermal collectors for preparation of domestic hot water and space heating were increasing. In most of these systems the collectors are used as a direct heat source for the load-side storage and thus only if the irradiation is high enough to reach the temperature level that is needed to increase the temperature of this storage. In this work it was analysed how low irradiation and the ambient can be used also as heat source. Therefore, three different systems were modelled and simulated in TRNSYS. One of the systems is a basic solar-heat pump (air source) combination which is sold today on the market. The other two systems use solar collectors in combination with an ice-storage as the only heat source of the heat pump. One of these variants uses unglazed selective coated absorbers and the other variant uses covered collectors with controlled natural ventilation behind and in front of the absorber. All systems have been sized to have the same costs for the end consumer. A single family house with boundary conditions according to the IEA SHC/HPP Task44/Annex38 was simulated with four different climates. The simulation results show that unglazed collectors and a brine heat pump in combination with a 400 litre ice storage can work reasonable and even reach a better performance than the reference. The free ventilated collector shows a benefit compared to the unglazed and standard glazed collector only for very warm climates and low energy demand.

Keywords: Selective Unglazed Collectors, Heat Pump, Natural Convection, Ice Storage

INTRODUCTION

Heat pumps are a favoured choice for providing heat for new buildings or for the replacement of old heating systems. However, their application is restricted: At some places, for example, it is forbidden to drill boreholes, and an air-source system may be unfavourable because of noise or aesthetic reasons. Alternatively, a heat pump system which uses uncovered selective collectors in combination with an ice storage as the only heat source might be used. The use of uncovered collectors instead of covered collectors gives the advantage that the ambient heat can be used additionally to the solar irradiation. The disadvantage is that uncovered collectors have higher heat losses at elevated temperature levels which mean that the direct contribution of these collectors at the temperature level of the heat demand is significantly lower than for covered collectors. In this work, a collector-design is investigated which is expected to combine the advantages of uncovered and covered collectors. This can be reached with a new type of covered collector with controllable free ventilation. It allows ventilation by natural convection between the glazing and the absorber as well as between absorber and insulation by additional openings that are passively controlled to open and only when needed (see Figure 3). In this article a reference solar and heat pump system was compared with two alternative heat pump systems that involve an ice storage and different collector concepts:

One with unglazed selective absorbers and the other one with passive controlled free ventilation collectors.

METHOD

TRNSYS 17 was used for all simulations. The boundary conditions were based on the IEA SHC/HPP Task44/Annex38 (T44A38) [1], but slightly adapted in order to include different climates and a more realistic DHW profile which was calculated according to Jordan & Vajen [2], detailed information can be found in Mojic et al. [3]. Table 1 summarizes the climates and the corresponding heat loads.

Location, Country Code	Heating Demand [kWh/(m^{2}a)]	Domestic Hot Water Demand [kWh/a]	Mean ambient Temperature [°C]
Zurich, CH	56.4	3038	9.1
Carcassonne, F	23.2	2691	13.2
Davos, CH	79.6	3571	2.8
Helsinki, FIN	93.3	3343	5.5

Table 1: Climates and heat demand for four different locations.

Reference System

In this simulation study a reference system was chosen that represents a state of the art system which is sold many times on the market according to its manufacturer. Figure 1 shows the hydraulic design of the reference. The collector area is 10 m^2 of standard glazed flat plate collectors (a_1 = 3.95 W/(m^{2}K), a_2 = 0.0122 W/(m^{2}K^2), η_0 = 0.793) with 45° inclination and south orientation. The heat storage has a volume of 750 litres with an internal coiled heat exchanger for the solar input (U = 1125 kJ/(hm^{2}K)). For the domestic hot water supply an external heat exchanger is used which is simulated without heat losses (UA = 19200 kJ/(hK)). The reference system includes an air-source heat pump with a power of 8 kW and a COP of 3.5 at A2W35. The heating distribution (floor heating) was simulated with a flow temperature of 35 °C and return temperature of 30 °C (Davos and Helsinki 40/35).

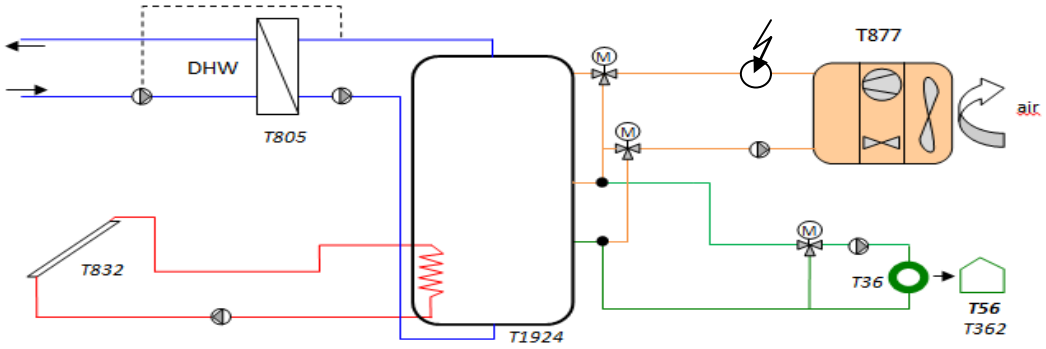

Figure 1: Hydraulic scheme of the reference system; Txy = TRNSYS Type number xy

Alternative Systems

The ***alternative systems*** (unglazed and ventilated) have different collectors, a different heat pump (brine source) and an additional ice storage. The hydraulic scheme can be seen in Figure 2. The heat pump was replaced by a brine-source heat pump with a power of 8 kW and a COP of 4.65 at B0W35 that is optimized for very low brine temperatures (minimal inlet temperature is -18 °C). The ice storage has a volume of 400 litres and is equipped with a coiled pipe heat exchanger (diameter 20 mm, 30 mm distance between the pipes).

For the ***unglazed system*** the collector field was replaced by selective unglazed absorbers with a total area of 18 m^2 (a_1 = 9 W/(m^2K), a_2 = 0 W/(m^2K^2), η_0 = 0.954) inclined at 45° and orientated south.

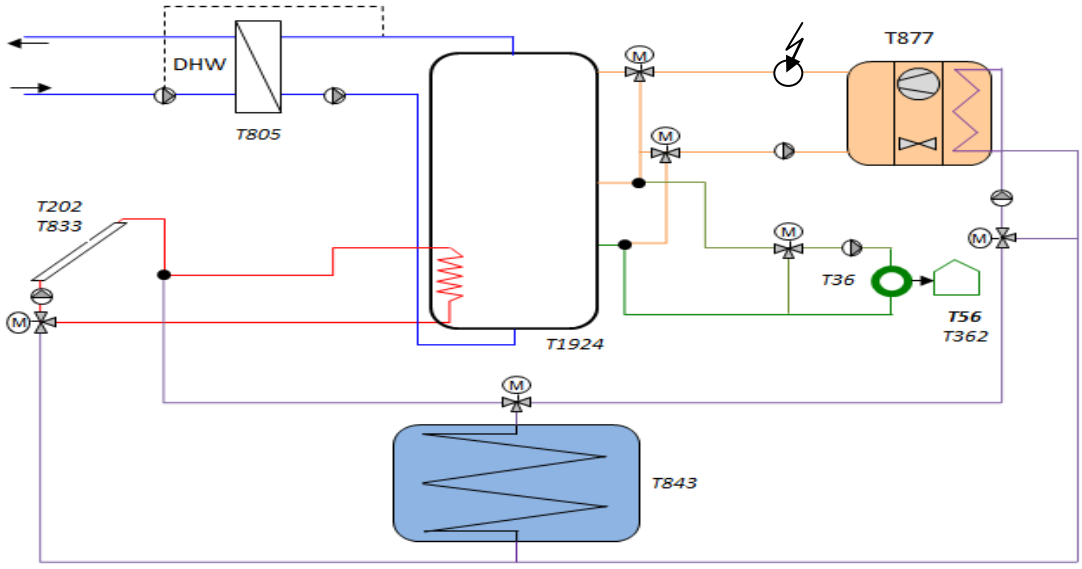

Figure 2: Hydraulic schema of the both alternative systems; Txy = TRNSYS Type number xy

The heat pump uses primarily the collectors as a heat source. If the collector outlet temperature gets too low, the heat pump switches to use the ice storage as a source. The main priority of the collectors is to charge the heat storage directly. Only if the required temperature cannot be reached, the collectors are heating the ice storage up to a maximum of 20 °C. In the case that the heat pump power output is too low an electric backup heater switches on which is placed downstream of the heat pump outlet.

The ***ventilated system*** has the same hydraulic scheme as shown in Figure 2. The only difference to the unglazed system is that another collector design is used as shown in Figure 3. This is basically a standard flat plate collector with the option to open channels which allow a natural convection between the absorber and the glazing as well as between the absorber and the insulation. The idea behind this concept is to additionally use ambient air as a heat source for the heat pump at low irradiations where direct collector heat use for the load-side storage would be inefficient or impossible.

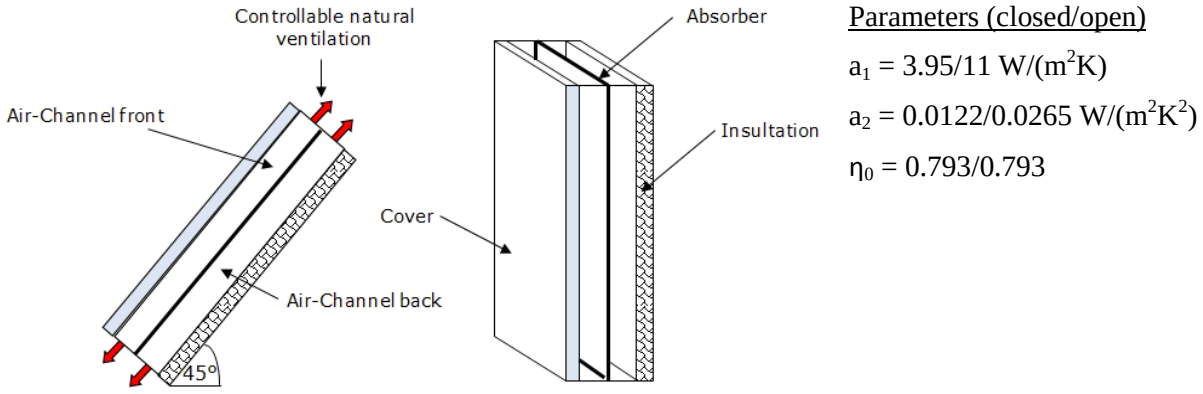

Figure 3: Design of the natural ventilated collector

The TRNSYS collector model (Type 832) [4] was modified to enable the ventilation feature. The collector parameters for the open air channels were calculated in EES (Engineering Equation Solver) based on equations from the Kolektor 2.2 software [5]. The free convection heat transfer was based on the theory of Klan [6]. A possible influence of wind on the air flow in the channels was not taken into account. For this first potential study the development of a mechanism for passively opening and closing the ventilation channels has not been developed yet. In these simulations it was assumed that this mechanism works perfect.

A fair comparison of the performance of the three different collector and system concepts can only be done if the investment cost for all three systems are equal. Therefore, the collector areas of the alternative systems have been sized in order to reach the same estimated investment cost as for the reference. Thus, the unglazed and the ventilated system have collector areas of 18 m² and 14 m² instead of 10 m² for the reference.

RESULTS

Table 2 shows the parameters which were used for the comparison of the three systems.

Parameter	Unit	Description	Boundaries
$SPF_{SHP+,pen}$	-	seasonal performance factor	complete system (T44A38) [3]
$Q_{solar,tot}$	MWh	collector gains	collector field without heat losses of the pipes
$W_{el.tot}$	MWh	electric demand of the total system	complete system, with space heating pump
$W_{el.Backup}$	MWh	electric demand of the backup heating	only backup heating device

Table 2: Overview of the comparison criteria for the simulation study

The SPF factor is the quotient of all energy gains contributed to the system divided by the total electricity consumption of all system components including the space heating pump and penalties for comfort losses because of not reaching the needed temperatures for space heating and domestic hot water, according to the definitions in T44A38 [3].

Figure 4 shows the results for the four different climates, all energies are in MWh.

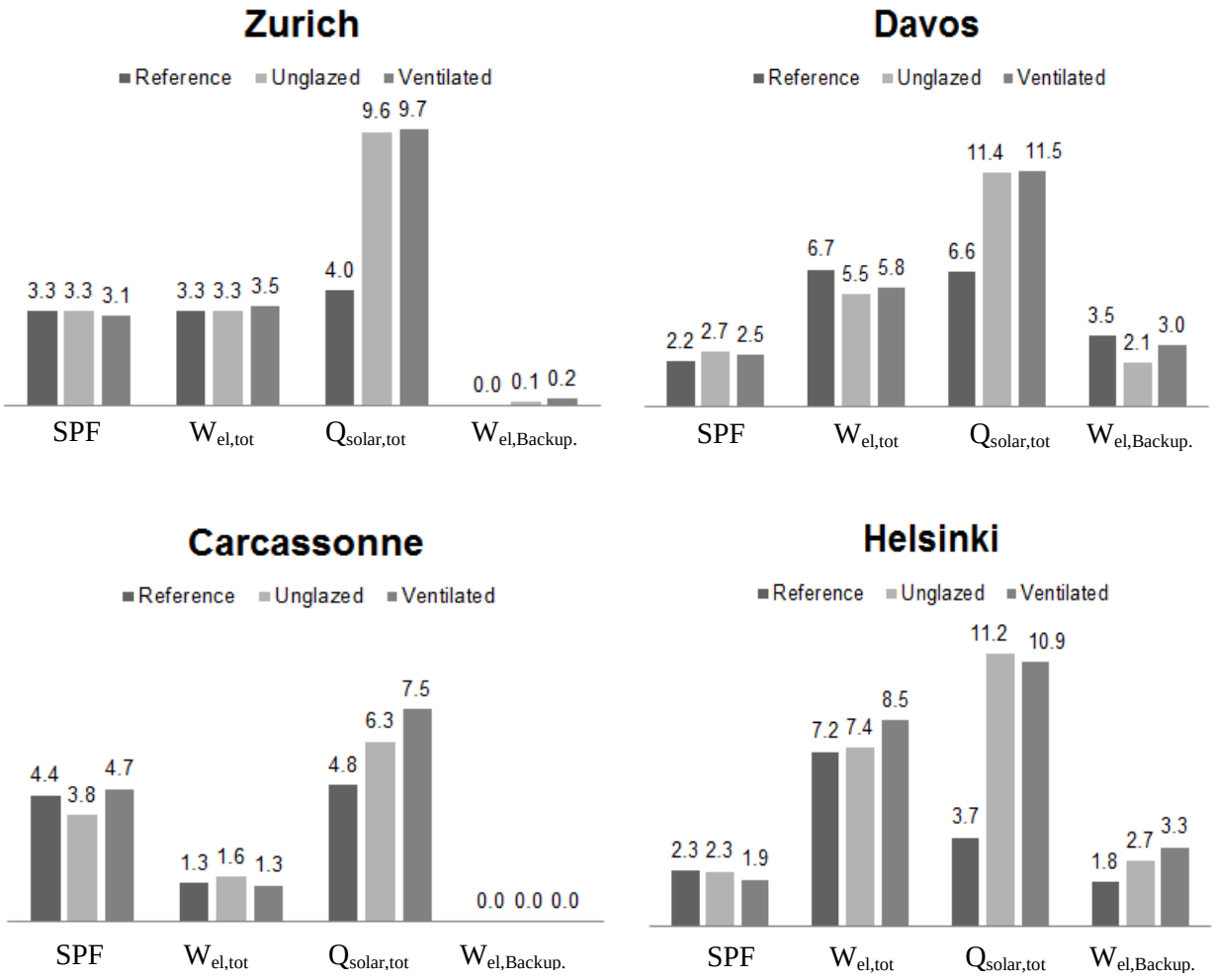

Figure 4: Result summary of the comparison of all three systems, all energies in MWh

The simulation results show that for Zurich the unglazed system can perform as good as the reference system, also for the very cold climate Helsinki the unglazed system has the same SPF as the reference. High differences between these two systems can be found for the climates Davos and Carcassonne, here the comparison shows that the unglazed system performs about 23% better in Davos and 14% worse in Carcassonne.

Compared to the reference, the ventilated system performs +14 % better for Davos and 7% better for Carcassonne, but only for Carcassonne the results are better than those of the unglazed system. Naturally, the heat delivered from the collectors is much higher (2-3 times) for the unglazed and the ventilated system then for the reference. However, only for Carcassonne the heat output of the ventilated collectors is significantly higher than for the uncovered collectors.

The electric backup heater contributes a lot to the total electric demand for the cold climates of Davos and Helsinki. This is an indication that the chosen heat pump is not suitable for these cold climates.

DISCUSSION AND CONCLUSION

The comparison of the simulated systems shows that their performance depends a lot on the climate. For none of the systems it can be claimed that it is the best for all cases. The ventilated system outperforms the others only for the climate of Carcassonne.

There is a possibility that the performance of this concept is underestimated because of the very basic simulation model of the collector that does e.g. not take into account the influence of wind on the air flow in the channels when they are open. On the other hand, the unglazed system leads to a good performance compared with the reference for many cases which makes it a good alternative. Only for Carcassonne the performance is significantly worse. The reason for this is the lower amount of heat that can be loaded directly to the load-side storage. A second one can be the low heating demand for this building and climate that leads to a high DHW share of the total heat load. It has to be mentioned also that for the unglazed collectors not all effects are taken in account, for example the loss of selectivity when the collector is covered by water droplets from condensation of moisture from the air [7] or the ice formation that may occur when the circulating fluid is at temperatures below 0 °C.

To conclude it can be said that selective unglazed collectors in combination with a small ice storage can lead to a good and reasonable SPF, which is in the same range or even better than a state of the art air source heat pump combined with standard glazed collectors. Additional benefits of the unglazed system compared to the reference air source heat pump are that noise emissions and outdoor ventilated air heat exchanger units can be avoided.

ACKNOWLEDGEMENTS

The research leading to these results has received funding from the European Union's Seventh Framework Programme FP7/2007-2013 under grant agreement n° 282825 – Acronym MacSheep.

REFERENCES

1. Haller, M., R. Dott, J. Ruschenburg, F. Ochs and J. Bony (2012) IEA-SHC Task 44 Subtask C technical report: The Reference Framework for System Simulations of the IEA SHC Task 44 / HPP Annex 38: Part A: General Simulation Boundary Conditions, IEA-SHC, Paris, www.iea-shc.org/task44.
2. Jordan, U. & Vajen,K., 2003. 3.4 Hot Water Consumption. In: W. Weiss, Ed. Solar Heating Systems for Houses - A Design Handbook for Solar Combisystems. James & James, London (UK). ISBN: 1-902916-46-8.
3. Mojic, I., Haller, M.Y., Thyssen, B. & Frank, E., (2013). Wärmepumpen-Systeme mit selektiven unabgedeckten und frei belüftbaren abgedeckten Kollektoren als einzige Wärmequelle. In: Proceedings of the 23th OTTI Symposium Thermische Solarenergie Regensburg 2013, Bad Staffelstein (Germany). CD.
4. Haller, M.Y., (2012). TRNSYS Type 832 v5.00 „Dynamic Collector Model by Bengt Perers" Updated Input-Output Reference. Institut für Solartechnik, Rapperswil. (Switzerland)
5. Matuska, T. & Zmrhal, V., (2009). KOLEKTOR 2.2 reference handbook. Available from http://www.fsid.cvut.cz/~matustom/kolektor.htm (27.02.2013), CTU in Prague.
6. Klan, H., (2006). Wärmeübergang durch freie Konvektion an umströmten Körpern. VDI-Wärmeatlas. S. Fd 1. Springer-Verlag Berlin Heidelberg New York ISBN: 3-540-25504-4
7. Philippen, D., Haller, M.Y. & Frank, E., (2011). Einfluss der Neigung auf den äusseren konvektiven Wärmeübergang unabgedeckter Absorber. In: Proceedings of the 21st OTTI Symposium Thermische Solarenergie, Regensburg 2011, Bad Staffelstein (Germany), CD.

A CONCEPT FOR INTELLIGENT FACADE SYSTEM

M.L. Otreba; K . Menzel; M . Siddig

University College Cork, IRUSE, 2.12 Western Gateway Building, Western Road, Cork, Ireland

ABSTRACT

Older buildings represent a significant percentage of total building stock in Europe, therefore their impact on energy consumption needs to be addressed. The integration of smart and renewable technologies is a widely accepted and chosen way to approach changes to these buildings. Most of existing buildings, commercial, require some form of changes and renovation could be the only choice considering different constraints (financial, listings order, etc.) to achieve a desirable level of the performance. One of the benefits of the approach presented in this paper is that each room or zone can be renovated independently of the rest of the building minimizing any disruptions to the operational processes of the building. The concept is based on an intelligent façade design and focuses mainly on four aspects of the design

1.The architectural aspect describes modularity on different levels: whole system level, component and sub-component level.

2.The structural section describes how the facade system and its application will influence the existing host structure of a renovated building. This part is split into three scenarios: facade replacement, application of a new skin, window unit replacement including integrated additional panels fixed to an existing wall.

3.The energy and control section will describe a process to establish the performance of the new concept deployed on a single zone. It will also verify the viability of the renovation.

4.The Control and monitoring section of the design describes the control logic of the system.

Finally the concept will be applied to a case study for one of the University College Cork campus buildings, Civil and Environmental Engineering (CEE). This case study will simulate a renovation process of the IT laboratory. The case study will involve replacement of existing single glazing windows with new modular units. Each unit will integrate an energy cogeneration or energy storage system with the ability to extend their harvesting capabilities through external wall based panels.

Keywords: Renovation, Modularity, BIM, Façade Design, Energy Performance, Single zone approach.

INTRODUCTION

Among some recently proposed plans endorsed by the EU Commissions is the Action Plan for Energy Efficiency. In this plan the main goals for the EU until 2020 are: to decrease greenhouse gas emissions by 20%, increase use of renewable energy by 20%,to reduce of energy consumption by 20%. The commercial and residential buildings sector have quite an impact on energy consumption in all these areas, responsible for about 40% of overall energy use and about 36% of CO2 emissions.[1,2] Furthermore residential sector accounts for 77% of CO2 from all buildings in the EU![2] . The main steps taken by the EU Commission to address the above issues were presented by Directive 2010/31/EU in February 2012 focusing on mandatory introduction of EPCs (Energy Performance Certificate).They are obligatory for each EU member to increase awareness of public bodies in areas of energy efficiency focusing on new buildings to apply near zero energy standards. Older existing buildings should be renovated to similar standards ensuring positive impact in future use.

According to the Building Performance Institute of Europe in 2011 about 75 % of total building stock is housing which accounts for over 230 million dwellings across 27 EU countries[3]. In 2010 the Ministry of the Interior and Exterior Kingdom Relations published statistics showing housing stock per EU country. This report indicates that in most of EU countries between 50 and 60% of current building stock was built before 1970 [4].
Currently there is a number of European projects that promote prefabricated units for facade renovation. International Energy Agency (IEA) in Energy Conservation in Buildings and Community Systems (ECBCS) Annex 50 introduces 4 systems that were used as renovation solutions for existing buildings[5].

System	Swiss	Austrian	French	Portuguese
Module structure	Multi layered	Multi layered	Multi layered	Multi layered
Integrated systems	Sun shading, Ventilation	Solar comb wall, solar thermal	Ventilation	Ventilation
U-values [W/m^{2}K]	0.10-0.15	Construction dependant	0.22	0.21 middle panel
Conclusions/ Suitable for	Yes	Yes	Yes	Yes

Table 1: Comparison of 4 Prefabricated Facade systems for renovation.[5]

CONCEPT

The main concept is focusing on a generic modular, prefabricated system where integration of new modules with existing buildings can be achieved on a single zone level.
The system is designed to integrate energy co-generation, storage capabilities, and a high level of control. Through a common interface, adapted for various constraints (structural, listing etc.) the system elements can be integrated, suitable for decentralised renovation on a zone by zone basis. The interface is designed to improve the flexibility of the connection and ease of replacement of outdated technologies in future years. Figure 1 presents the concept on very general level.

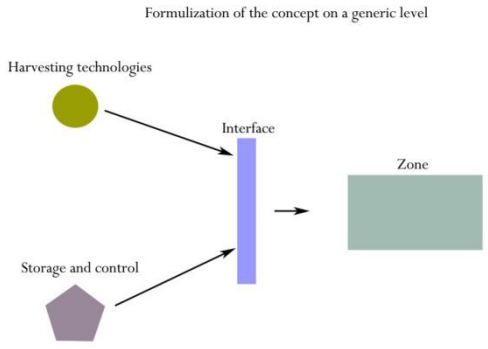

Figure 1: The concept on a generic level.

Architecture:

The system design is based on modularity concepts. It is composed of dimensionally and functionally coordinated modules that are linked through simple interfaces. Each module is decomposed into smaller components that are designed independently. This approach

minimizes the amount of alteration needed in the case of replacement or upgrade and provides the following advantages: improved productivity and efficiency, increased flexibility, improved components quality, facilitated design standardization, reduced production and construction time, reduced labour and material consumption. The modular architecture of the proposed system means that the functional and physical components are mapped on one-to-one bases. In other words, the interfaces among interacting physical components are decoupled. Changes made to a specific component can be done independently and do not require change to the other components in order for the system to function properly. This concept facilitates responding to changes required for upgrade, add-ons, adaptation and wear. Table 2 describes it in the following levels :

System level (figure2)	Modular unit level	Components level
- flexible dimensional range; increases geometric possibilities while complying with the building's boundary conditions. - standardization of the approach; dimensioning and interface allow future extension with minimum alterations to the structural frame.	- different components are combined to form a single independent unit. - single module can have multiple vertical and/or horizontal sub-modules. - ease of replaceability by other units with different functionalities.	-flexibility of the system for replacing existing components by new or more efficient ones. -integration of different technologies: PV panel, opaque panel, heating panel, window panel singular, window panel with extension

Table 2: Architectural description of the system.

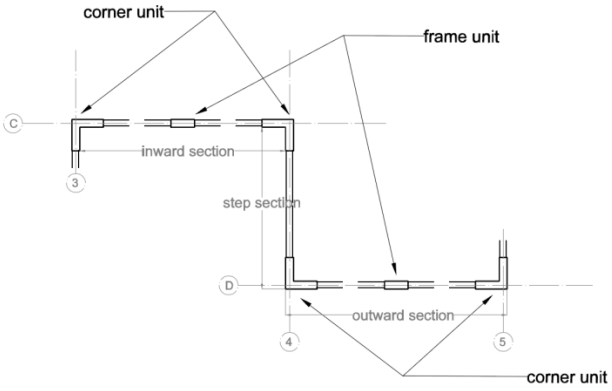

Figure 2: System level of the design. Different types of modules.

Structural:

This aspect of the design focused on different types of existing structures and the level of applicability of the new concept design. Amongst the structural types of buildings the system can be applied to. Table 3 describes in detail possible scenarios and applicable choice of the system type.

Type of building	Traditional wall			Existing modular facade	
Renovation process	Wall replacement	Extra skin	Window replacement (figure 3,4)	Replacement	Extra skin
System selection	Whole modular system	Whole modular system	Window module	Whole modular system	Whole modular system
Main Factor	Structural capacity before and after renovation	Structural capacity before and after renovation	Additional connection to a wall if module to be extended	Structural capacity before and after renovation	Structural capacity before and after renovation
Comment	Very work load and financially intense process	Might require additional footing or connection to existing structure	Extension possible with co-generation systems	Use of existing framing	Might require additional footing or connection to existing structure

Table 3: Structural approach of the systems .

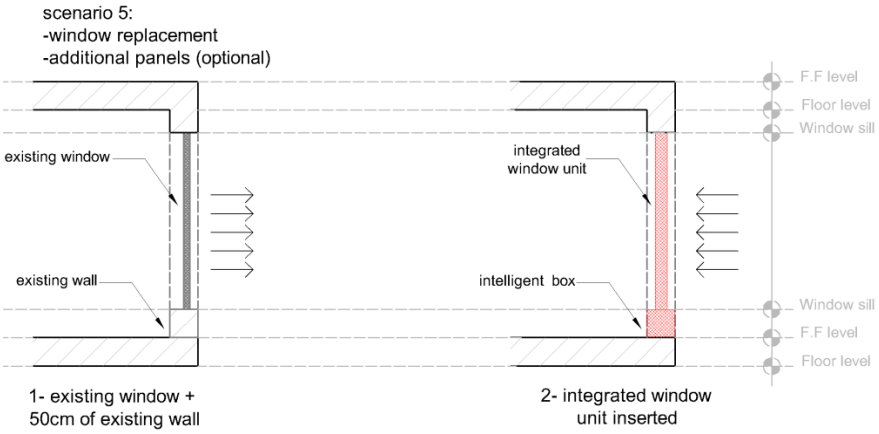

Figure 3:Section view of replacement of the window module unit.

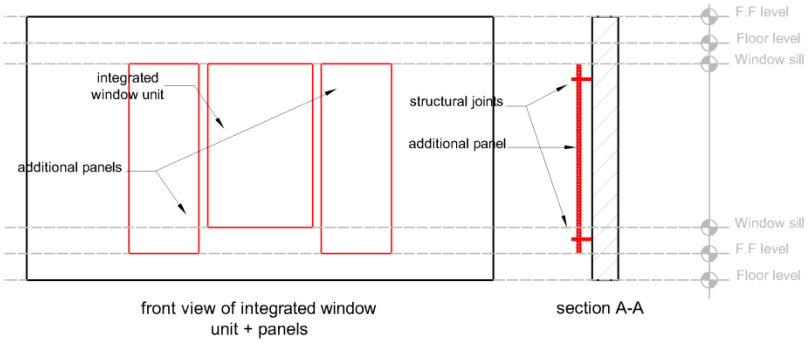

Figure 4:Window module unit with additional panels.

Energy and Control

The concept integrates energy co-generation and control capacity. There are a number different types of main modules. These can be used in three main scenarios: the whole system replacement, additional layer or window replacement. Technologies integrated are PV (Photovoltaic), solar thermal, and PCM (Phase Changing Material). Each one of the main modules integrates all aspects of sensing and control system. These systems not only control the facade performance but also provide data about internal and external conditions. The main controller is designed to have additional abilities to connect to existing wireless networks or to deploy additional in zone sensors. Figure below represent a window module with the integrated PV panel as an additional external panel. The integrated intelligent box includes storage capacity and controllers. Figure 5, 6 and 7 presents the intelligent box for window replacement tailored for PV integration.

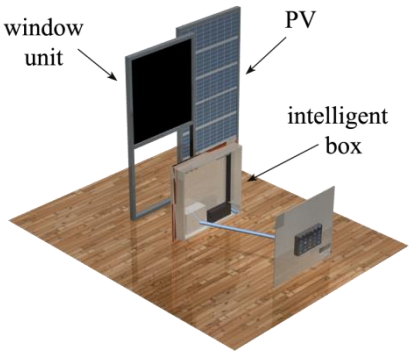

Figure 5: PV module

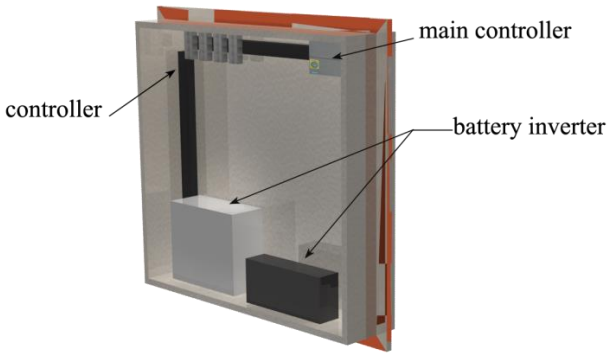

Figure 6: Detail of the intelligent box

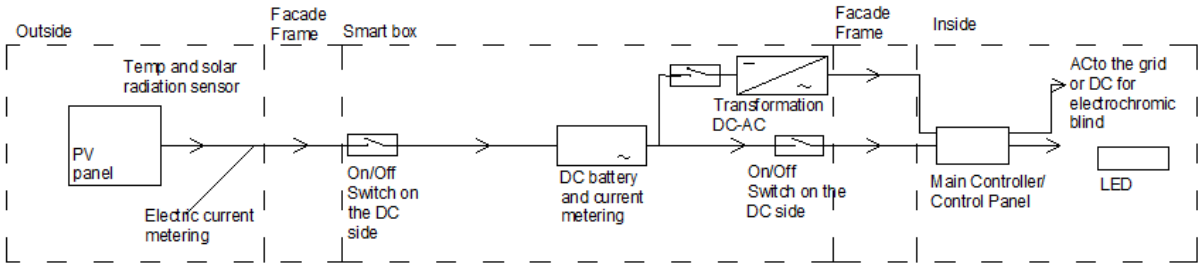

Figure 7: PID of PV window module

CASE STUDY

Computer lab CE108 of the Civil and Environmental Engineering building, University College Cork was chosen as a case study to determine the efficiency of the proposed PV based façade system. A simulation process was conducted using the proposed window module with integrated photovoltaic panels on the south façade of the building. In order to utilise the energy generated by the photovoltaic panels, a new lighting layout was proposed using LED lamps. Analysis were carried out to establish the room occupancy, lighting conditions, estimated solar radiation levels and estimated energy generation from the PV panels. The Sunpower E20/435 Solar Panel was chosen with a cell efficiency of 22.5% and module efficiency of 20.1%. In order to estimate the power produced by the panel, daily and monthly weather reports from Valentia Island Observatory (Met Éireann) were used. Overhead lighting in the room was downgraded to provide a luminance level of 200 lux, with manually controlled LED desk lamps providing additional luminance as needed by occupants in other words 12 overhead T8 lamps were reduced to 9 and individual desk lights were provided. The simulation results prove that the proposed lighting conditions provide a more adequate lighting level for the room and did so

using less power. The installation of the window module on the south face of the computer lab including 5 solar panels would provide more than enough electricity to offset the lighting power demand in the computer lab.It was assumed that all lighting in the remainder of the building is in full operation during the occupation of the building (10hours per day, 6 days a week). [5] Figure 6 presents results for electricity demand for room CE108 Apart from weeks 1-9 and 42 - 52 photovoltaic generated power will be more than sufficient to cover new lighting demand. However the mid weeks in a year are not densely populated by students (summer break) this power could be utilised by occupants of offices using the premises the whole year around.

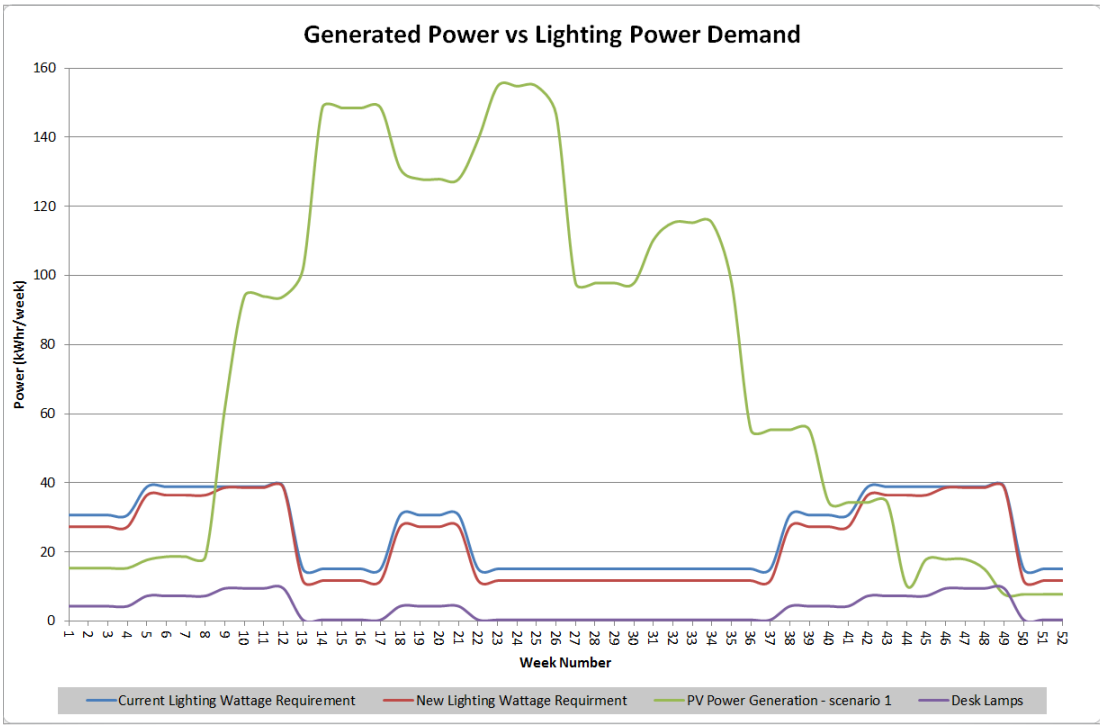

Figure 6: Generated Power vs. Lighting Power Demand [5]

REFERENCES

ACE, : National and Local Employment Impacts of Energy Efficiency Investment Programmes, Summary Report, London: Association for the Conservation of Energy, 2000

Itard, L. and F. Meijer: Towards a sustainable Northern European housing stock: figures, facts and future, Amsterdam: IOS Press. Odysee, 2008

BPIE (Buildings Performance Institute of Europe): Europe's buildings under the microscope A country-by-country review of the energy performance of buildings, October, Brussels. 2011

Ministry of the Interior and Kingdom Relations: Housing Statistics in the European Union", September, The Hague. 2010

IEA ECBCS Annex 50 : Prefabricated Systems for Low Energy Renovation of Residential Buildings, Retrofit Module Design Guide, March, 2011

K.Cullen and J.Meade: Evaluation of Retrofit Technologies for Building Renovations, 2013, Cork - not published.

EXPERIMENTAL AND MODELING ANALYSIS OF A URBAN SETTLEMENT SUPPLIED BY A DISTRICT HEATING SYSTEM BASED ON BIOMASS: A STUDY CASE IN SOUTH-TYROL

D. Prando; M. Renzi; A. Gasparella; M. Baratieri

Faculty of Science and Technology, Free University of Bolzano, piazza Università 5, 39100 Bolzano, Italy

ABSTRACT

The aim of this work is the energy efficiency assessment of a urban settlement supplied by a district heating system based on biomass located in Renon (Bolzano, Italy). The study investigates the energy performance of a 1 MW_{el} Organic Rankine Cycle (i.e., ORC) connected to a district heating network that provides heat to several domestic users. A wood chip boiler, fed by wood waste and forest residues, provides thermal energy to the ORC system. The electricity produced is delivered to the electric grid and the heat recovered in the condenser is delivered to domestic users.

A monitoring activity has been carried out to evaluate the energetic performance in different operating conditions; the system involves both the power plant, the distribution network and the users. Furthermore, a thermodynamic model that simulates the system operation has been developed in Matlab-Simulink environment using REFPROP 9. A preliminary test of the model has been carried out comparing the numerical results with the experimental data.

Keywords: CHP, district heating, ORC, biomass

INTRODUCTION

The current energetic scenario of South Tyrol involves 70 power plants based on woody biomass, most of them supplying heat to districts. The thermal power of these plants ranges from 100 kW to 10 MW and most of them are based on direct combustion. Some of the power plants set an Organic Rankine Cycle (ORC) for the combined generation of heat and power.

Organic fluids are particularly suitable for small scale power plant with heat source at low temperature [1,2]. The ORC is a standardised and reliable technology as opposed to gasification that is a promising technology but with uncertainty about performance and reliability. The ORC has a low power-to-heat ratio but a high turbine efficiency at partial load that favours the heat load tracking [3–7]. Beyond the energy technology systems, district heating systems play a key role to promote large scale renewable energy integration and can improve the matching between supply and demand. The efficiency of such systems can be improved by means of simulation tools that allow the operational optimization [8–10].

This work focuses on the experimental energy balance of a 1 MW_{el} ORC power plant with the main aim of determining the electrical efficiency with respect to the temperature of the network. A thermodynamic model that simulates the system operation has been developed in Matlab-Simulink environment using REFPROP 9 for determining the fluid properties and will support the design of the improvement management strategies of the system. A preliminary validation has been carried out comparing the numerical results with the experimental data.

METHOD

System characteristics

The investigated system is a district heating (DH) plant of the urban settlement located in Renon (Bolzano, Italy). The heat distribution network connects 250 users of different size (single buildings, apartment houses and hotels) with a supply temperature at approximately 90°C and a return temperature that depends on the user demand.

Figure 1 shows the schematic diagram of the power plant that provides heat to the district heating; the system is mainly based on a biomass boiler coupled with an organic Rankine cycle. The biomass boiler has a nominal power of 5.4 MW_{th} at a supply temperature of 310°C and a return temperature of 240°C. At nominal condition, the ORC produces 1 MW_{el} and 4 MW_{th} that is provided to the network at a mean temperature around 75°C. The boiler is fed with wood chip that consists of a main share of spruce forest residues from the surroundings (70%) and a small share of wood waste from sawmill (30%). Before feeding the boiler the feedstock is dried up to a water content around 15-25% on wet basis. Some samples collected on site show that the wood chips have a lower heating value ranging between 14-16 MJ/kg_{ar}.

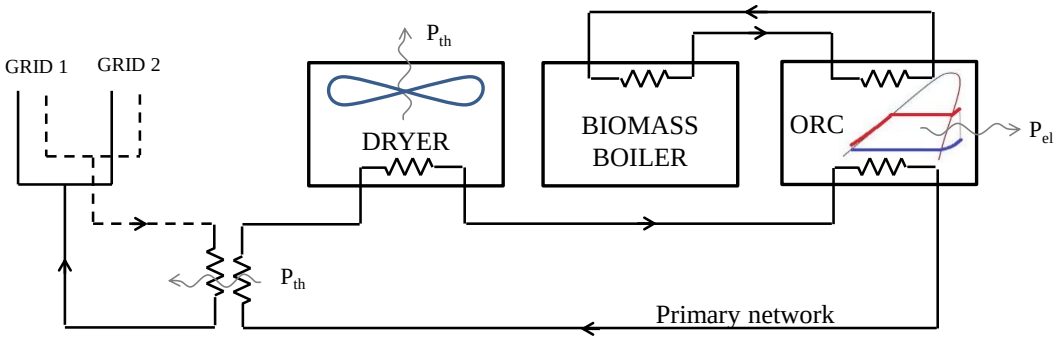

Figure 1: Schematic diagram of the power plant components.

As shown in Figure 1, the district heating has two main branches, the first branch supplies heat to the urban settlement of Klobestain (approx. 60% of total generated heat) and the second one to Oberbozen (approx. 40% of total generated heat). The length of the main network is about 23 km of steel pipe with diameter of 200 mm close to the power plant and 100 mm near the users. The water content in the network is approximately 500 m^3. The heat produced by the power plant is exchanged with the network and with the biomass dryer. The heat used by the dryer is around 53% on a yearly basis, but at lower temperature with respect to the network because the return stream from the network grid is used to supply the heat exchanger of the dryer.

Monitoring activity

The power plant has been monitored for the whole year 2012 with a time step of 1 minute to detect the operating performance of the different components. The supply temperature, the return temperature and the water mass flow rate have been recorded for the two branches of the district heating, the dryer, the biomass boiler, the input and output of the ORC. Also the electricity generation has been monitored to define the electrical efficiency of the organic Rankine cycle. A complete data set of the biomass mass flow to the boiler is not available, because the boiler inlet is not equipped with load cells.

The collected data have been pre-processed to filter data corresponding to unexpected or planned outages of the plant due to detected anomalies or to the maintenance program (which

is usually scheduled twice a year), that causes temporary arrest of the plant and, consequently, lack of data.

The accuracy of the temperature sensors embedded in the power plant has been checked by means of thermocouples (J and K type) and a portable multimeter (Agilent 34972A). The maximum deviation between the values detected by the plant sensors and the ones measured by the portable instruments has been verified to be lower than 1%.

ORC modelling

A basic thermodynamic analysis has been performed to define the main operating characteristics of the ORC generator. The working fluid used is octamethyltrisiloxane (MDM), which is a siloxane particularly suitable for low temperature power generation due to its thermophysical properties.

The biomass boiler provides heat to the thermal oil that flows to the evaporator and to the economizer where the working fluid of the ORC is pre-heated and vaporized. The organic vapour expands in a turbine, which is directly coupled to a synchronous electric generator. The exhaust vapour flows through a condenser and exchanges heat with the water flow of the primary circuit of district heating. Finally, the organic fluid is pumped to the regenerator before the next pre-heating and evaporation processes.

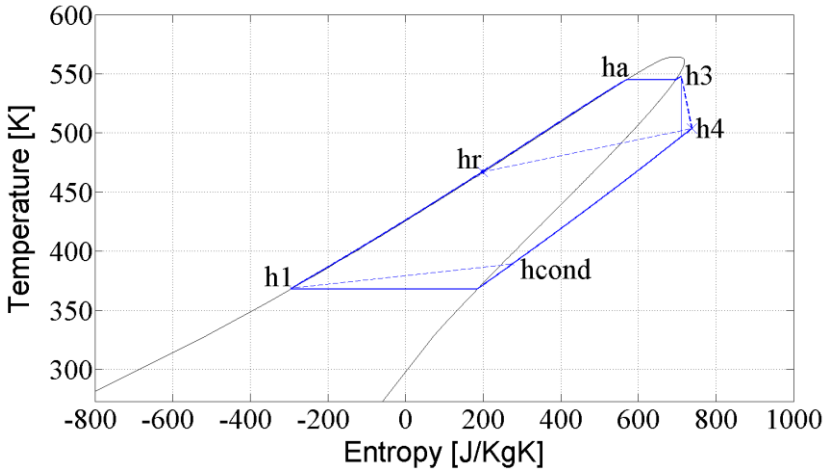

Figure 2: T-S diagram of the organic Rankine cycle with regenerator.

The values of the ORC working parameters are not stored in the control unit but values can be continuously recorded as they appear on the screen. By means of this data collection for different operating points, the thermodynamic cycle can be completely defined setting the values of the following parameters: condensing pressure, p_c; vapour evaporating pressure, p_v; superheating maximum temperature, t_3; pinch point at the Heat Recovery Vapour Generator (i.e., HRVG), t_{pp}. The thermal power provided to the ORC can be calculated as:

$$P_{th\_oil} = \dot{m}_{oil} \cdot c_{p\_oil} \cdot \left(t_{in\_oil} - t_{out\_oil}\right) \quad (1)$$

In order the define the evaporation temperature T_{ev}, in accordance with the experimental data, a pinch point of 20 °C was set in the evaporator heat exchanger between the thermal oil and the siloxane. The pinch point occurs at the beginning of the evaporation hence the siloxane mass flow rate ($\dot{m}_V$) can be evaluated as:

$$\dot{m}_V = \frac{P_{th\_pp}}{q_{in}} \tag{2}$$

where P_{th_pp} is the thermal power from the thermal oil till the pinch point and $q_{in} = h_3 - h_a$ is the heat conveyed to the siloxane. Since the plant embeds a regenerator, the vapour at the turbine outlet is used to preheat the liquid siloxane to the enthalpy h_r, so the thermal energy fed to the siloxane can be evaluated as:

$$P_{t\_rec} = \dot{m}_V \cdot (h_3 - h_r) \tag{3}$$

which equals the thermal power conveyed by the thermal oil, as reported in eq. (1).

The regenerator also cools down the vapour at the turbine outlet so the enthalpy of the siloxane at the inlet of the condenser is h_{cond}.

As regards the condensing pressure, the adopted procedure is analogous to what has been done for the evaporating section. The condensing pressure (p_c) and temperature (t_c) depends closely on the temperature of the cooling fluid:

$$t_c = t_{cf\_pinch} + \tau \tag{4}$$

where t_{cf_pinch} is the temperature of the cooling fluid at the pinch point and τ is the temperature difference between the condensing fluid and the cooling fluid at the pinch point. Since the conditions and the thermal power recovered in the water condenser are known, the siloxane condensing pressure is set by defining the temperature difference in the condenser heat exchanger to 10 °C. The thermal power recovered at the condenser can be defined as:

$$P_{cond} = \dot{m}_V \cdot (h_{cond} - h_1) \tag{5}$$

The thermodynamic properties of the organic fluid (siloxane) used in the ORC module has been provided by REFPROP 9.

$q_{out} = h_{cond} - h_1$	(heat output at the condenser per unit of mass)						
$l_{turbine} = h_3 - h_4 = (h_3 - h_{4is}) \cdot \eta_{is,t}$	(expansion work per unit of mass)						
$l_{pump} = h_2 - h_1 = (h_{2is} - h_1) / \eta_{m,p}$	(pumping work per unit of mass)						
$t_r = t_1 + \varepsilon(t_4 - t_1)$	(regeneration temperature)						
$P_{el} = \left[\left(l_{turbine} \cdot \eta_{m,t} \cdot \eta_{el,g} \right) - \left(\frac{l_{pump}}{\eta_{m,p} \cdot \eta_{el,p}} \right) \right] \cdot \dot{m}_v \cdot \eta_{aux}$	(ORC electric power)						
$\eta_{is,turb}$	0.8	$\eta_{el,gen}$	0.97	$\eta_{m,pump}$	0.98	$\eta_{regen.}$	0.73
$\eta_{m,turb}$	0.98	$\eta_{is,pump}$	0.70	$\eta_{el,pump}$	0.90	η_{aux}	0.90

Table 1: Equations adopted for the simulations and efficiency values assumed.

RESULTS

Figure 3 reports the electric load of the ORC as a function of the mean temperature of the primary network showing a correlation between the two parameters. The figure shows also a good agreement between the monitored data (dotted line) and the results of the model (continuous line). Nominal load operation refers to the winter period when the district heating demand is high and the return temperature from the network is the lowest. During summer the

plant manager keeps the district heating temperature as high as possible increasing the heat dissipated with the aim of maximizing the electricity generation, though causing a lower total conversion efficiency.

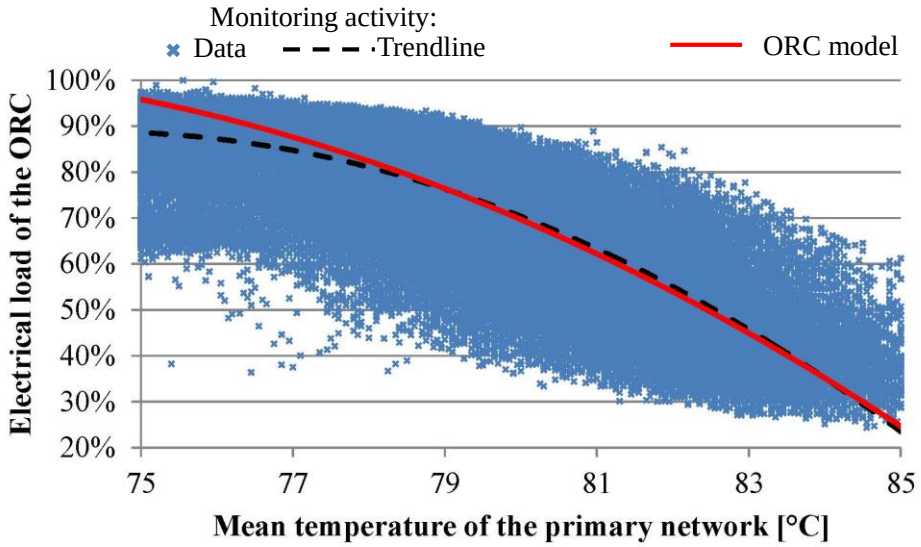

Figure 3: ORC electrical load depending on the mean temperature of the primary network.

Figure 4 shows the trend of the electric efficiency of the ORC as a function of the mean temperature of the primary network. The graph shows four levels provided with the ORC model considering different plant loads. A constant amount of feeding thermal power from the biomass boiler is considered for each load level. As the temperature of the primary network increases, also the condensing temperature of the thermodynamic cycle increases and the specific work of the cycle is reduced. For each degree of increase in the primary network temperature, the electric efficiency of the ORC generator lowers by about 0.1% and the thermal power discharged at the condenser increases.

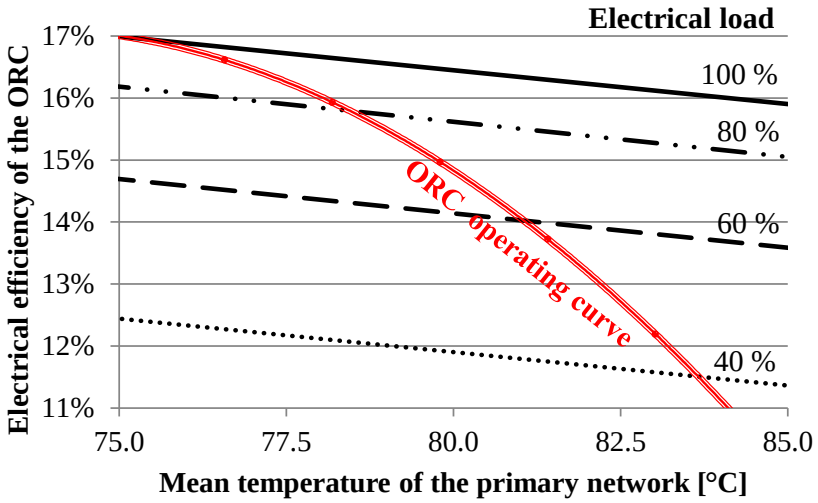

Figure 4: Electric power trend as a function of the mean temperature of the primary network

The ORC operating curve in Figure 4 represents the real operating conditions of the ORC and it crosses the black lines of the model in the corresponding operating point. The temperature at the condenser in the real plant is driven by the demand of thermal power from the district heating and the dryer: the lower the thermal power demand, the higher the return temperature

of the cooling water in the condenser. A lower thermal power demand also entails a lower power input from the biomass boiler because the heat output at the condenser cannot be discharged to the users.

DISCUSSION

The numerical results are in good agreement with the monitored data, hence - despite its preliminary features - the developed model shows some significant prediction capabilities. Since the power plant benefits of an incentive based on the electricity generation, the management of the power plant currently aims to maximize the electric power increasing the heat discharged to the network and then increasing the temperatures. However, a management of the power plant that aims to lower temperatures of the networks would probably lead to a smaller electricity generation but to a higher global efficiency. Moreover, a refurbishment of the buildings connected to the network e.g., upgrade to low-temperature systems, would allow a further improvement of the global efficiency. The future development of this work foresees the integration of the model of the plant with the model of the district heating and final users to evaluate and optimize the management strategy of the system.

ACKNOWLEDGEMENTS

The authors gratefully thank “Bioenergie Termocentrale Renon” for the data collected, Hansjörg Rottensteiner for his time and the Province of Bolzano that has funded the project.

REFERENCES

1. U. Drescher, D. Brüggemann, Fluid selection for the Organic Rankine Cycle (ORC) in biomass power and heat plants, Applied Thermal Engineering. 27 223-228, 2007.
2. Ufficio Risparmio Energetico Provincia Bolzano, Teleriscaldamenti a biomassa in Südtirol in Alto Adige, 2008.
3. F.J. Fernández, M.M. Prieto, I. Suárez, Thermodynamic analysis of high-temperature regenerative organic Rankine cycles using siloxanes as working fluids, Energy. 36 5239–5249, 2011.
4. D. Maraver, A. Sin, J. Royo, F. Sebastián, Assessment of CCHP systems based on biomass combustion for small-scale applications through a review of the technology and analysis of energy efficiency parameters, Applied Energy. 102, 1303-1313, 2013.
5. A. Algieri, P. Morrone, Comparative energetic analysis of high-temperature subcritical and transcritical Organic Rankine Cycle (ORC). A biomass application in the Sibari district, Applied Thermal Engineering. 36, 236-244, 2012.
6. A. Rentizelas, S. Karellas, E. Kakaras, I. Tatsiopoulos, Comparative techno-economic analysis of ORC and gasification for bioenergy applications, Energy Conversion and Management. 50, 674–681, 2009.
7. S. Quoilin, M. Van Den Broek, S. Declaye, P. Dewallef, V. Lemort, Techno-economic survey of Organic Rankine Cycle (ORC) systems, Renewable and Sustainable Energy Reviews. 22, 168–186, 2013.
8. I. Ben Hassine, U. Eicker, Impact of load structure variation and solar thermal energy integration on an existing district heating network, Applied Thermal Engineering. 50, 1437–1446, 2013.
9. NIST Reference Fluid Thermodynamic Database, REFPROP 9, 2012.
10. H. Li, S. Svendsen, Energy and exergy analysis of low temperature district heating network, Energy. 45, 237–246, 2012.

HEAT AND COLD SUPPLY FOR NEIGHBORHOODS BY MEANS OF SEASONAL BOREHOLE STORAGES AND LOW TEMPERATURE ENERGETIC CROSS LINKING

F. Ruesch[1]; M.Rommel[1]; M.Kolb[2]; T. Gautschi[2]

1: SPF Institute for Solar Technology, CH-8640 Rapperswil, Switzerland

2: Amstein + Walthert AG ; CH-8050 Zürich, Switzerland

ABSTRACT

To meet the ambitious goals for the reduction of greenhouse gas emissions of the EU, the demand of fossil energy for heating purpose has to be reduced drastically and additionally a growing demand for building air conditioning has to be provided. Novel neighbourhood based energy concepts can provide an important contribution to the achievement of this goal. In urban areas residential buildings with a demand of heat for domestic hot water and space heat during winter are sited in the neighbourhood of buildings with increasing cooling demand from the industry or service sector. A low temperature district heating network based on water-bearing uninsulated pipes can work as heat source for efficient heat pumps in the residential sector as well as cold source for the air conditioning of office buildings or other processes with large cooling demands (for example large data centres). Large borehole fields serve as thermal storages for heat respectively "cold" between the seasons. Thermal losses form the borehole storage as well as in the piping network can be minimized by keeping the temperature of the network close to the average temperature of the surrounding ground. One example of such a low-temperature district heating network, which has been engineered by Amstein+Walthert AG and is under construction at the at the time of composition of this contribution is described.

A project for developing the means for dynamically simulating the operation of low temperature networks was started at SPF, Amstein+Walthert AG and Vela Solaris AG with the aim of ameliorating the planning security for future networks and estimating the potential for energy savings by means of global regulation strategies or the implementation of other renewable and conventional energy sources.

In the contribution a literature review on existing concepts and simulation models for low temperature district heating networks is given. Then, one exemplary network is explained in more details. Furthermore, preliminary simulations of the borehole storage temperature evolution are done based on estimated load profiles and an outlook on planned work is given.

Keywords: low temperature district heating, low temperature networks, district cooling, heat pump, borehole storage, dynamic simulation, optimizing operation

INTRODUCTION

The residential sector accounts for about one fourth of the energy use of the EU and is dominated by fossil heat[1]. This demand has to be reduced and replaced by renewable energy sources or heat pumps driven by carbon free electricity to meet the goal of a reduced greenhouse gas emission of 80% below 1990 level by 2050 as announced by the EU und G8 members[2].

The European Technology Platform on Renewable Heating and Cooling predicts a decrease (80% SH and DHW, 20% Industry and others) in low temperature heat demand (<250°C)

until 2050 by 20..40% depending on the scenario[3]. In the meanwhile the cooling demand is foreseen to increase by a factor of nearly three by the same study. In urban areas, where domestic buildings and service buildings are present, the heat demand in winter can be compensated by the cold demands in summer on yearly bases.

One possibility of providing seasonal storage is the use of more or less densely drilled borehole fields with ground coupled heat exchangers which are called borehole thermal energy storages (BTES). A large BTES was built 2001/2002 in Sweden with 100 BHE with a depth of 65m, which was designed for the direct use of solar energy at elevated temperature levels for a small heating network. In the first years of operation quite high losses of 45..50% were reported[4]. In Canada a small district heating network has been realized, where Solar collectors and a BTES provided more than 90% of the heat demand of 52 homes. Due to the elevated ground temperatures the BTES efficiency is, depending on the year, at about 50%[5]. Several heating networks with large solar collector fields and seasonal storage have been realized in Germany[6] based on four different storage principles (hot water, gravel-water, borehole and aquifer thermal storage). Both installations with BTES have been equipped with heat pumps after the first years of operation[7] in order to increase the temperature spread and the exploitation of the storage volume and to reduce the temperature level and the according temperature losses. All these projects show that seasonal energy storage in the ground is possible and can be used for district heating, but it is coupled with elevated heat losses when temperatures at the user level of 45..65 °C is to be provided.

On the other hand BTES have been used for combined heating and cooling since 1980. A review on early projects is given by Sanner et al.[8]. Two of the largest borehole thermal energy stores were built in Norway, Nydalen Business Park and Akershus University Hospital with 180 resp. 228 boreholes with a length of 200m[9]. Both BTES serve for heat and cold supply and are running successfully since 2004 resp. 2007. Recently, design guidelines for geothermal cooling dominated BTES were elaborated by Pahud et al. [10] highlighting the need of dynamic simulations of the whole system for the definitive dimensioning. Most of the above cited BTES have been designed by means of dynamic simulations with models based on the work of Eskilson[11]–[13]. These models proved to be valid for the design and modelling of BTES.

The combination of seasonal BTES and a district heating and cooling network running at the low temperatures of the BTES is rarely reported, but similar low temperature networks distributing deep lake water for heating and mainly cooling purpose are installed in Toronto[14] and Geneva[15]. At ETH Zürich a new energy master plan has been announced, which is described in [16]. In the final phase a total of 800 boreholes provide heat and cold for the Campus Hönggerberg, which is distributed in a ring-like network of water bearing pipes. Up to now, 230 boreholes have been realized and are in operational state since spring 2012. Several similar networks have been planned by Amstein + Walthert. In this paper a network of the Familienheim Genossenschaft Zürich (FGZ) is described in more details.

DESCRIPTION OF THE FGZ-NETWORK

The network consists of a flow- and a return line of water containing uninsulated pipes. In its final state the network consists of a closed ring in which the flow direction is not a priori defined. From this central ring line there are several linear connection lines to access distant building blocks or energy sources. The flow in the network is generated by decentralized energy stations. These are on one hand energy stations equipped with highly efficient large heat pumps providing mainly heat for domestic buildings of entire building blocks. These energy stations are also equipped with local storage tanks and conventional heaters as back up and for peak loads. On the other hand also the energy supply, which is in this case mainly

provided by the cooling load of large data centre, is guided by decentralized energy stations. All pumping power for flow generation is included in the decentralized energy stations. If the flow rates of consumers and producers don't match, the excess flow is guided through the boreholes by charging or discharging the BTES. These borehole fields have no pumps for the flow generation, but are equipped with valves for connecting or disconnecting individual fields or subfields from the network. These valves provide the means to control the pressure drop between flow and return pipe and for a possible storage management with individual borehole fields held at different temperature levels if this is needed in a future running mode. A central control system called energy manager is installed with the aim of measuring the energy flow and controlling the working modes of each decentralized energy station. The connection of all decentralized energy stations to a central energy manager provides the possibility of implementing new control strategies for optimizing the energy efficiency of the whole network.

The first BTES (Grünmatt) with 153 boreholes of 250m length and the first energy station is planned to start operation in the end of 2013. By the end of 2014 the first construction phase with three energy stations with a cumulated power of about 3.4 MW will start its operation. The regeneration is provided mainly from the cooling loads of large data servers of the company Swisscom. In summer, the network is also used for air conditioning of the office building resulting in total heat rejection of more than 2 MW. This excess heat is reduced by internal heat recovery to about 0.9 MW during winter. The ability of net annual heat rejection of the Swisscom servers and building exceeds the heat demand of the first construction phase by a factor of two. There is still capacity for connecting more domestic buildings with additional heat demand to the network in further construction phases.

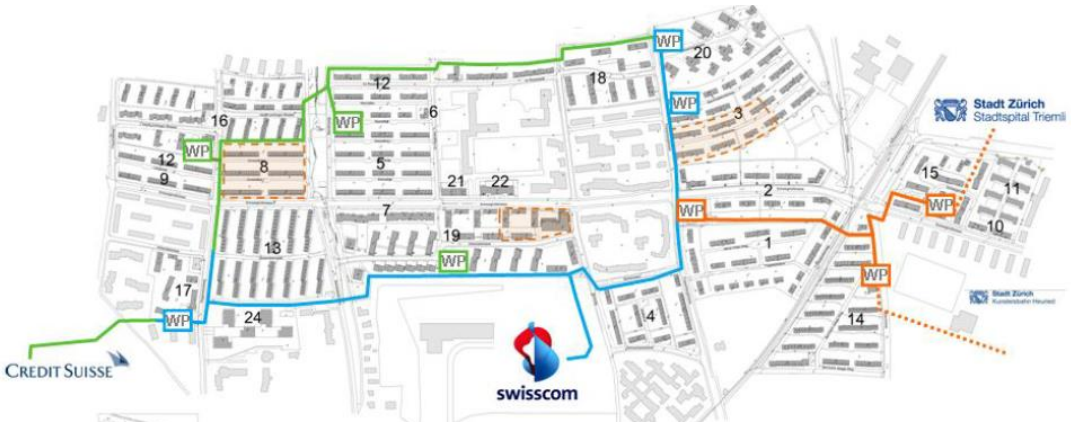

Figure 1: Overview of the planned low temperature network by construction phases. Blue: first construction phase, green: second construction phase, orange: third construction phase. Energy canters with heat pumps are marked with WP. (The coloured graph only available in the digital version of the paper)

SIMULATION OF THE GROUND STORAGE

The temperature evolution has been simulated based on estimated hourly load profiles from the first construction phase. The distribution of the space heat load was generated based on typical outdoor temperatures and the nominal powers of the planned heat pumps. For domestic hot water a constant load and for the recharging a profile constant monthly cooling loads from the company Swisscom where used. These load profiles are given in fig. 2. In addition to the energy load profiles, there are constraints on the temperatures, the lower limit was assumed to be 4°C and the upper limit was assumed to be 28°C. As the temperature level of the Swisscom cooling fluid is between 26°C and 38°C depending on the ambient temperature, there were no further temperature constraints applied, assuming that if

recharging is limited by 28°C (mainly in summer) this temperature can be provided by the Swisscom data centre. The ground properties have been evaluated by a thermal response test at a test borehole of 250m length (R_b=0.07KmW^{-1}; λ_{mean}=2.45Wm^{-1}K^{-1}) and were used for a ground simulation with a well-known superposition borehole model (SBM) developed by Eskilson[17] and adapted to TRNSYS[18] by Pahud[12]. A rectangular configuration of 6x25 (=150) boreholes with a distance of 6m has been used to decrease simulation time by taking advantage of symmetry. The real configuration of 153 boreholes slightly deviates from this idealized configuration. In fig.3 the temperature evolution of the BTES during this simulation is displayed. The minimal temperature of 4°C is reached several times in the year (only 15h in the fifth year) meaning that during this time, conventional backup heaters have to support the heat pumps. The displayed scenario results in coverage of the heat load of 99.8% by heat pumps resp. network. It can also be seen from this figure, that the summer mode (cooling of data centre resp. recharging of BTES) is limited by the maximal temperature of the network resulting in an excess heat of the Swisscom of still about 7.8 GWh/a which must be cooled in the conventional way (air exchangers) during the first construction phase. But during this phase the charging of the BTES still exceeds the discharging (118%) resulting in a slight temperature increase, which is hardly recognized in fig.3.

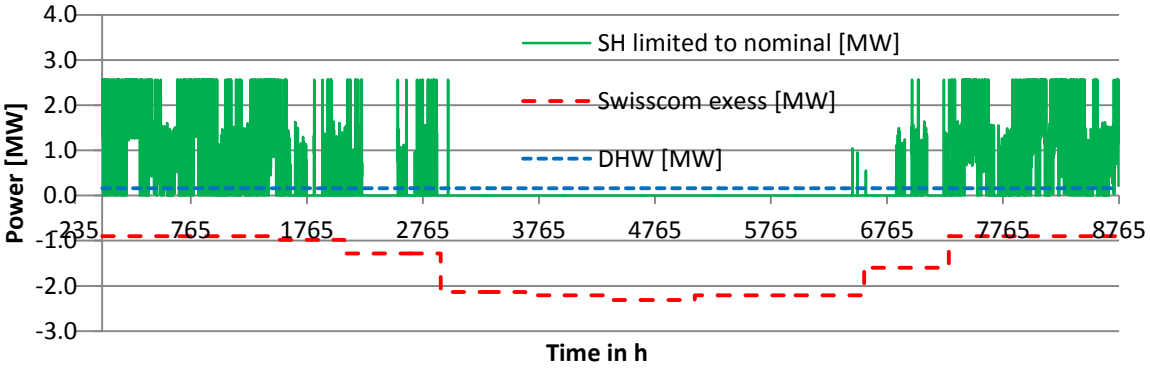

Figure 2: Estimation of the heating and regeneration loads at the "Grünmatt" ground storage after the first construction phase. (Coloured graph only available in the digital version of the paper)

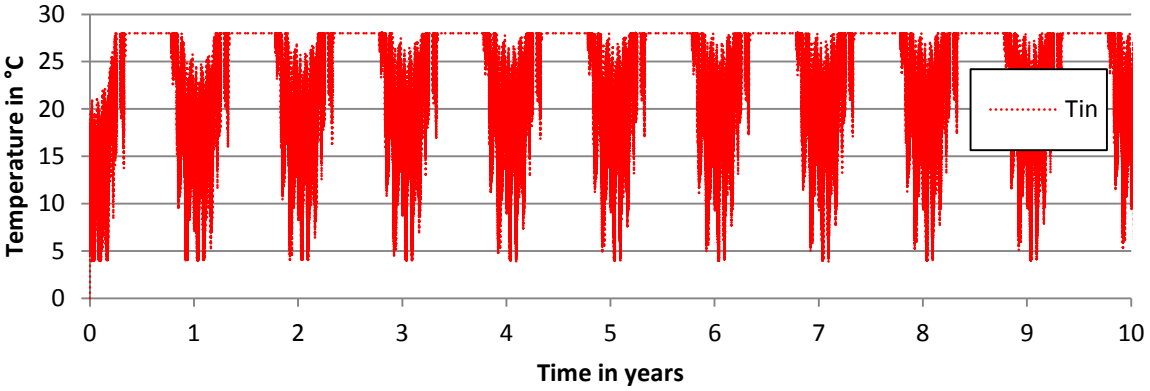

Figure 3: Input temperaturs at the "Grünmatt" ground storage simulated for ten years with the TRNSBM model based on a maximal temperature range of 4..28°C. (Coloured graph only available in the digital version of the paper)

OUTLOOK

The temperature simulation of the BTES is based on estimated constant load files, where only the ground storage is dynamically simulated. In further steps the dynamic behaviour of the network, and each energy centre containing heat pump, circulation pump, backup heater and local (water based) storage tank is going to be included in the dynamic simulation. The thermal capacities of local storage tanks, but also the networks and the buildings allow implementing a load management. Different control strategies will be investigated in order to increase the efficiency of the overall system by taking into account the coefficient of performance (COP) of heat pumps for DHW and SH, the cooling efficiency by free-cooling or by cooling units, the pumping power and the backup heaters.

DISCUSSION

Several low temperature district heating and cooling networks have been planned by Amstein+Walthert AG in the Region of Zürich. The first phase of the FGZ network is under construction and will start its operation in winter 2013. The waste heat from server cooling largely exceeds the demand of the attached buildings of the first construction phase on annual bases. It has been shown that the installed BTES capacity is sufficient to transform the summer excess heat to the space heat demand in winter in order to cover 99.8% of the heat demand. As there are still about 8 GWh of excess heat, which can't be distributed into the thermal network after the first construction phase, there is still capacity to add further BTES and energy consumers in the following construction phases.

The simulation of the entire network in order to optimize the control strategy is aimed in further steps of the project. From the first years of operation measured data will be available to validate simulation results and to increase simulation accuracy.

ACKNOWLEDGEMENTS

The support of the Swiss Federal Office of Energy (SFOE) for the presented investigations within the TARO project is gratefully acknowledged.

REFERENCES

[1] U. European, „EU Energy in Figures - Statistical Pocketbook 2012“. Publication Office of the European Union, 2012.

[2] „Roadmap 2050 - practical guide to a prosperous low carbon europe“. [Online]. Available: http://www.roadmap2050.eu/reports. [Accessed: 24-Apr-2013].

[3] B. Sanner, K. Ria, A. Land, M. Kari, P. Papillon, G. Stryi-Hipp, und W. Weiss, „2020–2030–2050 Common Vision for the Renewable Heating & Cooling sector in Europe“. Publications Office of the European Unio, 2011.

[4] M. Lundh und J.-O. Dalenbäck, „Swedish solar heated residential area with seasonal storage in rock: Initial evaluation“, *Renewable Energy*, Bd. 33, Nr. 4, S. 703–711, Apr. 2008.

[5] B. Sibbitt, D. McClenahan, R. Djebbar, J. Thornton, B. Wong, J. Carriere, und J. Kokko, „The Performance of a High Solar Fraction Seasonal Storage District Heating System – Five Years of Operation“, *Energy Procedia*, Bd. 30, Nr. 0, S. 856–865, 2012.

[6] D. Bauer, R. Marx, J. Nußbicker-Lux, F. Ochs, W. Heidemann, und H. Müller-Steinhagen, „German central solar heating plants with seasonal heat storage“, *Solar Energy*, Bd. 84, Nr. 4, S. 612–623, Apr. 2010.

[7] J. Nussbicker-Lux, W. Heidemann, und H. Müller-Steinhagen, „Validation of a Computer Model for Solar Coupled District Heating Systems with Borehole Thermal Energy Store“, Juni 2012.

[8] B. Sanner, E. Mands, und M. K. Sauer, „Larger geothermal heat pump plants in the central region of Germany“, *Geothermics*, Bd. 32, Nr. 4–6, S. 589–602, Aug. 2003.

[9] K. Midttomme, A. Hauge, R. S. Grini, J. Sterne, und H. skarphagen, „UNDERGROUND THERMAL ENERGY STORAGE (UTES) WITH HEAT PUMPS IN NORWAY“, presented at the Effstock, Stockholm, 2009.

[10] D. Pahud, M. Belliardi, und P. Caputo, „Geocooling potential of borehole heat exchangers' systems applied to low energy office buildings“, *Renewable Energy*, Bd. 45, Nr. 0, S. 197–204, Sep. 2012.

[11] P. Eskilson, „Thermal analysis of heat extraction boreholes“, PhD, Department of Mathematical Physics, University of Lund, 1987.

[12] D. Pahud, A. Fromentin, und J.-C. Hadorn, „The Superpositon Borehole Model for TRNSYS (TRNSBM) - User manual for the November 1996 version - Internal Report“, ÉCOLE POLYTECHNIQUE FÉDÉRALE DE LAUSANNE (EPFL), Lausanne, Switzerland, 1996.

[13] G. Hellström, „Duct ground heat storage model - Manual for Computer Code“, Department of Mathematical Physics, University of Lund, Sweden, 1989.

[14] F. M. Boyce, P. F. Hamblin, L. D. D. Harvey, W. M. Schertzer, und R. C. McCrimmon, „Response of the Thermal Structure of Lake Ontario to Deep Cooling Water Withdrawals and to Global Warming“, *Journal of Great Lakes Research*, Bd. 19, Nr. 3, S. 603–616, 1993.

[15] P.-A. Viquerat, „Utilisation de réseaux d'eau lacustre profonde pour la climatisation et le chauffage des bâtiments: bilan énergétique et impacts environnementaux. Etude de cas: le projet GLN (Genève-Lac-Nations) à Genève“, UNIVERSITÉ DE GENÈVE, Geneva, 2012.

[16] M. Sulzer und T. Gautschi, „ETH Zürich, Hönggerberg Masterplan Energie“, presented at the 15. Schweizerisches Status - Seminar «Energie - und Umweltforschung im B auwesen», Zürich, 2008.

[17] P. Eskilson, „Superposition Borehole Model - Manual for Computer Code“, Department of Mathematical Physics, University of Lund, Sweden, 1986.

[18] University of Wisconsin, „TRNSYS 17 - A Transient System Simulation Programm“. [Online]. Available: http://sel.me.wisc.edu/trnsys/default.htm. [Accessed: 24-Feb-2013].

SIMULATION STUDY OF A NATURALLY-VENTILATED BUILDING INTEGRATED PHOTOVOLTAIC ENVELOPE

Saadon S.[1,2]; Gaillard L.[1,2]; Ménézo C.[1,2]

[1]*INSA-Lyon, CETHIL, UMR5008, 69621, Villeurbanne, France*
[2]*Chaire INSA-EDF « Habitats et Innovations Energétique », 69100 Villeurbanne, France*

ABSTRACT

Ventilated double-skin photovoltaic (PV) facades can improve the thermal efficiency of a building whilst generating electricity. Such active building envelops are interesting in the context of goals to reduce the net energy footprint of buildings, yet to date remain underexploited, in part due to technical uncertainties concerning their real performance. This paper focuses on the simulation of a partially-glazed, ventilated PV facade designed for PV cooling in summer (with natural convection) and heat recovery in winter (mechanical ventilation). Air within the cavity is heated by transmission through glazed sections, and by convective and radiative exchange with PV elements and the primary wall. The system is simulated using a full-scale simplified physical model, developed for TRNSYS.

We present the model for the summer operating configuration, which is more challenging from a numerical perspective. The model describes the active envelop in terms of a simplified geometry, and includes parameters such as density of PV cells, relative coverage of semi-transparent/opaque surfaces, and the ratio of height/width of the double-skin. Surface and air temperatures, mass flow rate and PV power output are obtained via a calculation the thermal and aerodynamic balance, for a given set of meteorological conditions.

The current phase of the work is primarily concerned with model development. Validation of the model was carried out using experimental data from the Ressources project (ANR-PREBAT2007), comprising detailed in-situ measurements of a full scale prototype system installed in Toulouse, France, and monitored continuously with a sampling rate of 1/120 Hz for over a year.

Keywords: natural convection; double-skin; photovoltaic; building integration

INTRODUCTION

Building-integrated photovoltaic (PV) systems are typically designed with features to promote heat dissipation away from photovoltaic cells in order to limit temperature-dependant losses. Photovoltaic-thermal systems (PV-T) go further by exploiting this heat source. Chow et al. [1] showed that a significant fraction of the incident solar energy absorbed by a solar panel installed on a building wall can be recovered for hot water or space heating, and demonstrated the application of naturally ventilated PV glazing to shade indoor spaces whilst generating electricity [2].

The integration of photovoltaic (PV) panels into double-skin façades may be an effective solution to improve the energy-efficiency of existing structures and new builds. This hybrid system consists of PV panels incorporated into a double-skin with a thick air gap to the primary building wall. This gap acts as a solar chimney, and the air flow is driven by buoyancy (stack effect) and wind-induced pressure differences (if open to the exterior). In summer, the air gap can cool PV components, thereby enhancing power production, and act as a thermal barrier for the building. In winter, the same configuration can serve to pre-heat air entering the building (with the addition of mechanical ventilation).

In order to realise the potential of double-skin photovoltaic (PV) facades, system-level models are required to predict thermal and electrical performance under real conditions, taking into account natural convection and the wind effect on air flow within cavity. Moreover, simulations must be sufficiently robust to be applicable to the broad range of geometries that may result from building orientation, its surroundings, and other purposes of the double skin facade (such as sound protection and aesthetic criteria). [3]. In this context, rather than developing a detailed physical model with a faithful description of system geometry, thermal and aerodynamic behaviour can be adequately approximated using global models based on dominant physical features, such as that developed by Brinkworth et al. [4].

The present work concerns the simulation of partially opaque double-skin PV facades using TRNSYS. The starting point is the existing model for opaque BIPV systems with air cavities developed by TESS (type 567), which calculates the thermal state of the system for a given air flow rate. The model was adapted and extended to incorporate a calculation of mass flow rate due to natural ventilation, and allow for a semi-transparent double facade.

MODELLING A SEMI-TRANSPARENT SOLAR COLECTOR

Following the approach demonstrated by Guiavarch [5], a nodal model of a PV/T air collector was developed comprising PV cells integrated into partially opaque glazed facade. Figure 1 presents the resistive network for used by the model, which consists of six nodes, T_{ext}, T_0, T_1, T_f, T_2 and T_z, representing ambient air, PV cell, facade inner surface, cavity air, building primary wall and building interior temperatures respectively.

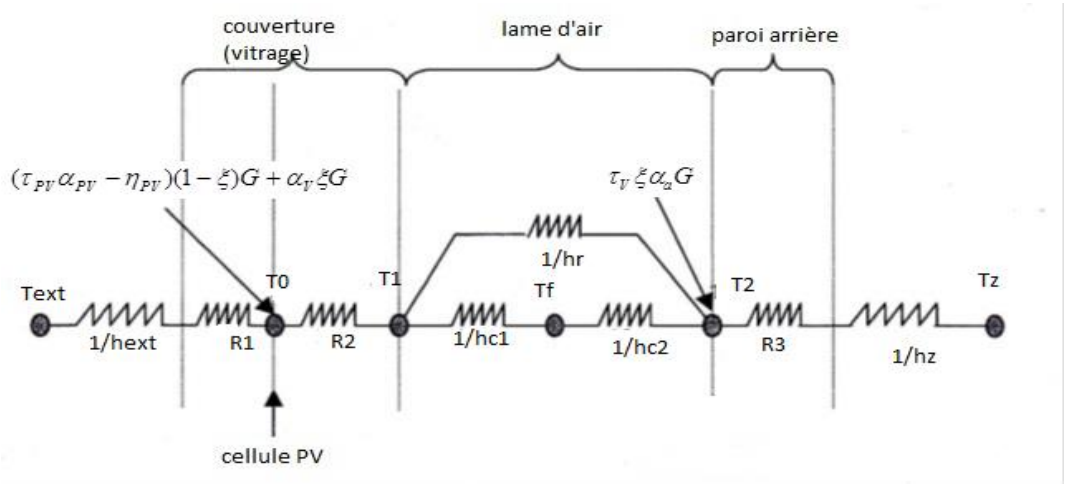

Figure 1: Nodal model of a ventilated PV double skin façade

Incident solar flux is hereafter represented by the symbol G. Parameters τ and α represent transmission and absorption coefficients for the surfaces indicated by subscripts, and η is the PV photo-conversion efficiency. Thermal resistances and heat transfer coefficients are represented by parameters R and h (subscripts r and c refer to radiative and convective transfer). In terms of energy balance, a key factor is the relative coverage of transparent and opaque surfaces, which determines the portion of solar radiation that is transmitted. Thus for the model, the facade is approximated as a uniform semi-transparent PV collector, characterised by a transparency factor, ξ, where $0 < \xi < 1$.

$$\xi = 1 - \frac{S_{cel}}{S_{tot}} \quad (1)$$

Where S_{cel} and S_{tot} are the area covered by PV cells and the total facade surface respectively. This factor is incorporated into the equations of energy balance for each node, which are resolved to determine the thermal and electrical performance of the system:

$$h'_{ext}(T_{ext} - T_0) + (\tau_{PV}\,\alpha_{PV} - \eta_{PV})(1-\xi)G + \alpha_v \xi G = \frac{T_0 - T_1}{R_2} \quad (2)$$

$$\frac{T_0 - T_1}{R_2} = \Phi_r + h_{C1}(T_1 - T_f) \quad (3)$$

$$\Phi_r + h_{C2}(T_f - T_2) + \tau_v \xi \alpha_a G = h_z'(T_2 - T_z) \quad (4)$$

with $$\Phi_r = h_r(T_1 - T_2), \frac{1}{h_z'} = \frac{1}{h_z} + R_3, \frac{1}{h_{ext}'} = \frac{1}{h_{ext}} + R_1 \quad (5)$$

The variable Φ_r is the heat flux by radiation between the cover and the absorber. The net heat gain by the air in the cavity is equal to the net enthalpy of the fluid, given by the product of mass flow rate, specific heat and inlet-outlet air temperature difference, the latter being determined by the mean fluid temperature and knowledge of its evolution along the cavity (stratification):

$$P_{th} = \dot{m} C_p \Delta T \quad (6)$$

IMPLEMENTATION OF THE CALCULATION OF THE FLOW RATE

A global description of air flow in a naturally ventilated cavity can be obtained by performing a one-dimensional 'loop analysis' of buoyancy forces, wind effect (coefficients C_w), frictional losses (f), and pressure drops near inlet and outlet (K_f). For the case of natural convection and laminar flow, Brinkworth et al. [4] showed that such a simplified model can reproduce empirically observed relationships between heat flux and mass flow rate for under controlled laboratory conditions. By adopting friction factors and internal heat transfer coefficients taken from studies of forced convection in ducts, and by introducing the stratification parameter δ_s to allow for a non-linear variation in air temperature, the following generalised equation was derived:

$$A\dot{m}^3 + B\dot{m}^2 + C\dot{m} + D = 0 \quad (9)$$

$$A = K_{f1} + K_{f2} + f_1, B = f_2 \upsilon(\rho w d)(\frac{L}{D_h{}^2}), \quad (10)$$

$$C = -(\rho w d)^2 (C_{W1} W_1{}^2 - C_{W2} W_2{}^2), D = -(\delta_S P_{th}) \frac{2(\rho w d)^2 g L \beta \sin(\theta)}{C_p}$$

Where ρ, β and υ are the kinematic viscosity, dilation coefficient and density of air. The length, width, depth, hydraulic diameter and inclination of the cavity are given by L, w, d, D_h, θ respectively. Parameter g is the acceleration due to gravity. Wind speed at the inlet and outlet are represented by the variable W. Note that a positive wind pressure coefficient at the inlet and a negative (suction) one at the exit will enhance the mass flow rate.

For turbulent flow, the Hypri model [5] provides a similar cubic relation for mass flow rate:

$$\dot{m}^3 + D' = 0 \quad (11)$$

with
$$D' = -(wd\rho)^3 \frac{\delta_S P_{th} \frac{g\beta \sin(\theta)}{\rho C_p}}{\frac{wd}{L}\left(f\frac{L}{D} + \frac{1}{2}((1+K_{f1})+1)\right)} \quad (12)$$

As the thermal model depends on mass flow rate, and the aerodynamic model provides mass flow rate as a function of heat flux, the equilibrium state is found numerically by iteration: starting from an initial value for flow rate, the Nusselt number and convective heat exchange coefficient are calculated, from which P_{th} is estimated. The mass flow rate is then recalculated using equation 9 or 11, and the loop is thus repeated until the results are found to converge.

EXPERIMENTAL VALIDATION

The model was configured to predict the behaviour of a full-scale prototype double skin PV facade constructed and monitored for the Ressources project, shown in figure 2. The installation, comprising a pleated, vertical facade, 7.7 m high, 4.5 m in width and (on average) 60 cm in depth, was fitted to the glazed South-West wall an occupied office building in Toulouse, France [6]. Following the instrumentation of the prototype, in the model, the air channel was divided into 3 macro-volumes with uniform temperature and pressure of 2.3m, 2.8m and 2.3m in height. Continuity of the flow is maintained between zones by conservation of the mass flow rate.

Figure 2: Left: Prototype pleated double skin PV facade designed and constructed for the Ressources project. Right: single prism element showing PV and glazed surfaces.

Other model parameters were chosen as follows. For heat exchange between the outer surface and the exterior, the standard wind-dependent correlation for convection presented by McAdams was used [7]. For friction, the form factor of the cavity suggests that flow should be primarily turbulent. An average constant friction coefficient f=0.0407 was estimated using experimental measurements of air speed and the following correlation for turbulent flow

$$f = 0.316\,\mathrm{Re}^{1/4} \quad (14)$$

Wind pressure coefficients where taken from reference data [8]: for a vertical wall and facing wind, inlet and outlet coefficients were set to 0.7 and -0.5 respectively. Singular pressure loss coefficients of K_{f1} = 0.5 and K_{f2} = 1 for inlet and outlet were estimated by tuning the model.

RESULTS

A sequence of 9 consecutive days in June (summer) was chosen to evaluate the model. A time step of 120 s was set to match the sampling rate of the data. Simulated and measured air flow rates are presented in figure 3. An order-5 (10 minute) moving average of experimental data is also shown. For most days the simulation agrees with the latter in magnitude and daily variation, but does not predict the short-term fluctuations that are likely caused by wind. Note that during this period wind speed could briefly reach as high as 10.3 m/s.

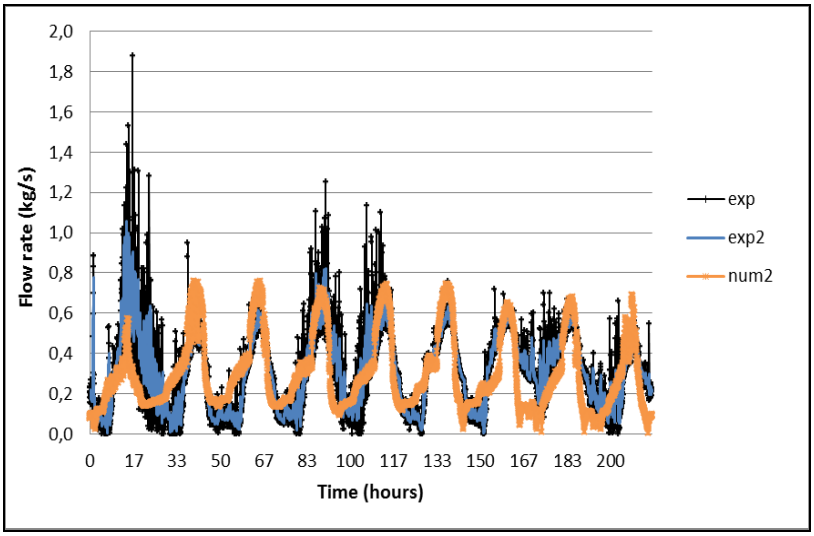

Figure 3: measured and calculated air flow rate during 9 consecutive days in June (summer). Data series "exp" and "exp2"refer to instantaneous and moving average values respectively.

In figure 4, outlet air temperature and PV surface temperature are shown for the same sequence. In the figure, data series "num2" refers to the new model and series "567" shows the results for the existing BIPV model.

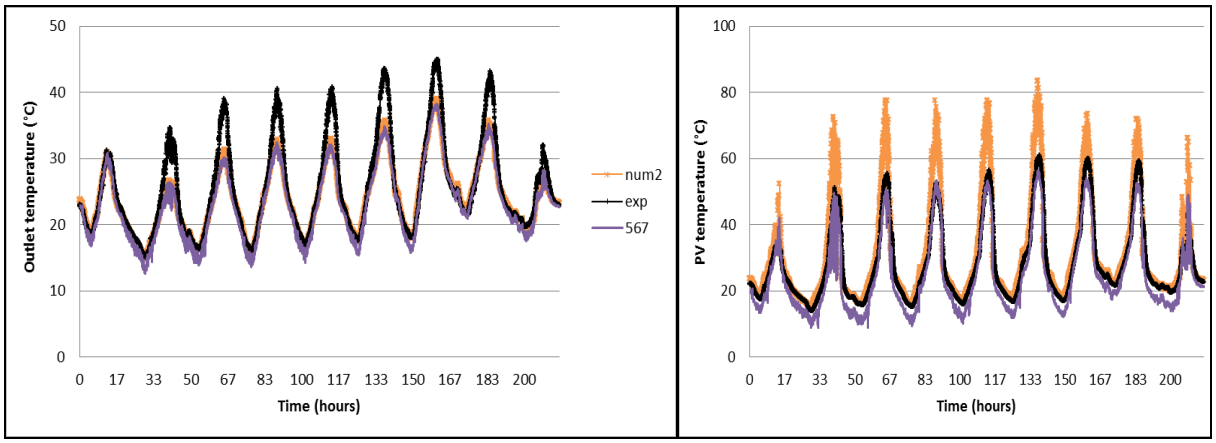

Figure 4 : evolution of outlet fluid temperature and PV cell temperature during 9 consecutive days in June (summer). Data series "num2" and "567" refer to the new and existing model.

In terms of the outlet temperature, the difference between the new model and the experiment varies from 2.4 K to as much as 12.8 K during the mid-afternoon when incident radiation is at a maximum. This discrepancy could be due to an oversimplification of air flow described by the models, although it may be possible to reduce this difference by further modifying pressure drop coefficients. Regarding the PV surface, the old model underestimates and the new model overestimates the temperatures during periods of high incident radiation. Since the

mass flow rate according to the two models are very similar (model 567 uses the experimental data), the difference in predicted PV temperatures is due to semi-transparency: the existing model corresponds to an opaque configuration whereas the new model assumed a constant degree of transparency of 30%. Considering the pleated geometry of the façade, a more accurate description would be provided by allowing the degree of transparency to vary during the day from nearly opaque when the sun is direct facing PV surface to nearly transparent in the late afternoon. Such a modification can be easily handled using TRNSYS.

CONCLUSION

We have presented a system-level model for a naturally-ventilated double-skin photovoltaic (PV) facade, the novel features of which include a calculation of air flow driven by the stack and wind effect, and an account of semi-transparency in energy balance equations. Validation with experimental data from a real full-scale system shows a reasonable agreement with mass flow rate, although discrepancies are observed in temperatures during periods of peak radiation. Some of these differences can be accounted for by further improvements to the model configuration, including allowing some parameters to vary with time of day. After making such refinements, in the following phase of work the model will be coupled to a more elaborate model in TRNSYS in order to evaluate the performance of double-skin PV facades as components of energy efficient buildings.

ACKNOWLEDGEMENTS

The authors would like to acknowledge the partners of project RESSOURCES (Convention ADEME 0705C0076): EDF R&D (R. Leberre), HBS-Technal (P. Lahbib, J. H. Fortier), Jacques Ferrier Architectes (O. Cornefert).

REFERENCES

1. Chow, T. T., He, W., Ji, J.: Dynamic performance of hybrid photovoltaic/thermal collector wall in Hong Kong. Building and Environment, Vol 38(11), pp 1327-1334, 2003.

2. Chow, T. T., Qiu, Z., Li, C.: Potential application of « see-through » solar cells in ventilated glazing in Hong Kong. Solar Energy Materials and Solar Cells, 93, pp 230-238, 2008.

3. M. A. Shameri, M. A. Alghoul, K. Sopian, M. Fauzi M. Zain, O. Elaye, Perspectives of double skin façade systems in buildings and energy saving, Renewable and Sustainable Reviews 15 (2011) 1468

4. Brinkworth, B. J., Marshall, R. H., Ibarahim, Z.: A validated model of naturally ventilated PV cladding. Solar Energy, Vol 69, No 1, pp 67-81, 1999.

5. Guiavarch, A.: Etude de l'amélioration de la qualité environnementale du bâtiment par intégration de composants solaires. Thèse de Doctorat, Ecole des Mines de Paris, 313 p, 2003.

6. L. Gaillard, S. Giroux, H. Pabiou, C. Ménézo, Full scale experimentation of building integrated photovoltaic component for naturally ventilated double-skin configuration, Journal of Fundamentals of Renewable Energy and Applications 2 (2012) R120316

7. McAdams, W. H., Heat transmission. 3rd Ed, New York, USA: McGraw-Hill, 532 p, 1954.

8. Commision Européenne (projet Altener): Natural ventilation in buildings. Editor: Allard F., James & James, 1998.

SOLAR AIR COLLECTORS FOR THE REFURBISHMENT OF FACTORY BUILDINGS. FIELD EXPERIMENT

B. Sicre[1]; M. Dürr[2]

[1]*Hochschule Luzern Technik & Architektur*
Technikumstrasse 21, CH-6048 Horw
Tel.: + 41 41 349 33 97, Fax: +41 41 349 39 34
E-Mail: benoit.sicre@hslu.ch

[2]*Montana Bausysteme AG, Durisolstrasse 11, CH-5612 Villmergen*
Tel.: + 41 56 619 85 85, Fax: +41 56 619 86 30
E-Mail: mduerr@montana-ag.ch

ABSTRACT

For the purpose of energy conservation, modern buildings are becoming more and more air-tight and generally rely on a mechanical ventilation system for the supply of breathing air in the rooms. According to literature, solar air heating systems can economize the heating and ventilation of commercial/factory/utility buildings. As they use ambient air as a heat carrier, they generally require less demanding production, fewer assembling techniques, and almost no maintenance. Therefore, they tend to be more cost-efficient than water based systems.

However, as air displays a very low heat capacity and therefore is not adapted for heat storage purposes, efficient solar air heating systems rely on interaction with the building and thus require a more complex system design.

In the Swiss Confederation, numerous factory buildings are allegedly reaching the end of their lifetime and need to have their façades refurbished. Refurbishment activity makes up around 30% of total factory construction activity. This presents a good opportunity for façade integrated solar air collectors to penetrate markets.

This paper describes the concept of combining solar air collectors, HVAC systems and building envelopes for use in factory building refurbishment. In addition, implementation at the Lucerne campus is depicted, including the monitoring concept.

Keywords: Façade-integrated solar hot air collectors, impact of integration on the building, costs and benefits

INTRODUCTION

Energy conservation and environmental protection in the built environment are not new research topics. But recently, far-reaching political decisions were taken in Switzerland in order to address climate change. The resulting program, called “Energy Transition 2050”, sets energy performance targets for buildings, industries, and mobility.

The building stock in the Swiss Confederation accounts for 40% of energy consumption. Potential energy savings are especially high for the retrofit market. Numerous non-residential buildings are allegedly reaching the end of their lifetime and need to have their façades refurbished. For instance, refurbishment activity makes up around 30% of factory construction activity. The total façade area of factory buildings amounts to nearly 3 Mio. m^2. This presents a good opportunity for innovative refurbishment techniques to penetrate markets.

Cost-efficient, façade integrated "transpired" solar collectors seem to be an attractive new market segment for façade manufacturers [1], [2]. However, this target group lacks the technical knowhow on integrating and connecting these with the ventilation system. As a centre of excellence for ventilation, the Lucerne University of Applied Science – Technique and Architecture was asked to assist in the design of a generic solar air heating system. A full-scale demonstration system with a ventilation system is currently under construction and will be extensively monitored in order to determine the performance characteristics under real operation conditions and to test different operation strategies.

In this paper the concept of combining solar air collectors, HVAC systems and building envelopes for use in factory building refurbishment will be described. Additionally, implementation at the Lucerne campus will be depicted and the first lessons learned during the construction will be presented.

BACKGROUND, MOTIVATION

Solar air heating systems are considered in the literature as an effective technology for the heating and ventilation of residential and commercial buildings. As they use ambient air as a heat carrier, they generally require less demanding production, fewer mounting techniques, and almost no maintenance. Therefore, they tend to be more cost-efficient than water based systems. Since modern building envelopes are becoming air-tighter for the purpose of energy conservation, a mechanical ventilation system is generally relied upon to supply breathing air in the building.

However, solar air collectors have to compete with other renewable energy sources. A study has shown that the most relevant competitor for solar air collector systems is the combination of PV panels and a heat pump, since it is assumed that PV costs will drop drastically in the coming years and earth coupled heat pumps are a well-established technology [3]. The most sensitive parameter in this competition is the investment costs. To become attractive for the market, solar air collectors need to be low cost [4]. A preliminary market study has shown that uncovered cladding, façade integrated solar air collectors are the collector type with the most potential in Switzerland for non-residential buildings [5]. It is called in the literature transpired solar collector (TSC) because outside air is sucked in through little holes. With high-efficiency at low temperature rise, TSC is well suited for the preheating of air in combination with commercial buildings and factories with a higher air change rate. Owing to its dual function as both an energy generating building envelope and a simple and low maintenance ventilation system, TSCs reach amortization periods of less than 3 years.

The coloured transpired collector is a façade upright solar collector, absorbing the solar energy striking it. The wall captures between 60% and 75% of the available solar energy, making it one of the most efficient solar collectors designed to date [6]. In addition to capturing direct solar radiation, the transpired collector collects the indirect, scattered, and reflected sunlight known as diffuse solar radiation. Typically, diffuse solar radiation, which includes a portion of the radiation on clear days and all the radiation on overcast days, makes up about 25% of the total annual radiation at the Earth's surface.

However, as air displays a very low heat capacity and therefore is not adapted for heat storage purposes, efficient solar air heating systems rely on interaction with the building and thus require a more complex design.

In Switzerland, it is mandatory to equip ventilation systems with a heat recovery unit. In central Europe, heat recovery in ventilation systems requires a pre-heating device to prevent frosting of the heat exchanger and the resulting disturbance in the air supply. A common energy saving solution is the ground-to-air heat exchanger ("earth tube"). In recent years

however, concerns have emerged about hygienic maters, since several studies found out that biofilm develops well in the buried tubes. A preferred solution nowadays is the direct electric defroster, which is low cost and easy to install. However, it dramatically increases the power bill and reduces the overall energy efficiency of the ventilation system. Therefore, there is an interest for high efficiency at low temperature rise as a solar preheating facility for the fresh air. Even if there is no sun, the heat transmission losses through the façade are recuperated by the façade integrated air collector and may be enough to keep the air above the freezing point.

Solar air collectors have less than 0.5% share of the solar thermal market in Germany (2009). In the last decade, there has been less effort to develop air collectors than water-based collectors. A lack of test standards and governmental subsidies has made the market roll-out difficult. However, normalisation efforts have been recently undertaken to produce EU-Standards for glazed solar air collectors [7].

Energy conservation and environmental protection in the built environment, especially non-residential buildings are indeed not new research topics. Nevertheless, recent far-reaching political decisions were taken in Switzerland in order to address climate change. The resulting program called "Energy Transition 2050", sets energy performance targets for buildings, industries, and mobility. This paves the way for the "2000 Watt and 1t CO_2 society" and potentially presents a good opportunity for innovative multifunctional façades to penetrate markets.

METHOD

In order to prove technical and financial feasibility, the Centre of Integral Building Technologies ZIG of the Lucerne University of Applied Science – Technique and Architecture and Montana Bausysteme AG jointly launched a demonstration project on the university campus in Horw, Central Switzerland. The objective is to build a full-scale demonstrator of a typical factory building, which meets the thermal requirements of the Swiss building standards Minergie in a pre-Alpine region. The demonstrator comprises the solar wall collector and a ventilation system. It is going to be extensively monitored in order to determine the performance characteristics under real operation conditions of the full system and to test different operation strategies.

Demonstration system

The dimensions of the test building correspond to average sized factory halls in Switzerland. The factory hall has got a useful floor area of 300 m^2 and a height of 8.2 m (s. Figure 1).

The factory hall is a typical industrial building consisting of a steel construction. It is equipped with large entrance gates that allow trucks to enter into the hall. The roof and the walls are thermally insulated according Minergie-Standards. The wall construction is done by means of liner trays, which are covered by a metal sheet cladding on the outside. A perforated metal wall will be installed in the top section of the south-facing side of a building, creating approximately a 9 cm confined gap between it and the building's structural wall. The coloured wall acts as a large solar collector that converts solar radiation to heat. It will receive the maximum exposure to direct sunlight during the fall, winter, and spring. Fans mounted at the top of the wall pull outside air through the transpired collector's perforations, and the thermal energy collected by the wall is transferred to the air passing through the holes. The fans then distribute the heated air into the building through ducts mounted near the ceiling. By preheating ventilation air with solar energy, the technology removes a substantial load from a building's conventional heating system, thus saving energy and money.

As shown in Figure 2, the transpired collector system also contains a bypass damper located directly in front of the fan inlet duct. During the summer months when ventilation air requires no heating, this damper opens, circumventing the air-heating system. The bypass damper automatically opens when the air outside reaches a predetermined temperature, usually about 20 °C.

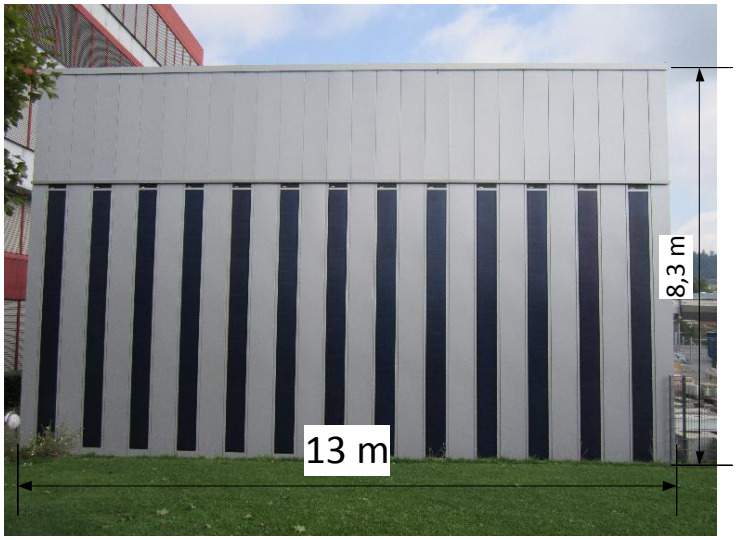

Figure 1: Cogeneration demonstration façade at Lucerne University of Applied Sciences. The TSC is placed in the upper part of the façade and supplies preheated outdoor air to the building. In the lower part, thin slice PV ribbons have been placed for solar power generation.

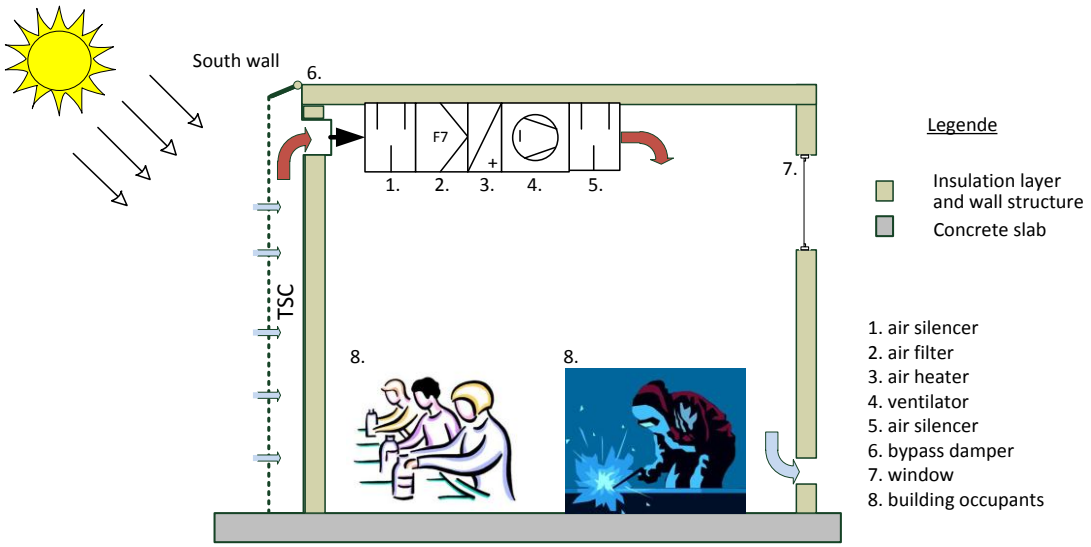

Figure 2: Schematics of the generic TSC system including ventilation system but without air-to-air heat recovery) (Illustration 8: © office.com)

Testing setup

The measurement at the demonstration facility aims at gaining knowledge about the energy performance of the overall system and to develop energy efficient operation strategies. The following aspects are of scientific relevance:

- Pressure losses in collectors at different air flow rates
- Temperature rise characteristics depending upon irradiation and air flow rate
- Collector efficiency line
- Optimal air flow rate through collector
- COP/EER of system

A metering plan has been developed in line with these factors (s. Figure 3 and Table 1). Nevertheless, only the most relevant parameters are going to be monitored due to budget constraints.

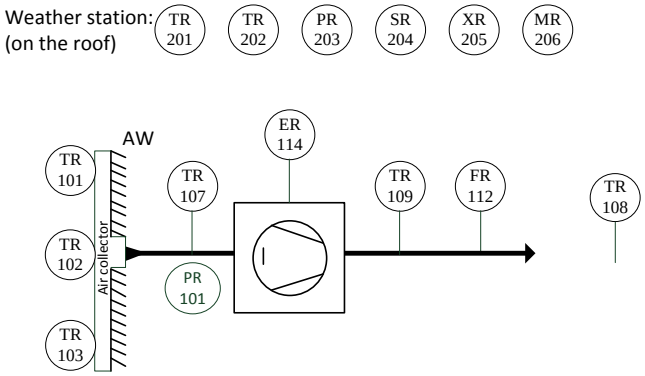

Figure 3: Schematics of the energy metering concept for the TSC system in Lucerne.

Sensor	Description	Sensor	Description
TR101-TR103	Local surface temperature of collector absorber	ER114	Power consumption of ventilator
TR104-TR106	Air temperature in collector plenum	TR201	Outdoor air temperature
TR107	Collector outlet air temperature	XR202	Global solar irradiation
TR108	Indoor air temperature	PR203	barometric pressure
TR109	Supply air temperature	SR204	Wind velocity
FR112	Air flow rate	XR205	Wind direction
PR101	Pressure	MR206	Outdoor air moisture

Table 1: Details of energy metering system for the performance analysis of TSC collector in Lucerne.

Further research issues in the project are static and dynamic issues related to construction engineering (wind pressure, waterproof ability against rain, thermal expansion, resistance to corrosion, fouling of wall collector, moisture formation in collector plenum, …). They will be reported in the framework of a long-term observation by façade experts.

CONCLUSION AND PROSPECT

A full-scale demonstration plant with a TSC collector and a ventilation system is under construction on the campus of Lucerne University of Applied Sciences. Its energy performance will be extensively monitored in order to obtain pertinent product specifications that can be used for instance in simulation (calibration of models). This paper describes the demonstrator and the measurement concept. Measurement results will be presented during the upcoming conference CISBAT 2013 in Lausanne and in future papers.

Future research issues will deal with system integration aspects, i.e. the interaction between TSC and air-to-air heat recovery or with storing heat in murocausts and/or hypocausts.

Considerations, such as simplifying and systemising façade refurbishment, providing knowledge based advice and tools to policy makers and industrial managers, elaborating rules and standards, and demonstrating feasibility will substantiate the technical and financial planning. As a result, more owners may decide to retrofit their facility rather than demolish and reconstruct it. This more environmentally friendly measure would save embodied energy and material, thus ensuring that TSC will have a far more reaching impact than simply reducing heating costs.

REFERENCES

1. C. Filleux, A. Gütermann, „solare Luftheizsysteme“, Ökobuch-Verlag, 2nd edition, Staufen, Germany, 2010
2. Stryi-Hipp, G. et al., Neue Perspektiven für Luftkollektorsysteme, proceedings of 20th Symposium “thermische Solarenergie”, pp. 37-41, bad staffelstein, 2010
3. Christen, R. : Solarluftkollektor - Vergleich mit einer Photovoltaikanlage, internal report, Lucerne School of Engineering and Architecture, Lucerne, Switzerland, 2012
4. Sicre, B.: Energetic and market potentials of solar air collectors for the refurbishment of factory building in switzerland”, Proceedings of the 10th international conference “Gleisdorf solar”, Gleisdorf, Austria, 2012
5. Sicre, B.: Solare Luftheizsysteme - Eine Marktstudie für die Schweiz und Europa, internal report, Lucerne School of Engineering and Architecture, Lucerne, Switzerland, 2011
6. Christensen, C.: Transpired collectors, Federal Technology Alert, DOE, Washington DC, 1998
7. Welz, C. et al.: Physikalische Modellierung und Simulation sowie detaillierte Vermessung von Luftkollektoren, proc. of 22th Symposium Thermische Solarenergie Bad Staffelstein, 2012

ANALYSIS OF THE PERFORMANCE GAP AND PERFORMANCE VARIATION FOR SOLAR THERMAL SYSTEMS

Adam Thirkill; Paul Rowley

CREST, Holywell Park, School of Electronic, Electrical and Systems Engineering, Loughborough University, Loughborough, Leicestershire, LE11 3TU

ABSTRACT

This paper describes the evaluation of both measured and modelled heat generation for 30 solar thermal systems in the UK. Variations in solar yield arising from simplified modelling methods are firstly analysed in terms of stochastic factors such as user behaviour regarding domestic hot water (DHW) demand, actual incident irradiation and the energy content of consumed hot water, along with other effects on the performance of real life solar thermal systems that cannot be easily incorporated into simplified model-based estimation. Additional statistical analysis shows evidence of performance variations arising from both technical and non-technical factors including system configuration, volumetric hot water consumption and hot water use profile. A number of techniques, including principal component analysis (PCA), were applied to explore the correlation between system performance and specific variables and a candidate Bayesian network (BN) has been developed which facilitates an effective means of both diagnosis and prognosis of system performance.

The results show that deemed heat generation calculated using a simple model-based approach exhibits significant variation (or performance gap) when compared to measured heat generation. Complex interactions between a number of factors such as the volumetric hot water consumption, hot water use profile and the timing of auxiliary heating systems result in a wide performance variation and this indicates that in order to maximise the contribution of solar thermal systems, a deeper holistic understanding of the impact of these factors for individual cases is required, along with the application of appropriate mitigation strategies, including more effective system control approaches. An evidence-based approach, such as via the use of Bayesian networks, offers the potential to use real life performance data to probabilistically predict the likely heat generated based on prior knowledge of the system.

Keywords: SAP, solar thermal systems, performance gap, Bayesian network

INTRODUCTION

The UK's Renewable Heat Incentive (RHI) is an energy yield tariff-based mechanism that aims to increase the take-up in renewable heat technologies. For domestic consumers, the scheme will be open to all those that meet minimum energy efficiency criteria, and will be payable based on deemed (or modelled) rather than measured energy generation. This estimated approach is based on the relatively high costs associated with measuring the performance of small-scale systems. Therefore, it is likely that the UK standard assessment procedure (SAP) for the energy performance of dwellings will play a central role in deeming the heat generated by domestic scale renewable heat systems [1], [2]. A key risk however, is the current lack of understanding and empirical evidence regarding the real-life performance of renewable heat technologies, and the resulting uncertainty regarding the accuracy of SAP-based deemed compared to actual heat generation. This in turn results in uncertainty as to the

impact of renewable heat technologies on the UK's carbon reduction targets [3], as well as investment risk for both Government and consumers alike.

METHOD

Field trial data

Data from the Energy Saving Trust's (EST) solar thermal field trial [4] was used to make an evaluation of the performance gap between SAP and actual heat generated and the variation in the performance of these systems. The field trial involved monitoring 88 systems throughout the UK, 30 of these were selected for the analysis presented in this paper.

Evaluating modelled SAP and measured heat generation for STS

The UK's standard assessment procedure (SAP) is a compliance tool used to evaluate building energy performance. In SAP, benchmark values for a range of variables that characterise specific dwellings are provided and steady state calculations are carried out in the form of a worksheet. In this study, the solar heat generated by the STS were calculated using the SAP 2009 methodology [5]. Using 30 installed systems monitored during the EST solar thermal field trial. Two types of SAP calculation were performed: SAP 1 and SAP 2. SAP 1 used basic knowledge about the STS size, orientation and efficiency as well as the occupancy level of the household but all other information was taken from the values provided in the SAP tables. SAP 2 used measured values from the EST field trial to replace simplistic assumptions made in SAP 1. The results for these calculations were compared to measured data from the field trial to evaluate the performance gap.

Evaluating the variation in performance using principal component analysis (PCA)

Principal component analysis (PCA) can be used to reduce a set of many correlated variables to a manageable number of uncorrelated variables. These are called principal components (PCs) and are obtained by orthonormal transformation of the original variables [6]. Eight variables from the 30 selected field trial systems were used in this analysis. Since the chosen variables have different units of measure the 'weighted' PCA method was used [7], carried out using the MATLAB programming environment. Transformations of the original variables were computed using the Pearson correlation matrix approach, as opposed to the covariance matrix.

Constructing the candidate Bayesian network (BN)

The candidate Bayesian network (BN) was constructed using a combination of a realist synthesis and causal mapping approach outlined in [8] and [9] respectively. The realist synthesis approach has the following steps:

1. Develop theories and questions about the STS performance and find evidence in literature and/or data to support or reject (this is termed realist synthesis);
2. Relationships and direction between the factors (variables) identified in the realist synthesis are determined;
3. The strength of the evidence supporting the relationships between the factors is considered, which indicates the confidence in the evidence;
4. The variables are discretised with the number of bins (states) being minimised to a level that maintains the correlations between the variables but reduces the number of conditional probabilities;

These four steps enable the structure of the BN and its initial conditional probabilities to be determined. After an initial realist synthesis of the literature, a causal map was developed showing the variables and related causality. This was transformed into a BN and data elicited from the literature was used to produce Bayesian priors and conditional probabilities. Where data was incomplete a heuristic approach to the derivation of the conditional probabilities was taken, which is an advantage of BNs compared to alternative methods [10]. Variables are represented by nodes and relationships by the linking arrows between them. Conditional probabilities are indicated by the distributions for each node. Distributions of heat generated by STS were generated by the BN using information about the domestic hot water (DHW) demand and system size (collector area and tank volume). Figure 1 shows the candidate BN used to generate distributions of annual solar heat generated (yield) in the current study.

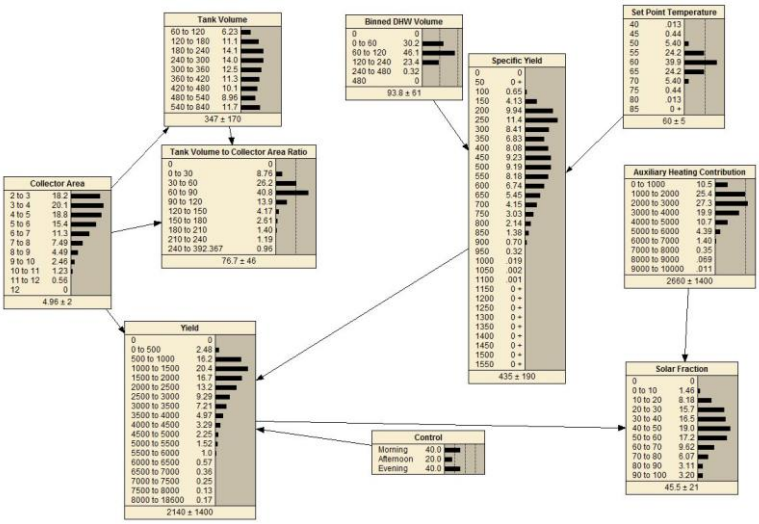

Figure 1: Candidate Bayesian network

RESULTS AND DISCUSSION

A comparison between SAP modelled and measured STS heat generation

A comparison between SAP modelled (or 'deemed') and measured STS heat generation is shown in Figure 2 where Delta Q_{sol} is defined as SAP deemed – measured STS heat generated. SAP 1 makes use of SAP assumptions whereas SAP 2 uses measured data in lieu of these. An underprediction of STS heat generation occurs when the SAP value is lower than the measured, the opposite represents an overprediction. Delta Q_{sol} ranges from -1500kWh/yr to 900kWh/yr.

Table 1 shows that there is a weak correlation between measured and either of the SAP estimates, whilst using measured data in place of SAP approximations improves correlation very slightly. This suggests that the use of SAP to deem heat generation for RHI accredited STS systems could be problematic; even by substituting known values in the calculation heat generated is poorly estimated. This may not be an issue related to the SAP procedure per se, but rather that user behaviour or other system factors are highly variable from system to system. Additionally, even if user behaviour for a particular system remains consistent over time, weather variations (and so variations in performance) are not accounted for by SAP. Thus, by not including uncertainty in the deeming method, confidence in the accuracy of modelled values is limited.

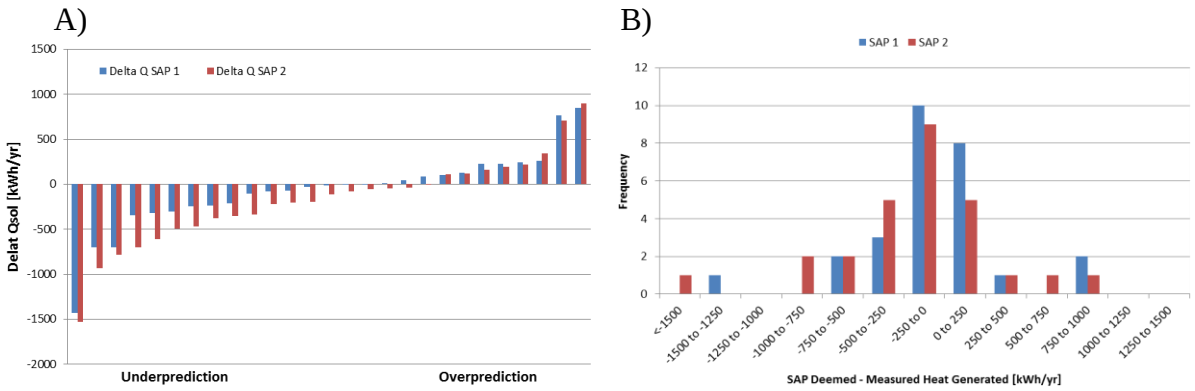

Figure 2: A) Individual Delta Q_{sol} B) Distribution of Delta Q_{sol}

	SAP 1	SAP 2	Measured Data
SAP 1	1		
SAP 2	0.005	1	
Measured Data	0.019	0.024	1

Table 1: Pearson correlation matrix for SAP deemed and measured STS heat generation

The results suggest that the inidcated instances of under-prediction of the heat generated by a RHI accredited installation could lead householders not being fully compensated for the initial cost of the system by the value of renewable energy actually generated. On the other, indicated instances of over-prediction of the heat generated poses a problem for policy makers in that this could result in consumers being over-compensated by the RHI scheme.

Evaluation of the variation in STS performance

Principal Component Analysis (PCA) was used to evaluate the annual variation in performance of the 30 monitored STS. Eight variables were included in the analysis and these are shown in Figure 3. Figure 3 shows the results of the PCA in the form of a bi-plot using the first three PCs, representing 82.2% of the variation in the data. A grouping of variables suggests that they are positively correlated whereas variables that are opposed on the plot are indicated to be negatively correlated. Variables that are orthogonal on the plot have no indicated correlation.

The results indicate a positive correlation between auxiliary water heater input and DHW demand. This is because for a given size of STS, greater DHW consumption volumes tend to require more auxiliary input to reach the desired temperature. There is a negative correlation between solar fraction and auxiliary input since solar fraction is a ratio of the solar input to the total input (solar and auxiliary). Solar fraction is therefore negatively correlated to DHW demand, due to the relationship between auxiliary input and DHW demand. Furthermore, the solar input is negatively correlated with auxiliary input and DHW demand on the second and third component axes. Higher auxiliary input can increase the temperature of the tank and therefore reduce the capacity for solar input [11], [12], whilst higher DHW loads can reduce the tank temperature and therefore increase the solar input [13], [14]. However if a system is poorly controlled in terms of auxiliary heating input, then the tank remains at a high temperature when the STS could otherwise make a contribution. Conversely, if optimally controlled, the DHW load can recharge the tank with cooler water before solar energy is available. Annual data might not show this relationship.

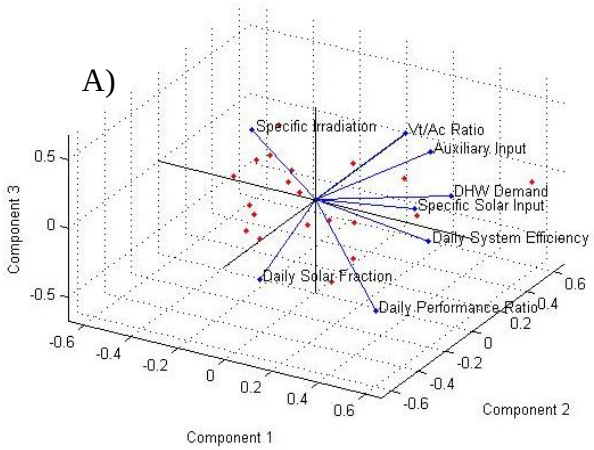

B)

Variables	Q_{solar}	I	Q_{aux}	DHW	η_{sys}	SF	V/A	PR
Q_{solar}	1							
I	-0.038	1						
Q_{aux}	-0.027	-0.225	1					
DHW	0.292	-0.194	**0.803**	1				
η_{sys}	**0.945**	-0.264	0.051	0.412	1			
SF	0.320	0.072	**-0.777**	-0.394	0.334	1		
V/A	**0.612**	-0.097	0.172	0.177	**0.509**	-0.096	1	
PR	0.436	-0.285	-0.086	0.265	**0.590**	0.350	-0.018	1

Figure 3: A) Bi-plot of the first three principal components, B) Pearson correlation matrix

Results from the Bayesian network

For each of the 30 systems, a distribution of the annual solar yield was produced using the BN. The results show that for the majority of the systems, the measured values were within the distribution of modelled annual yield. Only two systems did not fall within the predicted BN distribution, both of which had low annual yields of 671kWh/yr. and 357kWh/yr. Thus, the results show the potential for such a BN approach to manage uncertainty in performance prediction.

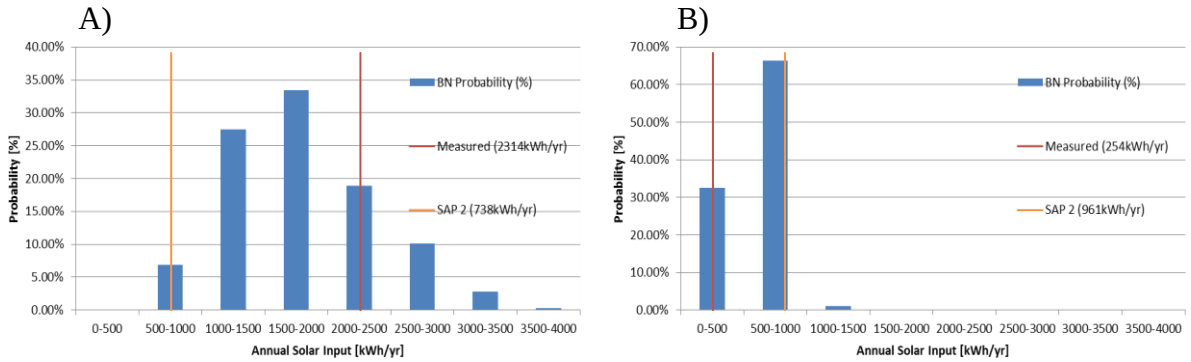

Figure 4: Distributions of annual heat generated A) under-predicted B) over-predicted

Finally, financial projections were carried out using the BN approach. Figure 4 shows annual heat generated by two STS: A) shows a system where SAP 2 under-predicts the yield and B) shows an over-prediction. Using the current RHI value of 17.3p/kWh, household A would receive £127.67 from the RHI, but measured data indicates an entitlement of £400.32. Household B would receive £166.25 when measured data suggests their entitlement is only £43.94. Therefore, there is little incentive for the user to adjust their behaviour to maximise system output. With the BN, since the distributions are skewed, a median value can be used. The median for A lies between 1500-2000kWh/yr, (1750kWh/yr), whilst for B it is between 500-1000kWh/yr (750kWh/yr). This would provide financial returns of £302.75 and £129.75 per year respectively. Thus, this represents an improved means for setting returns, since these are calculated using likely performance based on evidence.

In practice the BN based deeming method could be adopted during an RHI (or 'Green Deal') assessment: Information about a household's energy behaviour can be used in a BN to

provide a distribution of the likely performance of an STS. If the distribution is overly broad then a STS may not be the best technology for the household. A STS would be potentially a good investment if the distribution is narrow and at a reasonable level (such that the median yield would at least fully compensate the initial cost of the system over the investment period). SAP based models do not allow this kind of decision making under uncertainty to be performed and technology solutions cannot be tailored to fit householders' behaviour because variability is not fully considered. BNs incorporate uncertainty and variability and so allow households to be matched to suitable technologies. This is important because it allows a suitable tariff level to be set that will allow compatible households to see a positive return on investment and enables a mix of renewable heat technologies to be employed to meet carbon reduction targets.

REFERENCES

[1] Crowther, M., Charlick, H., Bates, B. and Green R.: Report to DECC on Heat metering for the RHI, 2010.

2. Kelly, S., Crawford-Brown, D. and Pollitt, M. G. Building performance evaluation and certification in the UK: Is SAP fit for purpose? Renewable and Sustainable Energy Reviews, Vol. 16, pp 6861-6878, 2012.

3. CMS Cameron McKenna: The Renewable Energy Directive: your Q & A guide. 2009.

4. EST: Here comes the sun: a field trial of solar water heating systems. 2011.

5. DECC: SAP 2009 The Government's Standard Assessment Procedure for Energy Rating of Dwellings. 2010.

6. Jolliffe, I. T.: Principal Component Analysis. Springer-Verlag New York Inc., New York, 1986.

7. MathWorks: Feature Transformation. Available: http://www.mathworks.co.uk/help/stats/feature-transformation.html#f75476. [Accessed: 15-Oct-2012].

8. Shipworth, D.: Synergies and conflicts on the landscape of domestic energy consumption: beyond metaphor. ECEEE 2005 Summer Study, pp 1381-1391, 2005.

9. Nadkarni S. and Shenoy P. P.: A causal mapping approach to constructing Bayesian networks. Decision Support Systems, Vol. 38, pp 259-281, 2004.

10. Fenton N. and Neil M.: The use of Bayes and causal modelling in decision making, uncertainty and risk. *CEPIS Upgrade*, Vol. 12, pp 10 - 22, 2011.

11. O'Flaherty F., Pinder J., and Jackson C.: Evaluating the performance of domestic solar thermal systems. Retrofit 2012, 2012.

12. Allen S. R., Hammond G. P., Harajli H. A., McManus M. C., and Winnett A. B.: Integrated appraisal of a Solar Hot Water system. Energy, Vol. 35, pp 1351-1362, 2010.

13. Knudsen S.: Consumers' influence on the thermal performance of small SDHW systems - Theoretical investigations. Solar Energy, Vol. 73, pp 33-42, 2002.

14. Furbo S., Andersen E., Knudsen S., Vejen N. K., and Shah L. J., Smart solar tanks for small solar domestic hot water systems. Solar Energy, Vol. 78, pp 269-279, 2005.

THE HYBRID SYSTEM OF RENEWABLE HEAT SOURCES - LOCAL THERMAL SMART GRID

Wójcicka-Migasiuk Dorota[1]; Chochowski Andrzej[2]

1: Lublin University of Technology, Faculty of Fundamental Technology, Nadbystrzycka 38,Lublin, Poland, d.wojcicka-migasiuk@pollub.pl

2:University of Life Sciences, Faculty of Production Engineering, Nowoursynowska 168, Warsaw, Poland, andrzej_chochowski@sggw.pl

ABSTRACT

The authors have been exploiting a hybrid energy supply for a hotel building since 1999. The cooperating sources are: solar energy, geothermal system and power mains supply. The basic task for this composition is to provide hot water. The system is composed of solar thermal flat plate collectors, heat-pipe vacuum collectors, a heat pump with a ground heat supply and a thermal accumulation system of water tanks aided by electric heating. The cooperation among various renewable energy sources is connected with the need to extend the systems with conversion devices and, even at first, with the need to accumulate the surplus of energy gain. It is important to optimise the fluxes of generated power and load in the way to distinctly reach energy savings in traditional energy carriers and energy efficiency of the whole solution.

The control software has the tasks: to measure control values, to analyze their dynamics of changes and to work out correct setup signals. Nowadays, these possibilities have remotely scattered automatics based on PLC controllers. This way an intelligent local network can be created to provide energy needs for e.g. a hotel and at greater size, for a district or even for a village.There is fully automatic monitoring and control based on PLC type S-7-300. The variety of algorithms have been tested to enable this system to work as a local smart grid and to select optimal parameters adjusted for current ambient conditions and thermal load. The adaptation control system has been used to allow for particular element diagnostics too. The described thermal energy supply system undergoes now exploitation tests after the modernization. Different control algorithms are tested but each test requires the whole year of operation, so the results are still expected.

Keywords: hybrid solar supply, automatic control, adjusted parameters, thermal accumulation system

INTRODUCTION

The reduction of traditional energy carrier sources and the tendency to raise the energetic effectiveness make people to search for more and more sophisticated techniques of cooperation between traditional energy sources and unconventional ones. The systems of hybrid supply have been composed recently. They incorporate energy sources of different character. Electric energy is aided by solar PV panels or wind turbines. Solar thermal collectors (flat plate and vacuum tubular) are used to prepare hot water and, e.g. shallow geothermal systems, for some other purposes. The combination of different renewable energy sources is not only the constructional composition of such elements as: solar collectors, PV panels, wind turbines, a heat pump and ground collectors but also the incorporation of a composed control system to enable the cooperation of these elements. The software component, i.e. a convenient control algorithm, is also of special importance.

The control of a renewable hybrid supply system requires the composition and construction of a measuring – monitoring system on a real time basis to enable monitoring either the possibility to gain the energy or to convert it, or also current demand.

This paper describes a hybrid supply of a hotel hot water system. This system has been in operation since 1998 yr and makes a local smart-grid incorporating devices supplied with electric energy, solar energy, geothermal energy and gasoil. The system operation is monitored and fully controlled by PLC S7-300 (Siemens) controllers in master/slave mode of operation, according to the introduced algorithms.

The system serves for the purposes to provide the needs for hot water system (SDHW) in a hotel and an auxiliary building. This system consists of several independent segments: flat-plate collectors, vacuum – tubular collectors, a compressor type heat pump with the bottom source in the form of a ground heat exchanger and a thermal accumulation tank of 2 m^3. This system is presented in Fig. 1 and cooperates with a gasoil boiler room and traditional electric water heaters which provide with thermal energy in the case when renewable energy supply is insufficient.

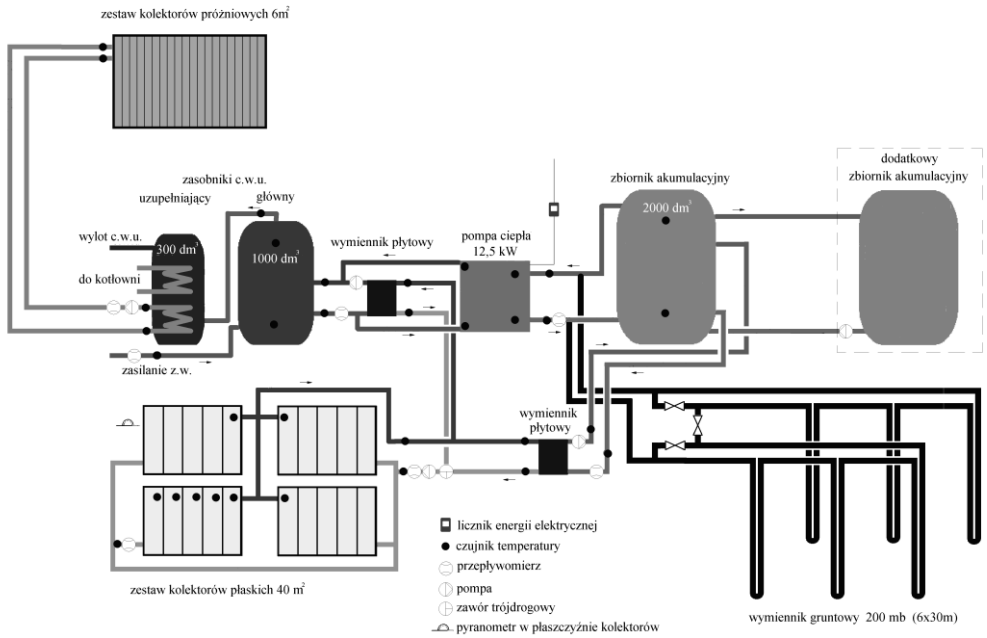

Figure 1: The hybrid system diagram composed of the following elements: vacuum-tubular collectors 6 m^2; 300 dm^3water accumulation with two coils, main water accumulation tank of 1000 dm^3, main flat plate heat exchanger, heat pump of 12.5 kW, accumulation tank of 2000 dm^3, additional auxiliary heat accumulation tank, flat plate solar collectors 40 m^2, flat plate heat exchanger, ground heat vertical exchanger 200 m long, additional symbols mean: electric power measurements, temperature sensor, flow meter, circulation pump, three-way valve, pyranometer on the plane of collectors.

The segment of flat plate collectors (also presented in Fig. 2) consists of 20 panels of total absorber surface of 40 m^2 placed on a construction on the ground, south oriented. Its load is in the form of main hot water accumulation tank of 1 m^3 and the auxiliary one of 2 m^3 that is used as the energy accumulator for the heat pump. Because of the use of *glikol* solution as medium in the solar system component the hot water tanks must be separated from the solar components by means of flat plate heat exchangers.

The sub-system of vacuum tubular collectors with heat-pipe elements consists of 60 tubes of total absorber surface of 6 m^2. These collectors are mounted on the roof of the auxiliary building, with the tilt angle of 40^0 and south – west orientation (see Fig. 2). This segment load is in the form of a two-coil 300 dm^3 tank connected in series with the main HW tank.

The stochastic character of solar radiation is the reason for high variation of thermal energy production intensity in collectors. This variation concerns either particular daytime hours or particular days and seasons. The compressor heat pump of nominal power 12.5 kW in cooperation with a vertical ground collector and its accumulation tank stabilize the supply of hot water.

The vertical ground collector is made of polyethylene tubes of 40 mm diameter, placed as double pipeline in 6 boreholes each 30 m deep. The total length is 360 m in the form of two parallel 180 m branches. The heat pump provides the temperature of hot water at the level of 50 C deg. There are some exemptions of intensive demand when a long time load exceeds the heat pump heating power. The reserve source (in the case of failure too) is a gasoil boiler which can be connected in the auxiliary tank loop. In practice, this happens only in winter season.

Figure 1: The solar segments in the hybrid system.

DISCUSSION

The described hybrid system supply has an extended measuring system. The monitoring consists in the constant registration of sensor indications in all nodes where the transformation, transport and the exchange of energy occurs and this makes possible to create the data basis. These bases collect the knowledge of the state and the waveform of phenomena occurring within the system and form the foundation to perform the short term prognoses. They can be used also to work out energetic efficiency diagnostic methods.

Initially, temperature in 40 measuring spots was measured by LM135 and LM335 sensors. Their advantages were low cost, linear characteristic, simple calibration and time constant not exceeding 1 minute. Their important disadvantage, however, was the fact that at high temperatures and simultaneous low load, they were damaged. That is why in 2010 yr., when

the system was modernized, they were substituted with Pt-1000 sensors o a bit longer time constant but of high durability.

Medium flow measurements were then performed by means of water flow meters equipped with pulse triggers (1 pulse per 2.5 dm^3). There were 7 such meters providing medium flux monitoring in all system segments and in heat exchangers. It followed from the research the sampling unit was insufficient at some detail analyses. That is why in both solar loops the flow meters have been substituted with higher precision ones, i.e.: 1 pulse per 1.5 dm^3.

Solar radiation intensity has been measured by means of two pyranometers for the measurements in both planes of collectors, i.e.: one for the flat plate collector plane and one for the roof mounted collectors. These pyranometers are of II^{nd} ISO class and their precision is sufficient for these exploitation measurements. The energy consumption of this hybrid system results from the need of power supply for the compressor type heat pump. Typical energy meter has been used to measure power used by the compressor electric motor (60 pulses per 1 Wh).

Initially, the control system consisted of 3 autonomous controllers that controlled separately the following segments: the flat plate collectors, the vacuum tubular collectors and the heat pump. That system enabled full remote monitoring through Internet of all current operation parameters (Fig. 3) but remote activation of regulator setups that were implemented in controllers was impossible those days. The circulation pumps in medium loops were not adjusted then to stimulate the flow. In 2011, the modernization of a measurement system and the control system of the whole was carried out. Then, the circulation pumps of changeable flows and controlled electromagnetic valves were installed to change hydraulic switch-over. At present, the superior controller – master controls the whole system. It receives the information directly from slave controllers and indirectly from measuring sensors, on current state of external inputs (e.g.: solar radiation, ambient temperature) and of current demand for hot water (Fig. 4). It also performs the analysis of the data and works out relevant valve settings (operation modes: flat plate collectors – accumulation tank; heat pump – accumulation tank; medium flow inside collectors, etc.). The method of task performance is determined by the algorithm uploaded to the controller memory. The algorithm can be changed remotely (through Internet) or control parameter values can be changed.

The previously exploited control system had several disadvantages and limitations, as the following: no possibility to extend thermal flux control, impossible modification of control algorithm, no possibility to change control settings remotely, no real time clock, impossible communication among controllers of particular system segments.

These limitations made impossible to maximize energy gain. The main problem was too low efficiency of particular segments and in the result - the whole efficiency of the system.

The newly modernized system has now SCADA (WinCC) software for the purposes of visualization and data storage, which is implemented at Windows on a PC computer. The card CP5611 with the protocol Profibus connects the controller. Besides the visualization, the technical features of WinCC make possible to read out the state of operation of particular devices and change settings of circulation pumps. Moreover, the remote monitoring through any Internet browser. Figure 5 presents the main screen of this system.

It is necessary to perform dynamic identification of all component devices to work out correct algorithms of system operation. These research has been carried out during the exploitation of such elements as: flat plate collectors, vacuum tubular collectors, heat exchangers, ground collector, accumulation tanks and the heat pump on the data basis. Dynamic properties have been determined by means of parametric identification methods. The appropriate model has

been selected and then used to determine transmittance and pulse characteristics. The selection of results and the methods were presented by the authors in some references [1,2,3,4].

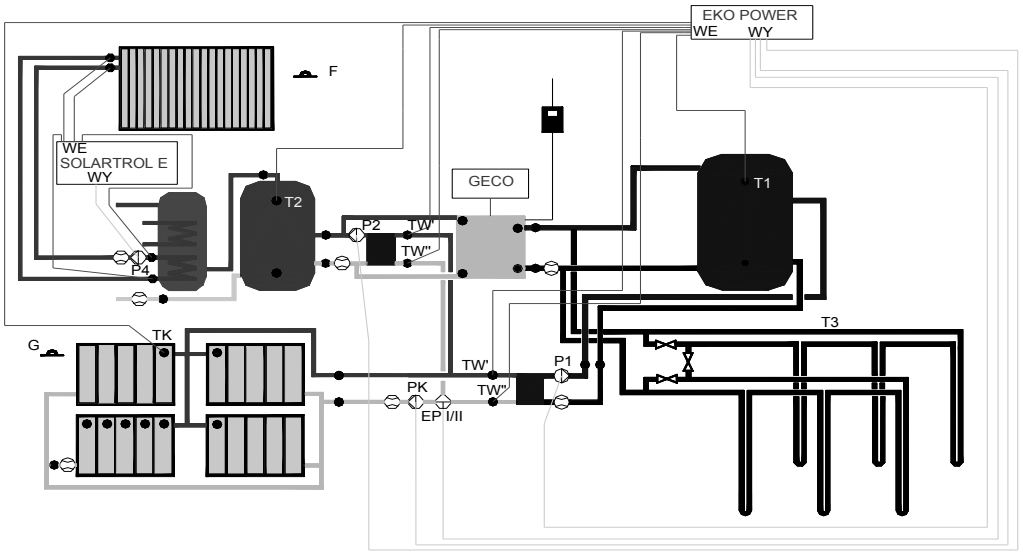

Figure 3. The principles of the initial hybrid system control in schematic layout.

The dynamic properties of some elements (e.g. collectors) are dependent not only on construction parameters but also on operation parameters. The example can be a set of collectors for which heat transfer resistance conditions their dynamics. They are strongly dependent on stochastic inputs, first of all on solar radiation. The determined dynamic properties let us use MATLAB Simulink all the way through the determination of all parameters and also of their character. One can carry out analyses of the system operation at different exploitation conditions when a hybrid system is modeled by means of dynamic blocks that reflect the cooperating elements.

The results of simulations make possible to work out a convenient control algorithm providing for the minimal renewable energy loss. The master/slave controllers steer energy flux flows, direct the surplus of energy to the auxiliary accumulation tank, select the priority of operation and control working medium flow. The method recognized as satisfying is adaptation control. It is important in this method to analyze the current state of operation on the basis of measurement history (result data basis) and smart short term prediction (1 to 3 hours ahead) of future states of operation. This is necessary to prepare operational devices to a relevant switch-over.

CONCLUSION

The described thermal energy supply system undergoes now exploitation tests after the modernization. Different control algorithms are tested but each test requires the whole year of operation, so the results are still expected.

The local network of cooperating different energy sources (solar, geothermal, electric, gasoil combustion) is to be the more intelligent the more predictive the control algorithm is and the prognoses enable to adapt the system to the users' need considering varying external inputs.

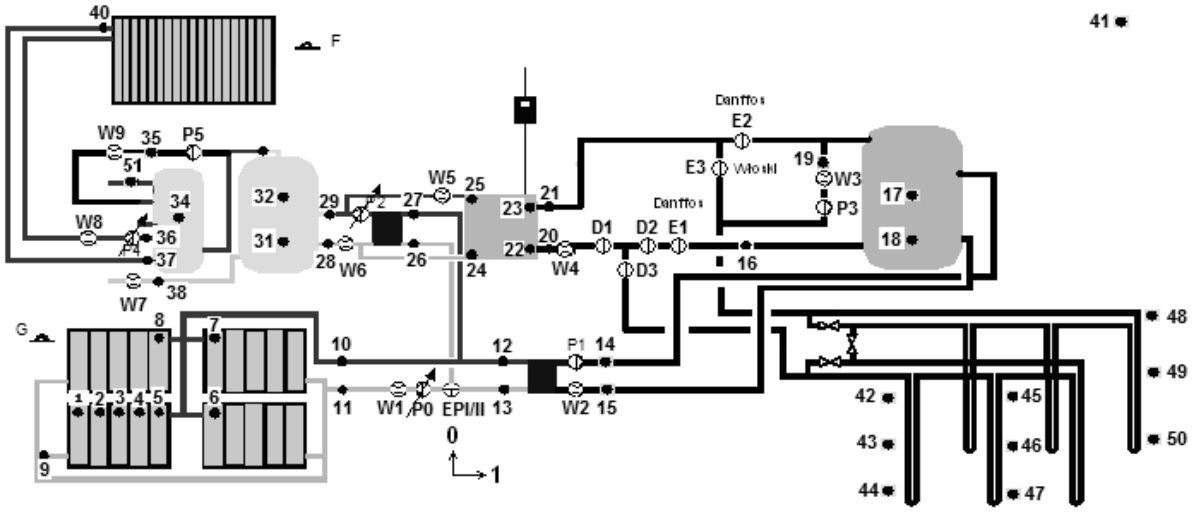

Figure 4. The principles of the modernized hybrid system control in schematic layout; D- hand operated valves, E - electric valves EP - three way valve, P circulation pumps.

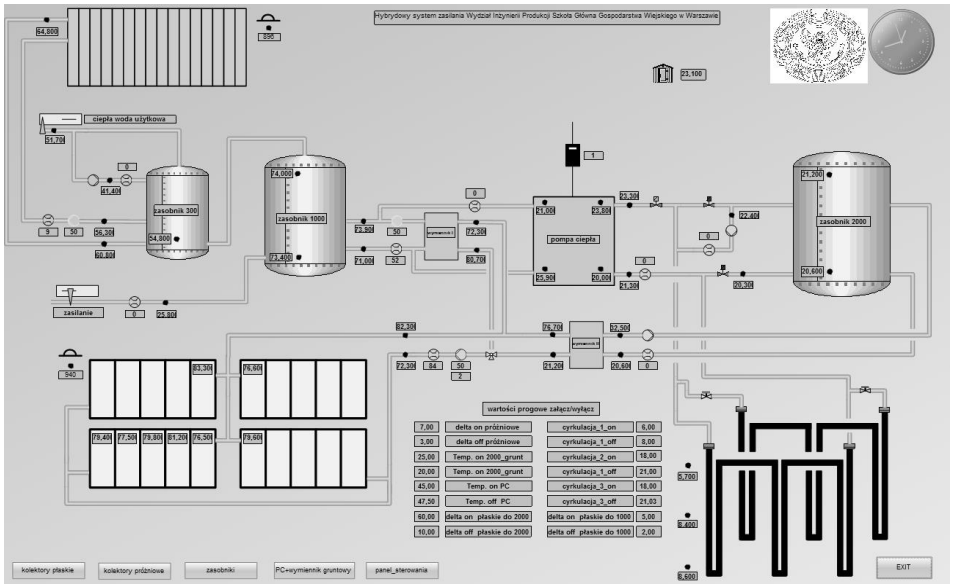

Figure 5. The main SCADA screen for the described system.

REFERENCES

1. Czekalski D., Chochowski A., Obstawski P.: Parametrization of daily solar irradiance variability. Renewable and Sustainable Energy Reviews 16 (2012) p. 2461-2467
2. Piotrowska E., Chochowski A.: Application of parametric identification methods for the analysis of the heat exchanger dynamics. Inter. Journal of Heat and Mass Transfer, 2012, Vol. 55, nr 23/24
3. Piotrowska E., Chochowski A.: Representation of transient heat transfer as the equivalent thermal network (ETN). International Journal of Heat and Mass Transfer 63 (2013) 113–119
4. Wójcicka-Migasiuk D.:Thermal system diagnostic through signal modelling. Environmental Engineering IV (2013) CRC Press Taylor and Francis Group (in printing)

Building and Urban Simulation

MODELLING THE URBAN MICROCLIMATE AND ITS INFLUENCE ON BUILDING ENERGY DEMANDS OF AN URBAN NEIGHBOURHOOD

J. Allegrini[1,2]; J. Kämpf[3]; V. Dorer[1]; J. Carmeliet[1,2]

1: Empa, Laboratory for Building Science and Technology, Dübendorf, Switzerland

2: ETHZ, Chair of Building Physics, Zürich, Switzerland

3: *EPFL, LESO, Lausanne, Switzerland*

ABSTRACT

In the past decades the portion of the population living in urban areas has continuously increased. Due to the high building density, the microclimate in urban areas changed significantly compared to rural areas. The temperatures measured in urban areas are, due to the urban heat island (UHI) effect, higher compared to the rural temperatures. The UHI intensities are increasing with higher building densities and growing cities. Space cooling and heating demands of buildings are strongly affected by the local microclimate at the building sites. Due to the climate change and the limited energy resources, energy saving and sustainability are nowadays important issues. A significant part of the global energy consumption is used for space cooling and space heating of buildings. Thus its minimization for buildings in urban areas has great energy saving potential.

Most building energy simulation (BES) models were developed for stand-alone buildings and therefore do not consider effects of the urban microclimate. This can lead to inaccurate predictions of the space cooling and heating demands for buildings in urban areas. The aim of this paper is to investigate the urban microclimate and its potential influence on the energy demand of buildings in an urban context by conducting detailed flow, radiation and building energy simulations at the urban neighborhood scale. CitySim is used for the radiation and building energy simulations. In CitySim detailed radiation models for solar and longwave radiation are implemented that can account for the radiation exchange between neighbouring buildings. The flow around the buildings is modelled by running CFD (computational fluid dynamics) simulations using OpenFOAM. As a result it is shown, how the temperatures and wind speeds can strongly differ within different urban areas. Further an approach is presented, to consider the local microclimate in the building energy simulation tool CitySim.

Keywords: Urban microclimate, Urban heat island effect, Building energy simulations, CFD

INTRODUCTION

Energy demand predictions for buildings in an urban context have to account for heat fluxes at several scales, considering interactions between surrounding buildings at local scale as well as urban heat island (UHI) effects at micro- and mesoscale [1]. Akbari et al. 1992 [2] reported that for US cities the peak electricity loads increase by 1.5 – 2 % for a temperature increase of 1 °F. As compared to an isolated building, a building in an urban area experiences (i) increased maximum air temperatures due to the urban heat island effect, (ii) lower wind speeds, and consequently reduced convective heat exchange, due to wind-sheltering effect, (iii) lower energy losses during the night due to reduced sky view factors, (iv) changed solar heat gains due to shadowing and a modified radiation balance. All these effects have an important impact on the energy demand of buildings [3-5], as they affect the conductive heat

transmission through the envelope, the energy exchange by means of ventilation [6] and the potential to employ passive cooling by night-time ventilation. Further the buildings influence the local microclimate in the urban area, because they change the local wind flow conditions and increase the local air temperatures. This shows that the local microclimate and the energy demand predictions of buildings have to be analysed in a coupled way. The changed local microclimate not only influences the energy demand of buildings, but also has an impact on the human comfort and health in urban areas.

In this study building energy simulations for a group of 14 buildings are conducted with CitySim [7]. For four weather conditions with high temperatures (high cooling loads), the surface temperatures determined with CitySim, accounting for detailed longwave and solar radiation exchange between the buildings, are used as boundary conditions for the CFD simulations. With CFD detailed temperature and velocity fields around the buildings are determined. These local air temperatures and wind speeds are then used for the building energy simulations of buildings in urban areas. In a second part of this paper an approach is presented to produce more accurate climatic data with CFD simulations, which can improve the energy demand predictions of building energy simulations.

NUMERICAL MODEL

The building energy simulations are conducted with CitySim for the climate of Zürich (Switzerland). CitySim is a simulation tool which models the energy fluxes from a small neighbourhood to an entire city. It includes a radiation model based on Perez All Weather [8] and Simple Radiosity Algorithm [9] to compute the hourly irradiation on the building surfaces. In this paper 14 office buildings are studied (Figure 1). The buildings have a height (H), a width (W) and a length (L) of 10 m, except buildings 6 and 9, which are 30 m or 25 m long depending on the cases. Two cases are studied with different distance (D) between the buildings to analyse the influence of the building density on the urban microclimate. The first case has an aspect ratio (H/D) of 1 and the second case an aspect ratio of 2. Each building consists of four thermal zones. Each thermal consists of one exterior building wall and a quarter of the buildings volume. The four zones are connected in such a way that they have the same inside air temperature. Space heating and space cooling are used to keep the inside air temperatures between 23 °C and 26 °C. The building walls have a glazing fraction of 25 % and a short wave reflectance of 50 %. The outside surfaces of the walls are made of bricks for simplicity. Therefore buildings with rather moderate surface temperatures are modelled here. Modern highly glazed office buildings using highly reflecting solar shadings will lead to significantly higher surface temperatures and influence the urban microclimate even more.

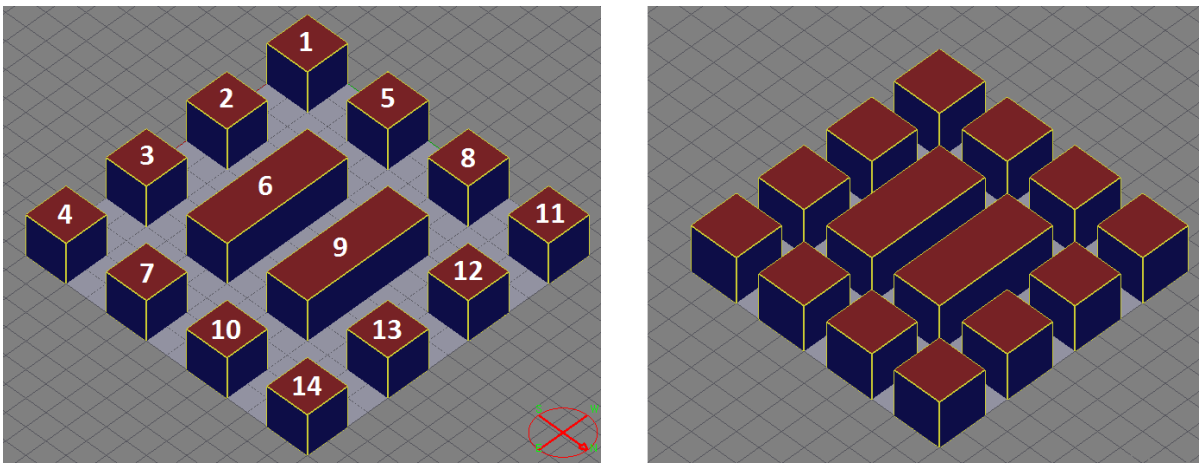

Figure 1: Arrangement of the 14 studied buildings (left: aspect ratio 1; right: aspect ratio 2).

For four weather conditions with rather high ambient temperatures CFD simulations are conducted with OpenFOAM (Table 1). These weather conditions are considered to be critical for space cooling.

	Wind speed	Wind direction	Air temperature
Weather condition 1	0.3 m/s	Normal	25.2 °C
Weather condition 2	5.5 m/s	Normal	25.5 °C
Weather condition 3	0.6 m/s	45 °	27.2 °C
Weather condition 4	4.7 m/s	45 °	25.9 °C

Table 1: Different studied weather conditions (Normal: Wind flow normal to large facades of buildings 6 and 9; 45 °: Wind direction with an angle of 45 ° between the wind direction and the surface normal of the large facades of buildings 6 and 9.).

Steady 3D RANS (Reynolds-Averaged Navier-Stokes) CFD simulations are conducted with a k-ε turbulence model. For the near-wall modelling wall functions are used to limit the computational costs. The possible overestimation of the convective heat flux at the building facades due to using wall functions is assumed to be smaller than the influence of different weather conditions on the urban heat island intensity. The aim of this study is not a detailed quantification of the urban heat island intensity, but presenting importance of the urban heat island effect and how it can be modelled with CFD. A structured grid is built based on a grid sensitivity analysis. At the inlet of the computational domain vertical atmospheric boundary layer profiles of the mean horizontal wind speed, the turbulent kinetic energy and the turbulence dissipation rate are imposed. At the inlet the air temperature is set equal to the temperature from the meteorological data for the condisered weather condition. At the ground and building surfaces the temperature from the BES are imposed. To model buoyancy the Boussinesq approximation is applied.

RESULTS

First the wind flow between the buildings is studied in more detail. The wind speeds around the buildings are needed to determine the convective heat fluxes at the building surfaces. For BES commonly the wind speeds from meteorological data are used for the determination of the convective heat transfer. However in urban areas these commonly used correlations are not correct, because they are based on measurements of stand-alone buildings.

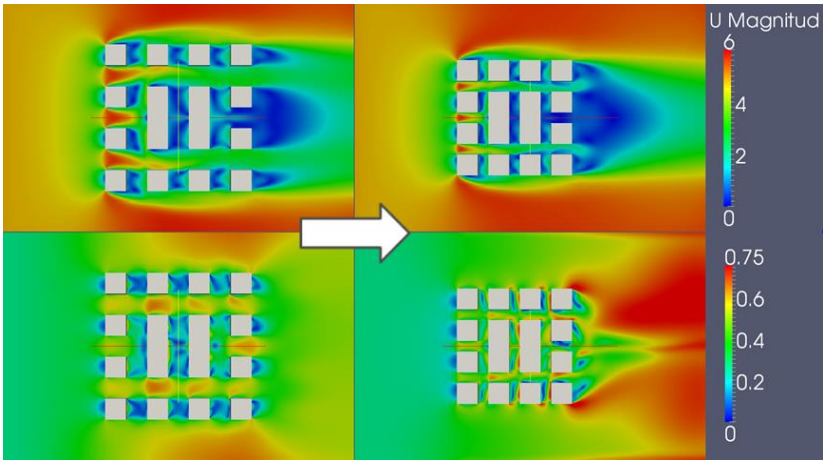

Figure 3: Contour plot of wind velocity 5 m above the ground for weather condition 2 (top) and 1 (bottom). Left: Aspect ratio 1; Right: Aspect ratio 2. Arrow indicates the wind direction.

Figure 3 shows contour plots of the wind speed for weather conditions 1 and 2. For weather condition 2 with high wind speeds, it can be observed that flow is accelerated around the buildings. For the first row of buildings there is also acceleration between the buildings, but further downstream the flow is slower between the buildings. For the determination of the convective heat transfer, different transfer coefficients have to be used for the different buildings. The convective heat losses are significantly lower for the buildings further downstream. The wind speeds are decreasing with higher building densities. For weather condition 1 the wind speeds are decreased to a lesser extent. For these low wind speeds the flow is mainly driven by buoyancy, what changes the flow fields and the wind flow between the buildings is less dependent on the approach flow.

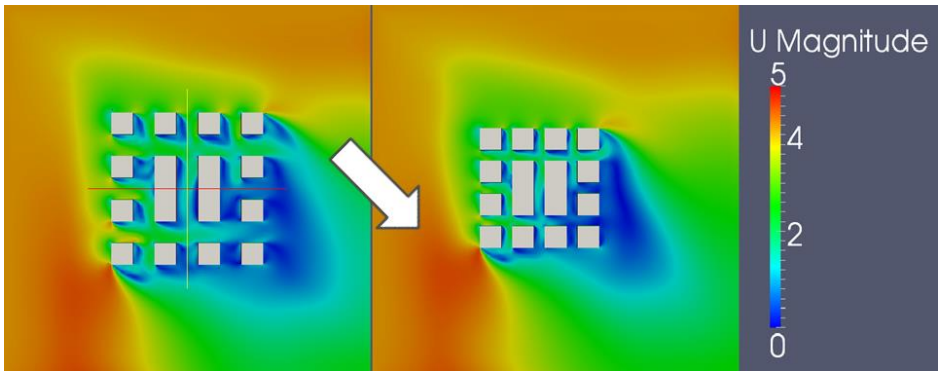

Figure 4: Contour plot of wind velocity 5 m above the ground for weather condition 4. Left: Aspect ratio 1; Right: Aspect ratio 2. Arrow indicates the wind direction.

Figure 4 shows the same contour plots for oblique wind flow directions. It can again be observed that the wind speed between the buildings is decreased. Further it can be seen that now the wind is flowing along the street canyon, in contrast to Figure 3, where the approach flow is normal to the street canyon and a vortex is generated inside the street canyon.The flow along the street canyon increases the removal of heat and increases the convective heat transfer at the building facades. It can be concluded that the wind flow around buildings in urban areas is complex and the convective heat transfer cannot be predicted only as a parameter of the wind speed of the approach flow. Either CFD simulations or local measurements are needed to accurately model the convective heat transfer for BES simulations.

From the same simulations the air temperature increase in an urban area, caused by the heated building surfaces due to absorption of solar radiation, is studied. In Figure 5 air temperature differences between the approach flow and the air inside a street canyon (between building 6 and 9) is presented for different weather conditions and different building geometries. As a first conclusion, it can be seen that the local heat island intensities can be modelled with CFD. Further it can be seen that the local heat island intensities for the chosen weather conditions can be up to 2.5 °C. This is a significant temperature increase that causes directly higher space cooling demands. Three parameters were varied in this study (wind speed, wind direction and building density). The results show that there is a complex interaction between these parameters. A higher building density decreases the solar gains inside the street canyon. This would lead to lower air temperatures. But at the same time, it also lowers the wind speed and therefore the removal of heat from the street canyon. Figure 5 shows that for weather condition 1 the shadowing effect is dominant compared to the effect of the wind. Therefore the air temperatures for the wider street canyon are higher. For weather condition 2 on the other hand, the effect of the wind is stronger and higher temperatures can be found in the narrower street canyon. For weather conditions 3 and 4 the wind direction is oblique to the

street canyon and therefore the wind can remove more heat by flowing along the street canyon. Here we can again see a stronger effect of the wind compared to the shadowing and therefore the temperatures inside the street canyons are higher for narrower street canyons. This shows that local heat island intensity cannot be predicted by analysing the three parameters independently. Therefore we propose to run CFD simulations with surface temperatures as obtain from BES as input to predict the air temperatures.

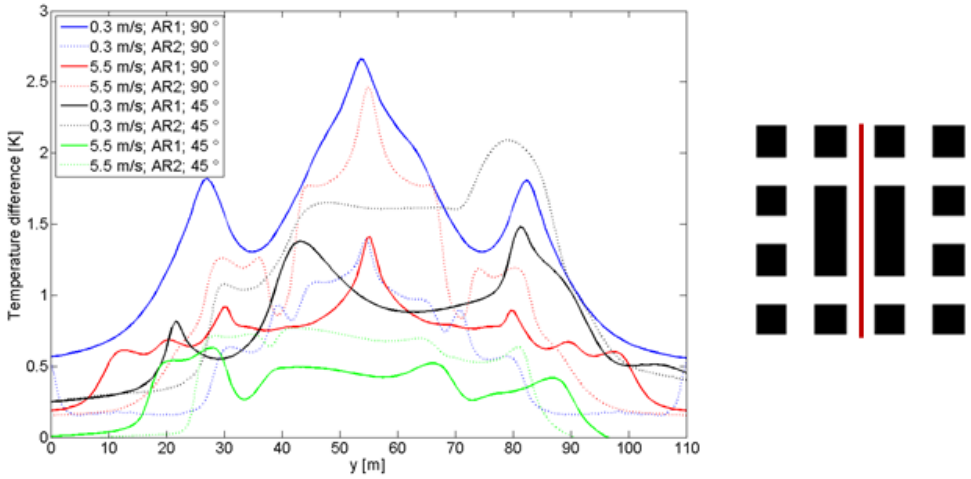

Figure 5: Temperature difference between the local air temperature on the red line (at 5 m above the ground) and the inlet temperature for the different weather conditions (Table 1) and aspect ratios (AR).

OUTLOOK

In the previous section we showed the importance of accounting for the urban microclimate, when simulating the space cooling and heating demands for buildings in urban areas. Here we give an outlook on an approach that will be used for CitySim simulations to consider the urban microclimate. Because the buildings and the local microclimate strongly influence each other, models for the urban microclimate and the building have to be conducted in a coupled way. The computational costs are much higher for CFD than for BES. Therefore the number of CFD simulations needs to be minimized. Figure 6 sketches an approach to model the interaction between the buildings and the urban microclimate. First a BES is conducted to get realistic temperature boundary conditions for the CFD simulations. Then for limited number of weather conditions CFD simulations are conducted. With CFD more accurate convective heat transfer coefficients (CHTCs) are determined and used for a second BES. Final CFD simulations with updated surface temperatures are used to analyse the urban microclimate. The CHTCs are again updated for the final BES to study the energy demands.

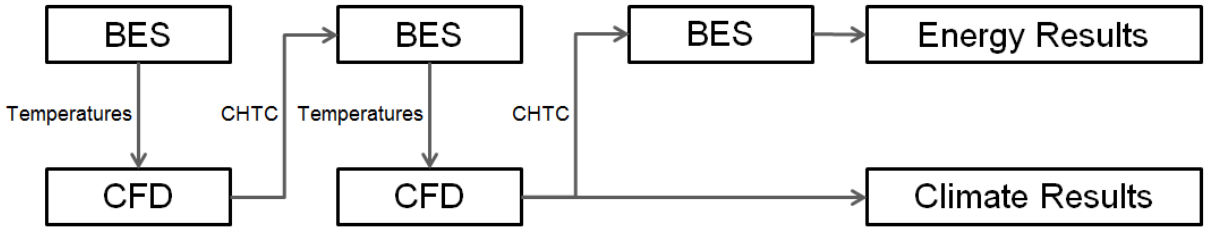

Figure 6: Sketch of approach to model the urban microclimate and its influence on buildings.

CONCLUSION

In this study the urban microclimate was modelled using CFD (computational fluid dynamics) and BESs (building energy simulations). BESs were used to model the surface temperatures and the radiative fluxes that the building surfaces. CFD simulations were conducted to model the wind flow around the buildings and the air temperatures in a small urban area. The results show there is a complex interaction between the buildings and the local microclimate. There is a large number of parameters that influences the local microclimate leading to local heat islands and complex wind flow structures, which need to be considered in BESs. The complex interaction makes it impossible to use simple rule of thumb to predict the influence of the neighbouring buildings, when conducting BES for a specific buildings. Therefore we propose here an approach to conduct CFD and BESs in a simplified coupled way to improve the predicted space cooling and space heating demand of buildings by BESs and the prediction of the local microclimate in an urban area.

ACKNOWLEDGEMENTS

Funding by the Swiss Federal Office of Energy (project no. 154 143), EU Climate-KiC (Project Smart Urban Adapt) and CCEM (Project Urban Multi-scale Energy Modelling) is gratefully acknowledged.

REFERENCES

1. Rasheed, A.: Multiscale Modelling of Urban Climate, PhD thesis 4531, EPF Lausanne, 2009.
2. Akbari, H., Davis, S., Dorsano, S., Huang, J.,Winett, S.: Cooling our communities – a guidebook on tree planting and light colored surfacing. US Environmental Protection Agency, 1992.
3. Santamouris, M., Papanikolaou, N., Livada, I., Koronakis, I., Georgakis, C., Argiriou, A., Assimakopoulos, D.N.: On the impact of urban climate on the energy consumption of buildings. Solar Energy, Vol 70, pp 201-216, 2001.
4. Kolokotroni, M., Giannitsaris, I., Watkins, R.: The effect of the London urban heat island on building summer cooling demand and night ventilation strategies. Solar Energy, Vol 80, pp 383-392, 2006.
5. Allegrini, J., Dorer, V., Carmeliet, J.: Influence of the urban microclimate in street canyons on the energy demand for space cooling and heating of buildings. Energy and Buildings, Vol 55, pp 823-832, 2012.
6. Ghiaus, C., Allard, F., Santamouris, M., Georgakis, C., Nicol, F.: Urban environment influence on natural ventilation potential. Building and Environment Vol 41, pp 395-406, 2006.
7. Robinson D., Haldi F., Kämpf J., Leroux P., Perez D., Rasheed A., Wilke U.: CitySim: comprehensive micro-simulation of resource flows for sustainable urban planning. Proc. of eleventh international IBPSA Conference, Glasgow, Scotland, 2009.
8. Perez R., Seals R., Michalsky J.: Allweather model for sky luminance distribution - preliminary configuration and validation. Solar Energy Vol 50 (3), pp 235-243, 1993.
9. Robinson D., Stone A.: Solar radiation modelling in the urban context. Solar Energy Vol (77) 3, pp 295-309, 2004.

URBAN ENERGY SIMULATION OF A SOCIAL HOUSING NEIGHBOURHOOD IN BOGOTA, COLOMBIA

A.V. Cifuentes Cuéllar[1], J. Kämpf[1]

1: Solar Energy and Building Physics Laboratory (LESO-PB), Swiss Federal Institute of Technology (EPFL), Station 18, 1015 Lausanne, Switzerland

ABSTRACT

High demographic dynamics and greater poverty in developing countries carry the urgent need to provide low cost housing to the poorest in urban regions. In Colombia the development of social housing settlements is characterized by two deficits, a quantitative one (related to urban density) and a qualitative one (related to indoor building conditions). It is therefore imperative to identify solutions that may lead to the adequate development of social housing in Colombia. This paper studies the relation between urban density and indoor thermal conditions of buildings of a social housing neighbourhood located in Bogotá, with the help of an urban energy simulator.

The particular location of the case study, close to the Equator, brought up many challenges. At first, remarkable differences were found when comparing the simulation results with the international norm CEN (EN 13790). The thermal model had to be slightly adapted for a good dynamic behaviour of the room temperatures. Moreover, as the constructional model of social housing is realised without any insulation, the thermal behaviour is very sensitive to the infrared exchanges with the environment, and as such the estimation of the ground temperature had to be refined. This latter point reinforces the idea of the importance of the infrared exchanges between adjacent buildings. Finally, satisfactory results were obtained from the models' improvements leading to an increase of confidence on the simulation results. With the optimised performance of the simulation tool, numerical simulations of radiatively interacting shelters were carried out heading to an analysis of the relation between different urban variables (such as site coverage, plot ratio, building and urban forms) and the thermal comfort of buildings' occupants. The study comprises the verification of the thermal model for simulations, the definition of a thermal discomfort indicator, and finally simulations of a social housing neighbourhood in Bogotá, the capital of Colombia. Results show that it is possible to maintain the same high human density and to improve thermal behaviour of the settlement by combining lower site coverage with higher buildings, which can provide architects and urban developers with helpful insights to improve social housing planning in Colombia.

Keywords: urban energy simulation, social housing, urban density, thermal comfort, Bogotá.

INTRODUCTION

By the horizon of 2050 urban areas are forecasted to hold almost 70% of the world's population. In developing countries the situation is even worse due to higher demographic dynamics and greater poverty rates that force governments to provide low cost housing to the poorest in urban regions. In Colombia's specific case, the social housing phenomenon has been characterized by two major deficits [1]. In one hand a quantitative deficit that carry the development of high density social housing settlements (macro-projects) [2], and on the other hand a high qualitative deficit that affects the well-being of inhabitants in comfort terms [3]. It seems therefore imperative to identify solutions that may lead to the adequate development of

social housing in Colombia. Thus, computer modelling happens to be an invaluable decision support tool as it potentially allows for a quick and somewhat precise evaluation of thermal performance associated to different urban scenarios.

For the first time, the urban energy simulator CitySim developed at EPFL [4] is used to simulate the thermal behaviour of a social housing neighbourhood located in Bogotá, the capital of Colombia.

METHODOLOGY

The aim of the study is to analyse the relation between urban density and thermal behaviour of buildings in a social housing neighbourhood in Bogotá. For this, the free floating dynamic thermal behaviour of the buildings has to be evaluated since Bogotá has a tropical highland climate with a yearly average temperature of 14.4°C, and no cooling nor heating are used to reach adequate internal thermal conditions. To gain confidence in simulation results, a verification of the urban energy simulator CitySim with the CEN (EN 13790) standard was carried out. It helped us to improve the solver and consequently a thermal discomfort indicator was defined in order to analyse three variations of the selected case study. As boundary conditions for the simulations, climatic data were obtained from MeteoNorm [5] and 2D and 3D information of the case study were obtained directly from the designers of the project [6].

Verification of the thermal model

As we rely on a software that has never been used exclusively for buildings without heating and cooling systems, results were verified through an inter-model comparison between CitySim and LESOSAI, the latter used for the certification and thermal balance calculation in buildings [7]. To acquire hourly thermal data for a complete year, calculation in LESOSAI was based on the CEN (EN 13790) standard. A simplified model of a typical building from the case of study was analysed using both simulation engines. Table 1 shows the input values associated to the virtual models.

BUILDING			
LOCATION	Country		Colombia
	Weather Station		Santa fe de Bogota
	Altitude of building site	m	2560
GEOMETRY	Volume	m^3	3217.4
	Large width	m	21.34
	Small width	m	10.47
	Height	m	14.4
	Net surface	m^2	223.42
OCCUPATION PROFILE	Living room, bedroom		
People	Quantity	P	142.5
	Metabolic activity	met	1.2
	Sensible heat	W/P	68.2
Electrical appliances	Specific power	W/m^2	12
Lighting	Specific power	W/m^2	56.46
HEATING AND COOLING	Summer	°C	60
	Winter	°C	-30
VENTILATION	Infiltration	m^3/hm^2	5.62
		v/h	0.4
	Window natural ventilation		no
PHYSICS	Thermal conductivity of soil	W/m·K	2
	Thermal capacity	$kJ/m^2·K$	511

ENVELOPE			
ROOF	Surface Area	m^2	223.42
	Calculated U-Value	$W/m^2·K$	5.1136
	Emissivity	%	90
	Absorption coefficient	%	90
	Shortwave Reflectance	%	42
	Glazing Ratio	%	0
FLOOR	Surface Area	m^2	223.42
	Calculated U-Value	$W/m^2·K$	3.9474
	Emissivity	%	90
	Absorption coefficient	%	90
	Shortwave Reflectance	%	42
	Glazing Ratio	%	0
East and West Facade	Surface Area	m^2	143.424
	Calculated U-Value	$W/m^2·K$	2.161
	Emissivity	%	90
	Absorption coefficient	%	90
	Shortwave Reflectance	%	50
	Glazing Ratio	%	0
North and South Facade	Surface Area	m^2	264.816
	Calculated U-Value	$W/m^2·K$	2.161
	Emissivity	%	90
	Absorption coefficient	%	90
	Shortwave Reflectance	%	30
	Glazing Ratio	%	40
	Surface Area	m^2	105.926
	Width	cm	1248
	Height	cm	849
	Simple Glass	mm	4
	Frame Fraction	%	30
	G-Value	%	92
	U-Global	$W/m^2·K$	5.87
	Blinds		no
	BlindsIrradianceCutOff	$W/m^2·K$	1385
	Shading Coefficient	%	0

Table 1: Main characteristics of the simplified model - Input values in LESOSAI and CitySim.

To illustrate the results obtained from the inter-model comparison a zoom was made on a period of the year in which we noticed significant differences in the internal building's temperature. The period starts from the 4105 hour of the year and ends in the 4205 hour which is essentially in the intermediate part of the year, from 21 to 24 June. In Figure 1, we present the results obtained with LESOSAI (labelled Lesosai) and CitySim (labelled CitySim_1), in which we notice important differences in the thermal behaviour. The major cause of the discrepancy was identified: the constructional model of social housing contains no insulation (as one can see from the U-Values in Table 1); therefore the buildings' thermal behaviour is very sensitive to the infrared exchanges with the environment. Consequently the radiant environment is of great importance in the thermal simulation, and as such a correct estimation of the surrounding buildings' and ground's temperature is necessary. After a modification on the ground temperature model that was implemented in CitySim for taking measured data instead of calculated ones, a more similar behaviour was found compared to LESOSAI (see the label CitySim_Tg in Figure 1). However, a presence of a phase shift between the results remained. To solve this issue, a last adjustment of the solver was carried out in order to distribute the thermal inertia to the air and wall temperature nodes according to the penetration depth δ_e of a 24 hours harmonic temperature variation in the material of the walls as calculated by Equation 1 in which λ, ρ, Cp and T are respectively the conductivity (W/m·K), density (kg/m^3), specific heat (J/kg.K) of the concrete, and T corresponds to the time period of 24 hours (given in seconds).

$$\delta_e = \sqrt{\frac{\lambda * T}{p * Cp * \pi}} \tag{1}$$

Figure 2 shows the variations in thermal results with the last adjustment (labelled CitySim_PD) compared with LESOSAI (labelled Lesosai). An acceptable thermal behaviour was achieved with CitySim, which allowed proceeding with the definition of the thermal discomfort indicator.

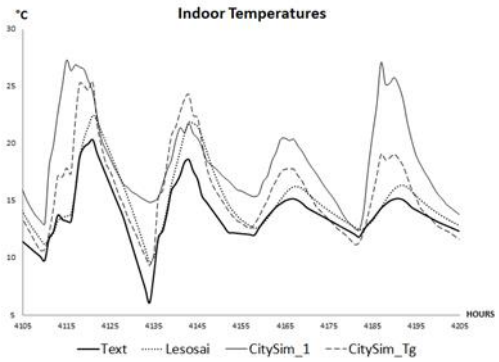

Figure 1: Inter-model comparison – Effect of ground temperature.

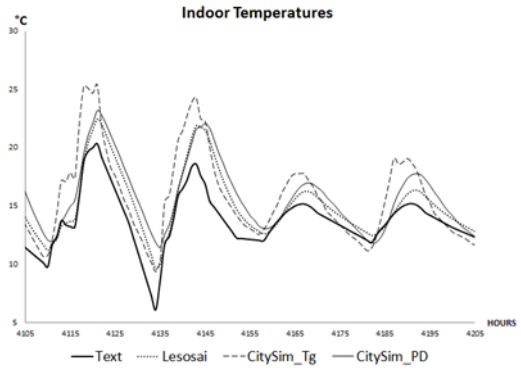

Figure 2: Inter-model comparison – Effect of penetration Depth.

Definition of thermal discomfort indicator

Based on Givoni's bioclimatic chart for Bogotá that aims at predicting the indoor conditions of the building according to the outdoor prevailing conditions [8] a comfort zone of internal temperatures between 18°C and 25°C was delimited. Consequently discomfort is understood as any indoor temperature (T_i in Equation 2) lower than 18°C or higher than 25°C. Hence to define a discomfort indicator that takes into account dynamic variation of internal building temperatures for each hour of a complete year, we calculated from Equation 2 the amount of

degrees-hour for hypothetical heating (to achieve 18°) and for hypothetical cooling (to achieve 25°C). The final result is the total yearly average of degrees-hour spent outside of the defined comfort zone during 8760 hours.

$$DH = \frac{1}{8760} \sum_{i=1}^{8760} [max(18 - Ti, 0) + max(Ti - 25,0)] \quad (2)$$

A scale from DH=0 to DH=3 was defined for the yearly average, where DH=0 means internal temperatures during the whole year in the comfort zone, DH=1 means internal temperatures on average 1° outside of the comfort zone, and DH=3 means internal temperatures on average 3° outside of the comfort zone. In this scale a DH until 2 is considered an acceptable difference, and a DH between 2 and 3 an unacceptable difference.

Case study

The project "Las Huertas" a social housing neighbourhood, located at the south of Bogotá (4°63', -74°08') was selected mainly for two reasons: First, because it is a macro-project that follows the actual Colombian social housing regulations that encourage building "the greater number of houses in the available area" [9]. And second, because of its very high human density. These specific conditions allowed us to better understand the problem of urban density in social housing in Colombia and to design a case study according to a real situation. For study purposes we selected 3 plots of land from the total macro-project. Figure 3 gives a 2D representation of the chosen area, and the density parameters are described in Table 2.

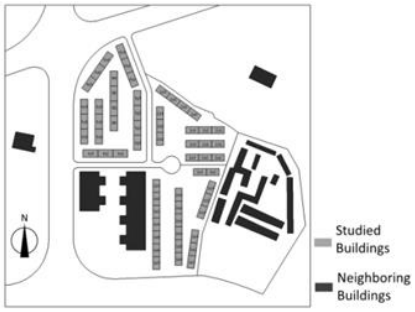

Figure 3: Selected plots of land.

CASE	Building Footprints	Site Area	Total Floor Area	Habitants
	m^2	ha	m^2	
1	11914.33	3.88	71485.98	4320

CASE	Number of Buildings	Buildings Height	Site Coverage	Plot Ratio	Human Density
		m	Building footprints / site area	Total floor area / site area	hab/ha
1	60.00	14.40	0.30	1.84	1113
2	30.00	28.80	0.15		
3	90.00	9.60	0.46		

Table 2: Density parameters for Las Huertas' selected plots and description of 3 case studies

We considered the quantitative deficit problem by studying three different urban scenarios with the same plot ratio but different site coverage (Figure 4) i.e., human density is the same in all cases. To conserve the same plot ratio build heights were modified as shown in Table 2.

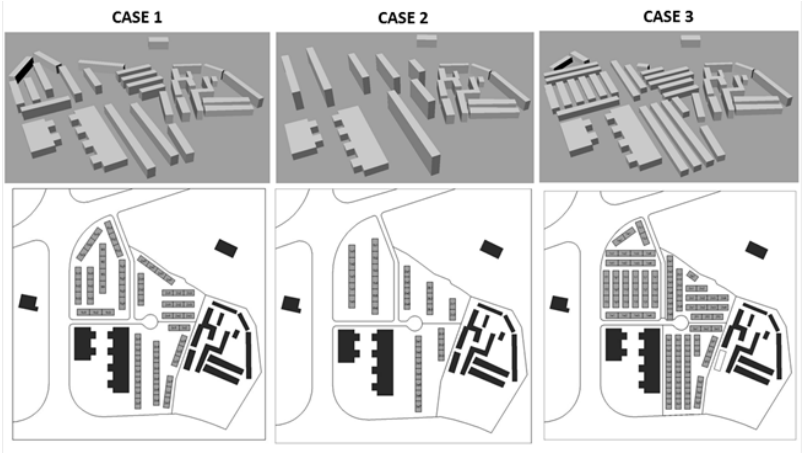

Figure 4: 3D and 2D representations of 3 urban scenarios

To evaluate the free floating dynamic thermal behaviour of the buildings it is compulsory to know the hourly occupancy profile related to the high human density. Since we only have the total number of potential occupants but not the variations of their presence, it was necessary to use for simulations standard profiles of occupancy, lighting and equipment. For this, and due to the lack of available data, the Swiss norm SIA 2024 was taken into account.

RESULTS

Simulation results take into account urban form, urban density, materials and thermal heat gains by occupants, lighting and equipment, according to the previously defined occupancy profiles. Figure 5 shows the influence of site coverage on thermal discomfort, the latter is illustrated with a colour scale from white to black where 1.7 was the lowest DH value obtained from simulations and 2.6 was the highest.

Case 3 with a site coverage of 0.46 (see Table 2), presents the highest discomfort rate with a DH=2.32, that is considered as an unacceptable difference. Case 2 with the lowest site coverage has the lowest DH. This can be explained by the effect of the larger vertical obstruction angle in case 2, which increases the distance between rows, and as a result more solar irradiation arrives to the buildings. In all three cases there is a better performance of buildings with a North-South orientation. Case 2 takes advantage of this privileged orientation allowing the settlement to achieve a lesser discomfort rate.

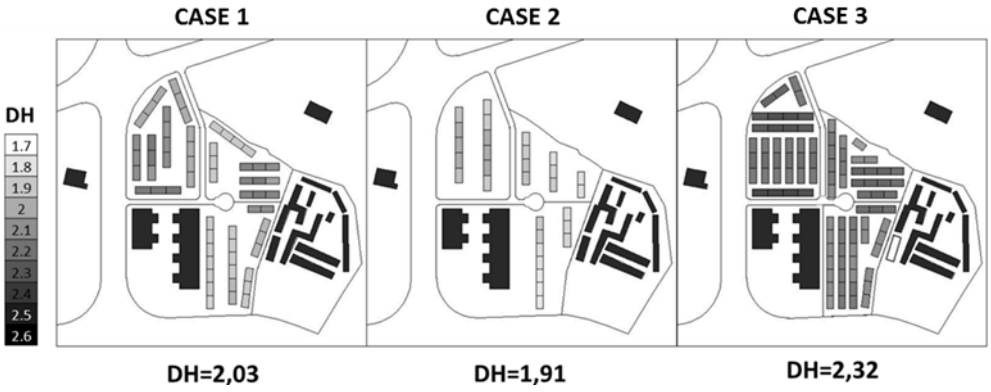

Figure 5: Yearly average discomfort indicators of three cases

Some interesting results were remarked in Cases 1 and 2; in the first case a zoom was made in order to see more clearly the influence of building's orientation (Figure 6). North-South oriented buildings show a considerably better thermal behaviour than those with an East-West orientation. In the second case the zoom aims to emphasize the effect of horizontal obstructions (Figure 7). A degradation of the scale of colours is evidently noticed i.e. DH values are affected by a reduction of the irradiation coming from the sides.

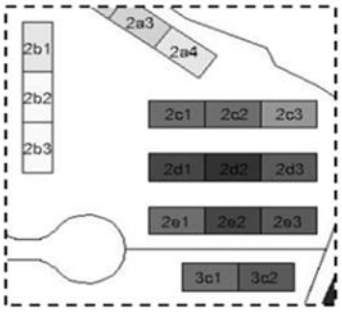

Figure 6: Zoom of case 1

Figure 7: Zoom of case 2

CONCLUSIONS

Three parameters associated with urban density have an influence on the average discomfort rate of urban settlements: vertical obstructions, horizontal obstructions and orientation of the buildings. Horizontal obstructions are related to site coverage (plan view), while vertical obstructions are related to plot ratio (elevation view). It was noticed that it is possible to reduce the discomfort rate of the neighbourhood and maintain the same high human density by combining lower site coverage with high rise buildings. In this way reducing vertical and horizontal obstructions of buildings can lead to more solar irradiation. Orientation is another important parameter that affects the thermal behaviour of buildings and therefore of urban settlement. North-South is the privileged orientation in Bogotá and architects and urban planners should take advantage of it in order to reduce the average discomfort rate of social housing neighbourhoods.

In a future perspective, further studies may analyse discomfort rates by floor levels defining one thermal zone per floor. It would be interesting to evaluate the effect of thermal inertia and glazing ratio on discomfort rates by changing some of the buildings' model parameters. Finally, architects and urban planners of Colombia have the challenge of creating sustainable urban habitats with a better environmental quality. To reach that objective, urban energy simulation is an invaluable support tool to manage the high urban and human densities that characterize cities in developing countries.

ACKNOWLEDGEMENTS

The authors gratefully acknowledge the CFBE (Comission Fédérale des Bourses pour Étudiants Étrangers) of the Swiss Confederation, who provided the scholarship of the first author.

REFERENCES

1. Departamento Administrativo Nacional de Estadística, DANE.: Metodología déficit de vivienda. Bogotá D.C. 2009

2. Decreto 4260 de 2007:
http://www.alcaldiabogota.gov.co/sisjur/normas/Norma1.jsp?i=27336, last visited 22.04.2013

3. Ceballos Ramos O.L.: Política habitacional y calidad de la vivienda. Revista Bitácora Urbano Territorial, vol. 1, núm. 10, enero-diciembre, 2006, pp. 148-157, Universidad Nacional de Colombia, Colombia

4. Robinson D. (ed.): Computer modelling for sustainable urban design – Physical principles, methods and applications. London, 2011

5. Remund J., Muller S.C.: Solar radiation and uncertainty information of meteonorm 7 (2011) 30th ISES Biennial Solar World Congress 2011, SWC 2011, 5, pp. 3773-3777

6. Constructora Apiros, http://www.apiros.com.co/, last visited: 15.02.2013

7. Favre D., Citherlet S.: Evaluation of environmental impacts of buildings with lesosai 6 (2009) IBPSA 2009 – International Building Performance Simulation Association 2009, pp. 1338-1343

8. Givoni B.: Man, climate and architecture 1st ed. Applied Science Publishers, London 1967

9. Decreto 2060 de 2004, Artículo 1, Densidad habitacional:
http://www.alcaldiabogota.gov.co/sisjur/normas/Norma1.jsp?i=14128, last visited 22.04.2013

EFFECT OF HOUSING DENSITY ON ENERGY PERFORMANCE OF SOLAR-OPTIMIZED RESIDENTIAL CONFIGURATIONS

C. Hachem; A. Athienitis; P. Fazio

Concordia University, 1455 Maisonneuve W., Montreal, Quebec, Canada, H3G 1M8

ABSTRACT

This paper presents a study of the effects of density of residential neighborhoods on their energy performance. Different scenarios are considered to accommodate increasing levels of residential density in 1 acre of land. The study is carried out for Montreal location, Canada (45ºN). All configurations considered assume a suburban environment that allows high solar exposure (Hachem et al, 2011). Energy performance is measured in terms of energy consumption, on the demand side, versus electricity production by means of integrated PV systems, on the supply side.

The first scenario consists of controlling density at the horizontal plan, through configurations of detached and attached two-story residential housing units of increasing degrees of density. A maximum density of 26 units/acre can be reached, while preserving a good solar access. Higher density levels are explored through apartment buildings - Low rise (3-5 floors), mid-rise (6-9 floors) and high rise (≥10 floors). In apartment buildings, integration of PV systems in facades, in addition to roof surfaces, is considered, in view of the reduced availability of roof surface per dwelling unit. The results indicate that densification of housing units in multiplexes enables the generation of excess of solar electricity over net-zero energy status. PV systems integrated in south and near south roof surfaces are capable of generating electricity in excess by some 25% over total energy consumption. Apartment buildings are relatively energy efficient for heating and cooling, while allowing a high level of residential density, but their solar potential is limited. Under the present study, a building of three stories can generate about 96% of its total energy use, if the roof design is optimized for solar energy generation. Above 3 floors, additional measures are required to approach net zero energy status. Employing PV on 50% of the south facades of three-storey buildings enables 14% excess production over consumption. Electricity production can be significantly increased by means of integration of PV systems on external structures in open spaces adjacent to the residential buildings themselves. This is particularly applicable to low-rise configurations.

Keywords: Density, energy performance, electricity generation, apartment buildings, multiplexes

INTRODUCTION

High density is conducive to viability and efficiency, while reducing infrastructure demand and greenhouse gas emission (GHC). On the other hand, increasing density affects negatively the solar potential of buildings and their energy efficiency (Hachem et al., 2012a). Land limitation in high density cities, restricts the availability of solar energy that can be used passively (passive space heating, daylighting, etc.) or actively to generate electricity and hot water.

Compact urban form with vertical zoning, combining multi-level and multi-functional clusters, offers an efficient high density development. However, roof and façade surfaces for integration of photovoltaic systems for sufficient electricity generation in such buildings are

restricted. To reach energy self-sustained communities, it is necessary to create development patterns that shift from individual buildings to a regional perspective of energy generation.

The current study investigates the level of residential density that can be reached per acre of land while maintaining a near net zero energy status. Increasing degrees of density are applied at the horizontal plan, through multiplexes of two story houses, and at the vertical plan using apartment buildings of increased height.

METHODOLOGY OF DESIGN

The objective of this research is to assess the effect of increasing residential density within an acre of land, on the overall solar potential and energy use of the development. Two general scenarios are explored: low rise- two story single family houses, and apartment buildings of varying height. A fixed floor area ($120m^2$) is considered for both residential houses and apartments. A family of four members is assumed to occupy these residential units. Buildings are designed to conform to passive solar design principles and to be highly energy efficient (e.g. insulation of 7RSI for the walls and 10RSI for the roofs, triple glazing low-e argon fill windows, airtight construction, etc.) (Hachem et al, 2012a). Housing units possess an aspect ratio - ratio of south façade to perpendicular façade - of about 1.3. This ratio is within the optimal range for passive solar design in northern climate, to maximize passive solar gains in winter (Athienitis and Santamouris, 2002). Total energy consumption in units is obtained by assuming energy use for appliances, lightings and hot water based on energy use in energy efficient houses (Hachem et al, 2012). Lighting energy consumption in rear apartments, where daylighting is limited, is based on published data of the average lighting usages in apartment buildings (NRCan, 2003). Elevators are considered in buildings with 5 floors and above.

Montreal (45^o N) is employed as the pilot location of the study, to represent northern cold climate. A heat pump with a coefficient of performance (COP) of 4 is assumed to supplement the passive and active solar heating systems. Simulations are performed employing Energyplus, to compute energy generation of the BIPV systems integrated on the south and near south facing surfaces (see below) and heating and cooling energy consumption.

Housing units

Housing units include configurations of rectangular housing units, attached and detached, and units with modified rectangular plans (hexagonal plans, see below).

Rectangular units: Detached housing units with minimum distance at the east west axis of 4m are designed. The one acre land can fit two rows of units distanced 20m apart (Fig.1a). This distance avoids mutual shading by rows (Hachem et al, 2011). A maximum of 16 detached units can be reached in this configuration. Attaching the units of each row allows increasing the density to 22 u/acre (Fig.1b). In all units PV systems are assumed to cover the total south facing area of a gable designed roof.

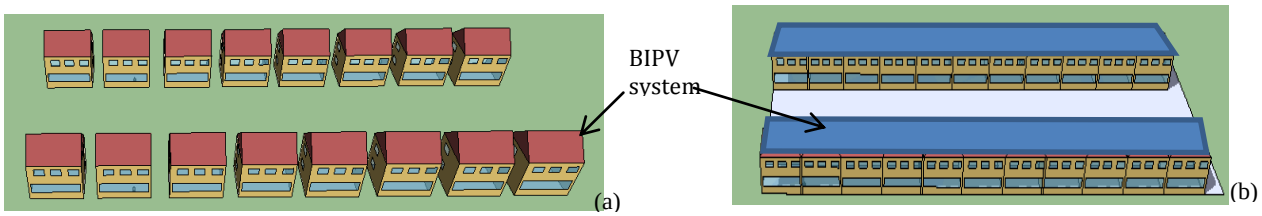

Figure 1 rectangular units, (a) detached, (b) attached

Hexagonal units: These are units of rectangular plan modified into hexagonal plan, to fit the outline of folded plate roof (Hachem et al., 2012b). In the configuration considered, facades

and roof surfaces are oriented at 15° east and west of south (Fig 2a).The folded plate roof provides enlarged surface for PV integration and spread of peak generation timing due to varying orientations of roof surfaces.

Some overlapping of units is incorporated in the design of multiplexes, for increased density (Fig. 2b), while ensuring that at least one near south façade is exposed. A maximum density of 26 units can be achieved through this method, while allowing solar access. The minimal distance between units of two rows is 12 m, resulting in some mutual shading of few units.

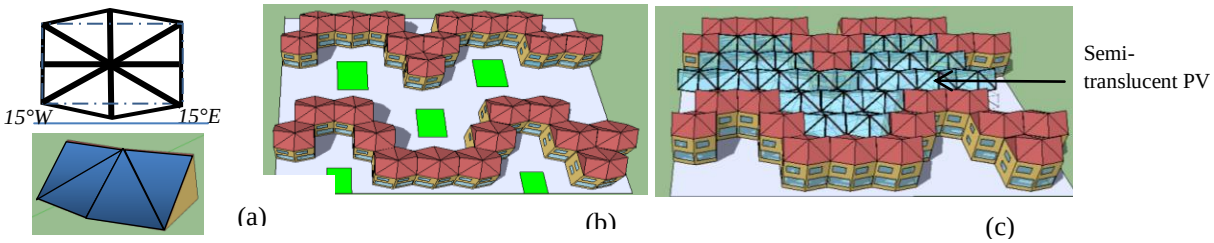

Figure 2 Hexagonal units; (a) roof design, (b) Configuration of multiplex, (c) multiplex with external structure

In the case of attached hexagonal units, an alternative design is considered, in which roofs are extended over the space between rows. The objective of this design is to enlarge the surface available for integration of PV systems. This roof extension consists of the same folded plates configurations of the housing units' roofs, and covers the outdoor space between the rows of units. The south facing plates of these roofs consist of semi-transparent PV. The outdoor covered areas can serve for individual purposes (e.g. garages) or for public and/or commercial areas. A similar option can be considered for the attached rectangular configuration, but is not included in the present study.

Apartment Buildings

The basic apartment building is designed with 8 apartments per floor (basic module), and a core area that serves for functions such as elevators and stairs. 1 Acre with a long layout can fit a building with up to 18 units per floor (Fig. 3d). Buildings ranging from 3 to 10 stories are designed and simulated.

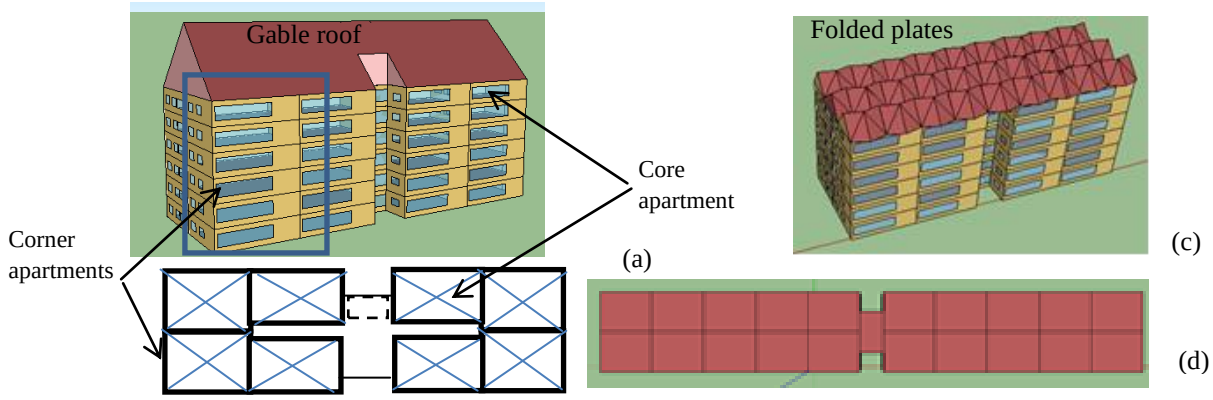

Figure 3 Apartment building: a) view with gable roof, b) Plan, (c) view with folded plate roof, (d) Maximum apartment buildings within an acre.

Design of south window area is based on sensitivity analysis of the effects of window size on heating and cooling loads. Window area larger than 30% of the south façade leads to a large cooling load especially in the upper floors, which may exceed the heating load. A south window area of 30% of the façade is therefore selected.

Roof design alternatives for integration of PV systems include a gable roof and folded plate roof (Fig.3c) with 45° tilt angles. In addition, up to 50% of south facades are PV integrated. Table 1 summarizes the main density aspects of the various studied configurations of houses and apartments.

Table 1, Density of houses and apartments.

	Housing units			Apartment buildings
	Rectangular detached	Rectangular attached	Hexagonal attached	
Units per acre	16	22	26	Height depending (54-144 units)
Land coverage	23%	32%	38.5%	62%

RESULTS

Low rise housing units

Results of energy production and consumption for the studied configurations are presented in Table 2. Average consumption refers to the total energy consumed by a given configuration, averaged over the total number of units. The configuration of detached rectangular units serves as reference for the multiplex configurations. Attaching the rectangular housing units can decrease heating load by up to 25% and cooling load by 8% while energy generation is not affected. Heating load is increased in the hexagonal configuration but this is counterbalanced by the larger density that can be obtained as well as the significantly larger energy generation (up to 1.46 more than the detached rectangular units). Scenario where semi-transparent PV is incorporated within an external structure can provide up to 2.5 more electricity than the overall energy use of the neighbourhood (Table 2).

Table 2, Results of energy performance: heating and cooling loads vs energy generation

Energy / Configuration	Total PV generation potential	Energy consumption				Energy generation to energy use
		Average Heating	Total Heating	Average cooling	Total cooling	
Detached (ref.) - kWh	7600	600	11853	149	2959. 8	1.02
Comparison to detached rectangular buildings						
Attached rectangles	1	0.75	0.75	0.94	0.92	1.10
Hexagonal Configuration	1.46	1.08	1.17	0.65	0.84	1.25
Hexagonal + external structure	2.82	1.17	1.37	0.61	0.84	1.47

Apartment buildings

Heating load in apartment buildings is lower than that in detached and attached houses, while cooling load is similar to attached houses. Average heating loads for each floor of buildings of varying heights are presented in Figure 4. It can be observed that the heating load in each of the top four floors does not differ much among buildings over five stories high, as indicated by the dotted lines. Heating load in the last floor increases by about 20% as compared to the floor below, due to the unheated attic. The rear apartments have an increased heating load of about 47% as compared to the front south facing apartments. Cooling load in such apartments is significantly lower than the front apartments (by 65%).

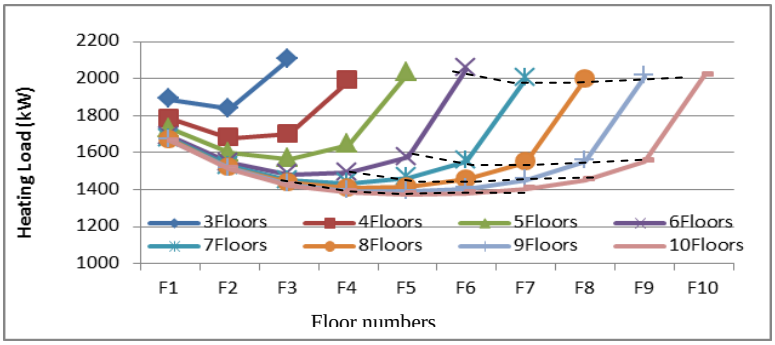

Figure 4, Average heating load for each floor in apartment buildings.

Results of energy generation versus consumption are presented in Figure 5. Figure 6 shows the relation between density and the ratio of energy generation to energy consumption. The relations for all roof configurations are also indicated in Figure 6 as regression lines. Electricity generation by a gable roof is limited, reaching a maximum of about 76% of the total energy use of a single 3-storey building. Replacing the gable roof by a folded plates PV roof enable to generate the approximate need of a 3-storey apartment building (Fig. 5).

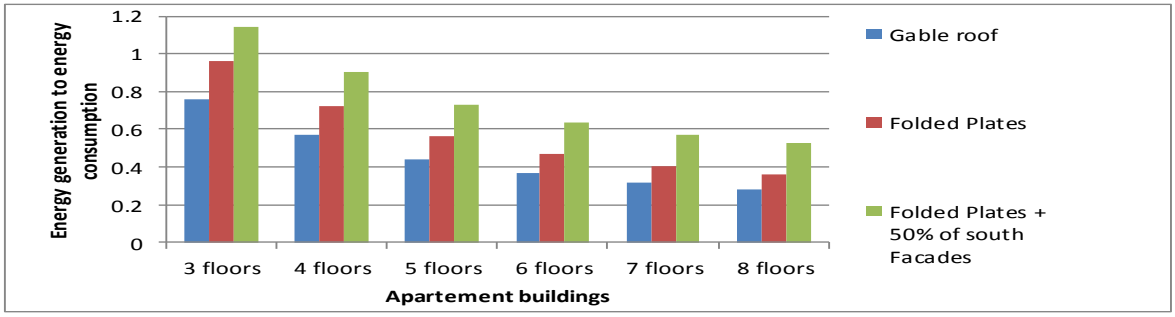

Figure 5, Comparison of generation to consumption for different design options.

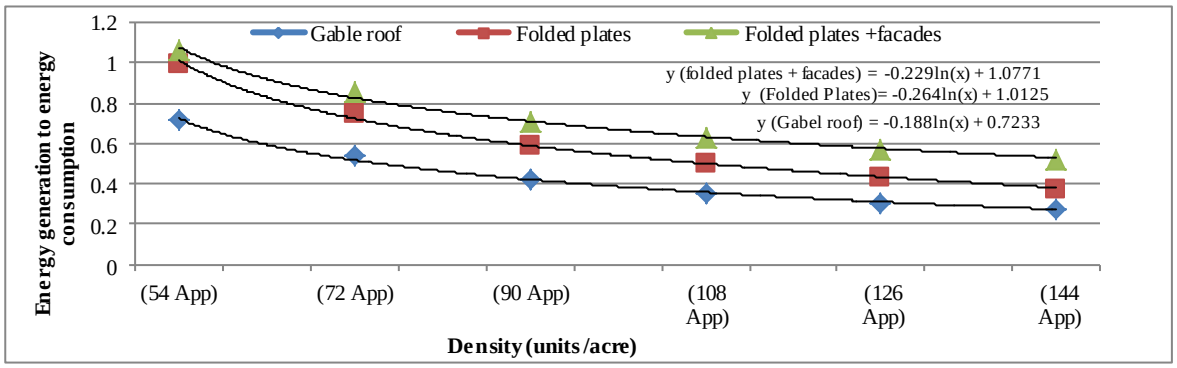

Figure 6, Energy balance vs density for different designs

SUMMARY AND DISCUSSION

This study investigates the densification of 1 acre of land and highlights the maximum electricity generation that can be achieved by different configurations of BIPV systems. Table 3 below generalizes the main findings of the study. The energy intensity of apartments and houses is included based on the assumptions of energy efficiency and passive design used in this study. Possibilities for enhancing electricity production by additional structures - either

horizontally as in the hexagon option, and/or vertically can be explored in order to improve the energy generation to energy consumption ratio.

Table 3, Summary

Studied scenarios		Multiplexes	Apartment buildings
Density		22-26 units	Height dependent (54 - 200 units in this study)
Intensity of energy consumption		62.5 kWh/m^2	68 kWh/m^2
Ratio of energy generation to energy use (Table 3 and Fig. 5)	Gables roofs	1.10	0.76 of energy use of 3 floor building (54 apartments)
	Folded Plates	1.35	0.96 of energy use of 3 floor buildings (54 apartments)

The study shows that energy generation within an acre is rather limited. The maximum number of housing units that can be fully supplied is about 32.5 using multiplex configurations with folded plates' roofs. For multi-storey buildings, the combined energy generated by a folded plate roof can almost supply the equivalent of energy consumed by around 54 apartments situated in 3 floor buildings (96%). This shows that low rise multi-story buildings can be more beneficial than multiplexes, due, partly, to regulations regarding clear space between rows of houses.

Strategies for increasing electricity generation should be explored, including design aspects such as the possibility of changing the design of tall buildings for increased energy generation. Possible options are use of curtain walls for integration of PV systems or supplementary structures – horizontal (e.g. between blocks), inclined, (e.g. over atria) or vertical, as free-standing towers with the sole purpose of electricity generation.

Design of land use and configurations within the land would play an important role in achieving optimal density and energy generation configurations. In the case of mix of different building types (low and high rise), the land design and positioning of the buildings should be optimized. For instance, high building should be on the north so as to avoid shading of the low-rise buildings. In all cases, policies and regulations affect the available options.

REFERENCES

1. Athienitis, A.K. and Santamouris, M., 2002. Thermal Anaylsis and Design of Passive Solar Buildings, London : James & James Ltd.
2. EnergyPlus. 2010. Version 5. 0. Lawrence Berkeley National Laboratory, Berkely, CA.
3. Hachem, C., Athienitis, A., Fazio, P., 2011. Investigation of Solar Potential of Housing Units in Different Neighborhood Designs, Energy and Buildings, 43 (9), 2262-2273.
4. Hachem C., A. Athienitis, P. Fazio, 2012a. Evaluation of energy supply and demand in solar , Energy and Buildings, Volume 49, June 2012, Pages 335–347.
5. Hachem C., A. Athienitis, P. Fazio, 2012b. Design of roofs for increased solar potential of BIPV/T systems and their applications to housing units. ASHRAE Transactions RNS-00226-2011.R1.
6. Natural Resources Canada (NRCan), Office of Energy Efficiency, 2003. Comprehensive Energy Use Database (CEUD). Visited on 11, Oct., 2010.

COMPARISON OF TWO STANDARD SIMPLIFIED THERMAL BUILDING MODELS

M. Lauster[1]; A. Constantin[1]; M. Fuchs[1]; R. Streblow[1]; D. Müller[1].

RWTH Aachen University, E.ON Energy Research Center, Institute for Energy Efficient Buildings and Indoor Climate, Mathieustr. 10, 52074 Aachen

ABSTRACT

Simplified thermal building models, especially thermal network models, are an interesting option to calculate buildings' energy demands at city district scale because of their comparably low requirements regarding parameterization and computational efforts. Several such models have been suggested, which vary in their number and interconnection of resistances and capacities. In order to contribute towards a comprehensive assessment of such models, the aim of this paper is to compare a model based on the widely used ISO 13790 with a model based on the German guideline VDI 6007.

For this comparison, both models were implemented in the object-oriented modeling language Modelica with the simulation environment Dymola. Four test cases were simulated to analyse the influence of several factors (outdoor temperature, solar radiation, and internal gains) on the inside air temperature and also to calculate the energy demand when using an ideal heater to keep the house at a constant set temperature. Because the results showed a crucial influence of the time period T describing the periodic depth of penetration for heat transfer through the walls, further tests using the same T for both models were carried out to quantify this influence.

The obtained results display different dynamic behaviour for the two models of ISO 13790 and VDI 6007, while the overall predicted heat demand for a longer time interval is similar for both methods. The model comparison shows that the differences in parameter calculation and thermal network design between the two models are outweighed by the influence of the time period T. These findings suggest that choosing the right parameter for the time period T can be more important than choosing which model setup to use for dynamic building performance simulations.

Keywords: simplified building model, city district dynamic simulation, ISO 13790, VDI 6007

INTRODUCTION

Simplified thermal building models are an interesting option to calculate buildings' energy demands at city district scale because of their comparably low requirements regarding parameterization and computational efforts. A broad range of research has been done in the field of dynamic building modelling and simulation [1, 2]. The application to city district scale often leads to simplified building models, of which thermal network models, based on the analogy with an electrical circuit, seem to be a wide-spread approach [3, 4].

The international norm ISO 13790 [5] specifies three related methods for thermal building models: a monthly method, an hourly method, and a dynamic method. Most research on this norm has been done to validate results obtained with the different methods (see e.g. [6, 7, 8]). For cases where this method failed validation, Jokisalo et al. [9] suggest that the hourly method can lead to more accurate results. A similar approach is described in the German guideline VDI 6007 [10]. The aim of this paper is to compare these two approaches in order to contribute towards a comprehensive assessment of thermal network based building models.

METHOD

Models

Figure 1 shows the thermal networks of ISO 13790 and VDI 6007 for a building modeled as one single thermal zone. They are based on different network designs and consider influences of energy sources in different ways.

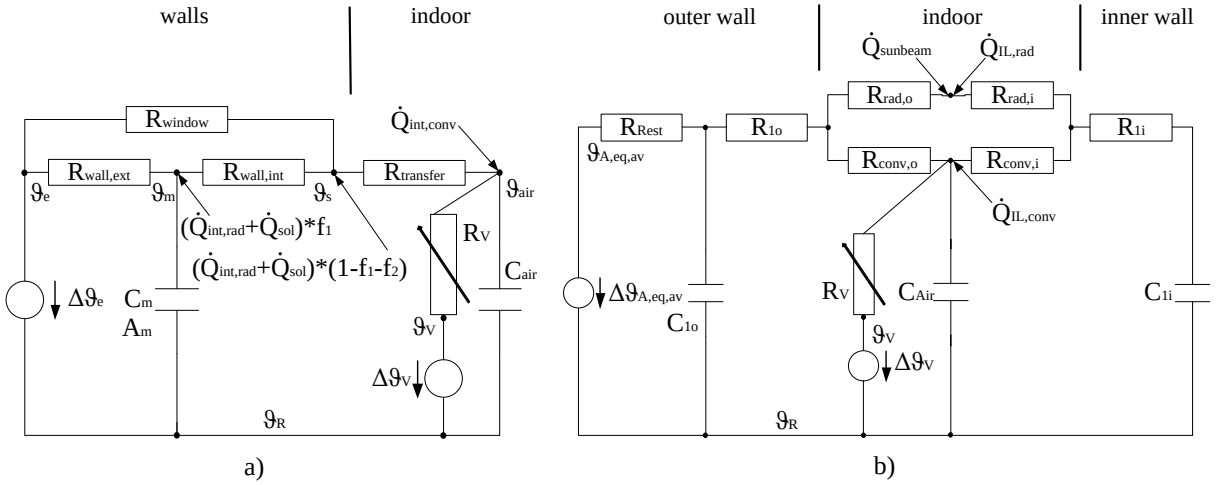

Figure 1: Thermal networks, a) ISO 13790 with air node, b) VDI 6007 with air node and adapted internal heat transfer

In general, both models calculate the indoor air temperature and the heat demand depending on the building physics, inner loads, solar gains, ventilation, occupancy, and weather conditions. Except the buildings physics all influences are considered as varying over time.

One main difference is the number of capacities used to model the thermal mass of the building. We added a capacity for the air volume in our versions of both models. The ISO-model uses one capacity to represent the overall active mass of the zone. In contrast, the VDI distinguishes between capacities for adiabatic inner walls and outer walls. More capacities can lead to a finer resolution regarding dependencies between different masses in a building. By defining more than one capacity, it is possible to distinguish masses that directly participate at the heat transfer to the surrounding and adiabatic masses. Yet, calculating the temperature of capacities always encompasses time derivatives which highly influence the CPU-time.

Concerning the heat transfer, both models use two resistances to model the transfer through the (outer) walls. In the ISO-model, one resistance is added for windows and one for the internal convective heat transfer. In the VDI-model, windows in terms of heat transfer are considered as walls without thermal mass. We adapted the VDI-model by using two resistances per wall to distinguish between convective and radiative heat transfer.

The dynamic parameters for resistances and capacities for the VDI 6007 model are calculated with the Beuken model defined in ISO 13786 [11]. The capacities as well as the resistances highly depend on the thermal mass of the building, which can be activated. This mass thus depends on the thickness of the wall, which can be used to store heat (periodic depth of penetration). The depth is described by a time period T that corresponds to the periodical loading behaviour. This time period thus highly influences the model's dynamic behaviour and should be chosen carefully. For the ISO-model, a time period of one day is recommended, while the VDI guideline specifies a time period of five days. In addition, the ISO 13790

proposes to use a simplified method derived from the Beuken model, while the VDI 6007 uses the detailed calculation method.

According to ISO 13790, the influence of solar radiation on the outer walls can be considered as an additional radiation or as an adapted outside temperature. Our ISO-model works with an adapted radiation while the VDI-model uses an adapted outside temperature. The radiative heat transfer in the ISO-model is divided in two parts. One part directly affects the inner wall node while the other part is taken into account on the inner surface of the wall.

Test Cases

As a test building a two storey single family dwelling with a living area of 150 m² was used. The walls are heavy and insulated according to the German Energy Savings Ordinance 2009 [12]. Two simplified models for the building were developed in Modelica, reducing the model in both cases to one thermal zone. For VDI 6007 two sets of parameters were calculated: one considering a time period T of five days and the other a T value of one day, for a better direct comparison with ISO 13790, where a time period of one day is used. This leads to two comparisons:

- Comparison "1-5": ISO 13790 with T=1 Day and VDI 6007 with T=5 Days
- Comparison "1-1": ISO 13790 with T=1 Day and VDI 6007 with T=1 Day

Parameter	**Unit**	**ISO 13790**	**VDI 6007**	
T	Days	1	5	1
$R_{indoor - outdoor}$	K/W	$65.13 \cdot 10^{-4}$	$64.20 \cdot 10^{-4}$	$59.15 \cdot 10^{-4}$
$R_{capacity- indoor}$	K/W	$5.03 \cdot 10^{-4}$	$3.32 \cdot 10^{-4}$	$2.39 \cdot 10^{-4}$
$C_{overall}$	J/K	$767 \cdot 10^{5}$	$1207 \cdot 10^{5}$	$839 \cdot 10^{5}$

Table 1: Comparison of overall heat capacity and combined resistances

As shown in Table 1, the values for resistances and capacities differ between the test setups, with 57% for comparison "1-5". The difference of about 10% for the overall capacity in comparison "1-1" can be explained by the different methods used for calculating the parameters. While the VDI-model uses a more complex calculation, the ISO-model parameters are calculated with a simplified method defined in the appendix of ISO 13786.

Differing values of the resistances between the setups for the VDI-model originate from differing masses for the inner walls which can be activated. Differences between ISO and VDI regarding handling and division of the overall resistance lead to different values for the individual resistances. In addition, the different calculation methods of the parameters also influence the resistances.

Four test cases were designed to investigate the behaviour of the models in a dynamic simulation. In order to achieve a clear result all influencing factors where set as constant at the beginning of the simulation: outdoor temperature 15 °C, ground temperature 10 °C, solar radiation 0 W/m², no ventilation / infiltration, no inner gains, no active heater. Once the simulation achieved steady-state, one of the selected factors was varied using a pulse signal, which lasted one day. After this the simulation continued until steady-state was reached again. This led to a simulation duration of 120 days/case, with the pulse taking place on the 60th day.

The first three test cases analyse the reaction of the indoor air temperature when:

- the outdoor temperature (Case 0) is set to 25°C

- the solar radiation (Case 1a) is set to 70 W/m² on all surfaces
- the inner loads (Case 1b) are set to 1125 W

The values were chosen in order to lead to a similar absolute increase in the indoor air temperature over all three cases. The last test case (Case 2) assesses the energy demand in keeping a set temperature of 22°C in the house. After achieving steady-state the indoor temperature was set to 22 °C until the end of the simulation and the energy demand of an ideal heater, which was conditioning the room air temperature, was measured.

RESULTS

Comparison "1-5"

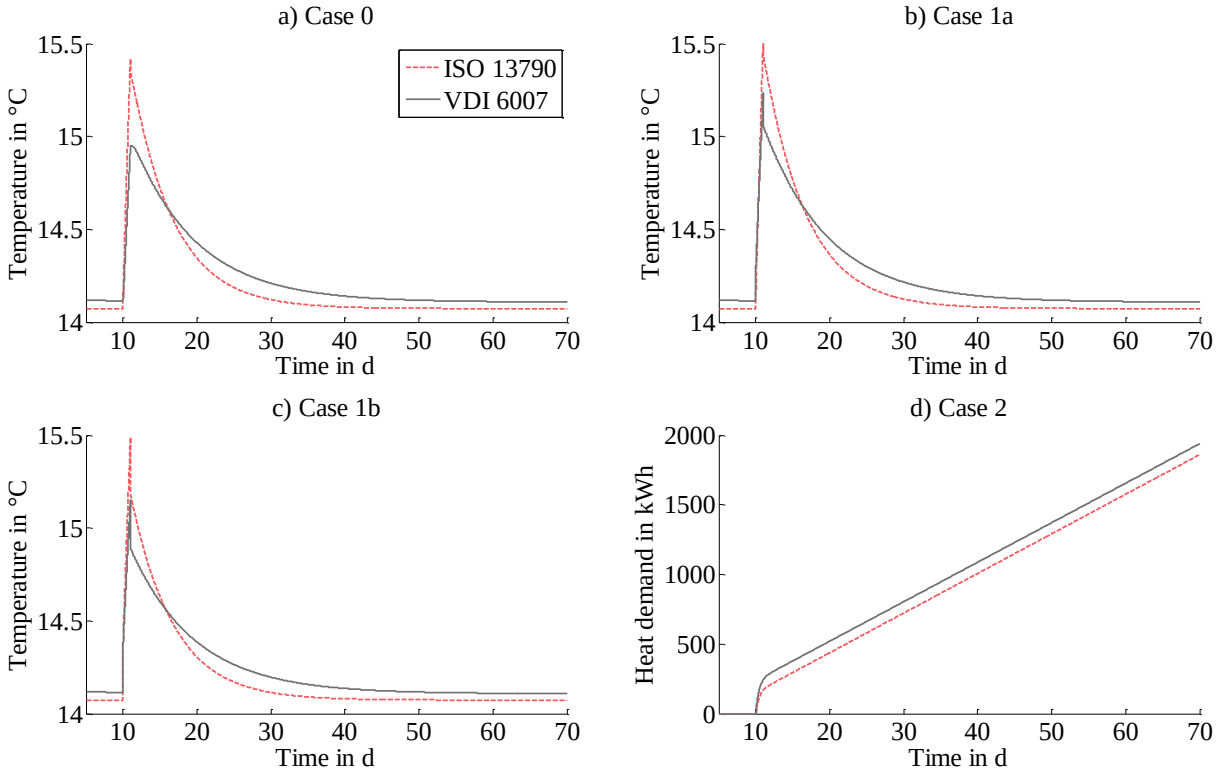

Figure 2: Comparison "1-5" of ISO 13790 (T=1 Day) and VDI 6007 (T=5 Day)

Comparison "1-1"

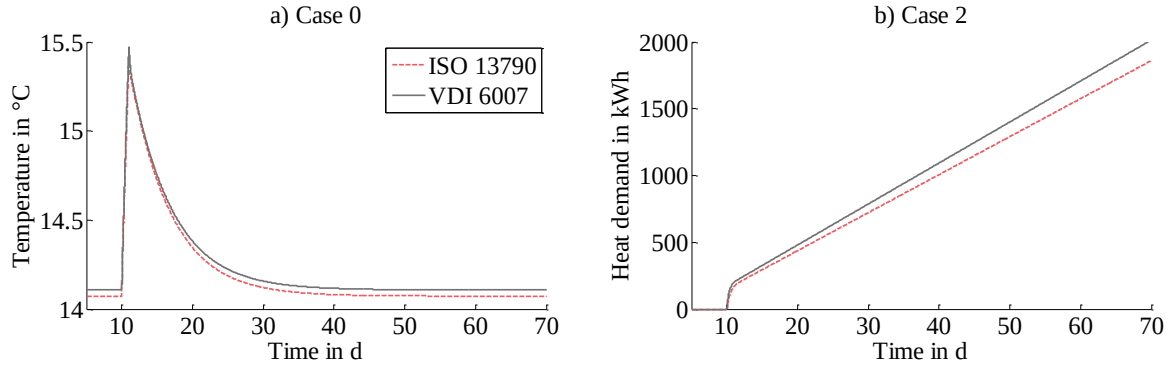

Figure 3: Comparison "1-1" of ISO 13790 and VDI 6007 with T=1 Day for both

Table 2 shows the results for the different test cases regarding the CPU-time and root mean square error (RMSE) as a value for the deviation. The ISO-model is on average 51% faster than the VDI-model. This can be explained by the lower number of capacities used, which in turn led to a reduced system of equations to solve.

Comparison	Test case	CPU-Time ISO	CPU-Time VDI	RMSE
"1-5"	0	2.43 s	5.06 s	0.09°C
	1a	2.62 s	5.61 s	0.08°C
	1b	2.41 s	4.95 s	0.07°C
	2	2.22 s	4.27 s	77.28 kWh
"1-1"	0	2.43 s	5.14 s	0.03°C
	2	2.22 s	4.35 s	91.5 kWh

Table 2: Results for the different test cases

DISCUSSION

All test cases in comparison "1-5" (see Figure 2) show a similar behaviour of both models, which leads to similar RMSE-values in Table 2. The maximum difference happens in test case 0, with the RMSE also having a higher value than for the other test cases. As the pulse of the outdoor temperature takes effect on the exterior side of the wall, the transfer to the interior is damped by the loading of the capacity, which for VDI 6007 is 57% higher than for ISO 13790. The radiant and convective loads in test cases 1a and 1b directly affect the inner side of the wall and the indoor air. Thus, the influence of different wall capacities is smaller on the indoor air temperature in these cases. The deviation visible in test cases 0, 1a and 1b at steady-state can be explained by the differing resistances between capacity and indoor air that lead to different heat flows. For test case 2, the deviation originates from the energy needed to load the different capacities. As the resistances between indoor and outdoor air are similar, the deviation remains nearly constant over time.

Comparison "1-1" (see Figure 3) shows that the influence of the time period T outweighs the network design. With the same time period T of one day, both models nearly provide similar results with a RMSE of 0.03°C. The small deviation originates from the different resistances between wall capacity and indoor air. As the resistance between indoor and outdoor air of the VDI-model is now 9.7% smaller than of the ISO-model (see Table 1), the VDI-model needs a higher heat flow to hold the set temperature in case 2.

CONCLUSION

The aim of this study was to analyse the differences between two simplified thermal building models (ISO 13790 and VDI 6007) using dynamic simulations. There are two main differences between the models, the numbers of capacities (one for ISO 13790 and two for VDI 6007) and the time period for the periodic depth of penetration for energy flows, T, (one day for ISO 13790 and five days for VDI 6007). For a more detailed comparison we also built an additional model according to VDI 6007 using a T of one day. The simplified models were set up for a well-insulated single family dwelling. Four test cases were simulated to analyse the influence of several factors (outdoor temperature, solar radiation and internal gains) on the inside air temperature and also to calculate the energy demand when using an ideal heater to keep the house at a constant set temperature.

Because of the extra capacity the CPU-time for simulations using the VDI 6007 model is higher (51%). When using a T of five days this model heats up less when a pulse for the

outdoor temperature is applied due to higher capacities. This difference disappears when using a T of one day. For the energy demand, the difference stays constant at 4.2% for T of five days, whereas for T of one day it increases over time to 8.3% after 60 days. The cause for this is the decrease in the resistance between outdoor and indoor with decreasing T. Slight differences (0.03°C) in the offsets of the temperature profiles are explained through different values in the resistances between capacities and indoor air.

The results show that the influence of the time period T outweighs the differences in the calculations of the dynamic parameters and the design of the thermal networks. These findings suggest that choosing the right parameter for the time period T can be more important than choosing which model setup to use for dynamic building performance simulations.

ACKNOWLEDGEMENTS

We gratefully acknowledge the financial support for this project by BMWi (German Federal Ministry of Economics and Technology) under promotional reference 03ET1004A.

REFERENCES

1. Hensen, J. ; Lamberts, R. : Building Performance Simulation for Design and Operation. Spon Press, London, 2011
2. Clarke, J. : Energy Simulation in Building Design. Butterworth-Heinemann, Oxford, 2001
3. Robinson, D. : Computer Modelling for Sustainable Urban Design. Earthscan, London, 2011
4. Kämpf, J. : A simplified thermal model to support analyses of urban resource flows. Energy and Buildings, Vol. 39, pp 445-453, 2007
5. ISO, International Organization of Standardization : ISO 13790 - Energy performance of buildings - Calculation of energy use for space heating and cooling. ISO, Switzerland, 2008
6. Corrado, V.; Mechri, H.E.; Fabrizio, E. : Building Energy Performance Assessment through Simplified Models: Application of the ISO 13790 Quasi-Steady State Method. Building Simulation 2007, Beijing, China, 2007.
7. Gratzl-Michlmair, M.; Heimrath, R.; Schranzhofer, H. : Einflussparameter auf Heizwärmebedarf und Kühlbedarf von Gebäuden in verschiedenen Berechnungsmethoden von EN ISO 13790. Bauphysik, Vol. 32, pp. 296-302, 2010.
8. Kokogiannakis, G.; Clarke, J.; Strachan, P. : Impact of Using Different Models in Practice – A Case Study with the Simplified Methods of ISO 13790 Standard and Detailed Modelling Programs. Building Simulation 2007, Beijing, China, 2007.
9. Jokisalo, J.; Kurnitski, J. : Performance of EN ISO 13790 Utilisation Factor Heat Demand Calculation Method in a Cold Climate. Energy and Buildings, Vol. 39, pp. 236-247, 2007
10. VDI, German Association of Engineers : Guideline VDI 6007-1 - Calculation of transient thermal response of rooms and buildings. VDI, Düsseldorf, 2012
11. ISO, International Organization of Standardization : ISO 13786 - Thermal performance of building components - Dynamic thermal characteristics - Calculation methods. ISO, Switzerland, 2007
12. Energieeinsparverordnung [German Energy Savings Ordinance] 2009, Beuth Verlag, Berlin, 2009.

SUSTAINABLE ENERGY PLAN FOR A NEIGHBORHOOD

K. Orehounig[1,2]; V. Dorer [2]; J. Carmeliet[1,2]

1: Chair of Building Physics, Swiss Federal Institute of Technology Zurich (ETHZ), Wolfgang-Pauli-Strasse 15, 8093 Zürich, Switzerland

2: Laboratory for Building Science and Technology, Empa, Überlandstrasse 129, 8600 Dübendorf, Switzerland

ABSTRACT

Current energy discussions involve reduction of fossil fuel consumption by improving the energy consumption of the building stock on the one hand and increasing the integration of energy from renewables on the other hand. Since renewable energy generation is known to be highly fluctuating in time, and as such energy demand and energy generation do not match necessarily, new concepts to manage these fluctuating power sources, like energy storage, energy conversion from one energy carrier to another, the integration of smart-, micro-grids, and energy-hubs have been developed. These concepts can be more effectively integrated at building block or quarter level then just taking individual buildings into account. Based on this background this paper outlines an approach for a simulation environment to evaluate and optimize energy flows within neighbourhoods. The envisioned simulation environment will integrate a city simulation tool with which different improvement scenarios of the energy performance of buildings can be investigated, and a simulation tool which manages and optimizes the energy flows within the community taking various energy carriers including renewables into account. The approach is presented based on a case study – a village in Switzerland. The intention of the village is to become an energy sustainable community, which relies on renewable energy sources, taking production, innovative energy networks, storage, and conversion into account, and fully reduce the consumption of fossil fuels. As a starting point the existing situation concerning the energy demand of the village with respect to different uses (heating, lighting, …), the different energy carriers (fossil fuel, gas, electricity, …), their origin (hydropower, combustion, …), their distribution and networks (e.g. district heating) is captured. In a next step the potentials for energy efficiency improvement of the existing building stock and the potential of decentralized energy generation is evaluated with the means of building energy simulation. Decentralized energy generation includes building integrated or local renewable energy generation by photo-voltaic, biomass, and small hydro power turbines. In a third step, different future energy scenarios towards an energy sustainable community are defined and analyzed with the energy hub concept aiming to optimize CO_2 emissions of the village.

Keywords: energy plan, energy hub, energy sustainable, neighbourhood

INTRODUCTION

A major share of the Swiss energy consumption is due to heating, cooling, and electricity consumed in buildings. To effectively reduce the energy consumptions of the built environment, concepts to sufficiently improve the energy efficiency of the building stock on the one hand and to manage energy from renewables on the other hand are necessary. Especially the energy performance of buildings can vary significantly depending on type, age, and integrated building systems, and not in all cases improvement options are feasible. There are historical buildings which are protected, and almost no improvement options of the

building envelope is possible, older buildings where the thermal performance of the building can be improved through a number of retrofitting measures, additionally the integration of renewables could be targeted, and there are new buildings which are listed as low, zero or even positive energy buildings which are highly equipped with renewable energy technologies. Renewable energy generation is known to be highly fluctuating in time, and as such energy demand and energy production do not match necessarily. Therefore new concepts to manage these fluctuating power sources, like energy storage, energy conversion from one energy carrier to another, the integration of smart-, micro-grids, and energy-hubs have been developed. These concepts can be more effectively integrated at building block or quarter level then just taking individual buildings into account. Based on this background this paper outlines an approach for a simulation environment to evaluate energy flows within neighbourhoods. It is targeted that the simulation environment should integrate a city simulation tool with which different improvement scenarios of the energy performance of buildings can be investigated, and a simulation tool which manages and optimizes the energy flows within the community taking various energy carriers including renewables into account. Within this paper the approach will be presented based on a case study. The intention is to develop a future energy concept for a village and convert it to an energy sustainable community, which relies on renewable energy sources, taking production, innovative energy networks, storage, and conversion into account, and fully reduce the consumption of fossil fuels.

APPROACH

The approach to effectively convert neighbourhoods to energy self-regulating entities is tested on an area within a village in Switzerland, and includes the following steps:

1) Investigation of the current situation

This area within the village, taken as a case study, consists of 20 buildings. The buildings are mainly built between 1970 and 1980s. As a starting point the existing situation concerning the energy demand of the village with respect to different uses (heating, lighting, …), the different energy carriers (fossil fuel, gas, electricity, wood, biomass), their distribution and networks (e.g. district heating) are captured. Additional collected information pertains to building characteristics such as age, type, construction method, insulation quality, and type of heating system. The majority of the buildings are equipped with electrical heating systems, additional energy sources are oil, biomass for a small district heating network, and wood for wood stoves. The village is connected to the electricity network. It has a small district heating network which is connected to a CHP unit fired by wood chips, which are brought to the village by trucks. To identify the energy consumption of the buildings information pertaining to annual electricity, oil, and wood consumption and delivered energy due to the district heating network was collected. For buildings were also electricity is used for space heating, the annual electricity consumption was divided into electricity used for appliances and lighting, and electricity used for space heating based on statistical values. Thereby assumptions for typical electricity demand for appliances [1] are subtracted from the actual electricity consumption; the remainder is defined as electricity consumption for space heating.

2) Energy performance of buildings

To identify the potential of increasing the energy efficiency of the building stock a simulation model of the buildings is generated with the city simulation model CitySim [2]. CitySim consists of a thermal model for simulating the energy performance of the building stock within an urban configuration. To identify the actual energy consumption of the building an

energy system model integrating heat pumps, boilers, cogeneration plants, as well as some renewable technologies are included in the simulation tool. Input assumptions for the simulation model are based on collected data such as type of construction and construction period, glazing area ratios, number of occupancy, and type of heating system. Internal conditions within the model are based on statistical values. Weather information is used from a locally installed weather station which collects information pertaining to temperature, relative humidity, global horizontal radiation, wind direction and wind speed. With the generated building simulation model first the actual energy performance of the buildings is investigated and results are compared to the collected energy consumption data from the period of October 2010 to September 2011. Once the simulation model is calibrated it can be used to evaluate alternative improvement options of the building stock and the building systems towards reducing the total energy consumption of the village.

3) Renewable potential

To evaluate the potential for decentralized energy production at building level, the generated city simulation model is used. Decentralized energy production includes building integrated or local renewable energy production by photovoltaic, solar thermal, geo thermal, wind, etc. Within this paper the potential for photovoltaic on roof surfaces is evaluated. Roof surfaces of the area with orientations from East, South, and West and inclinations from 0° to 45° have been investigated.

4) Energy hub model

To efficiently integrate fluctuating and distributed power sources from renewables within city quarters or communities, the concept of an energy hub is applied. The energy hub model was developed by Power Systems laboratory at ETH Zürich to manage energy flows within a large building complex, a city quarter, neighbourhood, or even countries. It gives the possibility to store energy, convert energy from multiple energy carriers to another (e.g. electricity to heat, natural gas to heat, thermal solar or bio-mass water heating and hot water storage, etc.) and sufficiently supply electricity, heat, cold, gases or fuels to the community. Thereby it is typically connected to electricity and gas infrastructures at the input port, gives the possibility to convert or store electricity, and provides energy services to the end-users at the output port. The advantage of the energy hub approach is an increase in reliability of the energy infrastructure since usually a number of options to provide heating or electricity to consumers is possible. Additionally it has the advantage to optimize the energy consumption, costs, emissions etc. by regulating conversion, storage, and distribution of energy. The energy hub concept can be applied at different levels of complexity whereby it doesn't imply that the energy hub is implemented as a physical entity but rather the concept can be used to optimize energy flows and evaluate the performance of different energy carriers within the community.

The general idea of an energy hub model is based on the following equation:

$$L = C * P + S * \dot{E} \quad (1)$$

Whereby L denotes the hub-output vector, P the hub-input vector, and Ė the vector of storage energies. C stands for the converter coupling matrix, and S for the storage coupling matrix.
Within this paper the "multi-carrier optimal dispatch" model is applied, which determines the optimal dispatch of the available energy carriers to effectively cover the load at the output of the hub. Thereby the power flows through the hub are optimized for a specific snapshot (e.g. annual energy consumption) [3]. Since the total input of one energy carrier might be converted into different forms of energy (e.g. electricity directly used, or converted to heat) so-called dispatch factors have to be determined. For the electricity consumption of the

village we assumed a lossless connection between delivered and net energy demand. In case of the heating energy demand a coupling matrix was used to account for energy losses due to conversion of energy carriers of electricity, oil, wood chips, or wood into net heating energy. Since the first version of the energy hub model does not consider multiple time periods but only a time integrated period of one year no energy storage possibilities were taken into account.

As a starting point for optimization we consider the time integrated energy consumption of the village area over the period of one year and optimize it aiming at minimal CO_2 emissions. A convex objective function that reflects the total emissions of the hub over the time period is assumed (Equation 2). The coefficients a_α assumed for this first example are given in Table 1. Coefficients are based on the following literature [4,5].

$$TE = \sum_{\alpha=e,p,o,h,b,w} (a_\alpha P_\alpha) \quad (2)$$

Energy carrier	**a_α[g CO_2/kWh]**	**Energy carrier**	**a_α [g CO_2/kWh]**
Electricity (mix)	122	Oil	698
PV	69.6	Biomass	21.6
Small hydro	4.7	Wood	21.6

Table 1. Assumed objective function coefficients (CO_2 emissions)

5) Development of Scenarios

Once the potential for different renewable energy sources are identified and the energy hub model is generated, a number of different energy scenarios for the area are identified which then are evaluated with the energy-hub model. The required annual load of the area, which has to be covered by the energy carriers, resulted in 224431 kWh electricity consumption for appliances and hot water, and 872452 kWh for net space heating. Note that the energy demand for space heating was identified with the city simulation model. As to the different energy scenarios, it is assumed that the village disposes of the existing energy carriers, namely a direct connection to the electricity network, oil for oil space heating, heat from the district heating network which is fired by wood chips, and wood for wood stoves. Additionally to the existing energy carriers, the calculated potential for building integrated photovoltaic (BIPV), and the potential of a small hydro power turbines are taken into account. It is assumed that electricity from the network, from PVs, and from the small hydro turbines could be directly used to cover the electricity demand of appliances or it can be converted by the energy hub to heat. In case of a direct use of electricity a lossless connection is assumed, whereas in case of a conversion to heat an efficiency of 0.95 is assumed. The other energy carriers (oil, wood chips, organic material, and wood) can be solely used to cover the space heating demand. The resulting scenarios are presented in the following table.

Energy carrier	**S1**	**S2**	**S3**	**S4**
Electricity	unlimited	unlimited	unlimited	unlimited
PV	266 MWh	266 MWh	266 MWh	266 MWh
Small hydro	-	-	-	176 MWh
Oil	unlimited	unlimited	unlimited	unlimited
Biomass	unlimited	-	184 MWh	184 MWh
Wood	201 MWh	201 MWh	201 MWh	201 MWh

Table 2. Scenarios with the maximum available amount of energy per energy carrier

RESULTS AND DISCUSSION

Figure 1 shows the simulated heating energy demand for all buildings of the village area, together with the actual energy consumption for a one year period from October 2010 to October 2011. The graph indicates a relatively good match for a number of buildings, whereas in other cases the simulated energy demand overestimates the real consumption significantly. Table 3 shows energy hub model results of the 4 different scenarios (as per table 2) together with the actual measured distribution of energy consumption per carrier. All scenarios show a reduction in total CO_2 emissions. As the best performing scenario shows, reductions in CO_2 emission of up to 80% can be achieved by completely replacing the oil space heating by more sustainable energy sources such as biomass and by electricity from PV and small hydro turbines.

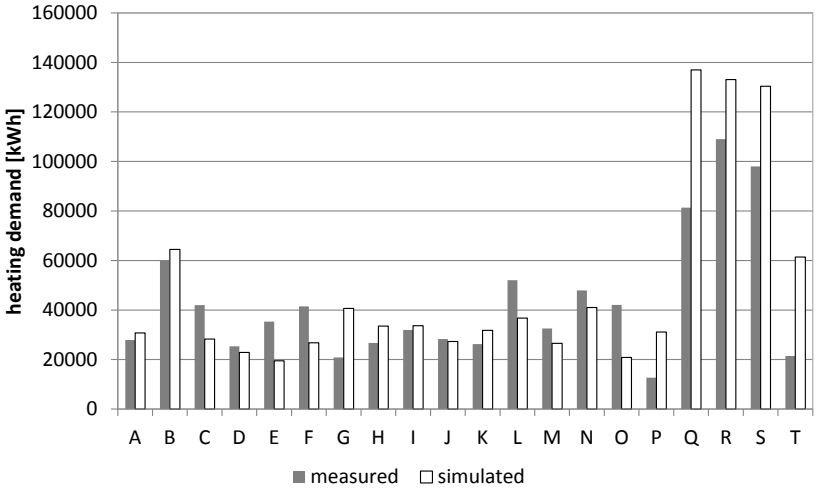

Figure 1. Comparison between measured and simulated heating demand of buildings

	Energy [MWh]					CO_2 emissions [t CO_2]				
	as is	**S1**	**S2**	**S3**	**S4**	**as is**	**S1**	**S2**	**S3**	**S4**
Electricity	479	-	728	544	410	58	-	89	66	50
BIPV	-	224	266	266	224	-	16	19	19	16
Small hydro	-	-	-	-	176	-	-	-	-	1
Oil	167	-	-	-	-	117	-	-	-	-
Biomass	184	918	-	184	184	4	20	-	4	4
Wood	201	-	201	201	201	4	-	4	4	4
Sum	1031	1143	1196	1196	1196	183	35	112	93	75

Table 3. Annual energy hub results (energy consumption per energy carrier and resulting CO_2 emissions)

CONCLUSION

This paper presents an approach for a simulation environment to evaluate energy flows within neighbourhoods. The simulation approach is applied at a pilot project – a village in Switzerland which aims to be energy sustainable by 2020. A number of conclusions can be drawn from the results presented:

Comparison between measured and simulated energy consumption shows a relatively good match for a number of buildings, whereas in other cases the simulated energy demand overestimates the real consumption significantly. Since detailed occupancy data are not

available, differences may occur due to higher occupants absence or presence compared to the assumed statistical values. Furthermore occupancy behaviour such as heating setpoint temperature, consumption of hot water, usage of electrical appliances etc. may contribute to additional deviations in energy consumption.

Initial results of the energy hub model are presented on the example of four different scenarios. In this case the dispatch of multiple energy carriers was optimized for system emissions. A CO_2 emission reduction of 80% could be achieved by increasing the consumption of biomass and PVs and decrease electricity from the network and the use of oil for space heating.

OUTLOOK

This paper presented the concept of an approach to develop an energy concept for a village. Further steps will include the identification of energy efficiency measures for the building stock using a more elaborated version of the city simulation model, and hence reduction of the total energy consumption of the buildings. Then further energy scenarios will be investigated. These will include also energy storage systems, both seasonal and short term storage, to efficiently overcome periods where the potential of renewables is low. To account for energy storage systems, a more advanced model of the energy hub will be developed. Finally the actual coupling of the city simulation model and the energy flow model is targeted. The resulting simulation environment will be tested at building conglomerations of different complexity, namely the development of a city quarter with options for new constructions, a city centre with historic buildings and more rigid boundary conditions, as well as further rural communities.

ACKNOWLEDGEMENTS

The research presented in this paper is supported in part by funds from ETH and KTI (Project leader: Prof. Kees Christiaanse and Michael Wagner). The authors also gratefully acknowledge members of the Architectural and Sustainable building technology group (Prof. Dr. Arno Schlüter) towards providing collected information regarding energy use, buildings, systems etc. The authors further acknowledge Prof. Dr. Göran Andersson, Dr. Thilo Krause, Govinda Upadhyay, Dr. Jerome Kämpf for providing the energy hub model and the CitySim tool.

REFERENCES

1. Nipkow, J., Gasser, S., Bush, E. 2007. Der typische Haushalt Stromverbrauch - Energieverbrauch von Haushalten in Ein- und Mehrfamilienhäusern. Bulletin SEV/AES 19/2007.
2. Robinson, D., Haldi, F., Kämpf, J, Leroux, P., Perez, D., Rasheed, A., Wilke, U. 2009. CITYSIM: Comprehensive micro-simulation of resource flows for sustainable urban planning. Eleventh International IBPSA Conference Glasgow, Scotland.
3. Geidl, M. 2007. Integrated Modeling and Optimization of Multi-Carrier Energy Systems, Diss. ETH No. 17141, Switzerland.
4. Frischknecht, R., Itten, R., Flury, K. 2012. Treibhausgas-Emissionen der Schweizer Strommixe. Bundesamt für Umwelt BAFU.
5. Moomaw, W., Burgherr, P., Heath, G., Lenzen, M., Nyboer, J., Verbruggen, A. 2011. Annex II: Methodology. In IPCC Special Report on Renewable Energy Sources and Climate Change Mitigation, Cambridge University Press, Cambridge, United Kingdom and New York, NY, USA.

MEU: AN URBAN ENERGY MANAGEMENT TOOL FOR COMMUNITIES AND MULTI-ENERGY UTILITIES

J. Rager[1], D. Rebeix[1], F. Maréchal[1], G. Cherix[2]; M. Capezzali[3]

[1] *LENI-IPESE, EPFL Station 9, CH-1015 Lausanne*
[2] *CREM, Av. du Grand-Saint-Bernard 4-CP 256, CH-1920 Martigny*
[3] *EPFL Energy Center, Station 5, CH - 1015 Lausanne*

ABSTRACT

In order to facilitate urban energy management and energy planning, the project MEU developed a web based tool as a decision support system for decision makers. Using a web based approach minimizes the effort on the client site as no software needs to be installed or be updated on the personal computer. First, data are collected based on the buildings in the federal land registry offices' data. The data contains all the relevant elements in the energy conversion chain of a given city over the last couple of years available on an annual basis: meteorological data, a list of accessible resources, energy conversion technologies, energy distribution networks and buildings as consumers of different energy services. Second, all buildings and networks are geo-referenced to allow plotting maps. This already gives a comprehensive overview of the current energy state of a city. Third, measurements of (annual) energy consumptions are introduced allowing the performance monitoring. Fourth, this data is structured and completed for the use in the energy simulation software: CitySim for the dynamic building energy demand simulation and EnergyTechnology for the calculation of the energy conversion technologies. As a set of default values is provided in the platform, it runs even if only a small data set is imported. When more information is available such as the energy consumption or the physical building data, the platform can easily be updated to increase the accuracy of the results.

With this approach, urban energy flows from resource to useful energy can be tracked and inefficiencies can be spotted easily along the conversion processes. Furthermore, the creation of scenarios based on a given actual year allows for example the quick comparison of different energy conversion scenarios for different technological measures introduced in a city or the evaluation of refurbishment strategies on the energy demand. The maps allow to geo-localize priority areas and help representing the results.

Keywords: urban energy planning, energy flows, gis, demand and supply

INTRODUCTION

Today, the planning of urban areas and their energy systems plays a key role towards reaching the goals of the mayors convention[1]. According to [2] over 35 percent of the final energy consumption is used to deliver space heating and hot water in developed countries such as Switzerland. Another 10 percent is used to deliver building related services such as lights, ventilation, air conditioning or other electrical appliances.

Even though significant efforts have been made over the last years, the primary energy use is still increasing[3]. With the introduction of smart metering, more and more data is available. However, different actors own this data in a more or often less structured way making it difficult to get the key information out of the data. In addition, the data quality

varies a lot between sources such as different cities. Only few publications[4] tackle the problem of the creation of urban scale data sets.

Being aware of the data related quality issues, MEU represents a consolidated effort to use a bottom up approach based on the available data on demand and supply simulation. MEU wants to help the partner cities in their energy planning. In the form of a cartographic web interface, different research tools can be accessed by partner cities.

Four cities have been studied in the validation process:

- La Chaux-de-Fonds (UNESCO World Heritage site) at 1000 meters altitude,
- Neuchâtel on the slope facing north-east on lake Neuchâtel,
- Lausanne facing south on the lake Geneva and
- Martigny (Bourg) with a lot of historic buildings behind a mountain ridge.

METHOD

The project MEU uses an energy flow graph for the evaluation, planning and monitoring of urban energy systems. In the current phase, only annual energy balances are calculated. The oriented graph traces all energy flows within the boundaries of the chosen district, that concern the following three services: heating, hot water production and electricity. From source nodes that represent resources, the energy flows towards energy distribution or conversion system nodes. Each distribution network node contains information about the physical connections and additional information about the type of contract. From there on, further edges can either connect to network nodes, energy conversion system nodes or directly to sinks that represent the building's energy demand.

Each node has one or many input flow edges and output flow edges. Each flow-edge contains a fraction equal to the amount of the start or stop node's total transported energy. A network node has a loss factor, therefore the input does not equal the output. Energy conversion system nodes rely on a separate set of simple energy conversion models for different technologies.

With the help of this graph, about 50 percent of the final energy use within the system's boundaries can be simulated.

Structure of the platform MEU

The website uses a carto-graphical user interface with underlying layers of an areal Orthophoto and official geometries of buildings to give access to the different modeled entities. Different layers can be activated to show the results such as specific consumption of each building or the Display Labels of each building.

The most important entities are the choice of the year or scenario, information about individual buildings and the possibility to calculate the energy flow graph in order to get global scene specific results such as primary energy use. All commands from the web interface are passed to the central meu service, which decides to either load a stored value or to calculate a value if necessary.

All the values are stored in a geo-spatial and temporal data base (PostgreSQL). For the calculation, the MEU service has the choice to either call the building simulation solver or the energy technology models.

In order to determine the heating demand of a building, CitySim[5] is called, a detailed

urban energy use simulation software. Once building demands are calculated, energy technology models are called to determine the final energy consumption. The energy technology models use also default efficiencies based on the current Swiss norms[6] when no other manual data has been entered.

Data and Default Data Sources

All cities provide the land registries office data, which contains basic information such as building footprint, height, usage and construction year[7]. From the local utilities, consumption data is added.

Most of the time when launching a simulation, whether on building or on scene level, the data set needs to be completed with default data. Data considered as measurement has the first priority. When no measurement exists, the default data set is used. The meta data traces whether the input data required for calculations is based on measurements or default values based on current norms and best practice values.

The electricity and hot water demand of a building are taken from the current Swiss norms[8]. The distribution networks have losses according to each local energy utility. All of the default values have been validated by the project partners[9].

Space Heating Demand: Estimation and Measurement

Space heating is the biggest part of the final energy demand. Therefore it is modeled with more detail. As an input, a complete physical model of the all the buildings is needed. Additional information such as occupant behavior can significantly improve predictions of the energy use. For MEU, standard profiles are used.

Most measurements are available for either heating and hot water demand of a residential buildings at the same time, these are analyzed in detail. With the help of these equations, measurements and simulation are put into relation with each other:

$$Measurement \quad *\eta_{technology} = \quad Simulation \tag{1}$$

$$Measurement \quad *\eta_{technology} * Fraction_{heating} = \quad Simulation \tag{2}$$

$$Measurement \quad *\eta_{technology} * Fraction_{heating} * Fraction_{Building} = \quad Simulation \tag{3}$$

First of all, the hot water use is excluded with the help of a statistical correction factor (Eq.:2). When the technology is connected to several buildings, only the building's fraction part is taken into account (Eq.:3). The $Fraction_{Building}$ is calculated based on the heat demand calculated by CitySim:

$$Fraction_{Building} = \frac{Building\ Heat\ Demand}{\sum Building\ Heat\ Demands} \tag{4}$$

With each simulation of an energy demand a scaling factor(SF) is calculated 5 between measurement and simulation to propagate the correct value in the energy flow graph:

$$SF = \frac{Measurement}{Simulation} \tag{5}$$

With the help of the scaling factor the simulation is corrected as the the measurement cannot be modified and is taken as a fixed value into the graph.

When no measurement is available, the simulation value of CitySim is taken as it is. This simple approach allows calculating all values within the graph from buildings to resources.

The final energy use or the green house gas emissions per building or for the whole scene are a result of the graph.

This approach is compared to a simplistic regression model: The space heating demand of all buildings is assumed to behave proportional to the outdoor temperature[10, 11]. The advantage of this approach is the simple usage and implementation. It does not need as much input data as a dynamic simulation nor as much computation time, but does not take the building physics into account.

RESULTS

The platform MEU can already be used as a monitoring tool to survey the annual energy consumption. The authors demonstrated that it is possible to let the platform MEU calculate urban indicators such as the annual final or primary energy demand (per building) as well as the green house gas emissions.

A proof of concept has been made for the proposed workflow: With the help of default data sets, the platform can perform its calculation. However, the results in figure 1 show a big gap between simulation and measured results for each case. Of course, all the factors of equation 3 could introduce errors in this calculation.

When looking at the overall picture, both generally over-estimate the consumption. Very old buildings as well as very new residential buildings seem to be difficult to estimate correctly as they are highly overestimated. New buildings represent only five percent of all available buildings, it is therefore difficult to evaluate these buildings in more detail. Residential buildings constructed between 1920 to 2000 are in average correctly simulated, however high standard deviations indicate that more knowledge of the building could help.

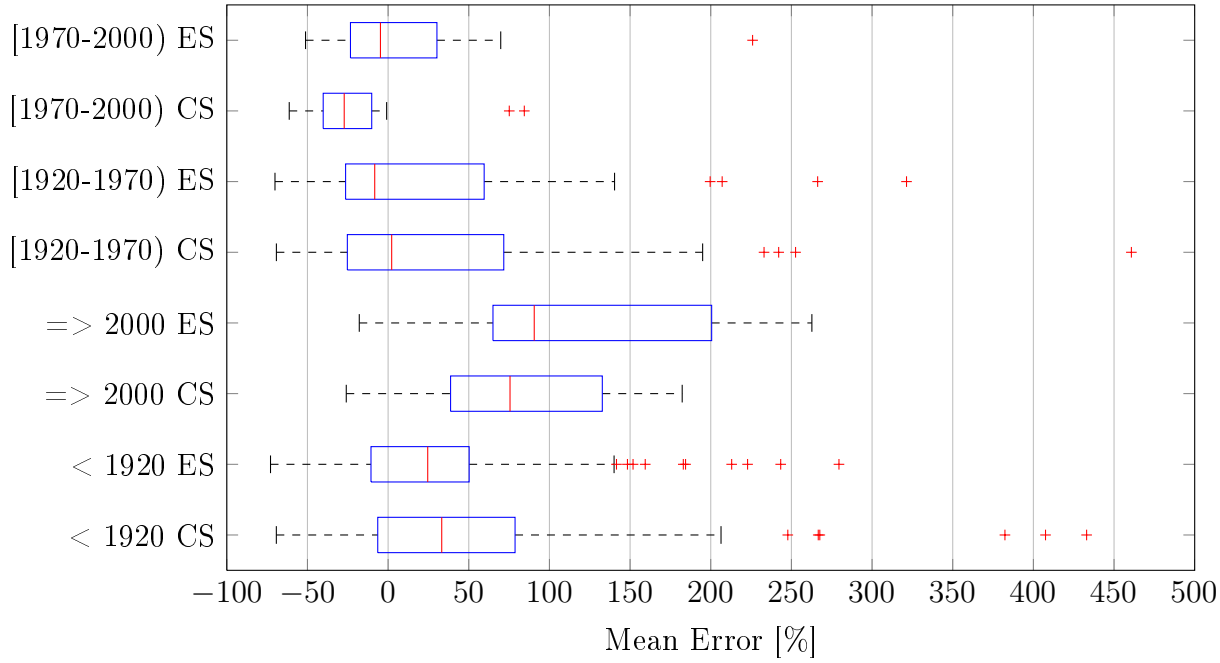

Figure 1: La Chaux-de-Fonds: Boxplot of the error between measurement and estimation with either the energetic signature(ES) or CitySim(CS) for different construction periods.

Comparing these results to other cities that provided data, the picture is confirmed. High standard deviations and high mean errors, show that more work on the individual

buildings is needed. With MEU specific error maps are be plotted to show the difference between estimation and measurement helping to identify poorly understood buildings. The tool might also identify faulty measurements on buildings which are well understood once better data was introduced. For the moment, it is highly likely that the error between the real and the estimated consumption for the buildings that do not have measurements, show the same differences. Therefore the platform is very likely to overestimate the total energy consumption by about the error shown in table 1.

City	Number of Measurements	Mean Consumption	Mean Error in % ± standard deviation	
			CitySim	Energetic Signature
La Chaux-de-Fonds	237 of 307	$126 \frac{kWh}{year*m^2}$	50% ± 131	33% ± 75
Neuchatel	104 of 152	$166 \frac{kWh}{year*m^2}$	74% ± 97	19% ± 54
Martigny	69 of 76	$78 \frac{kWh}{year*m^2}$	103% ± 88	20% ± 48

Table 1: Results across all cities that have introduced measured data.

CONCLUSION

First, the project demonstrates the possibility to generate a default data set in the absence of real measured data to get an idea about the current state of a city, if needed. Second, the data, measured or estimated, can then be used to calculate a set of urban performance indicators to compare the city over several years with itself (or with other cities): It is a monitoring tool measuring if the goals of the mayor's convention to cut down emissions and increase energy efficiency by 2020 are reached. Third, decision makers can use the results of the current state simulation or those of a scenario, such as overall primary energy consumption, part of renewable energy and greenhouse gas emissions, to quantify their choices. Local authorities can use it as a decision support. In addition, they can use MEU as a training tool to show the impact of typical scenario simulations.

One can conclude that making dynamic building simulations on scenes with very small measured data sets, leads to big errors. A simple method works at least as good as the sophisticated method for the already constructed building stock on the current data. Furthermore, the hypothesis of a fixed and on norms based first law efficiencies for the energy conversion systems needs to be re-evaluated. Varying the efficiency around a certain interval between 50 to 100 percent changes the overall result. Especially, when the efficiency is very low such as 50 percent, the overall results improve. However, these values are very unlikely.

For the short-term improvement, the following general steps for all cities should be undertaken:

- take the actual hemispherical view/horizon into account,
- introduce a basic numerical terrain model with all other obstacles,
- verify the user profiles for the residential buildings and introduce the number of inhabitants,
- consequently update physical building data for all buildings,
- create building types so that not general default values have to be used and
- measure technical efficiency of all technologies.

If these steps are not undertaken, it is very difficult to verify the taken approach and

adapt the default data set to correct values. One could change the air infiltration rate of a building or the u-values of a wall with the same result: But which change is correct? Such a platform can therefore only work correctly if the city takes consequently care of it, introducing correct data and default data sets.

As an alternative, one could accept the fact the correct retrofit is difficult to realize. Simple models require less data. For an annual energy consumption, they deliver at least the same precision for the old building stock, which represents the vast majority of all buildings, as more complex simulation approaches. Therefore simple models could be used for the retrofit where as dynamic approaches are used for new neighborhoods where all values are known. Especially new high performance buildings or neighborhoods can be precisely simulated and evaluated before being constructed.

REFERENCES

[1] Convenant of mayors. `http://www.eumayors.eu`, March 2013.

[2] Andreas Kemmler, Ale Piégsa, Andrea Ley, Mario Keller, Jakob Martin, and Giacomo Catenazzi. Analyse des schweizerischen energieverbrauchs 2000 - 2011 nach verwendungszwecken. Technical report, Swiss Federal Office of Energy, Bern, August 2012.

[3] OECD/IEA. Key world energy STATISTICS. Technical report, International Energy Agency, Paris, 2012.

[4] Diane Perez and Darren Robinson. Urban energy flow modelling: A data-aware approach. In *Digital Urban Modeling and Simulation*, volume 242 of *Communications in Computer and Information Science*, pages 200–220. Springer Berlin Heidelberg, 2012.

[5] Jérôme Henri Kämpf and Darren Robinson. OPTIMISATION OF URBAN ENERGY DEMAND USING AN EVOLUTIONARY ALGORITHM. In *Proceedings of the Eleventh International IBPSA Conference*, page 668–673, Glasgow, 2009.

[6] Swiss Society of Engineers and Architects. *Certificat énergétique des bâtiments selon SN EN 15217 et SN EN 15603 Cahier technique 2031*. SIA 2031. SIA, Zürich, January 2009.

[7] Federal land registry office. `https://www.housing-stat.ch`, June 2013.

[8] Swiss Society of Engineers and Architects. *L'énergie thermique(2009) et électrique (2006) dans le bâtiment*. 380/1 and 380/4. SIA, Zürich, January 2009.

[9] Massimiliano Capezzali, Gaëtan Cherix, Diane Perez, Jakob Rager, and Alain Duc. Swiss federal office of energy 102775 FP WKK, March 2013.

[10] Luc Girardin, François Maréchal, Matthias Dubuis, Nicole Calame-Darbellay, and Daniel Favrat. EnerGis a geographical information based system for the evaluation of integrated energy conversion systems in urban areas. *Energy*, 35(2):830–840, February 2010.

[11] Stig Hammarsten. A critical appraisal of energy-signature models. *Applied Energy*, 26(2):97–110, 1987.

TOWARDS SMART, SUSTAINABLE CITIES: THE APPLICATION OF HOLISTIC, ADAPTIVE MODELLING APPROACHES

P. Rowley[1]; N. Doylend[1] P. Dolado[2]; H. Madsen[3]; P Bacher[3]; A. Javadi[4]; M.Hartl[5]

1: CREST, Loughborough University, Leicestershire LE11 3TU UK

2: GITSE, I3A-University of Zaragoza, 50018, Zaragoza, Spain

3: Technical University of Denmark, Matematiktorvet, 2800 Kgs. Lyngby, Denmark

4: E.ON Energy Research Center, RWTH Aachen University, 52074 Aachen, Germany

5: Energy Department, AIT Austrian Institute of Technology, 1210 Vienna, Austria

ABSTRACT

This paper describes work carried out as part of the European Energy Research Alliance's (EERA) 'Smart Cities' joint programme, in which the aim is to apply advanced modelling approaches to support improved urban energy supply infrastructures. Additionally, a means to achieve medium and long term forecasting of possible scenario pathways to sustainable cities based on clear taxonomies, KPIs and benchmarks is a central goal. The paper illustrates the consortium's initial methodology from component to building scale, which includes development and integration of appropriate sub-system modelling approaches, whether empirical, stochastic, probabilistic or deterministic. Approaches for measured data integration are described in order to clarify potential routes towards cost-effective attainment of 'smart' sustainable urban environments within a pan-EU context. A particular focus is upon data-driven modelling for forecasting and control, especially the applications of grey-box modelling as bases for model predictive control for optimizing the operation of energy systems in cities. Specific aspects are described, along with testing and validation of the new framework by application to case studies.

One of the principal concepts behind the approach is the smart integration of a spectrum of various technologies into an urban environment applying an integrated, holistic methodology. This includes the smart integration of on-site renewable energy sources into buildings, the cascaded use of energy resources (or polygeneration) and the future coupling of electricity, heating and transport networks. This focus on the development of scientific tools for the optimal application of hybrid supply systems is demonstrated in the context of end-users' (such as building designers) requirements, with uncertainties in the outcome of complex system operation managed appropriately via various probabilistic and stochastic techniques.

A framework, or architectures, within which specific scenarios may be analysed quantitatively is also presented, in which multivalent energy sources and demand are considered as central modelling parameters. Beginning with an evaluation of the current practitioners' state-of-the-art, the modelling considers comparative assessments above and beyond the consideration for "single operation" approaches, which do not handle complex whole-system challenges arising on both system and component levels. Finally, the work discusses the practical aspects of creating adaptive, holistic models for the effective integration of distributed technologies on multi-scale levels, using techniques that are capable of dealing with complex integration issues such as sub-system control as well as that of whole-system design and operation.

Keywords: Simulation, control, smart cities, integrated modelling, renewable energy, demand management

INTRODUCTION

The European Strategic Energy Technology Plan (SET-Plan) outlines the crucial role of energy systems in successfully combating climate change and securing future energy supplies, and the importance of more efficient and new technologies in achieving these goals.

In response, leading Research Institutes across Europe have founded the European Energy Research Alliance (EERA), whose key aim is to accelerate the development of new approaches to energy system development by conceiving and implementing Joint Research Programmes. Key to this is the integration of activities and resources, combining national and Community sources of funding and maximising complementarities and synergies.

The Smart Cities EERA joint programme is focussed on energy efficiency and the integration of renewable and sustainable energy sources within urban areas. The main objective is the development of scientific tools and methods that will enable the intelligent design, planning and operation of energy systems of entire cities. An integrated transnational approach for the research is intended to capture best practice within national activities as they relate to all the relevant elements of the energy system, including thermal and electrical energy networks, buildings, energy supply technologies and the end-user.

The work presented in this paper sits within the context of the urban 'energy performance gap' that exists between predicted and actual performance of buildings, and is focussed upon a number of specific objectives, including:

- The creation of an integrated adaptive 'whole system' approach that is capable of incorporating holistic factors (both technical and non-technical) related to urban energy systems;
- The evaluation of the fitness-for purpose of current system and sub-system models, especially those currently used in building design and compliance contexts;
- The development of improved approaches to sub-system modelling that build upon international best-practice across the consortium;
- The use of national case studies to illustrate the testing and validation approach applied in the work.

METHOD

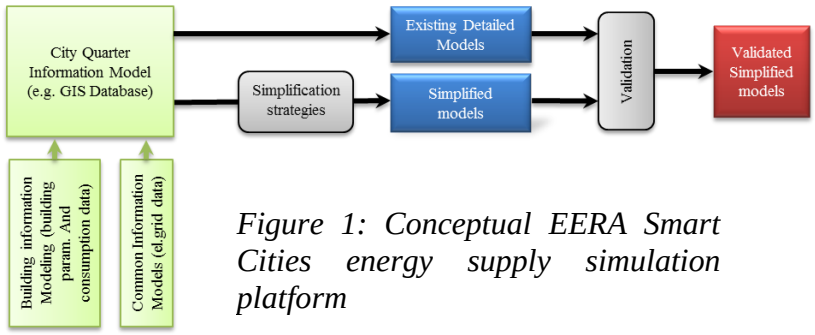

Figure 1: Conceptual EERA Smart Cities energy supply simulation platform

Central to the EERA Smart Cities joint programme is the development of a simulation platform integrating specific sub-system (or component) models, specialized around energy supply technologies as illustrated in Fig. 1. This concept includes the integration of models of different levels of detail to determine the interaction effects of large-scale implementation of renewable energy supply technologies in an overall Smart City context. Empirical validation of sub-system models utilizing appropriate national case studies underpins the achievement of reliable and accurate simulations. To this end, simulated effects of integration are progressively validated via comparison with data from continuously increasing numbers of national field experiments already running across the consortium. Aligning and integrating relevant national activities requires effective sub-system model

interoperability and temporal adaptation, according to the complexity of the simulation models. These may be relevant to large urban areas with different energy generation and distribution units, industrial and residential buildings and electricity grids. Thus, valid optimisation requires careful and reasonable definition at detail level for each component in order to achieve satisfactory dynamic system behaviour whilst concurrently reducing the simulation time, especially for thermal energy simulations, where higher numbers of variables may be involved. In order to promote these goals, clear pathways should be defined, such as where possible the use of validated simplified stochastic or probabilistic models instead of complex physical or empirical models. To this end, a key aspect is the development of a standardized database as input source of data for all different modelling approaches and the possibility of a co-simulation platform, in order to achieve a real-time simulation of the whole energy system, while integrating various models from different tools.

RESULTS

Construction of an adaptive, integrated framework

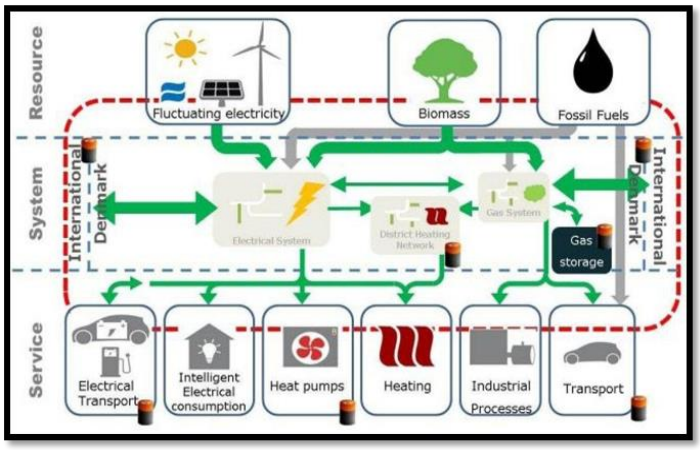

Figure 2: Modelling framework architecture.

Building upon the initial conceptual architecture, an integrated framework is developed which supports the creation of new strategies for the design, operation, and control of complex integrated urban-related energy supply and consumption systems. Figure 2, building upon a concept from DTU in Denmark, illustrates a framework for application within the EERA programme. This structure and the models within it need to fulfil several purposes, including simulation, forecasting and control. Within the framework, different modelling approaches are applied for various purposes depending on the context, ranging from deterministic physical models (white box models) through stochastic or probabilistic models to advanced dynamic stochastic modelling approaches, combining prior physical knowledge with data-driven statistical techniques (grey box modelling).

Baseline evaluation of current whole building and sub-system models

The frequent discrepancy that exists between design and post-occupancy energy use [1] arises not only due to inaccuracies in predictive deterministic modelling techniques, but also because practitioners' modelling assumptions are often poorly informed by what happens in real urban scenarios. From a whole-system perspective, the performance gap may arise from a combination of factors ranging from of poor client briefing, through sub-optimal design, construction, commissioning, management and system control. In turn, this problem is exacerbated by both a lack of feedback of actual monitored performance to designers and managers, as well as a shortfall in the capability of current pre-construction modelling techniques to reflect the complex interplay between various causal factors. Thus, an important aspect of the EERA work is to manage this complexity in order to address the need for new whole-system and component models that are fit-for-purpose.

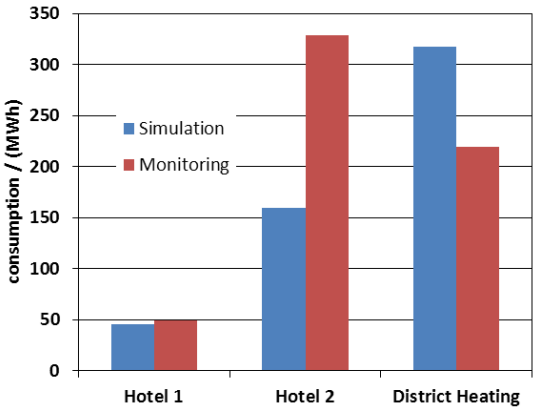

Figure 3: Simulated and monitored consumption for space heating and domestic hot water for the first year of operation for three example energy systems

An example is illustrated in Fig. 3, which shows data for a sample of non-residential energy systems in Austria monitored during their first year of operation. For the 50 systems in question, all utilize solar collectors with a gross area between 100 and 2000 m^2. Additionally, most of the systems are individual combinations of solar with heat pump, seasonal ground storage, and/or fossil back-up units respectively. Such complexity makes the design of optimised hydraulics and controls very challenging. Simulations performed on these systems in the planning phase were carried out with TRNSYS, T-Sol, GetSolar or PolySun, depending on the specific context [2].

Of the 8 systems that have already been monitored for an entire year of operation, the most important findings are:

1. Systems tend to be too complicated to apply general installation rules concerning hydraulics, controls and storage management. A total number of 32 optimization measures, such as increasing efficiency by hydraulic compensation, minimizing losses by lowering storage temperatures, avoiding unwanted circulations and for instance, resulting heat losses in the solar system during night time, could be applied to 17 systems. Some details can be found in [3]. Some of the errors were only for optimization purpose but some were fatal errors that caused significant harm to the system or led to stagnation of the solar part during the time of the largest solar yield.

2. The consumption for space heating and domestic hot water preparation estimated in the planning phase often significantly differs from the real operational consumption that has been monitored. An overall number of 8 systems showed an average miss-match in the order of 52%. However, this mismatch does not apply to a specific type of system configuration.

In the same context, the relevance of sub-system evaluation is illustrated in Fig. 4, which shows both an analysis of modelled and measured sub-system energy use intensity (EUI) for a commercial building in the UK. Both simulation environments utilised (TAS and IES) are regarded as ‘best-in-class’ dynamic simulation tools for such large and complex buildings.

The results show deviations in excess of 100% between modelled and monitored performance

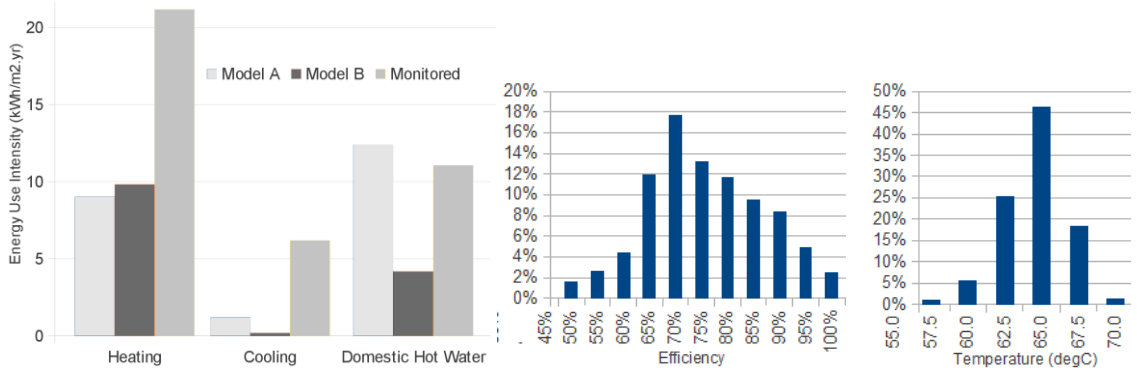

Figure 4: Comparison of (a) modelled and monitored sub-system EUIs and (b) frequencies of boiler efficiencies and water return-to-boiler temperatures measured at 15 minute intervals during operating period.

for both space heating and cooling energy. Thus, although reasonable agreement of modelled and measured whole-building energy performance may occur at a whole building level, this can be the result of significant sub-system modelling errors effectively cancelling each other out, reflecting the difficulty for existing models to effectively reflect post-occupancy reality. Fig. 4 also shows frequency distributions for both boiler efficiency and return water temperatures. A causal factor for the significant underperformance for this heating system is suggested by the frequency with which boiler return temperatures for the same plant are below the dew temperature of the flue gas, and points towards improvements in either system design or control approaches.

'Smart metering' for improved modelling and demand response management

An important enabler for the development of higher quality modelling approaches is the advance in metering technologies that facilitates the recording of sub-system energy generation and consumption at varying temporal resolutions. This allows insight into the behaviour of consumers and resulting consumption patterns as well as on the performance of energy equipment. Although the collection and distillation of this information into a useful form is a computational challenge, especially where real or near-time analysis is the goal, recent research [4,5] has shown that frequent recordings of the energy consumptions for heating or cooling can be used not only to characterize the energy performance of a building and identify 'low hanging fruit' for energy savings, but also in the identification of the time constants or thermal dynamics of buildings, which is very important for identifying how these thermal dynamics can be used in balancing consumption with fluctuating energy production.

In terms of whole-system modelling, this approach also paves the way for real time pricing of electricity. Information from frequent meter readings may also be useful for demand response management solutions, such as the control of electricity consumption through variable pricing, thereby utilising its latent flexibility [6]. The potential for peak load reduction of approximately 15% is apparent, and price-based demand response management can shift peaks by 5-10 hours in time by using the thermal capacity of buildings). An example from DTU Denmark of both a price response model concept and related measured consumption response is shown in Fig. 5. It should be noted that in the context of both renewable and traditional energy sources, the efficient management of such systems will require expertise in stochastic optimisation and modelling, statistics and computing. Forecasting will equally play a pivotal role for all stakeholders in the energy system and markets. An important example related to demand response management is a requirement for forecasting models describing the dynamic relation between price and consumption.

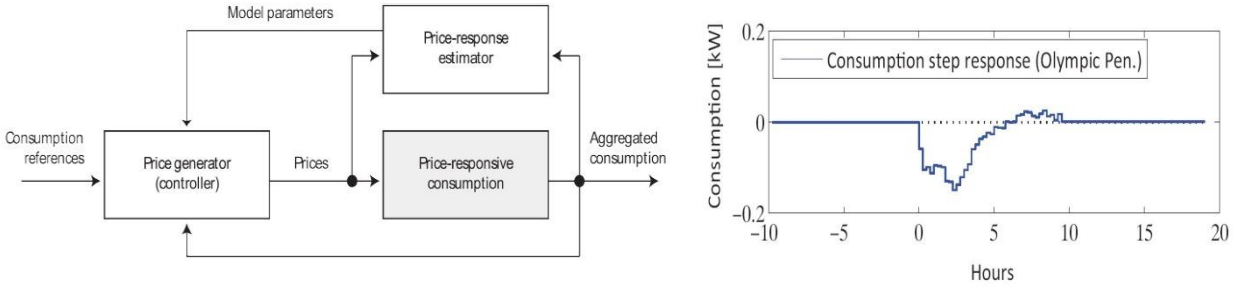

Figure 5: (a) Schematic of a system used to control electricity consumption in buildings using price signals and (b) Consumption response when the electricity price increases at hour 0.

DISCUSSION

The results described in this paper illustrate how holistic approaches to sub-system modelling and advanced data acquisition and analysis within an interoperable and adaptive framework can provide a foundation for the optimisation of urban energy supply infrastructures. Via careful selection and integration of sub-system modelling approaches (which include appropriate empirical, probabilistic, stochastic and deterministic methodologies) the means to achieve optimisation of multi objective outcomes emerges, along with identifying possible scenarios for cost-effective, 'smart' sustainable built environments within an international context. Specific aspects will be the focus of work within this EERA Smart Cities joint programme moving forward, including:

- Development of improved sub-system models and integration approaches for both energy supply technologies and for enabling technologies such as energy storage. This includes the capability to integrate non-technical factors such as human behaviour or tariff signalling using data-driven modelling, forecasting and control.
- The creation of an integrated data and model repository for use by research groups across the EERA network and beyond, utilising open standards for aspects such as data structures, provenance and usage permissions.
- Wider testing and validation of the framework by application to large-scale case studies across the EERA area, including for industry-urban integration.

In conclusion, this work illustrates a potential pathway for improving the 'smart' integration of a spectrum of energy technologies into complex built environments, with a focus on tool development for the optimal application of energy systems in light of a wide range of end-user and other stakeholder requirements, with uncertainties in the outcome of complex system operation managed appropriately via appropriate modelling techniques, whether empirical, deterministic, probabilistic or stochastic.

REFERENCES

1. Pollitt, G.: Building performance evaluation and certification in the UK: Is SAP fit for purpose. Ren. and Sust. En. Rev., vol. (2012), pp 6861-6878.
2. Fink, C.; Breidler, J.; Wagner, W.; Windholz, B.: Große solarthermische Anlagen in Österreich - Erste Ergebnisse zu einem Förderprogramm inkl. wissenschaftlicher Begleitung; in: 22. Symposium "Thermische Solarenergie, Ostbayerisches Technologie-Transfer-Institut e.V. (OTTI), Regensburg, 2012, ISBN: 978-3-941785-89-2
3. Windholz, B.; Zottl, A.; Fink, C.: Solarthermische Großanlagen kombiniert mit Wärmepumpen; Vortrag: 12. Internationales Anwenderforum Oberflächennahe Geothermie, Neumarkt i. d. Opf.; 19.03.2013 - 20.03.2013; in: 12. Internationales Anwenderforum Oberflächennahe Geothermie, Ostbayerisches Technologie-Transfer-Institut e. V. (OTTI), Regensburg (2013), ISBN: 978-3-943891-12-6; S. 50 - 57.
4. ENFOR: Analysis of energy consumption in single family houses. Technical report, Available at http://www.enfor.dk/pub/03EKS0009A002-A.pdf. 2010.
5. P. Bacher, P. and Madsen, H.: Identifying suitable models for the heat dynamics of buildings. Energy & Buildings, 2011, 43, 1511-1522
6. Corradi, O. & Ochsenfeld, H.: Integration of fluctuating energy by electricity price control Denmarks Technical University, 2011

TIME AND SPATIAL RESOLVED SIMULATION AS KEY INSTRUMENT TO DEVELOP SUSTAINABLE URBAN ENERGY SYSTEMS BASED ON RENEWABLE ENERGIES

G. Stryi-Hipp; J.-B. Eggers;

Fraunhofer Institute for Solar Energy Systems ISE, Heidenhofstr. 2, 79110 Freiburg, Germany

ABSTRACT

A growing number of cities worldwide become aware that they are key actors to tackle global challenges like climate change and energy scarcity. To support cities to become sustainable the German Fraunhofer Society on applied research formed a research network under the brand name »Morgenstadt – City of the future«. Urban energy systems are a relevant research topic since energy is very important for cities to become sustainable.

The transformation of an urban energy system to a sustainable energy system based on Renewable Energy Sources (RES) needs several years at least for large cities. New technologies, equipment and infrastructure must be developed and installed for generation, conversion, storage, distribution and consumption of electricity, heat and cold, and energy sources for transport.

At the beginning of the transformation, an ENERGY MASTER PLAN must be developed including the ENERGY TARGET SYSTEM and the ENERGY ROADMAP, which describes the path to achieve the ENERGY TARGET SYSTEM. A procedure to develop the ENERGY MASTER PLAN step-by-step is described. An extensive involvement of main stakeholders and strong governance structures are important to implement such a process successfully.

To identify the optimal ENERGY TARGET SYSTEM the ENERGY TARGET must be set precisely. Especially the origin of the RES and the balancing period must be well defined. Based on that ENERGY SYSTEM SCENARIOS can be simulated and the TARGET ENERGY SYSTEM identified.

Since the fluctuating solar energy and wind energy are usually the main RES used, temporally resolved simulations of ENERGY SYSTEM SCENARIOS are necessary. Therefore Fraunhofer ISE is developing the model »KomMod«, which allows to simulate detailed TARGET ENERGY SCENARIOS as a sound basis for decisions on the ENERGY ROADMAP.

To cover the interdependencies of the components of the energy system »KomMod« includes all four demand sectors and takes a macro-economic perspective. System design and operation are optimised simultaneously and the model is provided with perfect foresight. All components are implemented with the modelling environment AMPL, following a homogenous modelling approach and building one simultaneously solved equation system.

Keywords: urban energy system, energy system model, energy master plan, energy roadmap

INTRODUCTION

In the 21st century, mankind has to tackle serious challenges like the scarcity of conventional energy sources, scarcity of raw materials, climate change, an ageing society and growing population. A growing number of cities worldwide become aware that they are key actors to develop appropriate solutions since there is a strong tendency of urbanization worldwide. To support cities to become sustainable the German Fraunhofer Society on applied research formed a network under the brand name »Morgenstadt – City of the future« to do research in the sectors energy, buildings, mobility, water, production and logistics, security, information

and communication technologies (ICT) and governance. Urban energy systems are a relevant research topic in the network since energy plays a key role for cities to become sustainable.

Smart urban energy systems based on renewable energy sources (RES) are main pillars of sustainable cities, since they avoid CO_2-emissions, mitigate climate change, generate local added value and create jobs. Due to their decentralized structure, RES enable cities to generate energy on their own area and the surrounding region and become self-sufficient.

In Germany and several other countries a growing number of cites are setting ambitious goals regarding their future energy supply. For example, the city of Copenhagen with 650,000 inhabitants set the goal to become the first carbon-neutral capital by 2025, the city of Munich with 1.4 Mio inhabitants aims to supply the whole city with electricity from RES by 2025, and in the German city of Freiburg with 220,000 inhabitants a study was conducted which explains how Freiburg can become carbon-neutral by 2050.

Several decades are necessary to transform the energy system of a larger city to a sustainable energy system based on RES. New technologies, equipment and infrastructure must be developed and installed in generation, conversion, storage, distribution and consumption of electricity, heat and cold, and energy sources for transport. To run this transformation successfully a strategic long-term approach based on a well-defined target, a transparent governance structure, a strong political commitment, and the involvement and acceptance of the important stakeholder in the city are needed.

At the beginning of the transformation an ENERGY MASTER PLAN should be developed including the TARGET ENERGY SYSTEM and the ENERGY ROADMAP, which describes the path to achieve the TARGET ENERGY SYSTEM. To support these activities a standardized procedure of developing an ENERGY MASTER PLAN step-by-step is proposed. In this process the temporally and spatially resolved model for urban energy systems called »KomMod« can be a supportive tool, which allows to simulate detailed ENERGY SYSTEM SCENARIOS as a sound basis for decisions on the ENERGY ROADMAP.

PROCEDURE TO DEVELOP AN ENERGY MASTER PLAN

The challenge for cities to develop a sustainable urban energy system is twofold.

Firstly, most of the cities and their decision-making representatives and bodies are not experienced in designing the city's energy system. Most of them delegate the right to supply their citizens with energy to a utility company. But even if a city is owner of the local utility company the energy system is usually designed by experts of the utility company and only some framework conditions are set by the politicians.

Secondly, there is a lack of experiences on how a medium-sized or large city can mainly be supplied by RES. The vision of an urban energy system mainly based on RES has been a dream already for several decades, but the conviction that this is a realistic technological option which can be achieved within a few decades even in medium-sized and larger cities in industrialized countries is only some years old based on the strong growth of RES in countries like Denmark and Germany in the last decade. Nevertheless there are various issues unresolved yet: how a sustainable urban energy system will look like in detail, which technologies will be available at which costs, how stability and security of energy supply can be assured and how the energy market must be designed.

A systematic procedure for the development of an ENERGY MASTER PLAN is recommended as shown in Figure 1. In the first phase (step 1-5) a precise long-term ENERGY TARGET SYSTEM must identified by setting a precise ENERGY TARGET and calculating the ENERGY SYSTEM

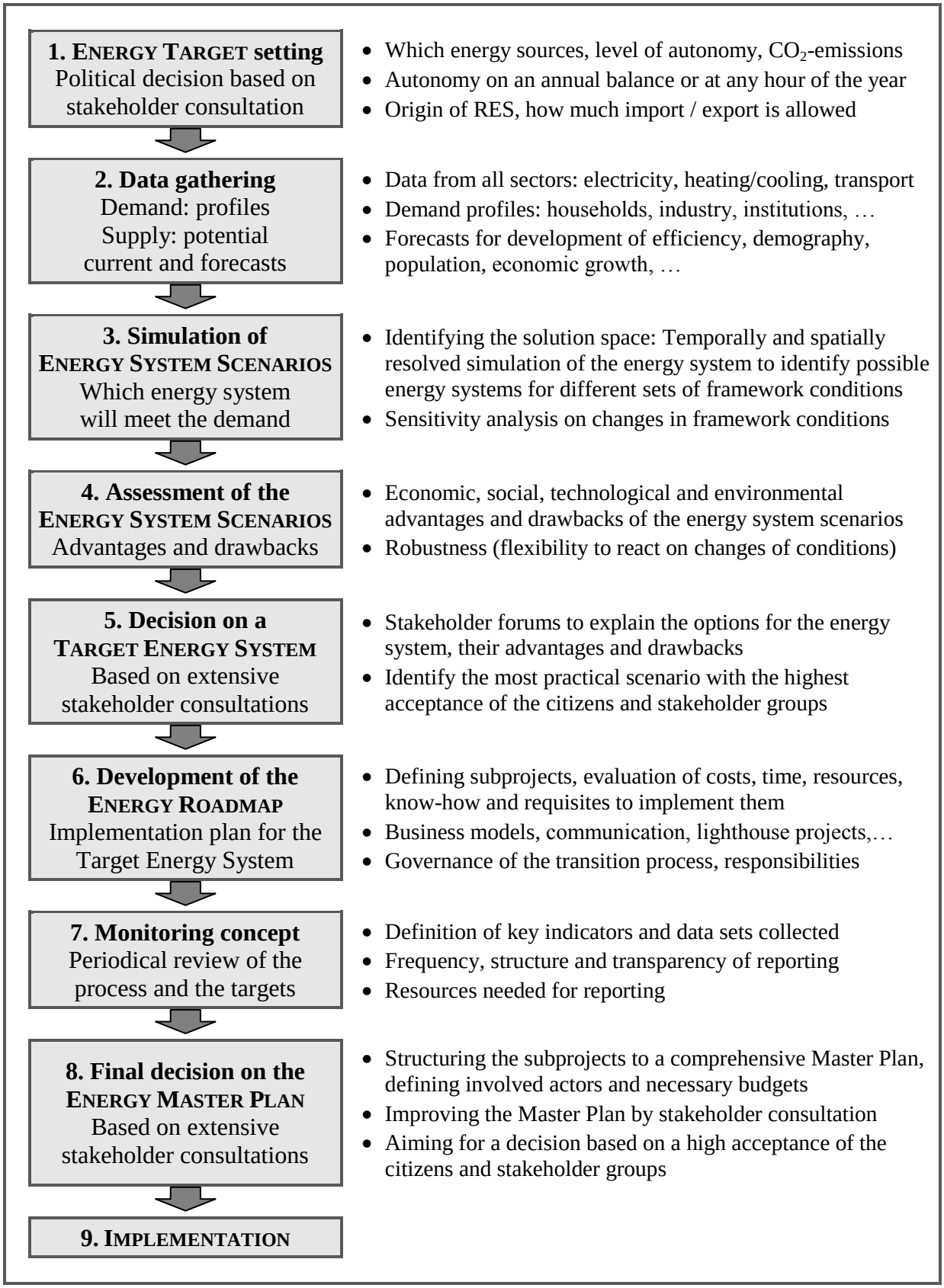

Figure 1: Procedure of the development of an ENERGY MASTER PLAN

SCENARIOS, with which the target can be achieved. This task is challenging, since the results are dependent on the predictions on the framework conditions e.g. the influence on the energy demand by improving efficiency, ageing society and growing or shrinking population. In the second phase (step 6-8) the ENERGY ROADMAP must be developed describing the steps to implement the TARGET ENERGY SYSTEM. In the third phase the ENERGY ROADMAP will be implemented.

Several aspects must be considered by implementing such a process. It must be accepted that it is not possible to identify the optimal TARGET ENERGY SYSTEM since a lot of conditions are unknown for the target year or not precisely predictable, regarding the development of the socio-economic data as well as of the available technologies. Therefore robust development paths must be identified and the implementation plan and its underlying assumptions must be regularly revised based on the progress achieved. This underlines the high importance of implementing a monitoring system (step 7) for energy consumption and CO_2-emissions to be able to measure the progress. Such a fundamental transition needs a strong backing by the majority of the citizens. Therefore, the ENERGY MASTER PLAN must be developed in an extensive stakeholder process to take into account the views of all stakeholder groups to get a high acceptance and a strong support for the implementation.

HOW TO IDENTIFY A TARGET ENERGY SYSTEM

Already the first step of the ENERGY MASTER PLAN development, the ENERGY TARGET setting is challenging. Typically a target like »Carbon-neutrality by 2025« or »100% RES by 2050« is set by a city. Since the corresponding TARGET ENERGY SYSTEM which fulfils this target is very much dependent on the set of boundary conditions like the definition and acceptance of carbon-neutral energy sources (nuclear power, waste incineration, fossil fuel with CCS or RES), the origin of the RES and the balancing period, these conditions must be defined precisely. Some consequences of different definitions are shown in Table 1.

Balancing period→ **Origin of the RES↓**	**Energy supply and demand balanced over the year**	**Energy supply and demand balanced every hour**
RES only from the city area and its surrounding region	**CALCULATED LOCAL AUTONOMY** Feasibility dependent on local RES (e.g. availability of wind power); large storage capacity or complementary energy generation needed in other regions to compensate seasonal imbalance;	**TRUE LOCAL AUTONOMY** Very difficult to achieve at least for larger cities; large on-site seasonal storage capacity needed; not optimal from the macroeconomic standpoint;
RES partly imported from other regions of the country	**CALCULATED LOCAL AUTONOMY WITH NATIONAL RES IMPORT** The use of RES from other regions of the country reduces seasonal imbalance and the need of storage capacity; beneficiary from the macroeconomic standpoint;	Not reasonable
RES partly imported from other countries	**CALCULATED LOCAL AUTONOMY WITH INTERNATIONAL RES IMPORT** Attractive RES sources in other countries can be used (e.g. solar power in southern Europe); transmission lines are needed; import dependency is increasing;	Not reasonable

Table 1: Types of ENERGY TARGETS *for an urban energy system*

To define the optimal TARGET ENERGY SYSTEM first the solution space must be identified by modelling ENERGY SYSTEM SCENARIOS, which correspond with the ENERGY TARGET. Based on well-defined criteria (e.g. costs or acceptance) the optimal TARGET ENERGY SYSTEM must be selected. How such a TARGET ENERGY SYSTEM principally looks like is shown in Figure 2. This graph shows that in energy systems with a high share of RES the energy sectors electricity, heating and cooling and gas are highly integrated and interacting strongly.

Since potential analysis shows that usually the fluctuating solar energy and wind energy are the main RES used, temporally resolved simulation of ENERGY SYSTEM SCENARIOS is necessary to identify the share of the different RES, the storage capacities and import/export of energy sources needed. Heating and cooling networks will play an important role in such systems since they allow the use of larger combined heat and power units, the transport of heat generated by RES to city areas without space of solar thermal collectors and the integration of large seasonal thermal storage. Therefore also spatially resolved simulations of ENERGY SYSTEM SCENARIOS are necessary as well.

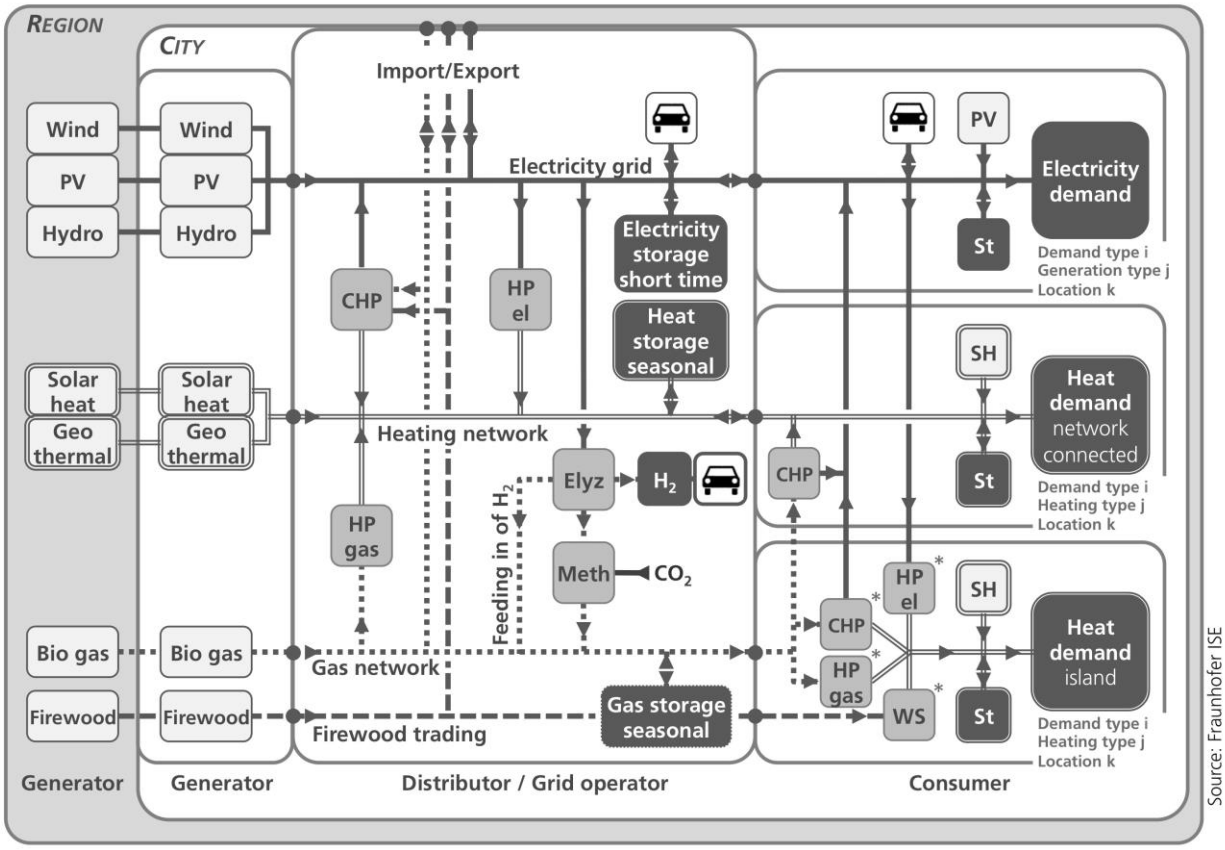

Figure 2: Structure of an urban energy system based on 100% RES

THE URBAN ENERGY SYSTEM MODEL »KOMMOD«

For the identification of optimal TARGET ENERGY SYSTEMS, Fraunhofer ISE is developing the urban energy system model »KomMod«, which allows to simulate temporally and spatially resolved ENERGY SYSTEM SCENARIOS [1]. »KomMod« is meant as a strategic tool, supporting cities with the structural analysis of their energy system and resulting strategic decisions. A major aspect within this task is the consideration of multiple interdependencies. Cross-sectoral interdependencies occur between all four demand sectors (electricity, heat/cold,

natural gas, and (local) transport), intra-sectoral interdependencies between different technologies, and furthermore interdependencies between structure (design) and operation of the components of an energy system as well as dependencies between technical and economical aspects have to be taken into account.

To cover these interdependencies »KomMod« includes all four demand sectors and takes a macro-economic perspective instead of calculating solutions optimal only for single stakeholders. System design and operation are optimised simultaneously and the model is provided with perfect foresight. This means that the model is able to adjust both, the capacities of the technologies used as well as their operation, under the premises of knowing the energy demand for every future time step, until it finds a well-balanced optimum. This process is dynamic in the way that the requirements of future time steps are already taken into account for current decisions. In contrast to short term operation planning, for strategic decisions it is sufficient to model every time step as a point of steady-state operation thus meaning that the dynamic behaviour of the components is only partly integrated.

All components are implemented with the modelling environment AMPL, following a homogenous modelling approach and building one simultaneously solved equation system. Technically, the component models include part-load efficiencies, load acceptance rates, minimal charging levels (reducing the net capacity of a storage) and self-discharge of storages for example. Grouping technologies into components of similar physical behaviour allows for their description with identical equations while differences between the elements of a technology are expressed by a change in the parameter sets.

To be able to model the requirements of high shares of RES properly, the temporal resolution is set to an averaging period of one hour, intended to be reduced to 15 minutes. This also enables »KomMod« to provide answers to questions with respect to the amount and operation of short-term storage. The spatial division into zones, sub-zones, and building types provides a finely graded basis to adjust the model to the specific needs of the respective municipality.

As a result »KomMod« enables the user to analyse and optimise urban energy systems and identify the optimal TARGET ENERGY SYSTEM. Different scenarios of possible technical, economical and/or socio-economic developments and their assessment as well as recommendations for the capacity and number of facilities to be installed, the relevant time series for their operation, and cost data can be included in the calculations.

CONCLUSION

The transformation of their energy system is a key element for cities to become sustainable. As a solution, a concept of an urban energy system based on renewable energy sources (RES) is presented. A standardized step-by-step approach is proposed to develop an ENERGY MASTER PLAN, including the TARGET ENERGY SYSTEM, which defines the target and the ENERGY ROADMAP, which describes a robust path to implement the concept. To identify the optimal TARGET ENERGY SYSTEM, temporally and spatially resolved simulations of ENERGY SYSTEM SCENARIOS are necessary. With the urban energy system model »KomMod«, Fraunhofer ISE provides a tool for cities to plan the transformation of their energy system on a sound basis.

REFERENCES

[1] J. B. Eggers, G. Stryi-Hipp: KomMod as a tool to support municipalities on their way to becoming Smart Energy Cities, Proc. of the Sustainable Building Conf. 2013, Graz, 2013.

URBAN FORM OPTIMIZATION FOR THE ENERGY PERFORMANCE OF BUILDINGS USING CITYSIM

T. Vermeulen[1]; J. H. Kämpf[2]; B. Beckers[1]

1: AVENUES, EA7284, Urban Systems Engineering, Université de Technologie de Compiègne (UTC), BP20529, 60205 Compiègne, France

2: Solar Energy and Building Physics (LESO-PB), Ecole Polytechnique Fédérale de Lausanne (EPFL), Station 18, CH-1015 Lausanne, Switzerland

ABSTRACT

The energy efficiency of the urban texture relies notably on the buildings' form, which characterizes its capability to take profit of the solar potential as well as its loss of energy through the envelope. Therefore, the general layout at the district scale has a significant impact on the global energy balance in a dense built environment, where the relative position of the adjacent buildings generate shadowing and inter-reflection on a large part of the incoming solar radiation.

In the current work, an urban energy simulator named CitySim is used together with a hybrid evolutionary algorithm. The physical model within CitySim features the computation of shortwave radiation including reflections, longwave radiation and a nodal thermal model for the building energy flows. The complete simulation leads to a rather precise evaluation of the annual heating needs, defined as the objective function to be minimized at the district scale. An existing district in Paris is taken as case study: the Bercy park front. Its buildings are disposed in several blocks surrounding courtyards with openings on the park's side (south-west). This district is recent (1994-2005) and located in a dense area of seven stories buildings. In its original design, the access to sunlight was taken into account by the planner, thus the initial intuition of the architect is compared with optimized configurations.

The paper describes a case of urban form optimization, with the formal description of the variables, constraints and objectives of the problem and the definition of the geometrical case for Bercy Front Park. The optimization variables focus on geometrical properties such as the height of the buildings and glazing ratios. The thermal properties of the building (insulation, glazing type) are set in accordance with the French standards of the thermal regulation (RT2005). The urban layouts resulting of the optimization process are analyzed and discussed.

Keywords: Urban form optimization, evolutionary algorithm, urban energy simulation, CitySim

INTRODUCTION

The use of simulation tools for the energy balance evaluation leads to a better understanding of what are the most important features of a good urban layout. The most common methodology consists in comparing different urban layouts considering one criterion, e.g. minimize the energy needs. In this context, combination of these tools with numerical optimization methods appears to be an efficient way to search within a large space of possible configurations those that best suit a given objective. Results are expressed as a set of values for each of the optimization variables which can be related to geometric and architectural characteristics (height and form of buildings, glazing ratio), materials properties (insulation, glazing), or building systems specifications for heating, cooling and HVAC [1]. Most of the

building optimization studies involves genetic or evolutionary algorithms to search for optimal solutions [1].

In the specific field of urban planning, the solar potential is a common criterion for design, either treated geometrically [2], by parametric studies of urban layouts [3], or by using optimization methods [4]. It has been shown that a significant improvement in the annual solar potential can be achieved compared to standard intuitive configurations [5]. While playing an important role in the solar transmitted energy, the design of windows is usually treated separately as a optimization problem in itself: glazed areas better transfer heat by conduction but allow the transmission of solar radiation which has an impact on daylighting, heating and cooling needs [6][7].

The present study describes a case of shape optimization at the urban scale based on the geometric parameterization of an existing district in Paris. The optimizer uses an evolutionary algorithm (hybrid CMA-ES/HDE) developed with the purpose to achieve urban optimization [8]. The annual energy needs for heating are defined as the objective function to be minimized. The evaluations of these needs are performed with CitySim, a software designed for the simulation of the energy fluxes at urban scales [9]. The cooling needs are not taken into account since they are not significant under Paris climate, assuming the possibility to open windows and to use blinds.

In a first optimization case, the heights of buildings forming a block are defined as optimization variables. The optimum configuration, obtained after the optimization process, is compared with the original layout with respect to their heating needs. An analysis of a set of good urban configurations is then performed with the aim to characterize the design subspace ensuring low heating demands. Finally, the glazing ratios of the four main block orientations are set as optimization variables together with the building heights to compare the importance of these two characteristics on the design subspace obtained.

METHODOLOGY

Optimizer

The optimization process is treated using an evolutionary algorithm developed as part of a work on urban shape optimization [8].

To this purpose, a vector of bounded continuous parameters, $\vec{x}$, is defined, encoding the characteristics of an urban configuration. In this scope, a set of values for these parameters defines an individual. A population corresponds to a group of individuals.

$$\vec{x} = \{x_1, \dots, x_n\} \qquad x_{i,min} \leq x_i \leq x_{i,max}$$

The optimization problem consists in minimizing the objective function $J(\vec{x})$, in our case the heating needs, given a parameter space *A*, ie:

$$\min_{\vec{x} \in A} J(\vec{x})$$

Case study

A district of Paris is considered as a case study: the Bercy Front Park. This district was built between 1988 and 2005 at the site of a former wine warehouse district, southeast of Paris. It is composed of seven stories housing blocks surrounding courtyards (24 m height). The area is bordered on the southwest side by the Bercy Park. Although the blocks were designed by different architects, consistency rules have been established by the architect responsible for the development of the area, Jean-Pierre Buffy. Thus, the blocks adjoining the park have a U-shape closed by two independent blocks, leaving visual openings on the park.

For this study, one single block is considered (Figure 1). To simplify the modeling, the block is discretized into 16 identical buildings around a courtyard (Figure 2). Trees and balconies are not taken into account, although they may have a significant influence on the reduction of solar radiation. The surrounding buildings are modeled in a simplified manner and influence the heating needs calculation. The heights of each of the 16 buildings of the modeled block constitute the parameters of the model, represented by the continuous variables $h_1, \dots, h_{16}$. The vector $\vec{x}$ of the optimization parameters can be written:

$$\vec{x} = \{h_1, h_2, \dots, h_n\}$$

The optimization problem is solved in two steps. At first, only the heights of the buildings are set as variables. Then, four parameters: r_{SW}, r_{SE}, r_{NE}, r_{NW} corresponding to the glazing ratio of the four directions of the block (for every surfaces) - respectively southwest, southeast, northeast and northwest - are added to the optimization parameters.

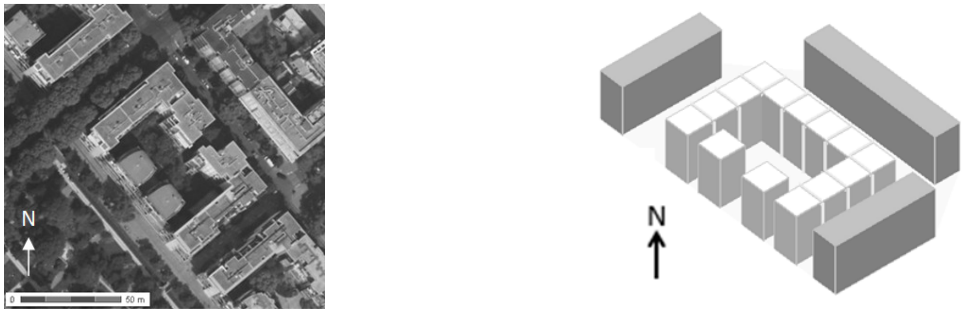

Figure 1: satellite view of the block (source: IGN) and simplified representation

Figure 2: representation of the block discretization with building numbering

Constraints

The Local Development Plan of the city of Paris sets the maximum allowable building height, which, for the studied block, is 31 m. In accordance with the regulation, and to work only with floors of 3 m, each height parameter is bounded:

$$3 \leq x_i \leq 30 \qquad i = 1,..,16$$

A constraint on the total volume of the block is defined with respect to the volume of the simplified original geometry of the block, V_{built} (Figure **1**):

$$\sum_{i=1}^{16} A_i h_i = V_{built} \pm 5\%$$

In the second optimization case, the glazing ratios, considered as variables, are bounded in order to prevent them from taking extreme values (no windows or fully glazed façades):

$$0.2 \leq r \leq 0.8 \qquad r \in \{r_{SW}, r_{SE}, r_{NE}, r_{NW}\}$$

Heating needs simulation

The annual heating needs are assessed using the software CitySim [9]. It features a nodal thermal model applied to each building. Heat gains from direct and diffuse solar radiation are taken into account, as well as shortwave reflections [10]. Longwave exchanges between the walls are also calculated. The calculations are based on weather data for the city of Paris from Meteonorm 6.1 [11].

The insulation of the buildings is defined in accordance with the French thermal regulation of 2005. Construction details are referenced in Table 1.

Location	Parameter	Unit	Value
Façades	Wall U value	W/(m².K)	0.36
	Wall solar reflectance	-	0.4
	Glazing U value	W/(m².K)	1.8
	Glazing ratio on all walls (1^{st} optimization case only)	-	0.25
	Glazing solar transmittance	-	0.7
Floor	U value	W/(m².K)	0.27
Flat Roof	U value	W/(m².K)	0.27
	Solar reflectance	-	0.2
Ground	Ground solar reflectance	-	0.2

Table 1: construction details

The air is renewed from ventilation and infiltration, with a coefficient of 0.4 volume/h. Thermal bridges are not taken into account in the calculation, which results in an underestimation of the heating needs. However, the corresponding losses are supposed constant with the geometric parameters (modification of heights), and therefore should not influence optimization results.

RESULTS

First case: optimization of the heights of the buildings only

In a first step, only the heights of the buildings are considered as optimization variables. A total of 5000 evaluations of the objective function are performed in the optimization process.

A decrease of 16.5 % of heating requirements is observed between the worst and the best individual. The best obtained configuration is presented in Figure **3**. The original design was simulated using the same simplified typology (Figure **1**), to ensure a comparable envelope surface and volume. The evaluation on CitySim results in a decrease of 12.1 % of the heating needs between the original configuration and the optimal case.

In order to evaluate the importance of each parameter, a set of good configurations is analyzed, using for this the 5 % best evaluations (about 250 unique individuals). These individuals are all within 2 % of the best individual with respect to the objective function computed with CitySim. For each parameter, a preferential range appears to gather the best configurations. The standard deviations and mean values are calculated for each variable (Figure **3**), giving information on the acceptable range ensuring low heating needs while leaving some flexibility to the urban planner for the design. It has to be mentioned that all the considered individuals have a total volume close to the minimum allowed ($V_{built} - 5\%$).

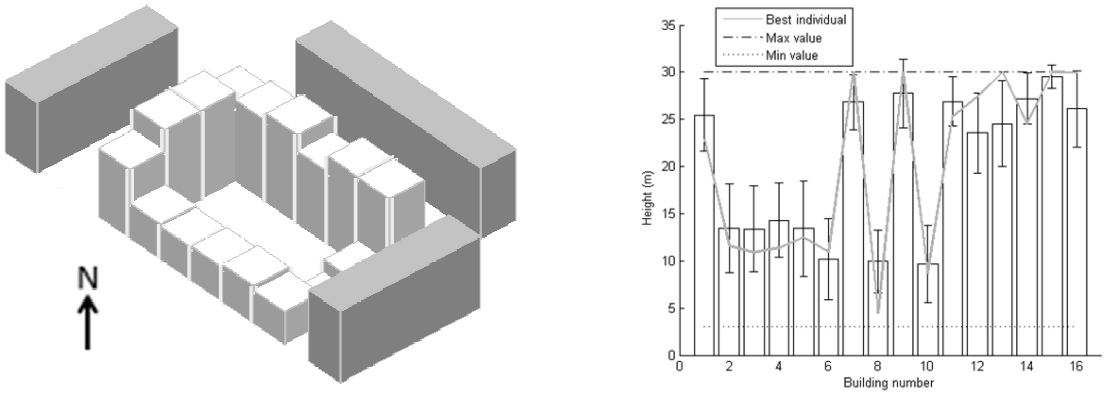

Figure 3: best configuration (left) and analysis of the 5% best individuals: mean values and standard deviations (right)

Second case: optimization of the building heights and the glazing ratios

The combined building height and glazing ratio optimization is also performed with 5000 evaluations of the objective function. The mean values and standard deviations, based on the 5 % best individuals, are shown in Figure 4. It appears that, for the analyzed set of individuals, the standard deviation of the glazing ratios is low relatively to height parameters. For the walls facing north (northeast and northwest) and for the obstructed orientation (southeast), the glazing ratio obtained corresponds to the defined lower bound. Solar gains are offsetting losses only for the southwest orientation which is unobstructed. Nevertheless, the obtained glazing ratio of 0.3 is still much lower than what was actually built (over 0.5). A possible explanation for these generally low values of glazing ratios is the lack of contradictory criteria such as daylight evaluation in the objective function.

The best solution found in this optimization case has a 2 % decrease heating requirements compared to that of the first optimization case, with optimal glazing ratios close to the value set in a first time. The height values of the best individual presents some similarities with the best configuration observed in the case where only heights are optimized (lower buildings to the south side and higher to the north side). Furthermore, the values for most of its parameters fit within the standard deviation around the mean value calculated for the 5 % best individuals of the first optimization case.

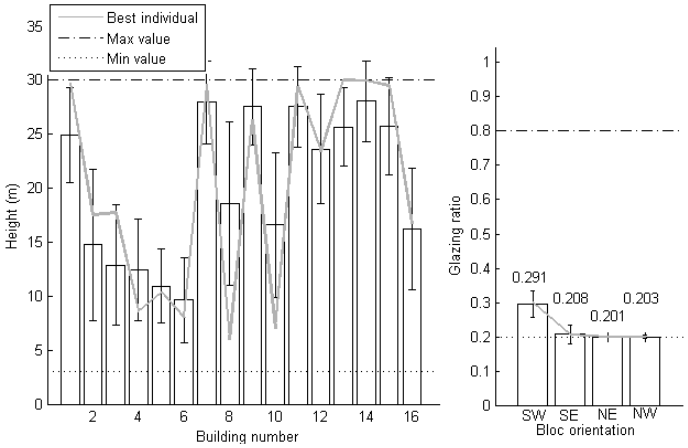

Figure 4: mean values and standard deviations for building heights and glazing ratios

CONCLUSION AND DISCUSSION

A study of urban form optimization was performed by coupling an evolutionary algorithm and CitySim for the calculation of heating needs. A city block based on a district of Paris was

used as a case study. For this purpose, the geometry of a block was simplified into elementary buildings of varying height. The optimization initially focused on the heights of the elementary buildings, then on the heights of buildings together with the glazing ratios of the different block façade orientations.

The results were analyzed by focusing on a set of good configurations with respect to the objective function. Thus, it was possible to define a design subspace in which urban configurations have low heating needs. After examining the combined building height and glazing ratio optimization, it was observed that the standard deviations of the glazing ratio parameters over a set of good configurations are lower than that of the height parameters. This could be explained by a higher sensitivity of the objective function to the glazing ratios than to the height parameters.

This study focused only on heating needs, which is the most important part of the energy consumption of residential buildings in Paris. However, notions of comfort, including the visual profit of daylight were not considered and would certainly lead to different results. Future studies might take these aspects into account, possibly in a multi-criteria optimization.

AKNOWLEDGEMENT

The authors would like to thank the Fondation Bâtiment Energie for the financial support to the present work through the project REPA-F4.

REFERENCES

1. Evins, R.: A review of computational optimization methods applied to sustainable building design. Renewable and Sustainable Energy Reviews 22, pp 230-245, 2013.
2. Knowles, R.L.: The solar envelope: its meaning for energy and buildings. Energy and buildings, pp. 15-25, 2003.
3. Hachem, C., Athienitis, A., and Fazio, P.: Parametric investigation of geometric form effects on solar potential of housing units. Solar Energy, pp. 1864-1877, 2011.
4. Kämpf, J.H., Montavon, M., Bunyesc, J., and Bolliger, R.: Optimisation of buildings' solar irradiation availability. Solar Energy, pp. 596-603, 2010.
5. Kämpf, J.H. and Robinson, D.: Optimisation of building form for solar energy utilisation using constrained evolutionary algorithms. Energy and Buildings, pp. 807-814, 2010.
6. Caldas, L.G. and Norford, L.K.: A design optimization tool based on a genetic algorithm. Automation in construction, pp. 173-184, 2002.
7. Wright, J. and Mourshed, M.: Geometric opimization of fenestration. 11th International IBPSA Conference, Glasgow, 2009.
8. Kämpf, J.H. and Robinson, D.: A hybrid CMA-ES and HDE optimisation algorithm with application to solar energy potential. Applied Soft Computing Journal, pp. 738-745, 2009.
9. Robinson, D., Haldi, F., Kämpf, J.H., Leroux, P., Perez, D., Rasheed, A. and Wilke, U.: CitySim: comprehensive micro-simulation of resource flows for sustainable urban planning. 11th International IBPSA Conference, Glasgow, 2009.
10. Robinson, D. and Stone, A.: Solar irradiation modeling in the urban context. Solar Energy, pp. 295-309, 2004.
11. METEONORM v.6.1. Meteotest, 2009.

EARLY DECISION SUPPORT FOR NET ZERO ENERGY BUILDINGS DESIGN USING BUILDING PERFORMANCE SIMULATION

Shady Attia[1,2], Elisabeth Gratia[2], Andre De Herde[2], Jan L. M., Hensen[3]

1: Interdisciplinary Laboratory of Performance-Integrated Design (LIPID), School of Architecture, Civil and Environmental Engineering (ENAC), École Polytechnique Féderale de Lausanne (EPFL), Switzerland

2: Université Catholique de Louvain, Architecture et climat, Louvain-la-Neuve, Belgium

3: Building Physics and Services, Eindhoven University of Technology, The Netherlands

ABSTRACT

This paper aims to investigate the use of building performance simulation tools as a method of informing the design decision of NZEBs. The aim of this study is to evaluate the effect of a simulation-based decision aid, ZEBO, on informed decision-making using sensitivity analysis. The objective is to assess the effect of ZEBO and other BPS tools on three specific outcomes: (i) knowledge and satisfaction when using simulation for NZEB design; (ii) users' decision-making attitudes and patterns, and (iii) performance robustness based on an energy analysis. The paper utilizes three design case studies comprising a framework to test the use of BPS tools. Two types of data were collected, mainly preference and performance data. The preference data were used to collect information from participants using self-reported metrics. The performance data were used to collect information on the energy performance of the final design. The energy evaluations were compared with the results of a quantitative assessment of the overall design performance. Finally the results were compared and presented. The paper provides results that shed light on the effectiveness of sensitivity analysis as an approach for informing the design decisions of NZEBs.

Keywords: decision support, early stage, net-zero, design, simulation, architects

INTRODUCTION

Building performance simulation (BPS) tools have the potential to provide an effective means to support informed design decision-making of NZEBs. However, certain barriers block architects' use of BPS decision support for NZEB design during early design stages. The most important barrier is informing design decisions prior to the decision-making and early on in the design process [1-2]. The barriers to informing the decision-making and providing guidance to architects during the early stages of NZEB design have been quoted by a number of previous studies around the world [3-5]. Currently, simulation tools are mostly used in the later stages of NZEB design by specialists as evaluation tools, rather than by architects as guidance tools. In this context, this paper aims to evaluate the effect of a simulation-based decision aid on achieving informed design decision-making by architects during early stages of the design of NZEBs.

DESIGNING AND CONDUCTING THE STUDY

Two types of data were collected, mainly preference and performance data. The preference data were used to collect information from participants using self-reported metrics. The performance data were used to collect information on the energy performance of the final design. Three workshops took place in Cairo to examine the effect of using the BPS tools and

sensitivity analysis technique in the design of NZEBs. The workshops were announced and three groups of participants were recruited.

Prior to starting the workshops, participants were asked to achieve proficiency in the use of geometrical modelling in DesignBuilder (DB) using the video tutorials provided online. Additionally, ZEBO, a Graphical User Interface developed for Egyptian, was installed and used by all participants [6]. At the beginning of the workshop, participants were given an introductory crash course in use of DB and ZEBO, requiring a time investment of eight hours. Throughout the crash course, participants were required to follow a guidebook checklist on how to carry out successful simulations. The checklist was developed after reviewing the work of Bambardekar [7] and Rocky Mountain Institute (RMI) [8] and was used to remind participants to use the minimum number of steps and to make the steps explicit. During the introductory tutorial participants were taught to: 1). create a simple building geometry model in ZEBO, 2). perform a simulation and sensitivity analysis exercise using ZEBO, 3). create a simple building geometry model in DesignBuilder, and 4). perform a simulation exercise in DesignBuilder, where the main building components as well as typical occupancy and equipment schedules were provided to the participants.

During the software instruction portion of the workshop, participants followed procedures as demonstrated by the checklist and instructor to create a model. The RMI Building_Model_Checklist was used to remind participants about the minimum steps of the simulation and to make them explicit [8]. The checklist offered the possibility of verification and instils a kind of discipline of higher input performance. The use of the checklist was established for a higher standard of baseline performance.

CASE STUDIES FRAMEWORK

This section describes three different design case studies for NZEBs in which simulation was used to test and measure the ability to achieve informed decision-making for design. Three design workshops were organized early in 2011 in Cairo to design and develop three case studies. One with the architects and engineers of the Egyptian Earth Construction Assoication EECA, one with the students from the Faculty of Fine Arts (FOFA) in Cairo and one with professional architects and engineers from different offices (OPEN). We provided all participants with rudimentary software training and asked for volunteers for more in-depth study of the BPS tools package. The aim was to provide opportunities for all participants to attain basic proficiency in using the software package with the help of a checklist developed to enable them to better understand the complexities of performing simulations. This introduction to BPS is meant to build a common-ground for future investigation of design decision-support by BPS during the design development of the case studies in the workshops.

Most participants participated in a previous introductory workshop on BPS tools in 2010 [9]. Before or parallel to that, all participants were instructed in various analysis techniques, including reading a sun path diagram, analysing thermal comfort, using the Database of Egyptian Building Envelop (DEBE) [10], and using the Weather Tool and Climate Consultant for climate visualization. Weather Tool is a visualisation and analysis program for hourly climate data. It recognises a wide range of international weather file formats as well as allowing users to specify customised data import formats for ASCII files. It also provides a wide range of display options, including both 2D and 3D graphs as well as wind roses and sun-path diagrams. The tool allows generating full psychrometric and bioclimatic analysis, which is a unique mechanism for assessing the relative potential of different passive design systems. Solar radiation analysis can be accurately determined and optimum orientations for specific building design criteria. The tool allows comprehensive pre-design climate/site

analysis. Climate Consultant is a graphic-based computer program that displays climate data in several of ways useful to architects, including temperatures, humidity, wind velocity, sky cover, solar radiation graphics and psychrometric charts for every hour of the year. Climate Consultant 5.0 also plots sun dials and sun shading charts overlaid with the hours when solar heating is needed or when shading is required. The psychrometric chart analysis shows the most appropriate passive design strategies in each climate, while the new wind wheel integrates wind velocity and direction data with concurrent temperatures and humidities and can be animated hourly, daily, or monthly.

RESULTS

The effects of the use of BPS and sensitivity analysis, was evaluated by means of three design case studies using a control trial and extended usability testing for preference and performance indicator. The following paragraphs identify the influence of BPS knowledge on the decision-making attitudes and patterns. Then the results of the scenario questionnaire are reported. Then the improved design through the energy performance comparison of the three case studies using BPS tools is verified. Finally, the outcome of the open-ended questions and workshop discussions together with associated material and observations are presented. An extended paper has been published including detailed analysis results [11].

Satisfaction: Using self-reported metrics, the background knowledge and understanding of NZEBs design and the satisfaction with the use of BPS decision-support were determined.

Knowledge: Evaluating the effectiveness of BPS tools in informing design required an understanding of the participants' pre- and post-simulation knowledge. Respondents completed pre- and post-simulation surveys to assess the value of the BPS tools to further the participants' understanding of NZEBs' design influences and their relation to the use of simulation. In order to assess participants' knowledge about NZEB design issues, participants were asked "How would you assess your ability to design NZEB?" Table 1 shows the paired t-test analysis of pre- and post-responses, showing a statistically significant increase. A significant increase in knowledge uptake was recorded for the three groups. Moreover, the repetition of this increase in all three group samples is strong evidence that the use of BPS increased the knowledge uptake. This indicates participant perception of growth in informative knowledge of the basic tenets of decision-making.

Table 1, Pre- and post-test analysis

ITEM	PRE-TEST MEAN	POST-TEST MEAN	MEAN DIFFERENCE	*T*	*P*	*N*
HOW WOULD YOU ASSESS YOUR ABILITY TO DESIGN NZEB? (EECA)	5.40	7.30	-1.900	-5.01	0.0007	10
HOW WOULD YOU ASSESS YOUR ABILITY TO DESIGN NZEB? (FOFA)	4.00	6.13	-2.130	-8.66	0.0318	23
HOW WOULD YOU ASSESS YOUR ABILITY TO DESIGN NZEB? (OPEN)	3.57	6.68	-3.110	-8.88	0.0001	19

Satisfaction (After-Scenario Questionnaire): The After-Scenario Questionnaire (ASQ) developed by Lewis (1995) was used to measure three fundamental areas of usability: effectiveness (question 1), efficiency (question 2), and satisfaction (all three questions). The results indicate a low level of satisfaction regarding the ease of completing the design using ZEBO and other BPS tools for all groups. Similarly results indicate a low level of satisfaction with the amount of time taken to complete the design using ZEBO and other BPS tools. On the other hand, participants' satisfaction with the information support was reported to be high. Surprisingly, the patterns of answers of the three groups almost match. These findings have unlimited generalizability because the sample size for the factor analysis was relatively large (52 participants). Also the resulting factor structure was very clear.

Figure 1, The After Scenario Questionnaire Results of the EECA, FOFA and OPEN groups respectively

Decision-making attitudes and patterns: Another self-reported usability metric was a post-workshop questionnaire that was administered to participants regarding how far using ZEBO and other BPS tools informed their decision-making and led to higher reliability and robustness of the NZEB design. Participants were asked to fill in an online questionnaire with six questions.

Informed decision-making: Figure 2a and 2b show that participants' questionnaire responses vividly indicate agreement with the statements "guides your decision-making" and "informs your decision-making". With regard to the "guiding" question, Most of Group 1 respondents strongly agreed or agreed while few were undecided. The results of Group 2 and Group 3 were similar. In total, 71.2% of participants recognized the importance of BPS tools in guiding the decision-making of NZEBs design even though 6.0% of all three groups disagreed with the statement. With regard to the "informing" question and as shown in Figure 2b most of participants recognized the importance of BPS tools in informing the decision-making of NZEBs design and none of the questionnaire respondents disagreed with the statement. In Group 1, 2 and 3, almost all respondents strongly agreed or agreed with the statement while few were undecided.

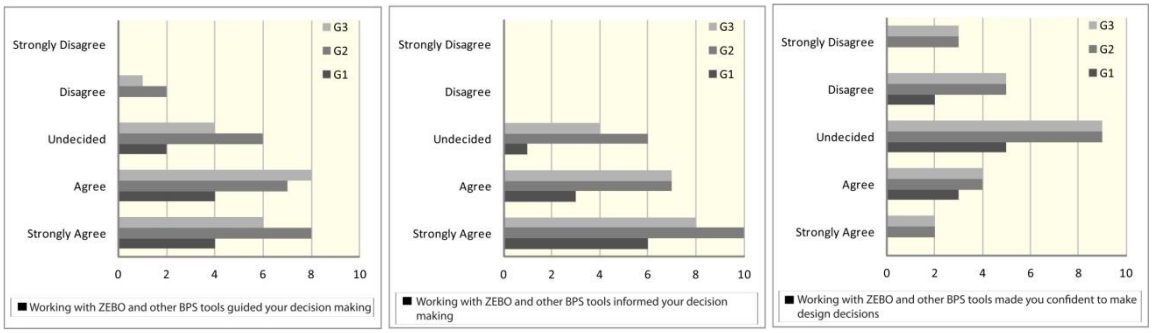

Figure 2, Participants' responses to a question related to guidance of decision making, informed decision making and confidence in decision making

However, as shown in Figure 2c, participants disagreed with the statement "makes you confident about your decision-making". In total one third of participants disagreed that the use of ZEBO and other BPS tools made them confident about their decision-making in NZEBs design while almost half of respondents were undecided. In the open-ended questions and discussion respondents indicated that the simulation process and the results have to be well presented and understood, so that they can gain confidence from the information.

Reliability and robustness of design: Figure 3a shows that participants' questionnaire responses indicate disagreement with the statement "allowed you to achieve the NZEB design target". In total more than half the participants disagreed that the use ZEBO and other BPS tools allowed them to achieve the NZEB design target while one third were undecided

According to Figure 3b, more than two third of participants agreed that the use ZEBO and other BPS tools is essential for NZEB design. More than half participants agreed that the use ZEBO produced reliable and robust NZEB design while one third of respondents were undecided (see Figure 3c). To avoid any ambiguity of the terminology the term reliable and robust was explained before the questionnaire. For most participants having to use ZEBO or DesignBuilder which are graphical user interfaces for EnergyPlus was sufficient to produce reliable and robust NZEB design.

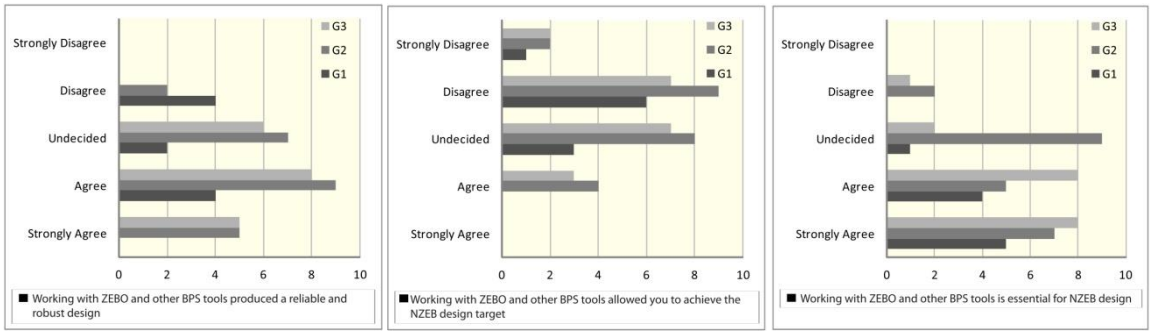

Figure 3, Participants' responses to a question related to the achieving the NZEB, importance of using BPS for NZEB design and BPS tools and the reliability and robustness of NZEB design

Verifying the effect of BPS: The impact of BPS is compared and summarized in Table 1. As shown in Table 1, a significant increase in knowledge uptake was recorded for the three groups. Also the new design incorporated optimised changes which were compatible, acceptable to the designers. Their introduction was a result of sensitivity analysis and parametric variation of the different design parameters listed below:

- The geometry was redesigned to reset the mass correctly with orientation close together.
- The solar protection was redesigned so that it maximizes the shading of openings and envelope.
- The openings ratio and glazing type were significantly improved in the third design round.
- Extra envelope insulation was added so that all envelopes thermal performance improved by at least 50%.
- The PV & ST sizing and architectural integration was optimised in all designs

DISCUSSION AND CONCLUSION

The use of BPS tools and the sensitivity analysis technique in the design of NZEBs demonstrated a strong correlation between increased usage and achieving informed decision-making. The main purpose of using BPS tools was to assess their ability on informing the decision making by using a simple parametric tool (ZEBO) and a detailed comprehensive tool (DesignBuilder). The aim of the study was not to compare those tools or expose participants to a broader composition of tools; rather it was assess the mechanics and process of using BPS tools to inform the decision making. In order to evaluate BPS and sensitivity analysis as a tool for informing decision-making, participants completed several questionnaires assessing their informative effectiveness. The questionnaires reveal participants' perceptions of the simulation's informative importance in their design decision-making. Specifically, the open-ended questions and group discussion addressed the value of and barriers to the use of simulation as a decision-support method. To validate the study findings a formal energy

analysis measure was employed in this respect. A group discussion was also used as an informal triangulation to facilitate the validation of the survey results reported below:

1). There is a relationship between BPS usage and better energy performance outcomes. 2). Parametric Analysis features were found to promote informed decision making. 3). The case studies revealed a significant difference in knowledge levels before & after. 4). NZEB design ambitions should be tempered by the complexity of design and design process.5). A more pre-decision approach is required to meet the uncertainty of decision making of designers. 6). Value of usability testing and other user experience measurements (self-reported metrics) is high as a research methodology. 7). Four factors that promote or inhibit the uptake of BPS as decision support in architectural practice: a) Interactional usability, b) Decision support (informative), c) Users' skills d) Contextual integration.

ACKNOWLEDGEMENTS

This paper is part of a PhD research funded by the Université catholique de Louvain.

REFERENCES

1. Charron, R., Athienitis, A. and Beausoleil-Morrison, I., 2006. A Tools for the design of zero energy solar homes, ASHRAE. Annual meeting, Chicago, vol. 112 (2), pp. 285-295.
2. Hayter, S., Torcellini, P. et al. 2001. The Energy Design Process for Designing and Constructing High-Performance Buildings, Clima 2000/Napoli 2001 World Congress.
3. Riether, G., and Butler,T. 2008. Simulation space. A new design environment for architects. In 26th eCAADe Conference Proceedings. Muylle M., ed., Antwerp, Belgium
4. Weytjens, L., et al. 2010. A comparative study of the 'architect-friendliness' of six building performance simulation tools, Sustainable Buildings CIB 2010, Maastricht, NL.
5. Attia, S., et al 2011. Selection Criteria for Building Performance Simulation Tools: Contrasting Architects and Engineers Needs, Journal of Building Performance Simulation, Taylor & Francis.
6. Bambardekar, S. and Poerschke, U., 2009. The architect as performer of energy simulation in the early design stage. In Proceeding of IBPSA, Glasgow, 1306-1313.
7. RMI, 2011, Rocky Mountain Institute, online at: http://bembook.ibpsa.us/index.php?title=Main_Page [accessed 1 April 2013].
8. Attia, S., 2012, A Tool for Design Decision Making-Zero Energy Residential Buildings in Hot Humid Climates, PhD Thesis, UCL, Diffusion universitaire , CIACO, Louvain La Neuve, ISBN 978-2-87558-059-7.
9. Attia, S., Gratia, E., De Herde, A, Hensen, J. 2012, Simulation-based decision support tool for early stages of zero-energy building design, Energy and Building, Vol. 49, June 2012, Pages 2-15, ISSN 0378-7788, 10.1016/j.enbuild.2012.01.28
10. Attia, S. and Wanas, O. 2012, The Database of Egyptian Building Envelopes (DEBE): A database for building energy simulations, SimBuild, August 2012, Madison, Wisconsin.
11. Attia, S., Gratia, E., De Herde, A, 2013. Achieving informed decision-making for net zero energy buildings design using building performance simulation tools, International Journal of Building Simulation, Tsinghua-Springer Press, Vol 6-1, P 3-21, 10.1007/s12273-013-0105-z.

CONSIDERING UNCERTAINTIES IN MODELLING THE ENERGY PERFORMANCE OF EXISTING NON-DOMESTIC BUILDINGS AT A LARGE SCALE

D. Godoy-Shimizu; P. Armitage

Martin Centre, Department of Architecture, University of Cambridge, 1-5 Scroope Terrace, Cambridge, CB2 1PX

ABSTRACT

In the UK, the non-domestic stock accounts for 19% of national CO_2 emissions. Due to a slow turnover of stock, efforts are required to make energy efficiency improvements to the existing building stock to have a chance of reaching national emissions reduction targets. However, there is still a lack of understanding of the compositions and energy use in this sector, partly due to a lack of good data, though disparate datasets do exist.

This paper details a study carried out on 150 non-domestic buildings in England, to evaluate the potential for sustainable improvements, taking swimming pools as a building type example. Simple external surveys were carried out online, and information gathered in this manner was combined with data from several sources of disaggregated information. The result of this data-gathering is a large database of information on the design, occupancy, system and construction of each of the buildings, along with actual energy use figures for the year 2008/2009. Naturally, the level of certainty for the different variables varies, and some factors have been estimated using proxies. For instance, envelope u-values have been assumed based on the survey, and building age information.

Simplified (monthly, steady-state) modelling was carried out for each building. To take account of the inaccuracy of the data, probability distributions were assigned to most variables, and Monte Carlo analysis was run for each building. Under this approach, the impact of different measures was calculated for each building not as a fixed 'annual emissions' reduction, but as a probability distribution instead. This paper presents the preliminary results of the analysis, at both the individual building scale, and the level of the overall swimming pool stock, and shows the benefits of using probability distributions to define uncertain variables, rather than 'typical' factors.

Keywords: energy performance, existing buildings, probabilistic analysis

INTRODUCTION

The UK non-domestic sector consists of over 2 million buildings [1], and accounts for a fifth of national CO_2 emissions [2]. Given the slow turnover rate, it is likely that over 70% of non-domestic buildings in 2050 already exist [3]. This makes improvements to the existing stock particularly important if the UK is to meet its stringent emissions reduction targets.

To happen efficiently, this requires a comprehensive understanding of both the current state of energy performance and the potential for improvement. Despite this need, there is acknowledged to be a relative lack of freely available, comprehensive data for non-domestic buildings [4] particularly when compared to the residential sector [e.g. 5]. Given the large diversity of form and function this means that, despite many years of research, further work is necessary in order to fully understand the non-domestic stock.

However, large-scale disaggregated sources of data on the non-domestic stock are indeed available, albeit with mixed levels of quality and coverage. Crucially, the introduction of Display Energy Certificates (DECs) in 2008 means that *actual* energy use data for thousands of public non-domestic buildings is collected, and made available, each year.

This paper presents the preliminary findings of an ongoing study into the energy performance of the non-domestic sector. The study considers 149 public swimming pools and leisure centres in England, using data from a number of sources in combination with a simple survey carried out online. Although swimming pools represent far fewer buildings than some non-domestic types, they account for the highest CO_2 emissions per m^2 in UK public buildings [7]. Furthermore, their large, concentrated, steady heat loads and typically public ownership can make them useful in improving local urban areas by acting as anchor loads for heat networks.

METHOD

Data Collection

The motivation for this study was to evaluate the potential for simple desktop studies to assess building performance at a large scale, using the data available without having to carry out detailed site surveys for each building.

Building information was collected from several sources of large-scale disaggregated data. Two of the main sources were the DEC and Active England databases. The DEC database (2008-2009) provides actual metered building energy use data (used to evaluate model outputs), alongside various building characteristics for many building types across the UK. Active Places is a comprehensive database of sporting venues within England, collected by Sport England [8]. Detailed information about the data gathering and processing for this data is available in a previous paper [9]

Due to differing motivations for collecting and publishing each dataset, mixed levels of quality and coverage were found, and some of the buildings were found to have inconsistencies across datasets, so significant processing was necessary on each raw dataset. Following the removal of buildings with unrealistic, conflicting or default data, a combined dataset was created for 149 leisure centres and swimming pools in England.

Surveys of the external characteristics of the building envelopes were also carried out using aerial and street level imagery collected from Bing Maps and Google Maps/Streetview, as well as image web searches.

Figure 1:Desktop external surveys were carried out using e.g. Digimap & Google Streetview.

Table 1 provides a summary of the disaggregated data that has been collected for this study for each swimming pool, grouped together based on the key factors that affect energy

consumption [10]. Where further information was necessary for building modelling, information from a small selection of the pools, or existing or typical data was used. This includes water temperatures (from Swimmers Guide), and 'typical' internal layouts and conditions [11, 12].

Info Type	Variable	Source(s)
Climate	Location (full address)	DECs
Building	Gross Internal Area (m^2)	DECs
	Age (proxy for fabric type, U-values)	Spogo
	Internal Layout (typical layout from Econ 78, assigned based on size/survey)	Econ 78, Spogo, Survey
	Swimming Pools (number and dimensions of pools)	Spogo
	Form (Building shape and footprint (m^2)	Digimap & Survey
	External Walls	Digimap
	Height *	Landmap & Survey
	Envelope Types & Glazing	Survey
	Shading	Survey
Systems	HVAC (HVAC type; Used to estimate system efficiencies)	DECs
	Primary Fuel Type (Used to estimate plant efficiencies, fuel CO_2 intensity)	DECs
	Pool Water Temperature (°C) *	Swimmers Guide
Operation	Opening Times (Typical winter opening timetable (hrs per wk))	Spogo
	Internal Conditions (Typical internal conditions & gains)	NCM
Performance	Annual Fossil-Thermal energy consumption (kWh/m^2)	DECs
	Annual Electrical energy consumption (kWh/m^2)	DECs
	Annual CO_2 emissions (kgCO2/m^2)	DECs

*Table 1: Summary of data gathered modelling (*not yet included in analysis)*

Uncertainty, Modelling and Calibration

Previous work examining the uncertainties in retrofitting the non-domestic stock has been carried out using both dynamic [e.g.13], and steady-state modelling techniques [e.g.14]. The relative advantages & disadvantages of the two approaches have been discussed in detail elsewhere; broadly, due to the ability of dynamic models to simulate a building and its internal environment in a more detailed transient fashion compared with steady-state approaches, they are commonly used for the design and specification of complex buildings. However for the purposes of comparing retrofit options at the macro level, the additional requirements in computation time and input data complexity mean that steady-state approaches may be preferable [7, 8].

For this study, a quasi-steady state energy model has been used. The model is based on an implementation of the EU CEN-ISO 13790 standard [15], specifically the UK SBEM (Simplified Building Energy Model, [16]). In order to account for the influence of swimming pool characteristics on water heat loss, the calculation has been adjusted to include the pool heat loss equations outlined in ASHRAE [17]. This enables the impact of swimming pool specific improvement options to be assessed; for example the addition of pool covers.

Uncertainties in the input data for this analysis can broadly be split into the three categories outlined in Table 1. The first two are fixed parameters that could potentially be found with detailed site surveys, while the last could vary in any given period of operation (two further key sources of uncertainty are model accuracy, but that is not considered here aside from simple model validation, and the climate data):

- Systems (e.g. boiler/chiller efficiencies, lighting power density)
- Building (e.g. fabric U-values [estimated based on age], infiltration)
- Operation (e.g. occupancy density, hours of occupancy)

A Monte Carlo analysis approach has been used, following previous work in understanding sensitivity and uncertainty in building thermal modelling [e.g. 18, 19]; this randomly samples variables determined by a probability density function, evaluating the model many times, producing a range of outputs. For this study this approach has also been used to estimate the impact of improvements to the buildings. This allows a better understanding of the uncertainty within the model, allowing the potential impact of different retrofit measures on a building's CO_2 emissions to be properly considered as a range of possible values, rather than a single definitive point. Furthermore, by evaluating the relationship between the variations in input data, and the different possible outcomes from improvement measures, it may be possible to identify the key drivers and, in turn, better identify the buildings most suitable for different retrofit measures.In this study, we have focused on fossil-thermal (FTh) energy use. The results for two types of building improvement have been presented; both the impact of the measures on an typical building, as well as the aggregated results for the sample. The measures were selected based on previous research [9, 11]; adding a swimming pool cover; and adding a pool cover + improving the heating system efficiency

Finally, it should be noted that at the time of writing this work is still ongoing, including some of the data collection. Consequently, the ranges and probabilities for any uncertain input data have been estimated based on existing studies and previous experience. Therefore, the results presented below should be considered as preliminary, and subject to change.

RESULTS

A total of 149 buildings were studied, which were categorised into swimming pools (25), leisure centres (64), and combined centres (69). Each building was modelled a thousand times with a range of random input variables. Figure 2 shows the comparison of the modelled FTh data for the building types against the actual FTh energy use from the DECs. In each of the cases, there is a strong overlap between the actual and modelled data.

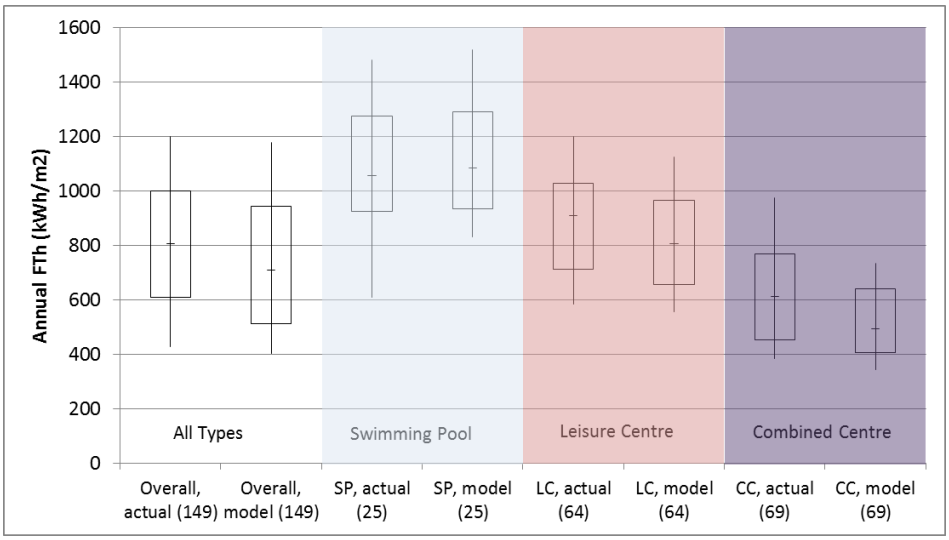

Figure 2: A comparison of actual Fossil-Thermal (FTH) energy use against modelled energy use, showing median, 10th, 25th, 75th and 90th percentiles, split by building type.

At this stage, the difference between the median actual and overall modelled FTh energy consumption is 12%. While ANOVA testing between the types does show that there is a statistical difference between the actual and modelled distributions, it is hoped that further data collection, and calibration of the model against monthly energy data, in the coming months will improve the model fit.

Improvements

The impact of the modelled improvements on the buildings are shown in Figure 3. This shows firstly the energy consumption distributions for the actual, modelled, and improved cases for all of the buildings in the study; secondly it shows the range of percentage reduction in emissions for a single building from the improvements, and for an example pool.

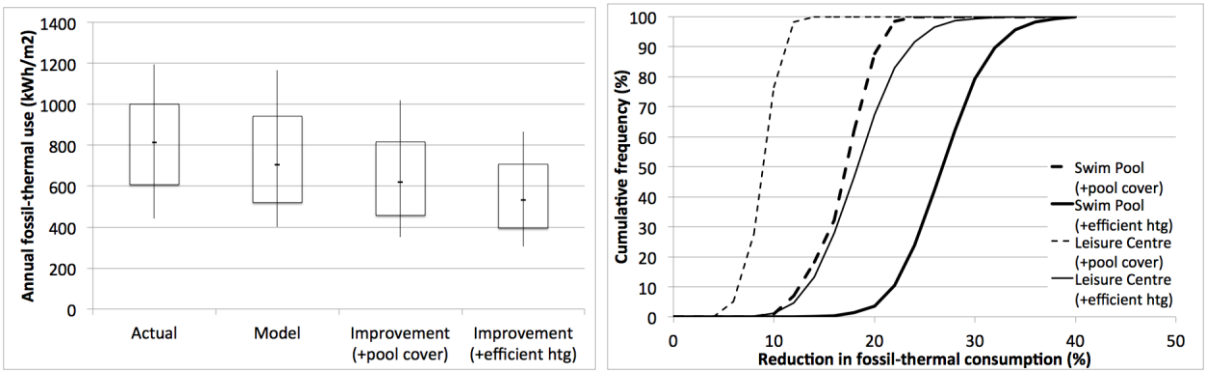

Figure 3: Impact of improvements on FTh consumption across all buildings (left); the range of % reduction in FTh consumption in an example swimming pool and leisure centre (right).

CONCLUSIONS AND FUTURE WORK

The analysis presented here includes the preliminary results from ongoing work that aims to use existing large-scale datasets and simple desktop building energy modelling studies in order to better understand the improvement options for the non-domestic building stock. The work considers uncertainties in building energy modelling, at a multi-building/stock level, using information for swimming pools and leisure centres, brought together from various sources in conjunction with a simple online survey.

The results show that even for individual buildings, the impact of improvement measures can vary significantly. This is in part a reflection of the limitations of carrying out building modelling without a detailed survey, but will also partly be due to factors that are very difficult to identify precisely; such as occupancy behaviour. Evaluating the relationship between input variables and building performance in more detail will be beneficial both for understanding the improvement potential for the wider swimming pool stock, and for prioritising data collection.

Further work will focus on improving the data that this modelling work is based upon, and the probability distributions used to define the building characteristics of the stock.

A similar project is also being undertaken at the stock level, for the EPSRC funded ReVISIONS project, considering retail, office, factory and warehouse sector non-domestic buildings. This incorporates building stock projections over the next 20 years, and allows a greater understanding of the uncertainty in non-domestic stock energy use.

ACKNOWLEDGMENTS

The authors gratefully acknowledge the funding provided by the EPSRC to carry out this research, and to their supervisors (Professor Koen Steemers and Professor Torwong Chenvidyakarn) for support on this paper.

REFERENCES

1. Brown, A.I. et al., 2009. Greening the UK building stock: Historic trends and low carbon futures 1970-2050. Tansactions of the Canadian Society for Mechanical Engineering, 33(1), pp.89–104.
2. Hinnells, M. et al., 2008. Transforming UK Non-Residential Buildings: Achieving a 60% Cut in CO2 Emissions by 2050. In Fifth International Conference on Improving Energy Efficiency in Commercial Buildings (IEECB'08).
3. UKGBC, 2007. Report on carbon reductions in new non-domestic buildings, London: Department of Communities and Local Government.
4. Bruhns, H., 2008. Identifying determinants of energy use in the UK nondomestic stock. In IEECB'08, Improving Energy Efficiency in Commercial Buildings Conference, Building Performance Congress. Frankfurt.
5. CLG, 2012. English Housing Survey (EHS). Available at: http://www.communities.gov.uk/housing/housingresearch/housingsurveys/englishhousingsurvey/ [Accessed May 17, 2012]
6. Godoy-Shimizu, D., Armitage, P., Steemers, K. and Chenvidyakarn, T., 2011, "Using Display Energy Certificates to quantify schools' energy consumption," Building Research & Information, Vol. 39 No. 6, pp. 535–552. doi:10.1080/09613218.2011.628457
7. Sports England, (2012), "Spogo: Active Places", Available at https://spogo.co.uk/developer-area (accessed Oct 2012)
8. Godoy-Shimizu, D., Armitage, P., Steemers, K. and Chenvidyakarn, T., 2013. Using Display Energy Certificates to quantify energy consumption in the UK non-domestic building stock. In: CIBSE Technical Symposium, 8-10 April 2013, Liverpool, UK.
9. Baker, N. & Steemers, K., 2000. Energy and environment in architecture: a technical design guide, Taylor & Francis.
10. BRECSU. (2001), "Energy Consumption Guide 78: Energy use in sports and recreation buildings", Watford.
11. BRE, 2011. National Calculation Methodology (NCM) modelling guide (for buildings other than dwellings in England and Wales). Available at: http://www.ncm.bre.co.uk/filelibrary/NCM_Modelling_Guide_2010_Edition_11Nov2011.pdf [Accessed November 30, 2011].
12. Thor Smith, S., 2009. Modelling thermal loads for a non-domestic building stock. Associating a priori probability with building form and construction - using building control laws and regulations. PhD Thesis. Nottingham University.
13. Heo, Y., 2011. Bayesian Calibration Of Building Energy Models For Energy Retrofit Decision-Making Under Uncertainty. PhD Thesis. Georgia Institute of Technology.
14. ISO:13790, 2008. Thermal performance of buildings - calculation of energy use for space heating and cooling.
15. BRE, 2013. SBEM: Simplified Building Energy Model. Available at: http://www.bre.co.uk/page.jsp?id=706 [Accessed April 30, 2013]
16. ASHRAE, 2011, ASHRAE Handbook – HVAC Applications, Atlanta, Georgia, USA
17. Lomas, K.J. & Eppel, H., 1992. Sensitivity analysis techniques for building thermal simulation programs. Energy and Buildings, 19(1), pp.21–44.

MODELICA-BASED MODELING AND SIMULATION OF AN OFFICE BUILDING WITH GEOTHERMAL HEAT PUMP SYSTEM

Roozbeh Sangi; Rita Streblow; Dirk Müller

Institute for Energy Efficient Buildings and Indoor Climate, E.ON Energy Research Center, RWTH Aachen University, Mathieustr. 10, 52074 Aachen Germany

ABSTRACT

In this study, dynamic modeling and simulation of a building with geothermal heat pump system has been performed. The simulated system is an office building located in Stuttgart and equipped with a heat pump, which is coupled to eleven vertical borehole heat exchangers. The system has been modeled in the object-oriented programing language Modelica. Dymola, which is a multi-domain modeling and simulation tool, has been used as simulation environment. The Modelica Standard Library 3.2 and the Modelica libraries for building simulation developed at the Institute for Energy Efficient Buildings and Indoor Climate, E.ON Energy Research Center, RWTH University have been applied to simulate the hydraulic and thermal behavior of the system. Sub-models for the hydraulic system have been developed and coupled with a model of the building to make a general model for simulating the performance of the whole system. To assess the validity of the model, the simulation results have been validated with the available measurement data. Reasonably good agreement has been obtained between the measurements and predictions.

Keywords: Building modeling and simulation, Dymola, Geothermal heat pump system, Modelica

INTRODUCTION

The amount of energy used for heating and cooling in the building sector is about one third of the total energy consumed in the world. The finiteness of natural energy resources on the one hand, and the ever-increasing demand for energy in the world on the other hand, necessitate the development of systematic approaches for improving the efficiency of building energy systems as well as minimizing the usage of primary energy resources and the damaging impacts and harmful effects on the environment. Dynamic modeling and simulation of heating systems, which are one of the most energy consuming parts of buildings, provides not only a convenient and low-cost tool for evaluating the performance of heating systems, but also makes engineers capable of developing new control and optimization strategies for such systems [1].

A geothermal heat pump, also known as ground source heat pump, is a central heating and cooling system that pumps heat to or from the ground. It uses the earth as a heat source in the winter or a heat sink in the summer. A geothermal heat pump system consists of a conventional heat pump coupled with a ground heat exchanger where water or a water-antifreeze mixture exchanges heat with the ground. This component accounts for a third to a half of the total system cost. Several major design options are available for these, which are classified by fluid and layout. Direct exchange systems circulate refrigerant underground, closed loop systems use a mixture of anti-freeze and water, and open loop systems use natural groundwater. Geothermal heat pump systems are attractive alternatives for both conventional heating and cooling systems because of their higher energy efficiencies. They have recently been applied to many residential and commercial buildings for heating and cooling purposes,

and they offer significant energy use and demand reductions on the power grid. Therefore, they are recognized to be energy efficient heating and cooling systems.

The objective of this research is to evaluate the dynamic performance of buildings with closed loop geothermal heat pump system. Therefore, in this study, a model for an office building and its energy system has been developed and the performance of the system has been simulated. The system has been modelled in the equation-based, object-oriented programing language Modelica. Models written in the Modelica language cannot be executed directly, and a simulation environment is needed to translate a Modelica model into an executable program. In this study, the models have been developed and simulated in the Modelica modeling and simulation environment Dymola version 7.4. To assess the validity of the model, the simulation results have been compared with the available measurement data.

SYSTEM DESCRIPTION

The simulated system is a model of the DS-Plan office building in Stuttgart and its energy systems [2]. The building is a five-floor office building with the total net area of 2500 m², which has been equipped with a reversible heat pump with a heating and cooling capacity of 68 and 52.3 kW, respectively. The heat pump has been coupled to eleven vertical borehole heat exchangers; each has about 100 m length. Six boreholes have the nominal diameter of 40 mm and the diameter of the rest five boreholes is 32 mm. The waste heat of the server room, which is about 6 kW, is also recovered for space heating. Figure 1a provides the façade of the simulated building and figure 1b depicts a schematic illustration of the system.

(a) *(b)*

Figure 1: a) Façade of the building b) Schematic illustration of the system

The building is heated and cooled through concrete core activation and edge strip heating elements. Concrete core activation is the concrete floor slab of a building having integrated water tubes. Through these tubes, heated or cooled water can circulate to heat up or cool down the slab. The heated or cooled slab exchanges heat with the room below and above, controlling the room temperature. It should be mentioned that concrete core activation and floor heating/cooling are not equal. Where in a floor heating/cooling system, the embedded pipes are separated from the building structure by a layer of insulation, with concrete core activation the pipes are embedded in the building structure. Thereby, the whole of the thermal mass of the building, which in modern office buildings is mostly situated in the floor, is

actively heated or cooled [3]. Due to the large thermal inertia of the concrete slab, this is a very slow process, and consequently room temperatures cannot be quickly changed. The edge strip heating provides additional heat for a fast response time. The building has been equipped with a monitoring system to gather local data.

MODELING

The Modelica Standard Library 3.2 and the Modelica libraries for building simulation developed at the Institute for Energy Efficient Buildings and Indoor Climate, E.ON Energy Research Center, RWTH University such as BaseLib, Database, Building and HVAC components libraries have been applied to simulate the hydraulic and thermal behavior of the system. The following paragraphs explain the developed sub-models of the general system in detail.

BUILDING MODEL

The components airload, wall, window, door, thermal and radiation interfaces, and solar radiation and wind speed ports have been used to model the building [4]. The airload model represents a heat capacity consisting of air described by its volume, density and specific heat capacity. The thermal and radiation connectors equate the temperatures and balance the convective and radiative heat flows, respectively. In order to reduce the simulation time, the offices with the same conditions in each floor has been considered in one zone. The floor plan, the zoning and the view of the first floor model in the graphical model editor of Dymola have been shown in Figures 2a, 2b and 2c, respectively.

(a) *(b)* *(c)*

Figure 2: a) Floor plan of the first floor b) Zoning of the first floor in the model c) Graphical user interface of the room model in Dymola

To simulate the internal heat gain, a component entitled HeatLoadFactor has been applied. The heat output of this component depends on the number of office workers and electronic devices in office rooms, which has been defined in a frame of time-dependent scenarios. Heat transfer by air exchange has been taken into account by using a component namely AirExchange. Furthermore, it has been considered that the main door of the building opens every half an hour, which causes a short but high air exchange.

WEATHER MODEL

To simulate the dynamic performance of the system under real climate conditions, the developed model has been coupled with a weather model that is capable of interpreting the weather data and integrating solar radiation, wind velocity, and ambient temperature into the simulation. The weather data of Stuttgart has been provided by the Federal Institute for Research on Building, Urban Affairs and Spatial Development (BBSR) [5].

HYDRAULIC SYSTEM MODEL

The components that have been used to model the hydraulic system are heat pump, expansion tank, pipe, valve and pump. Sensors for measuring temperature and mass flow rate have also been used. The sensors monitor the thermodynamic properties of the fluid passing their ports while they do not influence the fluid. The heat pump component is a table-based model which contains two simple heat exchangers.

GEOTHERMAL HEAT EXCHANGER MODEL

To model the field of borehole heat exchangers, models for the single borehole heat exchanger and the surrounding soil have been implemented and the interaction between these two models have been taken into account [6]. For the borehole heat exchanger an axial discretization has been chosen. The boundaries for this partial model are four fluid connectors for the upwards and downwards flowing streams and one thermal connector for the temperature of the soil at the borehole surface. The predominant heat transfer phenomena are heat conduction in the tube wall and in the concrete filling between soil and tube wall as well as heat convection in the pipe. In order to receive a one-dimensional problem in each element the distribution of heat capacities is assumed to be radial-symmetric. Each component consists of inlet and outlet pipes and concrete borehole fillings between the pipe and outside of the pipe. The surrounding soil is also modelled in a discretized way.

GENERAL MODEL

The hydraulic system model has been coupled with the model of the building in order to make the general model of the system. The thermal connectors that connect the building model to the distribution pipes equate the temperatures and balance the convective heat flows between distributor pipes and rooms. Also the solar radiation interfaces, thermal connections and wind ports of the building model have been connected to the weather model. The view of the general model in Dymola has been illustrated in Figure 3.

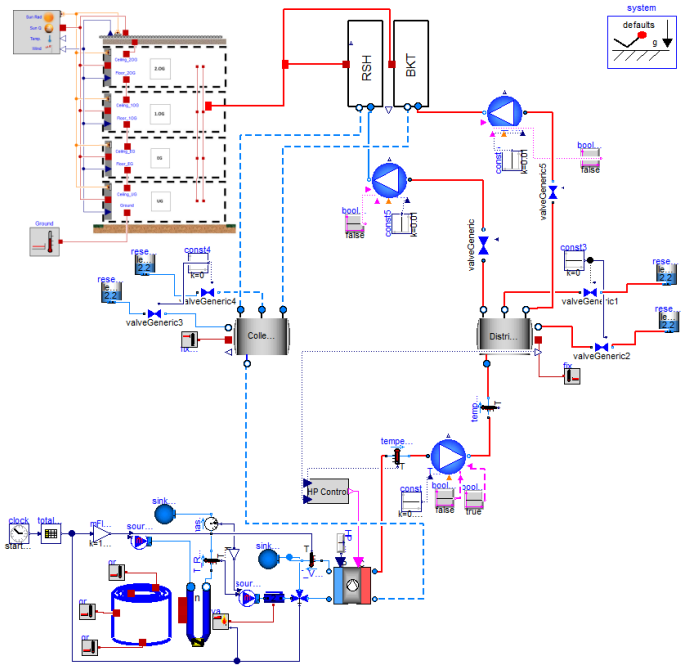

Figure 3: Graphical user interface of the general model in Dymola

RESULTS AND DISCUSSION

In the first stage, the developed model of the building has been validated on its own. The measured forward temperature of heat pump has been used as input for the model of building. The model has been simulated for a two-day heating period. Figure 4 compares the simulated and measured temperature at the outlet of the building. As it can be seen in Figure 4, reasonably good agreement has been obtained between the measurements and predictions. It should be mentioned that the model of geothermal heat exchanger has already been validated in another study [6].

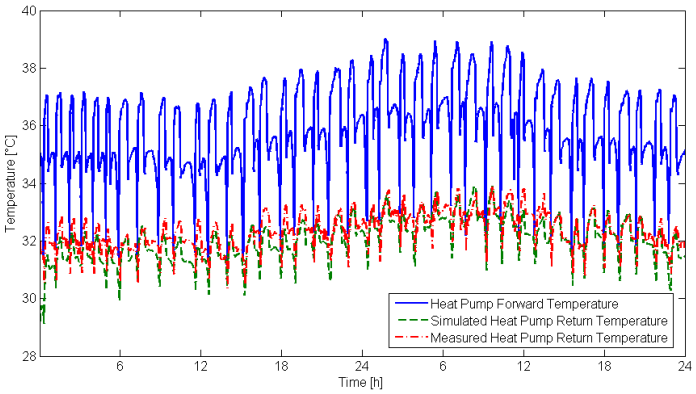

Figure 4: Heat pump forward and return temperatures

In the next step, the coupled model of building and hydraulic system has been simulated. The measured mass flow rate and inlet temperature of the borehole heat exchanger have been applied as inputs to the model. Fig. 5 illustrates the air temperature in zone 1a of each floor. It is evident from Figure 5 that top floor has the lowest temperature, which is caused by higher amount of heat loss from this floor to ambient in comparison with the other floors.

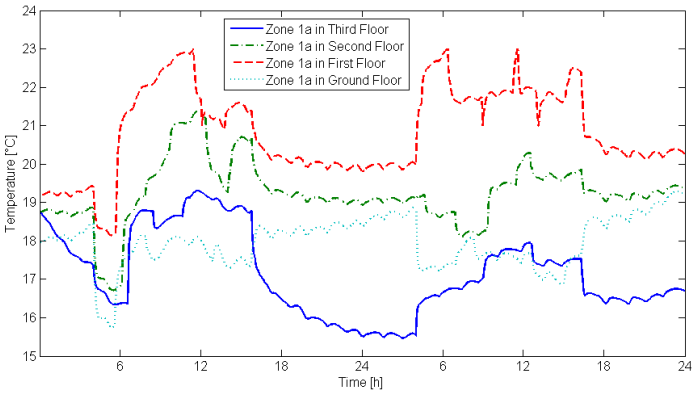

Figure 5: Air temperature in zone 1a of each floor

The predicted outlet temperature of the borehole heat exchanger has been compared with the measured data in Figure 6. The simulation results show a good correspondence with the measured data.

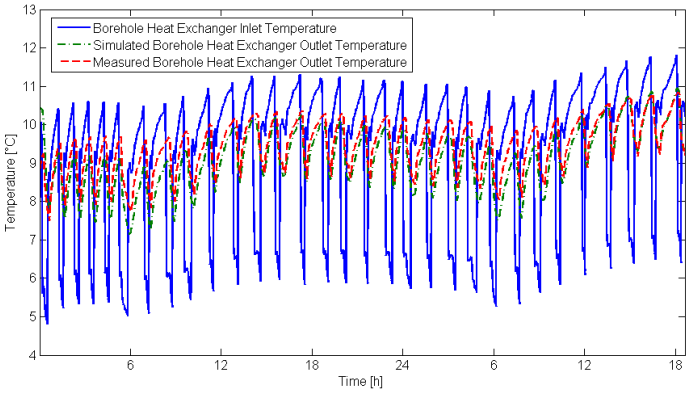

Figure 6: Borehole heat exchanger inlet and outlet temperatures

CONCLUSION

In this paper, the performance of a building with geothermal heat pump system was evaluated. The system was modeled in the object-oriented programing language Modelica. Sub-models for the hydraulic system were developed and coupled with a model of the building to make a general model for simulating the performance of the whole system. The developed model was simulated for a two-day heating period. To assess the validity of the model, the simulation predictions were validated with the available measurement data. The simulation results demonstrate the reliability and accuracy of the model. Developing a room temperature control system for the model can be the subject of the future research.

ACKNOWLEDGEMENTS

Grateful acknowledgement is made for financial support by BMWi (German Federal Ministry of Economics and Technology), promotional reference 0327466A.

REFERENCES

1. Sangi, R., Streblow, R., Müller, D. : Modelica-based modeling and exergy analysis of a central heating system. *3rd International Exergy, Life Cycle Assessment, and Sustainability Workshop & Symposium (ELCAS3)*, July 2013, Nisyros, Greece.
2. http://www.ds-plan.com/german/DS-Plan.htm
3. Sourbron, M.: Dynamic thermal behaviour of buildings with concrete core activation. PhD thesis, Katholieke Universiteit Leuven, Heverlee, Belgium, September 2012
4. Schummers, J., Kempkes, S., Zimmermann C. : Zonierung und Simulation eines Bürogebäudes: Entwicklung eines vereinfachten Gebäudemodells in MODELICA. Project thesis, Institute for Energy Efficient Buildings and Indoor Climate, E.ON Energy Research Center, RWTH Aachen University, Aachen, Germany, November 2011.
5. http://www.bbsr.bund.de
6. Comanns, T. : Modellierung und Simulation eines LowEx-Gebäudes in der objektorientierten Programmiersprache Modelica. Diploma thesis, Institute for Energy Efficient Buildings and Indoor Climate, E.ON Energy Research Center, RWTH Aachen University, Aachen, Germany, December 2011.
7. http://lowexmonitor.ise.fraunhofer.de/demonstrationsgebaeude/uwp_ds

SCENARIO ANALYSIS FOR THE ROBUSTNESS ASSESSMENT OF BUILDING DESIGN ALTERNATIVES – A DUTCH CASE STUDY

C.Struck [1]; J.L.M. Hensen[2]

1: Centre for Integrated Building Technology, Lucerne University of Applied Sciences and Arts, School of Engineering and Architecture
2: *Department of the Built Environment, Eindhoven University of Technology (TU/e), Eindhoven, The Netherlands*

ABSTRACT

This paper discusses the use of exploratory scenarios with environmental conditions on a case study in the Dutch context. The goal is thereby to assess the robustness of design alternatives during the lifetime of its building components. During building design it is common practice to use "normative" scenarios to prove compliance with design standards. The use of "exploratory" scenarios is less common. However, it is hypothized that the use of exploratory scenarios is a meaningful alternative, if no information is available on the uncertainty of input data such as climate and building use. This paper focusses particularly on the performance variability due to climate change.
The European Commission targets a 20% reduction of CO_2 emissions, a 20% increase of energy efficiency and a 20% increase in the use of renewable energy by 2020 still providing comfortable conditions within the buildings. As neither, building use nor environmental conditions are constants, it is necessary to quantify their influence on the energy use over the lifetime of its building components and subsequently on achieving the overall aim.
For the designer it is impossible to assess the contribution of his/her individual building project on achieving the goals posed by the European Commission. However, considering the performance of the building and its components under potential future conditions, conditions deviating from the design conditions, has the potential to support design by supporting the selection of design alternatives, provide comfortable conditions and reduce energy demand during building operation.
To integrate building use and environmental conditions into the computational performance assessment, their stochastic character needs to be taken into account, which is rarely possible due to limited availability of data. Still, in the absence of stochastic input data the use of exploratory scenarios represents a feasible alternative to map the variability of building use and environmental conditions. The paper concludes that exploratory scenarios present a feasible alternative to assess the future performance of potential design alternatives. Its application on the case study allows to identify the most robust out of three design alternatives by considering the performance indicators energy use and thermal comfort.

Keywords: design support, robustness assessment, performance simulation, climate change, occupancy pattern, future building performance

INTRODUCTION

The assessment of the future performance variability of design alternatives is an important aspect to consider during the design process. The goal is thereby to inform the client and design team about the design alternatives capacity to maintain comfortable conditions throughout the lifetime of the system components but also about its capacity to maintain the balance between energy supply (local generation) and demand as designed.

To integrate building use and environmental conditions into the computational performance assessment, their stochastic character needs to be taken into account. However this information is rarely readily available. In the absence of input data describing the stochastic behaviour the use scenarios represents a feasible alternative to map the variability of building use and environmental conditions onto its performance. It is common practice to use "normative" scenarios as input in building performance studies aiming to prove compliance with building regulations. The use of

"exploratory" scenarios is less common. Exploratory scenarios start with past and present trends, leading to a likely or unlikely future. Following Berkhout and Hertin [1] they are based on four assumptions. (1) The future is not a continuation of the past relationships and dynamics but is always shaped by human choice and action; (2) The future cannot be foreseen; however exploration of the future can inform the decisions of the present; (3) There is not only one possible future, uncertainty calls for a variety of futures mapping a "possibility space"; (4) The development of scenarios involves both relational analysis and subjective judgment.

Mietzner and Reger [2] identify two distinct disadvantages of using scenarios: (a) the necessity to collect expert knowledge and judgment to define comprehensive scenarios, as well as (b) the risk of diverting to wishful thinking, considering the most likely, best- and worst-case scenarios, only. Still, the use of scenarios also has four advantages: (i) potential to consider events with low probability but strong impact; (ii) the possibility of considering different futures side by side; (iii) the potential to recognize "weak signals" for discontinuities and disruptive events; (iiii) they function as vehicle to improve strategic communication about performance. The use of scenarios in building design practice is limited to normative scenarios. However, the robustness assessment of the future performance of design alternatives requires the provision of exploratory scenarios.

METHOD

To investigate the feasibility to use exploratory scenarios for providing design support the authors conducted a simulation study with a number of scenarios representing the projected climate change in the Netherlands across three temporal horizons now, over 15 years and in 30 years. To conduct the study a case study was defined, weather data sets generated and a robustness assessment in between three design alternatives undertaken.

Simulation study

The simulated case study considers one intermediate floor based on the layout of the office tower 'La tour' in Apeldoorn, The Netherlands. For the robustness assessment the performance of three conditioning concepts are investigated; top-cooling, floor cooling and the application of 4-pipe fan coil units. As climate change leads in the Netherlands to warmer and dryer summers, the investigation is limited to the period of April to September [3, 4].

The three concepts are sized to maintain an equal quality of the thermal comfort. The criterion used is zero hours above the adaptive temperature limit (ATL) of 80% for the reference year De Bilt 64/65. The cooling capacity is limited to maintain the target criteria. The concepts are then exposed to reference data sets derived from projected climate data. For the estimation of the uncertainty of the annual cooling, four data sets were used, representing the four change scenarios for the Netherlands W, W+, G and G+. For calculating the uncertainty in the number of hours above the ATL of 80%, 12 data sets were used; the three files 1%, 2% and 5% for each of the four change scenarios.

The *adaptive temperature limits* (ATL) differentiate building types into alpha and beta buildings. The differentiation is based on the degree of influence individuals can practice on their environment. Three performance bands of different quality, which are not to be exceeded, are defined. The central band, class B, indicates an acceptance of 80% of the building occupants over the use period of the building. The innerband, class A, represents the most stringent requirement and indicates a high quality thermal environment with an acceptance of 90% of the building occupants. The outer band, class C, is the most relaxed, only representing an acceptance of 65% of the occupants. Class C is not to be applied to new buildings. Exception can be granted e.g. to historic buildings to limit the technical and financial effort for refurbishments.

The performance bands are defined by the operative temperature and a derivative of the external air temperature; the four-days running mean outdoor temperature (RMOT). The RMOT is calculated from weighted daily means of the current and the three previous days (ISSO, 2004).

Performance indicators

The case study targeted considers the performance indicators the annual cooling demand and the number of hours above the adaptive temperature limit of 80% are applied.

The adaptive temperature limits differentiate building types into alpha and beta buildings. The differentiation is based on the degree of influence individuals can practice on their environment. Three performance bands of different quality, which are not to be exceeded, are defined for both building types. The central band, class B, indicates an acceptance of 80% of the building occupants over the use period of the building. The inner band, class A, represents the most stringent requirement and indicates a high quality thermal environment with an acceptance of 90% of the building occupants. The outer band, class C, is the most relaxed, only representing an acceptance of 65% of the occupants. Class C is not to be applied to new buildings. Exception can be granted e.g. to historic buildings to limit the technical and financial effort for refurbishments.

Future Climate data sets

Data sets generated based on historic weather data are unlikely to satisfactorily describe the external future climate conditions because they cannot account for global warming or cooling and heat island effect to be experienced in the future. To represent climate change in data sets for performance simulation, Guan [5] differentiates four methods: (1) Statistical extrapolation (Degree-day method); (2) Use of global climate models. (3) Imposed offset method; and (4) Application of stochastic weather models.

Of those four methods, the latter two are extensively used in research on building simulation and performance predictions the application of stochastic weather models by e.g., Wilde and Tian [6] and Kershaw [7] and the imposed offset method by e.g., Belcher et al. [8] Crawley [9], Degelman [10], Guan et al. [11]. As there is no information available yet to derive stochastic weather projections for the Netherlands the authors make use of scenarios for the robustness assessment.

Dutch climate change scenarios

The Intergovernmental Panel on Climate Change (IPCC) has formulated a common set of climate change scenarios based on assumptions about the likely future development of energy demand, emissions of greenhouse gases, land use change and future behavior of the climate system. The scenarios are based on results of Global Circulation Models (GCM). GCMs are numerical models for the simulation of physical processes in the atmosphere, ocean, cryosphere and land surface. The models describe the climate using a three dimensional grid with a typical horizontal resolution of 250-600km. Nested regional circulation models (RCM) are used to down-scale the climate change scenarios. Based on input of GCMs and RCMs, the Royal Dutch Meteorological Institute (KNMI) defined four likely climate change scenarios based on two observed phenomena: the global temperature increase and the change in airflow pattern over Western Europe. With respect to the temperature increase, the KNMI distinguishes between a global temperature rise of 1°C and 2°C for the period 1990 till 2050. With respect to air flow pattern, the temperature increase scenarios are associated with more westerly winds during winter and more easterly winds during summer, see Table 1.

Scenario	Global temperature increase in 2050	Change in atmospheric circulation
G	+1oC	Weak
G+	+1oC	Strong
W	+2oC	Weak
W+	+2oC	Strong

Table 1: Parameters values to identify climate change scenarios [12]

With the current knowledge it is not possible to indicate which of the four scenarios is most likely. All four are plausible and are therefore regarded with equal probability for performance simulations.

KNMI'06 Climate scenario data transformation

The KNMI website [13] provides the possibility to transform historic datasets for temperature and precipitation into projected future data sets for a specific location and temporal horizon. The transformation is based on three steps, taking into account the different changes in extremes and mean values over a given period.

Step1: Based on daily means of the standardized historic period the tool calculates the median 10th and 90th percentile for each month of the historic data set.

Step2: The tool determines the deviation of the future climate scenario for the specific time horizon from the historic dataset. The deviation is hardcoded for the horizons 2050 and 2100. Linear interpolation is used for other horizons.

Step3: The historic data series are transformed using the established deviation.

The difference between the projected daily mean air temperature and measured historic daily mean air temperatures was added to each hour of the corresponding day. By repeating the procedure, 20 projected data sets were created for the use with simulation tools. The work was accomplished in close cooperation between VABI BV and the TU/e.

Future projected and reference data sets for the Netherlands

The historic data sets were projected 30 years into the future, 2006 – 2035, using the most extreme KNMI climate change scenario, W+. The 30- year time horizon was chosen as this period corresponds to the expected lifetime of HVAC equipment. Using the projected data four artificial reference data sets were generated by selecting the corresponding months as defined in the NEN 5060. The four artificial reference data sets, one for energy and three for thermal comfort assessment, represent the 30-year projected reference period 1986 - 2005.

Design concepts

The presented simulation study only considered the summer period. That is why heating installation is not represented. The consideration of the system performance and its control in winter and mid-season is not considered.

Top cooling concept is a widely used conditioning concept in the Netherlands. Air is conditioned centrally and distributed over the floors to the rooms. The top-cooling capacity is used to lower the supply air temperature. It does not control the humidity. The supply air temperature is 18°C. However the supply air temperature linearly increases if the external air temperature rises above 28°C. The system maintains a maximum temperature difference between supply air and external air temperature of 10K. The system is expected to be critical with respect to climate change.

The second conditioning concept is *floor-cooling*. The system makes use of pipework installed within the top layer of flooring. Conditioned water is pumped through the pipes to temperate the floor as heat exchanger. The system is modelled to continuously maintain a water temperature of 17°C for cooling and 35°C for heating. Fresh air is provided centrally but unconditioned at the minimum flow rate.

The last conditioning concept considered is the traditional local air-conditioning via 4-pipe fan coils. The fan coil uses convection to via preconditioned air to heat ad cool the space. Different to a 2-pipe the 4-pipe fan coil has different set of supply and return pipes for heating and cooling. The supply water temperature for cooling is 6°C. Fresh air is provided centrally but unconditioned at the minimum flow rate.

RESULTS

Cooling demand

The results in Figure 1 and Figure 2 indicate that for top-cooling an uncertainty band exists which is twice as wide as that for the 4p-fancoil and floor-cooling concepts for the 30 years projection. Whilst it gives the smallest energy demand for the three concepts at 0 years, its mean gives the highest demand over 30 years with an increase of the factor 1.3. The floor cooling and 4p-fancoil concepts initially show a higher cooling demand than the top-cooling concept. However, for the 15 years of projected data the mean for top cooling shows the highest cooling energy demand of the three. The 30 year projections indicate the lowest energy demand for the 4p-fancoil units, followed by the floor cooling concept. Top-cooling gives the highest demand.

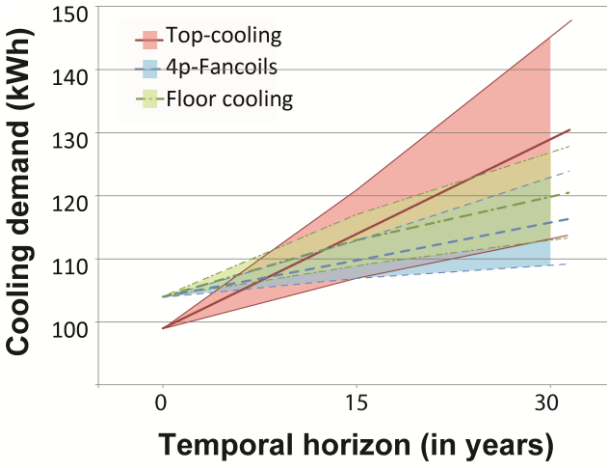

Figure 1: Uncertainty band ($\mu \pm 1\sigma$) of annual cooling demand for two temporal horizons, 15 and 30 years.

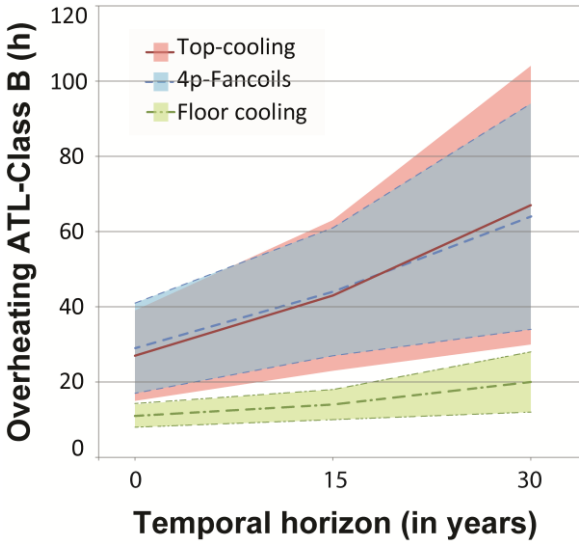

Figure 2: Uncertainty band ($\mu \pm 1\sigma$) of number of hours above ATL80% for two temporal horizons, 15 and 30 years.

Adaptive temperature limit 80%

The number of hours above the adaptive temperature limit of 80% shows a different ranking. The least number of hours are indicated by the floor cooling concept with a moderate maximal σ of 8h over 30 years. The uncertainty for the 4p-fancoils and top cooling are 4 and 4.5 times higher, respectively. The uncertainty band for floor cooling does not overlap with the bands for top-cooling and 4p-fancoils.

DISCUSSION

The concepts considered are floor cooling, top-cooling and 4p-fancoils. It was found that the reference data sets from the projected 15 and 30 years provide a good basis for a relative robustness assessment. From the concept comparison it can be concluded that the floor cooling concept provides the most stable and favourable condition with the least uncertainty within the office space during the considered summer period. This information has a high potential to inform the design process and subsequently reduce the impact of the climate on the energy use of the building. Although both diagrams show increasing trends it is not unfeasible that the opposite trend occurs if one takes use pattern and their impact on internal gains into account. The current trend towards lower specific office equipment could potentially offset the impact of the warming climate.

CONCLUSIONS & FUTURE WORK

Scenarios are commonly used in buildings design. It is common practice to use “normative” scenarios to prove compliance with design standards. The use of “exploratory” scenarios is less common. However, exploratory scenarios are required as input to assess the potential future performance of design alternatives as no information is available to quantify their likelihood of occurrence. In cooperation with VABI BV future climate data sets were generated. The data sets

were developed for different temporal horizons. The robustness assessment of three design alternatives shows that the floor cooling alternative performs most favourable compared with the two alternatives top-cooling and 4p-fancoils.

FUTURE WORK

Little is known about the severity of the response of specific performance metrics to the climate data used. Clarke [14] characterized residential buildings using the parameters: capacity, capacity location, window size, infiltration rate and insulation level to categorize typical constructions. Still, the work excludes HVAC system parameters that define the response of integrated building systems to climate variations. Hensen [15] highlighted problems associated with artificial reference data sets. He states that weather parameters, such as temperature, solar radiation and wind, are not necessarily correlated. When selecting days or months to compile an artificial reference data set, the specific applied parameter weights might not correspond to the sensitivities of the building under study. Hensen refers to different building types to illustrate the problem. A building with a high window to wall ratio – type: solar collector - might react most sensitively to variations in solar radiation, whilst a building with no windows - type: repository - is expected to be most sensitive to changes in temperature. As artificial reference data sets are typically purpose bound, e.g. annual energy demand and overheating risk assessment, they need to be carefully chosen for the specific type of performance study and "ideally" also for the type of building at hand.

REFERENCES

1. Berkhout, F. and J. Hertin, *Foresight Futures scenarios - developing and applying a participative strategic planning tool*. Greener Management International, 2003(37): p. 37-52.
2. Mietzner, D. and G. Reger, *Advantages and disadvantages of scenario approaches for strategic foresight.* Int. J. Technology Intelligence and Planning, 2005. **1**(2): p. 220–239.
3. Verkerk-Evers, J., et al., *Klimatiseringsconcepten voor de toekomst*, in *TVVL Magazine*2010, TVVL. p. 22-26.
4. Verkerk-Evers, J., et al., *Robuustheid voor Klimaatvariaties - Een Vergelijking van Klimatiseringsconcepten Met Behulp van Gebouwsimulatie*, in *Bouwfysica*2009. p. 2-7.
5. Guan, L., *Preparation of future weather data to study the impact of climate change on buildings.* Building and Environment, 2009. **44**(4): p. 793-800.
6. Tian, W. and P. de Wilde, *Uncertainty and sensitivity analysis of building performance using probabilistic climate projections: A UK case study.* Automation in Construction, 2011. **20**(8): p. 1096-1109
7. Kershaw, T., M. Eames, and D. Coley, *Assessing the risk of climate change for buildings: A comparison between multi-year and probabilistic reference year simulations.* Building and Environment, 2011. **46**(6): p. 1303-1308.
8. Belcher, S.E., J.N. Hacker, and D.S. Powell, *Constructing design weather data for future climates.* Building Service Engineering, 2005. **26**(1): p. 49-61.
9. Crawley, D. *Creating weather files for climate change and urbanization impacts analysis*. in *Building Simulation*. 2007.
10. Degelman, L.O., *Which came first – building cooling loads or global warming? – a cause and effect examination.* Building Services Engineering Research and Technology, 2002. **23**(4): p. 259-267.
11. Guan, L., J. Yang, and J.M. Bell, *A method of preparing future hourly weather data for the study of the impact of global warming on built environment*, in *QUT Research Week*, A.C. Sidwell, Editor 2005: Brisbane, Australia. p. 11.
12. Hurk, B.v.d., et al., *KNMI Climate Change Scenarios 2006 for the Netherlands*, 2006, Koninklijk Nederlands Meteorologisch Instituut (KNMI): De Bilt. p. 82.
13. KNMI, *KNMI'06 Climate scenario data transformator*, 2011, Koninklijk Nederlands Meteorologisch Instituut: De Bilt.
14. Clarke, J.A., *Energy simulation in building design*. 2nd ed2001, Oxford, UK: Butterworth-Heinemann. 362.
15. Hensen, J.L.M. *Simulation of building energy and indoor environmental quality - some weather data issues*. in *Int. Workshop on Climate data and their applications in engineering,*. 1999. Czech Hydrometeorological Institute in Prague.

PERFORMANCE ASSESSMENT OF HEAT DISTRIBUTION SYSTEMS FOR SENSIBLE HEAT STORAGE IN BUILDING THERMAL MASS

Henryk Wolisz, Ana Constantin, Rita Streblow, Dirk Müller

RWTH Aachen University, E.ON Energy Research Center, Institute for Energy Efficient Buildings and Indoor Climate, Mathieustr. 10, 52074 Aachen, Deutschland

ABSTRACT

With the growing share of renewable non-dispatchable energy generation the challenge of matching electricity production and consumption arises. To facilitate balancing excess renewable electricity generation (i.e. at times of strong wind) the potential for thermal energy storage in buildings is analyzed within our project. As of today pricing schemes for electricity in Germany and most other countries are either not time dependent at all, or a lower price for electricity is only provide at night. Considering the rising share of renewable electricity generation it is expected that dynamic electricity prices, driven by the actual availability and demand, will be introduced in the future creating demand for more storage capacities.

The focus of this analysis is the evaluation of energy storage in buildings thermal mass, comparing a conventional radiator heating with concrete core activation (CCA) as heat distribution system. Therefore within an accurately monitored room at our research center a field study was performed and the results were compared to simulation outcomes of a thermal model for the same room. Since the behavior of the simulation model proves to be close to the thermal behavior of the real room, the model is then used to simulate a scenario for activation of the buildings thermal mass according to a signal describing the availability of renewables.

For both systems a three hour overheating phase allowed to postpone further heating demand in winter by more than eight hours. The radiator based system lead to a room temperature increase of 3.1 K compared to only 0.2 K for the CCA. Thus, due to potential thermal discomfort the radiator based system would require either the limitation of permitted indoor temperature or a more complex control with occupancy monitoring / prediction. Furthermore, it is shown for the CCA system, that integration of an exemplary signal indicating high availability of renewable energies (RE) would have doubled the consumption of RE during our field test time, without compromising thermal comfort.

Keywords: demand side management, dynamic simulation, thermal storage, heating systems

INTRODUCTION

With the growing share of renewable non-dispatchable energy generation the challenge of matching electricity production and consumption arises. Thereby, residential and commercial buildings, accounting for up to 30 % of Germany's end energy consumption, could potentially provide flexibility to balance fluctuating electricity supply. Therefore, within the Dual Demand Side Management (2DSM) approach a concept is developed to manage the total energy demand (i.e. electrical and thermal) on city district level in a holistic way.

To facilitate balancing excess renewable electricity generation (i.e. at times of strong wind or high photovoltaic (PV) generation) the potential for thermal energy storage in buildings is analyzed within 2DSM. Thus, intending to use renewably generated electricity for heating purposes (i.e. through heat pumps (HP)) whenever it is abundantly available. Instead of prevalent hot water tank storage technologies this analysis focuses on the inherent thermal storage capacity of a building attributable thermal capacity of the used construction materials.

As of today pricing schemes for electricity in Germany and most other countries are either not time dependent at all, or a lower price for electricity is only provide at night [1], when lower room temperatures are preferred by residents anyway [2]. Fossil fuel powered heating systems have the same cost of operation at any time, therefore the effects of time dependent room heating were not subject of close analysis in the past. Nevertheless, the lower electricity prices at night were already used in the past to pre-cool non-residential buildings, thus lowering the electrical load throughout the day [3, 4]. Considering the rising share of renewable electricity generation it is expected that dynamic electricity prices, driven by the actual availability and demand, will be introduced in the future creating demand for more storage capacities.

However, the commonly used radiator based heat distribution systems seem not to be the optimal heat delivery method for thermal storage purposes. This can be accounted to the partially air based heat transfer between the radiator and the thermal mass as well as to infiltration and ventilation processes cooling the air down before it can reach the thermal mass. Hence, due to the direct heat transfer within the thermal mass e.g. floor heating or concrete core activation seem to be favorable heat distribution systems.

The focus of this analysis is the evaluation of energy storage in buildings thermal mass, comparing a conventional radiator heating with concrete core activation (CCA) as heat distribution system. Therefore within an accurately monitored room at our research center a field study was performed and the results were compared to simulation outcomes for a thermal model of the same room. Furthermore, the impact of thermal storage based demand side management (DSM) upon the integration of RE is shown through the integration of an binary "availability of renewables" signal into the simulation. In the next section the method is presented in detail, explaining the properties of the observed room, the implementation of the field study aw well as the modeling and simulation approach. Afterwards the obtained field test and simulation results are presented, compared and discussed.

METHOD

Measurement setup

The measurements are performed in an office within the E.ON Energy Research Center of RWTH Aachen University in Germany over one winter week in 2013. The building conforms to the requirements of the German energy directive 2009 [5]. The room is a corner office with a floor area of 41 m², two external walls (north-east and south-west orientation) and with a total window area of 24 m². In order to reduce the influence of solar radiation the external blinds were drawn throughout the experiment. The room was unoccupied.

The office room is conditioned using concrete core activation (CCA) within the ceiling, which is supplied by a HP. As the considered office is a reference room in the building, it is equipped with additional monitoring equipment, measuring the supply and return temperatures as well as the volume flow in the CCA. Additionally six tripods with air temperature sensors at four different heights were set up in the room, according to the ISO 7726 standard [6]. Also the ceiling surface temperature was measured at three positions. An electrical radiator with a maximum power of 2.0 kW was used to represent a conventional radiator based heating system for comparison with the CCA. The total electrical consumption of the set-up consisting of radiator and measuring equipment was constantly measured. Weather data (outdoor air temperature, wind speed, global and diffuse solar radiation) is available from our own weather station, situated on the roof of the nearby experimental hall.

At winter conditions (ambient temperatures in range of 3° C) the test room was repeatedly overheated for approx. 3 hours with the maximum power of either the CCA or the radiator system. Afterwards the cool down period was monitored till indoor temperature reached 0.5 K below the start values, with particular focus on the resulting postponement in heating demand.

Simulation setup

Two simulation setups are created: one for comparing the simulation with measurement data, and a second for simulating a scenario with intelligent activation of the thermal mass according to an "availability of renewables" signal.

The simulation model is build using the modelling language Modelica under the simulation environment Dymola by using components from our Modelica libraries [7]. Each wall, window and door is individually modelled and an additional thermal mass representing furniture is integrated. The air volume is modelled as one node. For the CCA a physical model is used, with the pipes inserted between the concrete layers. The electrical radiator is an ideal heat source with both convective and radiative heat transfer.

In order to compare the simulation with the measurement data, the relevant measurements (weather data, supply temperature and volume flow of the concrete core activation) were used as an input for the simulation and the response of the simulated system was compared against the real system, focusing mainly on the measured free flowing air temperature in the room.

Implication for the integration of renewable energies through DSM

Based on real energy generation data for the winter of 2012 collected from the European Energy Exchange AG (EEX) [8] an exemplary binary reference signal for availability of renewable energies (RE) is generated for a period equal to our field test (ten days). The electricity generation from renewables for the considered period was analysed and for all generation values among the top 20 % (approx. > 9.5 GW) the signal is set to one, while for all other values the signal remains zero. This results in a total of six intervals were the signal has a value of one, with a cumulated duration of 35 h over ten days. Thus, the availability of renewables is indicated for approx. 15 % of total field test time. This signal is then integrated into the performed simulation, where each time the signal turns to one a three hour overheating phase begins. The resulting DSM impact upon integration of RE is then analysed.

RESULTS

Measurement

The gathered temperature values from all sensors are aggregated to an average temperature value for the room temperature. Also, based on three sensors, an average surface temperature of the ceiling is calculated to monitor the status of heat stored into the concrete.

Out of several heating and cooling sequences performed with CCA as well as with the electric radiator, two measurement series were chosen due to their strong similarity of boundary conditions. For a clearer comparison, average values for the indoor and ambient temperatures are calculated over the time frame of overheating and cool down to the initial room temperature. Table 1 shows main characteristics of the analysed measurement series.

Measurement series (compare figure 1)	**CCA**	**Radiator**
start temperatures room/ ceiling	22.1 °C / 24.1 °C	22.2 °C / 23.9 °C
overheating time / energy input	3 h / 6.5 kWh	3⅓ h / 6.2 kWh
overheating temperatures indoor / ambient → resulting ΔT between indoor and ambient	22.2 °C / 2.5 °C 19.7 K	23.7 °C / 3.6 °C 20.1 K
maximum room temperatures reached → ΔT between start and maximum temperature	22.3 °C 0.2 K	25.3 °C 3.1 K
time until room temperatures return to start value	6 h	7.5 h
time until room reaches 0.5 K below start value	12 h	11.5 h

Table 1: Main characteristics of two series within the thermal storage field study

To allow for a comparison of these overheating processes the average heating demand of the observed room is calculated. Based on the actual heat delivery of the existing supply system a normalized heating demand is calculated for an indoor / ambient ΔT of 20 K. Thus, for the CCA approx. 910 W and for the electric radiator 650 W are needed. The difference between these values is explained by the fact that the CCA also delivers energy to the room above. Table 2 summarises the heating demand for the two measurement series compared above.

	CCA	**Radiator**
normalized heating demand	910 W	650 W
actual heating power during overheating	2190 W	1930 W
energy demand regular operation/with overheating	5.5 kWh / 6.5 kWh	4.9 kWh / 6.2 kWh
consumption overhead due to overheating	18 %	27 %

Table 2: Heating demand and energy balances for the analysed supply systems

Simulation

The first simulation is used for comparison with the measurement data in order to assess the suitability of using the simulation to produce realistic results when testing other scenarios.

Figure 1 shows the comparison between the simulation and measurement results for the room air temperature during a five day phase of the field study. The increase in the air temperature on the first day is due to overheating with CCA. The following four peaks are results of overheating with the radiator. At a first glance we recognise that the simulation follows a similar trend to the measurements and an overall similar temperature level.

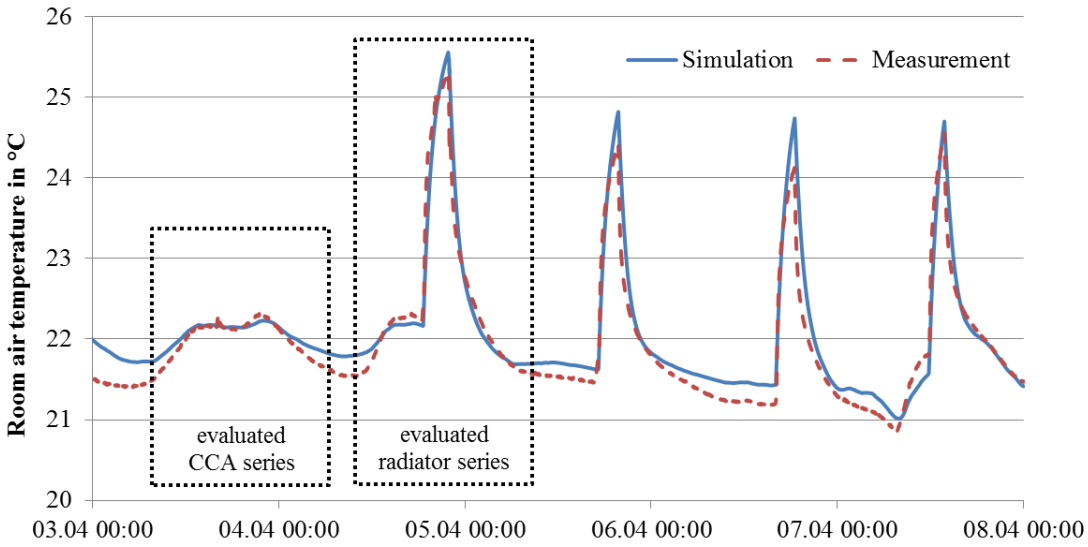

Figure 1: Comparison between simulation and measurement for the room air temperature

The simulation of the field test phase was repeated integrating the signal on availability of renewables. In the regular operating mode the CCA delivered 13 % of the total heating energy demand when the signal was one. In signal controlled operation, however, the CCA was able to incorporate 27 % of total heating demand into the renewable phases, thus approx. doubling the consumption of electricity available from renewable generation. In both cases the room temperature was kept between 21° C and 22° C.

DISCUSSION

Measurement shows that through energy storage in the thermal mass a considerable shift in thermal energy demand is possible for both tested heating systems. However, the temperature profiles and the storage behaviour vary distinctly between the CCA and the radiator based heating.

While the overheating phase causes only a room temperature increase by 0.2 K for the CCA system, the radiator setup induces 3.1 K temperature increase, thus heating the room to possibly inconvenient 25.3° C. However, this increase of room temperature enables thermal storage in all wall surfaces and other thermal masses (e.g. furniture), while the CCA mainly uses the capacity of the activated wall. This results in a many thermal masses just loaded in the surface layers for the radiator system, yielding an exponential temperature decrease in the cool down phase. For the CCA, however, the single thermal mass which is loaded up to the deeper layers leads to a linear temperature decrease.

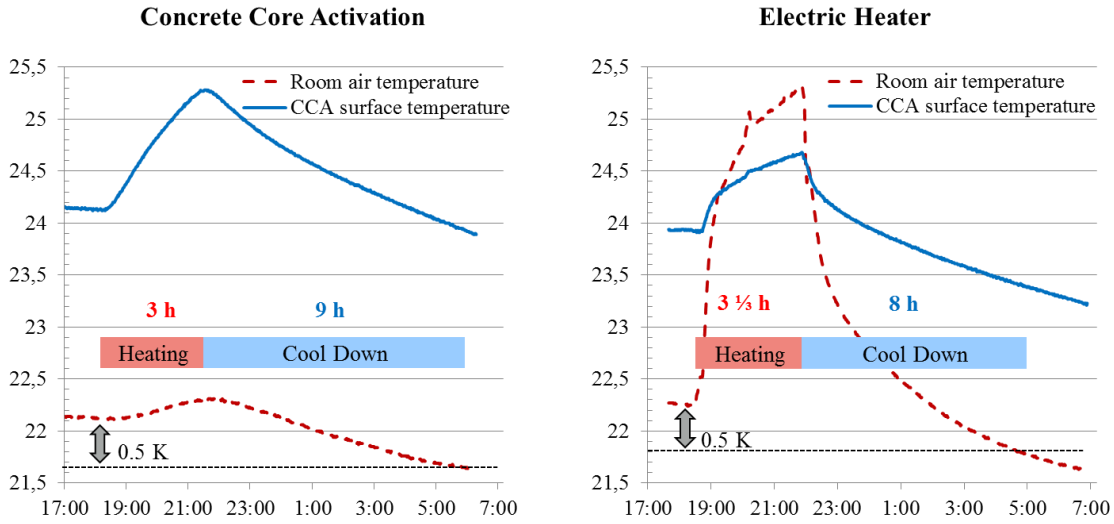

Figure 2: Comparison of measured overheating and cool down phases

It can be seen that both storage approaches allow more than eight hours without heating demand, if temperatures of 0.5 K below the start value are allowed. However, since the radiator system can interfere with thermal comfort expectations it would be preferable to schedule overheating phases at times without occupancy. Both systems have an increased energy demand due to overheating. However, the CCA system mainly loses energy to rooms adjacent to the activated ceiling while the radiator system loses heat to the ambient due to an increase temperature delta to the ambient. This results in 18 % higher energy demand for the CCA and 27 % higher energy demand for the radiator setup due to overheating (table 2).

The comparison between measurement and performed simulation shows a coefficient of determination of 0.94 with an absolute mean difference of 0.18 K and a standard deviation of 0.03 K. Since our goal is to test the similarity in the room reaction between simulation and measurements and not to exactly reproduce a set of measurements. We thus consider the model adequate.

The exemplary signal for availability of renewables was integrated in into our field test scenario. During regular operation the energy consumption from renewables corresponded to their relative availability (15 % of total time). When using the signal the CCA system was able to double the consumption of available RE. Considering that this increase in integration of RE is reached without violating strict comfort constraints, the theoretical potential is even larger.

CONCLUSION

For a state of the art thermally well isolated office within a building according to the German energy directive 2009 the potential for demand side management through heat storage within the buildings thermal mass was successfully shown. The thermal storage activation was performed with a CCA as well as with a radiator based supply system within a field test in winter time. For both systems a three hour overheating phase allowed to postpone further heating demand in winter by more than eight hours. The radiator system lead to a room temperature increase of 3.1 K compared to only 0.2 K for the CCA. Thus, due to potential thermal discomfort the radiator based system would require either the limitation of indoor temperature or a more complex control with occupancy monitoring / prediction. Furthermore, the radiator system had indeed a significant heating demand increase due to higher losses to the ambient. The CCA system, however, has a very low impact upon indoor temperature. Therefore heat loses to the ambient do not increase and even today's electricity pricing schemes could potentially be exploited, since overheating phases at night time are acceptable.

Thus, for thermal storage in building wall mass CCA or other heat delivery systems within the building structures seem favorable, especially since they are also suitable for cooling and pre-cooling of the thermal mass. Nevertheless, radiator systems which are by far more common and will still be the typical heating system for many years to come are also suitable for thermal storage. Still, the usage of radiator systems must be thoroughly planned to take higher energy demand into account and ensure comfortable indoor climate. Furthermore, it is shown that integration of an exemplary signal indicating high availability of RE would have doubled the consumption of RE during our field test phase, without compromising thermal comfort.

This analysis indicates considerable potential for thermal energy storage in building mass as well as the suitability of our simulative approach to investigate this process. Building on these results, analysis will be extended for further building structures and DSM algorithms based on thermal storage in building mass will be developed for different supply systems.

ACKNOWLEDGEMENTS

Grateful acknowledgement is made for the financial support by E.ON gGmbH.

REFERENCES

1. STAWAG, (2013). "Preisblatt - StromSTA Öko für Wärmepumpe". Available: online. http://www.stawag.de/. [accessed: 30.01.2013]
2. Peeters, L. (2009). "Thermal comfort in residential buildings: comfort values and scales for building energy simulation". Applied Energy, 86 (5), pp. 772-780.
3. Artmann, N. (2007). "Climatic potential for passive cooling of buildings by night-time ventilation in Europe". Applied Energy. 84 (2), pp. 187-201.
4. Kolokotroni, M. (1998). "Summer cooling with night ventilation for office buildings in moderate climates". Energy and Buildings, 27 (3), pp. 231-237.
5. Shettler-Köhler, H. (2009). "Energieeinsparverordnung 2009". Berlin: Beuth Verlag.
6. DIN, Deutsches Institut für Normung e.V. (2001). "DIN EN ISO 7726 Ergonomics of the thermal environment – Instruments for measuring physical quantities". Berlin: Beuth Verlag.
7. Müller, D., Hosseini Badakhshani, A. (2010). „Gekoppelte Gebäude- und Anlagesimulation mit Modelica". BauSim Conference, Vienna, Austria.
8. European Energy Exchange AG (2013). "EEX transparency platform". Available: online. http://www.transparency.eex.com/en/. [accessed:13.01.2013]

PREDICTING IMPROVED MICRO CLIMATE WITH REFLECTIVE ROOFS AND ITS IMPACT ON COOLING LOADS OF A TYPICAL COMMERCIAL BUILDING IN BENGALURU, INDIA

D E V S Kiran Kumar, MinniSastry

Centre for Research on Sustainable Building Science, The Energy and Resources Institute (TERI) Southern Regional Centre, Bengaluru, India; e-mail d.kumar@teri.res.in

There were several studies carried out in the recent past proving the existence of heat islands in many of the developing Asian cities. The temperature rise in urban areas influence the peak air conditioning energy consumption during hot days and thus increase the electricity demand of the entire city. Most of the cities in India face deficit in energy supply as the gap between demand and supply go up by almost 15 to 20% during summers. Local bodies should actively involve for implementing cool roofs for all new buildings in order to reduce the city electricity demand and to have a control on frequent power cuts.

The paper highlights a new methodology for the evaluation of urban environment and the impact of improved micro climate at building level cooling load demand. The study involves both experimental as well as simulation studies. Experimental part highlights the air temperature monitoring at city centre as well as city outskirts, along with the thermal performance of the reflective coatings. ENVI-met tool was used for modelling two urban locations in the city. Measured locations have been modelled in ENVI-met to predict the air temperatures. There is a good correlation (R^2= 0.96) found between measured and simulated data. Output data of these simulations is used to develop weather file format that is compatible for VisDOE.

A Box type building model for commercial office space has been developed for hourly energy simulation in Vis DOE. The updated weather files generated using the ENVImet output has been used for these simulations. This paper discusses the potential of cooling load reduction that is possible due to improved micro climates with the reflective roofs. It is observed that about 1.5^{0}C reduction in daily maximum temperature possible with improved micro climate due to reflective roofs. Also the study shows that there is almost 16.8% potential of peak load reduction possible due to the impact of reflective roofs.

Keywords: Heat Islands, Improved micro climate, reflective roofs, cooling load reduction

INTRODUCTION

Increase in population and consequent urbanisation leads to upsurge in urban built-up density. Buildings constructed with materials that absorb heat and emit back into atmosphere cause rise in temperatures. Due to higher built-up density at the core of an urban area and less open area and vegetation, it results in higher temperature than the surrounding suburban/ rural area and this phenomenon is known as Urban Heat Island (UHI) effect. The adverse effects of UHI include increase thermal discomfort (both indoor and outdoor) of people and thus results in higher energy consumption in air conditioned buildings.

The UHI issue is very prominent in many of the developing tropical cities of Asia where the ambient air temperatures and solar radiation intensities are normally high. Studies carried out

in the tropical cities of Asia like Tokyo, Hongkong, Singapore, Colombo, New Delhi, Pune and Chennai have confirmed the existence of heat island due to the rapid growth of these cities [1], [2], [3], [4], [5], [6], [7]. It is estimated that 3 to 8 % higher electricity demand in cities with populations greater than 1, 00,000 is used to confront the heat due to heat island effect [8]. Most of the cities in India face deficit in energy supply as the gap between demand and supply go up by 15-20% during summers. Although the issues of UHI are well documented in India, a very few mitigation measures have been implemented yet.

Implementation of Urban Heat Island (UHI) mitigation measures for various urban surfaces will reduce the ambient air temperatures. Energy savings in air conditioned buildings will possible due to improved micro climate around the buildings. ECO III- Cool Roof is one of the prevalent projects that are carried out in India addressing this issue. Simulations studies carried out as part of the project in Hyderabad [9] estimated maximum temperature reduction up to 2.5°C due to cool roofs. The study also highlighted that about 16% savings in annual cooling demand possible with the use high albedo paints over the buildings. The studies carried by Abkari & Konopacki[10] show upto 18-19% total energy savings are possible because of the improved micro climate due to high albedo roofs. These studies imply a sense to encourage passive cooling techniques and improve indoor conditions when the microclimate around the building is improved. With this background, the energy saving potential using cool roofs in context of the city of Bengaluru has been studied and presented in this paper.

METHODOLOGY

The study involves field experiments and use of simulation software to predict Urban Heat Island (UHI) in built environments, impact of mitigation measures to reduce UHI and its impact on reduction of building cooling demand has been established.

In the first phase, field experiments were carried out in Bengalurue to quantify urban heat island in the city. Field experiments were also carried out in locations where, UHI mitigation design measures were adopted. Thermohygro data loggers were used to monitor air temperature and relative humidity. Thermal infrared gun was used to take instantaneous surface temperature readings. The second activity was to use ENVImet software tool that can analyse urban microclimates. The software tool was validated for its results with the measured data from field experiments. The calibrated models were later used to carry out parametric simulations to study the impact of UHI mitigation measures on urban microclimate. Output data of these simulations was used to develop weather file format that is compatible for building simulation tools.

Finally, hourly energy simulation tool, VisDOE , was used to quantify the impact of UHI mitigation measures at building level and predict reduction in cooling demand of typical commercial building in Bengaluru. In this activity, using the ENVImet output for reflective roof modified Bengaluru weather file was used in VisDOE. Figure1 summarises the methodology adopted in the research project.

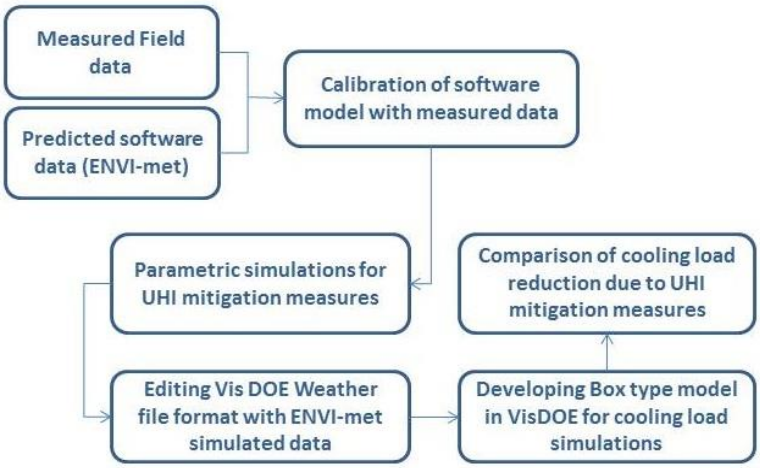

Fig. 1 Methodology followed to assess the impact of UHI mitigation strategies

EXPERIMENTAL STUDIES

Field studies were carried out for air temperature monitoring at one hour interval at Commercial Street (dense city centre) and Kodathi (sub urban area) for about one week during February. Higher air temperatures are recorded in case of Commercial Street when compared with Kodathi. Maximum of 5.3 degC observed between the two sites during the night. The difference in daily mean air temperature during the measured period (table 1) varies between 0.8 and 2 degC, where the commercial street remains at higher temperatures on all the days. Night temperatures at Commercial Street increase significantly as a result of the heat absorbed by the buildings during the day time. Kodathi gets cooled down drastically due to lesser built up and more vegetation. This, along with monitoring results at other locations confirms and proves the existence of heat island at the centre of the city where dense development and less vegetation is present.

Following to these studies, hourly measurements are carried out for reflective roofs at TERI Southern regional centre (TERI SRC). Surface temperatures (over and under the deck) are taken instantaneously at 1 hour interval during the daytime. It is observed that the under deck surface temperature for un coated and mass RCC roof remains constant at 29°C throughout the day. However, it got reduced from 29°C to 26°C after white coat is applied over it. It is very clearly noticed that difference in the average under deck and over deck surface temperature is 2.8degC and 16 degC for RCC mass roof with white coating, and conventional RCC roof respectively. Thus s significant reduction in heat flux is observed in case of coated RCC mass roof compared with the uncoated RCC roof.

Table 1 Daily mean air temperatures recorded at Commercial street and Kodathi

		Day1	Day2	Day3	Day4	Day5	Day6	Day7
Mean Air Temperature	**Kodathi**	24.8	23.5	23.6	24.5	24.8	23.8	23.3
	Commercial St.	25.6	24.7	25.1	26	26.3	25.6	25.3
	Difference	0.8	1.2	1.5	1.5	1.5	1.8	2

SIMULATION STUDIES

It is essential to compare the measurements with existing urban micro climatic models in order to carryout various parametric simulations. The ENVI-met tool which is used in this study is basically a three dimensional non- hydrostatic micro climate model for urban built environments. The tool helps to understand various UHI mitigation strategies and their levels of impact on the surroundings.

The hourly output data during the simulation period was compared with the measured data. Though the simulated data was found lower than the measured, a good correlation (R^2= 0.96 for Kodathi, R^2= 0.89 for Commercial street) was found. Thus the validity of ENVImet was confirmed to carry out the work. Simulation results of ENVI-met provide minimum, maximum and average temperatures possible in the studied area. When, ENVI-met predictions for Commercial Street are compared with the field monitored data, minimum temperatures were found similar with an average difference of +0.6°C. As the difference between the measured and simulated model is minimal, the software model is hence calibrated and used for further analysis.

The calibrated ENVI-met model for Commercial Street is used to carryout parametric simulations, where the roof type and its thermal properties are modified. High reflective roof is considered for all the buildings in the area of extent considered for ENVI-met model. Output data of these simulations was used to develop weather file format that is compatible for building simulation tools. Table 2 shows the thermal properties considered for these simulations. It is observed that there is 1.5^{0}C reduction in peak air temperatures possible with reflective roof when compared to the existing case. Figure 2 shows hourly air temperatures observed in ENVI-met for reflective roof in comparison with the existing (base case) scenario.

Table2. Input parameters considered for parametric simulations

Parameter	**High reflective roof case**
Heat Transmittance (U-Value) of roof	3.74W/m^{2}K
Reflectance of roof	0.9
Reflectance of wall	0.8
Simulation time	18.02.2012 & 06:00:00
Simulation interval and duration	1hr & 24hrs
Wind speed & Direction	3 m/s & SW
Ambient Temperature	17.9°C
Relative Humidity	85.8%
Indoor Building Temperature	19.9°C

Studies are carried out to observe cooling load patterns for a typical commercial building in commercial street area with the improved micro climate using VisDOE, a widely used and accepted commercial building energy analysis program. Providing a new weather data for modified micro climate was the most important in this task. Predicted ambient air temperatures from ENVI-met for reflective case is replaced in the weather file format (TMY2) that is currently available for Bengaluru. Thus, the modified weather data is converted in to the format that is readable for VisDOE tool. Table 3 shows the input data that is considered for the VisDOE simulations. Simulation results show that about 16.9% of peak cooling load reduction is possible in case of reflective roof.

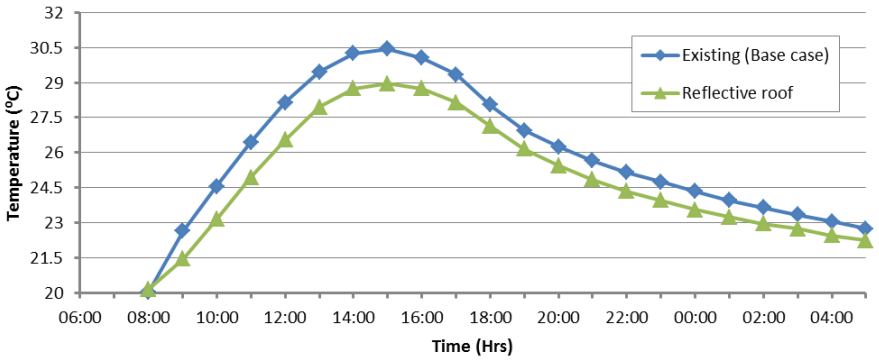

Figure2. Hourly air temperatures observed in ENVI-met for reflective roofs in comparison with the existing (basecase) scenario

Table 3. Input data considered for VisDOE simulations

Parameter	**Base Case**	**Reflective Roof**
Building Type	Commercial Office	Commercial Office
Zone Area	40000ft^2	40000Sft^2
Height	10ft	10 ft
Lighting power density	1.4 W /ft^2	1.4 W /ft^2
Equipment power density	0.75 W /ft^2	0.75 W /ft^2
Occupants	275 ft^2 / person	275 ft^2 / person
Occupancy Schedule	8 hours, 5 days a week	8 hours, 5 days a week
External wall	Uninsulated 230mm Brick Wall	Uninsulated 230mm Brick Wall
External Roof	Uninsulated 150mm RCC Roof	Uninsulated 150mm RCC Roof with reflective coat (albedo 0.9)
Glazing Specification	6mm clear glass	6mm clear glass

It is observed from the hourly load profile that the load reduction is possible throughout the day and it is maximum at 3PM when maximum temperature is recorded. Similar observations were made during the experimental studies where the reduction in heat flux was maximum in case of reflective white roof. Thus, it is clearly understood the impact of heat island mitigation options in reducing the cooling demand of air conditioned buildings.

CONCLUSIONS

Presence of heat island is thus clearly evident from the profile of the mean air temperature where, Commercial Street at centre of city with high development is 1.5degC higher than Kodathi which is located in the outskirts of Bangalore. The heat flux reduction incase of reflective white roofs on reduction of heat islands is also understood. It is observed that there is 1.5°C reduction in peak air temperatures possible with reflective roof when compared existing building scenario. It is clearly noted that about 16.9% of peak cooling load reduction is possible in case of reflective roof. It is thus understood the combined impact of improved micro climate and high albedo roofs. These studies encourage improvement of micro climate as a passive strategy to reduce the building loads and hence the methodology presented in this paper may be adopted to predict the same.

ACKNOWLEDGEMENTS

The research work presented in this paper was carried out with the grant of 13th round RRC by South Asian Network of Economic Research Institutes (SANEI), Bangladesh.

REFERENCES

1. CP TSO; A Survey of urban heat island studies in two tropical cities, Atmoshperc Environment, Vol 30, pp 507-519,1996
2. L Manawadu and NiroshaLiyanage ; Identifying surface temperature pattern of the city of Colombo,Engineer, Vol41 No.05, pp133-140, 2008
3. R Giridharan, S Ganesan and S S Y La ; study on nocturnal heat island effect in urban residential developments of hongkong- to achieve energy saving,Record No. 843-CIB 2004
4. P Pandey, D Kumar, A Prakash, K Kumar and V K Jain; A study of the summertime urban heat island over Delhi, International journal of sustainability science and studies, Vol1 No.1, pp27-34, 2009
5. B Padmanabhamurthy; Microclimates in Tropical Urban Complexes, Energy and Buildings,15-16, pp 83-92, 1990
6. Vrishali Deosthali; Impact of rapid urban growth on heat and moisture islands in Pune city, India, Atmospheric Environment, Vol34 pp 2745-2754, 1990
7. M D Devdas and Lily Rose; Urban Factors and Intensity of Heat Island in the city of Chennai, Proc. Of the seventh international conference on urban climate, 29 Jun-3Jul 2009, Yokohama, Japan 2009
8. A technical brief on ‘Green in Practice 103- cool communities’ by Portland cement association, 2012
9. Vishal Garg; Energy Savings by cool roofs- A case study of two buildings in Hyderabad, Centre for IT in Building Science, IIIT Hyderabad, 2007
10. Akbari, H., S. Konopacki and M. Pomerantz; Cooling energy savings potential of reflective roofs for residential and commercial buildings in the United States, Energy, vol 24, pp391–407, 1999

THE INFLUENCE OF FIELD ASSESSMENT ON THE ACOUSTIC PERFORMANCE OF DOUBLE-SKIN FACADES

Aireen Batungbakal[1]; Kyle Konis[1]; David Gerber[1]; Elizabeth Valmont[2]

1: University of Southern California School of Architecture, Watt Hall, Suite 204, Los Angeles, CA 90089 USA 1

2: ARUP, 12777 W. Jefferson Boulevard, Los Angeles, CA 90066 USA 2

ABSTRACT

This study assesses and validates the influence of measuring noise levels in the urban environment, site parameters, and glass façade components in responsively reducing sound transmission to the indoor environment. Among the most reported issues affecting workspaces, increased awareness to minimize noise led designers to reconsider the design of building envelopes and its site environment. Outdoor sound conditions, such as traffic noise, challenge building designers to accurately estimate the capability of glass façades in acquiring an appropriate indoor sound quality. Indicating the density of the urban environment, field-tests acquired existing sound levels in areas of high employment and traffic activity, establishing a baseline for sound levels common in urban areas. In this study, the city of Los Angeles is used to assess existing soundscapes common in urban areas. Field-measurements for sound transmission loss can establish a baseline performance in a context for sound levels common in urban areas. INSUL is a sound insulation software utilized as an informative tool correlating glass façade parameters with outdoor sound levels based on ISO 717 to predict indoor sound levels. Composed from the sound transmission loss of glass facades simulated through INSUL, results are utilized as an informative tool correlating glass façade components to respond to outdoor sound levels of a project site, achieving desired indoor sound levels based on occupancy. Field-measured sites in Los Angeles indicate the density and activity of the area and responds to the need in emphasizing the influence of site parameters in order to respond sound transmission from outdoor sound sources. This study also progresses to link the disconnection in validating the acoustic performance of building facades early in a project's design, from conditioned settings, such as field-testing and simulations, to project completion. Results from the study supports that acoustic comfort is not limited to a singular solution, but multiple design options responsive to its environment.

Keywords: acoustic, urban noise, sound transmission loss, indoor environmental quality, double-skin facade, design support

INTRODUCTION

Globally, urbanization continues to evolve, contributing to social, economic, and environmental issues, such as climate change, informal growth, energy consumption, congested infrastructure, and environmental pollution. Increased density makes zoning, site selection and planning impossible to avoid environmental noise. City planning and zoning regulations can no longer serve as the first response to informal growth. It is an unpredictable and uncontrolled force. Increased traffic congestion due to increased urban density results in noise pollution, a form of environmental pollution not as highly focused on like air pollution and water pollution. Noise pollution is one form of pollution resulting from urbanization. As the dynamics in the urban environments creates its own soundscape, designing a façade assembly to respond to urban noise is a challenge. Reported as one of the most common

issues of indoor environmental quality (IEQ) affecting workspaces, the unpredictable nature of environmental noise led designers to reconsider the design of the building envelopes in regard to its role in contributing to acoustic quality through the transmission of outdoor sound (Acoustics CEU 2009). In contrast to the available design guidance for other environmental aspects of the building façade, the influence of acoustics contributing to workspace comfort is not fully understood until after project completion. To determine and understand the acoustic performance for glass facades during the design phase remains a challenge for most projects, and is an area where designers have limited intuition to guide decision-making. With increased awareness of acoustic quality and its influence on occupant comfort, improved acoustic design guidance for building facades is needed to aid designers in making informed decisions for envelope design and material selection appropriate to the acoustic environment of the project site. While advances in design tools and facade performance criteria primarily focus on day lighting, thermal performance, and ventilation, acoustic design is often not the highest priority. The impact of acoustic performance in affecting workspace comfort is underestimated and confronted in every design project (Paradis 2012). Due to urban density, urban noise, and increasing levels of urbanization, designing towards acoustic comfort is an increasing design challenge. As urban environments vary, façade design solutions for one setting may not be applicable to, or effective in another. Each design project and each façade elevation requires sensitive consideration and response to site parameters and façade components.

METHOD

Applying field-tests enables building designers to identify its soundscape and façade components necessary to reduce sound transmission. The objective of this research is to provide acoustic design guidance to assist architects in designing glazed facades in areas where significant control of outdoor sound is needed. The approach is aimed at acoustic design support during early stages of design decision-making and voluntary implementation of building site and façade parameters. Methods included field-measurements using a hand-held sound meter device, Decibel 10th, and sound transmission simulations using INSUL, a sound insulation prediction software (INSUL 2011). As an iPhone application, Decibel 10th is utilized as a sound meter that measures sound pressure levels between 0dB and 110dB (Decibel 10th). Within the given timeframe, it identifies peak sound levels and maximum sound levels. Decibel 10th is not classified as Class I equipment; however, the iPhone application is used as a relative measurement tool and a diagnostic tool to compare the relative difference between measurements. Utilization of Decibel 10th encourages voluntary use and data collection of existing urban conditions. Sound data was organized to compile indoor conditions and outdoor conditions for an overall comparison. Comparing the indoor condition to its actual outdoor condition was also documented to determine the acoustic performance of each condition's building enclosure. Implementing field-measurements, INSUL simulations in compliance with ISO 717 standards, analytical simulations were obtained to provide realistic levels of traffic noise. While encouraging data collection of current urban conditions, this study identifies indoor sound levels to derive from sound transmission loss from the building façade. Graphs for each simulation, classified by glass type and thickness, display outdoor sound levels, amount of transmission loss, and resulting indoor sound levels below 5000 Hertz. Since the medium for field-test sound conditions were single-glazed facades, single-glazed facades were simulated to determine the acoustic performance a façade with a single glazing. In this study, single-skin facades are composed of an insulated glazing unit, IGU. For double-skin facades, graphs were also classified by glass type and glass thickness, along with air-cavity depth. Simulated single-glazed facades and single-skin facades of three glass types were classified into three graphs: (1)monolithic glass, (2)PVB laminated glass, and (3)TSC

laminated glass. With each graph focusing on a glass type, it displays the indoor sound levels for industry-standard glass thickness. Glass thickness is indicated by its shade of color, the darkest shade corresponds to the largest dimension and lightens as the dimension decreases. Double-skin facades followed the same format as sealed single-glazed facades and sealed single-skin facades.

Field-testing

Field-testing is performed to measure and establish baseline outdoor acoustic information, and to examine the efficacy of conventional curtain wall assemblies in reducing sound transmission. Measurements were taken at six existing sites in Los Angeles of office and study workspace occupancies (Table 1).

Condition	***Exterior***	***Interior***	***Area***	*Outdoor 4:00*	*Indoor*
1	Downtown LA Bunker Hill	Central	Business	60-100dB	49-67dB
2	Downtown	Office	Business	42-87dB	45-76dB
3	LAX Arrival	Arrival	Transit	65-90dB	57-75dB
4	LAX Depart DDeparture	Departure	Transit	68-84dB	57-82dB

Table 1: Field-test site conditions.

Figure 1: Map of employment density and congested traffic intersections indicating sound levels in Los Angeles

Sites were selected from mapping high employment density and midday vehicular traffic, indicating a concentration of activities that are common noise conditions in an urban environment (Fig. 1). Noise conditions at sites included vehicular traffic and aircraft noise. Indicating traffic congestion as red line segments, mapped street traffic was attained from Google Maps' interactive traffic feature. Each site was recorded and documented within closely related conditions. In measuring and recording indoor sound levels, an iPhone, utilized as a sound meter using the Decibel 10th application, was situated no more than 3 meters from glazed facades. In efforts to respond to sound levels affecting the workspace environment, all field tests were conducted on weekdays between 12:00–15:00, during active business hours. To compile a range of sound levels and reduce isolated test conditions, outdoor and indoor sound conditions were measured and recorded within a 4-minute timeframe (Fig. 2-3).

Figure 2: Field-tested outdoor sound levels of condition 1, Bunker Hill & LA Central Library

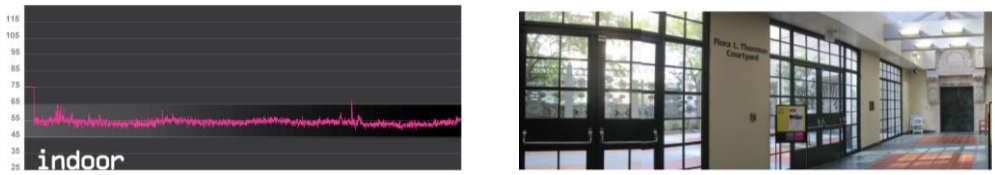

Figure 3: Field-tested indoor sound levels of condition 1, Bunker Hill & LA Central Library

It is fundamental to identify and understand the influence a façade design has on a workspace environment and its site conditions. Among the most challenging sound conditions is traffic noise, a common condition in the urban environment. Serving as initial measurements, the highest sound level obtained from field-testing- the most extreme condition, was implemented to weigh traffic sound spectrum simulated in INSUL. ISO 717, a rating of sound insulation in buildings and of building elements: airborne sound insulation, is defined as single-numbered values for airborne sound insulation in buildings and building elements, such as walls, flooring, doors, and windows (ISO 717). Field-measurements were used as a correction factor to INSUL's ISO 717 traffic noise prediction method to resemble the outdoor sound environment results in increasing the accuracy of simulations. Field-measurements provided single-figured dB levels. Implementing field-measurements in INSUL's ISO 717 traffic noise prediction method, a 1/3-octave band sound spectrum was obtained. This strategy aims toward enabling designers to determine design goals to reduce sound transmission through the facade.

Sealed Single-Glazed Facades, Sealed Single-Skin Façades, and Double-Skin Facades

The intent of assessing sound transmission loss from glass facades through simulations was to further analyze the performance of double-skin glass facades in reducing sound transmission from immediate distanced outdoor levels within frequencies to 5000Hz. Frequencies indicate the number of cycles-per-second (cps) a sound pressure wave repeats in hertz (Hz) and is used to determine the audible range of human hearing, 20Hz to 20,000 Hz. Within the audible range of human hearing, 20Hz to 20,000 Hz, INSUL simulated facades identifies sound transmission loss below 5,000 Hz. As a result, sound levels (dB) derive from the outdoor sound spectrum and simulated transmission loss. In accordance to EN ISO 717, varying conditions of sealed facades were simulated (British and International Standards 1997). Weighting ISO 717 sound levels with the maximum outdoor sound level from field-tests, 90dB, increased the accuracy of simulations to resemble a realistic setting as well as adjust sound levels to be audible Since field-test conditions consisted of single-glazed facades, 12 single-glazed facades were simulated in INSUL to determine the acoustic performance of a façade with single-glazing. In analyzing the acoustic performance of single-skin facades, 12 iterations derived from variables such as glass type and glass thickness (Fig. 4). Selected glass types, such as monolithic, PVB Glass (PVB), and Trosifol Glass (TSC), and glass thickness simulated for this study are typical models in the most glass manufacturing companies . Comparing transmission loss obtained from both forms of façade assemblies (single-glazed and single-skin) determined the amount of transmission loss improved by adding an additional glazing and increasing air-cavity dimension. In addition to comparing sound transmission loss in field-tested conditions and simulated conditions, data obtained from field-tests served to validate the accuracy range of INSUL's estimations. Demonstrated to provide sound transmission loss estimations within close range of single-glazed facades field-tested, double-skin glass facades were modelled and simulated within the same INSUL configurations used to simulate sealed single-glazed facades and sealed single-skin facades.

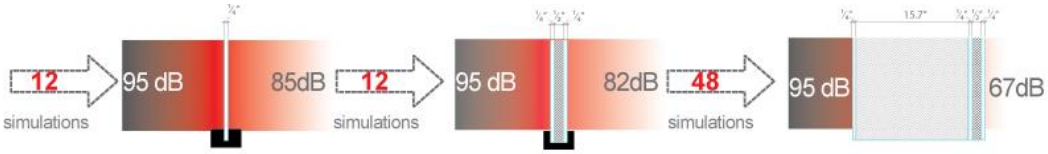

Figure 4: Progression from sealed single-glazed facades to sealed double-skin facades based on improved sound transmission loss from analysed simulations.

Using INSUL, sealed double-skin facades composed of three glass types were simulated under varied components. Considering standard parameters, three glass types, four thickness and four air-cavity depth, 48 were analysed (Fig. 4).

RESULTS

With field-measurements involving single-glazed facades as its enclosure, measured and recorded site conditions served as a baseline differentiating outdoor sound levels and indoor sound levels. Identifying differentiations between outdoor and indoor conditions in decibels (dB), its highest noise levels for traffic was implemented into simulated sealed single-skin facades and sealed double-skin facades. Obtained from field-tests, inputting the highest outdoor sound level to weight INSUL's standard traffic noise (ISO 717) provided a more realistic setting for the analysis. Sound transmission loss (dB) obtained using INSUL were ordered by four standard glass thickness and separated based on the three laminate types: monolithic, PVB, and TSC. Determining transmission loss due to varying parameters, all graphed simulations responds to the same outdoor sound level obtained from field-measurements. Simulated sealed double-skin facades were composed into 3 charts separated by glass type. Displaying the influence of glass type, glass thickness, and air-cavity depth in reducing sound transmission, indoor sound levels resulting from the remaining outdoor sound level transmitted correspond to a shade of a given color. The darkest shade of a given color indicates the thickest glass simulated. As the darkest shade indicates the largest glass thickness, lighter shades represent the smaller glass (Fig. 5). Comparison from single-glazed facades to single-skin facades, and single-skin facades to double-skin facades validated improved transmission loss resulting from double-skin facades.

Sealed Double-Skin Facades

Simulating sealed single-glazed facades, sealed single-skin facades, and sealed double-skin facades, increasing the air-cavity dimension provides increased sound transmission loss in comparison to glass thickness. As a result, increasing the air cavity depth for double-skin facades effectively reduced sound transmission within higher frequencies. Towards lower frequencies, air-cavity depth linked with maximum glass thickness improved sound transmission loss (Fig. 5).

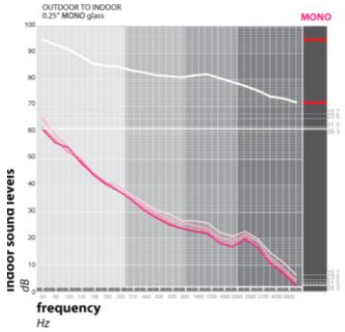

Fig. 5: Simulated sealed double-skin façade composed of monolithic glass under ISO 717.

DISCUSSION

Using Simulations configured to resemble realistic settings, sealed double-skin facades demonstrated to improve sound transmission loss. Field-testing is a fundamental procedure that reflects noise conditions in the current environment. In determining the parameters of a building's glass facade, measuring existing conditions of its site enables designers to specifically address to its sound environment. For instance, as field tests were conducted within Los Angeles' most concentrated commercial areas, the simulations and design support tool provides designers design solutions that would specifically respond to its current context. Mapping outdoor sound levels within an urban environment, highlighting high and low sound levels, designers can determine façade parameters that would reduce sound transmission loss with particular areas. Figure 6 displays high sound levels concentrated around commercial areas and streets with frequent traffic (Google Maps).

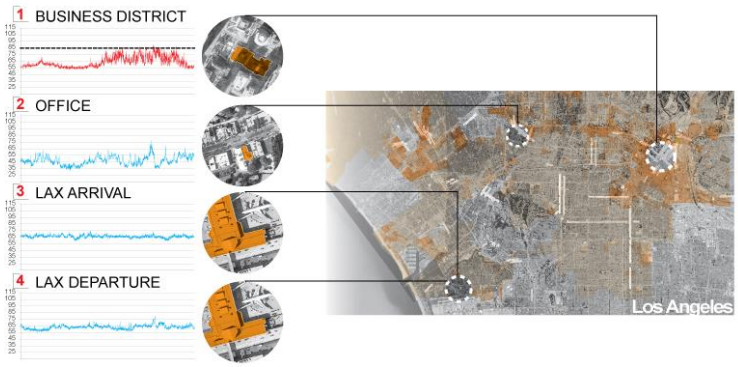

Fig. 6: Outdoor sound levels obtained from field-measurements to compose a mapping tool indicating façade parameters necessary to respond to indicated outdoor sound conditions.

Utilizing this study's approach can increase architectural designers' awareness in designing glass building enclosures and its response to its acoustic environment. This study approach demonstrates the careful consideration necessary to provide acoustic comfort. As the methods conducted in this study redefines acoustic design for glass facades, it provides designers the opportunity to collaborate with the city in continuing efforts to improve indoor acoustics as well as environmental acoustics.

ACKNOWLEDGEMENTS

Appreciation is expressed to thesis committee members, Dr. Kyle Konis, Dr. David Gerber, and Elizabeth Valmont. Their devoted assistance, along with foresight from thesis advisors Douglas Noble and Ilaria Mazzoleni, contributed in the study's development. Appreciation is also credited to INSUL for accommodating to the duration and verification necessary to attain simulated results.

REFERENCES

1. Acoustics: Continuing Education Unit 2003-2009, Acoustics in the Design Phase, viewed 25 September 2012, Current Online CEU. < http://www.acoustics.com/ceu.asp>.
2. Paradis, Richard 2012. 'Acoustic Comfort', Whole Building Design Guide: National Institute of Building Science, 24 April, viewed 25 September2012. <http://www.wbdg.org/resources/acoustic.php>.
3. British and International Standards, BS EN-ISO 717-1:1997 Rating of sound insulation in buildings and of building elements: airborne sound insulation, published 15 August 1997, viewed 15 September 2012.

STUDY OF A NEW CONCEPT BASED ON ELECTRICAL VEHICLE COUPLED WITH SOLAR PV BUILDING IN 2030

M. Cosnier[1]; D. Quenard[1]; F. Bougrain[2].

1: CSTB, DER/CPM, 24 rue Joseph Fourier, 38400 Saint Martin d'Hères

2: CSTB, DESH/ LSPI, Pst Descartes – Bâtiment « Le Bienvenüe » Plot A – 5ème étage 14 Boulevard Isaac Newton 77420 Champs sur Marne

ABSTRACT

Building and Transportation are the main consumers of final energy and emitters of GHG. In France, many efforts are made to improve energy performance of buildings, but the location of these buildings may erase the gains: 80 kWh/m²/yr of energy savings in a building is wiped off by 20 km by car every day for a year.

The present study aims to assess the impact of the concept based on electric vehicle (EV) coupled with solar photovoltaic building, on the power grid. TRNSYS software was used to assess the source of energy (PV, Grid, EV battery) involved when EV is used for commuting to work. The EV battery is used as a power source to minimize the energy needs from the power grid during peaks of electricity demand. Twelve scenarios have been examined in order to integrate assumptions on plug-in, climate and commuting distance. Finally, the influence of efficiency reduction due to aging of PV cells has been evaluated on a case.

Whatever the scenario is, the results show that, the annual PV energy production is greater than consumption, but as expected, does not match every time: for 50 to 70% of the time, the use of power grid is required. EV charging at work reduces drastically the need to the grid for consumption due to mobility. Moreover, the use of a plug-in station at home is particularly effective: EV battery acts as a source of additional electricity, it supplies the needs related to home electrical appliances and avoids the use of power grid during peak hours. Finally, the decrease of PV efficiency significantly reduces the energy sold to electricity supplier and increases the fraction of power grid in the energy supplied to the vehicle.

Keywords: Building, Electrical Vehicle, V2H, Energy Balance

INTRODUCTION

In France, Building and Transportation sectors are the main consumers of energy and the largest emitters of greenhouse gas [1]. To balance this, the French government has enacted the "Grenelle" laws including, among other key measures, the Sustainable Building Plan and the development of electric mobility. The first is to promote the diffusion of energy positive buildings after 2020, the second is to develop electric and plug-in hybrid vehicles with the objective of 2 million units sold in 2020 (30% of vehicle sales in 2020).

Considering these issues, development of solar mobility for individuals become a key point: energy positive buildings will be considered as production sites (PV) and become charging points for hybrid and electric vehicles. In addition, since on one hand, vehicles are parked on average 95% of the time and on the other hand the recharge time is long enough (a few hours), it seems interesting to take advantage of these periods of parking either in park lot of energy positive office buildings or on Park & Ride facilities equipped with PV [2]. Moreover, this Building-Transport convergence could be enhanced if EV batteries were used as energy

storage systems to cope with intermittent energy production and consumption (Vehicle-to-Home Concept - V2H).

This paper is the result of a part of the work made within the framework of POLINOTEN, a project funded by ADEME, whose purpose is to define how the French innovation policy towards solar mobility should be implemented. The study aims to assess the impact of the electric vehicle coupled with PV buildings on the power grid. Besides the energy used for moving, the EV battery also acts as a source of electricity to minimize the energy need from the power grid during peak electricity consumption. Plug-in scenarios, climate and commuting distance have been compared. The influence of aging of solar cells has also been investigated for one case.

METHOD

The study analyses the electric power balance of a French family living in an energy positive house (only household appliances consumption) located in suburban area. One of the adults goes to work during the day with an EV charged primarily by PV or otherwise by power grid.

Vehicle plug-in modes

Three modes were studied based on the location of PV and plug-in station (Figure 1).

1) PV and plug-in station at home

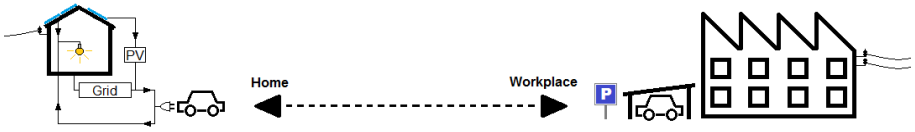

2) PV and plug-in station at work

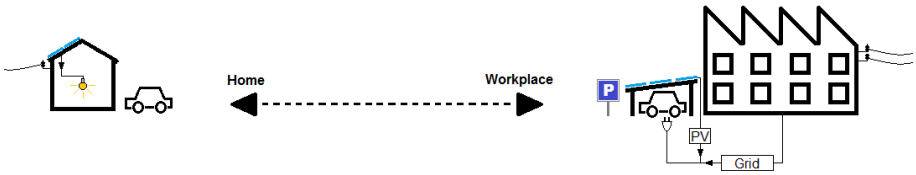

3) PV and plug-in station at home and at work

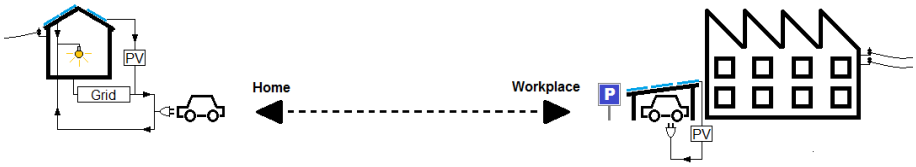

Figure 1: Plug-in modes

Commuting distance

Two kinds of weekday trips are considered: a 50 km round trip and a 16 km round trip which matches respectively the median and average commuting distance for French employees [4]. This parameter is quite important in terms of the overall balance since 80 kWh/m^2 of energy saved in building is wiped off by 20 km travelled by car every day for a year [5].

Climates

Two French climates have been studied to compare the influence of solar production: Trappes in the north of France and Carpentras in the south of France. The annual productivity for optimal solar orientation of PV panel is respectively, 973 kWh/kWp and 1320 kWh/kWp [3].

Electrical loads have been calculated through annual TRNSYS simulation with a 5 minutes time step. The assumptions for each component of the model are presented below.

ASSUMPTIONS

One relies on the high ranges of current performance. It was decided to adopt rather pessimistic hypothesis for 2030 by limiting the technological progress that can be expected. It is a way to prevent the risk of promoting a concept that would be unsustainable retrospectively.

PV cells

The model of PV panel used in the simulation is crystalline type (type 194a) of 140 Wp/m^2. The yield between the DC output of PV cells and the AC input of the power grid was set to 86%. It takes into account the efficiency of the inverter, the wire losses and unexpected disconnections due to power grid quality. The design of PV array at home is provided so that the house is energy positive over the year: for electrical appliances and mobility when plug-in at home is possible and only for appliances otherwise. Solar panels aimed to charge the vehicle at workplace cover 13 m^2 of the roof above the parking lot. A power grid supply at work for the car is possible only if it cannot be plugged-in at home.

Building and users

The investigated house is an energy positive house (BEPOS: Bâtiment Energie POSitive). Regulatory energy consumption items related to heating, cooling and domestic hot water have not been considered. Only electrical appliances consumption of the house has been taken into account. This assumption is justified since this item will be dominant in the future. Electricity consumption habits have been set for home equipment. As no projection in 2030 exists, consumption patterns from IEA for 2002 and 2005 have been used [6]. According to surveys conducted with a 5 minutes time step, the annual power consumption of the family is around 3028 kWh/year. At workplace, the power consumption has not been taken into account due to a lack of data. This strong assumption is realistic when you consider the alternative of park and ride facilities as a place to recharge the vehicle, disconnected from the workplace.

Electric vehicle

Electric vehicle is considered as a battery discharging when travelling. The battery model used in TRNSYS is a kind of lead battery (Type 47a) in which the state of charge (SOC) varies linearly for a constant power load or unload. The battery has a capacity of 25 kWh, depth of discharge (DOD) of 90%, a yield of load of 95%, a yield of unload of 90% and an estimated consumption of 0.2 kWh/km. One assumes the EV is only used to satisfy commuting distance (starting and returning times are respectively 8am and 5.30pm). The family does not use EV for travels during weekends. The actual journey duration is not taken into account; each trip is half an hour long (1 hour per day) and the vehicle's battery discharge more or less quickly depending on the length of the commuting distance.

Power grid

Power grid is modelled as a constant electric power of 3.7 kW (230 V and 16 A).

Practices rules

Practices rules modelled in TRNSYS by equations of Boolean type have been set up (figure 2). It is assumed that power grid parity will be reached by 2030. Consequently, self-consumption is favoured by assigning photovoltaic production primarily to home appliances, then load of the vehicle (if a plug-in station exists) and finally sale to the electricity supplier. Currently, considering Feed-In tariffs of solar electricity, priority is given to power grid. At

home and at work, the electric vehicle is loaded primarily by solar panels. Charging via the power grid is possible only if the SOC of the battery is too low to make one and a half times the daily commuting distance. Moreover, charging may only happen outside peak hours: at home between 10pm and 8am and at work between 10am and 12pm and between 2pm and 5.30pm to avoid peak hours.

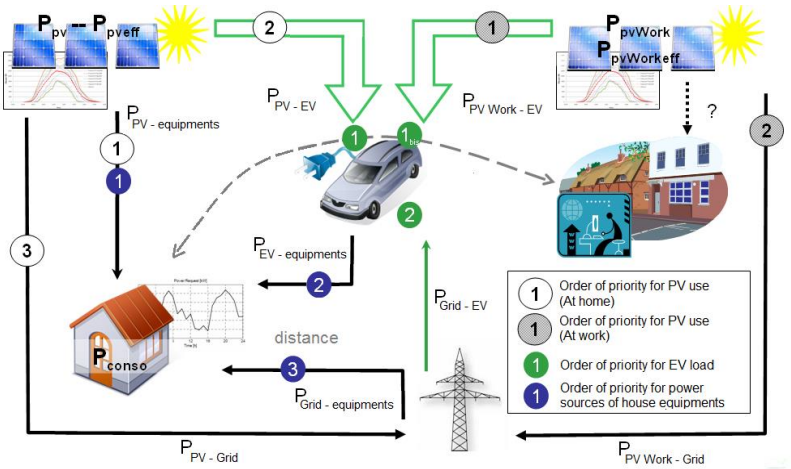

Figure 2: Electric flux and uses priorities

Between 6pm and 10pm, household appliances are supplied primarily through the car battery if its SOC is high enough (V2H concept). At workplace, this option is not available.

RESULTS AND DISCUSSIONS

Among the data, particular attention is paid to the use of PV production and the appliances and EV consumption. Besides, energy profiles from the power grid with a 15 minutes time step, consistent with French data of CO2 content of power grid, are available. These results were used in another study to quantify the environmental impact of the concept [7].

Figure 3 shows three main indicators for each scenarios: the percentage of solar energy consumed by EV compared with its total energy consumption, the percentage of time the building is autonomous and does not use power grid, and finally the percentage of energy provided by EV for appliances consumption during peak periods (concept V2H) versus the total energy consumed during this period.

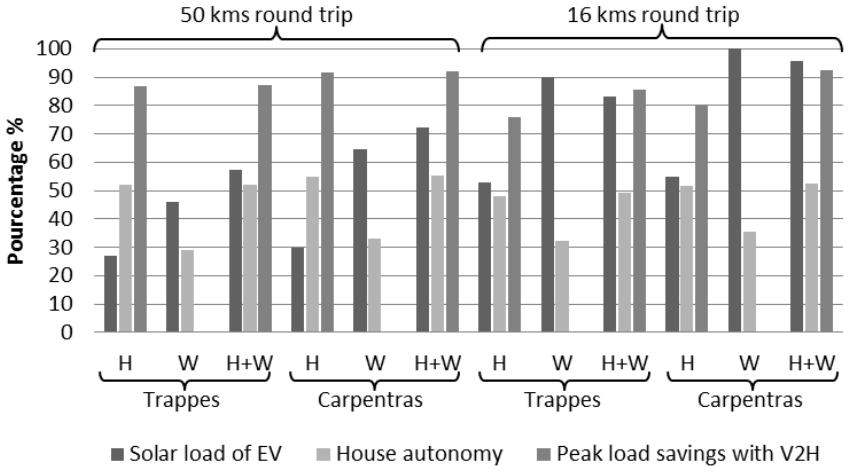

Figure 3: Solar load of EV, Building autonomy and Peak load savings with V2H for 3 plug-in modes – H (Home), W (Work) and H+W (Home & Work), 2 climates, 2 commuting distances

Whatever the scenario is, the annual energy production from PV panels is greater than the consumption of appliances and EV, but as expected, does not match the demand all along the year: for 50 to 70% of the time, the use of power grid for appliances consumption is required. Otherwise, the percentage of solar energy consumed by EV is between 28 and 100% depending on the scenario. Charging at workplace reduces drastically the use of the power grid for mobility. For the shortest trip and sunniest climate case, no power grid is even required. Finally, plug-in station at home is particularly effective for peak-shaving. When EV battery acts as an additional source of electricity during peak hours, it covers between 80 and 95% of the total energy consumed by electrical appliances of house during this period.

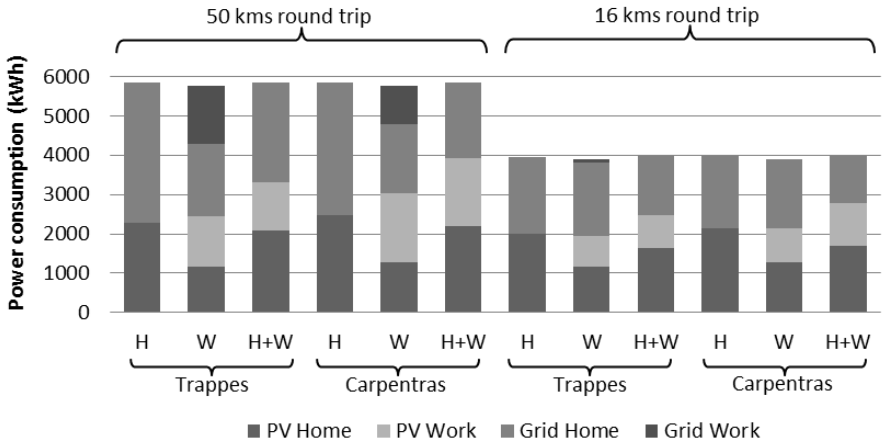

Figure 4: Distribution of energy consumed by appliances and EV for 3 plug-in modes – H (Home), W (Work) and H+W (Home & Work), 2 climates, 2 commuting distances

Figure 4 shows for each scenario, the source of energy consumed by appliances and mobility. Solutions combining plug-in station at home and at work (H+W) reduce the most the energy from power grid. The largest PV panels design also explains this result. An additional study was developed to examine the economic feasibility and the environmental impact of the aforementioned scenarios [7].

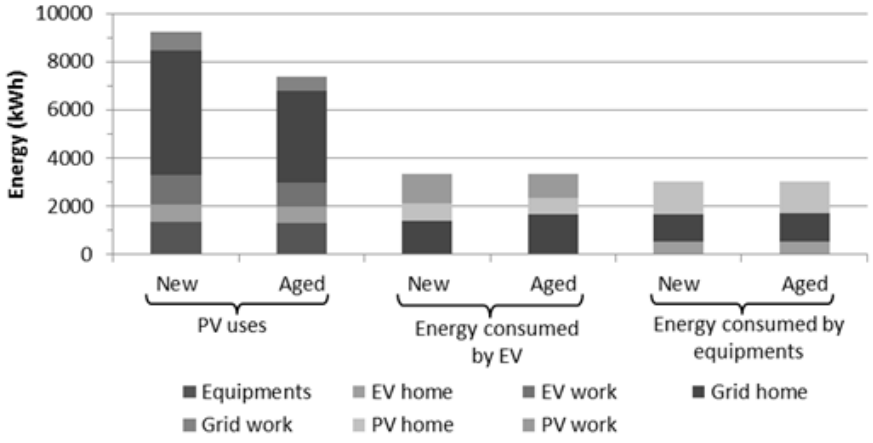

Figure 5: Distribution of solar production and energy consumed by EV and appliances for new and aged solar panels

Finally, to assess the impact of a decrease in performance of PV cells due to aging, an additional simulation has been run. It was based on the following hypothesis: a 20% decrease of PV yield, 50 km commuting distance, Trappes climates and plug-in station at home and at work.

Figure 5 compares the distribution of solar energy production and sources of energy consumed by electrical appliances and the vehicle for new and old PV cells. When energy produced decreases by 20%, energy sold to the electricity supplier is primarily affected with a 26% decrease. In addition, the power grid need for EV also increases by 17%; the percentage of solar load of EV varying then from 57 to 50%. For equipment, the decrease of PV yield does not affect the need to power grid. It is due to the fact that PV panels have been oversized as it has been designed for household appliances and mobility.

CONCLUSION AND PERSPECTIVES

This study examined the energy balance of the concept based on the Building - Transportation convergence. Several cases have been analysed according hypothesis on meteorological location, commuting distances and place of the plug-in station.

The results show that despite an annual solar energy production greater than the energy consumed by electrical appliances and electric vehicle, energy from power grid is still required in order to fit the demand every day. To minimize the energy supply from the power grid, a plug-in station at home and at work seems to be efficient. During the day, the vehicle is charged at the workplace parking lot, whereas when it is back home, the EV battery meets the needs for household appliances during the peak load period.

This energy study has served as a starting point for a larger study dealing with economic feasibility and environmental viability of solar mobility. Now, the aim is to define the best governmental policies in order to implement and develop this concept.

ACKNOWLEDGEMENTS

The authors gratefully thank ADEME (Agency of Environment and Energy Management) for its support in the framework of “Mettre l’innovation sur la trajectoire du facteur 4” program.

REFERENCES

1. DGEC (Direction générale de l’énergie et du climat) : Chiffres clés de l’énergie, Service de l’observation et des statistiques, 2012.
2. Quenard, D. : Vers l’autonomie énergétique, La Recherche, n°415, pp 76-79, 2008.
3. Meteotest: Meteonorm handbook, Parts I, II and III. Meteotest, Bern, Switzerland, 2003.
4. Baccaïni, B., Sémécurbe, F. et Thomas, G. : Les déplacements domicile-travail amplifiés par la périurbanisation, INSEE Première, n°1129, 2007.
5. Quenard, D. : Se loger, se déplacer : peut-on se libérer de l’addiction aux énergies fossibles ?, La chimie et l’habitat, EDP Sciences, les Ulis, pp 151-171, 2011
6. Knight I., Kreutzer N., Manning M., Swinton M. and Ribberink H.: European and Canadian non-HVAC electric and DHW load profiles for use in stimulating the performance of residential cogeneration systems », Annex 42 of the International Energy Agency – Energy Conservation in Buildings and Community Systems Programme, 2007
7. Taverdet-Popiolek N., Quenard D., Thais F., Vinot S., Wiss O. :Mettre l’innovation sur la trajectoire du facteur 4: la mobilité solaire en 2030, La revue de l’Energie, n°611, pp 23-40, 2013

THE USE OF BI-DIRECTIONAL SCATTERING DISTRIBUTION FUNCTIONS FOR SOLAR SHADING MODELLING IN DYNAMIC THERMAL SIMULATION: A RESULTS COMPARISON.

O. Dartevelle[1]; G. Lethé[2]; A. Deneyer[2]; M. Bodart[1]

1: Architecture et Climat, Université catholique de Louvain, Place du Levant 1, 1348 Louvain-la-Neuve, Belgium.

2: Belgian Building Research Institute, BBRI, Avenue P. Holoffe 21, 1342 Limelette, Belgium.

ABSTRACT

The evaluation of cooling needs and summer comfort in buildings requires an accurate quantification of solar gains through window systems (glazing and solar shading). However, in dynamic thermal simulation tools, the modelling of shading devices is usually simplified: angular dependency of properties is neglected; shading devices are considered as perfect diffuser; internal reflections between the slats of a venetian blind are neglected or considered only as diffuse. In some cases these simplifications bring significant inaccuracies on the evaluation of solar gains entering the building, and, consequently, on the building thermal behaviour. Bi-directional Scattering Distribution Functions (BSDF) allows a more detailed modelling of materials and systems which enhances the characterisation of the window behavior. The use of these functions appears to be an appropriate way to consider optical angular properties of shading devices in dynamic thermal simulations: it increases the accuracy of results without requiring excessive computation time.

This paper shows and discusses the results obtained when using-directional Scattering Distribution Functions in dynamic thermal simulation, for six common configurations of solar shading devices (external screen and venetian blinds of different characteristics), in comparison with those obtained by simplified modelling methods. The Window 7 software was used to generate BSDF data that were then used as input in the EnergyPlus V8 building energy simulation program. Results focus on transmitted solar energy through windows (double low E glazing) and cooling needs of a simple office room for the different solar shading devices.

In conclusion, this study shows for several solar shading types (and their characteristics), the importance of considering optical angular properties in dynamic thermal simulation and the accuracy gained obtained by BSDF characterisation.

Keywords: Solar shading, BSDF, dynamic thermal modelling, solar gains.

INTRODUCTION

One of the main purposes of dynamic thermal simulations is the evaluation of cooling needs and summer comfort in buildings. This evaluation requires an accurate quantification of solar gains through window systems (glazing and solar shading). However, modelling of shading devices is usually simplified in most of the tools.

For screens, the simplest models use fixed optical properties (with no dependence of incidence angle). For venetian blinds, more advanced models exist but present some simplifications. For example, EnergyPlus V8 [1] integrates a modelling inspired of ISO 15099 [2] standard which neglects the fine slat subdivision and the directional and spectral characteristics of the reflexion onto the slats [3]. In some cases these simplifications bring significant inaccuracies on the evaluation of solar gains entering the building, and, consequently, on the building thermal behaviour. This is especially the case for venetian blinds with highly reflective slats [4].

Characterizing the optical properties of glazing system by a Bidirectional Scattering Distribution Functions (BSDF) allows considering all these aspects in dynamic thermal simulation. Especially, the significant dependencies of angular properties on the profile angle for venetian blinds (obtained here from simulation), and on the solid angle for screens (here obtained from measurements) can be covered inside the more general formalism of BSDF.

METHODOLOGY

In EnergyPlus 8, a BSDF matrix can be input in order to define the angular optical properties (absorption, transmittance and reflectance) of the entire glazing complex (glazing and solar shading). This matrix can be generated using WINDOW 7 software.

For glazing equipped with screens, WINDOW 7 integrates a data base with angular optical properties measurements (BSDF) as an alternative for the simplified model (homogeneous diffusing shade). For glazing equipped with venetian blinds, an advanced radiosity calculation method (directional diffuse) and a more detailed slat subdivision and curvature is used to simulate the complex reflection between the slats of venetian blinds. This finally forms the BSDF pattern exported as input to EnergyPlus.

This study compares results obtained by the use of these WINDOW 7 BSDF representation (Complex Shade Model) with results obtained by common shading devices modelling methods in EnergyPlus, namely the *Shade modelling* (perfectly diffusing and non angle-dependant screen) and the *Blinds modelling* (roughly discretized and flat diffusing venetian blinds) [3].

CASE STUDY DESCRIPTION

For this study, a simple office room having a 60% glazed façade, south oriented, was considered [Figure 1]. Key hypothesis for simulations are presented in Table 1.

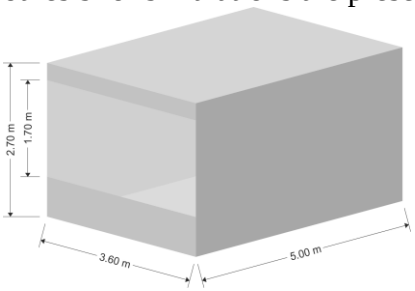

Figure 1: Geometry of the case study (office room).

U-values	South façade: U=0.32 W/m²K (EPBD requirements). The other walls are considered as adiabatic.
Window	Double Low E glazing (4-16-4) with a 90% argon gas layer. U=1.45 W/m²K; SHGC :0.58 Distance between shading layer and glazing: 50 mm. No top, bottom and sides openings considered.
Hygienic air flows	30m³/h.pers
Infiltration	12m³/h.m² (v50) (EPBD default value for Belgium [8]).
Internal gains	Occupation: 123 W/pers and 10m²/pers; Equipment: 7.11 W/m²; Lighting: 10 W/m².
Weather data	Brussels- IWEC [9]
Workings hours	Full occupation from 9a.m. to 5 p.m. (on weekdays).

Table 1: Key hypothesis considered for thermal simulations.

Two types of external shading devices have been tested (screens and venetian blinds). Table 2 and Table 3 gives respectively the screens and the venetian blinds properties.

Screen

	Sc1	**Sc2**
Openness Factor	5.24%	3.95%
Thickness	0.7mm	1mm
Solar Transmittance	13.73% (mainly diffuse)	4.59% (mainly directional)
Solar Reflectance	44.85%	35.04%
IR transmittance	5.24%	3.95%
Emissivity	85.3%	86.4%
Conductivity	0.15 W/m.K	0.15 W/m.K

Table 2: Description of screen properties (normal hemispheric optical properties)

BSDF characterising of glazing complex with screen were calculated using angular optical properties measurements (BSDF) included in the WINDOW 7 data base. Figure 2 and Figure 3 illustrate the angular behaviour of Sc1 and Sc2 in function of the incidence angle (normal plan).

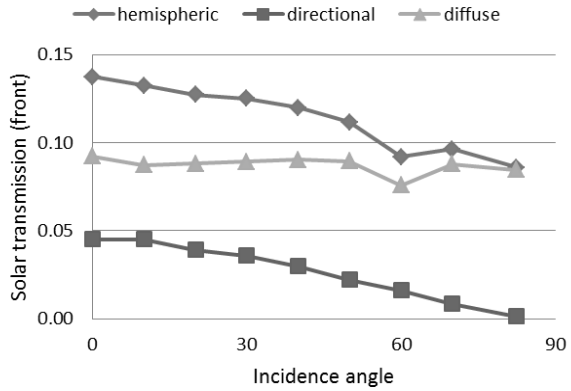

Figure 2: Hemispheric Front Solar Transmittance of Sc1

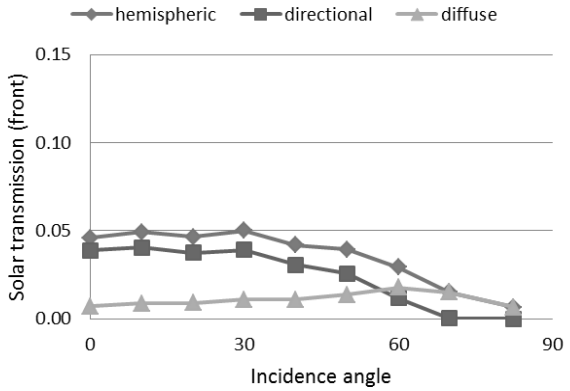

Figure 3: Hemispheric Front Solar Transmittance of Sc2

As can be seen, the solar transmission of the first screen is relatively higher and more diffuse than the solar transmission of the second screen which is mostly directional. Therefore, the relative difference between results using the BSDF or the simplified model is expected to be lower for the first screen than for the second.

Venetian blinds

Two slats types with two different slat angles were studied (see Table 3) (no curvature is considered). These two slats differ mainly from their level of solar reflectance and from the shape of the spectral curve which interferes specifically with the one of the glazing. Spectral slat properties were measured by the Belgian Building Research Institute (BBRI).

BSDF characterising of the glazing complex were then calculated from these measurements considering 5 subdivisions of the slat [6] while the *Energy Plus Blind modelling* is based on global coefficients and 2 subdivisions.

	Bl1_20	Bl2_20	Bl1_45	Bl2_45
Slat angle (from horizontal)	20°	20°	45°	45°
Slat width	65mm	65mm	65mm	65mm
Slat separation	55mm	55mm	55mm	55mm
Thickness	1mm	1mm	1mm	1mm
Slat Solar Transmittance	0%	0%	0%	0%
Slat Front Solar Reflectance	54%	4.8%	54%	4.8%
Slat Back Solar Reflectance	54.8%	5.2%	54.8%	5.2%
IR transmittance	0%	0%	0%	0%
Emissivity	84%	84%	84%	84%
Conductivity	100 W/m.K	100 W/m.K	100 W/m.K	100 W/m.K

Table 3: Description of venetian blinds properties

VARIABLES DESCRIPTION

Results are discussed through the transmitted solar energy (amount of beam and diffuse solar radiation entering through the window) and the cooling needs (calculated in order to maintain air temperature of maximum 24°C during occupancy).

RESULTS

Screen

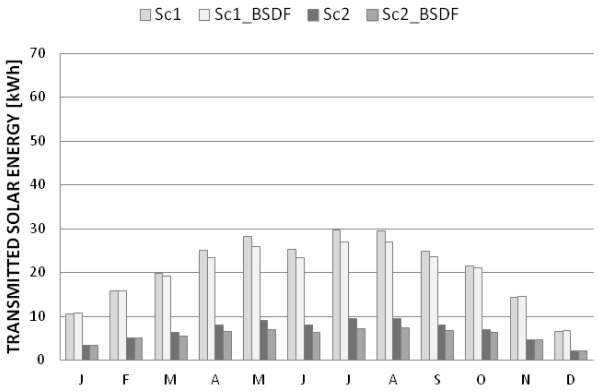

Figure 4: Monthly transmitted solar energy trough window for Sc1 and Sc2.

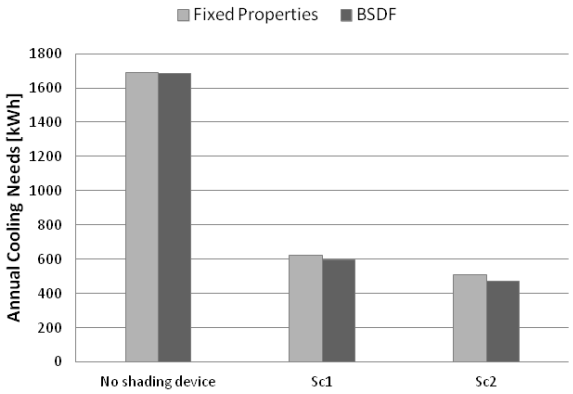

Figure 5: Annual zone cooling needs for Sc1 and Sc2.

	Fixed Properties	Complex Shade (BSDF)	
	December transmitted solar energy [kWh]		***Relative difference [%]***
Sc1	6.59	6.66	1.06%
Sc2	2.11	2.06	-2.37%
	July transmitted solar energy [kWh]		
Sc1	29.64	26.89	-9.28%
Sc2	9.51	7.11	-25.24%
	Annual cooling needs [kWh]		
Sc1	622.83	593.22	-4.75%
Sc2	508.75	469.57	-7.70%

Table 4: Comparison of main results for screens.

Venetian blinds

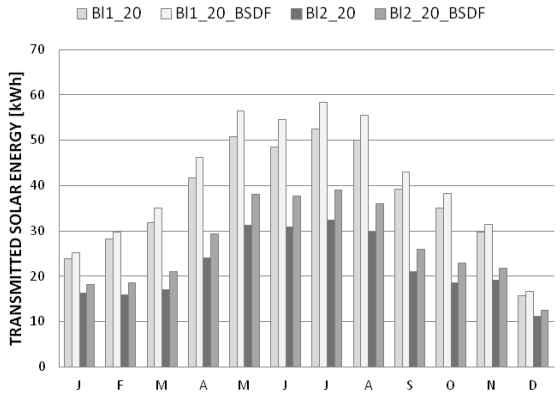

Figure 6: Monthly transmitted solar energy trough window for Bl1_20 and Bl2_20.

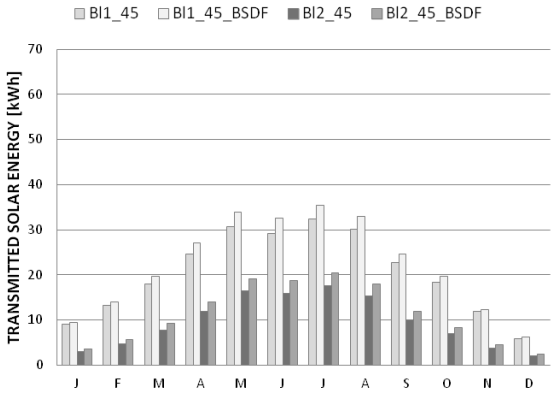

Figure 7: Monthly transmitted solar energy trough window for Bl1_45 and Bl2_45.

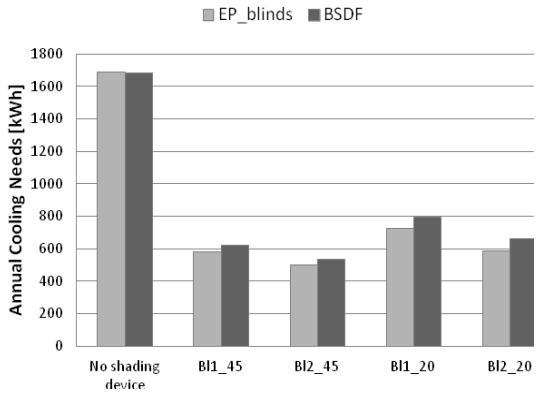

Figure 8: Annual zone cooling needs for Bl1_20, Bl2_20, Bl1_45 and Bl2_45.

	Blinds modelling	**Complex Shade (BSDF)**	
	December transmitted solar energy [kWh]		***Relative difference [%]***
Bl1_20	15.76	16.72	*6.09%*
Bl2_20	11.23	12.49	*11.22%*
Bl1_45	5.84	6.2	*6.16%*
Bl2_45	2.21	2.46	*11.31%*
	July transmitted solar energy [kWh]		
Bl1_20	52.54	58.3	*10.96%*
Bl2_20	32.34	39.09	*20.87%*
Bl1_45	32.42	35.49	*9.47%*
Bl2_45	17.59	20.39	*15.92%*
	Annual cooling needs [kWh]		
Bl1_20	724.65	791.84	*9.27%*
Bl2_20	596.57	660.15	*10.66%*
Bl1_45	581.4	621.1	*6.83%*
Bl2_45	498.29	537.4	*7.85%*

Table 5: comparison of main results for venetian blinds.

DISCUSSION

For screens, no significant difference of transmitted solar energy is noticed during the winter. Main difference appears in summer when the sun is high in the sky. In this case, simple modelling with fixed properties overestimates transmitted solar energy. This is particularly true for Screen 2 which presents properties with high angular dependency (25% of monthly values of transmitted solar energy. This provokes an overestimation of cooling needs (up to 7.7%). For Venetian Blinds, the common Energy Plus modelling globally underestimates transmitted solar energy. As seen previously for screens, main differences are noticed during the summer period. These differences appear to be more significant for low slat angle (closed to the horizontal) and are relatively more important for small values of glazing complex transmittance (up to 20.87% for Bl2). This provokes an underestimation of cooling needs (a difference of 10.66% was noticed).

CONCLUSION

This results comparison shows the importance of considering properly the angular dependency of optical properties for a precise evaluation of summer comfort and cooling needs with dynamic thermal simulation. BSDF characterizing of window complex represents a powerful way of introducing optical angular properties. This consideration allowed to highlight the under or over estimation of cooling needs generally obtained by simple modelling according to the type of shading device.

FUTURE WORKS

The enunciation of general rules concerning over- and under-estimations requires more in-depth studies and replication of the obtained results with other products. More parameters may also be varied, such as the positioning of the shading devices with respect to glazing (inside or outside), possible specularity of slats or other special products, as well as different shading controls.

REFERENCES

1. U.S. Department of Energy (DOE): EnergyPlus 8 simulation software, 2013.
2. ISO 15099: Thermal performance of windows, doors and shading devices, 2003.
3. U.S. Department of Energy (DOE): EnergyPlus 8 Engineering Reference Document, 2013.
4. Saelens D., Parys W., Roofthooft J., Tablada de la Torre A.: Assessment of modelling approaches for louver shading devices in office buildings. Proceedings CISBAT 2011, Lausanne.
5. Lawrence Berkeley National Laboratory: Window 7, 2013.
6. Carli, Inc. : Calculation of optical properties for a venetian blind type of shading device. Millers Falls, 2006.
7. Tzempelikos A., Laouadi A., Reinhart C., Athienitis A.: Determining the optical properties of shading devices: current modelling approaches and future directions. Canadian Solar Buildings Conference, Montreal, 2004.
8. Arrêté du Gouvernement Wallon : Performance Energétique des bâtiments, Annexe 2 - Méthode de détermination du niveau de consommation d'énergie primaire des immeubles de bureaux et de services et des bâtiments destinés à l'enseignement, 2008.
9. ASHRAE: International Weather for Energy Calculations. Atlanta, 2001.

SYSTEM EVALUATION OF COMBINED SOLAR & HEAT PUMP SYSTEMS

Ralf Dott; Thomas Afjei

Institut Energie am Bau, Fachhochschule Nordwestschweiz FHNW, St. Jakobs-Strasse 84, CH-4132 Muttenz, Switzerland

ABSTRACT

A local solar energy generation with solar thermal collectors or photovoltaic modules combined with the use of ambient heat by heat pumps can provides powerful solutions in building heat supply for a one hundred per cent renewable energy strategy.

This paper shows and characterises six heat generation system concepts with solar heat or electricity generation combined with heat pumps. The work is conducted as simulation study with Polysun® applying best available technologies. The systems range from a mainly direct use of solar irradiation for heat generation, thus requiring highly efficient components to overcome the seasonal mismatch of solar irradiation and heat demand in the building, over combined systems using either glazed collectors for direct use and unglazed absorbers as heat source for the heat pump or high efficient selective absorbers for both direct and indirect use. Furthermore a system that uses a solar absorber with cold storage as only heat source for a heat pump is evaluated and compared to a classical air/water heat pump system. The systems are applied to a single family house with three different thermal qualities of the building envelope, which has been defined in the "Solar and Heat Pump Systems" project of the International Energy Agency, to which these results also contribute.

The juxtaposition of the six systems shows and characterises solution pathways with its strength and weaknesses. The focus on solar thermal heat generation with seasonal heat storage reduces the electricity consumption to the lowest level. The heat generation only by heat pump comes with the highest electricity consumption but a combination with a PV generator leads to a high surplus electricity generation in summer. A combined solar heat and electricity generation with PVT modules reduces with a well-adapted control the electricity demand from the net to a comparable level to the seasonal solar heat storage and furthermore also produces surplus electricity.

Keywords: heat pump, solar heat, photovoltaic

INTRODUCTION

Future energy supply systems need to support the transition from a mainly fossil to a predominantly renewable energy generation. The heat generation for space heating and domestic hot water in buildings plays an important role. Therein solar energy systems as well as heat pumps are key technologies. This study investigates combinations of solar heat and air source heat pump systems striving for high renewable energy shares in systems that are still robust and can be realized with a reasonable technical effort at affordable cost. Aim of the paper is a juxtaposition of systems that use the roof as part of the building envelope to generate energy and to show their individual characteristics and respective strength and weaknesses. The work has been conducted in the frame of the International Energy Agencies (IEA) Heat Pump Program (HPP) Annex 38 / Solar Heating and Cooling (SHC) Task 44 "Solar and Heat Pump Systems" (A38T44) [1].

METHOD

The simulation study is conducted using Polysun® [2]. The generated heat is used for space heating and domestic hot water preparation of a single family house (SFH) which has been defined in IEA HPP Annex 38 / SHC Task 44 "Solar and heat pump systems" (A38T44) as reference heat load, c.f.[3]. Therein, three building types called SFH15, SFH45 and SFH100 are defined, where the numbers refer to the insulation quality and therewith the space heat demand of 15 kWh/m^2/a, 45 kWh/m^2/a or 100 kWh/m^2/a as described in detail in [4]. The heat demand is in this study implemented as load profiles where no interaction with the building, e.g. due to higher flow temperatures, could appear and thus the heat load for all compared systems is equal with the particular reference. In all systems the heat distribution and emission systems are equal and the heat is supplied via a buffer storage that is heated whether by the heat pump or by the solar thermal collectors. Six different heat generation systems have been defined to evaluate their respective characteristics and are applied to the three different heat loads of A38T44 each. All simulations use the moderate climate data set for Strasbourg, a French city in central Europe.

A south oriented and 45° inclined roof surface has been defined as possible area of up to 50 m^2 that could be covered either by solar thermal absorber area or photovoltaic panel area or photovoltaic-thermal absorber area (PVT) or a mixture of the named components. The photovoltaic generators in this simulation study supply the generated electricity to the grid. Furthermore all consumed electricity is taken from the grid. Hence, no electricity storage is considered, only the balance of electricity generation and consumption are evaluated on the bases of daily energy sums. The reason for the evaluation of a daily energy balance is that the heat storage is assumed to be able to store the heat for one day if an advanced control, which could not be modeled in the simulation environment, would be applied. The authors are well aware of the different handling of thermal and electric energy storage in this study, but concentrate on the system design for thermal energy supply and consider the photovoltaic generated electricity as potential use of the remaining roof area and as an estimation of a potentially own consumption of an own photovoltaic generator for SH and DHW heat demand.

Applied tools and parameter data sets

The used flat plate collector data set is the generic collector data set named “flat plate collector, premium quality” [2]. The storage tank model uses generic storage data with typical insulation thicknesses between 20 mm (e.g. for the heat pump source buffer in systems 5 and 6) up to 200 mm (e.g. for the 10 m^3 seasonal storage tank in system 3). For the air/water heat pump, performance data of a Viessmann Vitocal 350 A AWHI 351.A10 [5] are used. For the brine/water heat pump the data set “brine/water heat pump: heat pump 10 kW” [2] is taken. The photovoltaic generator is calculated with the “Photovoltaic polycrystalline PV module” which is identical to the one used in the PVT modules, which is taken from the data set “Photovoltaic thermal absorber: PVT collector 2” [2].

SYSTEMS

System 1 is the reference variant for the energetic efficiency since it only uses an air/water-heat pump (A/W-HP) without solar thermal heat generation. Hence all roof space remains for the PV system of 50 m^2 (c.f. Figure 1, left).

System 2 adds glazed solar thermal collectors of 8 m^2 aperture area for the heat generation that is otherwise supplied by the A/W-HP. Hence, the PV surface is reduced to 42 m^2 (c.f. Figure 1, right).

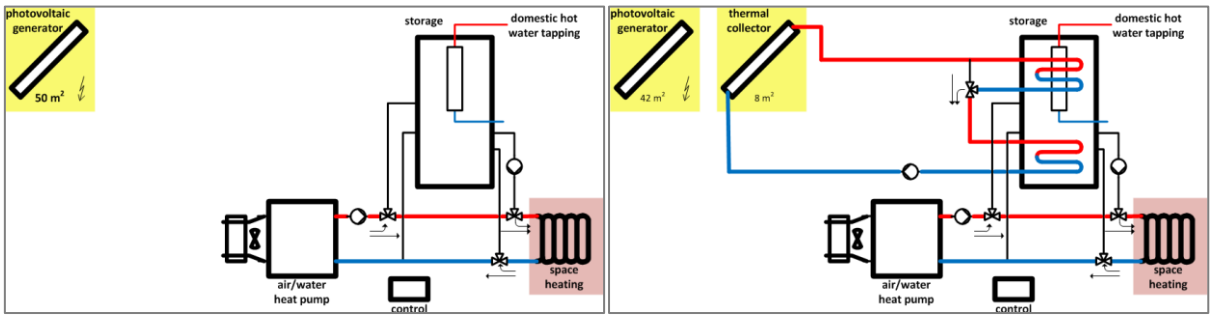

Figure 1 System and hydraulic scheme of system 1 (left) and system 2 (right)

System 3 uses the whole roof surface for glazed thermal collectors for direct heat generation and seasonal heat storage extended to 10 m^3 for this case. This leaves no space for PV (c.f. Figure 2, left).

System 4 employs PVT modules for combined electricity and heat generation on the whole roof surface. These modules supply heat as far as possible directly to the buffer storage and serve furthermore as heat source for the heat pump over a 0.6 m^3 brine buffer (c.f. Figure 2, right).

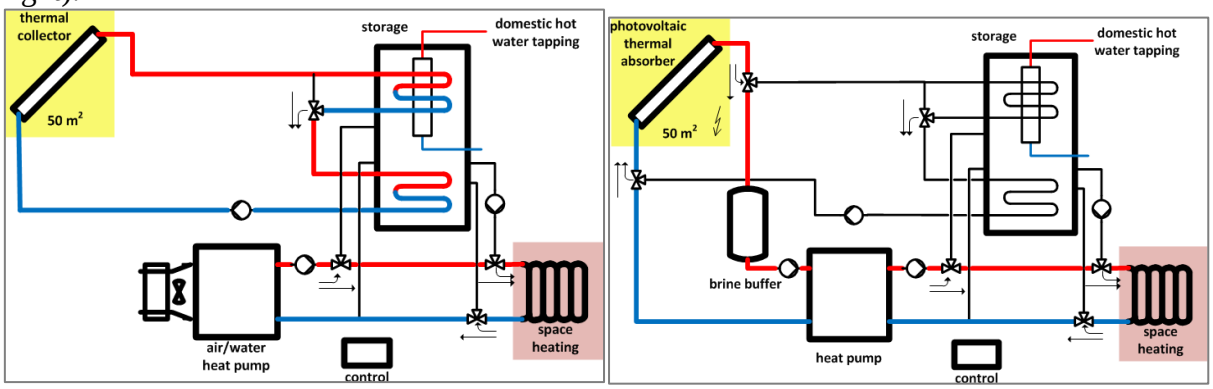

Figure 2 System and hydraulic scheme of system 3 (left) and system 4 (right)

System 5 keeps the hydraulic concept of system 4, but uses classic uncovered plastic absorbers as heat source. In this case no space is left for PV (c.f. Figure 3).

System 6 equals system 5, except that instead of the plastic absorber, now selectively coated steel absorber plates are used. Again no PV space is available (c.f. Figure 3).

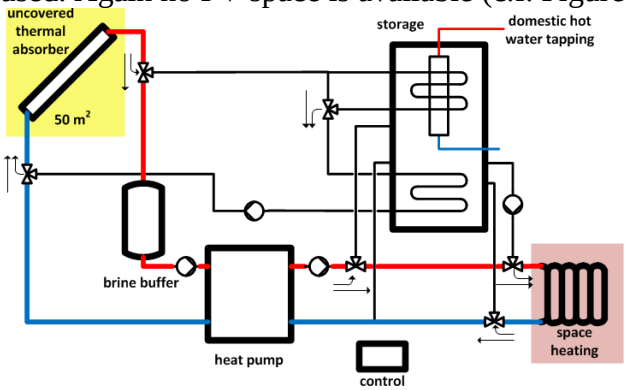

Figure 3 System and hydraulic scheme of system 5 and 6

RESULTS

Figure 4 shows the energetic evaluation results of the six systems for the building SFH15 on Minergie-P / passive house level; Figure 5 for the building SFH45 on new standard buildings level and Figure 6 for the building SFH100 an older existing building.

Systems with a low share of directly solar thermal generated heat, where the heat comes mainly from the heat pump (systems 1, 4 & 5), come with the lowest quantity of generated heat. On the other way around, a high share of directly solar thermal generated heat leads to high heat losses, for the SFH15 building nearly doubling the demand. This effect decreases with higher heat demands and leads for the SFH45 to an increase of 47% and for the SFH100 of 24%. This high quantity of generated heat for high solar thermal shares affects on the other hand the electricity demand only in a smaller degree because of the high efficiency of directly solar thermal heat generation. This leads to the smallest total electricity consumption for the systems 3 and 6 (in Figure 4 to 6 the sum of PV self-usage and grid electricity consumption). In contrast to this the systems with mainly heat pump heat generation (1, 4 & 5) result in the highest total electricity consumption due to their compared to solar heat lower efficiencies.

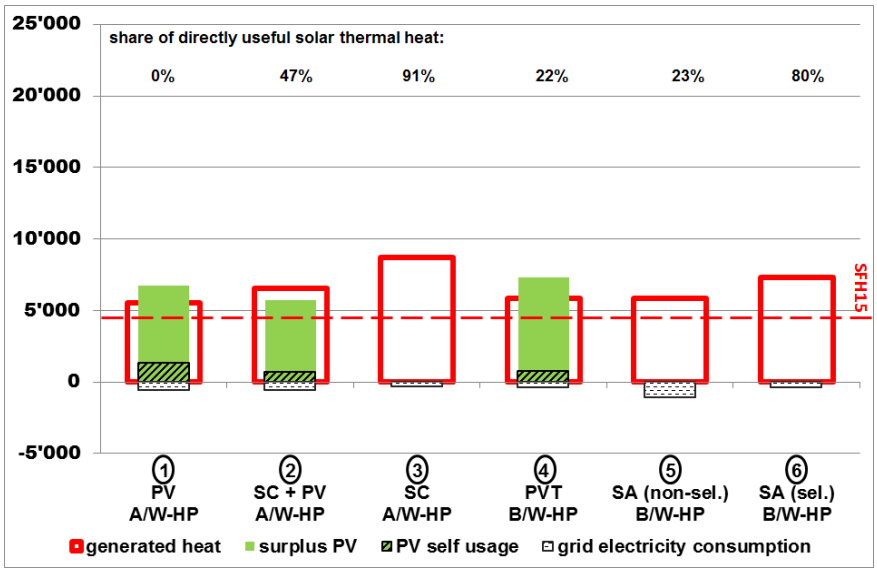

Figure 4 Results of the system comparison for the building SFH15

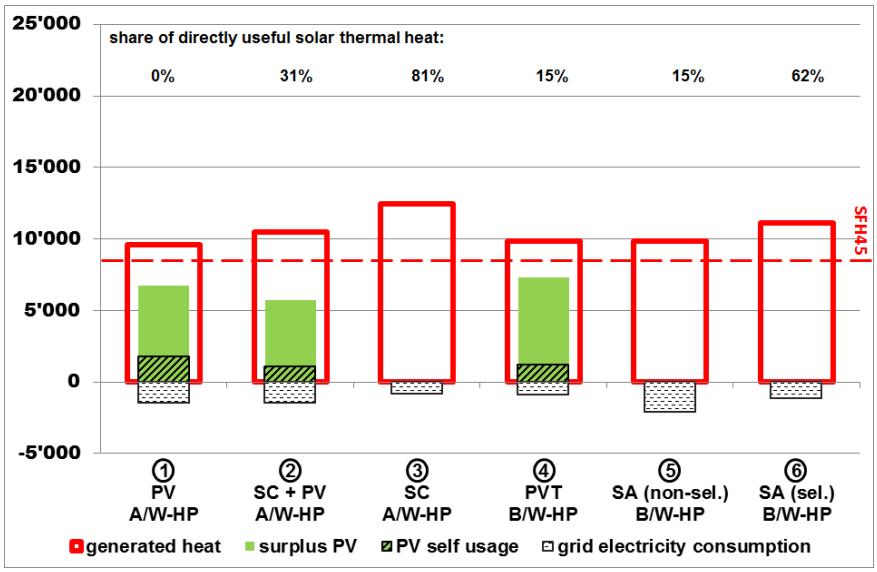

Figure 5 Results of the system comparison for the building SFH45

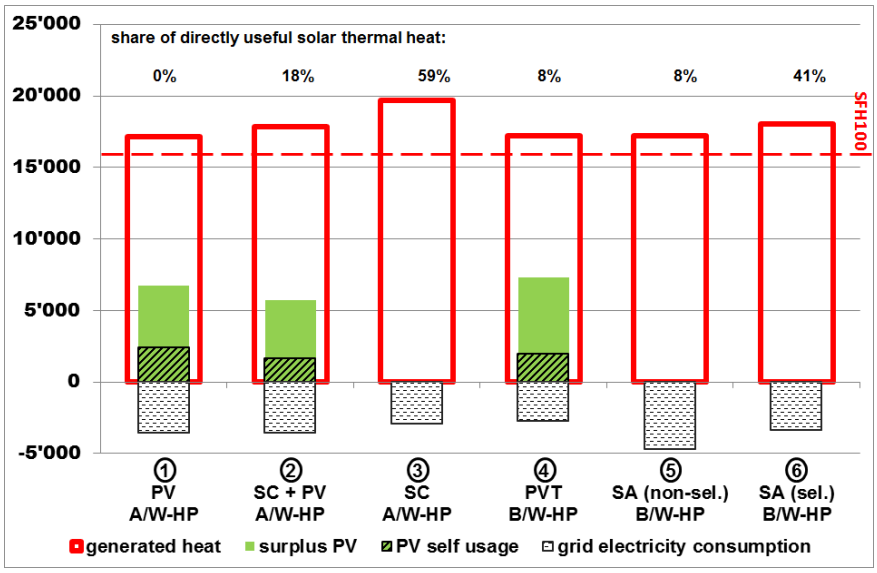

Figure 6 Results of the system comparison for the building SFH100

Considering the grid electricity consumption, where the self-generated and -used electricity from PV is yet subtracted, this result in a differing assessment of the systems, using the assumption of a restricted roof area. In systems 3, 5 and 6 the roof area is already completely covered with thermal collectors and hence no PV generator could be realised – so all electricity consumption comes from the grid. In systems 1, 2 and 4 a PV system can generate electricity at least partly in the roof area. This PV electricity is in this study primarily used for the heat generation system. The remaining electricity demand is then taken from the grid.

Table 1 summarises the relevant results for the electricity discussion of all three buildings and six heat generation systems with the following four resulting values:

- the ratio of generated heat in relation to the heat demand
- the surplus PV electricity that could not be used for the heat generation
- the total electricity consumption of the heat generation systems
- the electricity consumption from the grid

building / heat generation		SFH15		SFH45		SFH100	
HP + PV	1	123%	5'452 kWh	113%	4'980 kWh	108%	4'342 kWh
		1'888 kWh	590 kWh	3'224 kWh	1'454 kWh	5'958 kWh	3'550 kWh
HP + PV + SC-small	2	145%	5'021 kWh	123%	4'626 kWh	112%	4'042 kWh
		1'265 kWh	584 kWh	2'541 kWh	1'464 kWh	5'202 kWh	3'541 kWh
HP + SC-big	3	194%	0 kWh	147%	0 kWh	124%	0 kWh
		309 kWh	309 kWh	860 kWh	860 kWh	2'951 kWh	2'951 kWh
HP with PVT as source	4	130%	6'545 kWh	116%	6'120 kWh	108%	5'350 kWh
		1'107 kWh	362 kWh	2'068 kWh	886 kWh	4'695 kWh	2'730 kWh

legend:

generated heat / demand	surplus PV
electricity consumption	grid electricity

HP = heat pump; PV = photovoltaics; SC = solar thermal collector; PVT = photovoltaic-thermal collector; SFH = single family house;
The difference between the total electricity consumption and the electricity from net is met by self-generated PV electricity.

Table 1 System simulation results for the three building types and six heat generation systems

Comparing the grid electricity consumption of one building standard instead of the total electricity consumption it can be seen that, with the assumption / the aim of an as far as possible daily use of the PV electricity in the heat generation system, the grid electricity consumption could be reduced significantly. For the systems 1 and 2 with pure heat pump heat generation or a small solar thermal share, the grid electricity consumption could be reduced by two thirds. A combined heat and electricity generation with PVT collectors as heat source for the heat pump (system 4) reduces the grid electricity consumption to the level of a highly efficient solar thermal heat generation with seasonal heat storage as in system 3. Beyond that system 4 delivers surplus PV electricity in summer time.

CONCLUSIONS

A parallel heat generation with solar thermal collectors and a heat pump, both working on a combi-storage or buffer-storage for space heating and domestic hot water preparation, could reduce the electricity demand with increasing solar thermal heat share and be a robust solution if some rules like storage stratification or small temperature lift for the heat pump are respected. A combination of heat pump and photovoltaic represents a technically simple and flexible solution that could reduce the grid electricity consumption to a level slightly higher than a seasonal solar thermal heat storage system if an improved control strategy for high PV self-usage is used and furthermore supplies surplus PV electricity. A further developed and optimised combination of heat pump and PVT-collector as source for the heat pump delivers the highest specific energetic collector yield and is able to reduce the grid electricity consumption to the level of a seasonal solar thermal heat storage system with additional surplus PV electricity.

ACKNOWLEDGEMENTS

The authors are grateful for the project advising and funding by the Swiss Federal Office of Energy SFOE in the frame of the project SOFOWA. The project contributes to the IEA SHC Task 44 / HPP Annex 38 “Solar and heat pump systems”. The permission of Meteotest for using Meteonorm climate data for simulations within the IEA SHC Task 44 / HPP Annex 38 is gratefully acknowledged.

REFERENCES

1. IEA SHC Task 44 / HPP Annex 38 “Solar and heat pump systems”, International Energy Agency, http://task44.iea-shc.org/
2. Polysun Designer Simulation Software Version 5.9.6.16241, Velasolaris AG, Winterthur, Schweiz, 2012
3. M. Y. Haller, R. Dott, J. Ruschenburg, F. Ochs und J. Bony: The Reference Framework for System Simulations of the IEA SHC Task 44 / HPP Annex 38, 2011
4. R. Dott, M. Y. Haller, J. Ruschenburg, F. Ochs und J. Bony: Reference Buildings Description of the IEA SHC Task 44 / HPP Annex 38, 2011
5. Data set for Viessmann Vitocal 350 A AWHI 351.A10, in Planungsunterlagen für Wärmepumpen – Ausgabe 05/2012, Viessmann Deutschland GmbH, Allendorf, Germany, 2012. p. 502

AN EVALUATION OF THE EFFECTIVENESS OF PASSIVE DESIGN STRATEGIES IN A CHANGING TROPICAL CLIMATE

A Case of Nairobi's Central Business District, Kenya

L.N.Gichuyia

University of Cambridge, Department of Architecture, 1-5 Scroope Terrace Cambridge CB2 1PX. United Kingdom. Email: lng24@cam.ac.uk

ABSTRACT

There are quite a number of established passive design strategies geared towards indoor thermal comfort of spaces in the current climate for the many climatic zones in the world. It has been hard to fully answer the question on how effective these different approaches to passive indoor comfort will be in the future presuming that the climate, boundary conditions around the building, the future modification of space and its use in the building's life time may not remain stationary. In line with the fact that buildings and climate are inextricably linked and that indoor thermal performance of buildings is closely related to climate, it is becoming increasingly difficult to ignore the need for probabilistic analysis of the changing climate hand in hand with the analysis of thermal performance of indoor spaces over an extended time scale. There is need to ensure that indoor spaces remain thermally comfortable and energy efficient both in the short term and long term future while being subjected to the warming effects of climate change. Using defined parametric thermal simulations, this study presents results of work that characterize the potential of climate change in Nairobi, Kenya on a number of passive design pathways with regard to their effectiveness in minimising indoor overheating effects of the increase in atmospheric temperature caused by climate change. By quantifying the extent of thermal discomfort as a function of the ambient climate scenarios and properties for the various parameters investigated, the most effective passive measures in reducing or eliminating the negative impacts of climate change on indoor thermal comfort and cooling energy consumption were identified for future climate projection A2 (2080-2100) for Nairobi. All in all, if a space is able to passively reduce overall indoor overheating, carbon emissions from the use of active means to meet the remaining cooling energy is reduced. This therefore resonates with the idea of adaptive mitigation.

Keywords: Climate change, Passive thermal comfort, Adaptation, Mitigation

INTRODUCTION

Predictions of the world's climate point to an increasingly warmer world [1]. In recognition of the strong evidence that climate change is happening, the impact of climate change on our built environment is a subject generating considerable interest. With the inevitable effects of global warming and the awareness that that buildings have a relatively long lifespan which could easily reach 50 to 100 years, heightens the need to look towards the future and institute appropriate measures now. This therefore prompts the need to future-proof buildings against the effects of a changing climate.

The central objective of this study is to evaluate a range of established passive[1] design strategies used in a tropical urban climate with regard to reviewing their effectiveness in reducing indoor thermal discomfort which is set to get worse in the changing climate. This

[1] The term "Passive design" in this study's context applies to low energy design achieved not by electromechanical means, but by the building's particular morphological organisation to enable the indoor temperature of the building to be modified through natural and ambient energy sources in the natural environment. [4]

study seeks to answer the question: To what extent will passive means of achieving indoor thermal comfort be able to reduce overheating of spaces? How effective will different approaches to passive comfort cooling be under a changing climate? How can tropical urban designs be best adapted to reduce further impacts of climate change and withstand ongoing changes of the increase in atmospheric temperature? It will, in the end, determine which passive means of adaptation perform 'best' in the worst case climate scenario future projection A2[2](2080-2100).

This inquiry is based on the premise that by changing design parameters such as shape, orientation, and envelope configuration, a high-quality designed building can consume 40% less energy and adapt better to climate than a low-quality designed one [2]. Using defined parametric thermal simulations, this study presents results of work that characterize the potential of climate change in Nairobi, Kenya on a number of passive design parameters with regard to their effectiveness in minimising the negative impacts of increase in atmospheric temperature caused by climate change. By quantifying the extent of thermal discomfort as a function of the ambient climate scenario and properties of various parameters investigated, the most effective passive measures in reducing or eliminating the negative impacts of climate change on indoor thermal comfort and subsequent cooling energy consumption were identified.

PARAMETRIC STUDY

Introduction

Studies on various passive cooling techniques are extensive and different scholars have established preferred passive cooling techniques suitable for Nairobi's (1°17′S 36°49′) tropical climate for the current (21st century) atmospheric temperatures [3] [4] [5] [6]. This study will investigate nine of these preferred passive design parameters alongside 5-6 design variables for each parameter undertaken for both current and future climate scenario A2(2080-2100) as listed here below:

a. Floor plate shape: Circle, Ellipse, Rectangle, Rhombus, Square, Trapezium, Triangle
b. Floor plate configuration: Elongated, M-Plan, Rectangular courtyard, Square courtyard, U-Plan, W-Plan
c. Floor plate orientation: 5^{o}East of North, NEE-SWW, NWW-SEE, E-W, N-S, NE-SW, NW-SE
d. Window to Wall ratio: 100% solid, 15% glazed, 25% glazed, 50% glazed, 75% glazed, 100% glazed
e. Window Orientation: North window, South window, East window, West window, East + West window, North + South window, Window on all sides
f. Glazing material: 4mm single glazing, 6mm single glazing, 10mm glazing with cavity, Double glazing, Low-E Double glazing, Low-E Triple glazing, Triple glazing.
g. External wall material: Fully glazed, Brick faced concrete, Heavy weight concrete, Insulated concrete, Light weight concrete, Aluminium, Stone.
h. External Shading devices: Balcony, Horizontal shading, vertical shading, recessed windows, Not shaded.
i. Ventilation rate: 2 Air changes per hour, 4 Air changes per hour, 6 Air changes per hour, 8 Air changes per hour, 10 Air changes per hour, 12 Air changes per hour

[2] The A2 scenario family describes a very heterogeneous world. The underlying theme is self reliance and preservation of local identities. An increasing population. Economic development is primarily regionally oriented and per capita economic growth and technological change more fragmented and slower than other storylines [1]

Software used

IES-VE[3], a dynamic building energy simulation software was used to perform thermal simulations. It consists of a suite of integrated analysis tools, which can be used to investigate the performance of a building either retrospectively or during the design stages of a construction project[4]. Climatic data for the two climate scenarios under study was input as outdoor temperature in IES VE software to perform indoor temperature analysis for each model. The software calculated indoor temperatures for one design day for each month. This study's results present average indoor temperature data calculated for Monday (24hrs) for all months in the respective climate scenario modelled.

Climatic Data used

Average monthly minimum and maximum temperatures, for the 20th Century(1960-2000) and A2(2080-2100) climate scenarios for Nairobi's Dagoretti meteorological station were downloaded directly from the IPCC Data Distribution Website. This climatic data will present results for extreme indoor temperature that is Low (1960-2000) and high (A2-2080-2100).

Simulation Assumptions

All spaces simulated are assumed to be free running with a floor to ceiling height of 3 metres and a floor depth of 5metres. Additionally, partitioning, doors, beams and columns have been omitted from the data input in IES VE simulating software. Isolated single room enclosures highlighting the various parameters listed above were analysed, with an assumption that the room under investigation is single banked (with a one room deep section) as illustrated in fig.1 below. This is in the view that a single banked room is a more challenging space to design for when it comes to reducing indoor heat gain from the ambient climate compared to double banked rooms et al. This room will be modified to pick characteristics of parameters under investigation and in the end, the most resilient parameters to extreme climate will be picked out for further investigation. Internal heat gains have been taken into account and included in the room temperature analysis between 8am to 6pm (Normal office working hours). These values are as listed in the CIBSE-A [7], under benchmark allowances for internal heat gains in a typical office building for a density occupation of $12m^2$ of floor space per person. The values used are as summarised here below:

- Heat gain from people= $6.7W/m^2$
- Heat gain from lighting with dimming allowance = $8W/m^2$
- Heat gain from equipment = $15W/m^2$

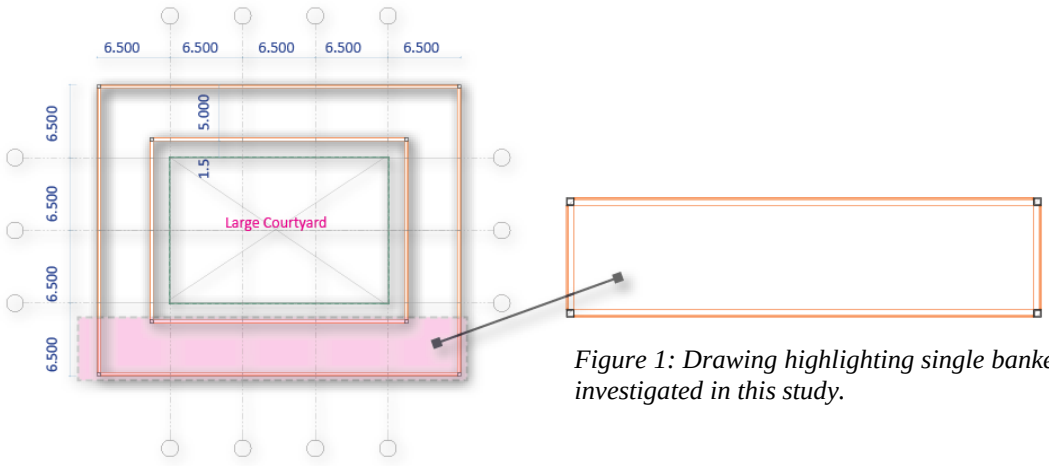

Figure 1: Drawing highlighting single banked room being investigated in this study.

[3] Virtual Environment by Integrated Environmental Solutions

[4] An overview of IES VE software is given online in :http://www-embp.eng.cam.ac.uk/software/iesve (Accessed March 2013)

Evaluation strategy:

To quantify the levels of thermal discomfort for each variable investigated, the thermal comfort temperature levels for each climate scenario was calculated using the Humphreys thermal neutrality formulae[5] for free running buildings [8]. The hourly values of indoor temperature above the thermal comfort levels per floor were then calculated over a 24 hour period of the design day for all the months and the net value of thermal discomfort in °C hours (°C h) was then calculated. Net thermal discomfort levels were used as the main performance index to pick out the most favourable passive strategies. The most favourable parameters were highlighted and later put together to perform an integrated effect.

RESULTS AND DISCUSSION

BEST PERFORMING PARAMETERS	NET VALUE OF THERMAL DISCOMFORT in °C hours (°Ch) 20TH CENTURY SCENARIO	NET VALUE OF THERMAL DISCOMFORT in °C hours (°Ch) A2(2081-2100_ SCENARIO
Trapezium	647.09	1096.61
Elongated Plan	650.36	1089.93
5 deg off NORTH SOUTH	754.28	1194.85
15% Glass	227.34	686.13
North Window	585.49	932.55
Double glazing	588.39	1046.92
Brick on Light weight Concrete	156.47	622.29
Recessed windows	244.46	1229.19
12 Air-change per hour	404.89	746.86

Table 1: A summary of the net values of thermal discomfort recorded for the best performing passive design parameters highlighted in Table 3.

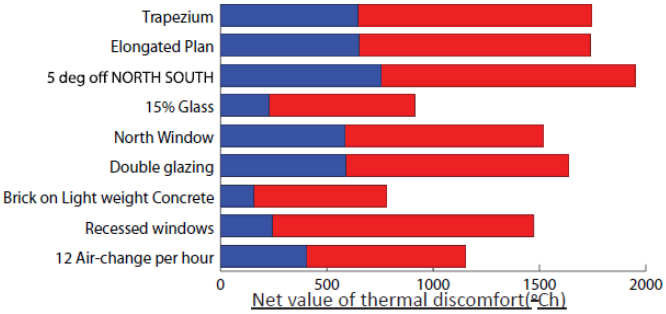

Graph 1: Graph illustrating the net values of thermal discomfort for the best performing passive design parameters highlighted in Table 3.

Table 1 and Graph 1 above summarize the results detailed in table 3. To investigate an integrated effect on indoor thermal comfort of the most favourable passive design strategies as identified above, a model with properties highlighted in table 1 was simulated in IES VE presenting results for 20th Century and A2(2080-2100) climate scenarios. Table 2 below summarises results of this integrated effect.

	NET VALUE OF THERMAL DISCOMFORT in °C hours (°Ch)	NO. OF HOURS ABOVE COMFORT TEMP	MIN. TEMP (deg C)	MAX. TEMP (deg C)	DIFF btw MAX n MIN (deg C)
20th CENTURY CLIMATE SCENARIO	236.05	126.00	15.61	23.06	7.45
A2(2081-2100) CLIMATE SCENARIO	568.35	168.00	20.80	30.54	9.74

Table 2: A summary of results for the integrated effect of the best performing passive design parameters

The results of an integrated effect of the most favourable passive parameters indicate that:

i. Although it doesn't completely eliminate the risk of overheating, an integrated effect of passive design strategies is more successful in reducing indoor thermal discomfort levels rather than one particular strategy in the two climate scenarios modelled.

ii. Thermal discomfort in A2 scenario is likely to be more than double that of the 20th Century scenario.

iii. We will have to persevere relatively high peak temperatures for longer in future climate A2(2080-2100) compared to the current scenario.

[5] Humphreys (1978) examined a large number of comfort studies, correlated thermal neutrality with the prevailing climate, and for free-running buildings suggested the equation Tn = 11.9 + 0.534 To.av (where To.av is the month's mean outdoor temperature), thus laid the foundation of the adaptability model. [6]

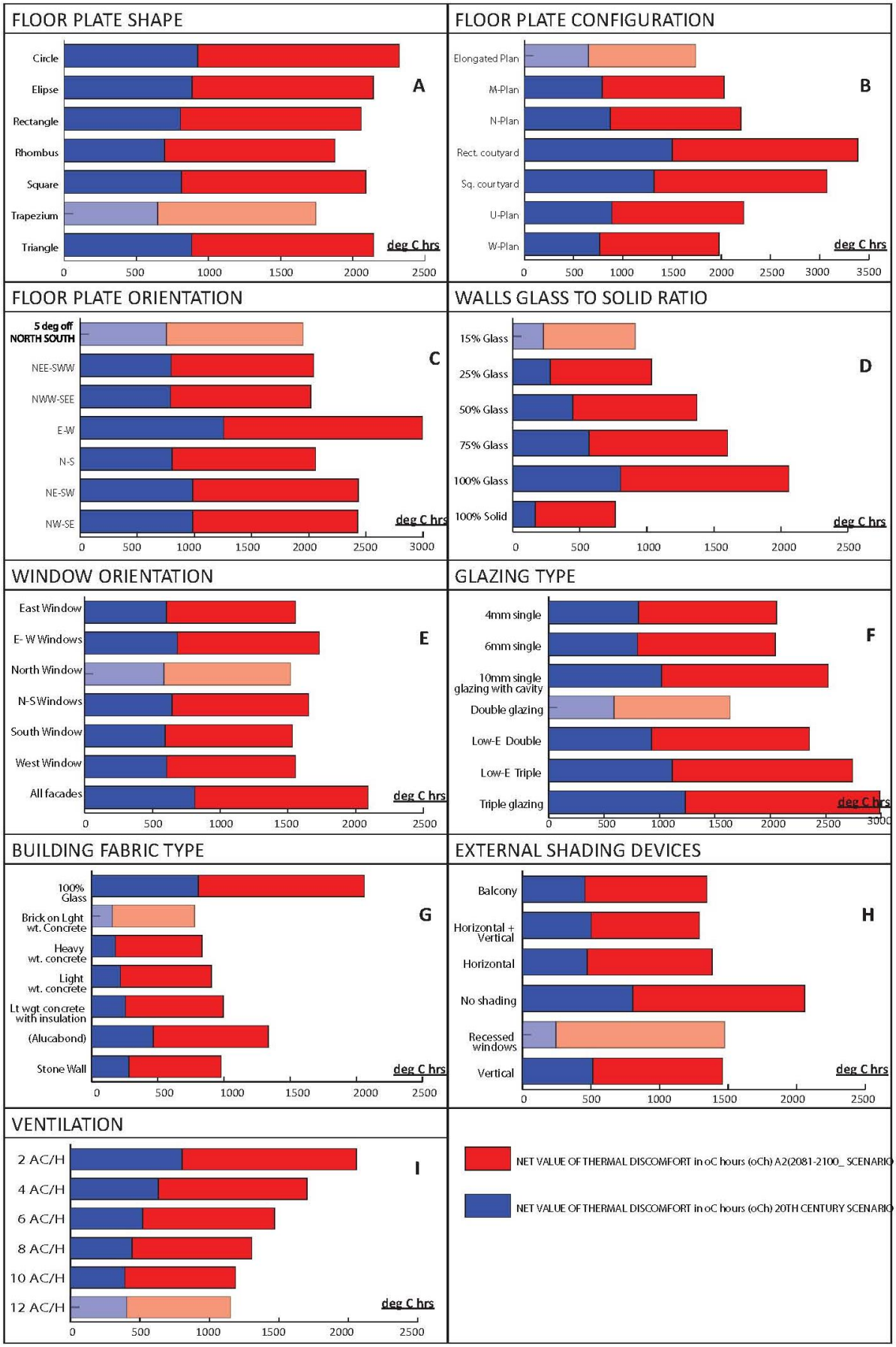

Table 3: Bar graphs summarising parametric results of the study. Highlighted in lighter shades are the best performing parameters under each design variable investigated.

.

CONCLUSION

The main purpose of this study was to gain a deeper understanding of the role of established passive design strategies outlined by various authors in the delivery of thermally comfortable indoor spaces in a changing tropical climate. Passive design parameters were evaluated within two clearly defined climatic contexts: The 20th Century and A2(2080-2100) climate projections specifically for Nairobi, Kenya. In summary, the results of this small study suggest that:

i. As expected, design elements such as the spatial layout of the building; its orientation; the number, size and location of windows; shading devices around it; the thermal resistance and heat capacity of its envelope as well as its orientation with respect to the sun path have a significant effect on indoor thermal comfort. However, no combination of passive design parameters is able to entirely eliminate the risk of overheating in the two climate scenarios investigated.

ii. The relationship between increase in external temperature due to climate change and increase in internal temperature and indoor thermal discomfort is linear.

iii. Even in the best performing buildings, compromise is an inevitable part of design and specification. Therefore, passive design considerations will no doubt be subject to the process of trade-off in achieving the right balance of priorities for a particular project. A balance of day lighting and visual comfort with the outdoors and natural ventilation should be achieved while at the same time trying to achieve the most favourable indoor thermal temperatures that requires a smaller window to wall ratio.

iv. There is need to cool the thermal mass of the external walls at night in Nairobi's climate given that external walls are likely to store a lot of heat energy from the sunlit hours during the day, which makes night cooling of the walls ideal. Light weight and low thermal mass envelope materials seemed to be most favourable for Nairobi's climate, especially the ones that display multidirectional heat effects that ensure the retarding of as much heat as possible during the day and at the same time having a higher rate of heat loss at night when the outdoor temperature is low.

This study was motivated by the world's increasing concern about the effect of global warming on the built environment. The presented work aims to contribute to the selection and application of building design strategies which aim to prevent and/or reduce indoor overheating of free-running office buildings in Nairobi's carbon constrained tropical climate.

REFERENCES

[1] IPCC, *Climate Change 2007 - The Physical Science Basis: Working Group I Contribution to the Fourth Assessment Report of the IPCC*. 2007.

[2] J. O. Lewis, *A Green Vitruvius: Principles and Practice of Sustainable Architectural Design*. Routledge, 1999, p. 152.

[3] B. Givoni, *The Passive and Low Energy Cooling of Buildings*. 1994.

[4] Ken Yeang, *The Green Skyscraper: The Basis for Designing Sustainable Intensive Buildings*. 1999.

[5] S. . S. Otto H. Koenigsberger, T G Ingersoll, A Mayhew, *Manual of Tropical Housing and Building: Climatic Design Pt. 1*. 1974.

[6] S. V Szokolay, *Introduction to Architectural Science: The Basis of Sustainable Design*. 2004.

[7] CIBSE, *Environmental Design (CIBSE Guide A) by Chartered Institution of Building Services Engineers*. 2006.

[8] ed M. Sala, *Architecture - Comfort and Energy: M. Sala: Books*. 1999.

POST OCCUPANCY EVALUATION AND ENERGY PERFORMANCE ASSESSMENT FOR ENERGY CONSERVATION AND OCCUPANT SATISFACTION

Jihyun PARK; Kevin LI ; Carl COVINGTON; Azizan AZIZ

School of Architecture, Carnegie Mellon University, Pittsburgh, PA 15213, USA

ABSTRACT

Energy performance modelling can provide insights into the efficiency and sustainability of commercial buildings, and also the achievement of certification standards such as USGBC LEED. However, the results from the modelling must be validated via a post-construction evaluation, which quantifies any discrepancies between the predicted energy usage and the actual energy consumed. In this study, an existing office building was examined to test how well the model predicts energy usage. The results from the model were com-pared with the actual usage of gas and electricity over two years (2010-2011). Our study showed a 123% higher in gas usage, and a 36% lower in electricity, compared with the simulation. This difference presents that occupant behaviour and building construction practices have significant impact on the energy usage of a building. For instance, the large discrepancy among gas usage is due to the office building's thermal envelope, which identifies the spots at which heat leaks out of the building, thereby forcing the heating unit to work more. Additionally, post occupancy evaluation study identified that indoor environmental conditions impact on energy consumption of the building.

Keywords:. Indoor environmental quality; Post occupancy evaluation; Energy simulation; Energy efficiency; User Satisfaction

INTRODUCTION

There is often a significant discrepancy between the designed and the actual total energy use in buildings. The reasons for this difference are generally poorly understood, and often have more to do with the role of human behaviour than the building design.

One limitation of current research would be that it focuses mostly on building-related factors, such as climate, building envelope and HVAC systems rather than human related aspects [7]. All of the factors, however, including building operation, occupants' activity and behavior, and indoor environmental quality, need to be analyzed using real measured energy consumption data [6,7].

Post occupancy evaluation (POE) is one of the most important efforts for energy consumption reduction while enhancing indoor environmental quality and occupant satisfaction. Raftery et al pointed out that user patterns would be a one of the important factors for total energy consumption modeling and adjustment of error [9]. Loftness et al showed that measured field data on IEQ, user satisfaction and the technical attributes of building systems (TABS) supports ongoing opportunities for energy conservation while meeting IEQ standards [2,6].

The goal of this study is to better understand and strengthen the knowledge for effective total energy usage in buildings by analyzing energy usage and expenses, sustainable practices and materials during construction, and the indoor environment quality.

We highlight areas of efficient performance, as well as deficiencies within the building. Following our assessment, we provide strategies that can improve its energy efficiency,

occupant comfort and the building's marketability through additional the U.S. Green Building Council (USGBC) Leadership in Energy and Environmental Design (LEED) certification. These strategies will also factor in the cost of adopting the recommendations to provide the building owner with insights into the return from such investments, since not all benefits are quantifiable.

METHODS

Our approach for assessing the overall performance of the commercial building is to focus on three areas: thermal envelope, energy usage and indoor environment quality. The energy usage comparison was conducted through the use of gas and electricity bills dating back to May 2010. This data was then compared to the energy simulation conducted using the eQUEST DOE-2 based simulation modelling tool [8]. Energy consumption was normalized for the heating and cooling degree-days to determine how well the building was actually performing.

To evaluate the thermal envelope, we used a thermo graphic camera to take pictures of the building exterior, work areas and the wall connections of the entire indoor space. This enabled us to identify areas of heat loss inside and outside the building. We also researched the materials of the building and their respective U-Values to compare with our actual findings from the pictures taken. Lastly, indoor environmental quality field measurements were taken over two days in the office building in Pittsburgh, PA. The first measurements were taken on April 2nd, 2012, and the second set on April 17 and 18, 2012. Both were workdays with a number of employees present in the office. On the first day, thermo graphic pictures, digital photos, surveys and NEAT cart measurements were taken for all rooms and spaces, including the basement. The subsequent days were used to capture additional thermo graphic and digital pictures, conduct interviews, distribute longer occupant surveys, and setup the 24-hour Airquity measuring system.

ANALYSIS OF CURRENT CONDITION

Building information, Equipment, and Controls

The building in this case study is Architectural building (Figure 1, Figure 2) in Pittsburgh, PA and is owner occupied. It has 1 ½ floor plus a basement. The total floor area is 1,650 ft^2 (153 m^2) with a conditioned volume of 23,100 ft^3 (654 m^2). The total wall and window area is 2,716 ft^2 (252 m^2) and 182 ft^2 (27 m^2), respectively. When the TAI+LEE group took over the building it had to be completely reconstructed since there was no insulation, and the roof had caved in. Therefore, they had to start from scratch by reconstructing the floor, walls and roof.

Figure 1. Exterior

Figure 2. Work area

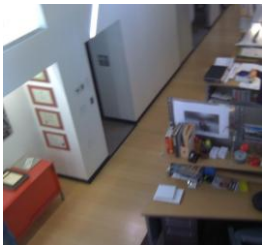

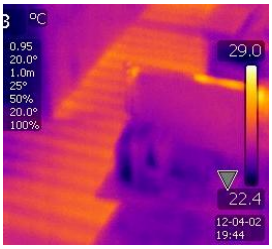

Figure 3. Radiant floor & thermal graphic image

The radiant floor system serves as the primary heating unit for the building (figure 3). It has a much smaller rated output of 42 kBTU/h versus 117 kBTU/h for the standard building. Its performance ratings are 96 for the EFF and 17 for the EER, compared to 80 and 8.9 for the traditional unit. TAI+LEE also installed a supplemental air heat pump to heat and cool the

building during extreme weather conditions. Although this system was installed to operate under the most extreme weather conditions, it is a high efficient system with a variable speed blower motor and is rarely used throughout the year.

The building is ventilated using two ERV systems, one in the basement (130cfm) and one on the first floor (200cfm) above the bathroom. The unit in the basement must be in constant operation to help control for humidity. However, the unit in the first floor is not used as often, since it is sufficient to manually ventilate the space by opening the windows on the north and south walls and the skylights.

Another controller is responsible for the ERV, AC and heater as a sub-system. Under normal conditions, passive techniques for ventilation are used, such as opening the skylights or front and rear windows. We noticed that the employees rarely used this control due to its multiple settings and the necessity to readjust once comfort level is reached. Although they prefer passive techniques, it has its own inconveniences, as workers tend to stay focused until the thermal comfort is unbearable. When the ceiling fan was turned on, it made a significant positive impact for air circulation.

Interviews conducted with the employees revealed that the indoor thermal controls were complicated to use, and most preferred to leave it alone. There are multiple devices for controlling various systems in the building. When the building was first finished, the central thermostat did not have an automated timer. This resulted in a significant time lag between when it was turned on and when the radiating floors would come into effect. A workaround for this was to turn on the heat pump while the radiating floor system took time to ramp up. Consequently, this resulted in higher electricity use until they installed an automated mechanism that set the temperature to 72°F (22.2°C) at 6 AM in the morning and 65°F (18.3°C) after 8 PM and on weekends

ENERGY ANALYSIS AND RESULTS

Thermal Envelop

One method to understand the large discrepancy among gas usage is to assess the office building's thermal envelope. This helps to identify the spots at which heat leaks out of the building, thereby forcing the heating unit to work more. A thermo-graphic camera identified multiple spots of heat loss on the front sidewall of the building.

A blower door test was performed for this building in 2008. The simulated infiltration was 0.3 ACH (Air exchange per hour), but the results from the test returned 0.4 ACH. The leaks, which were from the wire installations of the solar PV panels located on the second floor, were supposedly fixed shortly thereafter. However, Thermal graphic image shows some residual heat loss at the junction between the roof joist and the wall. Also, there are additional leaks in the conference room. Overall, the majority of the leaks occur in the north wall/area of the building (Figure 4, Figure 5)

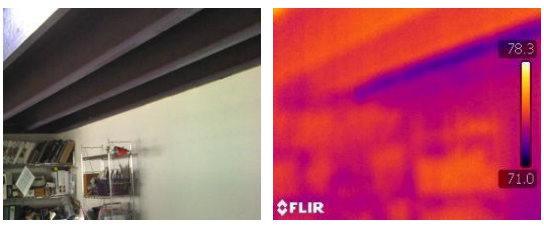

Figure 4. Images of loft ceiling area (Left: normal, Right: thermal Image)

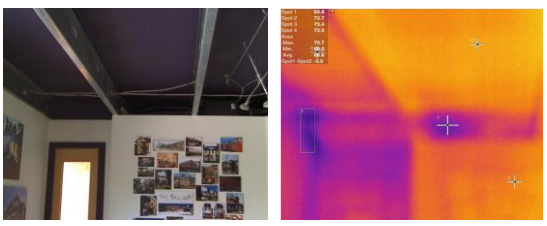

Figure 5 Images of conference area (Left: normal, Right: thermal Image)

Comparison of Simulation and Energy Bill

An energy simulation was conducted on this project via eQUEST software and was compared against a reference case commercial building with the same floor area, volume and weather conditions (Pittsburgh, PA, USA). This building has a 36% lower average u-value for the entire building (0.051 btu/hr-ft2-f), with increased R-values coming from the roof, floor and windows construction. In addition, it employs a more efficient and smaller HVAC system due to the improved thermal envelope. In addition, it contained only 2% total duct leak, compared with the expected 11% for the reference commercial building. Therefore, TAI+LEE outperforms the reference case by 52% on cost and 32% on electricity use over the course of the year.

Although the simulation shows that the building surpasses the reference commercial building, we wanted to compare the actual performance of the building to the simulated results. Based on the gas and electricity bills, this project used a total of 130,807 and 103,171 kBTUs for the years 2010-2011 and 2011-2012, respectively. The simulation estimated a total energy usage of 101,184 kBTUs. However, the heating degree day (HDD) and cooling degree day (CDD) for 2008 may be different than those for which we analysed. Therefore, we normalized each year's total energy usage by its respective HDD and CDD and separated it by electricity and gas use (Figure 6). Comparing their EUI to the 2003 CBECS data for office buildings, this building fell within the 25th percentile for electricity use (6.98 kWh/sq. ft.). However, their natural gas (47.09 cf/sq. ft.) put them in the 50-75th percentile range. This agrees with the findings above that they are using electricity efficiently, but gas use is suboptimal - possibly due to leaks within the thermal envelope.

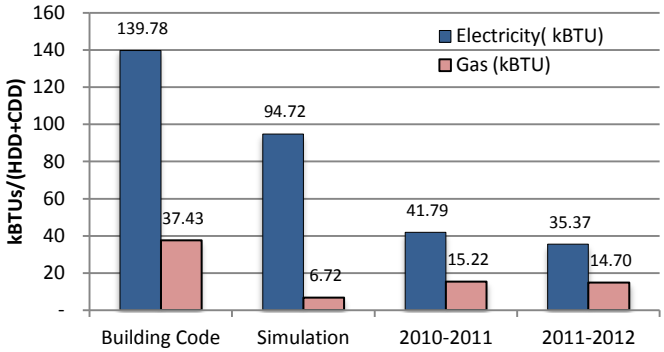

Figure 6. Normalized Energy Usage

Indoor Environmental Quality Evaluation: Thermal Comfort

In order to enhance the environmental profile of the work group beyond the descriptions possible with spot measurements, twenty-four hour continuous measurements were taken in one location of the office. An Aircuity Optima system is utilized to measure temperature, relative humidity, CO_2, CO, large and small particulates, TVOC, radon, and ozone. In this study, we are focused on thermal environmental qualities and findings.

Spot and 24 hour continuous air temperature measurements (1.1m, 0.6m, 0.1m) ranged between 68-78°F (20 - 25.6°C), average 73°F (22.8°C), comfortably within the seasonal comfort zone (Figure 7).

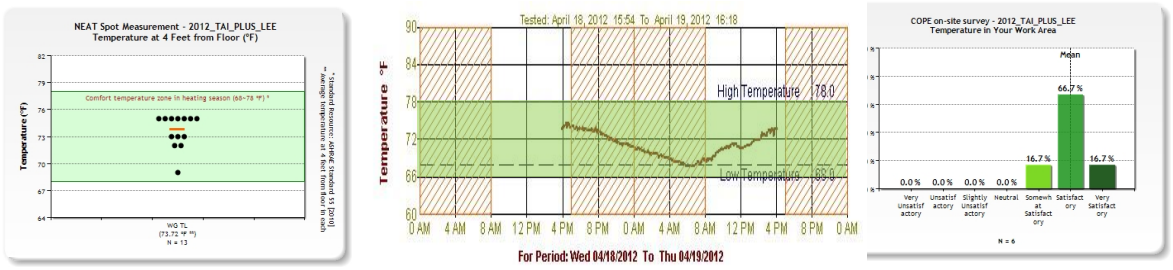

Figure 7. IEQ thermal comfort measurement and user satisfaction survey result

CONCLUSION AND DISCUSSION

Comparative analyses showed that energy usage discrepancies between the predicted and actual usages were significant. Based on the gas and electricity bills, the building used a total of 130,807 and 103,171 kBTU for the years 2010-2011 and 2011-2012, respectively, whereas the simulation predicted a total energy usage of 101,184 kBTU. The TAI+LEE commercial building was a well-thought out and executed retrofit on a dilapidated storage garage. Its use of high-quality, sustainable materials and selection of HVAC components are impressive. The electricity EUI was excellent as it fell within the 25th percentile of office buildings surveyed in the 2003 CBECS, and outperformed its energy simulation in 2008. In regards to the indoor environment quality, all measurements were within the comfort range and all employees enjoyed working in the building. With that said, there were some areas that could have been improved. The natural gas EUI did not perform as well, since it fell within the 50-75th percentile of the CBECS 2003 [3].

Since the HDD and CDD may vary year by year, each year's total energy usage was normalized by its respective HDD and CDD and separated it by electricity and gas use. Although the simulation predicted the total energy use relatively well, larger discrepancies were found after differentiating between electricity (36% lower than actual) and gas use (123% higher than actual). In general a building simulation analysis is expected to predict the usage in less than 10%. One method to understand the large discrepancy among gas usage is to assess the office building's thermal envelope. This helps to identify the spots at which heat leaks out of the building, thereby forcing the heating unit to work more. A thermo-graphic camera identified multiple spots of heat loss on the front sidewall of the building. It infers that that occupant behaviour and building construction practices may have significant impacts on the energy usage of a building. Accordingly, the design of a building needs to be incorporated with occupants' behaviours and interaction with their indoor environment. Additionally, it would be better that building codes and certification standards include requirements for best practice at construction sites to ensure proper installation and storage of materials.

Simplify Control Systems

The appearance of multiple controls mounted on the wall can be daunting for new and existing employees. Currently, the central thermostat control for floor heating does not need to be adjusted, since it is running on a timer and thermostat. The sub control can adjust the A/C, fan and heating, but is rarely used due to its complexity and the employees' aversion to making too many adjustments. Our first recommendation is to provide another training session solely for the Mitsubishi control and to educate them on the situations for appropriate use.

Although employing a consolidated automation control system would not be practical under current conditions, this could have been an option during the initial retrofit. Integrating once of these systems would remove the wall full of controllers and consolidate it into one touchscreen unit. The primary benefit of such a system would be difficult to quantify, but can provide much more convenience and comfort for employees, thereby increasing productivity, and additional security for the building.

ACKNOWLEDGEMENT

This material is based upon work supported by the Energy Efficient Buildings (EEB) Hub, an energy innovation hub sponsored by the Department of Energy under Award Number DE-EE0004261.

Authors acknowledge Stephen Lee, Yoko Tai, Erica Cochran, David Epley and Vivian for valuable support, discussions, and comments.

REFERENCES

1. ASHRAE. (2010). Performance Measurement Protocols for Commercial Buildings: American Society of Heating, Refrigerating and Air Conditioning Engineers
2. Aziz, A., Park, J., Loftness, V., & Cochran, E. (2012) Field measurement Protocols for Evaluating Indoor Environmental Quality and User Satisfaction in Relation to Energy Efficiency. U.S. DOE The Energy Efficient Buildings Hub, DOE, USA
3. CBECS. (2003). 2003 Commercial Buildings Energy Consumption Survey
4. Gundala, S. (2003). LEED Energy Performance Modeling and Evaluation of the ST Dana Building Renovations: A Practicum Submitted in Partial Fulfillment for the Degree of Master of Science (Natural Resources and Environment). University of Michigan, USA
5. Effinger, J., Effinger, M., and Kramer, H., PECI. (2012). Overcoming Barriers to Whole Building M&V in Commercial Buildings Paper presented at the ACEEE. http://www.aceee.org/files/proceedings/2012/data/papers/0193-000102.pdf
6. Loftness, V., Aziz, A., Choi, J., Kampschroer, K., Powell, K., Atkinson, M., & Heerwagen, J. (2009). The value of post-occupancy evaluation for building occupants and facility managers. Intelligent Buildings International, 1(4), 249-268. doi: 10.3763/inbi.2009.SI04
7. Yoshino, H. (2009). Total energy use in buildings-analysis and evaluation methods. In I. ECBSCS (Ed.), analysis and evaluation methods. UK
8. eQUEST, the Quick Energy Simulation Tool, http://www.doe2.com/equest
9. Raftery, P., Keane, M., & Costa, A. (2009). *Calibration of a detailed simulation model to energy monitoring system data: a methodology and case study.* Paper presented at the Proceedings of the 11th IBPSA Conference, Glasgow, UK

IMPACT OF THE SUN PATCH ON HEATING AND COOLING POWER EVALUATION: APPLIED TO A LOW ENERGY CELL

A.Rodler[1]; J.Virgone[2]; J-J.Roux[3], J.L.Hubert[4]

1-3: CETHIL, UMR5008, CNRS, INSA-Lyon, Université Lyon 1 20 Av A. Einstein, 69621 Villeurbanne Cedex, France

4: Site EDF R&D des Renardières, Avenue des Renardières – Ecuelles, 77818 MORET-SUR-LOING Cedex, France

ABSTRACT

In the context of low energy buildings we study the impact of the incoming radiation through a window (sun patch) on the heating and cooling demand. Existing studies have shown that not considering the sun patch and fast climatic variations (Figure 4, Global radiation) can lead to important differences in energy power evaluation [1, 2, 3]. In this paper we present a 3D envelope model taking into account the minute-wise sun patch evolution. Simulation results are analysed for a low energy cell.

A numerical model has been developed in order to simulate the transient thermal behaviour, with a refined spatial (3D) and temporal (down to one minute time step) discretization of the single room. For each node of the grid, the energy conservation equations are developed. They traduce balance between short-wave and long-wave irradiations, convection, air enthalpy and three-dimensional heat conduction. The particularities of the program are that it projects the sun patch on the inner walls, the conduction is treated in three dimensions and climatic minute-wise variations are taken into account.

As main results, the surface temperature evolution, the air temperature evolution and the heating or cooling power necessary to maintain an inner air set-point temperature are calculated at each time-step. Heating or cooling power is compared to the power calculated with no sun patch incorporation (solar loads only on the floor). Conclusions are made on the importance of the integration of the sun patch and its impact on the observed results.

Keywords: sun patch, fast climatic variations, heating and cooling power, insulated cell

INTRODUCTION

Electrical energy savings has become an important issue. Among the consumption sources, the building's sector represents 40% of the consumed energy in France. The heating power represents 2/3 of the total power consumption of the buildings sector [4] so that, in January 2009 for example, heating power represented a third of the total maximal power demand [5] (Figure 1). Therefore, a particular attention is given to the development of low energy buildings, which are strongly insulated and require less energy demand.

Very often, the overall power charged by the supplier is done according to simplified models, which do not evaluate the power peaks in time and do not integrate fast climatic variations in time [6]. On Figure 2, we can observe power discrepancies: the power charged by the supplier compared to the power measured does not overlap. The power charged by the supplier does not evaluate variations in time of the power consumption.

In dynamic simulations, the predominant method used to estimate the heat load is done by using the heat balance equation of the zone [7, 8, 9]. The heat is supplied to the air node by convection and/or radiation. Then, the heating load is estimated in order to reach the set-point

temperature. When the temperature of the zone is higher than its set-point, the value of the load is set to zero. This method is coupled to the transient behaviour of the zone. In TrnSys for example, in order to describe a building zone, the walls have to be defined. They are considered as "black boxes" and the "thermal history" of the walls is defined using the transfer function method [10]. Using TrnSys for simulations of high thermal inertia walls, when they reach a certain value of thickness, can lead to important problems [11, 12, 13]. Also, heat conduction transfer through a wall is evaluated in one dimension, only.

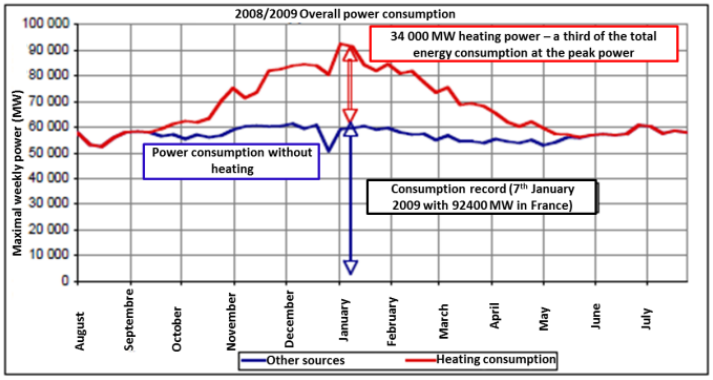

Figure 1: Heating power among the overall power consumption

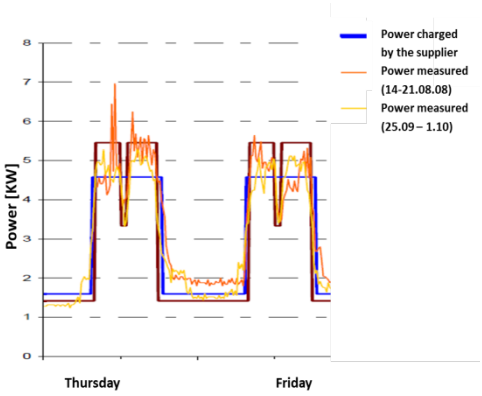

Figure 2 : Power charged by the supplier

The aim of the actual work is to better evaluate the power peaks for low energy buildings. In order to do this, it is important to better model the envelop so that it takes into account more accurately the weather variations in time. In order to consider weather variations in time we use one minute time-step weather data and the sun patch is located for each minute. In order to locate the sun patch, we have discretized the walls in control volumes and used the 3D heat conduction equation in order to model more accurately the heat exchanges through the walls. Then, the heating or cooling load is evaluated for given set-point temperatures.

METHOD

The building envelop is modeled following a three dimensional approach. The model represents a single room with a window.

The walls of the model are discretized. However, only a single air node is taken, considering that the air stratification has been neglected in this study in regard to the surface temperature distribution. The partial differential heat conduction equation in three dimensions for the temperature of the control volumes is applied to all the volumes of the cells. The heat conduction equation has been coupled to the convective and radiation exchanges.

$$CV\frac{\partial T}{\partial t} = \lambda_x\left(\frac{\partial T}{\partial x}\right)_{x+\frac{dx}{2}} dydz - \lambda_x\left(\frac{\partial T}{\partial x}\right)_{x-\frac{dx}{2}} dydz + \lambda_y\left(\frac{\partial T}{\partial y}\right)_{y+\frac{dy}{2}} dxdz - \lambda_y\left(\frac{\partial T}{\partial y}\right)_{y-\frac{dy}{2}} dxdz + \lambda_z\left(\frac{\partial T}{\partial z}\right)_{z+\frac{dz}{2}} dxdy - \lambda_z\left(\frac{\partial T}{\partial z}\right)_{z-\frac{dz}{2}} dxdy + \Phi_{TOT} \quad (1)$$

where

$$\Phi_{TOT} = \Phi_{SW} + \Phi_{LW} + \Phi_{CONV} \quad (2)$$

Φ_{CONV} is the convective heat flow between the surfaces and its environment and Φ_{LW} and Φ_{SW} are the long wave and short wave radiations. Thermal conductivities in the three directions are designated as $\lambda_x = \lambda_y = \lambda_z$ [W/mK] and the volumetric heat capacity is denoted by C [J/m^{3}K]. A particular attention is given to the short wave radiations absorbed by the surfaces of a control volume, as it will depend on the sun patch location. The short wave radiations absorbed by the surfaces of a control volume come together in the vector $\{\Phi_{SWI}\}$ and are calculated by:

$$\{\Phi_{SWI}\} = [S][a_{SWI}]\{E_{SW}\} \quad (3)$$

where [S] is the surfaces matrix and $[a_{SWI}]$ is the matrix of absorptivity of the internal wall for the short wave radiations. $\{E_{SW}\}$ is the vector of radiations received by the meshes obtained resolving:

$$[S]\{E_{SW}\} = [S]\{E^{\circ}_{SW}\} + [S][\rho][FF]\{E_{SW}\} \quad (4)$$

where $[\boldsymbol{\rho}]$ is the reflectivity matrix, $[FF]$ the view factors of the matrix which are calculated following the Nusselt analog. $\{E_{SW}^{\circ}\}$ is the vector composed by primary radiations received by the control volumes. It results from the horizontal beam radiation G_b and the diffuse radiation G_d received by the meshes:

$E^{\circ}_{SW,i} = \tau_b G_b R_b + \tau_d G_d R_d$, if the element i is in the sun patch

$E^{\circ}_{SW,i} = \tau_d G_d R_d$, if the element i is not included in the sun patch (5)

τ_b and τ_d are the direct and diffuse transmission coefficients of the glass and depend on the incidence angle of the beam, whereas R_b and R_d allow to calculate direct and diffuse radiation on titled surfaces, with p the slope of the surface. The sun patch position has been calculated by a geometrical test: the boundary of the window is projected on an orthogonal plane to the beam. The control volumes of the walls are projected on the same plane, and thus those projected cells belonging to the projection of the window are identified. The energy balance equation for the air in the cavity with temperature T_{ai} is:

$$\rho C_{air} V_c \frac{\partial Tai}{\partial t} = \sum_{n=0}^{N} Q C_{air}(T_{ae} - T_{ai}) + \sum_{j=1}^{NM} Sh_{ci}(T_{SI} - T_{ai}) \quad (6)$$

where T_{ae} is the exterior dry bulb temperature (°C), Q is the air flow (kg/s), C_{air} the heat capacity of the air (J/kgK), $\boldsymbol{\rho}$ the air density (kg/m^3), V_c the volume of the cavity, T_{SI} the interior surface temperature and h_{ci} the convective transfer coefficient. NM is the number of radiation balance equations corresponding to the number of surface mesh elements and N the number of zones (here N =1).

When wanting to maintain a set point temperature of 20°C for example, we maintain the set point temperature to 20°C and heat power is instantaneously injected on the air node.
Differential equations 1 and 2 are solved with a function of Matlab (ode23t). This function solves moderately stiff ordinary differential equations using the trapezoidal rule or Runge Kutta. This method solves the equations with an adapted and variable time-step, depending on the fluctuations of the data.

CASE STUDIES AND HYPOTHESES

We have modelled a single cell, similar to an existing in situ experimental set up. Five walls among the six are strongly insulated (U = 0.099 W/m²K) and therefore heat losses through

these walls are very small. Slightly higher losses take place through the south oriented wall, which has a window (U_{wall} = 0.277 W/m²K and U_{window} = 5.95 W/m²K). This room has a small thermal inertia and is highly insulated. The dimensions of the room are: 2.98 m in width, 2.89 m in depth and 2.83 m in height and the window's area measures 1.3×1.3m². The weather data is existing one minute time-step data from Vaulx-en-Velin of 2011[14]. The six walls and the window describing the cell contain 11000 control volumes, with a refined meshing near to the surfaces of the walls.

The first case study evaluates the cooling power necessary to maintain an inner set point temperature of 25°C, in July. Again, two models are studied: the first projects the incoming radiation on the floor (M1) and the second locates the sun patch throughout the day (M2).

The second case study consists in evaluating the power necessary to maintain an inner set point temperature of 20°C, in January. Two models are used: M1 and M2.

RESULTS OF DYNAMIC SIMULATIONS

For the first study, we evaluated cooling power for two days: 11th and 12th July 2011. Inside temperature was fixed to 25°C and cooling power was calculated for M1 and M2. For both models the incoming radiant flux is the same but it has been projected differently on the cells. On the 12thJuly (15h UTC) we observe the inside temperature distribution for the two models M1 and M2. Figure 3a/ shows that the sun patch touches some of the cells of wall 3 and 2. In Figure 3b/ the incoming radiation has been projected on all the cells of the floor. We can observe that the floor cells' are warmer than the other cells of the room. This last model follows the traditional taken hypotheses by most of the simulation tools.

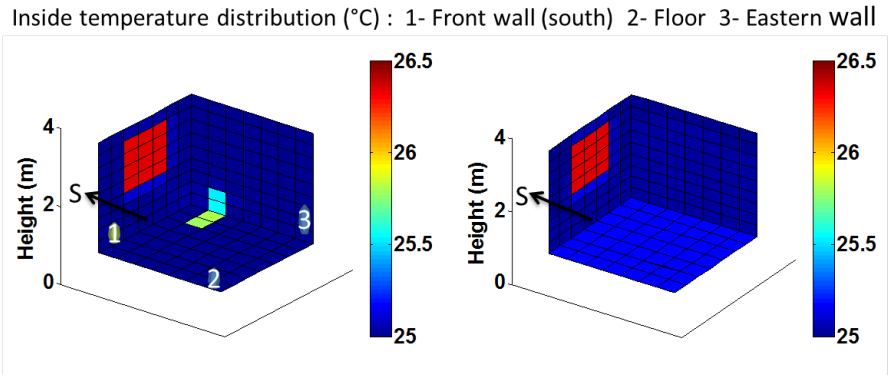

Figure 3: a/ with sun patch (M2) b/ incoming radiation projected on the floor (M1)

Despite the 25°C set point temperature, we notice differences on the temperature field (Figure 3) between both models. Maximal variations of 0.4°C are observed between the cells of the sun patch and the floor when comparing both models. This can explain the discrepancies between the two models when evaluating the power.

Cooling power is between 0 and 50W and gets more important when the temperature and the incident radiation is rises (Figure 4). Cooling power of M1 and M2 are compared. Discrepancies are observed, represented by the red area. Differences are larger when important solar fluctuations occur, during the day (red area). During this period the two models will project spatially the incoming radiation differently. With the sun patch model (M2) we have less cooling demand. For these two models and days of July, we have a relative difference of 83.9 %.

For the second case, we modelled the heating power necessary to maintain 20°C (Figure 5). Powers between 30 and 45 W are calculated. We observe discrepancies between these two models only during the day time, as for the other configuration. With the sun patch model, more heating is required during the day. A relative difference of 3.6 % is obtained between these two models.

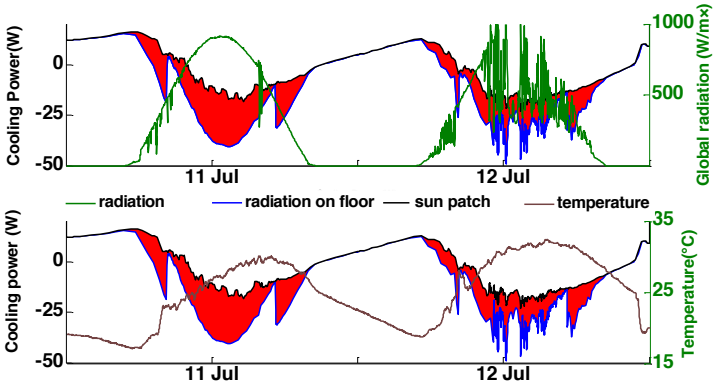

Figure 4: Cooling demand for M1 and M2

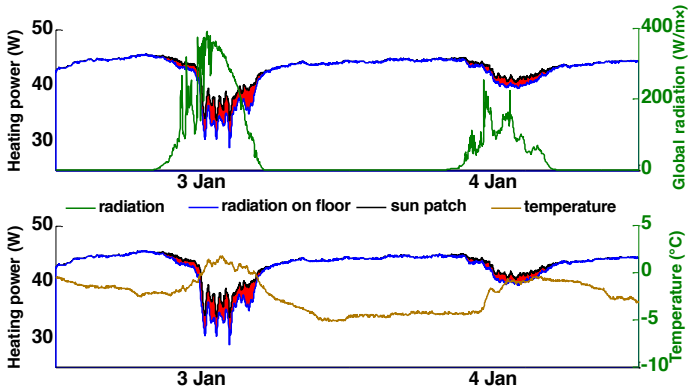

Figure 5: Heating power demand for a set point of 20°C for the two models

CONCLUSIONS

A 3D transient envelope model has been developed. In this model, we discretized the walls in small control volumes, with a refined meshing towards the surfaces. This spatial discretization enables to know where the sun patch is located at each time step. The weather data was sampled at a minute time-step, in order to take into account the fast climatic variations in time.

We applied this model to a low energy cell case, strongly insulated. A general similar trend between the results with the sun patch model and the results of S. Dautin [3] was found, knowing that we have a 3D model and in her work only 1D exchange were modeled. In the observed results of this paper, it seems important to consider the sun patch position for days with clear sky conditions. Higher discrepancies are observed between the two models for the cooling power demand than for the heating power demand. Taking too simplified hypotheses, like done with model M1, for clear sky conditions, could lead to important errors. These results were found for an important insulated cell but future studies for different configurations of cells will be realized in order to draw broaden conclusions on the impact of the sun patch on power demand.

These results have to be validated with experimental data, and therefore we are working on an in situ experimental set up.

REFERENCES

1. M. Wall, « Distribution of solar radiation in glazed spaces and adjacent buildings. Acomparison of simulation programs », Energy and Buildings, vol. 26, no 2, p. 129–135, 1997.
2. P. Tittelein, « Environnements de simulation adaptés à l'étude du comportement énergétique des bâtiments basse consommation », Thèse de Doctorat, Université de Savoie, 2008.
3. S. DAUTIN, « Réduction de modèles thermiques de bâtiments: amélioration des techniques par modélisation des sollicitations météorologiques », Thèse de Doctorat, Université de Provence, 1997.
4. Stratégie utilisation rationnelle de l'énergie, chapitre II : « Les bâtiments », Ademe, www2.ademe.fr
5. La pointe d'électricité en France, Dossier de Presse, 2009. www.negawatt.org
6. C. Weinmann, S. Pasche, F. Gass, J. Beck, et C. Grange, « Prévision et justification des consommations d'électricité pour 3 catégories de bâtiment », Echallens, Suisse, Weinmann-Energies SA et Ecost, Rapport annuel, 2008.
7. TRNSYS 16 documentation, 'Volume 6: Multizone Building modeling with Type56 and TRNBuild'
8. EnergyPlus, Energy Plus Engineering Reference, Lawrence Berkeley National Laboratory, 2009
9. CODYBA www.jnlog.com/codyba1.htm
10. G.P Mitalas, D.G. Stephenson, 'Calculation of Heat Conduction Transfer Functions for Multi-Layer Slabs', ASHRAE Annual Meeting, Washington, D.C., August 22-25, 1971.
11. J. Savoyat, K. Johannes, J. Virgone, 2011. Integration of thick wall in TRNSYS simulation. ISES solar world congress, Kassel, Germany, 2011
12. C. Flory-Celini, 'Modélisation et positionnement de solutions bioclimatiques dans le bâtiment résidentiel existant', Thèse de Doctorat, Université Claude Bernard Lyon 1, 2008
13. B. Delcroix, M. Kummert, A. Daoud, and M. Hiller, « Conduction Transfer Functions in TRNSYS multizone building model: Current implementation, limitations and possible improvements », Fifth National Conference of IBPSA-USA, Madison, Wisconsin, August 2012.
14. International Daylight Measurement Programme, Station de l'ENTPE de Vaulx-en-Velin, http://idmp.entpe.fr/vaulx/stafr.htm

ANALYSIS OF OPTIMAL FENESTRATION PARAMETERS FOR A PASSIVE SOLAR OFFICE BUILDING IN SERBIA

S. Stevanović[1,2]

1: University of Primorska, Institute Andrej Marušič, Muzejski trg 2, 6000 Koper, Slovenia

2: University of Niš, Faculty of Sciences and Mathematics, Višegradska 33, 18000 Niš, Serbia

ABSTRACT

Fenestration, important for adding aesthetics to the building design and providing adequate daylight illumination levels, also plays a vital role for thermal comfort in buildings and is easily considered as the most important individual strategy in passive solar design of buildings. Purpose of this work is to analyse and discuss optimal fenestration parameters for an office building located in Belgrade, Serbia. Office buildings are characterized by high internal gains due to the presence of people, computer equipment and lighting during the work hours, which may be beneficial in the heating season, but may pose a significant problem in the cooling season.

The case study is a four-story office building, rectangular in shape, with longer sides facing south and north. Windows are present at southern and northern walls only. The design parameters include six glazing types for southern and for northern windows each, seven values of windows-to-wall ratio for southern and northern facade each, presence of external shading at southern windows, as well as three U-values of external walls. In total, 10,584 parameter combinations have been simulated in EnergyPlus, with the building in a free running mode and with annual heating and cooling discomfort hours recorded at the output. The analysis is focused on the set of Pareto optimal solutions with heating and cooling discomfort hours as competing performance objectives.

The simulation results clearly demonstrate the importance of improved thermal insulation in the continental climate of Belgrade and the necessity of using superior triple, low-e, argon-filled glazing for all building variants with larger than minimal southern windows-to-wall ratio. The optimal choice of the southern windows-to-wall ratio turns out to be between 37,5% and 50%, with external shading of southern windows, while the optimal choice of the northern windows-to-ratio is between 25% and 37,5%.

Keywords: passive solar design, office building, fenestration, Pareto front, EnergyPlus.

INTRODUCTION

Passive solar design strategies aim to use solar energy to help establish thermal comfort in buildings, without the use of electrical or mechanical equipment. The greatest opportunities for integrating passive solar design strategies occur at the conceptual design level, by determining the values of building envelope parameters that have critical influence on its thermal performance. Building energy simulation plays a fundamental role in this process, since the building's future response to applied passive solar design strategies is highly sensitive to local climate factors.

Among the passive solar design strategies, fenestration may be considered as the most important, since it has the largest influence on the admission of solar energy into the building and, hence, plays a vital role in its thermal comfort. The purpose of this work is to analyse

and discuss optimal fenestration parameters for an office building located in Belgrade, Serbia. Belgrade has continental climate with hot summers (Dfa in Köppen classification), with average maximal monthly temperatures of 27,3°C in July and August and average minimal monthly temperature of -2,3°C in January [1].

CASE STUDY DESCRIPTION

Survey of the research on optimal passive solar design of low energy buildings [2] suggests two alternative optimal building plans: a square plan, which minimizes the ratio of the envelope surface and the interior volume and thus increases energy efficiency, or an elongated rectangle plan, with longer side oriented towards south, which enables better passive use of available solar energy during winter. The case study considered here has, therefore, a rectangular plan with dimensions 20m x 14m and four stories of 4m storey height. Office building is of open plan, so that the model has no internal partitions (except towards spaces that do not have large influence on thermal characteristics, such as staircases and restrooms).

By current Serbian legislative [3], exterior walls have U-value at most 0,3W/m^{2}K, while typical U-value for exterior walls of passive houses is around 0,1 W/m^{2}K. Three alternative U-values – 0,1 W/m^{2}K, 0,2 W/m^{2}K and 0,3 W/m^{2}K have been used in simulations. Exterior walls consist of plastic malter 0,5cm on the outside, expanded polystyrene of adequate thickness, hollow brick 25cm and cement stucco 2cm on the inside. The remaining opaque envelope components have fixed values: slab on the ground has U-value 0,246 W/m^{2}K, the construction between stories has U-value 0,416 W/m^{2}K, while the flat roof has U-value 0,147 W/m^{2}K. Concrete ceiling of each storey is stripped down, so that it serves as a thermal mass, while the insulating layer above it reduces the transfer of accumulated heat to upper stories. Infiltration rate is good and set to 0,5h^{-1}.

Glazing properties have significant impact on a number of building functions: its U-value is important for preservation of heat within the building, the solar heat gain coefficient (SHGC) determines the transmittance of solar energy, while the visible light transmittance coefficient (VL) influences the daylighting and reduces the needs for artificial lighting. Six common glazing types, whose properties are given in Table 1, have been considered in the case study.

Glazing	**U-value (W/m^{2}K)**	**SHGC**	**VL**
double, clear	2,742	0,743	0,801
double, clear, selective	1,628	0,421	0,682
double, tinted, selective	1,628	0,291	0,408
triple, clear	1,779	0,658	0,723
triple, low-e, argon-filled	0,893	0,495	0,651
triple, low-e, tinted	1,214	0,254	0,322

Table 1: Glazing types.

Windows-to-wall ratios (WWR) on southern and northern facade vary from 25%, necessary to satisfy minimal daylighting requirements, to 100% in steps of 12,5%. Windows shading is provided with external blinds. Blind slats are horizontal with 10cm depth and 10cm vertical distance between adjacent slats, which shade windows completely from May 20 to September 20, the period when maximal daily temperature is higher than 27°C in Belgrade [1].

Internal gains are determined by the presence of employees. Working hours are 8am-4pm, five days per week, although it is assumed that a half of the employees will be present from

7.30am-8am and also from 4pm-4.30pm. Each employee occupies area of $9m^2$ and has a 100W computer equipment. The metabolic rate for light office work, standing and walking, for a mix of equally many men and women, is 114,39W per person, which yields internal gains of 23,82 W/m^2 from presence of people and computer equipment. Artificial lighting uses T5 tubes, which in the absence of daylighting, use 13,2W/m^2 to provide 400lux light intensity. Since the glazing type and shading greatly influence availability of daylight, and respectively the energy needed for artificial lighting, the case study has a photosensor at desk height in the center of each storey and linear lighting control.

Natural ventilation is used as a passive cooling measure, as the oscillation between maximum and minimum daily temperatures in Belgrade is 10,4°-10,5° from May to July and 11,7°-11,9° in August and September [1]. Natural ventilation is available from Apr 15 to Oct 15 during working hours as necessary and during nighttime from 10pm to 6am, whenever the internal temperature is above 20°C and above the external temperature. It has maximum rate of $5,0h^{-1}$, with at most 20% of windows area allowed to open. Further, mechanical ventilation is used to provide minimum of 10l/s of fresh air per person during working hours.

SIMULATION RESULTS

The case study office building has several variable parameters: three exterior walls U-values (0,1; 0,2; 0,3 W/m^2K), six glazing types for southern facade (Table 1), six glazing types for northern facade (Table 1), seven WWR values for southern facade (25%; 37,5%; ...; 100%), seven WWR values for northern facade (25%; 37,5; ...; 100%) and the indicator of presence/absence of southern windows shading. In total, 10 584 building variants were simulated in EnergyPlus, using jEPlus [6] to automate simulation process.

The building variants were simulated in free running mode, with the simulation output consisting of heating and cooling discomfort hours. If $T_{zone,i,j,t}$ denotes operative temperature in zone i (i=1,2,3,4) during the working day j in a year and 15-minute long timestep t, then the heating discomfort hours are defined as

$$HDH = \sum_{i,j,t} \frac{1}{4} \max(20°\mathrm{C} - T_{zone,i,j,t}, 0°\mathrm{C}), \quad (1)$$

while the cooling discomfort hours are defined as

$$CDH = \sum_{i,j,t} \frac{1}{4} \max(T_{zone,i,j,t} - 26°\mathrm{C}, 0°\mathrm{C}). \quad (2)$$

Hence, the heating discomfort hours represent the number of degree hours that the operative temperature is below the heating setpoint of 20°C, while the cooling discomfort hours represent the number of hours that the operative temperature is above the cooling setpoint of 26°C. The discomfort hours have been used before in [4,5] as the heating and cooling energy indicators. Essentially, as pointed out in [5], it can be expected that the building minimizing heating and cooling discomfort hours will also minimize heating and cooling energy demand.

Natural ventilation was simulated using the EnergyPlus option Calculated, which takes into account wind and buoyancy effects. Simulation of each building variant took between 110s and 140s on Fujitsu Lifebook E782 with Intel Core i7-3612QM processor on 2.1GHz. Since the processor allows execution of eight EnergyPlus simulations in parallel, simulation of all 10 584 building variants took litlle more than 50 hours.

Figures 1-4 represent heating and cooling discomfort hours for all building variants, differently colored with respect to external wall U-value (Fig. 1), southern glazing type (Fig. 2), southern WWR (Fig. 3) and northern WWR (Fig. 4). These figures also show the Pareto front, made from those building variants for which no other variant has smaller both heating and cooling discomfort hours. The Pareto front, in this case, is made up of two parts: a steep line on the left with heating discomfort hours below 7 500°C, and an almost horizontal part with cooling discomfort hours below 2 500°C. Since heating requires substantially more primary energy than cooling, the five Pareto solutions situated at lower left peaks in the steep part of the Pareto front may be considered as the optimal choices. These five Pareto solutions all have:

- exterior walls U-value of 0,10 W/m^{2}K,
- triple, low-e, argon-filled glazing at both southern and northern windows,
- shading present at southern windows,
- northern WWR equal to minimal value of 25%,

while the southern WWR ranges from 87,5% for the variant with (*HDH*, *CDH*)=(5 172°C, 10 204°C) down to 37,5% for the variant with (*HDH*, *CDH*)=(7 365°C, 2 573°C).

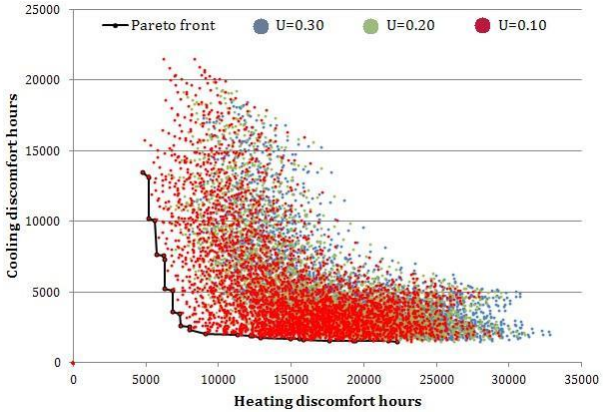

Figure 1: Building variants colored according to U-value.

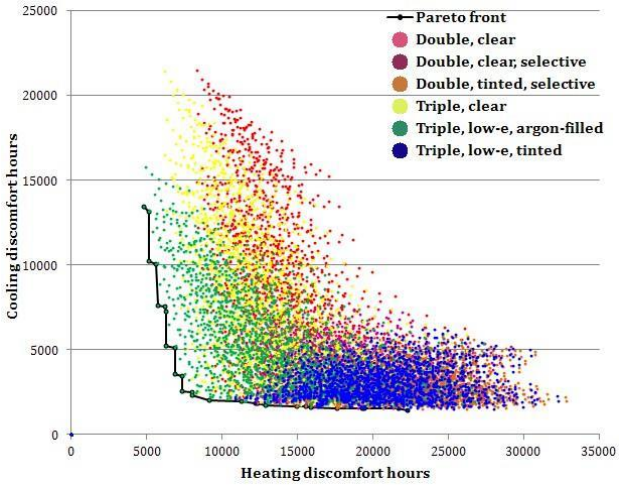

Figure 2: Building variants colored according to southern glazing type.

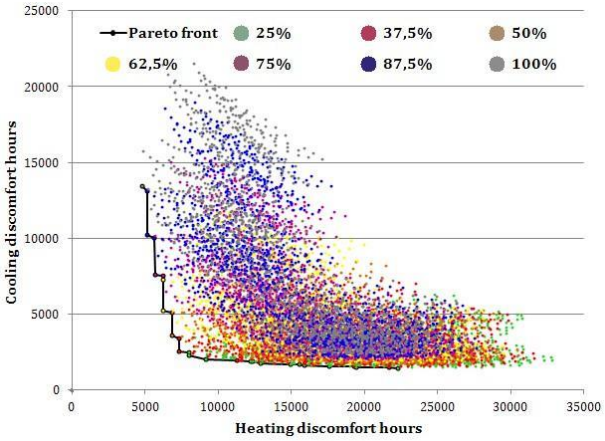

Figure 3: Building variants colored according to southern WWR.

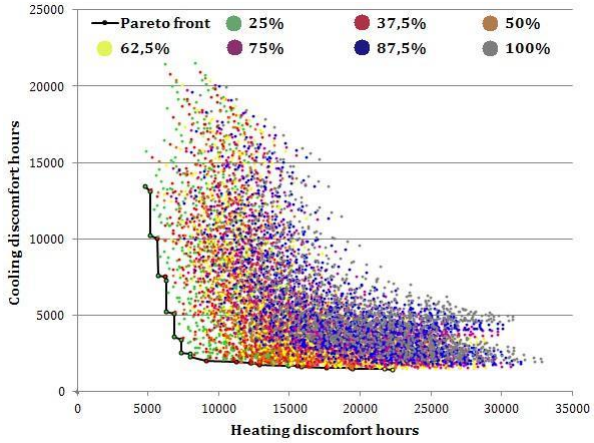

Figure 4: Building variants colored according to northern WWR.

DISCUSSION

It can be seen from Figure 1 that the building variants with smaller exterior wall U-value are generally closer to the Pareto front than the building variants with higher U-value. Together with the fact that all Pareto optimal variants have the exterior wall U-value of 0,1 W/m^{2}K, this clearly demonstrates the importance of thermal insulation in the continental climate of Belgrade. Nevertheless, large overlaps between areas with different U-values also show that the U-value itself is not the only decisive factor, as the numbers of heating and cooling discomfort hours largely depend on fenestration parameters as well.

The grouping of variants according to the type of southern glazing is easily noticeable from Figure 2. The smallest heating and cooling degree hours are generally obtained when triple, low-e, argon-filled glazing is used at the southern facade, and all Pareto optimal solutions with less than 10 000°C heating discomfort hours have this glazing type both at southern and northern windows, together with shading present at southern windows. The triple, low-e, argon-filled glazing is superior to other glazing types due to the smallest U-value, important for heat conservation during the heating season, and medium SHGC value. While it can be noticed from Figure 2 that some building variants, which use triple, clear or even double, clear glazing, are close to the lower left part of the Pareto front, such variants have minimal southern WWR, which limits the influence of glazing parameters.

Most Pareto optimal solutions have the southern WWR equal to either 25% or 37,5%. There is, however, a number of Pareto optimal solutions with the southern WWR between 50% and 100%, which all have triple, low-e, argon-filled glazing both at southern and northern facades and shading present at southern windows. These variants, due to the beneficial effect of winter solar gains have the smallest heating discomfort hours (less than 7 000), but at the same time have the largest cooling discomfort hours (from 3 574 for the southern WWR of 50% up to 13 436 for the southern WWR of 100%). The optimal choice of the southern WWR is between 37,5% and 50%, with shading present, which enables beneficial effect of solar gains during the heating season, without large negative impact on cooling discomfort hours.

The northern WWR has significant impact on heating and cooling discomfort hours, as visible from Figure 4. Building variants with larger northern WWR are generally further away from the Pareto front, while only variants with the northern WWR up to 50% appear close to the lower left part of the Pareto front. The fact that Pareto optimal solutions come in pairs, one of which has the northern WWR of 25% and the other 37,5%, suggests that these values are optimal choices for the northern WWR, which prevent large heat loss during the heating season, with appropriate influence on cooling of the interior space during summer months. The northern glazing type, with such WWR, does not appear to have large influence on the number of discomfort hours.

ACKNOWLEDGEMENTS

The author has been supported by the Research Project TR36035 “Spatial, environmental, energy and social aspects of the development of settlements and climate change – mutual influences” of the Ministry of Education, Science and Technological Development of the Republic of Serbia.

REFERENCES

1. Republic Hydrometeorological Service of Serbia: Meteorological yearbook – climate data 2011, Belgrade, 2012. Available at http://www.hidmet.gov.rs/podaci/meteo_godisnjaci/Meteoroloski%20godisnjak%201%20-%20klimatoloski%20podaci%20-%202011.pdf, accessed Apr 28, 2013.
2. Stevanović, S.: Optimisation of passive solar design strategies. Renewable and Sustainable Energy Reviews, 2013, accepted for publication.
3. Government of the Republic of Serbia: Regulation on energy efficiency of buildings. Official Gazette of the Republic of Serbia, Vol. 61, Belgrade, Aug 19, 2011.
4. Porritt, S., Shao, L., Cropper, P., Goodier, C.: Adapting dwellings for heat waves. Sustainable Cities and Society, Vol. 1 (2011), 81-90.
5. Bouchlaghem, N.: Optimising the design of building envelopes for thermal performance. Automation in Construction, Vol. 10 (2000), 101-112.
6. Zhang, Y.: JEPlus – An EnergyPlus simulation manager for parametrics. Leicester, 2012. Available at http://www.iesd.dmu.ac.uk/~jeplus/wiki/doku.php, accessed Apr 28, 2013.

SEASONAL PERFORMANCE OF A COMBINED SOLAR, HEAT PUMP AND LATENT HEAT STORAGE SYSTEM

Christian Winteler; Ralf Dott; Thomas Afjei

Institut Energie am Bau, Fachhochschule Nordwestschweiz FHNW, St. Jakobs-Strasse 84, CH-4132 Muttenz, Switzerland

ABSTRACT

This paper investigates the seasonal performance of a combined solar, heat pump and latent heat storage system for dwellings. This combination could provide a viable alternative to common brine-water heat pump systems with a borehole heat exchanger. (BHX). Since the latent heat storage, or ice storage, is filled with pure water, it can also be used in (but is not limited to) places where a BHX is prohibited, e.g. water protection areas. The aim of this work is to find and evaluate given system configurations for three different annual heat demands that reach seasonal performance factors (SPF) comparable to those of BHX heat pump systems, i.e. SPF ~ 4.0.

A simulation study using MATLAB®/SIMULINK® and the CARNOT Blockset is conducted. Technologies considered in the simulation study are a brine-water heat pump, unglazed solar collectors as source for the heat pump and a buried ice storage that serves as alternative source for the heat pump and is regenerated by the collectors. Unglazed collectors use solar irradiation and ambient heat (via convective heat exchange) for heat generation. Additionally, thermal coupling of the ice storage to the surrounding soil which also contributes to the regeneration of the system is considered. The simulation models of this system have been validated with laboratory and field test data. The heat generated by the heat pump is used for space heating and domestic hot water preparation of single family houses with different heat loads which have been defined in the framework of IEA SHC Task 44 / HPP Annex 38 "Solar and heat pump systems". To obtain the desired SPF for each building type the power output of the heat pump with the corresponding size of the collector field is varied.

For each building a configuration is found that yields a SPF ~ 4.0. A high SPF can only be reached as long as no backup heating is needed, which means, that the ice storage should never be completely discharged, i.e. completely frozen. This requires significant contributions from the solar collector, especially during the heating period.

Keywords: heat pump, solar heat, latent heat, ice storage

INTRODUCTION

The turnaround in energy policy demands energy supply systems to use predominantly renewable energy sources. Heat pumps in combination with solar energy are key technologies for heat generation for space heating and domestic hot water in buildings. Currently the most effective heat sources for heat pumps are borehole heat exchangers. Recently systems with large ice storages have been promoted as equally efficient at comparable cost without the need for deep drilling and the associated authorization and risks. Furthermore, ice storages can also be installed in areas where deep drilling is not possible or prohibited, even in water protection areas since the ice storage is filled with pure water.

Aim of this study is to investigate the seasonal performance of a combined solar, heat pump and ice storage system for buildings with different heat loads and compare it to the average seasonal performance factor of systems with borehole heat exchangers of ~ 4.0.

METHOD

The simulation study is conducted using MATLAB®/SIMULINK® [1] and the CARNOT Blockset [2]. Technologies considered in the simulation study are a brine-water heat pump, unglazed solar collectors as source for the heat pump and a buried ice storage that serves as alternative source for the heat pump and is regenerated by the collectors. Unglazed collectors use solar irradiation and ambient heat (via convective heat exchange) for heat generation. Furthermore, thermal coupling of the ice storage to the surrounding soil which also contributes to the regeneration of the system is considered. The heat generated by the heat pump is used for space heating and domestic hot water preparation of a single family house (SFH) which has been defined in IEA HPP Annex 38 / SHC Task 44 "Solar and heat pump systems" (A38T44) as reference heat load, c.f.[3]. Therein, three building types called SFH15, SFH45 and SFH100 are defined, where the numbers refer to the insulation quality and therewith the space heat demand of 15 kWh/m^2/a, 45 kWh/m^2/a or 100 kWh/m^2/a as described in detail in [4]. The implementation of these buildings in the presented simulation environment differs from the reference which can lead to an increase in the heat demand due to a different space heating control. However, the aim of the study is not to perfectly match the heat load to the reference, but to investigate the behaviour of the heat generation system for different system configurations.

Reference conditions

The reference conditions of A38T44 are applied using the following options for all systems:

- moderate climate of Strasbourg, a French city in central Europe
- a simplified domestic hot water (DHW) tapping profile of only three tappings per day (07:00, 12:00 and 19:00) corresponding to an average draw off of 140 l/d at 45 °C or 5.845 kWh/d (2133 kWh/a). The seasonal variation of the DHW energy demand is approximated with a sine-curve variation of the cold water temperature.

Domestic hot water preparation is delivered by a boiler with attached mixing valve to adjust the fixed tapping temperature and heated only by the heat pump.

The heat delivery system for space heating in SFH15 and SFH45 is a floor heating system, in SFH100 a radiator. The required flow temperatures needed to satisfy the heat demands are 30 °C for the SFH15 building, 34 °C for the SFH45 and 48 °C for the SFH100 building.

There is a range of heat pump models intended by the manufacturer for the solar ice storage system with thermal capacities of 6, 8, 10 and 13 kW. To study the behaviour of the heat generation system in combination with the aforementioned reference buildings, a heat pump is chosen for each building such that its thermal capacity exceeds the design heat load of the building (1.8 kW, 4 kW and 7.3 kW for SFH15, SFH45 and SFH100 respectively).

The heating characteristic of the heat pump controller defines the space heating return flow temperature as a function of the outdoor temperature. The heating characteristic is set such that the room temperature is kept around 20 ± 0.5 °C. If necessary, DHW preparation has priority over space heating.

Solar thermal absorber modules are installed on a south facing roof at an inclination of 40°. The collector area for the buildings SFH15 and SFH45 amounts to approximately 10 m^2, for building SFH 100 to 20 m^2.

Applied tools and parameter data sets

All simulations are performed with MATLAB®/SIMULINK® in combination with the CARNOT Blockset, an extension for the calculation and simulation of thermal components of heating systems. All simulation results are annual values from July to July with 300 days preconditioning, corresponding to one full heating period. Heat loads are simulated with the simple house model from the CARNOT Blockset, parametrized according to the building definitions from the IEA HPP Annex 38 / SHC Task 44. The Isocal solar ice system [5] consists of Isocal SLK-S pipe absorber modules and an Isocal SES ice storage.

The absorber is modelled as described in [6] and parametrized according to the data in [5]. Effects of condensation as well as freezing/frosting are not taken into account. The model has been validated through laboratory tests both with and without irradiation. For the brine/water heat pump the generic heat pump model from the CARNOT Blockset is used with performance data of Viessmann Vitocal 300 G BW series models [7] BW 301.A06 (6 kW) and BW 301.A08 (8 kW). The storage tank model is a CARNOT multiport model with specifications of a Viessmann Vitocell 100-V CVW [8]. All simulation models and applied parameter data sets have furthermore been validated through field test measurement data.

Schematic

Figure 1 shows a schematic depiction of the system and the hydraulic connections. The solar thermal absorber and the ice storage both serve as heat source for the heat pump. The buried ice storage is not insulated and can exchange heat with the surrounding soil. Additionally, the absorber also supplies heat for the regeneration of the ice storage. The heat pump is the sole supplier of heat for space heating as well as for domestic hot water preparation. The electric heater serves as backup in case the source temperature drops below the minimum operating temperature of the heat pump.

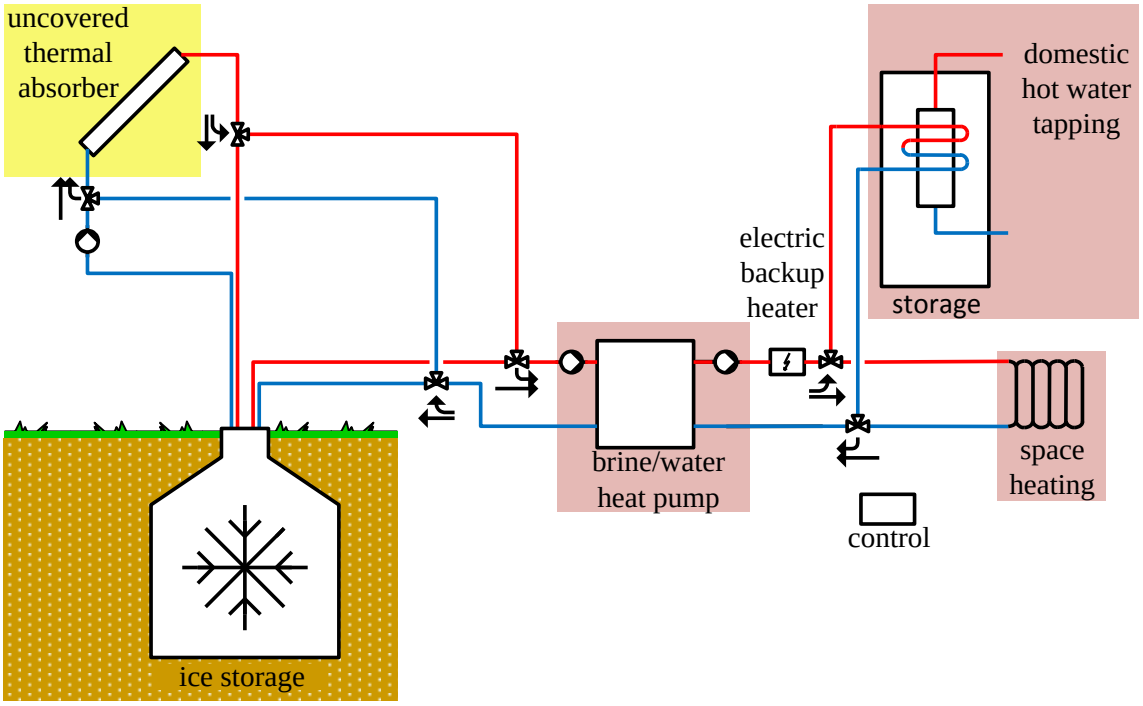

Figure 1 System and hydraulic scheme

RESULTS

A selection of results for the three chosen systems is presented in Figure 2 and Table 1. Therein, the following results are shown:

- The total generated heat for space heating and domestic hot water preparation in kilowatt-hours (kWh), divided into the different heat sources for the heat pump: electricity, solar collector or ice storage. The contribution from the ice storage is subdivided into a solar and a ground heat part, depending on how the heat extracted from the ice storage is restored. Since heat exchange between ice storage and ground works in both ways, the displayed value denotes the net annual energy balance. The latent heat contribution cannot be displayed here since its annual energy balance is zero.
- The total electric energy consumption of the whole heating system including all components in kWh.
- The seasonal performance factor (SPF) of the heat generation system as quotient of heat generated by the heat pump divided by the electricity consumption of the heat pump, the heat pump control, the pump between collector and ice storage, the pump for the heat pump source and the electric backup heater.

The variant SFH15, representing a building with very high energetic quality, has the lowest heating energy generation of 5'260 kWh. The major heat source for the heat pump is the solar absorber, providing 2'908 kWh of the 4'267 kWh needed. The rest of the energy is supplied by the ice storage, which in turn is regenerated by the absorber. On average the temperature of the ice storage is higher than the temperature of the surrounding ground. This excess heat is transferred from the ice storage to the ground which is indicated by the negative contribution in Figure 1. The SPF of 3.73 is slightly below the expected 4.0.

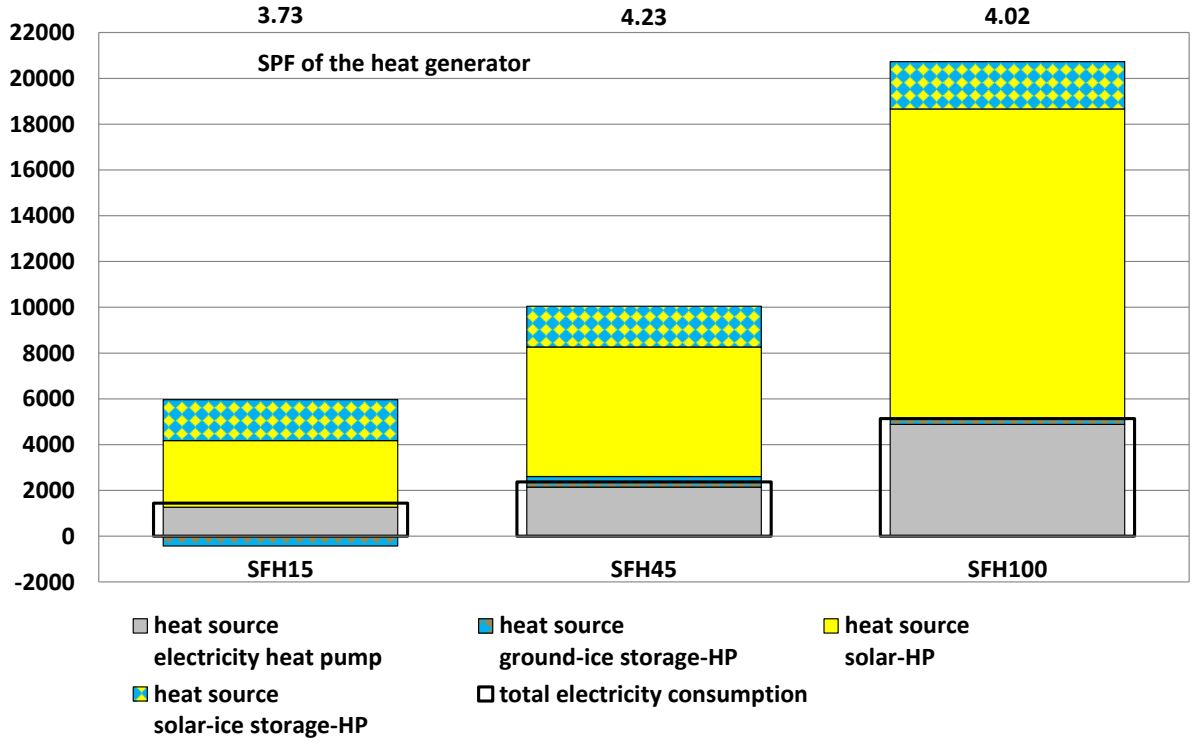

Figure 2 System simulation results for the three building types

The variant SFH45 represents a renovated building with good thermal quality of the building envelope that also satisfies current legal requirements. From the total 9'731 kWh of generated heat, 7'351 kWh are used for space heating. The predominant heat source for the heat pump is the solar absorber. Its contribution of 5'654 kWh to the total heat demand of 7'906 kWh is significantly larger than the 2'252 kWh extracted from the ice storage. On an annual balance the ice storage is not only recharged by the absorber, but also extracts 467 kWh heat from the surrounding ground. The thermal capacity of the heat pump of 6 kW matches the design heat load of the building quite well, resulting in the highest SPF of 4.23 among the presented simulations.

A38T44 building type	Solar absorber surface in m^2	Thermal power of heat pump in kW	Total generated heat in kWh	Design flow/return temperature in °C	SPF of heat generator	Total generator electricity consumption in kWh	Electricity consumption of auxiliaries in kWh
SFH15	10	6	5'260	30/25	3.73	1'412	150
SFH45	10	6	9'731	34/29	4.23	2'301	161
SFH100	20	8	20'249	48/38	4.02	5'040	158

Table 1 System simulation results for the three building types

The variant SFH100 represents a non-renovated existing building and has therefore the highest heat demand. From the total 20'249 kWh of generated heat 17'681 kWh are used for space heating. The 20 m^2 of thermal collectors deliver 13'549 kWh of heat as source energy for the heat pump. The remaining 2'298 kWh of source energy are supplied by the ice storage. The annual balance of the ice storage shows 233 kWh of heat that are extracted from the surrounding ground, the rest is provided by the collector. The heat generator reaches an SPF of 4.02.

DISCUSSION

For all three buildings the heat demand for space heating is significantly higher than the reference values given in [4]: 21 kWh/m^2/a for SFH15, 52.5 kWh/m^2/a for SFH45 and 126 kWh/m^2/a for SFH100. The main reason for this difference is the fact, that no thermostatic valves regulating the mass flow are used in the heat delivery system. This in turn leads on average to higher room temperatures and therefore more heat losses. However, the focus of this work is to study the performance of the solar ice storage system, i.e. the heat generation system, for different heat loads and not the optimal reproduction of the reference heat loads. The authors are well aware that this aspect could be optimized in future studies.

The most important result is that for all three buildings the solar ice system reaches an SPF close to or above 4.0. With a value of 3.73 the SFH15 variant is the only one with an SPF below 4.0. There are two main reasons for this discrepancy:

1. The heat pump thermal capacity of 6 kW is a factor 2-3 larger than the design heat load which leads to a lower SPF of the heat pump alone.

2. The fraction of electricity consumed by auxiliary systems (here the heat pump control, the pump between collector and ice storage, the source pump of the heat pump and the electric backup heater), 150 kWh, to total generator electricity consumption, 1'412 kWh, is around 11 % which leads to a rather large reduction of the SPF when extending the system boundary from the heat pump alone (SPF 4.17) to the heat generator (SPF 3.73).

From the range of available heat pumps intended for this system by the manufacturer, with thermal capacities of 6 kW and above, it is obvious that the ice storage system is not primarily designed for buildings with very low space heat loads like SFH15 (1.8 kW). In this context an SPF of 3.73 is still a remarkable result.

The SFH100 variant reaches an SPF of 4.02 which is only slightly above the desired value of 4. In this variant the heat pump SPF is reduced, because higher flow temperatures are needed to meet the heat load than in the variants with floor heating, see c.f. Table 1. To obtain these temperatures the heat pump needs more electricity which in turn reduces the SPF.

The highest SPF is reached for the SFH45 variant where the thermal capacity of the heat pump is close to the building heat load and heat is delivered at moderate temperatures with a floor heating system.

CONCLUSIONS

The study shows, that the solar ice system generates heat efficiently for different heat loads. It reaches SPF > 4 for buildings with moderate (SFH45) to high (SFH100) space heat demands with space heating or radiator heat delivery systems. The system is not primarily intended for buildings with very low heat loads (SFH15) but reaches a SPF close to 4 nevertheless.

ACKNOWLEDGEMENTS

The authors are grateful for the project advising and funding by the Swiss Federal Office of Energy SFOE in the frame of the project SOFOWA. They acknowledge the support of the component manufacturers Viessmann Werke GmbH & Co. KG and isocal HeizKühlsysteme GmbH. The project contributes to the IEA SHC Task 44 / HPP Annex 38 “Solar and heat pumps”. The permission of Meteotest for using Meteonorm climate data for simulations within the IEA SHC Task 44 / HPP Annex 38 is gratefully acknowledged.

REFERENCES

1. Matlab®/Simulink® Version R2011b, The Mathworks, Inc.
2. CARNOT Toolbox für Matlab/Simulink Ver. 5.2, August 2012
3. M. Y. Haller, R. Dott, J. Ruschenburg, F. Ochs und J. Bony: The Reference Framework for System Simulations of the IEA SHC Task 44 / HPP Annex 38, 2011
4. R. Dott, M. Y. Haller, J. Ruschenburg, F. Ochs und J. Bony: Reference Buildings Description of the IEA SHC Task 44 / HPP Annex 38, 2011
5. Das Wärmequellensystem SE 12 - Informationsblatt, isocal HeizKühlsysteme GmbH, Friedrichshafen, Deutschland, 2012
6. E. Frank, Modellierung und Auslegungsoptimierung unabgedeckter Solarkollektoren für die Vorerwärmung offener Fernwärmenetze, Kassel University Press, 2007
7. Data set for Viessmann Vitocal 300-G BW series , in Planungsunterlagen für Wärmepumpen - Ausgabe 05/2012, Viessmann Deutschland GmbH, Allendorf, Germany, 2012
8. Datenblatt Viessmann Vitocell 100-V Typ CVW - 06/2009, Viessmann Deutschland GmbH, Allendorf, Germany, 2009

THE ASSESSMENT OF DAYLIGHT REFLECTION FROM BUILDING ENVELOPES

Xiaoming Yang; Lars O. Grobe; Stephen K. Wittkopf

Lucerne University of Applied Sciences and Arts, CH-6048 Horw, Switzerland

ABSTRACT

Buildings could influence surrounding microclimate with their envelope designs. Reflective surfaces on the building envelopes could reflect daylight to the neighbourhood and cause problems such as glare and overheating. For the surrounding drivers, pedestrians and building occupants in the area, the reflected sunlight from the building envelope becomes the bright spot in their view which results visual discomfort or impairment. For building envelope designs, it is important to analyse the effect of daylight reflection to the neighbourhood at design stage. This could reduce the risk of environmental problems and minimize the consequences cost after construction.

A software tool to evaluate the reflected daylight from building envelopes has been developed. It is implemented on parametric design platform GRASSHOPPER using RADIANCE as background simulation engine. As shown in the case study, using the tool, the form of the assessed building envelope could be analysed and the critical areas around the assessed building including roads, pavements and façades of neighbouring buildings are examined for potential concentration of reflected daylight. Rich information is recorded for the critical areas: annual reflected solar radiation, period with irradiance value above threshold, origin of the reflected daylight on the assessed building envelope, etc. This information could help designers to optimize the form of the envelope and make façade material selection. The tool shows potentials for architects to understand the impact of their designs and avoid potential environmental problems.

Keywords: simulation, daylighting, building envelope, reflection, RADIANCE

INTRODUCTION

Buildings could affect surrounding microclimate with their envelope designs. Reflective surfaces on the building envelopes could reflect daylight to the neighborhood and cause problems such as glare and overheating. For the drivers, pedestrians and building occupants in the area, the reflected sunlight from the building envelope becomes the bright spot in their view which may result visual discomfort or impairment. With development of new glazing technologies, glass is increasingly being used on building envelopes. Additionally, in order to achieve the goal of energy conservation and lower the cooling load, glazing with high reflectance is preferred by façade designers. Both of these contributed to the more frequently encountered problems of reflected daylight from building envelopes. Another issue may lead to the problem of reflected daylight is the design of free formed or curved envelope. Without careful analysis, reflective materials on the curved surfaces could magnify sunlight in the same way as solar concentrators and cause problems more than annoyance to immediate neighbors. In extreme cases, scorched people's hair or even melted plastic cups are reported [1].

In literature, many approaches to evaluate and prevent the hazard from reflected daylight can be found. Planning authorities have enacted regulations to eliminate the problem of reflected daylight from building facade in several countries, mainly by controlling the use of building materials based on their reflectivity alone [2,3,4]. In practice, problems may rise because of such regulations. The policy may be possibly too restrictive with material selection, particularly in cases where proper architecture design can offset the additional reflected daylight from the envelope. In academia, researchers also developed methods to evaluate the effect of reflected daylight from building envelopes [5, 6]. These methods could only analyze a limited number of viewpoints in the simulation step and as a result, it is possible that viewpoints with severe glare problem in the neighboring area are overlooked. Building professionals also established methods to assess potential solar hazard from the proposed development in response to the requirement in building regulations. One methodology is widely adopted by Australia building consultants [7]. The application of this method is limited to constructed buildings and thus could not predict potential problems from reflected daylight in the design stage. This approach however ignores the duration of time over which reflections occur to the neighboring building.

With the aim of overcoming most of the drawbacks explained above, a new software tool for the evaluation of the reflected daylight from building envelope has been developed. Each building envelope design could be evaluated in the design stage. It allows detailed description of the assessed building envelope and the neighboring buildings with material reflection property. Positions in the neighborhood where reflected daylight is concentrated could be identified by the algorithm. With selected positions as viewpoints, using annual weather data in simulations, each time period when reflection occurs could be detected. The tool could also record the origin of the reflected daylight from the assessed building envelope and display it on the 3D model.

The tool presented may help architects to have a better understanding of the environmental impact of the building envelope at design stage. Additionally, it also provides information for designers to modify the form of the envelope and make material selections.

METHOD

For the task to assess reflected daylight from building envelopes, the presented method combines the two most commonly used lighting simulation method: forward ray tracing and backward ray tracing. Forward ray tracing method is more efficient in the situation to identify the areas in the neighborhood which are affected by the reflected daylight from the assessed building envelope. It could trace the whole transmission process of daylight: emission from the sun - reflection on the assessed building envelope – terminates on neighboring buildings. The distribution of reflected daylight from building envelopes follows angle of incident as well as ambient weather conditions and seasonal differences. Therefore, it is necessary to evaluate reflected daylight with annual weather data. Backward ray tracer in RADIANCE provides an efficient way for time-series simulations using daylight coefficient method [8]. It could avoid redundant computations and improve the overall speed of annual simulation by a large factor.

The working procedure could be divided into four steps. In the first step, the assessed building envelope and the neighbourhood models are required with their material reflection property. The next step is to localize reflected daylight distribution in the neighbourhood using forward ray tracing method. The critical positions are identified by density of intersections between reflected daylight and neighbouring buildings. This step works as a pre-selection step for

following backward ray tracing procedures and it also ensures that all positions in the neighbourhood where daylight is concentrated could be identified. The third step is to quantify the reflected daylight received at the critical positions with annual simulation. In the last step, the annual simulation result from the previous step is further processed to extract information of the origin of the reflected daylight on the assessed building envelope. With all the information from the above evaluation process, designers could modify the envelope design accordingly by changing the form, materials, orientation, etc. The design-evaluation process could be repeated until the design target is achieved.

CASE STUDY

Step 1

The presented reflected daylight evaluation tool has been applied to analyse performance of a building with curtain wall facade. The assessed building is located in Zurich and covered with a full glazing envelope. The model has been created in RHINO together with the neighbourhood. The assessed building envelope has been modelled with Double Pane Low-e glazing assuming reflectance of 29.3%. The neighboring buildings are 35% diffuse reflectors and the reflectance ground has been set to 20% (see Figure 1).

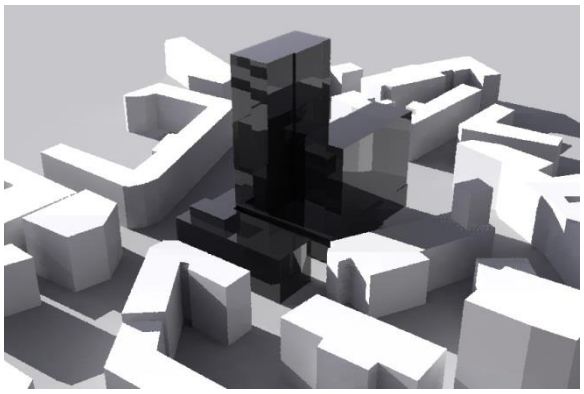

Figure 1: The assessed building with glazing envelope and the neighbouring buildings.

Step 2

With Zurich's sun path, forward ray tracing process has been carried out using half-hour time step throughout one year. Figure 12 (left) demonstrates the ray tracing process for one time step with reduced number rays while in the actual simulation, 10000 rays has been used for each time step. Figure 12 (right) shows the distribution of reflected daylight in the neighbourhood and 7 critical positions which have the highest density of ray intersections has been identified. Position 2 and 5 are located on the roof of the neighbouring buildings while the other positions are on the facades.

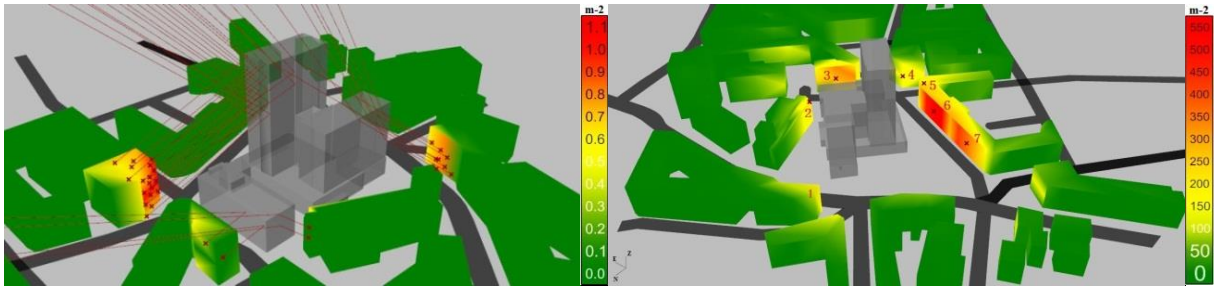

Figure 2: Left: Forward ray tracing for one time step using reduced number of rays. Right: Colour coded intersection density (number of intersection per square meter) for one year with critical positions numbered and marked with red crosses.

Step 3

With critical positions identified, the climate based simulation has been performed with luminance distribution of the sky according to measured data in Zurich and CIE clear sky model. The result with the sky model assumes sunny sky over the whole year which represents the worst case scenario for reflected daylight from the assessed building envelope. The simulation using weather data addresses the influence of weather condition for the location of the building and therefore it could be used to predict the reflected daylight in a local context. Some of the simulation results are presented in Figure 3. Position 2 receives the highest intensity of reflected daylight among all the tested positions because it is located the closest to the assessed building which constitutes a large part of the view at position 2. Position 3 only receives excess reflected daylight in the early morning. The reason consists in the fact that this position locates opposite southeast facing façade of the assessed envelope. Reflected daylight could only reach position 3 when the sun is to the east of the façade. Position 6 receive large amount of reflected daylight throughout the year around 3pm. This explained the high intersection density at position 6 in Figure 2. In the afternoon, intensive daylight is reflected by the southwest facing tower block toward the façade where position 6 is located.

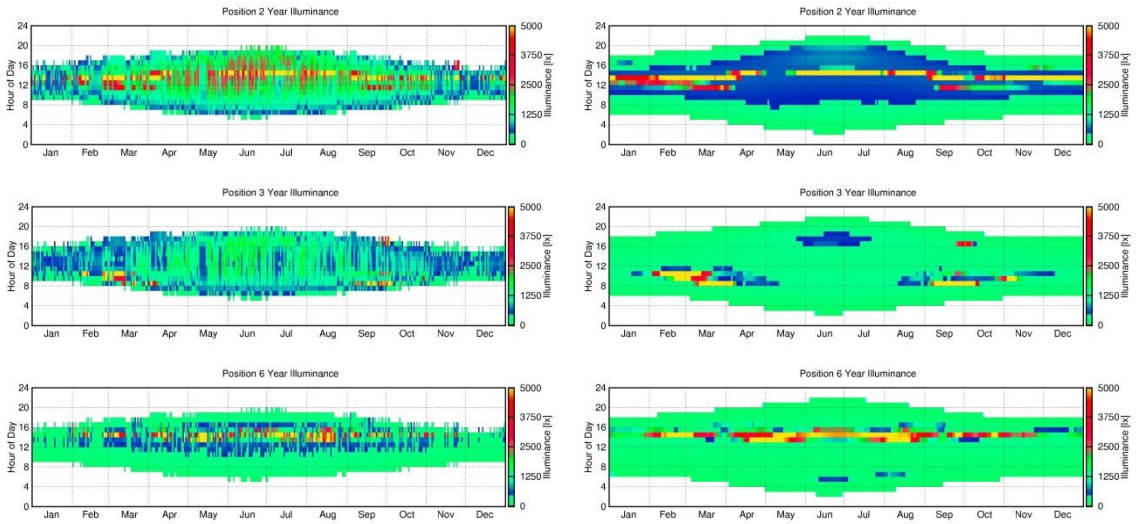

Figure 3: Heat maps of illuminance contributed from reflected daylight received at critical positions 2, 3 and 6 using Zurich weather data and CIE clear sky model.

Step 4

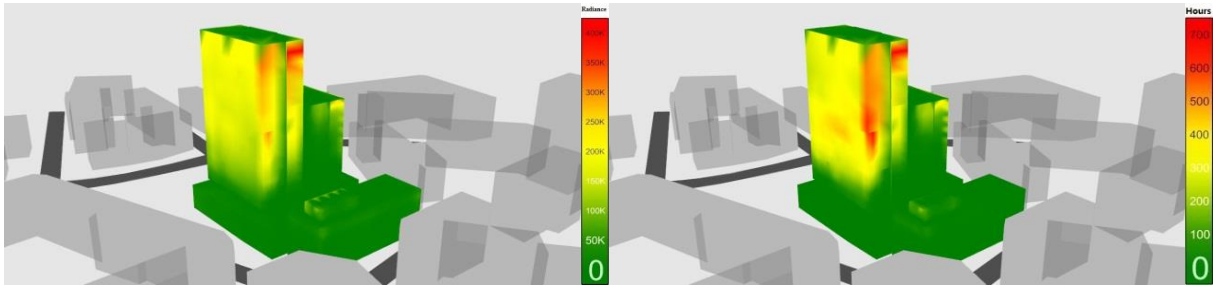

Figure 4: Left: Colour coded cumulative radiance on the assessed building envelope. Right: Hour count of luminance above threshold of 10000 cd/m^2 displayed on the assessed building envelope

After further processing of the time-series simulation results, the cumulative radiance of the reflected daylight from the assessed building envelope is calculated and displayed on the model (see Figure 4 left). The southwest facing façade of the tower block reflects intensive daylight and the extreme values occur at the highest levels of the southeast facing façade. The effect of the daylight reflection is also evaluated by counting hours when luminance is above threshold of 10000 cd/m^2 (see Figure 4 right). The color coded pattern is very close to the radiance distribution pattern in Figure 4 (left). The difference is that highest values are located around the medium height on the building rather than the highest levels.

Designers could focus the optimization work on the identified areas with extreme values in Figure 4. Whether to choose results from cumulative radiance assessment or radiance above threshold depends on the function of the neighbouring buildings and the potential effect of the reflected daylight.

CONCLUSION

A software tool for the assessment of reflected daylight from building envelopes has been developed. It overcomes the drawbacks of the existing assessment methods. Detailed model for the assessed building envelope and the neighboring buildings are accepted. Material reflection property is emphasized for the building models which should be based on verified or measured material models. Forward ray tracing is introduced to the evaluation procedure as a pre-processing step for the following annual simulation. It could identify all critical positions in the neighborhood where daylight is concentrated and make the later steps more efficient. Both weather data and CIE weather model could be used for the time-series simulation. For all viewpoints assessed in the neighborhood, rich information could be recorded including annual irradiance values contributed from the assessed envelope, period with irradiance value above a threshold, origin of the reflected daylight on the assessed building envelope, etc. With the assessment results displayed on the 3D model using color scale, designers could identify the critical areas on the envelope quickly and adjust the envelope design accordingly.

Further improvement of the presented method is possible. The assessment result could be linked to algorithms for mesh modification. With this feature, the whole design-assessment process could be repeated automatically. Ideally, the improved method could suggest optimized envelope design in which minimal modification is involved. Validation of the assessment results with more case studies is also planned.

REFERENCES

1. Whitely J, 2010. Vdara visitor: ‘Death ray’ scorched hair. *Las Vegas Review-Journal*, http://www.lvrj.com/news/vdara-visitor---death-ray--scorched-hair-103777559.html
2. Building and Construction Aothority of Singapore, 2010. Building Control Act. http://www.bca.gov.sg/BuildingControlAct/building_control_regulations.html
3. California Natural Resources Agency, 2007. Final Environmental Impact Statement / Environmental Impact Report. http://www.lbl.gov/Community/pdf/env-rev-docs/LRDP-final/FEIR-5.pdf
4. City Council of Busselton, 2010. Reflective building materials policy: consideration for adoption for community consultation. http://www.busselton.wa.gov.au/files/Draft%20Reflective%20Building%20Materials%20Officers%20Report.pdf

5. Schiler, M. and Valmont, E., 2005. MICROCLIMATIC IMPACT: GLARE AROUND THE WALT DISNEY CONCERT HALL
http://www.sbse.org/awards/docs/2005/1187.pdf
6. Shih, N.J. and Huang, Y.S., 2001. An analysis and simulation of curtain wall reflection glare, Building and Environment 36 (5): 619–626.
7. Hassall, D.N.H, 1991. Reflectivity: dealing with rogue solar reflections.
8. Reinhart, C.F. and Walkenhorst, O., 2001. Dynamic RADIANCE-based Daylight Simulations for a full-scale Test Office with outer Venetian Blinds. Energy & Buildings, 33(7): 683-697.

PLANNING FOR SOLAR SMART CITIES

M. Amado [1]; F. Poggi [2]

1: Civil Engineering Department, Faculdade de Ciências e Tecnologia da Universidade Nova de Lisboa, Campus da Caparica, 2829-516 Caparica, Portugal. ma@fct.unl.pt

2: GEOTPU - Faculdade de Ciências e Tecnologia da Universidade Nova de Lisboa, Campus da Caparica, 2829-516 Caparica, Portugal. f.poggi@fct.unl.pt

ABSTRACT

In order to respond to the growing urbanization process and subsequent energy demand, methodological approaches which implement alternative urban models are required to support the indispensable change towards more energy efficient cities. This paper discusses the solar energy potential of built environments and explores how urban planning can contribute to converting existing cities into Solar Smart Cities. To support this study, a performance-based analysis was done on an existing urban area taking into account the solar potential of roofs and the optimization of power distribution networks across the city neighbourhood. Using GIS and dynamic simulation software, urban morphological parameters and land use patterns have been identified and characterized to support the urban planning process. Statistical data of energy consumption at the neighbourhood level were used to estimate peak to off-peak periods taking into account current uses of buildings and their duration, frequency and temporal distribution during the day. This study shows the positive contribution that solar energy can offer at building block level and how urban planning and energy management supported by a solar smart grid can be important tools to reach the energy balance across a whole city.

Keywords: Solar Smart City, photovoltaic systems, GIS, urban planning, smart grids

INTRODUCTION

What are the determining factors and parameters that would turn an existing city into a Solar Smart City? This paper develops an approach that could be considered as a starting point for further discussions and research contributing to the global transition to renewable energy and more energy efficient cities.

Around 75% of global energy consumption occurs in cities and 80% of greenhouse gas emissions that cause global warming comes from cities [1]. These trends cannot continue along the same path and implementation of alternative urban models is required to support the indispensable change towards more energy efficient cities.

The Kyoto Protocol objectives to reduce global greenhouse gas emissions and, more recently, the emerging constraints on energy supply have increased the importance given to energy efficiency policies [2].

Furthermore with 40% of global energy consumption consumed in buildings [3] it is evident that the first step has to focus on actions to improve energy performances and efficiency in both new and existing buildings. Dealing with issues of energy security, access and demand, the generation of renewable energy within the city boundaries constitutes a substantial resource to be correlated with efficiency and conservation measures.

Whereas a global emergency regarding cities is their energy-consumption, several studies on renewable energy technologies show that urban areas have an enormous solar potential both for photovoltaic and thermal applications that at present is not exploited [4] [5] [6] [7].

In planning a solar smart city, the objective is to make the most of the solar photovoltaic potential on suitable rooftops and improve the energy balance setting out over a smart grid. On the other hand, urban planning can play a key role through integration and intensification, and thus manage the production of energy through the use of the solar potential on suitable built roof and façade areas.

In recent years this approach, which focuses on energy consumption and solar energy potential aiming to global city energy balance, has emerged as the name of Solar Urban Planning [8]. In this perspective, urban planning adopts the use of solar potential as a key urban design principle to improve energy efficiency in existing urban areas and promote Building Integrated Photovoltaics (BIPV) in new ones.

METHODOLOGY

In order to approach solar energy production and consumption at the urban scale, several studies have been considered. By reviewing them in comparison, it is evident that urban geometry has large impacts in both these domains.

The estimation of the solar potential on a suitable roof and façade area has to take into account factors such as the spacing between buildings to avoid overshadowing, their orientation and the type of roof [8] [9] [10] [11].

Likewise energy consumption is strictly related to urban form but also to other factors which depend on user activity in buildings including its duration, frequency and temporal distribution during the day [12] [13].

The proposed methodology is based upon a sequence of four steps which on one hand reflect the literature review and on the other hand focus on the urban planning role in ensuring the use of solar potential and managing the energy balance across the city.

Appling the case study method, a medium sized city localized in Portugal was selected to illustrate the methodological structure of the research.

Step 1: Data Collection

In conducting this research, the data collection aims to select and correlate indicative data which characterize the urban morphology and land-use patterns in the city.

Census data on population and buildings features were collected from the Information Reference Geographical Database (BGRI) released by the National Institute of Statistics (INE, Portugal) [14] and then combined with satellite imagery and topology across a GIS platform.

Step 2: Division of city into sub-spatial units

In this step the determining parameters that permit the energy consumption prediction and the solar potential estimation in the urban context are identified [8] [9] [12] [13].

According to this framework, the city was divided into Sub-Spatial Units that represent the "backbone" to evaluate and manage the energy performances across the city (Table 1).

Within the sub-spatial unit, the buildings blocks were then classified in order to build parametric elements and provide a common structure for the GIS platform to support and facilitate the urban planning approach from the local to the whole city scale (Table 2).

	**Neighbourhood Area (m²)**	71057
	Nº of Subdivision	13
	Nº of Buildings	60
	Resident Population	2615
	Pervious Area (m²)	5192
	Total flat roof area (m²)	18781
	Total pitched roof area (m²)	3955

Table 1: Sub-Spatial Unit

	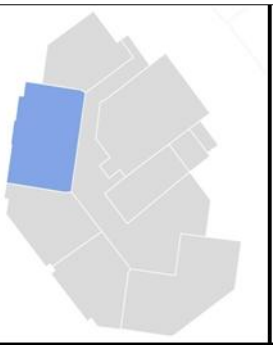	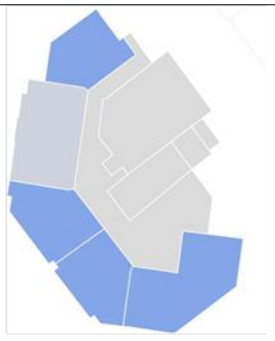	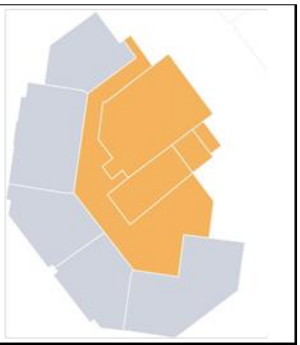
Year of Construction	1946 to 1960	1961 to 1970	1961 to 1970
Current use	Residential	Residential	Endosed Parking Garages
Resident Population	72	209	_
Nº of Buildings	1	4	3
Nº of Floors	8	8	1
Street orientations	8º N>O	52 º N>O / 35º N>E / 58º N>O	35º N>E

Table 2: Building block parameterization

Step 3: Energy Consumption Prediction

The energy consumption prediction at the urban scale is a quite complex process that depends on various factors [13].

To date, this study presents only the electricity consumption prediction based on statistical information for different building uses as shown in the Table 3 [14] but a considerable approximation is evident in this kind of approach.

Average annual electricity consumption by building use	1398 (Residential: kWh/inhab)		50 (kWh/m²)
Annual building energy consumption at the block level (kWh)	100620	292078	73000

Table 3: Energy consumption

According to this reflexion and using dynamic simulation software, the analysis of the constructive and geometrical aspects of buildings and occupant behaviour is already a work in progress to reach better results (Table 4).

3d Building model	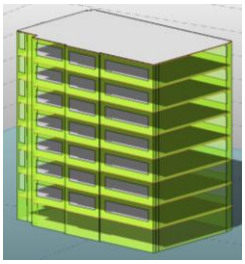	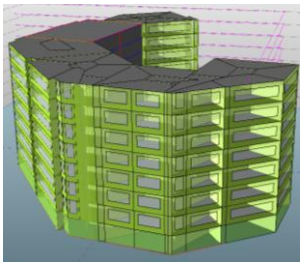	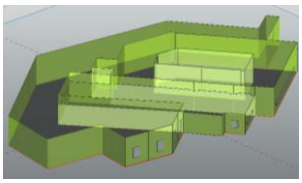
Total building height (m)	27.3	27.2	5.2
Typical floors height (m)	2.7	2.7	_
Single gross floor area (m²)	436	282 / 315 / 304 /493	1461
Resident Population	72	209	_
Total gross floor area (m²)	3860	11152	1460
Total gross façade area (m²)	1529	6681	1524
Volume (m³)	11848	39648	7058
Percentage of surface area which is glazed	21%	31%	2%

Table 4: Building parameterization at the building block level

Step 4: Solar Energy Production

According to related approaches to urban solar simulation, the net roof area available for a PV installation on the building block is determined assuming some reduction factors [8] [9] [11].

To estimate the annual energy production by PV systems the following equation [15] has been adopted:

$$Y = PR \times Me \times (Gr \times A) \quad (1)$$

PR is the Performance Ratio that considers the energy losses in the balance of system (adopted value in (1) | PR=75);

Me is the nominal module efficiency rating at Standard Test Conditions: air mass AM 1.5, irradiance 1 kW/m^2, cell temperature 25ºC reported by the selected manufacturer [16] (adopted value in (1) | Me = 13 %);

Gr is the sum of all global solar radiation values in each metric over a year (value obtained from Ecotect® simulation, see Table 5)

A is the net available roof area for PV installation (value calculated considering reduction factors [8] [9] [11]).

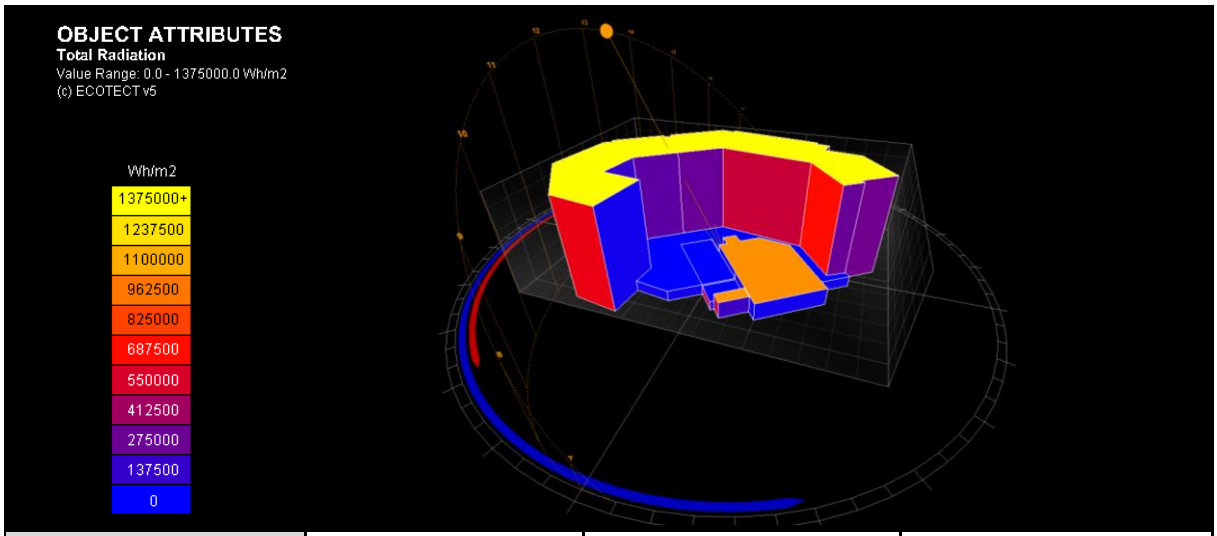

Gross roof area of building (m²)	436	1395	509
A | Net available roof area for PV installation considering reduction factors (m²)	371	1185	432
Gr | Sum of all global solar irradiation values over a year (kWh/m²)	1475	1449	1025
Mean annual global radiation on available roof area (kWh)	547225	1717065	442800
Predicted annual yield for PV systems on available roof area (kWh)	53354	167414	43173
Annual Solar Energy Supply	53%	57%	41%

Table 5: Solar energy production at the building block level

DISCUSSION AND CONCLUSIONS

"Will cities be able to be shaped by solar energy in the future?"

The concept of a Solar Smart City is likewise an atom structure: the neighbourhoods energetically behave as particles with positive, negative or no electrical charge and their energy balance is managed and improved by means of the solar smart grid that keeps the energetic performances of the whole city stable.

On this premise and as demonstrated by comparing energy consumption (Table 3) and solar energy production on roof areas (Table 5), the annual solar energy supply appoints at positive mean values of 50%. On the other hand, this result also shows how energy demand reduction is an indispensable step towards energy efficiency which has to include the adoption of measures at both the building and user behaviour level.

The construction of a GIS platform based on the proposed parametric elements allows the automatic approach to geometric and spatial characteristics of buildings, their energy performances and smart grid integration across all the sub-spatial units.

Following what has been described, further research will be carried out to understand how urban planning can play an important role improving energy consumption and production balance by means of mixed land use patterns and the utilization of smart grids, smart meters, and intelligent buildings across the city.

REFERENCES

1. Tibaijuka, A. K.: The Future in our Hands: Addressing the Leadership Challenge of Climate Change. Contribution of the United Nations human settlements programme, UN-HABITAT, New York, 2007.
2. World Energy Council.: Energy Efficiency Policies around the World: Review and Evaluation., World Energy Council, 2008.
3. WBCSD.: Energy Efficiency in Buildings – Transforming the Market., World Business Council for Sustainable Development;,ed : Atar Roto Presse SA, Switzerland, 2009.
4. Sarralde, J. J., Quinn, D., Wiesmann, D.: Urban modelling for resource performance analysis: estimating cities' renewable energy potential. In: Proceedings of Building Simulation 2011, Sydney, pp.1370-1377, 2011.
5. Eicker, U.: Renewable Energy Sources Within Urban Areas – Results From European Case Studies. In: Proceedings of Chicago Winter Conference 2012, Chicago, 2012.
6. Angelis-Dimakis, A., Biberacher, M., Dominguez, J., Fiorese,G.: Methods and tools to evaluate the availability of renewable energy sources. Renewable and Sustainable Energy Reviews, Vol.15, pp.1182-1200, 2011.
7. Jäger-Waldau, A., Szabó, M., Scarla, N., Monforti-Ferrario, F.: Renewable electricity in Europe. Renewable and Sustainable Energy Reviews, Vol.15, pp.3703-3716, 2011.
8. Amado, M., Poggi, F.: Towards Solar Urban Planning: A New Step for Better Energy Performance. Energy Procedia, Vol.30, pp. 1261-1273, 2012.
9. Gadsden, S., Rylatta, M., Lomas, K., Robinson, D.: Predicting the urban solar fraction: a methodology for energy advisers and planners based on GIS. Energy and Buildings, Vol.35, pp.37-48, 2003.
10. Wiginton, L., Nguyen, H., Pearce, J.: Quantifying rooftop solar photovoltaic potential for regional renewable energy policy. Computer, Environment and Urban Systems, Vol.34, pp.345-357, 2010.
11. Izquierdo, S., Rodrigues, M., Fueyo, N.: A Method for Estimating the Geographical Distribution of the Available Roof Surface Area for Large-scale Photovoltaic Energy-potential Evaluations. Solar Energy, Vol.82, pp.929-939, 2008.
12. Ratti, C., Baker, N., Steemers, K.: Energy consumption and urban texture. Energy and Buildings, Vol. 37, pp. 762-776, 2005.
13. Maïzia, M., Sèze, C., Berge, S., Teller, J., Reiter, S., Ménard, R.: Energy requirements of characteristic urban blocks. In: Proceedings of the CISBAT 2009 - Renewables in a changing climate - From Nano to urban scale, Lausanne, pp.439-444, 2009.
14. INE: Instituto Nacional de Estatística. Available at: http://www.ine.pt/xportal/xmain?xpid=INE&xpgid=ine_main
15. Bahaj, A., James, P.: Urban energy generation: The added value of photovoltaics in social housing. Renewable and Sustainable Energy Reviews, Vol.11, no. 9, pp.2121-2136, 2007.
16. Martifer Solar, Photovoltaic inverter manufacturer, http://www.martifersolar.com/pt

PALM TREES AS MODEL FOR SUSTAINABLE PLANNING IN THE SAHARAN REGIONS - CASE OF ZIBAN

Soumia BOUZAHER LALOUANI[1]; Moufida BOUKHABLA[2] Prof. Djamel ALKAMA[3]

1,2&3: Department of Architecture - Faculty of Science and Engineer's Sciences.

Med Khider-Biskra University, BP. 145 RP 07000 Biskra. Algeria.

ABSTRACT

This paper describes and analyzes a study regarding the requalification of palm trees as a sustainable instrument for urban planning. The objectives are to find a simulation of the sunspot under the palm trees, the optimal height of the palms and distance between them to promote an adequate shade on a defined surface. The study will confirm that the urban ecosystem can be restored by the reuse of palm trees to protect outdoor spaces.

Keywords: Sustainable urban planning, arid regions, palm trees

INTRODUCTION

Palms are the backbone of the oasis ecosystem and agricultural character of social life in Ziban. They have an ecological role that limits the advancing desert. Also, they create an essential microclimate for the proper development of understory crops. On the ground palm trees cover very large areas, minimizing the solar gain of the areas under palm trees, creating shaded areas identical to Saharan regions. The return to agriculture and palm trees, which is the original culture of Ziban particularly and the desert generally, becomes a necessity. In order to promote the use of palm trees, it must be integrated in development and urban planning.

Current situation of the case study, the Ziban (wilaya's Biskra):

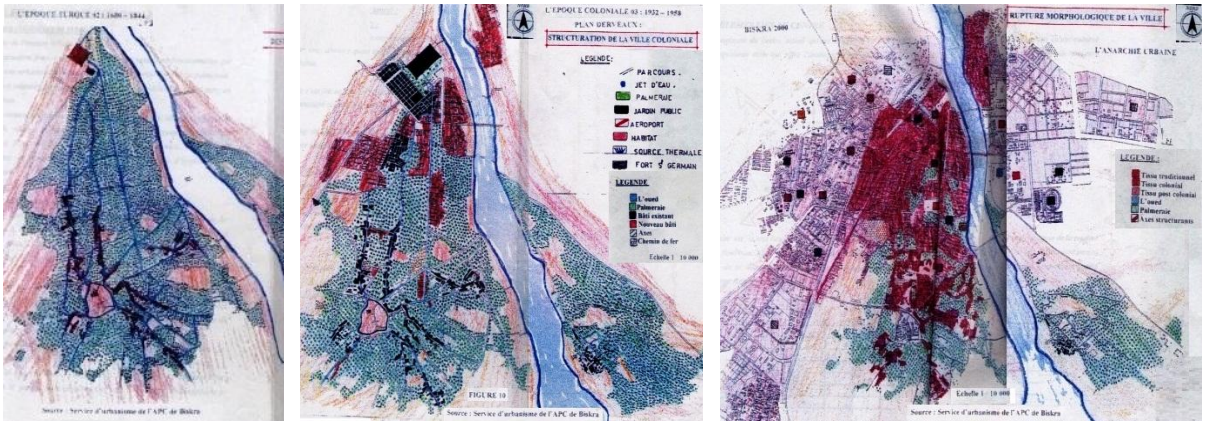

Figure 1: Maps show the mutation of oasis into urban space. Source: APC de Biskra.

These maps show the disappearance of palms from left to right; the first card presents the Turkish colonial period in 1844 , the second presents the period during the French colonialism from 1932 to 1958 and the third presents the post-colonial French period from 1962 into know. [1] We clearly see the continual loss of palm trees, natural heritage of this Zab, leading to an imbalance in the oasis ecosystem and consequently in the desert urban ecosystem. Urban growth in this Zab happens despite the palm groves which have undergone several transformations since the creation of the first cores till today.

Climatic Context

The climate of the micro-region is desert-prone arid and semi-arid, with a high temperature in summer reaching (48.8°C) in August, and a low temperature of (1.6°C) in February. Because of the desertification phenomena we get a longer and a hotter summer and a dry and shorter winter, with a 139, 8 mm / year of average rainfall [2].

In a previous research we have shown that palm trees are the sustainable armature of the oasis ecosystem. [3] Symbol of oasis agriculture, they are centers of life and a source of inestimable values: religious and moral, [4] cultural and economic. [5] To revitalize the use of this element and to restore the urban and oasis ecosystem we have proposed in this second part of work a project of local sustainable management module for outdoor spaces exposed to sunlight.

Calculation of Ziban overheated zone

This diagram highlights the diurnal and seasonal variability of air temperatures. To plot it, first we project the maximal and minimal monthly temperatures (Table1) on the calculator's hourly temperatures (Figure 2a). Then, in a table, we represent the temperatures for each month and draw lines linking between the maximal and the minimal.

Months	Jan.	Feb.	Mar.	Apr.	May.	Jun.	Jul.	Aug.	Sept.	Oct.	Nov.	Dec.
Max. t.	18°C	18°C	23°C	27°C	31°C	37°C	41°C	40°C	34°C	28°C	22°C	18°C
Min. t.	8°C	8°C	11°C	15°C	20°C	25°C	29°C	28°C	24°C	17°C	12°C	8°C

Table 1: Monthly temperature forecasts of Biskra (2011) Statements of the meteorological station of Biskra

The sunshine is significant; the number of hours of sunshine in warm periods exceeds 14 hours per day. In winter it is around 10 hours. (Figure 2a) This permits also considering the incidental energy on the ground that, by turns, is not negligible. "In the summer, the amount of incidental energy on a horizontal plane is 6682 Wh/m^2 [6] This solar potential offered by the climate of Ziban is promoting the integration of passive architectural processes. [7] Yet, a problem of overheating arises.

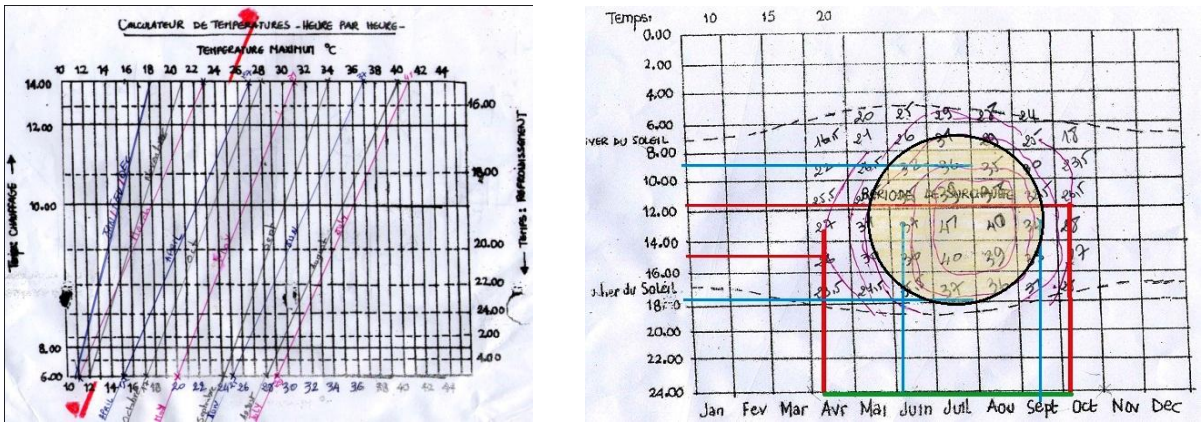

Figure 2(a): Hourly temperature calculator. (b): Ziban's matrix temperature per months and hours. *Source : S. Szocolay, (1979) [8]*

The thermo-isopleths presented in (Figure 2) show a close relationship between the average temperature and time of day (hour) and year (month), from which we can deduct three groups of zones: first one known as the zone of sub-heating, which lasts from December to February; second one known as the zone of comfort, which is defined by the neutral temperature 25 ° C and spans the months of March, October and November; third one known as the zone of overheating, which spans the months of May, June, July, August and September when the temperature exceeds 25 ° C, especially between 10 am and 6 pm, where the sun's intensity is high and requires solar control.

Once the temperatures are expressed in hours per month (Figre2b) we can carry them on the chart to determine the solar superheating zone. (Figure3)

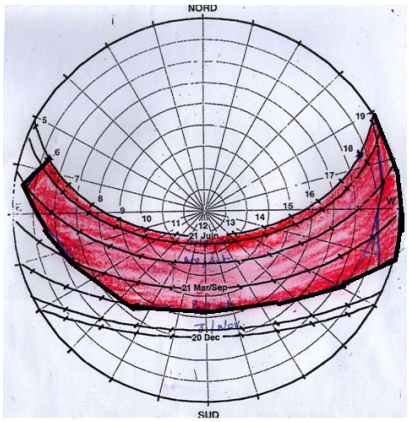

Figure 3: Polar diagram of Biskra, presentation of the superheated zone

The solar diagram of the micro region of Ziban latitude 35 ° confirms that the superheated zone is spread over all months of the year except winter. Summer is the overheating period. It starts from 6 am until 7 pm. This fact calls for the occultation of outdoor areas.

DATE PALMS - A TOOL OF SOLAR OCCULTATION IN ZIBAN

The proposed sustainable planning module counts with 15 palm trees per person [9]. For agricultural reasons, there are 2 palm tree planting methods in the Sahara (Figure 4), the "Quintral System" and the "Square System", which we will use it since it is the most common.

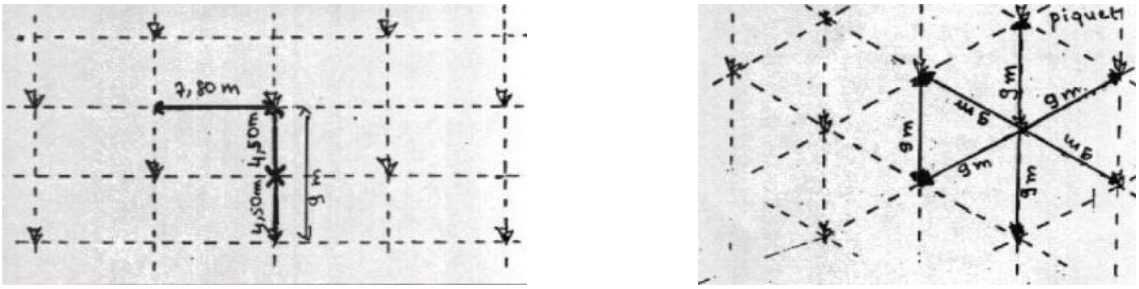

Figure 4: a) "the Square System" (b) the Quintral System Source: SECAAR

In this part of the study we have changed the orientation of "the square system" to southeast and southwest, the two orientations most exposed to solar radiations; three models of palm trees with varying distances are studied, and a height of approximately 10 m. The corresponding scale models were exposed under the sun of the hottest month of the year, June, simulated by the heliodon.

Figure 5: the simulation of palm trees Source: author

The 7 m x 7m module

Several studies in the field of agronomy found that a distance spaced from 7 m up to 10 m represents the best spacing in agricultural terms, [10] as a higher density has detrimental effects on yields and the ventilation of palm trees, since it hinders mechanization and handling inside the palm groves and makes difficult any development effort [11]. Besides, high density creates an unfavorable microclimate, and requires more work since the operations applied individually to each palm tree are even more numerous. [12]

The 5 m x 5 m module

This setting is chosen to to protect outdoor areas. The old palm groves were designed with such a dense spacing. It optimizes shade, compared with the new palm groves; but it does not foster the maintaining of palm trees and underlying cultures.

The 3 m x 3 m module

Traffic spaces in the region of Ziban are more or less narrow. Mmaximum distances in the streets and traffic lanes are 20 m for divided highways including pedestrian traffic areas. Pedestrian zones include an area of 3 m to 1.5 m, which is why we chose this as a third pattern for the study.

	3mx3m module	**5mx5m module**	**7mx7m module**
10 am			
12 am			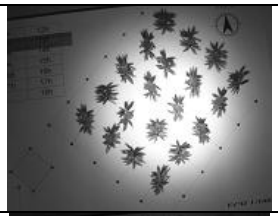
2 pm		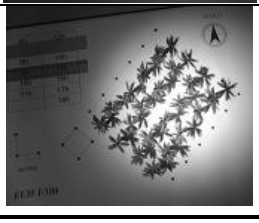	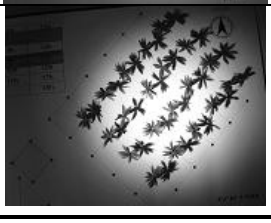

4 pm			
6pm			

Table 2: capture of the solar occultation of Jun 21st, the hottest month of the year by three different modules of palm groves (2012)

RESULTS

By comparing the three modules we notice that:

3 m x 3 m spacing allows more solar occultation over the whole day.

5 m x 5 m spacing: from 8 am till 12 am the spaces, under the palm trees, are shaded, from 12 am till 2 pm the spaces, under the palm trees, are less shaded, from 4 pm till 6 pm the spaces, under the palm trees, are also shaded.

7 m x 7 m spacing does not offer a great opportunity for occultation compared with the two other modules. But we note that: from 8 am till 12 am the spaces under the palm trees are enough shaded, from 12am till 4pm the spaces under the palm trees are not shaded, from 4pm till 6pm the spaces under the palm trees are less shaded.

5*5 m2 spacing can be used for solar occultation of public spaces, such as plazas and walkways, structuring and management of boulevards (more or less 20 m wide in arid regions). It serves as a Tool for channeling pedestrian traffic and provides a wide variety of planning possibilities (child play areas, fountains ... etc.).

As to the module 7*7 m2, it will be a good cover for vehicle stopping and parking spaces as well as for marking entrances of equipments such as universities, town hall, hospitals, and towns.
In both instances, palms will play an important role. The regular grid also allows easier surveillance for public security, and a good definition of visual landscape and perspective.

DISCUSSION

What happens in the urban context of the micro Ziban, which was one of the greatest oases, is public spaces desertion or worse, their mutations in to parking zones. As a result of the lack of inadequate development of outdoor spaces in the arid and semi arid area during the overheating period between 11 am and 3 pm they become places of aggression.

The integration of palm trees as a planning tool of outdoor spaces can promote their good practice. It will allow minimization of reflected solar radiation, absorption of sound noise, and consumption of CO2 emitted by vehicles, and finally the use of all the heat emitted for the maturation of dates.

Socially, the inhabitants of the micro region speak nostalgically about the atmospheres created in the oasis of the 80s (before they were burned or abandoned and sold as land) restoring this nostalgia can only encourage rooting society.

CONCLUSION

Sustainable planning, according to the Canadian Council of Forests Ministers intends "to maintain and improve the long-term ecosystem health ... for the benefit of all living beings ... while providing for present and future generations good environmental, economic, social and cultural prospects "[13]. Hence the need for this scientific approach to find the best density of “palm trees” for the studied oasis, which represents both the economic and environmental capital of Ziban and any Saharan regions.

This study has shown that the palm tree square system used by farmers to preserve the underlying cultures can be a tool of local and sustainable management of outdoor spaces for these regions. As we have seen, the module 5 m x 5 m is the most favorable for solar occultation in arid and semi arid regions.

The reuse of the palm tree as a tool of planning can help restore the oasis ecosystem through first the resumption between urban and natural heritage and second the rootedness of society itself in its natural context. This reuse must necessarily be a promoting factor to the recovery of the oasis identity of Ziban. It must also be a great developing project to prevent desertification. In order to promote the use of palm trees, they must be integrated in development and urban planning.

REFERENCES

1. Urbanism division of the APC of Biskra
2. La monographie de la wilaya de Biskra, 2009.
3. Soumia Bouzaher 2012 Palm trees reuses as sustainable element in the Sahara. The case of Ziban, as self-sustainable urban units in proceedings TerraGreen Lebanon,
4. Belguedji M, les ressources génétiques du palmier dattier : caractéristiques des cultivars du dattier dans les palmeraies du sud-est algérien Revue INRAA N°1/2002 ; pp 28-29
5. Scanagri, Etude des marchés des produits du palmier dattier du Maghreb : Analyse diagnostic du secteur du palmier dattiers en Algérie, Maroc et Tunnisie projet 2004 p.11-17
6. Capderou, M., Atlas solaire de l'Algérie énergétique, Tome 2 V 2, OPU Alger n: 2075-10-85. Alger, 1985, pp. 140-399.
7. Berghout, B. « Effet de l’implantation d’un bâtiment collectif sur le confort hygrothermique intérieur cas de Biskra », Algérie, MONTRÉAL. 2012 p. 37.
8. S. Szocolay, 1979
9. Soumia Bouzaher, The Ziban as Sustainable City in the Sahara in proceedings CISBET Lausanne, Switzerland 2011 pp.653-658.
10. SECAAR, http://www.secaar.org/. A10 Palmeraie - Comment créer une palmeraie sélectionnée. 2002.
11. Benziouche, S. 2008 L’impact du PNDA sur les mutations du système de production oasien dans le sud algérien. Revue des régions aride IRA Médenine, Tunisie,21, 1321-1330.
12. Conforti J. et Benmahmoud O. Zonage des oasis du Jérid. 1994. In Cahier du CIRAD. France .
13. Conseil canadien des ministres des forêts, 1992.

3-D GEOMETRICAL MODELLING AND SOLAR RADIATION AT URBAN SCALE - MORPHOLOGICAL OR TYPOLOGICAL DIGITAL MOCK-UPS?

Alessandra Curreli; Helena Coch Roura

Architectural Building Department, School of Architecture of Barcelona - Polytechnic University of Catalonia (UPC), Av. Diagonal 649, 08028 Barcelona (Spain)

ABSTRACT

Studies regarding solar energy at the neighbourhood scale always have to deal with the size and the complex geometry of a real built context. Three-dimensional modelling techniques allow visual reproduction of formal features and solar performance of a city portion. Nevertheless, the definition of the right level of detail (LOD) is always a crucial point when creating digital mock-ups.

On the one hand, currently available computational resources are not totally able to support the exact representation of a building cluster and the simulation of environmental phenomena is often based on parametrical analyses. On the other hand, a drastic geometrical abstraction could discard important information and affect the reliability of solar predictions.

This study aims to identify the most suitable LOD to simulate the solar performance at the *mesoscale* of the city. To do this, the direct radiation access within a building cluster is assessed by employing virtual models with different approximation degrees.

This comparison allows assessing the margin of error between different levels of detail and discussing about benefits and inconveniences of the two approaches. The results might be elaborated to define a rank of *deviation factors*, useful to evaluate the margin of error provided by generic models with regard to solar predictions.

Keywords: geometrical 3-D modelling, mesoscale, morphological and typological mock-ups, LOD, solar potential predictions, roughness

INTRODUCTION

The development and application of three-dimensional virtual models in the field of environmental studies offer great facilities to the research regarding solar access at the scale of the city district [1]. Traditional graphical methods [2] impose, in fact, a high degree of abstraction and provide information that is often limited to a schematic or two-dimensional representation of the urban context. Digital tools permit, instead, to handle large amounts of data and reproduce the complexity of a real urban structure considered as a whole system.

The employment of digital mock-ups for solar simulation allows for simultaneous evaluation of energy gains on different surfaces and ensures more accurate results. However, currently available hardware and software resources still have some limitations in exactly reproducing the complex interaction between the solar phenomenon and the extremely heterogeneous geometry of an urban portion. Therefore, a certain approximation degree is necessarily required by *mesoscale* modelling.

At the same time, applying drastic simplifications and assimilating the irregular urban fabric structure to a continuous array of identical blocks might cause the loss of relevant information and seriously affect the reliability of final outputs.

What is, therefore, the correct level of detail (LOD) for 3-D digital mock-ups at the neighbourhood scale? What is the relevant geometrical information to enclose, in order to get the right balance among calculating time, processing power and confidence of solar results?

Previous research was developed about the effectiveness of generic models for environmental analyses [3, 4] and about techniques for a simplified spatial representation of complex urban scenes [5, 6]. Outcomes of those studies commonly demonstrate the significant influence of morphological specificities on the amount and distribution of solar energy collected. Nevertheless, the possibility to exploit simple and synthetic models is not rejected at all, but it asks for some specifications.

The definition of a correct LOD for virtual models is firstly related to the final purpose of the solar analysis. Furthermore, it should be considered that the effects of any simplification action might differently affect solar predictions, depending on the *uniformity* of the original configuration and on the position of the exposed surfaces.

This paper deals with the assessment of solar potential on building façades and roofs by means of digital mock-ups with different levels of detail. The main purpose is to establish the most suitable LOD of 3-D models for solar simulation at the district scale. More specifically, it aims to evaluate the extent to which an identical simplification process might affect the solar potential of horizontal and vertical surfaces with regard to different degrees of *morphological roughness*. This kind of approach shall permit to identify the variable *deviation factor* associated to the application of generic models to different urban contexts.

METHOD

This study is based on the comparative analysis of solar predictions provided by the use of *morphological* and *typological* models. The former class keeps relevant geometrical specificities of the real urban form; the latter consists of a homogeneous simplified pattern, shaped according to the general and average spatial features deduced from experimental data.

Two urban fabric samples with very dissimilar formal structures were selected in the metropolitan area of Barcelona (Spain): the *Eixample* district (Case 1) is the result of a specific design and stands out for its ordered network; the *Barri Gotic* area (Case 2) keeps the typical features of an old city centre with narrow streets and irregular blocks (Figure 1).

Figure 1: Aerial view of the selected urban fabrics: Eixample (left) and Barri Gotic (right). Source: https://maps.google.es/

Morphological modelling

The *morphological* models (class A) were built on the basis of the cadastral plans which contain data about the number of floors, *patios*, courtyards and staircases of every block. Direct observation and photographical surveys were employed to complete and validate the available information. By assigning a height of 3m to each floor and extruding the plot footprint by computer-aided design techniques (software *AutoCad*), a 3-D reproduction of the existing buildings was therefore obtained.

The level of detail of these models is similar to level LOD2 of the CityGML official OGC Standard [7]. This means that the positional and height accuracy is about 2m and objects with a footprint of at least 4m x 4m are included (Figure 2).

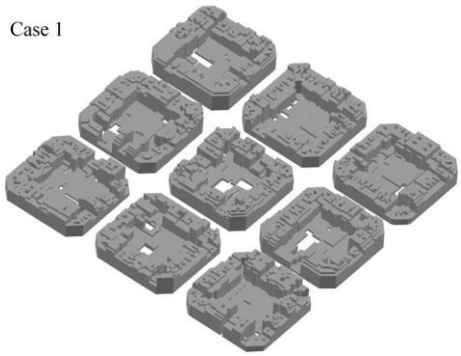

	Case 1	Case 2
Block volume	174.839	74.134 m³
Porosity	0,77	0,33

Figure 2: Morphological models of the Eixample (left) and Barri Gotic samples (right)

Typological shaping

The construction of the two *typological* models (class B) was based on the average dimensions determined by means of the *SpaceCalculator* method [8]. This tool allows calculating a series of indicators which express the abstract spatial properties of an urban area by mutually relating empirical data through mathematical functions (Fig. 3).

In order to reproduce the right proportion of full and empty spaces, the overall volume and the coefficient of *porosity* [9] were set equivalent to those of the *morphological* mock-ups (with a margin of error of about 2-3,5%); the proportions and distribution of voids were arranged according to the prevailing distinctive characteristics of the real urban fabric. The level of detail of typological models can be assimilated to LOD1 (see [7]), where the accuracy is about 5m and only major-scale objects are represented (Figure 3).

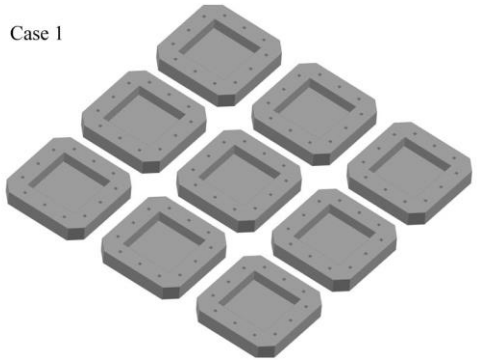

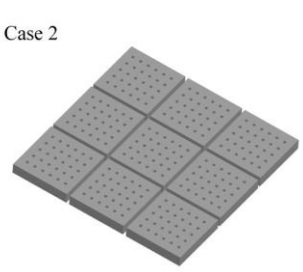

	Case 1	Case 2
Height	19,80	13,80 m
Side lenght	114,90	76,00 m
Street width	25,40	4,40 m
Block volume	179.539	76.716 m³
Porosity	0,78	0,34

Figure 3: Typological models of the Eixample (left) and Barri Gotic samples (right)

Assessment of solar potential and deviation factor

The **solar potential** is defined as the ratio of solar gains to exposure surface area of roofs and façades, independently. Horizontal ($\mathbf{SP_h}$) and vertical solar potential ($\mathbf{SP_v}$) were assessed in samples 1 and 2 with regard to the classes of model A and B, during the months with the highest and lowest level of irradiation: July and December, respectively. The solar simulation was implemented by means of the software *Heliodon 2* [10].

The **deviation factor** ($\mathbf{d_f}$) is computed as the percentage variation between solar potential values provided by the typological approach and solar potential values referred to the corresponding morphological method.

RESULTS AND DISCUSSION

Roofs

As a general tendency, the employment of *typological* mock-ups enhances the assessment of horizontal solar gains (Table 1). In fact, the flattening of height variations and the elimination of any protruding volumes considerably reduces the presence of obstructions on the roofs and improves their exposition to solar rays. The only surfaces that nearly do not receive any direct radiation are the covers of the minor *patios* located at a very lower level, but they do not affect the overall results, tahnks to their very limited extension.

In both case studies, the deviation factor between A and B in the month of December is more than double with respect to July (59% vs 23% in *Eixample* and 48% vs 21% in *Barri Gotic*), due to the greater impact of obstructions and of their cast shadows during the winter months.

Comparing the performances of the two urban patterns, it is observed that the values of d_f are slightly lower in Case 2 than in Case 1 (48% vs 59% in December and 21% vs 23% in July). This means that, when dealing with morphological models, the weight of shadowing on SP_h is more notable in the *Eixample* than in the *Gotic* district. This performance is attributable to the major presence of vertical projections on the roofs, that is to say to the higher level of *roughness* in the former case with respect to the latter.

Finally, it has to be noticed that the utter amounts of SP_h, are always higher in Case 2 than in Case 1. In other words, the simplification process does not modify the general tendency of behaviour: both morphological and typological models, in fact, evidence that covers in the *Barri Gotic* area have a bigger solar potential with respect to those in the *Eixample* district.

Case studies	Model A	Model B	**d_f** (%)
1_Eixample	17,40	27,61	**59**
2_Gotic	23,25	34,42	**48**

Case studies	Model A	Model B	**d_f** (%)
1_Eixample	155,00	191,07	**23**
2_Gotic	165,09	199,82	**21**

Table 1: Horizontal solar potential (SP_h) in kWh/m^2: December (left) and July (right)

Façades

Vertical surfaces show a more complex functioning with regard to the use of different LOD models, but some points in common with the performance of roofs can be found. The results confirm that the influence of actual geometry on solar potential is more important during the cold season: in absolute values, d_f decreases from 72% to 51% in Case 1 and from 34% to 4% in Case 2, in December and July, respectively (Table 2).

Once more, the deviation factor is more elevated in the *Eixample* than in the *Barri Gotic* neighbourhood and the difference between the two cases is more considerable than before: d_f is 72% vs -34% in the cold period and 51% vs -4% in the warm one. These data verify the tendency that was previously identified, that is to say the greater impact produced by the simplification process on SP_v in the sample 1 with respect to the sample 2.

However, while in the case of roofs the divergence was entirely attributed to the height variations, the performance of vertical surfaces is also affected by the *horizontal roughness*, that is understood as the presence of folds, protrusions and indentations with respect to the hypothetical "straight line" of a façade. Looking at the spatial distribution of the SP_v, the main differences between models A and B are effectively detected on internal fronts of the block, which show a very fragmented geometrical structure.

The most remarkable and probably unforeseen result is that the employment of typological models leads to an under-estimation of the solar potential on *Barri Gotic* façades, namely: -34% in winter and -4% in summer. This one constitutes the only case, among those which were studied, where the homogenization of irregularities (i.e. the inner outline and cavities of the block) improves possibilities for solar access.

Despite the contrasting results obtained in cases 1 and 2, it is important to point out again that the overall qualitative trend is not altered by the application of simplified models: in both A and B, in fact, the results display that the *Eixample* configuration supplies a higher vertical solar potential than the one provided by the *Barri Gotic* domain.

Case studies	Model A	Model B	$\mathbf{d_f}$ (%)
1_Eixample	11,42	19,65	**72**
2_Gotic	7,07	4,64	**-34**

Case studies	Model A	Model B	$\mathbf{d_f}$ (%)
1_Eixample	32,67	49,45	**51**
2_Gotic	24,65	23,67	**-4**

Table 2: Vertical solar potential (SP_v) in kWh/m^2: December (left) and July (right)

CONCLUSIONS AND FUTURE DEVELOPMENTS

This paper examines and compares the application of variable level-of-detail digital mock-ups with regard to the assessment of solar potential within different urban patterns.

In general terms, the results of the analysis demonstrate that the same LOD might produce changeable margins of error in evaluating possible solar gains, depending on the roughness and on the spatial characteristics of the urban pattern, on the period of the year and on the relative position of surfaces which are considered. It is, therefore, not possible to define an optimal LOD for solar simulation at urban scale nor identify a univocal deviation factor to be indistinctly applied to all classes of typological models. Nevertheless, some general considerations can be done:

- The simplification process mostly affects the three-dimensional virtual models of those urban fabrics which display a high degree of geometrical roughness.

In the present analysis, the highest deviation factor is detected in the case of the *Eixample*. The apparent morphological homogeneity that characterizes this pattern is actually limited to the street network and the external perimeter of the blocks, but the effective distribution of volumes is jagged. In fact, both the *compactness* and the *porosity* coefficients (see [9]) confirm that the *Eixample* sample has a lower level of mass concentration and a denser distribution of empty spaces with respect to the *Barri Gotic* one, which exhibits, instead, a smoother envelope.

- The employment of typological digital mock-ups might have dissimilar effects on quantitative predictions of solar potential, according to the vertical or horizontal position and to the *openness* of a surface.

In the case of roofs, the flattening of vertical projections generally produces an over-estimation of the energy collected. In the case of façades, the influence of roughness enhances or reduces the SP_v according to the greater or lesser *spaciousness* of the block internal surfaces. In fact, the deviation factor assumes positive values in wide and unobstructed spatial surroundings (i.e. the central courtyard in the *Eixample* block), but becomes negative when close and narrow spaces are considered (i.e. the resulting room within the *Barri Gotic* block). From the historical point of view, this performance might be related to the fact that the unplanned growth of the *Gotic* district probably allowed for an "instinctive" and spontaneous exploitation of available space, in order to get optimal solar exposure conditions.

- For both horizontal and vertical surfaces, the incorporation of specific details within the morphological 3-D modelling is definitely more impacting during the cold season because of the lower altitude of the sun in the sky vault and the greater impact of cast shadows.

In summary, it must be recognized that, in all the cases that have been studied, a lower approximation degree (from LOD2 to LOD1) does not modify the tendential relative solar performance of roofs and façades within a particular layout. Therefore, the employment of simplified models appears particularly suitable and helpful in comparative analyses aimed at evaluating the qualitative solar potential of different urban fabric archetypes. This kind of approach might be useful during the early decision steps of the design process, in order to fit urban design solutions and predicted daylight and thermal requirements.

However, specific attention should be paid to the simplification process, particularly to the definition of proper criterions and tools to regulate and implement the transition from a morphological reproduction to a typological representation of the city at the mesoscale. The manual method applied in this study proves to be valid and reliable, but displays some restrictions in the simultaneous handling of several dimensional and formal parameters. For this reason, the typological modelling necessarily requires a certain approximation degree.

A *parametrical* approach, supported by appropriate computational and modelling software, is strongly recommendable for further investigation about 3-D digital mock-ups and solar potential assessment. This kind of method would ensure a greater rigorousness with regard to the consistency between different level-of-detail models and to the assumption of generally applicable results. Furthermore, it would enable systematic processing of digital mock-ups and solar comparative analyses extended to a wider series of urban cases.

REFERENCES

1. Peckham, R.J.: Shading evaluations with three-dimensional models. Computer-Aided Design, Vol. 17, Issue 7, pp. 305-310, September, 1985.
2. Littlefair, P.: Passive solar urban design: ensuring the penetration of solar energy into the city. Renewable and sustainable energy reviews, Vol. 2, Issue 3, pp. 303-326, Sept., 1998.
3. Rasheed, A. et al.: On the effects of complex geometries on mesoscale modelling. ICUC-7 7th International Conference on Urban Climate, Yokohama, Japan, 29 June–3 July, 2009.
4. Beckers, B. et al.: About solar energy simulation in the urban framework: the model of Compiègne. 3rd International Congress Bauhaus Solar, Erfurt, Germany 10-11 Nov., 2010.
5. Adolphe, L.: A simplified model of urban morphology: application to an analysis of the environmental performance of cities. Environmental and Planning B Planning and Design, Vol. 28, Issue 2, pp. 183-200, 2001.
6. Ratti, C. et al.: Building form and environmental performance: archetypes, analysis and an arid climate. Energy and Buildings, Vol. 35, Issue 1, pp. 49-59, January, 2003.
7. Gröger, G., et al.: OpenGIS® City Geography Markup Language (CityGML) Encoding Standard. Open Geospatial Consortium Inc., 2008. www.opengeospatial.org
8. Berghauser Pont, M., Haupt, P.: Spacematrix. Space, density and urban form. NAi Publishers, Rotterdam, 2010.
9. Serra, R., Coch, H.: Arquitectura y energía natural. Edicions UPC, Barcelona, 1995.
10. Beckers, B., Masset, L.: Heliodon2. www.heliodon.net, 2011.

A DESIGN APPROACH FOR THE SOLAR OPTIMIZATION OF BUILT VOLUMES

Validation on a residential building's project in a historical district in Milan, Italy

Massimiliano Giani[1]; Cristian Belfiore[1]; Gabriele Lobaccaro[1]; Gabriele Masera[1]; Marco Imperadori[1]; Francesco Frontini[2]

1: Politecnico di Milano, Department of Architecture, Built Environment and Construction Engineering, Campus Leonardo, 20133, Milano, gabriele.lobaccaro@mail.polimi.it Phone: 0223996017

2: University of Applied Sciences and Arts of Southern Switzerland (SUPSI) CH 6952 Canobbio, Switzerland

ABSTRACT

This paper presents a process of solar potential optimization for residential buildings in high density urban areas. The process is validated through its application to the project of a mixed use, net zero energy building including public facilities and four levels of apartments. The optimization process concerns three phases: energy, solar and panelling optimization. The design approach combines parametric volume transformations (*Rhinoceros - Grasshopper*), solar dynamic analysis (*Daysim*) and solar maps analysis (*DIVA for Rhino*). The energy optimization regards the reduction of the heated volume, compared with the allowable volume defined by the regulations of the city of Milan, to a smaller one with lower internal heights, minimizing the building's energy demand. The solar optimization is focused on the transformation of the initial volume based on the local urban parameters (distance among buildings, allowable profile, building's height, plot ratio), in order to improve the solar exposure and maximize the solar access. The façades are modified to reduce the overshadowing effect of the nearby buildings, maintaining the same volume. The optimized volume derives from parametric studies about solar availability tilting the vertical facades away from the vertical. Solar dynamic annual analyses were conducted using *Daysim* and *DIVA for Rhino* in order to compare the initial and the solar optimized scenarios. The first set of simulations was carried out on both the isolated initial and optimized volumes, while the second set was carried out on the latter volumes placed in the district, thus affected by the surroundings. The loss in floor area due to the slope of the south and east façades is balanced by the addition of living areas facing the inner court without losing any commercial floor area. This choice allows a comparison of the two buildings, which have different shapes but the same volume. The annual solar mapping analysis is performed to localize the most irradiated parts of the building envelope, giving the possibility to design both a photovoltaic or thermal solar system with variable density elements. The results show the increase of available solar radiation in solar optimized design, while the panelling study permitted to optimize both technology and energy design of the solar systems required and furthermore to justify the architectural choices that led the building's design. The studies have demonstrated that through the optimization of the building shape, it is possible to obtain a huge improvement in the amount of solar radiation available on the façades, while keeping the same envelope surface. The next steps of the research will be focused on the analysis of both photovoltaic and solar thermal panels' efficiency, as well as the related assessment of increased surface temperatures on the façades, due to the solar energy system integration.

Keywords: Solar Potential, Energy optimization, Solar dynamic simulation, Panelling façade.

INTRODUCTION

Recent surveys show that 31% of the electrical energy and 44% of the thermal energy produced are consumed by houses, offices and commercial buildings causing 36% of CO_2 emissions in Europe. Most of this energy is used for heating (78%) and air-conditioning (25%) [1]. These data show how important it is to design self-sustainable buildings in order to fulfil the energy needs taking advantage of renewable sources and reducing the impact on climate. In the recast of the Energy Building Performance Directive (2010/31/EU), the European Commission has established that by 2020 all new buildings within the European Union should reach the nearly zero energy buildings standards [2]. In this scenario it is necessary to develop an integrated design process taking into account the most important technical aspects since the early design phases. Therefore the right orientation, exposure and design of the building envelope, as well as its performance and the choice of the solar integrated systems, should be considered since the preliminary design steps [3] [4]. The design process should be carried out evaluating different shapes and observing their effects in terms of solar access and irradiation onto the building itself, as well as the effects over the surroundings and from the surroundings to the building [5] [6] [7]. This paper shows a process of design optimization of a new building located in via Palermo, North of the city centre of Milan (Italy). This is a high density area composed of 4 or 5 storey buildings. Currently the site of construction, constrained within an L shape rotated 12° clockwise from the North direction, is a big hole in the urban texture. Therefore, because of its localization, the area is strongly restricted in terms of footprint of the ground floor, building height, limits for elevations' profile, plot ratio, and size of rooms.

AIMS OF THE RESEARCH

The study presented in this paper is a validation of a new solar design approach based on the optimization of the built volume. The work proposes guidelines for the assessment of solar potential in urban areas through a process of parametric modelling of the relationships between buildings and districts. The new design approach is the result of a wider process started with a first optimization of volumes within an intervention of demolition and reconstruction, in search of the shape with the highest solar access [8]. The work continued with a second study [9], where a sensitivity analysis of the levels of total solar radiation on the external envelope has been carried out for several geometrical transformations of the building shape; finally, the same analyses were developed through parametric transformations of complex shapes [10]. As was shortly written above, the process of the solar design optimization here presented is organised into two different but logically consequent steps. The first part is related to the estimation of the increment of solar access of the new building through a comparison between the initial building's volume and the solar optimized shape, defined by a parametric study and maintaining the same volume (5,409 m^3) and the same amount of the exposed surfaces (2,340 m^2). The second part is focused on the localization of the most irradiated areas of the building envelope, suitable for the installation of solar systems in order to produce energy and reduce the building's purchased energy demand. Therefore the aims of the study are:

- improve the solar access of the new building;
- maintain or improve the solar access of the nearby buildings;
- localize the best areas for the installation of solar systems.

THEORY AND METHODOLOGY

The approach starts from the maximum volume allowed by the city planning regulations, reducing the floor-to-floor height, from 3.80 m to 3.50 m changing the total height of the building from 19.20 m to 18.00 m. The preliminary transformation, which is permitted by the local regulations, allowed the reduction of the heated volume used for further parametric study for solar access optimization. This volume, called *Vol.A-ref*, is considered isolated and not inserted in any context.

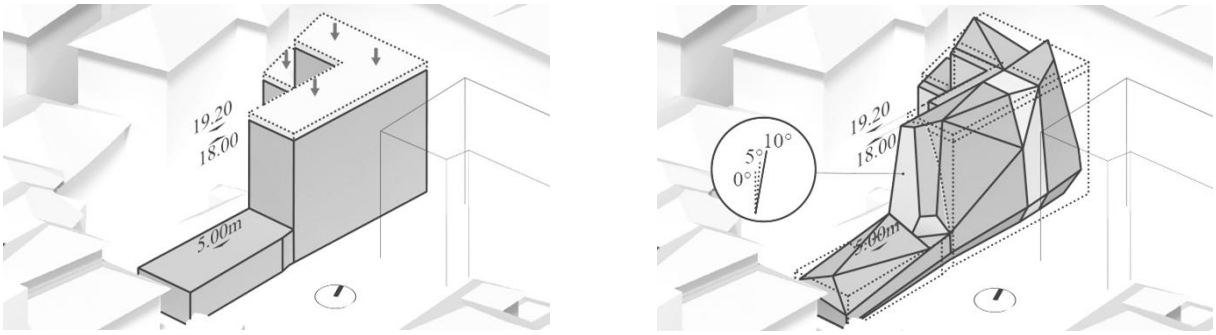

Figure 1. Comparison of the maximum allowable volume (Vol.0), initial volume (Vol.A) (on the left) and solar optimized volume (Vol.B) (on the right).

The approach is therefore based on the comparison, in different scenarios of analysis, between *Vol.A* and the Solar Optimized Volume, called *Vol.B*. The study started by fixing the urban parameters and modifying the shape of the building, varying them within the range indicated in the local urban planning regulations. All the transformations were conducted maintaining the volume of the building and the amount of surfaces exposed to the sky. Each transformation was applied taking into account parameters such as the orientation and inclination of the façades and the usability of the interior space. Figure 1 and Figure 2 summarize the different features considered for improving the solar exposure of the envelope surfaces. In particular the solar optimization process consists of an iterative parametric process that, for each façade, considers different slopes and orientations using generative modelling tools, such as *Rhinoceros* and *Grasshopper* [11]; the annual solar radiation analyses were run using a dynamic daylighting simulation tool, such as *Daysim* [12], considering all solar radiation components coming from sun (α), sky (β), reflections from the surroundings (λ) and from the ground (μ).

After the shape modelling based on the solar optimization process described above, same volumes with different shapes were obtained. The data of total annual radiation were filtered in order to choose the best shape with the highest value of solar access, limiting the overshadowing effect from the surroundings. Table 1 shows the final parameters used for all Radiance-based simulations, validated previously [10].

ambient bounces	ambient division	ambient super-sample	ambient resolution	ambient accuracy	specular threshold	direct sampling	direct relays
3	1000	20	300	0.1	0.15	0.20	2

Table 1. Set of "rtrace" parameters used for all radiance-based simulations.

Table 2 reports the radiance material adopted for surrounding buildings. All external surfaces of neighbouring buildings were treated with the average colour (pink) of existing districts. All simulations used the EnergyPlus weather statistical data climate file recorded for Milan-Malpensa Airport (latitude 45.27° N, longitude 9.11° E).

Material	Radiance Description	Number of values	R (refl.)	G (refl.)	B (refl.)	Specularity	Roughness
conc.plaster	void plastic	005	0.713	0.713	0.713	0.00	0.00

Table 2. list of radiance materials.

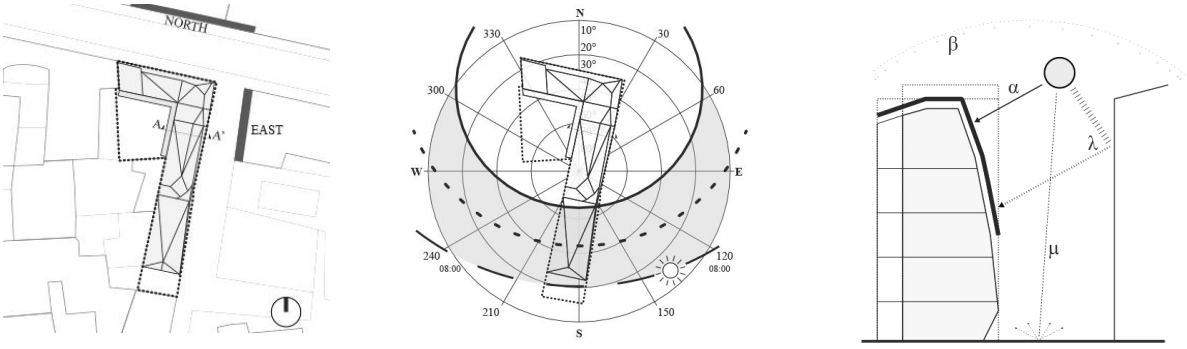

Figure 2. From the left side: site plan with the elevation of the analysed nearby buildings, the orientation of the building with respect to the sun path and section A-A' with different solar radiation components (sun (α), sky (β), surroundings reflections (λ), ground reflections (μ)).

The amount of solar radiation incident on the building envelope was calculated using the *Daysim* software. *Daysim* was developed by the National Research Council of Canada and the Fraunhofer Institute for Solar Energy Systems in Germany. It is one of the best software [13] to use for these kind of analysis. In a previous work [8], *Daysim* program was adopted and validated for a similar case of calculating solar radiation values on the external envelope of buildings.

The calculations have been performed using the DDS (dynamic daylight simulation) model, allowing for a more detailed analysis of direct solar radiation [13]. A detailed solar maps analysis, aimed at locating the most suitable area to install the solar energy system, was conducted using *DIVA for Rhino* [14]. It is a highly optimized daylighting and energy modelling plug-in for *Rhinoceros* and *Grasshopper*, based on *Radiance*.

RESULTS AND DISCUSSION

In the first part of the solar optimization process, regarding the improvement of the building's solar access, two different sets of simulations were run: in the first set, the total annual radiation on the building envelopes has been calculated, in the condition of simple isolated volumes, in order to define the design with the largest solar irradiation; in the second set of simulations, the analysed volumes were considered together with the existing urban environment, in order to estimate the overshadowing effects by nearby buildings.

Shape	ab	gr. refl.	R [kWh/yr]	R_A[kWh/m2yr]	Δ_{ref}[%]	Δ_{rel}[%]
Vol.A-ref	3	0	1,448,946.67	620.53	-	-
Vol.B	3	0	1,536,555.12	652.7	6.0	6.0
Vol.A	3	0.15	1,572,936.63	673.63	8.6	-
Vol.B	3	0.15	1,649,919.11	700.85	13.9	4.9

Table 3. Isolated Scenario - Results of solar radiation analysis. R: total solar radiation impacting on the external envelope. R_A: average solar radiation on the external envelope. $\Delta_{ref.}$: percentage of variation of solar radiation with respect to the initial reference volume (Vol.A-ref) and Δ_{rel}: with respect to the volume of the relative scenario analysed each time.

Shape	ab	gr. refl.	R [kWh/yr]	R_A[kWh/m2yr]	Δ_{ref}[%]	Δ_{rel}[%]
Vol.A	3	0	1,253,231.71	536.71	-13.5	-
Vol.B	3	0	1,366,164.2	580.32	-5.7	9.0
Vol.A	3	0.15	1,331,002.54	570.01	-8.1	-
Vol.B	3	0.15	1,440,993.46	612.11	-0.5	8.3

Table 4. Context Scenario - Results of solar radiation analysis. Legend: the same of Table 3.

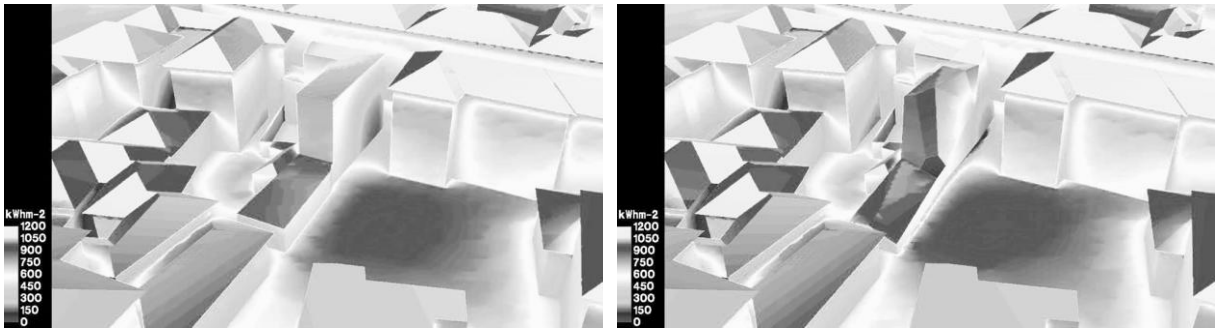

Figure 3. Comparison of solar radiation maps analyses between Vol.A (on the left) and Vol.B (on the right) in a Context Scenario – Elaboration data by DIVA for Rhino.

Each set of simulation includes two different scenarios: in the first, ambient bounces (ab) are set equal to 3 and ground reflectance (gr. refl.) equal to 0.0 in order to calculate only the solar reflection effect created by the surroundings, while in the second ab is considered equal to 3 and gr. refl. equal to 0.15, to calculate also the ground reflection contribution. The results are reported in Table 3 (*Isolated scenario*) and Table 4 (building inserted in a context – *Context Scenario*). The irradiation values obtained show that the solar optimization permits to increase the solar radiation on the building envelope up to 13.9% considering the isolated scenario. Moreover, the solar gains cover the reduction due to the surroundings (-0.5%) when the building is inserted in the context. It is important to underline that the ground reflectance affecting *Vol.B*, instead, does not provide the expected increment. The last column of Table 3 and Table 4 shows that the percentage of the scenario considering the ground reflection (ab=3, gr.refl.=0.15) is lower than the previous scenario (ab=3, gr.refl.=0.0). The increment of total solar radiation given by the ground reflected component is higher considering the *Isolated Scenario* (1.1%) and it is lower in the *Context Scenario* (0.7%). This is caused by the shape of the volume: the shape of the ground, visible in Figure 2, level has been designed in order to reduce the summer solar gains (both direct and reflected radiation) in the mediateca.

More solar access analyses were carried out on the context, in order to estimate if the amount of solar radiation on the façades of the nearby buildings would remain the same or would instead increase because of the new building. Considering the *Context Scenario* (ab=3, gr.refl=0.15) and the presence of *Vol.B*, the North and East façades of the closest building, are affected by an increment of solar radiation of 8.2% for the East façade and 0.7% for the North façade compared to the *Vol.A* case. The purpose of the second part of the solar optimization process was to localize the most irradiated surfaces of the building envelope; these would be the most suitable locations for the installation of the solar systems. The optimized volume includes North and East elevations tilted 6° away from the vertical direction. Starting from the South façade of the initial building, a new elevation is created by slicing the volume for the best exposure of South façade, which is sloped 10°. The "solar shell" (Figure 4) composed by 27% of the overall surface is able to harvest up to 45% of the total radiation incident on the building envelope, as estimated in the Context Scenario (ab=3, gr.refl.=0.15).

Figure 4. Views of the "Solar shell".

CONCLUSION AND OUTCOMES

The results confirmed that a new solar design approach can significantly contribute to the definition of the building's volume and the production of on-site renewable energy. Further studies are required to understand the consequences of the complex shapes deriving from the solar optimisation process, in terms of construction (panelling of surfaces) and cooling loads (increased surface temperatures due to solar panels).

REFERENCE

1. Ecofys Germany GmbH, Danish Building Research Institute (SBi), Principles for nearly zero-energy buildings - Paving the way for effective implementation of policy requirements, Buildings Performance Institute Europe (BPIE), 2011.
2. M. Hegger, M. Fuchs, T. Stark e M. Zeumer, Energy Manual. Sustainable architecture., Basel: Birkhäuser, Edition Detail, 2008.
3. M. Montavon, «Optimisation of Urban Form by the Evaluation of the Solar Potential,» École Politechnique Fèdèrale de Lausanne, Losanne, 2010.
4. V. Vannini, B. Turkienicz and A. Krenzinger, "Geometric optimization of building façades for BIPV," in Proceedings of the Energy Forum 2012, Bressanone, Italy, 2011.
5. R. Compagnon, «Solar and daylight availability in the urban fabric,» Energy and Buildings, vol. 36, pp. 321 - 328, 2004.
6. R. Compagnon and D. Raydan, "Irradiance and illuminance distributions in urban areas," in In Proceedings of PLEA 2000, Cambridge UK, July 2000.
7. M. Montavon, J. Scartezzini and R. Compagnon, "Comparison of the solar energy utilisation potential of different urban environments," in In PLEA2004, Eindhoven, The Netherlands, 2004.
8. G. Lobaccaro, G. Masera and T. Poli, "Solar district: design strategies to exploit the solar potential of urban areas," in Proceedings of the XVIII IAHS World Congress, Istanbul, Turkey, 2012.
9. G. Lobaccaro, F. Fiorito, G. Masera, Poli and T., "District Geometry Simulation: A Study for the Optimization of Solar Façades in Urban Canopy Layers," Energy Procedia, vol. 30, pp. 1163-1172, 2012.
10. G. Lobaccaro, F. Fiorito, G. Masera and D. Prasad, "Urban solar district: a case study of geometric optimization of solar façades for a residential building in Milan," in Solar 2012 Conference, Melbourne, 2012.
11. David Rutten and Robert McNeel & Associates., «Rhinoceros and Grasshopper software».
12. Harvard University, National Research Council Canada, Fraunhofer Institute for Solar Energy Systems, «Daysim version 3.1b,,» 2010.
13. D. Ibarra and C. Reinhart, "Solar availability: a comparison study of six irradiation distribution methods.," in Proceedings of Building Simulation 2011: 12th Conference of International Building Performance Simulation Association., Sydney, 2011.
14. Graduate School of Design at Harvard University - Solemma LLC, «DIVA for Rhino,» 2013.

MODELING APPROACH FOR CITY DISTRICT SIMULATION

Hassan Harb; Peter Matthes; Amir Javadi; Rita Streblow; Dirk Müller

RWTH Aachen University, E.ON Energy Research Center, Institute for Energy Efficient Buildings and Indoor Climate, 52074 Aachen

ABSTRACT

Renewable Energy Sources (RES) are set to be the pillar of the future energy supply in smart cities. However, the volatile generation of RES leads to challenges for matching the demand and supply. Hence, innovative energy management systems on a city district level are required to ensure the security of supply. A simulation environment is essential to investigate and assess the energy management concepts. This simulation environment comprises large numbers of buildings and different energy supply systems which result in extensive simulation time and thereby a great restriction to the research, especially for long simulation periods. Therefore, a modeling approach that ensures fast simulation times while simulating the thermal behavior accurately is developed. In this regard, simplified building as well as boiler, heat pump, storage heater and combined heat and power unit, table-based models are developed within the context of a Modelica-based library construed for city district simulation. The modeling and parameterization approach is presented in this paper. The feasibility of this approach is analyzed by a simulation of several dwellings. The results show that the approach enables fast simulation times while accurately simulating the thermal behavior of the buildings. Finally, further simplification of the models for the Energy Conversion Units (ECU) through eliminating the hydraulic components and reducing the model to thermal-based is investigated. This method results in reducing the simulation times of the ECU models up to 10 times.

Keywords: City district simulation, Parameterization of buildings, Modelica-based modeling

INTRODUCTION

Renewable Energy Systems (RES) are set to be the main contributor to energy supply in the near future. However, the weather dependent and volatile nature of RES allows only for throttling the generation and undermines the possibility of scheduling the energy generation. This leads to challenges for matching the demand and supply. Consequently, innovative energy management systems on city district level are needed to ensure the security of supply. In contrast to the conventional energy optimization strategies on a house level, a concept designed for city districts offers a higher degree of freedom and a large potential of flexibilities [1]. City district models can be used to assess the integration of RES in the supply structure and identify storage and load shifting potentials. Hence, City district simulations provide the investigation environment required to develop the different energy management strategies and analyze the feasibility of these solutions. The paper presents a parameterization and modeling approach of buildings and energy supply systems for city districts.

PARAMETERIZATION AND MODELING APPROACH

Parameters for Drafting a Building Model

The general set-up for the modeling of a building is illustrated in Figure 1. The heating demand in houses is mainly governed by the overall heat transfer coefficient of the house

envelope and its heat storage capacity. Therefore, the determination of the heat capacity and heat resistance of the building construct enable a rough simulation of the dynamic thermal behavior of a building. This requires the assessment of several parameters: a) the net area of the building which is deployed as the zone area of the simplified building model. The net area is equal to 85-90 % of the building gross area A_G which is computed according to eq. (1) from the construction area A_C of the building and the number of heated floors n_f b) the heated floor space A_N that is calculated using eq. (2) and (3) from the heated building volume V_e and the storey height h_f

$$A_G = A_C * n_f \tag{1}$$

$$A_N = V_e * 0.3/m \tag{2}$$

$$V_e = n_f * h_f \tag{3}$$

c) the construction configuration of the inner walls, outer walls, floor, ceiling, roof, flooring as well as the type of the windows d) the orientation and area of the outer walls and windows for the solar irradiations. Information on the building's dimensions is not always available and can be approximated through the analysis of pictures of the buildings and the usage of the aerial perspective in public web mapping service application. The construction configuration i.e. physical properties of the wall's layers, as well as the storey height is derived from the construction year as construction periods are characterized with a typical set up.

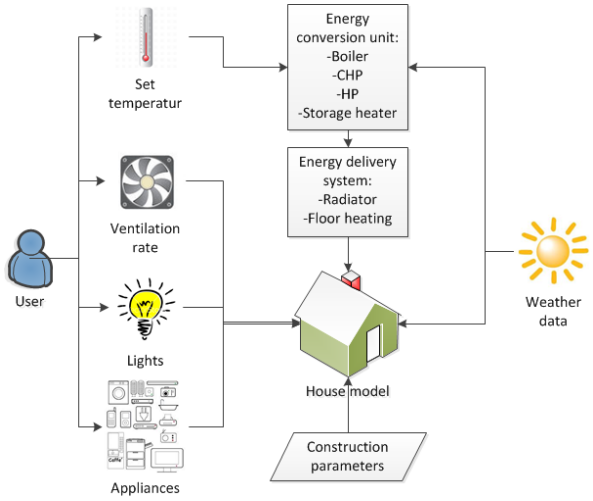

Figure 1: Set-up of a house model

Moreover, the heat demand depends on dynamic parameters i.e. the solar irradiation gains mainly through transparent areas, the inner thermal gain mainly the dissipation energy form light bulbs and electrical appliances i.e. computers, TV sets and refrigerators, the ventilation rates as well as the outdoor ambient temperature, the wind speed and the indoor temperature that define the potential of the heat losses to the environment. Furthermore, the outdoor temperature is an important parameter for the control of energy delivery system. This value is used to determine the feed temperature of the supply system with a characteristic heat curve. In this manner, a comfortable room temperature regardless of the outdoor temperature is ensured while minimizing the energy costs. The weather data can be derived from the measures of a weather station or from a test reference year. The ventilation rate and the inner thermal gains are users' dependent and cannot be accurately determined and must be approximated based on stochastic models for occupancy.

Sub-Models

Simplified building model: to simulate and investigate the thermal load performance of a large number of building models for a long period in parallel, a high computing capacity is required. The size of the equation system and the number of events are dominant factors for the simulation speed [2]. One feasible method to enhance the simulation speed without modifying the model is to parallelize the simulation and distribute it onto several nodes of a computer cluster. This might not be reasonable however, if the equations are strongly coupled – for example when the behavior of the heating system directly influences the thermal behavior of the building. A different approach is to reduce the complexity of the models. The more detailed the model is, the larger the number of equations to be solved. Events occur when a set of equations has to be changed during the simulation resulting in one or more non-differentiable function values at this point in time. Events normally occur in controller models because they use discrete variables but are also related to the complexity of physical models (switching between equations). Reducing the complexity of models can therefore result in less events and higher simulation speed. As a tradeoff, the accuracy of the simulation models normally is reduced as well. The developed simplified building model is based on the approach of the German industry guideline VDI 6007 [3]. The building is reduced to a single heating zone with two main components, thermal resistances and capacitors that describes respectively the heat transfer and storage in the building's wall mass. The implementation of this model requires a conversion of the original list of construction parameters of wall material layers and dimensions into equivalent thermal resistances and capacitors for outer and inner walls in a step prior to simulation. This approach decreases the model's number of equations as well as the computing time required to a reasonable level which enables city district simulation scenarios.

Energy conversion unit models: The energy supply system of a building is the link between the house and the energy grids (electrical, gas or thermal). Boilers are the standard heat generation in residential buildings. Heat pumps (HP) and combined heat and power (CHP) systems are increasingly installed due to their higher efficiency compared to standard boiler systems. HP and CHP coupled with thermal storage systems offer a load balancing potential for energy management. Similarly, electrical storage heaters gain attraction in an energy market with large amounts of renewable energy which can be stored as thermal energy for heating when the electrical energy supply is larger than the energy demand. The boiler system is modeled based on manufacturer data for the heat output. The control strategy used for this system is feed temperature control. Hence, the boiler controller minimizes the difference, between the set feed temperature according to the heat curve and the feed temperature measured value, by regulating the heater's power within the possible limits. The HP model is based on manufacturer data for heat and electrical power flow with two simple heat exchangers, the evaporator and the condenser. The temperature of the cold side in the evaporator and the warm side in the condenser determine the design thermal energy flow as known from manufacturer data. A continuous speed control concept is implemented to regulate the thermal power of the HP. A buffer storage is included in the system to reduce excessive on/off switching of the heat pump. In the CHP model, the conversion of the fuel into heat and electricity is determined based on manufacturer data. Both thermal- and electrical driven control are possible. Night storage heaters are used to take advantage of low electricity tariff during night and charge a storage mass to cover the heat demand for the next day. The charging time in the model is determined according to the outdoor temperature based on the manufacturer data. The output of the storage heater is controlled via a thermostat that regulates the revolution speed of the storage heater built in ventilator to ensure that the comfort set temperature is reached.

RESULTS AND DISCUSSION

Investigation of City District Simulation

In this section, the results of an investigation of 19 buildings in the region Bottrop in Germany are presented. Figure 2 depicts the complete model of these houses implemented in Dymola/Modelica. In this investigation, the buildings are modeled as a single heating zone according to the VDI 6007. The construction parameters of wall material layers and dimensions are approximated based on the parameterization approach presented earlier.

Figure 2: Snapshot of the buildings models in Dymola/Modelica

The supply systems are represented using the energy conversion models described in the previous section. A ventilation model is incorporated into the building. In this model, a selectable base air change rate increases due to occupancy, indoor and outdoor temperature. A higher occupancy leads to a higher additional air change rate. Also lower outdoor or indoor temperatures decrease the additional air change rate as people are less likely to leave windows open under these conditions. A discrete transient temperature profile ranging between 18 and 22 °C is chosen as the indoor set temperature which influences the radiators' thermostatic valve set point. This profile shows a night setback and normal daily temperature level. The occupancy and electrical consumption profiles for lights and appliances are generated stochastically while taking into consideration the number of apartments and residents to accommodate the internal heat gains according to [4]. The data form a test reference year is used for the weather parameters.

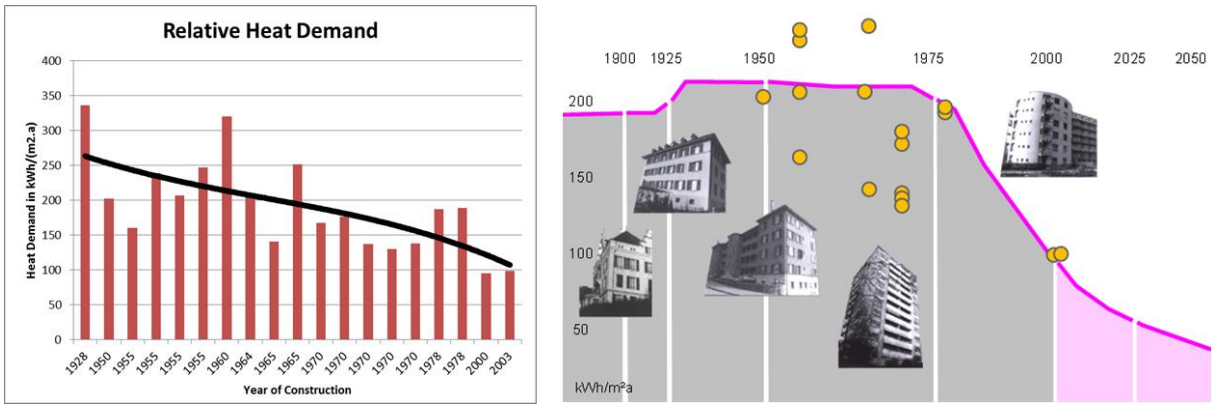

Figure 3: Evaluation of the simulation with the average annual specific energy demand with respect to the construction year based on [5]

The simulation execution time for the thermal performance of a single zone over a year period is estimated at 52 seconds. The simulated thermal behaviors of the houses are plotted in the

left diagram of Figure 3 as specific annual heat demand with respect to the building year construction. The results show a decreasing trend with increasing year of construction. This correlates with the increase in the thermal insulation requirements for buildings over the years.

The right diagram in Figure 3 illustrates the progress of the specific annual heat demand with respect to the construction periods with the simulation results presented as dots. The construction periods are characterized with a certain heat insulation standards for buildings. The results show a good agreement with the average progress of the annual specific energy demand. The negative deviation can be drawn back to refurbishment measures of the building or the energy supply system, or to a rational heat consumption pattern of the residents. The positive deviation can be explained through excessive heat consumption than the theoretical average due to an increased individual comfort standard, increased ventilation or inefficient operation of the energy supply system.

Investigation of Thermal Based Supply Models

For the simulation of city districts, the simulation time is a critical parameter. The energy supply systems are typically modeled with thermal-hydraulic components. However, the simulation of hydraulic models is computationally intensive, due to the higher number of variables involved. To further reduce the simulation time, two approaches are feasible. The first is to reduce the complexity of the medium model used and decrease the number of its physical properties that are continuously computed and result in long simulation time. The other is to eliminate the hydraulics and reduce the model to a thermal one. The investigation of this approach show that the elimination of the hydraulics results in several challenges in different segments of the energy supply model mainly the lack of a return temperature, due to the absence of the mass flow, as well the accommodation of the system's reaction time that depends on the hydraulics and of the thermal capacity of the heat carrier. These drawbacks are countered through regulating the heat supply's power, with no information about the return temperature, based on the energy balance of the building-supply system in which the power of the supply model is defined as the sum of the building heat losses. The time delays are accounted for by extracting the reaction times from the simulation of the hydraulic systems and implementing these in the thermal model. The consideration of the thermal capacity within the thermal models is essential to achieve an accurate behavior between the added energy and the temperature gradient. Therefore, the mass of the heat carrier is calculated directly from the manufacturer data of the supply unit and is replaced into the thermal model with an equivalent heat capacity.

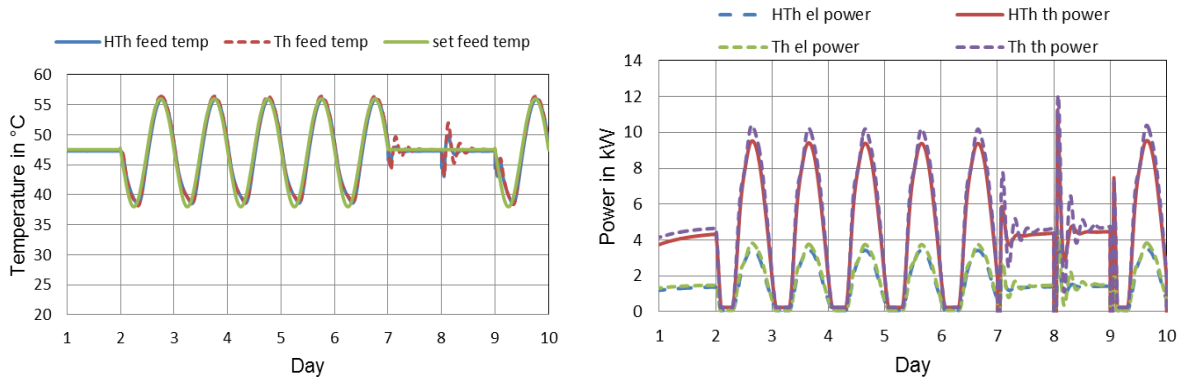

Figure 4: Comparison of the feed temperature and energy output

Figure 4 shows a comparison of the thermal-hydraulic (HTh) and thermal (Th) models of a CHP unit. This comparison is assessed while inducing several events during the simulation process, first under stationary condition followed by a period with a fluctuating desired feed temperature and finally two external on/off signal. The left diagram in Figure 4 displays the feed temperature delivered by the thermal and thermal-hydraulic models along with the set feed temperature during a 10 days simulation time. The absolute average error is 0.25 K while the standard deviation amounts to 0.46 K. The generated thermal and electrical energy with both models is depicted in right diagram of Figure 4. The absolute average error and standard deviation are respectively 0.144 and 0.155 kW for the electrical power and 0.295 and 0.4 kW for the thermal power. Hence, the performance of the thermal based supply models is validated. The simulation time for the thermal-based boiler and the CHP unit is around 11 times faster in comparison to the thermo-hydraulic models. The simulation time of the heat pump could be only improved about 4 times, due to the existence of many events.

CONCLUSION

The paper defines an approach for modeling city districts. A simplified building model as well as table-based boiler, heat pump, storage heater and combined heat and power units models are developed within the context of a Modelica-based library construed for city district simulation. The parameterization method for the building simulation is introduced and discussed in detail. This method enable an estimation of the construction parameters based on the construction year and through using web mapping service application. The residents' occupancy and internal thermal gain profiles are approximated based on a stochastic model. Accordingly, this approach is used to parameterize, model and simulate several buildings for a one year period. The simulated annual specific energy demands correspond to the average annual specific energy demand with respect to the construction period. The computing time for a one year simulation of a single zone model is estimated around 52 seconds. The results show that the modeling approach enables fast simulation times while accurately simulating the thermal behavior of the buildings. Finally, the first investigations on reducing the complexity of the models for the energy conversion units through eliminating the hydraulic components and reducing the model to thermal based show that the simulation time can be reduced up to 10 times for CHP and boiler systems and up to 4 times for HP. However, this method delivers several modeling drawbacks mainly the lack of the return temperature due to the absence of the transport medium. Therefore, a simplification approach based on reducing the number physical properties of the medium model could provide an improved solution.

REFERENCES

1. Molitor.C: "New Energy Concepts and Related Information Technologies: Dual Demand Side Management," Proceedings of 2012 IEEE PES Conference on Innovative Smart Grid Technologies
2. Liu, L.: Efficient simulation of hybrid control systems in Modelica/Dymola. Proceedings of the 6th Vienna International Conference on Mathematical Modelling (MATHMOD 2009), Wien, pp. 1344–1352, 2009.
3. Technical Division Building Services, VDI guideline, VDI 6007 part 1: Calculation of transient thermal response of rooms and buildings, March 2012.
4. Richardson, I.: Domestic electricity use: A high-resolution energy demand model, Energy and Buildings, vol. 42, no. 10, pp. 1878–1887, 2010.
5. Richner, P.: CO2-optimiertes Bauen als Grundlage für die Zukunft, plenary meeting of bauenschweiz, 2007.

SPATIAL BUILDING STOCK MODELLING TO ASSESS ENERGY-EFFICIENCY AND RENEWABLE ENERGY IN AN URBAN CONTEXT

M. Jakob[1]; H. Wallbaum[2]; G.Catenazzi[1], G. Martius[1], C. Nägeli[1], B. Sunarjo[1]

1: TEP Energy GmbH, Zurich, Switzerland

2: Chalmers University of Technology, Gothenburg, Sweden

ABSTRACT

The building stock has a decisive impact on energy consumption, greenhouse gas (GHG) emissions and sustainable development of urban areas. In previous studies the authors have assessed these impacts by applying a bottom up building stock model (BSM) including construction components and energy systems for different development scenarios. The goal of this work is to present novel improvements of the BSM which include a spatial differentiation of building characteristics, energy infrastructure and local potentials of renewable energy. As such the model is suitable to be used in the context of urban energy planning and to simulate different scenarios, for instance with regard to the feasibility of long term carbon mitigation and (primary) energy consumption reduction goals.

To simulate energy demand, carbon emissions and further key indicators of the building stock the bottom-up simulation methodology has been enhanced in terms of spatial differentiation. So far, to deal with the great complexity of building stock modelling, different building types of an urban context have been clustered into cohorts with similar characteristics. As compared to these earlier approaches, we combine specific data known on the level of each individual building with generic data that is known or assumed on the level of building or spatial cohorts. These cohorts are defined by variables such as construction period, building type and utilisation, and building location. However, model calculations are done on the level of specific building archetypes, building technologies, and building components. As such assumptions on technical characteristics and building stock alterations may be brought much closer to the decision processes. This new approach of spatial building stock modelling (SBSM) offers the advantage of being able to include specific, geo-referenced building data (e.g. from surveys or from building registers) and to represent results at the level of details needed. Hence, results may be represented by building type or other building attributes, but also by hectare or neighbourhoods, using geographical information systems (GIS).

Scientific results are achieved both with regard to methodology and with regard to content. Methodologically we demonstrate the feasibility of combining data and assumptions on different levels of aggregation such as building elements, individual buildings and cohorts. With regard to content we present results from a case study about feasibility of achieving the goals of the 2000-Watt- and 1-ton-CO_2-society in the city of Zurich, referring to spatially differentiated potentials of renewable energy and energy-efficiency.

Keywords: building stock, spatial simulation modelling, geographical information system (GIS), energy-efficiency, renewable energy, urban context

INTRODUCTION

The building stock is one of the largest energy consumer and emitter of greenhouse gases (GHG) in urban spaces. Even though buildings newly constructed in recent years have been using less and less energy, the average consumption of the building stock remains high as retrofitting rates of existing buildings remain low. Thus also potentials of renewable energies

should be taken into consideration to reach ambitious GHG mitigation goals. Yet, especially for urban areas tapping energy-efficiency and renewable energy potentials entail specific challenges. Models are adequate tools to improve the understanding of the development of the energy consumption of the building stock in different scenarios.

Several different methods of building stock modelling have been developed so far. Swan and Ugursal [1] and Kavgic et al. [2] give a general overview of the different modelling techniques. Especially bottom-up models have become more sophisticated with a trend towards spatially differentiated models related to geographical information systems (GIS). Markus et al. [3] use spatial data from a land use model in order to model the development of the energy demand distribution of city regions. A similar method is used by Howard et al. [4], who assess the current energy demand of New York by applying the results of a statistical regression model to the floor area distribution if the city. Biberacher et al. [5] combine spatially differentiated supply and demand modelling by optimizing local energy potentials with heat demand based on costs, efficiency and CO_2-emissions.

In previous studies the authors of this paper have assessed the impacts of the building stock on final energy consumption and GHG-emissions by simulating different scenarios with a bottom-up building stock model (BSM) that explicitly includes construction components, building technologies and energy systems [6-9]. The goal of this work is to present a further development of the BSM using a new approach of spatial building stock modelling with results from a case study about feasibility of achieving the goals of the 2000-Watt- and 1 ton CO_2-per-capita-society in the city of Zurich.

MODELLING CONCEPT

The bottom-up simulation methodology previously developed by the authors [6-9] in order to simulate energy demand, carbon emissions and further key indicators of the building stock is extended in terms of spatial differentiation. As such local heating (and potentially cooling) energy demand can be compared to locally bounded renewable energy potentials or current and future energy network infrastructure. With this modelling principle of matching locally demand and potentials or supply it becomes possible to assess energy policy scenarios in an urban context much more realistically.

The model adopts a cohort approach that aggregates data of individual buildings that are similar by building (construction) type, construction period, type of use (e.g. which mix of economic sectors within a building type) and location (right-pointing arrow in Figure 1). Thus, these cohorts are spatially differentiated in order to enable the modelling of spatially differentiated energy demand. Demand evolution is simulated using construction rates and retrofit measures, which differ across the city depending on urban development strategies. The demand is covered by spatially differentiated energy carrier mixes depending on the available supply infrastructure, renewable energy potentials and development strategies.

In order to deal with the great complexity and heterogeneity of the building stock, different building types of an urban context are clustered into cohorts with similar characteristics. As compared to the earlier approaches, we combine specific data known on the level of each individual building (from geo-referenced building registers) with generic data that is known or assumed on the level of building or spatial cohorts (right-pointing arrow in Figure 1). The heating and hot water heating demand is calculated for all cohorts based on the official Swiss norm SIA 380/1 (EN ISO 13790) [10]. The distribution of different heating systems, building technologies and appliances is modelled based on assumed diffusion rates, which depend on the different scenarios and are differentiated for all cohorts. Based on the building characteristics of each cohort and the assumed mix of heating systems, the model calculates

the final energy demand for all cohorts for each time step up to 2050. Based on the emission and primary energy factors (PEF)—which, in the case of electricity and district heating, depend on the break-down of primary energy input—the model then calculates greenhouse gas (GHG) emissions and primary energy use.

In a final step, cohort-specific results are allocated to the individual buildings of the geo-referenced building register in order to represent results in a geographical information system. The interface between the BSM and the GIS (left-pointing arrow in Figure 1) refers to attributes that uniquely identify the different cohorts of the BSM which are building type, construction period, zone, status of patrimonial protection, and others.

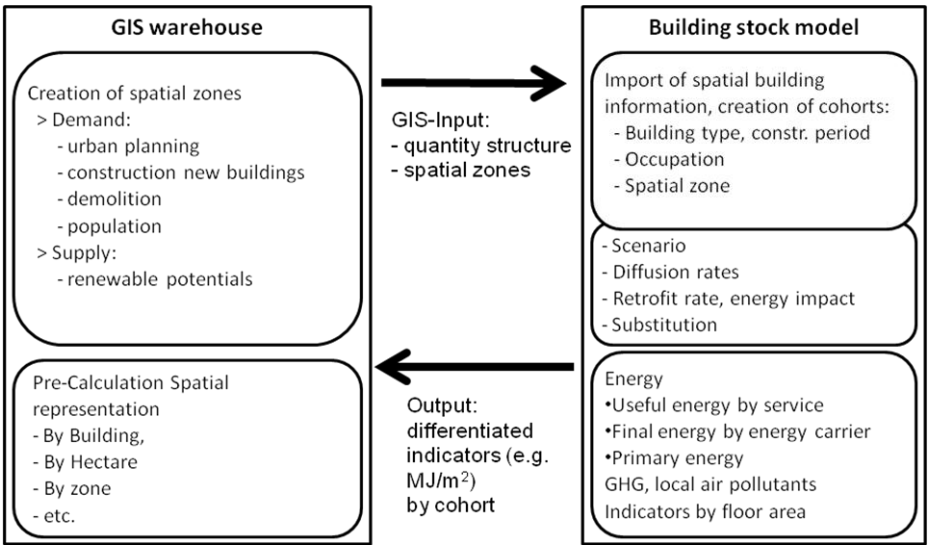

Figure 1: Interaction of the building stock model (BSM) with geo-referenced data and the GIS environment

IMPLEMENTATION

At the current stage technical implementation is quite heterogeneous: The BSM as such is implemented in MS Excel using Macros and VBA code, the interface between the BSM and the GIS environment is implemented in MS Access, and dividing the city area into different zones is done in ArcGIS.

Spatially differentiated development of heat demand

The development of heat demand of the buildings is carried out for all building types and is spatially differentiated. Geo-referenced data of the building stock, which covers all building types of a city, is aggregated to cohorts in GIS based on aforementioned characteristics.

Based on the local characteristics of the building stock and urban development considerations the city area is divided into different development zones. Zones can consist of the historic city core, traditional, pitoresque residential areas, reorientation areas or urban development areas. These zones differ in terms of the state of their buildings, their retrofit and new construction rates and the effect of energy efficiency measures, especially in the case of the facade (see Table 1 that exemplary show retrofit rates for two different cases and Table 2 as well as Tables 4 to 6 in [11] that illustrate how U-values of retrofitted façades are differentiated).

All buildings are grouped into different retrofit types based on the building type, building period, listed building status (patrimonial protection registry) and the construction zone, which includes specific assumptions about the renewal of their envelope and the building

technology (e.g. external insulation of the facade is often not possible for listed buildings and for the alternative internal insulation less insulation material can be applied resulting in a higher U-value). This results in spatially differentiated retrofit measures and efficiency potentials. The specific heat demand is then calculated for a limited number of building archetypes. Each of the cohorts is characterized by such an archetype. Archetypes are specifically defined in terms of geometry and building physics data for each of its main building envelope components (façade, windows, roof, etc). Results are then extrapolated to the whole building stock, relating resulting heating demand to the aggregated cohorts.

	With listed buildings (e.g. old city core area)				**Without listed buildings (e.g. reorientation area)**			
Construction period	2005	2020	2035	2050	2005	2020	2035	2050
Pre 1920	0.40%	0.58%	0.56%	0.45%	0.58%	0.84%	0.81%	0.65%
1920-46	0.54%	0.79%	0.76%	0.61%	0.69%	1.00%	0.96%	0.77%
1947-74	1.04%	0.96%	0.88%	0.75%	1.27%	1.17%	1.07%	0.92%
1975-1990	0.44%	1.22%	1.06%	0.38%	0.52%	1.44%	1.24%	0.45%
1991-2009	0.02%	0.21%	0.33%	0.41%	0.02%	0.25%	0.39%	0.48%

Table 1: Annual renewal rates [% floor area/year] for the building component "Facade" for Multifamily houses in the efficiency scenario as defined in [11]. The differences between the two areas stem mainly from the high percentage of listed buildings in city core areas. (Adapted from [11])

	With listed buildings (e.g. old city core area)				**Without listed buildings (e.g. reorientation area)**			
Construction period	2005	2020	2035	2050	2005	2020	2035	2050
Pre 1920	0.68	0.51	0.36	0.29	0.44	0.36	0.26	0.21
1920-46	0.50	0.39	0.27	0.22	0.38	0.31	0.22	0.18
1947-74	0.44	0.36	0.26	0.21	0.40	0.31	0.22	0.17
1975-1990	0.40	0.35	0.24	0.20	0.38	0.30	0.21	0.17
1991-2009	0.40	0.35	0.24	0.20	0.38	0.30	0.21	0.17
New buildings	0.24	0.20	0.15	0.14	0.24	0.20	0.15	0.14

Table 2: U-values [W/m^2/K] for the building component "Facade" for Multifamily houses in the efficiency scenario as defined in [11. The differences between the two areas stem mainly from the high percentage of listed buildings in city core areas. (Adapted from [11])

Spatially differentiated heat supply and renewable energy potentials

Additionally to zoning motivated by urban development and energy demand considerations the city area is also divided into different zones depending on the availability of renewable energy potentials suitable for heating purposes. The zones are differentiated according to the local availability of such potentials or use restrictions of thereof. Typical examples are ground water, perimeters of lakes and rivers, geothermal energy, waste water purification plants, and others. Many of these potentials require a (thermal) energy network infrastructure which implies that the existing district heating network and topological considerations (e.g. distance from lake and river, traffic infrastructure) are also influencing the zoning process.

Spatially matching heat demand, supply, and renewable energy potentials

Zones motivated by demand related considerations are than superposed with zones of supply infrastructure and potentials (see *"Abbildung 1"* in [11]). This allows for spatially matching supply and demand and to appraise to which extent locally available potentials may be sufficient to cover demand.

RESULTS

The spatial building stock model (SBSM) was applied in a case study covering the area of Zurich-Altstetten. Using specific, geo-referenced building data (from the building registry of Zurich) using geographical information systems (GIS) it became possible to represent results at the level hectares (see Figure 3). In Zurich-Alstetten areas of high demand coincide with groundwater energy potentials. Moreover it becomes apparent that high demand areas will be shrinking in the future and the demand in general is decreased in the scenario considered.

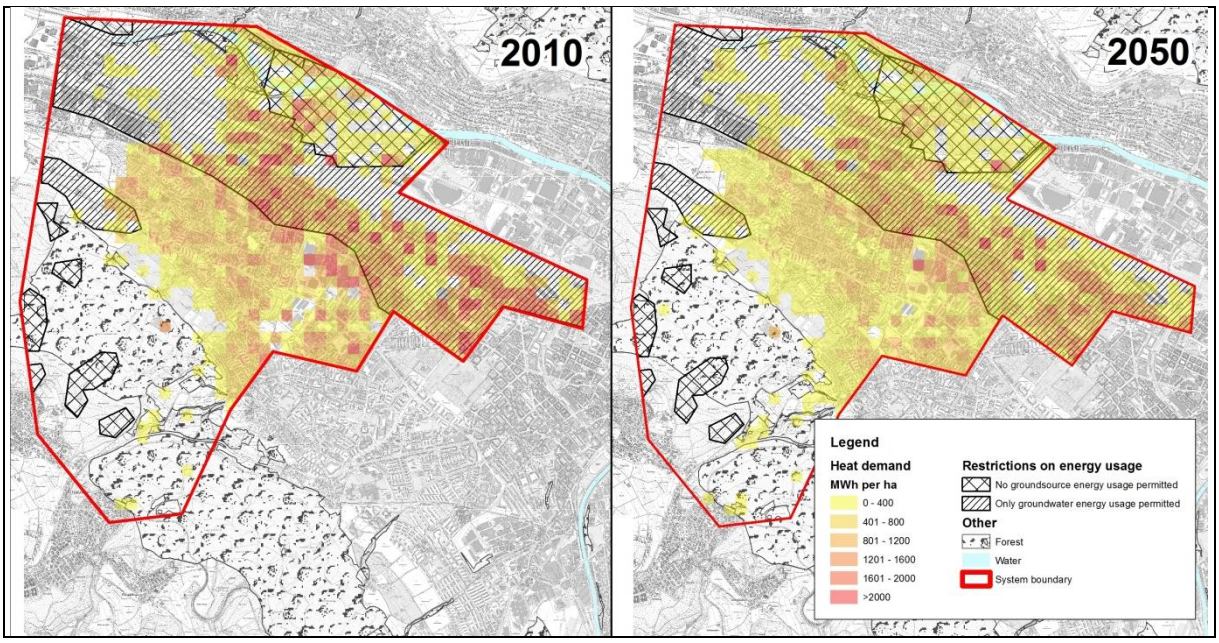

Figure 2: Exemplary results comparing the spatially distributed heat demand (space heating and warm water) of the neighbourhood of Altstetten in the city of Zürich in 2010 and 2050.

CONCLUSION

The new approach of spatial building stock modelling (SBSM) offers the advantage of being able to include specific, geo-referenced building and energy potential data (e.g. from surveys, building registers and geological maps), to locally match demand, existing energy infrastructure and potentials and to represent results at the level of details needed or desired. Obviously the approach and the level of disaggregation depend on the data availability of the place to be investigated. Hence, results may be represented by building type or other building related attributes such as building owner, but also by spatial attributes such as hectare, neighbourhoods, using geographical information systems (GIS) if data resolution is appropriated. The transferability of the SBSM to other cities is currently under investigation. For the case of London this is within the project Smart Urban Adapt (SUA) from which preliminary results are to be expected by the end of 2013 and for other cities within other activities of TEP Energy and Chalmers University of Technology. In parallel software implementation is being transferred to a more appropriate environment.

ACKNOWLEDGEMENTS

Results, underlying research and development summarized in this paper was predominantly enabled through financial contributions of the city of Zurich (represented by Energy Delegates Bruno Bébié and Felix Schmid and by Heinrich Gugerli, Municipal Building Department who, together with others, also were valuable discussion partners) and own funding of TEP Energy and partly by the Climate KIC project SUA (part of the interface between the BSM and the GIS) which we gratefully acknowledge.

REFERENCES

1. Swan L.G., Ugursal V.I. (2009). Modeling of end-use energy consumption in the residential sector: A review of modeling techniques. Renewable and Sustainable Energy Reviews. 13 (2009) 1819-1835.
2. Kavgic M., Mavrogianni A., Mumovic D., Summerfield A., Stevanovic Z., Djurovic-Petrovic M. (2010). A review of bottom-up building stock models for energy consumption in the residential sector. Building and Environment. 45 (2010) 1683-1697.
3. Markus P., Avci N., Girard S., Keim C., Peter M. (2009). Energy demand in city regions – methods to model dynamics of spatial energy consumption. ECEEE 2009 Summer Study. (2009) 705–714.
4. Howard B., Parshall L., Thompson J., Hammer S., Dickinson J., Modi V. (2012) „ Spatial distribution of urban building energy consumption by end use. Energy and Buildings. 45 (2012) 141-151.
5. Biberacher M. et al. (2010). Räumliche Modelle als Entscheidungsgrundlage für die Inwertsetzung regional verfügbarer Energiepotentiale zur CO_2-neutralen Deckung des lokalen Wärmebedarfs. 56 (2010).
6. Wallbaum H., Heeren N., Jakob M., Gabathuler, M. Gross N., Martius G. (2009). Gebäudeparkmodell SIA Effizienzpfad Energie Dienstleistungs- und Wohngebäude – Vorstudie zum Gebäudeparkmodell Schweiz – Grundlagen zur Überarbeitung des SIA Effizienzpfades Energie. ETH Zürich, TEP Energy i.A. Bundesamt für Energie, Bern, September.
7. Wallbaum H., Jakob M., Heeren N., Gross N., Martius G. (2010). Gebäudeparkmodell – Büro-, Schul- und Wohngebäude – Vorstudie zur Erreichbarkeit der Ziele der 2000-Watt-Gesellschaft für den Gebäudepark der Stadt Zürich. ETH Zürich und TEP Energy i.A. Stadt Zürich, Amt für Hochbauten, Fachstelle nachhaltiges Bauen, Zürich, Mai.
8. Heeren, N., Wallbaum, H., Jakob, M. (2012). Towards a 2000 Watt society – assessing buildings specific saving potentials of the Swiss residential building stock. International Journal of Sustainable Building Technology and Urban Development, May 2012: 43-49.
9. Heeren N., Jakob, M., Martius, G., Gross, N., Wallbaum, H. (2013). A component based bottom-up building stock model for comprehensive environmental impact assessment and target control. Renewable and Sustainable Energy Reviews, 20 (April 2013): 45-56.
10. SIA (2009). „SIA 380/1:2009 Thermische Energie im Hochbau“. Swiss society of engineers and architects, Zürich
11. Jakob M., Flury K., Gross N., Martius G., Sunarjo B., Bébié B., Heeren N., Wallbaum H. (2012). Energiekonzept 2050 für die Stadt Zürich - Auf dem Weg zur 2000 Watt tauglichen Wärme-Versorgung mit einem räumlich differenzierten Gebäudeparkmodell. 17. Status-Seminar «Forschen für den Bau im Kontext von Energie und Umwelt». 13./14. September 2012, ETH-Zürich

URBAN FORM AS A MAJOR ENERGY PARAMETER IN MODELING AN ECO-DISTRICT

Fabien Kuchler; Fabien Poumadère; Gaëtan Cherix

CREM – Center for Energy and Municipal Research, Av. du Grand-St-Bernard 4, 1920 Martigny

ABSTRACT

The real estate market tends to grow as cities are more and more populated and new buildings or districts are hatching. But a systemic vision of the realization of eco-districts is still lacking.

Current buildings have less thermal needs because of the technical improvements in the envelope and the heat distribution systems. Thus the morphological and geometric parameters of buildings have a significant impact on changes in energy needs, and it is possible to minimize the energy consumed while leaving ample liberty to planners and architects in their respective work. This can be done on one condition: the consideration of energy must take place at an early stage of the draft, when the first model is designed, in agreement with the planners, to assess its effects.

The objective of the "QuaD" project, driven by CREM in collaboration with the EPFL and the HES-SO Valais, is to develop a tool that can modelize a district and give energy, economic and sustainability indicators as the buildings, energy production and supply are defined by architects or urban planners on a 2D/3D software platform.

An ideal spacing between buildings, ideal compactness, optimum orientation, sustainable envelope elements and thoughtful supply aim at providing a more sustainable society. Sensibility calculations have been done on those parameters and many others to show their influence on the energy needs, that include heating, domestic hot water, embodied energy, electricity and energy induced by mobility. In parallel, providing a tool to urban planners represents a challenge as those people have typical workflows that can't be changed drastically. An analysis of the workflows of architects and urban planners has been done and the tool has been developed in order to meet their needs.

The difference of this tool compared to others is that it can modelize a district in 2D/ 3D, and immediately evaluate the impact of constructive, energy production and building choices. "QuaD" gives energy indicators that vary depending on those choices, and can integrate all the concepts of sustainability: from an economic comparison of solutions to the choice of the most efficient energy solution for energy supply, and taking social recommendations into account.

"QuaD" will give a new opportunity to planners who want to excel in building the new eco-districts of tomorrow, but could also be used by municipal architects, who want to elaborate scope statements for building projects on their parcels, or make district plans which contain energy criteria.

Keywords: sustainable districts, urban planning, energy efficiency, energy

INTRODUCTION

The Swiss real estate market tends to grow. It is well established that the choice of an urban project has a significant impact on the three pillars of sustainable development. However, it seems that some of these areas are neglected as actual processing for developing a district is not designed for being energy-/socially-/economically efficient.

Against this backdrop and in order to create new sustainable development standards, different tools have been developed and used to qualify or quantify whether a neighborhood is sustainable or energy efficient, but only when the architectural and urban concepts were endorsed.

In parallel, there are many communities that would make sustainable neighborhoods but who feel helpless when it comes to provide guidance for developers and investors, both technically and legally.

The CREM, in collaboration with the EPFL and the HES-SO Valais, want to solve this problem through the applied research project QuaD (Sustainable Neighborhoods). The goal is to create a software which allows to model the neighborhood showing energy indicators corresponding to the choice of the architect or another user, and that includes all the concepts related to energy efficiency.

METHOD

To identify issues related to the design of sustainable neighborhoods, it was first necessary to understand the current operation of projects that are undertaken, and assess the criteria that influence the energy performance of neighborhoods.

Cross approach bottom-up

Various players were included in this bottom-up approach to identify precisely the problem (architects, municipal councilors, housing service managers, responsibles for sustainable city development, urban planners, etc.).

These interviews and analytical work helped define and sketch a procedure for the neighborhood design competition.

Figure 1: Standard process of a neighborhood design competition. QuaD project, CREM

A short analysis of this scheme shows that many parameters that have a major influence on the energy performance of a neighborhood are set too early in the project, without having been analyzed as criteria involved in the selection of projects.

Evaluation of key energy parameters

The first step to solve this problem was to list all the parameters that influence the sustainability of a neighborhood based on the experience gained through many construction projects or renovations.

According to the "environment" dimension of sustainable development, the elements that have been identified are mainly related to:

- Invariable local context (there is a certain amount of fixed geographical data) that are for example the location, weather conditions, topology etc.
- The building's typology, depending on the type of construction, its assignment (residential, office, and all other categories of the SIA standard[1]), and also its shape and orientation.
- The behavior of the users for which it is possible to issue recommendations, but difficult to determine the representative criteria. The calculated heating needs are based on a 20°C inner temperature but real cases show that the inner temperature is closer to 22°C which causes a greater energy consumption.
- Mobility, responsible for a large share of greenhouse gas emissions. There are several ways to quantify the energy induced by mobility based on the use of buildings in the neighborhood. A calculation tool has been developed by the SIA.

For each identified parameter, experts have determined their relevance to be implemented in a help-designing tool, based on their experience and study results explained later.

In the "economic" aspects of sustainable development, a financial module allows to take into account the different costs that appear in the lifecycle of the neighborhood that has been created. This module also allows quantitative comparison of different solutions or concepts. The overall costs consist of investment costs, operating costs and decommissioning costs.

[1] www.sia.ch

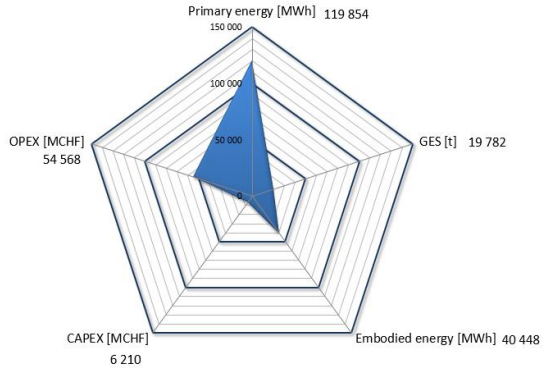

Figure 2: Economic analysis of a scenario. QuaD project, CREM

The data of a scenario can be showed in a web-diagram and those scenarios can be compared and include the CAPEX and OPEX. The costs taken into account here are:

- CAPEX: capital costs including the building costs and technical supply system costs. A standard cost has been assigned to types of construction: CHF 1'000.-/m3 for a standard construction, majored by 5% for Minergie label and 12% for Minergie-P. This is information communicated by the Minergie office concerning the actual construction costs. Concerning the supply systems, costs are based on experiences of municipal councilors that work in the "buildings commission".
- OPEX: operational costs consisting of energy costs, maintenance costs and amortization during the life-cycle of the different elements. They are related to the technology used for the scenarios. Energy costs are correlated with a standard inflation rate.

Finally, with the "social" aspect of sustainable development, it is not conceivable to set conditions that are evaluated in the QuaD tool. In this perspective, it makes sense to only offer recommendations. The social success of a neighborhood is depending on environmental factors, social diversity to promote social mix, and its functional diversity in order to create synergy, but also identification and ownership space for residents. Many studies show that for the moment, no tool is able to quantify social aspects on the basis of identified parameters.

Nevertheless. The QuaD tool could be coupled to other tools that give more information on social aspects that must be included during planification, as the SMeo[2] tool does.

Set of parameters

Developed for a use in the design phase, the number of inputs must be as low as possible while maintaining an acceptable accuracy in the final performance. In accordance with the working group, it was proposed that the tool QuaD has two levels:

- Level 1 – Summary model for a brief building assessment which includes
  - Location on a map or giving an address (weather station and solar mask are automatically calculated and retrieved).
  - Designing the main ground forms of the buildings
  - Introduce the height of the buildings, the number of floors and the ratio of glass surface
  - Choose the construction type (standard concrete, wood or mixed structure)
- Level 2 – Detailed model taking into account the specificities of each building in order to refine the previous results for the heating and associated costs.

Finally, the methodology for sensitivity studies was to model a neighborhood or a model building on which a parameter has varied. Then it is the result of the study to determine whether the tested parameter is significant or not.

[2] www.smeo.ch

A document of specification has been elaborated and the partners of the project, the HES-SO in Sion and the EPFL LESO-PB have simulated the sensitivity studies. Here is an example:

- Impact of existing buildings on solar gains
    - In studying different cases, a ratio could be found and give an ideal spacing between buildings in function of their height.
    - Varying parameters: distance between existing and planned buildings and height of buildings
    - Tool: CitySim
    - Output : ideal distance between buildings, in function of their height and margin of error
    - Priority: high
    - District model: planned district "Prés Magnin" located in Martigny

This was done for all the parameters influencing the energy performance of a building / neighborhood. All studies, given their numbers, cannot be presented individually in this paper but the main results from these many analyses are nevertheless presented below.

RESULTS

The parameters that must be considered when designing a neighborhood were divided into three distinct categories, which are planning and infrastructure, building and energy supply.

Planning and infrastructure

Urban form and geolocation are certainly essential for energy consumption in the area and therefore its environmental impact (greenhouse gas emissions).

- The mean angle of the solar mask must be optimized. Ideally, the mask angle should not exceed 20°.
- The orientation of buildings plays a significant role. By varying the orientation angle between 0 and 90 °, the consumption varies in the following manner :

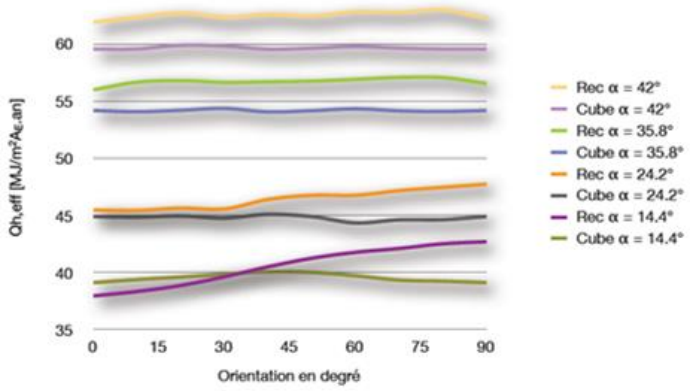

Figure 3: Energy-orientation correlation. Métamorphose project, Lausanne. The orientation of the buildings compared to a north-south axis implies a variation of the energy needs. The different colors represent the solar mask angle

In this diagram, different buildings have been simulated as « cubic » buildings or « rectangular » buildings. The orientation of the buildings compared to a north-south axis implies a variation of the energy needs. This is due to solar gains that change in function of the surfaces irradiated by the sun.

In consequence, for low solar masks, the orientation of rectangular buildings can change the energy needs up to 25%.

- The average solar mask is also related to geolocation. It is essential to be able to automatically retrieve the mask distant horizon based on the geolocation of the neighborhood.
- Finally, the average annual ambient temperature changes with altitude and location. It is expected to be able to automatically choose the weather station through the georeferencing tool QuaD.

Buildings

In addition to its aesthetic side, the architecture of a building is a basic component for the optimization of thermal needs. The shape of the building will play a role in the thermal decrease of the building, generating more or less heat losses, potential thermal bridges and discomfort associated with summer overheating.

- First, the shape of a building will define its compactness. This is what is called the form factor. It is the ratio of the surface of the heat losses and the energy reference area. Optimizing the form factor limits the need for heating. Thus, there may be a factor 2 or 3 on the heating needs between a compact and a building that is not for the same energy reference area (ERA)
- Changing the number of floors influences the form factor. The following graph shows that there is an optimal number of floors that varies depending on the ERA. Those data are calculated on a standard actual building.

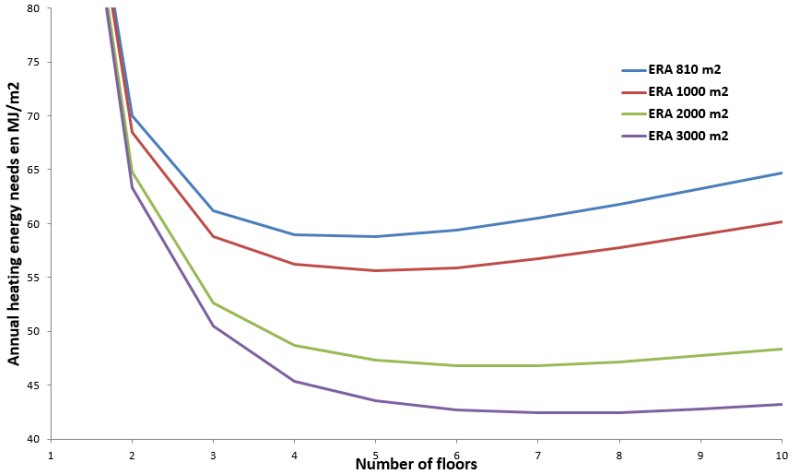

Figure 4: Influence of the number of floors and ERA. QuaD project, CREM

- The design of a building goes inevitably through the choice of materials. Thereby it is possible to be guided by their embodied energy. For example studies show that the concrete construction method has an equivalent embodied energy to one's generated by induced mobility.
- Finally, studies on the windows show that a good glass quality over the south facing glass surface reduces the heating needs. It should be noted however that these values were obtained by a static thermal calculation for each month of the year, which does not reflect the real dynamic behavior.

Energy supply

From a technological point of view, "improving the energy performance of a neighborhood is the result of the integration of four measures: improving the building envelope, use of distribution systems, use of indigenous resources and improved energy efficiency of conversion" [1].

Thus, even after optimization of the integration of building space and choices about the envelopes of these buildings, a quantity of energy is more or less required to meet remaining energy needs. This is ensured by energy supply systems which are mainly characterized by two distinct elements:

- The energy carrier (electricity, natural gas, oil, wood, geothermal energy, etc.)
- Technology or energy conversion systems that convert an energy carrier into another one or into useful energy.

The choice of energy supply systems has a major impact on the quantities of final and primary energy, [2] consumed to provide equivalent energy services. It is the same for GHG emissions.

In the case of QuaD project, it has been found that the energy supply systems, which ensure the needs of different consumer items, must in all cases be considered. This will calculate the amount of primary energy and greenhouse gas knowing the energy needs of the district.

Finally, Fig. 5 shows an example of analysis performed for a fictitious neighborhood showing the influence of different systems of energy supply on the primary energy consumption of the case study. This comparison is coupled with a presentation of the influence of the choice of constructive modes (wood or concrete) and energy performance related.

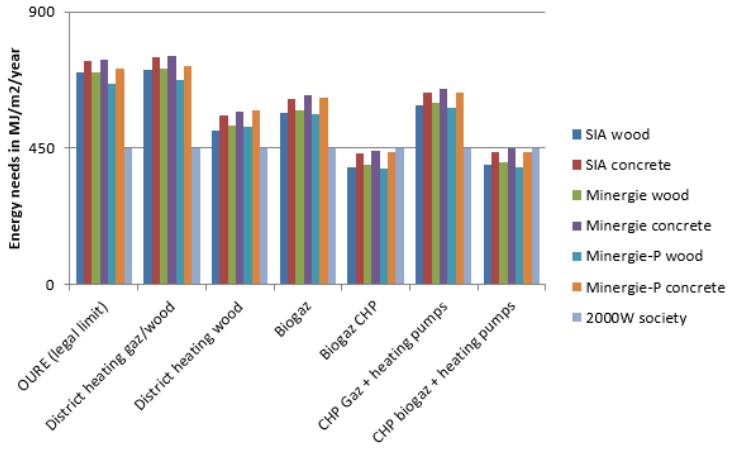

Figure 5: constructive modes and energy supply comparison. QuaD project, CREM

CONCLUSION

Following those works, broad prospects seem open to QuaD tool. In fact, that kind of help-designing tool would, on the one hand, facilitate the implementation of specifications including economic and energy efficiency criteria for the planning competition, and, on the other hand, evaluate draft district under energy-climate performances.

This assessment tool will be made available to district designers (architects, general contractors, etc.) giving them the opportunity to integrate economic and energy issues since design phase.

The example of a neighborhood in Martigny, taking into account different scenarios of energy supply, shows that the energy performance of the district, in terms of total primary energy (embodied energy included), varies by a factor 2.3.

Designing a neighborhood with high energy-climate performances requires considering energy issues, both for the urban design of the district, the architecture of the buildings and collective energy infrastructure.

REFERENCES

1. Girardin & al., EnerGis: A geographical information based system for the evaluation of integrated energy conversion systems in urban areas. Energy 1-11, 2009
2. Haldi & al., Methodological aspect of the definition of a 2 kW society. Energy, Vol.31 ,pp. 3159-3170, 2006

SUSTAINABLE URBAN DEVELOPMENT IN CHINA BY ADOPTING INTEGRATED RESOURCE MANAGEMENT APPROACH

J.Liang

Arup, 39F 1045 Huaihai Road (M) Shanghai PRC

ABSTRACT

In urban development projects, planners face significant challenges from the complexity of the urban system. Urban growth reflects the dynamic inter-connections among social, economic and environmental aspects. Land use arrangements have huge impacts on urban infrastructure, including energy, water, transport and waste, as well as on carbon emission levels. Traditionally, there is a communication gap between urban planners and technical teams. The former is centring on land use schedules while the latter focusing on proposing their individual strategies. This gap results in inconsistency that harms the potential of maximising the sustainability of urban development.

The Integrated Resource Management (IRM) approach was proposed by Arup London in 2005. This innovative and systematic approach integrates spatial and resource flow information from different technical disciplines through their internal linkages. Therefore, the model is able to process inputs from each technical team and quantifies performance outputs to provide a comprehensive indicator system for decision-makers. Since then, IRM has been further developed in the UK, the United States and Australian and has been applied for large scale projects globally.

During the unprecedented urbanization process, China has achieved great success in economic growth while facing severe environmental challenges in natural resources shortage and environmental pollution. With the slogan of "Shape a Better World", Arup has the mission and competence to drive Chinese cities' development into a sustainable path. Developing IRM within Chinese context is an essential part to achieving this goal. This paper provides a brief introduction to IRM China version by a case study in order to illustrating the benefits of its adoption in urban planning projects.

Keywords: urban development, integrated planning, sustainability

INTRODUCTION

City is defined as a relatively large and permanent settlement and is constituted of complex systems including housing, transport, land usage and utilities [1]. Cities accommodate lives of their residents and consequent business activities. High level concentration of developments brings prosperity to cities and attracts migrants and business moving to cities. This kind of urbanization process has taken place for decades globally and is extraordinarily remarkable in China during the past 30 years. Based on World Bank's prediction, there will be 350 million more people adding to China's 1 billion urban populations, and 221 cities with populations over one million by 2025 [2]. Not only the megacities such as Beijing and Shanghai, the second-tier cities, like Suzhou and Tianjin, call for integrated urban planning for their ambitious development goals.

Urban planning is both a political and technical process, with considerations of land use control and urban environment design. Expertises from policy makers, urban planners, architects and engineers all contribute to the planning process from concepts to detailed plans.

Traditionally in Mainland China, urban planning follows the designing process that has the similarity with an assembly line. Firstly, strategic development targets are set up by the central and local authorities. Urban planners then start to focus on land use schedules that reflect the high level targets. After that technical planners propose individual strategies on different disciplines accordingly. However, mass information is required to be processed within short time and the dynamic inter-connections generate urban complexity problems that are challenging urban development practitioners.

The Integrated Resource Management (IRM) model is created to provide a solution to urban complexity issues [3]. It interconnects data between land use and technical solutions in an Excel spreadsheet. It is able to process these technical inputs by integrating assumptions and calculations from energy, water, transport and waste sectors. All the outputs can be instantly quantified and sent to key performance indicator system, which can be used to appraise the performance of planning schemes.

Furthermore, the integrated design approach is developed along with the increasing emphasis on urban sustainability. With the adoption of IRM model, a sustainable design framework can be built up to guide the design and development from the very beginning. Work flow will be changed subsequently and so does the project management method.

Since 2005 when the first version came out, IRM has been used in various types of Arup projects all over the world, including eco-city planning in Dongtan masterplan (Shanghai, PRC) [4], greenhouse gas emissions estimation for waterfront Toronto (Canada) [5] and environmental impact assessment in Concord Community Reuse Plan (Northern California, US).

IRM CHINESE VERSION

IRM China version is further developed from its previous adoption in Australia with special considerations of the Chinese context. Framework of the model was re-structured according to Chinese coding system of land use while basic rates of resource consumption were collected by referring to national and local standards. In addition, an energy profile database for typical building types was established by using energy simulation tools.

In this paper, a case study is selected to introduce the China version model. All the information comes from a practical project which locates in a fast developing city of East China. The following sectors provide the details of using IRM to drive sustainable urban development.

i. Scenarios

The main purpose of using IRM is helping decision makers to efficiently assemble all the information together and make judgement and decision on optional scenarios. Therefore, scenario setting is the first and one of the most significant steps to build up framework of the project model.
There are two scenarios in the case study, BaU (Business as Usual) and Sustainability. BaU is developed according to national and local standards, and its strategy combination and the consequent results in its indicator system are regarded as the benchmarks to be compared with the counterparts of the Sustainability scenario.

ii. Indicators

As for sustainable urban development projects, a comprehensive indicator system is required to be established in order to be the guidance of the development. The indicators, as the performance results, are well linked with land use information and inputs of technical strategies.

Major indicators in this case are consumption and supply structure in energy and water sectors, waste generation and its breakdown after treatment, and transport mode share and the network performance, and carbon emission, which is the essential one to present overall result of both scenarios. In IRM, results are able to be calculated automatically, which makes the whole decision making process to be simplified by just clicking buttons in the input dashboard and choosing strategy combinations. Parts of the dashboard are shown in Table 1~3.

iii. Energy

Energy sector in IRM is divided into two parts, demand and supply. Energy demand focuses on calculating energy consumption according to land use arrangement and population, while supply structure and energy balance are considered in the latter one.

In terms of energy demand, an energy database is established by adopting e-Quest, the energy simulation software. There are five typical building models, including residential building, office, hotel, shopping mall and cultural buildings. Assumptions of each building model follow national codes and standards. As the results, the hourly energy profiles provide the demand baseline of electricity, heating and cooling.

Sustainable energy planning strategy calls for the reduction of energy demand and optimized supply option to minimize total carbon emission. In order to reduce energy demand, green building is the preferable option for the Sustainability case. In the Sustainability case, all the buildings are required to obtain the Three Star Certification, the highest Chinese green building standard. That means energy efficiency increasing 20% by comparison with national standard (GB).

As for energy supply, increasing renewable energy proportion are mainly considered. Compared to traditional grid supply, the priority of energy resource in Sustainability case goes from solar, to biomass, and to heat pump. In IRM, max yield of each supply option is provided and the desired proportion is testified to pursue for the optimized combination of solutions. Table 1 lists the results of the energy supply options. By replacing grid electricity with renewable energy, the structure of energy supply is changed totally (Figure 1 & 2). Hence the demand for national grid and natural gas is declined dramatically.

	Scenario =>	BaU		Sustainability	
2. ENERGY DEMAND	Residential	Select =>	GB	Select =>	3 Star
	Administration and Public Services	Select =>	GB	Select =>	3 Star
	Commercial Facilities	Select =>	GB	Select =>	3 Star
	Business Facilities	Select =>	GB	Select =>	3 Star
	Recreational & Public Service Facilities	Select =>	GB	Select =>	3 Star
3. ENERGY SUPPLY		Yield	Desired %	Yield	Desired %
	Solar PV (Building Roofs MWh)	141,447	0%	141,447	5%
	Solar PV (South elevation MWh)	34,537	0%	34,537	20%
	Solar HW (Building Roofs MWh)	599,66	0%	599,66	5%
	Bio-energy generation (MWh)	11,071	0%	11,071	80%
	Ground-source heat pump (KW)	263,74	0%	263,74	10%
	Water-source heat pump (KW)	2,500	0%	2,500	0%
		Consumption		Consumption	
	Grid Electricity (MWh)	108,171		48,569	
	Gas (GJ)	14,088		65	

Table 1: Dashboard of energy sector

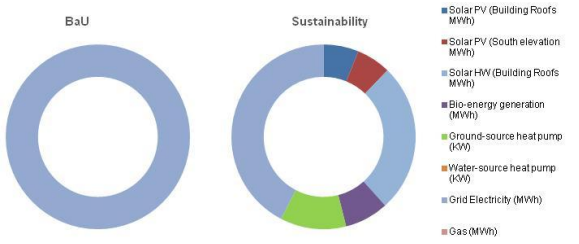

Figure 1: Energy Supply Type Proportions

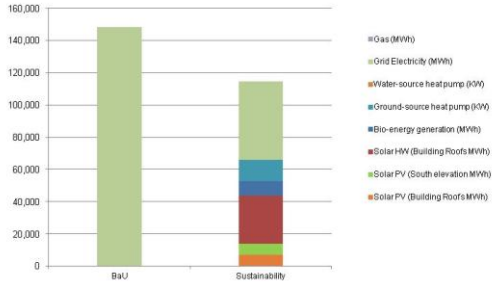

Figure 2: Energy Source Breakdowns (kWh supplied p.a.)

iv. Water

As the same as in energy sector, balancing water demand and supply are the main concern here. In BaU case, all the water usage counts on tap water supply and water consumption rates are identified in *National Water Saving Standard* [6].

The so-called sustainable water strategy focuses on introducing non-traditional water supply resource to diminish the demand of fresh water. By subdividing water use purposes, demand for toilet flushing and gardening can be satisfied by water regeneration and rainwater collection. Then the valuable fresh water is only required to meet the portable water needs. It should be mentioned that rainwater supply is regarded as backup because of its unreliability, although rainfall collection strategy is included in IRM water sector. Besides, pipeline leakage rate is also considered and its reduction is of significance to increase the efficiency of water supply network.

From Table 2 and Figure 3, it can be seen that 1/3 of tap water supply is saved by recycling 40% of waste water, collecting all the rainfall available and controlling pipeline leakage rate.

	Scenario =>	BaU	Sustainability
4. WATER	Regenerated Water Supply	0%	40%
	RainWater Supply	0%	100%
	Leakage Rate	20%	12%

Table 2: Dashboard of water sector

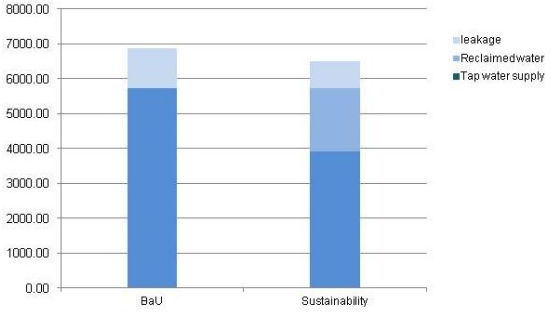

Figure 3: Water Demand by type (ML p.a.)

v. Waste

The current situation of waste sector from generation to treatment in China is quite different from that in western countries. There is no sophisticated garbage classification system. Total waste generation is divided into four classes: household refuse, big rubbish (waste furniture and electrical equipment), construction waste and hazardous waste.

Construction waste takes the biggest proportion due to the huge amount of new construction across China. Of them, 60% is able to be recycled [7]. As for household refuse, it can be separated into two parts, dry and organic waste. 50% of organic waste can be decomposed and contribute to bio-energy generation [8]. The 60% of dry waste, together with decomposed organic waste, disposed hazardous and big rubbish will also be recycled. Then, by considering combustible rate (90%) and combustion efficiency (90%), the amount of burning waste can be calculated, while the rest will be sent to landfill.

vi. Transport

In transport planning, the key indicators of network performance are total vehicle kilometres per year and total vehicle hours per year. Low vehicle kilometres and vehicle hours stand for high network efficiency. Those performance indicators are determined by total number of trips and transport strategies.

With the inputs of land use information and trip rates, daily trip amount can be obtained. Trip rates value in this model refers to Beijing statistics [9], which is the recognized source in Mainland when lack of local data. Two transport strategies are provided for this project, Metro/LRT provision and Transit Oriented Development (TOD). By adopting both of them and promoting the usage of public transport, mode splits are changed accordingly (Figure 4).

Then, by referring to local average travel distance and time, the performance indicators can be obtained (Figure 5 & 6). Moreover, environmental performance can also be assessed by calculating annual carbon emission from transport sector. In this case, assessment methods refers to Air Quality Assessment Screening Method in United Kingdom [10].

	Scenario =>	BaU		Sustainability	
5. TRANSPORT	Public Transport Mode Share	percentage	30.0%	percentage	50.0%
	Metro/LRT Provision	Select =>	X	Select =>	√
	Transit Oriented Development (TOD)	Select =>	X	Select =>	√
		Total Million Vehicle km/yr	Total Million Vehicle hr/yr	Total Million Vehicle km/yr	Total Million Vehicle hr/yr
	Network Performance	1,675	69	957	40

Table 3: Dashboard of transport sector

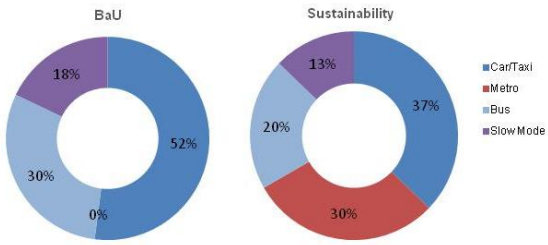

Figure 4: Mode splits

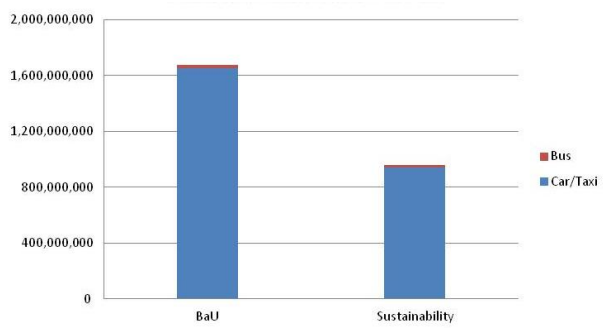

Figure 5: Total Million Vehicle km per Year

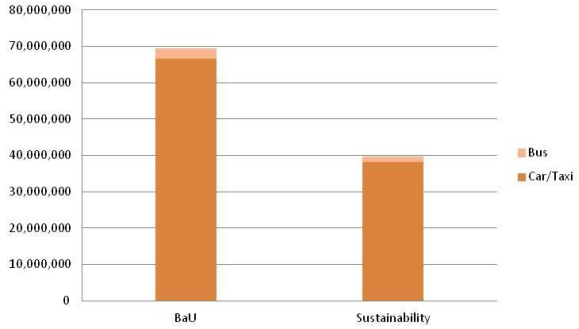

Figure 6: Total Million Vehicle Hours per Year

vii. Carbon

Carbon emission is an integrated indicator to evaluate the overall performance of the development plan. It constitute with three main parts, grid electricity, gas and transport.

The carbon emission factors refer to emission factors for regional power grids in China and IPCC report [11] [12]. By summarizing all the strategy illustrated above, total consumption of grid electricity and gas can be calculated. Figure 7 presents the fact that carbon emission is much smaller that BaU because of the replacement of grid electricity and introduction of green transportation.

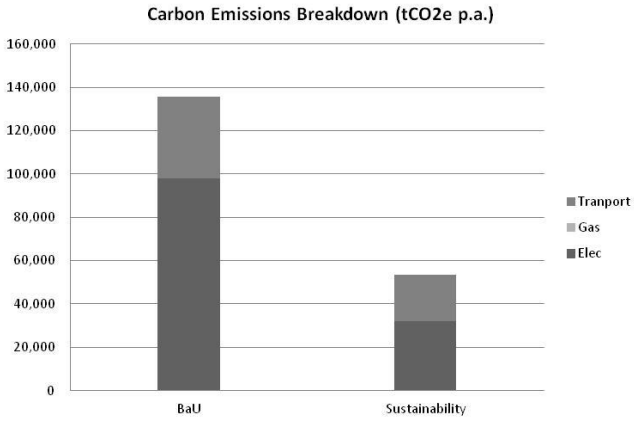

Figure 7: Carbon Emissions Breakdown

viii. Summary

From the case study, the whole process of adopting IRM in planning strategy decision is presented. By establishing database in advance, this approach provides an efficient way for decision making and project management. Most importantly, it is also a solution to realize sustainable planning when facing urban complexity.

FURTHER DEVELOPMENT

There are three parts which will be further developed in the next research phase.

Firstly, database needs to be strengthened in order to obtain full picture of energy consumption, especially those from industry and logistic. Secondly, financial appraisal is of significance in decision making. Construction cost and living expense data will be collected for each technical solution. Then the cost-benefit analysis is able to be presented to identify the best package of technical strategies. Third, the model will be used in urban design projects by equipped with 3D visualization function. Data link will be realized among AutoCAD, GIS, IRM and parametric design tool such as grasshopper.

ACKNOWLEDGEMENTS

This research project is sponsored by Arup's Design & Technical Fund, and has got support from Arup Melbourne office and Shanghai local expertises with background in urban planning, environment, energy, transport, carbon and GIS. I sincerely appreciate their contribution.

REFERENCES

1. Goodall, B., *The Penguin dictionary of human geography*. 1987: Penguin books London.
2. Baeumler, A., et al., *Sino-Singapore Tianjin Eco-City (SSTEC): a Case Study of an Emerging Eco-City in China.* World Bank TA Report, 2009.
3. Page, J., N. Grange, and N. Kirkpatrick, *The Integrated Resource Management (IRM) model - a guidance tool for sustainable urban design.* PLEA 2008 – 25th Conference on Passive and Low Energy Architecture, 2008.
4. Stanley, C., *ECO CITY: FROM CONCEPT TO IMPLEMENTATION WITH SHANGHAI DONGTAN AND BEIJING CHANGXINGDIAN AS CASES.* City Planning Review, 2008. 8: p. 011.
5. http://www.waterfrontoronto.ca/our_waterfront_vision/our_future_is_green/carbon_tool.
6. *Standard for water saving design in civil building* in *GB 50555-2010*, MoHURD, Editor 2010, China Architecture & Building Press.
7. Leng, F., et al., *Status and Development Trend of Construction Waste Resource at Home and Abroad.* Environmental Sanitation Engineering, 2009. 1.
8. Lu, F., et al., *Generation and treatment technologies of putrescible wastes.* Techniques and Equipment for Environmental Pollution Control, 2003. 4(8): p. 46-50.
9. Guo, J. and G. Wang, eds. *Trip Generation*. 2009, China Architecture & Building Press.
10. Techniques, A.Q.E.A., *Design Manual for Roads and Bridges (DMRB).* Highways Agency. 11.
11. NDRC, *2012 Baseline Emission Factors for Regional Power Grids in China*, 2012.
12. IPCC, *IPCC guidelines for national greenhouse gas inventories.* IGES, Japan, 2006.

A COMPREHENSIVE MODEL FOR THE GERMAN ELECTRICITY AND HEAT SECTOR IN A FUTURE ENERGY SYSTEM WITH A DOMINANT CONTRIBUTION FROM RENEWABLE ENERGY TECHNOLOGIES

Andreas Palzer[1], Hans-Martin Henning

Division Thermal Systems and Buildings
Fraunhofer Institute for Solar Energy Systems ISE, Heidenhofstraße 2, 79110 Freiburg, Germany

ABSTRACT

A clear consensus exists in the German society that renewable energies have to play a dominant role in the future German energy supply system. However, many issues are still under discussion; for instance the relevance of the different technologies such as photovoltaic systems and wind energy converters installed offshore in the North Sea and the Baltic Sea. The uncertain cost of a future energy system mainly based on renewable energies also gives rise to concerns. In this context, the presented work addresses the following questions: (1) Is it possible to reduce the emission of greenhouse gases of German energy sector by more than 90 % compared to 1990 within the limits of the available technical potentials of the main renewable energy resources? (2) What is the overall annual cost of such an energy system once it has been implemented? (3) What is the best composition of renewable energy converters, storages and energy saving measures?

In order to answer these questions we carried out many simulation calculations using REMod-D, a model we developed for this purpose. To date this model covers only part of the energy system, namely the electricity and heat sector, which correspond to about 62 % of Germany's current energy demand. The main findings of our work indicate that it is possible to supply the total electricity and heat demand of the total building sector within the given aim of reducing greenhouse gas emissions - on the precondition that the heat demand of the building sector is significantly reduced by at least 50 % or more compared to today's demand. Moreover, our analysis shows that once the transformation of the energy system has been concluded, supplying electricity and heat only from renewables is not more costly than the energy supply of today.

Keywords: Germany, energy system, optimization, renewable energies, space heating

INTRODUCTION

The current discussion on how or even if we should transform our fossil fuel based energy system to a renewable system is often based on emotions rather than facts. Political instruments like the German act for renewable energy technologies "Erneuerbare-Energien-Gesetz" (EEG) are discussed very controversially. Discussions are carried out about the number or the kind of needed power plants, the dimensioning of storage and the expansion of the electricity or district heating grids. In this paper we try to assess these issues based on

[1] Corresponding author: Tel.: +49 (0) 7 61/45 88-5903; fax: +49 (0) 7 61/45 88-9903.
E-mail address: Andreas.Palzer@ise.fraunhofer.de (A. Palzer).

numbers and assumptions from different reliable sources and based on a complex computer model that calculates hourly energy balances for the interaction of the German electricity and heat sector. We investigate different system configurations, the consequence of keeping a certain amount of fossil fuels in the system on the dimensioning of fluctuating renewable energy sources (RES) and the importance of energy retrofit measures in the building sector.

Various simulation models for national energy systems, which consider a high penetration of renewable energies, exist, but only a few models are able to combine the supply and demand from both the electricity and heat sectors. Many of the energy system models developed in the past focus on the electricity sector and its development but rather neglect the heat sector or do not cover it in detail. For example, the BALMOREL or the SIVAEL models cover the electricity sector but only district heating for the heating sector [1]. The EMCAS model focuses in detail on the operation of power systems [2]. A widely used example that covers both the electricity and the heat sector is the EnergyPLAN model developed in Denmark which has been applied to a number of different scenarios and regions [3-9]. A typical example for a model that focuses on the optimization of minimal energy system cost is the MARKAL model developed by the International Energy Agency (IEA) [10]. In contrast to the EnergyPLAN model, this model is used to optimize system cost and to represent the evolution of an energy system over a time period of several years. Other models with a comparable aim are, for instance, IKARUS which performs optimizations for a time period of up to 40 years in time steps of 5 years [11] or PERSUS which focuses on the minimization of energy supply system relevant expenditures [12]. These cost optimization tools cover the heat sector to a certain extent, but there is no detailed description of the related influences like building retrofit or alternative future heating technologies for centralized and decentralized systems. To our knowledge, there is only one tool that focuses on the detailed description of the heating and building sector in the context of a complex energy system. This model, called In*vert* [13], determines the influence of policy schemes in the field of heating, domestic hot water and cooling through a detailed description of this sector. Nevertheless, there is no cost optimization for a one year time period with hourly time-steps and also the interaction with the electricity sector is not treated in detail.

We developed the REMod-D model, introduced in this paper, to fill the gap with detailed modeling of the building sector in a complex energy system involving both the electricity and the heat sector. Further, the total cost optimization of a complex future energy system with a high penetration of renewable energy sources is carried out in hourly time-steps over a one-year simulation.

METHODOLOGY

The basic concept of the REMod-D model is to set up a fixed topology of energy producers, converters, storages and consumers and to optimize their sizing to meet the goal of minimized annual overall cost. The optimization rescinds – at least in this first step – completely from the existing infrastructure of the German energy system, i.e., the approach can be characterized as a “Green Field” simulation. A schematic of the implemented complete system is shown in Figure 1.

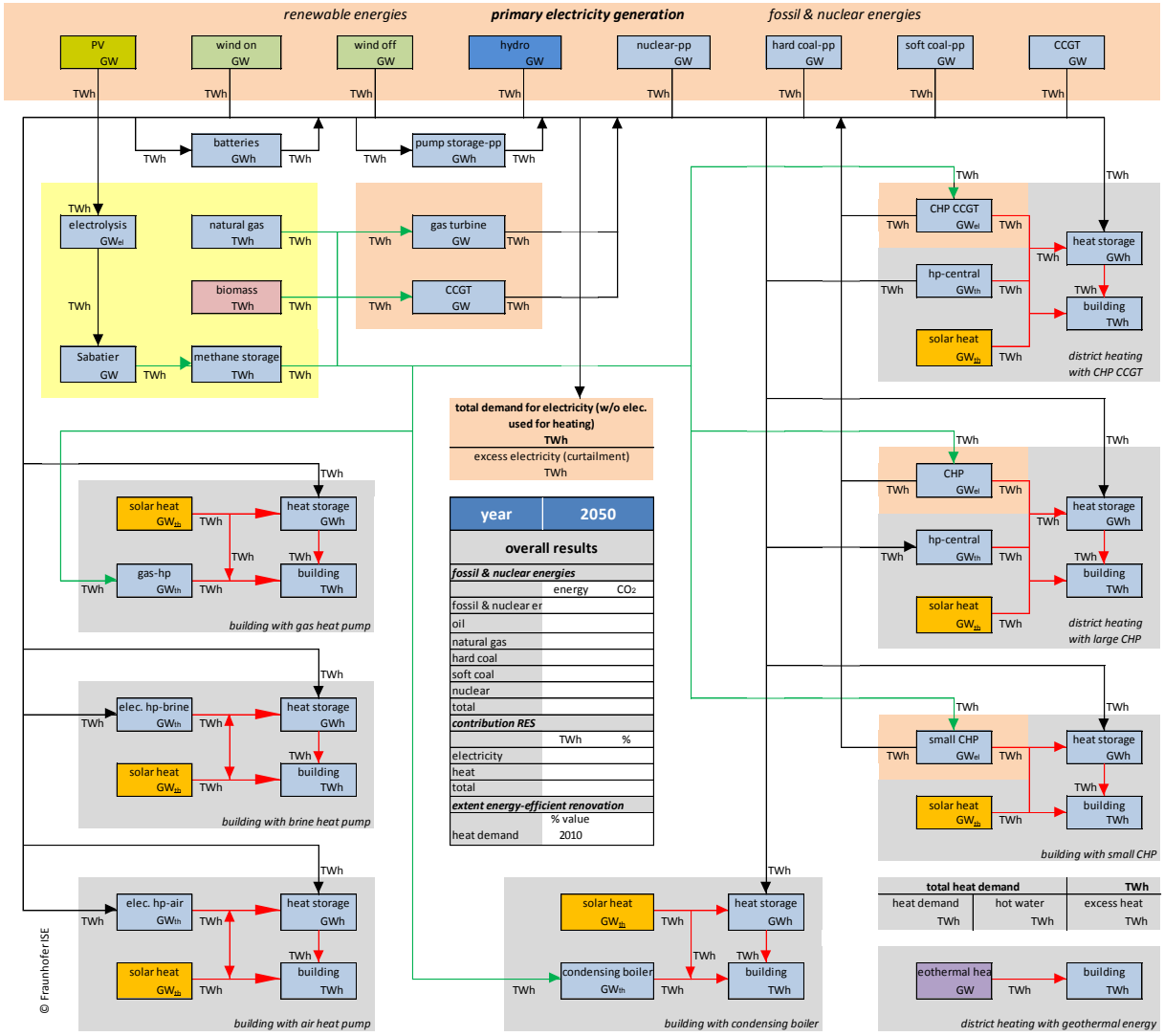

Figure 1: Topology of the model of the German energy system (electricity and heat sector) of the REMod-D model

The system contains photovoltaic power systems, on- and offshore wind generators and hydro power stations as primary renewable electricity generators. In addition, the expected residual amount of installed capacity for the year 2050 of nuclear and fossil fuel based power plants such as coal, natural gas and oil fired power plants are implemented in the system. Solar thermal collectors, connected either to central heating systems or to decentralized heating systems, act as primary heat generators. The secondary renewable electricity generators are combined heat and power systems (centralized, decentralized) and combined cycle power plants. Both use either natural gas, gas from biomass (value fixed here as: 50 TWh or gas produced from primary renewable electricity (power-to-gas). The total electric load is given by the overall load of all electricity consumers connected to the public grid (e.g. lighting, machinery, household electricity etc.) plus the electricity loads due to electrically driven compression heat pumps. Heat loads are separately treated for buildings which are connected to a centralized heat production (district heating networks) and buildings which have a decentralized heating system. For buildings having a decentralized heating system, different technologies are distinguished, namely electrically driven heat pumps, decentralized combined heat and power systems, gas driven heat pumps and conventional condensing boilers. Five different types of storage are included in the model: pumped hydro-power storage and batteries for the direct storage of electricity, gas storage (in Germany typically

large caverns) for storage of gas from renewables (power-to-gas) as well as centralized and decentralized heat storage.

RESULTS

In order to investigate different electricity and heat reduction scenarios and the influence of a certain amount of natural gas available for the electricity and heating sector, we selected corresponding boundary conditions.

> Two scenarios were used concerning the electricity demand: In the first one no electricity reduction is accomplished and thus still 500 TWh [14] of electricity is needed in the system. In the second one the electricity demand is reduced by 25 % down to 375 TWh.
> In order to cover the reduction of greenhouse gas emissions in a range of 80 to 95 % compared to 1990 we fixed the amount of available natural gas in the system with 0, 150, 300 and 500 TWh.

Table 1 gives an overview of the results. It can be seen that the required installed capacity of fluctuating RES strongly depends on the reduction in electricity consumption and on the amount of natural gas available in the system.

Electricity demand	**TWh**	**375**				**500**			
Natural gas	**TWh**	**0**	**150**	**300**	**500**	**0**	**150**	**300**	**500**
Wind offshore	**GW**	50	49	42	34	50	50	48	40
Wind onshore	**GW**	150	118	101	67	150	147	122	91
Photovoltaic	**GW**	221	141	93	68	257	233	173	123
Power-to-Gas	**GW**	70	29	0	0	75	46	10	0
Heat demand	**$\%_{2010}$**	72%	77%	82%	88%	45%	76%	78%	84%
CO_2-Emissions	**Mio t**	36	66	97	137	42	66	97	137
Reduction of CO_2 in	**%**	95%	90%	85%	79%	94%	90%	85%	79%

Table 1: Results of different optimization runs

With an amount of 300 TWh of natural gas in the system, no power-to-gas facilities are needed to store electricity and reducing heat in the building sector is less attractive. Analogously, the results suggest that smaller amounts of natural gas in the system promote higher reductions in heating energy demand. With a constant electricity demand of 500 TWh and no use of natural gas the cost optimal reduction in the heating sector amounts to about 55%, i.e. the space heating demand amounts 45 % of today's value. As boundary conditions for further calculations we choose 500 TWh of electricity, which seems reasonable assuming that the mobility sector switches at least partly from fuel to electricity in 2050. Furthermore we decided to fix the amount of natural gas to 150 TWh, because we expect natural gas to be used less in the low temperature heating sector and more for high temperature processes in the industry, which are not considered in the model yet. The influence of reduction for space heating in the building sector is investigated with a reduction ranging from 80 % down to 40 % compared to the space heating demand in Germany in the year 2010 (780 TWh [14]).

The effect of reducing the energy demand in the heating sector on the total annual cost and the amount of installed capacity of fluctuating RES can be seen in Figure 2. The minimal total annual cost is achieved with a reduction of the heat demand down to only 70 % of the 2010 value. At the same time, the installed capacity of fluctuating RES reaches almost 400 GW and an installed capacity of about 50 GW power-to-gas facilities is needed. With energy saving measures that lead to a heat reduction of 50 %, the total annual system cost increases by about 5 %, whereas the installed capacity of fluctuation RES decreases by about 18%. At the same time, the required installed capacity of power-to-gas facilities is reduced by almost 50 % from 41 GW to 22 GW. Thus a small increase in total annual system cost can decrease the number of installed energy facilities significantly and can thus be very helpful in increased societal acceptance concerning the expansion of fluctuation RES.

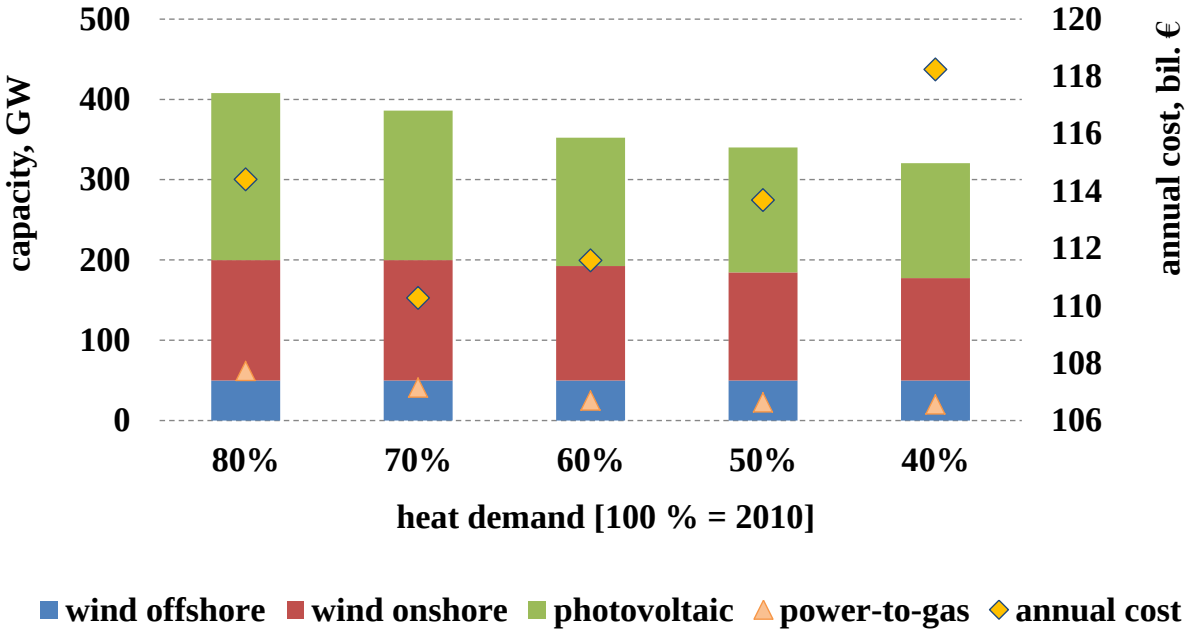

Figure 2: Installed capacity of different technologies and the total system cost depending on the amount of energy saving retrofit measures

SUMMARY AND OUTLOOK

Achieving the political goals of significant reduction of greenhouse gas emissions in Germany is technically possible and after the transformation of the energy system is completed, the overall annual cost will be comparable to today's cost. A complete supply of the energy system under these conditions, however, is dependent on a high energy efficiency standard of the building sector whereby the energy demand for heating is reduced by 50 % or more compared to the value in 2010. Therefore the costs for energy saving retrofit measures are a crucial value for the whole annual system cost. Furthermore, the installed capacity of RES and long term storage options like power-to-gas can be reduced significantly with an energy reduction for space heating down to 50 % of the 2010 value with only 5 % higher system cost. This is especially relevant for societal acceptance of large scale installation of RES.

With the model introduced in this paper we developed a powerful tool to assess different energy scenarios for national and regional energy systems. At the same time, the model is able to assess the impact of specific technologies in a future renewable energy system. Sensitivity analyses can help identify performance and cost dependencies of different technologies in a future energy system. For future work, several steps to further develop the model are planned:

- Integration of energy demand of the fuel based mobility and industry sector
- Calculation of system transformation cost to assess the expenses for conversion of today's energy system to a system relying on renewable energies
- A more detailed model of electricity exchange in a European context
- Diversification of the model, especially for space heating demand where the building structure in Germany will be implemented more in detail

1. REFERENCES

[1] ENERGINET.DK. 2012.

[2] ARGONNE National Labratory. *Electricity market complex adaptive system (EMCAS)* 2012 10.09.2012; Available from: www.dis.anl.gov/projects/emcas.html.

[3] Lund, H. and B.V. Mathiesen, Energy system analysis of 100% renewable energy systems—The case of Denmark in years 2030 and 2050. Energy, 2009. **34**(5): p. 524-531.

[4] Connolly, D., et al., *The first step towards a 100% renewable energy-system for Ireland.* Applied Energy, 2011. **88**(2): p. 502-507.

[5] Lund, H. and W. Kempton, Integration of renewable energy into the transport and electricity sectors through V2G. Energy Policy, 2008. **36**(9): p. 3578-3587.

[6] Connolly, D., et al. Ireland's pathway towards a 100% renewable energy-system: The first step. in 5th Dubrovnik conference for sustainable development of energy, water and environment systems, September 30 - October 3. 2009. Dubrovnik, Croatia.

[7] Lund, H., Large-scale integration of optimal combinations of PV, wind and wave power into the electricity supply. Renewable Energy, 2006. **31**(4): p. 503-515.

[8] Lund, H., Large-scale integration of wind power into different energy systems. Energy, 2005. **30**(13): p. 2402-2412.

[9] Lund, H. and E. Munster, Management of surplus electricity-production from a fluctuating renewable-energy source. Applied Energy, 2003. **76**(1-3): p. 65-74.

[10] Seebregts, A.J., G.A. Goldsten, and K. Smekens. Energy/Environmental modeling with the MARKAL family of models. in Operations Research Proceedings. 2001. Duisburg.

[11] Markewitz, P. and G. Stein, Das IKARUS-Projekt: Energietechnische Perspektiven für Deutschland, in Schriften des Forschungszentrums Jülich, Reihe Umwelt/Environment 2003, Forschungszentrum Jülich.

[12] Enzensberger, N., et al., PERSEUS-ZERT Systembeschreibung, Abschluss-Dokumentation einer Modellentwicklung für die RWE AG, Karlsruhe: Institut für Industriebetriebslehre und Industrielle Produktion. 2002.

[13] Kranzl, L., et al., Deriving efficient policy portfolios promoting sustainable energy systems—Case studies applying Invert simulation tool. Renewable Energy, 2006. **31**(15): p. 2393-2410.

[14] Bundesministerium für Wirtschaft und Technologie (BMWi) (Hrsg.). *Zahlen und Fakten. Energiedaten. Nationale und internationale Entwicklung*. 2012 21.08.2012]; Available from: http://www.bmwi.de/BMWi/Redaktion/Binaer/energie-daten-gesamt,property=blob,bereich=bmwi2012,sprache=de,rwb=true.xls.

SIMULATION OF URBAN ENERGY FLOW: A GRAPH THEORY INSPIRED APPROACH

D. Perez; J. Kämpf; J.-L. Scartezzini

Solar Energy and Building Physics Laboratory, École Polytechnique Fédérale de Lausanne, Switzerland

ABSTRACT

Following the increased consciousness regarding global warming and other environmental issues, there is a growing urge in cities for a more rational energy supply and use in buildings. In parallel, the range of possible actions has broaden, from building refurbishment and construction options, through local energy production (solar panels, heat pumps) to the larger scale re-use of waste heat, green electricity production or trading.

This evolution has increased the complexity of urban energy management, and more information regarding the energy efficiency of the energy demand and supply is required to evaluate possible improvements. Crude models fail to include all aspects of this complexity, while specialised simulation tools make global assessments and comparisons difficult. There is thus an opportunity for research to provide tools dealing with the increased complexity of urban energy flow to study the numerous options available to decrease the primary energy use of buildings and the related greenhouse gas emissions.

Focusing on the scale of a few hundred buildings, we model in this paper the disaggregated energy flow, from the resources through networks and energy conversion system towards the energy use in buildings for distinct services, as an oriented graph. Combining the limited available data with existing simulation tools and energy consumption data, a new graph theory inspired simulation method is formulated. The resulting detailed picture of energy flow can give access to a large amount of information but, most importantly, will provide a unified tool to compare energy efficiency scenarios regarding a broad range of technological aspects of energy demand and supply.

Keywords: disaggregated urban energy flow simulation, graph theory, factor graph, belief propagation, energy demand and supply, energy use measurements

INTRODUCTION

Graphical models is a framework used in various fields to represent and study probability distributions. Developed independently in statistical physics, coding theory and artificial intelligence, message passing algorithm are used to perform inference on such models and calculate marginal distributions [1].

Let Ψ be a probability density function of N variables $\mathbf{x} = \{x_1, x_2, ..., x_N\}$ that can be written as a product of M factors: $\Psi(\mathbf{x}) = \prod_{a=1}^{M} \psi_a(\mathbf{x}_{\partial_a})$. Each factor ψ_a depends on a subset of variables; the set of the corresponding variable indexes is noted ∂_a and the set of variables is noted $\mathbf{x}_{\partial_a}$. Factor graphs [1, 2] represent such functions as graphs composed of **variable nodes** associated with the variables x_i and **factor or function nodes** associated with functions ψ_a. There is an edge between the variable node i and the factor node a if and only if the function ψ_a depends on the variable x_i, i.e. iff $i \in \partial_a$.

Message-passing algorithms have been developed to compute the marginal or max-marginal distributions of the variables. This approach was proven to be very efficient in particular on tree graphs with discrete variables [1]. The message-passing algorithms operate by passing messages along the edges of the graph; the messages are probability distributions over the variable nodes' domains. Variable nodes inform neighbouring factor nodes of their probability distribution according to the other factor nodes they are connected to ($\nu_{i\to a}^{(t+1)}(x_i)$). In turn, each factor node send neighbouring variable nodes the distribution it would assign to them according to the other connected variable nodes ($\hat{\nu}_{a\to i}^{(t)}(x_i)$).

Considering in particular the **max-product** algorithm, the purpose of which is to find the configuration $\mathbf{x}$ maximising the probability $\Psi(\mathbf{x})$, the message update rules are given by the following equations:

$$\hat{\nu}_{a\to i}^{(t)}(x_i) \propto \max_{\mathbf{x}_{\partial_a \setminus i}} \left\{ \psi_a(\mathbf{x}_{\partial_a}) \prod_{j\in\partial_a\setminus i} \nu_{j\to a}^{(t)}(x_j) \right\} \tag{1}$$

$$\nu_{i\to a}^{(t+1)}(x_i) \propto \prod_{b\in\partial_i\setminus a} \hat{\nu}_{b\to i}^{(t)}(x_i) \tag{2}$$

(note that the message distributions need to be normalised). On a tree-graphical model, these updates converge to the correct max-marginals after at most $t^\star$ iterations, where $t^\star$ is the *diameter* of the graph, i.e. the maximum distance between two variable nodes [1].

While the numerical implementation of this algorithm is straightforward for binary or discrete variables, continuous variables prove to be more challenging. Loeliger [3] discusses options to treat continuous variables; of these the **max-product particle belief propagation** [4] consists in using a list of P samples to discretise the continuous domain. An optimisation can be performed iteratively using the max-product algorithm on the particle sample, and then choosing a more refined discretisation based on the results on the previous sample.

In order to fully define the algorithm, one must fix the number of particles to be used for each variable and their initial value. The initial messages $\nu_{j\to a}^{(0)}(x_j)$ of the variable nodes are set to a uniform distribution, although other initial conditions could be used. An update rule to define the new set of particles based on the results is also necessary, as well as a convergence criterion.

This paper presents an application of the factor graph formalism to the simulation of urban energy flow. Modelling the energy flow as a graph, the necessary simulation is formalised as an optimisation problem that can be solved using the max-product particle belief propagation algorithm.

METHODOLOGY

Modelling the disaggregated urban energy flow, from primary energy to energy services in buildings, naturally leads to an oriented graph representation, with *energy nodes* representing any grouping, transformation or distribution of energy, and edges corresponding to energy flows between nodes. In this conceptual graph, a distribution network is a node which collects the production of any number of energy conversion system (ECS) (or other networks) and distributes this energy, minus losses, amongst other nodes. ECS nodes are

similar, while the energy use of a building is represented by several "sink" energy service nodes. We consider distinctly the space heating, electricity and domestic hot water (DHW) services.

The N variables of interest $\mathbf{x} = \{x_1, x_2, ..., x_N\}$ are the quantities of energy passing through each edge in the chosen unit of time (we consider here annual energy flow, although the formalism is strictly identical for any unit of time). The energy nodes of the conceptual graph can be seen as constraints or information about these variables.

Provided enough information about the structure of the disaggregated energy system is available to build this conceptual graph, the available figures regarding the intensity of the energy flow are diverse:

- Energy losses at network and ECS nodes and energy conservation rules.
- Possible monitored energy flow for any edge (usually for billing purpose).
- Simulated values of energy demand per service.
- Estimated provision mode of each building's services (for instance, which fraction of a building's DHW service is provided by each ECS node).

The first two items correspond to hard constraints on the energy flow through the graph. However, the usually low availability of monitored data is insufficient to guarantee a determined problem. Using building simulation software or other methods to estimate the energy demands of building provide a consistent groundwork of data. Still, the system might be underdetermined where several edges provide the same service for instance. If the simulated demand of space heating for a building is known, and the model shows this service is provided both by a boiler and a heat pump, the system will only be determined once it is specified which part of the demand is provided by each ECS, or once a method (and enough data) to determine this information is defined.

Carefully building the model and setting rules about accepted structures can thus lead to a fully determined problem, which actually becomes overdetermined if monitored data is available together with simulated energy demands. Calculating the most coherent picture of the energy flow over the graph thus corresponds to an optimisation problem, satisfying (when possible) all the constraints regarding energy conservation and measurements, while approaching the simulated or estimated values as much as possible where degrees of freedom remain.

Optimisation problem

In order to formally define this optimisation problem, a cost or energy function E_a must be assigned to each node. The cost of a node is minimal when its constraints are satisfied and increases when the variables stray from the expected values. The variables for which measurements are available can either be fixed, or kept as variable to ensure that a solution might be found even in overdetermined cases (such a solution can be treated later and has the advantage to evidence the conflicting variables). The objective of the optimisation problem is then to find the configuration that minimises the total cost function; a robust method which allows the number of variables to become quite large (a few thousand to simulate a few hundred buildings zone) is preferred.

In a statistical physics analogy, the total cost function can be seen as an energy function $E(\mathbf{x})$. Finding the minimum energy configuration is then equivalent to finding the most probable configuration according to a (fixed low temperature) Bolzmann distribution $\mu_\beta(x) \propto \mathrm{e}^{-E(\mathbf{x})}$. This distribution has two properties supporting the use of factor graph:

- $E(\mathbf{x})$ being a sum of partial cost functions, $\Psi(\mathbf{x})$ can easily be factorized, each factor corresponding to a node: $\Psi(\mathbf{x}) \propto e^{-\sum_a E_a(\mathbf{x}_{\partial_a})} = \prod_a \psi_a(\mathbf{x}_{\partial_a})$, with $\psi_a(\mathbf{x}_{\partial_a}) = e^{-E_a(\mathbf{x}_{\partial_a})}$.
- Most factors concern only a small number of variables.

CASE STUDY

The methodology discussed above was applied to a test case representing a seven-storey apartment building. The conceptual model of the energy flow to supply electricity, space heating and domestic hot water in the building is represented in Fig. 1. The ECS are

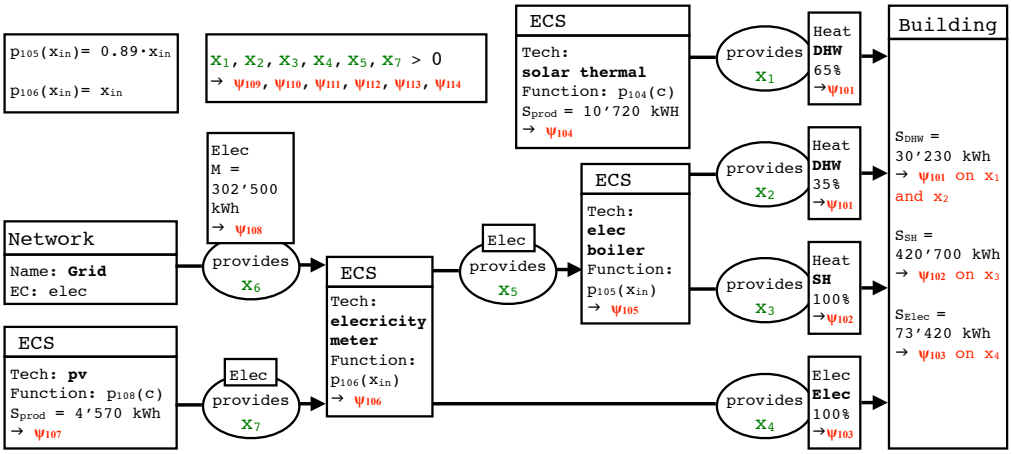

Figure 1: Example of conceptual graph representation of the energy flow concerning the provision of a building's energy services.

modelled through the p_a functions, estimating their energy production x_{out} based either on their consumption x_{in} or on climatic data c. The energy demands have been simulated by external means, as well as the solar panel production; the simulated values are noted S. Finally, the purchased electricity is known (M value). The sign of the energy flow variables x_i is fixed through the orientation of the graph from resources nodes to energy service sink nodes (building).

Each constraint or information is assigned a weight function $E_a(\mathbf{x}_{\partial_a})$ and a probability distribution $\psi_a(\mathbf{x}_{\partial_a}) \propto e^{-E_a(\mathbf{x}_{\partial_a})}$, resulting in the full probability distribution $\Psi(\mathbf{x})$. The corresponding factor graph is shown in Fig. 2, with the same x_i variable nodes and the ψ_a representing the factor nodes. The information available at the energy nodes of the

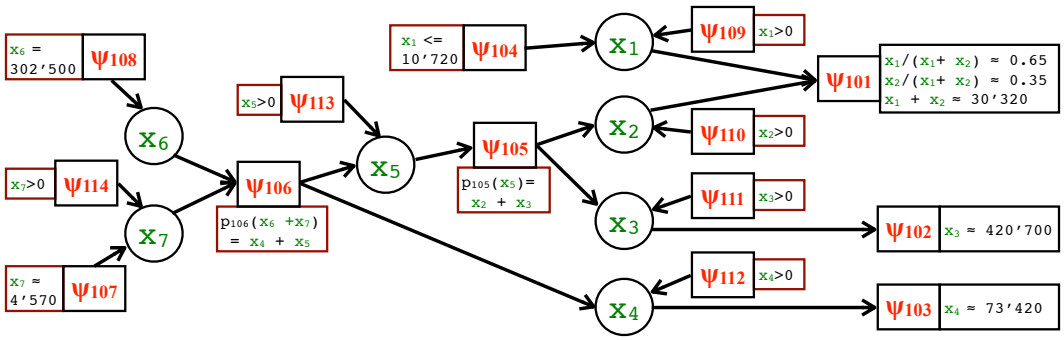

Figure 2: The factor graph corresponding to the test case energy flow.

conceptual model is embodied in the factor nodes ψ_{101} to ψ_{107}. These are completed by measurement data (ψ_{108}) and positive flow constraints (ψ_{109}-ψ_{114}) factor nodes.

The translation of the node properties as cost functions offers a large range of possibilities; the functions must however be chosen carefully in order to convey the intended behaviour. The selected cost functions $E_a(\mathbf{x}_{\partial_a})$ are detailed in Table 1.

Factor node type	Cost (or energy) function	Definitions
Positive flow	$E_{positive,a} = 100 \cdot \max\{0, -\mathbf{x}_{\partial_a}\}$	∂_a contains only one index i
Measurement	$E_{meas,a} = 1000\,\lvert m_{\partial_a} - \mathbf{x}_{\partial_a}\rvert$	∂_a contains only one index i, m_{∂_a} is the measured value of x_{∂_a}
Usual energy conversion systems	$E_{ECS,a}(\mathbf{x}_{\partial_a}) = \left\lvert p_a\left(\sum_{i\in\partial_a}\frac{1+o_{i,a}}{2}x_i\right) - \sum_{i\in\partial_a}\frac{1-o_{i,a}}{2}x_i\right\rvert$	$p_a(x_{in}) = x_{out}$ is the function linking the input and output energy flows of the ECS a, and $o_{i,a} :=$ {1 if orientation $i \to a$, -1 otherwise}
Solar energy production systems	$E_{SEPS,a} = \left\lvert S_a - \sum_{i\in\partial_a} x_i\right\rvert$	S_a is the simulated production of the energy system a
Building's service	$E_{service,a}(\mathbf{x}_{\partial_a}) = 10^{-3}\cdot\max\{T_a, S_a\}\cdot \left[\left(\max\{\frac{T_a}{S_a}, \frac{S_a}{T_a}\} - 1\right) + \left(\sum_{j\in\partial_a}\left(f_j - \frac{x_j}{T_a}\right)^2\right)^2\right]$	S_a is the simulated demand for the service, f_j the fraction of the service the edge (j,a) is expected to provide, and $T_a = \sum_{i\in\partial_a} x_i$

Table 1: Cost functions associated with the different kinds of node. These functions where adapted to avoid unwanted behaviour with zero or (forbidden) negative values.

RESULTS

First tests where performed with a sampling of $P = 3$ or $P = 5$ particles per variable, evenly spread on the domain chosen for this test case to $D_i^{(0)} = \{-100'000, 500'000\}$ for all variables (based on the available simulated and measured values). The parameter $s^{(u)}$ represents the size of the domain $D_i^{(u)}$. Once the belief propagation algorithm has converged, the most probable particle $x_i^{(u)}$ is chosen for each variable based on its max-marginal (given by Eq. 2 summing on *all* neighbouring factor nodes b). To force convergence, the search domain is decreased according to the rule $s^{(u+1)} = k \cdot s^{(u)}$, with k chosen at 0.7 for these tests, and the new particles are evenly distributed on the new domains $D_i^{(u)} = \{x_i^{(u)} - \frac{1}{2}s^{(u+1)}, x_i^{(u)} + \frac{1}{2}s^{(u+1)}\}$. These steps are repeated until $s^{(u)} \leq 0.1$.

The algorithm was found to be stable only if the cost functions are altered to match the granularity of the chosen discretisation, i.e. to ignore any variations in the values smaller than $\frac{s^{(u)}}{P}$: $E^{(u)}(\mathbf{x}) = \min\left\{E(\mathbf{x}') \mid x_i - x_i' \leq \frac{s^{(u)}}{P}\ \forall\, i\right\}$. As the types of cost function are in limited number, this can be performed easily. Using those adapted weight functions, the algorithm converges to the $\mathbf{x}$ values pictured in Fig. 3.

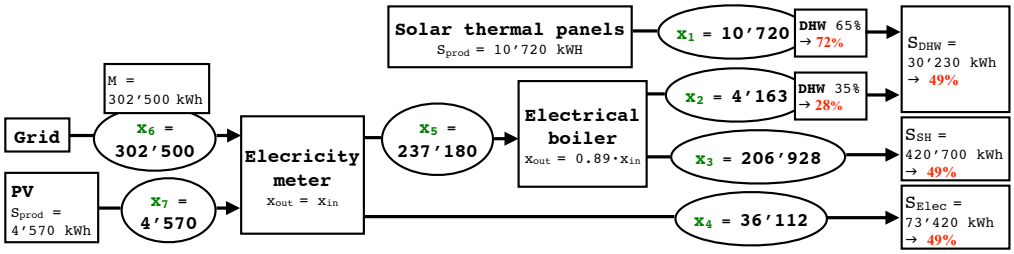

Figure 3: Simulation results: optimal energy flow according to available data.

The solution found fulfills the capital constraints regarding monitored data, energy conservation and simulated energy production. The second point of interest is the repartition

of the energy amongst the services. In this test case, the total supply is known and lower than the total simulated energy demand. As intended, this is reported evenly on all services, which are provided only 49% of the simulated demands. The indications about the production of DHW are intended to be influential only when other constraints are satisfied, and thus do not weight much in this example.

Despite the limited number and rough choice of particles discussed above, the algorithm converges correctly to the values expected given the available data. This is partly due to the deliberately "nice" nature of the energy functions used and their lowered sensibility. The convergence remains stable with small variations of k; smaller k can be used when the number of particle P is increased, however the computational cost increases faster with P than with k.

CONCLUSION

A conceptual model of urban energy flow considered as a graph has been developed. In order to simulate the disaggregated energy flow, the transformation in an optimisation problem through the building up of a factor graph is proposed. Using this formalism, the max-product particle belief propagation algorithm has been successfully applied to simulate the energy flow related to a test-case building. Based on a few other tests, this resolution method is expected to behave correctly in most situations, the main problems originating rather in the number of variables.

Still, in order to refine and possibly accelerate the simulation process, several aspects of the method can be further investigated. The robustness and efficiency of the algorithm in particular could be increase by exploring possible improvements:

- The domain of the variables does not need to be fixed beforehand if the parameter $s^{(u)}$ is not decreased after each iteration, but only once some convergence criterion has been met.
- The optimal combination of the parameters P and k requires more investigation.
- The properties of the cost functions have a dominating role: other possibilities and relative weighting need to be tested.

Nevertheless, the first concluding results encourage studies be carried out at a larger scale and on real cases, in order to assess the robustness and efficiency of the suggested algorithm.

REFERENCES

1. Mezard, M. and Montanari, A.: *Information, physics, and computation*. OUP Oxford, 2009.
2. Loeliger, H.-A.: An introduction to factor graphs. *Signal Processing Magazine, IEEE*, 21(1):28–41, 2004.
3. Loeliger, H.-A.: Some remarks on factor graphs. In *Proc. 3rd International Symposium on Turbo Codes and Related Topics*, pages 1–5. Citeseer, 2003.
4. Ihler, A. and McAllester, D.: Particle belief propagation. In *Proceedings of the Twelfth International Conference on Artificial Intelligence and Statistics (AISTATS)*, 2009.

A SMART APPROACH TO ANALYZE AT URBAN LEVEL BUILDINGS ENERGY DEMAND TO SUPPORT ENERGY SAVING POLICIES. AN ITALIAN CASE STUDY

Stefano Pili[1]; Massimiliano Condotta[2]

1: Dep. of Civil and Environmental Engineering and Architecture (DICAAR), University of Cagliari (IT), Via Santa Croce, 67 - 09124 Cagliari

2: *University Iuav of Venice. Dep. of Design and Planning of Complex Environments. Santa Croce 191 Tolentini. 30135 Venezia. Italy.*

ABSTRACT

Reducing cities energy consumption is a main target of the 20-20-20 communitarian policies, but effective strategies to promote existing buildings stock retrofitting need to be fostered and, on the same time, based on the specificity of the urban context.

The paper shows the preliminary results of an experimentation carried out on an Italian pilot case that has the purpose to define and test combined methodologies for the study, at urban scale, of the energy demand of buildings. The methodology is set on the Italian regulations [1] but can be easily adapted and replicated in any other geographic location.

The paper will describe two different methodologies: the “Energy Web Feltre” best practice, a project carried out in the pilot city of Feltre (Belluno, IT) that tested the use of survey data to analyse urban energy demand, and the "Urban EPC" experimentation that estimates the city energy demand using a bottom-up engineering model, developed on a GIS platform and based on the Italian standards for calculating the energy efficiency of buildings. [2]

In the end the results and the limits of the proposed study will be discussed by a comparison of the two different approaches. The paper ends with a preliminary hypothesis to solve some of the problems emerged during the experimentation using a social tool based on a web interface with the goal of using the knowledge of end users (eco-feedback) to improve the quality and quantity of data in order to improve calculation of buildings energy demand at urban level and to have a continuous update of information related to end-use energy consumption.

Keywords: energy demand, GIS, EPC, energy saving, urban regeneration, 3D city models

INTRODUCTION

The retrofitting process both of single buildings and entire districts is still an undeveloped and untapped solution that could considerably contribute to cut the energy consumption of cities; a process that, in any case, to be effective, needs to be associated with appropriate urban policies and actions that combine the opportunities of the mix of new available technologies with the complexity and particularity of urban systems. [3]

There is therefore the necessity of tools and methodologies able to define, assesses and represent the energy status of cities based on the energy demand of buildings that is the combined result of a number of micro energy utilities. For this reason its representation at urban level raises some problems due to the lack of available base data and to the strong variability of the factors that affect it.

In literature there are many approaches that, according to the purpose of the study, develop more or less detailed methodologies. [4] The recent availability of technologies for detailed urban survey (LiDAR, ground laser scanner, high resolution orthoimages), smart metering

and "*City Sensing*" [5], traces the path for overcoming the chronic lack of geo-referenced data about end users energy consumption, about the physical and facilities buildings characteristics and about the profile of the end-users (citizens).

To study these new opportunities we tested and compared two different methodologies: "Energy Web Feltre" best practice that calculates buildings energy demand on the bases of end users real consumption and behaviors and the "Urban EPC" experimentation that calculates buildings energy demand on the basis of technical standards to estimate buildings energy demand.

THE "ENERGY WEB FELTRE"BEST PRACTICE.

"Energy Web Feltre" is an experimental research project designed and conducted by the NT&ITA research group at University IUAV of Venice and its Spin-off Unisky s.r.l. It creates a shared knowledge system of the city focusing on the relationship between buildings energy consumption and the urban system. On it is built a networking between citizens, public administration and construction companies.

The strategy used is based on the union of two digital data structures. One - the "City Model" - refers to the physical and tangible field, like the morphological structure of the city, the geometric characteristics and the construction materials. The second - the "City Sensing" - includes the flow of social information matched with data about consumption, energy losses and families' behaviours.

We applied these methodologies to the Italian city of Feltre near Belluno. The construction of the *City Model* was made by the integration of high-resolution orthophotos, an airborne laser survey (LiDAR) and a 3D laser scanner survey. The fusion of these three levels of data leads to the creation of a geo-referenced high-resolution 3D model (*City Model).* From this it is possible to extract geometrical parameters that are useful in the verification of energy performance of buildings (e.g. surfaces extensions, volume, roof extension) and to analyse the urban territory by primitive elements like squares, roofs, green spaces and arboreal masses.

To this model we connected the *City Sensing* data structure that includes two different kinds of data: data from a survey work and data already collected in existing databases of public authorities or services companies.

Regarding the first kind of data, we performed a spread infrared thermal survey campaign of the buildings facades and a check of civic numbers of buildings.

Regarding data that comes from existing sources, thanks to the cooperation and the involvement of the City Administration we collected the data of the civil register. In this way we have information about the number of people living in each building, their age and family composition (young couples, elderly families, …). Also from the City Administration comes data about the kind of energy sources used for heating, while from the supply company, we obtain data about gas consumption. These structures of data give back the real energy consumption of the buildings. From the integration of the City Model and the City Sensing we created a new knowledge level, the Energy Model, an interactive data structure about energy consumption of buildings integrated in a collaborative geo-web portal that features also a social network with showcase of all city buildings. This system of notice boards is reserved to families, local construction companies, energy suppliers and city administration departments, and creates a space for networking and partnership between the different stakeholders. This common space, that becomes a sort of collective mind, is therefore inserted in a knowledge system where much information is stored and visualized about the energy status of the city. Information calculated for each building is the height, surface and volume. Elaboration of data

about gas consumption and kind of heating system used gives the possibility to estimate the total energy consumption in KW/year of each building and to express it per cubic meter (Figure 1). In this way it is possible to have a general view at urban level of the energy consumption of different city sectors, but also to have at the same time a clear view of the energy status of every building. The calculations done give a result that technically is quite coinciding with reality as the consumption data are not generated by standard procedure, but from real use of primary energy (gas). At the same time, they can be affected by many particular conditions that can distort the final consideration. For example, some people can use electricity to heat their apartment (and for this reason it is important to get also information about electricity data); some apartments in a building could be empty for some months, or only some rooms of the apartment are used. In any case, also considered these inconsistencies, the data that we get is the real trend of the city. The only carefulness that is necessary is to be aware of this situation and to crosscheck data in order to have a general view. This experience needs therefore other parameters and other levels of information to be compared with in order to validate results. One of these is the application that we have developed and that is described in the next paragraph.

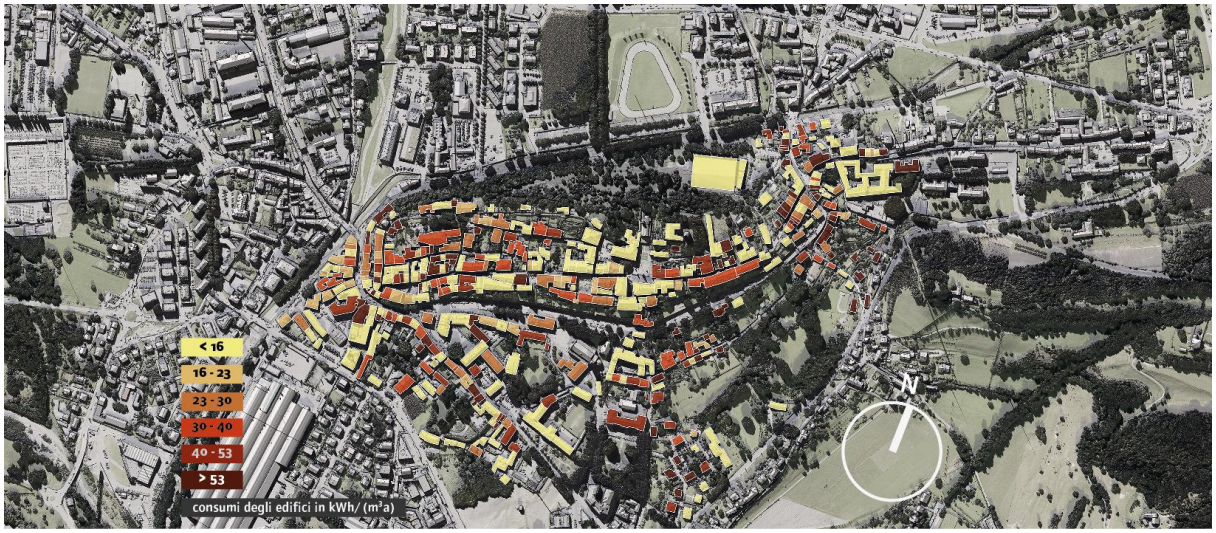

Figure 1: total energy consumption in KW/year per cubic meter of each building.

THE "URBAN EPC" EXPERIMENTATION.

The "Urban EPC" methodology focuses on the Energy Performance Certificate (EPC) calculation done according the "*asset rating"* procedure defined by Italian technical standards for the existing buildings [1,2].

The main outputs of the process are:

- The "Net Energy Need" of the building envelope for winter heating (NE), that means the heat energy required to maintain conditions of thermal comfort depending on the physical characteristics of the materials used and the geometry of the envelope;
- The "Primary Energy need" (PE), that is the energy needed to run mechanical systems and it represents the theoretical energy consumption taking into account the performance of the mechanical systems;
- The "Energy Performance Certificate" (EPC) labeling, an efficiency classification of the envelope-facilities system based on degree-day, the PE need and the ratio between loss surface and heated volume.

In the "Urban EPC" experimentation a GIS calculation procedure has been adopted to calculate these values at urban level starting from the available contextual data. The

procedure, developed using the "model builder" tool in the ArcMAP ESRI environment, defines a hybrid engineering model, based on standard calculation method and focused on residential buildings. The model assumes some simplification hypotheses:

- As suggested by asset rating calculation for multi-level buildings with similar dwelling units, sets the building envelope volume as thermal zone. This is also coherent with the scale of the end use data where, because of privacy protection, units consumption micro data has been aggregated at the building level;
- Adopt an archetypal approach for building physical characteristics according to the date of constructions. This well documented simplification for building stock energy need assessing is also suggested for existing buildings EPC calculation by the Italian standards, where it is not economically viable to provide measurements and materials testing.

Without going deeply into the calculation procedure, the workflow (Figure 2) shows how the data – coming from official open geodata source and from Energy Web Feltre project - have been combined into three different GIS toolsets. The first toolset uses the *City Model* topographical data and some manually input data to calculate the geometric attributes to carry out the asset rating calculation.

The second executes the calculation of "Neat Energy need" (NE), calculating by separately the factors of (1);

The third combines the neat heating need (NE) with the theoretical seasonal efficiency of heating and Domestic Hot Water (DHW) systems to calculate the PE need and the EPC label.

$$Need_h = (Q_{hve} + Q_{ht}) - fx\,(Q_{hint} + Q_{hsol}) \qquad (1)$$

where:

$Need_h$	= Neatheatingneed [kWh]	Q_{hint}	= Internal heat gains [kWh]
Q_{hsol}	= Solar heat gains [kWh]	Q_{hve}	= Ventilation heat loss [kWh]
Q_{ht}	= envelope heat loss [kWh]	f	= dynamic factor

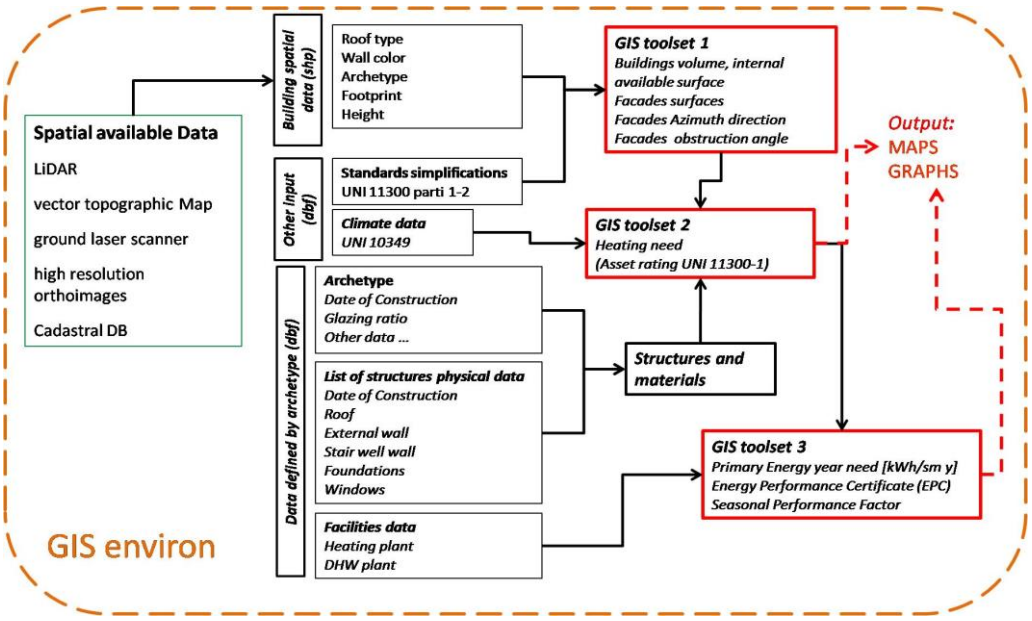

Figure 2: "Urban EPC" methodology logic schema and workflow

RESULTS AND DISCUSSION

Using the GIS procedure, the calculation has been provided for each building of the city center of Feltre. Considering the age of the building stock and the cold climate, common physical characteristics have been adopted: brick wall (0,45 meter wide), wood insulated roof,

windows with common thermal performance. Also building archetypes, identified by a local survey, show just a few types, while differences are mainly on the glazing ratio.

A spatial and statistical comparison has been done between the theoretical data coming from the "Urban EPC" experimentation and end users data coming from "Energy Web Feltre" methodology (Figure 3). As showed in a diagram of Figure 4, there are a lot of differences between theoretical and real consumption: as was predictable, theoretical PE need is higher than real consumption. This is because there are many houses not used or used just for the seasonal period, and because asset rating calculation gives precautionary results with an overestimation of about 20% of the theoretical need calculated by a dynamic algorithm. [6] It is also known that a percentage of the heating need is fulfilled by electrical heating systems, of which we totally lack consumption data. This hypothesis is confirmed by the difference between the number of residential buildings in the area and the number of buildings connected with the natural GAS network (Figure 4).

We also investigated the relationship between the shape parameter S/V ratio and the theoretical and real consumptions. The PE need is correctly strong related with S/V ratio while the solar heat gain that depends on glaze ratio and windows orientation explains a little variance. By contrast the real consumption does not show a strong relationship with geometrical parameters (Figure 4).

CONCLUSIONS

The two tools developed could be used to assess and design scenarios about building envelope refurbishment, mechanical facilities improvement and general retrofitting of the building stock. The proposed methodologies miss the consumption forecasting and monitoring, and end use data must be improved with electricity consumption. In any case, the proposed tools could be used in assessing and monitoring, in a preliminary way, the effectiveness of energy saving for urban policies and programs.

An important improving step, now under development, is to combine these two models with an eco feedback [7] web interface able to compare the theoretical energy needs trend with the dynamic trend of real consumption with the aims to improve users awareness and collect missing data from a voluntary generated information.

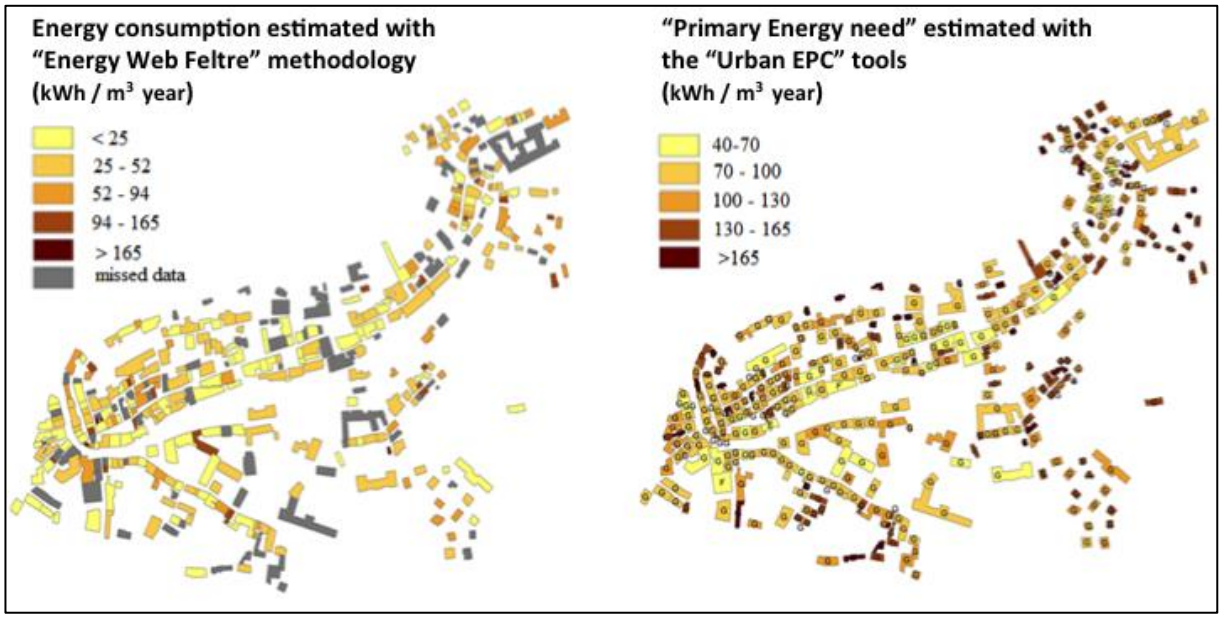

Figure 3: spatial representations of energy demand at urban level.

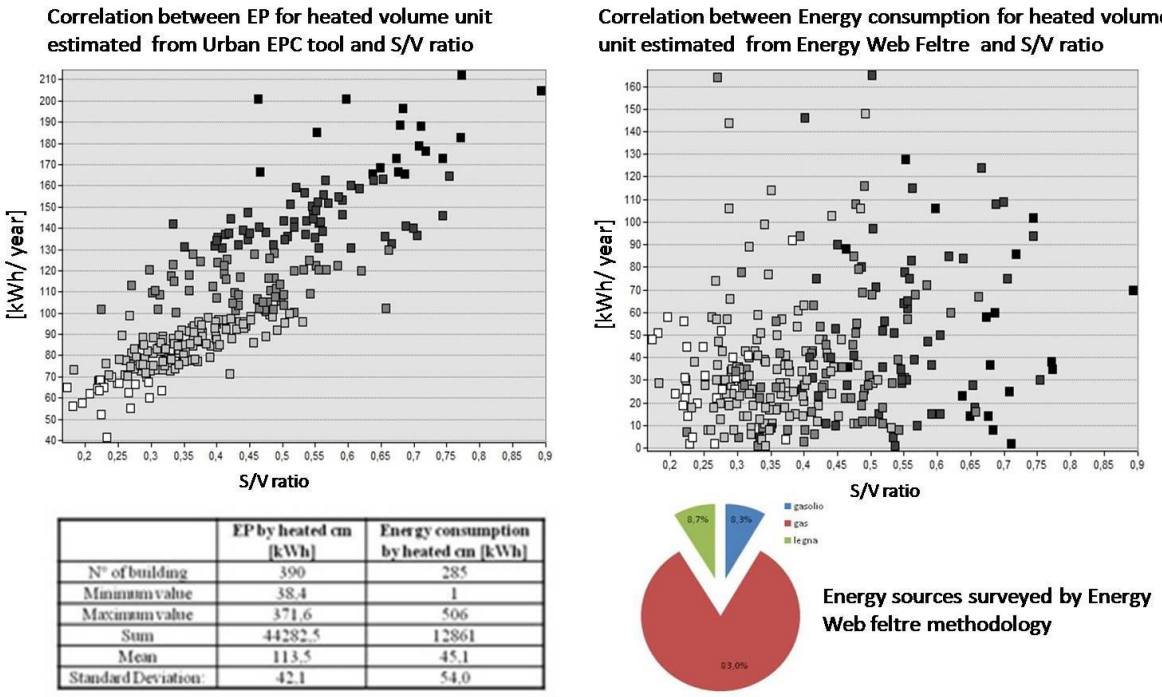

	EP by heated cm [kWh]	Energy consumption by heated cm [kWh]
N° of building	390	285
Minimum value	38,4	1
Maximum value	371,6	506
Sum	44282,5	12861
Mean	113,5	45,1
Standard Deviation:	42,1	54,0

Figure 4: Comparison between theoretical EP need and end-use consumption

REFERENCES

1. Dlgs. 192/ 2005 the Italian law that adopt the Energy Performance Building Directive, (EPBD) 2002/91/CE
2. UNI ISO 11300 parts 1-2, Italian standards based on ISO 13790:2008
3. Droege, P.: The renewable city: A comprehensive guide to an urban revolution. John Wiley & Sons, London, 2007
4. Swan,L.G., UrgursalV.I.: Modelling of end use Energy consumption in the residential sector: A review of modelling techniques. Renewable & Sustainable Energy Reviews, vol 13, 1819-1835,2009
5. Borga, G.: City Sensing. Aracne edizioni. Roma, (in publishing).
6. Baggio P., Cappelletti F., A. Gasparella, P. Romagnoni: *Il calcolo della prestazione energetica degli edifici. Gli esiti di un confronto*, Convegno AICARR: Riduzione dei fabbisogni, recupero di efficienza e fonti rinnovabili per il risparmio energetico nel settore residenziale, Rubano (PD), Giugno 2008
7. Jain, R.K., Taylor, J.E., Peschiera, G.: Assessing eco-feedback interface usage and design to drive energy efficiency in buildings. Energy and Buildings, vol 48, 8-17, 2011

DYNAMIC FINITE ELEMENT ANALYSIS OF THERMAL BEHAVIOR IN URBAN AREAS

Shanshan QU[1], Benoit BECKERS[1]and Catherine KNOPF-LENOIR[2]

1: AVENUES Research Team in Urban Systems Engineering, Compiègne University of Technology, Compiègne, 60200, France

2: ROBERVAL Laboratory in Mechanics, Compiègne University of Technology, Compiègne, 60200, France

ABSTRACT

The goal of this study is to analyze the effects of thermal exchanges (conductive, convective and radiative heat transfers) in some reference situations using finite element method. Usually, in space applications the thermal studies are performed using nodal methods. For instance, ESATAN is the standard European thermal analysis tool used to support the design and verification of space thermal control system. However, today, several finite element programs providers (SAMCEF®, ANSYS®, Siemens PLM Software…) are also proposing solutions in their general commercial offer. This new trend is potentially very advantageous because it allows analysis staffs working always in the same well known finite urban engineering, the two above cited laboratories of UTC are intending to develop a new generation of improved finite element software specialized in urban systems analyses. In this framework, they need to perform preliminary tests and to calibrate their product with standard finite elements software.

The first test of the benchmark corresponds to the case of an urban canyon oriented north – south and located at Equator. In these conditions the computation of solar radiation is drastically simplified and it is very easy to appreciate the influence of the different parameters: environment temperature, material properties and coefficients related to heat transfer. The solar radiation is calculated according to the equation based on the sun's position and the location of the city. The transient thermal simulation is performed in order to obtain the evolution of the temperatures on the facades in one day. The computation is realized with ANSYS®. More sophisticated situations will also be examined in the near future in order to build a set of benchmarks that will allow checking the quality and the performances of the other codes in development in the two UTC teams.

Keywords: Thermal finite element analysis; solar radiation; urban area

1. INTRODUCTION

The scope of this study is to analyze the effects of thermal exchanges (conductive, convective and radiative heat transfers) in some reference urban situations using finite element method.

In building applications, the thermal studies are usually performed with three main methods [1]: CFD (Computational Fluid Dynamics) approach, zonal approach and nodal methods. The application of CFD method is large but not specific to building model. FLUENT [2], COMSOL Multiphysics [3], etc are familiar CFD software. For example, a coupling program with a text-mode interface between building simulation and CFD simulation has been developed for thermal environment of natural ventilation in residential building, by Wang and Wong [4]. The zonal approach has the advantage of detailing the indoor environment and of estimating a zone thermal comfort. Jiru and Haghighat [5] have presented an application of the zonal approach for modeling airflow and temperature in a ventilated double skin facade. The last method is the nodal approach considered as a one-dimensional approach. TRNSYS

[5], ENERGYPLUS [6] etc. are the most popular software using this method in building simulations. For instance, Goyal and Barooah [7] have used a reduced order model to predict the temperature and humidity in multi-zone building.

Today, however, several finite element programs providers are also proposing solutions in their general commercial offer. This new trend is potentially very advantageous because it allows analysis staffs working always in the same well known finite element environment.

Finite element analysis is a numerical tool for determining approximate solutions to a large class of engineering problems [8]. It has large application in industrial engineering, especially for complex industrial problems, because of its diversity and flexibility as an analysis tool. Starting from the fundamentals of the finite element method for heat and fluid flow problems and the knowledge of urban engineering [9], developing a new generation of improved finite element software specialized in urban systems analyses is expected.

In this framework, preliminary tests are needed to be performed and to be calculated with aid of ANSYS Mechanical, simulation software using finite element analysis. It offers a comprehensive product solution for structural linear, nonlinear and dynamics analysis [10]. In addition, it provides powerful thermal analysis. Thereby, the dynamic analysis of thermal behavior in urban area is expected to be accomplished in ANSYS Mechanical.

This study tries to show the thermal behavior of an urban canyon oriented north – south and located at Equator on the 21th March using finite element analysis.

2. METHODOLOGY

2.1 Urban and Building Design Parameters

The street width between two buildings is equal to 12 meters. The street orientation is North-South. The first test corresponds to a single building oriented north – south and located at Equator. The flat roof has an elevation of 15 meters. The width of building is 14 meters and its length is 20 meters. Then a twin buildings model is studied considering the shadow part on the wall.

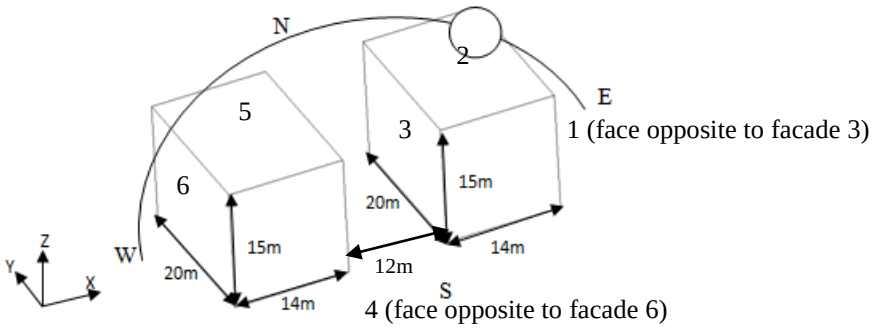

Figure 1: Street and building orientations with sun path

It is assumed that the material of the walls is uniform standard concrete. The density is defined as 2300 kg/m^3. The thermal properties are specific heat of 1000 J/kg*K and the thermal conductivity of 1.28 W/(m*K). The wall thickness is studied in two cases: 0.2 meters and 0.4 meters.

2.2 Finite Element Analysis

A finite element analysis usually consists of three principal steps: pre-processing, analysis and post-processing. In the pre-processing step, the geometry of the building model is created. It is an empty block without bottom surface, shown in Figure 1. Compared to the length of the

building, the wall thickness is small enough to allow a representation with shell element. It is a surface with the definition of thickness in ANSYS. Moreover, using shell element can reduce effectively the computation time compared to the solid element due to less nodes and elements. The type of shell element chosen in the study is a three dimensional thermal element with 4 nodes, having in-plane and through-thickness thermal conduction capability. The mesh for a building model has element size of 0.5 meters*0.5 meters with 5269 nodes and 5200 elements. The solar load on facades is computed every 30 minutes, so a dynamic thermal analysis is has to be performed. The time step varies from 0.5 seconds to 20 seconds. It is assumed that the initial temperature of each node is 15°C.

2.3 Solar Energy

The global irradiance on a surface of a scene consists of direct irradiance (sunbeam), diffuse irradiance (sky) and all the reflections. In this study, only the direct irradiance is calculated in Matlab. Then it is applied as load in building model. The amplitude of direct irradiance is obtained from 8 o'clock to 16 o'clock on the 21th March, representing spring and autumn equinoxes, under fair weather condition.

Direct irradiance is calculated in Matlab only for the roofs, and the facades facing east and west, because there is no thermal load on the facades facing north and south taking the sun path into account. The thermal loads to be applied on each element are then calculated. These values are distributed equally on the 4 nodes of each element. Table 1 shows the amplitude of direct irradiance on each facade. In the single building model, the east facade (facade 1) is exposed to the sunbeam only until noon, and the west facade (facade 3) only after noon. In the twin buildings model, the value of direct irradiance reaching the facades 3 and 4 varies with the time as well as the region where shadow part is taken into account. For instance, the whole facade 3 is exposed to the sunshine between noon and half past two in the afternoon. Then region A, shown in Figure 4, on the surface begins to be in shadow due to the obstacle of the other building. After half past three p.m., region B, shown in Figure 4, enters in shadow as well. The region C, shown in Figure 4, is always in the sun, without shadowing.

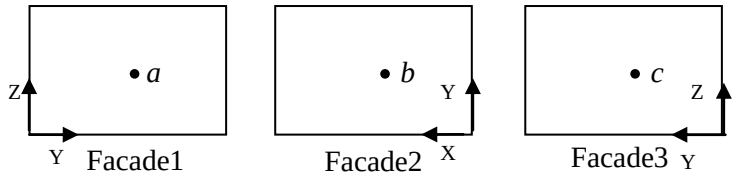

(a) *The single building model*

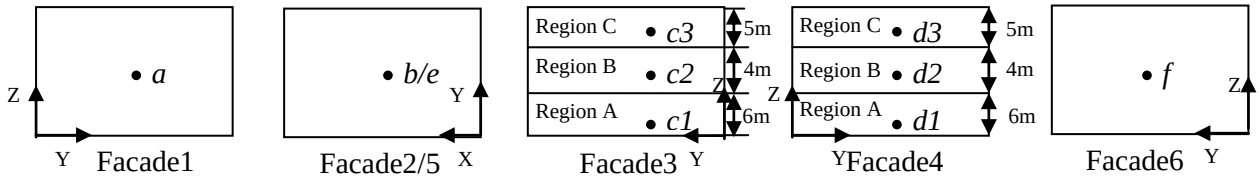

(b) *The twin buildings model*

Figure 4: Positions of nodes extracted from each facade

	Facade		Facade 3				Facade 4				Facade	
	1	2	Single building model	Twin buildings model			Single building model	Twin buildings model			5	6
				Region				Region				
				A	B	C		A	B	C		
8h	550.46	334.59	0	0	0	0	550.47	0	0	550.47	334.59	0
8.5h	603.64	463.19	0	0	0	0	603.64	0	603.64	603.64	463.19	0
9.5h	530.84	691.81	0	0	0	0	530.84	530.84	530.84	530.84	691.81	0
10.5h	355.59	858.46	0	0	0	0	355.59	355.59	355.59	355.59	858.46	0
11.5h	124.52	945.80	0	0	0	0	124.52	124.52	124.52	124.52	945.80	0
12h	0	945.80	0	0	0	0	0	0	0	0	945.80	0
12.5h	0	945.80	124.52	124.52	124.52	124.52	0	0	0	0	945.80	124.52
13.5h	0	858.46	355.59	355.59	355.59	355.59	0	0	0	0	858.46	355.59
14.5h	0	691.81	530.84	530.84	530.84	530.84	0	0	0	0	691.81	530.84
15.5h	0	463.19	603.64	0	603.64	603.64	0	0	0	0	463.19	603.64
16h	0	355.59	550.46	0	301.82	550.46	0	0	0	0	335.59	550.47

Table 1: Amplitude of direct irradiance (W/m²) reaching the facades

2.4 RESULTS

Figure 4 shows the positions of the nodes on each facade. In the single building model, node *a*, node *b* and node *c* are in the centre of each facade. In the twin buildings model, three nodes are positioned on the facade 3 in order to show the influence of the shadow. Node *c*1, node *c*2 and node *c*3 are situated in the centre of region A, region B and region C, respectively. The same happens to the facade 4. For the facade 1, 2, 5 and 6, only one node is located on each facade because of uniform change of temperature.

Figure 5 (figure on the left) shows the temperature of central nodes on the faces 1, 2 and 3 from 8 a.m. to 16 p.m. in the single building model. The sun appears in the east and faces to the facade 1 whose temperature rises up until noon. However, the facade 3 is shaded in the morning. Its temperature has no change. Similarly, in the afternoon, the sun is in the west, facing the facade 3 whose temperature increases after noon. The temperature of external surface of facade 1 decreases in the afternoon without direct irradiance, but the temperature of internal surface of this facade still increases due to conductive heat transfer through the wall. The roof face 3 warms up all the time.

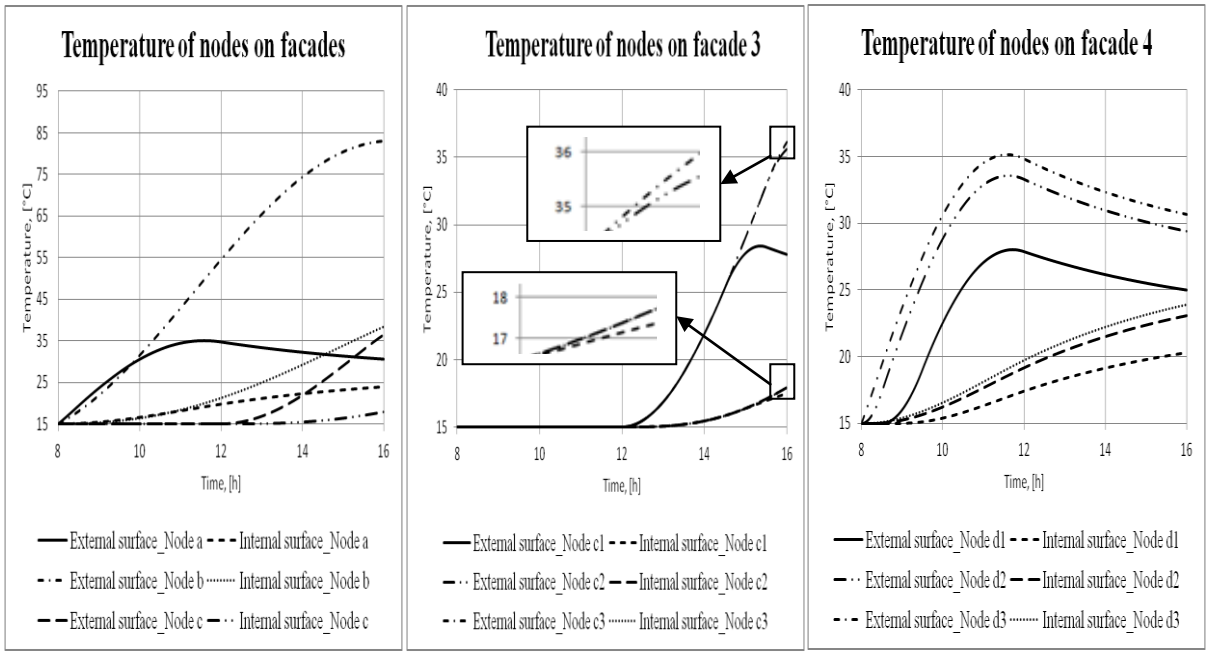

Figure 5: Temperature of central nodes on facades

In the twin buildings model, the temperature of node *a* has the same amplitude as in the single building model. Node *f* has the same temperature as node *c* in the single building model due to the identical value of irradiance. Similarly, the curves of temperature of node *b* and node *e* are the same as that of node *b* in the single building model. The only difference happens to the facade 3 and facade 4, shown in Figure 5 (central figure and figure on the right). For example, the temperature curve of external surface at node *c*1 decreases after half past three p.m. because it enters in shadow. But internal surface at node *c*1 warms up all the time due to conductive heat transfer. Similarly, the temperature curve of external surface of node *d*1 begins to increase until half past eight a.m., because region A is totally in shadow between 8 and half past 8 a.m.

Figure 6 shows the comparison of temperature of nodes on facades for different wall thicknesses of the single building model. The thicker the wall, the slower is the increase of its temperature.

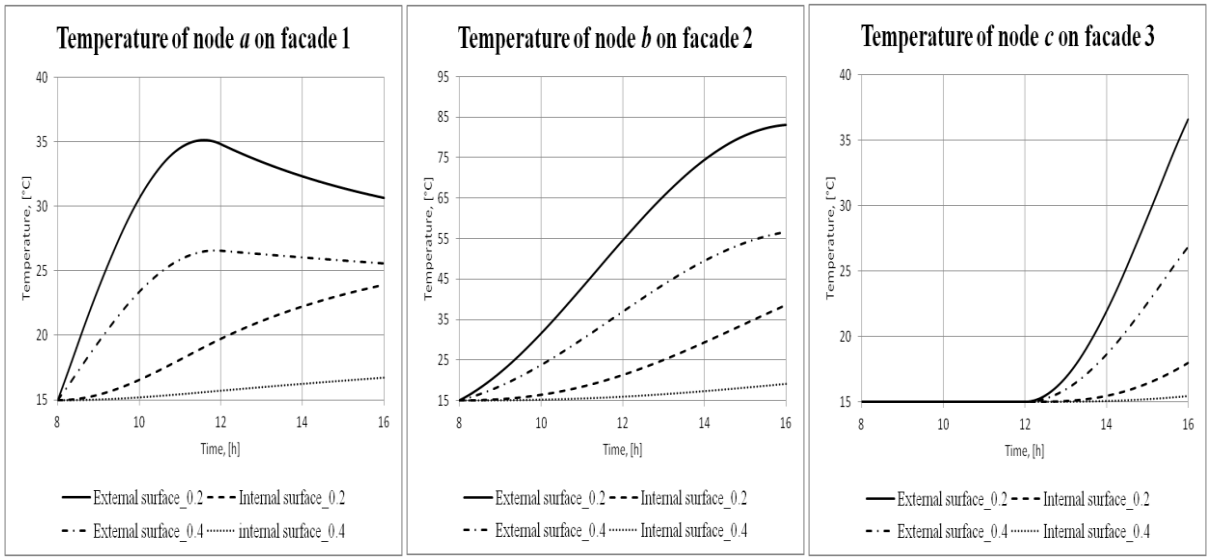

Figure 6: Comparison of temperature for different wall thicknesses

3. CONCLUSIONS AND PERSPECTIVES

The study shows the evolution of the temperature of external and internal surfaces on the facades in one day period taking solar energy and conductive heat transfer through the wall into account.

The temperature curves of walls in the cases of different wall thicknesses are also presented in this study. The results of the twin buildings model show clearly the influence of shadowing on the temperature of surface.

Different sun path, complete climate data and shortwave reflections are expected to be added in further work improve the quality of the results. In addition, further simulation should be accomplished considering convective heat transfer between the ambient air and the external surfaces, which has also important influence on the temperature of external surface of the walls. Radiation as a mode of heat transfer should also be presented. Furthermore, one advantage of the shell element is its ability to simulate non-uniform materials, because different layers can be defined easily in the direction of the thickness.

An urban area is a complex environment. Its thermal behavior is driven by lots of uncertain parameters. This study is a good preparation for the further research in the domains combining urban engineering and finite element method.

4. REFERENCES

[1] Aurélie Foucquier, Sylvain Robert, Frédéric Suard, Louis Stéphan, Arnaud Jay, State of the art in building modelling and energy performances prediction: A review, Renewable and sustainable energy reviews, 2013, 23:272-288.

[2] <http://www.ansys.com/Products/Simulation+Technology/Fluid+Dynamics/Fluid+Dynamics+Products/ANSYS+Fluent>, 2013

[3] < http://www.comsol.com/products/multiphysics/>, 2013

[4] Liping Wang, Nyuk Hien Wong, Coupled simulation for naturally ventilated residential buildings, Automation in construction, 2008, 17:386-398

[5] Teshome Edae Jiru, Fariborz Haghighat, Modeling ventilated double skin façade-a zonal approach, Energy and building, 2008, 40:1567-1576.

[6] <http://www.trnsys.com/>, 2013

[7] <http://apps1.eere.energy.gov/buildings/energyplus/>, 2013

[8] Goyal Siddharth, Barooash Prabir, A method for model-reduction of non-linear thermal dynamics of multi-zone buildings, Energy and buildings, 2012, 47:332-340.

[9] "Fundamentals of the Finite Element Method for Heat and Fluid Flow", Roland W. Lewis, Perumal Nithiarasu, Kankanhally N. Seetharamu, John Wiley & sons, 2004.

[10] "Solar Energy at Urban Scale", Benoit Beckers, John Wiley & sons, 2012.

[11] <http://www.ansys.com/Products/Simulation+Technology/Structural+Mechanics/ANSYS+Mechanical>

IMPACT OF CANYON GEOMETRY UPON URBAN MICROCLIMATE: A CASE-STUDY OF HIGH-DENSITY, WARM-HUMID CLIMATE

Tania Sharmin[1] and Linda Gichuyia[2]

1: Corresponding Author: PhD Candidate, University of Cambridge Department of Architecture, 1-5 Scroope Terrace, Cambridge, CB2 1PX, Tel: 01223 332950

2: PhD Candidate, University of Cambridge, Department of Architecture

ABSTRACT

Recent findings have demonstrated that microclimate inside urban canyons is largely controlled by its geometry. This study, intends to examine the impact of canyon geometry upon air temperature and radiant temperature in a high density warm humid context. For this study, two urban canyons in Dhaka city have been chosen with different street orientations. The microclimatic characteristic was observed through a high resolution CFD microclimatic model: ENVI-met Version 4. Important findings include reduced air temperature but increased Tmrt in deeper canyons while presenting apparently conflicting design options to achieve comfortable urban-microclimate. However, there are potentials to find a variety of canyon geometries that are harmonious with the apparently conflicting design objectives in a tropical city context.

Keywords: canyon geometry, sky view factor, height/width ratio, mean radiant temperature, air temperature

INTRODUCTION

Unbridled urbanisation in Dhaka has led to growth of disorganised and unplanned arrangement of built forms. Lack of effective urban planning has further worsened the situation. It is becoming increasingly difficult to ignore the unfavourable impact of urban pattern on city's micro-climate. Increased air temperature and reduced vegetation in this urban heat island exacerbated by the climate change scenarios, is directly affecting comfort levels in urban outdoor spaces. In this context, urban planning can play a substantial role to modify the microclimate of city's outdoor spaces. According to previous research [1] it is possible to control the urban microclimate through a careful arrangement of urban blocks. The study intends to find how urban geometry can affect the outdoor thermal environment in a high-density warm humid context. Outdoor open spaces in urban areas should be considered in relation to the built-form as they complement each other. Therefore, to create a comfortable urban microclimate, a harmonious balance between the built form and open space is necessary. The study is concerned with the quality of urban spaces adjacent to the buildings. This mainly includes pedestrian streets. These spaces not only affect the social life of the surrounding buildings but also comfortable atmospheric conditions in these areas will directly reduce the energy demand of the buildings. Promoting the idea of designing the city's outdoor spaces in relation to the neighbouring buildings will encourage the concept of city design and urban planning simultaneously with the design of urban spaces. The spaces will assist in vibrant social life in cities as well as accommodating myriads of activities which will in turn lead to a sustainable future of cities.

URBAN GEOMETRY AND CLIMATE

The main difficulty in designing a thermally responsive street is to achieve shelter from excessive solar gain, specially in a tropical context where the sun is very high in the sky most around the year. Shading has been identified as the main strategy to promote comfort

conditions in the warm climates [2]. Givoni [3] has also emphasised on the benefits of lowering solar and long-wave radiation to be the primary strategy to achieve cooler ambience in outdoor spaces. Inside an urban canyon (UC), the surface temperatures of the flanking buildings, the sensible heat flux transferred to air from building surfaces and consecutively the air temperature (Ta) is significantly affected by the presence or absence of direct solar radiation [1,4].

It is important to notice that air temperature inside the UC will vary temporarily but spatial difference is generally insignificant [4].Therefore thermal comfort studies explicitly depending on air temperature are imprecise as ascertained by Jendritzky and Nuber (1981) [cited in 5, p 48] specially in the outdoor context where mean radiant temperature (Tmrt) can be significantly different from air-temperature. Tmrt is identified as the most influencing factor to determine comfort level in outdoor thermal environment [6,7]. In fact, Tmrt is twice as important as Ta in case of tropical climates, whereas in cooler climates the impact of Ta and Tmrt are similar [8]. Therefore, the main strategy to enhance outdoor comfort should first aim to lower the amount of direct, diffused and reflected radiation. Tmrt is the average temperature of surrounding surfaces acting upon a standing person that represents its radiant heat exchange with the environment.In this study, Tmrt is calculated by ENVImet using the following formula [9]:

$$T_{mrt} = \left[\frac{1}{\sigma_B}\left(E_t(z) + \frac{\alpha_k}{\varepsilon_p}\left(D_t(z) + I_t(z)\right)\right)\right]^{0.25}$$

Tmrt calculation includes all radiation fluxes, i.e. direct irradiance It(z), diffuse and diffusely-reflected solar radiation Dt(z) as well as the total long-wave radiation fluxes Et{z} from the atmosphere, ground and walls.

In a high-density urban area with a H/W ratio of 4 or more, the amount of radiation reaching the ground is smaller in comparison to medium density areas (H/W = 1), as it is mainly absorbed high above the ground level [cited in 10]. Therefore, daytime air temperature increases with decreasing H/W ratio and larger view of the sky (SVF, Sky View Factor) [10]. This phenomenon is mainly applicable to mid-latitude cities. In case of equatorial climate the trend is rather reduced due to high solar altitude [11]. Despite the fact that deep canyons are able to cut large amount of direct solar radiation, it may on the other hand assist in entrapping the reflected short and long-wave radiation and reducing wind-driven cooling [12].

STUDY AREA

Dhaka is located at 23.24°N, 90.23°E which falls under tropical Monsoon climate with a distinct warm-humid rainy season, a hot-dry summer and a short cool-dry or winter season. In the outdoor spaces in Dhaka we see a preference for shaded spaces and exposure to air flow. Two different case study areas with different land-use patterns have been chosen for this study located in Baridhara and Sukrabad (Fig.1). Baridhara is a medium-density formal residential area with mostly uniform building heights (6 storied), while Sukrabad is an informal mixed-use residential area with a combination of different building heights and plot sizes.

METHODOLOGY

In this paper, the pedestrian level (1.5 m) thermal environment has been calculated and compared for two case-study areas with the aid of ENVImet Version 4. The climatic parameters include: air (Ta), radiant (Tmrt) and surface (Ts) temperature along with direct, reflected short-wave and long-wave radiation. Unlike the previous version (3.1), the latest

version of ENVImet is able to consider heat capacity of the walls into calculations [13]. As cloud coverage and its temporal variation is complex, a clear sky condition is assumed for all model situations. Air temperature and relative humidity was 'Forced' in the simulation with the data collected from local weather station. The input data for other parameters are shown in the Table. The building material was considered same for all buildings for easy comparison. The simulation was carried out for a typical day during the hot-humid season, in the mid-August when a high range of air temperature is coupled with high relative humidity and creates an uncomfortable environment.

Date of start of simulation	10 Aug 12
Time of start of simulation	7:00 am
Simulation period	18 hours
Wind speed at 10 m height	1.3(m/s)
Wind direction	135
Roughness length	0.01
Initial air temperature	30.15^0C
Specific humidity at 2500 m	14 (g/kg)
Relative humidity at 2 m	71(%)

Table 1: Input data for simulation

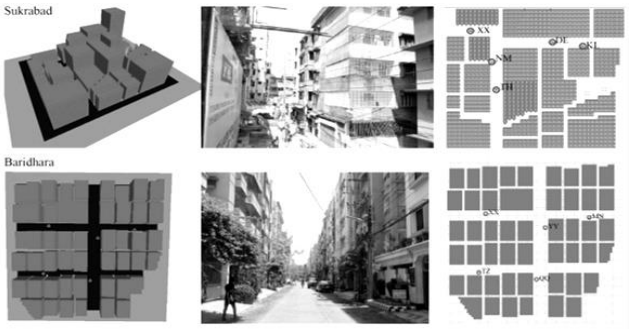

Figure 1:Case-study area and measurement points

RESULTS AND FINDINGS

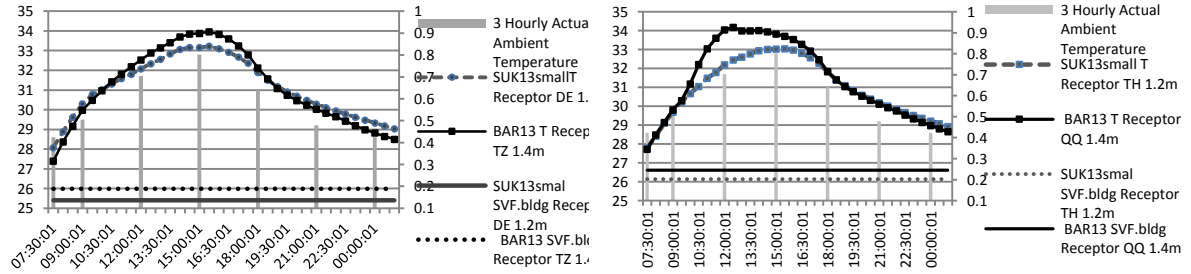

Figure 2: Comparison of Air Temp in Residential in E-W (a) and N-S(b) Street Canyons between Baridhara-DOHS and Sukrabad

Fig.2 (a) and (b) represents the relation between SVF and air temperature in two different sites. Higher temperature is observed in Baridhara DOHS which is a planned residential area in comparison to Sukrabad, an informal residential area. In case of N-S streets the temperature difference between the sites are almost 2^0C, whereas in E-W streets the difference is around 1^0C.

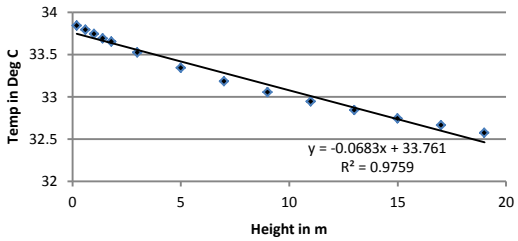

Figure 3: Temperature decreasing with height due to lapse rate

The temperature difference between different sites in Dhaka is not insignificant (2^0C) although the input data (collected from the local weather stations) was same for all simulations at different sites. In actual field the input data may be different due to different building materials, detail ground surface pattern and other complex parameters. Even a smaller reduction in outdoor air temperature has its implications on the building energy performance. For instance,

Wong et al [14] have reported a 5% saving in building energy consumption resulted from 1^0C reduction in outdoor air-temperature. Within the same canyon the temperature may also vary. Fig. 3 shows that air temperature decreases slightly (1.5^0C) with height due to lapse rate between the canyon surface (.2m) and roof (20 m). However, the correlation between air-temperature and SVF is clear from all figures above that air temperature decreases in deeper canyons with lower SVF. Both areas represent higher air-temperature than the ambient temperature.

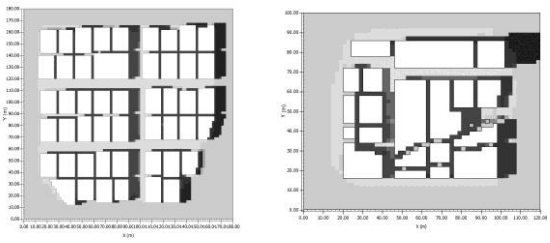

Figure 4: Comparison of MRT in Sukrabad and Baridharain N-S and E-W oriented streets

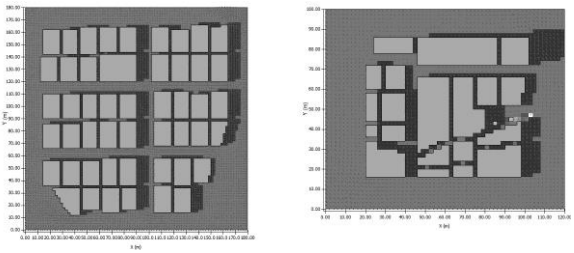

Figure 5: Comparison of Short-wave radiation at 14pm in Sukrabad and Baridharain N-S and E-W oriented streets

Comparing Fig.4 and Fig.5, it is clear that MRT is largely controlled by the amount of direct short-wave radiation and the presence of shade [6]. In Fig.4 , the MRT of sunlit areas in N-S street at 14:00pm (the hottest time of the day) in Baridhara is 35^0C higher than shaded parts.Findings from [7] also indicate similar differences in Colombo.The figure also indicates, N-S streets in Baridhara has lower MRT than E-W streets.The impact of orientation is also visible in Sukrabad area. In both sites, the spaces in between buildings which are constantly under shade are much cooler in comparison to the streets where H/W ratio is lower and SVF is higher. It indicates the importance of shade to lower MRT which ultimately results in better outdoor thermal comfort during daytime. MRT, however, is not governed by the presence of shade only. The ground surface temperature and longwave heat fluxes from building facades cannot escape easily due to restricted SVF. Inside deeper UCs mutual reflection and absorption of radiation tend to increase resulting in a lower albedo. Therefore, deeper canyons have higher day-time pick value of net radiation in comparison to shallower canyons [11,12].

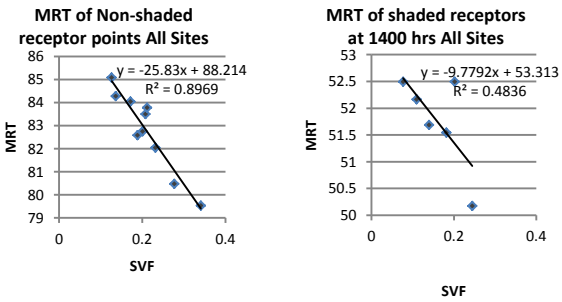

Figure 6: Comparison of SVF and MRT at 14pm in Sukrabad, and Baridharain in N-S and E-W oriented streets

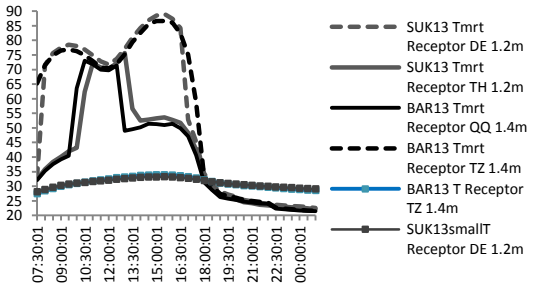

Figure 7: Comparison of MRT in Sukrabad and Baridhara

Fig.6 indicates this strong corelation between SVF and Tmrt. Fig. 7 also shows that the Tmrt for deeper canyons in Sukrabad area in both N-S and E-W orientations is atleast 2^0C higher than shallower canyons in Baridhara. Moreover, shade plays an important role in measuring Tmrt. Therefore, a shaded area although located in a wider canyon can have a lower Tmrt in comparison to a sunlit area in a deeper canyon. Fig.8 suggests that ground surface

temperature is almost 2^0C higher in the deeper canyon in Sukrabad in comparison to Baridhara. The increased surface temperature is mainly causing higher Tmrt (2^0C difference) in the deeper canyons. From Fig. 9 (a), (b) and (c) it is clear that in deeper canyon the amount of reflected short-wave radiation (Qsw.refl), long-wave emission of surface (Qlw.surf) and absorbed long-wave radiation from environment reaching the ground (Qlw.downTotal) is higher. This suggests a day-time urban heat-island effect in deeper canyons.

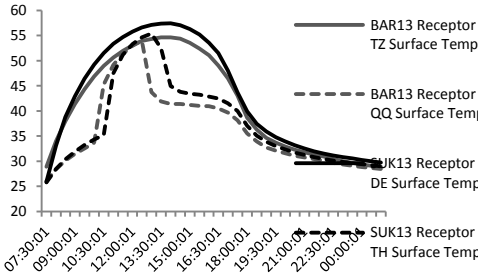

Figure 8: Surface temperature in Sukrabad and Baridhara

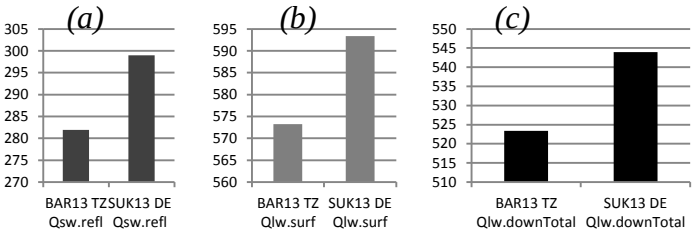

Figure 9: Comparison of Qsw.refl ,Qlw.surf and Qlw.downTotal between deeper (SUK13 DE) and shallower (Bar13 TZ) canyon

CONCLUSION

The important findings from above discussion can be summarised as follows:

- In a deeper canyon air-temperature decreased during daytime due to restricted SVF, (less than 2^0C).
- According to the simulation results, all urban canyons showed higher temperature values in comparison to ambient air-temperature over an 18 hour cycle, which suggests the impact of higher thermal storage and consequently elevated long-wave emission from the building mass in urban areas.
- The presence of direct solar radiation is the main guiding factor behind Tmrt and therefore thermal comfort. The study suggests a difference of 35^0C in Tmrt values between shaded and sun-lit areas. During the hottest time of the day at 15:00 hours, Tmrt is at least 50^0C higher for sun-lit areas and 20^0C higher for shaded areas in comparison to the air-temperature.
- Tmrt is also largely affected by orientation as orientation governs the presence of shade inside urban canyons. North-south canyons in the study areas were found more comfortable in comparison to east-west canyons.
- This result shows higher Tmrt in deeper canyons comparing different measurement points in different canyons with varying SVF values in the presence of shade. Matching correlation has been found from comparing all receptor points in the sun-lit area. This has resulted from the increase of net radiation inside deeper canyons as suggested in previous research [11,12].

It is important to note that impact of shade and the influence of H/W ration have to be dealt with separately to understand the resulting Tmrt. Several studies [2,6] have attempted to associate the reduction of Tmrt with reducing SVF or increasing H/W ratio, while this study suggests that the relation should refer to the presence/absence of shade. Increased H/W ratio can increase the mutual shading inside urban canyons and greater shade can reduce Tmrt when compared with Tmrt of sun-lit areas. It may be possible to achieve greater shade with a higher H/W ratio due to a reduction of direct solar radiation at street level. However, it has to be considered simultaneously that greater depth results in higher reflection of diffused short-wave radiation and trapping of long-wave radiation from the building mass, specially in a

high density context. The present arrangement in Dhaka is already very high-density, specially in terms of high land-coverage in the informal areas. Even, in planned formal residential areas like Baridhara, the FAR value is approximately 3.1 and percentage of land coverage is 61%. In this area the FAR and percentage of land coverage both are very high. Although modern urban planning intends to promote high-density and compact development to achieve sustainability, it does not discuss the consequences or upper limits of high-density. Therefore, any future steps should explore the implications of high density with the provision for increasing SVF which could provide sufficient density without impairing the street thermal comfort. Previous research [15] has shown that it is possible to produce high density and high SVF, as a result of a diverse urban geometry (i.e. variations in building heights and in spacing results in quite high densities and quite high SVFs compared to a traditional, more regular urban form). To conclude, the results and information from the current study can be integrated in the future urban planning processes.

REFERENCES

1. Santamouris,M. *et al* : On the Impact of Urban Climate on the Energy Consumption of Buildings. Solar Energy. 70(3),201-216.[online] Available from: Elsevier Science B.V. www.elsevier.com [Accessed 30 May 2011].2001
2. Emmanuel, R. *et al* : Urban shading – a design option for the tropics? A study in Colombo, Sri Lanka. International Journal of Climatology, 27, 1995–2004. .[online] Available from: Wiley InterScience(www.interscience.wiley.com)[Accessed on 26 June 2011].2007
3. Givoni, B. : Passive Low Energy Cooling of Buildings, Wiley.1994
4. Nakamura, Y. & Oke, T. R.:Wind, temperature and stability conditions in an east-west oriented urban canyon. Atmospheric Environment (1967), 22, 2691-2700.1988
5. Emmanuel, R.:An Urban Approach to Climate-Sensitive Design: Strategies for the Tropics, Spon Press.2005
6. Tan, C. L., Wong, N. H. *et al.:* Outdoor mean radiant temperature estimation in the tropical urban environment. Building and Environment 64(0): 118-129. 2013
7. Johansson,E. and Emmanuel,R. :The influence of urban design on outdoor thermal comfort in the hot, humid city of Colombo, Sri Lanka. International Journal of Biometeorology, 51, 119-133.2006
8. Szokolay, S. V. : Introduction to Architectural Science: The Basis of Sustainable Design, Elsevier Science & Technology Books.2004
9. Bruse M. : The influences of local environmental design on microclimate- development of a prognostic numerical Model ENVI-met for the simulation of Wind, temperature and humidity distribution in urban structures. Ph.D Thesis, University of Bochum, Germany.1999
10. Givoni, B. : Climate Considerations in Building and Urban Design, Wiley.1998
11. Erell, E., Pearlmutter,D. and Williamson, T. :Urban Microclimate: Designing the Spaces Between Buildings: Earthscan.2011
12. Pearlmutter, D., Berliner, P. and Shaviv, E. :Evaluation of urban surfaceenergy fluxes using an open-air scale model. Journal of Applied Meteorology;44:532–45. 2005
13. Huttner,S. and Bruse, M.:*Numerical Modelling of the Urban Climate- a Preview on ENVImet 4.0*,Johannes-Gutenberg-Universität, Mainz, Germany.2009
14. Wong, N.H., Alex, Y.K.T., Tan, P.Y., Wong, N.C.: Energy simulations on vertical greenery systems. Energy and Buildings 41,1401–1408. 2009
15. Cheng, V., Steemers, K., Montavon, M. & Compagnon, R. : Urban Form, Density and Solar Potential. PLEA .2006.

OBSERVATIONS OF THE URBAN HEAT ISLAND EFFECT IN OUTSKIRTS OF VENICE

V. Tatano [1], F. Spinazzè[1], F. Peron [2], M.M. De Maria[2].

1: Department of design, IUAV University of Venice, Santa Croce 191 Tolentini 30135 Venice, Italy.

2: Building Physics Laboratory, 30172 IUAV University of Venice, via Torino 153/A Venice Mestre, Italy.

ABSTRACT

In Italy, as in the rest of Europe, the base of cultivated lands contracts due to the opposite processes of rural abandonment and urbanization. In particular Veneto, the region around Venice, has undergone considerable land use and land cover change in the last decades. This work integrates field observations and numerical simulations to study the urban heat island (UHI) effect in the mainland part of Venice, in order to suggest possible mitigation strategies. The numerical study was performed using ENVI-met, an environment and micro-climatic simulation tool. Different mitigation scenarios are evaluated in a case study area. The focus of the analysis is, in particular, on the use of permeable surfaces vegetative soil or grassed parking instead of conventional asphalt or cement pavement as soil compensation mechanisms for soil loss and on the replacement of traditional roofs with cool or green ones. This study aims to explore the factors that contribute to urban heat island development proposing practical, feasible and specific solutions for mitigating their effects.

Keywords: urban heat island, surface energy balance, diurnal cycle, cool roof, Venice

INTRODUCTION

The world's population living in urban areas is more than 52%, with a much higher fraction (72.9%) in Europe and these percentages are expected to rise in the future [1]. This growth of urban population affects the land use and consequently the urban climate. A recent report presented by the Italian Institute for Environmental Protection (ISPRA) shows that the loss of rural land in Venice area from 1994 through 2006 amount to 24,00 km^2 and puts it in second place in the ranking of the Italian regions with the highest rates of building [2]. Is well known that in a city the atmospheric conditions are quite different compared to the surrounding rural environment. In urban areas, buildings, roads and paved surfaces store heat during the day, causing the surface temperature of urban structures to become 10-40 °C higher than the ambient air temperatures [3]. The surface heating throughout an entire area involves global increase in air temperature. This process known as the `urban heat island effect' is usually ascribed to many physical differences between urban and rural areas: absorption of sunlight and increased heat storage of buildings and streets surfaces, obstruction of re-radiation by buildings, less evapo-transpiration of water from soil for the lack of vegetation, obstacles in air circulation, and other phenomena [4]. The phenomenon can raise air temperature in a city, particularly in the night: on average, urban temperatures may be one to three degrees centigrade warmer, but under appropriate conditions air temperatures can be more than 10°C warmer than surrounding rural environments. Many studies have been conducted in order to mitigate discomforts associated with urban heat islands [e.g. 5,6,7] The climate effects associated with urban heat islands can adversely affect the health of the population. Therefore,

a method of mitigating UHI that is known to be effective is to increase areas of green-space, which lowers ambient temperatures mainly through increased evaporative cooling [8]. Moreover, the albedo of a city may be increased gradually replacing dark materials surfaces with high-albedo surfaces as cool roofs and cool pavements [9,10]. The aim of this study is to examine the urban heat island effect and to evaluate the effects of the mitigation strategies. A set of climate data, collected from a range of weather stations, are analyzed and used to evidence the UHI phenomenon. In a second phase a numerical analysis is performed to evaluate and quantify the possible additional benefits of large-scale use of roofs with both high reflectivity and high thermal emittance (cool roofs) and pavements that combine reflective materials and high water permeability (cool pavements). The microscale climate model ENVI-met v3.1 [11,12,13] was used to simulate a case study in Mestre, the part of Venice on mainland that has undergone a rapid and chaotic urbanization associated with the industrial expansion in mid to late 20th century.

EXPERIMENTAL STUDY OF UHI

With the aim to determine the spatial extent of urban heat island in the town of Mestre, temperature data collected by meteorological station in the area (owned by ARPAV the Regional Agency for Environmental Protection and by the Italian Air Force) were analysed. Mestre (45.49° N, 12.24° E) is the new part of Venice in the mainland with 176000 inhabitants. In the south-east it is limited by the lagoon, while in the north and north-western part the limit is given by a series of suburban centers. For the southern part, the border is given by the Northern Industrial Channel of Porto Marghera.

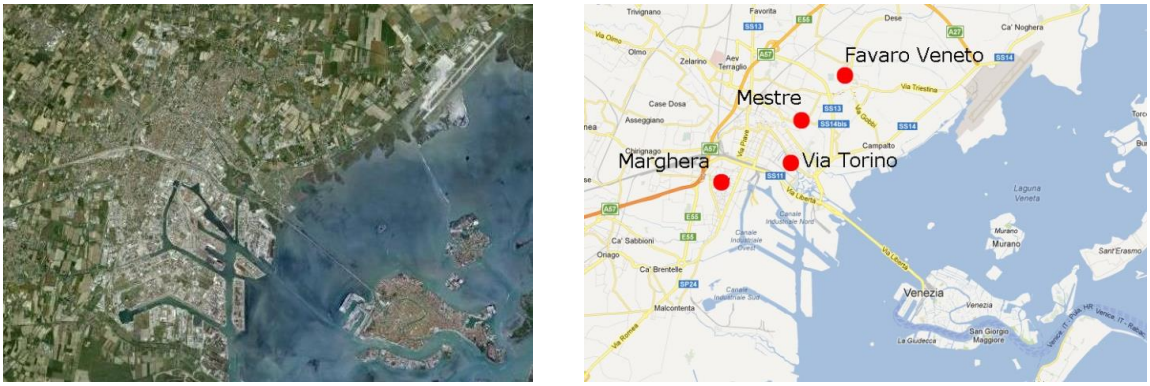

Figure 1. Satellite view of Mestre, Marghera and Venice area (left). Weather stations location map (right).

Figure 2 shows the behavior of air temperature in the area of Mestre over the period July 1st to August 31st 2012 using data from 3 weather stations distributed in the city center (Mestre, Via Torino and Marghera), and from one in a rural area (Favaro, 4 km east of Mestre). The lowest and highest mean daily temperature of 19,3°C and 28,9°C are observed at Favaro and Mestre respectively. Moreover there are two periods of high temperatures (above 26°C) one on late July to early August and ten days in the middle of August, each one followed by a rapid temperature drop of 5°C and 8°C. Observing the plot of the mean daily temperatures it is difficult to see the difference between the various sites. Using the rural Favaro station as reference it was possible to calculate the difference of mean daily temperature ΔT in order to highlight the heat island effect. Results are plotted in Figure 3. The difference ΔT between the rural site and urban sites is highest (2,5°C on August 28th) at Via Torino. Via Torino is in the center of Mestre and the cover of this area is mostly of buildings and thermally-absorbent artificial materials, confirming the "urban heat island effect". The difference is most of the time lower between Favaro and Marghera, a low density residential area.

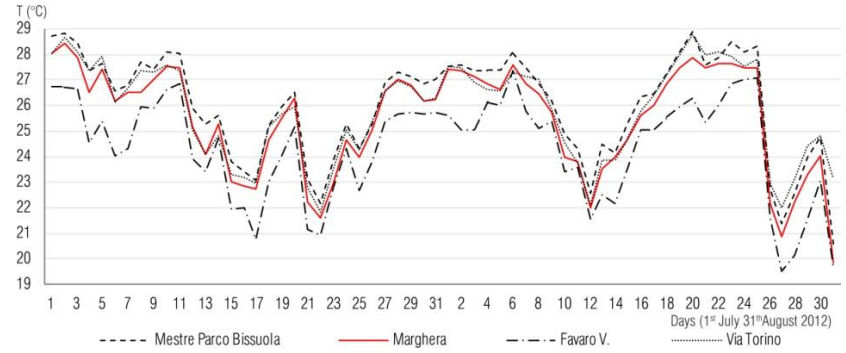

Figure 2 Mean daily temperatures of four weather stations 1st July-31st August 2012

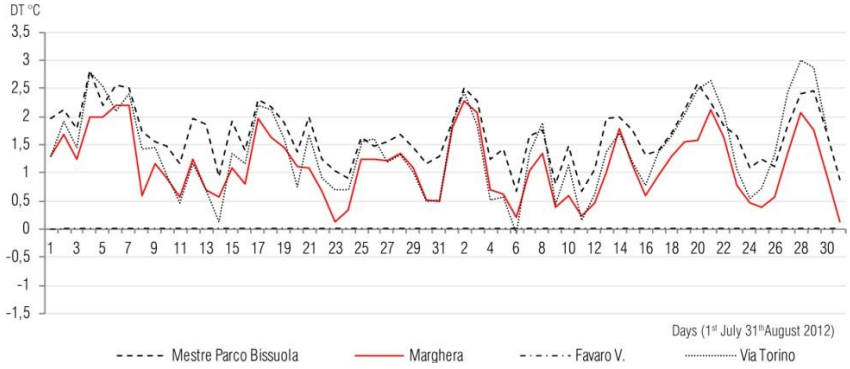

Figure 3. Mean daily temperatures differences ΔT 1stJuly-31thAugust 2012 for 4 weather stations with respect to Favaro station.

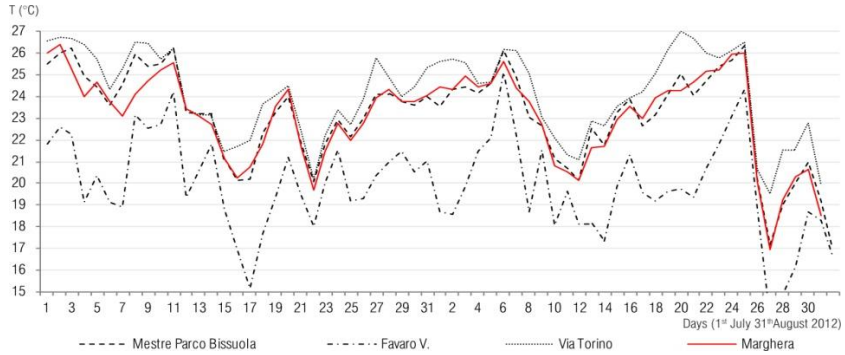

Figure 4. Mean temperatures between 9pm and 3am for four weather stations in the period 1st July-31th August 2012.

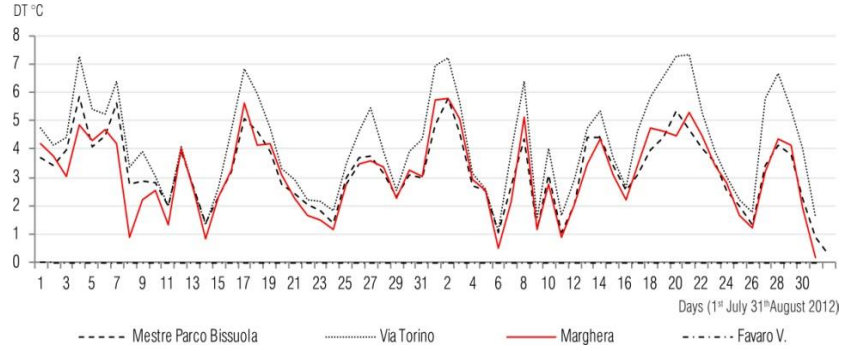

Figure 5. Mean night (9pm-3am) temperatures differences ΔT(°C) 1st July-31st August 2012 for three weather stations with respect to Favaro Veneto station.

As the UHI effect exhibits diurnal variations, most intense at night [4], analysis focused on the data of mean temperature collected at night-time in the range between 9 pm and 3 am (Figure 4). In this case, the temperature difference ΔT(°C) between urban areas in Mestre (Parco Bissuola and Via Torino weather stations) and the surrounding suburban or rural areas of Favaro Veneto, is on average always greater than 4°C, and sometimes reach values greater than 7°C (Figure 5). In particular the highest temperature difference ΔT=7,33 °C is recorded on August 21th in Via Torino weather station. The lowest temperature difference, ΔT about 0,53 °C, is on August 6th in weather station.

NUMERICAL ANALYSIS

Mitigation strategies were implemented as different plan scenarios using the numerical microclimate model ENVI-met. Simulations were run to analyse the effectiveness of the mitigation strategies for different urban surfaces. In the case study a real urban area in the center of Mestre, an unbroken pattern of buildings in a system of repetitive blocks, is used as a base map framework, in order to realise a theoretical optimal form of urban settlements as 'model area' for evaluation of mitigation strategies and produce generalizable results. According to Oke [14], the urban climate zone classification results as intensely developed high density urban in the class 2 of UCZ (Urban Climate Zone), with a fraction of ground covered (building, roads paved and other impervious areas) greater than 85% . The 'model area' defined complies with parameters suggested by Mestayer [15] to describe properties of urban surfaces as the percentage of total plan area. The urban morphology of the area used as model is about 15% permeable soil, impermeable of which 45% are buildings and 40% are streets, parking lots and paved areas.

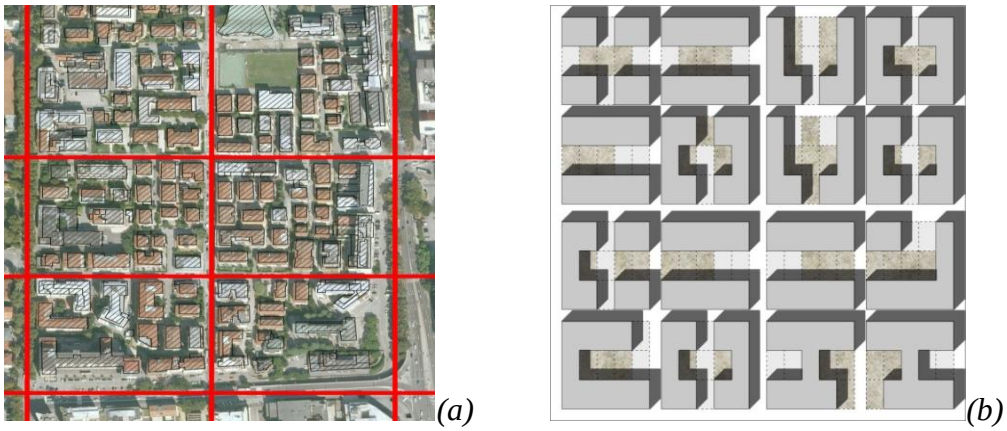

Figure 6. (a) Model area map and overlapped grid (b) model area (real scenario).

To assess the environmental impact of building on land use it has been defined a numerical index called "RIE" (Reducing the Impact Building Code). It varies between zero and ten. A values close to zero correspond to a full impermealized area with little or no green cover. In Italy it is used in building regulations of Bolzano and Bologna, which state that, in urban areas, the RIE index must be great than 4. The case study was analyzed in four different scenarios: real configuration (a); RIE index equal to 4 ('RIE configuration') (b); complete sealing of the soil (c); "cool materials" instead of existing pavements and roofs (d). In the simulation, the numerical model has been calibrated with data obtained from Mestre weather station. The figure 7 shows that the measured (solid line) and simulated average temperatures (dashed line) for 24 hours of August 2nd 2012 are in good agreement. The maximum in the measured temperature plot is lower and in advance than in the simulated one because the weather station is in an area where building density is lower than in the 'real scenario'. As

shown in Figure 7 and Figure 8, in *c* scenario, the temperatures are significantly higher than in the base case, while as both mitigation strategies (b and d) have led instead to a lowering of temperatures, with slightly better results using of permeable surfaces.

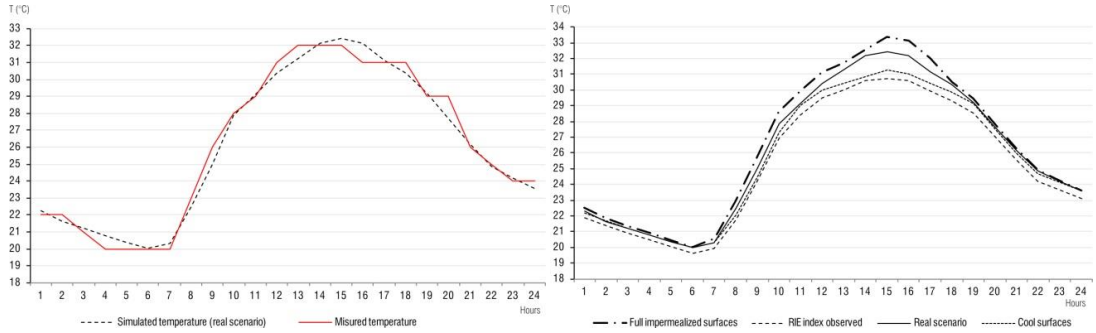

Figure 7. Measured (red line) and simulated hourly temperatures (dashed line) on *August 2 2012(left). Hourly temperatures simulation on August 2 2012 for four cases scenarios (right).*

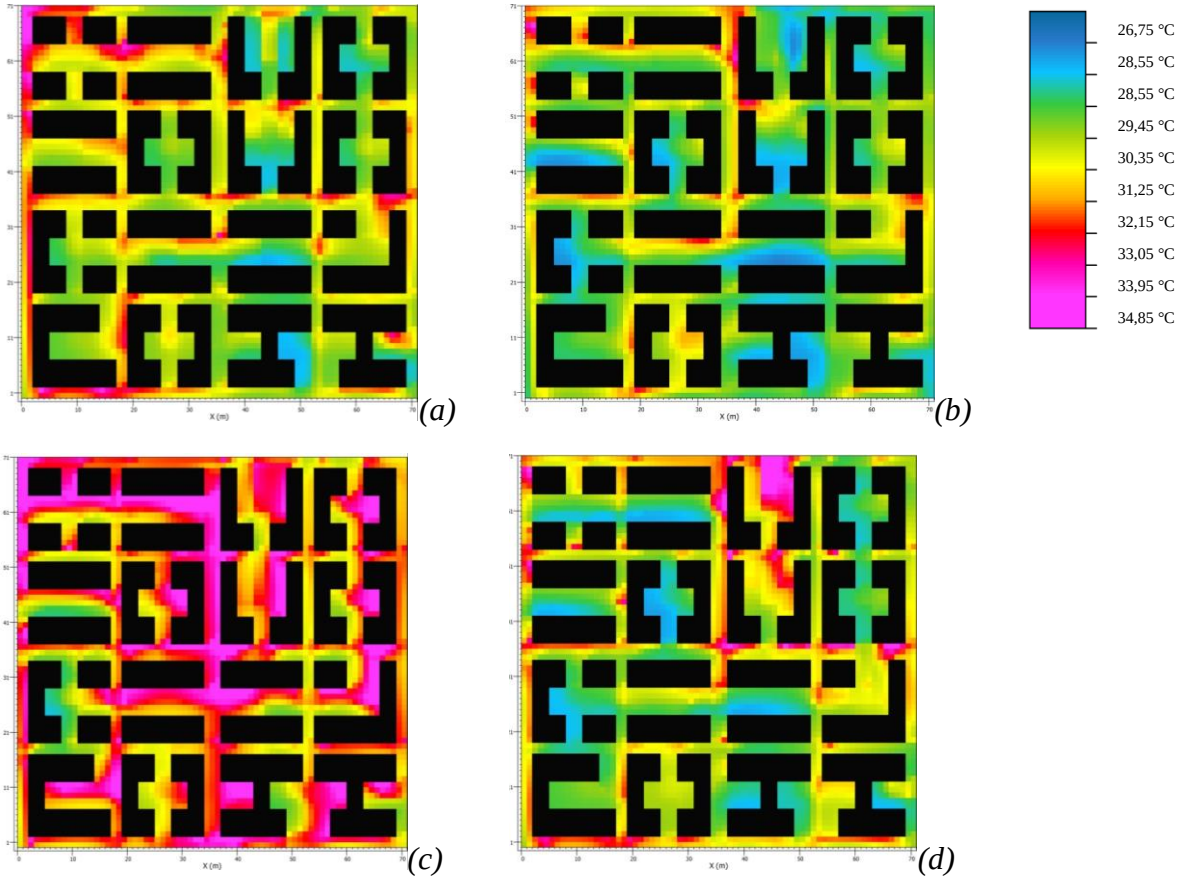

Figure 8. ENVI-met results urban air temperature, horizontal profile at 3m height in August 2nd, 3pm in four scenarios: (a) real, (b) RIE, (c) impervious surfaces, (d) cool surfaces.

CONCLUSIONS

Using data from weather stations distributed in city center and rural area nearby it has been possible to evidence the UHI phenomenon in the area of Mestre. In the night-time during the summer, the temperature difference between urban areas with high density building and the surrounding suburban areas is on average always greater than 4°C, and sometimes reach values greater than 7°C. A micro-scale climate model tuned with local environmental

conditions permitted to simulate as a case study a portion of Mestre area. The case study was analyzed in different scenarios and the use of "cool materials" and green permeable surfaces instead of existing pavements and roofs led to a lowering of the temperature around 4°C.

ACKNOWLEDGEMENTS

Authors gratefully acknowledge Centro Meteorologico ARPAV of Teolo, Venice Department of ARPAV and Servizio Meteorologico dell'Aeronautica Militare

REFERENCES

1. Population Division of the Department of Economic and Social Affairs of the United Nations Secretariat: World Population Prospects: 2009 Revision.
2. ISPRA http://www.isprambiente.gov.it/files/eventi/2013/convegno-consumo-del-suolo-2013/Foccardi.pdf (accessed on 13 February 2013).
3. Taha, H., Sailor D., and Akbari H.: High-albedo Materials for Reducing Building Cooling Energy Use, Lawrence Berkeley National Laboratory Report No. 31721, 1992
4. Oke T.: The energetic basis of the urban heat island., Quarterly Journal of the Royal Meteorological Society, 108, 455 (1982) 1.
5. Taha H., Chang C., and Akbari H.,: Meteorological and air quality impacts of heat island mitigation measures in three U.S. cities. LBL-44222, 2000.
6. Dandou A., Santamouris M., Tombrou M., Soulakellis N., Synnefa A., On the Use of Cool Materials as a Heat Island Mitigation Strategy, Journal of Applied Meteorology and Climatology Volume 47, Issue 11, pp. 2846-2856, 2008
7. Takebayashi H., Moriyama M.: Study on Surface Heat Budget of Various Pavements for Urban Heat Island Mitigation, Adv. Mat. Sci. Eng., Hindawi Pub. Corp., 2012.
8. Rosenfeld A. H., Akbari H., Bretz S., Fishman B. L,. Kurn D. M, Sailor D., Taha H., Mitigation of urban heat islands: materials, utility programs, updates, Energy and Buildings, Volume 22, Issue 3, pp 255-265, 1995.
9. Prokop G., Jobstmann H. and Schonbauer A., Overview of best practices for limiting soil sealing or mitigating its effects in EU- 27" , Environment Agency Austria, Final report on behalf of the Environment Directorate-General of the European Commission, 2011
10. Bowler D. E., Buyung-Ali L., Knight T. M., Pullin A. S., Urban greening to cool towns and cities: A systematic review of the empirical evidence, Landscape and Urban Planning, Volume 97, Issue 3, pp 147-155, 2010.
11. ENVI-met Homepage. Available online: http://www.envi-met.com.
12. Huttner, S., Bruse, M., Using ENVI-met to simulate the impact of global warming on the microclimate in central European cities, Met. Inst. Univ Freiburg,18, pp 307-312. 2008
13. Bruse, M. : Modelling and Strategies for improved urban climates. Invited Paper. In: Proceedings International Conference on Urban Climatology & International Congress of Biometeorology, Sydney, 8–12. Nov, 1999.
14. Oke TR.: Siting and exposure of meteorological instruments at urban sites. Proc. of the 27th NATO/CCMS international technical meeting on air pollution modelling and application, Kluwer, Banff, Canada, 2004.
15. Mestayer P., Joffre S., Baklanov A.: Parameterisation of the nocturnal UBL for NWP and UAQ models, D4.6 FUMAPEX Report. Danish Met. Ins., Copenhagen, Denmark, 2004.

Information Technologies and Software

LIGHTSOLVE - A FULL-YEAR GOAL-BASED TOOL FOR DAYLIGHTING PERFORMANCE EVALUATION

Marilyne Andersen[1]; Antoine Guillemin[1]; Lorenzo Cantelli[1]

1: Interdisciplinary Laboratory of Performance-Integrated Design (LIPID), School of Architecture, Civil and Environmental Engineering (ENAC), Ecole Polytechnique Fédérale de Lausanne (EPFL) – EPFL-IA-LIPID, BP 2229, Station 16, 1015 Lausanne, Switzerland

ABSTRACT

Lightsolve is an innovative tool that offers architects and lighting engineers a goal-based simulation platform for daylighting performance evaluation in early stages of building design. Users can import their own 3D model and define their own design goals for a comprehensive spectrum of daylighting performance perspectives regarding task illumination, visual comfort, overheating risks, health effects and visual interest of a space. The tool provides key information to the designer that is easy and intuitive to grasp thanks to a combination of unique, visual and interactive graphical display formats. Available visualization options include photo-realistic renderings, full-year temporal performance representation as color maps, and spatial performance distribution through false-color renderings. Both model orientation and localization can be user-defined, and weather data (e.g. TMY) can be used to get climate-specific results. Accuracy is ensured by the usage of the ubiquitous and extensively validated Radiance simulation tool.

INTRODUCTION

Designing spaces that are able to balance the many aspects of daylighting performance (workplane illuminance, visual comfort, overheating risks, visual interest, etc) over a whole year is a real challenge, yet a problem faced every day by building designers. A simulation framework for climate-based daylighting design support has been developed over the past few years, named Lightsolve, meant to address guidance at the early stages of the design process [1-3]. The adopted approach for this framework is to express performance from the perspective of user-defined goals fulfillment and with a strong emphasis on temporal dynamics and on displaying performance visually [2].

LIGHTSOLVE FOR DAYLIGHTING PERFORMANCE EVALUATION

The various research efforts have now been gathered into a new software platform for interactive, comprehensive daylighting analysis, available to architects and lighting designers and compatible with most 3D modeling softwares. The new embodiment for Lightsolve includes a Radiance calculation engine combined with an interactive user interface to visualize temporal and spatial 'distribution' of performance simultaneously. Annual performance is analyzed statistically over user-defined time intervals [4] (rather than time-steps directly derived from a TMY weather file) and is based on the validated ASRC-CIE sky model [5].

Daylighting performance is assessed from various perspectives based on metrics previously developed or under development and adapted for that purpose: Acceptable Illuminance Extent [2] for task (typically workplane) or surface (e.g. wall) illuminance, Daylight Glare Probability [6] for visual comfort – possibly extended to whole perimeters of interest [2], Solar Gains Surplus or Scarcity [2] for overheating risks and seasonal gains management, non-visual lighting effects [7,8] for health impacts (direct effects such as alertness and/or

circadian effects such as phase-shifting e.g. [9]), and perceptual daylight effects regarding contrast or variability [8,10].

These different types of performance metrics can be simultaneously visualized over time and over space on the Lightsolve interface, both in absolute terms using a linear color scale, and from a goal-based perspective using a triangular color scale [2].

LIGHTSOLVE OUTPUTS – ANALYSIS EXAMPLE

The Lightsolve interface and visualization framework (see Fig. 1) offers a very powerful support to reveal multi-faceted performance thanks to its time-based focus combined with a simultaneous visualization of renderings.

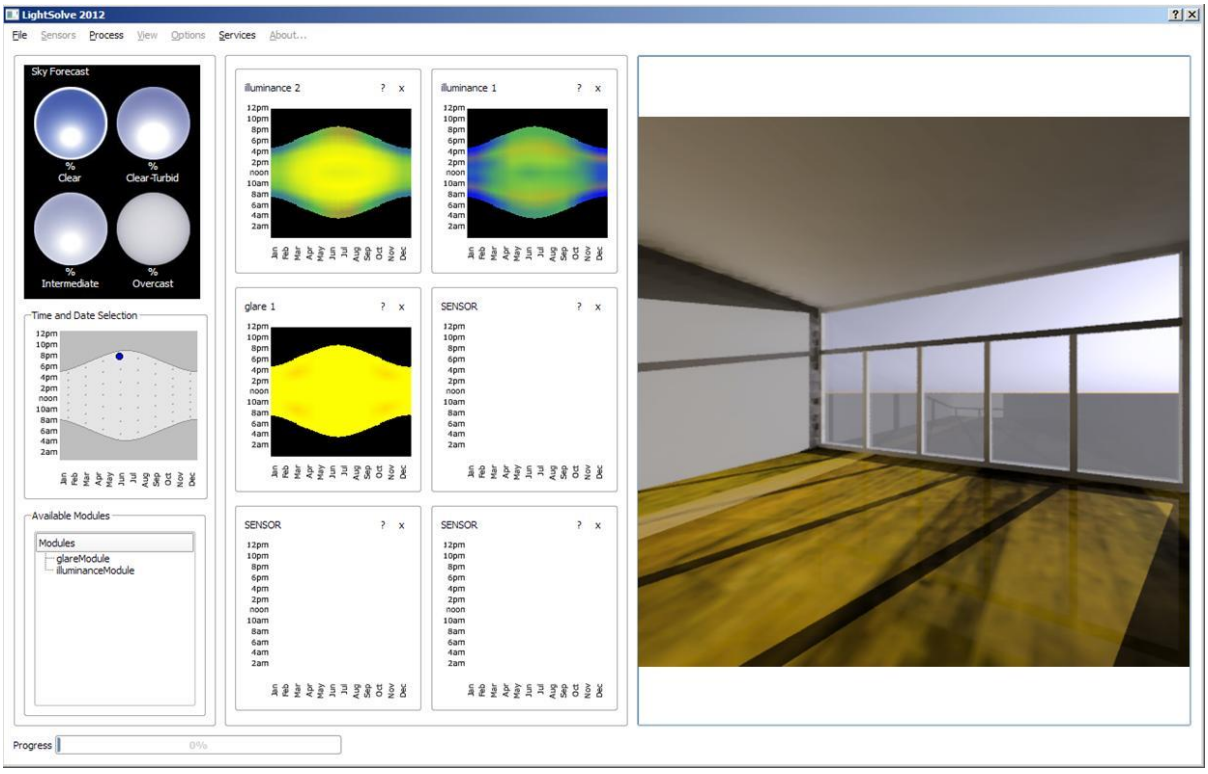

Figure 1: Lightsolve interface with a 3D model of a West-facing room, located at 41 degrees North (latitude). A real-time rendering is shown on the right.

As soon as a 3D model is uploaded in Lightsolve, the user can define his/her own design goals for each of the performance perspectives (metrics) of interest to the project. Then, the processing of the full-year analysis can be launched. It takes less than 1 minute to get results for all metrics. In Fig. 2 such results and their visualizations are depicted for a 3D model of a simple West-facing room.

There are two ways to visualize performance. Either using an absolute scale (most straightforward approach), where the respective metric's average value is displayed over a user-defined perimeter of interest, such as workplane illuminance [lux] in the example shown in Fig. 2a. Or using a goal-based scale, like in Fig. 2b, where what is represented is how closely prescribed goals are met. For both scales, two representations appear side-by-side on the Lightsolve interface to fully reveal annual, seasonal and daily performance over both time and space: a time-varied representation in the form of a temporal map (left) over which a cursor (cross in Fig. 2 left) can be moved to select a given moment over the year; and a rendering (right) associated to that specific moment, where the spatial distribution of the respective metric's values can be visualized in false-color on the user-defined sensors (areas

of interest). The type of sky (clear, clear-turbid, intermediate or overcast, see [4]) can be selected for visualization, while weather conditions are accounted for according to the selected weather data file.

The resulting "double combination" of absolute vs. goal-based and time-based vs. spatial visualization, further discussed in [8], makes the performance analysis particularly interactive and intuitive to the user.

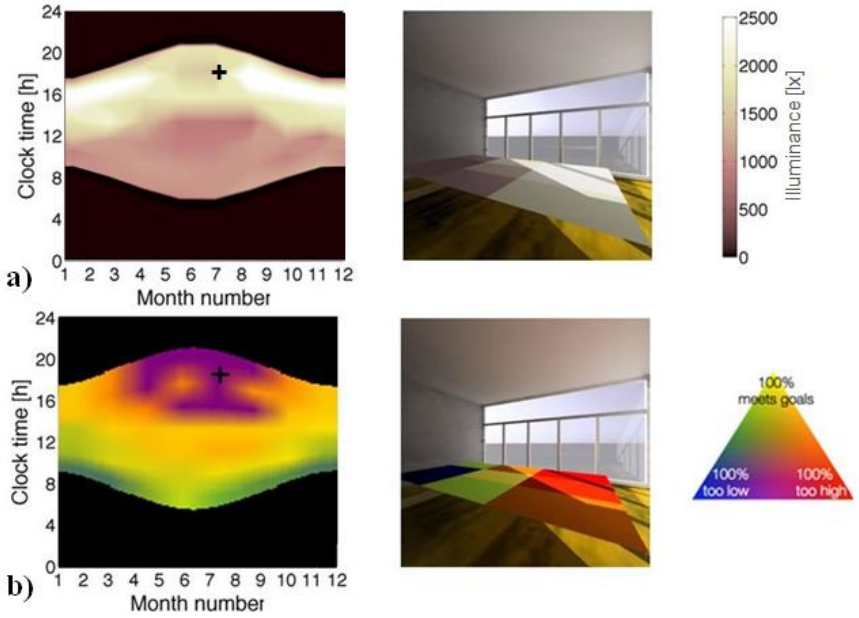

Figure 2: Time-based illuminance analysis (left) with associated rendering at given moment (right and cursor) on an absolute (a) and goal-based scale (b). Performances are evaluated on the visible sensor plane defined by the user (area of interest).

CONCLUSION

Lightsolve offers a set of innovative simulation resources that makes it a unique design support tool for comprehensive yet reactive and intuitive daylighting performance analysis. Such a tool could enable a desirable shift in schematic stage design practice and offer a more holistic approach to daylighting analysis by embedding its many aspects into a unique, interactive simulation framework.

REFERENCES

1. M. Andersen, S. Kleindienst, L. Yi, J. Lee, M. Bodart, B. Cutler, An intuitive daylighting performance analysis and optimization approach, Building Research and Information, vol. 36 (6), pp. 593–607, 2008
2. S. Kleindienst, M. Andersen, Comprehensive Annual Daylight Design through a Goal-Based Approach, Building Research & Information, vol. 40 (2), pp. 154-173, 2012
3. J.M.L. Gagne, M. Andersen, L.K. Norford, An Interactive Expert System for Daylighting Design Exploration, Building and Environment, vol. 46 (11), pp. 2351-2364, 2011
4. S. Kleindienst. M. Bodart, M. Andersen, Graphical Representation of Climate-Based Daylight Performance to Support Architectural Design, LEUKOS, vol 5 (1), pp. 39-61, July 2008

5. R. Perez, J. Michalsky, R. Seals, Modeling Sky Luminance Angular distribution for real sky conditions; experimental evaluation of existing algorithms. J. Illum. Eng. Soc. 21(2):84–92, 1992
6. J. Wienold, J. Christoffersen, Evaluation methods and development of a new glare prediction model for daylight environments with the use of CCD cameras. Energy and Buildings, 38, 743–757, 2006
7. M. Amundadottir, M. Andersen, S.W. Lockley, Simulation-based evaluation of non-visual responses to daylight: proof-of-concept study of healthcare re-design, In Proceedings IBPSA 2013, Chambéry, France, Aug 26-30, 2013
8. M. Andersen, A. Guillemin, M.L. Amundadottir, S. Rockcastle, Beyond illumination: An interactive simulation framework for non-visual and perceptual aspects of daylighting performance, In Proceedings IBPSA 2013, Chambéry, France, Aug 26-30, 2013
9. M.L. Amundadottir, M.A. St Hilaire, S.W. Lockley, M. Andersen, Modeling non-visual responses to light: unifying spectral sensitivity and temporal characteristics in a single model structure, In Proceedings CIE Midterm conference - Towards a new century of Light, Paris, France, Apr 15-16, 2013
10. S. Rockcastle, M. Andersen, Dynamic Annual Metrics for Contrast in Daylit Architecture, In Proceedings of SimAUD 2012 - Symposium on Simulation for Architecture and Urban Design, Orlando FL, March 26-30, 2012

SOFTWARE

LIGHTSOLVE A full-year goal-based tool for daylighting performance evaluation		***Available languages*** ☐ **Français** ☒ **English** ☐ **Deutsch** ☐ **…….** ☐ **Italiano** ☐ **……**
Editor **LIPID / EPFL** CH-1015 Lausanne	***Distributor*** **LIPID / EPFL** CH-1015 Lausanne	***Price*** 400€ (Free for academic use)

Description

Lightsolve offers architects and lighting engineers a goal-based simulation platform for daylighting performance evaluation in early stages of building design. It is seemlessly integrated into the design process through 3D modelling compatibility and targeted inputs focusing on design objectives. Key information regarding a large spectrum of daylight performance perspectives is provided to the user derived from his/her own goals, based on visual, interactive and intuitive graphical displays.

Key features of this first publicly available version are:

• A full-year analysis of all daylighting performances achieved in less than 1 minute (56 year moments)

• Performance analysis currently available:
Acceptable Illuminance Extent for task or surface illumination
Daylight Glare Probability for visual comfort
Solar Gains Surplus or Scarcity for overheating risks and seasonal gains management
Non-visual lighting effects for health impacts (alerting and phase-shifting effects e.g.)
Perceptual daylight effects regarding contrast or variability

• Results accuracy ensured by the usage of the lighting simulation tool RADIANCE

• Visualization over time and/or over space, either in absolute terms using a linear color scale, or from a goal-based perspective using a triangular color scale.

• Extremely fast photo-realistic renderings (few seconds) for better daylighting evaluation understanding

• Exact model orientation and localization, with TMY Weather data compatibility

• Robust import of own user pre-design 3D model using a standard format (OBJ)

• User-defined urban surroundings taken into account

Technical Data

Operating System ☒ **WINDOWS [**XP, Vista, 7**]** ☒ **MAC [**OS X 10.6+**]** ☐ **LINUX** ☐ **Others ……**	***Processor*** **x86 / x64 – NVidia GTX 5xx** ***Required memory*** **2GB of RAM** ***Required disk space*** **500 MB**

A COMPREHENSIVE INSTRUMENT TO ASSESS THE COST-EFFECTIVENESS OF STRATEGIES TO INCREASE ENERGY EFFICIENCY AND MITIGATE GREENHOUSE GAS EMISSIONS IN BUILDINGS

M. Jakob[1]; R. Bolliger[2]; S. von Grünigen[2]; S. Kallio[1]; W. Ott[2]; C. Nägeli[1]

1: TEP Energy GmbH, Rotbuchstrasse 68, CH-8037 Zürich, Switzerland

2: econcept AG, Gerechtigkeitsgasse 20, CH-8002 Zürich, Switzerland

ABSTRACT

The building sector is responsible for both direct and indirect energy consumption and related local and global environmental impacts. Apart from building envelope retrofit measures as such, a wide variety of options is available for building owners and policy makers to mitigate these impacts.

A comprehensive calculation tool was developed to assess trade-offs and synergies between different types of measures and to identify strategies aiming at reducing cost-effectively primary energy use and greenhouse gas emissions. The tool includes a database of empirical techno-economic characteristics of several types of measures. Measures are categorized in seven categories: (i) building envelope insulation, (ii) heating systems, (iii) ventilation system with heat recovery, (iv) electricity based services (lighting, cooling, and appliances), (v) energy supply mix, (vi) building automation control and regulation, and (vii) onsite energy production. Up to ten renovation packages of measures and related reference cases may be represented in terms of economic and environmental indicators: investment costs and life-cycle costs, total and non-renewable primary energy consumption, and greenhouse gas emissions. Using up-to-date empirical cost and price data the economic effectiveness and economic viability of advanced retrofit measures and up-stream options is assessed from a life-cycle-cost point of view. With the tool the impact of factors such as starting situation, scope and costs of measures, interest rate and energy price expectations can be revealed.

Concerning the output of the tool the user may develop guidelines and strategies for different building types and for different contexts to reach ambitious environmental targets at least life cycle costs. However, the tool is limited to a general approach and cannot be used in detailed design problems.

Keywords: energy-efficiency, renewable energy, cost-effectiveness, techno-economic database, assessment tool

INTRODUCTION

The building sector accounts for a large share of global final energy consumption in Switzerland. While energy related requirements for new buildings are constantly increasing, the improvement of energy performance of the building stock constitutes a major challenge for the future. The mastering of this challenge requires the identification of **cost optimal retrofit strategies** to achieve maximal reduction of energy consumption and carbon emissions within building renovation.

The economic effectiveness and viability of building retrofits, however, depend on many factors, e.g. scope of retrofit project, time horizon, costs of retrofit measures, including

information and transaction costs, performance risks, interest rate and energy price expectations as well as user preferences. Optimal energy related retrofit strategies for typical types of buildings to achieve ambitious targets for the reduction of primary energy (PE) use and greenhouse gas (GHG) mitigation haven't emerged yet nor have been systematically analyzed.

The purpose of a developed comprehensive calculation tool is to reveal trade-offs and synergies between different types of strategy measures and to identify strategies aiming at reducing cost-effectively primary energy use and greenhouse gas emissions. The tool includes a database of empirical techno-economic characteristics of several types of measures. Up to ten renovation packages of measures and related reference cases may be represented in terms of economic and environmental indicators: investments costs and life-cycle costs, total and non-renewable primary energy consumption, and greenhouse gas emissions. Using up-to-date empirical cost and price data the economic effectiveness and economic viability of advanced retrofit measures and up-stream options is assessed from a life-cycle-cost point of view. With the tool the impact of factors such as starting situation, scope, interest rate and energy price expectations can be revealed. Therefore the user may develop guidelines and strategies to reach ambitious environmental targets at least life cycle costs. The tool enables comparison between different renovation packages and strategies. As such this calculation tool is a complement for SIA 2040.

METHOD

Overview

The INSPIRE Tool focuses on residential buildings and simple office buildings without cooling needs. The methodology applied does neither account for building related mobility nor for co-benefits of retrofit measures, however, embodied energy use, up-stream life cycle primary energy use for energy carriers and related carbon emissions are included.

The software was developed as a Microsoft Excel spreadsheet, providing maximal flexibility and a familiar working environment for the user. For easy updating and maximum performance the data is stored in a separate file and accessed from Microsoft Excel by using industry-standard SQL commands.

Using a combination of programming in Visual Basic for Applications (VBA) and custom-build Excel functions, an interactive user interface was built. Options can be selected through drop-down menus and for most user inputs default values are provided which can be adjusted by the user. The interface is dynamic, as it reacts to the users input, e.g. if the option «building has a ventilation» is selected, the related input fields are shown and correct default values computed.

A schematic representation of the methodology to calculate the environmental and economic indicators (GHG emissions, PE and non-renewable PE use, and life cycle costs) is given in Figure 1. Building data and techno-economic data of GHG mitigation and PE efficiency measures are used to calculate heating energy need, final energy consumption, GHG emissions, PE use, and life-cycle-costs.

In Figure 1 input sections are shown with blue background (left side), calculation sections with yellow (middle), and the output sections with green (right side). The calculations and database are hidden. The arrows from the blue boxes refer to the user definition, which is used to derive corresponding data from the database as a default value. These default values can be overwritten. The arrows from databases and calculation boxes towards the input boxes refer to

default values. The arrow from the output box towards the calculations box refers to user preferences selected in the output sheet.

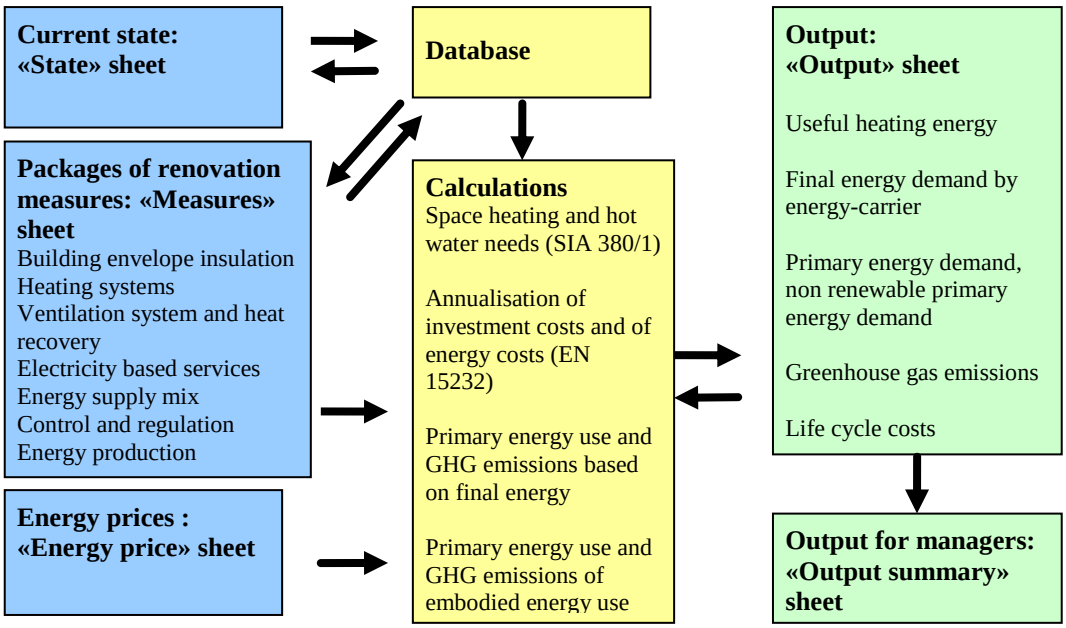

Figure 1: Schematic structure of the INSPIRE tool

The structure of the INSPIRE Tool

The Microsoft Excel spreadsheet is structured into the following five worksheets:

The «**State**» sheet is used to define a current situation of a building. Inputs related to building specific data, occupancy, building envelope area and previously undertaken building envelope measures, and building technology are provided by the user.

The measure packages and related reference cases can be defined in the «**Measures**» sheet. The possible measures are related to (i) building envelope insulation, (ii) heating systems, (iii) ventilation system and heat recovery, (iv) electricity based services (lighting, cooling, and appliances), (v) energy supply mix, (vi) building automation control and regulation, and (vii) onsite energy production.

The energy prices of the different energy carrier are defined in the **«Energy prices»** sheet using five interpolation values: default values are provided. From the interpolation values the tool calculates the annuities of the energy cost savings, depending on the interest rate and the life-time of the measures selected.

The two **«Output»** sheets are used to collect and present the results of the calculations. To cover different needs concerning the level of detail beside the comprehensive **«Output»** sheet a more manager-style «Output Summary» sheet is also available.

Database

The tool includes a comprehensive database of empirical techno-economic data concerning properties of building elements, energy systems and carriers, and a large range of measures that were collected from the companies and literature, such as CRB Elementarten-Katalog. Based on the dropdown selection made by the user (e.g. building type, building period, heating system) values from the database are used to automatically compute default values for a majority of the input values needed in the calculations. This approach enables also users,

with little knowledge of details and in an early project phase, to use the INSPIRE Tool and to generate at least preliminary results. Most of default-values derived from the database can be overwritten at any time if more accurate values are available.

Calculations

The information about the building and techno-economic data of GHG mitigation and PE efficiency measures are used to calculate the indicators in the **«Output»** sheet (see Figure 1). Calculation of energy needs takes into account energy performance of a building envelope, outdoor climate, target indoor temperature, and internal heat gains according to SIA 380/1. Optionally, the life-cycle impact in terms of energy need and greenhouse gas emissions of materials used in the renovation measures can be included. Greenhouse gas emissions and PE use are calculated by taking into account conversion efficiencies of the heating systems and emission factors as well as primary energy factors of the energy carriers including up-stream emissions or energy use. The life-cycle-cost and cost-effectiveness calculations are carried out dynamically with the annuity method. In order to compare the annuity of the investment with the increasing savings of energy costs, the savings of energy costs are discounted and converted to an annuity. The calculations are based on real prices, real interest rates and typical lifetimes of the building elements.

RESULTS

The tool can be used to compare renovation packages or build up a renovation strategy. An example of possible strategy is presented in the following steps.

- Step 1 Choice of energy supply mix (electricity)
- Step 2 Improvements of the thermal protection by insulation of building envelope (building element and efficiency level)
- Step 3 Choice of energy carrier/ Change in the heating system
- Step 4 On-site energy production: Implementation of solar thermal panels, PV or wind
- Step 5 Construction design and material choice with low embodied PE and GHG emissions

The steps above are implemented in the «**Measures**» sheet. The **«Output»** sheet shows graphically the results of the strategy that are presented in Figure 2.

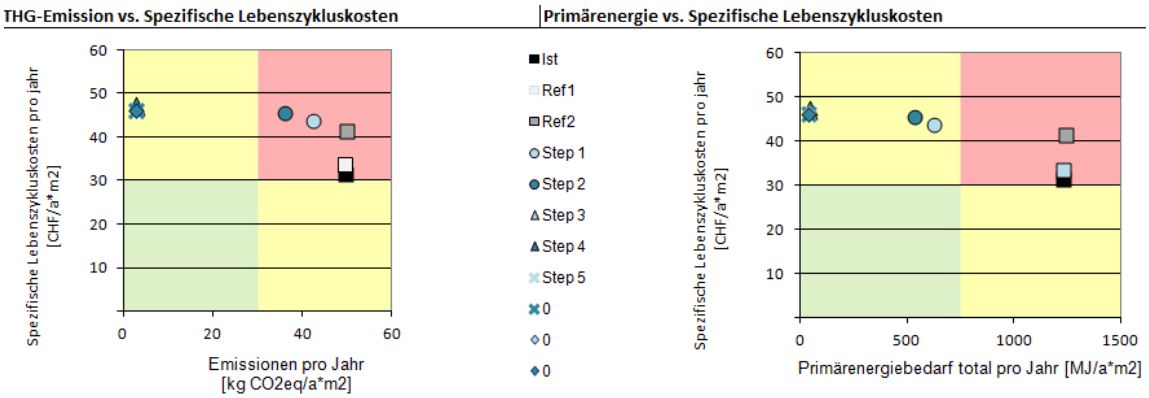

Figure 2: Emissions (left side) and primary energy use (right side) versus the life cycle costs for each strategy steps

In Figure 2 the GHG emissions (left side) and primary energy use (right side) versus the life cycle costs are presented. The Output- sheet includes also numerical results, for example, of the total life cycle costs per m^2 and year and a differentiation of costs in capital costs, operating and maintenance costs, and energy costs.

DISCUSSION

The novelty of the tool is to assess relations between GHG emissions or PE use vs. the life cycle costs. Typically, this kind of tools includes only the calculation of GHG emissions and PE use. The tool includes a wide variety of measure options to be investigated in terms of GHG emissions and PE use reduction. The strength of the tool is a possibility to compare different renovation packages with reference cases or to build up a renovation strategy with different steps. Four building categories are covered in the tool: single- and multi- family house, office building, and school. This makes the tool useful for different building owners, planners and other stakeholders. Finally, based on the result, the user may develop guidelines and strategies to reach ambitious environmental targets at least life cycle costs.

The tool is a simplified model and it is not developed to create energy certifications due to a lack of accuracy in modeling. However, the tool allows investigation of different renovation packages and strategies for specific buildings, taking into account particular characteristics of buildings or particular framework parameters. The user can either use the database or add case-specific data. The tool is currently made specifically to cover situations of building renovation. It could be envisaged to develop it further to cover also the case of new buildings.

ACKNOWLEDGEMENTS

The authors gratefully thank Swiss Federal Office of Energy, City of Zürich, Interessengemeinschaft privater, professioneller Bauherren, Credit Suisse, Allreal, Reuss Engineering (Implenia), W. Schmid AG, Belimo, Siemens Schweiz AG and Zürcher Kantonalbank for financing the project.

REFERENCES

1. Jakob M., Ott W., Bolliger R., von Grünigen S., Kallio S., Chobanova H., Nägeli C. (2013 forthcoming): Integrated strategies and policy instruments for retrofitting buildings to reduce primary energy use and GHG emissions (INSPIRE). TEP Energy GmbH, econcept AG.
2. Jakob M., Bolliger R., von Grünigen S., Kallio S., Ott W. (2013 forthcoming): INSPIRE Tool, Dokumentation für Aufwendung. TEP Energy GmbH, econcept AG
3. Jakob M., Bolliger R., von Grünigen S., Kallio S., Ott W., Nägeli C. (2013 forthcoming): INSPIRE Tool: Calculation tool for retrofit strategies

SOFTWARE

INSPIRE Tool		***Available languages*** ☐ **Français** ☐ **English** ☒ **Deutsch** ☐ **…….** ☐ **Italiano** ☐ **……**
M. Jakob, R. Bolliger, S. von Grüningen, , S. Kallio, W. Ott, C.Nägeli	***TEP Energy GmbH, econcept AG***	***Price: Free of charge from www.bfe.admin.ch***

Description

The building sector is responsible for both direct and indirect energy consumption and related local and global environmental impacts. Apart from envelope retrofit measures as such, a wide variety of options is available for building owners to mitigate these impacts. In this context building owners face the challenge of finding the adequate strategy to reduce energy use and greenhouse gas (GHG) emissions in the most cost-efficient way.

The purpose of the software is to provide a practical tool to reveal trade-offs and synergies between different types of measures and to identify strategies aiming at reducing cost-effectively energy use and GHG emissions. The software helps building owners not only to reach their energy and GHG goals but provides also a useful tool to secure the return on investment in an economic environment characterized by increasing energy prices.

The software includes a comprehensive database of empirical techno-economic data concerning several types of measures which were collected from companies and from the literature. This data enables even users with little detail-knowledge and users in an early project phase to use the tool and to generate (preliminary) results. All default-values from the database can be overwritten at any time if more accurate values are available. This approach makes the INSPIRE Tool a good choice in any phase of a retrofit project.

The software was developed as a Microsoft Excel spread-sheet, providing maximal flexibility and a familiar working environment for the user. For easy updating and maximal performance the data is stored in a separate file and accessed by using industry-standard SQL commands.

Measures are categorized into seven categories: (i) building envelope insulation, (ii) heating systems, (iii) ventilation system, (iv) electricity based services (lighting, cooling, and appliances), (v) energy supply mix, (vi) control and regulation, and (vii) onsite energy production. Up to ten measures or packages of measures may be analysed and are represented in terms of economic and environmental indicators: investments costs and life-cycle costs, total and non-renewable primary energy consumption, and greenhouse gas emissions. With the INSPIRE Tool the impact of factors such as scope, interest rate and energy price expectations can be revealed and presented both in a manager-style summary output sheet as well as in a more detail-oriented output sheet.

Technical Data

Operating System ☒ **WINDOWS [**Windows 7**]** ☐ **MAC [**Versions**]** ☐ **LINUX** **Microsoft Office 2007 or 2010 is required.** ☐ **Others ……**	***Processor*** n/a ***Required memory*** n/a ***Required disk space*** ***10 MB***

MIXED-DIMENSIONALITY APPROACH FOR ADVANCED RAY TRACING OF LAMELLAR STRUCTURES FOR DAYLIGHTING AND THERMAL CONTROL

Kostro A., Scartezzini J.-L., Schüler A.

Solar Energy and Building Physics Laboratory, Ecole Polytechnique Fédérale de Lausanne: LESO-PB, Station 18, Bâtiment LE, EPFL, 1015 Lausanne, Switzerland.

ABSTRACT

The appropriate choice of the type of glazing and glazed area in a façade depends on many factors. They include amongst other criteria: location, orientation, climatic condition, energetic efficiency, usage of the building, required user comfort, and the architectural concept. All requirements cannot be fulfilled at all times and priorities have to be set to find a compromise between occupant comfort, design objective, cost and energetic efficiency. An innovative glazing system combining daylighting, glare protection, seasonal thermal control and clear view was developed [1] and patented by the authors. This design was developed using a novel ray tracing approach to obtain a strongly angular dependent transmission with a specific angular distribution. Taking advantage of the changing elevation of the sun between seasons, a seasonal variation is created by a strongly angular dependent transmittance.

In this paper we present the mixed dimensionality approach used to achieve a very fast and accurate ray tracing of any lamellar structure that has a two dimensional profile. The originality of the presented Monte Carlo algorithm is the separation of intersection and interaction. Intersections are computed using only the two dimensions of the profile thereby increasing significantly computational speed. Interactions are computed using vector calculus in three dimensions and provide accurate results with very little computational load.

With such optimizations, the user interface could be designed to give an instantaneous idea of the light path in the modelled system. The model also calculates an accurate bidirectional transmittance distribution function that is used in a Radiance simulation to obtain a rendering of the daylighting distribution in an office space. Hereby we can compare the daylighting performances of the novel design based on optical microstructures with those of other CFSs. Finally the combination of simulated angular dependent transmittance and Meteonorm data provides an estimate of transmitted energy over the year and proves the efficiency of the presented optical microstructures for dynamic thermal control. The proposed working principles of redirection and angular dependent transmittance are thereby demonstrated. The software provides all the mentioned results in the user interface where the performances of different designs can also be compared, making the optimization process of a profile with a defined objective very intuitive.

Keywords: Microstructures, Daylighting, Thermal Control, Smart Windows, Complex Fenestration System, Ray Tracing, Monte Carlo

INTRODUCTION

In Switzerland, electric lighting, heating and air conditioning account for about 71 % of total energy demand in private housing (dominated by heating : 67%) and 31% of the overall Swiss electricity usage (dominated by lighting :13%) [2]. The novel complex fenestration system (CFS) proposed by the authors combines several functions and can contribute to significantly reduce energy consumption in buildings with favourably oriented glass façades. In winter, solar gains are used to reduce heating energy requirements; in summer, the proposed device blocks direct radiation and thus limits air conditioning load as well as overheating risks. Judicious use of daylighting furthermore reduces energy needs for artificial lighting and improves the well-being of occupants. These principles are illustrated in figure 1.

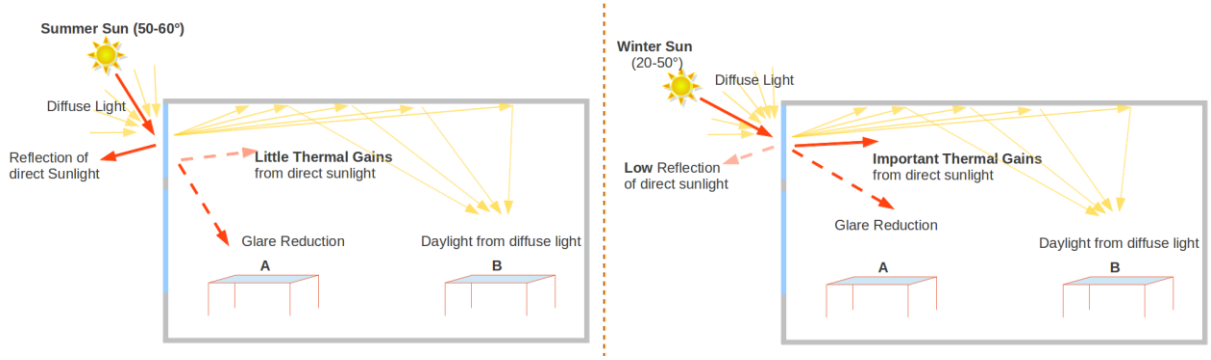

Figure 1 : Working principle of the CFS for daylighting, glare control and seasonal thermal control.

Ray tracing is a technique from geometrical optics to model the path taken by light in an environment by following rays of light. It may be use in the design of optical devices such as lenses and sets of lenses in microscopes, telescopes etc… Ray-tracing software is often used to calculate the Bidirectional Scattering Distribution Function (BSDF) of complex fenestration systems (CFS) [3, 4] but no dedicated tool was found for the modelling of CFSs combining geometry and material-dependent designs and integrating thin films. Also, existing commercial tools provide complete three dimensional characterisation but they are time consuming and the output is not adapted to the evaluation and comparison of CFS performances. For these reasons, a simple and efficient ray tracing tool for the study of laminar structures was developed with the possibility to directly compare glazing related performances and modulate designs. In this paper we describe the innovative concepts used in the algorithm, the user interface of the software and some of the CFS specific performance indicators provided.

Ray tracing is also used for graphical rendering in computer graphics and produces realistic illumination of virtual scenes. Amongst many, Radiance offers complete and flexible tools for the use of architects to render construction projects. More specifically and in relation to complex fenestration systems, rooms with different types of windows and electrical lighting sources can be modelled to study the illumination, be it natural or artificial, direct or indirect [5]. This however requires an accurate definition of the studied window. Such detailed description can be computed with the developed software.

Monte Carlo algorithms are stochastic and they are used to solve complex physical or mathematical problems. In a typical Monte Carlo algorithm, random draws define a chain of local events characterizing the global event and leading to a final state. Each draw follows a given distribution representative of the corresponding event. By repeating this iteration over random events numerous times, a probability distribution of the final states is obtained.

MIXED DIMENSIONALITY APPROACH

A two dimensional (2D) description of the designs is sufficient for most existing CFS products because they can be described as 2D extruded profiles. In a pure 2D ray-tracing of such a profile, with no scattering, transmittance is modelled accurately for zero degree azimuths because the rays are always in the same plane as the profile. For small deviations from this plane, the azimuth angle has little influence on the distribution of transmittance. However in some cases, for azimuth angles above 40°, using 2D only for reflection and refraction introduces errors above 20% in the angular distribution of transmittance. This is not acceptable for an evaluation of annual energetic transmittance that relies on three dimensional bidirectional Transmission and Reflection Distribution Functions (BTDF and BRDF). For an evaluation of daylighting using rendering software such as Radiance, complete and accurate BTDF are also required. For these reasons, the third dimension has to be considered.

In the proposed algorithm, all intersections are still computed in 2D. If a profile is defined in the x and y coordinates, the only loss of information is the z coordinate of the intersection. This information is of little use since we are interested mostly in the angular distribution of rays. Finding intersections between lines in two dimensions is very fast and can be efficiently done using a binary space partitioning tree [6]. For interactions however, all three dimensions are used. Reflection, refraction, scattering and absorption are precisely modelled using tree dimensional vector calculus and following physical rules. These principles are illustrated in figure 2.

Reflection and refraction probabilities are modelled following the Fresnel equations and Snell's law. Absorption follows the Behr Lambert law. The Fresnel equations for the calculation of reflectance and transmittance of thin films are derived from Maxwell's equations. Following the work of Macleod [7], a characteristic matrix can be used to compute these values. These behaviours all depend on the complex refraction indices of the implied materials. For accuracy, spectral values of these refraction indices are used.

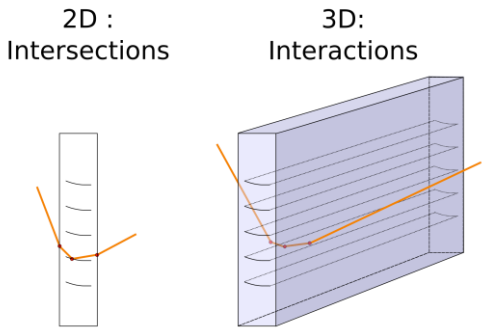

Figure 2: Illustration of the mixed dimensionality concept for ray tracing of profile defined geometries.

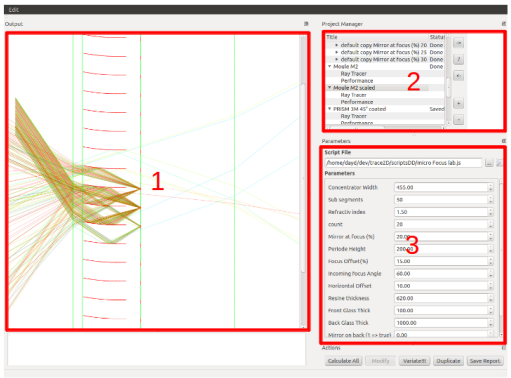

Figure 3: Graphical User Interface. Area 1 shows the output, in this case ray tracing. Area 2 shows the project list. Area 3 the parameters listed in the script.

OPTIMISATION OF GEOMETRY AND PARAMETERS

Besides accurate physical modelling and calculations, the developed software was also meant to be an intuitive and flexible design tool. For intuitive development, structures are parameterized and the parameters can be modified in the graphical user interface (GUI) with a direct rendering of the resulting rays distribution. The GUI can be used to change the angle of

incidence of the beam and visualize the angular distribution of transmitted and reflected light. To provide flexibility, the projects are described by a file containing the geometrical description of the design and parameters to modify and optimise the design. For example, a script describing an integrated flat mirror contains a description of how to draw the interfaces between the bulk material and air and where to include mirrors of a given width, tilt and at a specified interval. The scripts can use basic javascript language such as *for* and *while* loops, *if then else* statements, mathematical operands as well as more advanced data structures such as arrays. In addition to the javscript language, ray tracing specific functions are implemented to add interfaces, define materials and light sources. Another set of instructions was defined to add parameters, these are directly included in the graphical interface. Hereby almost any structure can be defined, modified and visualized.

In the process of designing a solution, new concepts need to be tested and parameters optimized. To facilitate the study and optimisation of CFS complying with complex requirements, the graphical user interface of the software was built around a list of projects and their variations. As shown in part 2 of figure 3, this gives a rapid overview and history of designs. As mentioned above, the projects are described by a javascript containing both the geometry of the design and the list of parameters. Each parameter can then be modified individually in the GUI -area 3 in figure 3- and the resulting ray path visualised immediately- area 1 in figure 3- . The resulting performances can also be visualized in area 1 of the GUI for each design. For a meaningful comparison and optimisation, a design can be varied according to a single parameter. The different variations are sub projects that can then be varied again or discarded. By selecting several projects in area 2 of the GUI, their performances can be directly compared in area 1 regarding different criteria. These criteria include transmission distribution, transmittance depending on incident angle, energetic transmittance and daylight rendering. This approach proved to be very useful to understand how complex geometries affect ray paths depending on the angle of incidence and it was used to find and optimize an original design described in the next section.

RESULTS AND DISCUSSION

The engineered geometry shall provide elevated daylight levels by redirecting the incoming light towards the depth of the room. This redirection simultaneously protects occupants from direct sun light and reduces glare risk. For an optimized usage of available solar radiation, the direct sunlight is transmitted in winter and reflected in summer. This complex set of objectives needs to be reached to achieve daylighting, seasonal thermal control and transparency simultaneously. In this section we briefly re-introduce the novel design proposed and patented by the authors [1] along some new results.

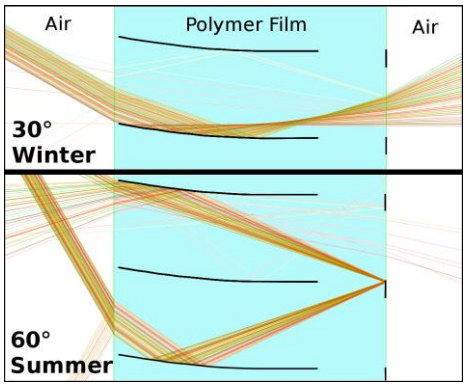

Figure 4: Structure as proposed with incoming beam at 60° and 30° elevation. Illustration of the focusing and resulting reflection in summer; and redirection for daylighting in winter.

The key of this new design is the focusing of light from a given angular interval by a first component onto a second component. To focus incoming light, the first component of the system should be a parabolic surface. The parabola has to be drawn in order to focus light incoming from a given range of incident angles on a second reflecting surface, which is located on the inner side of the system. This second mirror reflects lights from the selected range back through the system. The focus is achieved for angles corresponding to the summer elevation of the sun at the specified location (for example 60° in Lausanne). For this range the light is concentrated on the second surface and reflected. For angles out of the specified blocking range, the reflection on a parabolic shape distributes a parallel beam over a range of angles; this distribution is suited for daylighting. To achieve clear view, direct transmission without interaction for close to normal angles is maximized: the two elements have a minimal height and maximum overlap. The miniaturization of structures bellow a millimetre further reduces their impact on see-through property.

This principle is entirely based on a static structure and to be efficient, it has to be adapted to the geographical location where it will be installed. Depending on the latitude, the solar course changes and the two components have to be optimised to block radiation for the aestival elevations of the sun and transmit radiation from the winter sun.

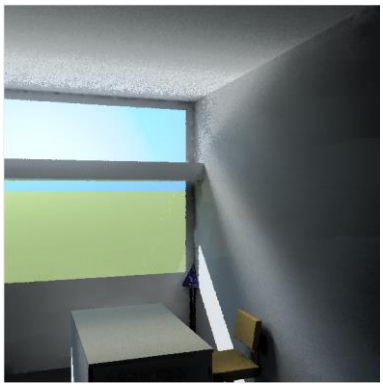

Figure 5: Radiance rendering of a scene with microstrucutred glassing following computed BTDF function using the bsdf primitive.

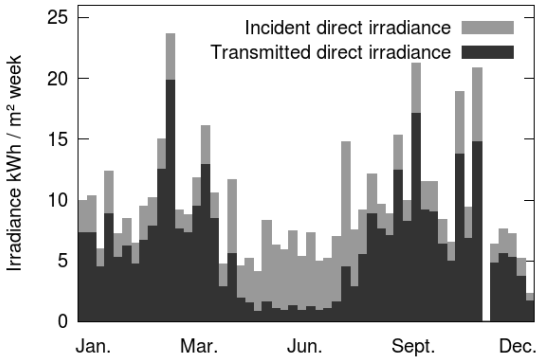

Figure 6: Simulated transmitted irradiance per surface area for a microstructured glass over the year compared to incident direct irradiance.

For seasonal thermal control, the defining value is the thermal gains. For each square meter of window, a portion of the incoming solar radiation is transmitted and this energy heats up the space behind the window. To calculate an estimate of this value, diffuse and direct transmission factors are calculated with the ray tracing simulation tool and used in combination with Meteonorm radiometric data. To combine these data, a common representation of space has to be used. For direct radiation the hourly solar position is used and for diffuse radiation, the hemisphere is divided into patches following Tregenza's subdivision of the sky. A Perez model of the sky is used to define the hourly radiation coming from each patch according to the corresponding climate file. The thermal gains due to direct and diffuse radiation were computed over the year and compared with other types of glazing. The designed glazing showed an energetic transmittance of direct sunlight lower than 20% during the summer period and higher than 70% during the winter period. Results are shown in figure 6.

Glare and illuminance on the work plane are the critical values for the evaluation of daylighting. Glare can be estimated using the Unified Glare Rating (UGR) or the Daylight Glare Index (GDI) and illuminance is measured in lux and should be between 300 and 1000

depending on the task. For common office work, values between 300 and 500 lux are required. To assess these values for the developed complex fenestration systems, the software is used to create the characteristic bidirectional transmittance distribution functions (BTDF). These BTDFs are then used to define a window in a Radiance scene and Radiance routines are used to render the scene, an example can be seen in figure 5. After careful alignment of the reference coordinates and of time, this radiance simulation was also used to compute hourly illuminance levels and glare indices on the defined workspaces over the course of a day, month or year in different sky conditions.

CONCLUSION

A simulation tool using a novel approach was developed for the modelling of CFSs. It was developed to find a new system that provides daylight, glare protection, seasonal thermal control and clear view. These aims were reached with the invention of a new design combining two reflective surfaces to achieve redirection of light and a strong seasonal dynamic in thermal gains. This design was characterised using Radiance simulations for the assessment of daylight and glare protection capabilities. An estimate of thermal gains for the evaluation of seasonal thermal controls was computed based on Meteonorm data. It was demonstrated that the simulated design reaches the set goals.

REFERENCES

1. A. Kostro, M. Geiger, N. Jolissaint, G. Lazo, M. Aymara, J.-L. Scartezzini, Y. Leterrier and A. Schueler. Embedded microstructures for daylighting and seasonal thermal control. SPIE 2012 International Symposium on Optical Engineering, San Diego, USA, August 13-16, 2012.
2. TEP Energy GmbH, Prognos AG, Infras AG. Swiss Federal Office of Energy. Analyse des schweizerischen Energieverbrauchs 2000-2011 nach Verwendungszwecken, 2012.
3. Wittkopf, S., Oliver Grobe, L., Geisler-Moroder, D., Compagnon, R., Kämpf, J., Linhart, F., and Scartezzini, J.-L. : Ray tracing study for non-imaging daylight collectors, Solar Energy 84 (6), 2010.
4. Andersen, M., Rubin, M., Powles, R., and Scartezzini, J.-L., Bi-directional transmission properties of Venetian blinds: experimental assessment compared to ray-tracing calculations, Solar Energy 78 (2), 2005.
5. J.H.Kämpf, J.-L.Scartezzini : Ray-Tracing simulation of Complex Fenestration Systems Based On digitally Processed BTDF Data, Proceedings CISBAT, pp 349—354, 2011.
6. Ize, T., Wald, I., and Parker, S.G. : Ray Tracing with the BSP Tree, IEEE/EG Symposium on Interactive Ray Tracing, 2008.
7. Macleod H.A. Thin-Film Optical Filters 2001.

"ENERGY PASSPORT" SOFTWARE PROGRAM FOR DESIGNING ENHANCED THERMAL PERFORMANCE OF THE BUILDING ENVELOPE AND ENERGY EFFICIENCY LABELLING

Karine Melikidze

Georgian Technical University (GTU), Building 1, #77 Kostava street, 0171 Tbilisi, Georgia

Sustainable Development and Policy (SDAP) Centre, #4 Besiki street, Office 202A, 0108 Tbilisi, Georgia

ABSTRACT

From a building physics perspective a building represents a single thermal unit with a vital relationship between the heat consumption and building envelope's thermal performance level that should be considered exclusively in connection with climatic conditions.

Four key principles should be under consideration with respect to thermal performance design of energy-efficient buildings:

- selection of a geometric shape for the building that reduces heat losses; a design approach that aims to lower the exterior surface area-to-volume ratio;
- reduction of energy consumption demand by increasing the thermal performance level with reduction of air permeability;
- provision of required air exchange with the help of organized air intake;
- meeting energy consumption needs of the building for heating purposes in the most effective manner.

The Energy Passport software program is a tool that enables a team of professionals including building physicists, architects and construction engineers to use an integrated design approach for assessing thermal performance by identifying the interaction of building envelope choices with other systems at the project planning and the design stage. Such an approach helps to make a decision for project implementation together with a cost benefit analysis for verification of reasonable cost.

The Energy Passport software program screens incorporate windows for climatic and building data that should be filled out. The program enables setting ofa normative/ recommended level for specific energy consumption for the type of building that is under assessment and calculates heating degree days for relevant climatic conditions based on best practices.

The above program provides flexibility to achieve the optimal thermal resistance values for exterior components and calculation of the designed specific consumption value based on the energy consumption requirement of the whole building through a variety of options selected for individual elements using normative/recommended value as a benchmark for results comparison. The selected thermal performance (design) level enables labelling/certification of a building by a specific energy consumption rating system and provides energy consumption figures that can be used to estimate energy savings and associated reduction of CO_2 emissions.

Keywords: "Energy Passport" software – tool, design of thermal performance of building envelope, energy efficiency, thermal balance of building, specific energy consumption value, labelling/certification of building, reduction of energy consumption and associated CO_2 emissions.

INTRODUCTION

One of the main goals of thermal performance design with enhanced energy efficiency is reduction of energy consumption in buildings. The sustainability approach for the building sector concerns reduction of the negative impact on the environment without compromising the internal level of comfort. The overall strategic vision on buildings' *energy efficiency* is to fill in the gap between the supply and demand sides, in terms of building sector energy balance and reduce energy consumption growth as well as associated CO_2 emissions by meeting the evolving energy needs while ensuring energy efficiency.

During the recent years research efforts in buildings energy efficiency have resulted in broad understanding of the implications of heat consumption in buildings and development of strategies and technologies for energy saving. The most comprehensive and advanced tool that should be used for designing a building's thermal protection level is the software tool, which enables assessment of energy consumption during the whole year.

The main aim in the application of a software tool for energy efficient design purposes is the achievement of the optimal balance between all the factors that affect minimisation of energy consumption. This approach enables engineers to examine energy consumption at the planning and the design stage. It is expected that an evaluation of thermal performance design should be supplemented with reliable economic calculations for the integrated energy performance measures for the building envelope aiming at identification of the cost optimal levels of energy efficiency.

However software tools are often not used by designers and developers for the following reasons: on the one hand due to the issue of accessibility of the software tools, on the other hand due to a lack of information on building energy consumption during the design stage.

METHODOLOGY

The concept of an advanced integrated approach to enhance the thermal performance level of buildings combines upgraded thermal resistance values - R for thermal properties for all exterior components of the building providing the set up level for reduced heat consumption with the consideration of air exchange and air permeability not exceeding the permissible limits. This approach enables designers to control indicators of the thermal protection level already at the design stage.

The "Energy Passport" software tool represents one of techniques that have been developed to reflect this advanced thermal performance design approach.

Software is developed based on a methodology that lays down a foundation for the advanced systematic approach in a building's thermal performance design and reflects requirements that are set not for the separate components that affect the heat balance of the building (walls, floors, ceilings, windows, et al.), but rather for the energy performance of the building as a whole. Energy performance is calculated as a function of envelope performance, building design and geometry, design and selection of heating and ventilation systems and passive solar gains intake over cardinal points of the building orientation with respect to the favourable volumetric-planning design solutions taking into account the efficiency of the heat supply system and climatic parameters. Based on this systematic approach the software tool calculates the specific energy consumption of the whole building over the heating season with the indication of heating system load for the heating season.

The above methodology envisages calculations that start from the calculation of heating degree -days DD by equation (1) that is given below:

$$\mathbf{DD= (t_{in} - t_{hs})x\ Z_{h} \quad (1)}$$

where: $\mathbf{t_{in}}$ – is the indoor temperature, ^{o}C; $\mathbf{t_{h.s}}$ – is the average temperature of heating season; $\mathbf{Z_{hs}}$ – the duration of heating season.

The normative/recommended thermal resistance values for exterior components of the building are calculated based on correlation results between DD and thermal resistance values of the building envelope components.

Methodology reflects integrated approach in thermal performance design by setting up normative/ recommended specific energy consumption values according to the type of building and number of storeys. This specific energy consumption parameter is proposed as a amount of heat required during the heating season per cubic meter of volume of a building, per degree day, measured in KJ/(m^3.^{o}C.day). In each particular case the normative/recommended specific energy consumption value is adjusted since it takes into consideration efficiency of heat distribution system.

The overall demand in energy/heat consumption for the heating period foresees thecalculation of thermal balance components and is calculated as a function of conductive heat losses, heat losses via air exchange, domestic and solar radiation intakes, coefficient of efficiency of automatic regulation of heat supply, as well as coefficient that considers additional heat consumption by theheating system.

In turn conductive heat losses -Qt are calculated as a function of degree -days, building envelope area and coefficient of heat transfer. Infiltration heat losses – Qv are calculated as a function of degree -days, building envelope area and conventional factor of heat transfer through infiltration and ventilation. Heat intake through solar radiation- Qs is calculated as a function of window area, passive solar gains intake over cardinal points of the building, and coefficient of relative penetration of solar radiation through the window as well as a coefficient that considers shading of windows with opaque elements. Domestic heat intake - Qi is calculated as metabolic heat per square meter, duration of heating season and rated heated area of the building.

Normative / recommended specific energy consumption value indicates benchmark level during design process and is very informative for its comparison with the designed specific consumption value that results from thedesign process aiming at selecting design solutions and insulation materials for exterior components of the building.

The Energy Passport software is a standalone desktop application. All required entrance data is divided into two parts: Climate Data and Building Data. Based on the methodology approach every input has its own purpose in performed calculations and in particular circumstances may or may not affect the result. The software calculates and shows several intermediate values. The main purpose of these calculations are design of the thermal performance of the building envelope and certification of the building by a specific energy consumption rating criterion based on the designed value of the specific energy consumption of the building for the heating season. Additionally the software creates the chart of the thermal balance components.

The software performs calculation tasks by steps in the following sequence: Climatic data such as designed outdoor temperature, average outdoor temperature for the heating season together with the internal temperature relevant to the type of the building, duration of heating period and solar radiation income on each side of the building according to its orientation

towards cardinal points as well as building geometry parameters are entered in the program and heating degree–days are calculated. For a given category of energy efficiency (A, B, C) the normative/recommended specific energy consumption value is determined based on the type of the building under design. Other building indicators as ratio of windows and balcony doors area to the total wall area, together with selected coefficients of window shading are also calculated. The software possesses special so-called energy "design" screen windows for entering coefficients of heat supply, efficiency of heat distribution, efficiency of regulation, and metabolic heat released from people. With the fulfilment of all building design parameters the software performes all calculations.

RESULTS

The thermal performance design of a new residential building designed by the Georgian company "ARCI" was performed with the aid of the "Energy Passport" software tool . The calculation was performed for the overall thermal resistance value for walls constructed from perlite blocks of 19 x 29 x 39 cm, and thickness: δ =29 cm. The figures for outdoor and indoor layers were taken as follows: for an outdoor plaster layer - cement sandy mortar with δ=0.02 m, λ=0.93 W/m K; for indoor plaster - complex mixture consisting from cement, sand and lime with: δ=0.02 m, λ=0.87 W/m K. In order to avoid thermal bridges in exterior walls it was suggested to smooth out joints with perlite cement mortar. The overall thermal resistance value – $\mathbf{R_{walls}}$ for walls from perlite blocks was identified as:

$$\mathbf{R_{walls} = R_{in} + R_{c} + R_{out} = 1/8.7+0.02/0.87+0.29/0.148+0.02/0.93+1/23=2.14\ m^2\ K/W}$$

Thermal resistance values for other exterior components have been selected and calculated in the same manner. Figure 1 presents software screen with results of thermal performance design calculations performed by "Energy Passport" software.

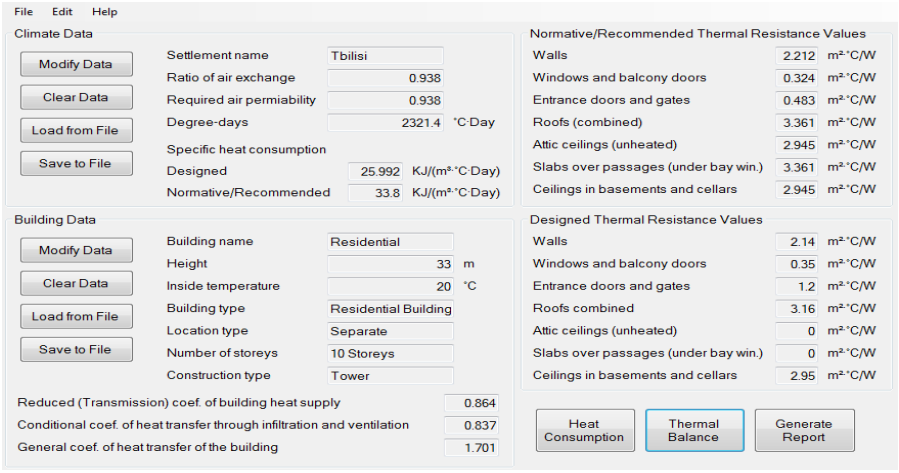

Figure 1 Software screen with the thermal performance design calculation results Figure 2 gives a chart with thermal balance components that have been calculated by software tool.

DISCUSSION

As of today Georgia has not adopted advanced thermal engineering codes which are in compliance with the European Energy Performance of Buildings Directive (EPBD). Assessment of the current construction sector shows that there is a great energy saving potential in the building sector, since the energy efficiency approach is not implemented and the construction sector in Georgia still continues to use old Soviet codes [1].

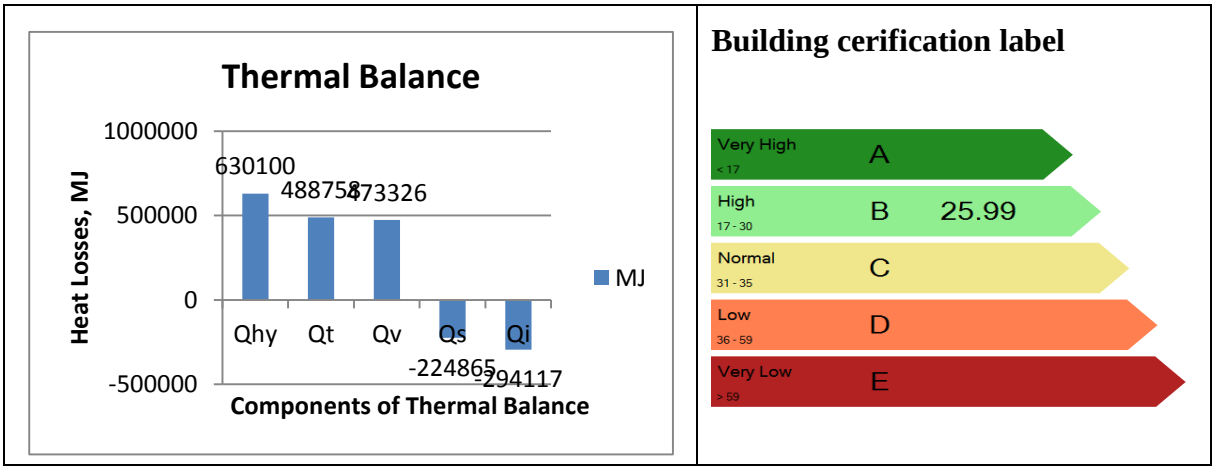

Figure 2 Thermal balance chart with certification label section

Results of thermal performance design based on an advanced approach have been compared for the prototype building designed with the old Soviet approach – an un-insulated house version that represents the current unfortunate construction practice in Georgia. This un-insulated version has also been calculated by the "Energy Passport "software. A comparison of heat consumption results is shown in Figure 3.

Calculations prove 53 % savings in heat consumption over the heating period, since R values of the un-insulated version are benchmarked by old Soviet codes and are rather low, for instance thermal resistance value for walls constitutes: $\mathbf{R_{walls} = 0.54\ m^2\ K/W}$
and is almost four times lower than the thermal resistance value $\mathbf{-R_{walls}}$ in insulated version."

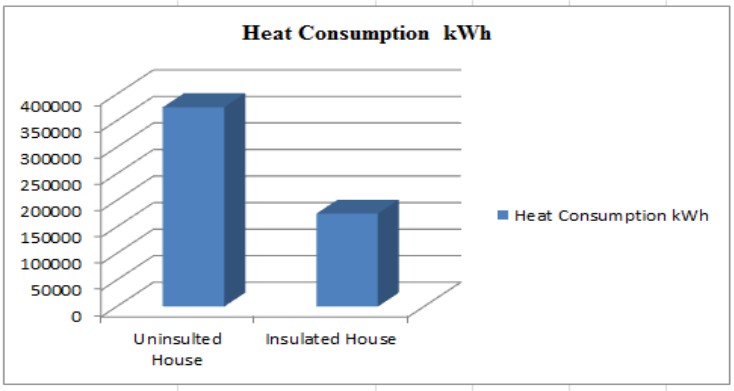

Figure 3 Heat consumption results calculated by software tool for un-insulated and insulated prototype building

The Energy Passport" software tool provides the opportunity for a quick assessment of a building design with the thermal protection level at the design stage and labeling with the wide possibility for evaluation of volumetric-planning indicators and thermal insulation solutions.

REFERENCES

1. Y. Matrosov, K. Melikidze, N. Verulava The energy efficiency perspective of the Georgian residential sector. http://www.sdap.ge/docs/microsoft_word_-_energy_efficiency_of_residential_sector.pdf

SOFTWARE

Energy Passport		*Available languages* ☐ **Français** ☒ **English** ☐ **Deutsch** ☐ **…….** ☐ **Italiano** ☐ **……**
Editor n/a	***Distributor tbd***	***Price pending***

Description

The Energy Passport software is a standalone desktop application based on Microsoft .NET Framework 4.0. The software is developed to calculate the thermal performance of the building envelope and labelling according to the requirements that are imposed by European Energy Performance of Buildings Directive. The data input is separated into Climate and Building windows. Every input has real-time impact on the results. The software is able to save and load the data as project file (*.epp), climate data file (*.stm) and building data file (*.bld). Also, software is able to generate report in Microsoft Word format (Microsoft Office required for operation). The Climate window includes the input boxes for climate data.
The gray boxes on the right side are designed for the read-only purposes.
These values should be updated according to the user's input in other sections of the software. The Energy Passport software - Building window includes the input boxes for the building data. The input boxes are grouped by subject. The first tab groups the general data of the building. The second tab groups the building geometry data (Area, Volume and Exposure). The third tab groups the design data of the building as well as coefficients attributed to heating system energy efficiency.

Technical Data

Operating System ☒ **WINDOWS XP/Vista/7/8** ☐ **MAC [**Versions**]** ☐ **LINUX** ☐ **Others ……**	***Processor*** ***1 GHz*** ***Required memory*** ***512 MB*** ***Required disk space*** ***10 MB***

DOMESTIC ELECTRICITY CONSUMPTION DATA FOR RESEARCH AND SERVICE DEVELOPMENT

Pierre Ferrez[1]; Philippe Renevey[2]; Andreas Hutter[2]; Pierre Roduit[1]

[1] *HES-SO Valais-Wallis, Route du Rawyl 47, CH–1950 Sion 2, Switzerland*
[2] *CSEM SA, Rue Jaquet-Droz 1, CH–2002 Neuchâtel, Switzerland*

ABSTRACT

During the last few decades, citizens around western countries became more and more sensible to energy saving. However, while home electricity consumption is a source of concern, the means to reduce this consumption are not easy to find and implement for private individuals. Different studies show that displaying the home consumption could lead to a reduction of electricity use. However, the global consumption doesn't provide the consumer with sufficient information about what counts for the main part of their electricity invoice. Systems able to display the energy used by the main appliances would greatly help the consumer to find out which equipment should be replaced and/or which behavior should be modified. Implementing such systems requires the disaggregation of the consumption of the main appliances. One solution consists in measuring the global electricity consumption and extracting the most important information from the general load curve using signal processing methods and detection algorithms.

The HES-SO Valais-Wallis (University of Applied Sciences Western Switzerland) and the CSEM (Swiss Center for Electronics and Microtechnology) are currently working in this direction. To develop recognition algorithms from an aggregated load curve, an acquisition system able to measure the three phases of a standard household has been built. This system has been deployed in seven households and has been acquiring data sampled at 1Hz for over two years for the first deployment site. In two households Ecowizz [1] plugs are used to acquire disaggregated data of the main appliances in parallel to the central measure. In parallel the HES-SO Valais-Wallis is deploying the system in fifty households for one month.

The collected data allow a better understanding of the main contributors to the load curve as well as the useful characteristics to recognize them. To first tackle the complexity of the aggregated load curve, a simulator of the main contributors (washing machine, dishwasher, tumble dryer, oven, stove, etc.) was also created, thus allowing to initially test the disaggregation algorithms with an *a priori* knowledge of the contributors. Both the database of real signals and the simulator are new tools that will allow for new research and development of algorithms for the analysis of aggregated load curves.

Keywords: Electricity Consumption, Energy Management, Non-Intrusive Load Monitoring (NILM), Load Signatures, Household Appliances, Household Appliances Simulator, Disaggregation Algorithms

INTRODUCTION

Since the first energy crisis in the early 1970s, populations of the western countries became progressively aware of the importance of sustainable development and energy saving for preserving the environment but also for reducing their energy bills. In 2010, households in Switzerland have consumed 19 TWh and a typical Swiss household of 4 people consume about 4500 kWh, representing a 1000 USD electricity bill [2]. Although Swiss households could potentially save 40% of their electricity bills by 2035, thanks for example to the optimization of the energy efficiency of appliances [2], efficient tools to reduce this consumption are not easy to find and implement for private individuals. Different studies show that providing pertinent information about the home consumption could lead to a reduction of electricity use between 4 and 15% [3]. However, the general consumption doesn't provide the consumer with sufficient information about what counts for the main part of his electricity invoice.

On another hand, systems able to display the energy used by the main appliances, in other words systems able to disaggregate the global consumption, would greatly help the consumer finding out which equipment should be replaced and/or which behavior should be modified. The disaggregation could be achieved using a measuring unit embedded in each appliance, in a similar way to the Web of Things [4]. This kind of solution is however very difficult to implement, especially with the already existing appliances, and generates high investments and operating costs. Another way to achieve this disaggregation is to measure the global electricity consumption of the household and to extract the most important information from this general load curve. This solution only requires one measuring unit but requires a system able to recognize in real time the main appliances.

The HES-SO Valais-Wallis (University of Applied Sciences Western Switzerland) and the CSEM (Swiss Center for Electronics and Microtechnology) are currently working in this direction. In order to develop recognition algorithms to disaggregate the general load curve, a representative consumption data set was needed. Given the lack of publicly available large data set and the relatively poor precision of already installed measuring systems we had to develop our own acquisition system able to measure the three phases of a standard household. As a example, the data of previously deployed smart meters were at our disposal, but the period (15 min) and the precision (1 kWh) were clearly insufficient for our purpose. The setup is recording values of voltage, current, active power, reactive power, power factor and energy at 1Hz. The system has already been deployed in seven households for up to two years. In two households a series of Ecowizz plugs able to record the electrical "signature" of a single-phased appliance [1] are used to record the electricity consumption of different appliances in parallel to the central measure. The acquisition system together with up to eight Ecowizz plugs are currently deployed in fifty households for one month in order to build a representative database.

The collected data allow a better understanding of the main contributors to the general load curve as well as the useful characteristics to recognize them. To first tackle the complexity of the aggregated load curve, a simulator of the main contributors (electric heating, boiler, washing machine, dishwasher, tumble dryer, oven, stove, etc) has been created. The simulator allows the aggregation of fully generated appliances as well as the aggregation of previously recorded appliances. This simulator is a powerful tool to initially test different disaggregation algorithms as it provides an *a priori* knowledge of the different appliances and therefore allows quantitative evaluations of the performances.

METHOD

The measuring unit is a power meter PowerLogic Series 800 PM810 from Schneider Electric. This power meter is equipped with 40/5 current transformers and with RS485 communications for integration into any power monitoring/control system. The PM810 is a true RMS meter capable of accurate measurement of highly non-linear loads. The sampling frequency is 6.4kHz (128 samples per 50Hz cycles) and the sampling technique enables accurate measurements through the 31^{st} harmonic [5-6]. The data is integrated and finally sampled at 1Hz and values of voltage, current, active power, reactive power and power factor for the three phases are recorded. The system also allows to store the value of the total active energy. The measurement accuracy is 0.325% from 1A to 10A for the current, 0.375% from 50V to 277V for the voltage and 0.2% for the power [5-6].

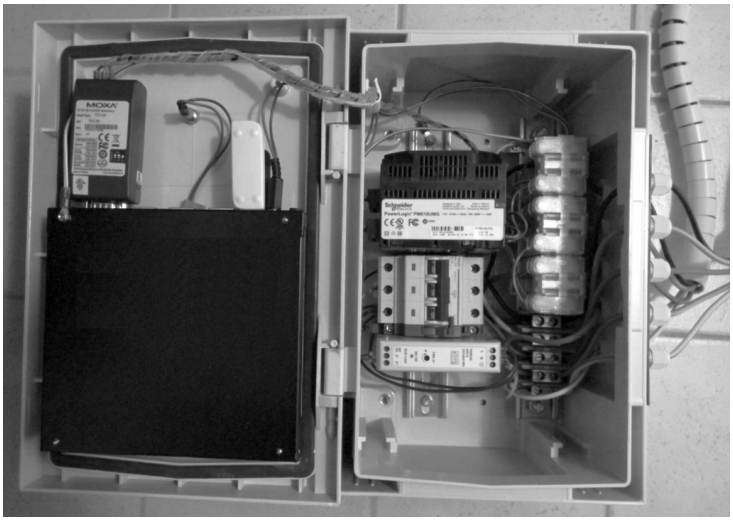

Figure 1: Data acquisition system.
The PC Engine can be seen on the left whereas the PM810 and the electric connections can be seen on the right.

The data is stored through a Modbus connection on a small PC platform (PC Engines [7]) running Voyage Linux [8], a very stripped-down Debian Linux. The data is stored in CSV files (Comma Separated Values) and is saved on two flash drives for redundancy. The data is composed of two timestamps (one from the PM810 and one from the PC Engine), the 3 voltages values, the 3 current values, the 3 active power values, the 3 reactive power values, the 3 power factor values and the cumulated active energy. The system generates one CSV files for every period of 24 hours, each CSV file consists thus of 86400 entries. The recordings are finally synchronized with a data server at the HES-SO Valais-Wallis that provides the final storage location. Figure 1 shows the details of the acquisition system, the PC Engine can be seen on the left whereas the PM810 and the electric connections can be seen on the right.

The simulator aims at producing realistic load curves by combining different electrical appliances. It is written in MATLAB and the format of the generated data is the same as the format of the "real-world" data recorded by the acquisition system. The simulator is based on configuration files defining the setup of the simulations (start and stop times, appliances to be used, phase(s) on which the appliances will appear, etc.) and models of the different appliances. Every electrical appliance used in the simulator is either gener-

ated using a statistical model or directly extracted from a database containing different measurements of the specific appliance. Two main aspects are modeled: the occurrence probability and the load curve. The occurrence probability varies during time (e.g. the dishwasher is more likely to be used around 1pm and/or 7pm rather than in the middle of the night). The statistical models contain parameters representing the appliance (number of cycles, duration of the cycle(s), duration of the different functioning states of the cycle, power levels of the different states, etc). The output of the simulation is stored in different files. The global load curves, similar to the "real-world" data, can be used to test different disaggregation algorithms. The particular load curves of every appliance used in the simulation can be used for quantitative evaluations of the disaggregation algorithms.

RESULTS

The acquisition system has been deployed in seven households and has been recording data sampled at 1Hz for over two years at the first deployment site. In two households Ecowizz plugs [1] are used to acquire disaggregated data in parallel to the central measure. In parallel the HES-SO Valais-Wallis is deploying the system in fifty households for one month to increase the statistical relevance of the database. Figure 2 shows a typical 24-hour recording of the active power for the three phases. A washing machine (over phase 1 & 2), a coffee machine, a tumble dryer (over phase 1 & 3), a dish washer and a fridge were used that day.

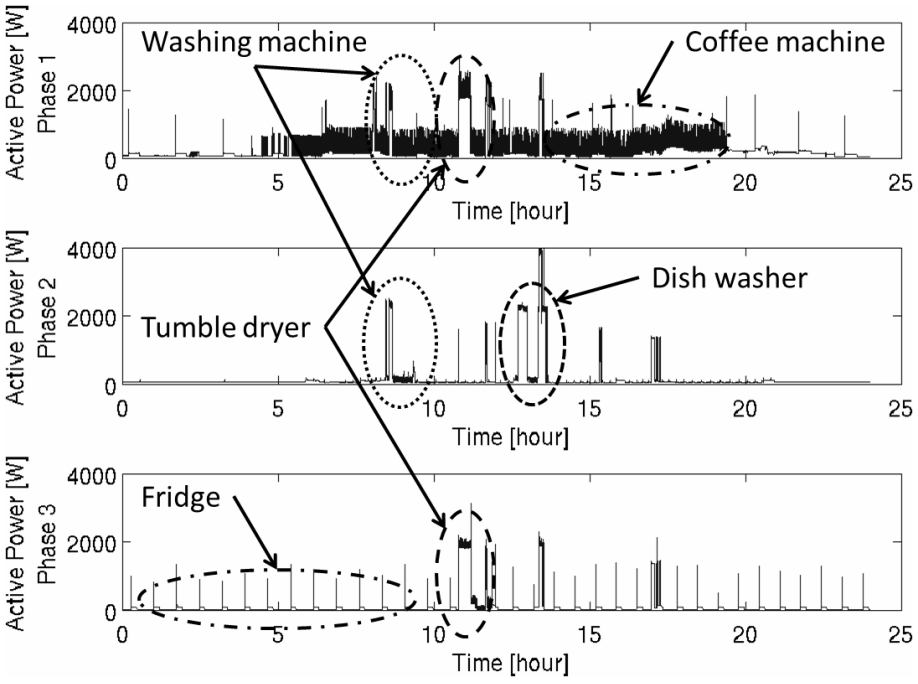

Figure 2: Typical 24 hour recording (active power, three phases).
A washing machine (over phase 1 & 2), a coffee machine, a tumble dryer (over phase 1 & 3), a dish washer and a fridge were used that day.

The simulator allows the aggregation of fully generated signals and/or the aggregation of previously recorded "signatures" of different high-consuming appliances. The user can choose to aggregate an electric heating, a boiler, a dish washer, a fridge, a heat pump

a tumble dryer, a washing machine, and cooking appliances. The user can also choose on which phase(s) the selected appliances will appear. Figure 3 shows a typical 24-hour simulation of the active power for the three phases. The simulation includes a heat pump (over phase 1 & 2), a washing machine, a fridge, a dish washer and a tumble dryer.

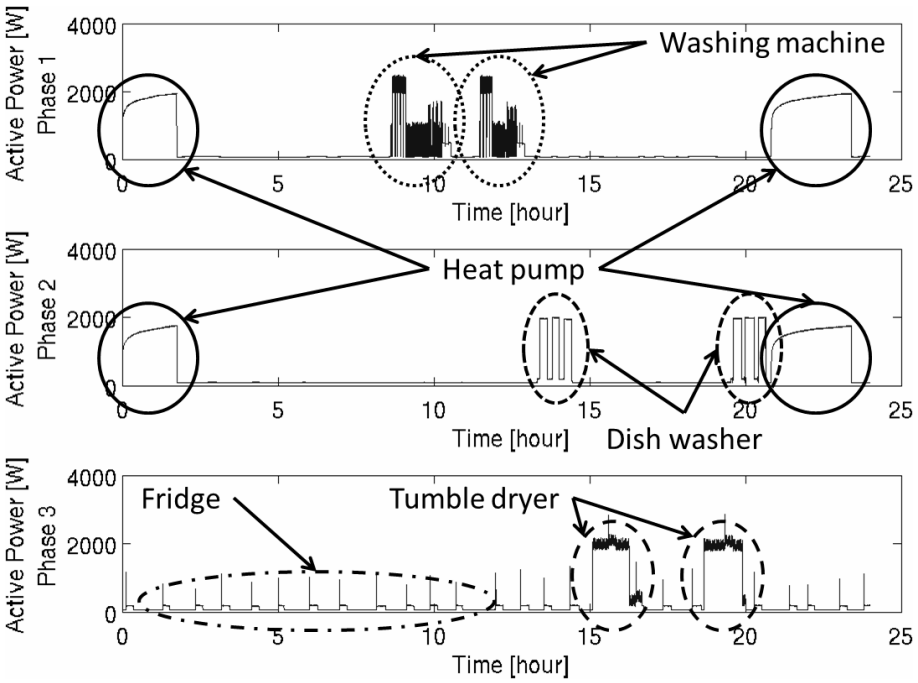

Figure 3: Typical 24 hour simulation (active power, three phases).
The simulation includes a heat pump (over phase 1 & 2), a washing machine, a fridge, a dish washer and a tumble dryer.

DISCUSSION

Research in this field is moving fast. Between our first measurements and the time this article was written (April 2013), a publicly available large data set of households electricity consumption appeared on-line [9]. Likewise, smart meters, which were initially developed for remote monitoring and billing purposes, are becoming more and more efficient, meeting the desired requirements (precision of a few Watts and data accessible each second). Moreover, solution such as the Solo II from Geo [10] counting the pulses from old smart meters should also provide the user with accurate enough data. All those low cost acquisition solutions would make data available for new services such as the analysis of aggregated consumption data.

Qualitative evaluations of different output of the simulator have shown a good match between simulated data and "real-world" measurement. Furthermore, the simulator is a powerful tool to test different disaggregation algorithms as it provides an *a priori* knowledge of the different appliances and therefore allows quantitative evaluations of the performances. This *a priori* knowledge could be obtained for "real-world" measurement using individual meters for each appliances, but generates higher investments and operating costs. Based on the recorded data and the simulator, different approaches for disaggregation algorithms are currently investigated with encouraging initial results.

ACKNOWLEDGEMENTS

This work was supported by the "The Ark Energy" project N^o 712-07 "i-BATs", the Commission for Technology and Innovation (CTI) project N^o 12553.2 PFIW-IW "Automatic Personal Energy Advising System (APEAS)" and the HES-SO project RCSO-TIC 29118 "Automatic Load Curve Automation (ALCA)".

REFERENCES

1. Ecowizz. http://www.ecowizz.net/
2. Office Fédéral de l'Energie (OFEN) - Statistiques de l'nergie. http://www.bfe.admin.ch/themen/00526/00541/00542/index.html?lang=en
3. J. Borstein and K. Blackmore, In-Home Display Unit: An Evolving Market, Part 1, March, 2008
4. Wikipedia, the Free Encyclopedia - Web of Things. http://en.wikipedia.org/wiki/Web_of_Things
5. Schneider Electric - Power Meter Series 800. http://www2.schneider-electric.com/resources/sites/SCHNEIDER_ELECTRIC/content/live/FAQS/140000/FA140345/en_US/PM800%20DataSheet.pdf
6. Schneider Electric - Power Meter Series 800. http://download.schneider-electric.com/files?p_File_Id=27600253&p_File_Name=63230-500-225A2_PM800_User_Guide_EN.pdf
7. PC Engines. http://www.pcengines.ch/
8. Voyage Linux. http://linux.voyage.hk/
9. J. Zico Kolter and Matthew J. Johnson. REDD: A public data set for energy disaggregation research. In proceedings of the SustKDD workshop on Data Mining Applications in Sustainability, 2011
10. Solo II, Geo. http://www.greenenergyoptions.co.uk/what-we-do/products/solo-2

BUILDING PERFORMANCE SIMULATION VISUALIZATION AS INVESTMENT DECISION MAKING ENABLERS FOR SUSTAINABLE BUILDINGS

N. Hamza[1]; P. DeWilde[2];

1: School of Architecture, Planning and Landscape, Newcastle University, UK, NE1 7RU

2: Environmental Design Group, Plymouth University, UK, PL4 8AA

ABSTRACT

Increasingly, companies strive to deliver project sustainability and indoor environments that are conducive to increasing human productivity in corporate buildings. Corporate environmental policies are underpinned by a strong nexus between business needs in an uncertain and resource constrained world, societal awareness, and governmental targets to decrease the economy's carbon footprint. Building Performance Simulation (BPS) is a key enabler for the realization of sustainable buildings, providing quantification of building performance for different design alternatives. Building performance simulation clearly has a role to play in the trend towards sustainable corporate buildings. Yet, it is ultimately in the boardroom that key decisions on investments in buildings are made. Boardrooms are arenas for human/social interaction as well as platforms for expert decision making. The decisions made on the board typically have different attributes, with performance needing to be balanced with other important issues such as cost, safety, capacity and others.
This paper explores how BPS results and their visualizations can aid key investment decision making in the boardroom regarding sustainable buildings. It uses an expert interviewing methodology to collect information from BPS experts in the field at senior management levels operating in large scale international companies and presenting BPS results to clients globally. Findings indicate that BPS experts often exchange knowledge by selecting and visualizing information from larger datasets of BPS results. They may use sophisticated information visualization techniques to overcome perceived cognitive limitations and information overload in the boardroom. It concludes that taking BPS results into the boardroom is a specialist and critical undertaking. While experts presently use advanced BPS visualizations to retain their competitive edge in the market, the interviews reveal that the level of economic funding for the project is changing methods in communicating building performance predictions in the boardroom

Keywords: boardroom decision making, building performance simulation visualizations

INTRODUCTION

Turkle (1995) states that '*We are moving towards a culture of simulation, in which people are increasingly comfortable with substituting representations of reality for the real*'. BPS tools present virtual predictions of environments that are communicated by experts to persuade board members, as the main financial decision makers, to invest in sustainable building.

High profile sustainable building projects are built statements of the corporate forward thinking and ethical responsibility towards combating climate change. Hamza (2011) analyses case studies of corporate sustainable buildings, where the ethical commitment, combined with ambitious corporate goals, provide impetus for building design teams to push design boundaries, allowing ample opportunity for the use of building simulation tools. Further analysis, discussions and examples of 2D-graphes and 3D-visual materials that are presented

in the corporate boardrooms and project developers can be found in (Hamza and DeWilde, 2013)

While building simulation is now making inroads into boardroom decision making, thus far there is no dedicated research into this particular use of simulation outputs, the underlying drivers, and the peculiarities that govern success in influencing boardroom decisions. Sheppard (2012) argues that information processing of issues related to climate change (buildings as contributors to carbon emissions in our case) have to be balanced and professionally crafted based on the receptors expertise, pre-existing knowledge, attitudes and values and the length of time given to this encounter. A desired effect of this encounter would be to affect cognition (knowing and learning). The main goal of using visualizations for building performance and building carbon emissions is to create a positive emotional and behavioural change to motivate the boardroom into decision making and action towards investment in sustainable buildings. Building performance information visualization needs to be *'technically defensible' and 'culturally palatable' to create a shared space of knowledge exchange and decision making'* (Loukissas 2012:11)

Corporate decisions to construct sustainable projects are governed by board members with diverse technical experiences, often from different industries and companies. These members will vary in their domain knowledge, the problems they have been exposed to and the problem-solving skills they have developed (Rindova, 1999). Boardroom meetings regarding these projects typically include the owner/representatives, company directors, building architects, sustainability consultants and, wherever possible, in-house building performance simulationists. As with investment decisions, the use of external building performance consultants to undertake building performance simulation (even if there is in-house experience) is attributed to the need for a second expert opinion to increase the credibility and success of decision-making, and as a 'shield for liability' (Waltin, 2012).

METHOD

This paper explores how BPS results aid key investment decision making in the boardroom regarding sustainable buildings, with a focus on the visualization of building performance. The term `visualization` is inclusive of graphs, 3D images and walkthroughs

The focus on experts and their high-performing teams is based on their track record of effective reasoning, reliable expert advice and effective communication in design teams that has led to the realization of award winning sustainable buildings in major national and international architectural projects. The paper applies a broad understanding to 'documentation', including traditional paper based reports and graphs, as well as state-of-the-art multimedia animations, probing the experts in terms of what data visualization techniques they use, and why. Expert interviews are typically used as a method of qualitative empirical research, and are suitable mechanisms for theory generalization, exploration of expert knowledge, and for augmenting a critical literature review. Pfadenhauer (2009) defines an 'expert' as an actor who has a good overview of the overall status as well as specialist knowledge in a given discipline. An expert thus is aware of what the specialists in this discipline know and how this relates to knowledge of other specialists. They have privileged access to information and the responsibility for planning and undertaking problem solving decisions regardless of their team's numbers or specialisms.

Semi-structured interviews were constructed based on the salient issues highlighted in the literature review on methods of facilitating knowledge exchange in the context of boardrooms. Telephone interviews were conducted with twenty eight directors and managers in five international companies, all with headquarters in the UK. The interviews or conference

calls lasted between 20-40 minutes and were thematically focussed on the use of building performance simulation tools in practice, and on the exchange of information and knowledge with stakeholders and colleagues in a boardroom decision context. Introductions were used to include activities and roles of team members, relevancies and maxims connected with various positions and functions. The team members themselves all had a range of 10-30 years of experience in practice. Interviews were taped with permission from interviewees and respondents annonymised, with this paper just stating their role in the team.

The semi-structured interviews were carried out to investigate six areas of interest:

- The knowledge background of those in the BPS teams within each company;
- The knowledge background of clients' representatives in boardroom meetings;
- The reasons for the use of BPS, and the need to use information visualization;
- Techniques and methods used for exchanging data output, and the complexity of visual structure techniques used and their temporal encoding.
- Extending the knowledge transfer beyond assurance of performance. Discussing design options explaining BPS data and outputs' uncertainties.

Data analysis followed a two tier classification, as suggested by Straus and Corbin (1990). 'Open coding' was carried out in which the various responses were categorized into key words; the second stage created a 'selective and thematic coding' in which a central storyline was created to better reflect current practices in processing building performance information and the communication of the results within a boardroom situation.

DISCUSSION

The Boardroom Scene:

Interviews reveal the mixed background of developers and their representatives in the boardroom requires strategic decisions on what and how to present BPS results. It is evident that presentation formats are affected by the consultants' perception of the level of the boardroom audience's understanding and knowledge of BPS. Also, this affects how consultants translate the projects' briefs to meet or exceed building energy saving targets.

'In the UK, we have stringent building regulations, I frequently present to knowledgeable people in BPS, working for large retailers and oil companies. They are regional managers and facilities managers, the architects and sometimes BPS specialists who work for the clients.' [Director]

'I work nationally and in the Middle East; when we meet clients there is an architectural team present. The clients may be there in person, with their financial representatives and sometimes representation from their estates departments, they might have not dealt with BPS before and we use different visualization tools to catch the clients' interest. Building performance simulation companies want to sustain their competitive edge and will endeavour to generate complex media for BPS information exchanges such as walk-throughs and 3D environmental models.' [Director]

The project brief may request prediction of future building performance under scenarios of climate change in which exceeding regulatory conformity is a target, extending the role of BPS visualizations.

'If clients are forward thinking and require proof that their buildings will continue to perform sustainably and resiliently, the work that we're doing with Land Lease on the Olympic Village, we use the software to make sure that residential units - or if you like hotel rooms-

are not only going to operate properly for the athletes, it's not only designing a building that will work in a year, but it's going to continue to perform for another 20 years. We need to present this to the clients and visualization of data is necessary'. [Director]

What To Present?:

Interviews reveal that the level and number of visualizations used in the boardroom are dependent on consultants' perceptions and understandings of their clients' information needs.

'A good consultant will know what the client needs to know and present it' [Team Manager]

The interviews also show that the decisions on inclusion of BPS visualization in presentations to the board were undertaken by the BPS teams intuitively. The consultants conceded that they were not graphic designers and depended on the default graphical presentations from simulation software. They highly valued the role of BPS visualisations:

'As boardroom members are increasingly knowledgeable about BPS, the tools and the possible outputs, we are increasingly depending on 2D graphs to show thermal conditions, and sometimes still 3D to show daylight and ventilation conditions. Sometimes we need to develop virtual walk-throughs to translate the environmental and technical performance' [Team Manager]

3D presentation of results relies on a combination of BPS tool outputs exported into visualization software tools using high computational power for rendering processes. However, time spent on generating 3D walkthroughs and detailed building simulation visualization has been reducing substantially over the last 5-6 years even before the economic downturn:

'It has to do with the economic situation and the project funding. We still need to retain a profit and if clients are more knowledgeable about the software capabilities and predictions we need less [sic]visualizations to externalize our knowledge. Verbal communication of expertize is used to answer any further queries on building performance' [Director]

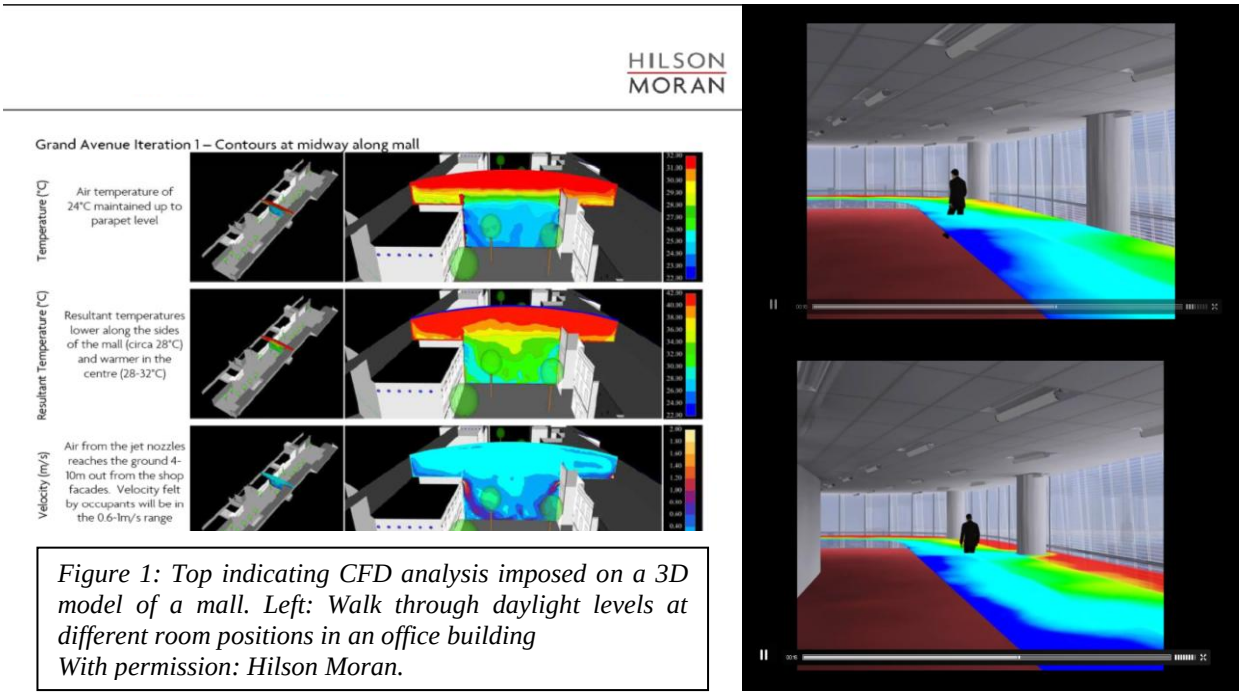

Figure 1: Top indicating CFD analysis imposed on a 3D model of a mall. Left: Walk through daylight levels at different room positions in an office building
With permission: Hilson Moran.

Interviews reveal that experts were intuitively aware of the main issues of reducing cognitive loads and also confirm that they made targeted presentations of BPS visualizations that would answer questions on performance but would not 'waste time' in proposing alternatives if the simulations of the proposed design indicated that they had met intended design targets. Also, the information exchange does not focus on uncertainties of the data outputs and scenarios of the building when in use leading to the possibility of the actual building deviating from predictions. However, there was an indication that these issues would be communicated verbally and more extensively in a detailed report to the board and the design team rather than in visualizations.

'This is a litigious issue. We need to protect ourselves by mentioning that the actual building will definitely perform differently as it will be occupied, have IT facilities and will change in its use over time' [Director]

'All tools have inherent errors and calculation limitations and approximations; this is a highly technical issue. The board members sometimes have to endure day-long design meetings of which many decisions on the building construction take place, we cannot waste the board's time' [Team Manager]

RESULTS AND KEY FINDINGS

This paper explores how building performance simulation visualization of outputs is an aid in key investment decision making regarding sustainable buildings in the boardroom. Through a series of interviews with elite consultants (experts) it gathers both opinions and examples of how building simulation results are presented to boards of directors. The results demonstrate how experts externalize what is normally seen as specialized and technical knowledge of building performance in a demanding context, where client interests, expertise, finance and litigation need to be taken into account.

Findings confirm that:

- Experts are aware that documentation that feeds into boardroom decisions needs to be of high quality; directors face both issues of data overload as well as of insufficient information. Interviews also suggest a preference for boardroom documentation that (1) is based on facts, evidence and analysis (2) makes explicit any uncertainties and (3) is transparent in terms of the logic used to prepare the documentation.

- The interviews and literature support the premise that different BPS outputs visualizations (graphs, tables, and animations) are sensory and perceptually effective tools for a wide-ranging audience in the boardroom. However, BPS results need to be combined with well-presented textual reports and physical architectural models and drawings when presenting to the boardroom.

- Experts actively manage the presentations of data outputs and sometimes 'tweak' and 'tune' it to highlight certain performance aspects. They confirm that visualizations are sensory and perceptually effective tools to a wide ranging audience in the boardroom. However, BPS visualizations need to be backed up by well-presented textual reports and physical architectural models and drawings when presenting to the boardroom.

- Visualizations do not normally highlight uncertainties in modelling, nor do they demonstrate the interlinked nature of cause and effect in results. Experts are aware that visualizations of high resolution and data contents may obscure issues of validity and the reliability of BPS results, and that these need to be communicated in boardroom presentations

and the final textual reports alike to avoid leading the focus of attention away from the relevant information and to avoid possible litigation actions in the future.

• While experts presently use advanced BPS visualizations to retain their competitive edge in the market, the interviews reveal that the level of economic funding for the project is changing methods of building performance communications. It remains to be seen how recent economic developments will impact the high end of building simulation result presentation in the boardroom in the long run, and whether a niche of special visualisation techniques will develop - or whether this will remain a domain that is mainly driven by experts combining the best from the building simulation and visualisation worlds.

ACKNOWLEDGMENT

The authors would like to thank building performance simulation teams in Hilson Moran, Fosters and Partners, AECOM, Buro Happold and ARUP's London for their valuable contributions and insights to this paper and dedicating the time for interviews. Acknowledgment is also extended to the late Dr.Sameh Shaaban for lengthy discussions on the importance of using information visualization techniques in communication.

REFERENCES

1. Hamza, N: Identity of Sustainability: from the technical to the sensory and experiential. 27th International Conference on Passive and Low Energy Architecture, pp.39-44, Louvain-la-Neuve, Belgium, 2011 (available on-line)
2. Hamza, N. and DeWilde, P: Building simulation visualization for the boardroom: an exploratory study. Journal of Building Performance Simulation, Taylor and Francis, Published on-line 14th of March 2013, DOI:10.1080/19401493.2013.767377
3. Loukissas, Y: Co-Designers, cultures of computer simulation in Architecture. Routledge, 2012
4. Pfadenhauer, M: At eye level: The expert interview-a talk between expert and quasi-expert, in Interviewing Experts, Bogner, A., Littig, B. And Menz, W.(Ed), Palgrave MacMillan, 2009
5. Rindova, V: What corporate boards have to do with strategy: a cognitive perspective, Journal of Management studies, Vol.36,pp 953-975 .
6. Sheppard, S: Visualizing Climate Change, A guide to visual communication of climate change and developing local solutions, Routledge, New York, 2012
7. Strauss, A. and Corbin, J: Basics of qualitative research; grounded theory procedures and techniques, SAGE Publications, California, 1990
8. Turkle, S: Life on the screen: Identity in the age of the internet. Simon &Schuster, 1995

THERMAL MODELLING OF A LOW EXERGY HVAC SYSTEM IN ENERGYPLUS: A CASE STUDY

C. Hersberger[1]; C. Sagerschnig[2]

[1] *Architecture & Sustainable Building Technologies (SuAT), Institute of Technology in Architecture (ITA), ETH Zürich, Building HPZ Floor G, Schafmattstr. 32, 8093 Zürich*
[2] *Roschi + Partner AG, Sägestrasse 73, 3098 Köniz*

ABSTRACT

Conditioning of buildings is responsible for a large part of the man-made greenhouse gasses; therefore low energy buildings can contribute a significant amount to the solution of the problem. Amongst low energy buildings, the low exergy approach has a high potential, because it is efficient, cost-effective and suitable for newly built houses as well as for retrofit projects.
Low exergy (LowEx) setups consist typically of water-based low temperature heating systems and high temperature cooling systems. In order to assess the energy performance and thermal comfort of buildings equipped with these systems, detailed modelling of HVAC equipment as well as their controls is required. Models have to represent these systems and their dynamical behaviour and impact on the thermal building mass and temperature with sufficient accuracy. In this case study we focus on LowEx zone equipment in EnergyPlus; we develop models namely for low temperature radiant heating and high temperature cooling panels and a decentralized ventilation system. Further we show an exemplary tuning process for those radiant panels and ventilation systems. The tuning process includes integration of manufacturer data and verification of the EnergyPlus component model, with very limited measured data available for comparison.
We conclude that modelling of LowEx zone equipment must be preceded by detailed component sizing and tuning; a procedure which currently cannot be automatized. Further the simulation results should be compared and validated with measurements. As a field of further research the development of a standardized process for model tuning and verification is recognized. In order to make LowEx simulations more convenient and feasible in terms of required time and modelling effort we suggest the development and integration of simplified idealized water-based equipment models into EnergyPlus.

Keywords: simulation, thermal modelling, EnergyPlus, heating, cooling, ventilation, low exergy, LowEx

INTRODUCTION

Motivation Heating and cooling processes in residential and non-residential buildings are responsible for a large part of the man-made greenhouse gasses [1]. Several strategies to use energy more efficiently were developed in the last years, i.e. passive houses or the low exergy strategy [2]. The latter is especially suitable for retrofit projects [3], as it lowers the requirements on the insulation of the building envelope (at the cost of an increased complexity of building systems). LowEx systems operate at very small temperature differences to the room air temperature, i.e. zone equipment that provides high-temperature cooling and low-temperature heating in order to use as little high quality energy (exergy) as possible.

Scope In this publication we discuss the thermal modelling of LowEx HVAC components used in a retrofit project. We present results of a study on energy and thermal comfort performance of radiant heating and cooling ceiling panels. This case study focuses on secondary LowEx systems (i.e. zone equipment); primary systems (e.g. heat pumps) and other plant-related devices are not treated. A main goal of the study was (i) the application of existing radiant systems models in the EnergyPlus simulation environment and (ii) assessing the suitability and potential obstacles for using these models for LowEx buildings.

HPZ BUILDING CASE STUDY

For this study the EnergyPlus building simulation environment was chosen. This environment provides models for radiant ceiling panels; however experiences and documentation of applying these models for LowEx building components are limited.

Case Description The HPZ building is located on the Hönggerberg campus of ETH Zürich. It contains offices of different chairs and was erected in the early 1970 and renovated from 2010 to 2012. The renovation was performed after the LowEx/low cost concept [4], thus only windows and HVAC systems were replaced; the opaque parts of the façade were left unchanged, even though their thermal insulation properties are poor.

HVAC System The newly installed HVAC zone equipment consists of low temperature heating/high temperature cooling panels that were mounted thermally coupled on the concrete ceilings (fig. 6). Radiant panels and ventilation units are connected to a common water circuit that supplies hot or chilled water, depending on the demand; the circuit is operated with a central pump and supplied with heat and cold from a central anergy network on the university campus.
The water flowrate in the ventilation unit coils is not controlled at room level. The radiant panels are individually controlled: depending on zone demand, decentralized pumps are pulling water from the water loop; the pumps have simple on/off controllers based on room air temperature.

MODELING

Implementation and Objectives The following sections give an overview of the modeling set-up. Focus is given to the radiant ceiling panels. Specific EnergyPlus sub-models mentioned are referenced in monospaced font (e.g. `DistrictHeating`). Detailed documentation on all EnergyPlus models is available in the online documentation [5].

Design Parameter	Abbr.	Heating	Cooling
Supply Water Supply Temperature	$T_{Water,sup}$	34 °C	18 °C
Supply Water Return Temperature	$T_{Water,rtn}$	31 °C	21 °C
Room Air Temperature	T_a	20 °C	26 °C
Water Temperature Difference	ΔT_{Water}	3 °C	3 °C
Temperature Difference Water To Room Air	$\Delta T_{Water,Air}$	12.5 °C	-6.5 °C
Heating/Cooling Rate	$\dot{q}'$	110 W/m^2	58 W/m^2

Table 1: Design properties of low temperature heating/high temperature cooling panels as given by the manufacturer [6].

Modeling of the radiant ceiling panels and ventilation units was based on very little available technical product specifications, see table 1. The goal of the study was to (i) develop plausible zone models based on limited available input data and (ii) reproduce design data for the ceiling panels as provided by the manufacturer.

Thermal Model The building simulation model for HPZ building consists of 22 thermal zones; corner offices were treated as separate zones, whereas other offices were grouped in one zone per orientation (fig. 3). As our model only treats secondary LowEx systems in detail, heat/cold supply (and thus primary systems) are represented with ideal energy suppliers using `DistrictCooling` and it's heating counterpart.

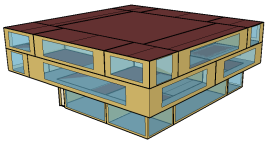

Figure 1: Sketchup 3D rendering of HPZ model.

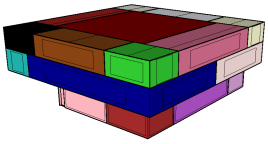

Figure 2: Sketchup rendering of HPZ thermal zones.

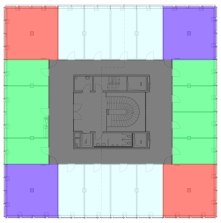

Figure 3: Exemplary floor plan with thermal zoning.

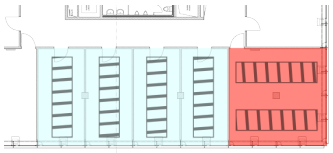

Figure 4: Floor plan detail: 2 zones with position of radiant panels.

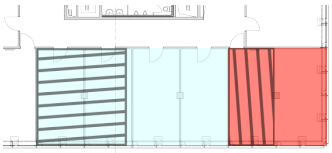

Figure 5: Radiant panel surfaces as represented in the model corresponding to Figure 4.

Radiant Panels Low temperature heating/high temperature cooling radiant panels were represented with `ZoneHVAC:LowTemperatureRadiant:VariableFlow` components (abbr.: LTRVF). The aluminum skeletal structure is relatively lightweight compared to the thermally activated concrete, therefore it was neglected. The radiant panel construction (model: `Construction:InternalSource`) was chosen to be identical to the rest of the ceiling, with one additional layer, a white painted steel-plate. The LTRVF tubing was placed right underneath the steel plate. The radiant panel sizes were chosen to match real-world panel sizes, however, multiple panels in the same zone were merged into one surface area and the exact localization was not represented (fig. 4, 5). LTRVF tubing length and inside diameter were also chosen as in real world. A simple thermostatic on/off control with hysteresis based on room air temperature was implemented with EnergyPlus' Energy Management System (EMS).

Ventilation Units The model for the decentralized ventilation units consists of a `ZoneHVAC:AirDistributionUnit` and a simple `AirLoopHVAC` with a corresponding outdoor air node for each thermal zone. The air flow rate is EMS-controlled, switching between two levels based on zone occupancy. The model's ventilation units run at 100% outdoor air rate. Water coils are used for air conditioning. Dimensioning of the coils was based on manufacturer data [6]. A custom EMS controller for the supply air temperature setpoint, based on outside and inside temperature and coil efficiency, was implemented.

Figure 6: Photograph of radiant panels in HPZ building.

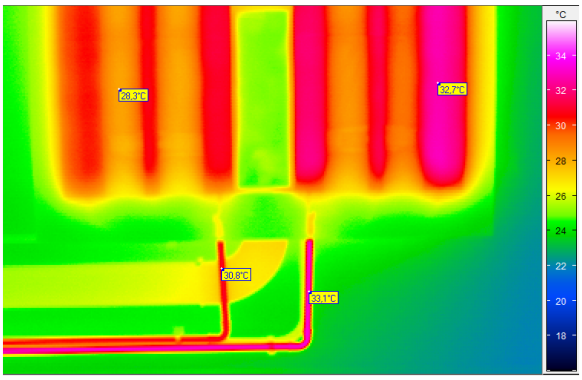

Figure 7: Thermal image of radiant panel in operation on an average winter day with $\Delta T(Water) = 2.3°$ C. Emissivity value $\varepsilon = 0.9$ assumed for all surfaces.

PARAMETER TUNING

Model tuning proved to be necessary for the radiant panels and for the decentralized ventilation units. In this paper we will focus on the radiant ceiling panels. Two parameters were identified to be most sensitive for panel performance: (i) tubing length as a main parameter for panel efficiency and (ii) surface convection coefficients for heat transfer to room air.

Convection Coeffcients The first simulations showed (fig. 8) that the difference of supply water temperature to return water temperature $\Delta T(Water)$ was much higher than expected and observed on thermal images (fig. 7). The first modification of the model was to change the surface convection algorithm used. We switched from the EnergyPlus default algorithm `TARP` to `AdaptiveConvectionAlgorithm` [5]. Further, as the observed convection coefficients for the radiating surfaces were much lower than expected from literature [7], we implemented EMS-controllers to specifically override EnergyPlus' default coefficients for the surface areas of the panels.

Panel Efficiency As the simulated temperature differences were still not matching manufacturer specs, namely the heating/cooling rates and therefore $\Delta T(Water)$ being too big, we modified the radiating panel efficiency using LTRVF's tubing length as a tuning parameter. In EnergyPlus, efficiency ε of the panels is modelled after the NTU-effectiveness method [8, 5]: $\varepsilon = 1 - e^{-NTU}$ with $U := (UA)/(\dot{m}_w \cdot c_w) = (h\pi DL)/(\dot{m}_w \cdot c_w)$ (with the number of transfer units NTU, the convection coefficient h, the tubing D and the tubing length L). The first simulations were performed with a tubing length corresponding to real-world dimensions (fig. 8, #1 to #4); later we reduced the tubing length by a factor of 30 (#5 and #6) while still keeping it variable (depending on panel surface area) from zone to zone. Further simulations were performed with constant tubing length over all zones independent of panel size (#7 to #14).

Discussion Reproduction of manufacturer data for the radiant ceiling panels turned out to be tricky as the panels' heating and cooling power was very sensitive to the chosen parameter sets. Heating power was more sensitive than cooling power regarding variation

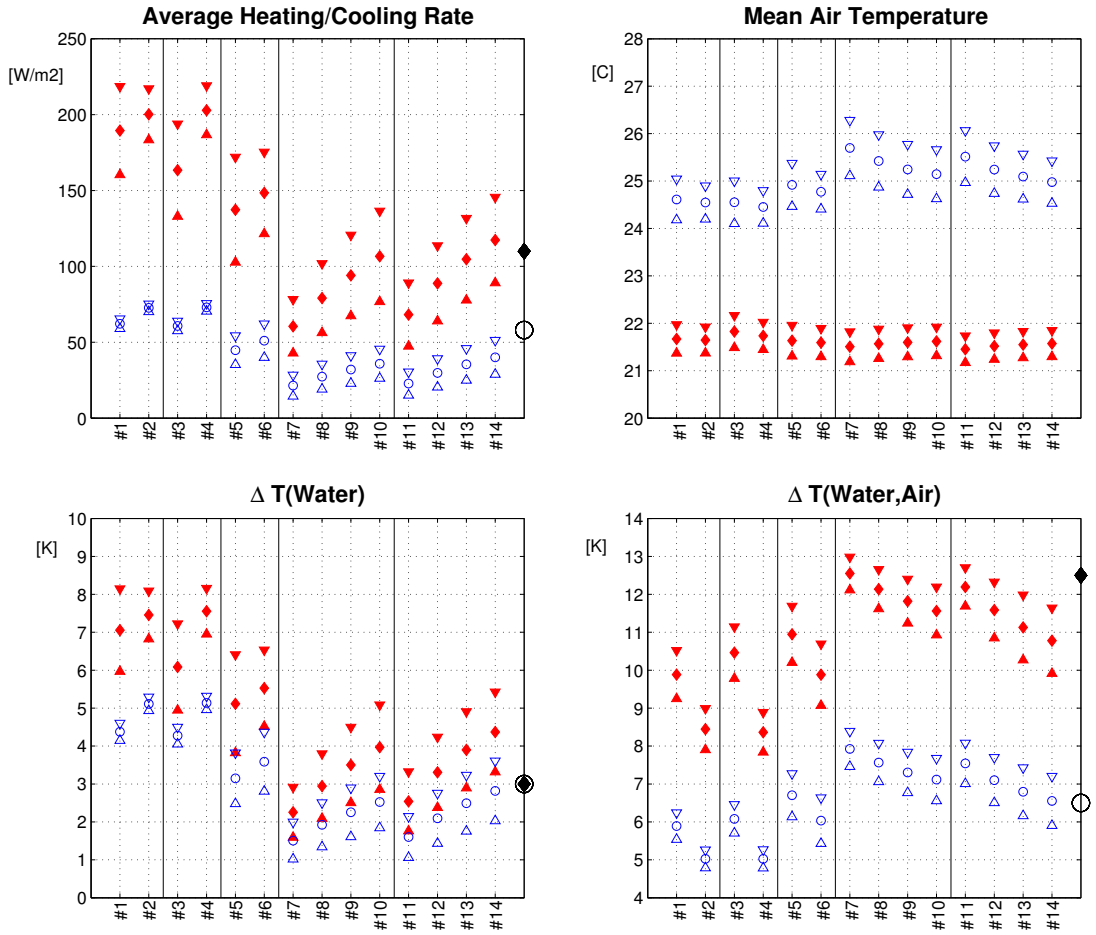

Parameter Set	#1	#2	#3	#4	#5	#6	#7	#8	#9	#10	#11	#12	#13	#14
Tubing Length [m]	original				short		1.0	1.5	2.0	2.5	1.0	1.5	2.0	2.5
Conv. Coeff. Algorithm	TARP		Adaptive		TARP									
EMS Conv. Coefficients	def.	EMS	def.	EMS	def.	EMS	default				EMS			
Heating: Avg. Conv. Coeff. [W/m2K]	1.3	2.8	0.5	2.9	1.3	3.2	1.2	1.2	1.3	1.3	4.6	4.0	3.7	3.4
Cooling: Avg. Conv. Coeff. [W/m2K]	2.3	7.9	1.7	7.9	2.0	9.5	1.6	1.7	1.8	1.9	10.8	10.5	10.1	9.9

Figure 8: Simulation results for different configurations of the radiant panels: heating (⧫) and cooling case (○). The values are area-weighted averages and variance (+/- 1 standard deviation). Black symbols on right y-axis represent design parameter values as listed in table 1.

of panel efficiency and surface convection coefficients. We suppose that this behaviour is driven by the higher temperature difference from water to room air in the heating case. In general, both temperature differences (supply to return water, mean water temperature to room air temperature, respectively) showed large spread. Design data given by the manufacturers could be reached by tuning the panel efficiency, even tough this meant to apply somewhat unrealistic tubing lengths for the panels.

Despite varying panel power, mean room air temperature, however, was very stable in the heating case. Additionally available heating devices (ventilation units, radiators in corner offices) balanced the panels missing heating energy. In the cooling period, mean room air temperature was more sensitive to the cooling power provided by the ceiling panels as there was only limited cooling available by the ventilation units. We conclude, that room air temperatures might be simpler to reproduce from measurements whereas assessment of the overall energy consumption is more difficult if zone equipment exceeds a single device.

Further Tuning Parameter modifications were also necessary for the decentralized ventilation units (not shown). As for the radiating panels, we needed to lower the efficiency (i.e. the calculated heating coil UA value) to achieve the design specifications, namely the low supply to return water temperature difference $\Delta T(Water)$.

CONCLUSIONS

The little amount of data available from the manufacturer - basically just the design points for heating and cooling operation - and the lack of monitoring data during panel operation proved to be hindering for a substantial validation of the model.
The available radiant ceiling panel models in EnergyPlus provide a great deal of flexibility. In combination with the supported algorithms for modeling convection coefficients, EnergyPlus proved to be a powerful tool for modeling this kind of LowEx systems. However, the complexity of the model and the sensitivity to the chosen convection algorithms lead us to conclude that a certain amount of uncertainty remains when modeling radiant ceiling panels. Especially, for practicioners with limited time for parametric studies and only limited data available (both from manufacturers and on-site measurements) sufficient model validation is tricky. In order to make LowEx simulations based on water-based equipment more convenient and feasible in terms of time and modelling effort, we suggest to enhance the available simplified equipment models in EnergyPlus by integration of simplified, idealized hydronic zone equipment; further, the modelling procedure for water-based systems could be simplified by providing templates or processes for automatted source code generation [9].

ACKNOWLEDGEMENTS

The authors would like to thank the chair of building physics for lending us the thermal imaging camera and instructing us how to use it.

REFERENCES

1. Metz, B., et al.: *Climate Change 2007: Mitigation of Climate Change.* Cambridge University Press, Cambridge and New York, 2007.
2. Shukuya, M.: *Exergy concept and its application to the built environment.* Building and Environment, 2009.
3. Meggers, F., et al.: *Low exergy building systems implementation.* Energy, 2012.
4. TEC21: *Modellfall Sanierung HPZ.* TEC21, Zurich, 2011.
5. EnergyPlus Website: *http://apps1.eere.energy.gov/buildings/energyplus/*
6. BS2: *HeptaSystem Technical Manual Version 2.1 / AirboxSystem Technical Manual Version 2.2.* 2010.
7. Glück, B.: *Heizen und Kühlen mit Niedrigexergie (LowEx) – Innovative Wärmeübertragung und Wärmespeicherung.* Clina Heiz- und Kühlelemente GmbH Berlin / Westsächsische Hochschule Zwickau (FH), 2008.
8. Incropera, F. P., et al.: *Fundamentals of Heat and Mass Transfer.* John Wiley & Sons US, 6th edition, 2001.
9. Miller, C., et al.: *Automation of Common Building Energy Simulation Workflows Using Python* IBPSA, 2013.

A QUALITATIVE MODELING APPROACH FOR FAULT DETECTION AND DIAGNOSIS - IMPLEMENTATION AT TWO EUROPEAN AIRPORTS

T. Müller; N. Réhault; T. Rist; F. Ohr

Fraunhofer Institute for Solar Energy Systems - ISE, Heidenhofstraße 2, 79110 Freiburg, Germany

ABSTRACT

The objective of the European project "CASCADE ICT for Energy Efficient Airports" is to develop an ISO 50001 Energy Management System supported by Fault Detection and Diagnosis (FDD) for heating, ventilating and air-conditioning (HVAC) systems and to implement and test it in two major European airports Milano Malpensa and Roma Fiumicino. FDD aims to recognize faults quickly, systematically and – as far as possible – automatically before too much energy is wasted. In the project, a model based approach using qualitative modelling of HVAC systems is developed and investigated. This paper describes the qualitative modelling approach developed for FDD purposes. A quantised system - describing the qualitative behaviour of a dynamical system - is established by transforming numerical inputs into qualitative values or states. Then, the qualitative model, based on a stochastic automaton, is used to determine system-states or outputs that may occur in the future. The supervision of the current states, inputs and outputs of the system allow the prediction of the future system states. The stochastic automaton determines the probability that a subsequent condition might occur. A stochastic automaton can then be used for FDD purposes by comparing the expected states of the faultless system with the occurring states of the real process. The development steps are first the construction of a model of the dynamic process that describes the faultless behaviour of the considered system, and then the abstraction of a qualitative model based on a stochastic automaton that describes the dynamic system. The algorithms are first developed and tested by using simulation models of faultless and faulty heating circuits under the simulation environment Dymola®/Modelica®. It is then planned to test the qualitative models against real data incoming from the airports pilot buildings and to assess their performance for FDD and their economic viability in terms of engineering efforts and costs by comparing them with a rule-based FDD system.

Keywords: heating, ventilating and air conditioning, FDD, qualitative modelling

INTRODUCTION

Large amounts of energy up to 30 % are currently wasted in commercial buildings due to insufficient maintenance, faulty equipment or wrong schedules or control loops setup. A significant part of this energy could be saved by the practical implementation of automated Fault Detection and Diagnosis (FDD) to support a condition-based maintenance [1]. Although big research efforts have been carried out in the last two decades, but there are only very few commercially available FDD tools for heating, ventilating, air conditioning, and refrigeration (HVAC&R) systems which are emerging on the market. The aim of the FP7 European project CASCADE is to develop an ISO 50001 Energy Management System supported by FDD for HVAC&R systems and to implement and test it in two major European airports Milan Malpensa and Rome Fiumicino. The developed methods and tools will be implemented and tested at the Malpensa Airport which is with 18.7 million passengers the second largest Italian airport behind Rome Fiumicino. In 2012, the energy consumption for heating was about 132.5 GWh and 112 GWh for cooling. Especially buildings of this size and complexity present a

special challenge for the application of FDD methods. The design of tools for automated support maintenance is especially challenging in the airport context due to the size and complexity of their different energy systems, and Building Automation Systems (BAS). Particularly in large buildings with many different systems, the most spread FDD approaches which are based on "If-Then-Else" rules often reach their limits due to the combinatory explosion of rules. The aim of this paper is to investigate and implement concretely a different approach, which allows to minimize the above mentioned problems. This approach uses a stochastic automaton as qualitative model and is referred to as "QuaMo". This method is mainly based on the work of Lichtenberg [2] and Schröder [3].

Figure 1 shows an overview of the most popular approaches of qualitative models for FDD purposes. It should be noted, that the classification of qualitative models is not uniform in the literature. The following overview of the different methods is based on the work of Katipamula [1]. Other classifications are described by Venkatasubramanian [4] and Isermann [5].

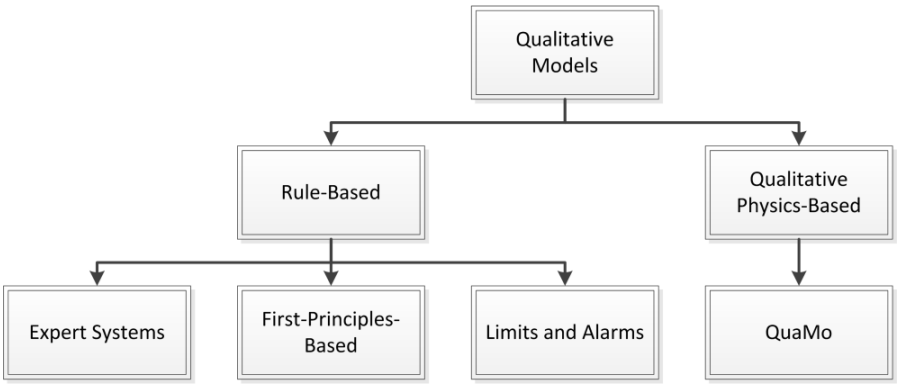

Figure 1: Classification of qualitative modelling approaches, based on [1]

The QuaMo approach can be used for supervision and FDD purposes of quantised systems. A quantised system uses quantisers to transform numerical inputs into qualitative values or states. Thus, a quantised system describes the qualitative behaviour of a dynamical system [2].

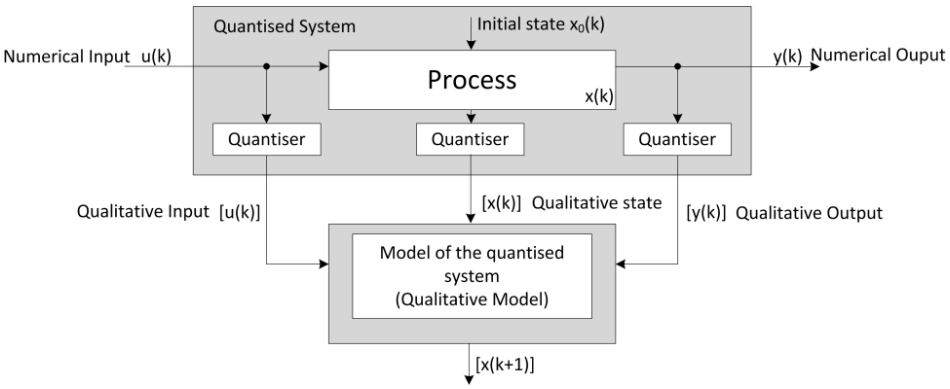

Figure 2: Supervision of a quantised system, based on [6].

Quantisation means reduction of information. Therefore the amount of information that needs to be processed by the supervisor is reduced to minimum [3]. The following Figure shows the

quantisation of a continuous-time and continuous-variable signal into a quantised signal. The value of the quantised signal can have a symbolic character like “high” or “low”.

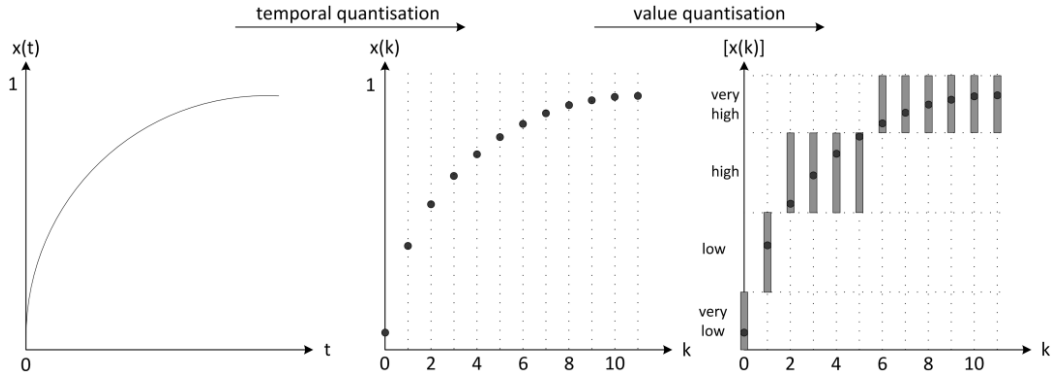

Figure 3: Signal quantisation, based on [3]

HOW CAN A QUALITATIVE MODEL BE USED FOR FDD?

A qualitative model based on a stochastic automaton can be used to determine system-states or outputs that may occur in the future. This prediction is based on the supervision of the current states, inputs and outputs of the system. The stochastic automaton determines the probability that a subsequent condition occurs (transition probability). For using the stochastic automaton for FDD it is possible to proceed as follows:

- Construct a model of the dynamic process that describes the faultless behaviour of the system.
- Thereof, abstract a qualitative model based on a stochastic automaton that describes the system as rough as possible and as precise as necessary [3]. It should be noted, that QuaMo can also be identified by using the measurement data of the real process [7]. The prerequisite therefor is that the system runs in a faultless mode under nominal conditions.
- Use the qualitative model for determining the transition probabilities and successor states of the faultless system.
- A comparison between the occurring states of the real process and the expected calculated states of the faultless system can be used to detect and to diagnose faults in the system.

ADVANTAGES OF THE QUAMO APPROACH

In contrast to quantitative or other FDD methods the QuaMo approach offers some notable advantages:

- Reduction of information: due to the quantisers the information flow is pared down to the minimum. The amounts of data to be processed by the qualitative model are correspondingly lower than by other methods. This affects positively the computing expenditure and the computing time [3].
- Low complexity in contrast to rule-based approaches: Rule-based methods include a large set of if-then-else clauses and these sets grow rapidly with the behavioural complexity of the system [8].

- QuaMo can deal with uncertain knowledge about the system: Rule-based methods do not have any understanding of the underlying physics of the system. If a new condition occurs that is not defined in the knowledge base, the rule-based approach fails [8].
- QuaMo can be applied to incompletely known systems or to systems whose inputs or initial states can be measured only roughly [9]. For example, many values are often not measureable and therefore it is only known whether they are “too high”, “too low” or “nominal”. In this case, a precise quantitative model can not be applied because the actual state or the input value of the system is not known [10].
- Based on the structure of QuaMo, the observation algorithm of the process can be applied under real-time conditions [11].

However, the approach also has drawbacks. The necessity to develop a time consuming model of the system to be supervised is one of them. Furthermore, systems with many physical states lead to a combinatory explosion of the state space of the automata. Therefore complex systems have to be subdivided into several systems. Afterwards a qualitative model of each subsystem has to be abstracted and linked as an automata network. The automata network can then be transferred into a equivalent single automaton that describes the qualitative behavior of the whole system (composition of automata) [3].

AREAS OF APPLICATION:

In general, QuaMo can be applied to many technical systems like HVAC&R Systems, Ciller’s, heating and cooling circuits. However, as a first step the QuaMo approach will be tested on a simple heating circuit that includes the most common parts like pump, pipework, thermal mass, 3-way mixing valve, thermostat valve and radiator. Therefore, a model of the heating circuit will be generated with the simulation environment Modelica®/Dymola® (see Figure 4). The reason for using Modelica® is the declarative and object-oriented property of the modelling language and the available interfaces to other scientific software. Especially the Python™ interface is useful, because the QuaMo algorithms are written using the Python™ language. For the building of the model of the heating circuit it is important to note, that every possible system state that can occur in the real process, has to be considered in the model. To consider all possible system states and their transition probabilities, we will investigate the use of a Monte Carlo simulation. As noted previously, the model has to describe the faultless behaviour of the heating circuit.

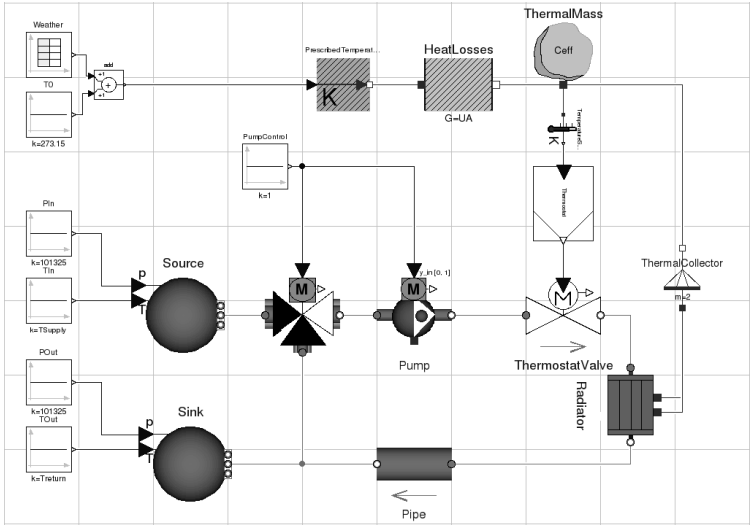

Figure 4: Scheme of the simple heating circuit model

After building the model, the qualitative model of the heating circuit can be abstracted. However, it must be ensured that the chosen partition boundaries of the state-, input- and output space are precise enough to describe the systems fundamental behaviour which means that when the flow temperature is defined as a state, it is reasonable to choose the partition boundaries so, that there are e.g. three partitions with the qualitative values "temperature too low", "temperature o.k." and "temperature too high". In order to keep the complexity of the system low, it makes sense to choose the smallest possible number of qualitative states.

The aim of the first tests in qualitative FDD is to identify potential weaknesses in the heating circuits and to diagnose the most common faults:

- Too low or too high flow/return temperature
- Too low or too high temperature spread
- Faulty valve positions or valve-leakage
- Leakages in the pipework
- Faulty operating state of the pump
- Wrong operating times of the whole system

After the first test with the Modelica-models, the QuaMo will be tested on a real system within the CASCADE project.The QuaMo will be applied to one of the heating circuits of a selected zone of the Milan Malpensa airport as shown in Figure 5. Therefore the whole heating circuit will be simulated in Modelica® to determine the transition probability's of the system states of the faultless system. After that, the QuaMo algorithm will be implemented at the real system to supervise the systems states and to compare them with the simulation results. Another point that will be investigated is the comparison between the results of the QuaMo method and a conventional method like a rule-based approach. Of particular interest here is the comparison of the results of the both methods regarding to the implementation and development efforts, accuracy of the FDD results and the transferability to other buildings.

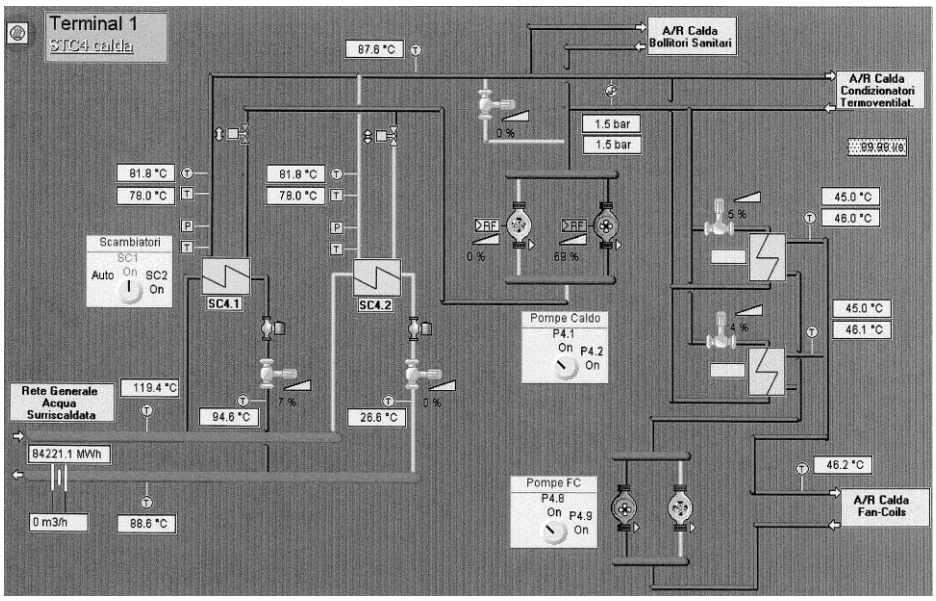

Figure 5: P&ID of a Heating Circuit in Terminal 1 of Mailand Malpensa Airport [12]

The research leading to these results has received funding from the European Union's seventh framework programme (fp7/2007-2013) under grant agreement n° 284920.

REFERENCES

1. Katipamula, S. and Brambley, M.R.: Methods for fault detection, diagnostics, and prognostics for building systems - A review, Part I. HVAC&R Research, Vol. 11(1), p. 3-25, 2005.
2. Lichtenberg, G.: Theorie und Anwendung der qualitativen Modellierung zeitdiskreter dynamischer Systeme durch nichtdeterministische Automaten. Vortschrittberichte VDI, Reihe 8: Mess-, Steuerungs- und Regelungstechnik, Vol. 686. VDI Verlag GmbH, Düsseldorf, 1998.
3. Schröder, J.: Modelling, State Observation and Diagnosis of Quantised Systems. Lecture Notes in Control and Information Sciences, Vol. 282. Springer-Verlag, Berlin, Heidelberg, New York, 2003.
4. Venkatasubramanian, V., Rengaswamy, R., Yin, K. and Kavuri, S.N.: A review of process fault detection and diagnosis Part I: Quantitative model-based methods. Computers & Chemical Engineering, Vol. 27(3), p. 293-311, 2003.
5. Isermann, R.: Fault-Diagnosis Systems. An Introduction from Fault Detection to Fault Tolerance. Springer-Verlag, Berlin, Heidelberg, New York, 2006.
6. Eginlioglu, P., Lichtenberg, G., Nixdorf, B., Schröder, J., Supavatanakul, P., Wassiliou, T. and Zacharias, M.: Qualitative Modelling Toolbox, Tutorial, Release 6.1. Ruhr-University Bochum, Fakultät für Elektrotechnik und Informationstechnik, 2002.
7. Lichtenberg, G.: Methoden der modellbasierten Fehlerdiagnose. ModQS Workshop. Technische Universität Hamburg-Harburg, Institut für Regelungstechnik, 2011.
8. Venkatasubramanian, V., Rengaswamy, R. and Kavuri, S.N.: A review of process fault detection and diagnosis Part II: Qualitative models and search strategies. Computers & Chemical Engineering, Vol. 27(3), p. 313-326, 2003.
9. Lunze, J.: Qualitative modelling of dynamical systems Motivation, methods, and prospective applications. Mathematics and Computers in Simulation, Vol. 46(5-6), p. 465-483, 1998.
10. Lichtenberg, G. and Lunze, J.: Prozessüberwachung mit Hilfe qualitativer Modelle. Fuzzy Duisburg '96, p. 44-66, Duisburg, Germany, 1996.
11. Lichtenberg, G. and Lunze, J.: Observation of unmeasurable states by means of qualitative models. 9th International Workshop on Qualitative Reasoning, p. 123-130, Amsterdam, Netherlands, 1995.
12. SEA S.p.A.: Produzione H2O Calda. Terminal 1, STC4 calda, 7.18.2012.

METHODOLOGY FOR ASSESSING THE ENERGY EFFICIENCY POTENTIAL OF ICT APPLICATIONS IN NEIGHBORHOODS

Emanuele Nastri[1]; Francesco Cricchio[2];

1: Smartcity SAS via Tufello 136 – Aprilia (LT) - 04011 Italy
2: D'Appolonia S.p.A. Innovation Consulting Division Via S. Nazaro, 19 - 16145 Genoa, Italy

ABSTRACT

We propose a methodology for assessing the energy efficiency potential of ICT applications used to manage energy systems in buildings, transports, manufacturing industry and electric power grids. This methodology, in order to overcome lacks of quantitative data, has a structure based on rigorous definitions and calculations, integrated by shared semi-quantitative estimations made by experts. By adopting this simple methodology policy makers could quickly simulate the impact of different policies, identifying the technologies that need more support, while investors could envisage the most promising opportunities of the growing green economy. This methodology is suitable to assess the energy efficiency potential not only of ICTs but also of other energy efficient technologies, manage energy systems in buildings, transports, manufacturing industry and electric power grids. This work contains results that have been elaborated and validated in the context of IREEN FP7 project during various workshop activities (IREEN ICT roadmap for energy efficient neighbourhoods - FP7 Coordination Action funded by the European Commission – grant agreement 285627). The IREEN (ICT Roadmap for Energy-Efficient Neighbourhoods) project is the European Coordination Action aiming to develop a comprehensive strategy for future European-scale innovation and take-up in the field of ICT for energy efficiency and performance in districts and neighbourhoods. The concept of energy-efficient neighbourhood has been defined in terms of relevant ICT technologies areas to be applied to identified neighbourhood application areas in order to improve their energy efficiency. The methodology proposed is suitable to assess the energy efficiency potential to various application areas identified in IREEN: data storage solutions for districts that require energy-efficient solutions in the implementation of data centre; the calculation of order effects of ICT on new integrated neighbourhoods with information technology; issues and problems of the smart grid at the neighbourhood scale.

Keywords: Energy Efficiency, ICT, Technology Assessment, Technology Foresight, Green Economy, IREEN FP7 project, smart neighbourhoods, scenario.

1 ENERGY EFFICIENCY

We assume to have a device (or a complex system) providing, in output, a work or a service $\mathbf{E_{out}}$. This work can be the light emitted by a lamp, the heat produced by a heating system, the amount of freights transported by a truck, etc. (If this work can be quantified in terms of Energy, it can be also expressed as a power by defining: Power = Energy / time). The considered system will consume – as input – an amount of energy $\mathbf{E_{in}}$ for performing that work. In case we have a system made by several devices, powered by a number "n" of energy sources, we should consider as input E_{in} the sum of all the energy inputs E_j (expressed in the same Measuring Unit). This can be generalised with the formula (1):

$$E_{in} = \sum_{j=0}^{n} E_j \qquad (1)$$

For example, for an ICT unit remotely managing path and load capacity of a truck, we should consider as E_{in} the petrol consumed by the truck plus the electric energy consumed by the controlling ICT unit, maybe expressing all the E_{in} components in Joule. The physical concept of "efficiency" (η) is the ratio between the work E_{out} produced in output from that system, and the total energy E_{in} required – as input – by the same system to produce that work:

$$\eta = \frac{E_{out}}{E_{in}} \tag{2}$$

When both E_{out} and E_{in} are expressed in the same measuring unit, efficiency is a pure number that can be also represented as a percent. For systems managing different input and output quantities, we can find efficiencies expressed as a ratio between measuring units, such as "distance travelled" versus "volume of fuel consumed" (km/litre) for car efficiencies, or "intensity of light" versus "power in input" (lumen/watt) for electric lighting (see Figure 1).

η = 70 lm/W

Figure 1 – Efficiency of a common compact fluorescent lamp

The definition of "Energy Efficiency" adopted by the European Union is perfectly matching with the physical concept reminded in (2). The EU directive 2006/32/EC on energy end-use efficiency defines energy efficiency: "*a ratio between an output of performance, service, goods or energy, and an input of energy*".

2 ENERGY SAVING DUE TO ENERGY EFFICIENCY COMPARISON

To raise Energy Efficiency (EE) of a system or a device means to perform the same work or service in output by consuming less energy in input. This is commonly simplified by the phrase: "do the same with less". From a physical point of view, if we intend to compare the energy efficiency η_1 of a system S_1 and the efficiency η_2 of a system S_2, we need to compare quantitative data describing their energy consumptions and performances. As a particular case, for two systems performing the same work in output, it is possible to say that a System 2 (i.e. ICT-driven) has a greater Energy Efficiency with respect to a reference System 1, if the Energy E_{in2} consumed in input by S_2 is less than the Energy E_{in1} consumed in input by S_1 (Figure 3). In this case we can also say that the Energy saved E_s by the system S_2 with respect to the system S_1 is:

$$E_s = E_{in1} - E_{in2} \tag{3}$$

The equation (3) easily explains how to assess energy savings from an "ICT for EE" application. However, this simple theoretical concept is not so trivial to be implemented in practical situations, because ICT systems are complex, and are often connected to other systems by mean of variables difficult to quantify and that can vary along time.

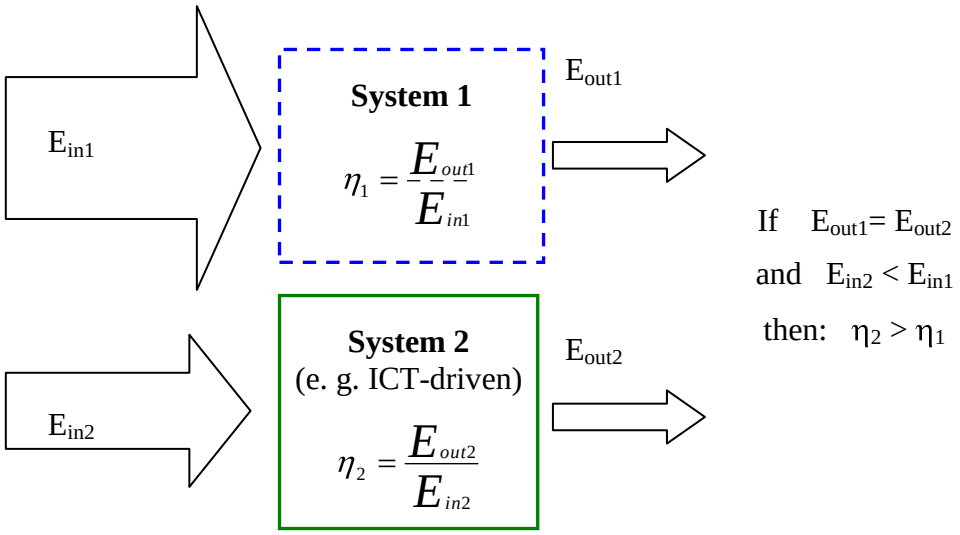

Figure 2 – Energy Efficiency comparison among two systems

Moreover, for several ICT driven systems (e.g. cooling systems) it is not simple to separate the energy saving contribution due to the ICT components (e.g. the inverter), to those given by other technological improvements embedded in the same system (better heat exchangers, improved refrigerant gas, etc.), or due to behavioural effects that is very difficult to assess.

3 BASELINE

The numerical value of the parameter "Energy saved" (E_s) obtained by the formula (3), can vary with the choice of the reference system. If we intend to assess E_s due to a particular ICT for EE application (e.g. a LED lamp light), we can compare its energy consumption to the one of an "old" technology (e.g. an incandescent bulb lamp) or to the consumption of a new (more efficient) competing technology (e.g. a fluorescent lamp light). This choice can bring to very different results and must be done considering the boundary conditions of our problem. Let's make an example: if a we intend to assess the convenience in buying or not a certain energy efficient device (e.g. a LED lamp light) for replacing an existing device that has still not reached its end of operating life ("early retirement"), we need to assess if, and in how much time, energy savings due to the replacement will re-pay the initial investment cost. So we must compare the energy consumptions of the new device (LED lamp) to those of the "old" one (incandescent lamp) we want to replace (see further in § 3.2). On the opposite, if we need to buy a brand new device, or to replace an old device that has already reached its end of life, we will compare costs and efficiencies of new devices present in the market, that are generally more efficient due to technology and regulatory improvements (see also § 6). In this case we can imagine to use as reference system an average lamp light with average efficiency present in the market ("market baseline", see § 3.1). These concepts are represented by the following Figure 3

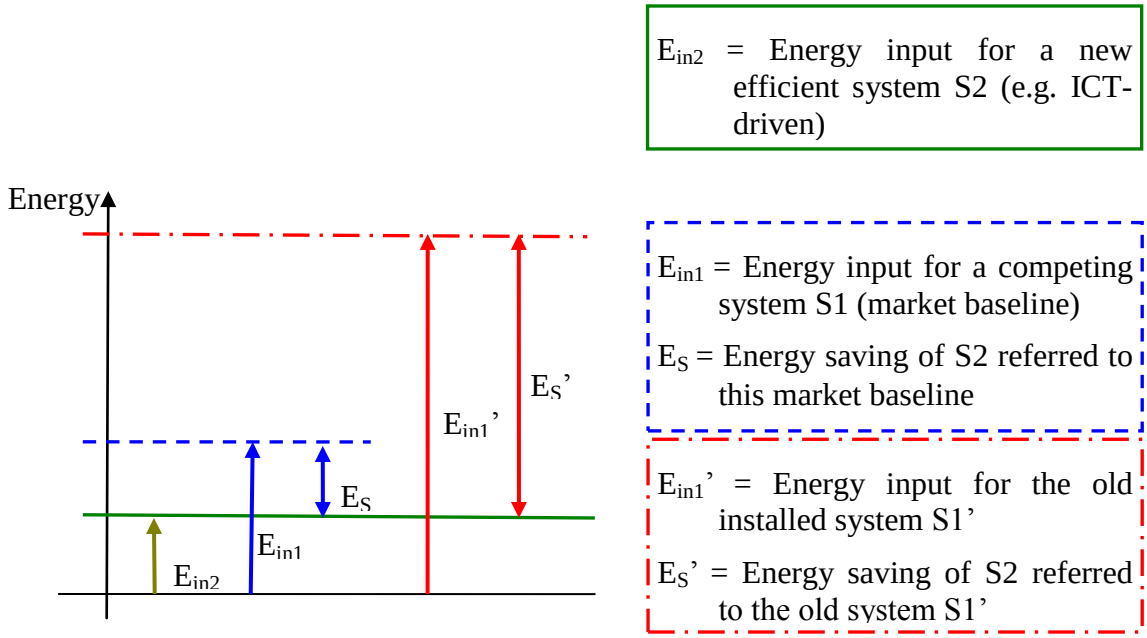

Figure 3 – Different energy savings for different baselines

3.1 Energy saving with respect to the Market Baseline

We define: Baseline technology, baseline system or baseline application the technology, the system or the application with average energy efficiency performances, available in the market in the year "t", and competing with the ICT for EE technology we intend to assess. The Energy saved (E_s) at year "t", by the ICT-driven system S_2, can be quantified by comparing the energy Ein1 consumed by the baseline system S1 to perform a certain service, with the energy E_{in2} consumed by S_2 to perform the same service. This can be represented by the formula:

$$E_s(t) = E_{in1}(t)\ (\text{baseline}) - E_{in2}(t)\ (\text{ICT}) \quad (4)$$

3.2 Energy saving respect the Installed Base

Another reference system for assessing the energy saved E_s could be the device with average efficiency in the Installed Base (also installed park). In this case, energy savings due to ICT applications could be calculated according to the formula:

$$E_s(t) = E_{in1}(t)\ (\text{installed}) - E_{in2}(t)\ (\text{ICT}) \quad (5)$$

This approach is suitable to be used while assessing interactions among EE and macroscopic economy indicators, as done in economic models for energy scenario planning.

3.3 Proposed reference system for the ICT for Energy Efficiency sector

In order to choose the reference system more suitable for an ICT for EE application, we need to consider the specific boundary conditions of the ICT for EE sector. In example, we should note that EU and global policies require a strong energy efficiency improvement, greater than the "natural" energy efficiency improvement due to the replacement of old devices with "average" new devices.

4 ENERGY SAVING PERCENT

The Energy saved **Es** at year "t" due to an ICT application, could be also expressed as the product among the energy saving in percent $\mathbf{E_{S\%}}$ and the amount of energy consumed in input $\mathbf{E_{in1}}$ by the baseline system:

$$Es = E_{S\%} \times E_{in1} \tag{6}$$

Where:

$$E_{S\%} = \frac{E_{in1} - E_{in2}}{E_{in1}} \tag{7}$$

This formulation is particularly useful if we cannot measure Es precisely but we need to use estimated data.

5 SCENARIO PLANNING

In order to quantify the Energy that could be saved by spreading a innovative ICT technology throughout society, we need to know the energy "Es" saved by a single application of that technology, and the number "N" of applications installed at a certain date in the considered geographic region. Each numerical value representing the Energy Efficiency Potential (EEP) of a technology is connected to specific politic, social and economic boundary conditions. A coherent set of boundary conditions could be also called "scenario". If we intend to simulate the impact (in terms of energy saved) of an action that could be made from a decision maker (e.g. a policy), we need to perform two specific EEP calculations for two different scenarios, and then to compare them. A first scenario should concern the EEPBAU, related to a Business As Usual (BAU) scenario, describing the impact of that technology if the decision maker does not acts in a particular way. Then, should be considered the specific scenario simulating the action undertaken by the decision maker. The difference among these two values of EEP will give us the quantitative impact of the particular action we intend to simulate. We can represent this concept with the following formula (8).

$$\text{Impact} = \text{EEP(action)} - \text{EEPBAU} . \tag{8}$$

Where:

Impact = The impact (in term of Energy saved) of the action or policy we intend to simulate; EEP(action) = Energy Efficiency Potential of the specific action or policy proposed; EEPBAU = Energy Efficiency Potential of the Business As Usual scenario (without the considered action).

6 NEW METHOD OF METRICS ICT FOR EE IN RELATION TO IREEN SCENARIOS

This paper proposes a methodology for assessing the energy efficiency potential of ICT applications used to manage energy systems in buildings, transports, manufacturing industry and electric power grids related to IREEN project application scenarios. The IREEN project (ICT Roadmap for Energy-Efficient Neighbourhoods) is an European Coordination Action aiming at developing a comprehensive strategy for future European-scale innovation and take-up in the field of ICT for energy efficiency and performance in districts and neighbourhoods. The methodology proposed in this paper is suitable to assess the energy efficiency potential to various IREEN application areas. Examples of relevant neighbourhood scenarios elaborated in the context of IREEN are summarized in the following:

- Data storage for the new districts require energy-efficient solutions in the implementation of data centres
- The calculation of order effects of ICT on new integrated neighbourhoods with information technology. Unlike many products and services sold in the world today ICT distinguishes itself by its double edged nature. On the one hand ICT has environmental impact at each stage of its life cycle e.g. from energy and natural resource consumption to e-waste. On the other hand, ICT can enable large efficiencies in life style and in all sectors of the economy by the provision of digital solutions that can improve energy efficiency, inventory management and business efficiency by reducing movement and transportation e.g. tele-working and video conferencing and by substituting physical products for digital information e.g. e –commerce. These different levels of impact are acknowledged in the academic literature as the three order effects of ICT: first order effects (or Environmental load of ICT): the impacts created by the physical existence of ICT and the processes involved, e.g. energy consumption and GHG emissions, e-waste, use of hazardous substances and use of scarce, non-renewable resources; second order effects (or Environmental load reduction achieved by ICT): the impacts and opportunities created by the use and application of ICT. This includes environmental load reduction effects which can be either actual or potential, such as travel substitution , transportation optimization, working environment changes, use of environmental control systems, use of e-business, e-government etc; other effects may include the impacts and opportunities created by the aggregated effects on societal structural changes by using ICT.
- Energy Footprint of ICT in Smart Grids at neighbourhood level. The implementation of smart grids will deploy many devices, in terms of both network equipment and data centres to create the communication infrastructures and host servers and data.

7 ACKNOWLEDGMENTS

The authors would like to thank the support and the collaboration with the whole consortium of IREEN project (ICT roadmap for energy efficient neighbourhoods - FP7 Coordination Action funded by the European Commission – grant agreement 285627). Finally the authors would like to thank the European Commission for the support that made possible the realisation of this work.

8 REFERENCES

1. Publications of ICT-21-EE available at http://www.ict21ee.eu/publications/
2. ITU-T Study Group 5, Question 18 – Methodology of environmental impact assessment of ICT.
3. R. Bolla, et al. IEEE Comm. Magazine, Vol. 49, No. 8, pp. 80-86, Aug. 2011.
4. Global e-Sustainibility Initiative (GeSI), http://www.theclimategroup.org/assets/resources/publications/Smart2020Report.pdf.
5. Code of Conduct on Energy Consumption of Broadband Equipment, European Commission, version 4, European Commission, D-G JRC, Ispra, Italy, 2011.
6. [b-EU Code of Conduct on data centers v2.0, European Union

ANALYZING THE DESIGN USE OF SCRIPTING INTERFACES FOR BUILDING PERFORMANCE SIMULATION

Julien Nembrini[1], Mark Meagher[2]; Adam Park[3]

[1] *Constructive Design and Structure Lab Universität der Künste Berlin, Germany*
[2,3] *School of Architecture, University of Sheffield, UK*

ABSTRACT

The paper documents an ongoing study in the use of Building Performance Simulation (BPS) as a source of feedback in the early stages of architectural design. Taking advantage of the specific affordances provided by *parametric scripting* for design, fine-grained data about design development is gathered from a group of architecture students with the aim to gain understanding into patterns of scripting in conjunction with BPS. By visualizing design activity for particular users, it is possible to recognize patterns of interaction between iterative cycles of parametric modification and simulation. Focusing on a single user, the paper documents this usage history, firstly at a macro level over the course of a semester, and in a second step closely analyzing each script modification during 24 hours. Using data visualization as a tool for analyzing the process of interaction between adjustments to the parametric model and feedback from simulation, this analysis outlines the role of examples in the design process: users tend to rely on examples to learn coding techniques, and then come back to them when engaged in design. It is expected that the method described in this paper will in the future allow us to achieve a detailed understanding of how users learn from and respond to simulation results in a parametric design process.

Keywords: Performance-based design, parametric scripting, BPS, usage analysis, data visualization

INTRODUCTION

In performance-based design, the digital model allows iterative evaluation of design decisions based on simulation [7]. As many current CAD software packages allow direct interaction with BPS tools such as Radiance, EnergyPlus and Ecotect, designers have started to use simulations in their design process, a development that raises questions about their expertise to assess the relevance of the obtained results [4, 8]. Using parametric design, factors that impact performance can be selectively explored by observing the influence of modifications on simulation results. In previous work it has been argued that *parametric scripting* — in which form is constructed with text-based instructions — presents further advantages when considering energy performance due to the complexity of simulation input as well as result analysis [6]. Such a scripting approach for design is gaining more and more adoption from architectural designers [2].

The goal of this study is to analyze in detail the design process followed by a group of architecture students in order to assess the potential of parametric techniques as a means for designers to test, adjust and better understand the results received from simulation

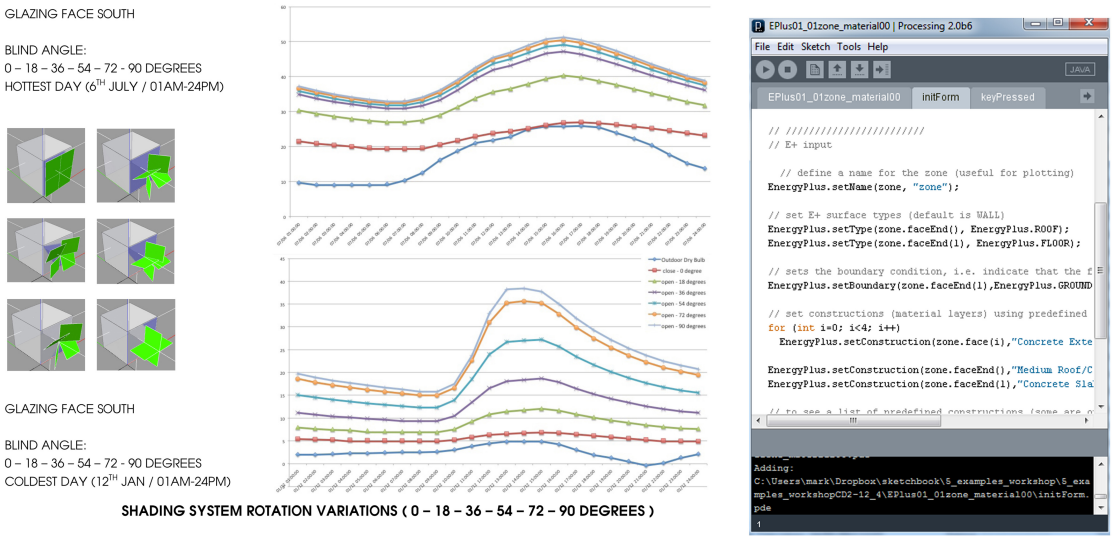

Figure 1: Final assignment: a parametric shading system adapting to different orientations. Example design and analysis produced by the students (Vinh Nhy Ly) (left). Example script within the Processing IDE, focused at EnergyPlus related functions (right).

engines. The present paper focuses on analysing the usage patterns of a single user.

There have been few systematic studies of BPS tool usage by designers [3, 1]. These are mostly qualitative, based on interviews/questionnaires of designers. Although several studies have discussed the impact of using thermal or daylighting simulation in design teaching [4, 8], none of these studies were based on a detailed recording of the designers' interaction with the design tools themselves.

METHODS

The tools used in the present research are all open-source or software made freely available on the web. The simulation engine is the EnergyPlus software provided by the US Department of Energy. The second tool is the Processing.org software which is firstly a very simple to use software Integrated Development Environment (IDE) as well as a widely-used scripting language aimed at a design audience. The study uses the library ANAR+, that provides functionality for producing associative parametric geometry through scripting [5]. This library also provides an extensive set of functions that interface with EnergyPlus, allowing geometrical elements to be supplemented with simulation data to automatically produce EnergyPlus input files, launch simulation runs and analyze results [6]. The script thus constitutes a complete description of the building model, including geometry and simulation parameters (Fig. 1, right). It is a text file, which means that users have to become accustomed to defining geometry and parameters related to simulation using a purely text-based approach.

In order to record usage data, the ANAR+ library was modified to log the following details on a server each time a script is run within the Processing IDE: (1) the user ID and time stamp, (2) the name of the script being run, (3) interface interactions such as simulation runs or parameter modifications, (4) the current state of the script's code.

Taking advantage of the text-based nature of the data recorded, source code version

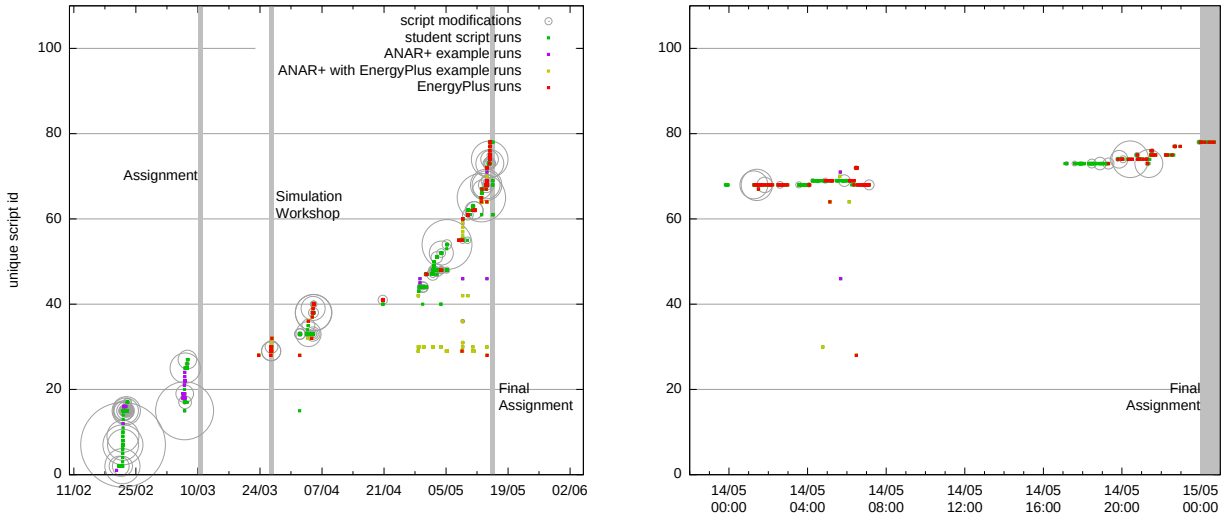

Figure 2: Time line of the Spring 2012 Workshop of user 03 *over approx.* 16 *weeks (left) and in the last hours before final assignment (right). Differentiation is made between running example scripts, example scripts including simulation functions, user's own scripts and the triggering of simulation runs. Empty circles of variable sizes indicate the number of code modifications between script runs.*

control software was used to store the usage history. With such a database it becomes possible in a second step to reconstruct the history of each user, especially the triggering of simulation runs. This approach allows us to easily identify any modifications to previously recorded scripts and allow the reconstruction of the development of each user's design process at a very fine-grained level.

The context for our study is a year-long course in computational design which was offered in the 2011-2012 academic year within the MSc in sustainable design at the Sheffield School of Architecture. The course included an initial revision of parametric design principles ending with an assignment; a workshop to introduce the use of simulation with an assignment exploring the influence of volume, orientation and window/wall ratio on performance; and a final assignment. The brief for the final assignment was to design a parametric shading system able to smooth out inside environmental conditions according to differing orientations. Example results produced by the students for the final assignment is illustrated in Fig. 1 (left).

EXPERIMENT

During the semester-long data recording, 49460 events were logged with 12509 individual script compilations, involving 297 different scripts. Among these different scripts, 121 contained EnergyPlus simulation functions and users triggered 1330 simulation runs. The data is thus of substantial volume and requires automated processsing for analysis. The presented results concentrate on a single user with the aim to determine such processing.

As a shortcoming, the data contains no output generated from the running of EnergyPlus simulations, initially to reduce the load on the logging server. This prevents us from discriminating between successful and unsuccessful EnergyPlus runs. Such additional data will be included in further work. Nevertheless, the data gathered still provides a

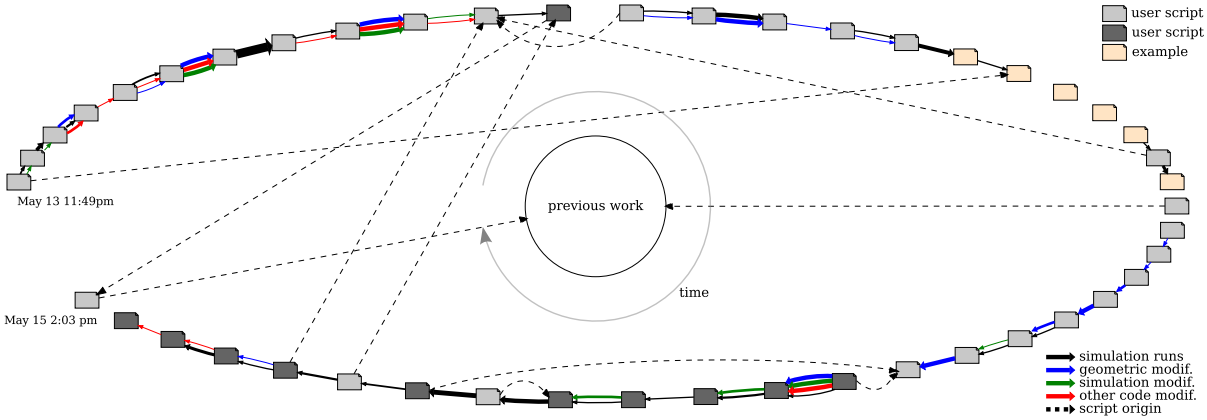

Figure 3: Detailed analysis of user 03's work during the 24 hours preceding the final assignment deadline, with each rectangle representing a unique version of a script. Several measures are depicted such as the amount of simulation runs between versions (black arrows), the amount of modifications between versions (blue, green, and red arrows). The dashed arrows indicate the script at the origin of a given script.

detailed insight into the unfolding of the design process.

The stage of data analysis presented here focuses on a single user to exemplify the kind of information about the design process that can be extracted from the kind of data logged. The analysis proceeds in two stages: firstly by displaying a time-based representation of the user data (Fig. 2), and in a second step by exploring the usage patterns of the user engaged in the final assignment (Fig. 3). Focus has been put on patterns of simulation usage in relation to script modifications.

Concentrating on a single user it becomes possible to visualize patterns, both for the usage of examples as for the relationship between simulation runs and code modifications. Fig. 2 represents the occurrence in time of script and simulation runs illustrating the difference between user-defined scripts, provided examples, examples including simulation functions, and simulation runs. In these graphs the unique ID assigned to each individual script is in the Y-axis, so horizontal lines of activity correspond to a particular script being run repeatedly by the user (scripts must be run to visualize the geometric relationships described in code). The concentric circles surrounding specific script runs indicate the number of lines changed compared to the previous run of that script.

Users tend to rely on examples to learn techniques and come back to them when engaged in the design phase. Most examples involving simulation were introduced in a workshop in late March (shown as a vertical line on Fig. 2, left). Straight vertical stacks of activity indicate users working with multiple scripts in rapid succession, while horizontal lines indicate activity within a single script over time.

In Fig. 2 (right) the final 24 hours before the final assignment are focused on. The user runs a number of different scripts during the last day before the deadline, most likely variants on the same script which have been given different names. Notably, he repeatedly check his design's consistency against simulation

Taking advantage of the data collected, the same time lapse is closely analyzed to unveil the relationship between code modifications and simulation runs. Fig. 3 schematically represents this analysis for the chosen user. Each rectangle represents a unique version

of each script while arrows between them indicate amounts of simulation being run and modifications to the scripts — manually categorized as modifications on geometry, on simulation definitions, and other changes to the script's code. Additional dashed arrows indicate on which previous script the new script is based. During this period of time 92 simulation runs were triggered by the user.

Starting on the left hand side and following the progress of time (clockwise), the unfolding of the user's design development can be traced with great precision. The dashed arrows make clear that the user does not follow a linear path. Instead, after developing a new script, he may fall back on the previous one, sometimes calling out a few examples, even starting again from older work. Looking at the sequence of simulation runs, it is clear that they tend to happen in bursts rarely accompanied with significant modifications. Thorough work on the scripts tend to precede or follow intensive simulation requests.

Focusing at the very beginning, the first script takes its origin from an example with some geometric changes, followed by a few changes in simulation parameters accompanied by simulation runs. Then significant change occurs over four script versions followed by an intense simulation testing. Such testing triggers further changes which are then tested before a new version is defined (dark grey box in the top middle of Fig. 3). This version is replaced by another which then follows a process of exclusively geometric changes accompanied by simulation testing.

Then the user decides to check again a variety of examples, and most notably the one at the origin of his work (Fig. 3, left). After this checking period, a new version is started from previous work followed by geometry modifications which are incrementally run for visual feedback and then tested through simulation, leading to further geometric refinement. Then the user engages in a new version with significant modifications which will be eventually thoroughly tested through numerous simulation runs.

DISCUSSION AND FURTHER WORK

One of the most important findings from the data is the importance of the provided examples in the process of designing through scripts. When engaged in the design phase, a majority of users periodically went back to examples, probably to understand/copy the code used to produce a certain functionality. Moreover, all contributions to the final assignment can be traced back to some provided example, sometimes even presenting quite a limited share of user-written code. This further confirms the importance of examples in the scripting approach.

An important weakness of the results presented is inherent in the data gathered, resulting from the relative simplicity of the task asked to the students.

The strength of the visualizations presented in this paper has been in providing a graphic representation of differing approaches to parametric design with simulation feedback. Using the visualizations of activity for a particular user, we have been able to recognize several distinct patterns of interaction between iterative cycles of parametric modification and simulation. In a future stage of the research, we will continue to examine this dataset and data collected in other classes and workshops with the goal of achieving through the data analysis a detailed understanding of how users learn from and respond to simulation results in a parametric design process.

CONCLUSION

This paper documents an ongoing study of simulation in the early stages of the scripting-based parametric design process. The goal of this study has been to analyze in detail the design process followed by students in order to assess the potential of parametric techniques as a means for designers to test, adjust and better understand the results received from simulation engines. Through an initial analysis of an unprecedented usage dataset, the work represents to our knowledge the first study of its kind on a design scripting framework in conjunction with BPS. Despite needing further work, the research already reveals a number of distinct design processes in relation with BPS usage. By outlining pitfalls and advantages of using scripting in this context, it is our expectation that this method will allow us to formulate specific guidelines required to integrate these tools in early stage design. Further work will concentrate on formulating more demanding tasks for students to induce greater need of BPS results interpretation and feedback in the design process. The approach presented here is believed to be of significant importance for the general aim to provide designers with explorative tools to consider sustainable construction in a systematic and informed manner.

Acknowledgement

The authors wish to thank Enrico Costanza and the University of Southhampton (UK) for providing their knowledge and infrastructure to record the students' data. Julien Nembrini is supported by the Swiss SNF grants PA00P1-129120 and PA00P1-142138.

REFERENCES

1. S. Attia, L. Beltran, A. D. Herde, and J. Hensen. "architect friendly": A comparison of ten different building performance simulation tools. In *Building Simulation 2009, 11th IBPSA Conf.*, pages 204–211, Glasgow, Scotland, July 2009.
2. M. Burry. *Scripting cultures: Architectural design and programming.* John Wiley and Sons, West Sussex, UK., 2011.
3. C. J. Hopfe, C. Struck, G. U. Harputlugil, J. Hensen, and P. D. Wilde. Exploration of the use of building performance simulation for conceptual design. In *IBPSA NVL symposium*, 2005.
4. D. I. Ibarra and C. F. Reinhart. Daylight factor simulations — how close do simulation beginners "really" get? In *Building Simulation 2009, 11th International IBPSA Conference*, Glasgow, Scotland, July 2009.
5. G. LaBelle, J. Nembrini, and J. Huang. Geometric programming framework: Anar+ geometry library for processing. In *Proceedings of eCAADe 2010, Future Cities*, pages 403–410, 2010.
6. J. Nembrini, S. Samberger, A. Sternitzke, and G. LaBelle. The potential of scripting interfaces for form and performance systemic co-design. In *Proceedings of Design Modelling Symposium*, Berlin, October 2011. Springer.
7. R. Oxman. Performance-based design: Current practices and research issues. *Int. Jour. of Architectural Computing*, 6(1):1–17, 2008.
8. C. F. Reinhart, T. Dogan, D. Ibarra, and H. W. Samuelson. Learning by playing — teaching energy simulation as a game. *Journal of BPS*, 5(6):359–368, 2012.

SOLAR FACTOR VERSUS DYNAMIC THERMAL CHARACTERISTICS OF OPAQUE COMPONENTS

R. Rabenseifer

KKPS SvF STU in Bratislava, Radlinskeho 11, 813 68 Bratislava, Slovakia

ABSTRACT

Occasionally, there are suggestions from professional public to use the total solar energy transmittance coefficient, *g* (solar factor), to describe not only transparent, but also opaque structures, particularly with regard to overheating of the under-roof spaces. The standard EN 410:1998 (Glass in building - Determination of luminous and solar characteristics of glazing) introduces the *g*-value as the sum of primary solar heat gain, g_1, due to the transparency of the glazing and the secondary solar heat gain, g_2, due to the absorption of solar radiation and its conversion into heat conduction and radiation over the total incident solar heat flux, φ_e. Nevertheless the value of g_1 may have zero or nearly zero value, e.g. in case of non-transparent glass. In addition to it, the standard ISO 15099:2003 (Thermal performance of windows, doors and shading devices - Detailed calculations) introduces equation for calculation of the frame *g*-value (actually the frame total solar energy transmittance), where window frames are clearly opaque components. What is then the difference between glass and "standard" opaque wall or roof? Why is in the latter case always introduced zero and in the first one some value different from zero? Won't it be practical, especially in time of large existing opportunities of computer use, to implement the use of *g*-values also in case of ordinary opaque structures and express their resistance to the absorption and conversion of solar radiation and thus overheating the adjacent interior spaces? This paper attempts, using EN ISO 13786 (Thermal performance of building components - Dynamic thermal characteristics - Calculation methods) and computer-aided models of transient heat transfer, to explain why the suggestion of using of the *g*-value in case of opaque components is not entirely correct and, why priority should be given to the dynamic thermal characteristics specified in this standard.

Keywords: dynamic thermal characteristics, solar factor, building structures, overheating

INTRODUCTION

Occasionally, there are suggestions from professional public to use the total solar energy transmittance coefficient, *g* (solar factor), to describe not only transparent, but also opaque structures, particularly with regard to overheating of the under-roof spaces. One of the arguments, standing behind this consideration lies in the fact that, for example ISO 15099:2003 (Thermal performance of windows, doors and shading devices - Detailed calculations) distinguishes between summer and winter *g*-value of the glazing, whereas the calculation of the first one states as boundary condition the intensity of solar radiation of 500 W/m^2 and for calculating the second one, the winter value, the intensity of solar radiation of 300 W/m^2. The standard respects the fact that during the day there is always some solar radiation, even on a cloudy day. Therefore, it should not happen that the denominator of the formula to calculate the *g*-value is zero. The formula introduced in the standard is:

$$\tau_S = \frac{q_{int} + q_{int}(I_S = 0)}{I_S} \qquad (1)$$

where

τ_S is the total solar energy transmittance (*g*-value), q_{int} is the net density of heat flow rate through the window or door system to the internal environment for the specified conditions, in W/m^2; $q_{int}(I_S = 0)$ is the net density of heat flow rate through the window or door system to the internal environment for the specified conditions, but without incident solar radiation, in W/m^2.

In addition to it, the standard introduces even equation for calculation of the frame total solar energy transmittance, where window frames are clearly opaque components. From subsequent equations for calculation of q_{int} and $q_{int}(I_S = 0)$ it is evident that τ_S must be equivalent to *g*-value introduced in EN410:1998 (Glass in building - Determination of luminous and solar characteristics of glazing). Otherwise both standards would negate each other. The formula for *g*-value calculation according to EN410:1998 is:

$$g = \frac{g_1 + g_2}{\varphi_e} \qquad (2)$$

where g_1 is primary solar heat gain due to the transparency of the glazing, g_2 the secondary solar heat gain due to the absorption of solar radiation and its conversion into heat conduction and radiation and φ_e the total incident solar heat flux in W/m^2.
Nevertheless the value of g_1 may have zero or nearly zero value, e.g. in case of non-transparent glass. What is then the difference between glass / window and "standard" opaque wall or roof? Why is in the latter case always introduced zero and in the first one some value different from zero? Won't it be practical, especially in time of large existing opportunities of computer use, to implement the use of *g*-values also in case of ordinary opaque structures and express their resistance to the absorption and conversion of solar radiation into convective and radiant heat and thus overheating the adjacent interior spaces?

DYNAMIC THERMAL CHARACTERISTICS

The answer to these questions gives especially standard EN ISO 13786:2007 (Thermal performance of building components - Dynamic thermal characteristics - Calculation methods (ISO 13786:2007)). The main thermal characteristics mentioned in this standard are periodic thermal admittance, its time shift and decrement factor. The periodic thermal admittance can be described as an amplitude of heat flux on the internal surface of the structure at varying outdoor air temperature (expressed as sine curve) and constant indoor air temperature (e.g. 0°C). The decrement factor is a ratio of the modulus of the periodic thermal admittance to the steady-state thermal transmittance *U* (see EN ISO 13786:2007). From many scientific studies, e.g. Physibel Pilot Books (2004 and 2010), it is clear that the time lag (and attenuation) of the amplitude of periodic thermal admittance of heavy construction is rather strong. In contrast, lightweight constructions are responding quite quickly. In both cases, however, we can say that the part of solar radiation, which is absorbed, gets by conduction and radiation into the interior with varying degrees of time lag. This means in my opinion that the value of g_2 in equation (2) may not be timely identical to the value φ_e, i.e. in an instant of given intensity of solar radiation the secondary solar heat gain must not correspond to this intensity, but may show up with a certain time lag and attenuation of the maximum value.

PROBLEM ILLUSTRATION

Perhaps the problem is best illustrated by an example of the three one-layer components of three different materials with the same *g*-value, e.g. concrete wall, glass pane and thermal insulation panel. The *g*-value was calculated according to Physibel Pilot Book (2013) in a manner similar to calculation of the frame total solar energy transmittance introduced in ISO 15099:2003 as:

$$g = \alpha_S \, . \, U / h_e \quad (3)$$

where α_S is the solar absorption, U the thermal transmittance of the component and h_e the global surface heat transfer coefficient at the exterior side. In case of glass pane a negligible primary heat gain was added. Table 1 shows the physical parameters of these materials, including U- and g-values.

Component	***d*** **[m]**	***λ*** **[W/mK]**	***R*** **[m²K/W]**	***N*** **[kg/m³]**	***c*** **[J/kgK]**	***τ*** **[-]**	***ε*** **[-]**	***ρ*** **[-]**	***α*** **[-]**
concrete wall	2.3	1.300	1.769	2300	840	0.00	0.90	0.29	0.71
glass pane	0.01	1.000	0.010	2500	750	0.01	0.90	0.97	0.02
insulation	0.1	0.040	2.500	30	1400	0.00	0.90	0.00	1.00

Table 1: Physical parameters of compared components.

The calculation of dynamic thermal characteristics was performed in accordance with requirements of EN ISO 13786:2007 using the software Capsol and method described in Physibel Software Pilot Book (2010) with following data input (according to the Physibel Pilot Book (2010)):

- The standard concerns a harmonic thermal analysis. A sinusoidal temperature (mean 0°C, amplitude 10°C, period 24h) is defined at one side (external or internal) and a constant temperature 0°C is defined at the other side (internal or external),
- Global surface heat transfer coefficients h_e = 25 W/(m²K) and h_i = 7.7 W/(m²K) are defined,
- Calculation duration of 1 day with start-up calculation duration of 5 days (in order to get a harmonic regime) is defined. A time step of 10 minutes and a maximum sub-layer of 0.01 m are specified, resulting in a reasonable precision of the numerical calculation,
- Graphic output (graphs and animations) and text output are defined. In order to derive the wall dynamic thermal characteristics the outputs of the heat flows at both wall surfaces are essential.

The CAPSOL text results were then processed in the Excel spreadsheet and are introduced in table 2.

Component	***g*-value [-]**	***U*-value [W/m²K]**	**Periodic thermal admittance, Y_{ie} [W/(m²K)]**	**Decrement factor, *f* [-]**	**Time shift [min]**
concrete wall	0.02	0.52	0	0.00	infinity
glass pane	0.02	5.56	5.55	0.99	-10
insulation panel	0.02	0.37	0.37	0.99	-30

Table 2: Results.

Figs. 1 to 3 show the charts with outdoor temperature [°C] and the heat flow at internal surface [W/m²] for each component (similarly to Physibel Software Pilot Book (2010)). The periodic thermal admittance, Y_{ie}, in [W/m²K] was obtained as:

$$Y_{ie} = - q_{i,max} / \theta_{e,max} \quad (4)$$

where $q_{i,max}$ is the complex amplitude of the density of heat flow rate through the internal surface [W/m^2] and $\theta_{e,max}$ is the complex amplitude of the outdoor temperature in °C (actually 10°C), when the temperature in interior is held constant at 0°C. The decrement factor, f [-], was calculated as:

$$f = Y_{ie} / U \quad (5)$$

Of course there might be an objection that the solar factor is used to assess the behaviour of surfaces exposed to solar irradiance and that the presented illustration does not take it into consideration. This is true, but the transfer of heat absorbed by opaque components is solely by conduction, convection and radiation and there is no direct light transmission. Hence, the source of temperature increase at the exterior surface can be defined as harmonic temperature curve, too.

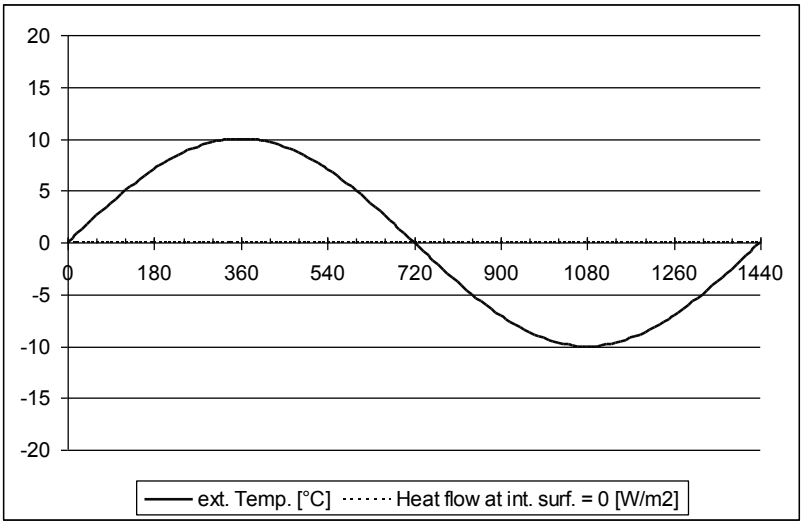

Figure 1 Concrete wall: heat flow rate through the internal surface [W/m^2] (dotted thin line) and outdoor temperature in °C (continuous thick line) over the period of one day (x-axis). In this case the heat flow rate equals zero.

RESULTS

The results show that the decrement factor of concrete wall is zero and the time shift close to infinity. This means that the concrete wall does not respond to temperature changes in the external environment at all. In the case of thermal insulation panel, the situation is exactly the opposite. The thermal insulation panel transfers these changes into interior fully equal to its *U*-value with 30 minutes time lag. Glass by its nature is close to the thermal insulation panel and shows similar result, though with time shift of 10 minutes. Actually, the thinner the glass pane the more immediate is the heat transfer. On the other hand, with increasing the mass of glass (thickness) and keeping the same *g*-Value (which is possible), the decrement factor decreases and also more significant time shift of the periodic thermal admittance occurs on the inside. All three components, however, have the same *g*-value (more or less according to standards), which indicates that it actually says nothing about the quality of these structures in terms of the attenuation and time shift of transmitted heat gains. In the simulation software Capsol the *g*-value is used just informatively as a benchmark value of glazing(s) in Wall Type Editor, whereas for the actual calculations of direct heat gains from solar radiation the value g_1, i.e. τ of glazing, and for the calculations of indirect solar heat gains a heat balance based on more detailed physical properties of materials, e.g. thermal conductivity, density and heat capacity, is used. This means that CAPSOL uses a variable solar factor.

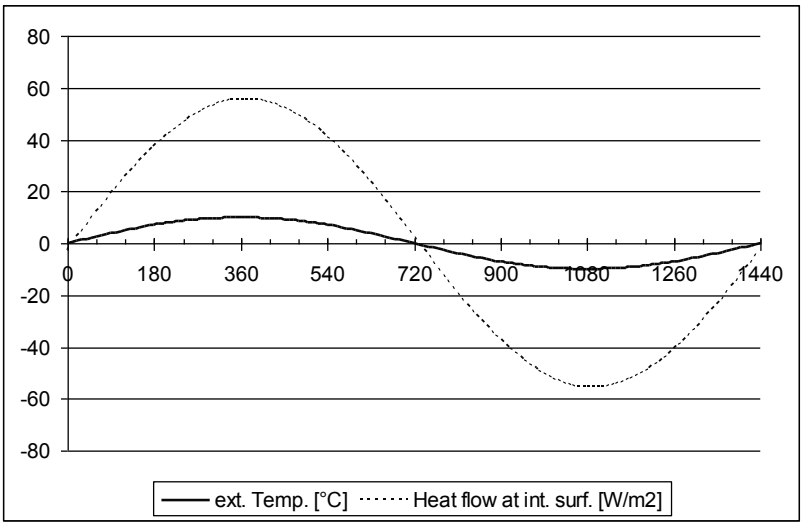

Figure 2 Glass pane: heat flow rate through the internal surface [W/m^2] (dotted thin line) and outdoor temperature in °C (continuous thick line) over the period of one day (x-axis).

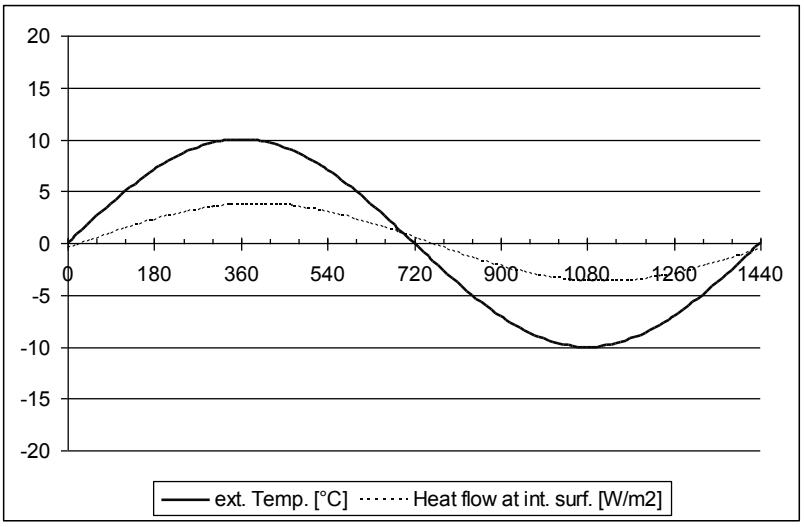

Figure 3 Thermal insulation panel: heat flow rate through the internal surface [W/m^2] (dotted thin line) and outdoor temperature in °C (continuous thick line) over the period of one day (x-axis).

According to Physibel Software Pilot Book (2004) this approach allows a more precise simulation, because the reflection of incident solar radiation can be angle dependent, the secondary component of the solar heat gains depends on the inside and outside temperatures, the thermal capacity of the construction causes a transient effect and the solar radiation reflected by internal walls can be transmitted back to the outdoors.

CONCLUSION

Given that the total solar energy transmittance coefficient, *g*-value (solar factor), is used in the steady state calculations of heat energy demand of buildings, it would not be very appropriate to apply it to the "normal" opaque components, as the heat gains it expresses, unlike glazing, may occur with significant and different time delay. In particular, the primary solar heat gain, which was not subject of this study, is in the case of glazing ensuring time consistency between cause and effect and makes the difference between transparent and opaque

components. Within steady-state calculations the use of *g*-values can be accepted in the case of glazing as it relatively correctly compensates for the transmission heat loss through it. In the dynamic, transient, calculations, where the problem of heat transfer is solved taking into account the thermal conductivity, density and heat capacity of materials, reflection, etc. the standardized simplified approach would be confusing. Hence, the *g*-value is more or less of no use for opaque components and a better way of simple expression of their quality, e.g. roofs, in addition to *U*-value, is introducing their periodic thermal admittance, time shift and decrement factor. It is also evident that from pragmatic point of view the use of *g*-values for assessing the opaque structures does not make too much sense, provided the *g*-values are based on equation (3) or the similar one for frame total solar energy transmittance in ISO 15099:2003. In the case of well-insulated components having *U*-value < 0.5 W/(m^2.K) namely, the *g*-value is a negligible number (see Table 3).

In my opinion the study also showed that standards mutually interact and should not be viewed in isolation, even though they do not refer to each other.

Mean *U*-value of component [W/(m^{2}K)]	0.01	0.05	0.1	0.5	1.0	2.0	3.0
Absorption α [-]	1.00	1.00	1.00	1.00	1.00	1.00	1.0
***g*-value [-] for h_e = 25 W/(m^{2}K)**	0.00	0.00	0.00	0.02	0.04	0.08	0.12

Table 3: g-values of opaque building components with low mean U-value and maximum solar absorption.

ACKNOWLEDGEMENT

At this time I would like to express my warmest thanks to Professor Dr. Ir. Arch. Piet Standaert from Physibel, Belgium, who kindly provided me with information regarding the Physibel software and explained many questions. The preparation of this article was supported by the TÁMOP-4.2.2.A-11/1/KONV-2012-0041 project. The project is co-financed by the European Union and the European Social Fund.

REFERENCES

1. ISO 15099:2003 Thermal performance of windows, doors and shading devices – Detailed calculations
2. EN ISO 13786:2007 Thermal performance of building components - Dynamic thermal characteristics - Calculation methods (ISO 13786:2007)
3. EN 410:1998 Glass in building - Determination of luminous and solar characteristics of glazing
4. Physibel Software Pilot Book - Practical problems solved using the Physibel Software © 2004 Physibel, Belgium (unpublished electronic version)
5. Physibel Software Pilot Book, Version 2, September 2010 - upgrade 07.10.2010 © 2010 Physibel, Belgium (unpublished electronic version)
6. Physibel Software Pilot Book, © 2013 Physibel, Belgium (unpublished electronic version)
7. CAPSOL, v.4.0 Computer Program to Calculate Multi-zonal Transient Heat Transfer, © 2002 PHYSIBEL

SIMULATION FRAMEWORK FOR DESIGN OF ADAPTIVE SOLAR FAÇADE SYSTEMS

Dino Rossi, Zoltan Nagy, and Arno Schlueter

Architecture & Sustainable Building Technologies (SuAT)
Institute of Technology in Architecture (ITA)
ETH Zürich
Schafmattstrasse 32
8093 Zürich, Switzerland
{rossi, nagy, schlueter}@arch.ethz.ch

ABSTRACT

Adaptive robotic systems have the potential to improve building energy performance and occupant comfort. For example, adaptive solar façade systems can provide multiple functionalities, including energy production, shading, glare reduction, etc. The design, and in particular the optimization of such systems requires detailed knowledge of the environmental conditions in which they operate. Some aspects of environmental knowledge required by these systems are too complex to be predicted accurately (e.g. user preferences and weather fluctuations), and require the implementation of online adaptive algorithms such as Q-learning in order learn appropriate response patterns. Other aspects can be modelled prior to deployment through suitable site-specific simulation frameworks with high spatiotemporal resolution. Such frameworks offer the potential to greatly decrease post-installation adaptation time compared to implementing adaptive building systems with no previous knowledge of their environments. While many simulation tools are currently available to architects, they are often computationally inefficient for the generation of the large data sets required in this context. In this research we develop a lightweight solar insolation framework for the simulation of site-specific solar radiation. Explicitly programming the required task allows us to significantly reduce computation time compared to a parametric simulation run through a 3D modelling environment, making this approach a viable option for the development of adaptive building systems. The framework can be extended to other environmental performance aspects, e.g. lighting/heating/cooling loads, and further improvements in computation time can be achieved through techniques such as porting to C and parallelization.

Keywords: adaptive, solar, façade, simulation, python

INTRODUCTION

Adaptive robotic systems, such as adaptive solar façade systems have the potential to improve building energy performance and occupant comfort. [1] As shown in Figure 1 these systems can provide multiple functionalities, including energy production, shading, and glare reduction. The design of these types of systems requires detailed knowledge of the environmental conditions in which they operate. Without the capacity for the system to make informed decisions potential energetic benefits would be lost. Some aspects of environmental knowledge required by these systems are too complex to be predicted accurately (e.g. user preferences and weather fluctuations), and require the implementation of online adaptive algorithms such as Q-learning in order develop appropriate response patterns. Other aspects can be modelled prior to deployment of the system through site-specific simulation. In order for these models to be of optimal use a high spatiotemporal resolution is required. In addition,

the many possible configurations of an adaptive façade leads to the problem of large simulation sets and potentially long simulation run times.

In this paper we introduce a fast solar simulation framework for use in design and control of adaptive solar façade systems. Such a framework offers the potential to greatly decrease post-installation adaptation time compared to implementing an adaptive building system with no previous knowledge of its environment. While many simulation tools are currently available to architects [2], they are often computationally inefficient for the generation of the large data sets required in this context. Our proposed framework is implemented as a lightweight Python based script for the simulation of site-specific solar radiation. Explicitly programming the required task allows us to significantly reduce computation time, making this approach a viable option for the development of adaptive building systems.

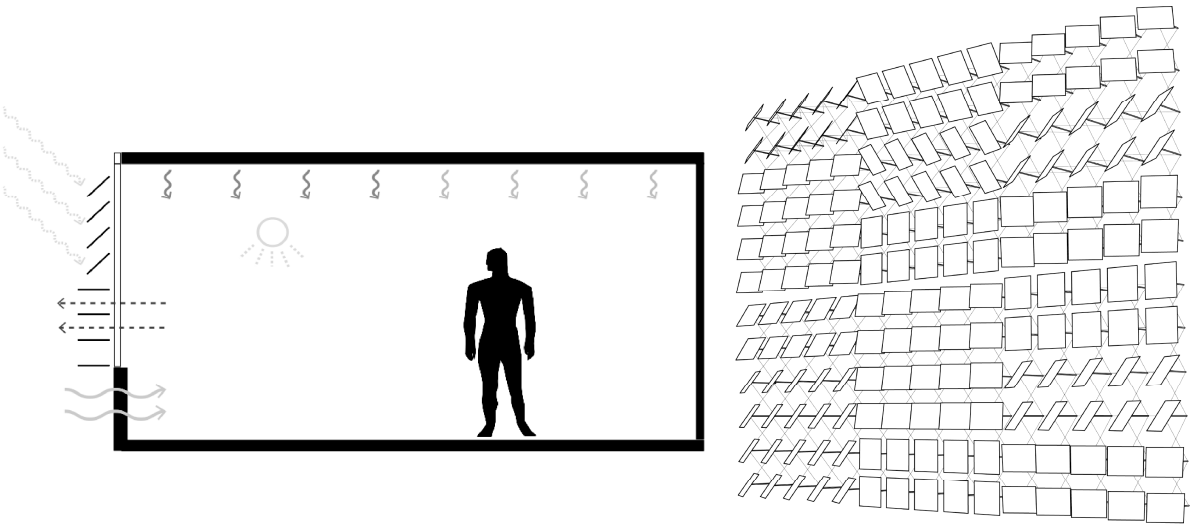

Figure 1: Environmental factors that can be influenced by adaptive solar façade systems include solar insolation, views, heating/cooling loads and artificial lighting loads (left). Adaptive solar façade elements in various orientations (right).

In addition to determining energy production the positioning of adaptive solar façade elements affects internal building energy dynamics including lighting, heating and cooling loads. In other research we address element orientation in relation to these dynamics. This paper specifically focuses on element orientation in relation to energy production.

COMPUTIAITON OF SOLAR INSOLATION

The task addressed by this research is to quickly calculate solar insolation on a surface at a specific location, time, and orientation. As a reference for computation time, we combined readily available software to perform the calculation through a parametric modelling/simulation setup (ParaSim) (Figure 2). The software packages used in the ParaSim include Rhinoceros [3], a 3D modelling environment, Grasshopper [4], a parametric modelling plug-in for Rhino, Geco [5], an add-on for Grasshopper that links to Ecotect [6], a simulation tool for calculating solar insolation, HoopSnake [7], an add-on for Grasshopper which allows for internal looping of model parameters, and finally Matlab [8] for cleaning and plotting the resulting data.

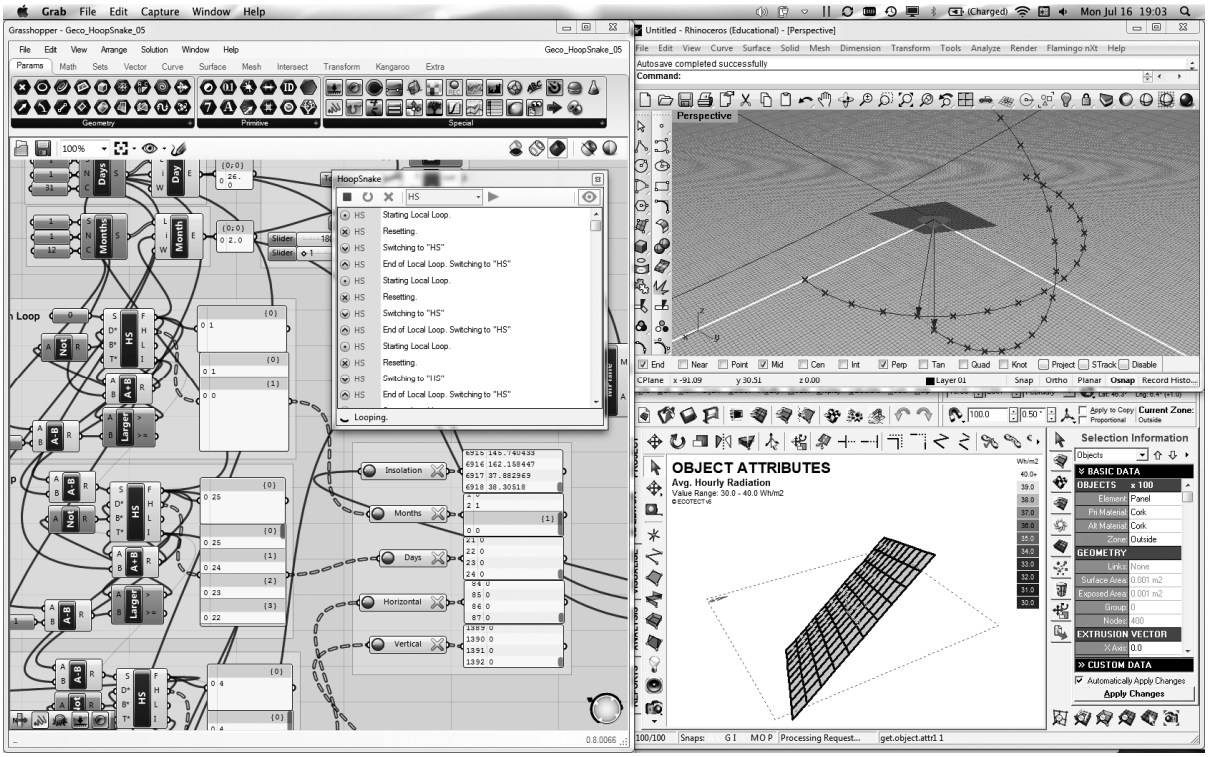

Figure 2: Screen shot of parametric modelling/simulation setup (ParaSim).

While the ParaSim is able to generate the desired results it has multiple aspects that are less than optimal. Being dependent on so many different software packages makes the simulation framework lack robustness. On multiple occasions during this study one or another of the packages was updated, which required reworking the setup to address the incompatibilities that arose. Additionally, while the ParaSim offers a high degree of flexibility regarding what can be modelled and simulated it is overly general, which translates to long simulation times. In response to these shortcomings we propose a lightweight solar insolation framework (LSIF).

The LSIF is written entirely in Python [9]. It uses the Pysolar library [10] to calculate solar position. The Pysolar library is built on a solar position calculation method developed by Reda and Andreas [13], which implements a reduced version of Meeus stellar/planetary position algorithm. [14] Once the solar position is calculated, Lambert's Cosine Law [11] is used to determine the solar insolation I [in W/m^2] on an element's surface that is not perpendicular to the solar angle, as

$$I = I_0 \cdot \cos\theta \tag{1}$$

where I_0 is the insolation on the perpendicular surface, and θ is the angle between the solar ray and the surface normal. If the difference in angle between the solar ray and the surface normal is greater than 90 degrees we set $I = 0$ to avoid calculating solar insolation on the back of a surface.

User inputs include geographic location (longitude, latitude), date time, and surface orientation. Figure 3 shows a flow diagram of the implemented algorithm. Once the calculations finish, Matplotlib [12] is used to plot the results.

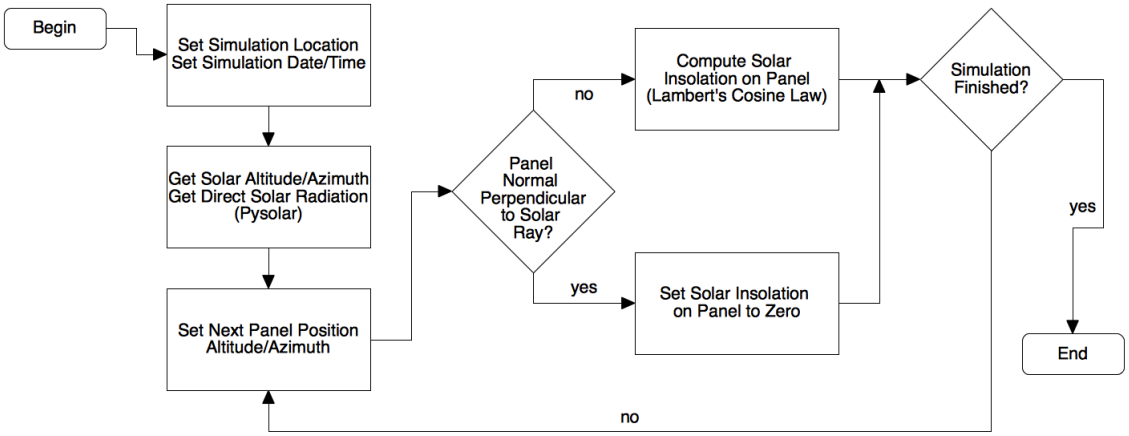

Figure 3: Flow diagram of the lightweight solar insolation framework (LSIF).

RESULTS

The proposed LSIF is able to complete the task of quickly calculating solar insolation on a surface given a geographic location, date time, and surface orientation. The location used in the study is the ETH Hönggerberg, Zürich, CH (longitude 8.510, latitude 47.408).

Table 1 shows the results of a sample of runs for both the parametric modelling/simulation setup and the LSIF. The LSIF proved to be in excess of 3,400 times faster than ParaSim. Simulation times for the ParaSim do not include plotting of results, but the times for the LSIF do include plotting. If this were included in the comparison it would further increase the speed improvement of the LSIF over the ParaSim. Additionally, the LSIF allows for a time resolution on the order of microseconds, while the finest resolution allowed by the parametric modelling setup is hourly. Sub-hourly resolution is beneficial for control applications.

	Simulations	Total Time	Time per Simulation
ParaSim	324	~113 sec.	0.3488 sec.
LSIF	32,400	~3.4 sec.	0.0001 sec.

Table 1: Comparison of simulation speeds between the Parametric modelling /simulation setup (ParaSim) and the lightweight solar insolation framework (LSIF).

Figure 4 shows a subset of simulation runs for every day of the year 2013 at 12:00:00. The plots are the results from the 21st day of each month. Note that the plots are scatter plots comprised of 32,400 data points each, they are not filled contour plots.

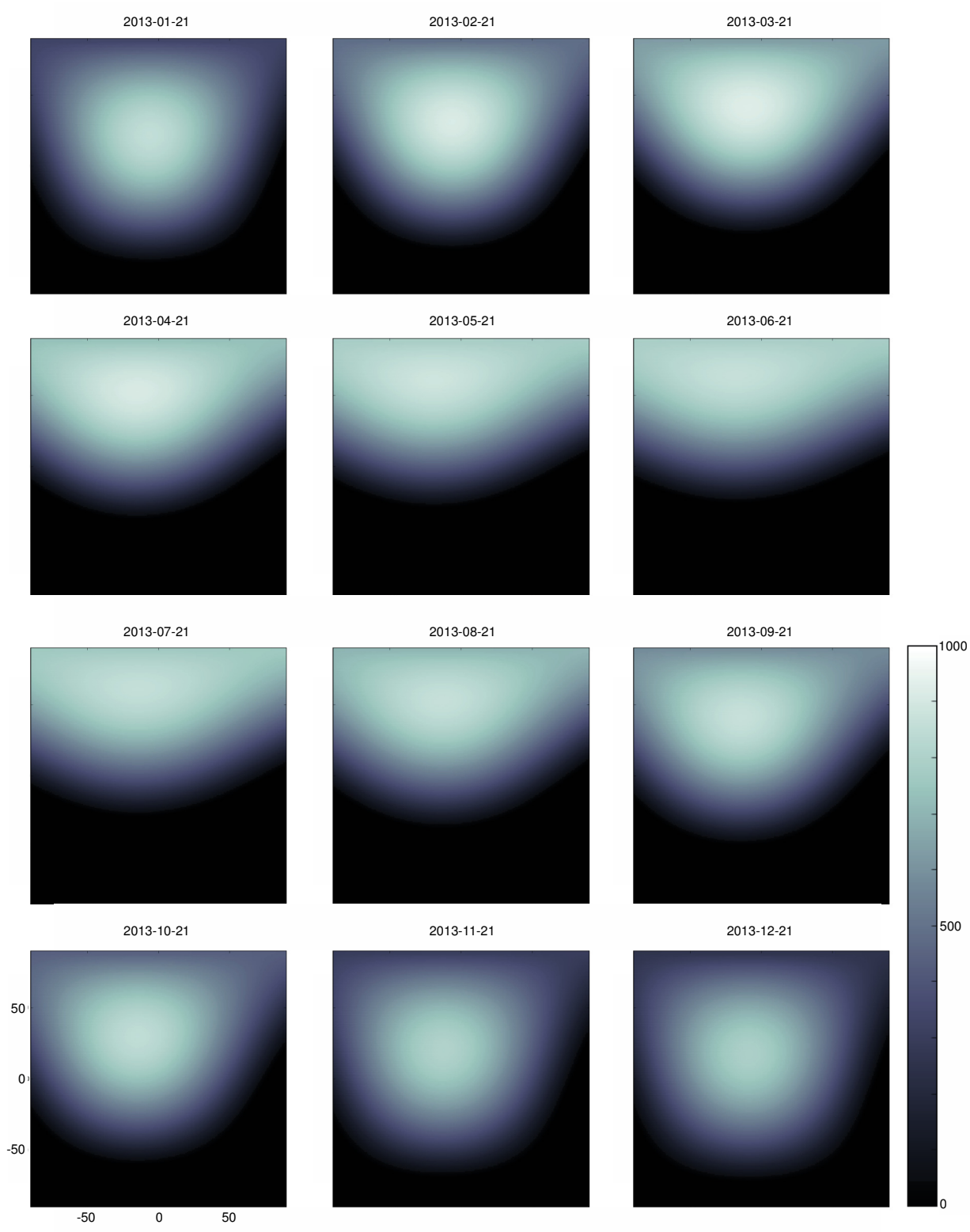

Figure 2: Scatter plots of solar scan results at 12:00:00 on the 21st day of each month. The x-axis represent the horizontal orientation of the panel and the y-axes represent the vertical orientation of the panel. Both x and y axes have a range from -90 to 90 degrees. Each plot is comprised of 32,400 data points. The colormap scale represents W/m^2.

CONCLUSIONS & OUTLOOK

In this paper we present a lightweight solar insolation framework (LSIF) for evaluating energy potential of adaptive solar façade elements. We demonstrate considerable decrease in computation time compared to a parametric modelling/simulation setup (ParaSim). The LSIF offers increased spatiotemporal resolution. High-resolution scatter plots can be generated from the calculations at desired time steps. These results can be used for optimal control of adaptive solar façade elements. This can be done through the creation of lookup tables from results, or calculations can be done on the fly if the required computational power is available. One drawback of the LSIF compared to the ParaSim is that in its current state surrounding geometry (e.g. buildings, landscape, vegetation) are not taken into account. This can be accounted for in the implemented adaptive system by updating lookup tables based on in situ sensor readings. In our continued research we plan to extend this lightweight framework to include internal energy dynamics (e.g. daylighting/electrical lighting, heating/cooling loads) as additional calculations. When used to define the control of adaptive solar façade systems, these calculations combined with user interaction and online learning will lead to increased occupant comfort and reduced energy consumption.

ACKNOWLEDGEMENTS

We would like to thank Daren Thomas for his help in refining the code, and Brandon Stafford for his effort in developing Pysolar and useful discussion.

REFERENCES

1. Rossi, D., Nagy, Z., Schlueter, A., “Adaptive Distributed Robotics for Environmental Performance, Occupant Comfort and Architectural Expression”, Int’l Journal of Architectural Computing, issue 01, volume 10, 2012
2. Dubois, M., Horvat, M., “State-of-the-art of digital tools used by architects for solar design”, IEA SHC Task 41 – Solar Energy and Architecture, Report T.41.B.1, 2010
3. http://www.rhino3d.com (Retrieved 2013-04-25)
4. http://www.grasshopper3d.com (Retrieved 2013-04-25)
5. https://sites.google.com/site/utotoolswiki/gecogh (Retrieved 2013-04-25)
6. http://usa.autodesk.com/ecotect-analysis/ (Retrieved 2013-04-25)
7. http://yconst.com/computation/hoopsnake/ (Retrieved 2013-04-25)
8. http://www.mathworks.com/products/matlab/ (Retrieved 2013-04-25)
9. http://www.python.org (Retrieved 2013-04-25)
10. http://pysolar.org (Retrieved 2013-04-25)
11. Lambert’s Photmetrie (Photometria, sive De mensura et gradibus luminus, colorum et umbrae), 1760, Lambert, available at Open Library : http://openlibrary.org/books/OL23743622M/Lamberts_Photometrie
12. http://matplotlib.org (Retrieved 2013-04-25)
13. Reda, I., Andeas, A., “Solar Position Algorithm for Solar Radiation Applications”, National Renewable Energy Laboratory, Golden, Colorado, USA, 2008. Available online: http://www.nrel.gov/docs/fy08osti/34302.pdf
14. Meeus, J. “Astronomical Algorithms”. Second edition 1998, Willmann-Bell, Inc., Richmond, Virginia, USA

NON-INTRUSIVE LOAD MONITORING TECHNIQUES FOR ENERGY EMANCIPATION OF DOMESTIC USERS

G.M. Tina; S. Gagliano; V. Amenta

DIEEI: Department of Electrical, Electronics and Information Engineering, University of Catania, Italy.

ABSTRACT

Consumer systems for home energy management can provide significant potential energy saving. But most people have only an approximate idea of how much energy they are using and what impacts they could make by changing day-to-day behavior. On the other hand, detailed information about energy consumption is crucial especially when a PV system is also locally connected, if the overlapping of load and PV generation curves is an economical objective. Hence it is important to develop systems, based on Non Intrusive Appliance Load Monitoring (NIALM) algorithms, in which individual appliance power consumption information is disaggregated from single-point measurements, that provide a feedback in such a way to make energy more visible and more amenable to understanding and control. This paper presents a new algorithm which detects the load curve of each appliance in a domestic context based on power consumption. The system successfully detects two-state (on-off) appliances by means of measurements performed by a commercially available power meter.

Keywords: NIALMS, power meter, loads identification.

INTRODUCTION

Today when resources are getting increasingly scarce, leading to an increase of prices charged by utility providers, there's currently a renewed interest in understanding and reducing energy use. Commercial interest in Non Intrusive Load Monitoring (NILM) includes Google PowerMeter [1], a system developed by Greenbox [2] and the established NILM products from Enetics [3]. Commercial solutions to improve the management of energy demand have centred on the deployment of smart meters and in-home energy displays that can provide whole-house real-time energy monitoring and dynamic pricing from suppliers in an attempt to motivate users to shift or reduce their energy consumption [4]. Digital electricity meters (e.g. power meters) measure total electricity consumption of a household at a fine temporal granularity. Using this data, the consumption of individual appliances can be retrieved and used to provide novel services, such as personalized energy consulting. There are two approaches to monitoring household energy. The first uses a single NILM meter to measure aggregate energy use as power enters the home. The second approach measures each load in the home separately, using complex instrumentation systems that individually meter each device's energy consumption [5-8] Although this approach provides accurate data for each device, it requires a significant investment in monitoring equipment. The first approach with a single NILM meter is attractive because it's easy, requiring only one meter to monitor whole-house energy consumption. This approach analyzes the whole-house data and matches step changes in power use to a load database—for example, a 500-watt step might represent a refrigerator turning on. This works remarkably well for large (more than 150-W) loads that operate as simple on/off devices or have simple operating states [9]. However, because there are many possible combinations of appliances contributing to the electricity consumption at the same time, these centralized, single-sensor approaches usually achieve limited accuracy in real deployments [10, 11]. Also, low-power loads and devices with numerous states, such as a

dishwasher, or continuously variable energy use, such as an electric stove, are difficult to extract from whole-house measurements. On the other hand the effectiveness of the disaggregation algorithms are strictly correlated with the information that the house's owner is available to provide to the monitoring system. Some data are reported on the technical documentation of the appliances whereas others can be recovered only by means of specific electrical characterization of each appliances. The available NIALM methods, though based on different techniques, have several common principles. First, specific appliance features, or signatures, need to be selected and mathematically characterized. Next, a hardware installation (sensor and data acquisition system) that can detect the selected features, is required. Lastly, a mathematical algorithm detects the features in the overall signal. Here, we describe NILM approach with a single and commercially available power meter and the related new and simple algorithm for disaggregating the overall consumption into individual appliances. The paper will be structured as follows: the hardware installation will be explained in system description paragraph, the algorithm description and lastly the results. The algorithm is suitable for detection of two-state (on-off) appliances and the algorithm does not require detailed information about the equipment.

SYSTEM DESCRIPTION

The Monitoring Local System (SML) allows to acquire and to elaborate locally electrical measurements (e.g. voltage, current, power factor, so on). The measurements are acquired at the point of delivery of electricity from the company distributing electricity. After a properly processing the data can be transmitted via the web to a server, named Central Monitoring System (SMC) where data processing at higher level are performed. Both data collected locally and those drawn from the central server will then be made available to the user through an appropriate informatics platform and userfriendly interface. Figure 1 shows a simply system architecture SML, which is composed of a tool for the acquisition and processing of the voltage and current detected at a point in the system ("power meter"). For operational and safety reasons the current cannot be detected directly, it is necessary to use a current transformer (TA). PM1 and PM2 are two devices used to monitor locally electrical loads. In fact, two power meters have been used in such a way to compare their performances, strictly related to NILM algorithms applications.

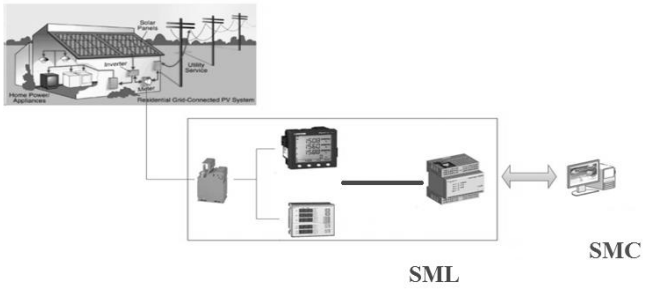

Figure 1: System Architecture of a NILM system.

In Fig.2 the experimental set up, up installed in IDRILAB laboratory at DIEEI (University of Catania-Italy), is shown.

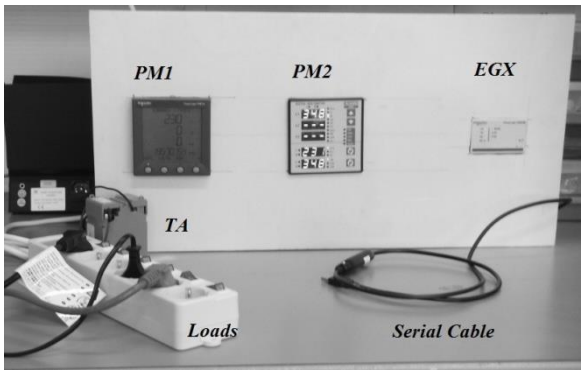

Figure 2: Experimental set up.

The measurements acquired by the power meters must be either transferred to a local computer or directly to the Internet, in order to transfer them to the SMC via WEB. For this purpose it is possible to use a serial cable, or an intelligent Ethernet gateway that provides fast, reliable Ethernet-to-serial line connectivity between intelligent power meters. The system shows in this paper does not require the access to individual devices, therefore, does not require the installation of sensors distributed along the plant. The Power meter data will be sent to low frequency (1 Hz) and the data are average values with respect to a sampling period set in advance in the above-mentioned equipment. The effectiveness of NILM algorithms is guaranteed by the quality of the data we get from Power meters. In this way have been experimented and compared two different devices: PM1 and PM2.

ALGORITHM DESCRIPTION

In order to decompose the total load into its components, we need the model of each appliance and its main characteristics. The appliances can be modeled by a power constant load. Some appliances contain more than one electrical load (for example, a front loader washing machine contains a heating element and a motor – each component drawing very different loads). Preliminary in this project we consider only two state (on / off) appliances. The system uses two different power meters for voltage (V), current (I) and active and reactive power (P, Q) measurement. The data for developing the algorithm were collected at 1s intervals in the laboratory IDRILAB (DIEEI-University of Catania). Two power meters were used to measure and record the current (I), the voltage (V) and active and reactive power (P), (Q) in the following appliances: (1) lamp, (2) personal computer, (3) refrigerator and (4) radio. Due the pretty constancy of the voltage over the day, in the disaggregation algorithm have not been introduced a procedure to cope with it. Preliminary data analysis consisted of observing how the electric demand of each appliance varies over time and then comparing it to the total electric demand. For example, the refrigerator has a long low rectangular profile with a relatively large initial spike and a short period of decreasing demand at the end of the switching event. Each appliance event is characterized by an ON signal, an OFF signal and a duration. The NILM program is written in the Matlab programming language and it is descript in Fig. 3. The input are: an Excel data files (Appliance data.xls) which contain a series of information: the number of the appliance, the active nominal power (P), the reactive nominal power (Q) and a file with the information coming from the measurement system. This information can be preprocessing before enter in NILM algorithm. These algorithms are called signal preprocessors (linearize P, linearize Q) because they filter the total demand signal before appliance load recognition is used. The preprocessor program aims to smooth

out small or erratic variations in the total demand signal. The final filtered signal consists of distinct rectangular shapes where each increase or decrease in demand is more likely to represent a significant ON or OFF signal. To eliminate small or erratic variations it is necessary to set up: ΔP, ΔQ, and the related ΔT (time interval). If the variations ΔP, ΔQ is greater than a fixed value (Tolerance, that depends on the appliance) and this variation continues for a time interval greater than ΔT a steady-state value is detected. The filtered signal from the preprocessors are the input for the NILM algorithm. The algorithm compares each change in the P total signal to each appliance operating range (coming from Appliance data.xls). If the magnitude of the change is within the range of an appliance operating level, that is, the mean demand plus or minus two standard deviations, the change is attributed to that appliance. Therefore, assuming that there are no coincident ON or OFF signals, at least 95% of the ON and OFF signals should be recognized. If an increase is within both two different appliances range, a new comparison in change in the Q total signal has been applied. In figure 3 algorithm's flowchart is presented.

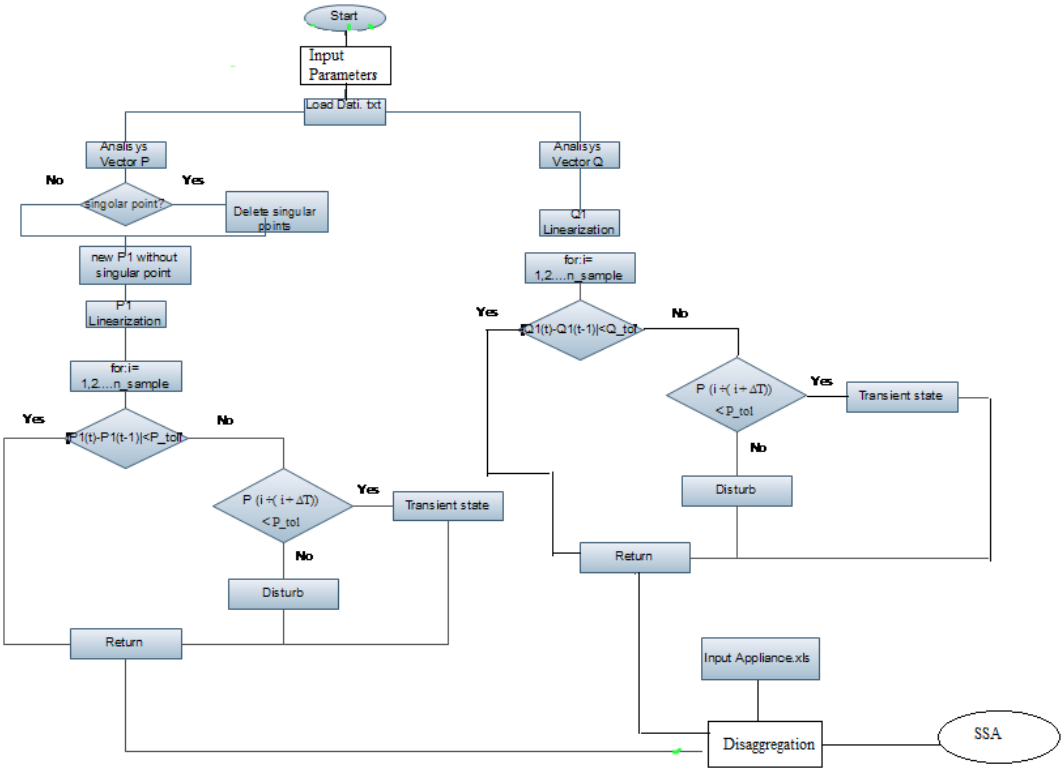

Figure 3: Flowchart of the proposed NILM algorithm

RESULTS AND CONCLUSIONS

The measurements of active and reactive power coming from the developed system have been linearized and the results have been reported in Figs. 4 and 5. Of course the results of linearized process depend on the parameters values. Specifically, they are the minimum step of P and Q, named respectively P_tol and Q_tol, and the minimum duration of the variation of the considered variables (e.g. P and Q), named Delta_T, that can be considered as a switching on and off of an appliance. Of course, as far as the Delta_T tends to zero the precision of the linearization increases, but, on the other hand, it does not allow to distinguish adequately a transition from noise in the variables. This condition affects greatly the process

of disaggregation. The samples have been recorded every second. Fig. 6 shows the results for four appliances: lamp, personal computer, refrigerator and radio.

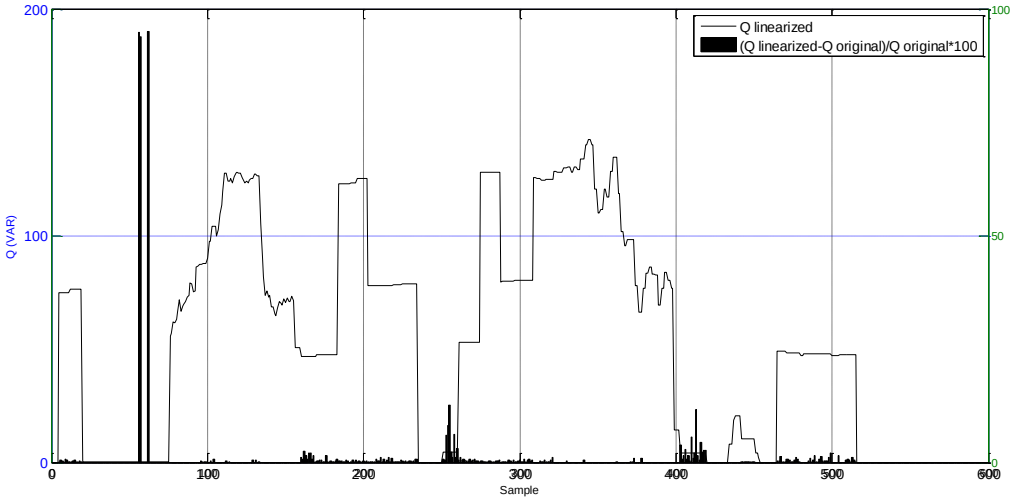

Figure 4: Reactive Power: measurements and percentage error

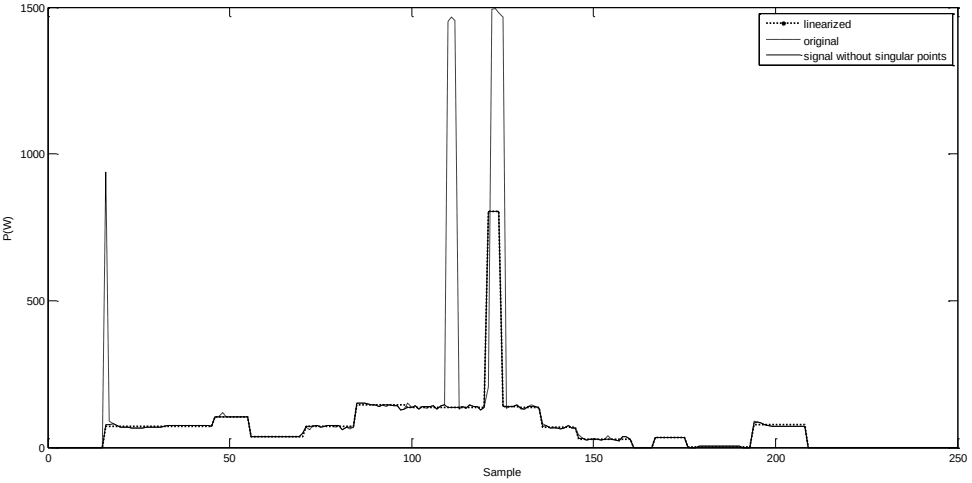

Figure 5: Active Power: measurements, corrected, linearized

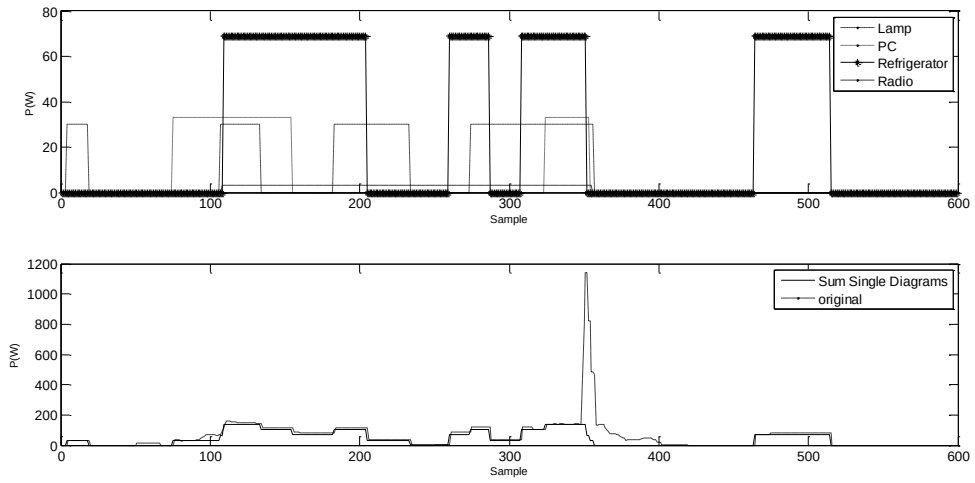

Figure 6: load curve: single appliances (above), total load (below)

From the analysis of Fig. 6, the disaggregation algorithm seems to perform adequately but some problems have arisen, it is worth mentioning the treatment of the switching on spikes of some appliances (e.g. refrigerator and coffee machine). In fact in the linearization process they are almost always eliminated but in this way important information for disaggregation process are lost.

ACKNOWLEDGEMENTS

This work is developed under the SEEE project funded by the POR FESR Sicilia 2007-2013 program.

REFERENCES

1. www.google.org/power meter
2. http://getgreenbox.com
3. www.enetics.com
4. Ramchurn, P. Vytelingum, A. Rogers and N. Jennings, "Putting the "smarts" into the smart grid: A grand challenge for artificial intelligence." CACM (2011).
5. Y. Agarwal , T. Wang, R. K. Gupta, "The Energy Dashboard: Improving the Visibility of Energy Consumption at a Campus-Wide Scale" BuildSys'09, November 3, 2009, Berkeley, CA, USA
6. X. Jang et al. Experiences with a high Fidelity Wireless Building Energy Auditing Network" Proc. 7th ACM Conf. Embedded Network Sensor Systems (SenSys 2009) ACM Press 2009, pp 113-126.
7. M. Kazandjieva et al. PowerNet: A Magnifying Glass for Computing System Energy," Proc. Stanford Energy & Feedback Workshop: End-Use Energy Reductions through Monitoring, Feedback, and Behavior Modification, 2008.
8. www.tendrilinc.com
9. Alan Marchiori, Douglas Hakkarinen, Qi Han, Lieko Earle, "Circuit-Level Load Monitoring for Household Energy Management" IEEE 2011
10. O. Parson, S. Ghosh, M.Weal and A. Rogers, "Using Hidden Markov Models for Iterative Non-intrusive Appliance Monitoring." In Proc. 2011 Machine Learning for Sustainability Workshop (MLSUST 2011), Sierra Nevada, Spain.
11. J. Z. Kolter and M. J. Johnson, "REDD: A Public Data Set for Energy Disaggregation Research." In Proc. 2011 KDD Workshop on Data Mining Applications in Sustainability (SustKDD 2011), San Diego, CA, USA.
12. L. Farinaccio, R. Zmeureanu, "Using a pattern recognition approach to disaggregate the total electricity consumption in a house into the major end-uses", Energy and Buildings, vol. 30, pp. 245-259, 1999.
13. M. L. Marceau, R. Zmeureanu., "Nonintrusive Load Disaggregation Computer Program to Estimate the Energy Consumption of Major End Uses in Residential Buildings", Energy Conversion & Management, vol. 41, pp. 1389-1403, 2000.
14. J. Powers, B. Margossian, B. Smith, "Using a Rule-Based Algorithm to Disaggregate End-Use Load Profiles from Premise-Level Data", IEEE Computer Applications in Power, pp. 42-47, 1991.

FROM LIGHTING INTENTION TO LIGHT FILTERS

Vincent Tourre[1], Eduardo Fernández[2]; Gonzalo Besuievsky[3]

[1] *LUNAM, École Centrale de Nantes, CERMA UMR CNRS 1563, Nantes, France*
[2] *Centro de Cálculo, Universidad de la República, Uruguay*
[3] *Geometry and Graphics Group, Universitat de Girona, Spain*

ABSTRACT

Lighting intentions are the goals and constraints that designers would like to achieve in an illumination design process. Light filters can be used as an architectural element to obtain such intentions by inserting them into walls or roofs. Defining correctly the filter shape is a challenge. In this work, we present a novel method to design optimal filters from a given lighting intention. Our methodology, which could be completely integrated within a computer aided architectural design framework, it is based on a global illumination and optimization approach. Our test results show that optimal filter shapes can be obtained in a short time.

Keywords: Lighting intention, Inverse lighting, CAD, Building envelope

INTRODUCTION

As light reveals architecture, the natural lighting is a critical feature in architecture design. For the designer, the problem comes from the management of the natural lighting during the design process. Some design approaches have focused on keeping the intention of the designer as the project is going on. As an example, the design by intent approach is based on a lighting description, expressed by texts or by drawings, taking into account the user comfort or the energy savings. In general, the whole process to design an architectural illumination space may achieve several steps that go from revealing the general use of the space to the special light accentuation that must be obtained [10].

The goal of the Computer Aided Architectural Design (CAAD) developers is to keep the mentioned intents as a guideline through the design process by a connection between the lighting description and the geometric or optic properties of the building. In this work, we propose to link the designer's lighting concepts and the building matter through the natural lighting simulation used in an inverse approach. Through our approach architects and engineers could set up constraints parameters about lighting needs and an inverse lighting model optimizes some of the geometric properties of the built spaces. Previous work proposing solution for this problem can be found in [1], and an approach with a case-study application can be found in [12, 7].

In this paper, we present a methodology for computing optimal filters from a given lighting intention. An architectural real-case example is shown in Figure 1. The paradigm of our method is to focus on potential light filtering areas such as walls, openings or architectural elements. The key of our method is to find a compact representation of the lighting equations derived, so we can applied an inverse lighting approach to solve the design constrain problems. The main contribution of our work is to provide a flexible lighting design approach intended for searching both, fast and accurate solutions to the inverse lighting problem. The method is presented as a framework approach that could

be extended for many lighting filtering purposes. We present here results for applying it for designing filters using pattern that the designer provide as a draw.

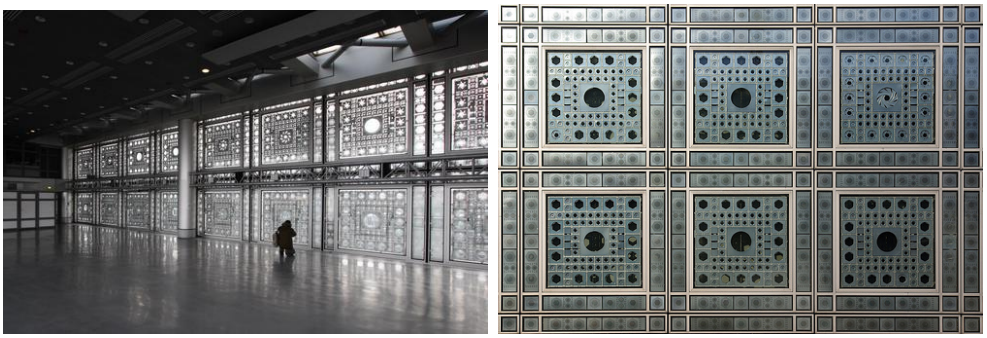

Figure 1: Lighting filter examples in modern architecture. Institute du monde Arabe (Paris), by Jean Nouvel. The holes of the filter (right) can vary to achieve a desired intention.

RELATED WORK

Our work deals with an inverse lighting problem. Direct methods calculate data from a specific configuration of model parameters. In contrast, inverse problems generally infer the properties of a physical system from desired data. Inverse problems are usually numerically complex and are of interest in a wide range of fields in lighting engineering and lighting design.

In our work we focus on inverse problems considering global illumination solution, for such purpose we use the radiosity computation. In this context, several works driven by different motivations and assumptions were proposed [2, 8, 5]. We based our solution on work done in [5], where the low-rank radiosity method is used to solve the inverse lighting problem integrating skylights and artificial Lambertian sources.

PROBLEM DEFINITION

The main goal of our proposal is to provide a tool for efficient lighting design of filters. We consider diffuse environments, that is, all of the surfaces have perfectly diffuse materials with no specular component. For skylight filters we also consider that a diffuser with a homogeneous transmittance coefficient is used. This kind of diffusers are currently used systems in real buildings. They provide diffuse and controllable sunlight, which creates a desirable ambient light [10]. These kinds of skylights, because they scatter light homogenously, can also be considered as Lambertian emitters. The filters we use in this work are defined as holes of this kind of emitters.

Lighting intention

Lighting intentions can be defined as the goals and constraints that designers must provide to achieve a desired illumination. Regarding the reference focus and motivation, they could be classified in different ways by:

- Lighting representation (incoming or reflected light).
- The set of surfaces considered (the overall scene or a specific set of surfaces).
- The kind of target goal to achieve (optimize specific lighting levels or contrast be-

tween surfaces, or satisfy several constraints).

- The light transport level (only direct lighting or global illumination).

Designers have freedom to set as many lighting intention as necessary. Possible examples are: "Guarantee a minimum of irradiance in a wall" or "Maximize the incoming light into the room". An example of restriction may the size of the opening or any other architectural constraint (see Figure 2(a)). In an inverse lighting problem we must obtain the "best" lighting position that also satisfies both the constraints and the lighting intentions. Usually, a goal related to the energy-consumption should be minimized.

Filter Design

In order to specify the filter design we use a pattern drawing. First, the designer has to decide which is the wall or roof where to install the filters. Then, a pattern is associated. The designer has complete freedom to use any draw. This draw will be mapped to the associated surface as lambertian holes emitters in the constructive surface. Of course they may be many ways for expressing a possible shape of a filter, we just decide to use this simple one in order to test our optimization engine.

System Overview

The pipeline design of our approach is described in Figure 2(b). Given an architectural interior model for lighting design, the user first configures both the parameters of the filter and lighting intentions. These parameters specify where to install the filters as well as the pattern they may have. In the example of Figure 2(a), a homogeneous filter with holes was used with a maximum rectangular area to provide the opening. Before the optimization process begins, we first pre-process the scene to obtain a compact representation of the form-factor matrix of the elements of the scene. For this purpose, we use a low-rank radiosity method. The optimization method works by getting the compact representation found and a design configuration, to obtain efficiently the optimal shape. The results can be visualized interactively and the direct lighting computation can be assured. The designing process may iterate if the designer wants to change or explore other solutions by modifying parameters.

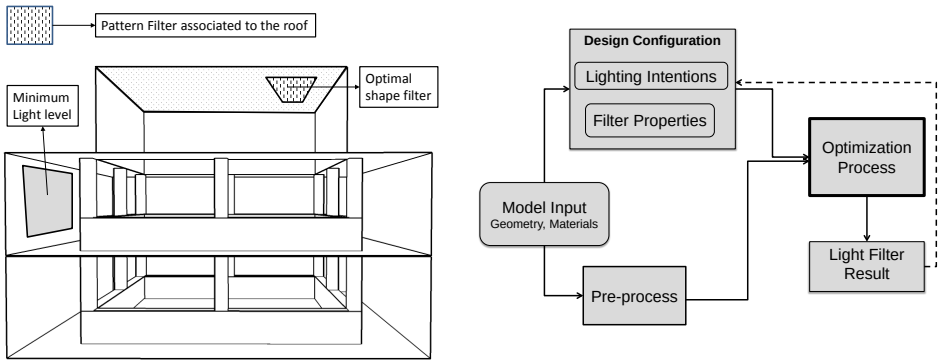

(a) Design example scene. (b) System overview.

Figure 2: From a given design specification and filter pattern (a), our pipeline uses an optimization process to compute the optimal filter shape (b).

OPTIMIZATION PROCESS

In this section we summarize our mathematical method to obtain the filter optimization. The method is based on direct computation through the use of the low-rank radiosity method and the same inverse lighting method as in [5].

Direct Radiosity Computation

In the discrete radiosity formulation, the radiosity of the scene is computed by solving a linear system that can be expressed as:

$$(\mathbf{I} - \mathbf{RF})B = E \tag{1}$$

where $\mathbf{I}$ is the identity matrix with dimension $n \times n$ (n is the number of patches or polygons), $\mathbf{R}$ is a diagonal matrix that stores the reflectivity index of the patches, $\mathbf{F}$ is the form factor matrix, B is a vector with the radiosity value of each patch, and E is the emission vector. B and E are measured in W/m^2.

Regardless of the optimization method used, the radiosity must be evaluated many thousand times before finding a converged solution. For this purpose an efficient method should be used. The low-rank radiosity method [4], offers the advantage of obtaining directly the radiosity values through an inverse matrix approximation:

$$\widetilde{B} = \widetilde{\mathbf{M}}_B E \tag{2}$$

where $\widetilde{\mathbf{M}}_B$ is an approximation of $(\mathbf{I} - \mathbf{RF})^{-1}$. The detailed process on how to obtain this matrix is described in [4]. The key of the method is to explore the coherence in the scene to reduce the numerical rank of the form factor matrix $\mathbf{F}$. This matrix can be approximated by the product of two matrices with dimension $n \times k$ ($n \gg k$), without loss of relevant information. The memory requirement for both matrices is $O(nk)$, which is significantly less than $O(n^2)$ required to store $\mathbf{F}$ of Equation 1. This memory saving allows storing the information in the main processor memory for scenes with several hundred thousand patches.

For static scenes with dynamic lighting, the required matrices are computed once, therefore, the calculation of $\widetilde{B}$ has complexity $O(nk)$. This result allows to perform many radiosity calculations per second, motivating it uses for inverse problems.

Optimization Algorithms

The lighting intentions and the objective, can be formulated as an optimization problem. The problem consists of finding the emission configuration E that optimizes a goal function $f(E)$, subject to a set of constraints $G(E)$ that must be satisfied:

$$\min f(E), \text{subject to } G(E) \tag{3}$$

Although optimization is a well known topic, there is no computational algorithm that provides the global optimum for a general non-linear objective function. Finding the optimal solution by *brute force* is usually not feasible in a reasonable time because of the huge search space of the possible states. Heuristic algorithms avoid visiting the whole search space, by means of designing rules that drive the search towards optimal solutions. There is a large number of heuristic search algorithms in the literature, which can potentially be used to solve lighting problems [9, 11].

In our work, we used the Variable Neighborhood Search (VNS) method [6]. This methodology is based on the idea of successive explorations of a set of neighborhoods. The method explores, either at random or systematically, a set of neighborhoods to obtain different local optima. Each neighborhood has its own local optimum, and it is expected that the global optimum is the same as a local optimum for a given neighborhood. We adapted the mention algorithm for finding the optimal filter shapes. We used a closed polygon (for example a rectangle) as a clipping figure to find the best holes configuration that would achieve the intentions. The algorithm shakes over the extremes of the polygon, that are used as variables in the optimization algorithm (see Figure 4).

RESULTS AND CONCLUSSION

We implemented the proposed method and test it with different pattern filters and lighting intentions. We choose a patio scene , where filters should be installed in the roof (see Figure 3 and 4). All simulations were performed in a Matlab environment using a standard PC (Intel Core i7 2.2 Ghz processor and 8 GB memory).

Scene : Patio. Size ($n \times k$): 23744×1484.

Goal : Maximize power light in the marked areas

Constraints : The light emitters must lie in the ceiling, and
$B_{min} \leq B(P) \leq B_{max}, \forall P \in$ red surface
$A_{min} \leq Area_{Emitter} \leq A_{max}$

Variables : 8 (Four 2D-coordinates that delimit the sources position)

Processing time :
Pre-processing: The low-rank pre-computation takes 18 minutes.
Optimization: 570 seconds for 100000 radiosity evaluations

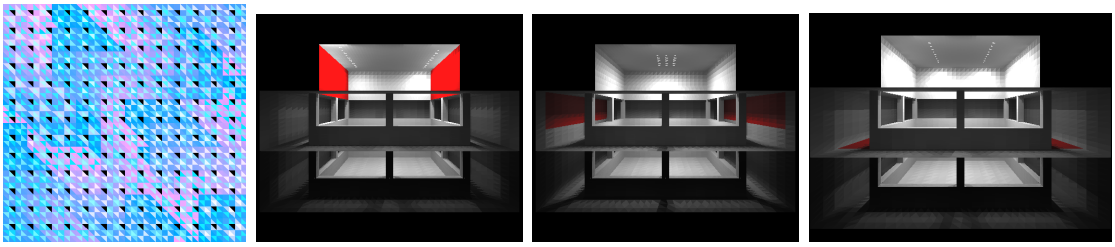

Figure 3: Filter optimization for an homogeneous filter (left), the black triangles represent the pattern and the rest of triangles, the associated mesh. Three different lighting intentions (form left to right: lateral upper walls, first floor walls and first floor) where designed to obtain the corresponding filters.

We presented a new method for designing optimal filters from a given lighting intention. We believe that it could be a useful method for opening design, where singular installation in buildings are unpredictable. Our test results show that optimal filter shapes, using a global illumination approach, can be obtained in a short time, This considerable time reduction could promote it use for interactive applications and it inclusion in standard illumination design tools, as for example [3]. For future work, we would like to extend our model for including time-dynamic variable holes as in Figure 1.

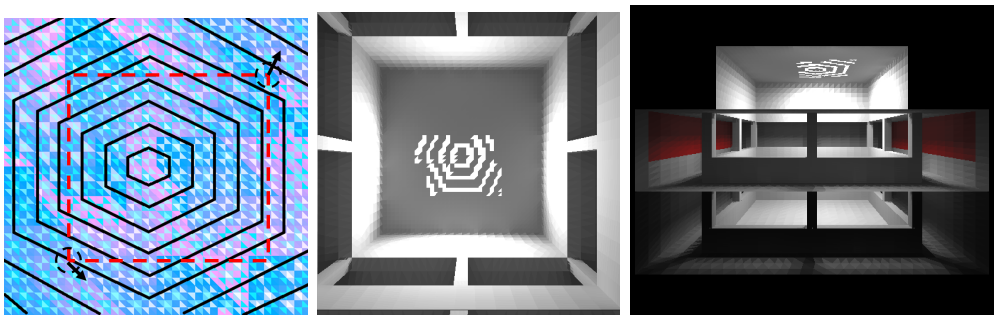

Figure 4: Filter optimization using an hexagonal pattern filter (left) and the resulted filter (middle) for given lighting intention at the lateral (in red) walls (right).

ACKNOWLEDGEMENTS

This work was partially funded by the TIN2010-20590-C02-02 project from Ministerio de Ciencia e Innovación, Spain, and LiPaD project (PICS 5786) from CNRS, France.

References

[1] G. Besuievsky and V. Tourre. A daylight simulation method for inverse opening design in buildings. In *Proceedings of the IV Iberoamerican Symposium in Computer Graphics*, pages 29–46, June 2009.

[2] Magali Contensin. Inverse lighting problem in radiosity. *Inverse Problems in Engineering*, 10(2):131–152, 2002.

[3] DIALux. Dial. light, building, software. www.dial.de, Apr 2013.

[4] Eduardo Fernández. Low-rank radiosity. In *Proceedings of the IV Iberoamerican Symposium in Computer Graphics*, pages 55–62, June 2009.

[5] Eduardo Fernández and Gonzalo Besuievsky. Inverse lighting design for interior buildings integrating natural and artificial sources. *Computers & Graphics*, 36(8):1096–1108, 2012.

[6] Pierre Hansen and Nenad Mladenovic. Variable neighborhood search: Principles and applications. *European Journal of Operational Research*, 130(3):449–467, May 2001.

[7] Frdric Imbert, KathrynStutts Frost, Al Fisher, Andrew Witt, Vincent Tourre, and Benjamin Koren. Concurrent geometric, structural and environmental design: Louvre abu dhabi. In *Advances in Architectural Geometry 2012*, pages 77–90. 2013.

[8] J. K. Kawai, J. S. Painter, and M. F. Cohen. Radioptimization - goal based rendering. In *ACM SIGGRAPH 93*, pages 147–154, Anaheim, CA, 1993.

[9] David Luenberger and Yinyu Ye. *Linear and Nonlinear Programming*. International Series in Operations Research & Management Science. Springer, 2008.

[10] S. Russell. *The Architecture of Light: Architectural Lighting Design, Concepts and Techniques: a Textbook of Procedures and Practices for the Architect, Interior Designer and Lighting Designer*. Conceptnine, 2008.

[11] El-Ghazali Talbi. *Metaheuristics: From Design to Implementation*. Wiley Publishing, 2009.

[12] Vincent Tourre and Francis Miguet. Lighting intention materialization with a light-based parametric design model. *International Journal of Architectural Computing*, 08(4):507–524, 2010.

AUTHOR INDEX

AUTHOR INDEX

E

F

G

H

N

O

P

Q

R

S

T

V

W

X

Y

Z

ACKNOWLEDGEMENTS

CISBAT 2013 would not have been possible without the efficient contribution of the secretariat of the Solar Energy and Building Physics Laboratory as well as that of our scientific and technical staff.

Our scientific partners from Cambridge University and the Massachusetts Institute of Technology as well as the members of the international scientific committee and the session chairs have enthusiastically supported the conference and ensured its quality. We would like to express our sincere thanks for the time and effort they have spent to make it a success.

CISBAT can only exist thanks to the patronage of the Swiss Federal Office of Energy. We are grateful for their continuing support.

We also owe sincere thanks to the Zeno Karl Schindler Foundation, whose financial support was vital for the conference.

Finally, we cordially thank all speakers, authors and participants who have brought CISBAT 2013 to life.

Prof. Dr J.-L. Scartezzini

Chairman of CISBAT 2013

Head of EPFL Solar Energy and Building Physics Laboratory